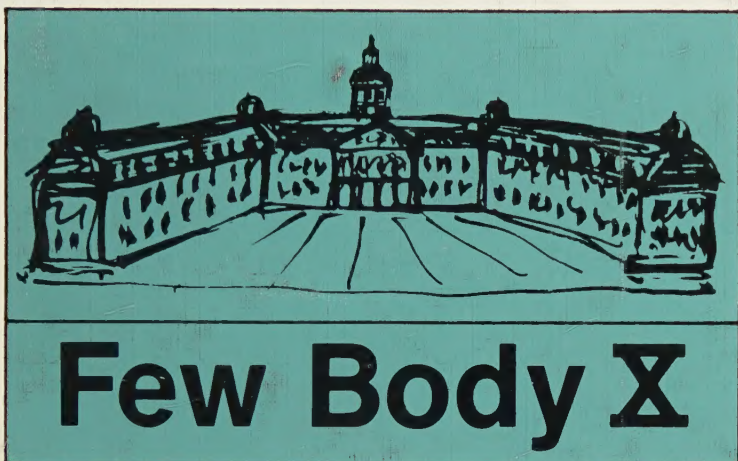


# Few Body Problems in Physics



Volume I    Invited Review Talks and Reports  
on the Discussion Sessions

edited by  
**B. Zeitnitz**

North-Holland

QC  
174.17  
.P7  
I58  
1983  
v.1





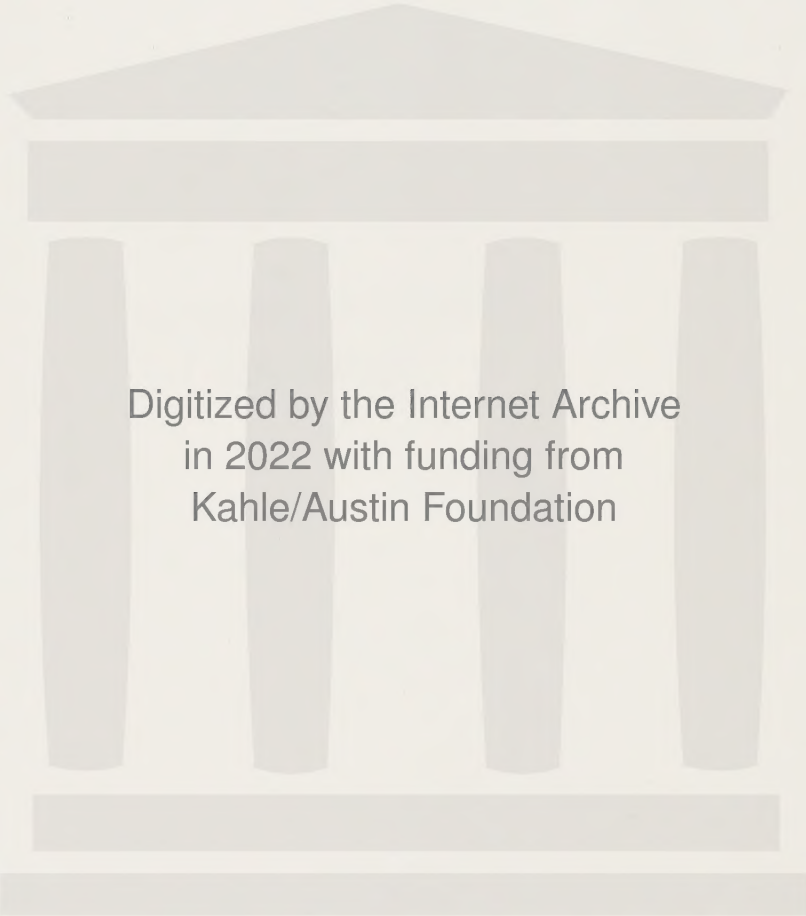
RETURNING MATERIALS:

Place in book drop to  
remove this checkout from  
your record. FINES will  
be charged if book is  
returned after the date  
stamped below.

[REDACTED]  
[REDACTED]  
MICHIGAN STATE UNIVERSITY  
LIBRARY

APR 25 2017

WITHDRAWN



Digitized by the Internet Archive  
in 2022 with funding from  
Kahle/Austin Foundation







FEW BODY PROBLEMS  
IN PHYSICS



# FEW BODY PROBLEMS IN PHYSICS

Proceedings of the Tenth International IUPAP Conference on  
Few Body Problems in Physics,  
Karlsruhe, Germany, 21-27 August, 1983

Volume I

Invited Reviews Talks and  
Reports on the Discussion Sessions

Edited by

**B. ZEITNITZ**

Kernforschungszentrum Karlsruhe  
University of Karlsruhe

organized at

**The University of Karlsruhe**

sponsored by

Union of Pure and Applied Physics  
Kernforschungszentrum Karlsruhe  
Deutsche Forschungsgemeinschaft



1984

NORTH-HOLLAND  
AMSTERDAM · OXFORD · NEW YORK · TOKYO



© Elsevier Science Publishers B.V., 1984

*All rights reserved. No part of this publication may be reproduced, stored in a retrieval system, or transmitted, in any form or by any means, electronic, mechanical, photocopying, recording or otherwise, without the prior permission of the copyright owner.*

ISBN: 0 444 86901 8

*Published by:*

North-Holland Physics Publishing  
a division of  
Elsevier Science Publishers B.V.  
P.O. Box 103  
1000 AC Amsterdam  
The Netherlands

*Sole distributors for the U.S.A. and Canada*

Elsevier Science Publishing Company, Inc.  
52 Vanderbilt Avenue  
New York, NY 10017  
U.S.A.

## **Reprinted from Nuclear Physics A416 (1984)**

### **Library of Congress Cataloging in Publication Data**

International IUPAP Conference on Few Body Problems in  
Physics (10th : 1983 : University of Karlsruhe)  
Few body problems in physics.

Includes indexes.

Contents: v. 1. Invited reviews, talks, and reports  
on the discussion sessions -- v. 2. Contributed papers.

1. Few-body problem--Congresses. 2. Quarks--  
Congresses. 3. Nuclear reactions--Congresses.  
I. Zeitnitz, B. (Bernhard), 1929- . II. International  
Union of Pure and Applied Physics. III. Kernforschungs-  
zentrum Karlsruhe. IV. Deutsche Forschungsgemeinschaft.  
V. Title.

QC174.17.P7I58 1983 530.1'4 84-1681

ISBN 0-444-86901-8 (v. 1 : U.S.)

ISBN 0-444-86902-6 (v. 2 : U.S.)

Printed in The Netherlands

# ORGANIZATION

This conference was organized at the campus of the University of Karlsruhe. It was sponsored by the International Union of Pure and Applied Physics, the Kernforschungszentrum Karlsruhe and the Deutsche Forschungsgemeinschaft.

## Conference Organizers

H.O. Klages and B. Zeitnitz

## Scientific Organizing Committee

J. Domingo	P.U. Sauer
W. Glöckle	F. Scheck
H.M. Hofmann	E. Schmid
H. Koch	H. Schmitt
W. Sandhas	W. Weise
	B. Ziegler

## International Advisory Committee

E.O. Alt	Sing Nan King	A. Rinat
G. Backenstoß	B. Kühn	T. Sasakawa
V.B. Belyaev	F.S. Levin	G. Schierholz
F.P. Brady	I. Lovas	I. Sick
W. Breunlich	L. Lovitch	M. Simonius
S. Brodsky	Th. Mayer-Kuckuck	Yu.A. Simonov
R.H. Dalitz	I.E. McCarthy	I. Slaus
J.A. Edgington	J.S.C. McKee	I.H. Sloan
H. Fiedeldey	B.H.J. McKellar	R.J. Slobodrian
A.C. Fonseca	A.N. Mitra	A.W. Thomas
W. Grüebler	M.J. Moravcsik	J.A. Tjon
L. Heller	G.R. Plattner	R. van Wageningen
A. Johansson	M. Rho	R.L. Walter
Y.E. Kim	J.R. Richardson	H. Zingl

## Local Organizing Committee

P. Doll	H.O. Klages
W. Heeringa	B. Zeitnitz

## Conference Secretaries

G. Grundel and V. Lallemand



## PREFACE

The Tenth International Conference on Few Body Problems in Physics was held August 21 - 27, 1983 at Karlsruhe, Germany. The series of conferences on Few Body Problems was opened with a meeting in London in 1959. It was followed by the International Conferences at Brela, 1967; Birmingham, 1969; Budapest, 1971; Los Angeles, 1972; Quebec, 1974; Delhi, 1976; Graz, 1978 and Eugene, 1980.

During these years the community of scientists working in the field has developed some traditional rules. But besides the discussion of classical nuclear few body systems like the three nucleon bound state problem each conference had its specific new and exciting topics which attracted colleagues from different fields of physics. One important reason for this surprising vitality was the tradition to confine the programme to basic problems of microscopic understanding and description of the inner structure and dynamics of few body systems in nuclear, atomic and molecular physics. The field of few body physics has become even much broader during the last decade and it is now covering important new aspects in elementary particle physics on one side and in chemistry and even in celestial mechanics on the other side.

The scientific field has been again broadened compared to earlier conferences. Here we followed a suggestion of the IUPAP committee. On the other hand the space given to the different topics has been considerably changed. This was partly due to my individual opinion but it followed also a statistics which was obtained from the first application forms where nearly 600 colleagues answered the question on their "main field of interest". Therefore, I think that the final programme which was worked out in close cooperation with the Scientific Organizing Committee follows recent developments in physics.

The number of participants of the conference has considerably grown to nearly 450. There was also a corresponding large number of interesting contributions. Those contributions accepted by the referees are presented in Volume II.

The format of the conference has been considerably changed. There were plenary sessions only. We had 32 invited review talks and 6 discussion sessions for the discussion of more common questions. As a result most fields could only be covered by one talk. Therefore, the speakers were asked to present a critical but fair and complete review on their field.

The discussion sessions were organized by the moderators and the rapporteurs of the corresponding fields. The reports on the discussion sessions were not presented orally but are published in Volume I together with the manuscripts of the review talks.

I am very grateful to Professor E. Lomon who accepted to take over the difficult task of presenting the Closing Remarks only one day before the end of the conference. Volume I contains also summarizing reports on two workshops preceding the conference.

Thanks is due to the members of the Scientific Organizing Committee for all their advice on the programme of the conference and for their assistance in organizing the refereeing procedure for the contributions. The extraordinary energy and skill of my co-organizer Dr.H.O.Klages was most important for the successful organization of the conference. The valuable assistance of Drs. P.Doll and W.Heeringa is gratefully acknowledged.

B. Zeitnitz



## TABLE OF CONTENTS

PREFACE	ix
CHAPTER I	
FEW QUARK PROBLEMS	1c
Quantum Chromodynamics in Few Nucleon Systems	
S.J. Brodsky	3c
Nonperturbative Quantum Chromodynamics	
J. Kuti	25c
Gluonic Excitations in Hadron Spectroscopy	
F.E. Close	55c
Chiral Symmetry and the Bag Model	
A.W. Thomas	69c
Quantum Mechanical Scattering with Confining Interaction	
K. Yazaki	87c
P-Matrix Analysis of Nucleon-Nucleon Scattering	
P.J. Mulders	99c
Nucleon-Nucleon Interaction and the Quark-Compound-Bag-Model (QCB)	
Yu.A. Simonov	109c
Future Experiments on QCD Effects in Few Nucleon Systems with High Energy Electrons	
R.G. Arnold	119c
Few Quark Problems: A Summary of the Discussion Session DS2	
Moderator: L. Heller	
Rapporteur: C. Detar	129c

## CHAPTER II

## PION-NUCLEON INTERACTION

## MESON-FEW NUCLEON SYSTEMS

139c

Meson-Deuteron-Scattering Experiments:

The Polarization Era

J. Arvieux

141c

Pion Absorption and Production in Few Nucleon Systems

G. Jones

157c

Pion-Nucleon Elastic Scattering

B.M.K. Nefkens

193c

First Workshop on Pion-Nucleon Scattering

G. Höhler

209c

Discussion Session on

Mesonic Degrees of Freedom in Few Nucleon Systems

Moderator: F. Lenz

Rapporteur: Y. Avishai

211c

## CHAPTER III

## NUCLEON-NUCLEON INTERACTION

225c

Nucleon-Nucleon Experiments and  
Phenomenology

D.V. Bugg

227c

Analysis of Experimental Information on the  
Dibaryon Resonance Problem

M.P. Locher

243c

Nucleon-Nucleon Scattering at Medium Energies

I.R. Afnan

257c

Symmetries and the N-N Interaction

W.T.H. van Oers

267c

The Deuteron Properties

T.E.O. Ericson 281c

Semiphenomenological Nucleon-Nucleon Potentials

J.J. de Swart, W.A. van der Sanden, W. Derks 299c

The Nucleon-Antinucleon Interaction

C.B. Dover 313c

Discussion Session on

Two Nucleon Problems

Moderator: A.M. Green

Rapporteur: P.U. Sauer 335c

CHAPTER IV

THEORY AND CALCULATIONS IN FEW BODY SYSTEMS 345c

Theoretical Description of Few-Cluster Systems

E.W. Schmid 347c

Resonating Group Calculations in Nuclear Few  
Cluster Systems

H.M. Hofmann 363c

Effective Interactions in Two- and Three-Cluster  
Systems

Report on Preceding Workshop

E.W. Schmid 379c

Relativistic Effects in Few Nucleon Systems

Moderator: W. Glöckle

Rapporteur: F. Gross 387c

The Green's-Function Monte-Carlo Method in  
Few-Body Calculations

J.G. Zabolitzky 401c

Random Number Method in Few Body Calculation	
Y. Akaishi	409c
Recent Results of Calculations in the Four Nucleon System	
A.C. Fonseca	421c
Three-Nucleon Forces	
Invited Talk and Report on Preceding Workshop	
B.H.J. McKellar and W. Glöckle	435c
Recent Developments in Few Particle Scattering Theory	
K.L. Kowalski	465c
Discussion Session on Trends in Theoretical Few Body Physics	
L.P. Kok, A.S. Rinat	481c
 CHAPTER V	
SPECIAL TOPICS	489c
 Few Body Problems in Atomic and Molecular Physics	
T.K. Lim	491c
Electromagnetic and Weak Interactions in Few-Nucleon Systems	
B.F. Gibson	503c
Molecular Systems with Muons or Monopoles	
G. Fiorentini	519c
Few-Body Problems in Celestial Mechanics	
S.F. Dermott	535c

CHAPTER VI	
EXPERIMENTS ON FEW NUCLEON SYSTEMS	551c
Few Body Experiments with Polarized Beams and Polarized Targets	
J.E. Simmons	553c
Nuclear Few Cluster Studies	
G.-R. Plattner	565c
Electron Scattering and Few Nucleon Systems	
B. Frois	583c
Discussion Session on Trends in Experimental Few Body Physics	
Moderator: J.S.C. McKee	
Rapporteur: I. Sick	605c
Concluding Remarks	
E. Lomon	613c
TABLE OF CONTENTS OF FEW BODY PROBLEMS IN PHYSICS - BOOK OF CONTRIBUTED PAPERS	621c
LIST OF PARTICIPANTS	649c
AUTHOR INDEX	675c





Chapter I  
FEW QUARK PROBLEMS



## QUANTUM CHROMODYNAMICS IN FEW NUCLEON SYSTEMS\*

Stanley J. Brodsky

Stanford Linear Accelerator Center  
Stanford University, Stanford, California 94305

### 1. INTRODUCTION

One of the most important implications of quantum chromodynamics (QCD) is that nuclear systems and forces can be described at a fundamental level.<sup>1,2</sup> The theory provides natural explanations for the basic features of hadronic physics: the meson and baryon spectra, quark statistics, the structure of the weak and electromagnetic currents of hadrons, the scale-invariance of hadronic interactions at short distances, and evidently, color (i.e., quark and gluon) confinement at large distances. Many different and diverse tests have confirmed the basic predictions of QCD; however, since tests of quark and gluon interactions must be done within the confines of hadrons there have been few truly quantitative checks. Nevertheless, it appears likely that QCD is the fundamental theory of hadronic and nuclear interactions in the same sense that QED gives a precise description of electrodynamic interactions.

QCD is a renormalizable non-Abelian gauge theory of color-triplet quark and color-octet gluon fields invariant under color-SU(3) transformations. The fundamental degrees of freedom of nuclei as well as hadrons are postulated to be the spin-1/2 quark and spin-1 gluon quanta. Nuclear systems are identified as color-singlet composites of quark and gluon fields, beginning with the six-quark Fock component of the deuteron. An immediate consequence is that nuclear states are a mixture of several color representations which *cannot* be described solely in terms of the conventional nucleon, meson, and isobar degrees of freedom: there must also exist "hidden color" multi-quark wavefunction components—nuclear states which are not separable at large distances into the usual color singlet nucleon clusters. There are also a number of new perspectives for nuclear dynamics:

---

\* Work supported by the Department of Energy, contract DE-AC03-76SF00515

1. The electromagnetic and weak currents within a nucleus are carried solely by the quark fields at any momentum transfer scale  $Q^2 = -q_\mu^2$ . In the deep inelastic, large  $Q^2$ , large  $p \cdot q = M\nu$  domain, the lepton scatters essentially incoherently off of the individual quark constituents of the nucleus, giving point-like cross sections characteristics of Bjorken scaling, modified by logarithmic corrections to scale-invariance due to QCD radiative corrections. At low momentum transfer the quark currents become coherent, giving cross sections characteristics of multi-quark, nucleonic, or mesonic currents.
2. The nuclear force between nucleons can in principle be represented at a fundamental level in QCD in terms of quark interchange (equivalent at large distances to pion and other meson exchange) and multiple-gluon exchange.<sup>3</sup> Although calculations from first principles are still too complicated, recent results derived from effective potential, bag, and soliton models<sup>4</sup> suggests that many of the basic features of the nuclear force can be understood from the underlying QCD substructure. At a more basic level one can give a direct proof<sup>5</sup> from perturbative QCD that the nucleon-nucleon force must be repulsive at short distances (see Section 3).
3. Because of asymptotic freedom, the effective strength of QCD interactions becomes logarithmically weak at short distances and large momentum transfer

$$\alpha_s(Q^2) = \frac{4\pi}{\beta_0 \log(Q^2/\Lambda_{\text{QCD}}^2)} \quad (Q^2 \gg \Lambda^2) . \quad (1.1)$$

[Here  $\beta_0 = 11 - \frac{2}{3} n_f$  is derived from the gluonic and quark loop corrections to the effective coupling constant;  $n_f$  is the number of quark contributions to the vacuum polarizations with  $m_F^2 \lesssim Q^2$ .] The parameter  $\Lambda_{\text{QCD}}$  normalizes the value of  $\alpha_s(Q_0^2)$  at a given momentum transfer  $Q_0^2 \gg \Lambda^2$ , given a specific renormalization or cutoff scheme. Recently  $\alpha_s$  has been determined fairly unambiguously using the measured branching ratio for upsilon radiative decay  $\Upsilon(b\bar{b}) \rightarrow \gamma X$ .<sup>6,7</sup>

$$\alpha_s(0.157 \text{ M}_\Upsilon) = \alpha_s(1.5 \text{ GeV}) = 0.23 \pm 0.13 . \quad (1.2)$$

Taking the standard  $\overline{MS}$  dimensional regularization scheme, this gives  $\Lambda_{\overline{MS}} = 119^{+52}_{-34}$  MeV. In more physical terms, the effective potential between infinitely heavy quarks has the form [ $C_F = 4/3$  for  $n_c = 3$ ]

$$V(Q^2) = -C_F \frac{4\pi\alpha_V(Q^2)}{Q^2} \quad (1.3)$$

$$\alpha_V(Q^2) = \frac{4\pi}{\beta_0 \log(Q^2/\Lambda_V^2)} \quad (Q^2 \gg \Lambda_V^2)$$



where<sup>7</sup>  $\Lambda_V = \Lambda_{\overline{MS}} e^{5/6} \simeq 270 \pm 100 \text{ MeV}$ . Thus the effective physical scale of QCD is  $\sim 1 \text{ fm}^{-1}$ . At momentum transfers beyond this scale,  $\alpha_s$  becomes small, QCD perturbation theory becomes applicable, and a microscopic description of short-distance hadronic and nuclear phenomena in terms of quark and gluon subprocesses becomes viable. In this lecture we will particularly emphasize the use of asymptotic freedom and light-cone quantization to derive factorization theorems,<sup>8-10</sup> rigorous boundary conditions, and exact results for nuclear amplitudes at short distances.<sup>5,11,12</sup> This includes the nucleon form factor at large momentum transfer,<sup>10</sup> meson photoproduction amplitudes, deuteron photo- and electro-disintegration,<sup>12</sup> and most important for nuclear physics, exact results for the form of the form factor of nuclei at large momentum transfer.<sup>5,11</sup> Eventually it should be possible to construct fully analytic nuclear amplitudes which at low energies fit the standard chiral constraints and low energy theories of traditional nuclear physics while at the same time satisfying the scaling laws and anomalous dimension structure predicted by QCD at high momentum transfer.

4. Since QCD has the same natural length scale  $\sim 1 \text{ fm}$  as nuclear physics it is difficult to argue that nuclear physics can be studied in isolation from QCD. Thus one of the most interesting questions in nuclear physics is the transition between conventional meson-nucleon degrees of freedom to the quark and gluon degrees of freedom of QCD. As one probes distances shorter than  $\Lambda_{\text{QCD}}^{-1} \sim 1 \text{ fm}$  the meson-nucleon degrees of freedom must break down, and we expect new nuclear phenomena, new physics intrinsic to composite nucleons and mesons, and new phenomena outside the range of traditional nuclear physics. One apparent signal for this is the experimental evidence<sup>13</sup> from deep inelastic lepton-nucleus scattering that nuclear structure functions deviate significantly from simple nucleon additivity, much more than would have been expected for lightly bound systems. Further, as we discuss in Section 5, there are many areas where QCD predictions conflict with traditional concepts of nuclear dynamics.

## 2. EXCLUSIVE PROCESSES IN QCD

One area of important progress in hadron physics in the past few years has been the extension of QCD predictions to the domain of large momentum transfer hadronic and nuclear amplitudes including nuclear form factors, deuteron photodisintegration, etc.<sup>8</sup> A key result is that such amplitudes factorize at large momentum transfer in the form of a convolution of a hard scattering amplitude  $T_H$  which can be computed perturbatively from quark-gluon subprocesses multiplied by process-independent “distribution am-

plitudes"  $\phi(x, Q)$  which contain all of the bound-state non-perturbative dynamics of each of the interacting hadrons. To leading order in  $1/Q$  the scattering amplitude has the form [see Fig. 1(a)]

$$\mathcal{M} = \int_0^1 T_H(x_j, Q) \prod_{H_i} \phi_{H_i}(x_j, Q) [dx_j] . \quad (2.1)$$

Here  $T_H$  is the probability amplitude to scatter quarks with fractional momentum  $0 < x_j < 1$  from the incident to final hadronic directions, and  $\phi_{H_i}$  is the probability amplitude to find quarks in the wavefunction of hadronic  $H_i$  collinear up to the scale  $Q$ , and

$$[dx_j] = \prod_{j=1}^{n_i} dx_j \delta\left(1 - \sum_k x_k\right) \quad (2.2)$$

A key to the derivation of this factorization of perturbative and non-perturbative dynamics is the use of a Fock basis  $\{\psi_n(x_i, \vec{k}_{\perp i}, \lambda_i)\}$  defined at equal  $\tau = t + z/c$  on the light-cone to represent relativistic color singlet bound states.<sup>9</sup> Here  $\lambda_i$  is the helicity;  $x_i \equiv (k^0 + k^z)/(p^0 + p^z)$ , ( $\sum_{i=1}^n x_i = 1$ ), and  $\vec{k}_{\perp i}$ , ( $\sum_{i=1}^n \vec{k}_{\perp i} = 0$ ) are the relative momentum coordinates. Thus the proton is represented as a column vector of states  $\psi_{qqq}$ ,  $\psi_{qqqg}$ ,  $\psi_{qqqq}$ , ... In the light-cone gauge,  $A^+ = A^0 + A^3 = 0$ , only the minimal "valence" Fock state needs to be considered at large momentum transfer since any additional quark or gluon forced to absorb large momentum transfer yields a power-law suppressed contribution to the hadronic amplitude. For example at large  $Q^2$ , the baryon form factor takes the form<sup>10</sup> [Fig. 1(a)]

$$F_B(Q^2) = \int_0^1 [dy] \int_0^1 [dx] \phi_B^\dagger(y_j, Q) T_H(x_i, y_j, Q) \phi_B(x_i, Q) , \quad (2.3)$$

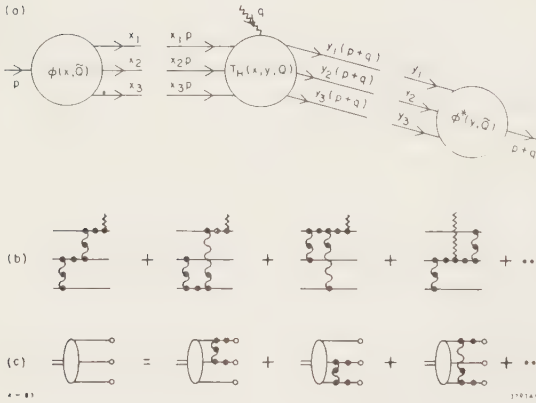


Fig. 1. (a) Factorization of the nucleon form factor at large  $Q^2$  in QCD. The optimal scale  $Q$  for the distribution amplitude  $\phi(x, \tilde{Q})$  is discussed in Ref. 8. (b) The leading order diagrams for the hard scattering amplitude  $T_H$ . The dots indicate insertions which enter the renormalization of the coupling constant. (c) The leading order diagrams which determine the  $Q^2$  dependence of  $\phi_B(x, Q)$ .

where to leading order in  $\alpha_s(Q^2)$ ,  $T_H$  is computed from  $3q + \gamma^* \rightarrow 3q$  tree graph amplitudes: [Fig. 1(b)]

$$T_H = \left[ \frac{\alpha_s(Q^2)}{Q^2} \right]^2 f(x_i, y_j) \quad (2.4)$$

and

$$\phi_B(x_i, Q) = \int [d^2 k_\perp] \psi_V(x_i, \vec{k}_\perp) \theta(k_\perp^2 < Q^2) \quad (2.5)$$

is the valence 3-quark wavefunction evaluated at quark impact separation  $b_\perp \sim O(Q^{-1})$ . Since  $\phi_B$  only depends logarithmically on  $Q^2$  in QCD, the main dynamical dependence of  $F_B(Q^2)$  is the power behavior  $(Q^2)^{-2}$  derived from scaling of the elementary propagators in  $T_H$ . Thus, modulo logarithmic factors, one obtains a dimensional counting rule for any hadronic or nuclear form factor at large  $Q^2$  ( $\lambda = \lambda' = 0$  or  $1/2$ )<sup>14</sup>

$$F(Q^2) \sim \left( \frac{1}{Q^2} \right)^{n-1}, \quad (2.6)$$

$$F_1^N \sim \frac{1}{Q^4}, \quad F_\pi \sim \frac{1}{Q^2}, \quad F_d \sim \frac{1}{Q^{10}}, \quad (2.7)$$

where  $n$  is the minimum number of fields in the hadron. Since quark helicity is conserved in  $T_H$  and  $\phi(x_i, Q)$  is the  $L_z = 0$  projection of the wavefunction, total hadronic helicity is conserved<sup>15</sup> at large momentum transfer for any QCD exclusive reaction. The dominant nucleon form factor thus corresponds to  $F_1(Q^2)$  or  $G_M(Q^2)$ ; the Pauli form factor is suppressed by an extra power of  $Q^2$ . In the case of the deuteron, the dominant form factor has helicity  $\lambda = \lambda' = 0$ , corresponding to  $\sqrt{A(Q^2)}$ . The general form of the logarithmic dependence of  $F(Q^2)$  can be derived from the operator product expansion at short distance or by solving an evolution equation for the distribution amplitude computed from gluon exchange [Fig. 1(c)], as we discuss in Section 3 for the deuteron. The result for the large  $Q^2$  behavior of the baryon form factor in QCD is<sup>8,10</sup>

$$F_B(Q^2) = \frac{\alpha_s^2(Q^2)}{Q^4} \sum_{n,m} d_{nm} \left( \ell n \frac{Q^2}{\Lambda^2} \right)^{-\gamma_m - \gamma_n} \quad (2.8)$$

where the  $\gamma_n$  are computable anomalous dimensions of the baryon 3-quark wave function at short distance and the  $d_{mn}$  are determined from the value of the distribution amplitude  $\phi_B(x, Q_0^2)$  at a given point  $Q_0^2$ . Asymptotically the dominant term has the minimum anomalous dimension. The predicted sign of  $G_M^p(Q^2)$  at large  $Q^2$  is the same as  $G_M^p(0)$ . The dominant part of the form factor comes from the region of the  $x$  integration where each quark has a finite fraction of the light cone momentum; the end point region where the struck quark has  $x \simeq 1$  and spectator quarks have  $x \sim 0$  is asymptotically suppressed by quark (Sudakov) form factor gluon radiative corrections.

As shown in Fig. 2 the power laws (2.6, 2.7) predicted by perturbative QCD are consistent with experiment.<sup>16</sup> The behavior  $Q^4 G_M(Q^2) \sim \text{const}$  at large  $Q^2$  provides a direct check that the minimal Fock state in the nucleon contains 3 quarks and that the quark propagator and the  $qq \rightarrow qq$  scattering amplitudes are approximately scale-free. More generally, the nominal power law predicted for large momentum transfer exclusive reactions is given by the dimensional counting rule  $M \sim Q^{4-n_{TOT}} F(\theta_{cm})$  where  $n_{TOT}$  is the total number of elementary fields which scatter in the reaction. The predictions are apparently compatible with experiment. In addition, for some scattering reactions there are contributions from multiple scattering diagrams (Landshoff contributions) which together with Sudakov effects can lead to small power-law corrections, as well as a complicated spin, and amplitude phase phenomenology. Recent measurements<sup>17</sup> of  $\gamma\gamma \rightarrow \pi^+\pi^-$ ,  $K^+K^-$  at large invariant pair mass appear to confirm the QCD predictions.<sup>18</sup>

In principle it should be possible to use measurements of the scaling and angular dependence of the  $\gamma\gamma \rightarrow M \bar{M}$  reactions to measure the shape of the distribution amplitude  $\phi_M(x, Q)$ . An actual calculation of  $\phi(x, Q)$  from QCD requires non-perturbative methods such as lattice gauge theory, or more directly, the solution of the light-cone equation of motion

$$\left[ M^2 - \sum_{i=1}^n \left( \frac{k_{\perp}^2 + m^2}{x} \right) \right] \Psi = V_{\text{QCD}} \Psi \quad (2.9)$$

The explicit form for the matrix representation of  $V_{\text{QCD}}$  and a discussion of the infrared and ultraviolet regulation required to interpret (2.9) is given in Ref. 9.

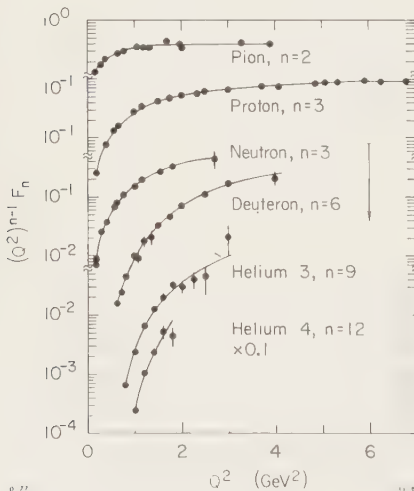


Fig. 2. Comparison of experiment with the QCD dimensional counting rule  $(Q^2)^{n-1} F(Q^2) \sim \text{const}$  for form factors. The proton data extends beyond  $30 \text{ GeV}^2$  (see Ref. 16).

Thus far experiments has not been sufficiently precise to measure the logarithmic variation from dimensional counting rules predicted by QCD. Checks of the normalization of  $(Q^2)^{n-1}F(Q^2)$  require independent determinations of the valence wavefunction. The relatively large normalization of  $Q^4 G_M^p(Q^2)$  at large  $Q^2$  can be understood if the valence 3 quark state has small transverse size, i.e., is large at the origin.<sup>9,19</sup> The physical radius of the proton measured from  $F_1(Q^2)$  at low momentum transfer then reflects the contributions of the higher Fock states  $qqqq$ ,  $qqq\bar{q}q$  (or meson cloud), etc. A small size for the proton valence wavefunction (e.g.  $R_{qqq}^p \sim 0.3 \text{ fm}$ ) can also explain the large magnitude of  $\langle k_\perp^2 \rangle$  of the intrinsic quark momentum distribution needed to understand in hard-scattering inclusive reactions. The necessity for small valence state Fock components can be demonstrated explicitly for the pion wavefunction, since  $\psi_{qq}/\pi$  is constrained by sum rules derived from  $\pi^+ \rightarrow \ell^+ \nu$ , and  $\pi^- \rightarrow \gamma\gamma$ . One finds a valence state radius  $R_{qq}^\pi \sim 0.2 \text{ fm}$ , corresponding to a probability  $P_{qq}^\pi \sim 1/4$ . A detailed discussion is given in Ref. 19.

### 3. THE DEUTERON IN QCD

Of the five color-singlet representations of six quarks, only one corresponds to the usual system of two color singlet baryonic clusters. (Explicit representations are given in Ref. 20). Notice that the exchange of a virtual gluon in the deuteron at short distance inevitably produces Fock state components where the 3-quark clusters correspond to color octet nucleons or isobars. Thus, in general, the deuteron wavefunction should have a complete spectrum of hidden-color wavefunction components, although it is likely that these states are important only at small internucleon separation.<sup>21</sup>

Despite the complexity of the multi-color representations of nuclear wavefunctions, the analysis<sup>5</sup> of the deuteron form factor at large momentum transfer can be carried out in parallel with the nucleon case outlined in Section 2. Only the minimal 6-quark Fock state needs to be considered to leading order in  $1/Q^2$ . The deuteron form factor can then be written as a convolution (see Fig. 3),

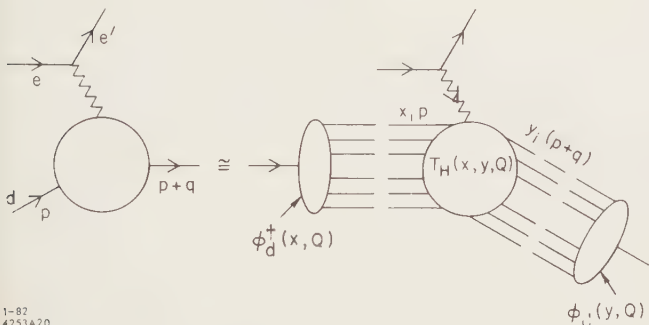


Fig. 3. Factorization of the deuteron form factor at large  $Q^2$ .



$$F_d(Q^2) = \int_0^1 [dx] [dy] \phi_d^\dagger(y, Q) T_H^{6q+\gamma^* \rightarrow 6q}(x, y, Q) \phi_d(x, Q), \quad (3.1)$$

where the hard scattering amplitude scales as

$$T_H^{6q+\gamma^* \rightarrow 6q} = \left[ \frac{\alpha_s(Q^2)}{Q^2} \right]^5 t(x, y) [1 + \mathcal{O}(\alpha_s(Q^2))] \quad (3.2)$$

The anomalous dimensions  $\gamma_n^d$  are calculated from the evolution equations for  $\phi_d(x_i, Q)$  derived to leading order in QED from pairwise gluon-exchange interactions: ( $C_F = 4/3$ ,  $C_d = -C_F/5$ )

$$\prod_{k=1}^6 x_k \left[ \frac{\partial}{\partial \xi} + \frac{3C_F}{\beta} \right] \tilde{\Phi}(x_i, Q) = -\frac{C_d}{\beta} \int_0^1 [dy] V(x_i, y_i) \tilde{\Phi}(y_i, Q). \quad (3.3)$$

Here we have defined

$$\Phi(x_i, Q) = \prod_{k=1}^6 x_k \tilde{\Phi}(x_i, Q), \quad (3.4)$$

and the evolution is in the variable

$$\xi(Q^2) = \frac{\beta_0}{4\pi} \int_{Q_0^2}^{Q^2} \frac{dk^2}{k^2} \alpha_s(k^2) \sim \ln \left( \frac{\ln \frac{Q^2}{\Lambda^2}}{\ln \frac{Q_0^2}{\Lambda^2}} \right). \quad (3.5)$$

The kernel  $V$  is computed to leading order in  $\alpha_s(Q^2)$  from the sum of gluon interactions between quark pairs. The general matrix representations of  $\gamma_n$  with bases  $\prod_{i=1}^5 x_i^{m_i} >$  are given in Ref. 20. The leading anomalous dimension  $\gamma_0$ , corresponding to the eigenfunction  $\tilde{\Phi}(x_i) = 1$ , is  $\gamma_0 = (6/5)(C_F/\beta_0)$ .

In order to make more detailed and experimentally accessible predictions, we will define the “reduced” nuclear form factor<sup>11,12</sup> in order to remove the effects of nucleon compositeness (see Section 4):

$$f_d(Q^2) \equiv \frac{F_d(Q^2)}{F_N^2(Q^2/4)}. \quad (3.6)$$

The arguments for the nucleon form factors ( $F_N$ ) are  $Q^2/4$  since in the limit of zero binding energy each nucleon must change its momentum from  $\sim p/2$  to  $(p+q)/2$ . Since the leading anomalous dimensions of the nucleon distribution amplitude is  $C_F/2\beta$ , the QCD prediction for the asymptotic  $Q^2$ -behavior of  $f_d(Q^2)$  is<sup>5</sup>

$$f_d(Q^2) \sim \frac{\alpha_s(Q^2)}{Q^2} \left( \ln \frac{Q^2}{\Lambda^2} \right)^{-\frac{2}{5} \frac{C_F}{\beta}}, \quad (3.7)$$

where  $-(2/5)(C_F/\beta) = -8/145$  for  $n_f = 2$ .

Although this QCD prediction is for asymptotic momentum transfer, it is interesting to compare (3.7) directly with the available high  $Q^2$  data<sup>16</sup> (see Fig. 4). In general one would expect corrections from higher twist effects (e.g., mass and  $k_\perp$  smearing), higher order contributions in  $\alpha_s(Q^2)$ , as well as non-leading anomalous dimensions. However, the agreement of the data with simple  $Q^2 f_d(Q^2) \sim \text{const}$  behavior for  $Q^2 > 1/2 \text{ GeV}^2$  implies that, unless there is a fortuitous cancellation, all of the scale-breaking effects are small, and the present QCD perturbative calculations are viable and applicable even in the nuclear physics domain. The lack of deviation from the QCD parameterization also suggests that the parameter  $\Lambda$  in (3.7) is small. A comparison with a standard definition such as  $\Lambda_{\overline{MS}}$  would require a calculation of next to leading effects. A more definitive check of QCD can be made by calculating the normalization of  $f_d(Q^2)$  from  $T_H$  and the evolution of the deuteron wave function to short distances. It is also important to confirm experimentally that the helicity  $\lambda = \lambda' = 0$  form factor is indeed dominant.

The calculation of the normalization  $T_H^{6q+\gamma^* \rightarrow 6q}$  to leading order in  $\alpha_s(Q^2)$  will require the evaluation of  $\sim 300,000$  Feynman diagrams involving five exchanged gluons. Fortunately this appears possible using the algebraic computer methods introduced in Ref. 22. The method of setting the appropriate scale  $\hat{Q}$  of  $\alpha_s^5(\hat{Q}^2)$  in  $T_H$  is given in Ref. 7.

We note that the deuteron wave function which contributes to the asymptotic limit of the form factor is the totally antisymmetric wave function corresponding to the orbital Young symmetry given by [6] and isospin ( $T$ ) + spin ( $S$ ) Young symmetry given by {33}. The deuteron state with this symmetry is related to the  $NN$ ,  $\Delta\Delta$ , and hidden color ( $CC$ ) physical bases, for both the  $(TS) = (01)$  and  $(10)$  cases, by the formula<sup>23</sup>

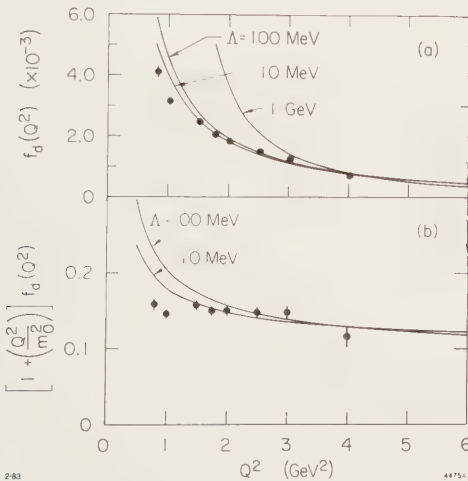


Fig. 4. (a) Comparison of the asymptotic QCD prediction (3.7) with experiment (16) using  $F_N(Q^2) = (1 + Q^2/0.71 \text{ GeV}^2)^{-2}$ . The normalization is fit at  $Q^2 = 4 \text{ GeV}^2$ . (b) Comparison of the prediction  $[1 + (Q^2/m_0^2)] f_d(Q^2) \propto (\ln Q^2)^{-1-2/5} C_F/\beta$  with data. The value  $m_0^2 = 0.28 \text{ GeV}^2$  is used.

$$\psi_{[6]\{33\}} = \sqrt{\frac{1}{9}} \psi_{NN} + \sqrt{\frac{4}{45}} \psi_{\Delta\Delta} + \sqrt{\frac{4}{5}} \psi_{CC} . \quad (3.8)$$

Thus the physical deuteron state, which is mostly  $\psi_{NN}$  at large distance, must evolve to the  $\psi_{[6]\{33\}}$  state when the six quark transverse separations  $b_{\perp}^i \leq O(1/Q) \rightarrow 0$ . Since this state is 80-percent hidden color, the deuteron wave function cannot be described by the meson-nucleon isobar degrees of freedom in this domain. The fact that the six-quark color singlet state inevitably evolves in QCD to a dominantly hidden-color configuration at small transverse separation also has implications for the form of the nucleon-nucleon ( $S_z = 0$ ) potential, which can be considered as one interaction component in a coupled channel system. As the two nucleons approach each other, the system must do work in order to change the six-quark state to a dominantly hidden color configuration; i.e., QCD requires that the nucleon-nucleon potential must be repulsive at short distances<sup>3,5</sup> (see Fig. 5). The evolution equation for the six-quark system suggests that the distance where this change occurs is in the domain where  $\alpha_s(Q^2)$  most strongly varies.

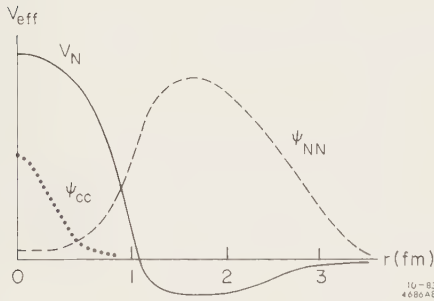


Fig. 5. Schematic representation of the deuteron wavefunction in QCD indicating the presence of hidden color 6-quark components at short distances.

#### 4. REDUCED NUCLEAR AMPLITUDES

One of the basic problems in the analysis of nuclear scattering amplitudes is how to consistently account for the effects of the underlying quark/gluon component structure of nucleons. Traditional methods based on the use of an effective nucleon/meson local Lagrangian field theory are not really applicable (see Section 5), giving the wrong dynamical dependence in virtually every kinematic variable for composite hadrons. The inclusion of *ad hoc* vertex form factors is unsatisfactory since one must understand the off-shell dependence in each leg while retaining gauge invariance; such methods have little predictive power. On the other hand, the explicit evaluation of the multiquark hard-scattering amplitudes needed to predict the normalization and angular dependence for a nuclear process, even at leading order in  $\alpha_s$ , requires the consideration of millions of Feynman diagrams. Beyond



leading order one must include contribution of non-valence Fock states wavefunctions, and a rapidly expanding number of radiative corrections and loop diagrams.

The reduced amplitude method,<sup>11,12</sup> although not an exact replacement for a full QCD calculation, provides a simple method for identifying the dynamical effects of nuclear substructure, consistent with covariance, QCD scaling laws and gauge invariance. The basic idea has already been introduced in Section 3 for the reduced deuteron form factor. More generally if we neglect nuclear binding, then the light-cone nuclear wavefunction can be written as a cluster decomposition of collinear nucleons:  $\psi_{q/A} = \psi_{N/A} \prod_N \Psi_{q/N}$  where each nucleon has  $1/A$  of the nuclear momentum. A large momentum transfer nucleon amplitude then contains as a factor the probability amplitude for each nucleon to remain intact after absorbing  $1/A$  of the respective nuclear momentum transfer  $\sqrt{-t}/A$ . We can identify each probability amplitude with the respective nucleon form factor  $F(t_i = \frac{1}{A^2} t_A)$ . Thus for any exclusive nuclear scattering process, we define the reduced nuclear amplitude

$$m = \frac{\mathcal{M}}{\prod_{i=1}^A F_N(t_i)} \quad (4.1)$$

The QCD scaling law for the reduced nuclear amplitude  $m$  is then identical to that of nuclei with point-like nuclear components: e.g. the reduced nuclear form factors obey

$$f_A(Q^2) \equiv \frac{F_A(Q^2)}{[F_N(Q^2/A^2)]^A} \sim \left[ \frac{1}{Q^2} \right]^{A-1}. \quad (4.2)$$

Comparisons with experiment and predictions for leading logarithmic corrections to this result are given in Refs. 5 and 12. In the case of photo- (or electro-) disintegration of the deuteron one has

$$m_{\gamma d \rightarrow np} = \frac{\mathcal{M}_{\gamma d \rightarrow np}}{F_n(t_n) F_p(t_p)} \sim \frac{1}{p_T} f(\theta_{cm}) \quad (4.3)$$

i.e., the same elementary scaling behavior as for  $\mathcal{M}_{\gamma M \rightarrow q\bar{q}}$ . Comparison with experiment<sup>26</sup> is encouraging (see Fig. 6), showing that as was the case for  $Q^2 f_d(Q^2)$ , the perturbative QCD scaling regime begins at  $Q^2 \geq 1 \text{ GeV}^2$ . Detailed comparisons and a model for the angular dependence and the virtual photon-mass dependence of deuteron electrodisintegration are discussed in Ref. 12. Other potentially useful checks of QCD scaling of reduced amplitudes are

$$\begin{aligned} m_{pp \rightarrow d\pi^+} &\sim p_T^{-2} f(t/s) \\ m_{pd \rightarrow H^3\pi^+} &\sim p_T^{-4} f(t/s) \\ m_{\pi d \rightarrow \pi d} &\sim p_T^{-4} f(t/s). \end{aligned} \quad (4.4)$$

It is also possible to use these QCD scaling laws for the reduced amplitude as a parametrization for the background for detecting possible new dibaryon resonance states.

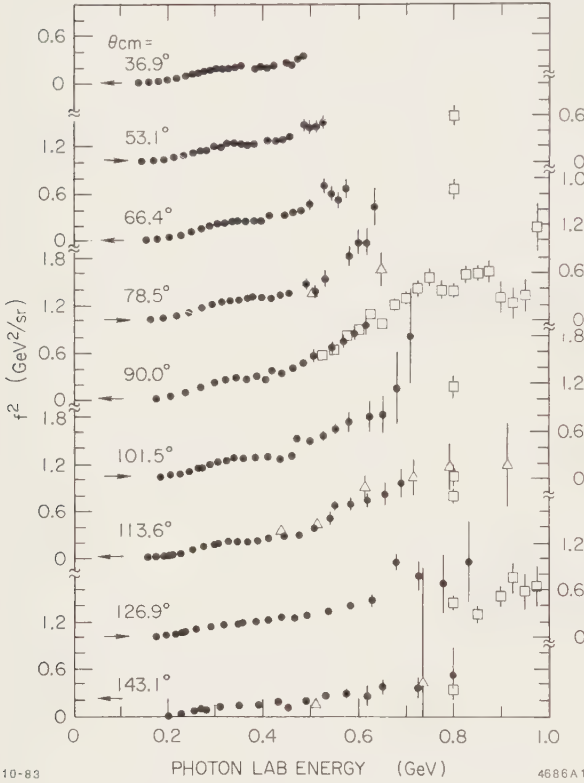


Fig. 6. Comparison of deuteron photodisintegration data<sup>24</sup> with the scaling prediction (4.3) which requires  $f^2(\theta_{cm})$  to be independent of energy at large momentum transfer.

## 5. LIMITATIONS OF TRADITIONAL NUCLEAR PHYSICS<sup>27</sup>

The fact that the QCD prediction for the reduced form factor  $Q^2 f_d(Q^2) \sim \text{const}$  appears to be an excellent agreement with experiment for  $Q^2 > 1 \text{ GeV}^2$  provides an excellent check on the six-quark description of the deuteron at short-distance as well as the scale-invariance of the  $qq \rightarrow qq$  scattering amplitude. It should also be emphasized that the impulse approximation form used in standard nucleon physics calculations

$$F_d(Q^2) = F_N(Q^2) \times F_{\text{Body}}(Q^2) \quad (5.1)$$

is invalid in QCD at large  $Q^2$  since off-shell nucleon form factors enter [see Fig. 7(a)]. The

region of validity<sup>25</sup> of (5.1) is restricted to  $Q^2 < \lambda_H^2$  where  $\lambda_H^2$  is a hadronic scale. The traditional treatment of nuclear form factors also overestimates the contribution of meson exchange currents [Fig. 7(b)] and  $N\bar{N}$  contributions [Fig. 7(c)] since they are strongly suppressed by vertex form factors as we shall show in this section.

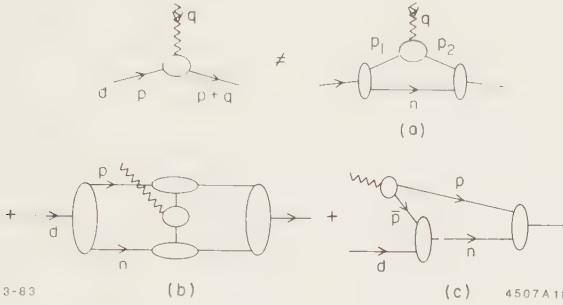


Fig. 7. Critique of the standard nuclear physics approach to the deuteron form factor at large  $Q^2$ . (a) The effective nucleon form factor has one or both legs off shell  $|p_1^2 - p_2^2| \sim q^2/2$ . (b) Meson exchange currents are suppressed in QCD because of off shell form factors. (c) The nucleon pair contribution is suppressed because of nucleon compositeness. Contact terms appear only at the quark level.

At long distances and low, non-relativistic momenta, the traditional description of nuclear forces and nuclear dynamics based on nucleon, isobar, and meson degrees of freedom appears to give a viable phenomenology of nuclear reactions and spectroscopy. It is natural to try to extend the predictions of these models to the relativistic domain, e.g. by utilizing local meson-nucleon field theories to represent the basic nuclear dynamics, and to use an effective Dirac equation to describe the propagation of nucleons in nuclear matter.<sup>26</sup> An interesting question is whether such approaches can be derived as a “correspondence” limit of QCD, at least in the low momentum transfer ( $Q^2 R_p^2 \ll 1$ ) and low excitation energy domain ( $Mv \ll M'^2 - M^2$ ).

As we have discussed in Sections 2 and 4, the existence of hidden-color Fock state components in the nuclear state precludes an exact treatment of nuclear properties based on meson-nucleon-isobar degrees of freedom since these hadronic degrees of freedom do not form a complete basis on QCD. Since the deuteron form factor is dominated by hidden color states at large momentum transfer, it cannot be described by  $np$ ,  $\Delta\Delta$  wavefunction components on meson exchange currents alone. It is likely that the hidden color states give less than a few percent correction to the global properties of nuclei; nevertheless,

since extra degrees of freedom lower the energy of a system it is even conceivable that the deuteron would be unbound were it not for its hidden color components!

Independent of hidden color effects, we can still ask whether is it possible—in principle—to represent composite systems such as meson and baryons as local fields in a Lagrangian field theory, at least for sufficiently long wavelengths such that internal structure of the hadrons cannot be discerned. Here we will outline a method to construct an effective Lagrangian of this sort. First, consider the ultraviolet-regulated QCD Lagrangian density  $\mathcal{L}_{\text{QCD}}^\kappa$  defined such that all internal loops in the perturbative expansion are cut off below a given momentum scale  $\kappa$ . Normally  $\kappa$  is chosen to be much larger than all relevant physical scale. Because QCD is renormalizable,  $\mathcal{L}_{\text{QCD}}^\kappa$  is form-invariant under changes of  $\kappa$  provided that the coupling constant  $\alpha_s(\kappa^2)$  and quark mass parameter  $m(\kappa^2)$  are appropriately defined. However, if we insist on choosing the cutoff  $\kappa$  to be as small as hadronic scales then extra (higher twist) contributions will be generated in the effective Lagrangian density:<sup>9</sup>

$$\begin{aligned} \mathcal{L}^\kappa = & \mathcal{L}_0^\kappa + \frac{em(\kappa)}{\kappa^2} \bar{\psi}_N \sigma_{\mu\nu} \partial^\mu \psi_N A_{\text{em}}^\nu + e \frac{f_\pi^2}{\kappa^2} \phi_\pi^\dagger \overleftrightarrow{\partial}_\mu \phi_\pi A_{\text{em}}^\mu \\ & + e \frac{f_p^2}{\kappa^2} \bar{\psi}_N \gamma_\nu \psi_N A_{\text{em}}^\nu + \frac{f_p^2 f_\pi}{\kappa^8} \partial_\nu \bar{\psi}_N \gamma_5 \gamma^\nu \psi_N \phi_\pi + \dots \end{aligned} \quad (5.2)$$

where  $\mathcal{L}_0^\kappa$  is the standard Lagrangian and the “higher twist” terms of order  $\kappa^{-2}$ ,  $\kappa^{-4}$ , ... are schematic representations of the quark Pauli form factor, the pion and nucleon Dirac form factors, and the  $\pi - N - N$  coupling. The pion and nucleon fields  $\phi_\pi$  and  $\psi_N$  represent composite operators constructed and normalized from the valence Fock amplitudes and the leading interpolating quark operators. One can use Eq. (5.2) to estimate the effective asymptotic power law behaviors of the couplings, e.g.,  $F_{\text{Pauli}}^{\text{quark}} \sim 1/Q^2$ ,  $F_\pi \sim f_\pi^2/Q^2$ ,  $G_M \sim f_p^2/Q^4$  and the effective  $\pi \bar{N} \gamma_5 N F_{\pi N \bar{N}}$  coupling:  $F_{\pi N \bar{N}}(Q^2) \sim M_N f_p^2 f_\pi / Q^6$ . The net pion exchange amplitude for  $NN - NN$  scatterings thus falls off very rapidly at large momentum transfer  $M_{NN \rightarrow NN}^\pi \sim (Q^2)^{-7}$  much faster than the leading quark interchange amplitude  $M_{NN \rightarrow NN}^{qq} \sim (Q^2)^{-4}$ . Similarly, the vector exchange contributions give contributions  $M_{NN \rightarrow NN}^\rho \sim (Q^2)^{-6}$ . Thus meson exchange amplitudes and currents, even summed over their excited spectra, do not contribute to the leading asymptotic behavior of the  $N - N$  scattering amplitudes or deuteron form factors once proper account is taken of the off-shell form factors which control the meson-nucleon-nucleon vertices.

Aside from such estimates, the effective Lagrangian (5.2) only has utility as a rough tree graph approximation; in higher order the hadronic field terms give loop integrals highly sensitive to the ultraviolet cutoff because of their non-renormalizable character. Thus an effective meson-nucleon Lagrangian serves to organize and catalog low energy constraints

and effective couplings, but it is not very predictive for obtaining the actual dynamical and off-shell behavior of hadronic amplitudes due to the internal quark and gluon structure.

Local Lagrangians field theories for systems which are intrinsically composite are however misleading in another respect. Consider the low-energy theorem for the forward Compton amplitude on a (spin-average) nucleon target

$$\lim_{\nu \rightarrow 0} \mathcal{M}_{\gamma p \rightarrow \gamma p}(\nu, t=0) = -2 \hat{\epsilon} \cdot \hat{\epsilon}' \frac{e^2}{M_p} . \quad (5.3)$$

One can directly derive this result from the underlying quark currents as indicated in Fig. 8(b). However, if one assumes the nucleon is a local field, then the entire contribution to the Compton amplitude at  $\nu = 0$  would arise from the nucleon pair  $z$ -graph amplitude, as indicated in Fig. 8(a). Since each calculation is Lorentz and gauge invariant, both give the desired result (5.3). However, in actuality, the nucleon is composite and the  $N\bar{N}$  pair term is strongly suppressed: each  $\gamma p \bar{p}$  vertex is proportional to

$$\langle 0 | J^\mu(0) | p \bar{p} \rangle \propto F_p(Q^2) = 4M_p^2 ; \quad (5.4)$$

i.e.: the timelike form factor as determined from  $e^+e^- \rightarrow p\bar{p}$  near threshold. Thus, as would be expected physically, the  $N\bar{N}$  pair contribution is highly suppressed for a composite system (even for real photons). Clearly a Lagrangian based on local nucleon fields gives an inaccurate description of the actual dynamics and cannot be trusted away from the forward scattering, low energy limit.

We can see from the above discussion that a necessary condition for utilizing a local Lagrangian field theory as a dynamical approximation to a given composite system  $H$  is that its timelike form factor at the Compton scale must be close to 1:

$$F_H(Q^2 \simeq 4M^2) \simeq 1 . \quad (5.5)$$

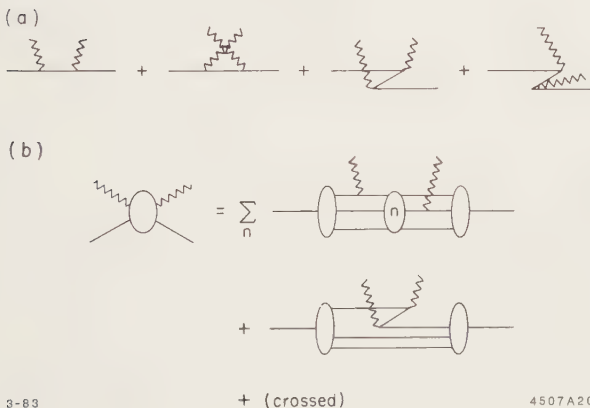


Fig. 8. Time-ordered contributions to (a) The Compton amplitudes in a local Lagrangian theory such as QED. Only the  $z$ -graphs contribute in the forward low energy limit. (b) Calculation of the Compton amplitude for composite systems.



For example, even if it turns out that the electron is a composite system at very short distances, the QED Lagrangian will still be a highly accurate tool. Equation (5.5) fails for all hadrons, save the pion, suggesting that effective chiral field theories which couple point-like pions to quarks could be a viable approximation to QCD.

More generally, one should be critical of any use of point-like couplings for nucleon-antinucleon pair production, e.g. in calculations of deuteron form factors, photo- and electro-disintegration since such contributions are always suppressed by the timelike nucleon form factor. Note  $\gamma N \bar{N}$  point-like couplings are not needed for gauge invariance, once all quark current contributions including pointlike  $q \bar{q}$  pair terms are taken into account.

We also note that a relativistic composite fermionic system, whether it is a nucleon or nucleus, does not obey the usual Dirac equation—with a momentum-independent potential—beyond first Born approximation. Again, the difficulty concerns intermediate states containing  $N \bar{N}$  pair terms: the identity of the Dirac equation requires that  $\langle p | V_{\text{ext}} | p' \rangle$  and  $\langle 0 | V_{\text{ext}} | p' \bar{p} \rangle$  be related by simple crossing, as for leptons in QED. For composite systems the pair production terms are suppressed by the timelike form factor (5.4). It is however possible that one can write an effective, approximate relativistic equation for a nucleon in an external potential of the form

$$(\vec{\alpha} \cdot \vec{p} + \beta m_N + \Lambda_+ V_{\text{eff}} \Lambda_+) \Psi_N = E \Psi_N \quad (5.6)$$

where the projection operator  $\Lambda_+$  removes the  $N - \bar{N}$  pair terms, and  $V_{\text{eff}}$  includes the local (seagull) contributions from  $q \bar{q}$ -pair intermediate states, as well as contributions from nucleon excitation.

An essential property of a predictive theory is its renormalizability, the fact that physics at a very high momentum scale  $k^2 > \kappa^2$  has no effect on the dynamics other than to define the effective coupling constant  $\alpha(\kappa^2)$  and mass terms  $m(\kappa^2)$ . Renormalizability also implies that fixed angle unitarity is satisfied at the tree-graph (no-loop) level. In addition, it has recently been shown that the tree graph amplitude for photon emission for any renormalizable gauge theory has the same amplitude zero structure as classical electrodynamics. Specifically, the tree graph amplitude for photon emission caused by the scattering of charged particles *vanishes* (independent of spin) in the kinematic region where the ratios  $Q_i/p_i \cdot k$  for all the external charged lines are identical.<sup>28</sup> This “null zone” of zero radiation is not restricted to soft photon momentum, although it is identical to the kinematic domain for the complete destructive interference of the radiation associated with classical electromagnetic currents of the external charged particles. Thus the tree graph structure of gauge theories, in which each elementary charged field has zero anomalous

moment ( $g = 2$ ) is properly consistent with the classical ( $\mathbf{K} = 0$ ) limit. On the other hand, local field theories which couple particles with non-zero anomalous moments violate fixed angle unitarity and the above classical correspondence limit at the tree graph level. The anomalous moment of the nucleon is clearly a property of its internal quantum structure; by itself, this precludes the representation of the nucleon as a local field.

The essential conflict between quark and meson-nucleon field theory is thus at a very basic level: because of Lorentz invariance a conserved charge must be carried by a local (point-like) current; there is no consistent relativistic theory where fundamental constituent nucleon fields have an extended charge structure.

## 6. CONCLUSIONS

The synthesis of nuclear dynamics with the quark and gluon processes of quantum chromodynamics is clearly a basic fundamental problem in hadron physics. The short distance behavior of the nucleon-nucleon interaction as determined by QCD must join smoothly and analytically with the large distance constraints of nuclear physics. As we have emphasized, the fundamental mass scale of QCD is comparable with the inverse nuclear radius; it is thus difficult to argue that nuclear physics at distances below  $\sim 1$  fm can be studied in isolation from QCD: meson and nucleon degrees of freedom of traditional nuclear physics models must become inadequate at momentum transfer scales  $\gtrsim 200$  MeV where nucleon substructure becomes evident.

Thus the essential question for nuclear as well as particle physics is to understand the transition between the meson-nucleon and quark-gluon degrees of freedom. There should be no illusion that this is a simple task; one is dealing with all the complexities and fascinations of QCD such as the effects of confinement and non-perturbative effects intrinsic to the non-Abelian theory. Such considerations also enter the physics associated with the propagation of quarks and gluons in nuclear matter and the phenomenology of hadron and nuclear wavefunctions.<sup>29</sup>

Despite the difficulty of the non-perturbative domain, there is reason for optimism that "nuclear chromodynamics" is a viable endeavor. For example, as we have shown in Section 4 we can use QCD to make predictions for the short distance behavior of the deuteron wavefunction and the deuteron form factor at large momentum transfer. The predictions give a remarkably accurate description of the scaling behavior of the available deuteron form factor data for  $Q^2$  as low as  $1 \text{ GeV}^2$ . The QCD approach also allows the definition of "reduced" nuclear amplitudes which can be used to consistently and covariantly remove the effect of nucleon compositeness from nuclear amplitudes. An important feature of such predictions is that they provide rigorous constraints on exclusive nuclear amplitudes which

have the correct analytic, gauge-invariant, and scaling properties predicted by QCD at short distances. This suggests the construction of boundary condition model amplitudes which simultaneously satisfy low energy and chiral theorems at low momentum transfer as well as the rigorous QCD constraints at high momentum transfers.<sup>30</sup> In addition, by using the light cone formalism, one can obtain a consistent relativistic Fock state wave function description of hadrons and nuclei which ties on to the Schroedinger theory in the non-relativistic regime. One can also be encouraged by progress in non-perturbative methods in QCD such as lattice gauge theories or chromostatics;<sup>31</sup> eventually these approaches should be able to deal with multi-quark source problems.

It is essential to have direct experiment guidance in how to proceed as one develops nuclear chromodynamics. A high duty factor electron accelerator<sup>32</sup> with laboratory energy beyond 4 GeV is an important tool because of the simplicity of the probe and the fact that we understand the coupling of the electron and quark current in QCD. It is also clear that

1. One must have sufficient energy to extend electron scattering measurements from low momentum transfer to the high momentum transfer region with sufficient production energy such that Bjorken scaling can be observed. One certainly does not want to stop at an intermediate momentum transfer domain—a regime of maximal complexity from the standpoint of both QCD and nuclear physics. The recent EMC and SLAC data<sup>13</sup> showing breakdown of simple nucleon additivity in the nuclear structure functions also demonstrates that there is non-trivial nuclear physics even in the high momentum transfer domain.
2. One must have sufficient electron energy to separate the longitudinal and transverse currents. The  $\sigma_L/\sigma_T$  separation is essential for resolving individual dynamical mechanisms; e.g. single quark and multiple quark (meson current) contributions.
3. One wishes to study each exclusive channel in detail in order to verify and understand the emergence of QCD scaling laws and to understand how the various channels combine together to yield effective Bjorken scaling. Helicity information is also very valuable. For example QCD predicts that at large momentum transfer, the helicity-0 to helicity-0 deuteron form factor is dominant and that for any large momentum transfer reaction, total hadronic helicity is conserved.<sup>15</sup>
4. One wishes to make a viable search for dibaryon states which are dominantly of hidden color. The argument that such resonances exist in QCD is compelling just from counting of degrees of freedom. The calculation of the mass and width of such resonances is clearly very difficult, since the detailed dynamics is dependent on the degree of mixing with ordinary states, the availability of decay channels, etc. Since hidden color states have suppressed overlap with the usual hadronic amplitudes it



may be quite difficult to find such states in ordinary hadronic collisions. On the other hand, the virtual photon probe gives a hard momentum transfer to a single struck quark, and it is thus more likely to be sensitive to the short-distance hidden color components in the target wave function. Adequate electron energy is essential not only to produce dibaryon resonances but also to allow sufficient momentum transfer  $Q^2$  to decrease backgrounds and to provide  $\sigma_L/\sigma_T$  separation.

5. One wishes to probe and parametrize the high momentum transfer dependence of the deuteron  $n - p$  and  $\Delta - \Delta$  components, as a clue toward a complete description of the nuclear wavefunction.
6. One wishes to measure the neutron, pion, and kaon form factors.
7. The region well beyond  $x = 1$  for deep inelastic electron-nucleus scattering is important QCD physics since the virtual quark and gluon configurations in the nuclear wave function are required to be far off shell. Understanding the detailed mechanisms which underlie this dynamics will require coincident measurements and the broadest kinematic region available for  $\sigma_L/\sigma_T$  separation. The  $y$ -variable approach which attributes the electron scattering to nucleon currents is likely to break down even at moderate  $Q^2$ . Coincidence measurements which can examine the importance of the nucleon component are well worth study.
8. One wishes to study the emergence of strangeness in the nuclear state.

The fact that QCD is a viable theory for hadronic interactions implies that a fundamental description of the nuclear force is now possible. Although detailed work on the synthesis of QCD and nuclear physics is just beginning, it is clear from the structure of QCD that several traditional concepts of nuclear physics will have to be modified. These include conventional treatments of meson and baryon-pair contributions to the electromagnetic current and analyses of the nuclear form factor in terms of factorized on-shell nucleon form factors. On the other hand, the reduced nuclear form factor and scattering matrix elements discussed in Section 4 give a viable prescription for the extrapolation of nuclear amplitudes to zero nucleon radius. There is thus the possibility that even the low momentum transfer phenomenology of nuclear parameters will be significantly modified.

#### ACKNOWLEDGEMENTS

Parts of the talk are based on collaborations with J. R. Hiller, C.-R. Ji, and G. P. Lepage. I also wish to thank F. Gross and C. Shakin for helpful conversations.

## REFERENCES

1. Reviews of QCD are given in A. J. Buras, *Rev. Mod. Phys.* **53**, 199 (1980); A. H. Mueller, *Phys. Rep.* **73C**, 237 (1981); and E. Reya, *Phys. Rept.* **69**, 195 (1981).
2. For additional discussion of applications of QCD to nuclear physics and references, see S. J. Brodsky, published in the proceedings of the conference "New Horizons in Electromagnetic Physics", University of Virginia, April 1982; S. J. Brodsky, T. Huang and G. P. Lepage, SLAC-PUB-2868 (1982) published in *Springer Tracts in Modern Physics*, Vol. **100**, "Quarks and Nuclear Forces", ed. D. Fries and B. Zeitnitz (1982); S. J. Brodsky and G. P. Lepage, in the proceedings of the Eugene Few Body Conference 1980: 247C (*Nucl. Phys.* **A363**, 1981) and S. J. Brodsky, to be published in the proceedings of the NATO Pacific Summer Institute Progress in Nuclear Dynamics, Vancouver Island (1982).
3. For a recent discussion of progress in the derivation of nuclear forces from QCD-based models, see K. Maltman and N. Isgur, *Phys. Rev. Letters* **50**, 1827 (1983), E. L. Lomon, MIT preprint CTP No. 1116 (1983); and references therein. The quark interchange mechanism for  $N - N$  scattering is discussed in J. F. Gunion, S. J. Brodsky, and R. Blankenbecler, *Phys. Rev.* **D8**, 287 (1983). Qualitative QCD-based arguments for the repulsive  $N - N$  potential at short distances are given in C. Detar, HU-TFT-82-6 (1982); M. Harvey (Ref. 7); R. L. Jaffe, *Phys. Rev. Lett.* **24**, 228 (1983); and G. E. Brown, in Erice 1981, Proceedings, Quarks and the Nucleus. The possibility that the dueteron form factor is dominated at large momentum transfer by hidden color components is discussed in V. A. Matveev and P. Sorba, *Nuovo Cimento* **45A**, 257 (1978); *Nuovo Cimento* **20**, 435 (1977).
4. See, e.g. G. Adkins, C. R. Nappi, and E. Witten, Princeton preprint (1983); G. E. Brown, *Nucl. Phys.* **A374**, 63C (1982); C. Shakin, Brooklyn College preprint 82/081/115; M. C. Birse and M. K. Banerjee, University of Maryland preprint 83-201.
5. S. J. Brodsky, C.-R. Ji, G. P. Lepage, *Phys. Rev. Lett.* **51**, 83 (1983).
6. C. Klopfenstein, et al., CUSB 83-07 (1983).
7. S. J. Brodsky, G. P. Lepage, P. B. Mackenzie, *Phys. Rev.* **D28**, 228 (1983).
8. S. J. Brodsky, G. P. Lepage, SLAC-PUB-2294, published in "Quantum Chromodynamics" (AIP, 1979). G. P. Lepage and S. J. Brodsky, *Phys. Rev.* **D22**, 2157 (1980) and G. P. Lepage and S. J. Brodsky, *Phys. Rev.* **D22**, 2157 (1980). See also S. J. Brodsky, Y. Frishman, G. P. Lepage, and C. Sachrajda, *Phys. Lett.* **91B**, 239 (1980), A. Duncan and A. H. Mueller, *Phys. Rev.* **D21**, 1636 (1980), M. Peskin, *Phys. Lett.* **88B**, 128 (1979), and A. V. Efremov and A. V. Radyushkin, *Phys. Lett.* **94B**, 245 (1980).
9. Details of light-cone Fock methods are given in G. P. Lepage, S. J. Brodsky, T. Huang, and P. B. Mackenzie CLN3-82/522, published in proceedings of the Banff Summer Institute on Particle Physics, Alberta, Canada, S. J. Brodsky and G. P. Lepage, *Phys. Rev.* **D24**, 1808 (1981) and S. J. Brodsky, in proceeding of Quarks and Nuclear Forces, Springer **100**, Bad Liebenzell (1981).

10. S. J. Brodsky and G. P. Lepage, Phys. Rev. Lett. **43**, 545, 1625(E) (1979). S. J. Brodsky, G. P. Lepage, S.A.A. Zaidi, Phys. Rev. **D23**, 1152 (1981).
11. S. J. Brodsky and B. T. Chertok, Phys. Rev. Lett. **37**, 269 (1976); Phys. Rev. **D14**, 3003 (1976). S. J. Brodsky, in Proceedings of the International Conference on Few Body Problems in Nuclear and Particle Physics, Laval University, Quebec (1974).
12. S. J. Brodsky and J. R. Hiller, Phys. Rev. **C28**, 475 (1983). Figure 6 is corrected for a phase-space factor  $\sqrt{s/(s-m_d^2)}$ .
13. R. T. Aubert, et al., Phys. Lett. **105B**, 315, 322 (1981); Phys. Lett. **123B**, 123, 275 (1983). A. Bodek, et al., Phys. Rev. Lett. **50**, 1431; **51**, 524 (1983). For recent theoretical discussions and references to the EMC effect see e.g., M. Chemtob and R. Peschanski, Saclay preprint SPh.T/83/116 (1983), and E. Lomon (this proceedings).
14. S. J. Brodsky and G. R. Farrar, Phys. Rev. Lett. **31**, 1153 (1973), and Phys. Rev. **D11**, 1309 (1975); V. A. Matveev, R. M. Muradyan and A. V. Tavkhelidze, Lett. Nuovo Cimento **7**, 719 (1973).
15. S. J. Brodsky and G. P. Lepage, Phys. Rev. **D24**, 2848 (1981).
16. M. D. Mestayer, SLAC-Report 214 (1978) F. Martin, et al., Phys. Rev. Lett. **38**, 1320 (1977); W. P. Schultz, et al., Phys. Rev. Lett. **38**, 259 (1977); R. G. Arnold, et al., Phys. Rev. Lett. **40**, 1429 (1978); B. T. Chertok, Phys. Lett. **41**, 1155 (1978); D. Datz, et al., Phys. Rev. Lett. **43**, 1143 (1979). Summaries of the data for nucleon and nuclear form factors at large  $Q^2$  are given in B. T. Chertok, in Progress in Particle and Nuclear Physics, Proceeding of the International School of Nuclear Physics, 5th Course, Erice (1978), and Proceedings of the XVI Rencontre de Moriond, Les Arcs, Savoie, France, 1981.
17. H. J. Behrend, et al., CELLO collaboration preprint (1983). W. J. Stirling, DAMTP 83/17 to be published in the proceedings of the 5th International Workshop on Photon-Photon Collisions (1983).
18. S. J. Brodsky and G. P. Lepage, Phys. Rev. **D24**, 1808 (1981).
19. S. J. Brodsky, T. Huang, G. P. Lepage, SLAC-PUB-2540 (1980), and T. Huang, SLAC-PUB-2580 (1980), published in the Proceedings of the XXth International Conference on High Energy Physics, Madison, Wisconsin (1980).
20. S. J. Brodsky, C.-R. Ji, and G. P. Lepage (to be published).
21. See also A. Matveev and P. Sorba, reference 3.
22. G. R. Farrar and F. Neri, Rutgers preprint RU-83-20 (1983).
23. M. Harvey, Nucl. Phys. **A352**, 301, 326 (1981).
24. H. Myers et al., Phys. Rev. **121**, 630 (1961); R. Ching and C. Schaerf, Phys. Rev. **141**, 1320 (1966); P. Dougan et al., Z. Phys. **A276**, 55 (1976).
25. S. J. Brodsky, C.-R. Ji and G. P. Lepage (to be published).
26. See the proceedings of the meeting "New Horizons in Electromagnetic Physics", Virginia (1983).

27. A more detailed discussion of the material of this section is given in S. J. Brodsky, to be published in the proceedings of the NATO Pacific Summer Institute "Progress in Nuclear Dynamics", Vancouver Island (1982), and references 2 and 9.
28. S. J. Brodsky and R. W. Brown, *Phys. Rev. Lett.* **49**, 966 (1982). R. W. Brown, S. J. Brodsky, and K. L. Kowalski, *Phys. Rev.* **D28**, 228 (1983), and references therein.
29. For a discussion and references to QCD effects of quarks and hadrons in nuclear matter, see reference 27 and S. J. Brodsky, SLAC-PUB-3219 (to be published in the proceedings of the Third International Conference on "Physics in Collisions", Como, Italy (1983).
30. For related methods see, e.g. P. Hoodbhoy and L. S. Kisslinger, Carnegie-Mellon preprint (1983). V. G. Ableev, et al., JINR preprint E1-83-487 (1983).
31. S. Adler, IAS preprint (1983), to be published in the proceedings of the Workshop on Non-perturbative QCD. J. Hiller, *Ann. Phys.* **144**, 58 (1982).
32. P. Barnes, et al., NSAC Subcommittee report (1983).

## NONPERTURBATIVE QUANTUM CHROMODYNAMICS

Julius Kuti

Department of Physics  
University of California at San Diego  
La Jolla, California 92093

### ABSTRACT

A powerful stochastic method for the numerical evaluation of path integrals in quantum mechanics and quantum field theory is reviewed. Known as the Monte Carlo method it is directly applicable to the detailed numerical study of Quantum Chromodynamics with lattice regularization. Important results on non-perturbative quantities, like the confining force between a heavy quark-antiquark pair, the critical temperature of thermal quark liberation and the mass gap are reviewed first within the pure gauge sector of the theory in the absence of quark vacuum polarization effects. The numerical calculation of the hadron spectrum in this approximation is discussed. The stochastic treatment of quark vacuum polarization effects is also reviewed.

### 1. INTRODUCTION

After so many years there is now a general belief that Quantum Chromodynamics (QCD) is the correct theory of the strong interactions. This theory is remarkably consistent with deep inelastic phenomena<sup>1</sup> and provides a solid framework for probing hadron structures at short distances. The great success of QCD is explained by asymptotic freedom<sup>2</sup> which tells us that the quark-gluon coupling becomes weak at short distances and perturbation theory is applicable in a systematic fashion. The bare coupling constant  $g(a)$  will vanish logarithmically as a function of the space-time cut-off parameter  $a$ ,

$$g(a) \approx \ln^{-1} a\Lambda \quad (1.1)$$

in the limit  $a \rightarrow 0$ . The value of the lattice scale parameter  $\Lambda$  in MeV units sets the strength of the bare quark-gluon coupling.<sup>3</sup> It directly relates to the widely used deep inelastic scale parameter  $\Lambda_{\overline{MS}}$ <sup>4</sup> by some numerical conversion factor,<sup>3</sup>

$$\Lambda_{\overline{MS}} = 28.8 \Lambda . \quad (1.2)$$

Asymptotic freedom in Eq. (1.1) is indicated in a somewhat symbolic fashion without putting in some coefficients and higher order logarithmic terms.

On the scale of 1 fermi the coupling becomes strong, perturbation theory breaks down and the most interesting hadron parameters (mass spectrum, decay widths, wave functions, ...) are not calculable by analytic methods. In fact, it has been deduced from QCD on quite general grounds that any hadron mass  $M_h$  will depend on the bare quark-gluon coupling constant  $g(a)$  non-perturbatively,

$$M_h = c_h a^{-1} \left[ \frac{24 \pi^2}{11 g^2(a)} \right]^{51/121} \exp \left[ \frac{-b}{g^2(a)} \right] . \quad (1.3)$$

The space-time cut-off  $a$  carries the dimension of the hadron mass in Eq. (1.3). It is the only dimensional parameter which appears in the regularized equations of the theory in the limit when all quark masses vanish. The constant  $b$  in the exponent is known analytically. Without quark vacuum polarization contributions it is given by

$$b = \frac{12 \pi^2}{11} . \quad (1.4)$$

In contrast, the non-perturbative coefficient  $c_h$  in front of the exponential expression in Eq. (1.3) varies from hadron to hadron and has to be calculated by numerical methods. This type of calculation is the main topic of the lecture.

Asymptotic freedom for the bare coupling leads to the transmutation of Eq. (1.3),

$$M_h = \text{const}_h \Lambda_{\overline{MS}} , \quad (1.5)$$

where the hadron mass  $M_h$  does not depend on the cut-off  $a$  anymore.



The dimension of the mass is carried now by the physically measurable quantity  $\Lambda_{\overline{\text{MS}}}$ . The constant relating the hadron mass to  $\Lambda_{\overline{\text{MS}}}$  must be calculated non-perturbatively, as we noted before.

The experimental value of  $\Lambda_{\overline{\text{MS}}}$  is only poorly known from short distance physics<sup>1</sup> to be somewhere between  $100 \text{ MeV} < \Lambda_{\overline{\text{MS}}} < 400 \text{ MeV}$ . The main difficulty is that the predicted experimental scaling violation effects are logarithmically slow functions of the momentum transfer. In the non-perturbative theoretical study of QCD we hope to determine  $\Lambda_{\overline{\text{MS}}}$  accurately, and perhaps less costly. Since the relation in Eq. (1.5) is linear, a few percent relative accuracy in the determination of the constant would lead to the same small error in setting the scale parameter in MeV units.

I would like to emphasize here that the detailed quantitative understanding of QCD is very important beyond the investigation of strong interaction phenomena. The tests of grand unification theories of weak, electromagnetic and strong forces require non-perturbative solutions in QCD. The illustration of this statement is as follows. The unification scheme with SU(5) makes a prediction for the proton lifetime,<sup>5</sup>

$$\tau_p \approx 10^{32 \pm 2} \left[ \frac{\Lambda_{\overline{\text{MS}}}}{\text{GeV}} \right]^4 \text{ year} , \quad (1.6)$$

with dominant decay modes into  $e^+ \pi^0$  type channels. The theoretical error from the unknown proton structure and uncertainties from extrapolation to the unification scale is guessed to be about two orders of magnitude as indicated by the error bars in the exponent. The proton lifetime depends on the fourth power of  $\Lambda_{\overline{\text{MS}}}$ , a non-perturbative quantity again. With the current experimental lower bound,<sup>6</sup>

$$\tau_p(e^+ \pi^0) > 10^{32} \text{ year} , \quad (1.7)$$

the standard SU(5) prediction seems to be in serious trouble if  $\Lambda_{\overline{\text{MS}}} \approx 100\text{-}200 \text{ MeV}$ . The seriousness of the problem depends on the details of the proton structure and the accurate value of the scale parameter  $\Lambda_{\overline{\text{MS}}}$ . The answer is expected to come from the non-perturbative solution of QCD.

The non-perturbative method I am going to describe is in a way the theorists' experiment. With computer simulation, we can create

now interesting experiments, like the investigation of quark-gluon matter under extreme conditions with thermal quark liberation at high temperatures. The same technique allows us to calculate the hadron spectrum directly from first principles of Quantum Chromodynamics.

To understand the method, I will describe it first in detail as applied to a simple quantum mechanical problem. In Quantum Chromodynamics I will only summarize the most important results without going into technical details. This presentation was prepared for those who want to get a first idea about the Monte Carlo method with some review on lattice QCD applications.

## 2. THE PATH INTEGRAL AND THE MONTE CARLO METHOD

I will briefly describe now a powerful stochastic method for the numerical evaluation of path integrals in quantum mechanics. The method is easy to generalize to Quantum Chromodynamics with lattice regularization.

Consider a non-relativistic particle of mass  $m$  moving in some one-dimensional potential well  $V(Q)$ . The particle is described by the Hamiltonian

$$H = \frac{P^2}{2m} + V(Q) . \quad (2.1)$$

The transition amplitude,

$$Z_{fi} = \left\langle Q_f \left| e^{-\frac{i}{\hbar} H(t_f - t_i)} \right| Q_i \right\rangle , \quad (2.2)$$

plays a fundamental role in quantum mechanics. It describes the probability amplitude of propagating from the initial position  $Q_i$  of the particle at time  $t_i$  to some final position  $Q_f$  at time  $t_f$ .

### 2.1 Feynman's Path Integral

The time interval  $t_f - t_i$  in Eq.(2.2) can be divided into  $n+1$  segments with  $t_f - t_i = (n+1)\epsilon$ , where  $\epsilon$  is the length of the time slice along the time-like axis in Fig. 1. The time direction is discretized this way as in lattice calculations. It is easy to show that  $Z_{fi}$  in



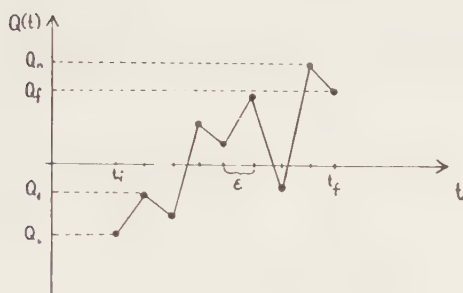


Fig. 1

Eq. (2.2) can be represented as the limit of the  $n$ -dimensional integral,

$$Z_{fi} = \text{const} \cdot \lim_{n \rightarrow \infty} \int \prod_{k=1}^n dQ_k \cdot \quad (2.3)$$

$$\cdot \exp \left\{ \frac{i}{\hbar} \sum_{j=1}^{n+1} \epsilon \left[ \frac{1}{2} m \frac{(Q_j - Q_{j-1})^2}{\epsilon^2} - \frac{V(Q_j) + V(Q_{j-1})}{2} \right] \right\},$$

with the notation  $Q_0 = Q_i$  and  $Q_{n+1} = Q_f$ . The normalization constant in Eq. (2.3) is not relevant for our considerations. Eq. (2.3) can be derived by writing

$$\left\langle Q_f \left| e^{-(i/\hbar) H(t_f - t_i)} \right| Q_i \right\rangle$$

in Eq. (2.2) as

$$\left\langle Q_f \left| \prod_{k=1}^{n+1} e^{-(i/\hbar) H \epsilon} \right| Q_i \right\rangle$$

and inserting a complete set of states  $n$  times.

The integration over  $n$  variables in Eq. (2.3) corresponds to the sum over all zig-zag paths of Fig. 1 connecting  $Q_i$  to  $Q_f$  in the time interval  $t_f - t_i$ . The limit  $n \rightarrow \infty$  defines Feynman's path integral,

$$Z_{fi} = \text{const} \int dQ \exp \left[ \frac{i}{\hbar} \int L(\dot{Q}, Q) dt \right], \quad (2.4)$$

where  $L = \frac{1}{2} m \dot{Q}^2 - V(Q)$  is the Lagrangian of the particle. The transition amplitude  $Z_{fi}(Q_f = Q(t_f), t_f; Q_i = Q(t_i), t_i)$  is given by the sum of exponential phases along the paths from  $Q_i$  to  $Q_f$ . The phase of a path is determined by the value of the action integral  $S = \int L(\dot{Q}, Q) dt$  along the path.

For the numerical evaluation of the path integral we will keep  $n$  finite and work on a time lattice as depicted in Fig. 1. With sufficiently dense slicing (large  $n$ ) the results of the calculation will meet any prescribed accuracy.

It is very difficult to sum the rapidly oscillating phases of the path integral, even in simple quantum mechanical applications. We follow the standard trick and rotate to Euclidean time. In practice, this rotation corresponds to the substitution  $\epsilon \rightarrow -i\epsilon$  in the integrand of the zig-zag approximation of Eq. (2.3). This eliminates the imaginary phase from the exponent.

The Euclidean transition matrix element with  $n$  segments in the zig-zag paths is given by

$$Z_{fi}^{(n)} = \int \prod_{k=1}^n dQ_k \exp \left[ -\frac{1}{\hbar} S_E(Q_i, Q_1, \dots, Q_n, Q_f) \right], \quad (2.5)$$

where we dropped the normalization factor of the integral. This factor always cancels in physical quantities. The Euclidean action in Eq. (2.5) is given by

$$S_E(Q_0, \dots, Q_{n+1}) = \sum_{k=0}^n \left[ \frac{1}{2} m \epsilon \frac{(Q_{k+1} - Q_k)^2}{\epsilon^2} + \epsilon \frac{V(Q_{k+1}) + V(Q_k)}{2} \right]. \quad (2.6)$$

There is no integration in Eq. (2.5) over the end points  $Q_0 = Q_i$  and

$$Q_{n+1} = Q_f .$$

One can study the Euclidean correlation functions of the quantum mechanical particle, like the two-point function

$$\langle Q_I Q_J \rangle = \frac{\int \prod_{k=1}^n dQ_k Q_I Q_J \exp \left[ -\frac{1}{\hbar} S_E(Q_0, \dots, Q_{n+1}) \right]}{Z_{fi}^{(n)}} , \quad (2.7)$$

or more complicated ones. The relevant physics has to be extracted from averages like the correlation function in Eq. (2.7).

## 2.2 The Monte Carlo Method

Feynman's path integral in Euclidean time shows some interesting formal analogy with a classical one-dimensional crystal. In the approximation of  $n$  integration variables,  $Z_{fi}^{(n)}$  in Eq. (2.5) can be viewed as the partition function of a chain of  $n+2$  particles in a crystal lattice. There is some potential energy  $\epsilon V(Q_k)$  for the  $k$ -th particle where  $Q_k$  designates the displacement of the particle. The interaction between two neighboring particles along the chain is given by  $m/2\epsilon (Q_{k+1} - Q_k)^2$ . The displacements  $Q_0$  and  $Q_{n+1}$  of the first and the last particles, respectively, are fixed. The other particles can move in the crystal lattice.

The energy of this classical system is given by the Euclidean action  $S_E$  and the temperature of the crystal is  $\hbar$  following our formal analogy. The correlation function in Eq. (2.7) is interpreted as the thermal average of  $Q_I Q_J$  over the classical one-dimensional crystal at temperature  $\hbar$ . The probability distribution of the configurations is given by

$$dP \approx \frac{\exp \left[ -\frac{1}{\hbar} S_E \right]}{Z_{fi}^{(n)}} dQ . \quad (2.8)$$

The expectation value  $\langle Q_I Q_J \rangle$  can be calculated as follows. We generate configurations according to the probability distribution  $dP$  in Eq. (2.8) by bringing the crystal to thermodynamical equilibrium at temperature  $\hbar$ . Taking samples from the probability distribution,

the correlation function  $\langle Q_I Q_J \rangle$  will be given simply by the statistical average of  $Q_I Q_J$  over the sample configurations.

There are Monte Carlo computer simulation techniques to accomplish this. The computer would cycle through the crystal lattice changing the position of the particles sequentially. When a particle is updated its new displacement is generated according to the probability distribution of Eq. (2.8) keeping the other particles fixed at their previous position. This probability distribution is the Boltzmann factor of the particle at temperature  $\hbar$  when all the other particles are kept frozen. The physical picture is that we bring every particle in contact with a local heat bath, sequentially. The repeated procedure will eventually bring the system to thermal equilibrium.

A sufficient number of sweeps will bring the crystal lattice to thermal equilibrium in the sense that at the end of each cycle a new configuration is generated with the correct probability distribution of Eq. (2.8), for all particles simultaneously. The statistical average of  $Q_I Q_J$  over the configurations will determine  $\langle Q_I Q_J \rangle$  within statistical errors. The error will decrease proportional to  $N^{-1/2}$  where  $N$  is the number of sweeps through the crystal lattice used for averaging in the computer simulation.

### 2.3 Particle in Double Well Potential

A simple application of the above described method will demonstrate the power of the stochastic procedure. It will also help us to understand the thermodynamics of a quantum mechanical particle in heat bath at temperature  $T$  using the path integral formulation of the problem. The same procedure is followed in QCD in the study of the properties of hot quark-gluon matter.

In thermodynamics the partition function of the particle is given by

$$Z = \text{Tr} e^{-\beta H}, \quad \beta = \frac{1}{kT}. \quad (2.9)$$

The trace can be written as

$$Z = \int dQ \langle Q | e^{-\beta H} | Q \rangle. \quad (2.10)$$

The evaluation of Eq. (2.10) proceeds as before. The operator  $e^{-\beta H}$  is written as the product of  $e^{-\epsilon H}$  factors. Complete sets of states

are inserted and the trace is reduced to the  $n$  dimensional integral of Eq. (2.5). One also has to integrate over the end point variable  $Q = Q_f = Q_i$  because of the presence of the trace operation in Eq. (2.10).

We learn therefore that the thermodynamics of a quantum mechanical particle at inverse temperature  $\beta$  is equivalent to the sum of periodic Feynman paths with period  $\beta$ . Furthermore, the summation of the Feynman paths is equivalent to the classical partition function of a periodic one-dimensional crystal. The inverse of temperature  $T$  appears as  $\beta = (n+1)\epsilon$  where  $\epsilon$  is the length of the periodic crystal. It is important to distinguish between the physical heat bath which is the environment of the quantum mechanical particle in the thermal problem and the fictitious heat bath of the Monte Carlo procedure in generating the probability distribution of Eq. (2.8).

We apply now the machinery to the double well potential<sup>7</sup>

$$V(Q) = -\frac{1}{2}\mu^2 Q^2 + \lambda Q^4, \quad (2.11)$$

with two minima as depicted in Fig. 2. When the temperature is low so that  $kT$  is much smaller than the ground state energy  $E_0$ , we can extract information about the ground state properties of the system. Fig. 3 shows a typical configuration as generated by the Monte Carlo simulation of the one-dimensional crystal lattice.<sup>7</sup> We can see quantum mechanical tunneling here between the two potential minima for  $kT \ll E_0$ .

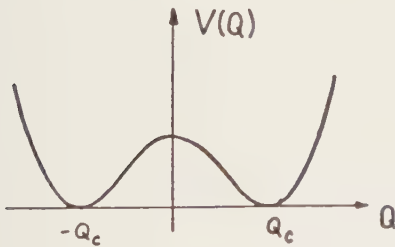


Fig. 2

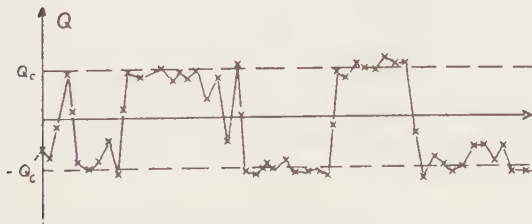


Fig. 3

The histogram of the  $Q$ -distribution as cumulated over many configurations is shown in Fig. 4. With proper normalization it gives the absolute value square of the wave function for the quantum particle in ground state. The Monte Carlo points of Creutz and Freedman are sitting right on the dashed line of the exact curve. The ground state energy can be extracted from correlation functions.

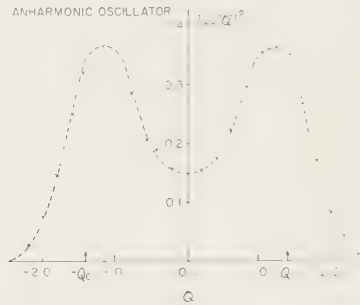


Fig. 4

Though the above procedure may appear somewhat peculiar for the solution of quantum mechanics, it is the only tool today to attack non-perturbative QCD.

### 3. OBSERVABLES IN THE PURE GAUGE SECTOR

The spirit of the calculation in QCD is the same as in our simple quantum mechanical example. The functional integrals are now four-dimensional in Euclidean space-time. We take some finite volume in this 4d space and introduce Wilson lattice regularization.<sup>8</sup> Gauge fields live on links in lattice QCD and quark fields live on lattice sites. The lattice system has a finite number of degrees of freedom. The relevant  $n$ -dimensional integrals can be evaluated again using the above described Monte Carlo technique. In practice, we integrate now over the order of a million variables. A remarkable technical achievement, indeed.

A hypercubical lattice in four Euclidean space-time dimensions is used in the calculations. The link connecting the nearest neighbor

sites  $i$  and  $j$  is designated by  $[i, j]$ . An  $SU(3)$  matrix  $U_{ij}$  is associated with every link of the lattice such that

$$U_{ji} = (U_{ij})^{-1} . \quad (3.1)$$

The partition function is defined by

$$Z(\beta) = \int \prod_{[i,j]} \exp[-\beta S_E(U)] dU_{ij} . \quad (3.2)$$

where  $\beta$  is the inverse coupling constant squared as given by  $\beta = 6/g^2(a)$ . Here  $g(a)$  is the bare coupling constant of the theory for lattice cut-off  $a$ . The measure in the integral of Eq. (3.2) is the normalized invariant Haar measure. The action  $S_E$  is defined as a sum over all unoriented plaquettes,

$$S_E(U) = \sum_{\text{plaquettes}} S_{pl} = \sum_{\text{plaquettes}} \left( 1 - \frac{1}{3} \text{Re Tr } U_{pl} \right) , \quad (3.3)$$

where the plaquette  $U_{pl}$  is the smallest rectangular Wilson loop. Rectangular Wilson loops<sup>8</sup> are defined by the expectation value

$$W(I, J) = \frac{1}{3} \langle \text{Re Tr } U_C \rangle , \quad (3.4)$$

where  $C$  is a rectangle of rectangular dimensions  $I$  and  $J$  and  $U_C$  is the product of link variables along the loop  $C$ .

The use of Monte Carlo techniques in lattice QCD was first suggested by Wilson.<sup>9</sup> The first calculation of the string tension in the pure gauge sector of the theory with  $SU(2)$  color was carried out by Creutz.<sup>10</sup> It came after the pioneering work of the Brookhaven group<sup>11</sup> and triggered great interest in the subject.

### 3.1 String Tension

The potential energy  $V(r)$  between a heavy quark-antiquark pair at large separation  $r$  defines the string tension  $K$  in the gluon sector of the theory,

$$V(r) = - \frac{4 \alpha(r)}{3r} + Kr . \quad (3.5)$$



The Coulomb term in Eq. (3.5) describes asymptotic freedom at short distances and the linear potential is associated with permanent quark confinement. One often pictures the confining force as a chromoelectric flux tube between the quark-antiquark pair. The energy stored per unit length in this flux tube is given by  $K$ .

$K$  also relates phenomenologically to the slope  $\alpha'(0)$  of Regge trajectories. If high angular momentum excitations are described as rotating strings, one derives the relation

$$K \approx \frac{1}{2\pi\alpha'(0)} \quad (3.6)$$

Heavy particle spectroscopy, which is based on the potential of Eq. (3.5), and the universal Regge slope  $\alpha'(0)$  are consistent with a value for  $K$  somewhere around

$$K \approx \frac{1 \text{ GeV}}{\text{fermi}} \quad (3.7)$$

The string tension was the first physical quantity determined by the above described Monte Carlo technique, first in  $SU(2)$ ,<sup>10</sup> and later in  $SU(3)$ .<sup>12</sup> To extract the string tension, one has to calculate the logarithmic ratios

$$\chi(I, J) = -\ln \left\{ \frac{W(I, J) W(I-1, J-1)}{W(I, J-1) W(I-1, J)} \right\} \quad (3.8)$$

For large  $I$  and  $J$ , the ratio  $\chi(I, J)$  is identified with the dimensionless string tension  $Ka^2$  in lattice spacing units. Since  $K$  is a dimensional physical quantity with dimension  $\text{mass}^2$ , it must depend on the bare coupling constant  $g(a)$  as

$$K = \text{const} \frac{1}{a^2} \left[ \frac{24\pi^2}{11g^2} \right]^{102/121} e^{-\frac{2b}{g^2(a)}} \quad (3.9)$$

This non-perturbative behavior on the bare coupling constant is similar to that described in the Introduction for hadron masses.

Interesting progress has been made recently by Tomboulis in proving quark confinement in the pure gauge sector of the theory.<sup>13</sup> He proves that in  $SU(2)$  lattice gauge theory, the energy of a heavy



quark-antiquark pair is bounded from below by that calculated from the approximate Migdal-Kadanoff renormalization group transformation. This transformation generates a linear confining potential with a string tension of the form of Eq. (3.9). The Tomboulis bound therefore can be interpreted as a rigorous proof of quark confinement on the lattice.

Unfortunately, the parameter  $b$  in the exact form of Eqs. (3.9) and (1.4) is smaller than the one generated by the Migdal-Kadanoff transformation. This has a serious consequence. In the limit when the lattice spacing  $a$  goes to zero the Tomboulis bound becomes trivial. The lower bound for the string tension becomes zero in this limit. We have to turn to Monte Carlo calculations for practical results.

The latest Monte Carlo results of Creutz and his collaborators<sup>14</sup> on the string tension is shown in Fig. 5. The lattice size is

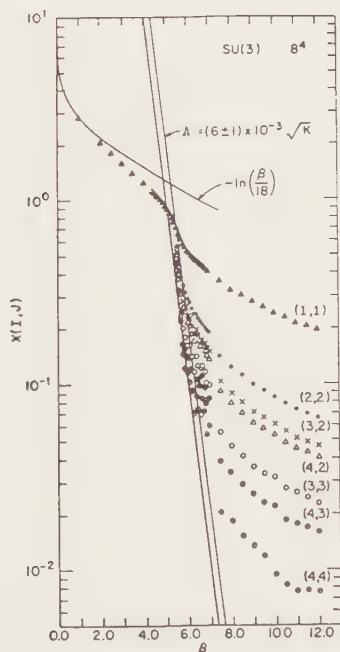


Fig. 5

$8^4$  in the calculation. The straight line on the logarithmic plot is the envelope of the logarithm of Wilson loop ratios to project out the expression  $Ka^2$  from the Monte Carlo data. The slope of the straight line is fixed by the renormalization group and given by the exponent of Eq. (3.9). The data strongly departs from the leading strong coupling result

$$Ka^2 = -2n \frac{\beta}{18} \quad (3.10)$$

around  $\beta = 5.5$ . It is indicative that continuum renormalization group behavior is seen in the data above  $\beta = 5.7$ . The relation between the string tension and the lattice scale parameter from the intercept of the straight line and the horizontal axis is given by

$$\Lambda = (6 \pm 1) 10^{-3} \sqrt{K} \quad (3.11)$$

This result is being challenged by some recent calculations.<sup>15,16</sup> Stack<sup>15</sup> measures  $K$  on a lattice of size  $8^3 12$ . The long time direction allows him to measure longer Wilson loops, as dictated by the theory, for fixed spatial separation of the heavy quark-antiquark pair. Also, Stack calculates the heavy  $q\bar{q}$  potential from short distances to one fermi and beyond. He finds scaling behavior as expected from the renormalization group in the limit  $a \rightarrow 0$ .

The calculated points of the potential are shown in Fig. 6. Since the potential  $V$  is plotted against a scaling variable  $x$ , the fact that all the points are on a single scaling curve is interpreted as continuum limit renormalization group behavior.<sup>15</sup>

The solid line is a fit to the Monte Carlo points with the phenomenological form of Eq. (3.5). The dashed line is the running Coulomb potential at short distances. Around  $1/2$  fermi the non-perturbative behavior sets in and the Monte Carlo points depart from perturbation theory. The best estimate between  $\Lambda$  and  $K$  is reported to be

$$\Lambda = (11 \pm 3) 10^{-3} \sqrt{K} \quad (3.12)$$

in clear discrepancy with Eq. (3.11). The two calculations differ by about a factor of two.

Recently, another determination of the conversion factor was reported.<sup>16</sup> The authors of that paper work on a lattice of size

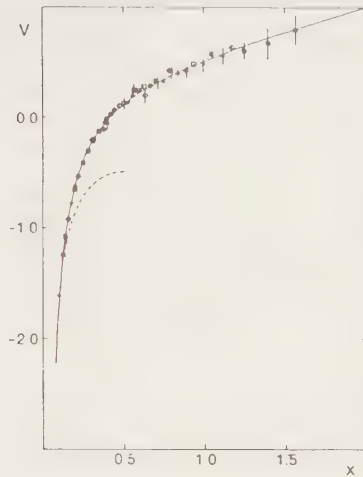


Fig. 6

$10^3$ 20. They measure the string tension from the correlation function of thermal Wilson loops (Section 3.2) which are periodic along one of the directions with ten links. The reported value

$$\Lambda = (11.9 \pm 0.6) 10^{-3} \sqrt{K} \quad , \quad (3.13)$$

is very close to the result of Stack.

In a contribution to the conference<sup>17</sup> a new calculation of the conversion factor (with a value 7.9) was reported for data above  $\beta = 5.5$  on a lattice of size  $10^4$ .

At  $\beta = 5.7$  there is another recent calculation<sup>18</sup> on a large lattice of size  $16^4$ . The reported value is 6.9 close to the number in Eq. (3.11). Since scaling is not seen at that coupling in the calculation, the result is interpreted as a lower bound on the conversion factor. I should also note that Stack would agree with the number 6.9 at  $\beta = 5.7$  using square-like Wilson loops.

The controversy of the string tension calculation has to be clarified in the near future. It has serious consequences in setting the

physical scales in the theory. Taking  $\sqrt{K} \approx 450$  MeV the scale parameter  $\Lambda_{\overline{MS}}$  is about 80 MeV with a conversion factor of 6. With the new values 11 or 11.9,  $\Lambda_{\overline{MS}}$  would be about 150 MeV. Accordingly, the lattice spacing at  $\beta = 6$  would decrease from 0.2 fermi to 0.1 fermi.

### 3.2 Hot Gluon Plasma

There has been a long-standing conjecture<sup>19</sup> that a phase transition occurs as a function of temperature between the low temperature confining phase of QCD and the deconfined hot gluon plasma phase. Quarks can move freely in the hot gluon plasma.

Recent Monte Carlo calculations<sup>20</sup> gave strong numerical evidence that the quark liberating phase transition indeed occurs in the gauge sector of QCD. The calculation goes as follows.

We insert a heavy quark-antiquark pair in the vacuum at large separation. At zero temperature some chromoelectric flux develops between the quark and antiquark, and we experience some confining force law with linear potential energy. Now we heat up the system and repeat the calculation at finite temperature.

One finds a critical temperature  $T_c$  where the confining force between the heavy quark and antiquark suddenly disappears. What happens somehow is that the vacuum as a medium which supports the confining chromoelectric flux gradually fills up with glueballs as the temperature increases. At a critical temperature  $T_c$  suddenly some gluon plasma forms and the string tension becomes zero. The quark and antiquark are not permanently bound anymore.<sup>1</sup>

The finite temperature calculation proceeds similarly to that of the simple quantum mechanical example in Section 2.3. The static quark is represented by the thermal Wilson loop  $W_t$ . It is defined as the expectation value of the trace of the U-matrix product along the temperature direction for fixed spatial position of the quark.<sup>20</sup> There is a similar thermal loop for the antiquark. The string tension at finite temperature can be extracted from the correlation function of the thermal loops for the quark-antiquark pair.

The phase transition is a bulk property of the system and therefore relatively easy to detect in Monte Carlo calculation. The order parameter  $W_t$  of the phase transition,

$$W_t = \exp(-\beta F) , \quad (3.14)$$

where  $F$  is the free energy of an isolated heavy quark in heat bath, can be continuously monitored as the temperature  $T$  ( $\beta = 1/kT$ ) is increased in the Monte Carlo calculation. An abrupt change in the order parameter  $W_t$  is observed<sup>20</sup> at the critical temperature as shown in Fig. 7.<sup>21</sup>

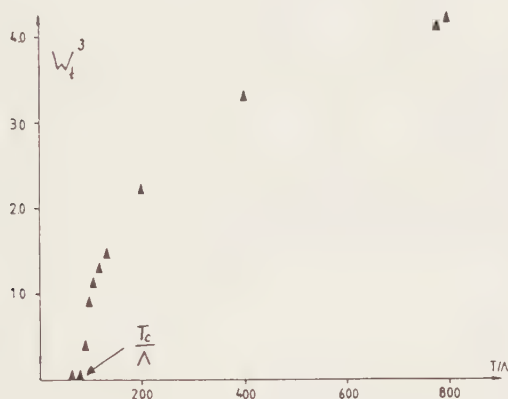


Fig. 7

Below  $T_c$  the color field around the isolated quark forms a collimated chromoelectric flux. Above  $T_c$  we find a Debye screened Coulomb field as shown in Fig. 8. The change in the chromoelectric



Fig. 8

field energy of the isolated quark is infinite at the critical temperature  $T_c$ , even for finite cut-off  $a$ . This infinite change in the free energy of the isolated quark makes the order parameter vanishing in the confining phase below the critical temperature.

The critical temperature is a physical quantity of mass dimension. Therefore,  $T_c$  depends on the bare coupling the same way as  $\sqrt{K}$  or any hadron mass. This is clearly demonstrated in Fig. 9<sup>22</sup>

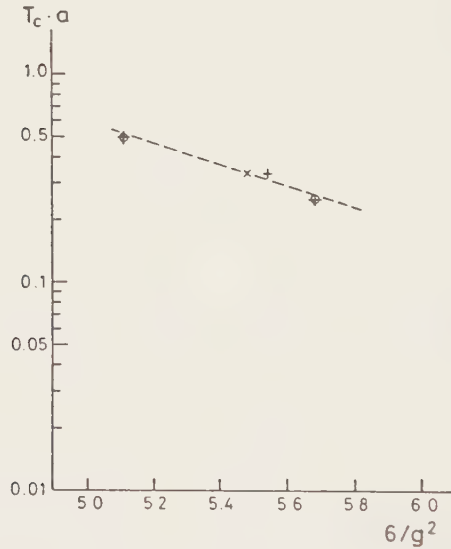


Fig. 9

where the intercept of the straight line (with the right slope) yields the relation between  $T_c$  and the lattice parameter  $\Lambda$ . With the old value of the string tension one finds

$$T_c \approx \frac{1}{2} \sqrt{K} \quad . \quad (3.15)$$

The numerical value of  $T_c$  would be around 200 MeV, a very interesting temperature for the heavy ion community.

If, however, the string tension is close to the new value of Eq. (3.12), the relation becomes

$$T_c \approx \sqrt{K} \quad (3.16)$$

pushing  $T_c$  to about 400 MeV a very large temperature to access in heavy ion physics.

The nature of the phase transition is rather well established by now. It appears to be strongly first order<sup>23</sup> with a measurable latent heat. The presence of quark vacuum polarization is expected to destroy the first order nature of the phase transition. In fact, there has been a conjecture<sup>24</sup> that the phase transition may be completely smeared out by the presence of light vacuum polarization quarks.

### 3.3 Mass Gap and Glueball Excitations

It would be very interesting to determine numerically the mass spectrum of lowest glueball states. Previous attempts<sup>25</sup> were based on the study of the exponential decay of correlation functions, like

$$\langle 0 | G_{\mu\nu}^2(0) G_{\mu\nu}^2(x) | 0 \rangle \quad (3.17)$$

where  $G_{\mu\nu}$  designates the field strength of the gluon field. The exponential decay of the correlation function at large separation is governed by the lowest glueball state which can be excited from the vacuum by the composite operator  $G_{\mu\nu}^2$ .

A new scheme was proposed recently<sup>26</sup> which allows the extraction of glueball masses from correlation functions of composite operators in combination with a variational principle.<sup>27</sup> Results are reported for the mass of the  $0^{++}$  glueball to be

$$m(0^{++}) \approx 2 \sqrt{K} \quad , \quad (3.18)$$

if the value in Eq. (3.11) is used for the string tension. With the new string tension results the mass of the  $0^{++}$  glueball would be around

$$m(0^{++}) \approx 4 \sqrt{K} \quad . \quad (3.19)$$

The numerical value of the  $0^{++}$  glueball mass is predicted to be somewhere between 1 GeV and 2 GeV, subject to a more consistent determination of the string tension.



Putting that aside, I still feel somewhat worried about the reliability of glueball mass calculations, since the lattice sizes involved are disturbingly small.

To improve the quality of Monte Carlo calculations on a given size lattice at some coupling (around the cross-over into the scaling regime), Symanzik suggested<sup>28</sup> the modification of the lattice action adding properly chosen irrelevant operators to the Lagrangian. The method seems to improve the Monte Carlo results significantly.<sup>29,30</sup> Fig. 10 shows the mass gap in the 2d  $O(3)$  model using Symanzik's improved action.<sup>29</sup>

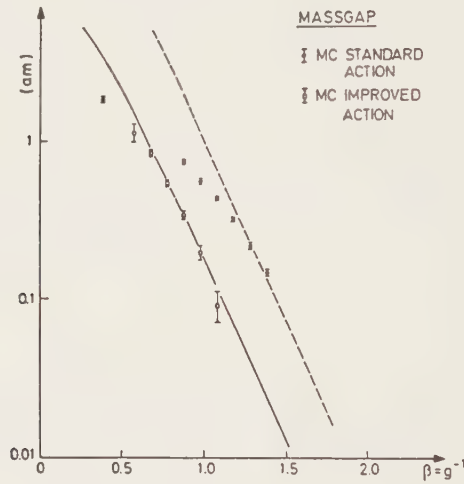


Fig. 10

Apparently, the onset of scaling is much more rapid with the improved action which has the same continuum limit as the old one. The approach is very promising for future applications. A glueball calculation with the new improved action in the  $SU(2)$  gauge model was reported recently.<sup>30</sup>

### 3.4 Gluon Condensate in the Vacuum

The vacuum state of Quantum Chromodynamics, even in the absence of quark vacuum polarization, is a complicated medium whose physical properties are only poorly known.

Unfortunately, we have learned only very little so far about the detailed structure of the vacuum from Monte Carlo calculations. We know that the vacuum as a medium is responsible for confinement, and when heated it suffers deconfining phase transition at some critical temperature. Very little is known about the nature of the gluon condensate which is responsible for those phenomena.

We are impressed by simple pictures which describe so elegantly some of the simple spin models. Fig. 11 shows the two-dimensional x-y model as it evolves from some chaotic configuration to a low temperature state in a few hundred Monte Carlo sweeps.<sup>31</sup>



Fig. 11

One can clearly see the Koesterlitz-Thouless vortices as they emerge from the initial configuration. The important role of the Koesterlitz-Thouless vortices is well known in the 2d x-y model. It

would be very satisfying to see that sort of qualitative (and also quantitative) insight into the vacuum structure of Quantum Chromodynamics.

#### 4. THE FERMION PROBLEM

During the last two years considerable effort went into Monte Carlo methods for the numerical study of quantum systems with fermionic degrees of freedom. This outstanding problem is of great importance for applications in quantum field theories, condensed matter physics, and nuclear physics.

We will follow here the standard strategy of quantum field theory and work directly with the effective action of the gluon fields when the fermionic degrees of freedom are all integrated out. Though the effective action becomes non-local and very complicated in the presence of the fermion determinant, a considerable effort has been made to extract results from QCD in the presence of quark degrees of freedom.

##### 4.1 Fermion Determinant

For a general presentation, I will consider now the Euclidean action

$$S = S_0(U) + \sum_{ij} \bar{\psi}_i M_{ij}(U) \psi_j \quad (4.1)$$

in four dimension. It describes the interaction of the gluon field  $U$  with the quark field  $\psi_i$ , and the subscripts on the fields refer to the lattice points. Spin and internal symmetry indices are suppressed, for simplicity. The matrix  $M_{ij}(U)$  designates both the kinetic and mass terms for the quark field, and coupling to the gluon field.  $S_0(U)$  describes the pure gluon part of the Euclidean action.

It is interesting to note that most of the important models in quantum field theory, condensed matter physics and nuclear physics can be brought to a bilinear form in the fermion fields.

The fermion Green's functions can be calculated by inserting sources into the path integral

$$Z(\bar{\eta} \eta) = \int D\bar{\psi} D\psi DU \exp \left[ -S + \sum_i (\bar{\eta}_i \psi_i + \bar{\psi}_i \eta_i) \right]. \quad (4.2)$$

By taking the functional derivatives and integrating out the Grassman variables of the fermions, the quark correlation function can be written as

$$\begin{aligned} \langle \bar{\psi}_i \psi_j \rangle &= \frac{\delta^2}{\delta \eta_i \delta \bar{\eta}_j} \ln Z(\bar{\eta} \eta) \Big|_{\eta = \bar{\eta} = 0} \\ &= \frac{1}{Z} \int DU M_{ij}^{-1}(U) \exp[-S_{\text{eff}}(U)] , \end{aligned} \quad (4.3)$$

where  $Z$  is the partition function of the quark-gluon system. The effective action is given by

$$\exp[-S_{\text{eff}}(U)] = \det[M(U)] \exp[-S_0(U)] . \quad (4.4)$$

The fermion determinant with Wilson fermions is always positive definite.

We apply now the Metropolis Monte Carlo method to the evaluation of the functional integral in Eq. (4.3). A local change  $U \rightarrow U + \delta U$  in the gauge field implies<sup>32</sup>

$$\begin{aligned} \frac{\exp[-S_{\text{eff}}(U + \delta U)]}{\exp[-S_{\text{eff}}(U)]} &= \det[1 + M^{-1}(U) \delta M(U)] \cdot \\ &\cdot \frac{\exp[-S_0(U + \delta U)]}{\exp[-S_0(U)]} . \end{aligned} \quad (4.5)$$

With local quark-gluon coupling the non-trivial change  $\delta M$  in the fermion matrix is restricted to the neighborhood of the updated lattice link. Consequently, we need only a few inverse elements of the large matrix  $M$  in each updating step of the Metropolis procedure. Since the results of a Monte Carlo calculation are always subject to some statistical inaccuracy, it is reasonable to evaluate the inverse matrix elements stochastically.<sup>33, 34</sup>

## 4.2 Chiral Symmetry Breaking

Recently, some challenging results were reported concerning chiral symmetry breaking and the spectrum of light hadrons. In the quenched approximation<sup>35, 36</sup> the fermion determinant ( $\det M$ ) is set

to one in the Monte Carlo calculation. The hope is that quark vacuum polarization will not play an important role in the mechanism of chiral symmetry breaking, or in light hadron spectroscopy.

The observation of spontaneous chiral symmetry breaking was reported in the Monte Carlo evaluation of  $\langle \bar{\psi} \psi \rangle$  in the absence of quark vacuum polarization loops. Later quark loops were added to the calculation<sup>37</sup> using the pseudo-fermion method<sup>33</sup> for the evaluation of the quark determinant.

The difficulty with spontaneous chiral symmetry breaking is twofold. First, there is no satisfactory way of putting fermions on the lattice and maintaining the chiral symmetry of the Lagrangian. This problem is partially cured by the introduction of staggered fermions on the lattice. Second, even if we had satisfactory lattice fermions, the limit of vanishing quark mass has to be taken to demonstrate spontaneous chiral symmetry breaking. With present Monte Carlo techniques one has to do the calculation for finite fermion mass and extrapolate to the zero quark mass limit empirically.

The restoration of chiral symmetry at finite temperature was studied recently by the Urbana group<sup>38</sup> in the quenched approximation. At zero temperature they confirm the appearance of spontaneous chiral symmetry breaking using staggered fermions in the calculation. As the system is heated a critical temperature  $T_{\text{chiral}}$  is found where chiral symmetry gets restored. Fig. 12 shows their Monte Carlo results.

The thermal Wilson loop  $W_t$  and  $\bar{\psi} \psi$  are plotted on the same figure as a function of  $\beta$ . For their fixed lattice size  $8^3.4$  the variation of the coupling constant corresponds to the variation of the temperature: The length of 4 of the thermal direction is fixed in lattice spacing units but the cut-off  $a$  varies in physical units as we vary the bare coupling constant. Fig. 12 demonstrates that the phase transition of thermal quark liberation and restoration of chiral symmetry take place at the same critical temperature within the error bars of the Monte Carlo calculation.

Some results were also reported on the restoration of chiral symmetry as a function of quark density<sup>39</sup> in the absence of quark vacuum polarization effects.

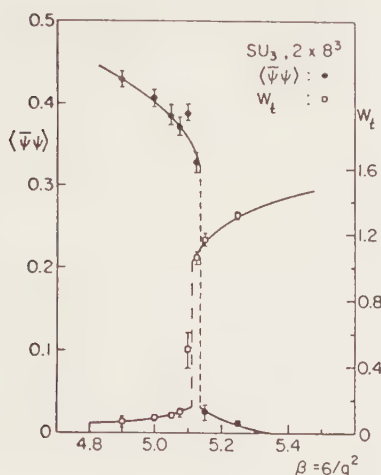


Fig. 12

### 4.3 Hadron Spectrum without Internal Quark Loops

At the beginning of this game optimists and sceptics were worlds apart. Very good results were reported for the light hadron spectrum in the quenched approximation.<sup>35</sup> The lattice size was small ( $6^3 10$ ) and  $\beta = 6$  was chosen, where the continuum approximation should be reasonable. Equally good results were reported at  $\beta = 5.7$  on the same size lattice.<sup>36</sup> Since the results were so good, the optimists thought that the only remaining little step was to show that bringing in the internal quark loops would not change the results.

Unfortunately, the results changed without bringing in quark loops at all. The small lattice and  $\beta = 6$  brings the gluon system close to the boiling point of the confinement phase and the hadron masses fluctuate wildly as a function of Monte Carlo sweeps through the lattice. Due to those thermal fluctuations results on hadron masses would fluctuate accordingly, within a factor of two or more depending on where you stopped the Monte Carlo run. This is clearly seen in Fig. 13 of some recent work<sup>40</sup> where a large lattice of size  $10^3 20$  was used.



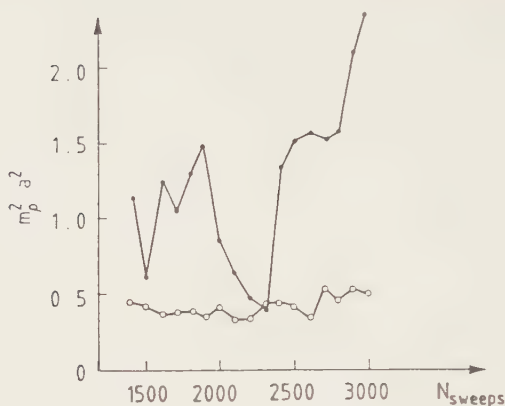


Fig. 13

Doubling the lattice size (approximately) in every direction is a great technical improvement. The new  $\rho$  meson mass now appears to be stable while the old one on the small lattice wildly fluctuates as a function of Monte Carlo sweeps. The mean value of the old mass calculation differs from the new one by about a factor of two.

Good agreement of the quenched approximation with observed hadron masses is still claimed, since a new conversion factor between the lattice scale parameter and the string tension was measured on the big lattice<sup>16</sup> as reported before in Eq. (3.13). The previous calculation on the small lattice<sup>35</sup> used a conversion factor in agreement with the value in Eq. (3.11). If the new string tension measurements turn out to be the accurate ones, we still have a problem. The lattice spacing  $a$  for the same coupling  $\beta = 6$  would be about 0.1 fermi, about half of the previous value. Though the lattice size was substantially increased, 10 links only add up to 1 fermi, a disturbingly small value again.

I should point out that the calculation<sup>36</sup> with  $\beta = 5.7$  is probably free of the above problem, since the gluon system is far from its boiling point at stronger coupling. However, the scaling properties of this calculation remain to be investigated. The coupling seems to me dangerously strong.

I should also mention that another interesting way of calculating hadron masses in lattice QCD has been developed by Hasenfratz



et al.<sup>41</sup> The hopping parameter expansion of the quark propagator is combined there with careful Padé analysis to extract the poles of hadron correlation functions at the location of hadron masses. The latest results of this analysis for meson masses was reported very recently<sup>42</sup> on a large lattice of  $16^4$ .

#### 4.4 Quark Vacuum Polarization

The first results on quark vacuum polarization effects just begin to appear.<sup>37, 43-46</sup> The most interesting to me is a recent calculation of quark vacuum polarization effects in the phase transition of thermal quark liberation.<sup>45</sup> It is reported that heavy quarks seem to smear out the first order phase transition. It is argued on the basis of Monte Carlo calculations that vacuum polarization quarks as heavy as 1 GeV may wash out the phase transition completely. Similar conclusions were reached in a paper<sup>46</sup> submitted to this conference.

#### ACKNOWLEDGMENTS

This work was supported in part through funds provided by the U.S. Department of Energy under Grant No. DE-AT03-81ER-40029. I wish to acknowledge the kind hospitality of the Institute for Theoretical Physics at Santa Barbara where a large part of this talk was prepared and supported by funds provided by the National Science Foundation under Grant No. PHY77-27084.

## REFERENCES

1. G. P. Lepage.
2. D. J. Gross and F. Wilczek, *Phys. Rev. Lett.* 30, 1343 (1973);  
H. D. Politzer, *Phys. Rev. Lett.* 30, 1346 (1973).
3. A. Hasenfratz and P. Hasenfratz, *Phys. Lett.* 93B, 165 (1980);  
R. Dashen and D. Gross, *Phys. Rev.* D23, 2340 (1980).
4. W. Celmaster and R. J. Gonsalves, *Phys. Rev.* D20, 1420 (1979).
5. J. Ellis.
6. E. Fiorini.
7. M. Creutz and B. Freedman, BNL 28588 preprint (1980).
8. K. G. Wilson, *Phys. Rev.* D10, 2445 (1974).
9. K. G. Wilson, Cargese lectures (1979).
10. M. Creutz, *Phys. Rev.* D21, 2308 (1980).
11. M. Creutz, L. Jacobs, and C. Rebbi, *Phys. Rev. Lett.* 42, 1390 (1979).
12. M. Creutz, *Phys. Rev. Lett.* 45, 313 (1981); E. Pietarinen, *Nucl. Phys.* B190, 349 (1981).
13. T. Tomboulis, Princeton preprint (1983).
14. R. W. B. Ardill, M. Creutz, and K. J. M. Moriarty, *Phys. Rev.* D27, 1956 (1983).
15. J. D. Stack, Santa Barbara preprint (1983).
16. G. Parisi, R. Petronzio, and F. Rapuano, CERN-TN 3596 preprint (1983).
17. M. Fukugita, T. Kaneko, and A. Ukawa.

18. F. Gutbrod, P. Hasenfratz, Z. Kunszt, and I. Montvay, CERN-TH 3591 preprint (1983).
19. A. M. Polyakov, Phys. Lett. 72B, 477 (1978); L. Susskind, Phys. Rev. D20, 2610 (1979).
20. L. D. McLerran and B. Svetitsky, Phys. Lett. 98B, 195 (1981); J. Kuti, J. Polonyi, and K. Szlachanyi, Phys. Lett. 98B, 199 (1981); K. Kajanti, C. Montonen, and E. Pietarinen, Z. Physik C9, 253 (1981); J. Engels, F. Karsch, I. Montvay, and H. Satz, Phys. Lett. 101B, 89 (1981).
21. I. Montvay and E. Pietarinen, Phys. Lett. 115B, 151 (1982).
22. T. Celik, J. Engels, and H. Satz, BI-TP83/04 preprint (1983).
23. J. Kogut et al., ILL-(TH)-83-9 preprint (1983); T. Celik, J. Engels, and H. Satz, BI-TP83/07 preprint (1983); B. Svetitsky and F. Fucito, Paper C-235 submitted to this conference.
24. T. Banks and A. Ukawa, Stanford preprint (1983).
25. B. Berg, Phys. Lett. 97B, 401 (1980); G. Bahnot and C. Rebbi, Nucl. Phys. B180[FS2], 469 (1980).
26. K. G. Wilson, Abingdon meeting (1981).
27. For the latest results and earlier references, see, K. Ishikawa, A. Sato, G. Schierholz, and M. Teper.
28. K. Symanzik, DESY83-016 and 83-026 preprints (1983).
29. B. Berg, S. Meyer, I. Montvay, and K. Symanzik, Phys. Lett. to be published.
30. B. Berg, A. Billoire, S. Meyer, and C. Panagiotakopoulos, DESY preprint (1983).
31. C. Kawabata and K. Binder, Solid State Comm. 22, 705 (1977).
32. D. J. Scalapino and R. L. Sugar, Phys. Rev. Lett. 46, 519 (1981).

33. F. Fucito et al., Nucl. Phys. 180[FS2], 369 (1981).
34. J. Kuti, Phys. Rev. Lett. 49, 183 (1982).
35. H. Hamber and G. Parisi, Phys. Rev. Lett. 47, 1792 (1981); E. Marinari, G. Parisi, and C. Rebbi, Phys. Rev. Lett. 47, 1795 (1981).
36. D. Weingarten, Phys. Lett. 109B, 57 (1982); Nucl. Phys. B215[FS7], 1 (1983).
37. H. Hamber, E. Marinari, G. Parisi, and C. Rebbi, BNL 32456 preprint (1983).
38. J. Kogut et al., Urbana preprint (1983).
39. J. Kogut et al., ILL-(TH)-82-39 preprint (1983).
40. H. Lipps, G. Martinelli, R. Petronzio, and F. Rapuano, Phys. Lett. 126B, 250 (1983).
41. A. Hasenfratz et al., Phys. Lett. 110B, 289 (1982).
42. P. Hasenfratz and I. Montvay, DESY83-072 preprint (1983).
43. J. Kuti and J. Polonyi, Proceedings of the Florence Workshop, 15 (1982).
44. C. B. Lang and H. Nicolai, Nucl. Phys. B200, 135 (1982).
45. P. Hasenfratz, F. Karsch, and I. O. Stamatescu, CERN TH. 3636 preprint (1983).
46. T. A. DeGrand and C. E. DeTar.

## GLUONIC EXCITATIONS IN HADRON SPECTROSCOPY

Frank E CLOSE

Rutherford Appleton Laboratory, Chilton, Didcot, Oxfordshire OX11 0QX  
England

### 1. INTRODUCTION

Quarks possess colour charge and these charges appear to be the source of the forces that cluster quarks together to form the bound states that we collectively call "hadrons". The hypothesised similarity in the behaviour of colour and electrical charge is well known, as is the consequent similarity between QCD - the relativistic quantum field theory of colour - and its electromagnetic counterpart QED. Indeed we have already seen at this conference how QCD is now being applied to nuclear problems, not merely single hadrons.

The more deeply we study the mathematics of QCD the richer and more profound it appears. Although it is very similar to QED at the perturbative level, in the non-perturbative regime of confinement it is utterly different and only hazily understood. The analogy between hadronic (QCD) and atomic spectroscopy (QED) and the current conundrums are nicely highlighted by Gottfried<sup>1</sup> "Hadrons, hadronic spectroscopy, and the quark model of hadrons, all came before we had a viable theory of the strong interaction. While we believe that the Yang-Mills equations of QCD are the analogues of Maxwell's equations, we do not yet know how to extract the equivalents of the Coulomb and Biot-Savart laws from this field theory, though we are on the verge of attaining a precise semi-empirical knowledge of these interactions from the data. And there is as yet no clear-cut spectroscopic evidence for gluonic excitations --as if we were puzzling over atomic spectra without direct evidence for photons".

The existence of gluonic excitations<sup>2</sup> - "glueballs" - and hybrid excitations of gluons and quarks - "hermaphrodites or meiktons"<sup>4-7</sup> is a necessary consequence of QCD. I shall concentrate on this important area in this talk as there has been a sudden rush of papers during the last year. For the current status of conventional quark spectroscopy and what we are learning about QCD see Gottfried's excellent review<sup>1</sup>; if your colleagues merely want to know the general basics of quarks see reference 8.

Models which give successful descriptions of quark spectroscopy and incorporate QCD are natural tools to exploit in seeking expectations for gluonic spectroscopy. Lattice QCD and bag models appear to establish the important fact that gluonium states are immersed in a swamp of conventional mesons. In the absence of detailed theory do we have hope of isolating and identifying gluonic candidates? I believe the answer is yes modulo three working hypotheses.

1 States that are prominent in gluonic processes (such as  $\psi$  decays) and are absent or hardly visible in conventional hadronic data are *prima facie* candidates.

Conventional hadronic experiments involve beams of quarks and targets of quarks, so dominantly quark clusters are produced. To produce glue we first destroy the quarks, the ensuing colour radiation - gluons - can then form gluonic clusters. Such a case is  $\psi \rightarrow \gamma + \mathbb{X}$ . In QCD perturbation theory this process is triggered by  $\psi \rightarrow \gamma +$  two gluons. This predicts that 1 in 7 decays of the  $\psi$  should be of this form, and indeed they are. The qualitative suspicion that glue is around is quantitatively validated so if the state  $\mathbb{X}$  resonates, and has not been seen in quark experiments, the onus is on people to say why it is not a gluonic candidate.

The models so far have discussed gluonium<sup>9</sup>, having the constituents GG, GGG etc ... and hybrids with constituents  $q\bar{q}G$  as well as familiar  $q\bar{q}$ ,  $qq\bar{q}\bar{q}$  etc. The distinction between these tends to disappear once interactions are included. So one can shuffle one's feet and argue that mesons contain gluonic components in their wavefunction but also have  $q\bar{q}$  and so are not pure glueballs. The whole picture then gets very murky: "is this state or that dominantly glue; which one is dominantly  $q\bar{q}$ " etc. In the present state of affairs this is hardly the right attitude. Let me make hypothesis 2.

2 If, as time and data progress, more and more hitherto unobserved states of low spin (in particular  $0^{-+}$ ) emerge in  $\psi$  (or  $\tau$ ) decays, quark degrees of freedom will be insufficient to explain the abundance.

Recent reports on new structures in  $\psi \rightarrow \gamma\chi$  have not yet forced us into this position, but we are getting uncomfortably near to it. Gluonic degrees of freedom may be manifested in the totality of states even though ideal gluonium may be absent or unidentified. A survey of states in  $\psi \rightarrow \gamma\chi$  which were not clearly seen in hadronic data include the following channels  $\chi$ : 1,9,10,11,12

a)  $K\bar{K}\pi$  1(1440) is clearly seen with a width of 50 to 100 MeV. It is probably  $0^{-+}$ . It is the favourite candidate<sup>9,13</sup>.

b)  $\eta\pi\pi$   $\iota(1440)$  is not seen here. Crystal Ball <sup>12</sup> report a broad enhancement  $1770 \pm 45$  with  $\Gamma = 520 \pm 110$ , probably containing more than one resonance. Mark III also see this structure <sup>11</sup>.

c)  $\delta\pi$  ( $\eta\pi\pi$ ) Mark III see an enhancement below 1400 that is not the  $\iota(1440)$ . It can be fitted with two Breit Wigners; one  $m = 1280$ ,  $\Gamma = 26$  MeV tantalisingly similar <sup>14</sup> to the  $\zeta(1275)$ . The partner is  $m = 1380$ ,  $\Gamma = 27 \pm 18$ . These widths are comparable to  $\iota(1440)$ . There is a catch 22: the  $\iota$  is not seen in  $\delta\pi(\eta\pi\pi)$ , yet its  $0^{-+}$  assignment supposed that  $KK\pi$  is dominantly  $\delta\pi$ .

d)  $\gamma\rho$  Mark III and Crystal Ball both see a 1270 structure (this could be  $f(1270)$  if  $\Gamma(f \rightarrow \gamma\rho) \approx 1$  MeV) and a state whose mass is consistent with  $\iota(1440)$  or the 1380 state in  $\delta\pi$ . However both groups find large widths, order 150 MeV, so this is not  $\iota(1440)$ . If better statistics confirm these structures then one may be forced into accepting several states in the 1300-1450 mass range. This total structure has a radiative width of order 1 MeV but it could consist of several states with rather smaller individual radiative widths. It is important to establish what is going on here as pure gluonia cannot couple directly to photons, quark contamination is required (models that give quantitative estimates for gluonia radiative widths uniformly incorporate  $q\bar{q}$  mixing).

e)  $KK$  The  $\theta(1700)$ ,  $\Gamma(100 - 150$  MeV) is now well established even though its constituency remains controversial. The startling new result comes from Mark III who find <sup>10</sup> also a very narrow state  $\xi(2217)$ ,  $\Gamma = 28 \pm 15$  MeV. Decays into  $K^+K^-$  and  $K_S^0 K_S^0$  are seen so the allowed quantum numbers are  $0^{++}, 2^{++}$  etc. This state is so far above  $K^+K^-$  threshold that its stability is astonishing. It is difficult to believe that  $d\bar{d}$ ,  $u\bar{u}$  or  $s\bar{s}$  quarks are significant in its Fock State and it is surely something new.

f)  $\phi\phi$  Nothing is seen in  $\psi \rightarrow \gamma X$  (other than  $\eta_c(2980)$ ) but three broad states are claimed <sup>15</sup> in  $\pi N \rightarrow \phi\phi N$ , masses 2.1 to 2.4 GeV and widths of 200-300 MeV. As this process is *prima facie* mediated by glue there have been claims that these are gluonia.

So there are plenty of candidates (and there are others claimed in hadronic experiments <sup>16</sup>). Can we bring further order into the game?

Hypothesis 3. Very Broad States couple strongly to quarks and so cannot be ideal gluonium.

They may well have GG in their Fock State but the strength of their coupling to quark matter undermines the possibility of them being "pure glue".

It is possible that all states are mixed - I am thinking of failure of "ideal" mixing, where "ideal" now is generalised to mean  $\frac{1}{\sqrt{2}}(u\bar{u} + d\bar{d})$ ;  $S\bar{S}$ ;  $Q\bar{Q}$ ; GG .... If so life will be tough and hypothesis 2 will be our fall back



position. But there are examples of near ideal mixing in  $q\bar{q}$  space, might we not hope for some kindness in nature for GG too? Could  $\xi(2200)$  be this gift?

## 2. MODELS OF GLUONIC STATES

### 2.1) Glueballs : Lattice QCD with no fermions

At the Brighton Conference Teper<sup>17</sup> reported the following states below 2 GeV, masses in MeV.

$0^{++}$	$750 \pm 50$
$0^{-+}$	$1400 \pm 200$
$2^{++}$	$1600 \pm 100$
$1^{-+}$	$1700 \pm 200$

all of which have  $\pm 20\%$  systematic errors to be added due to the uncertain string tension. These results are qualitatively and even quantitatively, similar to those of bag models when  $O(\alpha)$  energy dependent forces are included.

### 2.2 Bag Models of Glueballs and Hybrids

The idea is that inside a finite sphere of radius  $R$  QCD perturbation theory can be applied to confined quarks and gluons. Confining these fields forces them into discrete eigenstates<sup>2,3</sup> which for the vector gluons are essentially the familiar TE and TM eigenmodes of classical electrodynamics in cavities.

The lowest modes are,

TE <sub>1</sub>	: $1^{+-}$	$\omega = 2.7/R \approx 460 \text{ MeV}$
TE <sub>2</sub>	: $2^{--}$	$\omega = 4.0/R \approx 680 \text{ MeV}$
TM <sub>1</sub>	: $1^{--}$	$\omega = 4.5/R \approx 750 \text{ MeV}$

where the explicit energies correspond to a typical bag radius of  $R \approx 1.2 \text{ fm}$ .

The lowest mass colour singlets are formed from two gluons

$$\begin{aligned} \{TE\} &= 0^{++}, 2^{++} \\ \{TE\}, \{TM\} &= 0^{-+}, 2^{-+} \end{aligned}$$

Note that there is no light oddball  $1^{-+}$ , nor a  $1^{++}$ . Some authors make models where the gluon is treated as a massive vector particle with three degrees of freedom. They obtain  $1^{-+}$  and  $1^{++}$  but this seems to be a further model assumption beyond the QCD Lagrangian.

To put this on a firmer footing one can form gauge invariant combinations

of  $G_{\mu\nu}$  which act as interpolating fields between the vacuum and physical states.

$$\langle j^P \mid G_{\mu\nu} G_{\alpha\beta} \mid 0 \rangle$$

one finds<sup>2</sup> that  $J^{PC} = 0^{\pm}, 2^{\pm}$  but not  $1^{\pm}$  exist. To form  $1^{\pm}$  requires  $G_{\mu\nu} G_{\alpha\beta} G_{\zeta\sigma}$ . (at least three gluons in bag models).

In the early bag papers<sup>2</sup> two non-interacting gluons were considered. The  $0^{++}$  and  $2^{++}$  were degenerate at 0.96 GeV; the  $0^{-+}$  and  $2^{-+}$  degenerate at 1.3 GeV. These papers made an important contribution, gave us our first orientations into possible gluonia spectrum and stimulated a lot of people. This early work led to a richer literature and their initial estimates have been superceded. In particular, we know that there are important spin dependent forces that split N and  $\Delta$  quark states and it is to be expected that gluon systems are also split.

During 1979-81 the technology for perturbative QCD in a cavity was developed<sup>18-20</sup> (tree level only; no loops). If  $\alpha_s$  is  $\geq 0.5$  the  $0^{-+}$  falls below the  $2^{++}$ . The unknown energy shifts due to loops can raise or lower the overall mass scale. This is the major source of any apparent differences among the papers in the literature.

All groups<sup>3,7,18</sup> are now agreed on the tree level technology. (CHP<sup>18</sup> have gone further by including Coulomb interactions and part of the Coulomb contributions to the self energy). The phenomenological differences are that ref<sup>3</sup> implicitly assumed that the self-energies of TE and TM are the same. The later work of refs<sup>7,18</sup> relaxed this constraint. CS<sup>7</sup> assume that  $\psi(1440)$  is  $0^{-+}$  gluonic meson to fix the sum of TE and TM and let their ratio vary between  $\frac{1}{2}$  and 2.

Today the possibility arises that even the loops may be within reach. Two independent groups<sup>19</sup> have computed the self energy for a confined massless s-wave quark and agree that is some hundreds of MeV. When the analogous results for gluons are known, or at least the (TE) - (TM) differences, then much of the present uncertainty will disappear.

If the (TE) - (TM) self energies are not too different from one another, the pattern of states in bag and lattice<sup>17</sup> are very similar. Everyone seems to agree that  $0^{++}$  lies lowest ( $1.0 \pm 0.2$  GeV typically in the bag, 750 MeV  $\pm$  ? in the lattice). The  $0^{-+}$  lies higher with  $2^{++}$  higher still. Various authors in desperation have suggested that  $S^*(980)$  may have significant gluonic content.<sup>3,16</sup> Indeed the CERN axial field spectrometer group<sup>14</sup> find evidence for central  $S^*$  production in  $pp \rightarrow pp + X$  - a process where the  $X$  may be expected to be produced by gluons. Yet there is no evidence

for  $S^*$  in  $\psi \rightarrow \gamma\chi$ , the "canonical" glue factory.

A 1 GeV  $0^{++}$  may be a problem if you believe that  $\psi \rightarrow \gamma\chi$  is a glue meson factory. One way out in bag models is to exploit the unknown  $^{TE}/^{TM}$  self energy ratio. CS fix the sum to fit  $\chi(1440)$ . We could pump up the TE at the expense of TM and so push the  $(^{TE})^2 0^{++}$  up (but go too far and the  $(^{TM})^2 0^{++}$  passes it coming down). The extreme is where two  $0^{++}$  occur at about 1700 MeV, in which case there are two  $2^{++}$  in the 2.2 - 2.4 GeV region. These latter would mix with the radial  $3^3P_2(q\bar{q})$  states which should also be in this region and may help explain the  $\phi\phi$  data reported by Lindenbaum<sup>15</sup>.

But this seems rather ugly. Everyone but the experimentalists seems to want a light  $0^{++}$  glueball. Jaffe and Pennington<sup>20</sup> have made an interesting observation. If the  $0^{++}$  is around 600-700 MeV in mass, and has a width less than 5 MeV then it would have escaped detection in  $\pi\pi$  phase shifts.

Moreover on a rising background it would generate a sudden dip rather than a spike. It is important to reexamine the  $\pi N \rightarrow \pi\pi N$ ;  $\psi \rightarrow \gamma\pi\pi$   $T'' \rightarrow T\pi\pi$ , and at LEAR to study  $\bar{p}p \rightarrow \pi\pi X$  with as fine a resolution as possible. The importance of establishing or refuting a light  $0^{++}$  glueball cannot be overstressed. And the  $\phi$  width is only 4 MeV, so it is not at all unreasonable that  $0^{++}$  glueball could be order 5 MeV. We may simply be missing it for lack of resolve.

### 3. HYBRID MESONS IN BAG MODELS

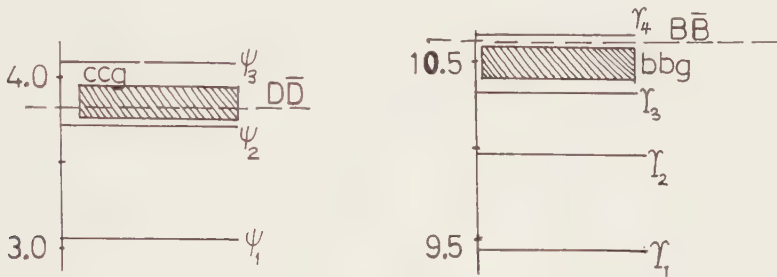
During the last twelve months there has been a sudden growth in the literature on hybrid hadrons<sup>4-7,21-29</sup> - overall colour singlets where the quarks form a colour octet; the gluonic fields are also in an octet representation<sup>4,5</sup> and can be dynamically excited. In a bag model the simplest example consist of  $q\bar{q}$  and a (TE) gluon:

$$(q\bar{q})_8 \quad x(G)_8 \quad \longrightarrow \quad \left\{ \begin{array}{c} 2^{--} \\ 1^{--} \\ 0^{--} \end{array} \right. ; \quad 1^{--}$$

Note the presence of the exotic  $J^{PC} = 1^{--}$  here:<sup>5-7</sup> this arises because the vector combination of  $q\bar{q}$  can be in any of three helicity states (contrast the restriction to two for gluons and hence the absence of  $1^{--} GG$ ). The phenomenological importance of hybrids is that a flavour nonet of  $1^{--}$  states would be a clear signature; gluonia nor  $q\bar{q}$  would fit. As we shall see there are some other distinctive properties of  $q\bar{q}G$  that may aid their identification.

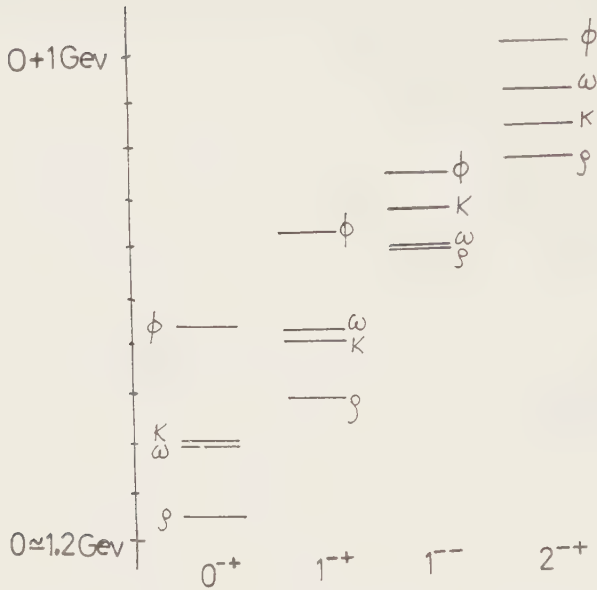
Although the new literature has been concerned with  $q=u,d,s$  (where the

confined perturbation theory techniques are applicable) the first papers<sup>5</sup> dealt with heavy quarks. As nice data are now emerging on T spectroscopy it is opportune to review the  $c\bar{c}G$  and  $b\bar{b}G$ . Hasenfratz et al.<sup>5</sup> noted that an exotic  $1^{--}$  would occur but did not discuss spin dependent splittings. The system's radius decreases with increasing quark mass, so the energy of a confined gluon in  $b\bar{b}G$  (ie  $m(b\bar{b}G)-m(b\bar{b})$ ) is greater than in  $c\bar{c}G$ . But the distances to the heavy flavour production threshold is also greater in  $b\bar{b}$  than  $c\bar{c}$ . The result is that for heavy enough flavours  $Q\bar{Q}G$  is below the heavy flavour continuum. This is illustrated in fig 1.



Detailed studies of the spin dependent energy shifts in  $Q\bar{Q}G$  have not yet been made. It is important to know whether these are expected below threshold; if so whether they can be detected in radiative transitions among  $b\bar{b}$  states.

For light quarks the detailed calculations of such energy shifts have been performed. Two independent groups<sup>6,7</sup> are agreed on the results, the only remaining question is the magnitude of the gluon self energy and hence the overall mass scale. Thus the splitting pattern is settled though the precise masses are still unknown. The calculations of  $O(\alpha_s)$  splittings were done in Coulomb gauge. There is an important effect due to  $q\bar{q}$  annihilation and instantaneously (Coulomb) reappearance. This shifts  $I=0$  states up by about 100 MeV relative to their  $I=1$ , counterparts. This arises because  $q\bar{q} \in g^C$  and is absent for conventional  $(q\bar{q})$  mesons. The " $\omega g$ " is nearly degenerate with " $K g$ ", not with " $\rho g$ " (see fig 2).



This is a pattern which should be clearly noticeable in the spectrum (unless nature has been so unkind as to make it invisible by complicated mixing effects - even so we hope that some remnant of it will show through).

Indeed, this pattern is already well known in the  $0^{-+}$ :  $\pi$ ;  $\eta \approx K$ ;  $\eta'$ . Maciel-Monaghan<sup>21</sup> and also Donoghue and Haqq<sup>22</sup> have effectively mixed the  $0^{-+}$  ( $q\bar{q}$ ) with  $q\bar{q}g$  and qualitatively<sup>21</sup>, or even quantitatively<sup>22</sup>, described the  $\eta$   $\eta'$  masses as a result. Vector mesons receive no contribution from this Coulomb annihilation effect and, (empirically!) are ideally mixed.

If confined perturbation theory is any guide, magnetic (TE) gluon modes are physical but electric (TM) tend to be dominated by nonphysical Coulomb  $q\bar{q}$  annihilation/creation. Some of our OZ1, ideal mixing and glueball production folklore might need to be revaluated.

In particular the folklore that " $\psi \rightarrow \gamma X$  is a good glueball factory" might not be true for negative parity  $X$ . The negative parity state is

$$X \neq G_M G_E ; X = G_M(q\bar{q})$$

ie negative parity hybrid states may be produced in  $\psi \rightarrow \gamma X$ . Note that the lightest hybrids (in bag models) are  $0^{-+}$  not  $0^{++}$ , in contrast to glueballs. So here we have another compelling reason to determine whether we have missed

finding light  $0^{++}$  ( $2^{++}$ ) glueballs in data.

If the TE and TM gluon self energies are similar then the  $0^{--}$   $q\bar{q}G$  nonet masses will be  $\pi(1300)$ ,  $K(1400)$ ,  $\eta(1400)$  and  $\eta^{\prime}(1700)$ , these show a tantalising similarity to states in the particle data tables. The  $\eta(1400)$  should be produced in  $\psi \rightarrow \gamma X$ . Before identifying it with  $\iota(1400)$  we should remember that the TE/TM self energies have been chosen such that  $\iota(1400)$  is identified as  $0^{--}$  glueball<sup>7</sup>. The  $\iota$  and  $q\bar{q}G$  may mix: the  $q\bar{q}G$  state will decay to  $\gamma V$  ( $V = \rho, \omega$ )<sup>26</sup> something that GG will not do. (Claims that GG can have substantial radiative decays seem to exploit the large phase space available. However form factors will more than compensate for the large phase space. And intuitively, it is all wrong to claim that flavourless states couple to photons strongly: the largest radiative decay width involving quarks is  $\omega \rightarrow \pi\gamma$  - surely one cannot exceed that.) Thus it would be interesting to seek a radiative decay  $\psi \rightarrow \gamma X$  :  $X \rightarrow \gamma\gamma$  where  $X$  is near to, but distinct from, the  $\iota(1440)$ . A  $\gamma\rho$  signal has been seen around 1.4 GeV. If this is a hybrid  $\omega G$  state, then a  $\phi G$  will yield  $\gamma\phi$  around 1.7 GeV. Even if there is  $\omega G$ - $\phi G$  mixing we expect two masses for the radiative signals as against one mass for a glueball.

#### 4 HYBRID MESONS : (NON-BAG)

QCD sum rules have been applied to the  $1^{--}$  sector through  $J_{\nu} \equiv \psi \gamma_{\mu} G_{\mu\nu} \psi$ . Balitsky et al.<sup>28</sup> claimed that this yields 1.3 GeV for the lightest  $1^{--}$  hybrid resonance. The Louvain group<sup>28</sup> obtain 1.65 GeV. This is in line with the bag model above (for which the  $0^{--}$  are around 1.4 GeV).

Lattice calculations by the Liverpool group<sup>29</sup> yield a rich hybrid spectroscopy. Their " $E_U$ " states correspond to the lowest bag model states discussed above, and are predicted to lie between 0.5 GeV to 1 GeV above the ground state  $q\bar{q}$  as in the bag model. In particular the light quark  $q\bar{q}G$  should be in the vicinity of  $q\bar{q}$  radials; the  $c\bar{c}G$  and  $b\bar{b}G$  near the second and third radials. This is as in bag models.

The only model that has heavy hybrids is the string model of Isgur-Paton<sup>30</sup>. All gluonic hadrons are above 2 GeV (with the possible exception of  $0^{++}$  at about 1.5 GeV).

#### 5 HYBRID BARYONS

Analogous to mesons one forms hybrid baryons,<sup>23-26</sup>

$$(q^3)_8 \otimes (G)_8 \longrightarrow (q^3 G)_1$$

Antisymmetry among the quarks causes a  $\underline{70}$  plet of flavour SU(6) for the ground state hybrids, and in a bag model (where  $G \equiv TE$  with  $J^P = 1^+$ ) this  $\underline{70}$  plet has positive parity, and contains

$${}^4\bar{8} \left( \frac{1}{2}^+, \frac{3}{2}^+, \frac{5}{2}^+ \right); \quad {}^2\bar{8} \left( \frac{1}{2}^+, \frac{3}{2}^+ \right); \quad {}^2\bar{10} \left( \frac{1}{2}^+, \frac{3}{2}^+ \right); \quad {}^2\bar{1} \left( \frac{1}{2}^+, \frac{3}{2}^+ \right)$$

The superscripts denote the  $(2S+1)$  of the quark-content spins. The non-strange spectroscopy, including  $O(\alpha_s)$  energy shifts, has been studied in refs 23/24. There is a tantalising similarity between the model and states in the particle data tables (fig 3 taken from GHK, ref 24). However one can show that this is misleading, in particular the Roper  $P_{11}$  (1470) cannot dominantly be  $q^3G$ . The reason is that there is a selection rule<sup>23</sup> forbidding  $\Upsilon P \rightarrow (q^3G) e^+ \bar{e}^-$  - reminiscent of Moorhouse's old quark model rule<sup>31</sup>. Yet the Roper is photoproduced from both p and n, so it is not  $(q^3G) e^+ \bar{e}^-$ . The mass scale of hybrids must be higher than ref<sup>24</sup> supposed, which suggests that TE self energy is important (omitted in ref 24). A similar problem arises in ref 25 where the  $\Lambda G$  singlet was studied. The  $O(\alpha)$  shifts cause the  $\frac{1}{2}^+$  to be low, near to the lightest non strange NG. The candidate state,  $\Lambda(1600)$ , chosen in ref 25 is surely in  $\bar{8}$ , partnered by  $\Sigma(1660)$  and  $N(1440)$ .

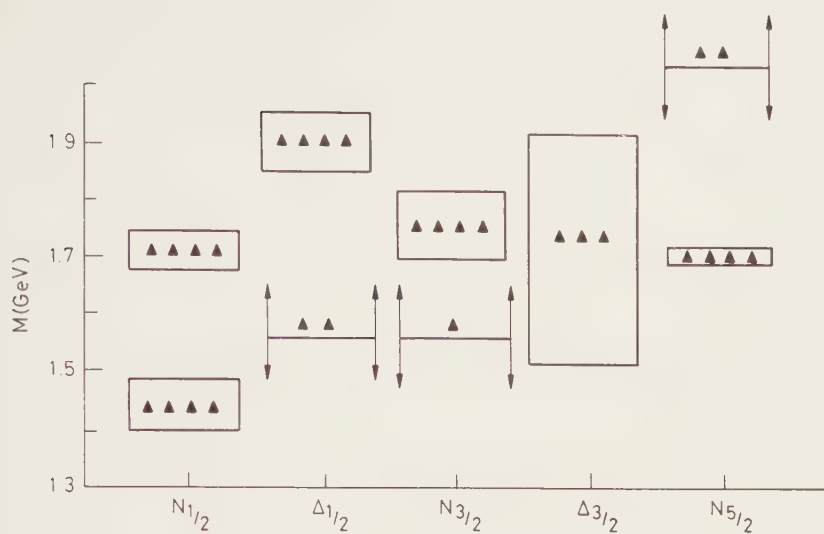
The  $q\bar{q}G$  and  $q^3G$  relative mass scales are independent of TE self energy<sup>23</sup>. The absence of  $0^{++}(q\bar{q}\bar{G})$  low lying places a lower limit on  $q^3G$  such that at most  $\frac{1}{2}^+$  and maybe  $\frac{3}{2}^+ NG$  will be below or near 2GeV.

The radiative decays of the lightest  $q\bar{q}\bar{G}$  do not vanish, in contrast to  $q^3G$ . Thus  $\psi \rightarrow \gamma(q\bar{q}\bar{G}) \rightarrow \gamma(\gamma\pi \text{ or } \gamma V)$  should be looked for.

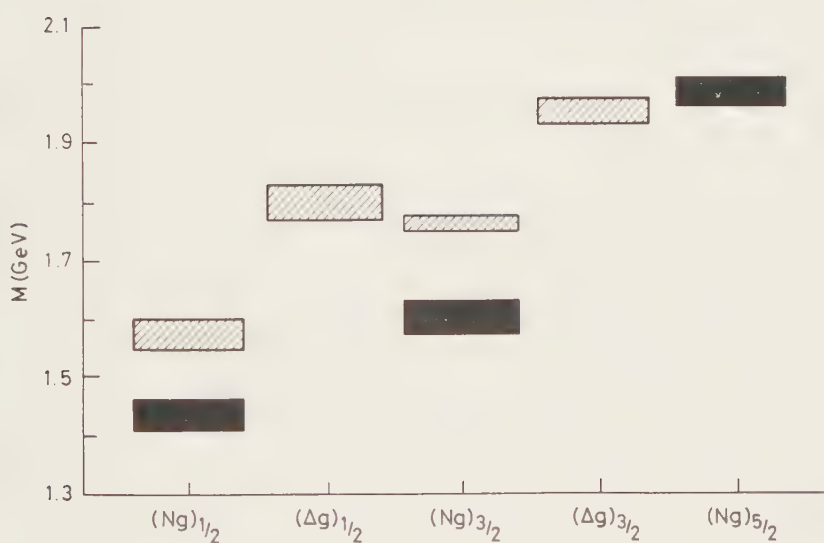
Detailed studies of production and decay channels have been made in ref 6,7. Early studies of  $\pi N$  width and electromagnetic interactions are being made<sup>26-27</sup>. One possible way of isolating  $q^3G$  could be in  $\pi p \rightarrow K^0 \Lambda$ . Quark model states in  ${}^4\bar{8}$  decouple from  $K\Lambda$  so it may be possible that a  $q^3G$ , hidden by  ${}^4\bar{8}$  in  $\pi p \rightarrow \pi p$ , could be revealed in  $\pi p \rightarrow K\Lambda$ . There are some tantalising signals here<sup>32</sup> but one does not necessarily need to invoke  $q^3G$  as the answer.

In twelve months we have seen a lot of work opening up this phenomenology. The first challenge is to make experimentalists aware of it. For theorists, I would like to see more "theory" - lattice studies and QCD sum rules. The bag is a useful guide but is only a model. But if its suggestions can be underwritten by other model/theory then it may need to be taken seriously. Indeed, I am encouraged by the first lattice results<sup>29</sup>, and hope that more study will follow.





(a) Data



(b) Model

## ACKNOWLEDGEMENT

I am indebted to B Zeitnitz and the organizers of Few Body X for their hospitality in Karlsruhe, and to the many participants whose interest and questions helped frame the form of this written version of my talk.

## REFERENCES

1. K Gottfried, Proc. of EPS Internat. Conf. on High Energy Physics Brighton 1983; (J Guy ed.)
2. R Jaffe and K Johnson, Phys. Lett. 60B, 301 (1976)  
J Donoghue, K Johnson, B. Li. Phys. Lett. 99B 416 (1981)
3. T Barnes, F Close, S Monaghan, Phys. Lett. 110B, 159 (1982); Nucl. Phys. B198, 380 (1982)
4. T Barnes, Ph.D. thesis, Caltech 1977; Nucl. Phys. B158, 171 (1979)  
F Close, Proc Kupari Summer School 1980; ed. J Ellis, RL-80-095  
F de Viron and J Weyers, Nucl. Phys. B185, 391 (1981)
5. D Horn and J Mandula, Phys. Rev. D17, 898 (1978)  
P Hasenfratz, R Horgan, J Kuti, J Richard, Phys. Lett. 95B, 299 (1980)
6. T Barnes and F Close, Phys. Lett. 116B, 365 (1982)  
T Barnes, F Close, F de Viron, Nucl. Phys. B224, 241 (1983)
7. M Chanowitz and S Sharpe, Nucl. Phys. B222, 211 (1983)
8. F Close, chapter 7, "The Cosmic Onion", (Heinemann, London 1983)
9. E Bloom, Proc. of XXI Intl. Conf. on HEP, Paris 1982
10. K Einsweiler, in ref 1
11. D Hitlin Proc of International Symposium on Lepton and Photon Interactions at high energies, Cornell Univ. August 1983
12. C Edwards et al., Phys. Rev. Letters 51, 859 (1983)  
K Ishikawa, Phys. Rev. Letters 46, 978 (1981)
13. M Chanowitz, Phys. Rev. Letters 46, 981 (1981)  
M Chanowitz, Proc. SLAC Summer Institute 1981
14. W Stanton et al. Phys. Rev. Letters 42, 346 (1979)
15. S Lindenbaum, in ref 1
16. T Akesson et al. CERN - EP/83 - 108
17. M Teper, in ref 1
18. T de Grand et al., Phys. Rev. D12, 2060 (1975), C Thorn unpublished  
T D Lee, Phys. Rev. D19, 1802 (1979)  
F Close and R Horgan, Nucl. Phys. B164, 413 (1980)

- F Close and S Monaghan, Phys. Rev. D23, 2098 (1981)  
 C Carlson, H Hanson, C Peterson, Phys. Rev. D27, 1556 (1983)
19. J Baacke, Y Igarishi, G Kasperidus, Dortmund D0-TH 82/13  
 H Hanson and P Jaffe, MIT reports in preparation
  20. R Jaffe and M Pennington (in progress)
  21. A Maciel and S Monaghan, Oxford TP25/82 (1982)
  22. J Donoghue and E Haqq, (unpublished)
  23. T Barnes and F Close, Phys. Lett. 123B, 89 (1983)
  24. E Golowich, E Haqq and G Karl, Phys. Rev. D28, 160 (1983)  
 I Duck and E Umland, "Gluonic Nucleons in a Valon Model", Rice University (1983)
  25. C Carlson and H Hanson, MIT Report CTP 1074 (1983)
  26. T Barnes and F Close, Phys. Lett. 128B, 277 (1983)  
 F Wagner, Munich report MPI-PAE/PTH 4/83 (1983)
  27. M Tanimoto, Phys. Lett. 116B, 198 (1982)  
 E Golowich (in progress)
  28. I Balitsky, D Dyakanov, A Yung, Phys. Lett. 112B, 71 (1982)  
 J Govaerts, F de Viron, D Gusbin, J Weyers, Z Phys (1983)
  29. L Griffiths, C Michael, P Rakow, Liverpool Report LTH 106 (1983)
  30. N Isgur and J Paton, Phys. Lett. 124B, 247 (1983)
  31. R Moorhouse, Phys. Rev. Letters 16, 772 (1966)
  32. K Bell et al. Nucl. Phys. B222, 389 (1983)



## CHIRAL SYMMETRY AND THE BAG MODEL

Anthony W. THOMAS

Theoretical Physics Division, CERN  
1211 Geneva 23, Switzerland\*

We give a brief review of the connection between QCD and the more phenomenological, chiral bag models, which have generated so much excitement recently. Some recent results from the cloudy bag model are then presented, together with a discussion of the evidence from deep-inelastic scattering which supports this choice. We close with a few comments on the relevance of these ideas in interpreting the EMC effect.

### 1. INTRODUCTION

There is now an almost universal acceptance that quantum chromodynamics (QCD) is the theory of strong interactions. It is therefore the only truly fundamental starting point from which to develop a consistent theoretical description of nuclear phenomena. Unfortunately it is too difficult to solve the QCD equations except in some limits. At high  $Q^2$  it has been established (using the renormalization group) that QCD is "asymptotically free". That is, if we determine the strength of the quark-gluon coupling,  $\alpha_s(Q_0^2)$ , at some momentum scale  $Q_0^2$ , then  $\alpha_s(Q^2)$  decreases logarithmically as  $Q^2$  increases beyond  $Q_0^2$ . Thus at high  $Q^2$  (or small distances) quarks should behave essentially like free particles. This is the main reason for the success of the naïve quark-parton model for deep inelastic scattering (DIS)<sup>1,2</sup>.

Another limit where it is believed that we know something about QCD is in the infra-red - large separation. There the non-Abelian nature of QCD is supposed to lead to confinement of coloured objects. On a time scale of many years it is possible that brute-force numerical work on a space-time lattice may unambiguously yield the structure of the nucleon implied by QCD. However, even the most ardent lattice advocates do not foresee the day when one could calculate (e.g.) the properties of finite nuclei in this way. For that we need phenomenological models. A great variety of such models exist, ranging from the non-relativistic quark models<sup>3</sup>, through variants of the kind proposed by Shuryak<sup>4</sup>, to the relativistic bag models<sup>5-7</sup>.

Our discussions will concern only the recent generalizations of the MIT bag model, but it should be realized that this is largely a matter of taste. The

---

\*Permanent address from March 1984, Physics Department, University of Adelaide, P.O.Box 498, G.P.O. Adelaide, 5001, South Australia, Australia.

major advantages of the bag model are that it incorporates two key features of QCD, namely confinement and asymptotic freedom in a simple, phenomenological Lagrangian. As with essentially all other phenomenological models proposed by high energy theorists, the radius of the region within which the quarks are confined is of order 1 fm. This brings us to the question of what is meant by short-range nuclear physics. A very natural definition would be that inter-nucleon separation at which it is no longer sufficient to describe nucleon-nucleon scattering in terms of nucleons and pions alone. Within conventional nuclear theory the exchange of the massive  $\omega$  meson leads to a repulsive core at distances of order 0.3 to 0.5 fm. Because of its large mass, the  $\rho$  meson does not contribute much beyond 1 fm. Nevertheless, there is tremendous model dependence in (for example) the calculation of short-range exchange currents because of the interplay between correlations and heavy meson exchange ( $\rho$ ,  $\rho\pi$ ,  $\omega\pi$ , etc.). (These ambiguities are even worse in calculations of electromagnetic processes because of the difficulty of imposing gauge invariance in the presence of *ad hoc* form factors at the meson-nucleon vertices.) Within this framework the no-man's-land of uncontrolled short-distance corrections is typically 0.3 to 1.0 fm.

On the other hand, if one thinks of nucleons as composite bags of quarks with a radius of order 1 fm, it is clear that short-distance physics begins at 2 fm ! Certainly at an inter-nucleon separation of 1 fm nuclear phenomena should deeply involve quark degrees of freedom. Rather than being more complicated than the conventional meson exchange picture, because of the property of asymptotic freedom, there is reason to hope that calculations at the quark level might prove simpler and less ambiguous.

With these long-term aims in mind we now turn to the most recent extensions of the bag model, which have centered on incorporating a third fundamental property of QCD - namely chiral symmetry.

## 2. CHIRAL BAG MODELS

It is firmly established empirically<sup>8</sup> that the masses of the  $u$  and  $d$  quarks are very small (less than about 10 MeV) compared with the typical hadronic energy scale. Thus to a good approximation the strong interactions should preserve chiral symmetry. Simply put, this implies that the equations of motion should be invariant under separate  $SU(2)$  transformations for left- and right-handed particles [i.e., under  $SU(2)_L \times SU(2)_R$ ]. Unfortunately, the MIT bag model necessarily violates this third fundamental property of QCD<sup>9</sup>. The reason, illustrated in Fig. 1, is simply that the very act of confining the quarks mixes the left-handed and right-handed sectors.



FIGURE 1  
Illustration of the intrinsic violation  
of chiral symmetry in the MIT bag model

A possible solution to this problem is suggested by the following general consideration<sup>10</sup>. The Goldstone theorem tells us that if  $SU(2)_L \times SU(2)_R$  is an exact symmetry, either all the particles occurring in nature come with degenerate, negative parity partners or the symmetry must be realized in the Goldstone mode. There are very good reasons for believing that the pion, with its remarkably low mass, is very close to being a Goldstone boson. Unfortunately, one of the mysteries of QCD is that we do not yet understand the dynamical mechanism whereby this collective  $q\bar{q}$  state appears. Certainly the one-gluon exchange is extremely strong in the pion channel - without it the  $\rho$  and  $\omega$  would be degenerate at  $\sim 650$  MeV in the MIT model, and in first order, one-gluon exchange lowers the pion mass to some 280 MeV. Several groups have been led by this to suggest that iterated gluon exchange could be the mechanism for dynamical symmetry breaking<sup>11</sup>. Others have shown that instanton effects can produce a strong attraction in the pion channel<sup>12,13</sup>. Whatever the mechanism for producing the pion, all of the recent extensions of the MIT bag model which restore chiral symmetry, do so (by analogy with the work of Gell-Mann and Levy<sup>14</sup>) by coupling an elementary pion field to the confined quarks<sup>14,15</sup>. Of course, this does not mean that we expect to see pointlike, pseudoscalar objects in deep inelastic lepton-nucleon scattering<sup>16,17</sup>. Instead, we are constructing a phenomenological model meant to be applied at momentum transfers low compared with the internal structure of the pion. There are many examples in physics where the introduction of such collective pairing effects are essential in order to describe observed phenomena.

Whereas these very general arguments tell us that pions are intimately involved in the restoration of chiral symmetry, it is unfortunate that QCD gives little practical guidance in constructing phenomenological models. (For a much more detailed discussion, see Ref. 17.) There is therefore room for quite different phenomenology and hence considerable controversy. In the absence of any higher authority the ultimate test of which model is best must be a comparison with as much experimental data as possible.

Essentially all of the chiral bag model calculations performed so far correspond to one of two main working hypotheses, the little bag model (LBM)<sup>14</sup> or the



cloudy bag model (CBM)<sup>6,15</sup>. In the latter it is *assumed* that hadron sizes are determined by non-perturbative QCD effects which are not significantly altered by pionic corrections. Then it makes sense to calculate pionic corrections as a small perturbation about the MIT bag model solutions. In the former, on the other hand, the pionic effects are supposed to be intimately linked with the process of confinement, compressing the bag to perhaps one tenth the volume of the MIT model. In this way, one would of course revive the conventional nuclear physics picture of essentially pointlike nucleons exchanging heavy mesons.

A second difference between the models, which has recently faded to insignificance<sup>18</sup> was the original insistence in the LBM on excluding the pion from the interior of the bag - a strict two-phase model. In the CBM, this was not the case. The pion was allowed throughout all space for two reasons. Firstly, the theoretical case for a strict two-phase picture is by no means universally accepted, and secondly the exclusion of the pion field destroys one of the major successes of the MIT bag model, namely the quite accurate prediction for the axial charge of the nucleon<sup>19</sup>. In the CBM this correct prediction is preserved in a very simple and natural way<sup>6,15</sup>.

Since the mathematical details of the pion coupling to confined quarks in both models have been described in great detail elsewhere<sup>2,20</sup> we shall not repeat that material here. Instead, in the next section we review a few of the more recent results obtained in the CBM. Only then shall we discuss the recent test of these models using DIS, which strongly supports the CBM.

### 3. RECENT RESULTS IN THE CLOUDY BAG MODEL

A fairly recent summary of results from the CBM can be found in Refs. 6 and 17. It is not unreasonable to say that in every case where pionic corrections have been computed the agreement with experiment is as good as, and usually better than, the original MIT bag model. Of course, the major underlying defect of the bag, namely the spurious centre-of-mass motion, is not solved by adding pionic corrections. Thus for magnetic moments, and particularly for the charge radii, there are corrections at the level of 10% or so, upon whose sign there is no general agreement. It remains to be seen whether a thorough theoretical analysis can lead to a generally acceptable correction procedure, or whether what we really need is a better relativistic model of confinement. For the present, agreement of any bag model calculation at a level better than (5-10)% must be regarded as random. At that level, however, its success is still striking.

Because of the fact that the CBM results have been reviewed elsewhere, we shall only discuss those cases where there has been a significant new development.

### 3.1. The $\Sigma^-$ magnetic moment

This is of particular interest for the chiral bag models because of the so-called Pilkuhn-Eeg effect<sup>21</sup>. That is, the pionic correction for the  $\Sigma^-$  is twice as big as one might naïvely expect, because as well as the process  $\Sigma^- \rightarrow \Sigma^0 \pi^-$ , one has also  $\Sigma^- \rightarrow \Lambda \pi^-$ . In the CBM, using the same bag parameters as the MIT bag model, we find  $\mu(\Sigma^-) = -1.08 \mu_N$ <sup>22</sup>. This answer is quite insensitive to the actual strange quark mass or bag radius<sup>23</sup>. (For comparison the corresponding value without pionic corrections is about  $-0.81 \mu_N$ .) On the other hand the LBM prediction is of the order  $-0.58 \mu_N$ <sup>24</sup>.

Until recently, the experimental situation was unclear, with older atomic physics measurements giving  $-1.41 \pm 0.27 \mu_N$ , and a  $\Sigma^-$  beam measurement giving  $-0.89 \pm 0.14 \mu_N$ . The new generation of  $\Sigma^-$  atom measurements made by the William and Mary group have made an order of magnitude improvement in this. Indeed, the accuracy of the most recent value of  $\mu(\Sigma^-)$ <sup>25</sup>, namely  $-1.09 \pm 0.03 \mu_N$ , is too good for the present theory! Nevertheless, the confirmation of the CBM prediction is very welcome.

### 3.2. The axial form factor of the nucleon

For reasons explained in detail in Ref. 6, in the CBM only the quarks contribute to the axial (as opposed to the induced pseudoscalar) current of the bag. Thus, unlike the electromagnetic properties for which there are pionic contributions, the axial form factor is a direct measure of the quark distribution in the nucleon. At present the data on  $g_A(q^2)$  come from two sources, the reaction  $\nu_\mu + n \rightarrow \mu^- + p$  and pion electroproduction - see, e.g., Ref. 26. It is usually represented as a dipole

$$g_A(q^2) = (1 + q^2/m_A^2)^{-2}, \quad (3.1)$$

with  $m_A = 0.95 \pm 0.14$  GeV.

If we calculate  $g_A(q^2)$  for the CBM we find this corresponds to a bag radius  $R = 1.16 \pm 0.20$  fm<sup>27</sup>. Clearly there should be corrections to this value arising from centre-of-mass and recoil effects, but as a first estimate this strongly suggests a bag size similar to that expected in the original MIT bag model.

Guichon et al.<sup>27</sup> also investigated  $g_A(q^2)$  in the hybrid model of Chin and Miller and Vento, where the pion is excluded from a region  $r < R_{ch}$  inside the bag [i.e.,  $\xi = R_{ch}/R \in (0,1)$ ]. For  $\xi \neq 0$  the pion also contributes to  $g_A(q^2)$ . However, as shown in Ref. 27, the slope of  $g_A(q^2)$  changes by less than 10% over the whole range of values of  $\xi$ . Thus the result  $R = 1.16 \pm 0.20$  fm is a general result for all chiral bag models.

Finally we note that we can also calculate the  $\pi NN$  form factor in the hybrid model. If we parametrize  $g_A(q^2)$  as  $[1 - q^2 r_A^2/6]$  and  $g_{\pi NN}(q^2)$  as  $[1 - q^2 r_\pi^2/6]$ , then for all values of  $\xi$ ,  $r_\pi > r_A$ . That is, the  $\pi NN$  form factor in all chiral bag models is softer than  $g_A(q^2)$ . In the CBM, where  $\xi = 0$ ,  $g_{\pi NN}(q^2)$  would correspond to a dipole of mass  $0.90 \pm 0.14$  GeV ( $r_A/r_\pi \sim 0.9$ ), which is very soft. For  $\xi$  in the range 0.0 to 0.8 this hardly changes, but in the range 0.8 to 1.0  $g_{\pi NN}(q^2)$  becomes rapidly softer, with  $r_A/r_\pi$  dropping to 0.65 and the corresponding dipole mass to about 0.76 GeV!

Clearly it would be very valuable to have more precise data for  $g_A(q^2)$ . Nevertheless, even at the present accuracy, we regard the arguments which we have just reviewed as the most direct indication (apart from the discussion of DIS in Section 4) that the nucleon bag is of the order of 1 fm in radius.

### 3.3. Exotic states

One of the more exciting possibilities raised by the MIT bag model was that there might be stable, exotic states. For example, it was suggested that the so-called H dibaryon (a  $\Lambda\text{-}\Lambda$  state) might be bound by (50-80) MeV<sup>28</sup>. In view of the relatively large self-energy corrections associated with pions for single hadrons, it is reasonable to ask how those corrections affect the masses of exotic states.

In order to check this in a scheme consistent with the philosophy of the CBM, Mulders and Thomas refitted the usual hadron spectrum with the phenomenological form<sup>29</sup>

$$E(R) = E_Q + E_V + E_M + E_p \quad (3.2)$$

Here  $E_Q$ ,  $E_V$  and  $E_M$  are respectively the standard kinetic energy, volume and colour magnetic contributions to the bag energy. The last term  $E_p$ , is a phenomenological representation of the pion self-energy which has the form

$$E_p = \frac{-1}{pR^3} \sum_{i,j} (\vec{\sigma} \cdot \vec{\pi})_i \cdot (\vec{\sigma} \cdot \vec{\pi})_j \quad (3.3)$$

The spin-isospin structure corresponds to keeping only the lowest orbital in the intermediate state, and treating all such states as degenerate. Finally,  $p$  is a phenomenological constant.

There were several notable features associated with the best fit parameter. The rather large value of the colour coupling constant  $\alpha_s$  in the bag model was reduced by some 35%, which is a step in the right direction. The strange quark mass also came down to 218 MeV (from 279 MeV) - a little closer to the usual current algebra value of 150 MeV. Lastly, we observe that, although treated as an adjustable parameter, the value of  $p$  agreed very well with that calculated

for a nucleon in the chiral bag models.

For the non-strange,  $B = 2$ , exotic bag states, the pionic corrections had little effect. In  ${}^3S_0$  and  ${}^1S_0$  the bag masses were 2.18 and 2.24 GeV respectively (cf. 2.16 and 2.23 in the original MIT bag model<sup>28,30</sup>). Since these lie well above the appropriate thresholds they will be quite broad, and should not have dramatic experimental consequences.

On the other hand, for the doubly strange  $H$  dibaryon the change is dramatic. The combination of decreased colour attraction (smaller  $\alpha_s$ ), and the  $R^{-3}$  dependence of the pionic self-energy result in a larger mass for the  $H = 2.22$  instead of 2.15 GeV. From this, Mulders and Thomas conclude that the  $H$  is almost certainly unbound, and thus it is no mystery that experimental searches have failed to find it. In conclusion, we must remark that this matter is not yet completely closed, as Kerbikov<sup>31</sup> has recently claimed that the coupling of the six quark bag to hadronic channels could lower the mass again. This deserves further study.

### 3.4. Pion photoproduction

The initial motivation for, and the first success of, the CBM was to reconcile<sup>32</sup> the two orthogonal views of the  $\Delta(1232)$  which existed side by side - namely the Chew-Wick and the quark models. Next it was established that the CBM also reproduced  $s$  wave  $\pi N$  scattering at low energy<sup>33,34</sup>. Given these successes with the elastic channel it is natural to ask whether the model is also able to reproduce existing pion photoproduction data. This is of particular interest because of the claims in the LBM of a very large  $d$  wave component in the small nucleon bag which could lead to a sizeable  $E2$  amplitude<sup>35</sup>.

As shown by Kälbermann and Eisenberg<sup>36</sup> the CBM does indeed provide a "consistent and reasonable" picture of the  $M1$  photoproduction amplitude in the  $\Delta(1232)$  energy region. The same calculation yields a ratio of  $E2/M1$  amplitudes of  $-0.9\%$  of which only a fifth comes from the  $d$  state admixture in the  $\Delta$ . Most importantly this rather small result is quite consistent with existing experimental data, which could of course be profitably improved.

### 3.5. Other developments

While the coupling of the pion to the bag is uniquely determined up to order  $\phi^2$  in Refs. 33 and 34, the terms of next order can be altered by redefinitions of the physical pion field<sup>6,37</sup>. The  $\pi N \rightarrow \pi\pi N$  reaction near threshold provides an interesting testing ground for alternative versions of the CBM which differ at that order. For an initial discussion of this problem, which indicates that Weinberg's choice<sup>37</sup> for the pion field may be preferable at order  $\phi^3$ , we refer to the recent discussion of Kälbermann and Eisenberg<sup>38</sup>.

Another very exciting development, based on the Thomas formulation of the CBM<sup>33</sup>, is the work of Miller and Singer<sup>39</sup>. Whereas the CBM was initially applied

to baryon properties, they have been able to successfully derive (e.g.) the  $\omega\pi\pi$ ,  $\rho\pi\pi$ ,  $K^*K\pi$  and  $K^*K^*\pi$  coupling constants. A more recent extension to radiative decays of the vector mesons also seems to agree very well with existing data<sup>40</sup>.

There are a number of other interesting developments related to the CBM which we simply do not have space to describe here. Instead we refer to the recent review by Miller for details<sup>41</sup>.

#### 4. A TEST USING DIS

The phenomenon of Bjorken scaling in deep inelastic scattering (DIS) of leptons from nucleons was discovered at SLAC in the late 60's. We now understand fairly well why scaling violations must occur if QCD is the theory of the strong interactions, and these violations have been studied systematically<sup>1,2</sup>. Nevertheless the property of asymptotic freedom also explains why the naïve quark-parton model works so well over a large range of  $Q^2$ . For our purposes it will be sufficient to use this language. For a relatively simple and up-to-date review of the present knowledge of the nucleon structure function, and its interpretation in the naïve quark-parton model we refer to Ref. 17.

In order to relate what is known about DIS to chiral bag models we begin with the observation by Sullivan that there is a contribution to the nucleon structure function arising from the process shown in Fig. 2<sup>42</sup>. This contribution can be written as

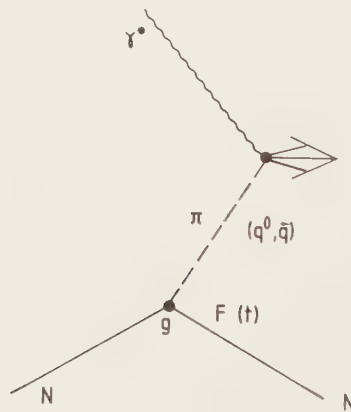


FIGURE 2  
The contribution of the pion  
to the structure function of the nucleon

$$\delta F_{2N}(x) = \int_x^1 dy f(y) F_{2\pi}(x/y), \quad (4.1)$$

where  $F_{2\pi}$  is the pion structure function and  $f(y)$  is the momentum distribution of the pion in an infinite momentum frame. (For the present purposes we can omit the  $Q^2$  dependence of  $\delta F_{2N}$  and  $F_{2\pi}$ .)

The physical interpretation of Eq. (4.1) is that we sum over all  $y$  the product of the probability  $[f(y)]$  of finding a pion carrying a fraction  $y$  of the momentum of the nucleon, with the probability  $[F_{2\pi}(x/y)]$  of finding a quark in the pion with a fraction  $x$  of the nucleon's momentum. Since  $F_2(\xi)$  has been measured by the NA3 collaboration at CERN in the Drell-Yan process<sup>43</sup>, all we need is  $f(y)$ . This is very easily calculated in terms of the  $\pi NN$  coupling constant  $g$ , and the  $\pi NN$  vertex function  $F(t)$  with  $t = \vec{q}^2 - q^0{}^2 =$  minus the four-momentum transfer. For simplicity, we take a simple exponential for  $F(t)$

$$F(t) = \exp[-\lambda(t + m_\pi^2)/m_\pi^2] \quad (4.2)$$

and seek to put some bounds on  $\lambda$ . However, we should point out that in the CBM the form factor is very well approximated by Eq. (4.2) if  $\lambda = 0.106 m_\pi^2 R^2$  with  $R$  the bag radius<sup>6,23</sup>. The final expression for  $f(y)$  is

$$f(y) = \frac{3g^2}{16\pi^2} \int_{m_N^2 y^2}^{\infty} \frac{dt t |F(t)|^2}{(t + m_\pi^2)^2} \frac{1}{1-y} \quad (4.3)$$

A straightforward numerical calculation of Eq. (4.3) reveals two essential features. First,  $f(y)$  peaks at about 0.25 for any reasonable value of  $\lambda$ . Second the maximum value of  $f(y)$  increases rapidly as  $\lambda$  decreases. Returning to Eq. (4.1) we see that the pion structure function is evaluated at  $x/y$ . As usual we expect that the valence component of the pion should dominate for  $x/y > 0.1$ . Since  $y$  is typically 0.25, this implies that the pionic contribution to the nucleon structure function for  $x > 0.03$  involves only non-strange quarks. Thus, if the pion is an important component of nucleon structure, it should contribute to breaking the  $SU(3)$  flavour symmetry  $[SU(3)_F]$  of the sea. Of course, it is generally expected that  $SU(3)_F$  will be broken because of the larger strange quark mass, and it would be unreasonable to attribute the entire excess of non-strange sea quarks to the pion. Nevertheless, it seems quite reasonable to use any evidence for  $SU(3)_F$  breaking to impose a limit on the pionic contribution to the nucleon structure function.

Integrating Eq. (4.1) over  $x$ , we find that

$$\int_0^1 \delta F_{2N}^{\Pi}(x) dx = \left[ \int_0^1 F_{2\pi}^{\Pi}(\xi) d\xi \right] \left[ \int_0^1 dy y f(y) \right]. \quad (4.4)$$

Using the Drell-Yan data for the pion structure function we find the first integral on the right of Eq. (4.4) is  $0.015 \pm 0.004$ . From the physical interpretation of  $f(y)$ , the second integral - which we denote  $\langle y \rangle_{\pi}$  - is the average fraction of the momentum of the nucleon carried by pions. Clearly if we use the observed excess of non-strange over strange quarks<sup>17,44</sup> to give an upper bound on the value of the left-hand side of Eq. (4.4), we obtain an upper bound on  $\langle y \rangle_{\pi}$ <sup>16</sup>. Modulo some discussion of nuclear corrections to the experimental value of  $\bar{S}/(\bar{U}+\bar{D})$ <sup>44</sup>, which was obtained in Fe, we find  $\langle y \rangle_{\pi} \leq 5 \pm 1.5\%$ .

In Fig. 3, we show the average fraction of the momentum of the nucleon carried by pions,  $\langle y \rangle_{\pi}$ , as a function of the cut-off parameter  $\lambda$ , at the  $NN\pi$  vertex.

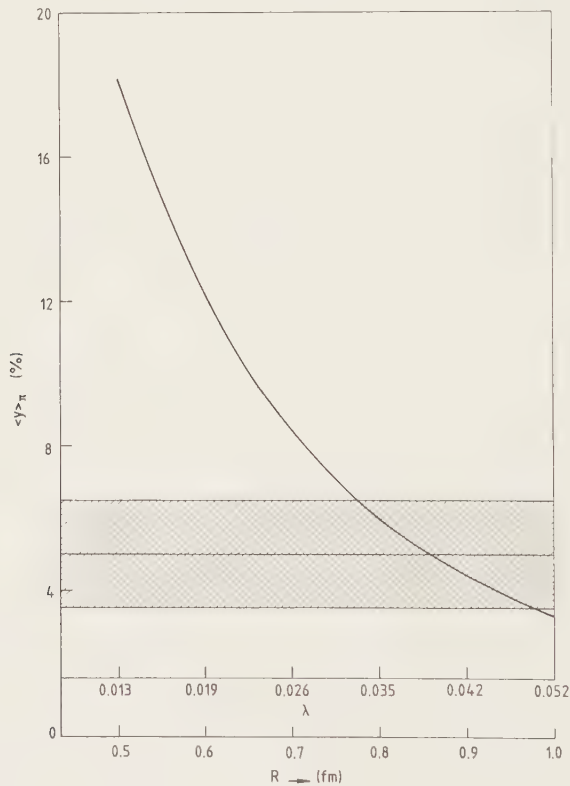


FIGURE 3  
The average fraction of the nucleon's momentum carried by the pions as a function of  $\lambda$  (or bag radius  $R$ ). The shaded area represents the bound obtained in Ref. 16



Clearly our bound is a very strong constraint on that parameter. It is not possible to accept a value of  $\lambda$  smaller than  $0.039^{+0.012}_{-0.006}$ . We also show in Fig. 3 the CBM radius corresponding to each value of  $\lambda$ . The lower bound on the bag radius in the CBM is  $R = 0.87 \pm 0.10$  fm. Of course, there are many defects in the static bag model, and one cannot insist too strongly on an absolute value of  $R$ . One expects the bag to have some surface thickness, and this together with centre-of-mass and recoil corrections could change the simple relationship between  $R$  and  $\lambda$ . Nevertheless, we expect this upper bound to be a good indication of the size of the region within which quarks are confined in the nucleon. The concept of a little bag with a size of order (0.3-0.5) fm is definitely excluded.

For a nuclear audience, it is worthwhile to put this result in perspective. From the measurements on Fe we know that the valence quarks carry some 36% of the momentum of the nucleon, while the whole sea carries about 10%. Our bound says very simply that the pionic contribution should not be more than about 20% of the sea. (The quarks carry about 40% of the pion's momentum, and  $0.40 \times 0.05 / 0.10 = 0.20$ .) Even this may seem quite large to a number of high energy physicists!

In conclusion we note one corollary to this discussion, which may turn out to be more important. The study of the evolution of structure functions is quite an industry at present. Within experimental errors this evolution is consistent with the Altarelli-Parisi equations<sup>1,45</sup>. However, the evolution of the sea is inextricably linked to the unmeasurable gluon momentum distribution, and one must solve for these self-consistently<sup>45</sup>. From the earlier discussion of Fig. 2 we know that it is the *valence* distribution in the pion which is mainly responsible for the pionic contribution to the *nucleon sea*. The former should decrease as  $Q^2$  goes up, whereas the latter is known to increase. We intend to investigate the consequences of this intriguing observation in the next few months.

## 5. THE EMC EFFECT

In the early part of this lecture we gave as one of the major motivations for the development of the CBM that it might lead us to a somewhat deeper understanding of the nuclear many-body problem. Indeed a rather natural picture which one might consider involves a collection of relatively large nucleons ( $R \sim 0.8$ - $1.0$  fm) moving independently some of the time, but also merging and fissioning. Thus at any given instant there will be a non-negligible probability of finding a given quark in a six-quark rather than a three-quark bag. It is therefore quite gratifying that recent data from the European Muon Collaboration (EMC)<sup>46</sup> has revealed a dramatic difference in the effective structure function of a nucleon in Fe compared with that in D. (Throughout the rest of this discussion,

we shall not distinguish between the structure function of a free-nucleon and that of a nucleon in deuterium - because of the latter's low density.)

Essentially the EMC data, which has been partially confirmed at SLAC<sup>47</sup>, shows a softening of the structure function in Fe. For  $x \lesssim 0.1$ ,  $F_{2N}^U(x)$  is enhanced by about 15%, while at  $x \sim 0.6$ , it is depressed by the same amount. Eventually at large  $x$  fermi motion takes over and the ratio rises above one.

Late last year, it was suggested by Llewellyn Smith<sup>48</sup>, on the basis of Eq. (4.1), that an increase in the number of pions per nucleon in Fe could explain the enhancement at small  $x$ . To see this we evaluate Eq. (4.1) at  $x = 0$ , with the result

$$\frac{\delta F_{2N}(0)}{F_{2N}(0)} = \int_0^1 \delta f(y) dy. \quad (5.1)$$

Here  $\delta f(y)$  is the change in the distribution of pions (per nucleon) in Fe compared with a free (isoscalar) nucleon. Thus, the right-hand side of Eq. (5.1) is the extra number of pions per nucleon in Fe, and in order to explain the extrapolated experimental value at  $x = 0$  of  $0.18 \pm 0.07$ , one would need between 6 and 14 extra pions in Fe.

Having said this we should immediately add a caution about interpreting this extra number of pions too literally<sup>49</sup>. Equation (4.1) is meaningless if one goes too near  $x = 0$ , firstly because of shadowing, but also because additional processes where a nucleon turns into a pion and a baryon resonance should be considered inside  $x \sim 0.05$ <sup>42</sup>. Thus, while the argument of Llewellyn Smith was very important in motivating further work, the only reasonable way to use the EMC data is to calculate  $\delta F_{2N}(x)$  using a model of the nuclear response to a pionic excitation<sup>50</sup> and compare directly with the data for  $x \gtrsim 0.05$ . Of course if a fit is found one could a posteriori calculate the number of extra pions. Even then this "number" is defined in an infinite momentum frame<sup>42,48,50</sup> and does not correspond to the simple expectation value of the number operator in the rest frame<sup>49,51</sup>.

Explicit calculation with Eq. (4.3) reveals that the most important contribution comes from pions with a three-momentum,  $|\vec{q}|$ , of order 300 to 400 MeV/c and low energy ( $\omega \sim -|\vec{q}|^2/2m_N$ ). This region has been of tremendous interest in medium energy physics for the past decade in connection with possible pion condensation<sup>52-54</sup>. The mechanism for this enhancement of the pion field is shown in Figs. 4b and 4c. If iterated in RPA these processes would lead to pion condensation at nuclear matter density if it were not for a short-range repulsive interaction which is conventionally parametrized as the Landau-Migdal parameter  $g'$  - shown in Figs. 4d and 4e.

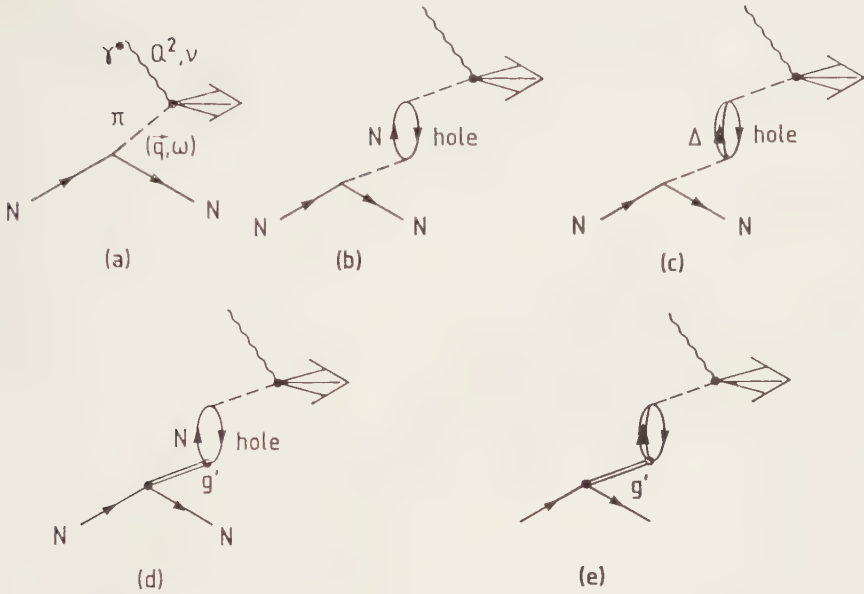


FIGURE 4

Illustration of (a) the basic pion contribution to the nucleon structure function (the  $\gamma^*\pi$  vertex involves the structure function of the pion itself); (b) and (c) other coherent processes involving pion rescattering in the nucleus which lead to enhancement for  $|\vec{q}| \sim 300-400$  MeV/c; (d) and (e) the phenomenological short-range repulsion which damps the enhancement arising from (b) and (c) - from Ericson and Thomas<sup>50</sup>.

Our intention is not to pursue the justification of the Landau-Migdal force, or to discuss its consequences in the famous suppression of Gamow-Teller strength<sup>52,53</sup>. We merely note that as shown by Ericson and Thomas<sup>50</sup> it is possible to generalize Eq. (4.1) to the nuclear case by introducing the nuclear spin-isospin response function. Then, within the conventional RPA with  $g' \sim 0.7$ , we obtain the solid curve of Fig. 5. Clearly, the shape and magnitude of the enhancement of the sea is reproduced. In view of the controversy over the microscopic calculation of  $g'_{N\Delta}$ , we point out that any value of this parameter significantly less than 0.7 would give an enhancement that was far too big.

Obviously the model which we have described says nothing directly about the decrease in the structure function of Fe in the valence region ( $x \sim 0.6$ ). On the simple grounds of momentum conservation, if the momentum carried by pions

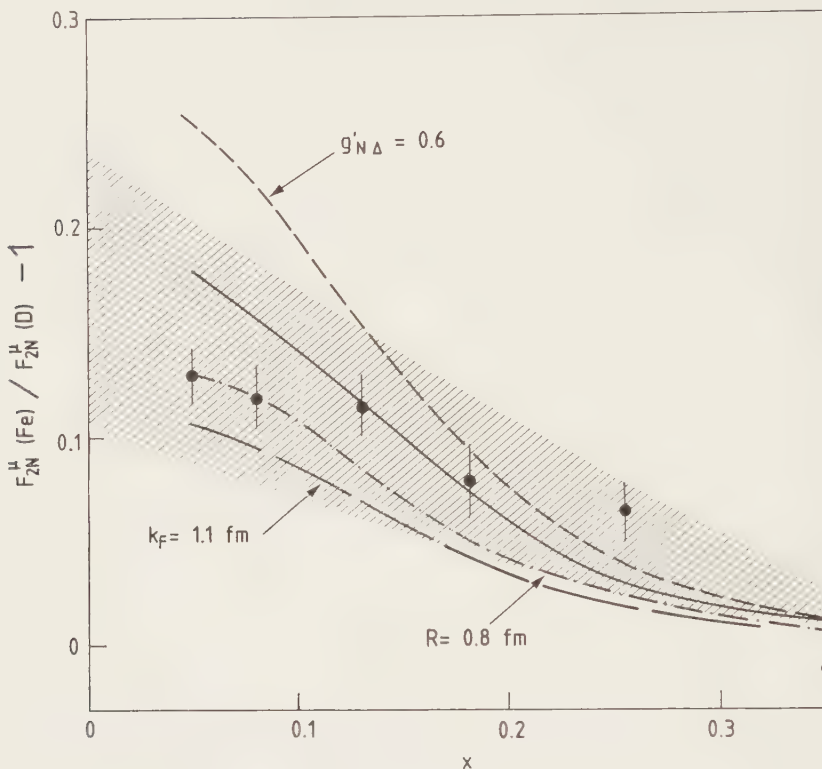


FIGURE 5

The fractional increase in the ratio of the structure function in Fe compared with D, as a function of  $x$  ( $= Q^2/2m_N\nu$ ), caused by the multi-nucleon pion emission graphs of Figs. 4b-e. The data are from the EMC collaboration, and the shaded area indicates possible systematic errors. The standard input (solid curve) for Fe is  $k_F = 1.30 \text{ fm}^{-1}$ ,  $g'_{NN} = g'_{N\Delta} = g'_{\Delta\Delta} = 0.7$ , a bag radius of  $0.7 \text{ fm}$  in  $F(q^2)$ , and  $\Gamma(q^2)$  is a dipole of mass  $1.67 \text{ GeV}$ . We show in the other curves the effect of altering any single one of these parameters - taken from Ericson and Thomas<sup>50</sup>

goes up, something else must lose momentum. Simple estimates of this effect have been made by several groups - either by lowering the average momentum per nucleon<sup>48</sup>, or by a naive calculation of the photon coupling to the nucleon instead of the pion in Fig. 3<sup>49,55</sup>. Both methods give similar results, depressing the structure function at  $x \sim 0.6$  in agreement with the data, but also lowering it at  $x \sim 0.2$ , thereby worsening the fit there.

In Ref. 50, we decided to calculate only the processes shown in Fig. 4, for the following reasons. These terms are gauge invariant by themselves. They represent the modification of the longest range part of the structure of the nucleon. Calculating all of the couplings of the photon to the baryons in Fig. 4

would hopelessly complicated. Finally a mechanism for balancing a large part of the momentum taken by pions had already been suggested by Jaffe<sup>56</sup>. Since that mechanism matches perfectly with the picture of the nucleus which we have advocated as a consequence of the CBM, we prefer to pursue that first. Only after it has been calculated, if there is still some small momentum imbalance, would we resort to purely phenomenological corrections.

Although Jaffe's suggestion was based on the MIT bag model the result is more general<sup>57,58</sup>. All one needs is that there is a significant probability of finding a given quark in a six-quark rather than a three-quark bag. The Drell-Yan-West relation<sup>1,2</sup> then tells us that the structure function of a six-quark state must behave as  $(1-x/2)^9$ , while that of a three-quark bag goes as  $(1-x)^3$ . It is then trivial to show that

$$\frac{F_{2,6q}(x)}{F_{2,3q}(x)} \sim \frac{(1 - x/2)^9}{(1 - x)^3}, \quad (5.2)$$

has a minimum at  $x = 0.5$  - exactly as in the data.

Clearly the essential qualitative features of the data can be understood. The real difficulty is to make the analysis quantitative. For example, even the fermi motion corrections seem to be fairly model-dependent. A program of experiments to map out the dependence of this effect on atomic number has just been completed at SLAC, and we eagerly await the results. This information, together with a measurement of whether the enhancement of the sea is SU(3) symmetric or not, should distinguish between most of the numerous theoretical models which have appeared in the last few months<sup>48-51,56,58,59</sup>.

While it will be some time before the EMC effect is fully understood, we should take some pleasure in what has been achieved. It is quite conceivable that we are seeing confirmation of a new and deeper understanding of the structure of the nucleus than we have ever had before. Through phenomenological models of hadron structure, like the CBM, we may at last be near to a unified theoretical description of nuclear and particle physics.

## REFERENCES

- 1) A.J. Buras, Rev. Mod. Phys. 52 (1980) 199.
- 2) F.E. Close, An introduction to quarks and partons (Academic Press, New York, 1979).
- 3) N. Isgur, Proceedings of BARYON '80 (University of Toronto Press, 1980).
- 4) E.V. Shuryak, CERN Report 83-01 (1983).

- 5) K. Johnson, *Acta Phys. Polonica* B6 (1975) 865.
- 6) A.W. Thomas, *Adv. Nucl. Phys.* 13 (1983) 1.
- 7) C.E. DeTar and J.F. Donoghue, *Ann. Rev. Nucl. and Part. Sci.* 33 (1983), to appear.
- 8) J. Gasser and H. Leutwyler, *Physics Reports* 87 (1982) 77.
- 9) T. Inoue and T. Maskawa, *Progr. Th. Phys.* 54 (1975) 1833.  
A. Chodos and C.B. Thorn, *Phys. Rev.* D12 (1975) 2733.
- 10) H. Pagels, *Physics Reports* 16 (1975) 220.  
M. Gell-Mann, R. Oakes and B. Renner, *Phys. Rev.* 175 (1968) 2195.
- 11) T.J. Goldman and R.W. Haymaker, *Phys. Rev.* D24 (1981) 724.  
V. Miransky and P. Fomin, *Phys. Lett.* 105B (1981) 387.
- 12) G. 't Hooft, *Phys. Rev.* D14 (1976) 3432.
- 13) R. Brockmann, W. Weise and E. Werner, *Phys. Lett.* 122B (1983) 201.
- 14) G.E. Brown and M. Rho, *Phys. Lett.* 82B (1979) 177.
- 15) G.A. Miller, A.W. Thomas and S. Th  berge, *Comm. Nucl. Part. Phys.* 10 (1981) 101.
- 16) A.W. Thomas, *Phys. Lett.* 126B (1983) 97.
- 17) A.W. Thomas, *Lectures at the 7th International School of Nuclear Physics, Erice (1983)*, CERN Preprint TH. 3668 (1983), *Rep. Progr. Phys.* in print.
- 18) S.A. Chin and G.A. Miller, *Phys. Lett.* 121B (1983) 232.  
V. Vento, *Phys. Lett.* 121B (1983) 370.
- 19) F. Myhrer, G.E. Brown and Z. Xu, *Nucl. Phys.* A362 (1981) 317.
- 20) G.E. Brown, in *Progress in Particle and Nuclear Physics*, Vol. 8, ed. D. Wilkinson (Pergamon, London, 1982) p. 147.
- 21) J.O. Eeg and H. Pilkuhn, *Z. Phys.* A287 (1978) 407.
- 22) S. Th  berge and A.W. Thomas, *Phys. Rev.* D25 (1982) 284.
- 23) S. Th  berge and A.W. Thomas, *Nucl. Phys.* A393 (1983) 252.
- 24) G.E. Brown, M. Rho and V. Vento, *Phys. Lett.* 97B (1980) 423.
- 25) L. Roberts and R. Welsh, Private communication.
- 26) E. Amaldi, S. Fubini and G. Furlan, *Pion electroproduction at low energy and hadron form factors*, in *Springer Tracts in Modern Physics*, Vol. 83 (Springer-Verlag, Berlin, 1979).
- 27) P.A.M. Guichon, G.A. Miller and A.W. Thomas, *Phys. Lett.* 124B (1983) 109.
- 28) R.L. Jaffe, *Phys. Rev. Lett.* 38 (1977) 195.
- 29) P.J. Mulders and A.W. Thomas, CERN Preprint TH. 3443 (1983), *J. Phys. G.* in print.

- 30) A.T. Aerts, P.J. Mulders and J.J. de Swart, *Phys. Rev.* D17 (1978) 260.
- 31) B.O. Kerbikov, ITEP Preprint 42 (1983).
- 32) S. Th  berge, A.W. Thomas and G.A. Miller, *Phys. Rev.* D22 (1980) 2838, D23 (1981) 2106(E).  
A.W. Thomas, S. Th  berge and G.A. Miller, *Phys. Rev.* D24 (1981) 216.
- 33) A.W. Thomas, *J. Phys.* G7 (1981) L283.
- 34) A. Szymacha and S. Tatur, *Z. Phys.* C7 (1981) 311.
- 35) V. Vento, G. Baym and A.D. Jackson, *Phys. Lett.* 102B (1981) 97.
- 36) G. K  lbermann and J.M. Eisenberg, *Phys. Rev.* D28 (1983) 71.
- 37) S. Weinberg, *Phys. Rev. Lett.* 18 (1967) 188.
- 38) G. K  lbermann and J.M. Eisenberg, *Phys. Rev.* D28 (1983) 66.
- 39) G.A. Miller and P. Singer, CERN Preprint TH. 3609 (1983), *Phys. Lett.* in print.
- 40) G.A. Miller, Private communication.
- 41) G.A. Miller, CERN Preprint TH. 3516 (1982), to appear in the Proceedings IUCF Workshop (November 1982).
- 42) J.D. Sullivan, *Phys. Rev.* D5 (1972) 1732.
- 43) J. Badier et al., CERN-EP/83-48 (1983).
- 44) H. Abramowicz et al., *Z. Phys.* C15 (1982) 19.
- 45) F. Bergsma et al., *Phys. Lett.* 123B (1983) 269.  
H. Abramowicz et al., *Z. Phys.* C17 (1983) 283.
- 46) J.J. Aubert et al., *Phys. Lett.* 123B (1983) 275.
- 47) A. Bodek et al., *Phys. Rev. Lett.* 50 (1983) 1431.
- 48) C.H. Llewellyn Smith, CERN-83-02 (1983) p. 180, and Oxford Preprint 18-83 (1983), *Phys. Lett.* in print.
- 49) E. Berger, F. Coester and R. Wiringa, ANL Preprint ANL-HEP-PR-83-24 (1983).
- 50) M. Ericson and A.W. Thomas, CERN Preprint TH. 3553 (1983), *Phys. Lett.* in print.
- 51) B.L. Friman, V.R. Pandharipande and R.B. Wiringa, University of Illinois Preprint ILL-(NU)-83-15 (1983).
- 52) M. Ericson, in *Proceedings 8 ICOHEPANS*, eds. D.F. Measday and A.W. Thomas, *Nucl. Phys.* A335 (1980) 309 ; *Lectures at Erice* (1983), see Ref. 17).
- 53) E. Oset, H. Toki and W. Weise, *Physics Reports* 83 (1982) 281.
- 54) J. Meyer-ter-Vehn, *Physics Reports* 74 (1981) 324.
- 55) M. Ericson and A.W. Thomas, unpublished.



- 56) R.L. Jaffe, Phys. Rev. Lett. 50 (1983) 228.
- 57) A.W. Thomas, Invited talk at the 3me Journées d'Etudes Saturn (April 25-29, 1983), CERN Preprint TH. 3600 (1983).
- 58) H.J. Pirner and J.P. Vary, Heidelberg Preprint UNI-HD-83-02 (1983).
- 59) C.E. Carlson and T.J. Havens, Phys. Rev. Lett. 51 (1983) 261.  
F.E. Close, R.G. Roberts and G.G. Ross, Rutherford Preprint RL-83-051 (1983).  
S. Date, Waseda Preprint WU-HEP-83-4 (1983).  
H. Faissner and B.R. Kim, Aachen Preprint (1983).  
W. Furmanski and A. Krzywicki, Orsay Preprint LPHE 83/11 (1983).  
O. Nachtmann and H. Pirner, Heidelberg Preprint HD-THEP-83-8 (1983).  
J. Szwed, Jagellonian Preprint TPJU-1/83 (1983).

## QUANTUM MECHANICAL SCATTERING WITH CONFINING INTERACTION

Koichi YAZAKI

Department of Physics, Faculty of Science, University of Tokyo,  
Bunkyo-ku, Tokyo 113, Japan

Following two topics on the scattering problem with confining interaction will be discussed. a) Nucleon-nucleon scattering based on the quark cluster model with two-body confinement. b) A new type of confining interaction and its application to simple scattering systems.

### 1. INTRODUCTION

Description of low energy hadron-hadron interaction based on the quark model is one of the challenging problems in the recent development of the strong interaction physics. Although the Monte-Carlo simulation<sup>1</sup> based on the lattice gauge theory of the quantum chromodynamics (QCD) seems to give qualitative explanation of the ground state properties of an isolated hadron, it has not yet attained the stage of calculating the excited spectra of hadrons and is far from being able to treat multi-hadron systems. Several models<sup>2,3</sup> have therefore been proposed to describe the low energy strong interaction phenomena. They can be classified into two groups according to their descriptions of confinement. One is the bag model<sup>2</sup> which describes the confinement either by boundary conditions (MIT bag, chiral bag, cloudy bag) or by an additional field (soliton bag). The other is the potential model<sup>3</sup> in which the confinement is described by an interaction between quarks. Both have been reasonably successful in explaining the ground state properties and the excited spectra of hadrons and there have been many attempts<sup>4,5,6</sup> to apply them to the low energy hadron-hadron interaction.

In this talk, I will discuss two topics on hadron-hadron scattering based on the potential model. The first one concerns with the short range part of baryon-baryon interaction in the quark cluster model with a two-body potential for confinement, and is mainly based on the works<sup>6</sup> with M. Oka. A problem related to the long range color Van der Waals force<sup>7</sup> in the case of two-body confining potential is also briefly discussed. The second is based on the work<sup>8</sup> with F. Lenz, T. Londergan, E. Moniz, R. Rosenfelder and M. Stingl. A new type of confining interaction, which is free from the Van der Waals problem, is proposed and applied to simple scattering system.

General discussions on the non-relativistic quark model are given in section

2. The short range part of the baryon-baryon interaction is discussed in

section 3 and the new type of confining interaction is discussed in section 4.

## 2. NON-RELATIVISTIC QUARK MODEL

### 2.1. Excuses for the non-relativistic kinematics

It is well known that the bare (or current) masses of the u- and d-quarks, which are relevant for non-strange hadrons, are of the order of several MeV. On the other hand, the renormalized (or constituent) masses are usually said to be around 300 MeV and this has been the basis of using non-relativistic kinematics as the zeroth order approximation. In fact, there is no clear way of defining the constituent mass since a quark cannot be isolated. The mass, the form of kinetic energy and the interaction can only be tested by comparing their predictions with the experiments. In that sense, the non-relativistic model<sup>3</sup> has been quite successful in describing the observed baryon and meson spectra. A favorable feature of the non-relativistic kinematics is the clear separation of the center-of-mass variables from the internal variables, which is very important in the scattering problems. For heavy quarks, such as c- and b-quarks, the non-relativistic treatment is certainly considered to be a good approximation.

### 2.2. Wave function for a single hadron

A meson consists of a quark and an anti-quark and the wave function is given by

$$\psi_M(1, \bar{1}) = \phi_M(\vec{r}_{1\bar{1}}) S_M(\xi_1, \xi_{\bar{1}}) C(\eta_1, \eta_{\bar{1}}) \quad (1)$$

where  $\phi_M$ ,  $S_M$  and  $C$  are the orbital, spin-flavour and color parts, respectively.  $C$  is the unique color singlet state while  $\phi_M$  and  $S_M$  depend on the meson,  $M$ .

A baryon consists of three quarks and has a wave function of the form

$$\psi_B(1, 2, 3) = [\phi_B(\vec{r}_1, 23, \vec{r}_{23}) S_B(\zeta_1, \zeta_2, \zeta_3)] C(\eta_1, \eta_2, \eta_3) \quad (2)$$

where  $C$  is the totally anti-symmetric color singlet state while the orbital ( $\phi_B$ ) and spin-flavour ( $S_B$ ) parts are to be combined to form a totally symmetric state. For non-strange baryons, the lowest orbital state is considered to be totally symmetric and, combined with the totally symmetric spin-isospin part, gives the nucleon and  $\Delta$ -isobar, i.e.  $N(S = 1/2, T = 1/2)$  and  $\Delta(S = 3/2, T = 3/2)$ . The excited orbital states may have other symmetries (mixed or totally anti-symmetric) and the corresponding spin-isospin part  $S_B$  is to have the same symmetry.

### 2.3. Wave function for two hadrons

A two-meson system consisting of two quarks and two anti-quarks is described by a wave function of the form

$$\Psi(1, \bar{1}, 2, \bar{2}) = \sum_{M, M'} A [\psi_M(1, \bar{1}) \psi_{M'}(2, \bar{2}) \chi_{MM'}(\vec{r}_{1\bar{1}}, 2\bar{2})] \quad (3)$$

where  $\chi_{MM'}$  describes the relative motion between the two mesons,  $M$  and  $M'$  and  $A$  is the anti-symmetrizer for quarks and anti-quarks. One can show<sup>6</sup> that any state for a color singlet two-quark-two-anti-quark system is given by a wave function of the form (3) although the corresponding  $\chi_{MM'}$  may not be unique. The Schrödinger equation for such a system, therefore, takes the form of a coupled integral equation for  $\chi_{MM'}$ .

A two-baryon system consisting of six quarks is described by a wave function of the form

$$\Psi(1, 2, \dots, 6) = \sum_{B, B'} A [\chi_B(1, 2, 3) \chi_{B'}(4, 5, 6) \chi_{BB'}(\vec{r}_{123}, 456)] \quad (4)$$

where  $A$  is the anti-symmetrizer for quarks. One can again show that any state for a color singlet six-quark system is given by a wave function of the form (4), and the Schrödinger equation is expressed as a coupled equation for  $\chi_{BB'}$ .

### 3. SHORT RANGE PART OF BARYON-BARYON INTERACTION

#### 3.1. Hamiltonian with two-body confinement

The hamiltonian in the non-relativistic quark model is usually taken as

$$H = \sum_i K_i + \sum_{i < j} V_{ij}, \quad K_i = m + \frac{\vec{p}_i^2}{2m} \quad (5)$$

where the two-body interaction consists of the confinement term  $V_{ij}^{\text{CONF}}$  and the one-gluon-exchange term  $V_{ij}^{\text{OGE}}$ , i.e.

$$V_{ij} = V_{ij}^{\text{CONF}} + V_{ij}^{\text{OGE}}. \quad (6)$$

The confinement term is assumed to be linear, i.e.

$$V_{ij}^{\text{CONF}} = (\lambda_i \cdot \lambda_j) a r_{ij} \quad (7)$$

while the one-gluon-exchange term is given by

$$V_{ij}^{\text{OGE}} = (\lambda_i \cdot \lambda_j) \frac{\alpha_s}{4} \left[ \frac{1}{r_{ij}} - \frac{\pi}{2} (1 + \frac{2}{3} (\sigma_i \cdot \sigma_j)) \delta(\vec{r}_{ij}) \right] \quad (8)$$

where the tensor and the velocity dependent terms have been omitted.

#### 3.2. The resonating group method (RGM)

The wave function (4) can be rewritten as

$$\Psi(1, 2, \dots, 6) = \sum_{\beta} A [\psi_{\beta}(123; 456) \chi_{\beta}(\vec{r}_{123}, 456)] \quad (9)$$

where  $\beta$  stands for  $(B, B')$  combined to give a definite total spin and isospin state, i.e.

$$\psi_{\beta}(123; 456) = [\psi_B(123) \psi_{B'}(456)]_{\beta} \quad (10)$$

The Schrödinger equation for  $\Psi$  then takes the form

$$\sum_{\beta'} \int d\vec{r}' \{ E N_{\beta\beta'}(\vec{r}, \vec{r}') - H_{\beta\beta'}(\vec{r}, \vec{r}') \} \chi_{\beta'}(\vec{r}') = 0 \quad (11)$$

where the overlap kernel  $N_{\beta\beta'}$  and the hamiltonian kernel  $H_{\beta\beta'}$  are defined by

$$\begin{aligned} \begin{pmatrix} N_{\beta\beta'}(\vec{r}, \vec{r}') \\ N_{\beta\beta'}(\vec{r}, \vec{r}') \end{pmatrix} &= \int d\tau \psi_{\rho}^+(123:456) \delta(\vec{r} - \vec{r}_{123,456}) \begin{pmatrix} 1 \\ H \end{pmatrix} \\ &\times A [\psi_{\rho}(123:456) \delta(\vec{r}' - \vec{r}_{123,456})] \end{aligned} \quad (12)$$

Eq. (11) is nothing but the coupled RGM equation and is exact if the sum over  $\beta'$  is not restricted. In practice, the sum must be truncated and, in the case of two-body confinement (eq. (7)), reasonable results can be obtained only if the sum is truncated, as will be discussed later in connection with the color Van der Waals force.

### 3.3. Results

In the actual calculations,<sup>6</sup>  $\beta$  is restricted to the lowest orbital clusters, i.e. NN,  $N\Delta$  and  $\Delta\Delta$ . The orbital wave function  $\phi_{\beta}$  is taken to be Gaussian with the size parameter  $b$ . The results for the S-wave baryon-baryon scattering are summarized in Table 1. In most cases, the phase shift behaves like that of a hard core scattering. Large hard core radii ( $r_c = 0.7 \sim 0.8$  fm) are obtained in the cases where the 0s state for  $\chi_{\beta}$  is forbidden by the Pauli principle. The situation is similar to the case of  $\alpha$ - $\alpha$  scattering<sup>9</sup> where the Pauli principle gives rise to the hard core like behaviour in the phase shifts. Relatively small hard core radii ( $r_c = 0.4 \sim 0.5$  fm) are obtained in other cases including the most interesting cases of NN scattering and the strong repulsion arises as a combined effect of the color magnetic interaction and

Table 1. Summary of the S-wave baryon-baryon scattering

BB'	T		interaction	
	S	T		
NN, $\Delta\Delta$	1	0	hard core like	$r_c = 0.39$ fm
NN, $\Delta\Delta$	0	1	"	$r_c = 0.41$ fm
$N\Delta$ $\Delta\Delta$	2	1	"	$r_c = 0.44$ fm
$N\Delta$ $\Delta\Delta$	1	2	"	$r_c = 0.48$ fm
$N\Delta$	1	1	"	$r_c = 0.74$ fm
$N\Delta$	2	2	"	$r_c = 0.77$ fm
$\Delta\Delta$	3	2	"	$r_c = 0.75$ fm
$\Delta\Delta$	2	3	"	$r_c = 0.78$ fm
$\Delta\Delta$	3	0	attractive	
$\Delta\Delta$	0	3	weakly repulsive	

The parameters used in the calculation are,  $m = 300$  MeV,  $b = 0.6$  fm,  $\alpha_s = 1.39$ ,  $a = 141$  MeV fm<sup>-1</sup>.

the Pauli principle. Unlike the usual vector meson exchange model, the repulsion is not universal and there are cases where the interaction is weakly repulsive or even attractive. These features of baryon-baryon interaction can be in principle tested against the experiments by the detailed studies of di-baryon systems.

### 3.4. Color Van der Waals force

The two-body confinement represented by eq. (7) is known to have a problem of color Van der Waals force.<sup>7</sup> For a large separation of two baryons, the virtual excitations of color octet dipole states in both clusters gives rise to a long range attractive interaction with the behaviour  $r^{-3}$ . In general, the two-body confinement of the form  $r_{ij}^n$  gives the color Van der Waals interaction with the behaviour  $r^{n-4}$ . Although there is no immediate experimental evidence against such a force in the case of weak confinement ( $n \sim 0$ ), the universal long range attraction between hadrons is generally considered to be an unfavourable feature of the two-body confinement.

The problem did not appear in the previous calculation because the sum over  $\beta$  in eq. (9) was truncated. In fact, the configuration of well separated two color octet dipole states can only be expressed as a sum of highly excited orbital states for  $\beta$ . The truncation thus provides an automatic screening of the Van der Waals force, and one may argue that the hamiltonian (5) can only be used in such a restricted space. This is certainly unsatisfactory unless a reasoning and a criterion for the truncation is given. The problem is clearly demonstrated by a recent calculation of reference 10, where the color octet dipole channel is explicitly included in the coupled RGM equation.

## 4. NEW TYPE OF CONFINING INTERACTION

### 4.1. Construction of the interaction

The previous arguments indicate that, although the potential model seems suitable for treating hadron-hadron interaction, the confinement by the two-body potential has an unfavourable feature. There are also arguments that the confinement is an essentially many-body effect.<sup>11</sup> We have tried to construct a new type of confining interaction,<sup>8</sup> taking these arguments into consideration. The criterions we impose on the interaction are,

- (a) quark confinement within a hadron and asymptotic separability of hadrons
- (b) exchange symmetry among the quarks and among the anti-quarks
- (c) absence of the long range color Van der Waals force between hadrons

Let us consider a simple two meson system consisting of two quarks (1, 2) and two antiquarks ( $\bar{1}$ ,  $\bar{2}$ ). The spin, flavour and color degrees of freedom are

suppressed for the moment. The hamiltonian for a single meson consisting of a quark (1) and anti-quark ( $\bar{1}$ ) can be written as

$$H = K_1 + K_{\bar{1}} + v(r_{1\bar{1}}) \quad (13)$$

where the confinement is ensured by the requirement  $v(r) \rightarrow \infty$  ( $r \rightarrow \infty$ ). For simplicity, we also assume that  $v(r)$  is monotonic. A generalization of the hamiltonian (18) to the two meson system, which is consistent with the criteria (a)  $\sim$  (c), is

$$H = K_1 + K_{\bar{1}} + K_2 + K_{\bar{2}} + V \quad (14)$$

where the interaction,  $V$ , is given by

$$V = \min_s u_s, \quad (15)$$

$$u_1 = v(r_{1\bar{1}}) + v(r_{2\bar{2}}), \quad (16)$$

$$u_2 = v(r_{1\bar{2}}) + v(r_{2\bar{1}}).$$

For a given spatial configuration of the quarks and antiquarks, the interaction is a sum of two-body interactions, either  $u_1$  or  $u_2$ , and the interacting pairs are selected by the minimization in eq. (15). It is similar to the interaction in the string flip-flop model<sup>12</sup> proposed by Miyazawa. Another way of writing eq. (15) is

$$V = u_1 \theta(u_2 - u_1) + u_2 \theta(u_1 - u_2) \quad (15)$$

where  $\theta$  is the step function, i.e.

$$\theta(x) = \begin{cases} 1 & (x \geq 0) \\ 0 & (x < 0) \end{cases} \quad (17)$$

It can be easily confirmed that the interaction given by eq. (15) (or (15')) indeed satisfies the criteria (a)  $\sim$  (c).

The color degree of freedom can be included in the following way. We assume the SU(N) color in general and introduce a projection operator,  $P_{1\bar{1}}$ , onto the color singlet state for the (1,  $\bar{1}$ ) system. A meson consisting of 1 and  $\bar{1}$  is always in a color singlet state and its hamiltonian is again given by eq. (13). A possible form of the interaction,  $V$ , for the two meson system is

$$V = u_1 + u_2 - u_1 \theta(u_1 - u_2) P_2 - u_2 \theta(u_2 - u_1) P_1 \quad (18)$$

where the projection operators  $P_1$ ,  $P_2$  are defined by

$$P_1 = P_{1\bar{1}} P_{2\bar{2}}, \quad P_2 = P_{1\bar{2}} P_{2\bar{1}} \quad (19)$$

If  $u_2 > u_1$  for a given spatial configuration, the interaction is  $u_1$  when  $1\bar{1}$  and  $2\bar{2}$  are both in color singlet states while it becomes  $u_1 + u_2$  (i.e. the system is completely confined) when  $1\bar{1}$  and  $2\bar{2}$  are both in color non-singlet



states. The completely confined part can be modified without affecting the asymptotic part and a simple generation is obtained by

$$V = \frac{1}{1+\epsilon} \{u_1 + u_2 - (u_1 - \epsilon u_2)\theta(u_1 - u_2)P_2 - (u_2 - \epsilon u_1)\theta(u_2 - u_1)P_1\}, \quad (20)$$

where  $\epsilon$  is a real number larger than  $-1$ .

As mentioned previously, the wave function for the two meson system is given by eq. (3) and the Schrödinger-equation becomes a coupled equation for  $\chi_{M,M'}$  analogous to the RGM equation (11) for the two baryon system. The convergence of the summation over  $M, M'$  and the existence of a solution to the coupled equation depend on whether the hamiltonian (14) with the interaction (15) or (20) gives a physically reasonable scattering system or not. In the following, we show that a special simplification arises in the case of harmonic oscillator confinement, i.e.  $v(r) \propto r^2$ , and allows an essentially exact treatment of the four-body problem. We shall also see that the interaction (15) or (20) with such a special choice of  $v(r)$  indeed gives a rich and interesting scattering system.

#### 4.2. Harmonic oscillator confinement

Let us take a harmonic oscillator form for  $v(r)$ , i.e.

$$v(r) = \frac{m\omega^2}{4} r^2 \quad (21)$$

We also introduce the following variables which are appropriate for the present scattering problem.

$$\begin{aligned} \vec{x} &= \frac{1}{2}(\vec{r}_1 + \vec{r}_2 - \vec{r}_1 - \vec{r}_2) \\ \vec{y} &= \frac{1}{2}(\vec{r}_1 + \vec{r}_1 - \vec{r}_2 - \vec{r}_2) \\ \vec{z} &= \frac{1}{2}(\vec{r}_1 + \vec{r}_2 - \vec{r}_1 - \vec{r}_2) \\ \vec{R} &= \frac{1}{4}(\vec{r}_1 + \vec{r}_2 + \vec{r}_1 + \vec{r}_2) \end{aligned} \quad (22)$$

The hamiltonian (14) in the new variables is

$$\begin{aligned} H &= K_R + K_x + K_y + K_z + V \\ K_R &= 4m + \frac{\vec{p}_R^2}{8m}, \\ K_x &= \frac{\vec{p}_x^2}{2m}, K_y = \frac{\vec{p}_y^2}{2m}, K_z = \frac{\vec{p}_z^2}{2m} \end{aligned} \quad (23)$$

and the interaction (15) becomes

$$V = \frac{m\omega^2}{2} [x^2 + y^2\theta(z^2 - y^2) + z^2\theta(y^2 - z^2)] \quad (24)$$

The variable  $\vec{x}$  in addition to the center-of-mass variable  $\vec{R}$  decouples and the essential part of the hamiltonian is

$$\hat{H} = K_y + K_z + \frac{m\omega^2}{2}[y^2\theta(z^2 - y^2) + z^2\theta(y^2 - z^2)] \quad (25)$$

One also sees that the angular momenta for  $\vec{y}$  and  $\vec{z}$  variables conserve separately so that, after the partial wave decomposition, the problem is reduced to a two-dimensional problem.

A similar decoupling of the  $\vec{x}$ -variable arises in the case of SU(N) color for the interaction (20) with  $\epsilon = 1$ , i.e.

$$V = \frac{m\omega^2}{4}[2x^2 + y^2 + z^2 - (y^2 - z^2)\theta(y^2 - z^2)P_1 - (z^2 - y^2)\theta(z^2 - y^2)P_2] \quad (26)$$

One can again use the flexibility in the completely confined situation and add quark-quark and antiquark-antiquark interactions of the form

$$\Delta V = \alpha \cdot \frac{m\omega^2}{4} \cdot (y^2 + z^2)[1 - \theta(y^2 - z^2)P_1 - \theta(z^2 - y^2)P_2]. \quad (27)$$

The ratio,  $\lambda$ , of the interaction strength in the color non-singlet channel to that in the color singlet channel is

$$\lambda = \frac{1 + \alpha}{2} \quad (28)$$

and can be used as a parameter to change the completely confined part of the interaction.

#### 4.3. Method of solution

We illustrate here the method of solving the scattering problem with the interaction  $V$  of eq. (24) or  $V + \Delta V$  of eqs. (26) and (27), for the simplest case of the S-wave scattering without the color degree of freedom. The Schrödinger equation for the two dimensional problem is

$$\{E + \frac{1}{2m}(\frac{d^2}{dy^2} + \frac{d^2}{dz^2}) - \frac{m\omega^2}{2}[y^2\theta(z^2 - y^2) + z^2\theta(y^2 - z^2)]\}\psi(y, z) = 0. \quad (29)$$

Since the equation is invariant with respect to the interchange of  $y$  and  $z$ , the solutions are classified into symmetric and antisymmetric ones,  $\Psi_s$  and  $\Psi_a$ , i.e.

$$\Psi_s(y, z) = \Psi_s(z, y), \quad \Psi_a(y, z) = -\Psi_a(z, y) \quad (30)$$

In the region  $y > z$ , the Schrödinger equation takes a simple form

$$\{E + \frac{1}{2m}(\frac{d^2}{dy^2} + \frac{d^2}{dz^2}) - \frac{m\omega^2}{2}z^2\}\Psi(y, z) = 0. \quad (31)$$

and the asymptotic form of  $\Psi$  is given by

$$\Psi(y, z) \sim \sum_n \phi_n(z)[\delta_{n0} e^{-ik_n y} - S_{n0} e^{ik_n y}], \quad (y \rightarrow \infty) \quad (32)$$

where  $\phi_n$  is an eigen function for the harmonic oscillator,

$$(\epsilon_n + \frac{1}{2m} \frac{d^2}{dz^2} - \frac{m\omega^2}{2} z^2) \phi_n(z) = 0, \quad \epsilon_n = (2n + \frac{3}{2})\omega, \quad (33)$$

$k_n$  is defined by

$$\epsilon_n + \frac{k_n^2}{2m} = E \quad (34)$$

and an incoming wave in the ground state channel ( $n = 0$ ) is assumed.  $S_{n0}$  is the S-matrix element for the transition to the  $n$ -th excited state. A similar expression is obtained in the region  $z > y$ , and the main problem becomes the matching of the wave function along the diagonal  $y = z$ . With the observation that each term in the expansion (32) satisfies the Schrödinger equation (31) in the region  $y > z$ , a naive way of matching is to use the expression (32) in the neighbourhood of the diagonal  $y = z$ . This is mathematically a little shaky because of the convergence problem of the sum over  $n$ , but is actually justified by the better founded Green function method.<sup>8</sup> For the antisymmetric solution, the wave function vanishes along the diagonal and the equation to determine  $S_{n0}^{(a)}$  becomes

$$\sum_n \phi_n(y) [\delta_{n0} e^{-ik_n y} - S_{n0}^{(a)} e^{ik_n y}] = 0. \quad (35)$$

For the symmetric solution, the normal derivative of the wave function vanishes and the equation for  $S_{n0}^{(s)}$  becomes

$$\sum [\delta_{n0} e^{-ik_n y} [\phi_n'(y) + ik_n \phi_n(y)] - S_{n0}^{(s)} e^{ik_n y} [\phi_n'(y) - ik_n \phi_n(y)]] = 0. \quad (36)$$

The actual calculation of  $S_{n0}^{(a)}$  and  $S_{n0}^{(s)}$  was done by expanding the functions along the diagonal with a complete set of the harmonic oscillator eigenfunctions,  $\{\phi_n\}$  and reducing eqs. (35) and (36) to algebraic equations for  $S_{n0}^{(a)}$  and  $S_{n0}^{(s)}$ . More detailed descriptions of the methods as well as the other methods of using Green functions or the coupled channels approach are given in reference 8.

#### 4.4. Results and discussions

We will show here some of the numerical results for the harmonic oscillator confinement described previously.

The S-wave scattering without color is the simplest case and the elastic S-matrices for the symmetric and antisymmetric cases,  $S_{00}^{(s)}$  and  $S_{00}^{(a)}$ , are shown in Figure 1. There is a shallow bound state (binding energy = 0.04  $\omega$ ) for the symmetric case and the phase shift starts from  $\pi$ . Thresholds for inelastic scatterings are at  $k_0 = \sqrt{2n} b^{-1}$  ( $b^{-1} \equiv \sqrt{m\omega}$ ) and one sees sharp resonances near the thresholds in the symmetric case. For the antisymmetric case, the phase shift behaves like that of the hard core scattering with small structures at thresholds. The hard core like behaviour is due to the Pauli principle which excludes the harmonic oscillator 0s state from the relative motion between

clusters. It is interesting to note the similarity between the present scattering system and the electron-hydrogen (e-H) system. One sees that the e-H interaction in monopole approximation has the same structure as the present one. A shallow bound state ( $H^-$ ) and sharp resonances near thresholds are indeed observed in the e-H system.<sup>13</sup>

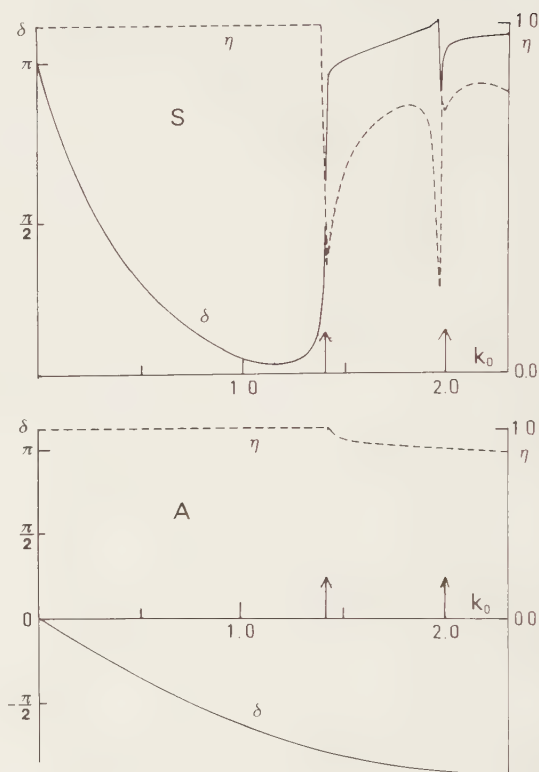
The cases with color have much more varieties due to the flexibility in the completely confined "hidden color" configuration. The results depend on the interaction strength ratio,  $\lambda$ , (see eq. (28)) and the number of colors,  $N$ . They can be summarized as follows.

a) For small  $\lambda$  ( $\lambda < \sqrt{2}$ ), the low lying "hidden color" states manifest themselves as bound and resonance states in the scattering system.

b) For large  $\lambda$  ( $\lambda > \sqrt{2}$ ), the "hidden color" part of the wave function becomes small, and, in the limit  $\lambda \rightarrow \infty$ , where the "hidden color" part is completely excluded, the scattering system becomes equivalent to that of the antisymmetric case without color.

c) The difference between the symmetric and antisymmetric cases becomes smaller as  $N$  increases and, in the limit  $N \rightarrow \infty$ , the two cases become equivalent.

d) The present model gives a finite scattering in the limit  $N \rightarrow \infty$ , but there is another way of modifying the "hidden color" part of the interaction, for



FIGURE

S-wave elastic S-matrix ( $ne^{2i\delta}$ ) for symmetric (S) and antisymmetric (A) cases without color degrees of freedom.  $k_0$  is the wave number for the elastic channel in unit of  $b^{-1}$ . The arrows indicate the inelastic thresholds.

which the scattering amplitude behaves as  $1/N$  for large  $N$ .<sup>14</sup>

In conclusion, we have demonstrated that the new type of confining interaction proposed here gives physically acceptable and interesting scattering system. They even share some features with the observed hadron-hadron interaction. For quantitative discussions, however, missing factors such as spin and flavour degrees of freedom as well as the short-range part of the interaction should be taken into account.

#### ACKNOWLEDGEMENT

I would like to thank F. Lenz, T. Londergan, K. Masutani, E. J. Moniz, M. Oka, R. Rosenfelder and M. Stingl for letting me discuss the results of their works prior to publication.

#### REFERENCES

- 1) M. Creutz, L. Jacobs and C. Rebbi, Phys. Rep. 95 (1983) 201.
- 2) T. DeGrand, R. L. Jaffe, K. Johnson and J. Kiskis, Phys. Rev. D12 (1975) 2060.  
G. E. Brown, M. Rho and V. Vento, Phys. Lett. 84B (1979) 83.  
S. Th  berge, A. W. Thomas and G. A. Miller, Phys. Rev. D22 (1980) 2838  
R. Goldflam and L. Wilets, Phys. Rev. D25 (1982) 1951.
- 3) A. De R  jula, H. Georgi and S. L. Glashow, Phys. Rev. D12 (1975) 147.  
W. Celmaster, Phys. Rev. D15 (1977) 1391.  
N. Isgur and G. Karl, Phys. Lett. 72B (1977) 109.
- 4) C. De Tar, Phys. Rev. D17 (1978) 323.  
P. J. Mulders, Phys. Rev. D26 (1982) 3039.
- 5) D. A. Liberman, Phys. Rev. D16 (1977) 1542.  
M. Harvey, Nucl. Phys. A352 (1981) 301, 326.
- 6) J. E. T. Ribeiro, Z. Phys. C5 (1980) 27.  
M. Oka and K. Yazaki, Prog. Theor. Phys. 66 (1981) 556, 572.  
A. F. Faessler, F. Fernandez, C. L  beck and K. Shimizu, Phys. Lett. 112B (1982) 201.  
M. Oka and K. Yazaki, in preparation.
- 7) R. S. Willey, Phys. Rev. D18 (1978) 270.  
P. M. Fishbane and M. T. Grisaru, Phys. Lett. 74B (1978) 98.  
S. Matsuyama and H. Miyazawa, Prog. Theor. Phys. 61 (1979) 942.  
O. W. Greenberg and H. J. Lipkin, Nucl. Phys. A370 (1981) 349.
- 8) F. Lenz, T. Londergan, E. J. Moniz, R. Rosenfelder, M. Stingl and K. Yazaki, in preparation.
- 9) R. Tamagaki and H. Tanaka, Prog. Theor. Phys. 34 (1965) 191.  
S. Okai and S. C. Park, Phys. Rev. 145 (1966) 787.
- 10) K. Maltman and N. Isgur, Phys. Rev. Lett. 50 (1983) 1827.

- 11) A. T. Aerts and L. Heller, Phys. Rev. D25 (1982) 1365.
- 12) H. Miyazawa, Phys. Rev. D20 (1979) 2953.
- 13) B. L. Moiseiwitch, "Atom and Molecular Processes" (D. R. Bates, ed.)  
P. 280 - 333, (1962) Academic Press, New York
- 14) K. Masutani, private communication.

## P MATRIX ANALYSIS OF NUCLEON-NUCLEON SCATTERING

P. J. MULDER

Center for Theoretical Physics, Laboratory for Nuclear Science,  
Massachusetts Institute of Technology, Cambridge, MA 02139, U.S.A.

The P matrix is useful to establish the connection between the short range quark and gluon, and the long range nucleon and meson degrees of freedom which play a role in the interactions between hadrons. It can be used as a phenomenological tool in data parametrization but, more important, it contains information about the short range interaction.

### 1. INTRODUCTION

The theory for the strong interactions is believed to be quantum chromodynamics (QCD). Unfortunately we do not know how to solve it. We do know, however, some of its consequences. The theory is asymptotically free: quarks and gluons are almost free at short distances. Over distances larger than  $\Lambda_{\text{QCD}}^{-1} \approx 1$  fm, however, the theory becomes complicated. Color charges get screened because gluons themselves are charged. There may be a phase transition: (colorless) bubbles of the perturbative vacuum containing the valence quarks and gluons are emerged in the complicated global vacuum. In the perturbative vacuum inside the hadrons virtual quark-antiquark pairs can be created, which when they are colorless can leave the hadrons and become the virtual mesons that are exchanged between hadrons and that are responsible for the long range interaction.

The meson exchange picture has been very successful in explaining the low energy interaction between two nucleons. Beyond  $\sim 2.5$  fm this interaction is dominated by one pion exchange (OPE). The short range part of the interaction obviously is much more complicated, involving fusion and fission of two hadrons. Nevertheless, the interaction effectively may be described by meson exchange, even up to intermediate energies (momenta  $\sim \pi/R_H$ , where  $R_H$  is the hadron radius). Such a representation may be extremely useful in nuclear physics applications, but it will not lead to a more fundamental understanding. E.g. in a short range process as simple as an exchange of two gluons, not only  $q\bar{q}$ , but also  $q\bar{q}G$ -mesons and glueballs are exchanged in the baryon-baryon (BB) t-channel.

---

This research has been supported by the U.S. Department of Energy under contract DE-AC02-76ER03069.



The question thus arises how to describe the interaction using the proper degrees of freedom? Leaving out lattice calculations, there are two quark models that are "based on QCD" and have been extensively used to describe the spectrum and properties of hadrons, namely quark bag models and quark potential models. In both models attempts have been undertaken to understand the NN force. DeTar<sup>1</sup> calculated the energy of a bag in which the center of mass coordinates of the three quark clusters had been fixed. His calculations show that a six quark bag is unstable, since it is energetically favorable to form two nucleon clusters. The potential model calculations have one very serious drawback, namely the confining force generates a long range van der Waal's force that is quite different from the OPE force.

In both of the above calculations attempts to use the proper degrees of freedom for the short range part of the interaction, quarks (and gluons), have been made, but in both cases there is no way to get to the baryon and meson degrees of freedom for the long range part of the interaction. For instance in potential models the presence of a continuum of two gluon exchanges in the t-channel starting at  $t = 0$  is the reason for the van der Waal's force. The physics of the two gluons coalescing into (heavy) glueball mesons is missing. While there is not one model covering all interaction ranges, one needs to use different models for different regions and match the interactions. Here the P matrix as a specific example of a boundary condition matrix becomes useful.

## 2. THE P MATRIX

The use of boundary condition models is well known in nuclear physics (R matrix theory<sup>2</sup>) when it is convenient to describe the scattering of particles off nuclei in terms of eigenstates of the compound system. In the NN interaction an (almost) energy independent boundary condition (f matrix<sup>3</sup>) provided a good description of the core. The P matrix<sup>4</sup> is identical to the f matrix, but it is not the boundary condition at the core radius, but rather at the quark-gluon domain radius that is considered.

The P matrix is the logarithmic derivative of the (scattering) wave function or actually (in a spherically symmetric case) the function  $\phi(r) = u(r)/(2\mu)^{1/2}$ , where  $u$  is the radial wave function and  $\mu$  is the reduced mass in the scattering channel,

$$b(d\phi/dr)_b = P(s,b) \phi(b). \quad (2.1)$$

$P$  depends on the choice of boundary (matching radius  $b$ ) and the energy ( $s$  = center of mass energy squared). The poles in  $P$  correspond to solutions in the internal region ( $0 \leq r \leq b$ ) that satisfy a boundary condition,  $\phi_n(b) = 0$ . In the case of two body scattering, one can write down a once subtracted expansion,

$$P(s) = f + s \sum_n \frac{r_n}{s_n(s - s_n)} \quad (2.2)$$

An instructive example is the square well potential  $V(r) = -V_0$  for  $r \leq b$ ,  $V(r) = 0$  elsewhere. The natural choice of the boundary is the square well radius. Then the logarithmic derivative at  $b$  is  $P = k'b \cot(k'b)$  where  $k'^2 = 2\mu(E+V_0)$ . This has an expansion like (2.2) with  $f=1$  and  $k_n'^2 = n^2 \pi^2 / b^2$ .

From (2.1) one can deduce the relation between  $P$  and the scattering matrix  $S$ . In the absence of infinite range potentials, like Coulomb,

$$\phi(r) = k^{-1/2} (H_2 + H_1 S) \quad (2.3)$$

where  $H_1$  and  $H_2$  are those scattering solutions that approach free outgoing and incoming waves for  $r \rightarrow \infty$ ,

$$H_i(r) \rightarrow kr h_\ell^{(i)}(kr) \quad (2.4)$$

for  $i=1,2$ . From (2.1) and (2.3) it follows

$$P = x^{1/2} [H_2'(x) + H_1'(x) S] [H_2(x) + H_1(x) S]^{-1} x^{1/2} \Big|_{x=kb} \quad (2.5)$$

(Note  $xH'(x) \rightarrow b(dH/dr)_b$  if  $H$  is not a function of  $kr$ ). If there is no interaction for  $r > b$ ,  $H_1$  and  $H_2$  become equal to the Hankel functions for  $r > b$ . This was the case in our square well example, and for  $S$  waves (2.5) becomes

$$P = kb \cot(kb + \delta), \quad (2.6)$$

which is (with  $P$  in terms of  $k'$ , see above) the well known first year quantum mechanics solution for the square well  $S$ -wave scattering phase shift.

I will summarize the most important properties of  $P$ . For more details references 2-4 may be useful. Most properties are easily derived from (2.5) and the analytic properties of the  $S$  matrix and the scattering solutions.

- (a) The matrix  $P$  is symmetric and real for real energies ( $\text{Im } k^2 = 0$ ).
- (b)  $P$  has no cut for real energies and no two body threshold singularities. In general it has simple zero's and poles for real energies (see 2.2).
- (c) From the relation between  $P$  and  $S$ , and the fact that  $S$  is independent of  $b$ , one finds that for a pole in  $P$ ,  $P \approx r_n(b)/[s-s_n(b)]$ , the residue satisfies

$$r_n(b) = [-b(ds_n/db)] \times \text{projection operator}. \quad (2.7)$$

- (d)  $P$  satisfies the Wigner condition,

$$dP/ds \leq 0. \quad (2.8)$$

In the limit that  $P(r_0, s) = f = \text{constant}$ , the interaction is maximally nonlocal within  $r_0$ ; semiclassically there is an infinite signal velocity over this distance.<sup>3</sup> Note that for  $S$  waves (2.6) and (2.8) imply  $d\delta/dk \leq r_0$ . For the equal sign this means semiclassically that the scattered wave starts to emerge when the center of the incoming wave packet is still a distance  $r_0$  from the target.

### 3. QUARK BAGS AND THE P MATRIX

Bag models led in a natural way to the prediction of colorless multiquark states, e.g. six quark states. The absolute confinement that is imposed on the quarks, however, is not correct, since in general fission into colorless subsystems is not prohibited. Jaffe and Low<sup>4</sup> (JL) pointed out that the multiquark states (e.g.  $q^6$ ) correspond to P matrix poles in the corresponding scattering channels (e.g.  $(q^3)(q^3) = BB$ ).

The position of the poles in P depend on the matching radius  $b$ . At this radius a condition on the BB wave function is imposed. In the MIT bag model confinement is achieved by a (linear) boundary condition on the Dirac spinors. JL proposed to compare the density of two clusters (with  $N_1$  and  $N_2$  quarks respectively) in an N-quark bag with the density of a confined BB wave function  $\phi(r) \sim \sin(\pi r/b)$ . This yields

$$b \approx 1.37 (N/(N_1 N_2))^{1/2} R, \quad (3.1)$$

where  $R$  is the N-quark bag radius.

If the pole position is known as a function of  $b$ , an estimate of the residue can be obtained from (2.7). For values of  $b$  less than the value corresponding to  $R_m$ , which minimizes the bag energy, one then obtains  $-b(ds_o/db) = 2M(M - 4BV)$ , where  $M$  is the bag mass at  $R$  corresponding to  $b$ ,  $s_o = M^2$ , and  $BV$  is the bag volume energy. This estimate will be reliable for  $R \ll R_m$  (and then becomes essentially  $2s_o$ ), but it is not reliable for  $R \approx R_m$ , where it gives zero. Since the system can fission into color singlet clusters, the volume term should not be present for them. JL showed that without seriously affecting the bag mass, this leads to  $r(b) \approx 1.5 s_o(b) \xi_o \xi_o$ , where the  $\xi_o$ 's are the fractional parentage coefficients for the  $q^6$  wave function,  $|q^6\rangle = \sum_i \xi_i |BB\rangle_i$  (the sum runs over color singlet (o) and color octet (c) channels). Therefore, an estimate for values of  $b$  corresponding to  $R \leq R_m$  is

$$r(b) \approx (1.5 - 2) s_o(b) Q \quad (3.2)$$

where  $Q$  is a projection operator onto all BB channels ( $Q_{ij} = \xi_i \xi_j$ ).

At this stage it is necessary to consider the fact that many channels are closed channels, i.e. the energy is below the thresholds for those channels (for instance color octet channels). Only in the open channels scattering can take place and only a (unitary) submatrix  $S_{oo}$  of the S matrix is relevant. The P matrix in the open channels, related to this submatrix through (2.5) is called the reduced P matrix  $\tilde{P}_{oo}$ ; it is related to the full P matrix by

$$\tilde{P}_{oo} = P_{oo} - P_{oc} [P_{cc} - x_c H_c^1 H_c]^{-1} P_{co}, \quad (3.3)$$

where  $H_c$  is the outgoing wave in the closed channel (exponentially damped). Because  $-x_c H_c^1 H_c$  is usually positive ( $\kappa b$  for  $H_c(i\kappa r) = \exp(-\kappa r)$ ) the pole in the reduced P matrix is in general lower than the real P matrix pole. In the

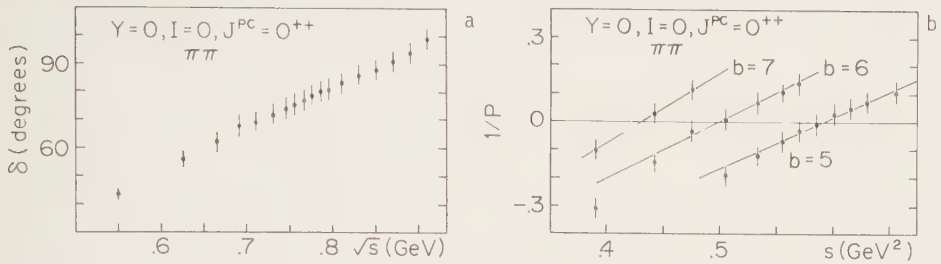


FIGURE 1

A smooth  $\pi\pi$  S-wave phase shift (a) and the poles in  $P$ , shown as zero's in  $1/P$ (b) for  $b = 5, 6$ , and  $7 \text{ GeV}^{-1}$  (see ref. 4 for details).

case that all closed channels are far removed the reduced  $P$  matrix becomes the restriction of the real  $P$  matrix to the open channels.

#### 4. REVIEW OF ANALYSES OF SCATTERING DATA

The  $P$  matrix may be obtained from the  $S$  matrix (2.5), if the latter is completely known. This has been applied to meson-meson,<sup>4</sup> baryon-meson,<sup>5</sup> and baryon-baryon<sup>6,7</sup> channels. The method is illustrated for a  $\pi\pi$  S-wave channel in fig. 1. The smooth (structureless) phase shift in (a) yields clear poles in  $P$  (b). The results will be discussed in section 5.

In many cases the complete  $S$  matrix is not known, and (2.5) cannot be used. The solution is well known from e.g. baryon spectroscopy. One assumes a parametrization for the  $S$  matrix and fits the parameters to the available data. Grach et al.<sup>8</sup> have used such an  $S$  matrix parametrization of the coupled  $NN(^1D_2) - N\Delta(^5S_2)$  system to obtain the  $P$  matrix (see section 5 for the results).

Instead of parametrizing  $S$  one also can parametrize  $P$ . As has been pointed out independently by Mulders<sup>9</sup> and Jaffe<sup>10</sup>, the starting point for such a parametrization should be the  $P$  matrix for the no-scattering case ( $S = 1$ ); from (2.5) one sees that then  $P = P^{(0)}$ , where

$$P^{(0)} = kb \frac{j'_\ell(kb)/j_\ell(kb)}{S\text{-wave}} - kb \cot(kb). \quad (4.1)$$

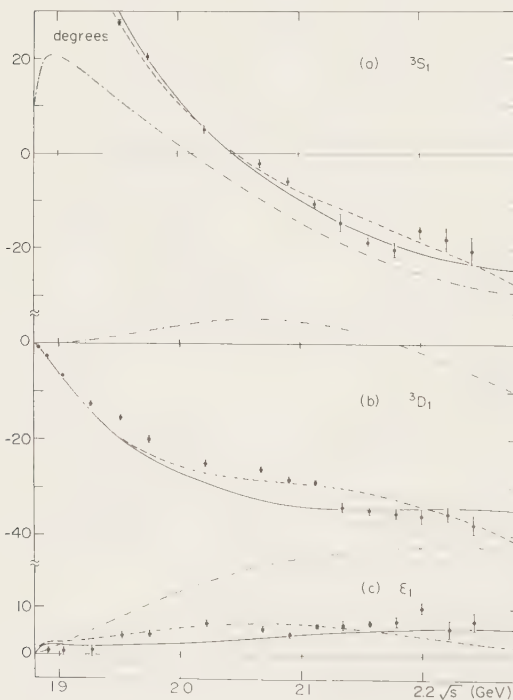
This  $P^{(0)}$  matrix already has an infinite number of poles (called compensation poles). To obtain a parametrization for  $P$  one modifies the constant and the relevant poles in  $P^{(0)}$ . As an example, for  $b = 6 \text{ GeV}^{-1}$  the only relevant compensation pole in  $NN$  scattering is the S-wave pole at  $2.15 \text{ GeV}$ , so for the  $NN \ ^3S_1 - ^3D_1$  wave a good parametrization may be

$$P = \begin{bmatrix} x \cot(x) - \frac{2\pi^2}{x^2 - \pi^2} & 0 \\ 0 & x j_2'(x)/j_2(x) \end{bmatrix} + f + \frac{r}{s - s_0} \quad (4.2)$$

where  $x=kb$ , and  $f$  and  $r$  are  $2 \times 2$  matrices. At low enough energies a one pole approximation (without higher compensation poles) for  $P$  still gives a good result. The results are shown in fig. 2. One pole approximations to  $P$  have been used by Simonov<sup>11</sup> for NN S-waves. Forms like in (4.2) have been used by Jaffe<sup>10</sup> for the  $I = 2 \pi\pi$  S-wave, and by Mulders<sup>12</sup> for various nonstrange baryon-baryon waves. An example for the NN  ${}^3S_1$ - ${}^3D_1$  waves is shown in fig. 2 (see ref. 7 for details).

Two remarks should be made at this point. About the long range interaction: in order to find the  $P$  matrix which connects to the interaction for  $r < b$ , one has to include the long range interaction. Without accounting for it  $P$  in general will violate the Wigner condition (2.8), especially at low energies.

Secondly, about the poles that are put in the parametrization: in the baryon number 1 systems the compensation poles in the BM system are identified with confined  $q\bar{q}$  states. Of course also excited  $q^3$  states will show up in an analysis. They are not accounted for by modifying compensation poles, but by putting in *additional* poles. As an example, the  $P$  matrix for the  $N\pi$  P33 wave



in the  $\Delta$ -resonance region is accurately parametrized by the form  $P = kb j_1'(kb)/j_1(kb) + f + r/(s-s_0)$  for  $b = 6 - 7 \text{ GeV}^{-1}$  (e.g. for  $b = 6.5 \text{ GeV}^{-1}$ ,  $f = -0.16$ ,  $r = 0.46 \text{ GeV}^2$  and  $\sqrt{s_0} = 1.31 \text{ GeV}$ ). Noteworthy is also the fact that the  $P$  matrix automatically gives the correct threshold behavior. No barrier factors are needed in the residue! In the MM systems additional poles are necessary for excited  $q\bar{q}$ -mesons and possibly glueballs.

FIGURE 2  
P matrix parametrization (4.2) for the NN  ${}^3S_1$ - ${}^3D_1$  waves (solid line). A one pole approximation has also been shown (dashed line). A long range OPE potential has been taken into account. The dot-dashed line shows how the (solid line) result changes when the external potential is taken zero.

## 5. DISCUSSION OF THE RESULTS

In this discussion I will consider a few specific examples. Comparisons are made with the MIT bag model.<sup>13</sup> The first example is the  $\pi\pi$  S-wave, considered in fig. 1 of section 4. The P matrix pole position and residue for values of  $b$  between 4 and 10  $\text{GeV}^{-1}$  are shown in fig. 3; it has been assumed that there is no interaction for  $r > b$ , so (2.6) is valid. The lowest bag state (marked  $q^2\bar{q}^2$ ) has  $M = 0.65 \text{ GeV}$ , and  $R = 4.4 \text{ GeV}^{-1}$ . From section 3 we thus expect a pole in  $P$  at this energy for  $b = 6.1 \text{ GeV}^{-1}$  with a residue  $r \approx 0.3 \text{ GeV}^2$  ( $\xi_{\pi\pi}^2 = 0.41$ ). This last estimate is obtained from (3.2) and assumes that the reduced  $P$  is the restriction of  $P$  to the open channels. The agreement between the predictions and the experimental results is very reasonable.

If the  $\pi\pi$  system matches on to a  $q^2\bar{q}^2$  bag at  $6 \text{ GeV}^{-1}$ , one cannot go to smaller  $b$  values and determine the position and residue without taking the residual interaction for  $r > b$  into account. Nevertheless, there probably is a transition region in which the results still make sense, since the scattering structure at some energy  $E$ , e.g. a pole in  $P$ , will not significantly change before the strength of the residual interactions becomes comparable to the energy difference between pole and threshold.

It is interesting to compare the position of the pole in  $P$  with that of the lowest pole in  $P^{(0)}$  (compensation pole). The pole in  $P$  is considerably lower, due to the strong one gluon exchange (OGE) attraction in the  $q^2\bar{q}^2$  system. This is reflected as an attractive phase shift as can be seen from (2.6): since the pole is at  $kb < \pi$ , we must have  $\delta > 0$  at that energy.

The next examples are the NN S-waves. The positions and residues for the lowest pole in  $P$  are shown in figs. 4 and 5. For large values of  $b$  the pole positions are the same as for the compensation poles. This is what we expect, since short range repulsive effects barely alter the pole positions for large  $b$  and the pion exchange interaction is very weak on the scale in figs. 4 and 5; indeed, we see (figs. 4, 5) that inclusion of the OPE interaction for  $r > b$  does

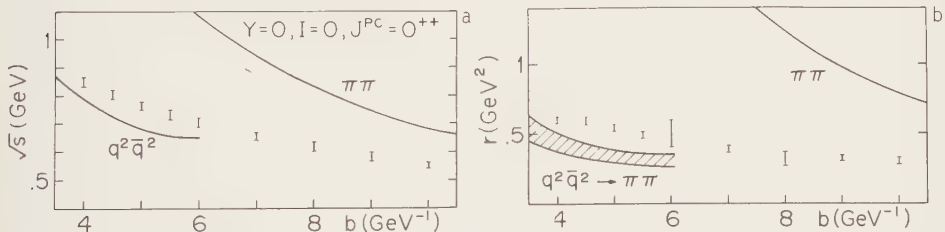


FIGURE 3

Lowest pole in  $P$  for  $I = 0, \pi\pi$  S-wave, compared with compensation pole ( $\pi\pi$ ) and bag model predictions ( $q^2\bar{q}^2$ ). (a) Pole position, (b) residue of pole.

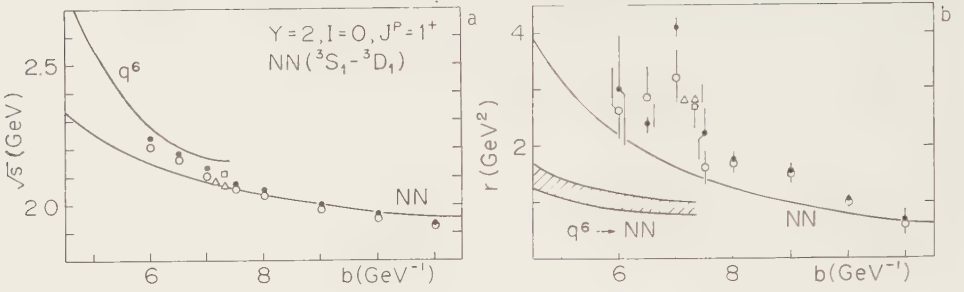


FIGURE 4

Lowest pole in P for  $(I, J^P) = (0, 1^+)$  NN channels, compared with compensation pole (NN) and bag model predictions ( $q^6$ ). Circles are our points (open/filled are without/with OPE from phase shifts in ref. 14), triangles from ref. 11, squares from ref. 6. (a) Pole position, (b) total residue of pole (without potential  $\xi_D^2 \approx 0.04$ , with potential  $\xi_D^2 \approx 0.14$ ).

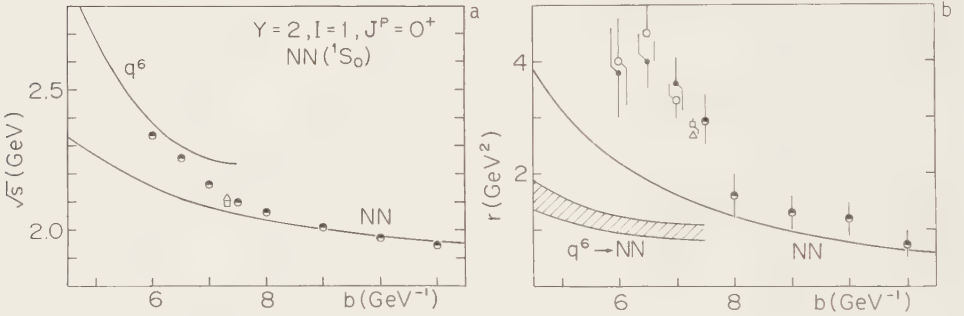


FIGURE 5

see caption of fig. 4, but for  $(I, J^P) = (1, 0^+)$  NN channel.

not significantly change the pole parameters (especially for the  $1S_0$  wave the effect is extremely small). The influence of different NN potentials has been considered in ref. 15. The bag model predictions for the positions of the pole are in good agreement with the experimental positions. We see a gradual transition from the NN compensation mass to the  $q^6$  bag mass going from  $b = 8$  to  $b = 6$  GeV $^{-1}$ . The difference in energy for the poles in triplet and singlet S-waves agrees nicely with the difference between bag masses due to OGE interaction. The residues do not agree with the predicted residue for bags. Of course, inside the bag the quarks not only couple to NN ( $\xi_{NN}^2 = 1/9$ ), but also to  $\Delta\Delta$  ( $\xi_{\Delta\Delta}^2 = 4/45$ ), and color octet channels ( $\xi_{CC}^2 = 4/5$ ). It is, however, not possible to get an enhancement for NN in the reduced P matrix by taking into account the presence of closed channels through (3.3) without having ridiculously large values for the constant matrix  $f^7$ . More likely, the



enhancement indicates that for the largest cluster separations in the bag the color singlet clusters are dominant. Noteworthy is that there was no such enhancement in the  $\pi\pi$  S-wave (fig. 3). This difference can be understood mathematically: because of (2.7) the enhancement is stronger for a multiquark bag with mass higher than the compensation mass; it also can be understood physically,<sup>16</sup> since the repulsive OGE will enhance color singlet correlations.

Next, consider the coupled  $NN(^1D_2) - N\Delta(^5S_2)$  system (fig. 6). Between  $b = 8$  and  $9 \text{ GeV}^{-1}$  the NN D-wave and  $N\Delta$  S-wave compensation poles cross (at  $\sqrt{s} \approx 2.29 \text{ GeV}$ ). This is also observed in the residues of the poles. For  $b > 9 \text{ GeV}^{-1}$   $r_{N\Delta} \ll r_{NN}$ , while for  $b < 8 \text{ GeV}^{-1}$   $r_{NN} \ll r_{N\Delta}$ . Because of the coincidence of the bag mass and the  $N\Delta$  compensation pole (both position and residue) no striking effects of the six quark system are expected.

As a last example consider the H dibaryon ( $Y = I = 0, J^P = 0^+$ ), which couples to the  $\Lambda\Lambda$ ,  $\Xi N$ , and  $\Sigma\Sigma$  S-waves ( $\epsilon_{\Lambda\Lambda}^2 = 1/40$ ,  $\epsilon_{\Xi N}^2 = 1/10$ ,  $\epsilon_{\Sigma\Sigma}^2 = 3/40$ ). The bag model predicts a bound state (fig. 8). So far there is no evidence for this. A possible trajectory for position and residue in the three channel P matrix is shown in fig. 7. Noteworthy is that a pole at  $b = 6 \text{ GeV}^{-1}$  with  $\sqrt{s}_0 = 2.3 \text{ GeV}$  (above  $\Lambda\Lambda$  threshold) and  $r = 1 \text{ GeV}^2$  still does give a bound state.

Summarizing, the P matrix yields information about the short range, which is relevant for our knowledge of the interactions between quarks. Exotic channels, like NN, that do not couple to resonances through  $q\bar{q}$  annihilations, are particularly useful. The data seem to indicate that for  $b \approx 6 \text{ GeV}^{-1}$  color singlet correlations are important. One, thus, may want to evaluate P at a smaller radius, where a simpler bag description may work<sup>17</sup> but this implies more complicated residual interactions between the baryons. What is more challenging in view of the elementarity of the interactions is trying to improve the understanding of the interactions in terms of the quarks.

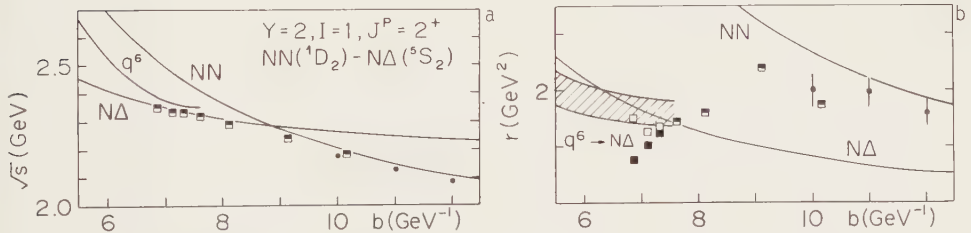


FIGURE 6  
Lowest pole in P for  $(I, J^P) = (1, 2^+)$  NN -  $N\Delta$  system, compared with compensation poles (NN,  $N\Delta$ ) and bag model predictions. Squares are from ref. 8. (a) Pole position, (b) total residue of pole (see ref. 8 for  $r_{NN}$  and  $r_{N\Delta}$  separately).

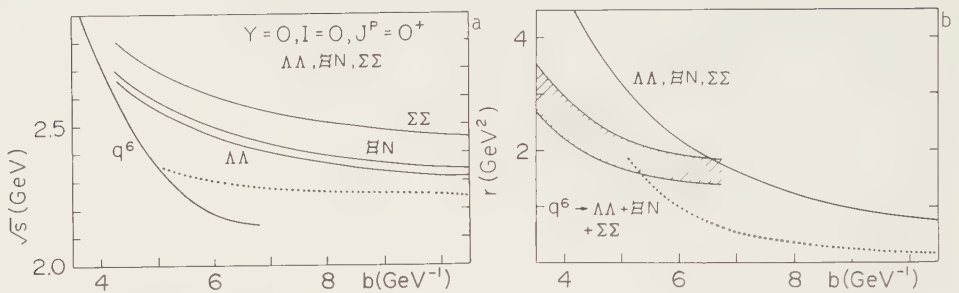


FIGURE 7

Bag model predictions for H dibaryon and the S-wave compensation poles. One out of many possible trajectories for  $s_0(b)$ , and corresponding  $r(b)$ , that would correspond to a bound state at the  $\Lambda\Lambda$  threshold, is shown (dotted lines).

## REFERENCES

- 1) C. DeTar, Phys. Rev. D17 (1978) 323, and D19 (1979) 1451.
- 2) see review by A.M. Lane and R. G. Thomas, Rev. Mod. Phys. 30 (1958) 257.
- 3) H. Feshbach and E. L. Lomon, Ann. Phys. (N.Y.) 29 (1964) 19.
- 4) R. L. Jaffe and F. E. Low, Phys. Rev. D19 (1979) 2105.
- 5) C. Roiesnel, Phys. Rev. D20 (1979) 1646.
- 6) R. L. Jaffe and M. Shatz, Caltech report CALT-68-775 (unpublished).
- 7) P. J. Mulders, Phys. Rev. D28 (1983) 443.
- 8) I. L. Grach, I. M. Narodetsky and M. Zh. Shmatikov, ITEP report ITEP-32 (1983).
- 9) P. J. Mulders, Phys. Rev. D25 (1982) 1269
- 10) R. L. Jaffe in: Proceedings of 1981 International Symposium on Lepton and Photon Interactions at High Energies, ed. W. Pfeil (University of Bonn, Bonn, 1981), p. 395.
- 11) Yu. A. Simonov, Phys. Lett. 107B (1981) 1.
- 12) P. J. Mulders, Phys. Rev. D26 (1982) 3039.
- 13) T. A. DeGrand et al., Phys. Rev. D12 (1975) 2060; R. L. Jaffe, Phys. Rev. D15 (1977) 267 and 281; R. L. Jaffe, Phys. Rev. Lett. 38 (1977) 195; A. T. Aerts, P. J. Mulders and J. J. de Swart, Phys. Rev. D17 (1978) 260.
- 14) R. A. Arndt et al., Phys. Rev. D28 (1983) 97.
- 15) B. L. G. Bakker and M. van der Velde, this conference.
- 16) R. L. Jaffe, private communication.
- 17) E. L. Lomon, private communication, Phys. Rev. D26 (1982) 576, and this conference.

# NUCLEON-NUCLEON INTERACTION AND THE QUARK-COMPOUND-BAG (QCB) MODEL

Yu. A. Simonov, ITEP, Moscow

Recent results for NN interaction in the QCB model are reviewed including the P matrix NN analysis as a tool of the QCB potential construction, admixture of six quark bags in nuclei, weak NN QCB interaction.

## 1. INTRODUCTION

The nature of NN interaction still is an open question, especially at small distances,  $r < 1F$ , where nucleon bags overlap. We all believe now that QCD lies at the foundation of strong interaction and gluon and quark degrees of freedom play crucial role for very small distances<sup>1</sup>. A fundamental question arises: can one explain NN forces in terms of quark and gluon degrees of freedom and interaction between them? Three main directions are used nowadays to answer this question:

- i) "energy deformation method", in the framework of the MIT-bag picture<sup>2</sup>;
- ii) nonrelativistic (constituent) quark model (NQM)<sup>3</sup>;
- iii) the QCB model<sup>4,5,6,7,8,9,10,11,12</sup>.

It is the purpose of this talk to answer the above question in the framework of the QCB model. For detailed analysis of experimental data and additional formulas the reader is referred to an extended version of this talk<sup>12</sup>.

## 2. OUTLINE OF THE MODEL

There are two basic observations in the physical picture of the QCB model: i) when two nucleon bags overlap a new 6q bag is formed, ii) two nucleons exist inside the 6q bag (we shall call it QCB throughout the paper), as a  $N(3q)N(3q)$  term in the formal cluster decomposition of the QCB wave function (w.f.). In this way the NN w.f. is made continuous both inside and outside of the QCB.

In the first version<sup>4-6</sup> of the QCB model only the point i) was taken into account in the two-channel approach. An additional (but

not necessary) assumption was made in<sup>4-12</sup> and will be pursued throughout this talk for simplicity reasons; namely:

iii) the transition of NN into the QCB takes place in the narrow region at the boundary of the QCB, we call this distance between nucleon bags a "transition radius"  $r = b \approx 1.14R_{6q} = 5.7M^{1/3} \text{ GeV}^{-1}$  13-14. For  $M = 2 \text{ GeV}$  we get  $b' = 1.44F$ .

In what follows I present the latest version of the QCB model 8,12 incorporating i) and ii), which contains as a limiting case the first version<sup>4-6</sup>; the assumption iii) will be done at the final stage to get explicit results. For details of derivation see 8,12.

We write the 6q w.f. as in the resonating group formalism (RGF) 15

$$\Psi = \Psi_q + \Psi_{cl}; \quad \Psi_{cl} = A \{ \phi(r) [\psi_N(3q) \psi_N(3q)]_{S,I} \} \quad (1)$$

where  $\Psi_q$  is the w.f. of QCB, while  $\Psi_{cl}$  describes motion of two nucleons - 3q clusters.  $\Psi_{cl}$  is fixed by its asymptotics,  $\Psi_q$  is necessary in (1) since physically at  $r < b$  colored clusters (and gluons) are present not taken into account in  $\Psi_{cl}$ . The resulting equation for the w.f. of the NN relative motion  $\phi(r)$  is obtained in the usual RGF<sup>15</sup>

$$(T - E + V + V_{NqN}) \phi = 0, \quad (2)$$

where  $V$  is in general a nonlocal interaction comprising the direct and crossed contributions from qq potentials, while  $V_{NqN}$  is due to the intermediate QCB formation. We approximate  $V$  outside of QCB by an OBEP, whereas inside the QCB nucleons exist only as an intrinsic part of QCB w.f. and the qq interaction is already taken there into account. Hence we can write:

$$V(r) = V_{OBE}(r) \Theta(r - b). \quad (3)$$

$\Psi_q$  can be decomposed into a sum of the QCB eigenfunctions  $\Psi_n$  (with energy eigenvalues  $E_n$ ),  $n = 1, 2, \dots$ . For  $\Psi_n$  one can use the cluster expansion<sup>16</sup> ( $i$  denotes the type of 3q clusters,  $i = N, \Delta, C$ )

$$\Psi_n = \sum_i \phi_{i1}(123) \phi_{i2}(456) y_n^i(R_{123,456}) g_n^i \quad (4)$$

$y_n^i$  and its radial part  $\eta_n^i(r)$  is the normalized w.f. of cluster-cluster motion,  $g_n^i$  is the c.f.p., measuring the probability amplitude of clusters  $i$  inside the QCB w.f. in the state  $n$ . For the  $s^6$  state  $g_n^i$  was calculated in<sup>16</sup>; in the case of NN clusters the result is  $|g^{NN}|^2 = 0.11$ , whereas  $|g^{CC}|^2 \approx 0.8$ .

We should stress, that the 80% probability of colored clusters means that the QCB w.f.  $\Psi_n$  is much different from  $\Psi_{cl}$  and contains additional degrees of freedom which should be taken separately, as e.g. in (1). Below we show that the presence of QCB explains main features of NN interaction, both apparent repulsion at smaller distances and attraction at intermediate distances, the role of external OBE interaction being the subsidiary one. The main part,  $V_{NqN}$  is given by<sup>8</sup>:

$$V_{NqN}(\vec{r}, \vec{r}') = \frac{1}{rr'} \sum_n Y_{JM\ell S}^* \frac{f_n^*(r, E) f_n(r', E)}{E - E_n} Y_{JM\ell S} \quad (5)$$

$Y_{JM\ell S}$  are the spin-angular normalized w.f., while

$$f_n(r, E) = -c_n a_n(r) + x_n \eta_n(r)(E_n - E) \Theta(b - r). \quad (6)$$

Here  $\eta_n$  normalized as  $\int_0^b [\eta_n(r)]^2 dr = 1$ ,  $x_n = \sqrt{10} g_n^{NN}$ , and  $c_n$  is a real constant, giving the probability amplitude for the transition  $NN \rightarrow$  QCB at the boundary of the QCB; we take for simplicity  $a_n(r) = \delta(r - b)$ .

### 3. PROPERTIES OF THE NN POTENTIAL IN THE QCB MODEL

The total NN interaction is according to (3), (5) (apart from angular factors):

$$V_{NN} = V_{OBE} \Theta(r - b) + \sum_n \frac{f_n^* f_n}{E - E_n} \quad (7)$$

If  $X(r)$ ,  $Y(r)$  and  $G(r, r')$  denote the regular, irregular solutions and the Green function for the Schroedinger equation (S.eq.) with  $V_{NN} = V_{OBE} \Theta(r - b)$ , then the general solution of S.eq. with interaction (7) can be written as (we keep in the sum (5) for simplicity only one QCB term)

$$\phi(r) = X(r) + \frac{\int G(r, r') f_n(r') dr' + \int f_n(r) X(r) dr}{E_n - E - \iint f_n(r) G(r, r') f_n(r') dr dr'} \quad (8)$$

From (6) and (8) one can deduce the following properties of the NN w.f.  $\phi(r)$  <sup>4, 5, 8</sup>:

- a)  $\phi(r) = 0$  for  $E = E_n$  and  $r \leq b$  ;
- b) at  $E = E_n$  the P matrix has a pole:

$$P(E) = \frac{\phi'(r)}{\phi(r)} \Big|_{r=b+\delta, \delta>0} = \frac{Mc_n^2}{E - E_n} + P_0 \quad (9)$$

The first property means that the interaction (7) acts as an infinite core inside QCB for  $E = E_n$ . Even for  $E \neq E_n$ , e.g.  $E = 0$ , the w.f. is strongly suppressed for  $r \leq b$  if  $c_n$  is large. When the NN-QCB transition is not sharp, i.e.  $a(r)$  is smeared off near  $r = b$ , the w.f. is nearly zero inside QCB for  $E = E_n$ . The physical reason of this w.f. damping is that  $V_{NqN}$  acts as a barrier, preventing nucleons from entering the QCB. Thus  $V_{NqN}$  constitutes a universal mechanism for the NN repulsive core: the main ingredient is the existence of the strong (large  $c_n$ ) NN-QCB transition to a nearby QCB state with energy  $E_n$ . A similar repulsion exists in the  $I = 2\pi\pi$  system, where  $c_n$  is also large, whereas in the  $I = 1\pi\pi$  system  $c_n$  is small and repulsion is restricted to a narrow region near the  $\rho$ -meson mass. All that is in contrast to a suggested in <sup>17, 18</sup> nonuniversal explanation of the NN repulsive core, based on the specific role of the  $s^4p^2$  state.

The property b), Eq. (9), is the basis of the P matrix analysis, which enables one to find  $E_n$  and  $c_n$  from experiment, as was originally suggested by Jaffe and Low <sup>13</sup>. The QCB model is to our knowledge the only explicit model, which realizes the fruitful idea of the P matrix analysis given in <sup>13</sup>. Other important properties of  $V_{NN}$  (7) are: it is nonlocal (separable) and strongly energy dependent. Since the lowest QCB states for NN are widely separated in energy  $|E_2 - E_1| \gtrsim 0.5$  GeV, one can retain in the sum (7) one or two terms. For  $x_n = 0$  we obtain the first version of

the QCB model<sup>4</sup>, in that case it was realized that one should add to  $V_{NqN}$  some additional interaction inside QCB, linear in energy to reproduce the  $^1S_0$  and  $^3S_1$  data. It is rewarding to obtain exactly this term from the correct treatment of QCB, as is exemplified by (7).

#### 4. P MATRIX ANALYSIS AND THE QCB MODEL

P matrix analysis plays a special role in the QCB model since it enables to obtain all QCB potential parameters from the experiment. The P matrix analysis is to be done using the experimental phase shifts and solutions in the chosen OBEP at  $R < r < \infty$ , to find "experimental" P matrix at  $r = R$ . This can be compared to the theoretical P matrix, found from the potential (7). The latter depends on the function  $\eta_n(r)$ . A convenient choice for  $\eta_n(r)$  is

$$\eta_n(r) = N_n j_\ell(\beta_n r) \beta_n r \quad (10)$$

where  $N_n$  is defined by the normalization condition and  $j_\ell$  is the Riccati-Bessel function. The OBE parameters are held fixed and the parameters to be found from the fit to the experiment are  $E_n$ ,  $c_n$ ,  $x_n$ ,  $b$  and  $\beta_n$ .  $E_n$  and  $c_n$  can be found from the P matrix analysis in a narrow energy region around a P-matrix pole, as was done first for the NN case by Jaffe and Shatz<sup>14</sup> and demonstrated a good agreement of  $E_n$  with MIT predictions. Next step was done in<sup>4</sup> where the representation (9) with  $P_0 = \text{const}$  was used in the energy region  $0 \leq T_L \leq 515$  MeV to describe the experimental S-wave data with good accuracy. The value of  $P_0$  was found from the position of the deuteron (or singlet deuteron) pole. No OBE part was used in<sup>4</sup> and<sup>14</sup>. In<sup>4</sup> the agreement was worse with low energy data ( $T_L < 10$  MeV) and  $r_{\text{eff}}$  value (15% too low as compared to exp.), suggesting the importance of OBE contribution in that region. We note at this point, that  $b$ , as a transition radius, is of course fixed at some physical value, but the P matrix analysis can be done at any radius  $R$ , in general  $R \neq b$ , and  $E_n$  is a function of  $R$ ,  $E_n = E_n(R)$ . Only at  $R = b$ ,  $E_n(b)$  should be compared to the MIT-bag energy values. At present there are extended P matrix analysis done by several groups<sup>19-25</sup>. The main conclusion of<sup>20</sup> is that the type of OBE is not essential for pole characteristics in agreement with<sup>14</sup>. The results of<sup>21,24,25</sup> display a strong dependence of  $E_n(R)$  on  $R$ . This fact was exploited further in<sup>23</sup>



to define the transition radius  $b$  : the curves  $E_n(R)$  and  $c_n^2(R)$  obtained in a potential model close to (7) strongly change their behaviour at  $R \approx b$  and  $\frac{\partial}{\partial R} c_n^2(R)$  even has a bump at this point.

Inelasticity in the  $^1S_0$  channel was treated in<sup>24</sup> as due to  $^5D_0$  NA channel and the inclusion of the latter was shown to influence strongly the pole position. The important point discovered in the analysis of single channels<sup>21</sup> and coupled  $^3S_1$ - $^3D_1$  channels<sup>22</sup>, is that the sign of  $\frac{\partial P}{\partial E}$  may be positive at  $T_L \leq 100$  MeV in contradiction with the Wigner condition, as discussed in<sup>24</sup>.

A small change in phases and mixing parameters usually cures the situation<sup>22,26</sup>, in this way the P matrix analysis may serve as an indicator of data accuracy. An extended review of the work done at ITEP and The Free University of Amsterdam is contained in<sup>28</sup>, where also further discussion of the Wigner condition violation can be found. For the  $^3S_1$  -  $^3D_1$  waves the P matrix analysis<sup>22</sup> done at  $R = 1.44F$  finds only one pole for each element ( $P_{11}$ ,  $P_{12} = P_{21}$ ,  $P_{22}$ ) at the same energy. It is in agreement with the QCB model, where the pole is due to one and the same QCB state with energy  $E_n$ , coupled to both  $^3S_1$  and  $^3D_1$  waves. In contrast to that, in the general matrix potential one gets two poles in each channel; thus the analysis<sup>22</sup> confirms the validity of the QCB model in this case.

## 5. SOME EXPLICIT EXAMPLES OF THE QCB NN POTENTIAL

Already the early BCM P matrix analysis has revealed<sup>24</sup> that the data up to  $T_L \approx 300$ -400 MeV are in agreement with the constant value of the  $P = P_0$ . On the other hand, as was shown in<sup>27</sup> for that the internal potential should grow linearly in energy  $E$  with a coefficient close to one. That kind of internal potential ( $r \leq 0.8F$ ) was used in Paris potential<sup>28</sup> on phenomenological grounds. The QCB potential (7) provides a clue to this energy dependence. From (6) and (7) one can see that  $V_{NN}$  contains a linear energy dependence with a coefficient  $E x_n^2 \eta_n(r) \eta_n(r') \Theta(b-r) \Theta(b-r')$ . Since  $\eta_n$  are normalized to one, one needs  $x_n^2 = 1$  to get the constant  $P_0$ <sup>8</sup>. Now using the theoretical value of  $g^{NN}$ <sup>16</sup> we obtain  $x_n^2(\text{theor}) = 1.1$ . Thus the quark structure of QCB, used in<sup>16</sup>, may explain the observed energy dependence of the NN interaction. (Note, that real experimental value of  $x_n^2$  should be smaller than the theoretical one due to deformation of nucleon clusters inside

QCB not taken into account in<sup>16</sup>).

The value  $x_n^2 = 1$  was used to construct the simplified version of the  $^3S_1$  and  $^1S_0$  NN potentials in<sup>8,12</sup>. Those potentials reproduce the experimental phase shifts with 10%-15% accuracy in the energy interval  $0 < T_L < 515$  MeV. Note that these potentials do not contain the OBE part, so the nontrivial conclusion is that one can describe the NN interaction in S-waves using QCB term only. In a more elaborated version  $x_n^2$  is taken as a fitting parameter together with  $\beta_n$ ,  $c_n$ ,  $E_n$ ,  $b$ . Work in this direction for lowest NN waves is in progress.

## 6. ADMIXTURE OF QCB IN NUCLEI

The "static" admixture in deuteron is defined by normalization as follows:

$$B_{QCB} = \frac{\int |\Psi_q|^2 d\tau}{\int |\Psi|^2 d\tau} = \sum_n B_{QCB}^n \quad (11)$$

where

$$B_{QCB}^n = \left[ x_n \int_0^b \eta_n(r) \phi_d(r) dr + \frac{c_n}{E_d - E_n} \phi_d(b) \right]^2. \quad (12)$$

Using the parameters of the  $^3S_1$  QCB potential and the deuteron w.f. from<sup>8</sup> we obtain

$$B_{QCB} \approx (0.53 - 0.37)^2 = 2\% \quad (13)$$

Note that this small number is a result of a strong cancellation between the "volume" and "boundary" terms in (12). It is curious, that all NN interaction is here due to QCB in contrast with the small admixture (13). Analogously, for a nucleus, assuming the Fermi-gas model, we obtain for the  $^3S_1$  type of QCB and a set of realistic QCB parameters

$$B_{QCB}(A) \approx (1.3 - 1.9) 10^{-2} A \quad (14)$$

## 7. P-MATRIX POLES AND DIBARYONIC RESONANCES

There is a simple connection between S and P matrices, e.g.

see (A.1) of<sup>12</sup> and if one disregards OBEP and uses (9) with  $P_0 = \text{const}$ , one can obtain a simple connection between a P-matrix pole and S-matrix pole. For  $^3S_1$  wave it was found in<sup>7</sup> that the S matrix contains 3 poles, two of them correspond to a dibaryon with a very large width,  $E_p = 147 \pm i218$  MeV, the third is a deuteron pole. For the  $^1D_2$  state the P-matrix analysis<sup>21</sup> reveals a pole in the P matrix at  $\sqrt{s} = 2.33$  GeV in agreement with MIT prediction and the corresponding pole in the S-matrix is at  $M_R - \frac{i\Gamma}{2} \approx 2.16 - i0.07$  GeV. A similar situation occurs for the  $^3F_3$  state. In addition in  $^1D_2$  and  $^3F_3$  there are nearby pseudoresonances due to  $\Delta N$  intermediate state, so to a dibaryonic state there correspond a P matrix pole, an S matrix pole and a pseudoresonance.

#### 8. RELATIVISTIC EFFECTS AND OTHER SYSTEMS

Relativistic treatment of S and P waves was done in<sup>29</sup>, the role of P matrix poles played by CDD poles, with good description of data up to  $T_L = 1$  GeV. Poles in the YN and YY systems have been treated in<sup>30</sup> in the same way as the NN system in<sup>7</sup>. The P matrix analysis of KN system in terms of QCB parameters was done in<sup>31</sup>.

#### 9. PARITY VIOLATING (PV) NN FORCES

The calculation of PV NN amplitudes in the QCB model was done in<sup>9-10</sup> for PV NN asymmetry and in<sup>11</sup> for PV effects in thermal neutron capture by protons. It is an important check of the model, since no parameters are introduced for PV amplitude in addition to known parity conserving NN QCB parameters, provided known Weinberg-Salam Lagrangian is used. Unfortunately two near QCB states contribute to both processes which interfere with unknown phase, so that the results for  $P_\gamma$  and  $A_{pp}$  lie in some region of possible values:  $-10.8 \cdot 10^{-8} \leq P_\gamma \leq -2.9 \cdot 10^{-8}$ ,  $-2.26 \cdot 10^{-7} \leq A_{pp} (15 \text{ MeV}) \leq -0.75 \cdot 10^{-7}$ . If one takes the combination of QCB states minimally coupled to the  $\Delta\Delta$  channel, the results for  $A_{pp}$  at 15 and 45 MeV well agree with experiment.

#### 10. CONCLUSIONS

Applications of the QCB model even in the simplest approximations (no external OBE, sharp transition) are reasonably successful, showing that this model takes into account the most essential quark structure of NN interaction. One of the most important checks of the QCB NN potential - the calculation of 3N and 4N obser-

vables and the generalization of the QCB model to include the  $9q$ ,  $12q$ , ... bags in nuclei - are now in progress.

## REFERENCES

- 1) S.Brodsky, QCD in nuclear few body systems, this volume.
- 2) C.De Tar, Phys.Rev. D17 (1978) 302, 323; D19 (1979) 145.
- 3) A. Faessler, How should or will QCD influence nuclear physics? In Quarks and Nuclear forces, eds. D.C. Fries and B. Zeitnitz. Springer, v. 100, 1982, L. Heller, *ibid*; F. Close, *ibid*.
- 4) Yu.A. Simonov, Phys.Lett. 107B (1981) 1.
- 5) Yu.A. Simonov, preprint ITEP-142 (1981).
- 6) Yu.A. Simonov, Yad.Fiz. 36 (1982) 722 .
- 7) A.M. Badalyan, Yu.A. Simonov, Yad.Fiz. 36 (1982) 1479.
- 8) Yu.A. Simonov, preprint ITEP-73 (1982), Yad.Fiz. 38 (1983) 1542.
- 9) Yu.A. Simonov, preprint ITEP-31 (1982).
- 10) I.T. Obukhovskiy, Yu.A. Simonov. M.Z. Shmatikov, Yad.Fiz. 38 (1983) 1248.
- 11) V.M. Dubovik, I.T. Obukhovskiy, M.Z. Shmatikov, Yad.Fiz. 3<sup>c</sup> 1984) in press.
- 12) Yu.A. Simonov, preprint ITEP-93 (1983).
- 13) R.L.Jaffe and F.E. Low. Phys.Rev. D19 (1979) 2105.
- 14) R.L.Jaffe and M.P.Shatz, preprint CALT-68-775 (1980).
- 15) K. Wildermuth and Y.C. Yang, A unified theory of the nucleus, Vieweg, Braunschweig, 1977.
- 16) V.A. Matveev and P. Sorba, Lett.Nuovo Cim. 20 (1977) 435.
- 17) A. Faessler, Contribution to the 10-th Int. Conf. on Few Body Problems in Physics. Karlsruhe, 1983.
- 18) V.G. Neudatchin et al. Yad.Fiz. 35 (1982) 288.
- 19) P. Mulders, P matrix analysis of NN interaction, this volume.
- 20) B.L.G. Bakker and M. van der Velde, Contribution to the 10-th Int. Conf. on Few Body Problems. Karlsruhe, 1983.
- 21) I.L. Grach, I.M. Narodetskii, M.Zh. Shmatikov, preprint ITEP-32 (1983).

- 22) A.I. Veselov, I.L. Grach, I.M. Narodetskii, preprint ITEP-56 (1983).
- 23) Yu.S. Kalashnikova, I.M. Narodetskii, A.I. Veselov, preprint ITEP-
- 24) I.L. Grach, N.B. Konyukhova, M.Zh. Shmatikov, A.I. Veselov, preprint ITEP-126 (1983).
- 25) V.N. Efimov, preprint Dubna P4-82-202.
- 26) B.L.G. Bakker et al. Sumb. to Nucl. Phys. A and preprint ITEP to be published.
- 27) H. Feashbach and E.L. Lomon, Ann.Phys. 29 (1964) 19, *ibid.* 48 (1968) 94.
- 28) M. Lacombe et al. Phys.Rev. D12 (1975) 1495.
- 29) A.N. Safronov, Phys.Lett. 124B (1983) 149.
- 30) B.O. Kerbikov, preprint ITEP-26 (1982), ITEP-42 (1983).
- 31) Yu.S. Kalashnikova, preprint ITEP-116 (1982), ITEP-80 (1983).

## FUTURE EXPERIMENTS ON QCD EFFECTS IN FEW NUCLEON SYSTEMS WITH HIGH ENERGY ELECTRONS

R. G. ARNOLD\*

*The American University, Washington, D.C. 20016 and  
Stanford Linear Accelerator Center  
Stanford University, Stanford, California 94305*

### 1. INTRODUCTION

A central question in the study of the few nucleon systems today is how to understand nuclear structure in terms of the quark degrees of freedom. It is now clear that nucleons are composite, and that QCD, the gauge theory of colored quarks and gluons, is probably the correct theory of hadronic matter. The question is: At what points in our description of nuclear structure do we have to abandon the conventional meson-nucleon theory in favor of quarks? In this talk I review some of the evidence for quarks in nuclei from previous high energy ( $E > 1$  GeV) electron scattering experiments.<sup>1-6</sup> There is a great need for more electron data on nuclear targets. In response to that need there are now plans for more experiments in the near future.

### 2. WHERE TO LOOK FOR QUARKS?

Examination of the present high energy electron scattering data on the nucleons and the  $A \leq 4$  nuclei yields the following observations:

A. There appears to be a gradual transition from the conventional nuclear physics regime to the quark regime in the high energy electron data. As the energy and momentum transfer to the hadronic system increases from the MeV range to the GeV range, there is a gradual change from coherent scattering off collections of quarks (nucleons, mesons, isobars) to scattering from individual point-like quarks (scaling region). This transition takes place in the momentum transfer  $Q^2$  range up to approximately  $4 \text{ (GeV/c)}^2$ , and can be seen in both the elastic and inelastic data. In Fig. 1 the elastic form factors of the nucleons and the nuclei  $A \leq 4$  are observed to gradually approach the power law fall-off with increasing  $Q^2$  predicted by the quark counting rules.<sup>7</sup> The power law behavior follows directly from the dominance at large  $Q^2$  of the minimal  $n$  quark component of the hadronic wave function, and the scale invariance of the quark-quark interaction at short distances (quarks are point-like), up to logarithmic corrections. Figure 2 shows a schematic<sup>8</sup> of the proton structure

---

\*This work was supported by the Department of Energy under contract DE-AC03-76SF00515, and by the National Science Foundation under grants PHY-8108484 and PHY83-40337.

functions derived from  $ep$  data<sup>9</sup> covering the elastic peak, the nucleon resonances, and the deep inelastic region. The peaks from coherent scattering sink into the continuum of incoherent scattering from individual point-like quarks as the  $Q^2$  is raised to 3 or 4 (GeV/c)<sup>2</sup>. For inelastic scattering from nuclei the picture is similar except the nucleon resonant structures are smeared out due to Fermi motion and interactions in the nuclear medium.

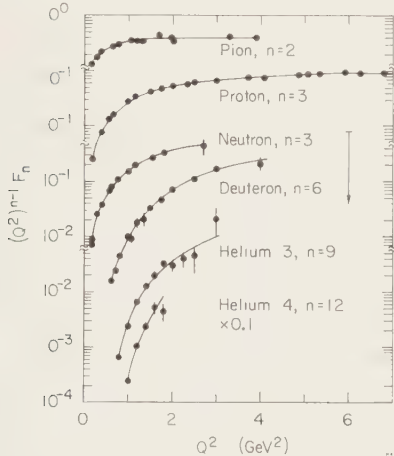


FIGURE 1. Elastic form factors  $F = \sqrt{A(Q^2)}$  of the hadrons and  $A \leq 4$  nuclei multiplied by the power of  $Q^2$  determined for each  $n$  quark system by the dimensional scaling quark model (ref. 7).

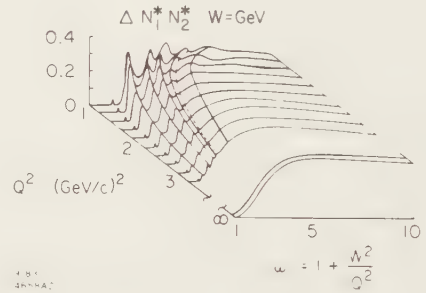


FIGURE 2. Schematic representation of the electron proton structure functions  $\nu W_2$  at high energies. The figure is from ref 8, based upon data in ref. 9.

B. There is a systematic pattern of deviations of the present high energy electromagnetic structure function data from the predictions of the conventional meson-nucleon models. These models generally give too small values for the cross sections at large  $Q^2$ . In the deuteron  $A(Q^2)$ , for example, the conventional nonrelativistic models<sup>10</sup> fall below the data by factors of 2 to ten at  $Q^2 = 4$  (GeV/c)<sup>2</sup>, and the relativistic corrections make the agreement worse.<sup>11</sup> Similarly the charge form factor of  $^3\text{He}$  is poorly described. Figure 3 shows one of the recent calculations<sup>12</sup> based on the best available Faddeev 3-body wave functions. When contributions from meson exchange (MEC) and isobars are included, there is improvement in the size and shape of the diffractive features, but the theory still falls below the data at the largest  $Q^2$ . This pattern of too-low predictions can also be seen in the inelastic data. In Fig. 4 the momentum space wave function  $\psi^2(k)$  for nucleons in the deuteron extracted<sup>13</sup> from quasi elastic  $ed$  scattering lies considerably above the conventional 2-body wave functions above  $k = 200$  MeV/c. Similarly for  $^3\text{He}$  the Faddeev predictions<sup>14,15</sup> of the inclusive electron spectra at large  $Q^2$  and small energy transfer (corresponding to large internal momentum  $k$ ) are all smaller than the measurements<sup>4</sup> by factors of 2 or more.



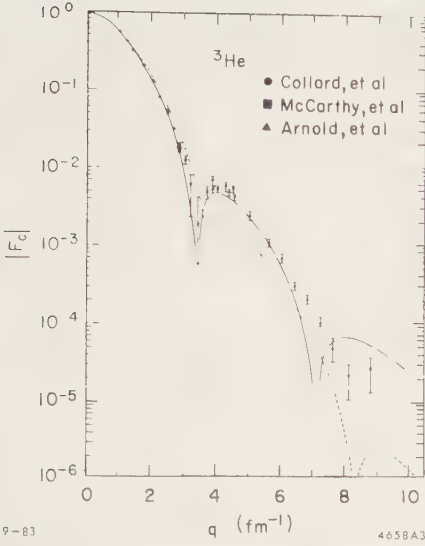


FIGURE 3. The charge form factor of  ${}^3\text{He}$  taken from ref. 12. The dashed curve is the impulse approximation, the solid curve includes MEC.

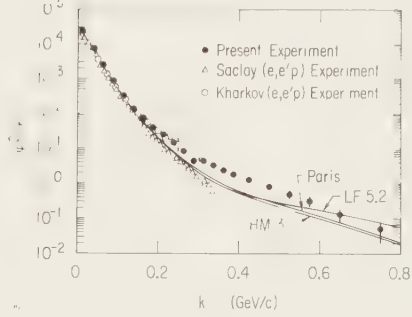


FIGURE 4. Experimental deuteron wave functions compared to three nonrelativistic models. The figure and the solid points are from ref. 13.

These deviations of the conventional models from the high  $Q^2$  data have been interpreted to be possible due to various deficiencies of the models: not enough high momentum components in the wave functions; the need for inclusion of MEC and isobar contributions; and relativistic effects. Unfortunately the present status of the conventional models is far from satisfactory. We do not yet have a completely consistent relativistic treatment of few nucleon structure including meson and isobar currents. In some cases the addition of these terms seems to bring the theory closer to the data. However closer examination prompts us to proceed with caution. The *ad hoc* way the higher order terms are presently patched into the nonrelativistic theory is open to question.<sup>11,18</sup> The theoretical results also have a large sensitivity to a large number of unknown parameters (nucleon form factors, meson-nucleon couplings and form factors, relativistic effects).

It is also possible that what we are seeing is the slow breakdown of the conventional picture and the gradual emergence of the quark degrees of freedom. In the  $Q^2$  range up to  $4 (\text{GeV}/c)^2$  we are looking at a transition region where on the one hand nucleons become strongly overlapping at short distances and lose their identity, and on the other hand the quarks are moving in the long range region dominated by nonperturbative dynamics. In this dual region it is possible that both theoretical pictures will have some approximate validity, and that a major goal of our study ought to be to understand one description in terms of the other. To make progress in this program we need to continue to develop, if possible, a

completely consistent conventional relativistic theory<sup>16</sup> so as to have a basis for identifying the breakdown and the possible emergence of quark effects. It is also essential to press on with more explicit QCD calculations<sup>17-22</sup> of cross sections including the normalizations in addition to the predictions of asymptotic form factors.<sup>7</sup> Eventually from intercomparison of these competing models and the data we may begin to understand how the constituents of nuclear matter at short distance can best be described. Clearly what is needed for this program to succeed is extensive high quality data in this transition region. It is also essential to make comprehensive comparisons with all available structure function data, not just subsets of it. This leads to my third observation:

C. Much of the necessary electromagnetic structure function data on the nucleons<sup>23</sup> and the few body nuclei is poorly known or entirely missing. Of all the possible 24 single arm elastic and inelastic structure functions for the nucleons and  $A \leq 4$  nuclei ( $G_E$  and  $G_M$  for nucleons,  $G_C$ ,  $G_Q$ , and  $G_M$  for deuterium,  $F_C$  and  $F_M$  for  ${}^3\text{He}$  and  ${}^3\text{H}$ ,  $\nu W_2$ ,  $W_1$  for all) for  $Q^2 \geq 1$  (GeV/c)<sup>2</sup>, we have no information at all for eleven of them and in many cases the others are not well measured at large  $Q^2$ . This situation makes impossible the kind of comprehensive comparison necessary to narrow the theoretical choices. Consider the following cases:

Proton: In many processes the dominant contributions in the impulse approximation arise from terms proportional to  $G_{Mp}$ . At present for most purposes the error arising from the 2-3% error on  $G_{Mp}$  out to 4 (GeV/c)<sup>2</sup> is not the dominant uncertainty. However, eventually we will need to know  $G_{Mp}$  more precisely, especially as we move toward more detailed questions about the difference between on-shell and off-shell form factors and the extent of distortion of the free nucleons in the nuclear medium.  $G_{Ep}$  is poorly known.<sup>24</sup> The errors at  $Q^2 = 2$  (GeV/c)<sup>2</sup> are  $\pm 20\%$  and nothing is known above 3.8 (GeV/c)<sup>2</sup>. The lack of knowledge of  $G_{Ep}$  is a serious problem for nuclear structure calculations in the transition region.

Neutron: The 5% uncertainty<sup>6</sup> in  $G_{Mn}$  out to 4 (GeV/c)<sup>2</sup> contributes to the overall uncertainty of many calculations. As with the proton, eventually we will need more accurate measurements of  $G_{Mn}$  as our tests of models become more refined.  $G_{En}$  is very poorly known,<sup>25</sup> partly because it is nearly zero. The present values extracted from elastic and quasi elastic  $ed$  scattering have experimental errors of 50% to 100%, and they are subject to large uncertainties from deuteron model dependence. There is no data above  $Q^2 = 1.5$  (GeV/c)<sup>2</sup>. This lack of knowledge is a major problem for few nucleon studies. In the deuteron  $A(Q^2)$ , for example, large differences are possible depending on which values for  $G_{En}$  are assumed.<sup>11</sup>  $G_{En}$  is also of high intrinsic interest because it tells about the charge distribution of the neutron. This we now believe to arise from a delicate balance between the charge on the +2/3 and the two -1/2 valence quarks and the cloud of ocean quarks resulting in a spacial distribution of charge that is not everywhere zero.<sup>26</sup> Measurements of  $G_{En}$  will provide important tests of nucleon structure.

**Deuteron Elastic:** The major experimental goals here are measurement of the magnetic form factor  $B(Q^2)$  (or  $G_M$ ) beyond<sup>27</sup>  $Q^2 = 1$  (GeV/c)<sup>2</sup> and a separation of the charge  $G_C$  and quadrupole  $G_Q$  form factors. The  $G_M$  and  $G_C$  are each predicted in the impulse approximation<sup>10,11</sup> to have sharp diffractive features which get shifted or even totally obliterated when MEC<sup>10</sup> or 6-quark<sup>18,20</sup> contributions are included. A major advance in our understanding of the relevant degrees of freedom at short distances for two nucleons will be made when these functions are measured.

**Deuteron Inelastic:** Threshold electrodisintegration of the deuteron is already identified<sup>28</sup> as a sensitive place to see effects MEC, and this data<sup>29</sup> needs to be extended to  $Q^2$  above 1 (GeV/c)<sup>2</sup> to see if the trends continue. In general a complete Rosenbluth separation of the longitudinal and transverse response functions from threshold out into the nucleon resonance region will be very useful for helping to identify the relevant scattering mechanisms.<sup>30</sup>

**Helium and Tritium:** Separation of the complete set  $F_C$ ,  $F_M$ ,  $\nu W_2$ , and  $W_1$  in the 3-body nuclei over the whole kinematic domain accessible with high energy electrons is essential for progress in this field. We have already seen the rich information contained in  $F_{ch}$  and  $\nu W_2$  for  ${}^3\text{He}$ . The magnetic elastic form factors are especially important as they are predicted<sup>12</sup> to be very sensitive to many ingredients of the conventional models. At present nothing is known of  ${}^3\text{H}$  above 0.3 (GeV/c)<sup>2</sup>. Eventually  ${}^3\text{H}$  and  ${}^3\text{He}$  structure function data at large  $Q^2$  will give powerful constraints as the models are required to simultaneously reproduce the diffractive features in all the structure functions in a consistent picture.

In addition to the single arm structure functions, we eventually will need measurements of as many of the coincidence cross sections as possible. Of particular interest are measurements of the type  $(e, e'p)$  which can be interpreted in terms of the spectral functions<sup>15</sup> (convolutions of the initial and final state wave functions). The present measurements<sup>31</sup> are limited to nucleon momentum  $k \leq 300\text{-}400$  MeV/c and separation energy  $E_s \leq 60\text{-}80$  MeV primarily by the background of accidental coincidences. For extension of these experiments it is essential to have high-intensity high-duty electron beams in the GeV region.

### 3. FUTURE EXPERIMENTS

There are two recent developments in the U.S. that promise to help provide the missing data outlined above. First is the recent approval and appropriation of funds for construction of a new injector at SLAC. The other is a recent recommendation<sup>8</sup> by a DOE-NSF review panel for construction of a new high duty 4 GeV electron machine in Newport News, Virginia, as proposed by the South Eastern University Research Association (SURA).

The SLAC injector is a project originated by the American University Group at SLAC to add a new electron gun and injector near the downstream end of the two mile long SLAC linac to provide high intensity (35  $\mu\text{A}$  average), good quality beams in the energy range 0.5 to approximately 5 GeV. The construction project is now getting underway (October

1983), and we expect to have beam for testing in early 1985. This new beam will be used for a program of nuclear structure measurements using the existing facilities of SLAC End Station A. The primary emphasis will be on elastic and inelastic electron scattering in the  $A \leq 4$  nuclei. These experiments will take full advantage of the high energy and beam current but do not need high duty factor. An example of the extension in sensitivity is shown in Fig. 5 where the  $Q^2$  range accessible for a measurement of the deuteron  $B(Q^2)$  is plotted. In this case the elastically scattered electrons will be measured in coincidence with the recoil nuclei. Similar extension of the separation of  $F_C$  and  $F_M$  for  ${}^3\text{He}$  and  ${}^3\text{H}$  will be possible as well as separation of  $\nu W_2$  and  $W_1$  in all these nuclei.

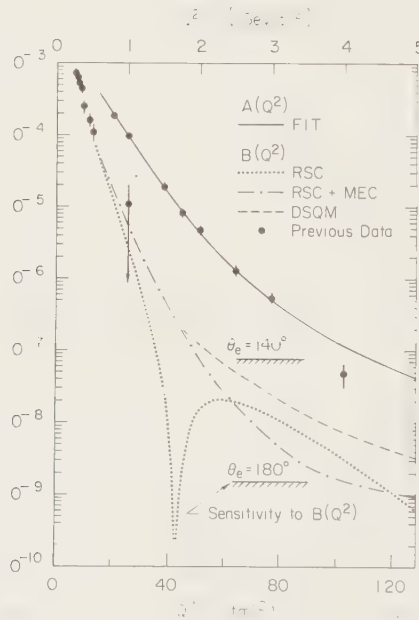


FIGURE 5. Sensitivity of experiments proposed with the new injector at SLAC for measurements of the deuteron  $B(Q^2)$ .

In addition to standard scattering measurements we are particularly interested in the possibility to use polarized electrons to separate elastic form factors.<sup>32</sup> In the case of scattering longitudinally polarized electrons from nucleons, the polarization transferred to the nucleons depends upon the form factors:

$$I_0 P_x = -2 [\tau(1 + \tau)]^{1/2} G_M G_E \tan\left(\frac{1}{2} \theta\right) ; \quad \tau = \frac{Q^2}{4m^2}$$

$$I_0 P_z = 2\tau \left\{ (1 + \tau) \left[ 1 + \sin^2\left(\frac{1}{2} \theta\right) \right] \right\}^{1/2} G_M^2 \sec\left(\frac{1}{2} \theta\right) \tan\left(\frac{1}{2} \theta\right)$$

A measurement of the recoil nucleon polarization offers a new experimental method in addition to the Rosenbluth method to separate  $G_E$  from  $G_M$ . It appears feasible to make recoil neutron polarization analyzer/detectors based upon elastic  $np$  scattering with efficiency adequate to make measurements of  $G_{En}$  in the  $Q^2$  range 0.5 to perhaps 2 (GeV/c)<sup>2</sup>. A similar technique using  $pp$  scattering could be used to improve the knowledge of  $G_{Ep}$  above 2 (GeV/c)<sup>2</sup>. It should be noted that for the neutron a measurement of  $P_x$  is a direct signature for  $G_{En}$  that can be made in a ratio experiment (up-down asymmetry) completely independent of models for deuteron wave functions and measurements of neutron detection efficiencies or any absolute counting rates. Measurement of  $G_{En}$  for any  $Q^2 > 0$  would be extremely helpful, and experimenters at low and medium energy electron facilities should explore the possibilities for such experiments, perhaps using elastic neutron-helium scattering for the analyzer.

In the case of elastic  $ed$  scattering with longitudinal beam polarization  $a$ , the cross section for  $ed$  scattering followed by a second analyzing reaction is:

$$\begin{aligned} \frac{d^2\sigma}{d\Omega d\Omega_2} = \frac{d^2\sigma}{d\Omega d\Omega_2} \bigg|_0 & \left\{ 1 + \frac{3}{2} a p_x A_y \sin \phi_2 + \frac{1}{2} p_{zz} A_{zz} \right. \\ & + \frac{2}{3} p_{xz} A_{xz} \cos \phi_2 \\ & \left. + \frac{1}{6} (p_{xx} - p_{yy}) (A_{xx} - A_{yy}) \cos 2\phi_2 \right\} \end{aligned}$$

The term proportional to  $p_x$ , the vector polarization transferred to the recoil deuterons (perpendicular to the recoil momentum and in the scattering plane), is present only when the beam is polarized.  $p_x$  depends upon different combinations of  $G_C$  and  $G_Q$  than does the cross section, and it could be measured in an up-down asymmetry in a second scattering provided the analyzing power  $A_y$  ( $2/\sqrt{3} i T_{11}$ ) is known. If a recoil polarization analyzer were available with full azimuthal symmetry, as for example using elastic scattering from carbon with track reconstruction before and after the scattering, then with sufficiently accurate data a Fourier decomposition would allow separation of the  $\phi_2$  dependent terms. In particular the ratio of the amplitude of the  $\sin \phi_2$  and  $\cos \phi_2$  components would yield:

$$\frac{p_x}{p_{xz}} = \frac{4}{3} [\eta(1+\eta)]^{1/2} \frac{M_d}{E+E'} \left( \frac{G_C}{\eta G_Q} + \frac{1}{3} \right), \quad \text{where } \eta = \frac{Q^2}{4M_d^2}.$$

Before such measurements can be undertaken, it is essential to have more precise and extensive measurements of the analyzing powers for a suitable reaction. There are now underway an important series of measurements<sup>33</sup> at Saturne in Saclay on  $dp$  and  $dC$  scattering that hopefully will yield the required analyzing powers and make possible and eventual separation of  $G_C$  and  $G_Q$ .

The low duty factor of SLAC ( $10^{-4}$ ) will not allow performance of any inelastic coincidence experiments, such as  $(e, e'p)$ . For these we eagerly await the development over the



next few years of high duty electron facilities. This will open up a vast new area for experimental exploration of the inelastic final states and provide much new evidence for discussion at future few body conferences.

#### 4. WATCH FOR SURPRISES

I conclude with a reminder that we must continue to be awake for surprises that may come along to modify our points of view and perhaps reorder the priorities of our experimental programs. A recent example is the discovery by the European Muon Collaboration at CERN,<sup>34</sup> and confirmed by old SLAC data,<sup>35</sup> that deep inelastic scattering from the quarks in deuterium is not the same as in iron. This discovery has sent big ripples across the boundary between nuclear and particle physics. The data indicate that the quark distributions are distorted when nucleons are embedded in a large nucleus compared to those in (nearly) free nucleons. This effect provides an important new signature for quark degrees of freedom in nuclei.

There have been several recent theoretical papers suggesting possible mechanisms for the distortion of quark distributions in nuclei. These include nucleon overlap into multiquark bags,<sup>36</sup> the presence of quasi pions<sup>37</sup> and isobars<sup>38</sup> in nuclei, and changes in the effective mass and radius of nucleons found in nuclei.<sup>39</sup> In the region  $x \leq 0.2$  there are apparently effects due to photon shadowing, and the region  $x > 1$  (forbidden to free nucleons) will be the place to look for cumulative effects.<sup>21,22,40</sup>

#### 5. CONCLUSION

The field of high energy electron scattering from nuclear targets is at the threshold of an exciting new era. High energy electron experiments are particularly good ways to look for QCD effects in nuclear systems because they provide clean measurements of the charges and currents carried by the quarks in nuclei. We look forward in the near future to much more data that that will provide important new tests of our understanding of the underlying quark degrees of freedom in nuclei.

#### REFERENCES

1. R. G. Arnold, et al., Phys. Rev. Lett. **35** (1975) 776.
2. W. P. Schütz, et al., Phys. Rev. Lett. **38** (1977) 259.
3. R. G. Arnold, et al., Phys. Rev. Lett. **40** (1978) 1429.
4. D. Day, et al., Phys. Rev. Lett. **43** (1979) 1143.
5. S. Rock, et al., Phys. Rev. C **26** (1982) 1592.
6. S. Rock, et al., Phys. Rev. Lett. **49** (1982) 1139.
7. S. Brodsky and B. Chertok, Phys. Rev. D **14** (1976) 3003.
8. DOE/NSF Nuclear Science Advisory Committee, "Report of the Panel on Electron Accelerator Facilities," DOE/ER-0164 (April 1983).

9. E. D. Bloom, F. J. Gilman, Phys. Rev. D **4** (1971) 2901;  
G. Miller, et al., Phys. Rev. D **5** (1972) 528.
10. M. Gari and H. Hyuga, Nucl. Phys. **A264** (1976) 409.
11. R. G. Arnold, C. E. Carlson, and F. Gross, Phys. Rev. C **21** (1980) 1426;  
M. J. Zuilhof, and J. A. Tjon, Phys. Rev. C **24** (1981) 736.
12. H. Hadjimichael, B. Goulard, R. Bornais, Phys. Rev. C **27** (1983) 831.
13. P. Bosted, et al., Phys. Rev. Lett. **49** (1982) 1380.
14. I. Sick, D. Day, J. S. McCarthy, Phys. Rev. Lett. **45** (1980) 871.
15. H. Meir-Hajduk, et al., Nucl. Phys. **A395** (1983) 332.
16. J. L. Friar, Proceedings of International Conference on Nuclear Physics with Electro-magnetic Interactions, Mainz, eds., H. Arenhövel and D. Drechsel, (1979) 445; Phys. Rev. **C22** (1980) 796.
17. S. J. Brodsky, Tao Huang, and G. P. Lepage, SLAC-PUB-2868, published in Springer Tracts in Modern Physics, Vol. 100, "Quarks and Nuclear Forces," ed., D. Fries and B. Zutnitz (1982);  
S. J. Brodsky and J. R. Hiller, Phys. Rev. C **28** (1983) 475;  
S. J. Brodsky, Chueng-Ryong Ji, and G. P. Lepage, Phys. Rev. Lett. **51** (1983) 83.
18. A. P. Kobayshikin, Sov. J. Nucl. Phys. **28** (1978) 252.
19. M. Beyer, D. Drechsel and M. M. Giannini, Phys. Lett. **122B** (1983) 1.
20. L. S. Kisslinger, Phys. Lett. **112B** (1982) 307.
21. L. L. Frankfurt, M. I. Strikman, Phys. Rep. **76** (1981) 217.
22. H. J. Pirner, J. P. Vary, Phys. Rev. Lett. **46** (1981) 1326.
23. G. Höhler, et al., Nucl. Phys. **B114** (1976) 505.
24. J. Litt, et al., Phys. Lett. **31B** (1970) 40.
25. S. Galster, et al., Nucl. Phys. **B32** (1971) 221.
26. A. W. Thomas, S. Théberge, and G. A. Miller, Phys. Rev. D **24** (1981) 216.
27. B. Frois, Saclay, invited paper III.6, at this conference.
28. J. Hockert, et al., Nucl. Phys. **A217** (1973) 14;  
W. Leidemann and H. Arenhövel, Nucl. Phys. **A393** (1983) 385.
29. M. Bernheim, et al., Phys. Rev. Lett. **46** (1981) 402.
30. W. Fabian and H. Arenhövel, Nucl. Phys. **A314** (1979) 253.
31. M. Bernheim, et al., Nucl. Phys. **A365** (1981) 349;  
E. Jans, et al., Phys. Rev. Lett. **49** (1982) 974.
32. R. G. Arnold, C. E. Carlson, F. Gross, Phys. Rev. C **23** (1981) 363.
33. J. Arvieux, Saclay, private communication and Discussion Section DS4, this conference.
34. J. J. Ambert, et al., Phys. Lett. **123B** (1983) 275.
35. A. Bodek, et al., Phys. Rev. Lett. **50** (1983); Phys. Rev. Lett. **51** (1983) 534.



36. R. L. Jaffe, Phys. Rev. Lett **50** (1983) 228;  
C. E. Carlson and T. J. Havens, Phys. Rev. Lett. **51** (1983) 261.
37. C. H. Llewellyn Smith, Phys. Lett. **128B** (1983) 107;  
M. Ericson and A. W. Thomas, Phys. Lett. **128B** (1983) 112;  
E. L. Berger, F. Coester, R. B. Wiringa, Argonne Preprint ANL-HEP-PR-83-24 (June 1983).
38. J. Szwed, Phys. Lett. **128B** (1983) 245.
39. F. E. Close, R. G. Roberts, and G. G. Ross, Rutherford Laboratory Preprint RL-83-051 (1983).  
L. L. Frankfurt and M. I. Strikman, Leningrad Preprint (1983) (to be published in Physics Letters).
40. L. L. Frankfurt and M. I. Strikman, Phys. Lett. **114B** (1982) 345;  
A. M. Baldin, Dubna, presentation at this conference.

## FEW QUARK PROBLEMS: A SUMMARY OF THE DISCUSSION SESSION DS2

C. E. DETAR

Department of Physics, University of Utah, Salt Lake City, UT 84112, USA

The discussion session on few quark problems was conducted by posing a few questions under four topical headings allowing approximately fifteen minutes for each topic, followed by a fifteen minute period for topics chosen by the audience. Each prearranged topic was introduced with a brief discussion by the rapporteur (i.e. the provocateur). What follows is my reconstruction of the discussion. I have inserted a few editorial remarks and placed them in brackets.

### 1. HADRON-HADRON SCATTERING IN BAG-LIKE MODELS: Matching the short range quark component and the long range hadron component.

It is generally agreed that the short range hadron-hadron interaction should be described with quark and gluon degrees of freedom, whereas the long range component is most economically described with hadronic degrees of freedom. There are, of course, differences in opinion about the dividing line. In order to calculate scattering amplitudes or phase shifts it is necessary to have a satisfactory description of the hadron-hadron interaction at all ranges. Bag models attempt to describe the short range quark component in a framework characteristic of QCD, but it has not been possible to compute bag model phase shifts without embellishing the model with elaborate assumptions<sup>1</sup>. An alternative approach has been to find methods for matching a long-range two body hadronic wave function on to a short range quark-bag component. To construct the quark component and keep it at short range, it is necessary to introduce an artificial constraint. In the P-matrix approach of Jaffe and Low<sup>2</sup> it was intended to impose a constraint that corresponds approximately to a sharp barrier at a hadronic separation comparable to the bag radius, requiring the matching exterior wave function to have a node at a scattering energy equal to the energy of the interior "primitive" state, i.e. the P-matrix is required to have poles at these energies. [The P-matrix poles are related precisely to nodes in the relative hadronic wave function and therefore to interior eigenstates with a sharp barrier in the relative coordinate. This barrier should not be confused with the bag boundary, which limits the extent of the one-body quark wave functions. In fact there is no precise way in the bag model to

introduce a barrier in the relative coordinate. Therefore, one is limited to an approximate relationship between the bag size and the separation at the node.] Two other approaches have been proposed recently. Henley, Kisslinger, and Miller hope that it may be possible to define a conserved baryon current in the relative two quark cluster coordinate, and from current conservation they relate the normalization of the quark component to an expression involving the exterior hadronic wave function at the matching surface<sup>3</sup>. [Their approach is a promising start, but more work needs to be done to ensure that a particular choice of the interior quark wave function matches in all respects and not just in normalization.] Kim and Orłowski have similar ambitions, but require further assumptions to reach their conclusions<sup>4</sup>. [Their assumptions appear to give an undeserved physical status to an artificial constraint.] Simonov introduces a coupling to the interior quark "channel" and obtains the P-matrix phenomenology, and he also obtains an explicit effective two hadron potential<sup>5</sup>.

In all P-matrix applications to date the phenomenologically determined primitive energies are compared with quark primitive energies that are taken from bag model calculations with all quarks placed in the spherical cavity  $S_{1/2}$  orbitals<sup>6</sup>. Such a constraint corresponds to an arbitrary truncation of the Hilbert space without reference to any physical observable related to an interhadronic coordinate. The resultant state is in no sense an eigenstate of the cavity hamiltonian. One could argue that merely restricting the six-quark configuration to a spherical cavity, but allowing any orbital configuration, comes closer to a geometrical restriction on the interhadronic separation. Indeed in the six-quark problem it has been found that the energy of the spherical state is substantially lowered by mixing in the configurations  $S_{1/2}^4 P_{3/2}^2$  in the Young symmetry class [4,2]<sup>7</sup>. Similar results are obtained in nonrelativistic quark models<sup>8</sup>. Thus we come to the question:

"Why do we use  $S^6$  [6] when  $S^4 P_{3/2}^2$  [4,2] is important?"

The answer must, of course, also deal with the question, how should we formulate the constraint so that it corresponds to a restriction on the "relative separation" of three quark clusters? My opinion is that the constraint should be formulated in terms of physical observables, such as moments of baryon charge densities, rather than by manipulating wave functions. Constraining the quadrupole moment, for example, is preferable to truncating the Hilbert space or to measuring the separation of two centers that serve only as a reference point for defining a set of basis wave functions.

In the discussion that followed, Simonov and Lomon stressed the utility of the P-matrix as a phenomenological parameterization of the low energy scatter-

ing data. In Lomon's view the phenomenology serves as a guide for distinguishing among different approaches to defining the constraint; he also cited his recent successful treatment with a reduced bag radius and the  $S^6$  configuration<sup>9</sup>. More pertinent to the question of configuration mixing per se, Viollier commented on the repulsive character of the  $S^4_{P_{1/2}^2}$  (as opposed to  $S^4_{P_{3/2}^2}$ ) configuration based on his recent work and Duck expressed concern that the P orbitals of the cavity might be contaminated by spurious c.m. translational modes, the true orbitals having much higher energies, thereby putting these configurations out of action. The latter remark is easily answered by noting that the removal of spurious modes is done at the level of configurations and not orbitals. The translation operator has a Young symmetry [6] and when acting upon the  $S^6$  [6] configuration results, again, in a [6] which is orthogonal to a [4,2].

A question of great importance to the matching of relative wave functions is this:

"What is the relative cluster coordinate and how do we determine the relative nucleon-nucleon wave function for six relativistic quarks?"

A related question:

"Is there any unambiguous meaning to the concept 'wave function for the hidden color component'?"

In the discussion it was observed by Redish that the same question arises in non-relativistic, non-confined problems and it still has not been resolved in a satisfactory way, although there have been promising developments. Simonov remarked that at least for intercluster separations less than  $1F$  there is no unambiguous definition, making matching hopeless, and requiring the sort of procedure that he adopted. [Miller's contention (expressed outside of the discussion) was that the ambiguities in the NN wave function are certainly less severe at large cluster separation and that some sort of cluster model wave-function should do. The reader should also note the talk by Schmid on related questions in non-relativistic problems.<sup>10</sup>] Concerning the hidden color component, Brodsky remarked that evolution equations for the amplitude of the elastic charge form factor at high  $Q^2$  show that the [6] dominates by powers of  $\log Q^2$  over the [4,2] in determining the high  $Q^2$  component." The hidden color component of the [6] is defined naturally by the fractional parentage coefficient expansion.

## 2. HADRON-HADRON INTERACTIONS FROM POTENTIAL MODELS: THEORETICAL UNCERTAINTIES

If we want the non-relativistic and quasi-relativistic two-body potential models to reflect properties of QCD, then we should be concerned about the following problems. Constituent quarks are extended objects (they include a gluon field, etc.) and as such their "masses" are undoubtedly dependent upon their environment--i.e. different for mesons, baryons, and NN--indeed, in the NN interaction they may depend on the cluster separation. Moreover, extended objects may be subject to non-local interactions, and many quark interactions may be important. The question posed was

"In view of the above mentioned theoretical uncertainties, aren't there large uncertainties in the predictions of these models? In particular, a predicted bound state may just as predictably be unbound. Phase shifts may be off by many degrees."

In the ensuing discussion an objection was raised regarding the importance of size effects--mesons and baryons may well have the same size [although the case of two separating hadronic clusters may pose special problems]. The discussion was further stimulated by Simonov, who asked why we should believe these models at all, since we know that the QCD vacuum plays an important role in confinement, and it is certainly not manifested as a two-body interaction. Heller remarked that in the bag model for heavy quarks the confining part of the interaction is a many-body potential. Richard also cited evidence for non-locality from the bag model.<sup>12</sup> Moravcsik commented that the potential model or additive quark model works remarkably well, but unjustifiably so--the reason remains a mystery. Pirner cited recent work on low energy  $K^+N$  scattering in a potential model, where again the model seems to be working surprisingly well.<sup>13</sup> K. F. Liu, claiming there was no mystery, said many of the successful predictions (e.g. static properties of hadrons) were based on simple, general principles. Coester also defended the utility of the model, saying at least they admit the possibility of describing states in a Poincaré invariant framework (in some sense). Thomas recalled work by Shuryak that attempted to justify the non-relativistic model from QCD.<sup>14</sup> [Models with two-body confining interactions also produce unwanted van der Waals forces. Yazaki described a new approach that avoids this difficulty.<sup>15</sup>] Finally, in response to a question, whether the potential models didn't indeed follow from lattice calculations, Kuti observed that what is known is based on quarks of infinite mass<sup>16</sup>, a result perhaps appropriate to bound states of heavy quarks; nothing is known about potentials for light quarks or whether the concept is meaningful.

### 3. THE RELATIVISTIC FEW BODY PROBLEM

If we take the point of view that quarks are light enough that a relativistic potential model treatment is required, then we ask

"How do we (or should we) formulate a model with a 'reliable' wavefunction of the relative coordinates, where 'reliable' means incorporating confinement and other QCD features?"

Kuti asked why one should even be posing such a question for quarks, since it is unlikely that we can get such a model from QCD. In defense of the approach Mitra argued that because we can't have the perfect model, we must make tactical concessions, and cited his work on the Bethe-Salpeter equation with a confining interaction<sup>17</sup>. Coester commented about his work with Polyzou that shows some promise<sup>18</sup>. Gross speculated on the possibility that a  $1/q^4$  interaction could easily be handled in a relativistic calculation, but, as Bolsterli observed, it would lead to long range van der Waals interactions. Namysłowski was optimistic that the Weinberg light-cone equations could be generalized to include a confining term, following his recent work. Brodsky, even more optimistic, thought that ad-hoc confining terms were unnecessary, since there already is an exact, consistent light-cone formulation of QCD that should, in principle, give a correct Fock-space description of bound states<sup>19</sup>. Further discussion of this topic took place in session DS3.

A second question under this topical heading dealt with the problem of correcting for the c.m. motion in the bag model. In the cavity approximation to the model the usual shell model problem arises: the states are not eigenstates of the total momentum. This is an old and well-known problem, but is repeated here:

"How do we remove effects of the bag c.m. motion? How accurately?"

[In a contribution to the conference Goldflam and Betz describe a novel semi-classical procedure for correcting the charge form factor of a soliton bag for recoil effects.<sup>19</sup> The method does not, however, carry out a proper quantization of the total momentum and apparently ignores the momentum spread due to localization.] In the discussion Bolsterli remarked that in principle the soliton bag model permits a solution to the problem, but Kuti observed that such a solution exists only for very low momenta. The problem of quantizing the soliton in three dimensions has been with us for a decade and remains unsolved. Liu recalled a Peierls-Yoccoz technique for the bag model--one of several phenomenological approaches requiring added assumptions.<sup>21</sup>



#### 4. ASYMPTOTIC NUCLEAR FORM FACTORS AND THE EMC EFFECT

Quarks and gluons should certainly manifest themselves when nuclei are probed at short distances--e.g. in elastic form factors and in deep inelastic scattering at high  $Q^2$ . At lower values of  $Q^2$  a description in terms of hadronic degrees of freedom is more economical. The question, slightly rephrased from the original is

"How far can we go in  $Q^2$  with conventional hadronic degrees of freedom before we are forced to accept a quark model description?"

The discussion dealt with the "EMC effect" and the elastic form factors. The EMC effect refers to an apparent A-dependence of quark momentum distributions in nuclei.<sup>22</sup> The deep inelastic lepton scattering structure function at a given  $Q^2$  for a large nucleus, say  $^{56}\text{Fe}$ , is compared with that of a deuteron at the same  $Q^2$  and the same value of a scaling variable  $x$ , defined so that a nucleon at rest in the nucleus has  $x=1$ . The ratio of the iron to deuteron structure functions, renormalized by a factor of  $56/2$  would be exactly 1 if the nucleus consisted of a loose collection of A nucleons at rest with respect to each other. However, because of Fermi motion, the range  $0 < x < A$  is kinematically allowed. Experimental results are shown in figures 1-2 including experimental results of the Dubna group presented in the discussion by Baldin.<sup>23</sup> For  $x < 1$  there is an apparent enhancement at small  $x$  and depletion at large  $x$ . For  $x > 1$  there is again an enhancement. Several phenomena could produce these effects. There are violations of Björken scaling. Thus, it may be appropriate to compare the data at different  $Q^2$ , as suggested in the discussion by Close.<sup>24</sup> Pirner mentioned his work with Nachtmann, which attempts to justify an explicit relationship between the nuclear radius and the scale change.<sup>25</sup> Indeed much of the effect for  $x < 1$  can be accounted for in this way. The effect can also be explained in part by supposing that there are more pions per nucleon in the nucleus compared with the deuteron. Since the pions would tend to enhance the low  $x$  region, a higher  $x$  region would be depleted by momentum conservation. Various authors have attempted this approach. Coester commented that from his work it was not possible to account for the whole effect in this manner.<sup>26</sup> Close asked whether the results of Coester et al. didn't conflict with those of Llewellyn Smith<sup>27</sup>. Thomas answered that he thought the calculations agreed, but that the interpretation of the discrepancy was different, with Coester et al. insisting upon a stricter reading of the experimental error bars.<sup>28</sup> [A further complicating factor, not brought out in the public discussion, but developed in private conversations, is that all of these calculations have



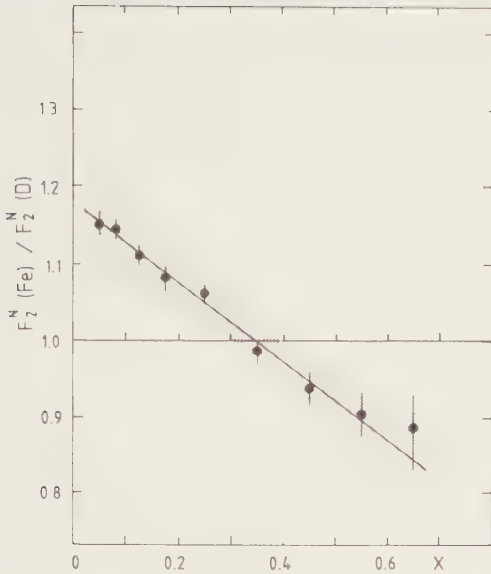


FIGURE 1

The ratio of the nucleon structure functions  $F_2^N$  measured on iron and deuterium as a function of  $x = Q^2/2M_p \nu$  from the EMC collection<sup>22</sup>.

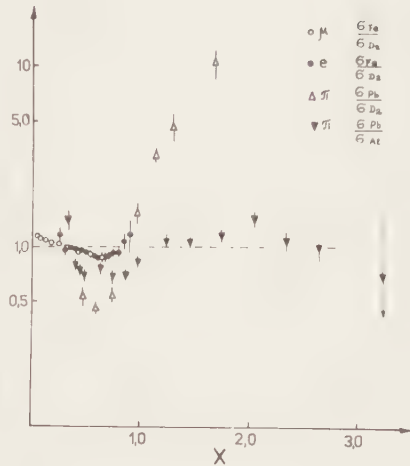


FIGURE 2

The same ratio as in Figure 1, compiled by the Dubna group<sup>23</sup>. The structure functions labeled  $\pi$  are reconstructed from pion fragmentation.

assumed that the pions and nucleons behave as naive partons--i.e. that they act incoherently.<sup>29</sup> Because they are composite objects, it is probably important to take into account interference terms in calculating the square of the nuclear and pion "wave function". These "shadowing" terms could lead to a growth of  $A^{2/3}$  as opposed to  $A$  in the contribution to the structure function for smaller values of  $x$ , depending upon kinematic considerations. The net result might give a trend opposite to what is observed. Thus the theoretical situation is somewhat confusing at the moment.] At  $x > 1$  the enhancement can be explained as due to multi-quark clusters. Vary cited his work with Pirner.<sup>30</sup> The effect may also be accounted for in conventional language by modifying the momentum distribution of nucleons in the nucleus, giving more nucleons with high momenta. The reaction  $eA \rightarrow ep$  ( $A-1$ ) is also sensitive to this high momentum tail, puts restrictions on it, and probably does not allow the whole effect to be explained in this way.

As for the elastic form factors, Sick despaired of ever reaching a sufficiently high value of  $Q^2$  that the asymptotic forms would be valid, since, for example, in the deuteron,  $Q$  must be absorbed by each of six quarks, and  $Q/6$  should be larger than at least the mean Fermi momentum. Brodsky replied that by dividing by the appropriately scaled nucleon form factors to get the "reduced form factor", these problems disappear and we can use  $Q^2 > 1 \text{ GeV}^2$ . Vary observed that the current studies leading to a theoretical determination of the normalization of the asymptotic form factors should put constraints on the multiquark clusters in his and Pirner's model and might allow a determination of the form factors over the whole range of  $Q^2$ .

#### V. MISCELLANEOUS

The miscellaneous session was devoted to topics proposed by the audience. The audience chose to devote a substantial portion of the session toward further discussion of the fourth topic above. Three further items were discussed.

Thomas proposed the question, "What is the pion, a collective state or a  $QQ$  state?", remarking that lattice gauge theories should give some hints. Weise, noting his work with the Regensburg group, observed that if the pion is to be a Goldstone boson, it is a collective state.<sup>31</sup>

Rinat, taking Brodsky's optimism about the QCD light cone evolution equations literally, pleaded with him to give us NN wavefunctions and to relate higher quark clusters to pairing forces. Brodsky remarked that we are close to knowing at least the part of NN relevant to the high  $Q^2$  elastic form factors.

In his talk earlier in the day Kuti reviewed recent evidence from lattice gauge theories suggesting that the QCD renormalization scale  $\Lambda$  should be increased by about a factor of two over the old value. The new value of  $\Lambda/\sqrt{T}$ , the ratio of the lattice QCD renormalization scale to the square root of the string tension is  $0.011 \pm 0.003$ .<sup>32</sup> In the miscellaneous session Schierholz mentioned his recent work calculating hadron masses using "staggered fermions" in the "quenched approximation", showing that the results are consistently interpreted using the old value of  $\Lambda$ .<sup>33</sup>

#### REFERENCES

- 1) S. Furui and A. Faessler, Nucl. Phys. A 397 (1983) 413.
- 2) R. L. Jaffe and F. E. Low, Phys. Rev. D19 (1979) 2105. See Mulders' talk, this conference.
- 3) E. M. Henley, L. S. Kisslinger, and G. A. Miller, Univ. of Washington, Seattle report 40048-22-N2 (May, 1983).
- 4) Y. E. Kim and M. Orlowski, Purdue Univ. report PNTG-83-8 (July 1983).

- 5) Yu. A. Simonov, Phys. Lett. 107B (1981) 1; Yad. Fiz. 36 (1982) 268; See Simonov's talk, this conference [ITEP-93 (1983)].
- 6) P. J. Mulders, this conference.
- 7) C. E. DeTar, Phys. Rev. D 17 (1978) 323.  
M. Harvey, Nucl. Phys. A352 (1981) 301, 326 uses a language that does not link the [4,2] component to a physical separation of the baryonic clusters, but he finds the same effect.
- 8) I. T. Obukhovskiy, V. G. Neudatchin, Yu. F. Smirnov, and Y. M. Tchuvilsky, Phys. Lett. 88B (1979) 231.  
I. T. Obukhovskiy, Z. Phys. A308 (1982) 253.
- 9) E. Lomon, contribution to this conference.
- 10) See Schmid's talk, this conference.
- 11) S. J. Brodsky, Chueng-Ryong Ji, and P. LePage, SLAC-PUB-3064 (Feb. 1983).
- 12) H. Høgaasen, J. M. Richard, and P. Sorba, Phys. Lett. 119B (1982) 272.
- 13) I. Bender, H. G. Dosch, H. J. Pirner, and H. G. Kruse, Univ. Heidelberg report (1983).
- 14) E. V. Shuryak, Nucl. Phys. B 203, 116 (1982).
- 15) K. Yazaki, this conference. See also D. Robson, contribution to this conference.
- 16) J. D. Stack, Institute for Theoretical Physics, Santa Barbara report, ITP-UCSB (1983).
- 17) A. N. Mitra et al., Z. Phys. C8 (1981) 25, 33.
- 18) F. Coester and W. Polyzou, this conference.
- 19) S. J. Brodsky and G. P. LePage, Phys. Rev. D 22 (1980) 2157.
- 20) R. Goldflam and M. Betz, this conference.
- 21) C. W. Wong, Phys. Rev. D 24 (1981) 1416.
- 22) J. J. Aubert et al (EMC) Phys. Lett. 123B (1983) 275.  
A. Bodek et al., SLAC-PUB-3041 (1982).
- 23) A. M. Baldin, Dubna report E2-83-415 (1983).
- 24) F. E. Close, R. G. Roberts, G. G. Ross, Phys. Lett. B (1983, to be published). See also H. Rith, talk at the European Physical Society Conference on High Energy Physics, Brighton, 1983.
- 25) O. Nachtmann and H. J. Pirner, Z. Phys. C (1983, to be published).
- 26) E. L. Berger, F. Coester, and R. B. Wiringa, ANL-HEP-PR-83-24 (1983).
- 27) C. H. Llewellyn Smith, Phys. Lett. B (1983, to be published).
- 28) M. Ericson and A. Thomas, Phys. Lett. B (1983, to be published).

- 29) S. Brodsky and F. Close, private communication (1983) stimulated by a remark by Jaffe at the European Physical Society Conference on High Energy Physics at Brighton.
- 30) J. P. Vary and H. J. Pirner, this conference and references therein.
- 31) V. Bernard, R. Brockmann, M. Schaden, W. Weise, and E. Werner, contribution to this conference.
- 32) See 16. Stack's figure also agrees with G. Parisi, R. Petronzio, and F. Rapuano, CERN-TH-3596 (May 1983).
- 33) Schierholz et al., DESY report (1983, in preparation).

## Chapter II

# PION-NUCLEON INTERACTION MESON-FEW NUCLEON SYSTEMS



## MESON-DEUTERON SCATTERING EXPERIMENTS : THE POLARIZATION ERA

Jacques ARVIEUX

Laboratoire National Saturne, 91191 Gif-sur-Yvette Cedex and  
Institut des Sciences Nucléaires, 38026 Grenoble Cedex, France

### 1. INTRODUCTION

At the time of the Eugene Conference in the summer of 1980 the core of accurate pion deuteron scattering data was formed by the very precise (1-2% accuracy) total cross-sections obtained at SIN in the range  $T_\pi = 70 - 370$  MeV and by extensive  $\pi d$  differential cross-sections also from SIN<sup>2</sup>, which were available as preprints. These were complemented by some measurements at backward angles<sup>4</sup> and 180 degrees<sup>3</sup> in the same energy region and by a few data sets at lower (25 and 47 MeV<sup>5-7</sup>) and higher (up to 512 MeV<sup>8</sup>) energies. Polarization data were limited to a single deuteron tensor polarization  $t_{20}$  (180°) measurement at 140 MeV from a pioneering work done at LAMPF<sup>9</sup>. Elaborate calculations within the Fadeev equations formalism were in good agreement with the experimental data up to  $T_\pi \sim 180$  MeV but there was (and there is still !) discrepancy at and above 256 MeV. At about the same time a surprising behaviour was confirmed in the polarized proton-proton total cross sections as a function of energy<sup>10</sup>. Although the detailed Nucleon-Nucleon (NN) data were subject to some controversy the undisputed conclusion was that NN polarization parameters could vary very fast with incident energy (even when unpolarized observables had a relatively smooth behaviour) and that they were very important for the understanding of the underlying dynamics. Most naturally deuteron polarization data were called for in  $\pi d$  scattering. The last three years have been dominated on the experimental side, by the advent of a wealth of polarization data and on the theoretical side, by a dispute over their interpretation in terms of dibaryon resonances. Since the latter subject is treated by M. Locher at this conference<sup>11</sup> we shall mainly concentrate on experimental problems which are serious enough to deserve a critical examination. In section 2 we review the experimental situation for cross-section data and examine the consistency between available data sets. We then analyze some recent results on  $\pi^\pm d$  comparison and their relation with charge symmetry breaking. Polarization data are reviewed in Section 3 and discrepancies between tensor polarization data sets are discussed.



A comparison with some theoretical models is made in Section 4.

## 2. DIFFERENTIAL CROSS-SECTIONS

### 2.1. Consistency between different data sets

Around 80, 120 and 140 MeV, the  $180^\circ$  measurements of Holt et al.<sup>9</sup> are consistent with lower angle data<sup>2</sup> and, for 142 MeV, with Stanovnik et al.<sup>4</sup> (CERN). At 143 MeV  $\pi^\pm$ -d cross-sections have recently been published by Masterson et al.<sup>12</sup> and they are in very good agreement with Gabathuler et al.<sup>2</sup> (SIN) (figure 1).

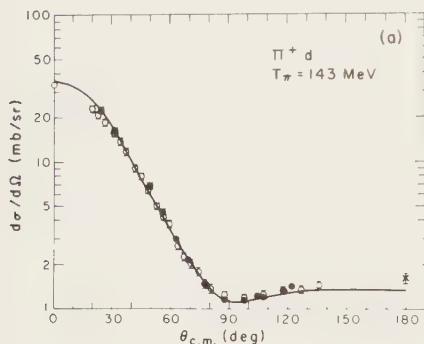


FIGURE 1

Comparison between SIN<sup>2</sup> (open dots) and LAMPF (black dots<sup>12</sup> and crosses<sup>9</sup>) data. The solid line is a three body calculation<sup>18</sup> without any free parameters.

At 180 MeV the CERN data<sup>4</sup> fall somewhat below the SIN data<sup>2</sup> and the  $180^\circ$  point of Frascaria et al.<sup>3</sup>. At 254 MeV the backward CERN data<sup>4</sup> extrapolate well from the SIN data<sup>2</sup> but they are in disagreement by a factor of 2 with the  $180^\circ$  point<sup>3</sup>. At 292 MeV new data by Minehart et al.<sup>13</sup> are again in excellent agreement with the SIN data<sup>2</sup>.

In conclusion the experimental situation for  $\pi$ -d differential cross-section is very gratifying with an impressive agreement between data obtained at different labs (LAMPF<sup>9,12,13</sup>, SIN<sup>2,3</sup> and CERN<sup>4</sup>) with different methods (spectrometer or recoil techniques) except at  $180^\circ$  where the direct measurements of Frascaria et al.<sup>3</sup> lie somewhat higher than straight extrapolations of the CERN<sup>4</sup> backward angle data. In view of the availability of extensive polarization data triggered by the great dibaryon hunt, some backward angle ( $130$ – $180^\circ$ ) cross-sections would be worth remeasuring.

### 2.2. Tests of charge symmetry

Charge-independence breaking (CIB) effects are most readily observed in the 3.3% difference between the  $\pi^\pm$  mass (139.57 MeV) and the  $\pi^0$  mass (134.96 MeV). Charge symmetry breaking (CSB) is more subtle as apparent in the much smaller mass difference between the neutron and the proton

$$(m_n - m_p) / \frac{1}{2} (m_n + m_p) = 0.14\%$$

(the fact that  $m_{\pi^+} \approx m_{\pi^-}$  is not due to charge symmetry but to TCP invariance since  $\pi^+$  and  $\pi^-$  are anti-particle to each other).

Further confirmation from CIB comes from the large difference between np and pp (Coulomb corrected)  $^1S_0$  scattering lengths. A recent estimate by Henley<sup>14</sup> gives (in fermis)

$$a_{np} = -23.715 \pm 0.015$$

$$a_{nn} = -16.4 \pm 1.2$$

$$a_{pp} = -7.823 \pm 0.011$$

$$a_{pp} \text{ (Coulomb corrected)} = (-17.2 \pm 3.0)$$

On the other hand the near equality of  $a_{nn}$  and  $a_{pp}$  (Coulomb corrected) is compatible with no CSB within large uncertainties on  $a_{nn}$  coming from the analysis of 3-body final states and on  $a_{pp}$  coming from electromagnetic corrections. Since the uncertainty on the pp Coulomb correction, as quoted by the same author<sup>15</sup>, has been multiplied by 1.5 in ten years, there is not much hope to find some CSB evidence from this system in the near future. Another approach is a comparison of binding energies in mirror nuclei which seems to leave some differences not accounted for by Coulomb effects<sup>14</sup> (e.g.  $^3\text{H}$ - $^3\text{He}$ ) but they need to be confirmed by other sources. Comparisons of  $\pi^+d$  and  $\pi^-d$  cross-section provide a sensitive test of CSB since electromagnetic corrections might be easier to calculate for scattering systems than for bound nuclei. Indeed evidence for CSB has been found<sup>1</sup> in total  $\pi^\pm d$  total cross-sections were asymmetries  $A = \frac{\sigma_{\pi^+} - \sigma_{\pi^-}}{\sigma_{\pi^+} + \sigma_{\pi^-}}$  of the order of 3-8% have been deduced after Coulomb and nuclear Coulomb interference corrections.

Two precise comparisons of  $\pi^\pm d$  scattering at 65 MeV<sup>16</sup> and 143 MeV<sup>12</sup> have since been published. At the lowest energy Coulomb effects are important which result in large experimental asymmetries but also in a greater dependence of CSB to electromagnetic corrections. The results shown in figure 2 are compared with theoretical models : Fadeev type 3-body calculations<sup>18,19</sup> (curves a and b) and single scattering via  $\Delta$ -isobar excitation<sup>17</sup> (curves c and d), all including Coulomb corrections. These calculations reproduce the overall asymmetry shape except in the 90°-110° region but since they do not fully fit the separate  $\pi^+$  and  $\pi^-$  data in this angular range it is too early to talk of evidence for CSB from this result.

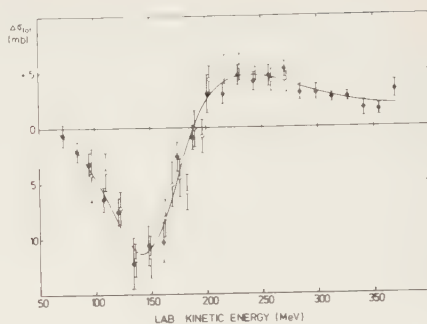
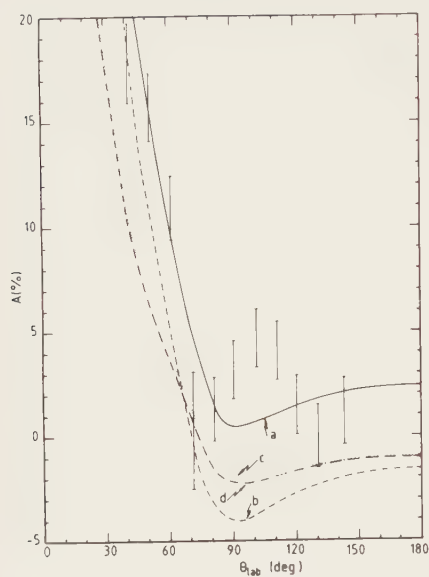


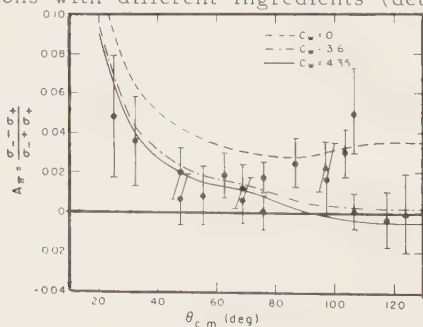
FIGURE 3

Difference between  $\pi^+d$  and  $\pi^-d$  total cross-sections as function of incident energy<sup>1</sup> after electromagnetic corrections

FIGURE 2

Asymmetry parameter in  $\pi^\pm d$  scattering at 65 MeV<sup>16</sup>. The curves are described in the text

The energy of 143 MeV may be more adequate for CSB studies for multiple reasons 1) Coulomb effects are weaker and electromagnetic corrections should be less critical, 2) theoretical models<sup>19-21</sup> reproduce well the experimental cross-sections and 3) at this energy the largest difference was found in  $\pi^\pm d$  total cross-section measurements<sup>1</sup> (figure 3). This feature is probably related to the fact that at these energies  $\pi d$  scattering is dominated by excitation of  $\Delta$ -resonances in intermediate states. To lowest order  $\pi^+d$  scattering is then dominated by  $\Delta^{++}(\pi^+p)$  and  $\Delta^+(\pi^+n)$  excitation;  $\pi^-d$  scattering by  $\Delta^0(\pi^-p)$  and  $\Delta^-(\pi^-n)$  excitation. Since the masses of the  $\Delta$ -isobars are not the same in different charge states, they must consequently produce CSB effects. The angular distribution of the asymmetry parameter  $A$  is shown in figure 4 where it is compared to Fadeev calculations with different ingredients (deuteron wave-function, pion absorption,



etc...) all including Coulomb effects.<sup>12</sup>

FIGURE 4

Asymmetry parameter  $A(\theta)$  at 143 MeV compared to 3-body calculations with external ( $c_w = 0$ ) and internal Coulomb corrections

When assuming charge symmetry of the strong interaction (curve  $C_w = 0$ ) the large forward angle asymmetry and overall shape is satisfactory reproduced with external Coulomb corrections except for the angular region  $\theta_{cm} = 90^\circ - 110^\circ$ . A better fit is obtained if one allows CSB by varying the mass of the intermediate  $\Delta$  isobar through the isobar mass difference parameter  $C_w = W_- - W_{++} + \frac{1}{3} (W_o - W_+)$  where  $W_-$  is the mass of the  $\Delta^-$  and so on. The best fit is obtained for  $C_w = 4.35 \pm 0.50$  MeV in very good agreement with the value of  $4.6 \pm 0.2$  MeV obtained in the total cross-section comparison<sup>1</sup> and with quark-model predictions of 4.3 MeV<sup>22</sup> or 3.9 MeV<sup>23</sup>. On the other hand Rinat et al<sup>24</sup> concluded to no CSB evidence from a recent analysis of the same data so the problem of data interpretation in terms of CSB is essentially a theoretical one.

Since the  $\pi d$  vector-analyzing power  $iT_{11}(\theta)$  is well fit at this energy by theoretical 3-body calculations (see Section 3) a precise  $\pi^\pm$  comparison for this parameter would bring useful complementary information. One set of accurate  $\pi^\pm d$  cross-section data at an energy over the (3,3) resonance (e.g. around 260 MeV) where Coulomb effects would be even smaller could also be helpful.

Finally it should be stressed that at this high level of data precision, radiative correction might become significant as emphasized by Saghai in a recent contribution<sup>42</sup>. At 200 MeV effects up to 4% have been computed for  $\pi^+d$  scattering and 7% for  $\pi^-d$  scattering which, if not corrected, would result in a 3% false  $\pi^\pm$  asymmetry.

In conclusion 1) there exists a fairly extensive body of accurate cross-section data over the region 25-500 MeV for which, except for some minor discrepancies, good agreement exists between different data sets, 2) precise  $\pi^\pm d$  comparisons are available for total and differential (at 65 and 143 MeV) cross-sections, 3) the raw data exhibit large  $\pi^+/\pi^-$  asymmetries, mostly explained by external Coulomb correction, 4) after removal of electromagnetic effects, asymmetries at the level of a few per cent are still present and they can be parametrized with different masses and widths of the  $\Delta$ -isobars in different charge state (inner electromagnetic corrections).

### 3. DEUTERON POLARIZATION MEASUREMENTS

Besides total and differential cross-sections two spin dependent parameters have been studied, namely the vector analyzing power  $iT_{11}(\theta)$  and tensor polarization parameter  $t_{20}^{lab}(\theta)$ . Following the Madison Convention analyzing powers  $T_{kq}(\theta)$  are deduced from asymmetry measurements with a polarized deuteron target and  $t_{kq}(\theta)$  are polarization parameters of the recoil deuteron in scattering of pions by an unpolarized deuteron target.

3.1. Vector analyzing power  $iT_{11}(\theta)$

An impressive set of data has come out from the Karlsruhe-Erlangen-SIN collaboration<sup>25,26</sup>. The first data were obtained at 142 and 256 MeV. The 142 MeV data showed a smooth angular behaviour in good agreement with available theoretical calculations<sup>19-21</sup>; on the contrary the 256 MeV exhibited marked oscillations (figure 5) which were predicted by Kubodera et al<sup>37</sup> if dibaryon resonance amplitudes were added to 3-body Fadeev amplitudes. Although there were some difficulties to understand both the 142 MeV and 256 MeV data with the same theoretical assumptions, these results caused a great excitement and prompted some new measurements which extended the angular and energy range.

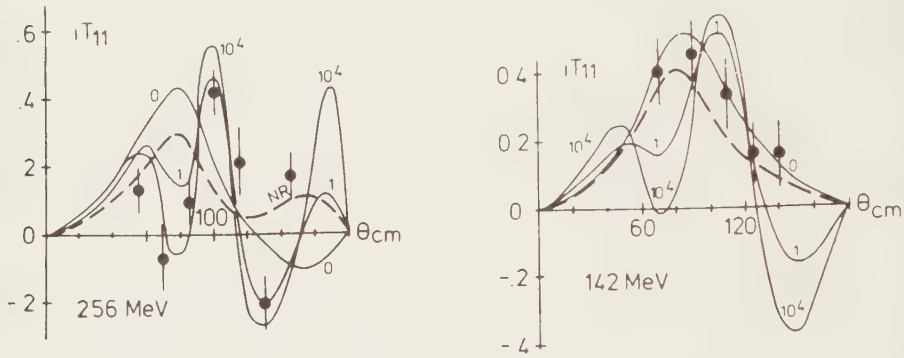


FIGURE 5  
Earlier  $iT_{11}(\theta)$  data at SIN<sup>25</sup>. The dotted curve is a calculation without explicit dibaryon, for the solid curves diverse dibaryon resonances have been added.

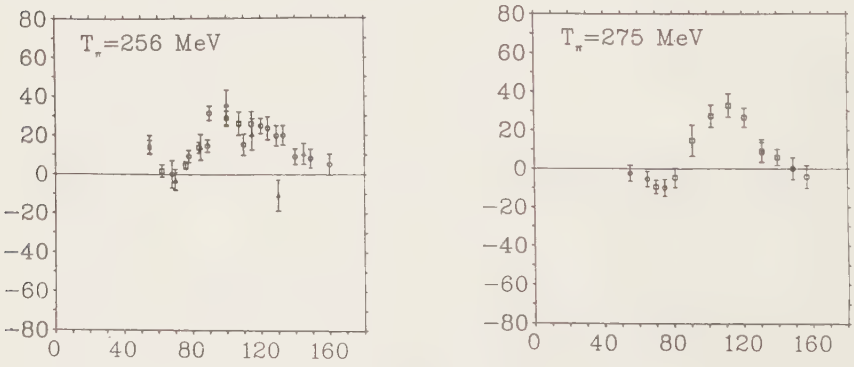


FIGURE 6  
New  $iT_{11}(\theta)$  data from SIN<sup>44</sup> (preliminary)

Apart from a renormalization of the complete set of data by a factor 2/3 coming from a different definition of the target polarization, the new data (figure 6) essentially confirm the previous ones except for the single negative point at 256 MeV and 130° where  $iT_{11}$  is now all the way positive. This changes somewhat the picture since it removes the wild backward oscillation which caused so much speculation. The new data are still not reproduced by existing calculations up to 90° but there is now more hope to understand these data.

### 3.2. Tensor polarization

The tensor polarization parameter  $t_{20}^{\text{lab}}(\theta)$  is measured by double scattering techniques. The pion beam first hits an unpolarized deuteron target ( $\text{CD}_2$  or liquid deuterium). The pions are scattered at an angle

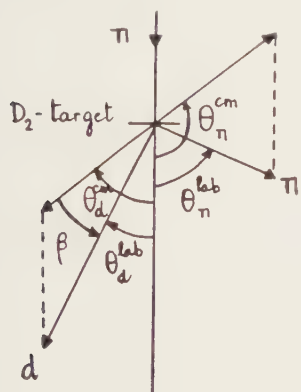


FIGURE 7  
Definition of the scattering angles  
in the measurement of  $t_{20}^{\text{lab}}(\theta)$

$\theta_{\pi}^{\text{lab}}$  in the lab system to which corresponds an angle  $\theta_{\pi}^{\text{cm}}$  (in short  $\theta$ ) in the c.m. system (figure 7).

The deuterons recoiling at an angle  $\theta_d^{\text{lab}}$  are focussed by a system of quadrupole lenses onto a secondary gaseous  $^3\text{He}$  target where they initiate the  $^3\text{He}(d, p)^4\text{He}$  reaction. The outgoing protons are detected at 0° in scintillator telescopes and/or Si(Li) detectors. The parameter  $t_{20}^{\text{lab}}$

is extracted from the relation

$$\epsilon = \epsilon_0 [1 + t_{20}^{\text{lab}}(\theta) T_{20}(0^\circ)]$$

where  $\epsilon_0$  and  $\epsilon$  are respectively efficiencies for an unpolarized or a polarized beam ;  $T_{20}(\theta)$  is the analyzing power of the  $^3\text{He}(d, p)$  reaction which is known to be large in

this energy region<sup>29</sup>. In order to determine the effective efficiency of the polarimeter<sup>18</sup> one has to make an experimental calibration at a low-energy machine (Berkeley cyclotron or SIN injector) where  $\epsilon_0$ ,  $\epsilon$  and  $T_{20}(\theta)$  (effective) are measured with a deuteron beam having a well known polarization  $t_{20}$ .

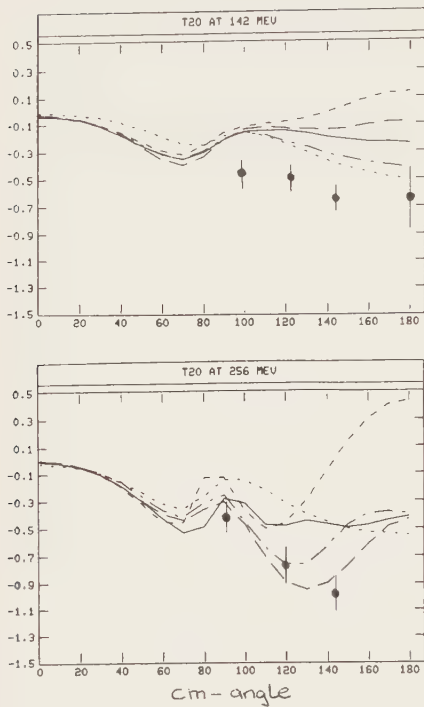


FIGURE 8:  
 $t_{20}(\theta)$  at 142 and 256 MeV<sup>30</sup>. The curves are theoretical calculations by Blankleider and Afnan (solid line) Betz and Lee (dots), Rinat (dash dots), Fayard et al. (short and long dash)

Experiments have been done in two independent labs using the same type of polarimeter but differing in some details. The latest results of Holt et al<sup>30</sup> at 142 MeV and 256 MeV are shown in figure 8. They confirm previous data by the same group. All values are negative and have both a smooth angular and energy dependence. Although the agreement with 3-body calculations including absorption, is not perfect the overall trend is reproduced by most models (with the exception of the calculations of Betz and Lee<sup>32</sup>).

The other set of data has been obtained at SIN by a Zurich group. In a first measurement at 138 MeV (later corrected for 134 MeV) a strong positive oscillation was found between 130° and 180° which, except for the 150° point, could have been in some agreement with the LAMPF data. Subsequent measurements<sup>34,35</sup> confirmed the first oscillation and exhibited a second positive oscillation, now in definite disagreement with Holt's results (figure 9). These oscillations are smoothed out at 117 and 151 MeV although the overall trend is still positive as shown in the excitation function at 150° (figure 10). Both sets of data can only be exactly compared at 142 MeV where



$t_{20}(150^\circ) = +0.35 \pm 0.05$  for the SIN data which cannot be reconciled with  $t_{20}(145^\circ) = -0.65 \pm 0.05$  for the LAMPF data.

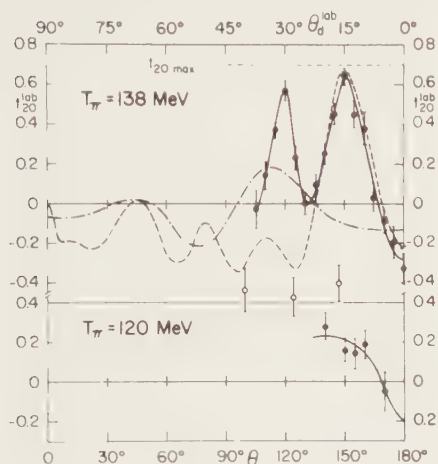


FIGURE 9

$t_{20}(\theta)$  at 117 MeV and 134 MeV<sup>35</sup> (energies corrected by the authors). Black dots are SIN data<sup>34</sup> and open circles are LAMPF data at 142 MeV<sup>31</sup>. The solid curve is a guide for the eye only.

In conclusion there is a clear case of data incompatibility in the measurement of  $t_{20}^{lab}(\theta)$  around 140 MeV which can only be solved by further measurements.

These measurements should better control the experimental conditions (e. g. extensive use of MWPC's to better trace the apparatus acceptance and check for any accidental losses). The results of an experiment proposed at TRIUMF<sup>36</sup>, although using the same polarimeter technique, are awaited with interest. A strong improvement would be to use a polarimeter which does not rely on absolute yields but on asymmetry measurements.

#### 4. COMPARISON WITH THEORY

##### 4.1. Introduction

Pion (spin 0)- deuteron (spin 1) scattering is completely described by a  $3 \times 3$  helicity amplitude matrix  $M(\theta)$ . If one takes time-reversal invariance and parity-conservation into account only 4 complex amplitudes are independent but they are related through an overall phase so that 7 independent experiments are required at each angle and energy to fully determine the scattering matrix. We are far from this goal since only the cross-section  $\frac{d\sigma}{d\omega}(\theta)$  and two spin parameters  $iT_{11}(\theta)$  and  $t_{20}^{lab}(\theta)$  have been measured

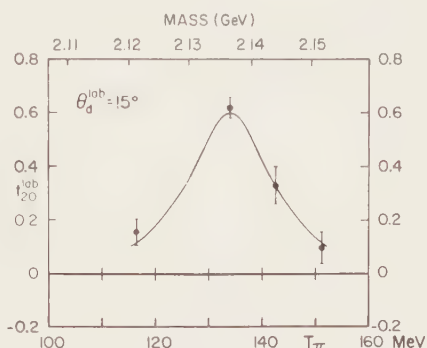


FIGURE 10

Excitation function of  $t_{20}(150^\circ)$ <sup>35</sup>. The solid line is a visual guide

over a limited range of angles and energies. They nevertheless bring useful information on the reaction dynamics through a direct comparison with theoretical models or through a phase-shift analysis (PSA). These two approaches have a common feature : they don't impose dibaryon constraints as a start.

#### 4.2. Theoretical models

There are now many theories<sup>19-21</sup> which are : exact (unitary in two and three body channels), relativistic (they are potential theories but fully covariant) and realistic (in the way NN and  $\pi$ N interaction are taken into account). They all include pion-absorption through the  $\pi$ N  $P_{11}$  pole term, so they can treat  $\pi d \rightarrow d$ ,  $\pi d \rightarrow NN$  and  $NN \rightarrow NN$  (long and medium range part) on the same footing. These calculations contain dibaryon effects only if they are generated by the input  $\pi$ N and NN amplitudes (e.g. through  $NN \rightarrow \Delta N$  intermediate states). There are a few groups working independently and an impressive feature is the agreement between the different calculations despite the complexity of the computational problems and differences in input (parametrization of the  $\pi$ N and NN amplitude, NN vertex form factors, inclusion or not of  $\rho$ -exchange etc...).

As can be seen<sup>19</sup> in figure 11, the agreement is very good with the 142 MeV data, marginal at 180 MeV in view of the uncertainty of the backward angle data, (see Section 2.1.) and definitely bad above 90° at 256 MeV. The same conclusion could be drawn from all 3-body calculations. One interesting fact is the better agreement when the  $P_{11}$   $\pi$ N pole term, responsible for pion absorption, is neglected. There are at least two independent confirmations of this feature 1) in a phase shift analysis<sup>28</sup> including  $iT_{11}(\theta)$  at 142 MeV and 256 MeV but not  $t_{20}$  it was found that the  $f_{LL}^J = f_{11}^0(S_1)$  and  $f_{00}^1(P_0)$  amplitudes which are most sensitive to absorption effects were experimentally closer to the no-absorption theoretical values, 2) more recently the  $t_{20}^{lab}$  data obtained by Holt<sup>30</sup> are also better reproduced by no absorption calculations. This converging evidence deserves more attention from the theoreticians.

Concerning  $iT_{11}$ , the same satisfactory agreement is observed at 142 MeV (figure 12) which does not persist at 256 MeV and above. There may be two types of explanations for this discrepancy 1) assume that the theory is essentially correct but that some ingredients are lacking, e.g. pion-nucleon  $P_{13}$ ,  $P_{31}$  or higher partial waves, which become more and more important as the energy increases, 2) suppose that some dynamical effects are missing from the theory (e.g. exotic dibaryon states not mediated by standard  $\pi$ N and NN interaction) which are then added to 3-body amplitudes (but some

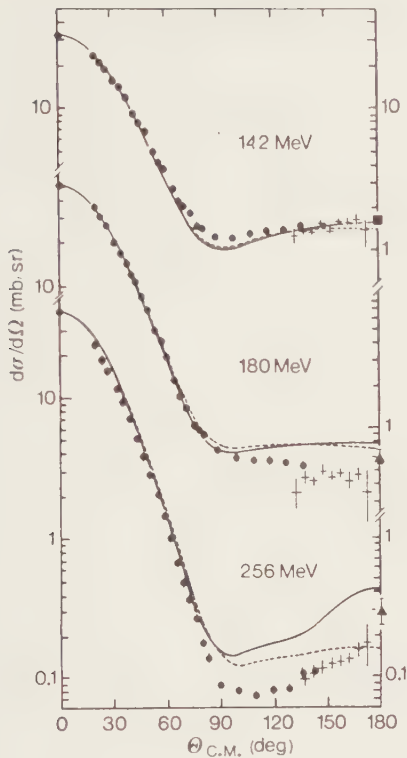


FIGURE 11  
Comparison of 3-body calculations<sup>19</sup> with experimental differential cross-sections. The solid line includes pion absorption, the dotted line does not.

#### 4.3. Phase shift analysis (PSA)

In a PSA exotic phenomena would appear in the behaviour of the experimental phase-shifts (or amplitudes). There are currently 3 PSA including some of the most recent polarization data. Hiroshige et al<sup>38</sup> tried to fit earlier  $\text{SIN } t_{20}^{\text{lab}}$  data together with the LAMPF data points although they somewhat disagree. Moreover there was an error in their calculation of  $t_{20}$ . Since the scattering matrix is usually defined in the c.m. system it is necessary to derive the parameter  $t_{20}^{\text{lab}}$  as a function of the polarization in the cm system of the deuteron obtained by a rotation  $\beta = (\theta_d^{\text{lab}} - \theta_d^{\text{cm}})$  of the quantization axis around the perpendicular to the scattering plane (figure 7). One gets

care has to be taken with unitarity since Fadeev amplitudes are themselves unitary).

The agreement of all 3-body calculations at low energy is consistent with a large  $2^+$  amplitude with counterclockwise Argand plot. This behaviour has been sometimes associated with a  $^1D_2$  dibaryon at 2.14 GeV (which correspond to  $T_\pi \sim 140$  MeV) with width  $\Gamma \sim 75$  MeV. There seems now to be a consensus in favor of an effect due to the opening of the S-wave  $N\Delta$  channel. Concerning the discrepancy at higher energies more investigation are needed both experimentally (e.g. forward angle polarization data would be useful) and theoretically before deciding in favor of exotic phenomena. One step in this direction is a recent contribution in which Rinat shows<sup>43</sup> that some oscillatory behaviour for  $T_{11}(\theta)$  can be generated at 256 MeV by using the

cloudy bag model to calculate  $\pi d$  amplitudes.

$$t_{20}^{\text{lab}}(\theta) = \frac{1}{2} (3\cos^2 \beta - 1)t_{20}^{\text{cm}}(\theta) - \left(\frac{3}{2}\right)^{\frac{1}{2}} \sin 2\beta t_{21}^{\text{cm}}(\theta) + \left(\frac{3}{2}\right)^{\frac{1}{2}} \sin^2 \beta t_{22}^{\text{cm}}(\theta)$$

If the pion cm angle  $\theta$  is counted positive counter-clockwise, then the angle  $\beta$  is also positive. This formula was first derived in ref. 31 (in which the angle  $\alpha$  is counted negatively). Unfortunately due to a printing error the exponent 1/2 was missing twice and although the error was corrected in an erratum<sup>31</sup> it apparently escaped the attention of the Japanese group<sup>39</sup>. Their results at 142 MeV are then doubtful otherwise the amplitudes ( $J = 2, L = L' = 1$ ) and ( $J = 3, L = L' = 2$ ) which couple to the  $^1D_2$  and  $^3F_3$  NN states have a fairly smooth behaviour with energy and show counter-clockwise looping. A K-matrix analysis of  $\pi d + \pi d$ ,  $pp + pp$  and  $pp \rightarrow \pi d$  amplitudes concludes to a pole in the  $^1D_2$ -state at  $s^{1/2} = 2.20$  MeV with total width  $\Gamma = 173$  MeV which is dynamically related to the  $N\Delta$  channel. Gruebler et al have performed a PSA of their results around 140 MeV and they reproduce this fast variation of  $t_{20}^{\text{lab}}$  between 117 and 151 MeV. They suggest that this behaviour is the signal from a dibaryon resonance not compatible with effects of the well-known  $N\Delta$ -resonance<sup>35</sup> but give no resonance parameter assignment.

A third PSA<sup>39</sup> includes total and differential cross-sections and the most recent polarization data. Three-body amplitudes are used as inputs for the high-partial waves in the same way OPEP was used in nucleon-nucleon PSA to constrain the long-range part of the NN interaction. The conflicting  $t_{20}^{\text{lab}}(\theta)$  data were analyzed separately. If Holt's data are used a smooth behaviour is obtained in all-partial waves resulting in counter-clockwise looping with widths 100-200 MeV which can be interpreted as pseudo resonances in  $N\Delta$  intermediate states<sup>40</sup>. When Gruebler's data are included at 142 MeV, many amplitudes (including the dominant ones for which  $L = L' = J - 1$ ) have to be drastically changed from the theoretical values to get an acceptable fit (figure 12). This difficulty in fitting the SIN data is to be related to the fact that when  $t_{20}^{\text{lab}}(\theta)$  reaches its maximum value  $+1/\sqrt{2}$  (at 134 MeV and  $\theta = 150^\circ$ )  $iT_{11}(\theta)$  must be equal to zero<sup>33</sup> which is not the case as seen in figure 13. Moreover if there were a fast amplitude variation in a small energy region due to a resonance of the compound  $\pi d$  system there should be a corresponding effect in  $pp + \pi d$  amplitudes. These have been determined at  $90^\circ$  by a Geneva group<sup>40</sup> at SIN between 450 and 580 MeV proton kinetic energy (555 MeV corresponds to the same c.m. energy as 134 MeV in  $\pi d$  elastic scattering) and they show no resonance except if it were very sharp (figure 14).

# Vector Analyzing Power

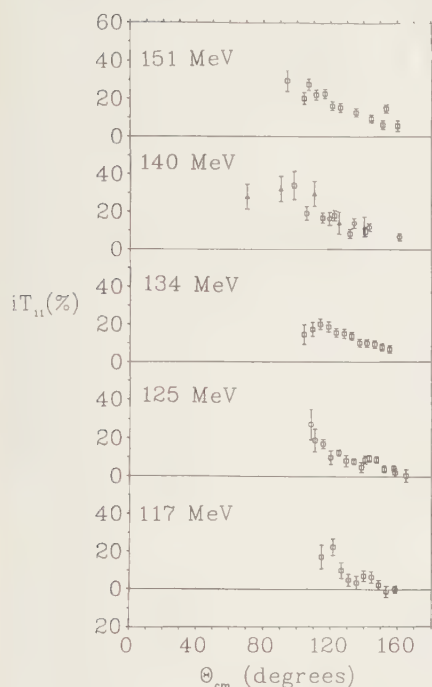


FIGURE 12

$iT_{11}(\theta)$  in  $\pi d$  scattering around 140 MeV (preliminary SIN data<sup>44</sup>)

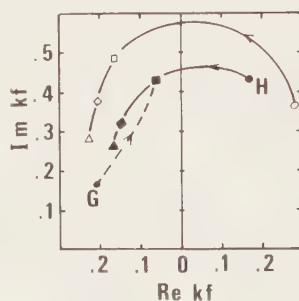


FIGURE 13

Argand plot of the  $P_2$  amplitude ( $J = 2, L = L' = 1$ ) from a phase shift analysis of  $\pi d$  scattering<sup>39</sup> 19. Open symbols are theoretical values ( $\circ$  140 MeV,  $\square$  217 MeV,  $\diamond$  256 MeV,  $\Delta$  292 MeV). For the points at 142 MeV labelled G and H the  $t_{lab}$  data of Gruebler et al<sup>35</sup> and 20 Holt et al<sup>30</sup> respectively have been analyzed

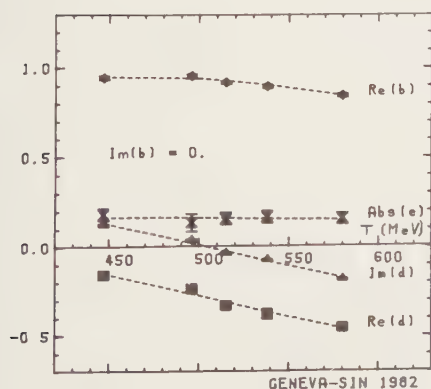


FIGURE 14

Amplitudes for the  $pp + \pi d$  reaction at  $90^\circ$  as a function of the proton incident energy

## 5. CONCLUSIONS

Pion-deuteron scattering illustrates the degree of accuracy (cross section data) and ingenuity (polarization data) achieved at meson factories with beams of unstable particles. Experimental progress has been accompanied by sophisticated 3-body calculations which would probably not have been done if there had been no hope to check them against good data. All these calculations are in good agreement with the existing data up to 140 MeV (except for one  $t_{20}^{\text{lab}}$  set). It is gratifying for the mind that a complex 3-body problem can be understood in terms of 2-body ( $\Delta N$  and  $NN$ ) interactions but it pleases our curiosity that some mysteries are still to be solved both experimentally and theoretically. The most urgent problem concerns  $t_{20}^{\text{lab}}(\theta)$ . If LAMPF data were confirmed  $\pi d$  scattering would well be represented by  $\pi NN$  elementary interactions coupling to  $N\Delta$  states although details of the theory still need to be refined. If the sharp structure of the  $SIN$  data were real then it could be a strong indication for long sought exotic effects.

## REFERENCES

- 1) E. Pedroni et al. Nucl. Phys. A300 (1978) 321
- 2) K. Gabathuler et al. Nucl. Phys. A350 (1980) 253
- 3) R. Frascaria et al. Phys. Lett. 91B (1980) 345
- 4) A. Stanovnik et al. Phys. Lett. 94B (1980) 323
- 5) B. Saghai in IKO Summer Studies on "Physics with low energy beams of pions and muons". ed. by R. Van Dantzing et al, Amsterdam (1978) p. 17
- 6) B. Balestri et al. AIP Conf. Proc. 54 (1979) 515
- 7) D. Axen et al. Nucl. Phys. A256 (1976) 243
- 8) R. H. Cole et al. Phys. Rev. C17 (1978) 681
- 9) R.J. Holt et al. Phys. Rev. Lett. 43 (1979) 1229
- 10) A. Yokosawa, Phys. Reports 64 (1980) 49
- 11) M.P. Locher and M.E. Sainio, Phys. Lett. B121 (1983) 227 and M.P. Locher, this volume
- 12) T.G. Masterson et al. Phys. Rev. C26 (1982) 2091
- 13) R.C. Minehart et al. Phys. Rev. Lett. 46 (1981) 1185
- 14) E.M. Henley and G.A. Miller in "Mesons in Nuclei", Eds. M. Rho and D.H. Wilkinson, North-Holland Publishing Company, 1979, p. 406
- 15) E.M. Henley in "Isospin in Nuclear Physics", Ed. D.H. Wilkinson, North-Holland Publishing Company, 1969, p. 16

- 16) B. Balestri et al. Nucl. Phys. A392 (1983) 217
- 17) R.M. Rockmore, Phys. Rev. C21 (1980) 2678
- 18) N. Giraud et al. AIP Conf. Proc. 54 (1979) 590
- 19) C. Fayard et al. Phys. Rev. Lett. 45 (1980) 524
- 20) B. Blankleider and I.R. Afnan, Phys. Rev. C22 (1980) 1638
- 21) A.S. Rinat and Y. Starkand, Nucl. Phys. A397 (1983) 313
- 22) H.R. Rubinstein et al. Phys. Rev. 154 (1967) 1608
- 23) N.G. Deshpande et al. Phys. Rev. D15 (1977) 1885
- 24) A.S. Rinat and Y. Alexander, preprint WIS-82/33, june PH, Weizmann Institute, Rehovot, Israel
- 25) J. Bolger et al. Phys. Rev. Lett. 46 (1981) 167
- 26) J. Bolger et al. Phys. Rev. Lett. 48 (1982) 1667
- 27) J. Arvieux et A.S. Rinat, Nucl. Phys. A350 (1980) 205
- 28) J. Arvieux, Phys. Lett. 103B (1981) 99
- 29) W. Gruebler et al. Nucl. Phys. A334 (1980) 365
- 30) R.J. Holt, private communication
- 31) R.J. Holt et al. Phys. Rev. Lett. 47 (1981) 472 and 47 (1981) 1862 (erratum)
- 32) M. Betz and T.S.H. Lee, Phys. Rev. C23 (1981) 375
- 33) J. Ulbricht et al. Phys. Rev. Lett. 48 (1982) 311
- 34) W. Gruebler et al. Phys. Rev. Lett. 49 (1982) 444
- 35) W. Gruebler et al. Contribution to 5th International Symposium on High Spin Physics, Brookhaven, Sept. 1982, AIP Conf. Proc.95(1983)234
- 36) W. Shin, private communication
- 37) K. Kubodera et al. J. Phys. G : Nucl. Phys. 6 (1980) 171
- 38) N. Hiroshige et al. Prog. Theor. Phys. 68 (1982) 327 and private communication
- 39) M. Meyer and J. Arvieux, to be published
- 40) E. Aprile et al. SIN Newsletter n° 15, p. NL15, 1983 and to be published
- 41) Y.A. Simonov and M. Van der Welde, J. Phys. G : Nucl. Phys. 5 (1979) 493
- 42) B. Saghai, Internal Report D.Ph-N/HE 83-2, Saclay 1983, to be published
- 43) A.S. Rinat, Phys. Lett. 126B (1983) 151
- 44) E. Boschitz, private communication.





## PION ABSORPTION AND PRODUCTION IN FEW NUCLEON SYSTEMS

Garth JONES

Physics Department, University of British Columbia, Vancouver, B.C. Canada

### 1. Introduction

Investigations of pion production and absorption in few nucleon systems is clearly the means for studying both the elementary pion creation and annihilation processes and the associated problem of the propagation of pions and excited nucleons within nuclear matter. In this paper I wish to discuss those aspects of the subject which have received most attention by the contributors to this conference. Since David Bugg has discussed the  $NN \rightarrow NN\pi$  situation in some detail, I shall restrict my treatment of the  $NN$  system to involve only the specific reaction  $\pi d \rightarrow 2p$ . In addition, I will discuss a few selected topics concerning pion production and absorption in few nucleon systems, primarily to point out areas in which significant activity is currently in progress. I shall also restrict all discussion to those situations in which only one pion is involved, excluding any mention of multi-pion processes.

### 2. $NN \rightarrow d\pi$

#### 2.1. Theoretical situation

The  $NN \rightarrow NN\pi$  reaction is the fundamental pion production reaction. The particular example,  $pp \rightarrow d\pi$ , is the simplest to study experimentally because of the 2-body final state. The strength of the final state interaction of the two nucleons (a bound state, in fact) permits this reaction to dominate the pion production process up to about 600 MeV. Some simplification in the theoretical description of the reaction also results from the fact that the isospin of the nucleon pairs in the initial and final states are well defined.

This reaction (and its inverse) thus constituted the earliest pion production (absorption) process investigated experimentally. The experimental effort was matched by corresponding vigorous theoretical activity. An extensive review of the current status of the theory was presented at Bloomington by Betz et al.<sup>1</sup>(1982).

In this paper, I should like first to paraphrase their presentation by providing simply a qualitative description of the various theoretical approaches. The first realistic field-theoretic treatment of the  $pp \rightarrow d\pi$  reaction based on the Chew-Wick model of  $\pi N$  dynamics was published in the mid 50's by Lichtenberg<sup>2</sup>. In that paper, he extended an earlier model of pion

emission to include pion rescattering through the  $(3,3)$  resonance. The relevant terms are illustrated diagrammatically in Fig. 1a. This model yielded reasonably good agreement with the experimental data available at that time. It should be noted that Lichtenberg recognized the importance of the large longitudinal momentum transfer characterizing the process and was one of the first to point out the resulting importance of the D state of the deuteron. This basic picture was subsequently refined by a number of workers, to include N-N distortions, explicit calculation of pion rescattering for all s- and p-wave spin-isospin channels,  $\rho$  exchange etc. Until the early 70's the theoretical treatment consisted primarily of non-relativistic first-order perturbation theory (non-relativistic except possibly for the pion kinematics) involving at most only one re-scattering of the pion. Clearly, for such a strong interaction, multiple scattering (as shown in Fig. 1b) is at least as important as the usual distortions considered between the initial nucleons and between the final pion and deuteron. Including both effects however can lead to over-counting problems because the distortions are themselves manifestations of the multiple scattering already referred to. Improvements in the theoretical description have resulted from several different approaches.

One technique, introduced by the Helsinki group, (principally Green and Niskanen<sup>3</sup>) involved the development of a coupled-channels technique illustrated diagrammatically in Fig. 1c. Such coupling of the NN and N $\Delta$  channels included  $\rho$  exchange implicitly and provided a full summation over pion multiple scattering. The approach, however, was non-relativistic involving static channel-coupling potentials. For the first time, however, theory was able to provide predictions<sup>4</sup> which compared well with experimental measurement (not only of the differential and total cross-sections, but also of a variety of polarization observables). This group was the first to include up to f-wave angular momentum channels for the pions (f-wave arising from the  $^1G_4$  pp state which couples to the D-wave N- $\Delta$  intermediate state). This theoretical approach was a forerunner of the current  $\Delta$ -hole models used in considerations of pion interactions with nuclei.

An alternative approach based on the application of Faddeev techniques (Afnan and Thomas<sup>5</sup> and Mizutani and Koltun<sup>6</sup>) enabled exact summation over all multiple scatterings of the pion (albeit with the restriction that no more than one pion at a time be involved in the intermediate state). This technique is illustrated diagrammatically in Fig. 1d. A major result of this technique was the achievement of exact two- and three-body unitarity. In this way, NN scattering, the NN  $\rightarrow \pi d$  reaction, NN  $\rightarrow$  N $\Delta$  coupling and  $\pi d$  elastic scattering are all related within a single framework. It is illustrated diagrammatically in Figs. 1e-g.

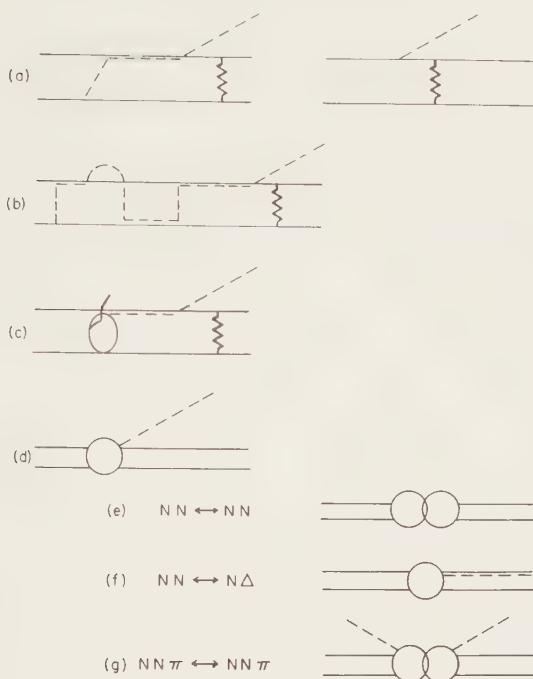


Fig. 1 (a) Pion rescattering and single emission graphs.

(b) Typical example of pion multiple scattering graph.

(c) Graph illustrating coupled-channels approach. The elliptical blob represents the  $NN\text{-}N\Delta$  coupling.

(d) 3-body unitary approach. The circle represents exact summation over all pion rescattering.

(e,f,g) Schematic representations of the application of the 3-body unitary approach to  $N\text{-}N$  scattering,  $NN \rightarrow N\Delta$  coupling, and  $\pi d$  scattering.

This approach was developed further by three principal groups: the Flinders' group of Afnan and Blankleider<sup>7</sup>, the Lyons group of Fayard et al.<sup>8</sup> and that of Rinat<sup>9</sup>.

The latter two groups have developed fully relativistic approaches based on Blankenbecler-Sugar reduction techniques. Full sets of amplitudes for the  $pp \rightarrow d\pi$  reaction, however, have been published only by the Rinat and Flinders'

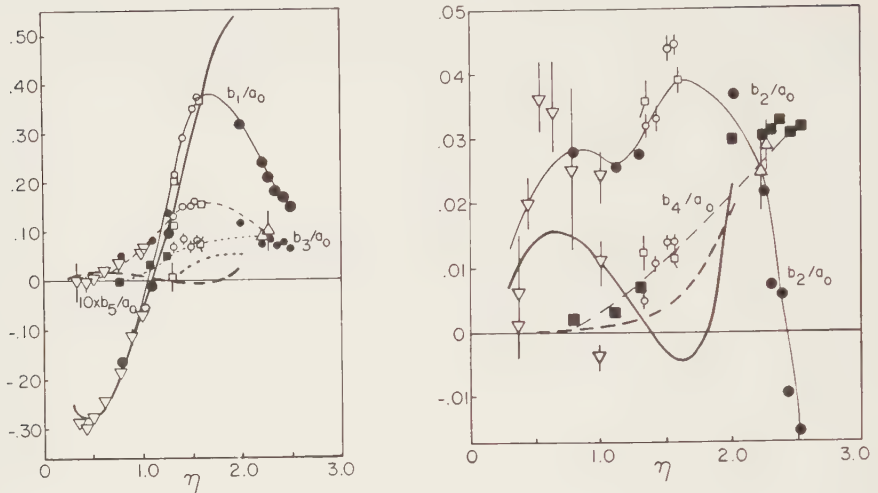


Fig. 2. Coefficients of an expansion of the polarization-dependent cross-section in terms of associated Legendre polynomials are shown as a function of  $\eta$ , the pion centre-of-mass momentum in units of  $m_\pi c$ .  $a_0$  is the total cross-section. Open symbols represent "old" data. The solid symbols show recent data (refc. 55 for  $\eta < 1.5$  and refc. 57 for  $\eta > 1.5$ ). The errors for the new data are generally within the size of the symbol. The full lines (solid and dashed) show predictions of the coupled-channel model of Niskanen<sup>4</sup>. The thin lines are merely to guide the eye.

groups. The partial wave amplitudes from these two groups, appropriate to an incident energy of 578 MeV are shown in Fig. 6. (The amplitudes of Rinat have been normalized by a factor of 11/9 in order to obtain reasonable agreement with the experimental values for the differential cross-section). Aside from questions concerning the inherent limitations of such an approach (questions relating to the limitation to three-particle intermediate states, for example) it is clear that there are significant differences between the theoretical predictions of the different groups. Such differences arise from use of different  $\pi$ -N parameterizations (particularly in the  $P_{11}$   $\pi$ N channel), use of

relativistic versus non-relativistic formalisms, etc.). From the point of view of the experimentalist, it would be very useful if the theorists involved attempted to provide with their final results some estimate of the 'error' or uncertainty characterizing their results.

Other recent developments have centered around explicit relativistic effects. Locher et al.<sup>10</sup> at S.I.N. have completed an extensive study of relativistic effects within the single-scattering framework shown in diagram 1a. In this approach, multiple-scattering effects were approximated in the usual way by including distortions in both the initial and final states.

Presumably the next major development will involve inclusion of some explicit quark dynamics possibly via a cloudy bag model. A preliminary attempt in this direction has already been provided by Miller and Kisslinger<sup>11</sup>.

## 2.2. Overview of Recent Data

A review of the experimental situation up to 1981 was presented at Bloomington<sup>12</sup>. A further update has been provided by Watari in the list of data references accompanying his Partial Wave Analysis update<sup>13</sup> for the  $pp \rightarrow d\pi$  reaction. In this paper, I would like to provide an indication of the experimental explosion which is currently characterizing this subject area. In the contributions to this meeting alone, there are over ten experimental submissions (as well as two theoretical). Table 1 lists those results (published results as well as contributions to this meeting) which have appeared within the last year. The Table lists the observables measured ordered according to initial proton kinetic energy.

There are many new measurements. Some of them are of observables measured earlier by different techniques. Aside from the higher statistical precision which usually characterizes the newer results, the existence of several sets of measurements of the same observable obtained using different experimental techniques is very useful in providing information concerning the extent of systematic errors. For example, there are now good measurements of differential cross-section and analyzing powers, some obtained using single-arm systems usually incorporating a magnetic spectrometer and others involving double-arm counter systems. Double-arm systems are free of the acceptance solid angle problems characterizing spectrometers but have their own specific problems, usually related to background definition. As a result of the recent work, the analyzing power as well as differential cross-section is now well defined over a large energy range. The improvement since 1981 as far as analyzing power is concerned is illustrated in Fig. 2. Additional precision measurements of the analyzing power between 550 and 800 MeV have been performed by the Northwestern group at LAMPF as illustrated in a contribution to this

meeting<sup>14</sup>. This contribution emphasizes a failure common to both the coupled-channel and unitary three-body theories in their descriptions of the analyzing power. Although these theories provide reasonable predictions of the odd terms in an Associated Legendre polynomial expansion of the polarization-dependent cross-section, they fare very poorly in their ability to predict the even terms.

The last section of the table points out a rather novel measurement which is reproduced in Fig. 3, namely an excitation function of the  $\pi d \rightarrow 2p$  differential cross-section at  $90^\circ$  (cms) from (equivalent) proton energies of 409 to 889 MeV in 3-5 MeV steps<sup>15</sup>. This data should provide the final definitive description of the excitation function of this important reaction within this energy range.

Important new data close to threshold are also described in the contributions. Complete angular distributions of the isospin-related reaction  $np \rightarrow d\pi^0$  have been measured by the Freiburg group at SIN for pion

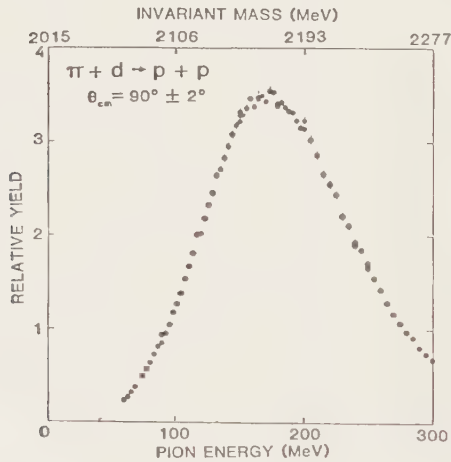


Fig. 3. Excitation function of the  $\pi d \rightarrow 2p$  reaction at  $90^\circ$  (cms).



TABLE 1  
Table of Reference for Recent  $pp \rightarrow d\pi$  Measurements

$T_p$ (MeV)	$\sigma_T$	$d\sigma$	$A_{NO}$	$A_{NN}$	$A_{SS}$	$A_{LL}$	$A_{SL}$	$it_{11}$	$K_{NN}$
325	54								
375			55						
(419)	56	56							
433	54								
(434)	56	56							
447			22	22	22	22	22		
(449)	56	56							
450			55						
(479)	56	56							
496			22	22	22	22	22		
500			23, 55	25		24	24		
(509)	56	56							
515			22	22	22	22	22		
516	54	62	63				58		
529		62							
538			22	22	22	22	22		
(539)	56	56							
542		62	63				58		
547			59						
556		62							

$T_p$ (MeV)	$\alpha_T$	$d\sigma$	$A_{NO}$	$A_{NN}$	$A_{SS}$	$A_{LL}$	$A_{SL}$	$it_{11}$	$K_{NN}$
(569)	56	56							
569		62	63						
575		62							
582		62	63				58		
597	54								
598			59						
600			23	25		24			
(630)		64							
648			59						
650			23	25		24	24		
684	54								
698			59						
700			23	25		24			
(705)		64							
725		57	57						
733			23	25					
750						24			
765		57	57						
767	54								
793			59						
(799)								19	
800	59	57	57, 59, 23	25		24	24	17	17

$T_p$ (MeV)	$\sigma_T$	$d\sigma$	$A_{NO}$	$A_{NN}$	$A_{SS}$	$A_{LL}$	$A_{SL}$	$it_{11}$	$K_{NN}$
825		57	57						
(847)	60	60							
850		57	57						
857	54								
(860)		54							
875		57	57						
(889)	60	60							
900		57	57						
940		57	57						
(949)	60	60							
992	54								
1000		57	57						
(1001)	60	60							
(1067)	60	60							
1078	54								
(1129)	60	60							
1168	54								
(1189)	60	60							
1262	54								
(410)-(890)		61 $d\sigma(90^\circ)$							
286-590		16 $np \rightarrow d\pi^0$							

Entries characterized by parentheses in column 1 refer to  $\pi d \rightarrow 2p$  measurements. The bracketted energy is the equivalent proton energy for the inverse reaction.

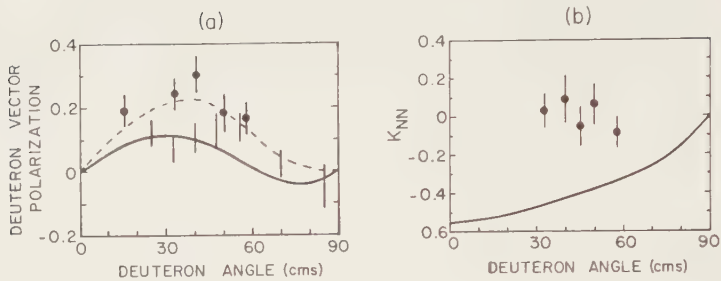


Fig. 4 (a) Deuteron vector polarization as a function of angle for unpolarized protons incident on an unpolarized target. The vertical lines represent data obtained from measurements of proton asymmetry obtained when pions are absorbed on a polarized deuteron target<sup>19</sup>.

(b) The spin transfer parameter,  $K_{NN}$ , for the  $\vec{p}p \rightarrow \vec{d}\pi^+$  reaction plotted as a function of angle.

The solid lines are predictions of Niskanen while the dashed line is that of Rinat.

centre-of-mass kinetic energies from 120 MeV down to 5 MeV!<sup>16</sup> A particularly noteworthy development has been the initiation of measurements of "spin transfer parameters" as exemplified by the work of Bonner's group at LAMPF shown in Fig. 4. This figure differs somewhat from that in the contribution<sup>17</sup> to this Conference. The sign of the theoretical values of Niskanen has been changed (private communication). In addition, the data of Smith et al. have been scaled by a factor of 2/3 to correct an error<sup>18</sup> in their publication<sup>19</sup>. This renormalisation somewhat worsens the agreement. Clearly, additional measurements are needed to clarify the situation regarding this important observable.

### 2.3. Amplitude Analysis

Since the  $pp \rightarrow p\pi$  reaction is described by a  $3 \times 4$  T-matrix, eleven measurements are required to determine the six independent amplitudes to within an arbitrary phase. However, as recently pointed out by Moravcsik<sup>20</sup> the magnitudes of all six transversity amplitudes can be unambiguously determined by independent measurements of only six observables,  $d\sigma$ ,  $P_N$  (vector

polarization of the deuteron), the analyzing powers  $A_{NO}$  and  $A_{ON}$ , the  $A_{NN}$  spin correlation parameter, and  $K_{NN}$  the spin transfer parameter. If the measurements are made as a function of angle, only five observables need be determined, as  $A_{NO}$  and  $A_{ON}$  are simply related ( $A_{ON}(\theta) = -A_{NO}(\pi - \theta)$  in the Madison convention). Additional experiments ( $A_{LL}$ ,  $A_{SS}$  and a triple spin correlation parameter) are needed in order to fully determine three of the relative phases. Finally, four additional experiments (with at least one involving measurement of a deuteron tensor polarization) are required to determine the remaining two phases. Because of the identity of the two protons, a significant simplification results at  $90^\circ$ .<sup>20,21</sup> At this angle only three of the amplitudes contribute. For this case then, the magnitudes of these three amplitudes can be determined from just three different measurements ( $d\sigma$ ,  $A_N$  and  $A_{NN}$ ). Additional measurement of either:  $A_{LL}$  and  $A_{SS}$  or  $A_{LS}$  then provides the information required to determine the relative phase between two of these amplitudes.

Extensive measurements of six observables ( $d\sigma$ ,  $A_{SS}$ ,  $A_{NN}$ ,  $A_{LL}$ ,  $A_{LS}$ , and  $A_{NO}$ ) have been performed at 447, 496, 515, 538 and 578 MeV by the Geneva group at S.I.N.<sup>22</sup>. In addition, from the LAMPF contributions to this meeting we have learned that the four observables ( $A_{NO}$ ,  $A_{NN}$ ,  $A_{LL}$ ,  $A_{SL}$ ) have also been measured at 500, 650, 700, 750 and 800 MeV.<sup>23,24,25</sup> Analysis of the  $90^\circ$  values of these observables together with interpolated estimates of  $d\sigma(90^\circ)$  provides an unambiguous determination of the magnitudes of three amplitudes at  $90^\circ$  ( $T_2$ ,  $T_6$  and  $S$  in Foroughi's notation<sup>21</sup>) and the relative phase between two of them ( $T_6$  and  $S$ ). The result of such an analysis is illustrated in Fig. 5. It is very interesting to note that none of these amplitudes exhibit a significant resonance structure over this energy range!

#### 2.4. Partial Wave Amplitude Analysis

An alternative approach involves analysis of the data in terms of partial wave amplitudes, quantities which are related to a spherical harmonic decomposition of the amplitudes referred to in the previous section. Here the rotationally invariant character of such amplitudes is utilized to "interpolate" between incomplete sets of data. In addition, as long as the energies are not too high, centrifugal barrier effects limit the number of partial wave amplitudes which can contribute. At higher energies, however, the number of terms in such an expansion can become unmanageable.

Partial wave analyses of the existing data base are now being carried out by several groups. Watari<sup>13</sup> provides two basic choices of amplitudes, each of which fits the data. He obtained his solutions by performing an energy-

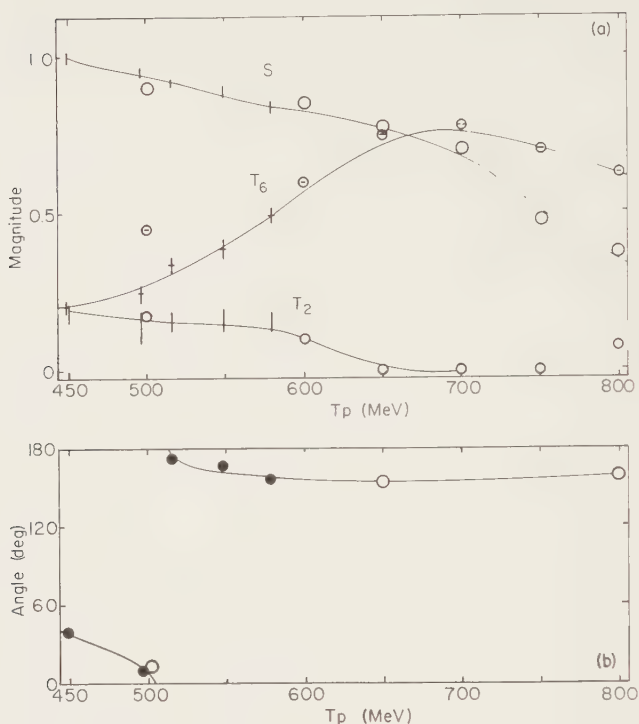


Fig. 5 (a) Magnitudes of three helicity amplitudes<sup>21</sup> at 90° as a function of incident proton energy.

(b) Included angle between two of the amplitudes ( $T_6$  and  $S$ )<sup>21</sup> at 90° as a function of proton energy.

For both diagrams, the lines are only to guide the eye.

dependent analysis of the data, one in which the amplitudes are required to be continuous functions of energy. In addition, a threshold momentum dependence expected on the basis of centrifugal penetrability was imposed. He provides two basic fits, one having a dominant DP2 amplitude (called fit D), and the other a dominant SP0 amplitude (called fit S). (See Table 2a for a definition of these amplitudes.) At this meeting, we have also learned of a similar energy-dependent partial wave analysis being carried out at Leningrad<sup>26</sup>. The energy range covered in the latter analysis is rather higher than for the others, extending from 400 MeV to 1235 MeV.

TABLE 2  
 Categorization of  $NN \rightarrow \pi NN$  Channels

Isoscalar final nucleon states

a) Mandl-Regge<sup>28</sup>

Isovector initial nucleon states

2N $2s+1 \begin{pmatrix} l_N \end{pmatrix}_J^T$	N $\Delta$ (intermediate state) $2s+1 \begin{pmatrix} l_J \end{pmatrix}^T$	$\pi NN$ $2s+1 \begin{pmatrix} l_\pi \end{pmatrix}_J^T$	Amplitude
$1_{S_0}^1$		$3_{P_0}^0$	$a_0 = \text{SPO}$
$3_{P_1}^1$	$3,5_{P_1}^1$	$3_{S_1}^0$ $3_{d_1}^0$	$a_1 = \text{PS1}$ $a_3 = \text{PD1}$
$1_{D_2}^1$	$5_{S_2}^1$	$3_{P_2}^0$ $3_{f_2}^0$	$a_2 = \text{DP2}$ $a_7 = \text{DF}_2$
$3_{P_2}^1$	$3,5_{P_2}^1$	$3_{d_2}^0$	$a_4 = \text{PD2}$
$3_{F_2}^1$	$3,5_{P_2}^1$	$3_{d_2}^0$	$a_5 \equiv \text{FD2}$
$3_{F_3}^1$	$5_{P_3}^1$	$3_{d_3}^0$ $3_{g_3}^0$	$a_6 = \text{FD3}$ $a_9 \equiv \text{FG3}$
$3_{F_4}^1$	$3,5_{F_4}^1$	$3_{g_4}^0$	$a_{10} \equiv \text{FG4}$
$1_{G_4}^1$	$5_{D_4}^1$	$3_{f_4}^0$ $3_{h_4}^0$	$a_8 \equiv \text{GF4}$ $a_{13} \equiv \text{GH4}$
$3_{H_4}^1$	$3,5_{F_4}^1$	$3_{g_4}^0$	$a_{11} \equiv \text{HG4}$
$3_{H_5}^1$	$5_{F_5}^1$	$3_{g_5}^0$	$a_{12} \equiv \text{HG5}$
$1_{I_6}^1$	$5_{G_6}^1$	$3_{h_6}^0$	$a_{14} \equiv \text{IH6}$



Isovector Final Nucleon States

## b) Isovector initial nucleon state

${}^3P_0^1$	${}^3P_0^1$	${}^1s_0^1$
${}^3P_2^1$	${}^{3,5}P_2^1$	${}^1d_2^1$
${}^3F_2^1$	${}^{3,5}P_2^1$	${}^1d_2^1$
${}^3F_4^1$	${}^5D_4, {}^{3,5}F_4$	${}^1g_4^1$
${}^3H_4^1$	${}^5D_4, {}^{3,5}F_4$	${}^1g_4^1$

## c) Isoscalar initial nucleon states

${}^3S_1^0$	$T = 0$	${}^1p_1^1$
	$\therefore$ no $\Delta$ -N	
${}^3D_1^0$		${}^1p_1^1$
${}^3D_3^0$		${}^1f_3^1$
${}^3G_3^0$		${}^1f_3^1$

At TRIUMF, we (Blankleider et al.)<sup>27</sup> have also begun such an analysis. Fits to the data at 578 and 515 MeV, using purely random initial estimates for the amplitudes have been made. Argand plots of such amplitudes for the 578 MeV case are shown in Fig. 6. The solutions shown correspond to  $\chi^2/n_D < 2.5$ . The incompleteness of the data base is particularly noticeable in terms of the

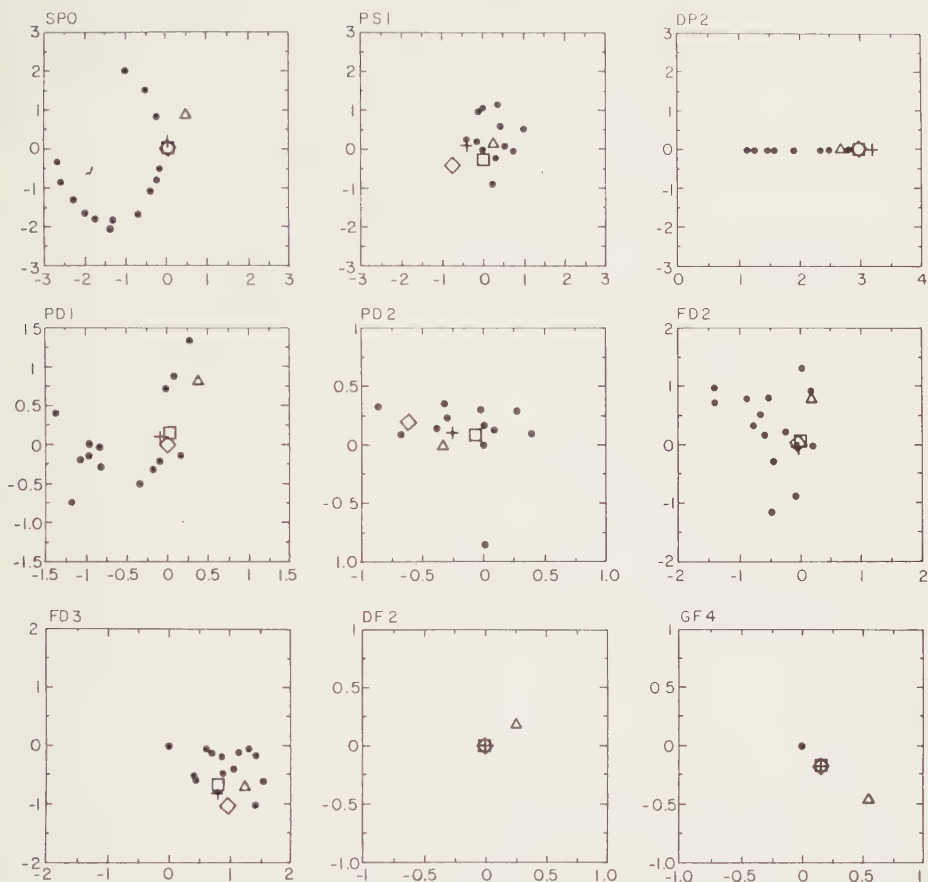


Fig. 6. Argand plots of nine partial wave amplitudes labelled according to the convention described in Table 2a. The solid points indicate the results of fits to the existing data when initial values were chosen purely randomly.

$\Delta$  - Watari "D" amplitudes<sup>13</sup>

$\diamond$  - Bugg amplitudes<sup>29</sup>

$+$  - Blankleider amplitudes<sup>7</sup>

$\square$  - Rinat amplitudes<sup>9</sup>

"circles of confusion" which characterize some of the less well-defined amplitudes such as the SPO. The partial wave amplitudes shown are defined as originally described by Mandl and Regge<sup>28</sup>, and listed in an extended version in Table 2a.\*

An extensive amplitude fit has recently been performed by DAVID Bugg<sup>29</sup>. As indicated in his talk, he considered only those amplitudes corresponding to channels containing S- or P-wave  $\pi\Delta$  intermediate states. As well, the SPO amplitude (expected to be small) was arbitrarily set equal to zero. Whereas the relative phases of Watari's energy-dependent solutions fluctuate with energy, Bugg imposed an additional "continuity" constraint which required the phases to vary uniformly and in a fashion simply related to NN and  $\pi\pi$  scattering phase shifts. Given the incompleteness of the existing data, such a condition was required in order to constrain the problem sufficiently to yield a unique solution. There has, however, been some doubt expressed regarding the validity of the particular prescription employed. In addition, he constrained the higher partial waves (corresponding to high impact parameter) to be equal in value to those predicted by the unitary theory of Blankleider<sup>7</sup>.

In Fig. 6 it is seen that the higher partial wave amplitudes predicted by both Blankleider and Rinat for 578 MeV incident energy are in good agreement, thus providing further justification for Bugg's assumption. The extent to which the different partial wave solutions are consistent with the existing data is shown in Fig. 7a. Predictions of other observables associated with deuteron polarization are shown in Figs. 7b and 7c.\*\*

Although the experimental situation is far from complete it has improved markedly with inclusion of the recent data. Because  $A_{LS}$  and  $A_{NO}$  both depend on the same bilinear combination of amplitudes (the first depending on the real

\* The units are such that:

$$4\pi \frac{d\sigma}{d\Omega_{J,K}} = \sum_{\ell} C_{\ell}^{JK} P_{\ell}^m(\cos \theta)$$

with  $C_{\ell}^{JK}(I, I') = \sum_{I < I'} C_{\ell}^{JK}(I, I')$  Bilinear  $(a_I a_{I'}^*)$

where the  $C_{\ell}^{JK}(I, I')$  is the product of all the relevant vector-coupling coefficients and angular momentum factors. The kinematics and phase space factors are contained in the definition of the amplitudes,  $a_I$ .

\*\* For the spin transfer observables shown here, the direction of the quantization axis is that of the pion direction in the centre-of-mass. This is not the natural extension of the Madison convention where the quantization axis is in the direction of the momentum of the particle in question.

part and the second on the imaginary), determination of both of these two observables provides a very stringent constraint on the relative phases between the amplitudes. It is therefore important for both these observables to be measured when an experiment is performed. Calculations of the observables shown in Figs. 7b and 7c obtained using the various amplitude 'fits' displayed in Fig. 6 yield a wide variety of predictions. Some of the observables are more sensitive to the choice of amplitudes than others. On the basis of such a study it is clear which additional experiments are required to optimally constrain the existing uncertainties in the amplitudes.  $it_{11}$  (0011 in Fig. 7b) (vector polarization of the deuteron) is an obvious first choice. It is very sensitive to the choice of SPO, primarily because, unlike most of the other observables, SPO depends essentially on an interference between two (initial state) singlet amplitudes. Most of the other observables depend more on the interference between the dominant singlet  $DP_2$  amplitude and those associated with the triplet initial states. Other additional experiments of importance for reducing the uncertainties in the amplitudes are those involving spin transfer. As Bugg has pointed out<sup>29</sup>, those associated with sideways proton spin and vector deuteron polarization normal to the reaction plane are important. Other sensitive observables are those relating normal proton spin orientations with deuteron tensor polarization.

### 3. Pion Absorption in Few-Nucleon Systems

Pion absorption in a nucleus is characterized by the subsequent emission of fast nucleons and/or clusters of nucleons. Such clusters, may, in fact, include a sufficiently large fraction of the total nucleons available that it is more appropriate to speak of a pion-induced "fission" process.

In this paper, I shall restrict my attention to the case of nucleon emission. In particular, I shall consider only the following:

- a) Two Nucleon Emission
- b) Single Nucleon Emission

#### 3.1 Two Nucleon Emission

Quasi-free absorption of a pion on two nucleons can be preferentially selected by experimentally insisting that the outgoing nucleons are sufficiently energetic and that they are emitted at the appropriate 'conjugate' angles determined by the kinematics associated with absorption on free nucleon clusters. In this regard,  $^3\text{He}$  and  $^4\text{He}$  have been favourite target choices because they are characterized by having all their target nucleons in a relative S-state. Aside from the obvious fact that pion absorption on two nucleons within a nuclear environment is very interesting in its own right,

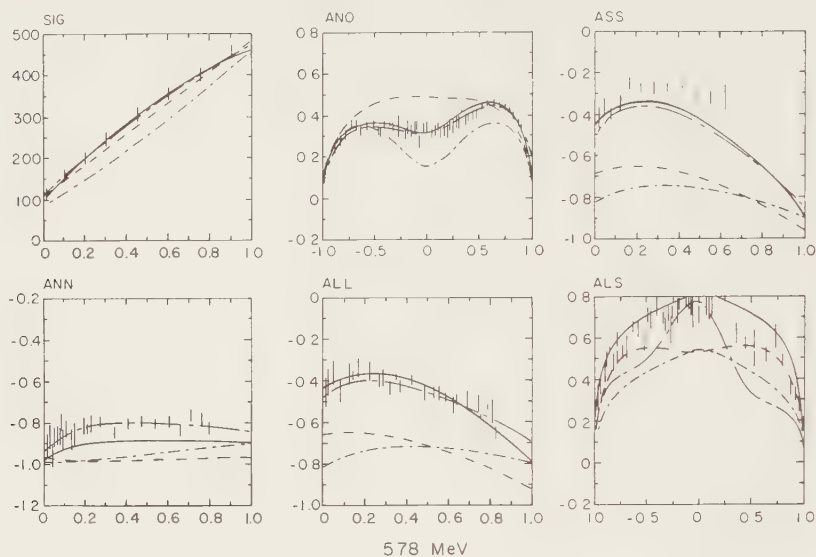
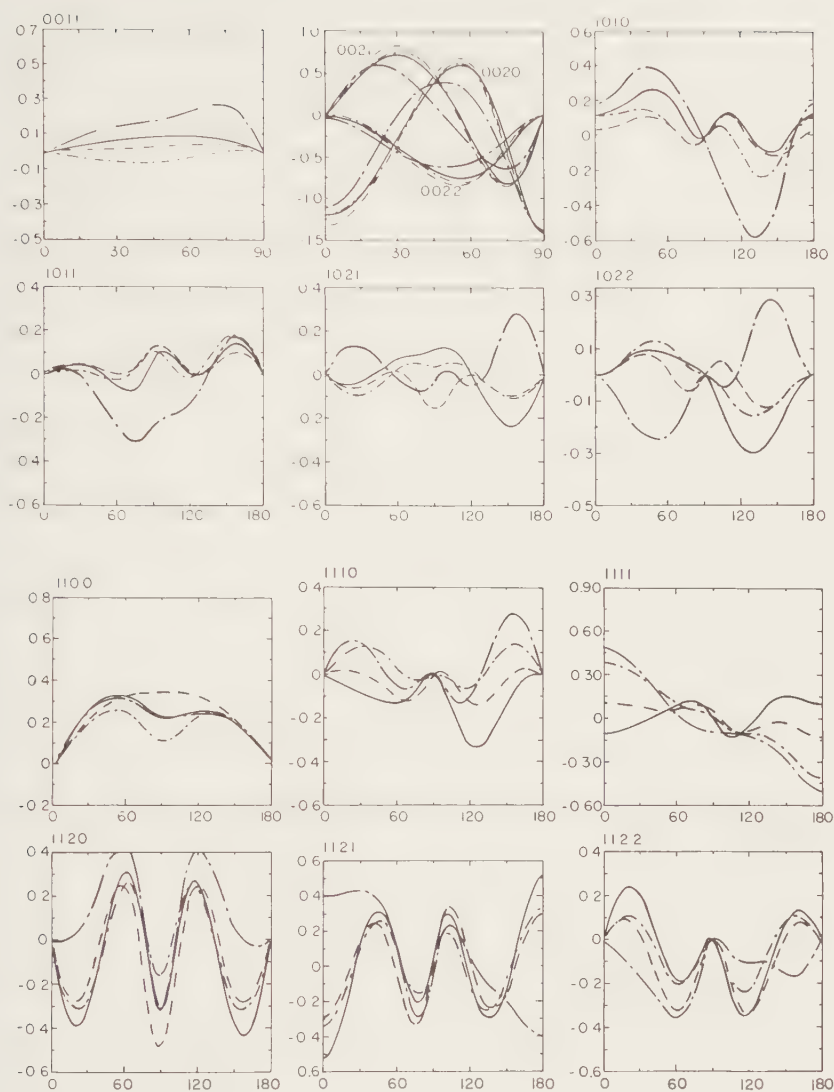


Fig. 7 (a) Angular dependences of spin-dependent observables for the  $pp + d\pi^+$  reaction generated by the amplitudes shown by open symbols in Fig. 6. Vertical bars indicate experimental data.

— — — — — Watari "D" amplitudes<sup>13</sup>  
 ————— Bugg amplitudes<sup>29</sup>  
 - - - - - Blankleider amplitudes<sup>7</sup>  
 - · - · - Rinat amplitudes<sup>9</sup>

For X coordinates labelled  $0 \rightarrow 1$ , the relevant variable is  $\cos^2 \theta$ .  
 For X coordinates labelled  $-1 \rightarrow 1$ , the variable is  $\cos \theta$ .  
 SIG indicates differential cross-section. The remaining observables are analyzing powers or spin correlation functions labelled in the usual way.



(b) & (c) Spherical tensor spin transfer parameters for the  $\vec{p}p \rightarrow \vec{d}\pi^+$  reaction as generated by the amplitudes corresponding to the open symbols in Fig. 6. X coordinate values refer to the centre-of-mass angle in degrees.

The lines are defined as described in the caption to Fig.

this type of reaction also affords the opportunity to study pion absorption on nucleon pairs having quantum numbers different from those of the deuteron. In particular, interest has centred on a comparison of absorption on isovector (spin singlet) nucleon pairs to that on isoscalar (spin triplet) pairs obtained by comparing the  ${}^3\text{He}(\pi^+, 2p)p$  with  ${}^3\text{He}(\pi^-, pn)n$  reactions<sup>30,31</sup>. The transition amplitudes which contribute (in addition to those already described for the  $pp \rightarrow d\pi$  reaction) are listed in Tables 2b and 2c. For an isovector (spin singlet) relative S-wave final nucleon pair configuration (in pion production), the total angular momentum  $J$  for the channel is simply  $\ell_\pi$ . Parity conservation then forbids  $\ell_N = J = \ell_\pi$  in the initial NN state. Thus only spin triplet initial state nucleon pairs can contribute, with  $J = \ell_N \pm 1$ .

One of the principal reasons for the great interest in these particular absorption reactions is the (unexpectedly) large ratio observed for pion absorption on isoscalar nucleon pairs compared to isovector (especially for pion kinetic energies greater than 100 MeV). The original observations by Ashery et al.<sup>30</sup> and Backenstoss et al.<sup>31</sup> had only recently been announced at the time of the Versailles meeting and were thus highlighted by Ingram<sup>32</sup> in his review on pion nuclear interactions. The momentum developed in this subject is evident by the additional experimental results contributed to this conference<sup>33,34</sup>. The energy dependence obtained for the isovector/isoscalar ratio for incident pions between zero and 165 MeV is shown in Fig. 8.

An obvious explanation for such a strong isospin dependence is that of dominance by  $N\Delta$  intermediate states. Since it is impossible for an  $N\Delta$  state to have zero isospin,  $N\Delta$  dominance discriminates against any of the transitions involving coupling of an isovector nucleon state with a pion to give zero total channel isospin (Table 2c). On the other hand, for pion absorption on an isovector nucleon state where the total isospin is unity only  $N\Delta$  intermediate states with  $\ell$  greater than or equal to 1 can be involved, as shown in Table 2b. Thus, there are far fewer channels available for absorption on isovector NN pairs than there are for isoscalar (Table 2b plus 2c versus 2a). In addition to such arguments based simply on the number of channels available, none of the channels listed in Table 2b or 2c include the dominant S-state  $\Delta N$  channel (channel DP2 of Table 2a). Thus it is easy to understand an isoscalar enhancement for the pion absorption reaction. Lee and Ohta<sup>35</sup> showed that the experimental result could be understood in terms of a model in which both  $\Delta N \rightarrow NN$  and  $\Delta NN \rightarrow NNN$  transition amplitudes are considered. They concluded that the P-wave  $N\Delta$  intermediate state of Table 2b dominates for isovector pion absorption. At this conference, Silbar and Piasetzky<sup>36</sup> argue that the energy dependence of this ratio requires that the  $NN'$  intermediate states of Table 2c must also be included. The actual form of the energy dependence of the



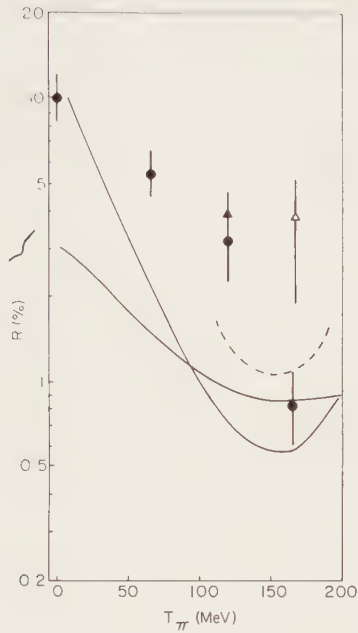


Fig. 8. Ratio of the pion absorption cross-sections on isovector to isoscalar nucleon pairs in a  $^3\text{He}$  target as a function of pion kinetic energy. The circular points indicate measurements corresponding to outgoing angles of  $\sim 75^\circ$ , whereas the triangles correspond to  $\sim 55^\circ$ . The solid points refer to data described in the literature<sup>30,31</sup> and in the contributions to this meeting<sup>33,34</sup>. The open circle indicates a very preliminary result communicated at this meeting. The lines refer to various theoretical predictions (as described in refs. 30, 34, 35 and 36).

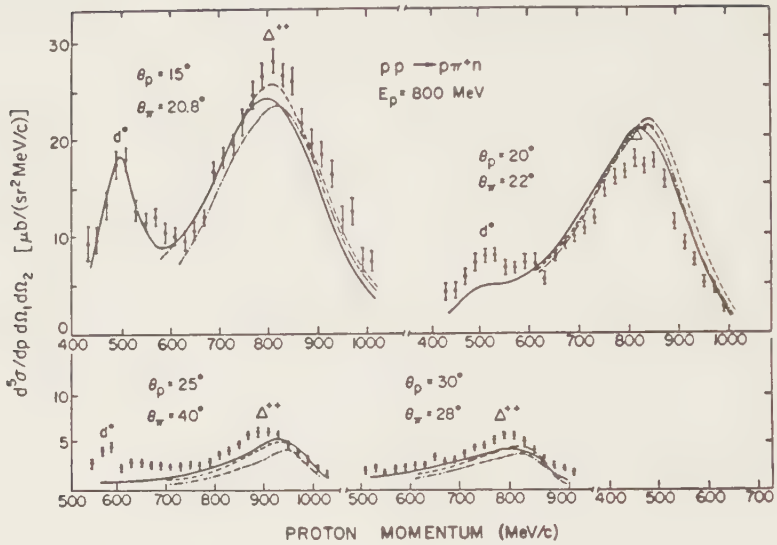


Fig. 9. Differential cross-sections for the  $pp \rightarrow pn\pi^+$  reaction<sup>38</sup> as a function of outgoing proton momentum for 800 MeV incident kinetic energy. The solid lines indicate various theoretical fits including  $np$  final state interaction (labelled by  $d^*$ ).

isovector to isoscalar ratio is still far from clear, however. As shown in Fig. 8, recent preliminary data from SIN indicate a much smaller ratio at 165 MeV than was previously measured at LAMPF. How much of this discrepancy between the different results can be attributed to differences in the methods of analysis (assumed contribution from "three-body" absorption, for example) rather than simply reflecting a strong angular dependence remains to be established. Certainly more detailed measurements, including complete angular distributions, are very much in order.

As pointed out by Ingram<sup>32</sup>, a full understanding of this phenomenon requires an understanding of the corresponding situation involving free nucleons. One way of obtaining such information involves measurement of the  $pp \rightarrow (pn)\pi^+$  reaction in the kinematic region corresponding to the  $np$  final state interaction. Very little experimental information exists for this reaction, however. Since only isovector nucleons participate in the initial state of the production process, only parts a) and b) of Table 2 apply. Again, the assumption of  $N\Delta$  dominance (especially that of the S-wave  $N\Delta$  state) would

preclude a significant contribution to the reaction from a spin-singlet final state interaction. Fig. 9 shows the final state interaction peak for the  $pp \rightarrow pn\pi^+$  reaction observed<sup>38</sup> at 800 MeV incident energy. In order to fit this peak a spin triplet/singlet ratio of  $\sim 2$ -2.5 was required. Although the NN pairs in such a final state interaction are in a relative S-state, very large pion angular momenta with respect to the NN pair are possible at incident energies of 800 MeV. Other  $pp \rightarrow pn\pi$  measurements have been performed, both at LAMPF and at TRIUMF, but to date no detailed analyses of the differential cross-sections appropriate to this final state interaction region have been carried out.

At TRIUMF, we have investigated pion line shapes as measured in a small magnetic spectrometer by using the  $pp \rightarrow d\pi$  reaction for protons of 400 and 450 MeV kinetic energy. During this investigation, we also recorded a substantial part of the continuum from the  $pp \rightarrow pn\pi$  reaction as shown in Fig. 10. The shape of the continuum clearly necessitated inclusion of a final state interaction in order to account for the contribution in the region of the two-body tail. By folding in the instrumental line shape to a continuum containing both spin singlet and spin triplet final state interactions, we fitted the whole spectrum as shown by the smooth curves in Fig. 10. The instrumental resolution (dominated by the kinematic shift associated with the acceptance of the spectrometer) precluded obtaining a definitive result from this data. As shown in the figure, our resulting  $\chi^2$  values tolerate a fairly wide range of triplet/singlet ratios. However, all the results we have examined thus far (at both 400 and 450 MeV) show a clear preference for a triplet/singlet ratio  $\sim 3:1$ , close to the simple statistical ratio and consistent with the higher energy results of Hudomalj-Gabitzsch et al.<sup>38</sup>. Results such as these indicate the role played by  $NN'$  intermediate states (and also non S-wave  $N\Delta$  states) in the free pion production (absorption) reaction and do so without the complexity introduced by attempting such measurements in a nuclear environment.

However, no results are available near 600 MeV where the  $N\Delta$  intermediate states should have the greatest effect. Detailed measurements of the np final-state interaction channel are very much needed over the energy range encompassing the  $N\Delta$  intermediate state.

It is clear that more extensive measurements of both types of reaction are required: the true  $pp \rightarrow (pn)\pi$  to determine the nature of the elementary production (absorption) process, and pion absorption in nuclei to elucidate the complicating effects of the nuclear environment. More work is also needed on the theoretical front. In addition to the growing attention being directed towards the problem of pion absorption on few nucleon systems, we need a better understanding of the reaction mechanisms involved in pion absorption on a free isovector nucleon pair.

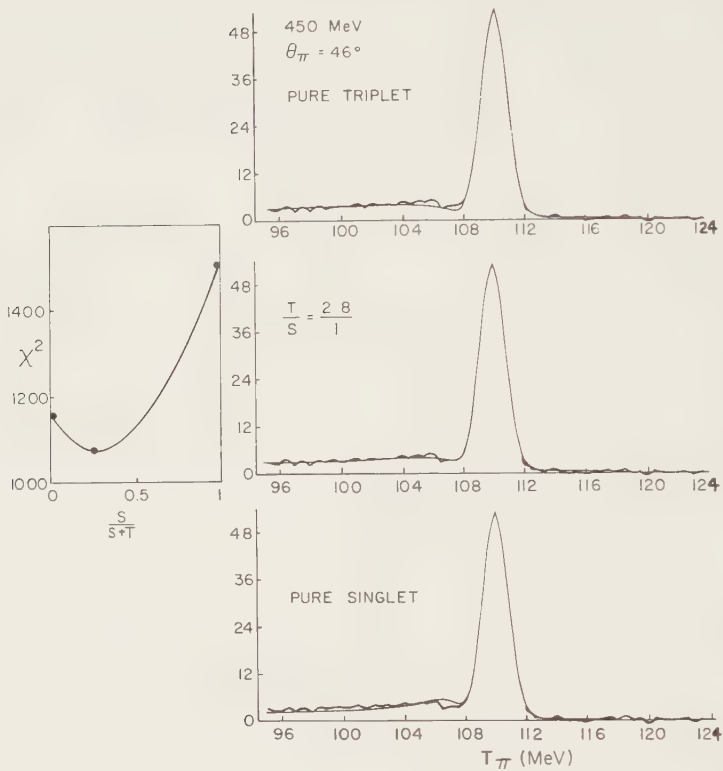


Fig. 10. Relative differential cross-sections for pion production by the  $pp \rightarrow (pn)\pi^+$  reaction at an incident kinetic energy of 450 MeV. The dominant peak corresponds to the mono-energetic pions produced by the  $pp \rightarrow d\pi$  reaction (at  $46^\circ$  lab). The lower energy continuum corresponds to the three-body phase space modified by the  $np$  final-state interaction. The thin line indicate the result of folding in the theoretical line-shape to a sum of the two contributions, one corresponding to a singlet and the other a triplet final state interaction (calculated in the usual way; eg. Goldberger and Watson). The three separate diagrams refer to different values for the spin triplet to spin singlet ratios in the final state interaction.

### 3.2 Single Nucleon Emission

We now turn to the last type of reaction I wish to discuss, that of single nucleon emission. The subject will, in fact, be treated in terms of the inverse reaction:  $p + A \rightarrow (A + 1) + \pi^+$ . I shall subdivide this subject into two general categories: (a) Traditional (b) New.

'Traditional' refers to the general program of measurement of differential cross-section (together with spin dependent observables such as analyzing power) designed to test our understanding of the pion production process in a nuclear environment. Conversely, 'new' refers to observations of behaviour which deviate significantly from expectation.

#### 3.2.1 Traditional

The theoretical understanding of pion production in nuclei [ $pA \rightarrow (A+1)\pi$  reaction] has been plagued by problems similar to those characterizing the theoretical development of the  $pp \rightarrow d\pi$  reaction. The longitudinal momentum transfer in such a reaction is very large,  $\sim 500$  MeV/c. Here, as in the  $pp \rightarrow d\pi$  reaction much effort has been expended on attempting to unravel the relative importance of single-nucleon to multi-nucleon mechanisms. The two processes are illustrated diagrammatically in Fig. 11. The similarity to Fig. 1a is very apparent. However, a realistic two-nucleon calculation in a nuclear environment is much more difficult than it is for free nucleons. Again, one encounters double-counting problems involved in trying to treat nucleon and pion optical model distortions separately from the basic pion rescattering processes. No really satisfactory solution (akin to the Faddeev technique for the NN case) has yet been developed. Instead, most work has been directed to the simpler problem of summing the simple rescattering diagram of Fig. 11 coherently over all the nucleons in the nucleus. Additional difficulties arise due to the nuclear aspects of the problem. An important example is the treatment of off-shell effects. Severe unphysical enhancements tend to appear when the pion is far off-shell (the "pionic wave distortion" of the Kisslinger potential). Also, and again paralleling the free NN situation, the importance of specifically relativistic effects is not at all well understood. Cooper and Sherif<sup>39</sup> obtained some very major changes to the simple single-nucleon predictions when they carried out a relativistic treatment.

Finally, much effort has been directed in the last few years towards developing a completely consistent treatment including both two-nucleon and single-nucleon mechanisms with all significant diagrams included. Keister and Kisslinger<sup>40</sup> have treated the  $(p, \pi)$  reaction on nuclei within the framework of an isobar-doorway model, a treatment which includes features of both one- and



Fig. 11. Diagrammatic representations of two-nucleon and single-nucleon pion production mechanisms.

two-nucleon models. The theory, however, is not simple and involves many features which are currently poorly understood (pion vertex cut-off, proper handling of distortion, off-shell nature of pion in exchange terms, etc.). In spite of all the sophistication involved, the theoretical predictions still differ qualitatively from experiment even for such spin averaged observables as the differential cross-section. Another approach of this type is being developed at Indiana by Dillig and co-workers.<sup>41</sup> It is an ambitious program involving extensive numerical computation. It includes a large number of elements known to be important (one- and two-nucleon mechanisms, *s*- and *p*-wave rescattering (including  $\sigma$ - and  $\rho$ - exchange), off-shell corrections, short-range correlations etc.). Even here, however, proton distortions have to be introduced explicitly. Unfortunately, this program has not yet been developed to a level where comparison with experiment is possible.

In view of the problems associated with development of a realistic theoretical description of pion production in nuclei, perhaps more attention should be directed to studying pion production in few-nucleon systems from a microscopic point of view. The Helsinki group, (Green and Sainio<sup>42</sup>) tried applying their coupled-channel technique (developed originally for the  $pp \rightarrow d\pi$  reaction) to the case of  $pd \rightarrow t\pi$ . Unfortunately, the approach was much less successful here than for the elementary pion production reaction. In order to explore some of the reasons for this failure, Sainio is re-examining some older techniques associated with relating the  $pd \rightarrow t\pi$  reaction more directly to the elementary  $pp \rightarrow pn\pi$  reaction<sup>43</sup>. In a contribution<sup>44</sup> to this meeting, Dutty et al. present data for both  $nd \rightarrow t\pi^0$  and  $nd \rightarrow {}^3\text{He}\pi^-$ . They also demonstrate the extent to which the various theoretical models developed to date fail in their ability to describe the data.

Recently, Hirata and Masutani<sup>45</sup> performed calculations of the  ${}^4\text{He}(\pi^-, n){}^3\text{H}$  reaction in terms of a  $\Delta$ -hole model, incorporating both two- and single-nucleon mechanisms. Again, the theoretical results do not compare well with data. In general, the theoretical predictions exhibit much more angular structure at back angles than is observed experimentally.

It is important to recognize however that structureless differential cross-sections which vary only slowly with energy do not necessarily imply that the spin-dependent amplitudes also follow suit. Abegg et al.<sup>46</sup> show that over an angular range where the differential cross section for the  $pd \rightarrow t\pi$  reaction varies only slowly with energy, the analyzing power exhibits a very strong energy dependence. Probably significant progress will have to await the experimental determination of the spin-dependent amplitudes themselves over an energy and angular range appropriate for a definitive confrontation with theory. A recent theoretical development worth noting is that of Avishai and Mizutani<sup>47</sup> who are developing a connected kernel technique for handling the coupled  $\pi NN \rightarrow NN$  system, a technique which is intended to be applied to reactions of the type discussed above.

In view of the difficulties which theorists have encountered in attempting to provide an understanding of pion production in nuclei, it is particularly important for experimentalists to provide guidance to their theoretical colleagues by exploring the general features of the reactions. While endeavouring to elucidate the systematic features of such reactions, a frequently recurring question concerns the selection of the relevant parameters or kinematical variables for describing the results. Frequently, certain features are more prominent when displayed against one parameter rather than another. In fact, systematic trends may only be apparent when the parameters are defined appropriately. In this regard, Nefkens<sup>48</sup> has for some time now been encouraging experimentalists to both:

i) Utilize relativistic invariants (in particular, the Mandelstam variables) when presenting their data, and

ii) To eliminate trivial kinematic dependences from the observables selected for presentation. For example, he prefers to depict the dependence of an invariant matrix element versus  $t$  rather than a differential cross-section versus centre-of-mass angle. Figure 12 illustrates this point. The first diagrams are a comparison of the energy dependence of the  ${}^3\text{He}(\gamma, p)d$  reaction at two different angles. The last is a comparison of the angular dependence of the inverse reaction at two different energies. It is clear that the systematics of the reaction are much more apparent when plotted in the way Nefkens suggests. Couvert has pointed out<sup>49</sup> similar situations where such ideas can be usefully applied to the  $(p, \pi)$  reaction. Fig. 13 is a collection of published differential cross-sections for the  $pd \rightarrow t\pi$  (and, using isospin invariance,  $pd \rightarrow {}^3\text{He}\pi^0$ ) reactions for incident proton energies between 375 and 810 MeV, an energy range which should show significant  $s$ -dependence if the reaction is dominated by  $\Delta$  production in the intermediate state. The data displays an almost universal shape when the invariant matrix element is plotted



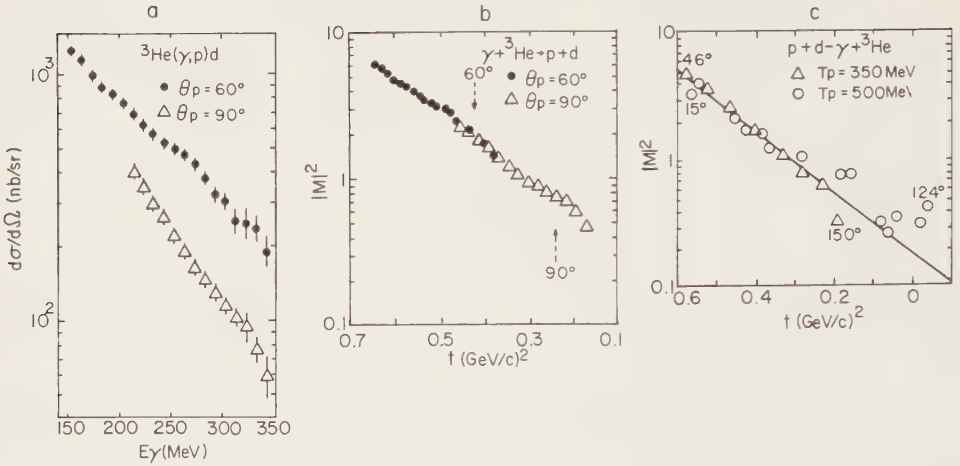


Fig. 12 (a) Excitation functions for the differential cross-section for photo-disintegration of  ${}^3\text{He}$  (at  $60^\circ$  and  $90^\circ$  in the cms).

(b) The data of (a) plotted so that the invariant matrix element is presented as a function of  $t$  (four-momentum transfer).

(c) Angular dependence of the radiative capture reaction,  $pd \rightarrow {}^3\text{He}\gamma$  for two different incident energies presented in terms of the invariant matrix element as a function of  $t$ .

against the four-momentum transfer! Interestingly, very little  $s$ -dependence is observed. At forward angles, it would appear that the matrix element achieves its maximum value for incident energies of  $\sim 450 \text{ MeV}$ . At backward angles, very little systematic behaviour is evident.

Another illustration<sup>49</sup> of the application of such ideas to  $(p, \pi)$  reactions is obtained by considering the momentum transfer bounds for the  $(p, \pi)$  reaction in nuclei. Plotted in the usual way<sup>50</sup> as shown in Fig. 14a, the ranges of the variables shown are very dependent on the masses of the nuclei involved. Couvert and Nefkens have pointed out, however, that if instead of  $q_{\text{cm}}$  and  $T_p$  one chooses the Lorentz scalars  $t$  and  $[\sqrt{s} - m_f]$ , (i.e.  $\epsilon_p^*$ , the total cm kinetic energy in the final state) one obtains the results shown in Fig. 14b. The result is a very much reduced dependence on the nature of the nuclei involved. Essentially all of the bounds overlap. The minimum value of  $-t$  at  $(0^\circ)$  is identical for all nuclei, namely  $t_{\text{min}}(0^\circ) = (m_p - m_\pi)^2$  and this minimum occurs at a bombarding energy approximately 30 MeV above threshold. Thus one



Fig. 13. Differential cross-sections for the  $pd \rightarrow t\pi^+$  and  $pd \rightarrow {}^3\text{He}\pi^0$  reactions covering a range of incident energies, from 375 to over 800 MeV, presented in terms of the invariant matrix element as a function of  $t$ .

samples at  $0^\circ$  smaller values of momentum transfer in the nuclear form factor as the energy increases above threshold for the first 30 MeV or so. Above this energy, the momentum transfer then starts to increase with increasing energy.

Another interesting example involves the application of these ideas to the case of analyzing powers. Which kinematic variables should be used when comparing the polarization analyzing powers from various  $(p, \pi)$  reactions? Fig. 15 shows the analyzing powers for the three reactions:  $pp \rightarrow d\pi^+$ ,  $pd \rightarrow t\pi^+$ , and  $p^{12}\text{C} \rightarrow {}^{13}\text{C}\pi^+$ . Only data leading to ground state excitation of the final nuclei are shown. The incident proton energies are chosen in each case so that similar centre-of-mass kinetic energies characterise each reaction (about 44 MeV in the final state). Fig. 15a is a comparison in terms of center-of mass

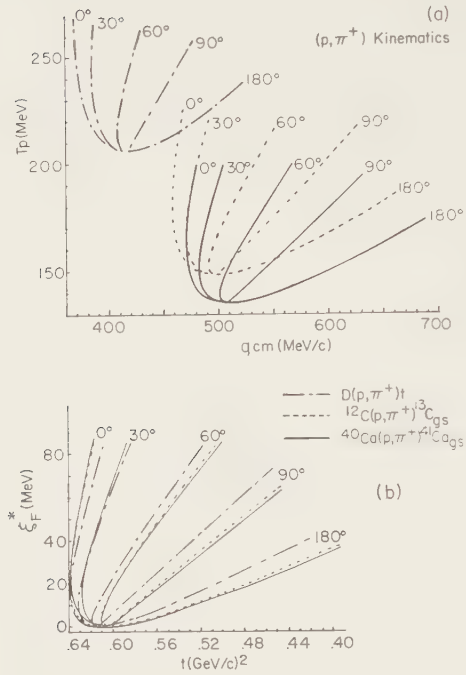


Fig. 14. Momentum transfer bounds for the  $(p, \pi)$  reaction on nuclei.

(a) shows the usual type of plot<sup>50</sup>, with the relationship between  $T_p$ ,  $q_{cm}$  and angle displayed<sup>49</sup>.

(b) here the same bounds as displayed in (a) are presented, except now appropriate relativistic invariants are used in place of  $T_p$  and  $q_{cm}$ <sup>49</sup>.

production angle. One would be tempted to conclude that the  $pp \rightarrow d\pi$  and  $pd \rightarrow t\pi$  reactions behave similarly whereas the reaction involving the heavier nucleus is considerably different. Plotting as a function of center-of-mass momentum transfer as shown in Fig. 15b, however, leads to a completely different conclusion. Now the nuclear reactions,  $pd \rightarrow t\pi$  and  $p^{12}C \rightarrow ^{13}C\pi$  are very similar while the elementary  $pp \rightarrow d\pi$  reaction is the one that differs. In Fig. 15c, the analyzing power is plotted as a function of four-momentum transfer. Now, very little difference is apparent between any of the three reactions, and we can infer that analyzing powers depend primarily on four-momentum transfer in this energy range, with rather little dependence on the

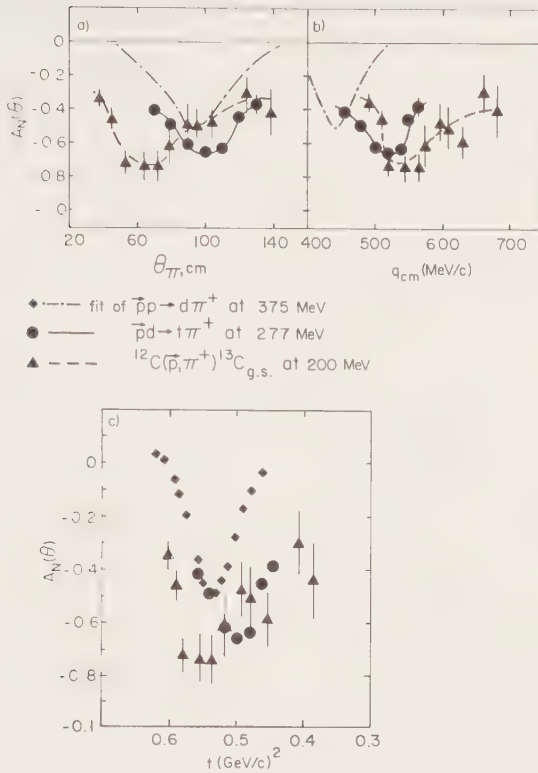


Fig. 15. Analyzing powers for the  $\pi^+$  reactions on hydrogen, deuterium and carbon-12, for similar centre-of-mass kinetic energies. In (a) the data are plotted as a function of the pion angle (cms), in (b) as a function of momentum transfer  $q$  (cms) and in (c) as a function of four-momentum transfer.

structure of the nuclei involved. It will be interesting to see whether this very preliminary conclusion is borne out by more extensive investigations involving other nucleus and over a wider energy range. We also look forward to the theoretical developments required to understand such basic systematic dependences.

### 3.2.2 New

At this meeting, Seth's group provided a contribution<sup>51</sup> showing remarkable energy dependent structure at back angles in both the analyzing power and the

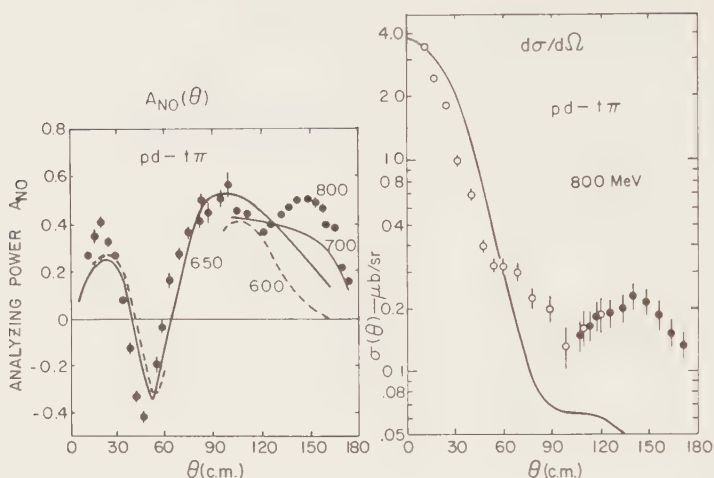


Fig. 16. Angular distributions of the analyzing power and differential cross-section for the  $pd + t\pi^+$  reaction at a number of energies between 600 and 800 MeV. In the diagram for analyzing power, the curves are merely lines to guide the eye. For the case of the differential cross section, the line shows a theoretical expectation based on impulse approximation.

differential cross section for the  $pd + t\pi$  reaction for incident energies of 650–800 MeV. Preliminary results are reproduced in Fig. 16. Perhaps this is no different in principle (other than in magnitude) from the energy dependent structure at back angles mentioned earlier for the analyzing power data of Abegg et al.<sup>46</sup> at about 450 MeV. The feature discovered by Seth et al., however, stands out prominently in both differential cross section and analyzing power. In this respect the structure is indeed very unusual. It is interesting that the back angle structure in the differential cross-section was not detected in previous work in this energy range<sup>52</sup> (this previous work involved a study of the isospin-related reaction,  $pd + t\pi^0$ ). However, preliminary results from a SACLAY/TRIUMF collaboration<sup>53</sup> for both analyzing power and differential cross-section at 1000 MeV tend to confirm the structure observed by Seth et al. The energy threshold at which the effect begins to become evident is in the region suggestive of a two pion effect (the threshold for two pion production in the free  $pp$  reaction is  $\sim 600$  MeV). Seth et al.

suggest, in fact, that the effect is related to the role played by two  $\Delta$  isobars in the reaction.

Because of the unexpected nature of these results and the fact that they are at variance with earlier results from an (isospin) related reaction, further experimental investigations of both the isospin and kinematic (including spin) dependences of this reaction are required. Hopefully, the theorists will also soon accept the challenge and provide us some insight into the possible mechanisms responsible for the effect, and in particular to provide us the guidance needed for mounting optimal experimental investigations of the phenomenon.

It is the possibility of making unexpected observations of this kind that provides the on-going incentive to experimentalists. There is always the enticing possibility that one has found the elusive dibaryon or equivalently exciting - some specific quark or cloudy bag effect. Whether something of this kind will indeed be discovered in investigations of few body systems is a question whose resolution will probably have to await the results to be presented at a later meeting of this series.

#### REFERENCES

1. M. Betz, B. Blankleider, J.A. Niskanen, and A.W. Thomas, "Pion Production and Absorption in Nuclei - 1981", ed. R.D. Bent, AIP Conference Proceedings No. 79 (1982) 65.
2. D.B. Lichtenberg, Phys. Rev. 105 (1957) 1084.
3. A.M. Green, J.A. Niskanen and M.E. Sanio, J. Phys. G4 (1978) 1055.
4. J.A. Niskanen, Nucl. Phys. A298 (1978) 417.
5. I.R. Afnan and A.W. Thomas, Phys. Rev. C10 (1974) 109.
6. T. Mizutani and D. Koltun, Ann. of Phys. 109 (1977) 1.
7. B. Blankleider and I.R. Afnan, Phys. Rev. C24 (1981) 1572.
8. C. Fayard, G.H. Lamot and T. Mizutani, Phys. Rev. Lett. 45 (1980) 52
9. A.S. Rinat and Y. Starkand, Nucl. Phys. A397 (1983) 381.
10. W. Grein, A. Kunig, P. Kroll, M.P. Locher, A. Svarc, SIN Report: PR-83-08 (1983).
11. G.A. Miller and L.S. Kisslinger, Phys. Rev. C27 (1983) 1609.
12. G. Jones, "Pion Production and Absorption in Nuclei - 1981", ed. R.D. Bent, AIP Conference Proceedings No. 79 (1982) 15.
13. W. Watari (1983) Osaka City University Report, OCUPWA-003.

14. K. Seth, "Few Body X Contributions", ed. B. Zeitnitz
15. K.K. Seth et al., "Few Body X Contributions"
16. J. Franz et al., "Few Body X Contributions"
17. S.E. Turpin et al., "Few Body X Contributions"
18. E.L. Mathie, private communication, 1983.
19. G.R. Smith, J. Bolger, E. Boschitz, E.L. Mathie, G. Proebstle, M. Meyer, F. Vogler, and S. Mango, Phys. Rev. C25 (1982) 3228.
20. G.R. Goldstein and M.J. Moravcsik, private communication, 1982, Oregon Institute of Theoretical Science (Report OITS 198)
21. F. Foroughi, J. Phys. G: 8 (1982) 1345.
22. E. Aprile-Giboni, Thesis (1982), Geneva.
23. W.B. Tippens et al., "Few Body X Contributions".
24. D.B. Barlow et al., "Few Body X Contributions".
25. W.B. Tippens et al., "Few Body X Contributions".
26. A.V. Kravtsov, M.G. Ryskin, and I.I. Strakovsky, "Few Body X Contributions".
27. B. Blankleider, R.S. Stoddard, G. Jones, private communication, 1983.
28. F. Mandl and T. Regge, Phys. Rev. 99 (1955) 1478.
29. D.V. Bugg, private communication (1983), and invited talk at this meeting.
30. D. Ashery et al., Phys. Rev. Lett. 47 (1981) 895.
31. P. Gotta et al., Phys. Lett. 112B (1982) 129.
32. C.H.Q. Ingram, Nucl. Phys. A374 (1982) 319c.
33. K.A. Aniol et al., "Few Body X Contributions".
34. G. Backenstoss et al., "Few Body X Contributions".
35. T.-S.H. Lee and K. Ohta, Phys. Rev. Lett. 49 (1982) 1079.
36. R. Silbar and Piasetzky, "Few Body X Contributions".
37. H. Ullrich, "Few Body X Contributions" and private communication.
38. Hudomalj-Gabitzch et al., Phys. Rev. C18 (1978) 2666.
39. E.D. Cooper and A. Sherif, "Pion Production and Absorption in Nuclei - 1981", ed. R.D. Bent, AIP Conference Proceedings No.79 (1982) 231.
40. B.D. Keister and L.S. Kisslinger (1983) private communication.



41. M. Dillig, F. Soga and J. Conte, "Pion Production and Absorption in Nuclei - 1981", ed. R.D. Bent, AIP Conference Proceedings, (1982) 275
42. A.M. Green and M.E. Sainio, Nucl. Phys. A329 (1979) 477.
43. M.E. Sainio, Nucl. Phys. A389 (1982) 573.
44. W. Dutty, J. Fran, E. Rossle, H. Schmitt and D. Dumbrajs, " Few Body X Contributions"
45. M. Hirata and K. Masutani, private communication, 1983.
46. R. Abegg et al., "Few Body X Contributions"
47. Y. Avishai and T. Mizutani, Nucl. Phys. A393 (1983) 429.
48. B.M.K. Nefkens, contribution to "Symposium on Delta-Nucleus Dynamics at Argonne National Lab., 1983"
49. P. Couvert, Invited talk, Univ. of Alberta/TRIUMF Workshop on "Studying Nuclei with Medium Energy Protons", Edmonton, Alberta, July, 1983.
50. B. Hoistad, "Pion Production and Absorption in Nuclei - 1981", ed. R.D. Bent, AIP Conference Proceedings No. 79 (1982) 105.
51. D. Kielczewska et al., "Few Body X Contributions".
52. J.W. Low et al., Phys. Rev. C23 (1981) 1656.
53. J. Arvieux, R. Abegg et al., private communication (1983).
54. F. Shimizu et al., Nucl. Phys. A386 (1982) 571.
55. G. Giles et al., "Few Body X Contributions".
56. B.G. Ritchie et al., Phys. Rev. C27 (1983) 1685.
57. R. Bertini et al., private communication (1983)
58. J. Hoftiezer et al., private communication, 1983.
59. K.K. Seth, "Few Body X Contributions".
60. M.J. Borkowski et al., "Few Body X Contributions" and private communication.
61. K.K. Seth et al., "Few Body X Contributions".
62. J. Hoftiezer et al., Nucl. Phys. A402 (1983) 429.
63. J. Hoftiezer et al., private communication: (to be published in Nucl. Phys.) 1983.
64. E.L. Mathie, G.R. Smith, E. Boschitz, J. Hoftiezer and M. Meyer, Z. für Phys. A313 (1983) 105.



## PION-NUCLEON ELASTIC SCATTERING

B.M.K. NEFKENS

Physics Department, UCLA, Los Angeles, California 90046

Pion-Nucleon scattering is reviewed. Positive results include: 1) good agreement between the  $\pi N$  resonance parameters of the Karlsruhe-Helsinki, K-H, and Carnegie-Mellon-Berkeley, CMU-LBL, partial wave analyses; 2) no sizable isospin violation near the Roper resonance; 3) a  $10^{-20}$  isospin violation in the region of the  $\Delta(1232)$ ; 4) the u- and d- quark mass difference is small, with  $m_d > m_u$ ; 5) forward dispersion relation predictions agree with experiment up to 300 GeV/c; 6) there are no good candidates for  $\pi N$  hermaphrodites; 7) the Isgur-Karl quark model calculations are useful up to  $m \approx 1800$  MeV. Negative findings are: 1) there is urgent need for spin rotation measurements to verify the correct use of theoretical constraints in all partial wave analyses; 2) existing data is insufficient to establish the fate of 24  $\pi N$  resonance candidates; 3) 3 strong and 7 weak  $\pi N$  resonances with mass above 1800 MeV predicted by the Isgur-Karl quark model are not seen; 4) the experimental result for the  $\pi N$   $\sigma$ -term is  $64 \pm 8$  MeV while the QCD inspired prediction is  $35 \pm 5$  MeV. Finally, there is some evidence for clustering of  $\pi N$  resonance poles in the complex energy plane, it is unknown if this is accidental or new physics.

## I. INTRODUCTION

According to a hypothesis of Gell-Mann<sup>1</sup> and Zweig<sup>2</sup> all baryon resonances consist of three quarks, thus qualifying for a review at a Few Body Conference. The lightest  $\pi N$  resonance, the  $\Delta^{++}(1232)$ , is made up of three u-quarks,  $|\Delta^{++}\rangle = |uuu\rangle$ . If this hypothesis is correct the u-quark must have two remarkable properties, namely a fractional electric charge,  $Q(u) = +\frac{2}{3}e$  and parastatistics of order three, known as the "color degree of freedom".<sup>3</sup>

The general acceptance of the quark hypothesis comes partly from the fact that quarks provide a simple, qualitative basis for understanding the over 200 known hadron resonances. All baryon resonances can be arranged in a few series, the N,  $\Delta$ ,  $\Lambda$ ,  $\Sigma$ , etc. series, each characterized by quantum numbers I, S, C, as illustrated in Fig. 1. This picture is based on the Table of Resonances from the Review of Particle Properties,<sup>4</sup> RPP, our only regularly updated and generally accepted data compilation. A property of a long-lived particle listed in RPP, for example the mass of the  $\pi^+$  meson, is the weighted average of different experimental measurements; in contrast, the mass, width, and quantum numbers of the  $\pi N$  resonances are not measured directly, their values are determined from the partial wave analyses, PWA. This may come as a surprise to many faithful users of the RPP Resonance Tables. It needs to be

emphasized that the Resonance Tables are still rather incomplete listings, furthermore, the quality of one or two star resonances is not equivalent to the standing of a one or two star restaurant; to the contrary, one and two star resonances are not well established, and several may disappear when better experimental data become available while new resonances may very well show up.

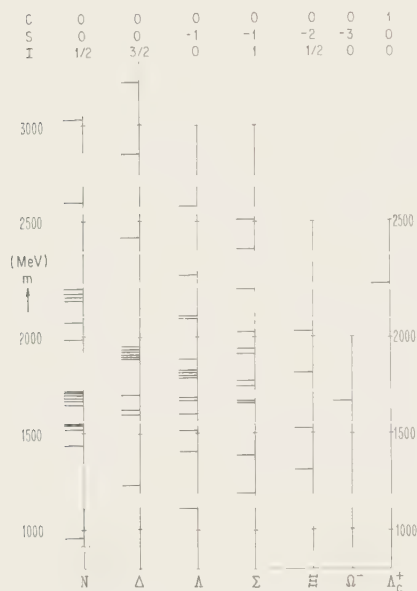


Fig. 1. Baryon resonances arranged in groups with the same I, S, C. The ordinate shows the mass. Data from Review of Particle Properties,<sup>4</sup> 3 and 4 star resonances only.

Because of the important role that the  $\pi N$  resonances play in any quantitative quark theory it was deemed useful to have a workshop on  $\pi N$  scattering to discuss the many nagging uncertainties and the problems currently facing the  $\pi N$  PWAs. The workshop was held here in Karlsruhe on the Saturday preceeding this conference. Since a PWA is not better than its data base much of the discussion was centered around establishing criteria for evaluating the quality of the entries to the data base. A proposal was made for grading the experimental data assigning three, two, one, or zero stars to indicate the quality as outlined in Table 1.

A report on the workshop appears elsewhere in the proceedings and more information is available from G. Höhler and myself.

As an example of the confusing status of several resonance parameters consider the  $P_{11}$  (1420)  $\pi N$  resonance. It is narrow in Germany and Finland as the Karlsruhe-Helsinki<sup>5</sup> PWA gives a width of 135 MeV, it is broad in the United States where CMU-LBL<sup>6</sup> gives  $\Gamma = 340$  MeV, and the Roper resonance is split in two in France<sup>7</sup> and Russia.<sup>8</sup> This divergence of opinions is a direct consequence of the poor quality of the  $\pi N$  scattering data in the region of the Roper resonance as discussed in the  $\pi N$  workshop. Until the needed three star data become available, the  $P_{11}$  (1420) parameters remain ill-defined and should not be used in support of theoretical work.

TABLE 1  
Outline of  $\pi N$  Data Base Star System

Data category	Data quality	Standards
A: ***	Impeccable	5/5
B: **	Good	4/5
C: *	Iffy	3/5
D: no star	Questionable	$\leq 2/5$

#### Standards:

1. Sufficient detail on calibrations, errors, ... 2. Full length article in good, refereed journal. 3. Modern measurement, published after about 1972.
4. No measurement shortcomings, e.g., lack of counter calibrations. 5. No inconsistencies with reasonable theoretical considerations, e.g., very rapid variations of  $d\sigma/d\Omega$ .

## II. $\pi N$ ELASTIC SCATTERING AMPLITUDES

A complete representation of  $\pi^+p$  elastic scattering free of ambiguities requires two independent amplitudes, e.g., the spin-nonflip,  $F$ , and the spinflip amplitude,  $G$ . The proof of this statement is based on rotation and reflection invariance<sup>9</sup> and does not require time reversal invariance unlike nucleon-nucleon scattering.

The three reactions,  $\pi^+p \rightarrow \pi^+p$ ,  $\pi^-p \rightarrow \pi^-p$ , and  $\pi^-p \rightarrow \pi^0n$  are related by isospin invariance. The scattering amplitude may be divided further into two independent isospin parts as discussed below.

To determine the two complex amplitudes,  $F$  and  $G$ , without ambiguity, leaving aside the isospin decomposition, one needs three independent measurements namely the cross section,  $d\sigma/d\Omega$ , the left-right asymmetry,  $A_N$ , measured using a transverse polarized target, and the spin rotation angle,  $\beta$ , measured using a longitudinal polarized target. The connections with the amplitudes are:

$$d\sigma/d\Omega = |F|^2 + |G|^2, \quad (1)$$

$$A_N = 2 \operatorname{Im} (F^*G) / (|F|^2 + |G|^2), \quad (2)$$

$$\beta = \arg \left( (F - iG \sin\theta) / (F + iG \sin\theta) \right). \quad (3)$$

There is a wealth of experimental data on  $d\sigma/d\Omega$  and  $A_N$  but most is not of three star quality. There is no data on  $\beta$  below 6 GeV/c; consequently, the determination of  $F$  and  $G$  from Eqs. 1 and 2 above is racked with ambiguities. For example, both  $d\sigma/d\Omega$  and  $A_N$  are invariant under the transformation:

$$F \pm iG \rightarrow (F \pm iG) \exp \left( \pm \frac{1}{2} i\phi \right), \quad (4)$$

with  $\phi$  ( $\theta=0$ ) = 0. An especially disturbing case known as the generalized Minami ambiguity occurs when  $\phi = -\theta$  changing all scattering waves by one unit

of angular momentum, e.g.,  $S_1 \leftrightarrow P_1$  and  $P_3 \leftrightarrow D_3$ .

To compensate for the lack of data on the spin rotation angle all PWAs introduce some theoretical constraints to eliminate the many ambiguities and to select a solution in cases where there are several acceptable fits to the experimental data. The theoretical constraints used are: a) unitarity via the unitarity bounds on the scattering amplitudes; b) analyticity expressed in the form of forward, fixed- $t$  or hyperbolic dispersion relations; c) isospin invariance. There is no need to worry about the validity of the unitarity bounds. The application of dispersion relations, which requires evaluating the dispersion integral including a contribution of the unknown distant part of the left hand cut, has been questioned since the forward scattering amplitude measured in  $\pi^-p \rightarrow \pi^-p$  around 20 GeV/c by Foley et al.<sup>10</sup> does not agree with the predictions of forward dispersion relations. Recently new measurements have been reported by Fajardo et al.<sup>11</sup> and Burq et al.<sup>12</sup> up to 300 GeV/c incident  $\pi^-$  momentum which are in good agreement with the most recent dispersion relation evaluation by H hler and Kaiser,<sup>13</sup> see Fig. 2. This justifies our relying on the use of dispersion relations until spin rotation angle measurements become available.

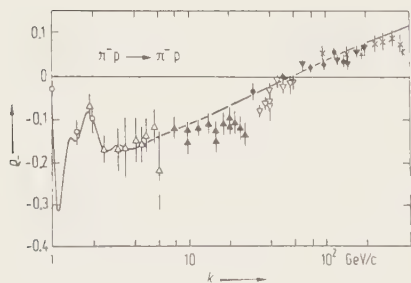


Fig. 2. Test of forward dispersion relations. The solid line is the calculation by H hler et al.<sup>13, 23</sup> for  $\pi^-p \rightarrow \pi^-p$ . The experimental points are:  $\blacktriangledown$  Fajardo et al.,<sup>11</sup>  $\bullet$  and  $\star$  Burq et al.,<sup>12</sup> and  $\blacktriangle$  Foley et al.<sup>10</sup>

Isospin invariance is expected to be valid down to the level of the Coulomb corrections and the effects of the u- and d-quark mass difference. There are only two isospin amplitudes in  $\pi N$  scattering,  $A_{1/2}$  and  $A_{3/2}$ , see Table 2.

Table 2

#### Isospin Decomposition

$$A(\pi^+p \rightarrow \pi^+p) \equiv A^+ = A_{3/2} \quad \text{and} \quad \sigma^+ \equiv |A^+|^2 = d\sigma/d\Omega(\pi^+p \rightarrow \pi^+p)$$

$$A(\pi^-p \rightarrow \pi^-p) \equiv A^- = \frac{2}{3} A_{1/2} + \frac{1}{3} A_{3/2} \quad \text{and} \quad \sigma^- \equiv |A^-|^2 = d\sigma/d\Omega(\pi^-p \rightarrow \pi^-p)$$

$$A(\pi^-p \rightarrow \pi^0n) \equiv A^0 = -\frac{1}{3} \sqrt{2} (A_{1/2} - A_{3/2}) \quad \text{and} \quad \sigma^0 \equiv |A^0|^2 = d\sigma/d\Omega(\pi^-p \rightarrow \pi^0n)$$

Isospin invariance in  $\pi N$  elastic scattering implies the relation:

$$A^+ - A^- = \sqrt{2} A_0, \quad (5)$$

This amplitude equality which holds at every energy and every scattering angle can be converted directly into triangle inequalities for the differential cross sections:

$$(\sqrt{\sigma^+} - \sqrt{\sigma^-})^2 < 2\sigma_0 < (\sqrt{\sigma^+} + \sqrt{\sigma^-})^2. \quad (6)$$

These relations provide a model independent test of isospin invariance. They hold for spin-averaged cross sections measured with an unpolarized proton target and also apply to the cross sections obtained using a transverse polarized target, separately for spin up and spin down, the so called transversity cross sections,  $Z_{\pm} = \sigma(1 \pm A_N)$ .

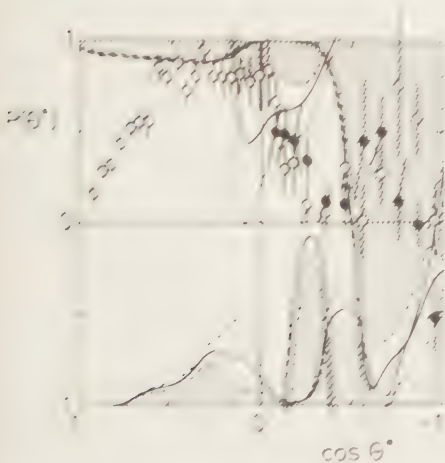


Fig. 3. Violation of isospin invariance reported by the Gatchina group. The data points are  $A_N(\pi^-p + \pi^0p)$  at  $T_\pi = 550$  MeV from Ref. 16. The shaded region is forbidden by isospin conservation, it is calculated using the triangle inequality relations and the data from Ref. 14.-16.



Fig. 4. Test of isospin invariance using the triangle inequalities, Eq. 6, at 625 MeV/c. The squares are  $d\sigma/d\Omega(\pi^-p + \pi^0n)$ . The shaded area is obtained using  $\pi^\pm p + \pi^\mp p$  measurements and is forbidden by isospin conservation. Input data are from the UCLA group at LAMPF.<sup>17</sup>

It was somewhat of a surprise when the Leningrad group<sup>14, 15</sup> hinted that the bounds of Eq. 6 tested using transversity cross section measurements,



were violated in the region of the Roper resonance at backward angles, see Fig. 3, implying isospin violation. The data used for this surprise announcement were a mixture of recent Gatchina<sup>14,15</sup> and some questionable Rutherford data.<sup>16</sup> The UCLA group at LAMPF is in the process of measuring the three relevant cross sections and the three left-right asymmetries. Their preliminary results contributed at this conference,<sup>17</sup> see Fig. 4, do not show a violation of the triangle inequalities in support of the approximate validity of isospin invariance in the region of the Roper resonance.

To alleviate the dependence of PWAs on theory and to check that the existing PWAs are on the right track, it is absolutely necessary that measurements of the spin rotation angle  $\beta$  be made. This is now realized at Gatchina<sup>18</sup> and at LAMPF<sup>19</sup> where measurements are being prepared.

### III. COMPARISON OF $\pi$ N PARTIAL WAVE ANALYSES

There are three major, modern partial wave analyses. The largest project, covering the momentum region from threshold to 10 GeV/c, is by the Karlsruhe group which is updating and expanding the original Karlsruhe-Helsinki PWA.<sup>5</sup> Fixed- $t$  and fixed- $\theta$  dispersion relations are used to compensate for the lack of spin rotation data and sometimes for imprecise experimental results. The second effort is spearheaded by R. Cutkoski who is continuing the original Carnegie-Mellon University-Lawrence Berkeley Laboratory PWA, CMU-LBL 79 and 80.<sup>6</sup> This work covers the momentum region from 0.4 to 2.5 GeV/c and uses continuity along certain hyperbolas in the Mandelstam plane as theoretical input. The third and relatively new group is from VPI.<sup>20</sup> Aside from a report<sup>21</sup> covering the low momenta region up to 0.4 GeV/c, no detailed information is available as yet. There are also several outdated PWAs and some special, fixed energy analyses.<sup>8,22</sup> An encyclopedic treatise of all aspects of  $\pi$ N scattering by Höhler<sup>23</sup> in which these PWAs are included has just become available. We restrict ourselves here to a comparison of the results obtained by the K-H and CMU-LBL analyses.

There is good agreement between the resonance parameters obtained by both PWAs. Of the 26 3 or 4 star N and  $\Delta$  resonances 23 agree in the mass value within the quoted error, 19 agree in the width and 24 in the elasticity, and for the others the differences are minor. The situation for the 1 and 2 star "resonances" is almost opposite: mass and width differ typically by 100 MeV and there is no agreement on the existence of 5 one star resonance candidates.

Finally, we compare both PWAs with experiments performed recently and not included in the data base. Shown in Fig. 5 is  $d\sigma/d\Omega$  ( $\pi^-p \rightarrow \pi^-p$ ) at  $p_\pi = 586$  MeV/c measured at LAMPF by the UCLA group.<sup>24</sup> The systematic uncertainties in the data are about 2%. The agreement of both PWAs with the data is reasonable

except in the dip near  $\cos\theta = -0.4$ . The K-H result is slightly better than CMU-LBL. The left-right asymmetry,  $A_N$ , measured by the same group,<sup>25</sup> is shown in Fig. 6 for  $\pi^-p \rightarrow \pi^-p$  elastic scattering, again the agreement is reasonable except near  $\cos\theta = -0.5$  where the old data used in the PWAs has large errors. This goes to illustrate that a PWA is not better than its data base.

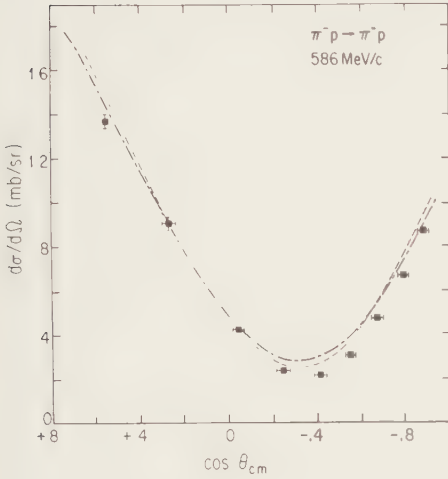


Fig. 5. Comparison of recent  $d\sigma/d\Omega$  ( $\pi^-p \rightarrow \pi^-p$ ) data<sup>21</sup> with predictions based on K-H<sup>5</sup> (dashed) and CMU-LBL (dashed-dotted) PWA.

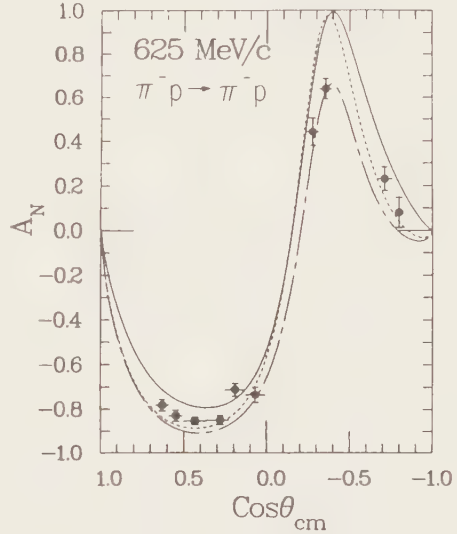


Fig. 6. Comparison of recent  $\pi^-p \rightarrow \pi^-p$  asymmetry<sup>25</sup> data with predictions based on PWA, solid line is K-H,<sup>5</sup> dotted is CMU-LBL,<sup>6</sup> and dashed is VPI.<sup>20</sup>

It is noted that K-H lists 24  $N$  and  $\Delta$  1 and 2 star resonance candidates. In general, the existing experimental data are insufficient and/or inaccurate to assert the true nature of these 24 resonance candidates. More and better data are required before we can become confident about knowing the baryon resonances with natural flavor.

#### IV. CLUSTERS OF RESONANCE POLES

In his new  $\pi N$  handbook,<sup>23</sup> Höhler has made an interesting observation. It appears that many  $\pi N$  resonances have, within the quoted error, the same pole positions. This clustering of resonances has potentially interesting

consequences for the quark model and other theories of the strong interaction.

When there are several overlapping resonances with large inelastic channels, a unique and theoretically palpable definition of a resonance is non-trivial. The energy dependence of the elastic partial wave amplitude, in the ideal case, is given by a pure Breit-Wigner type formula:

$$A(W) = R_1 / (M - W - \frac{1}{2}i\Gamma) . \quad (7)$$

This equation implies that the resonance amplitude in an Argand diagram follows a counter-clockwise rotation, that the resonance phase shift increases rapidly near  $\delta = \pi/2$  and that the speed of the resonance amplitude  $|dA/dW|$  has a clear maximum. However, resonances are not purely elastic and besides the resonance part,  $A_R$ , there is a background component,  $A_B$ :

$$A = A_R (1 + 2i A_B) + A_B . \quad (8)$$

The modified Breit-Wigner resonance formula is:

$$A_R(s) = R(q) / [M^2 - s - iM \Gamma(q)] . \quad (9)$$

Most compilations characterize a resonance by the parameters  $M$ ,  $\Gamma$ , and  $\eta$  where the resonance mass,  $M$ , is the c.m. energy at which the real part of the denominator of Eq. 9 vanishes; the resonance width,  $\Gamma$ , is taken at  $W = M$  and so is the elasticity,  $\eta = \Gamma_{e1} / \Gamma_t$ . A resonance can also be specified by the location of the complex pole of  $A$  which occurs in Eq. 7 when  $W = M - \frac{1}{2}i\Gamma$  and by the value of the complex residue  $R_1$  of Eq. 7. The difficulty with this definition is that one has to perform an analytic continuation of the scattering amplitude into the second sheet over an appreciable distance. Such an analytic continuation has been carried out by Cutkosky.<sup>6</sup> The values for the real parts of the pole position are shifted in comparison with the values of the mass parameters,  $M$ , by different amounts in the range 0 to 100 MeV. When H hler arranged the  $\pi N$  resonances according to their pole positions, he noticed several distinct clusters of resonances, as summarized in Table 3. It is important that selected new  $\pi N$  experiments be done to reduce the spread in uncertainty of the pole positions so the extent of the resonance pole clustering can be probed. It would, of course, be very interesting to determine the pole positions of the various  $\Lambda$  and  $\Sigma$  resonances to see if there is a similar clustering.

If further experimentation would strengthen the case for clustering rather than proving that Table 3 is a mere accident, it would have interesting consequences for the Isgur-Karl and other quark models.

TABLE 3  
Clusters of  $\pi N$  Resonance Poles in the Complex Plane

N	Pole Position		Isospin	Name
	Re (MeV)	Im (MeV)		
6	1665 $\pm$ 25	-55 $\pm$ 15	1/2	S <sub>11</sub> , P <sub>11</sub> , P <sub>13</sub> , D <sub>13</sub> , D <sub>15</sub> , F <sub>15</sub>
6	1880 $\pm$ 30	-120 $\pm$ 30	3/2	S <sub>31</sub> , P <sub>31</sub> , P <sub>33</sub> , D <sub>35</sub> , F <sub>35</sub> , F <sub>37</sub>
5	2110 $\pm$ 50	-180 $\pm$ 50	1/2	D <sub>13</sub> , D <sub>15</sub> , G <sub>17</sub> , G <sub>19</sub> , H <sub>19</sub>

N = number of 3 and 4 star resonances

#### V. THE u- AND d- QUARK MASS DIFFERENCE

There are strong theoretical prejudices for the case of the u- and d-quarks having different bare masses. Weinberg<sup>26</sup> estimates  $\Delta m = m(d) - m(u) \approx 3$  MeV and  $m(d)/m(u) = 1.8$ ; a recent calculation by Gasser and Leutwyler gives  $m(d)/m(u) = 1.76 \pm 0.13$  and  $\Delta m$ , which is more difficult to evaluate, about the same as Weinberg's value. Different u- and d- quark masses imply isospin violation; this holds also in QCD. Consider the usual QCD Lagrangian

$$L = L_0 - m(u) \bar{u} u - m(d) \bar{d} d - \dots \quad (10)$$

$L_0$  contains the quark and gluon kinetic energy and the interaction terms and is invariant under chiral  $SU_N \times SU_N$  transformations. If  $m(d) \neq m(u)$  this Lagrangian is manifestly isospin noninvariant. As  $\Delta m$  is only a few MeV the expected isospin breaking is of the same order of magnitude as the one induced by the isospin violating Coulomb interactions. It would be interesting to see some experimental manifestations of this intrinsic isospin violation, originating from the quark mass difference.

In the quark model  $|\Delta^{++} (1232) \rangle = |uuu\rangle$  and  $|\Delta^- \rangle = |ddd\rangle$ . Naively we have  $m(\Delta^-) - m(\Delta^{++}) = 3\Delta m$  or about 9 MeV. More refined estimates<sup>29-31</sup> yield about 2/3 of this value, see Table 4.<sup>32, 33</sup> There are as yet no reliable measurements of this mass splitting. Fortunately, one can check a related, less sensitive mass difference namely  $m(\Delta^0) - m(\Delta^{++}) = 2 \Delta m$  which is experimentally accesible using  $\pi^\pm p$  scattering; the status is shown in Table 4. The best determination is by Koch and Pietarinen<sup>33</sup> based on an update of the K-H PWA. The evaluation by Zidell et al.<sup>21</sup> is not listed in Table 4 as the nearby left hand cut singularities were not included in the original  $\pi N$  partial wave parametrization, and the PWA is being updated.<sup>20</sup> Table 4 shows that the experiment favors  $m(d) > m(u)$  with  $\Delta m$  having the expected magnitude, though there is room for a better determination.

TABLE 4  
Mass and Width Differences between Members of the  $\Delta(1232)$  Quartet

Theory		Ref.	Experiment		Ref.
mass $\Delta^- - \Delta^{++}$ MeV	mass $\Delta^0 - \Delta^{++}$ MeV		mass $\Delta^0 - \Delta^{++}$ MeV	width $\Gamma^0 - \Gamma^{++}$ MeV	
4.5	1.6	28	$2.7 \pm 0.3$	$6.6 \pm 1.0$	32
6.9	3.0	29	$2.7 \pm 0.6$	$2.0 \pm 1.8$	33
4.5	1.3	30			
4.5	1.3	31			

Related to the preceeding discussion is the direct measurement of an isospin violation in  $\pi^+p$  elastic scattering above the peak of the  $\Delta(1232)$  which is experimentally easier. A group at SIN<sup>22</sup> has carefully measured the asymmetry parameter,  $A_N$ , in  $\pi^+p$  elastic and  $\pi^-p$  charge exchange scattering and used their new data as input in a new simplified PWA. They have found a small, but clear difference in the  $P_{33}$  phases measured in  $\pi^+p$  and  $\pi^-p$  scattering:

$$\begin{aligned} \text{at } T_\pi = 238 \text{ MeV} \quad & \delta_{33}(\pi^+p) - \delta_{33}(\pi^-p) = 1.61^\circ \pm 0.55^\circ \quad \text{and} \\ \text{at } T_\pi = 292 \text{ MeV} \quad & \delta_{33}(\pi^+p) - \delta_{33}(\pi^-p) = 1.95^\circ \pm 0.44^\circ . \end{aligned}$$

This is currently our best available evidence for an intrinsic -- not of Coulombic origin -- violation of isospin invariance.

VI. THE QUARK MODEL OF ISGUR AND KARL

At the "Baryon 1980" Conference, the Isgur-Karl, I-K, quark model<sup>34</sup> was hailed as the most successful quark model calculation of the baryon resonances made thus far. The model is an extended version of the early non-relativistic three-quark models of baryons based on an ad hoc flavor-independent confinement perturbed by hyperfine interactions that originate from one gluon exchange.<sup>30</sup>

A review of both pre- and post- QCD quark models has just appeared<sup>35</sup> together with a discussion of existing experimental data and data analysis.

It is of interest to determine the level of agreement between the published  $\pi N$  resonance parameters, which are the best known set of resonance parameters and the I-K model calculations. The interest is enhanced by H hler's observation<sup>23</sup> about resonance pole clustering. A global comparison between the Koniuk-Isgur<sup>36</sup> I-K model calculations and the  $\Delta$  and  $N$  parameters listed in RPP<sup>4</sup> is given in Table 5. Below about 1800 MeV all predicted resonances are observed, though often with a mass or  $\pi N$  decay amplitude just outside the quoted uncertainties. This is certainly a very nice accomplishment. The weak

aspect of the I-K model calculations occur at higher energies where there are three resonances predicted with a strong  $\pi N$  channel as well as seven weak ones that have not been seen, see Table 6. New  $\pi N$  scattering experiments are needed to clarify this matter.

TABLE 5  
Comparison of Isgur-Karl Quark Model Predictions from Ref. 36  
with Experimental Data from RPP, Ref. 4

Family	Mass		$\pi N$ Amplitude		$n N$ Amplitude	
	Correct	Incorrect	Correct	Incorrect	Correct	Incorr
N	6	5	8	3	7	4
$\Delta$	5	3	4	4		

TABLE 6  
Resonances Predicted by Isgur-Karl Quark Model, Ref. 36,  
not seen by RPP, Ref. 4

Family	Strong	Weak	Name
N	2		P <sub>13</sub> (1870), P <sub>11</sub> (1890)
N		5	P <sub>13</sub> (1955), F <sub>15</sub> (1955), P <sub>13</sub> (1980), P <sub>11</sub> (2055), P <sub>13</sub> (2060)
$\Delta$	1		P <sub>31</sub> (1875)
$\Delta$		2	P <sub>33</sub> (1975), F <sub>35</sub> (1975)

TABLE 7  
Comparison of the Experimental Radiative Decay Amplitude of some light  
 $\pi N$  Resonances with the Predictions<sup>36</sup> of the Isgur-Karl, I-K, Model

Resonance	Isospin	$A_p$		$A_n$	
		"Exp"	I-K	"Exp"	I-K
P <sub>33</sub> (1232)	1/2	-141±6	-103		
P <sub>33</sub> (1232)	3/2	-258±8	-179		
P <sub>11</sub> (1420)	1/2	-70±9	-24	+42±19	+16
D <sub>13</sub> (1520)	1/2	-17±11	-23	-69±14	-45
D <sub>13</sub> (1520)	3/2	+166±7	+128	-136±14	-122
S <sub>11</sub> (1535)	1/2	+67±15	+147	-78±29	-119
S <sub>11</sub> (1650)	1/2	+45±17	+88	-23±33	-35
D <sub>15</sub> (1675)	1/2	+13±8	+12	-37±24	-37
D <sub>15</sub> (1675)	3/2	+22±12	+16	-54±24	-53

Amplitudes are given in the unit of  $10^{-3} \times [\text{GeV}]^{-1/2}$

The radiative decay of the  $\pi N$  resonances is of particular interest as the magnitude as well as the sign can be determined using pion photoproduction. In the case of the neutral resonances it is preferred to use the inverse reaction,  $\pi^- p \rightarrow N^* \rightarrow n \gamma$  to avoid the deuteron corrections that trouble  $\gamma n \rightarrow \pi N$  experiments. Table 7 gives a detailed comparison between the I-K model and experiment for the 6 lightest resonances. The agreement for the sign of the decay amplitude is very good but the magnitude is usually well outside the quoted error, particularly disturbing are the discrepancies seen in the lowest two resonances, the  $\Delta(1232)$  and the Roper, showing little improvement over the work of the pre-one-gluon-exchange era.

## VII. HERMAPHRODITE BARYONS

In the early years of the quark age the pivotal role in understanding hadron spectroscopy was played by the quarks. All baryons were identified by the type and configuration of the three constituent quarks; the gluons were used only for binding and otherwise had a passive role. The introduction of the "color degree of freedom"<sup>3</sup> has brought the emancipation of glue: 2 or 3 colored gluons can form a colorless and, therefore, observable object called a glueball, G. The experimental search for glueballs is just getting into full gear; the expected mixing with conventional ( $q^3$ ) systems and possible occurrence of radially excited ( $q\bar{q}$ ) or even ( $q\bar{q}q\bar{q}$ ) states may make it hard to discover these glueballs.

TABLE 8

Comparison of the Mass of Positive Parity  $\pi N$  Resonances  
Predicted for Hermaphrodites ( $q^3 G$ ) and I-K Three Quark ( $q^3$ )  
States with Experimental Data from RPP, Ref. 4

Mass in MeV				
# stars	Name	Exp	( $q^3 G$ )	( $q^3$ )
4	P <sub>11</sub>	1440±40	1430±20	1405
4	F <sub>15</sub>	1680±10	1980±30	1715
3	P <sub>33</sub>	1700±200	1600±30	1780
4	P <sub>11</sub>	1710±30	1680±30	1705
4	P <sub>13</sub>	1745±55	1770±20	1710
4	P <sub>31</sub>	1900±50	1800±30	1875
3	P <sub>33</sub>	2010±15	1960±20	1925



If glueballs exist then there must also be hybrids of quarks and glueballs, ( $q^3G$ ), called hermaphrodite<sup>37</sup> or meikton<sup>38</sup> matter. Since the  $\pi N$  system is the best known resonance system, it is a natural system to give us evidence for or against this proposed new hadronic matter. Golowich et al.<sup>39</sup> have calculated the expected ( $q^3G$ ) spectrum of positive parity states using harmonic oscillator and a bag model. The result is shown in Table 8 and compared to the previously discussed Isgur-Karl three quark calculation.<sup>36</sup> On the basis of this table there is no need to invoke the existence of hermaphrodite baryons.

Barnes and Close<sup>40</sup> have considered the photoproduction of hermaphrodite baryons finding that the photoexcitation of the lightest candidates from a proton target is strongly suppressed but allowed from neutrons, not unlike the Moorhouse selection rule in the old quark model. They suggest that this eliminates the Roper resonance as a hermaphrodite baryon candidate as the radiative decay  $P_{11}^+(1420) \rightarrow \pi\gamma$  is not suppressed, see Table 6. Instead, they propose the  $P_{11}(1710)$  as a new candidate. We consider the case of the Roper candidacy not yet closed: suppose the new pion scattering experiments would find that the Roper actually has a double peak as originally suggested by Aved.<sup>7</sup> Finding a single peak, charged radiative Roper and a double peak, neutral radiative one would be indicative of a ( $q^3G$ ) state. New experiments on the radiative decay from the  $P_{11}(1420)$  and  $P_{11}(1710)$  from both the neutral and charged states will be very helpful in probing the proposed existence of the hermaphrodite baryons.

### VIII. THE $\pi N$ SIGMA TERM

Important among the low-energy results stemming from theories with broken chiral symmetry is the so-called  $\pi N$  sigma term, i.e., the nucleon expectation value of the equal-time (sigma) commutator of the axial-vector current with its divergence. The importance of the  $\sigma$ -term stems from the fact that it is directly proportional to the strength of chiral symmetry breaking. In the framework of QCD this can be calculated directly from the quark bare mass term:

$$\sigma = \frac{1}{2} (m_u + m_d) \langle N(p) | \bar{u}u + \bar{d}d | N(p) \rangle + \text{small isospin breaking term} . \quad (11)$$

Gasser and Leutwyler<sup>27</sup> recently have reviewed and updated the available calculations; they find  $\sigma(\text{QCD}) = 35 \pm 5$  MeV, where older calculations give values from 20 to 40 MeV.<sup>41</sup>

The "experimental" value of the  $\sigma$ -term can be obtained from on-shell  $\pi N$  scattering amplitudes extrapolated to an unphysical point in energy<sup>42</sup> using dispersion relations. Extrapolations published since 1973 have yielded values for the  $\sigma$ -term from 56 to 86 MeV.<sup>41</sup> Recently R. Koch<sup>43</sup> has obtained  $\sigma(\text{exp}) = 68$

$\pm 8$  MeV; in this new evaluation he makes use of hyperbolic dispersion relations and the  $K$ - $H^b$  PWA phases.

The  $\sigma$ -term is one of the few cases where a numerical prediction based on QCD together with a few reasonable dynamical assumptions can be tested experimentally at low energy. Thus, the discrepancy between "experiment" and theory looks interesting. Upon close inspection it turns out that the low energy PWA is not at all certain as it is based on no-star data. There is urgent need for new, accurate low energy  $\pi N$  data. A Karlsruhe group<sup>44</sup> at SIN is planning a careful measurement of the difference between  $\pi^+p$  and  $\pi^-p$  scattering in the Coulomb region with the aim of obtaining a reliable value for the  $\sigma$ -term.

#### IX. CONCLUDING COMMENTS

The salient features of this  $\pi N$  review have been summarized in the abstract. We want to stress here the need for new  $d\sigma/d\Omega$ ,  $A_N$ , and  $\beta$  data at intermediate energies: a) to resolve the fate of the 24 tiny peaks in various partial waves found by the partial wave analyses and euphemistically called one or two star resonances by RPP; b) to strengthen or dismiss the potentially very interesting case of resonance pole clusters; c) to provide a strong test of the Isgur-Karl quark model by settling the case of the 3 strong and 7 weak resonances predicted but not seen; d) to probe the possible existence of hermaphrodite baryons; e) to provide a new value for the  $\pi N$  sigma term.

It is a pleasure to acknowledge stimulating discussions with G. H hler on the theoretical aspects of  $\pi N$  scattering and PWA.

This work was supported in part by the United States Department of Energy.

#### REFERENCES

1. M. Gell-Mann, Phys. Lett. 8 (1964) 214.
2. G. Zweig, CERN reports 8131/TH.461 and 8419/TH.412 (1964), not accepted for publication.
3. More appropriate would be "color degree of constraint".
4. Review of Particle Properties, M. Roos et al., Phys. Lett. 111B (1982).
5. G. H hler, F. Kaiser, R. Koch, and E. Pietarinen; Handbook of pion-nucleon scattering, Physik Daten Vol 12-1, Karlsruhe 1979; Low energy update, R.Koch and E. Pietarinen, Nucl. Phys. A336 (1980) 331.
6. R.E. Cutkosky, C. Forsyth, R. Hendrick, and R.L. Kelly, Phys. Rev. D20 (1979) 2839; also ibid 2732 (1979) and 2804 (1979); update R.E. Cutkosky in Proc. IVth Conf. on Baryon Resonances, Toronto 1980, ed. N. Isgur.
7. R. Ayed, CEA-N-1921, Saclay 1976.
8. V.V. Abaev et al., Leningrad Nucl. Phys. Inst. preprint No 438 (1978).

9. P.L. Csonka and M.J. Moravcsik, Phys. Rev. 152 (1966) 1310.
10. K.J. Foley et al., Phys. Rev. 181 (1969) 1775.
11. L.A. Fajardo et al., Phys. Rev. D24 (1981) 46.
12. J.P. Burq et al., Phys. Lett. 109B (1982) 111; *ibid* 77B (1978) 438.
13. G. Höhler and F. Kaiser, KFK 3027 (1980) Karlsruhe.
14. V.S. Bekrenev et al., Nucl. Phys. A364 (1981) 515.
15. V.V. Abaev et al., Z. Phys. A311 (1983) 217.
16. R.M. Brown et al., Nucl. Phys. B117 (1976) 12, *ibid* B144 (1978) 287.
17. M. Sadler et al., Contr. Few Body X, Karlsruhe (1983).
18. V.S. Bekrenev et al., Contr. Few Body X, Karlsruhe (1983).
19. LAMPF proposal #806 by UCLAG (= UCLA-CUA-LAMPF-ACU-GWU) collaboration.
20. R.A. Arndt, private communication.
21. V.S. Zidell, R.A. Arndt, and R.D. Roper, Phys. Rev. D21 (1980) 1255.
22. J.C. Alder et al., Phys. Rev. D27 (1983) 1040.
23. G. Höhler, Pion-Nucleon Scattering, Landolt-Bornstein Vol I/9b, part 2 (Springer-Verlag, Berlin, 1983).
24. M.E. Sadler et al., Phys. Lett. 119B (1982) 69.
25. D.H. Fitzgerald et al., Contr. Few Body X, Karlsruhe (1983).
26. S. Weinberg in Festschrift for I. Rabi, N.Y. Acad. of Sc. 185 (1978).
27. J. Gasser and H. Leutwyler, Physics Reports 87 (1982) 78.
28. R.P. Bickerstaff and A.W. Thomas, Phys. Rev. D25 (1982) 1869.
29. N. Isgur, Phys. Rev. D21 (1980) 779.
30. A. de Rújula, H. Georgi, and S.L. Glashow, Phys. Rev. D12 (1975) 147.
31. W. Thirring, Acta Physica Austriaca Suppl. 8 (1965) 205
32. E. Pedroni et al., Nucl. Phys. A300 (1978) 221.
33. R. Koch and E. Pietarinen, Nucl. Phys. A336 (1982) 331.
34. N. Isgur and G. Karl, Phys. Rev. D19 (1979) 2653 and references quoted therein.
35. A.J.G. Hey and R.L. Kelly, Physics Reports 96 (1983) 72.
36. R. Koniuk and N. Isgur, Phys. Rev. D21 (1980) 1868.
37. T. Barnes and F.E. Close, RL-82-088 T 311.
38. M. Chanowitz and S. Sharpe, LBL-14865 (1982).
39. E. Golowich, E. Hagg, and G. Karl, Amherst preprint 1982.
40. T. Barnes and F.E. Close, Phys. Lett. 128B (1983) 277.
41. C.A. Dominguez and P. Lanacker, Phys. Rev. D24 (1981) 1905.
42. R. Dashen and M. Weinstein, Phys. Rev. 188 (1969) 2330.
43. R. Koch, Z. Phys. C 15 (1981) 161.
44. H. Degitz et al., SIN proposal (1982).



# FIRST WORKSHOP ON PION-NUCLEON SCATTERING

Gerhard HÖHLER

Institut für Theoretische Kernphysik, Universität Karlsruhe, P.O.Box 6380,  
D-7500 Karlsruhe 1, Federal Republic of Germany

A summary is given of a workshop held on the eve of the "FEW BODY X"  
Conference at Karlsruhe (August 20, 1983).

The purpose of the workshop was to discuss the status of the experimental information on  $\pi N$  scattering, plans for new experiments, and methods and results of  $\pi N$  partial wave analysis. The workshop was organized by G. Höhler, B. Nefkens and H.M. Staudenmaier.

B. Nefkens proposed to introduce a star system for  $\pi N$  scattering experiments<sup>1</sup>, which makes it easier to assign an appropriate weight to the existing data in partial wave analysis. - A collaboration of the CMU, Virginia and Karlsruhe groups plans to compare the different  $\pi N$  data banks and to produce a combined and corrected version, which can be used in forthcoming partial wave analyses. The new data bank will include "Comments" on experimental methods, procedures used for the data analysis and discrepancies between different data sets.

A survey of the existing data was given by M.E. Sadler (0 - 1.0 GeV/c), J. Malos (1.0 - 2.5 GeV/c) and H.M. Staudenmaier (>2.5 GeV/c). J. Malos explained the reason why the important data set of the Bristol-Southampton-Rutherford group has not yet been published. He promised that a detailed paper will be available soon.

Plans for new  $\pi N$  scattering experiments at meson factories were described by A. Triol (TRIUMF), W.J. Briscoe (LAMPF) and W. Kluge (SIN).

The last topic was introduced by R. Koch, who compared the results of the most recent partial wave analyses. In general, the agreement between the CMU-LBL<sup>2</sup> and KH<sup>3</sup> solutions is good, although the methods are quite different. Some discrepancies are due to different compromises in cases where data sets are contradictory. Others occur in the tail of high partial waves. - A large discrepancy between the KH<sup>3</sup> and VPI<sup>4</sup> solutions is caused by the fact that the Virginia group ignored the existing information on the nearby left hand cuts of the partial wave amplitudes. - The Leningrad solution<sup>5</sup> is not compatible with the forward dispersion relation<sup>6</sup>.

My talk on the "Methods of  $\pi$ N Partial Wave Analysis" appears elsewhere in these Proceedings<sup>7</sup>. The main point is that the existing solutions can be improved by using the prediction for the tail of high partial waves that follows from the Mandelstam hypothesis. Other consequences of this hypothesis have to be applied anyway in order to obtain a unique solution.

If Mandelstam analyticity is ignored, partial wave analysis is not well-defined in a generally accepted way. One can derive a unique solution only by introducing various ad hoc assumptions which have no theoretical justification (sharp cut-off of the partial wave expansion, a special parametrization of the energy dependence, etc.).

It is planned to include the other contributions to this workshop in an informal report called " $\pi$ N Newsletter", and to distribute it to the participants and to others who are interested. The "Newsletter" will also contain further "Comments" on  $\pi$ N scattering experiments, partial wave analyses or applications of partial wave amplitudes, and information on new experiments and new partial wave analyses. Copies can be obtained from our institute or from B. Nefkens, Dep. of Physics, University of California, Los Angeles.

#### ACKNOWLEDGMENT

B. Nefkens and I would like to thank R. Cutkosky, R. Arndt and D. Fitzgerald for detailed discussions on the topics of this workshop during the LAMPF II meeting in July 1983.

#### REFERENCES

- 1) B.M.K. Nefkens, Few Body Problems X (Book of Contributed Papers).
- 2) R.E. Cutkosky et al., Phys. Rev. D20 (1979) 2840. "Baryon 1980", Proc. 4th Int. Conf. on Baryon Resonances, ed. N. Isgur, p. 19.
- 3) G. Höhler, F. Kaiser, R. Koch and E. Pietarinen, Handbook of Pion-Nucleon Scattering, Physics Data 12-1 (1979).  
R. Koch and E. Pietarinen, Nucl. Phys. A336 (1980) 331.
- 4) V.S. Zidell, R.A. Arndt and L.D. Roper, Phys. Rev. D21 (1980) 1255, 1289.
- 5) V.V. Abaev, S.P. Kruglov and Y.A. Malov, Leningrad Report 438 (1978).
- 6) J. Stahov, Karlsruhe preprint TKP 81-5 (1981).
- 7) G. Höhler, Few Body Problems X (Book of Contributed Papers). See also my book "Pion-Nucleon Scattering" in Landolt-Börnstein I/9b2, ed. H. Schopper (Springer 1983).

## MESONIC DEGREES OF FREEDOM IN FEW NUCLEON SYSTEMS

Moderator F. Lenz SIN

Rapporteur Y. Avishai Beer Shava

### 1. Introduction.

Mesonic degrees of freedom (MDF) in few nucleon systems are the corner stone of nuclear physics since the emergence of the Yukawa theory. Thus, nucleon structure, NN interaction (strong, electromagnetic and weak) are all based on MDF. The mounting evidence of quark structure and the belief that quantum chromo-dynamics (QCD) is the underlying field theory of strong interactions confronted nuclear physicists with a great challenge: to construct a unified theory of nuclear forces at long and short distances.

In the present few body conference, we have had many contributions and discussions pertaining to this goal. Yet, in this discussion session we will not touch this subject directly. Rather, we shall discuss the MDF in few nucleon systems with special attention focused on the coupling to excited states of the nucleon ( $\Delta$  and  $N^*$ ). Evidently, the relative simple description of these states in quark terms and existence of coupling schemes such as  $\Delta\pi$  indicate that the study of MDF in connection with  $N, \Delta, N^*$  is an important ingredient on the way to the main goal.

Before entering into the subjects of discussion, it is worthwhile to remind ourselves how deeply MDF are interlaced with few nucleon systems. This we shall do briefly, focusing on one nucleon,  $\pi N$  interaction, two nucleon and few nucleon systems.

Let us then start with the nucleon. The mesonic cloud around the nucleon determines its interaction range (e.g. the pion compton wave length  $\approx 1.4$  fm). Unlike QCD, the strong coupling made it very difficult to predict short distance behaviour and to get valuable information on the "inside" of the nucleon. This later ignorance is now being eliminated after the discovery of quark degrees of freedom. The structure of the nucleon and its excited states ( $\Delta, N^*$ ) are now explained in relatively simple terms. The size of the nucleon is determined by the bag model radius. Notice however that at distances greater than 1 fm, the pionic cloud prevails. A unified theory (of the nucleon and its surrounding mesons) which is based on QCD still does not exist.

Next, let us mention the  $\pi N$  interaction. This was one of the most extensively studied systems. The strong  $\pi N$  interaction is intimately related to



nucleon structure. In the past, the Chew-Low theory was successful in the low to medium energy range but nucleon-structure effects have been replaced by cut-offs. From the MDF point of view, the treatment of the  $\Delta$  state has undergone a crucial change in the passage to the quark picture. Furthermore, Chiral (little and cloudy) bag models should be able to account for  $\pi N$  scattering with nucleon structure effects built in. Still, there are several open problems like e.g. the non-resonant partial waves, effects of other mesons, and above all, understanding  $\pi N$  scattering up to very high energies.

It is also worth mentioning the role of MDF in weak interaction. The existence of strangeness conserving non-leptonic weak interaction (which is the origin of parity non conservation in nuclei) has now been established. Theoretical models of weak meson nucleon vertices based on quark  $SU_6$  models have been suggested recently. Such models can be tested by  $\pi + \bar{p}$  scattering experiments.

The role of MDF in the NN interaction cannot be overestimated. The meson exchange potentials describe rather well the long and medium distance interaction. A beautiful example of pion physics in the deuteron has been recently demonstrated. The short range behaviour has now started to be unravelled thanks to the quarks picture. Still, a unified theory at all distances does not exist. Should it be established, we will be able to build nuclear physics from prime principles.

MDF play also an important role in NN weak interaction. The mesons carrying the force meet one nucleon in a strong vertex and the other one in weak vertex. Evidently, MDF appear also in studying electromagnetic probes on the NN system. Meson exchange currents modify the electromagnetic properties of free nucleons such as magnetic moments and form factors.

Finally, MDF in few nucleon systems are of much importance. The dual role of the pion as a physical particle (which can serve as a probe in scattering experiments) and an agent of the nuclear force led to special interest in reactions involving scattering, absorption and production. In particular, it has been suggested that understanding of the absorption on two nucleon states can shed some light on the controversial dibaryon resonance question. The confrontation of multiple scattering predictions with those of theories based on quark models may illuminate important issues such as off shell effects, overlapping nucleons, color excitations etc. It is likely that the familiar multiple scattering theory will be replaced by a new theory based on QCD.

Having presented a telegraphic compendium of the main issues, we now proceed to the points to be discussed. It has recently been realised that pionic excitation of the nucleon via processes like  $N+N \rightarrow N+\Delta$  is an essential element in intermediate energy ( $E_L \sim 400$  MeV) NN reactions. This concept is now used in models of nucleon-nucleon dynamics as well as in reactions involving absorption and production of pions on light nuclei. A critical discussion of this point is then worthwhile. We will then address the following questions:

- 1) Mesonic degrees of freedom in the two nucleon system beyond meson exchange potentials (short range parameters, coupling to isobar states etc.).
- 2) The role of  $\Delta \leftrightarrow \pi N$  process, how far it can be pursued in few nucleon systems (NN scattering,  $\pi d$  scattering, three nucleon bound states form factors etc.).
- 3) Dynamics of pion absorption in few nucleon systems; is the  $\pi NN \rightarrow \Delta N \rightarrow NN$  process dominant? What about non-resonant partial waves? Can one explain the suppression of absorption on  $T = 1$  NN pairs? Are there signatures of dibaryon resonances related to these reactions?

In section II, coupling to isobar states in the two nucleon system is discussed by E. Lomon. In this context the MDF enter only through virtual pions mediating the forces between nucleons and isobars ( $\Delta, N^*$ ). A unified description of NN force,  $\pi d$  scattering, three nucleon bound-states and electromagnetic structure of three nucleon bound-states is discussed in section III by P.U. Sauer. Finally, pion absorption by  ${}^3\text{He}$  and  ${}^3\text{H}$  is discussed in section IV by T.S.H. Lee. The absorption on  ${}^3\text{He}$  has been the subject of recent experimental investigations, which have been reported in this discussion session by the Basel group. Some concluding remarks are drawn after section IV.

## II Deuteron Properties of Models with Isobar coupling, with implications for the $N^*(1440)$ Magnetic Moment (Earle Lomon)

### 1. INTRODUCTION

Previous studies of the roles of the  $\Delta\Delta$  isobar in the deuteron have indicated anywhere from 0.3% to 3.5%  $\Delta\Delta$  component.<sup>1</sup> Theoretical constraints used included single pion and, sometimes,  $\rho$  meson exchange transition potentials, while low energy scattering data was used as a phenomenological constraint. As two-pion exchange range transition potentials are likely to be important, and have not yet been calculated, these investigations were over-constrained theoretically. On the other hand they did not use the experimental information from intermediate energy scattering data above elastic threshold, which is particularly sensitive to the isobar channel coupling. A model has recently been published<sup>2</sup> which fits the nucleon-nucleon data for all partial waves (including the  $^1D_2$  and  $^3F_3$  structures) for laboratory energy  $E_L \leq 800$  MeV. It uses a field theoretical NN potential and one-pion exchange plus phenomenological two-pion range transition potentials to the  $N\Delta, \Delta\Delta$  and  $NN^*(1440)$  isobars outside a boundary condition core. The constraint of the energy dependence of  $\delta_{10}$ ,  $\delta_{12}$  and  $\epsilon_1$  removes much of the arbitrariness of previous coupled channel calculations of deuteron properties.

The amount of coupling to higher mass channels required to give the correct energy dependence to the intermediate energy  $^3S_1$ - $^3D_1$  phase shifts and coupling parameter is substantial<sup>2</sup> and implies that the amount of isobar channel in the deuteron is about 2.7%, on the high end of the range previously considered. But the proportion of coupling to different isobar states is not well determined by the elastic data (In the future, comparison with  $n$   $p$  inelastic data will restrict it.). The resulting difference in deuteron properties does, as we see below, remove much of the uncertainty.

In the model developed for the NN scattering data the  $\Delta\Delta(^3S_1)$  and  $NN^*(^3S_1)$  channels were coupled to the  $NN(^3S_1$ - $^3D_1)$  channel, as their relatively low threshold and angular momentum barrier gives them the most influence on the  $^3S_1$ - $^3D_1$  energy dependence. As the  $\Delta\Delta$  and  $NN^*$  channels have nearly the same threshold their influence on NN scattering is interchangeable. In Ref. 2 the

phenomenological short range ( $\frac{1}{2} \mu^{-1}$ ) transition potentials and the boundary condition coupling used were in approximate proportion to the OPE transition potentials. However different amounts of  $\Delta\Delta$  or  $NN^*$  dominance can be achieved by changing the proportions of these short range transition interactions. Furthermore the  $\Delta\Delta(^7D_1)$  state, which has less influence on the scattering because of the angular momentum barrier, importantly affects the deuteron magnetic moment  $\mu_D$ .

As detailed below,  $\mu_D$  is incompatible with  $\Delta\Delta$  dominated isobar components, but can be accommodated by plausible values of the  $N^*$  magnetic moment if the  $NN^*(^3S_1)$  channel is the major part of the isobar component. There are presently several competitive models of  $N^*$  structure whose predicted magnetic moments need to be compared with the range allowed by  $\mu_D$ .

## 2. THE MODEL

We keep the NN potential and the OPE transition potentials to the S states of  $\Delta\Delta$  and  $NN^*$  exactly as described in Ref. 2. The NN potential is obtained from single  $\pi$ ,  $\rho$ ,  $\omega$  and  $\eta$  exchange and from a non-relativistic calculation of  $2\pi$  exchange with nucleon intermediate states<sup>3</sup>. The isobar intermediate states are included through the explicit channel coupling. The OPE transition potentials are of the form

$$V_{\pi}^{ab} = \frac{1}{3} \frac{f_a f_b}{4\pi} \mu \tau_a \cdot \tau_b [\sigma_a \cdot \sigma_b V_0(\mu r) + S_{ab} V_2(\mu r)]$$

where  $V_0(x) = x^{-1}e^{-x}$ ,  $V_2(x) = (x^{-1} + 3x^{-2} + 3x^{-3})e^{-x}$  and the operators are either ordinary (iso)spin one-half or transition (iso)spin one-half to three-halves operators. The OPE transition potentials from the  $\Delta\Delta(^7D_1)$  channel are

$$V_{\pi}[NN(^3S_1) - \Delta\Delta(^7D_1)] = 0.276 \mu V_2(\mu r)$$

$$\text{and } V_{\pi}[NN(^3D_1) - \Delta\Delta(^7D_1)] = -0.056 \mu V_2(\mu r)$$

## 3. RESULTS

In case 1 we omit the  $\Delta\Delta(^7D_1)$  channel altogether and keep approximately equal strength two-pion range transition potentials and boundary condition couplings to the  $\Delta\Delta(^3S_1)$  and  $NN^*(^3S_1)$  channels. This resembles the  $^3S_1$ - $^3D_1$  model of Ref. 2, but a new fit to the data was obtained because of a numerical error in the published result (the sign of  $\epsilon_1$  is opposite to that shown). A good fit to the data for  $E_L \leq 800$  MeV is obtained with

$$V_{2\pi}[NN(^3S_1) - \Delta\Delta(^3S_1)] = 2.4r^{-1}e^{-2\mu r}$$

$$V_{2\pi}[NN(^3D_1) - \Delta\Delta(^3S_1)] = 2.95r^{-1}e^{-2\mu r}$$

$$V_{2\pi}[NN(^3S_1) - NN(^3S_1)] = -0.7r^{-1}e^{-2\mu r}$$

$$V_{2\pi}[NN(^3D_1) - NN(^3S_1)] = -2.15r^{-1}e^{-2\mu r}$$

and  $f_{S,S} = 12.3134$ ,  $f_{S,D} = 1.5$ ,  $f_{D,D} = 2.5$ ,  $f_{S,\Delta\Delta} = 4.6$ ,  $f_{D,\Delta\Delta} = -0.4$ ,  $f_{\Delta\Delta,\Delta\Delta} = 3.5$ ,  $f_{S,NN^*} = -5.7$ ,  $f_{D,NN^*} = 0.4$ ,  $f_{NN^*,NN^*} = 3.5$ , and  $f_{\Delta\Delta,NN^*} = 0.0$ .

This results in a deuteron with 2.2245 MeV binding energy,  $P_D = 6.0\%$ ,  $P_{\Delta\Delta}(s) = 1.2\%$ ,  $P_{NN^*} = 1.6\%$ ,  $Q^{IA} = .289 \text{ fm}^2$  and  $\eta = .0270$ . The  $Q$  and  $\eta$  agree with measurements, neglecting meson exchange current corrections<sup>4,5</sup> but  $Q$  may be too large when the corrections are computed for this model.

Assuming the quark model value of the  $\Delta$  magnetic moment,  $q_\Delta\mu_p$ , the deuteron magnetic moment is

$$\begin{aligned} \mu_D = & \mu_{MEC} + \mu_p + \mu_n + \left[\frac{3}{4} - \frac{3}{2}(\mu_p + \mu_n)\right]P_D - \mu_n P_{\Delta\Delta(S)} \\ & + (\mu_p - \mu_n - \frac{1}{2} M/M_\Delta)P_{\Delta\Delta(D)} + (\mu_p + \mu_n + \mu_S^*)P_{NN^*}. \end{aligned}$$

The average of the magnetic moments of the two isospin states of the  $N^*$ ,  $\mu_S^* = (\mu_p^* + \mu_n^*)$ , is experimentally unknown. Taking into account MEC corrections<sup>4</sup>,  $\mu_{MEC} \approx 0.006$  requires  $\mu_S^* \approx -1.0$ , for this case. We note that this case already has somewhat less  $\Delta\Delta$  than  $NN^*$  component, and the  $\Delta\Delta$  is all in the  $^3S_1$  state. The above equation shows that the coefficients of  $P_{\Delta\Delta}$  are positive, and that the coefficient of  $P_{\Delta\Delta(D)}$  is substantially larger than the coefficient of  $P_{\Delta\Delta(S)}$ .

In case 2, the  $\Delta\Delta(^7D_1)$  channel has been added with the OPE coupling described above. A good fit to the  $E_L \leq 800$  MeV data was obtained which minimized interaction with the  $\Delta\Delta$  channels, using

$$V_{2\pi}[NN(^3S_1) - \Delta\Delta(^7D_1)] = -2.0r^{-1}e^{-2\mu r}$$

$$V_{2\pi}[NN(^3D_1) - \Delta\Delta(^7D_1)] = 0.4r^{-1}e^{-2\mu r}$$

$$V_{2\pi}[NN(^3S_1) - \Delta\Delta(^3S_1)] = -0.2r^{-1}e^{-2\mu r}$$

$$V_{2\pi}[NN(^3D_1) - \Delta\Delta(^3S_1)] = 0.8r^{-1}e^{-2\mu r}$$

$$V_{2\pi}[NN(^3S_1) - NN(^3S_1)] = -2.1r^{-1}e^{-2\mu r}$$

$$V_{2\pi}[NN(^3D_1) - NN(^3S_1)] = -0.5r^{-1}e^{-2\mu r}$$

and  $f_{S,S} = 9.3774$ ,  $f_{S,D} = 1.4$ ,  $f_{D,D} = 2.5$ ,  $f_{\Delta\Delta(D),\Delta\Delta(D)} = 2.0$ ,  $f_{\Delta\Delta(S),\Delta\Delta(S)} = 3.0$ ,  $f_{S,NN^*} = -4.0$ ,  $f_{NN^*,NN^*} = 1.0$  and all other  $f$ 's vanishing.

The resulting deuteron has 2.2245 MeV binding energy,  $P_D = 5.7\%$ ,  $P_{\Delta\Delta(D)} = 0.4\%$ ,  $P_{\Delta\Delta(S)} = 0.0\%$  and  $P_{NN^*} = 2.3\%$ ,  $Q^{IA} = .284 \text{ fm}^2$  and  $\eta = .0261$ . The value of  $\eta$  is consistent with experimental indications, but  $Q^{IA}$  may still be too close to the experimental  $Q$  to allow for the meson exchange current corrections (which are yet to be calculated for this model).

Using the above formula for  $\mu_D$ , we find that  $\mu^* = -0.1$  for case 2. We note that a fit that eliminated completely the  $\Delta\Delta$  components would fit  $\mu_D$  with  $\mu^* = +0.5$ . As large negative values for  $\mu^*$  would require very special models the experimental value of  $\mu_D$  seems to favor  $NN^*$  dominated deuteron models with  $\Delta\Delta$  components constituting less than half of the total isobar content of  $\sim 2.7\%$ .

As the  $N^*(1440)$  mass is not easily obtained in a bag model there are several competing models containing one or more of the following quark configurations;  $[(1S_{1/2})^2, 2S_{1/2}]$ ,  $[(1S_{1/2})^3, 1P_{1/2}, \overline{1S_{1/2}}]$ ,  $[(1S_{1/2})^3, \text{gluon}]$ ,  $[(1S_{1/2})^3, \text{monopole vibration of bag}]$ . The  $\mu^*$  of these models have not been published, but should be examined to determine if they satisfy  $\mu^* < 0.5$  and what proportion of  $\Delta\Delta$  components is implied.

### 3. CONCLUSIONS

The constraints of a field theoretic  $NN$  potential and one pion exchange transition potentials to isobar channels together with scattering data from threshold into the inelastic region are sufficient to determine the overall strength of the two-pion exchange range transition potentials and boundary condition coupling. The resulting deuteron has about 6% D state and about 2.7% total isobar component. The predicted values of  $Q$  and  $\eta$  are close to the experimental values without meson exchange current corrections.

The proportions of  $\Delta\Delta$  and  $NN^*$  isobar components are not determined by the elastic scattering, but may eventually be determined by inelastic data. The value required of the isospin sum of the  $N^*$  magnetic moment,  $\mu^*$ , to fit  $\mu_D$  is very sensitive to their proportions. If one expects that  $\mu^* \geq -1.0$  then the  $NN^*$  component needs to be about one-half or more of all the isobar content of the deuteron. Model values of  $\mu^*$  are required to be less than 0.5.

### REFERENCES

- 1) H.J. Weber and H. Arenhövel, Physics Reports 36, 277 (1978).
- 2) E.L. Lomon, Phys. Rev D26, 576 (1982).
- 3) E.L. Lomon and H. Feshbach, Ann. Phys. (NY) 48, 94 (1968).

- 4) E. Hadjimichael, Nucl. Phys. A312, 341 (1978).  
 5) J.A. Tjon and M.J. Zuilhof, Phys. Lett. 84B, 31 (1979).

### III Two Nucleon Force Model with $\Delta$ and $\pi$ Degrees of Freedom (P. Sauer).

Above  $r=1$  fm, the N-N interaction is understood in terms of meson exchange. The long range is dominated by OPE while the medium range attraction is generated by the scalar part of the irreducible  $2\pi$  exchange in which intermediate nucleons can be excited to  $\Delta$  isobars. The  $\rho$  and  $\omega$  exchanges generate the shorter range part. At  $r<1$  fm, quark degrees of freedom become important and account for repulsion of the core through color magnetic interaction. Attempts to unify quark and meson exchange picture for the nucleon-nucleon interaction are so far not successful.

Meson exchange and internal nucleonic excitation in a relativistic description are important for the derivation of the two nucleon potential. The derivation usually results in an instantaneous two body potential. In the model suggested, the potential can excite a nucleon to a bare  $\Delta$  isobar. It couples through a vertex

$$\Delta \begin{array}{c} \nearrow \pi \\ \searrow N \end{array} = f' \frac{p}{(2\omega(p))^{1/2}} \left( \frac{\Lambda^2 - m_\pi^2}{\Lambda^2 + p^2} \right)^2$$

to  $P_{33}$  pion nucleon states and thereby build up the physical  $P_{33}$  resonance, which is energetically the most easily excited baryon resonance. For the NN interaction the instantaneous potential contains all meson exchanges, except half the OPE which arises from the energy dependent coupling to the  $NN\pi$  channel. Thus, it includes both  $\Delta$  isobar excitation and pionic degrees of freedom. It is flexible enough to describe, on the one side, NN scattering below and above the inelastic threshold as well as  $\pi d$  scattering but on the other side, remains simple enough to be used also in nuclear structure calculations.

In the introduction we have mentioned the special role of the  $\Delta$  in the quark bag models together with its characteristics as a baryon resonance. This picture is implied in the present model where the  $\Delta$  is a quark bag which receives its dressing as Physical baryon resonance due to its coupling to the pionic channel through the  $\pi N\Delta$  vertex.

I shall now describe some consequences of the present model when applied to a three-nucleon system<sup>1</sup>. This has been done by including wave-function components containing a single  $\Delta$  isobar in the three nucleon wave-function. Multiple  $\Delta$ -effects are ignored. The two-nucleon interaction acts in all partial waves up to total angular momentum  $J=2$ . The presence of a  $\Delta$ -isobar increases the three-nucleon binding energy by about 0.3 MeV, 0.6 MeV repulsion being a dis-



persive two-body effect, and 0.9 MeV attraction arising from the three-nucleon force with an intermediate  $\Delta$ -isobar. The effect of the  $\Delta$  on the three-nucleon charge and magnetic form factors and on the weak decay is investigated.

The model revives the  $\Delta$ -isobar degrees of freedom for the three-nucleon bound state. It uses the coupled channel approach as a clean and consistent method for calculating the nuclear structure corrections due to the  $\Delta$  isobar. We observe and emphasize that a complete calculation of  $\Delta$  effects is crucial, because the different  $\Delta$  mechanisms compete and often tend to cancel. For example, the attractive binding-energy contribution of the  $\Delta$  mediated three-nucleon force is partly balanced by the repulsive two-nucleon dispersive effect. We are also concerned about the standard calculations of exchange current corrections for e.m. and weak properties. We expect the observed competition between  $\Delta$  corrections to persist when multiple  $\Delta$  excitations and other baryon resonances besides the  $\Delta$  were considered.

Qualitatively the corrections due to single  $\Delta$  excitation reduce the disagreement between theory and experiment, but quantitatively they are disappointingly small. The description of the e.m. and weak properties of the three-nucleon bound states will be improved by the inclusion of mesonic exchange current contributions. However, the hope that the discrepancy between experimental  $^3\text{H}$  binding energy could be overcome by a  $\Delta$  mediated three-nucleon force has not been fulfilled, and this hope was the driving motive for the calculation. We consider the problem of the missing binding energy as grave.

We would like to ask, using the three-nucleon bound state as a substitute for the heavier and more complicated nuclei : does the picture of the nucleus as a nonrelativistic system of interacting nucleons, baryons resonances and mesons work quantitatively ? Even after the rather ambitious  $\Delta$  treatment, we are still unable to answer this question.

Other features of the model together with its success in describing two nucleon data,  $\pi$ d differential cross-section, three nucleon bound-states and  $^3\text{He}$  charge form factors are detailed in the contribution by Pöping, Sauer and Xi-Zhen to this conference.

The conclusion is then a reconfirmation of the traditional fact that the treatment of the virtual  $\Delta$  in bound systems of nuclear structure as a stable particle is a valid approximation. It remains to be seen to what extent this approach can, in general, cure the existing problems in the microscopic theory of nuclear structure, where three body forces are essential. In the treatment of three body forces here, an attempt is made to unify aspects of intermediate energy physics and low energy nuclear physics.

IV Isospin Dependence of Pion Absorption on  $^3\text{He}$  (T.S.H. Lee)

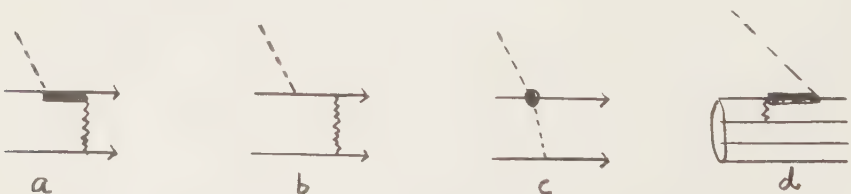
The following discussion is focused on  $\Delta N \longleftrightarrow NN$  dynamics in pion absorption reactions on  $^3\text{He}$ . Experimental measurements of  $(\pi^+, pp)$  and  $(\pi^-, pn)$  on  $^3\text{He}$  have been reported by several groups. In the present discussion session we learned about the results of the Basel group (Reported by Ulrich). The reason for going from deuterium target to  $^3\text{He}$  target is that due to spin and isospin constraints on the deuteron wave-function the  $\pi d \rightarrow NN$  process only probes  $T=0$  NN pairs. Our interest in  $\Delta N \longleftrightarrow NN$  dynamics therefore requires heavier targets in which nucleon pairs with various spin-isospin configurations are accessible. Only then we will be able to get a complete microscopic understanding of pion absorption reactions.

All the pertinent measurements have shown that pion absorption on a  $T=1$  NN pair of nucleons in  $^3\text{He}$  target is strongly suppressed and its strength relative to a  $T=0$  pair of nucleons does not follow a simple isospin arguments. This is reflected in a quantity  $R(E, \theta)$  defined by

$$R(E, \theta) = \frac{d\sigma/d\Omega(\pi^+, pp)}{d\sigma/d\Omega(\pi^-, pn)}$$

Since nucleons in  $^3\text{He}$  are predominantly in the relative  $S$  states, the intermediate  $\Delta N$  in the  $^5S_2$  state, which dominates absorption for a  $T=0$  nucleon pair is forbidden for a  $T=1$  pair. It is clear that we need a sufficiently detailed  $\Delta N \longleftrightarrow NN$  dynamics to explain these important data. I want to stress the point that any theoretical approach must take into account the dependence of  $R$  on energy and angle. It is also crucial that each cross-section is reproduced separately and not only their ratio  $R$ .

In a work completed recently (with K. Ohta and M. Thies) it has been shown that a model Hamiltonian for  $N, \pi, \Delta$  can successfully be constructed to describe both the magnitude of the  $(\pi^+, pp)$  and  $(\pi^-, pn)$  cross-sections as well as their ratio  $R$ . The general considerations pertaining to the absorption mechanism at  $E_\pi \gtrsim 50$  MeV were as follows; absorption is a two body process which is divided into isobar excitation (fig. 1a) plus corrections. These corrections include a).  $P_{11}$  nucleon pole term (fig. 1b) b).  $S$  wave absorption (fig. 1b) and c). "pre-existence" of  $\Delta$  in nuclei (fig. 1d)



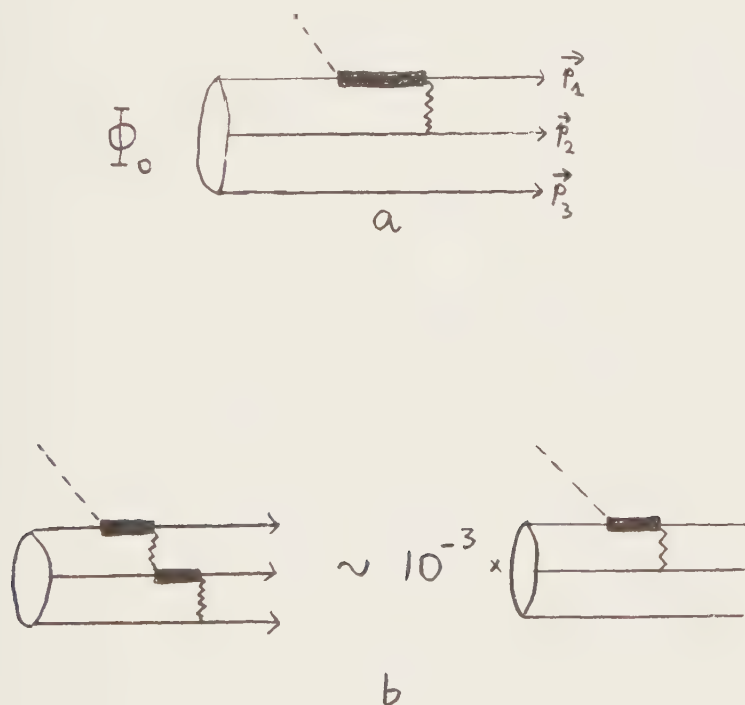
The crucial point in our approach is concerned with the determination of the input parameters to the  $\pi, N, \Delta$  Hamiltonian beyond the OBE. In the present work they are chosen to fit all data of the reactions

$$\pi N \rightarrow \pi N \quad (E \leq 300 \text{ MeV})$$

$$NN \rightarrow NN, NN\pi \quad (E \leq 1000 \text{ MeV})$$

(including  $\pi d \rightarrow \pi d, pp, \pi pn$ ). The model Hamiltonian is chosen with attention to the following points 1) Simplicity, namely, we keep only  $\pi N \Delta$  coupling and account for two body processes like  $NN \longleftrightarrow NN$ , and  $NN \longleftrightarrow N\Delta$ .  $\pi N, NN$ , and  $\pi d$  data are all quantitatively described. 2) Consistency with meson exchange mechanism. We start from the Paris potential, and include  $\pi, \rho$  exchange for  $NN \rightarrow N\Delta, \Delta\Delta, NN^*$ . In this way,  $\pi N$  ( $E \leq 1 \text{ GeV}$ ) and  $NN$  ( $E \leq 2 \text{ GeV}$ ) are well described.

The calculations of the absorption cross-section involve graphs as in fig. (2a). Two important points must be stressed here ; 1). Exact integration over the  ${}^3\text{He}$  wave-function is needed to get accurate prediction of the theory. For example  $\pi^+/\pi^-$  ratio of  $d^5\sigma/d\Omega_1 d\Omega_2 d\vec{p}_1 d^2\sigma/d\Omega_1 d\Omega_2$  are all sensitive to the accuracy of this integration (partial-wave dependence is strong). 2). Three body rescattering terms can be neglected (see fig. 2b).



Calculations based on the model of Betz and Lee show that the ratio  $R$  can be understood successfully from the  $\pi NN \rightleftharpoons \Delta N \rightleftharpoons NN$  dynamics determined from the  $\pi N$  and  $NN$  scattering data. No additional absorption mechanisms are necessary. It is important to note that by fitting  $NN$  inelasticities given by phase-shift analysis the essential dynamics of the  $\pi NN \rightleftharpoons \Delta N \rightleftharpoons NN$  process is incorporated in the model. In fact, the  $NN \rightleftharpoons \Delta N$   $t$  matrix (calculated from the model) in the channel  ${}^1D_2(NN) \rightleftharpoons {}^5S_2(\Delta N)$  is much stronger than those in other channels. This simply reflects the fact that  $NN$  scattering in  ${}^1D_2$  has the largest inelasticity. The consistency of the  $\pi NN \rightleftharpoons \Delta N \rightleftharpoons NN$  dynamics with the  $NN$  scattering is essential for the understanding of pion absorption on  ${}^3\text{He}$ .

Kinematics of  $\pi NN$  coincidence measurements indicates that the two ejected nucleons can come from either (A) an interacting nucleon pair or (B) one from an interacting pair and one spectator or (C) the genuine three body process. A careful investigation of the data indicates that the three body term (C) can practically be neglected in any region. It is now possible to investigate the ratio  $R$  under the assumption that only two body processes dominate. The differential cross-section for  $(\pi^-, pn)$  looks very similar to that of  $(\pi^+, pp)$  except that the maximum of the lump is shifted by about  $5^\circ$  and the magnitude is much smaller. As shown in our work these differences are brought about by the fact that the  $(\pi^+, pp)$  reaction is dominated by the  $S$  wave  $\Delta N$  state while the  $(\pi^-, pn)$  reaction is dominated by the  $P$  wave  $\Delta N$  state. Clearly, the ratio  $R$  is a function of angle and not an overall constant which one would have expected from isospin consideration alone.

In conclusion, the essential physics of the pion absorption by  ${}^3\text{He}$  can successfully be described by the two body mechanism provided that the essential  $N\Delta \rightleftharpoons NN$  dynamics in different partial waves is determined from  $NN$  scattering. Three body absorption mechanism (mediated by two body interaction) is found to be very small. The two body process  $\pi NN \rightleftharpoons \Delta N \rightleftharpoons NN$  seems to be essential absorption mechanism.

## REFERENCES

- 1) T.S.H. Lee and K. Ohta, Phys. Rev. Lett. 49 1079 (1983).
- 2) T.S.H. Lee and K. Ohta, Phys. Rev. C25 3043 (1982).
- 3) T.S.H. Lee, Phys. Rev. Lett. 50 1511 (1983).
- 4) M. Thies, T.S.H. Lee and K. Ohta, to be published.

## CONCLUDING REMARKS.

There is a general feeling that the nucleonic degrees of freedom alone fail to account for all the experimental data and that before we will have a QCD formulation of nuclear physics, the necessary ingredient is supplied by MDF. In this context, few nucleon systems are the most appropriate theoretical laboratory. The message of our discussion session is that coupling of nucleons to  $\Delta, N^*$  through meson exchange is rather essential at intermediate energies. A natural question now arises of whether the success of this idea is short lived, or it will become a part of textbooks. Apparently consistence with QCD requirements will determine the answer. If, as we hope, success is not accidental (in spite of the fact that the "true" degrees of freedom are quarks and gluons) then an overlap between these two concepts is called for. This is the realm of bag models and large  $N_c$  (number of colors) QCD. It is likely that this aspect of MDF in few nucleon systems will open new channels both in theory and in experiment. Hence, this domain of nuclear physics is worth being explored.

## ACKNOWLEDGMENT

I would like to thank the participants of the discussion for sending me their notes; I am grateful to Prof. A. Rinat for guidance and encouragement. Finally Prof. B. Zeitnitz should be thanked for giving the opportunity and for his flawless work in organizing the conference. I have also learned a lot from the works cited below.

## GENERAL REFERENCE

- Mesons in Nuclei* edited by M. Rho and D.H. Wilkinson (North Holland, Amsterdam 1979).
- J.M. Eisenberg and D.S. Koltun, *Theory of Meson Interactions with Nuclei* (Wiley, New York, 1980).
- W. Weise, Nucl. Phys. A374 (1982) 505<sub>c</sub>.
- J. Delorme, Nucl. Phys. A374 (1982) 541<sub>c</sub>.
- D.S. Koltun, Com. Nucl. Part. Phys. 11 (1983) 171.



## Chapter III

# NUCLEON-NUCLEON INTERACTION





## NUCLEON-NUCLEON EXPERIMENTS AND PHENOMENOLOGY

D. V. BUGG

Queen Mary College, Mile End Rd., London E1 4NS, UK

Recent experimental results on NN elastic and inelastic scattering up to 1 GeV are discussed. A unique amplitude analysis of  $NN \rightarrow D\pi$  is now possible up to 580 MeV, if one uses reasonable assumptions about phases and high partial waves; results agree qualitatively with predictions of Blankleider and of Niskanen, but exhibit quantitative disagreements for  $^3P_1$  and  $^3P_2$ . BASQUE (TRIUMF) data at 425, 465 and 510 MeV on  $pp \rightarrow np\pi^+$  are presented and discussed. They exhibit considerable similarities with  $pp \rightarrow d\pi^+$ , but an important difference in  $A_{SL}$ . They demand small (negligible) inelasticity in  $^3P_0$  and a sizeable amplitude for  $^3P_1 \rightarrow nZ^{++}$ , where Z stands for the  $\pi N S_{31}$  wave. Data on  $A_{NO}$ ,  $A_{ON}$  and  $A_{SL}$  indicate a final state  $N\Delta$  phase of about  $45^\circ$  for the dominant  $^1D_2 \rightarrow N\Delta$  at all three energies. A shortlist of crucial outstanding experiments up to 800 MeV is compiled.

### 1. INTRODUCTION

Data will be discussed in order of increasing interest: (a) elastic, (b)  $NN \rightarrow D\pi$  and (c)  $NN \rightarrow NN\pi$ .

### 2. ELASTIC SCATTERING

New results submitted to this conference are discussed briefly here. The non-partisan reader is advised that elastic scattering is now well enough known that these data are pinning down fine detail rather than fresh qualitative features. Figures displaying the new results are to be found in contributed papers.

#### 2.1. Below 100 MeV

New np P and  $A_{NN}$  data of impressive accuracy between 14 and 50 MeV are presented by groups from Karlsruhe<sup>1,2</sup>, Wisconsin<sup>3</sup> and Erlangen<sup>4,5</sup>. These data will improve our knowledge of the longest range part of the spin-orbit potential. However, below 142 MeV, the major phenomenological uncertainty remains the value of  $\bar{e}_1$ , which is horribly correlated with  $^1P_1$  in present data. The experiment which would resolve this is an accurate measurement of  $A_{LL}$ <sup>6,7</sup>. An interesting preprint of Grach et al.<sup>8</sup> fits P matrices of  $^3S_1$ ,  $\bar{e}_1$  and  $^3D_1$  up to 800 MeV, and concludes that Arndt's values of  $\bar{e}_1$  below 100 MeV disagree with any reasonable theory having a long-range OPE tail.

The Louvain group presents data<sup>9-11</sup> on elastic and capture differential cross sections between 45 and 75 MeV, and finds results disagreeing with previous data and (therefore) Arndt's analysis. In view of the uncertainties in  $^1P_1$ , this is

not necessarily surprising.

## 2.2. 500-1000 MeV

The Geneva group has completed very extensive and accurate measurements at SIN of pp spin-correlation, Wolfenstein and triple-spin parameters at 448, 494, 515, 536, 560 and 578 MeV<sup>12</sup>. New results at 560 MeV, with accuracies of  $\sim 0.03$  from  $34$  to  $122^\circ$  c.m., are presented at this conference.<sup>13</sup> There are no surprises and results agree with the Saclay-Geneva phase shift analysis<sup>14</sup> and with my analysis and Arndt's. Amplitudes from 425 to 580 MeV are now determined very securely, both by phase shift analysis and by direct reconstruction of amplitudes from the data, bypassing phase shifts<sup>15</sup>.

Also from SIN, there are measurements of  $d\sigma/d\Omega$  for np charge exchange from 200 to 590 MeV<sup>16</sup>. These results need to be scaled up by 5% in normalisation (within the errors) in order to agree with BASQUE data<sup>17</sup> and the conventionally accepted<sup>18</sup> value of  $f^2$ .

From TRIUMF, there are valuable measurements of pp  $d\sigma/d\Omega(90^\circ)$  from 300 to 500 MeV<sup>19</sup>. These establish absolute normalisations ( $\pm 1.8\%$ ), which previously have been rather poorly known, except for the accurate data of Chatelain et al.<sup>20</sup> from 515 to 580 MeV. The two experiments agree well.

From LAMPF, there are accurate pp measurements of (i)  $D_{NN}(90^\circ)$  from 380 to 800 MeV<sup>21</sup>, and (ii) P and Wolfenstein parameters at 699 and 750 MeV<sup>22</sup>. There are no surprises in these data, but it is likely that they will complete firm phase shift solutions bridging the 650-800 MeV gap, where previously there were very few spin-dependent data except P.

The Saclay group<sup>23</sup> presents new  $\Delta\sigma_L$  results from 550 to 2400 MeV. It is interesting that their results lie systematically about 10% higher than earlier ZGS<sup>24</sup> and LAMPF<sup>25</sup> results, although they do not quote a normalisation error. TRIUMF data from 200 to 520 MeV<sup>26</sup> also lie systematically 10-20% higher than ZGS and LAMPF results. My current phase shift solutions agree well with Saclay data for both  $\Delta\sigma_L$  and  $\Delta\sigma_T$  from 550 to 970 MeV.

My phase shift analysis<sup>27</sup> and Arndt's<sup>28</sup> now agree closely up to 970 MeV (including Gatchina data), except for one detail to be discussed here. My belief is that the current Saclay-Geneva solution also agrees closely, except for a few minor wiggles (associated with instabilities in high partial waves) where data have been sparse (650-1000 MeV). For  $I=1$ , the details on which there has been disagreement are the magnitudes of inelasticities in  $^3P_0$  and  $^1S_0$ , where Arndt has always favoured rather large inelasticities, and I have had almost none. The origin of this has been mainly that Arndt has fitted ZGS-LAMPF  $\Delta\sigma_L$  and  $\Delta\sigma_T$  data and has discarded TRIUMF results; I have fitted both, allowing the normalisation uncertainty quoted by each experiment, and resulting

in a fit roughly midway between the two<sup>26,27</sup>. As I will show in Section 4, inelastic data up to 510 MeV now conclusively limit the inelasticity in  $^3P_0$  to 20% of Arndt's 1982 value.

The pp amplitudes are now secure and accurate up to 800 MeV, and anyone proposing further elastic experiments must justify them against this background. Some tidying up is desirable at Gatchina energies, where some Wolfenstein parameters are out of line with phase shift solutions and with the trend of data from lower energies. The np data give secure  $I=0$  phase shift solutions from 140 to 515 MeV and a very shaky solution at 800 MeV. There is a dearth of np data around  $90^\circ$  above 495 MeV, and a crying need for measurements of  $A_{LL}$  and  $A_{SS}$  across the full range  $30-160^\circ$  at 650 and 800 MeV. These measurements will begin shortly at LAMPF<sup>29</sup>. My belief is that, in order to close this story, it will also be essential to measure  $D_t \approx K_{NN}$  and possibly  $R_t \approx K_{NN}$ .

At this point, the Bonn group<sup>30</sup> have published a paper by Z. Bialas and J. Bonner<sup>30</sup>. They show explicitly how to derive all amplitudes from  $d\sigma/d\Omega$ ,  $P$ , Wolfenstein and spin-correlation parameters. They remark that triple-spin parameters are not needed in principle. This coincides with my own observation that the limited accuracy of triple-spin parameters is in practice such that they have little impact on phase shift analysis up to 800 MeV.

### 3. $NN \rightarrow D\pi$

There are several contributions to this conference on  $pp \rightarrow d\pi^+$  data from 500 to 800 MeV. Comment on these data will be deferred to other speakers. Here, results will be presented of my analysis of earlier data from threshold to 580 MeV<sup>31</sup>.

There has been an earlier analysis of this channel by Watari and collaborators<sup>32-35</sup>. They have done an energy dependent analysis up to 800 MeV, freeing both amplitudes and phases of most waves up to  $^1G_4$ . However, many features of their solutions look odd. For example, they find a larger amplitude for  $^3P_1 \rightarrow d\pi(L=2)$  than for  $^3P_1 \rightarrow L=0$ , despite the centrifugal barrier in the final state, and also amplitudes for  $^1D_2 \rightarrow L=3$  and  $^1G_4 \rightarrow L=3$  much larger than theory (which one expects to be reliable for high partial waves). Since there are only eight types of data and six complex amplitudes, it seems likely that the data are as yet incapable of supporting so much freedom.

In my analysis, Blankleider's calculations<sup>36</sup> are used (a) to fix high partial waves with  $L \geq 3$  in both initial and final states (and also the small amplitude for  $^3P_1 \rightarrow L=2$ ), (b) to constrain loosely phases of most low partial waves (the exception being  $^3P_1 \rightarrow L=0$ , where cancellations are expected to lead to large uncertainty in the theoretical phase). The motivation for this latter

constraint is Watson's theorem, which says that if  $NN, \pi d$  and  $NN\pi$  are weakly coupled, partial wave amplitudes are given by

$$a(NN \rightarrow \pi d) = |a| e^{i\phi} = |a| \exp i(\delta_{NN} + \delta_{\pi d}),$$

where  $\delta$  are phase shifts for  $NN$  and  $\pi d$  elastic scattering respectively. This result is independent of the detailed internal dynamics of the  $NN$  and  $\pi d$  channels; in practice,  $\delta_{\pi d}$  is poorly known experimentally, and the coupling between  $\pi d$  and  $\pi NN$  channels is sufficiently strong that  $\phi$  has to be taken from theory. The phase constraints are applied by including in the  $\chi^2$  minimisation contributions of the form

$$\chi^2 = \sum \left( \frac{\phi_{\text{expt}} - \phi_{\text{theory}}}{\delta\phi} \right)^2$$

where  $\delta\phi$  are arbitrarily set to values of  $1-3^\circ$  near threshold (where Watson's theorem is accurately true) and  $7-10^\circ$  near 580 MeV.

The conclusions are:

- (i) the phase constraints have little effect on  $\chi^2$ , i.e. the data are compatible with them; they act so as to eliminate solutions with phases wildly different to theory;
- (ii) all amplitudes up to  $^3F_3$  are quite well determined, except for the  $^1S_0$  amplitude, which, for special reasons, is poorly determined; however, it must be small up to 580 MeV;
- (iii)  $^1D_2$ ,  $^3F_2$  and  $^3F_3$  amplitudes agree well with predictions of both Blankleider and Niskanen<sup>37</sup> (Figs. 1-2);
- (iv)  $^3P_2$  and  $^3P_{1 \rightarrow L=0}$  amplitudes show qualitative similarity to predictions, but both are larger than theory (Figs. 1 and 3).

An important conclusion is that the phase of the  $^1D_2$  amplitude agrees closely with theory. The relative phase of  $^1D_2$  and  $^3F_3$  (the largest two amplitudes at 580 MeV) is determined by the data  $+5^\circ$ . This is because  $P$  is given by the imaginary part of the interference between a particular bilinear combination of amplitudes, and  $A_{SL}$  is given by the real part of exactly the same combination. The extensive and accurate data on these parameters of the Geneva group<sup>38</sup> and Hoftiezer et al.<sup>39</sup> fix phases of  $^3P_1$  and  $^3F_3$  relative to  $^1D_2$  very well. Since the phase of the  $^1D_2$  amplitude agrees closely with theory, there is no call for coupling to a dibaryon resonance in this wave up to 580 MeV. The observed phase variation of the  $^1D_2$  amplitude originates purely from the  $\pi N$  interaction, through the  $\Delta(P_{33})$  resonance between the pion in the final state and both nucleons in the deuteron.

It is desirable to remove the theoretical props (i.e. phase constraints) on which these results are based. The crucial measurements needed are:

- (a)  $iT_{11}$ , the vector polarisation of the deuteron, which fixes the  $^1S_0$  wave<sup>40</sup>,

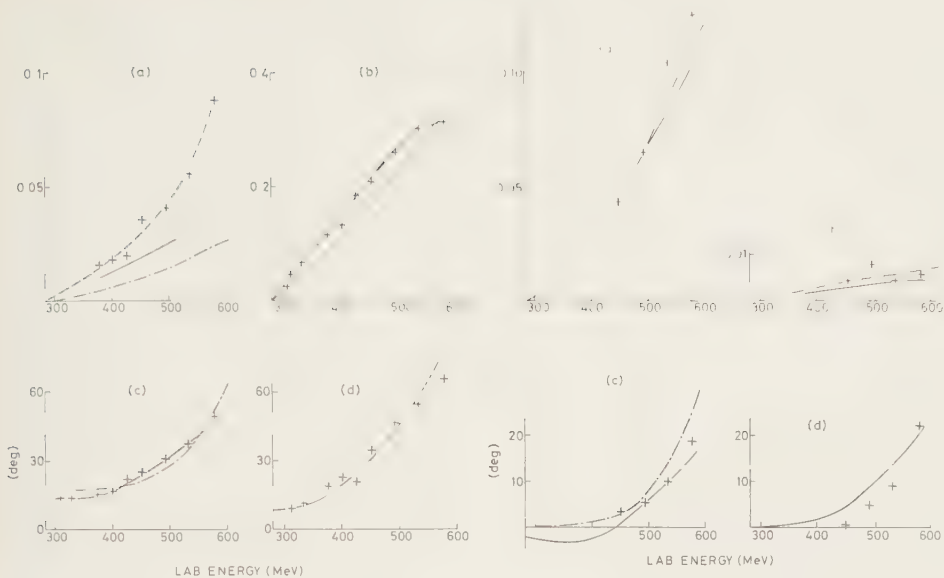


FIGURE 1

(a)  $|a(^3P_2)|$ , (b)  $|a(^1D_2)|$ , (c)  $\phi(^3P_2)$  and (d)  $\phi(^1D_2)$ . Full lines are predictions of Blankleider and chain curves those of Niskanen. The dashed lines are to guide the eye.



FIGURE 2

(a)  $|a(^3F_3)|$ , (b)  $|a(^3F_2)|$ , (c)  $\phi(^3F_3)$  and (d)  $\phi(^3F_2)$ . Curves are as in Fig. 1.

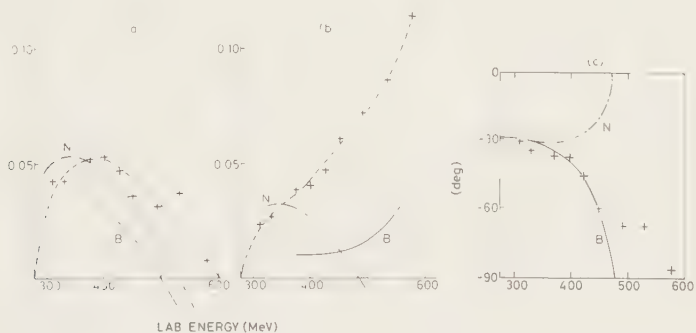


FIGURE 3

(a)  $\text{Re } a(^3P_1 \rightarrow L=0)$ , (b)  $\text{Im } a(^3P_1)$  and (c)  $\phi(^3P_1)$ . Curves are as in Fig. 1.

(b)  $\sigma(S0|iT_{11})$ , the same quantity measured with a proton beam polarised in the transverse direction  $S$  in the plane of scattering; this determines the small  $^3F_2$  amplitude and the small  $^3P_1 \rightarrow L=2$  amplitude.

4.  $NN \rightarrow NN\pi$ 

There are extensive new data from TRIUMF and LAMPF on the spin dependence of  $pp \rightarrow np\pi^+$  and  $pp \rightarrow pp\pi^0$ . These data are important for their information on (a) possible dibaryon resonances<sup>41,42</sup> in  $^1D_2$  at a nucleon lab energy of 570 MeV and in  $^3F_3$  at  $\sim 800$  MeV, (b) inelasticities, many of which are poorly determined by elastic data. I shall concentrate on the BASQUE (TRIUMF) data because they are sufficiently complete that, with a little help from theory, they give a complete picture of the partial waves contributing. The theory on which I lean is that of Silbar, Kloet, Dubach and Cass<sup>43-45</sup>, based on  $NN \rightarrow N\Delta$  and  $NN \rightarrow NN'$  via  $\pi$  exchange; here  $N'$  refers to the  $\pi N$   $P_{11}$  wave and  $\Delta$  to the  $P_{33}$  resonance. The theory includes rescattering via Fadeev equations, and therefore includes both 2 and 3-body unitarity.

The BASQUE data are measurements at 425, 465 and 510 MeV of  $A_{NO}$ ,  $A_{ON}$ ,  $A_{NN}$ ,  $A_{LL}$ ,  $A_{SS}$  and  $A_{SL}$  in  $pp \rightarrow np\pi^+$ . The experiment used a polarised beam of  $2 \times 10^6/s$  and a polarised target, and detected all three particles in the final state<sup>46</sup>. Including a time of flight measurement on the neutron, this resulted in a 2C fit; the background of carbon events and other inelastic channels was typically 15%, and could be subtracted cleanly by extrapolation under the kinematic peak (Fig. 4).

It is a tortuous process to relate partial waves to a five dimensional display of the data. Therefore, conclusions will be presented first, and will be justified by reference to the data; the computer carries out a five dimensional fit.

The process will be displayed graphically and discussed as  $pp \rightarrow nX^{++}$ , where  $X$  may stand for  $\Delta = P_{33}$  or  $Z = S_{31}$  in the  $\pi N$  system. The theory includes interfering amplitudes from  $pp \rightarrow pX^0$ . The kinematic variables will be as follows. The neutron has polar angle  $\beta$  and azimuthal angle  $\alpha$  around the incident beam in the overall centre of mass; in the  $X$  rest frame,  $X$  decays to a pion with polar angle  $\theta$  and azimuthal angle  $\phi$  with respect to the neutron direction. The fifth kinematic variable is  $M$ , the rest mass of  $X$ . The experimental configuration is such that  $\alpha \approx 0$  and is symmetrical about zero. Hence the  $\alpha$  dependence has been removed from the data by averaging over  $\alpha$  and using the fact that  $A_{NO}$ ,  $A_{ON}$  and  $A_{SL}$  are proportional to  $\cos \alpha$ , while  $A_{NN}$ ,  $A_{LL}$  and  $A_{SS}$  depend on  $\cos^2 \alpha$ ; in the

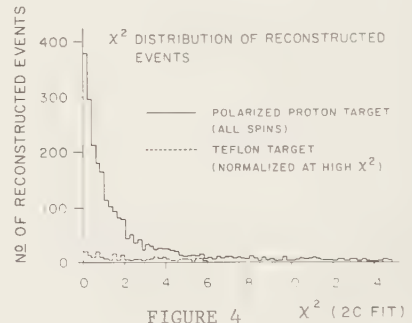


FIGURE 4  
The  $\chi^2$  distribution of  $pp \rightarrow np\pi^+$  events from the BASQUE experiment at 465 MeV. The full black histogram shows carbon background.



latter case, perturbations to  $A_{NN}$  from  $A_{SS} \sin^2 \alpha$  are removed by calculation, and vice versa for  $A_{SS}$ . In principle, for  $\phi=0$  there are terms  $A_{NL}$ ,  $A_{NS}$ ,  $A_{SN}$ ,  $A_{SO}$  and  $A_{OS}$  (conserving parity and time-reversal) present in the data, but all are proportional to  $\sin \alpha$ , and disappear when the data are summed over  $\alpha$ .

Because of the coils of the polarised target, coverage of phase space is incomplete. Coverage of  $\beta$  is complete but biased towards  $180^\circ$  both because of the geometry for detecting forward  $p$  and  $\pi^+$  and because of the energy dependence of neutron detection efficiency. Acceptance in  $\phi$  is biased towards the horizontal plane because of  $p$  and  $\pi^+$  geometry, but does cover  $90^\circ$  and  $270^\circ$  for some values of the other variables. Acceptance in  $M$  is reasonably uniform, and the peak in Fig. 5 is due to the  $\Delta(1230)$  resonance. Acceptance in  $\theta$  is incomplete, being restricted to two regions (a)  $0$  to  $60^\circ$  (both  $p$  and  $\pi^+$  forward) and (b)  $105$ - $150^\circ$  ( $\pi^+$  sideways). Despite these non-uniformities, enough of phase space is sampled to allow isolation of partial wave amplitudes. Asymmetries, hence spin-dependent observables, are independent of constant geometrical non-uniformities.

In the comparison with experiment, partial waves for  ${}^3F_3$  and higher waves are taken unadulterated from the calculations of Silbar et al. For lower waves, the phase is adjusted by  $\{\delta_{NN \rightarrow NN}(\text{expt}) - \delta_{NN \rightarrow NN}(\text{theory})\}$ , to correct for inadequacies in the initial state interaction ( $\rho$ ,  $\omega$ ,  $\phi$  and  $\eta$  exchange). This is important for  $A_{NO}$ ,  $A_{ON}$  and  $A_{SL}$  which are strongly phase dependent. This model is the origin of the dashed curves compared with the data on the figures which follow. Discrepancies between theory and the data are then to be accommodated by varying the magnitudes of amplitudes from initial  $NN$   ${}^1S_0$ ,  ${}^3P_0$ ,  ${}^3P_1$  and  ${}^3P_2$  states as adjustable parameters. The magnitude of the dominant  ${}^1D_2 \rightarrow N\Delta(L=0)$  amplitude would in principle be taken from the well known integrated cross section for  $pp \rightarrow p\pi^+$ ; in practice, no adjustment is necessary. The phase of this amplitude is treated as a variable, in order to allow for the possibility of a dibaryon resonance in this wave. At the time of writing, the computer programme does not include  $pp \rightarrow N\Delta$ , and therefore conclusions must be regarded as tentative.

The data demonstrate clearly that the  ${}^1D_2$  amplitude really is dominant. If this were the only amplitude present, it is easy to show that

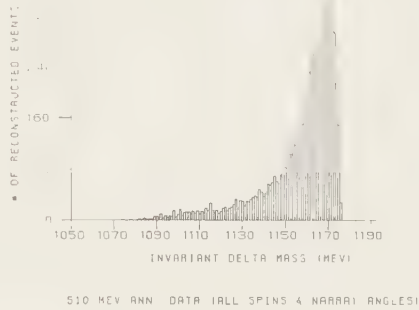


FIGURE 5

Projection of BASQUE data on  $M$ , the mass of the  $p\pi^+$  pair, at an incident energy of 510 MeV.

$$A_{NN} = A_{SS} = A_{LL} = -1.$$

This is true for any singlet state. Fig. 6 shows projections of the data at 510 MeV against  $\cos\theta$ , and the transverse momentum of the neutron,  $p_n^T = p_n \sin\theta$ . The data are consistent with  $A_{NN} \approx A_{SS} \approx -0.7$  and  $A_{LL} \approx -0.5$ . Results at 425 and 465 MeV are very similar. The discrepancy between theory and experiment may be taken up by increasing  ${}^3P_1$  and  ${}^3P_2$  amplitudes.

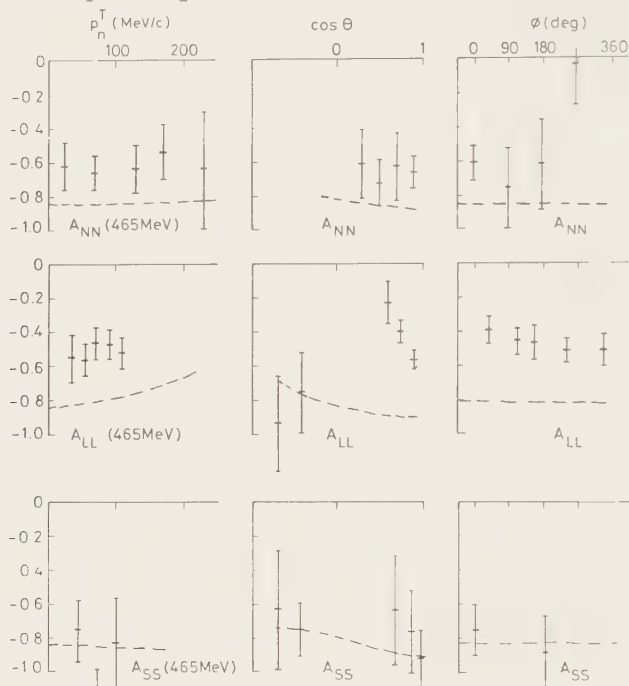


FIGURE 6

Projection of BASQUE  $A_{NN}$ ,  $A_{LL}$  and  $A_{SS}$  data against (a) neutron transverse momentum, (b)  $\cos\theta$  and (c)  $\phi$  at 465 MeV. The dashed curves are predictions of the model of Silbar et al. after adjustment of phases to experimental NN values.

Fig. 7 shows the dependence on  $M$ , the mass of the  $p\pi^+$  pair. There is a tendency for all parameters to go more positive at low values of  $M$ ;  $A_{LL}$  shows this effect more strongly than  $A_{NN}$  and  $A_{SS}$ . This result is not predicted by Silbar et al. However, it may be understood very simply, and was indeed anticipated. Near threshold, the  $\pi N S_{31}$  wave ( $Z$ ) is stronger than the  $\pi N P_{33}$  wave. Hence, for low  $M$  one expects a strong  ${}^3P_1$   $NN \rightarrow nZ^{++}$  amplitude. For  ${}^3P_1$  alone,  $A_{LL} = +1$ ,  $A_{NN} = A_{SS} = 0$ . There is no interference in  $A_{NN}$ ,  $A_{SS}$  and  $A_{LL}$  between

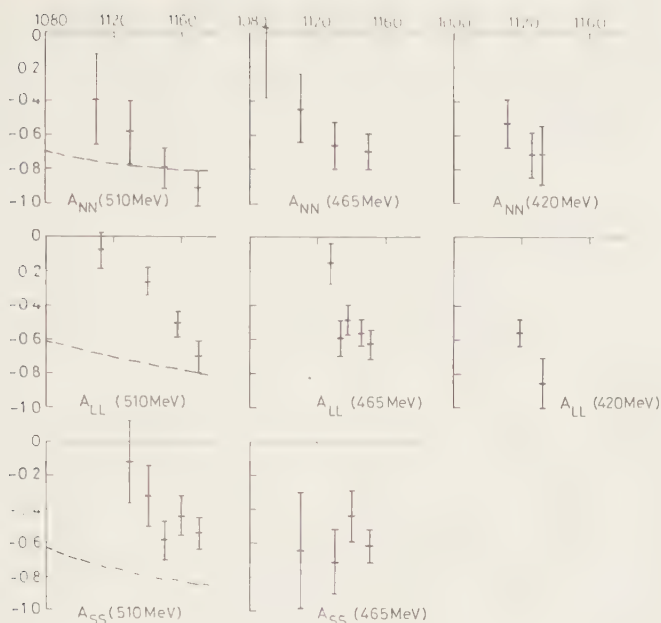


FIGURE 7

Projection of BASQUE  $A_{NN}$ ,  $A_{LL}$  and  $A_{SS}$  data against  $M$ , the mass of the  $p\pi^+$  pair. Curves are as in Fig. 6.

$^3P_1$  and  $^1D_2$  amplitudes (because of initial state Clebsch-Gordan coefficients). The observed  $M$  dependence of  $A_{NN}$ ,  $A_{LL}$  and  $A_{SS}$  is consistent with  $^1D_2$  dominance near the  $\Delta$  resonance and an increasing proportion of  $^3P_1 \rightarrow nZ$  near threshold. This parallels closely the energy dependence of the  $^3P_1$  and  $^1D_2$  amplitudes in  $NN \rightarrow D\pi$ .

The data of Fig. 6 also demonstrate that the  $^3P_0$  amplitude is weak. For this wave alone,  $A_{LL} = -1$ ,  $A_{NN} = A_{SS} = +1$ . Again there is no interference with  $^1D_2$ . In his phase shift analysis, Arndt has a  $^3P_0$  inelasticity nearly as large as in  $^1D_2$ . This must come entirely from  $NN\pi$ , since  $^3P_0$  is forbidden by conservation of angular momentum and parity in  $NN \rightarrow D\pi$ . Arndt's inelasticity would require  $A_{NN} \approx A_{SS} \approx A_{LL} + 0.5$ , in contradiction to the data. Fits indicate that the  $^3P_0$  inelasticity cannot be more than 20% of Arndt's value, and the optimum is zero.

The polarisation parameters  $A_{NO}$  and  $A_{ON}$  are displayed in Figs. 8 and 9. They are large and approximately equal and opposite. Again, this result may be understood very simply. For interference between any two states of the same parity,  $A_{NO} = A_{ON}$ , while for interference between states of the opposite parity  $A_{NO} = -A_{ON}$ . The data clearly demand dominant interference between  $^1D_2$  and P or F waves. Calculation reveals that the polarisation arises largely from interference of  $^1D_2$  with  $^3P_1$  and  $^3F_3$  (with possible small contributions from  $^3P_2$ ).

The sign of the polarisation is correctly predicted by the model of Silbar et al, but theory is too small. The  $\phi$  dependence (Fig. 10) can also be seen in the theory, but is sensitive to small variations of parameters. The polarisation data provide a second argument against a large  $^3P_0$  amplitude, which would seriously upset the observed relation  $A_{NO} \approx -A_{ON}$  and would introduce a large  $\cos\beta\cos\phi$  term which is not observed in the data.

The most important result, shown on Fig. 11, is that  $A_{SL}$  is everywhere compatible with zero or may be slightly positive. This is very different from (a) the model of Silbar et al. and (b)  $A_{SL}$  in  $pp \rightarrow d\pi^+$  (Fig. 12). In both cases, large negative values arise largely from interference between  $^1D_2$  and  $^3F_3$ . One finds formulae for  $A_{NO}$ ,  $A_{ON}$  and  $A_{SL}$  of the form

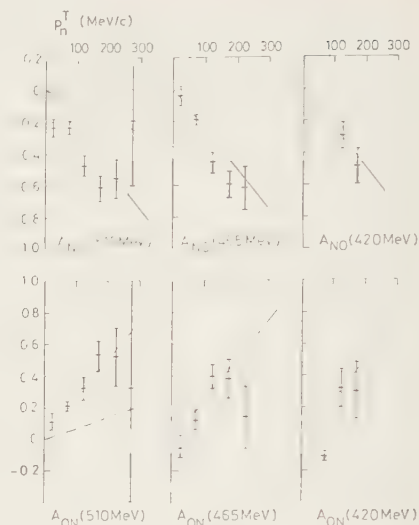


FIGURE 8

Projection of BASQUE  $A_{NO}$  and  $A_{ON}$  data against neutron transverse momentum at 425, 465 and 510 MeV. The line is to guide the eye and has the same slope on all plots. The dashed curve is as in Fig. 6.

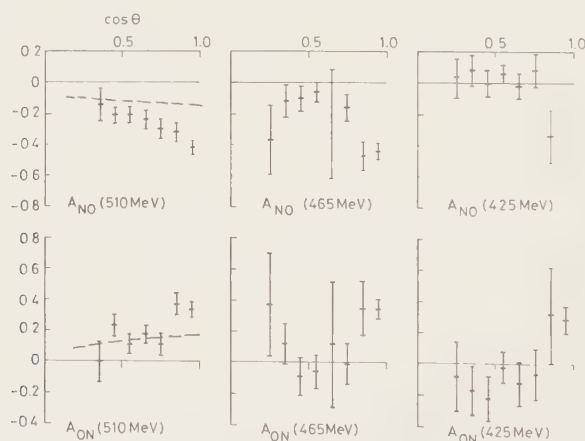


FIGURE 9

Projections of BASQUE  $A_{NO}$  and  $A_{ON}$  data against  $\cos\theta$ . Curves are as in Fig. 6.

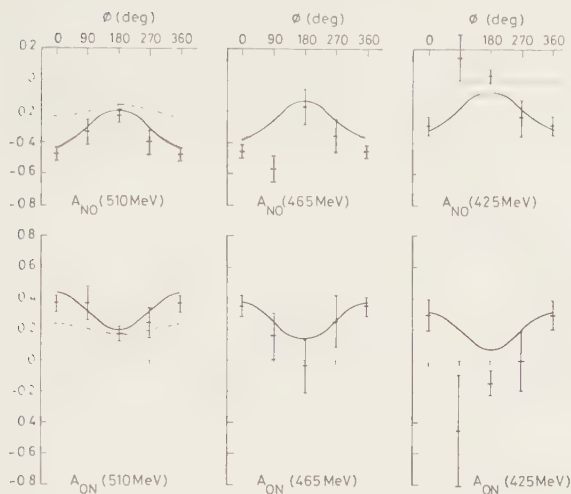


FIGURE 10

Projection of BASQUE  $A_{NO}$  and  $A_{ON}$  data against  $\phi$ . The dashed curves are as in Fig. 6 and the full curves are to guide the eye; they have the same modulation on all diagrams.

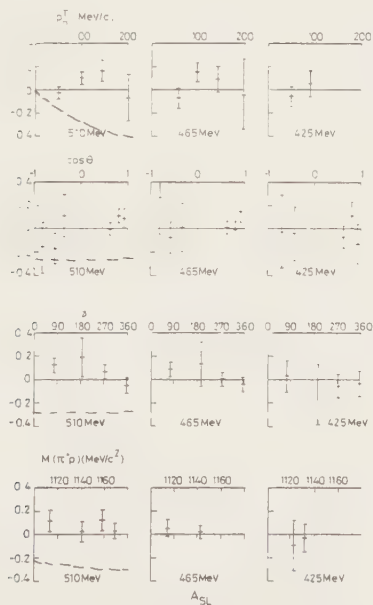


FIGURE 11

Projection of BASQUE  $A_{SL}$  data against (a) neutron Transverse momentum, (b)  $\cos\theta$ , (c)  $\phi$  and (d)  $M$ . The S subscript refers to the beam and L to target polarisation. Dashed curves as in Fig. 6.

$$\begin{aligned}\sigma A_{NO} &= -\sigma A_{ON} = \text{Im}\{a(^1D_2)a^*(^3F_3)\}Y(\beta, \theta, \phi) \\ \sigma A_{SL} &= -\sigma A_{LS} = \text{Re}\{a(^1D_2)a^*(^3F_3)\}Y(\beta, \theta, \phi)\end{aligned}\quad (1)$$

with the same  $Y(\beta, \theta, \phi)$  in both expressions. It is immediately apparent that both  $A_{NO}$  and  $A_{SL}$  are sensitive to the relative phase of the amplitudes. If amplitudes for  $NN \rightarrow N\Delta$  are written

$$a = |a| \exp i(\delta_{NN} + \delta_{N\Delta}), \quad (2)$$

they are sensitive to  $\delta_{N\Delta}$  and hence any dibaryon resonance. If the  $NN \rightarrow N\Delta$  interaction is weak,  $\delta_{N\Delta}$  is the phase of  $N\Delta$  elastic scattering, by Watson's theorem. If the coupling is strong,  $\delta_{N\Delta}$  is no longer the phase of elastic scattering, but has a complicated relation to the K matrix.

Numerical experiments show that fits to the data demand either (a) a negligible  $^3F_3$  amplitude, which seems very unlikely, or (b)  $\delta_{N\Delta}(^5S_2)$  close to  $45^\circ$  at all three energies, 425, 465 and 510 MeV. The latter result is a direct consequence of the fact that  $P$  and  $A_{SL}$  show no energy variation. Final arithmetic awaits introduction into the computer programme of the amplitude for  $NN \rightarrow NZ$ , where  $Z = \pi N(^3S_1)$ .

It is not surprising that one finds an attractive phase shift for the  $N\Delta$  interaction. The data suggest that this takes the form of an attractive scattering length, giving constant  $\delta_{N\Delta}$  like the  $NN\ ^1S_0$  interaction near threshold. The vital question is whether a resonance develops near 570 MeV. This question could be answered by measurements of  $A_{NO}$  and  $A_{SL}$  at 580 and 650 MeV, over the position of the supposed resonance, which would lead to dramatic variations in  $A_{NO}$  and  $A_{SL}$  if  $\delta_{N\Delta}$  moves rapidly through  $90^\circ$ . Even if both  $^1D_2$  and  $^3F_3$  resonate, the presence of strong  $^3P_1$  amplitudes guarantees that one could isolate a  $^1D_2$  resonance from the  $Y(\beta, \theta, \phi)$  dependence.

A fundamental question is whether one can correctly use a value of  $\delta_{N\Delta}$  independent of  $\Delta$  mass. If the  $NN \rightarrow N\Delta$  coupling is weak, equn (2) takes the form

$$a = \frac{A}{M_0 - M - i\Gamma(M)} \exp i(\delta_{NN} + \delta_{N\Delta}),$$

where the propagator is that of the  $\pi N \rightarrow \Delta$  interaction. In this case, it is appropriate to take  $\delta_{N\Delta}$  as constant, since  $\Gamma$  simply reflects the lifetime of the

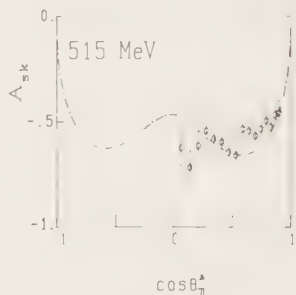


FIGURE 12

$A_{SL}$  data for  $pp \rightarrow d\pi^+$  at 515 MeV from Aprile-Giboni, ref. 38.

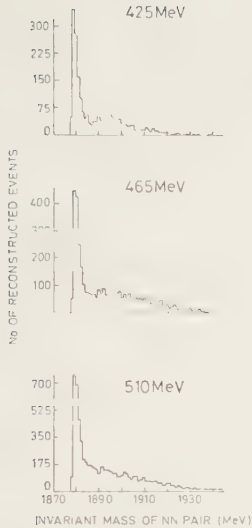


FIGURE 13

Projection of BASQUE data in the  $A_{NN}$  configuration against the mass of the NN pair at 425, 465 and 510 MeV

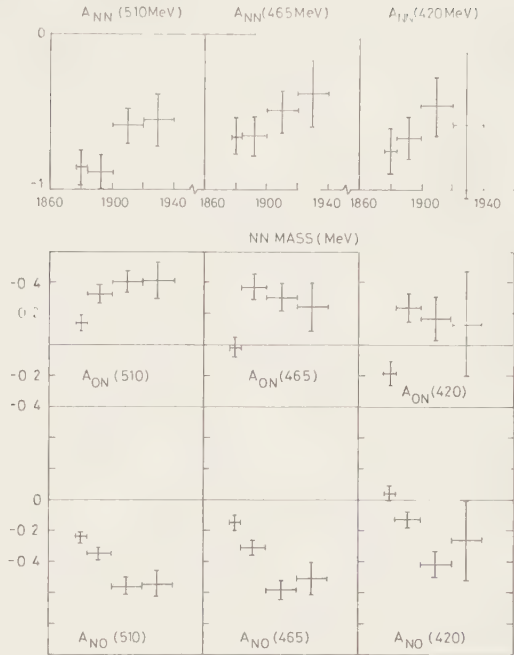


FIGURE 14

Projection of BASQUE  $A_{NN}$ ,  $A_{NO}$  and  $A_{ON}$  data against the mass of the NN pair at 425, 465 and 510 MeV.

$\Delta$ . If the  $NN \rightarrow N\Delta$  interaction is strong, one must solve the Fadeev or similar equations.

A final interesting result is shown on Figs. 13 and 14.

In the former, there is a clear peak due to the threshold  $NN$  final state interaction. By itself, this is hardly surprising. In Fig. 14,  $A_{NN}$ ,  $A_{NO}$  and  $A_{ON}$  are plotted against  $NN$  mass. The lowest bin is chosen to bracket the peak. One sees a slow variation of  $A_{NN}$  with  $NN$  mass; this is a reflection of the variation with  $M$  on Fig. 7. What is interesting is that there is no significant change in  $A_{NN}$  between the lowest bin and its neighbour, but a large change in  $A_{NO}$  and  $A_{ON}$ . This implies that the  $NN$  final state interaction occurs dominantly in the  $NN \rightarrow N\Delta$   $^1D_2$  wave. The drop in  $A_{NO}$  and  $A_{ON}$  is readily understood, since  $A_{NO} \propto \text{Im}\{a(^1D_2)a(^3P_1)\}/|a(^1D_2)|^2 \propto 1/|a(^1D_2)|$ , and  $|a(^1D_2)|$  is enhanced in the  $NN$  peak. This implies that the dominant  $^1D_2$   $n\Delta$  amplitude originates from a cooperative three-body interaction arising via attractive final-state interaction between all three pairs  $\pi^+$  and  $p$ ,  $\pi^+$  and  $n$  and  $n$  and  $p$ .

In my opinion, we shall soon know  $NN$  inelasticities up to 515 MeV better from direct analysis of  $NN$  inelastic interactions than from  $NN$  elastic phase shift



analysis. It is already clear that (i) the sum of  $NN\pi$  and  $D\pi$  inelasticities in  ${}^3P_2$ ,  ${}^3F_2$  and  ${}^3F_3$  agree remarkably closely with my elastic phase shift analysis, (ii)  ${}^3P_1$  inelasticity is slightly larger than in either my phase shift analysis or Arndt's, and (iii)  ${}^3P_0$  inelasticity is close to zero.

There are several experiments at LAMPF which have produced data on the spin dependence of  $NN \rightarrow NN\pi$ . Hancock et al.<sup>47</sup> have measured cross sections and  $A_{NO}$  at selected angles for exclusive kinematics in  $pp \rightarrow np\pi^+$  at 800 MeV. Results disagree with theory. From the same experiment, preliminary (unpublished) data have been derived for  $A_{NO}^0$  in  $pp \rightarrow pp\pi^0$ , and this time are in spectacularly good agreement with Dubach, Kloet and Silbar. At this conference, Bonner et al.<sup>48</sup> present results on  $A_{NO}$ ,  $D_{NN}$  and  $P=2iT_{11}/(3)^{1/2}$ . Bhatia et al.<sup>49</sup> have a preprint on  $A_{NN}$  in  $pp \rightarrow np\pi^+$ . Because of the limited geometry in which all these data have been taken, it is difficult to interpret them without a complete model of the inelastic process. Silbar<sup>50</sup> discusses them in a recent preprint.

## 5. WHAT EXPERIMENTS ARE NEEDED?

A few well chosen experiments could now complete our understanding of  $NN$  elastic and inelastic scattering up to 800 MeV. In summary, the measurements required are:

- (i)  $A_{LL}(np \rightarrow np)$  at 25 and 50 MeV, to determine  $\bar{\epsilon}_1$ ,
- (ii)  $A_{LL}$ ,  $A_{SS}$ ,  $D_t \equiv K_{NN}$  (and possibly  $R_t \equiv K_{ss}$ ) for  $np$  elastic scattering at 650 and 800 MeV, to determine  $I=0$  phase shifts,
- (iii)  $iT_{11}$  and  $\sigma(S0|iT_{11})$  in  $pp \rightarrow d\pi^+$  from 450 to 800 MeV to determine the small  ${}^1S_0$ ,  ${}^3F_2$  and  ${}^3P_1 \rightarrow L=2$  amplitudes,
- (iv)  $A_{NO}$  and  $A_{SL}$  in  $pp \rightarrow np\pi^+$  at 580, 650, 725 and 800 MeV to determine the phases of possibly resonant amplitudes in  ${}^1D_2$  and  ${}^3F_3$ .

## 6. ACKNOWLEDGEMENTS

I am greatly indebted to DR. R. R. Silbar for his help and computer programmes in interpreting BASQUE  $pp \rightarrow np\pi^+$  data. I am also grateful to the SERC for a Senior Research Fellowship.

## REFERENCES

- 1) F.P. Brady et al., "Measurements of the Proton-Neutron Analyzing Power between 17 and 50 MeV", this conference.
- 2) R. Aures et al., "Measurement of the Spin Correlation Parameter  $A_{YY}$  for  $\vec{n}-\vec{p}$  scattering in the Energy Range up to 50 MeV", this conference.
- 3) M.D. Barker, D. Holslin, P.A. Quin and W. Haeberli, "Polarization in Neutron-Proton Scattering at 25 MeV", this conference.

- 4) M. Schüberl et al., "A Neutron-Proton Spin Correlation Experiment at 14 MeV using a Polarized Proton Target", this conference.
- 5) H. Obermayer, H. Kuiper, B. Seidler and K. Frank, Nucl. Phys. A344(1980) 75.
- 6) J. Binstock and R. Bryan, Phys. Rev. D9 (1974) 2528.
- 7) D.V. Bugg, J. Phys. G: Nucl. Phys. 6 (1980) 1329.
- 8) I.L. Grach et al., ITEP-56 preprint (1983).
- 9) A. Bol, P. Leleux, P. Lipnik and P. Macq, "A measurement of the Extreme Backward Angle Neutron-Proton Elastic Scattering between 45 and 75 MeV", this conference.
- 10) A. Bol et al., "The  $170^{\circ}$ -to- $90^{\circ}$  Cross Section Ratio for Neutron-Proton Elastic Scattering", this conference.
- 11) A. Bol et al., "Neutron-Proton Capture at Extreme C. M. Angles", this conference.
- 12) E. Aprile et al., AIP Conf. Proc. 95 (1983).
- 13) E. Aprile et al., "Measurements of Polarization Parameters in pp Elastic Scattering at 560 MeV", this conference.
- 14) J. Bystricky et al., Saclay report No. 82-12 (1982).
- 15) E. Aprile et al., Phys. Rev. Letts. 46 (1981) 1047.
- 16) J. Franz et al., "Elastic and Inelastic Scattering of Neutrons on Protons at SIN", this conference.
- 17) R.K. Keeler et al., Nucl. Phys. A377 (1982) 529.
- 18) D.V. Bugg, A.A. Carter and J.R. Carter, Phys. Letts. 44B (1973) 278.
- 19) D.F. Ottewell et al., "The Differential Cross Section for Proton-Proton Elastic Scattering at  $90^{\circ}$  C.M. between 300 and 500 MeV", this conference.
- 20) P. Chatelain et al., J. Phys. G.: Nucl. Phys. 8 (1982) 643.
- 21) C.L. Hollas et al., "The Energy Dependence of the  $D_{NN}$  Parameter and of the Moduli of the Transversity Amplitudes at  $\theta_{CM}=90^{\circ}$  for pp Elastic Scattering between 0.9 and 1.5 GeV/c", this conference.
- 22) D.J. Cremans et al., " $D_{SS}$ ,  $D_{LS}$  and  $D_{LL}$  and P for pp Elastic Scattering at 699 and 750 MeV", this conference.
- 23) F. Lehar, "N-N Experiments with Polarized Beam and Target at Saturne II", this conference.
- 24) I.P. Auer et al., Phys. Lett. 67B (1977) 113; 70B (1977) 475.
- 25) I.P. Auer et al., Phys. Rev. D24 (1981) 2008.
- 26) J.P. Stanley et al., Nucl. Phys. A (to be published).
- 27) R. Dubois et al., Nucl. Phys. A377 (1982) 554.
- 28) R.A. Arndt et al., VPI preprint "Nucleon-Nucleon Partial Wave Analysis to 1 GeV", (1982).
- 29) H. Spinka, private communication.
- 30) R.F. Rodebaugh and B.E. Bonner, "Amplitude Reconstruction for pp Scattering

- at 800 MeV", this conference.
- 31) D.V. Bugg, QMC preprint , submitted to J. Phys. G: Nucl. Phys.
  - 32) H. Kamo and W. Watari, Prog. Theor. Phys. 62 (1979) 1035.
  - 33) H. Kamo, W. Watari and M. Yonezawa, Prog. Theor. Phys. 64 (1980) 2144.
  - 34) N. Hiroshige, W. Watari and M. Yonezawa, Prog. Theor. Phys. 68 (1982) 2074.
  - 35) W. Watari, Osaka report OCUPWA-003 (1983).
  - 36) B. Blankleider, Flinders report FIAS-R-72 (1980).
  - 37) J.A. Niskanen, Nucl. Phys. A298 (1978) 417.
  - 38) E. Aprile-Giboni, University of Geneva Ph. D. Thesis No. 2066 (1982).
  - 39) J. Hoftiezer et al., Sin preprint PR-83-06.
  - 40) Ch. Weddigen, Nucl. Phys. A312 (1978) 330.
  - 41) K. Hidaka et al., Phys. Lett. 70B (1977) 479.
  - 42) N. Hoshizaki, Prog. Theor. Phys. 58 (1979) 716.
  - 43) W. Kloet and R. Silbar, Nucl. Phys. A338 (1980) 231; A338 (1980) 317.
  - 44) J. Dubach et al., Phys. Lett. 106B (1981) 29.
  - 45) J. Dubach, W.M. Kloet and R.R. Silbar, J. Phys. G: Nucl. Phys. 8 (1982) 475.
  - 46) R. Shypit et al., Phys. Lett. 124B (1983) 314.
  - 47) A.D. Hancock et al., Phys. Rev. C27 (1983) 2742.
  - 48) B.E. Bonner et al., "The Polarization Observables  $D_{NN}$ , P and A for  $\overrightarrow{pp} \rightarrow \overrightarrow{pn}\pi^+$  at 800 MeV", this conference.
  - 49) R.R. Silbar, "Spin Dependence of NN and NN $\pi$  Reactions and the Question of Dibaryon Resonances", submitted to Comments on Particle and Nuclear Physics, (July, 1983).
  - 50) T.S. Bhatia et al., LAMPF preprint LA-UR-83-215 (1983).

## ANALYSIS OF EXPERIMENTAL INFORMATION ON THE DIBARYON RESONANCE PROBLEM

R.P. LÜCHER

SIN, Swiss Institute of Nuclear Research, 5234 Villigen,  
Switzerland

### INTRODUCTION

This survey is concerned with the situation regarding dibaryons, i.e. states with baryon number  $B = 2$  and with strangeness  $S = -2, -1$  or  $0$ . All these states (and a few more) are possible in the six quark system. Some of them have exotic quantum numbers. In fact, since the quarks carry color it would be natural in the framework of QCD and its approximate bag model representation to have states containing hidden color subclusters. Those states might have color  $\bar{8}-\bar{8}$ ,  $3-\bar{3}$  or  $6-\bar{6}$  configurations, representations which exist only for systems containing more than three quarks. Whereas the possibility of such states is a rigorous consequence of the color group symmetry properties any predictions for their mass spectrum depend on model assumptions<sup>1</sup>. In particular one usually assumes that the colored clusters are kept apart simply by an angular momentum barrier. The correspondence of (extended) bag model states to phenomena in physical scattering channels is not straightforward either, due to the difficulty of formulating the confining surface for a multiquark bag. In fact, primitive bag model states<sup>2</sup> need not correspond to resonances at all. A connection to scattering observables is offered by the P-matrix formalism<sup>2</sup>. The corresponding quantum mechanical matching problem is technically very involved especially for quarks in higher bag model orbitals. Generally, the many states predicted in such models are expected to be very broad and overlapping. Yet there exists the possibility of moderately narrow states ( $\Gamma \gtrsim 100$  MeV) and perhaps of some really narrow ones ( $\Gamma < 10$  MeV) with or without exotic quantum numbers. The present analysis attempts to assess the evidence for dibaryon resonances beyond those driven by conventional NN dynamics or conventional one

boson exchange which is based on color neutral objects. Whether one uses the more modern language of QCD at this level is more a question of semantics than of principle (due to our poor understanding of the confining mechanism). Even if these resonances are found, it will be a difficult second step to establish their relation to the more exotic possibilities of QCD (colored substructures in multi-quark bags). In the absence of clear-cut predictions for multi-quark systems the analysis necessarily proceeds by comparing the experimental information in all the  $B = 2$  channels, particularly the available spin observables, to the best available calculations. This procedure is delicate and risky but unavoidable.

#### CHANNELS WITH STRANGENESS

In the bag model the strange dibaryon H with configuration uuddss, having charge and isospin  $Q = I = 0$ , strangeness  $S = -2$  and  $J^P = 0^+$  was estimated<sup>3</sup> at a mass  $m_H (\sim 2.15) < m_{\Lambda\Lambda}$ , stable against strong decay. In the experiment by Carroll et al.<sup>4</sup> no signal in  $pp \rightarrow K^+ K^+ m_H$  has been seen, within statistics. The upper limit for the production cross-section is  $\sigma_H < 30$  to  $130$  nb (for  $2 < m_H < 2.5$  GeV). This is not very restrictive for a two-step production mechanism. As suggested in ref.<sup>5</sup> it might be worthwhile to look for the production of the H particle on  ${}^3\text{He}$  which is the smallest nucleus, having a pp subsystem. The cross-section for  $K^- {}^3\text{He} \rightarrow K^+ nH$  is estimated to be  $1 \mu\text{b}$  at  $2 \text{ GeV/c}$  incident momentum.

Still in the  $S = -2$  channel a charged dibaryon  $H^-$  with  $I = 1$  was searched for in the reaction  $K^- d \rightarrow K^+ H^-$  at  $1.4 \text{ GeV/c}$  by the Rome-Saclay-Vanderbilt collaboration<sup>6</sup>. No narrow signal was seen with a limit to the cross-section of some nanobarns.

In the  $S = -1$  channel the same collaboration and several earlier experiments have studied the  $(\Lambda p)$  mass spectrum in  $K^- d \rightarrow \pi^- (\Lambda p)$ . A narrow peak  $\Gamma = 5.9 \pm 1.6 \text{ MeV}$  at  $M_{\Lambda p} = 2129.0 \pm 0.4 \text{ MeV}$  has been observed<sup>7</sup>. This peak sits right on top of the  $\Sigma^+ n$  threshold (not  $\Sigma^0 p$ ). The coincidence with a threshold speaks rather in favor of a cusp interpretation due to the open channel. However, threshold effects might also hide an underlying resonance<sup>7</sup> which could be broad and shifted in energy. It should be clear from these remarks that the study of the strange channels has only just started. The single

strange valence quark of the kaon should be particularly helpful for the analysis.

#### THE NUCLEON-NUCLEON CHANNEL

Much effort in recent years has been devoted to the NN channel with  $S = 0$ . It is clear that the study had to concentrate on rather subtle effects involving spin observables since the gross structure of total and differential cross-sections is smooth. The only nuclear bound state is the deuteron (its spin zero counterpart is nearly bound only). Because of its size, however, the deuteron is well described by two nucleons held together by conventional color singlet forces, with the possible exception of small  $6q$  bag-state admixtures<sup>8</sup>.

In the NN channel the situation with respect to polarization observables (total cross-sections in pure spin states, angular dependence of spin correlations) has progressed only slightly, comp. ref.<sup>9</sup> and <sup>10</sup>. This means, e.g., that some minor but disturbing inconsistencies between different cross-section experiments for  $\Delta\sigma_T [= \sigma_{\uparrow\downarrow} - \sigma_{\uparrow\uparrow}]$  and  $\Delta\sigma_L [= \sigma_{\uparrow\downarrow}^+ - \sigma_{\uparrow\downarrow}^-]$  are still present. Figure 1 shows the situation. The most annoying feature until recently was the need for matching different experiments at masses  $\sim 2.1$  GeV (limit of TRIUMF and SIN energies). This mass range, however, is exactly where the spin triplet projector  $\Delta\sigma_T - \Delta\sigma_L$  shows possible structure, usually assigned to  ${}^3F_3$  (2.22), see Fig. 2. Until the Saturne meeting<sup>10</sup> the situation was ambiguous. With the first preliminary data<sup>11</sup> for  $\Delta\sigma_L$  ( $\Delta\sigma_T$  was available before<sup>17</sup>) the difference can now be formed over the critical energy range (crosses in Fig. 2 at energies marked by dashed arrows). The triplet structure around 2.2 GeV seems to be confirmed, the final analysis must be awaited, however.

The status of the remaining two Argonne candidates in the  $I = 1$  channel is as follows. The  ${}^1D_2$  (2.14) is clearly seen, right on top of the  $N\Delta$  threshold and therefore most likely a measure of the degree to which we are able to calculate the threshold effect. There is at present no established need for an extra resonance on top or near the  $N\Delta$  threshold. The case for a  ${}^1G_4$  (2.43) from pp scattering alone is presently somewhat weakened<sup>10</sup> by the reduced

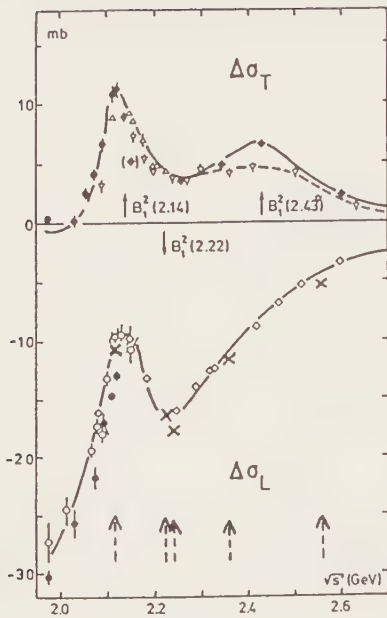


FIGURE 1

The total cross sections  $\Delta\sigma_T$  and  $\Delta\sigma_L$  for pp scattering from ref.10. Five preliminary values (x)11 for  $\Delta\sigma_L$  are added (at energies marked by dashed arrows). Data symbols match references as follows: (●)12, (○)13, (◊)14, (Δ)15, (◆)16 and (▽)17.

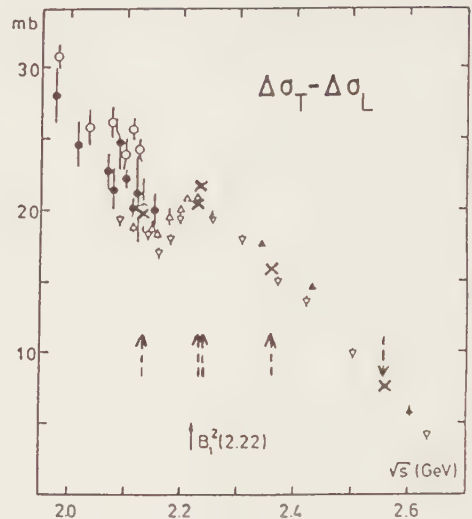


FIGURE 2

The triplet projector  $\Delta\sigma_T - \Delta\sigma_L$  from10. Data combinations marked as follows: (○)ref.12 only, (●)ref.12 with 13, (Δ)ref.14 with 15, (▲)ref.14 with 16, (▽)ref.14 with 17, and (x)ref.11 with 17 [energies for preliminary  $\Delta\sigma_L$  values11 marked by dashed arrows].

peaking of the new data<sup>17</sup> for  $\Delta\sigma_T$  in this energy range, see Fig.1. This disregards possible superposition effects and evidence from other channels (see the discussion of the vector polarization in  $\pi d$  elastic scattering further below). Recently, in ref.<sup>17</sup> a singlet structure has been attributed to the peaking of  $A_{nn}$  ( $90^\circ$ ) at somewhat lower energy,  $T_p \sim 750$  MeV or  $\sqrt{s} \sim 2.2$  GeV. However, whilst the singlet cross-section is indeed proportional to  $1 - A_{nn}$  the triplet cross-section is proportional to  $1 + A_{nn}$  and any structures are inextricably correlated. The behaviour of the small singlet amplitude in the presence of the dominant triplet contribution around 750 MeV requires therefore further study.

The status of possible  $I = 0$  resonances<sup>10</sup> in the NN channel depends crucially on the interpretation of the  $I = 1$  pp data, since



the pn amplitudes are obtained from pd scattering by a subtraction procedure. (No data with polarized neutron beams in the relevant energy range exist.) The analysis of existing data is still proceeding but no final conclusions are presently possible.

#### PIONIC CHANNELS

We start with *elastic  $\pi d$  scattering* as there are new polarization data (partly preliminary). We recall that the theoretical analysis is particularly stable and reliable in the forward hemisphere ( $\theta < 80^\circ$ ) where the elastic reaction is peripheral and involves moderate momentum transfer. Even so, since we are discussing sensitive observables, only the best available calculations should be used. The backward hemisphere is more difficult to interpret, the cross-section is down by two to three orders of magnitude and is sensitive to small effects. A similar degree of caution is needed in the interpretation of all pion production and absorption processes where the momentum transfer is large at all angles.

New data for the vector polarization  $iT_{11}$  in  $\pi d \rightarrow \pi d$  for  $140 < T_\pi < 325$  MeV have been contributed to this conference, Smith et al.<sup>18</sup>. The data show improved statistics and a finer angular mesh, see the figure in ref.<sup>18</sup>. The dominant feature for energies  $T_\pi > 250$  MeV is the steep rise of the data between  $70^\circ$  and  $90^\circ$  in contrast to Faddeev predictions<sup>19</sup> which are maximal where experiment is small, comp.<sup>20</sup>. In the analysis of ref.<sup>20</sup> this rise is attributed to the admixture of a  ${}^1G_4(2.48)$  resonance and the energy dependence was found to be consistent with a Breit-Wigner form. The situation is illustrated at 294 MeV in Fig. 3. The details of resonance parameters will have to be refitted because the experimental normalization has changed and because the negative data point at  $130^\circ$ ,  $T_\pi = 256$  MeV has been replaced by a series of positive values (all other measurements have been confirmed within statistics). Note that upper couplings of resonance,  $L_\pi = J+1$ , generally lead to oscillations in  $iT_{11}$  and hence are an indication for the presence of a resonance if the energy dependence is right. *The converse, however, is not true.* Full strength Argonne type resonances with lower coupling produce very

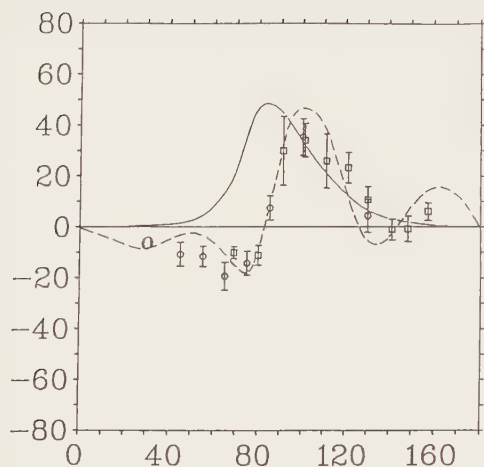


FIGURE 3  
The vector polarization  $iT_{11}(\%)$  in  $\pi d$  elastic scattering at  $T_\pi = 294$  MeV. The data are from<sup>18</sup>. The solid line is the Faddeev calculation<sup>19</sup>, the dashed line a resonance admixture, mostly  ${}^1G_4(2.48)$  from<sup>20</sup>.

little structure in  $iT_{11}$  as has been shown already in the exploratory calculation of ref.<sup>21</sup>. For the quantitative analysis it will be important to have the detailed behaviour at smaller angles. Measurements are presently being done at SIN. The discussion so far is based on the analysis of the cross-section (well understood for  $\theta < 80^\circ$ ) and the vector polarization. In the forward hemisphere no other observables are available. It would of course be highly desirable to have a complete set of seven observables which would allow direct amplitude reconstruction. This would serve as a test of our understanding of the underlying dynamics.

Any further information at present comes from the backward hemisphere where differential cross-sections and some tensor polarization data are available. The cross-section is well measured for  $T_\pi \lesssim 300$  MeV and well described by coupled channel calculations except for the upper energies where theory is too high<sup>19,22</sup> even if the effects of genuine pion absorption are included. Yet it seems dangerous to advocate specific resonance effects<sup>23</sup> to remove the remaining discrepancy. At higher energies there is a recent high precision excitation curve at  $180^\circ$  from KEK<sup>24</sup> for  $2.2 < \sqrt{s} < 2.8$  GeV. The curve shows two distinct structures at masses around 2.43 and 2.72 GeV. Assuming a smooth ad hoc background amplitude the corresponding Breit-Wigner width is 100 and 220 MeV, respectively. Of course, a reliable dynamical treatment

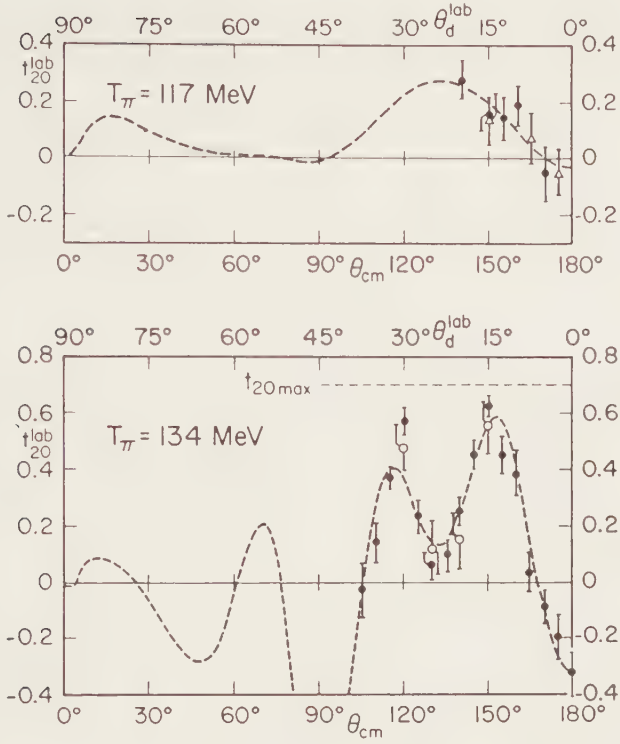


FIGURE 4

The tensor polarization  $t_{20}^{lab}$  for  $\pi d$  elastic scattering<sup>25</sup>. The dashed curves correspond to fitted phase shifts from the same reference.

of the background amplitude is necessary to establish such an interpretation. This will be difficult.

We turn to a discussion of the tensor polarization  $t_{20}$  where we have a conflict of data at present. Two strong peaks have been reported<sup>25</sup> at  $\theta \sim 120^\circ$  and  $\sim 150^\circ$ , see Fig. 4. These structures occur at  $T_\pi = 134$  MeV and disappear rapidly within  $\pm 20$  MeV. The data of<sup>26</sup> have  $t_{20}$  negative ( $< -0.4$ ) and smooth, similar to the trend of Faddeev predictions. A preliminary excitation curve from<sup>26</sup> at  $\theta = 144^\circ$ , see Fig. 5, shows no structure around 134 MeV (the peaking angles<sup>25</sup> of  $120^\circ$  or  $150^\circ$  have not been measured yet). At the nearby angle of  $\theta = 140^\circ$  the excitation curve from the group<sup>25</sup> is also flat<sup>27</sup> (although very different in magnitude), while it is strongly peaked<sup>25</sup> for  $\theta = 150^\circ$ . Theoretically, the angular structures seen in<sup>25</sup> are unexpected. The algebra of spin

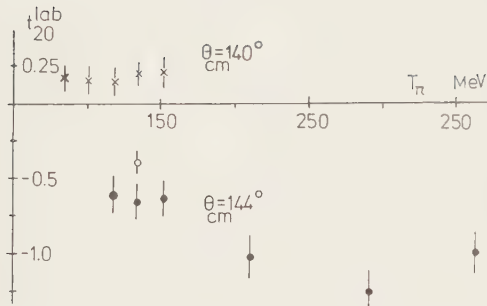


FIGURE 5  
Excitation curves for the tensor polarization  $t_{20}^{lab}$  in  $\pi d$  elastic scattering. The circles are from<sup>26</sup> for  $\theta_{cm} = 144^\circ$ , the crosses are from<sup>27</sup> for  $\theta_{cm} = 140^\circ$ . All data preliminary!

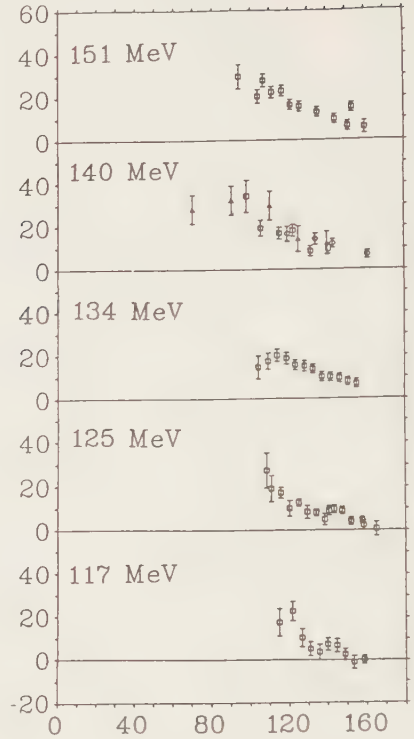


FIGURE 6  
The vector analyzing power  $i T_{11}(\%)$  for  $\pi d$  elastic scattering from<sup>30</sup>. Kinetic pion energies (lab) in MeV.

observables<sup>28,20</sup> relates peaks of  $t_{20}$  to zeros of  $i T_{11}$  (rigorously in the cms, if  $t_{20}$  is maximal). Such a behaviour is indeed observed in the analysis of<sup>29</sup> based on a limited set of data. On the other hand, the expected structure(s) in  $i T_{11}$  have not been seen experimentally<sup>30</sup> in a special run matched to the energies of ref.<sup>25</sup>, see Fig. 6. The vector polarization in the backward hemisphere is smooth in angle with little energy dependence. However, since  $t_{20}$  from<sup>25</sup> is not quite maximal, the data are not in a direct conflict. On more general grounds one should be aware that it is difficult to produce the sharp peaks seen in ref.<sup>25</sup> by the admixture of a single additional (and narrow) resonance. Such a reson-

ance (which could be extraneous to the  $pp$  channel,  $J^P = 1^+$ , e.g.) would have to conspire with several big partial waves in  $\pi d$  scattering ( $JL_\pi = 01, 10, 21, 32, \dots$ ) in order to annihilate rapidly two out of four complex helicity amplitudes. The confirmation of such a signal would be so much more challenging. Further experiments to resolve the difficulties are planned at different laboratories. The group of ref.<sup>25</sup> is testing a new polarimeter. However, no final answers can be expected before next spring.

*Pion production processes:* Extensive calculations have been made for the two-body reaction  $pp \rightarrow d\pi^+$  in the framework of Faddeev-type multi-channel scattering equations<sup>19b, 22, 31-33</sup>. A similarly thorough calculation based on a relativistic perturbation theory with effective vertex functions and subamplitudes has been made recently<sup>34</sup>. A detailed comparison with an almost complete set of observables is possible at  $T_p = 578$  MeV. Both types of calculations<sup>22, 34</sup> fare rather well on the gross features of the reaction but there is a definite discrepancy in the spin correlation parameters  $A_{yy}$  and  $A_{xx}$  common to both analyses. The difficulty can be traced<sup>34</sup> to the amplitudes which couple to spin triplet states in the  $pp$  channel. Their calculated magnitude is too small (see also the phenomenological analysis of<sup>35</sup>). The energy of  $T_p = 578$  MeV is too low to be of relevance for the higher dibaryons. The only spin observable available<sup>36</sup> at higher energies is the sensitive asymmetry  $A_{y0}$ . It is at variance with the available Faddeev calculations. We are looking forward to complete sets of data at the higher energies as well.

At energies around  $T_p \sim 800$  MeV there are indications for discrepancies between theory and experiment from other sources. For the continuum pion production  $pp \rightarrow \pi np$  a Deck model calculation<sup>37</sup> predicts too small inelasticities for  $pp$  triplet waves. Similarly in the analysis of<sup>38</sup> the inelasticities for  $^3F_3$ ,  $^3F_2$ ,  $^3P_2$ ,  $^3P_3$  are systematically low. Some features of the Saclay data<sup>17</sup> might in fact be related to a similar problem, as we have discussed in the NN section.

## ELECTRO-MAGNETIC CHANNELS

The best studied reaction is the deuteron disintegration

channel. Historically, the observation<sup>39</sup> of a large recoil proton polarization  $P$  in  $\gamma d \rightarrow \vec{p}n$  at  $E_\gamma \sim 550$  MeV, contrary to theoretical expectations, was the first evidence for the possible existence of a resonance. The original explanation<sup>40</sup> of the data called for a contribution from the usual  $I = 1$ ,  $J^P = 3^-$  ( $\sim 2.26$ ) state in combination with an  $I = 0$ ,  $3^+$  (or  $1^+$ ) resonance with mass  $\sim 2.36$  GeV. More data on  $P$  are now available<sup>41,42</sup>. They are compatible with the above interpretation as long as  $P$  is considered in isolation. However, with more data on further (spin) observables no consistent picture emerges. In particular the recent measurements<sup>43</sup> of the differential cross-section with tagged photons do not agree with any of the calculations in<sup>41</sup> at angles below  $30^\circ$ . For the asymmetry  $\Sigma$  from linearly polarized photon beams the situation is even worse. New data<sup>44</sup> for  $80 < E_\gamma < 600$  MeV combined with the existing ones disagree with calculations<sup>41,45</sup> at all energies, see Fig. 7. The measurements of the target asymmetry  $T$  presented similar difficulties of interpretation already at the time of the review<sup>46</sup>. In particular the Bonn and the Tokyo analysis differ substantially in their non-resonant predictions. The asymmetry  $T$  is generally of small magnitude<sup>46,47</sup>, but there is considerable angular structure<sup>48</sup> at  $E_\gamma = 550$  MeV, e.g. It is clear that the resolution of the present difficulties requires a major theoretical effort to stabilize the predictions for similar physics input. On the experimental side systematic measurements of spin correlation and spin transfer parameters are highly desirable to constrain the enormously rich spin structure of photodisintegration.

As far as pion photoproduction is concerned evidence for a resonance at 2.23 GeV stems<sup>49</sup> from the analysis of  $\gamma d \rightarrow p p \pi^-$ . The isospin would have to be zero since nothing has been seen<sup>50</sup> in the similar reaction  $d(\pi^\pm, p)\pi N$  at SIN.

#### CONCLUDING REMARKS

A careful comparison of the available experimental information in the  $B = 2$  channels shows systematic differences with respect to the best available dynamical calculations. This happens in particular also for those cases where the predictions or con-

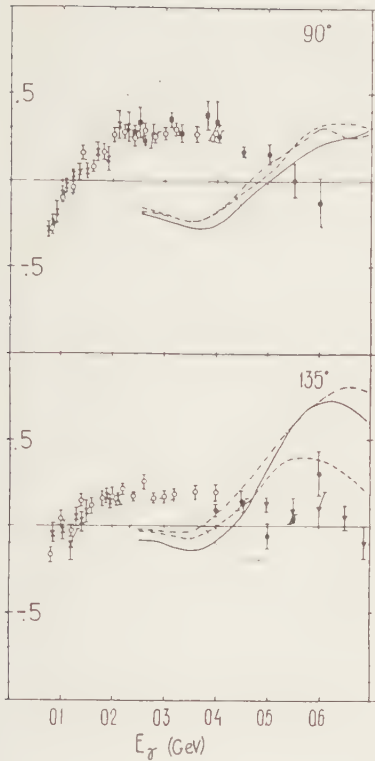


FIGURE 7

The beam asymmetry  $\Sigma$  in photo-disintegration as a function of photon energy taken from<sup>44</sup> for  $\theta_{cm} = 90^\circ$  and  $135^\circ$ . The dotted curve is a calculation from<sup>45</sup>, the remaining curves are from<sup>41</sup> with and without dibaryon admixtures.

straints from conventional dynamics are considered reliable ( $\sigma_{NN}^{\rightarrow}, pp$  inelasticities,  $\pi d - \pi d$  in the forward hemisphere). The interpretation in terms of relatively broad ( $\Gamma > 100$  MeV)  $B = 2$  resonances is consistent with the established data but further multichannel analysis is required both on the theoretical and on the experimental side. For reactions involving the deuteron, kinematics with low momentum transfer to the deuteron are more promising for an unambiguous interpretation. Furthermore certain contradictions need clarification (measurements of  $t_{20}$  in  $\pi d$  elastic scattering, theory of photo-disintegration). Ultimately we shall need much more spin information for all the  $B = 2$  channels to achieve direct amplitude reconstruction in a range of energies. Even in the best measured channels the spin information is still incomplete. In many channels experiments have barely started (reactions with strange particles, reactions with polar-



ized neutron beams, channels with neutral final state pions, electroproduction, etc.).

I am very indebted to all the experimental colleagues working in the field for supplying me very generously with their most recent, partially unpublished results. Without their friendly support such a review would be impossible. Helpful discussions with Alfred Švarc are acknowledged.

#### REFERENCES

- 1) A. Aerts, P. Mulders and J. de Swart, Phys.Rev.D21 (1980) 2653.
- 2) R.L. Jaffee and F.E. Low, Phys.Rev.D13 (1976) 1295.
- 3) R.L. Jaffee, Phys.Rev.Lett.38 (1977) 195.
- 4) A.S. Carroll et al., Phys.Rev.Lett.41 (1978) 777.
- 5) A. Aerts and C.B. Dover, in preparation. See C.B. Dover, Proc.Second LAMPF II Workshop (1982) p.80.
- 6) G. d'Agostini et al., Nucl.Phys.B209 (1982) 1.
- 7) D. Braun et al., Nucl.Phys.B124 (1977) 45 and references quoted.
- 8) V.A. Matveev and P. Sorba, Lett.Nuovo Cim.29 (1980) 405; H. Høgaasen, P. Sorba and R. Viollier, Z.Phys.C4 (1980) 131; V.G. Ableev et al., JETP Lett.37 (1983) 196 and Nucl.Phys.A393 (1983) 491; S.J. Brodsky and B.T. Chertok, Phys.Rev.D14 (1976) 3203.
- 9) D. Bugg, Proc. 9 ICOHEPANS, Paris 1981, p.350. (North-Holland, 1982).
- 10) P. Kroll, "Dibaryons", preprint Wuppertal University WU B83-8 (1983), contr. to SATJRNE meeting, Fontevraud 1983.
- 11) F. Lehar et al., contr.to 10th Few Body Conference, Karlsruhe 1983 and private communication.
- 12) J.P. Stanley et al., preprint, London (1982).
- 13) E. Aprile et al., contr. to Intern.Symp. on High-Energy Physics with Polarized Beams and Targets, Lausanne (1980).
- 14) I.P. Auer et al., Phys.Rev.Lett.41 (1978) 354.
- 15) J. Bystricky et al., contr. to 9th ICOHEPANS, Versailles (1982).

- 16) E. Biegert et al., Phys.Lett.73B (1978) 235.
- 17) J. Bystricky et al., preprint Saclay (1982), DPhPE 82-09.
- 18) G. Smith et al., contr. to 10th Few Body Conference, Karlsruhe 1983.
- 19) a) J. Bystricky, G.H. Lamot and L. Vignani, Phys.Rev.Lett.45 (1980) 524 and priv.comm.  
b) T. Mizutani, C. Fayard, G.H. Lamot and R.S. Nahabetian, Phys.Lett.107B (1981) 177.
- 20) A.F. Titard and R.C. Eisele, Phys.Lett.106 (1982) 327.
- 21) K. Kubodera, M.P. Locher, F. Myhrer and A.W. Thomas, J.Phys.G6 (1980) 171.
- 22) A.S. Rinat and Y. Starkand, Weizmann Institute (1982), preprint WIS-82/31.
- 23) K. Kuboi et al., Prog.Theor.Phys.62 (1973) 153 and 65 (1981) 266.
- 24) M. Akemoto et al., Phys.Rev.Lett.50 (1983) 400.
- 25) V. Knöig et al., subm. to J.Phys.G (1983) and contrib. to 10th Few Body Conference, Karlsruhe 1983.
- 26) R. Holt et al., Argonne Nat.Lab., private comm. and W. Freeman et al., contr. to 10th Few Body Conference, Karlsruhe, 1983.
- 27) W. Gruebler et al., priv. comm.
- 28) W. Grein and R.P. Locher, J.Phys. A7 (1981) 1355.
- 29) N. Hiroshige, W. Watari and M. Yonezawa, Prog. Theor.Phys. Lett.68 (1982) 327.
- 30) E.L. Mathie et al., subm. to Phys.Rev.C.
- 31) J.A. Nishkhaner, Nucl.Phys.A296 (1978) 417; 5th Int. Symp. on Polariz. Phenom. (1980), Santa Fé, p.62; Phys.Lett.82B (1979) 167.
- 32) B. Blankleider and I.R. Afnan, Phys.Rev.C24 (1981) 1572.
- 33) M. Betz and T.-S.H. Lee, Phys.Rev.C23 (1981) 375.
- 34) W. Grein, A. König, P. Kroll, M.P. Locher and A. Švarc, SIN-preprint 83-08 (May 1983), subm. to Ann.of Phys.
- 35) D. Bugg, "NN- $\pi$ d amplitudes up to 580 MeV", in preparation (1983).
- 36) K.K. Seth et al., Phys.Lett.126B (1983) 164.

- 37) A. König and P. Kroll, Nucl.Phys.A358 (1981) 345; A. König and P. Kroll, in preparation.
- 38) A.S. Rinat and R.S. Bhalerao, Weizmann Institute, preprint WIS 82-55 Nov-Ph. (1983).
- 39) T. Kamae et al., Phys.Rev.Lett.38 (1977) 468.
- 40) H. Hidaka et al., Phys.Lett.70B (1977) 479; N. Hoshizaki, Prog.Theor.Phys.56 (1977) 716.
- 41) H. Ikeda et al., Nucl.Phys.B172 (1980) 509.
- 42) A.S. Bratashvskii et al., Yad.Fiz.32 (1980) 418 [Sov.J.Nucl. Phys.32 (1980) 216].
- 43) K. Baba et al., Phys.Rev.Lett.48 (1982) 729.
- 44) V.G. Gortenko et al., Nucl.Phys.A351 (1981) 181.
- 45) J.M. Laget, Nucl.Phys.A312 (1978) 265.
- 46) W.J. Schwille, Intern.Symp. on Lepton and Photon Physics, Bonn (1981).
- 47) T. Ishii et al., Phys.Lett.110B (1982) 441.
- 48) W.J. Schwille et al., priv.comm.
- 49) P.E. Argan et al., Phys.Rev.Lett.48 (1981) 96.
- 50) G. Tamas et al., Saclay-SIN collaboration, SIN Newsletter No. 13 (1980) 28.

## NUCLEON-NUCLEON SCATTERING AT MEDIUM ENERGIES

I.R. AFNAN <sup>†</sup>

School of Physical Sciences, The Flinders University of South Australia,  
Bedford Park, S.A. 5042, Australia.

A model of the N-N potential, at medium energies, in the frame work of the BB- $\pi$ BB equations, is presented. The derivation is based on the Cloudy Bag Model Hamiltonian. Recent N-N calculations are reviewed in the frame work of the model. Theoretical methods for the analysis of dibaryon resonances are compared.

### 1. INTRODUCTION

The interest in N-N scattering, above the pion production threshold, has been considerably enhanced by the observed structure in  $\vec{p}\text{-}\vec{p}$  scattering, and the possible existence of dibaryon resonances<sup>1</sup>. The fact that such resonance behavior might also be manifest in  $\pi$ -d scattering and in particular, in the recent vector polarization measurements<sup>2</sup>, may enhance the need for a theory that describes the full A=2 system, i.e. NN $\rightarrow$ NN, NN $\rightarrow$  $\pi$ d and  $\pi$ d $\rightarrow$  $\pi$ d. Furthermore, the failure of a theory based on the conventional pionic degrees of freedom (i.e. N, $\Delta$ , $\pi$ , $\rho$ ,...) to reproduce the observed structure, may be considered as evidence for the need of quark degrees of freedom to describe N-N and  $\pi$ -d scattering.

The present talk will be divided into three parts: (i) I will present a theory for N-N scattering, based on an effective Lagrangian, that could be derived from a chiral bag model<sup>3,4</sup>. In this way, I will maintain consistency with QCD without increasing the degrees of freedom of the problem. To maintain contact with established N-N phenomenology, I will demonstrate how the present theory includes most of the features of the standard N-N potentials<sup>5,6</sup>. (ii) In an attempt to review the work done on N-N scattering above the pion production threshold since the last conference, I will describe what features of the present theory have been included in existing calculations. In this way, I will illustrate the similarities and differences of the recent calculations. (iii) I will summarize some of the methods used to find the resonance poles in the complex energy plane.

---

<sup>†</sup> Work supported by the Australian Research Grants Scheme.

## 2. THEORY

The effective Lagrangian used, is basically similar to that used in the cloudy bag model (CBM)<sup>4</sup>, in that

$$L = L_0 + L_I \quad (1)$$

where  $L_0$  includes the kinetic energy of the pion and the bare baryons ( $B=N, \Delta, \dots$ ). The latter can be considered as three quarks in the bag. At this stage, the  $\Delta$  has no width for decay to  $\pi$ -N. Here,  $L_I$  is the interaction Lagrangian for the baryons and the pion, and can be non-linear in the pion field. The vertices in  $L_I$  have form factors associated with them. These are determined from the internal structure of the baryon, i.e. the quark wave function in the bag. The  $\pi$ BB form factor will get some further dressing from the scattering of the pion from the baryon. This further dressing has to be consistent with the measured rms radii and electromagnetic form factor of the neutron and proton.

In principle, one could extend this Lagrangian to include the coupling of the baryon, or bag, to other mesons. But for the present analysis, I will restrict the meson to the  $\pi$  and the baryon to the N and  $\Delta$ .

To derive the equation for the N-N amplitude, I have used the methods previously used to derive the NN- $\pi$ NN equations<sup>7-9</sup>. This involves the classification of the diagrams in perturbation theory, that contributes to the amplitude according to their irreducibility, using the last-cut-lemma<sup>13</sup>. The advantage of this method is that the detail form of the Lagrangian need not be specified. The final equations for N-N scattering, are a set of coupled Bethe-Salpeter type equations for the channels N-N, N- $\Delta$  and  $\Delta$ - $\Delta$ , where the  $\Delta$  is the physical  $\Delta$ . In operator form, the equation is given by,

$$T^{(2)} = T^{(3)} + T^{(3)} G_0 T^{(2)} \quad (2)$$

where  $T^{(i)}$  is the sum of all connected diagrams that are i-particle irreducible. The propagator  $G_0$  is a diagonal matrix of dressed propagators, i.e.  $\langle a | G_0 | a \rangle = d_a d_b$ ;  $a, b = N, \Delta$  where  $d_a$ , the dressed propagator for baryon a, is given by  $d_a^{-1} = d_a^{(0)-1} - \Sigma_a^{(2)}$ . Here,  $d_a^{(0)}$  is the undressed propagator that arises from  $L_0$ , while  $\Sigma_a^{(2)}$  is the dressing that results from the coupling of the bag to the pion. The contribution to  $\Sigma_a^{(2)}$ , in the case of the CBM, is given by,

$$\Sigma^{(2)} = f^{(3)} g f^{(3)\dagger} + f^{(3)} g m^{(2)} g f^{(3)\dagger}, \quad (3)$$

where  $f^{(3)}$  is the  $\pi$ BB form factor, as given by the CBM, g is the  $2 \times 2$   $\pi$ -B propagator with  $\langle a | g | a \rangle = d_a d_\pi$  ( $a = N, \Delta$ ). Here,  $m^{(2)}$  is the non-pole part of the  $\pi$ -B amplitude as would arise from the crossed diagram in Fig. 1. The  $\Delta$ , with propagator  $d_\Delta$ , is the physical  $\Delta$  and has a width for decay into  $\pi$ -N.

In Eq. (2),  $T^{(3)}$  plays the role of the N-N, N- $\Delta$  and  $\Delta$ - $\Delta$  potentials and includes all diagrams that are three particle irreducible. A detailed examination of the diagrams that contribute to  $T^{(3)}$ , using the last-cut lemma, gives an expression for  $T^{(3)}$  in terms of the more basic parameters in our effective Lagrangian. For the case where the interaction Lagrangian is linear in the pion field (e.g. CBM),  $T^{(3)}$  is given by



FIGURE 1

$$T^{(3)} = \sum_{ij=1}^2 F_d^{(3)}(i) \bar{\delta}_{ij} G_1 F_d^{(3)\dagger}(j) + \sum_{ij=1}^2 \sum_{\alpha\beta=1}^3 F_d^{(3)}(i) \bar{\delta}_{i\alpha} G_1 M_{\alpha\beta}^{(3)} G_1 \bar{\delta}_{\beta j} F_d^{(3)\dagger}(j), \quad (4)$$

where  $G_1$  is the  $\pi$ BB propagator,  $\bar{\delta}_{ij} = 1 - \delta_{ij}$ , and  $F_d^{(3)}$  is the disconnected part of the  $\pi$ BB $\rightarrow$ BB amplitude, i.e. it is related to the  $\pi$ BB dressed vertex  $f^{(2)}$  by the relation

$$F_d^{(3)}(i) = \sum_j f^{(2)}(i) d^{-1}(j) \bar{\delta}_{ij}. \quad (5)$$

Here, the  $\pi$ BB dressed form factor is given by:

$$f^{(2)}(i) = f^{(3)}(i) + f^{(3)}(i) g m^{(2)}(i) \quad (6)$$

In eq. (4),  $M_{\alpha\beta}^{(3)}$  is the three-particle irreducible amplitude for  $\pi$ BB $\rightarrow$  $\pi$ BB and can be taken as the Faddeev amplitude for the  $\pi$ BB system, as was the case in the NN- $\pi$ NN equations<sup>8-12</sup>. In lowest order,  $M_{\alpha\beta}^{(3)}$  is the  $\pi$ -B or B-B amplitude. In that case, Eq. (4) reduced to,

$$T^{(3)} = \sum_{ij=1}^2 f^{(2)}(i) d_{\pi} \bar{\delta}_{ij} f^{(2)\dagger}(j) + \sum_{ij=1}^2 f^{(2)}(i) d(i) t^{(2)} d_{\pi} d(j) f^{(2)\dagger}(j) + \sum_{ij=1}^2 f^{(2)}(i) d_{\pi} d(i) m^{(2)}(j) d_{\pi} f^{(2)\dagger}(i). \quad (7)$$

We first observe that all  $\pi$ BB vertices are dressed and thus depend on the energy and momentum. The first term on the r.h.s. of Eq. (7) is the one pion exchange potential, with the added feature that it does not require any

regularization as all the form factors are predetermined. In the second term on the r.h.s. of Eq. (7),  $t^{(2)}$  is the B-B amplitude and could be approximated by the one pion exchange potential. In that case, for  $i \neq j$ , this term is the crossed two pion exchange contribution to the N-N potential and is commonly represented by the diagrams in Fig. 2. On the other hand, had we replaced  $t^{(2)}$  by the B-B amplitude  $T^{(2)}$ , we would have a bootstrap problem and the resultant equations would be non-linear in  $T^{(2)}$ . The justification for breaking this bootstrap situation is the result of two observations: (a) Because of the parity and iso-spin of the pion, the B-B amplitude  $t^{(2)}$  is required in partial waves other than that of  $T^{(2)}$ . (b) The energy at which we need the B-B amplitude  $t^{(2)}$ , in the  $\pi$ BB space, is at least  $m_\pi$  less than in  $T^{(2)}$ . Thus, at medium energies, we need the B-B amplitude predominantly below the pion production threshold and this I can describe by a real potential such as the Paris potential<sup>5</sup>. Finally, by including the contribution from this term, we get a contribution to the N-N potential from the coupling to the  $\pi$ -d channel.



FIGURE 2

Since we have included the  $\Delta$  as an explicit channel, the contribution of the last term on the r.h.s. of Eq. (7) is due to the smaller  $\pi$ -N partial waves and the non-pole part of the amplitudes in the  $P_{11}$  and  $P_{33}$  channels. Since these amplitudes are in general small, we don't expect a large contribution from this term.

Although Eq. (7) can be considered as an N-N potential for use above the pion production threshold, some calculations to date have used only the first term in conjunction with N-N potentials commonly used below the pion production threshold. Alternatively, I can proceed from Eq. (4) with  $M_{\alpha\beta}^{(3)}$  given by the Faddeev equations for the  $\pi$ NN system. In that case, the equations can be recast into a set of coupled integral equations for all the  $2 \rightarrow 2$  amplitudes in the  $A=2$  system. This approach guarantees that two- and three-body unitarity are satisfied.

### 3. RECENT RESULTS

Since the last conference in Eugene, there have been a number of calculations of the N-N scattering above the pion production threshold. Within the frame work of the theory presented above, these calculations can be divided



into two classes. (1) Those that satisfy two- and three-body unitarity<sup>14-20</sup>. (2) Coupled channel calculations, in which the coupling is between the N-N and N- $\Delta$  channels<sup>21-24</sup>. In the following, I will review some recent results.

### 3.1. Three-body calculations

All these calculations<sup>14-20</sup> have several features in common: (i) They all include the  $\Delta$  resonance by introducing a  $\pi$ -N amplitude that fits the phase shifts in the  $P_{33}$  channel. In this way, they have the correct N- $\Delta$  threshold and the  $\Delta$  is a genuine  $\pi$ -N resonance. This feature leads to N-N phase shifts that have the characteristic of a resonance (see Fig. 3). (ii) The  $\pi$ NN and  $\pi$ N $\Delta$  vertices have form factors that have been adjusted to fit the experimental  $\pi$ -N phase shifts in the  $P_{11}$  and  $P_{33}$  channels. As a result of this, there is no need to introduce cut-off into the theory. However, the  $\pi$ -N phase shifts don't uniquely determine the form factor for the  $\pi$ NN vertex (i.e. the off-shell behavior of the  $\pi$ -N amplitude) and the results are very sensitive to the choice of form factor. This is illustrated in Fig. 3, where we present the  $^1D_2$  phase shifts for two different  $\pi$ NN form factors.

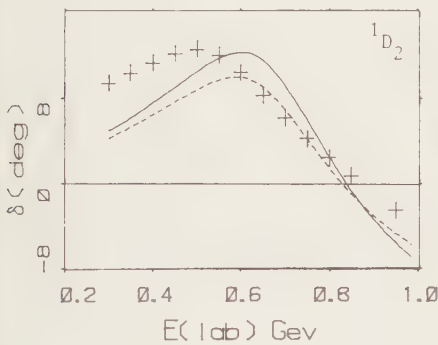


FIGURE 3

The  $^1D_2$  phase shifts for two different  $\pi$ N form factors.

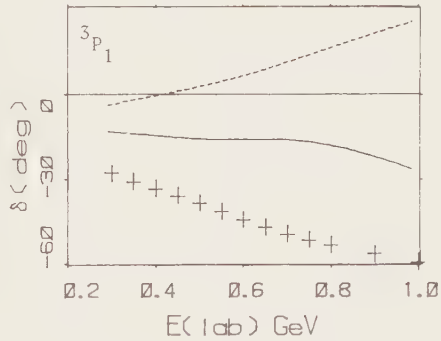


FIGURE 4

The effect of the N-N interaction in the  $\pi$ N space on the  $^3P_1$  phase shifts.

The early calculations<sup>25</sup> using this approach were pure three-body models in which the nucleons were not treated on equal footing. This problem is still present in the work of Araki et al.<sup>19</sup> and Kloeet and Silbar<sup>14</sup>. Araki et al. overcome this problem by increasing the strength of the  $P_{11}$  interaction. Unfortunately, that increases the cross section for  $pp \rightarrow \pi d$  and  $\rho$ -exchange is introduced to compensate for this abnormally large production cross section. On the other hand, Kloeet and Silbar add a static one pion exchange with half the normal strength to build the one pion exchange strength. Both of these

calculations use the pole part of the  $P_{11}$   $\pi$ -N amplitude and thus do not fit the phase shifts. In their calculations, Kloet and Silbar have no coupling to the  $\pi$ -d channel. As a result of this, they have no effective cross two pion exchange in their calculations. While Araki et al. included the coupling to the  $\pi$ -d channel and have included all three terms on the r.h.s. of Eq. (7).

The work of Blankleider and Afnan<sup>16</sup>, Mizutani et al.<sup>18</sup> and Rinat et al.<sup>20</sup>, use the same equations<sup>8-11</sup> and in this case the nucleons are treated on equal footing, since the equations were derived from field theory<sup>8,9</sup>. All three of these calculations restrict the baryon to the nucleon and the  $\Delta$ -resonance is included through the third term in Eq. (7). Furthermore, they solve the full set of NN- $\pi$ NN equations. Although the first term on the r.h.s. of Eq. (7) is included in all cases, the parametrization of  $f^{(2)}$  is different in the three calculations. This explains part of the difference in their predictions for the  $pp \rightarrow \pi d$  total cross section and N-N phase shifts (see Fig. 3). Better agreement could be achieved if the constraint imposed by the CBM, the nucleon rms radius and the electromagnetic form factor of the nucleon, on the  $\pi$ NN form factor, could be implemented.

For the second term on the r.h.s. of Eq. (7), all three groups have included the  ${}^3S_1$ - ${}^3D_1$  amplitude in terms of a separable potential. In this way, the coupling to the  $\pi$ -d channel is established. In addition, Rinat et al. include the  ${}^1S_0$  for the T=0 channels, while Blankleider and Afnan included the S-, P- and D-waves and thus the crossed two pion exchange. In Fig. 4, I illustrate the contribution of the N-N partial waves other than the deuteron, in the  $\pi$ NN Hilbert space, to the  ${}^3P_1$  phase shifts. This shows the importance of the second term in Eq. (7). Rinat et al. have compensated for this term by including heavy meson ( $\rho, \omega$ ) exchange. Finally, all three calculations include s- and p-wave  $\pi$ -N interaction through the third term in Eq. (7).

The most complete calculation to date using these equations<sup>8-11</sup>, is the work of Rinat et al., who have examined all three reactions in the A=2 system. In addition to one pion exchange, they have included  $\rho$ - and  $\omega$ -exchange. Their fit to the data is impressive, considering the few free parameters that go into the calculations and the fact that the same equations with the same input give good agreement with experiment for  $\pi$ -d elastic scattering and  $pp \rightarrow \pi d$ . In Fig. 5, I present their fit to the  ${}^3P_1$  and  ${}^1D_2$  channels which gives the best agreement. The largest discrepancy is in the  ${}^3P_2$ - ${}^3F_2$  channel, which is the most difficult to reproduce by any of the theories. Here I should point out that  $\rho$ -exchange is taking the role of the crossed two pion exchange.

### 3.2. Coupled channels calculations.

These calculations are basically an extrapolation of the static N-N

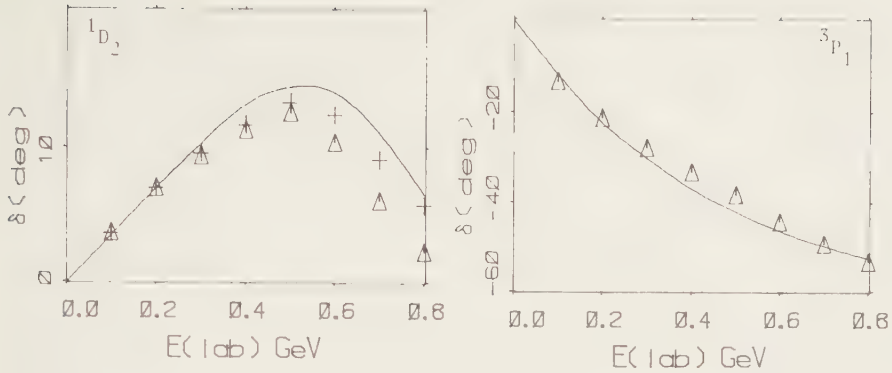


FIGURE 5

The  $1D_2$  and  $3P_1$  phase shifts from the calculations of Rinat et al.<sup>20</sup>.

potentials to medium energies. Since the pion production cross section is dominated by  $NN \rightarrow N\Delta \rightarrow NN\pi$ , the N-N equations used at low energies are replaced by Eq. (2), in which the  $\Delta$  has acquired a  $\pi$ -N decay width. In this way, the main mechanism for inelasticity in N-N scattering has been included. The coupling potential in these calculations is basically the first term in Eq. (7) with the added feature that both  $\pi$ - and  $\rho$ -exchange are included, and the form factors  $f^{(2)}$  are taken as a dipole with a cut-off.

The main difference between the calculations to date has been the choice of kinematics, the description of the width for the  $\Delta$ -resonance, and the N-N potential extrapolated. The early work of Green and Sainio<sup>21</sup> have used the Reid<sup>26</sup> potential and the non-relativistic Schrodinger equation. Here, the threshold is given the correct momentum dependence and the parameters for the width were adjusted to fit the  $\pi p$  total cross section. More recently, Tjon and van Faassen<sup>23</sup> have performed a similar calculation using the Bethe-Salpeter equation and the extrapolation of the one-boson exchange potential. In both of these calculations, since the  $\Delta$  is included explicitly, the third term of Eq. (7) has been neglected, while the second term in Eq. (7) is replaced by the heavy meson ( $\omega, \eta, \dots$ ) exchange for the N-N part of the potential only. This latter approximation is similar to that of Rinat et al.<sup>20</sup>.

An alternative to the coupled channel calculations, is to explicitly include the third term in Eq. (7) into the N-N potential. In this way, the  $\Delta$  and the  $N^*$  can be included without increasing the number of coupled equations. This approach has been pursued by Lee<sup>22</sup>, who has extended the Paris potential above the pion production threshold. The new feature of this calculation is

that the  $\Delta$  and  $N^*$  have their width for decay to  $\pi N$  and  $\pi\pi N$  adjusted by the  $\pi$ - $N$  phase shifts via a separable type potential. In this case, the first and second term on the r.h.s. of Eq. (7), are placed by the Paris potential, with a subtraction to avoid over counting. One problem with the above procedure for including the  $N^*$ , is that the third term in Eq. (7) includes only the non-pole part of the  $P_{11}$  amplitude, which should not fit the phase shifts. Although this procedure for including the  $\Delta$  and  $N^*$  also determines the  $\pi NN$  and  $\pi N\Delta$  form factor, the latter are not included in the calculation of the transition potential.

Both of the above coupled channel calculations give a good fit to the phase shifts; however, the cut-off in their  $\pi NN$  and  $\pi N\Delta$  form factor differ by almost a factor of two.

### 3. DIBARYON RESONANCES

The main problem in establishing the existence of the dibaryon resonance, has been the unfolding of the  $N$ - $\Delta$  threshold from the experimental data to see if there is a resonance pole. Most calculations to date can be divided into three classes; (i) Those that fit the data with K-matrix theory<sup>27</sup> and analytically continue the amplitude into the complex energy plane in search of a resonance pole. (ii) Models of  $N$ - $N$  scattering described above, for which the on-shell amplitude is examined in terms of an Argand diagram<sup>28,16</sup>. (iii) Attempts at finding the pole of the amplitude, in the complex energy plane, for a given model<sup>29,30</sup>. Although the last approach is the most reliable, it presupposes that the model gives a correct description of the physics.

To compare the above three methods, consider a three-body model of  $\pi$ - $d$  scattering in the  $2^+$  channel. The position of the resonances are then determined by examining the eigenvalues of the Faddeev kernel. The phase shifts for this model are then used to test the first two methods. The results are present in Fig. 6 for two cases. We observe that for resonances with width less than the  $\Delta$  width, all three methods predict the same result. However, when the  $\Delta$  width is smaller than the resonance width, the three methods give different results. In particular, the K-matrix approach is sensitive to the choice of unitarity branch points included in the analysis. Thus, including the elastic and breakup through the  $\Delta$  channel (B), using the K-matrix method gives a different result from that of including both breakup channels (C). Part of the discrepancy between B, C and F (the Faddeev result), is due to the fact that the K-matrix approach involves assuming a constant amplitude in reducing the unitarity equations from three-body to quasi two-body equations. A more detailed analysis of this approximation might give us a clue, to improve

the K-matrix approach for dibaryon analysis.

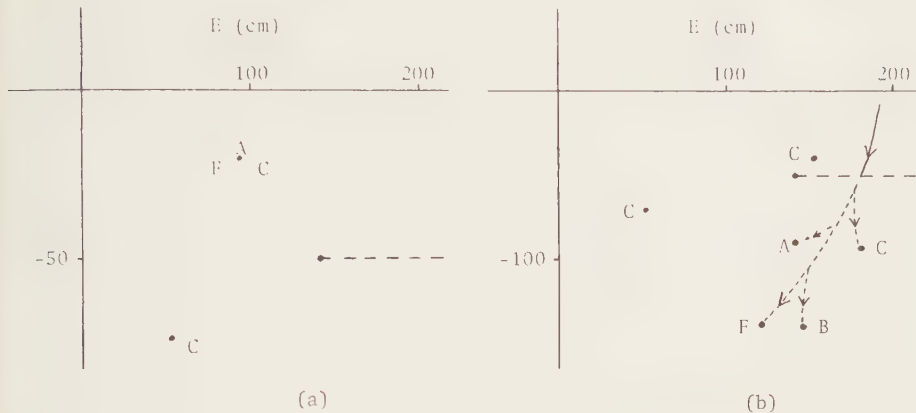


FIGURE 6

The position of the dibaryon pole as predicted by K-matrix (B,C), Argand (A) and Faddeev (F) method, for non-relativistic (a) and relativistic (b)  $\pi$ -d scattering in the  $2^+$  channel.

#### ACKNOWLEDGEMENT

I would like to thank Bruce Pearce and Bob McLeod for their assistance in the numerical calculations. I also would like to thank Bruce Pearce for reading the manuscript prior to publication.

#### REFERENCES

- 1) A. Yokosawa, Phys. Rep. 64 (1980) 47.
- 2) J. Bolger et al., Phys. Rev. Lett. 46 (1980) 167; 48 (1982) 1667.
- 3) G.E. Brown and M. Rho, Phys. Lett. 82B (1979) 177;  
G.E. Brown, M. Rho and V. Vento, Phys. Lett. 94B (1979) 383; 97B (1980) 423; C. De Tar, Phys. Rev. D42 (1981) 752, 762.
- 4) A.W. Thomas, Advances in Nuclear Physics, ed J. Negele and E. Vogt (Plenum Press N.Y.); S. Theberge, A.W. Thomas and G.A. Miller, Phys. Rev. D22 (1980) 2838; Can. J. Phys. 60 (1982) 59.
- 5) M. Lacombe et al., Phys. Rev. C21 (1980) 861.
- 6) K. Holinde, Phys. Rep. 68C (1981) 122.
- 7) A.W. Thomas and A.S. Rinat, Phys. Rev. C20 (1979) 216.
- 8) I.R. Afnan and B. Blankleider, Phys. Rev. C22 (1980) 1638.
- 9) Y. Avishai and T. Mizutani, Phys. Rev. C27 (1983) 312.

- 10) Y. Avishai and T. Mizutani, Nucl. Phys. A526 (1979) 352; A535 (1980) 377; A552 (1981) 399.
- 11) I.R. Afnan and A.T. Stelbovics, Phys. Rev. C23 (1981) 1584.
- 12) A.S. Rinat, Phys. Rev. C22 (1980) 2156.
- 13) J.G. Taylor, Nuovo Cim. Suppl. 1 (1963) 934.
- 14) W.M. Kloet and R.R. Silbar, Nucl. Phys. A338 (1980) 281, 317; A364 (1981) 346.
- 15) I.R. Afnan and B. Blankleider, Phys. Lett. 93B (1980) 367.
- 16) B. Blankleider and I.R. Afnan, Phys. Rev. C24 (1981) 1572.
- 17) M. Betz and T.-S.H. Lee, Phys. Rev. C23 (1981) 375.
- 18) T. Mizutani et al., Phys. Lett. 107B (1981) 177.
- 19) M. Araki, Y. Koike and T. Ueda, Nucl. Phys. A369 (1981) 346; A389 (1982) 605; M. Araki and T. Ueda, Nucl. Phys. A379 (1982) 449.
- 20) A.S. Rinat and Y. Starkand, Nucl. Phys. A397 (1983) 381; A.S. Rinat and R.S. Bhalerao, Weizmann Preprint (1982).
- 21) A.M. Green and M.E. Sainio, J. of Phys. G5 (1979) 503.
- 22) T.-S.H. Lee, Phys. Rev. Lett. 50 (1983) 1571; Argonne National Laboratory Preprint (1983).
- 23) J.A. Tjon and E. van Faassen, Phys. Lett. 120B (1983) 39; University of Utrecht Preprint (1983).
- 24) J. Cote et al., Nucl. Phys. A379 (1982) 349.
- 25) I.R. Afnan and A.W. Thomas, Phys. Rev. C10 (1974) 109.
- 26) R.V. Reid, Ann. of Phys. 50 (1968) 191.
- 27) R. Bhandari et al., Phys. Rev. Lett. 46 (1981) 1111; B.J. Edwards and G.H. Thomas, Phys. Rev. D22 (1980) 2772.
- 28) W.M. Kloet, J.A. Tjon and R.F. Silbar, Phys. Lett. 99B (1981) 80.
- 29) I.R. Afnan and B.C. Pearce, contributed paper to the conference.
- 30) T. Ueda, Phys. Lett. 119B (1982) 281.

## SYMMETRIES AND THE N-N INTERACTION

W.T.H. van Oers

University of Manitoba, Winnipeg, Manitoba, Canada R3T 2N2 and  
 TRIUMF, Vancouver, B.C., Canada V6T 2A3

A new generation of precision experiments to study symmetries in the N-N system is being undertaken at various laboratories. A short discussion of the background to some of these experiments is presented.

### 1. PARITY

The weak, strangeness-conserving part of the hadronic interaction should manifest itself through the parity-violating signature inherent to the weak interaction. Since parity is conserved in the hadronic and electromagnetic interactions any parity violation in nuclear scattering or in nuclear reactions indicates a weak interaction contribution. Most directly interpretable are studies of parity violation in nucleon-nucleon scattering since such studies are not subject to the complications of nuclear structure.

#### 1.1 Parity Violation in Proton-Proton Scattering

Measurements of parity violation in proton-proton scattering are based on the relative changes in the total cross section or the integrated differential cross section (over a suitable angular range) if the polarization direction of the incident polarized beam is changed from positive to negative helicity. The longitudinal analyzing power ( $A_z$ ), can be expressed as

$$A_z = \frac{1}{|p_z|} \frac{\sigma^+ - \sigma^-}{\sigma^+ + \sigma^-}$$

Here  $p_z$  is the polarization of the incident proton beam, while the superscripts refer to positive and negative helicity.

Assuming rotational and time-reversal invariance (TRI), but not parity conservation, the centre-of-mass scattering amplitude for two like particles can be written<sup>1</sup>

$$M = \frac{1}{2} \left[ (a+b) + (a-b)(\vec{\sigma}_1 \cdot \vec{n})(\vec{\sigma}_2 \cdot \vec{n}) + (c+d)(\vec{\sigma}_1 \cdot \vec{m})(\vec{\sigma}_2 \cdot \vec{m}) + (c-d)(\vec{\sigma}_1 \cdot \vec{\ell})(\vec{\sigma}_2 \cdot \vec{\ell}) + e(\vec{\sigma}_1 + \vec{\sigma}_2) \cdot \vec{n} + r(\vec{\sigma}_1 - \vec{\sigma}_2) \cdot \vec{\ell} + s \left\{ (\vec{\sigma}_1 \cdot \vec{n})(\vec{\sigma}_2 \cdot \vec{\ell}) - (\vec{\sigma}_1 \cdot \vec{\ell})(\vec{\sigma}_2 \cdot \vec{n}) \right\} \right]$$

Here  $\ell$ ,  $m$  and  $n$  are unit vectors defined as

$$\ell = \frac{\vec{k}_i + \vec{k}_f}{|\vec{k}_i + \vec{k}_f|} ; m = \frac{\vec{k}_f - \vec{k}_i}{|\vec{k}_f - \vec{k}_i|} ; n = \frac{\vec{k}_i \times \vec{k}_f}{|\vec{k}_i \times \vec{k}_f|} ;$$

with  $\vec{k}_i$  and  $\vec{k}_f$  the initial and final state centre-of-mass nucleon momenta. The



quantities  $a, b, c, d, e, r$  and  $s$  are functions of centre-of-mass energy  $E$  and scattering angle  $\theta$ . Invoking also parity conservation the last two terms will drop from the equation.

The longitudinal analyzing power can be expressed as<sup>2</sup>

$$A_z(\theta) = \frac{1}{2\sigma_0} \left[ \{ \text{Re}((a+b-c+d)^*r) - \text{Re}(e^*s) \} \cos\theta/2 + \{ \text{Im}((-a+b-c+d)^*s) + \text{Im}(e^*r) \} \sin\theta/2 \right],$$

with  $\sigma_0$  the differential cross section for the scattering of unpolarized particles

$$\sigma = \frac{1}{2} (a^2 + b^2 + c^2 + d^2 + e^2 + r^2 + s^2) .$$

From the detection of a non-vanishing analyzing power one obtains information on the parity non-conserving amplitudes  $r$  and  $s$ , provided that the other interfering amplitudes ( $a, b, c, d$ , and  $e$ ) are known through standard p-p phase-shift analyses.

The experiments are extremely difficult and require elimination of systematic errors to the level of  $10^{-7}$ . The most important instrumental effects which need to be considered are: beam intensity modulations, beam position and direction modulations, beam emittance modulations (in particular if these modulations are correlated with spin flip), residual transverse polarizations, double scattering effects,  $\beta$ -decay (and hyperon decay) asymmetries, and electronic asymmetries. Measurements span the range from 15 MeV to 5.13 GeV (see Table 1.1).

Table 1.1 Measurements of the parity-violating analyzing power  $A_z$ .

	$T_1$	$A_z$	ref	$A_z^{\text{theor}}$	ref
p+p	15 MeV	$-(1.7 \pm 0.8) \times 10^{-7}$	3	$-1.3 \times 10^{-7}$	8
p+p	45 MeV	$-(2.3 \pm 0.8) \times 10^{-7}$	4	$-2.3 \times 10^{-7}$	8
p+p	46 MeV	$-(1.3 \pm 2.3) \times 10^{-7}$	5	$-2.3 \times 10^{-7}$	8
p+p	800 MeV		6		
p+H <sub>2</sub> O	800 MeV	$(6.6 \pm 3.2) \times 10^{-7}$	6		
p+H <sub>2</sub> O	5.13 GeV	$(2.65 \pm 0.60) \times 10^{-6}$	7		

The low-energy results are in good agreement with theoretical predictions for the longitudinal analyzing power based upon a distorted wave approach with the weak interaction part parametrized by  $\rho, \omega, \pi$ , and  $2\pi$  exchanges.<sup>8,9</sup> If one writes the scattering amplitude as  $\mathcal{F} = \sum_J [F^J + f^J]$ , with  $F^J$  and  $f^J$  the parity-conserving and parity-violating parts for total angular momentum  $J$ , respectively, then for sufficiently low energy, where  $^1S_0$ - $^3P_0$  mixing is dominant, the analyzing power can be written as<sup>9</sup>

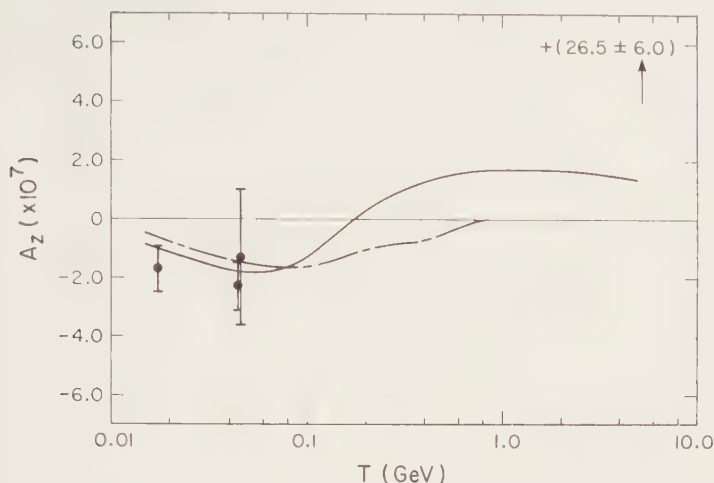


Fig. 1. Energy dependence of the longitudinal analyzing power  $A_z$ . The solid and dashed curves are predictions from Refs. 9 and 10, respectively.

$$A_z \approx \frac{2\text{Re}[F_{00}^{0*}f_{01}^0 + F_{11}^{0*}f_{10}^0]}{1/4(|F_{00}^{0*}|^2 + |F_{11}^{0*}|^2)}.$$

With  $f_{01}^0$  and  $f_{10}^0$  monotonically increasing functions of energy, and with  $F_{00}^0$  proportional to  $\sin[\delta(^1S_0)]$  and  $F_{11}^0$  proportional to  $\sin[\delta(^3P_0)]$ , the energy behaviour shown in Fig. 1 becomes clear. Both the  $^1S_0$  and  $^3P_0$  phase shifts become negative just above 200 MeV. When the energy increases the higher angular momentum contributions become more important, in particular  $J=2$  and  $J=4$  (corresponding to  $^3P_2$ - $^1D_2$  and  $^3F_4$ - $^1G_4$  mixing). These contributions have the opposite sign to the  $J=0$  contribution and therefore partially cancel it below 200 MeV. Because of the crucial role of the short-range interaction the boson exchange models are less satisfactory.

Theoretical predictions have also been obtained within the framework of a hybrid multi-baryon-quark shell model giving satisfactory agreement with the low-energy results but a change in sign only at about 800 MeV.<sup>10</sup> The experimental value at 5.13 GeV,  $A_z = (2.65 \pm 0.60) \times 10^{-6}$ , disagrees with the prediction of the boson exchange model by more than one order of magnitude. However, newer theoretical predictions<sup>11</sup> taking into account parity-violating effects of the quark constituents of the nucleons predict values of  $A_z \sim 2 \times 10^{-6}$  at 6 GeV, but these same theoretical predictions extended to the lower energies overestimate the measured analyzing powers.

## 2. TIME REVERSAL

Time-reversal invariance (TRI) is only known to be broken in neutral K decay. The resulting TRI-violating parameters are consistent with current superweak theories. Time-reversal invariance is an assumed symmetry which must rest on an experimental basis (as is the case for all symmetries). For the large number of hadronic tests of TRI giving a null result, the attained accuracy is in general not much better than one per cent. Thus, even though there exists at present very little theoretical support for millistrong interactions leading to TRI violation in parity-conserving nuclear processes, experimental tests should receive consideration provided they lower the upper limit of possible TRI-violating effects to the level of less than a few parts in  $10^3$ .

## 2.1 Time-Reversal Invariance Tests in the N-N System

Most tractable in terms of determining an upper limit to a TRI-violating amplitude are polarization analyzing power equality tests (P-A tests) for N-N scattering. Assuming invariance under rotations and space reflections the n-p centre-of-mass scattering amplitude can be written<sup>12</sup>

$$M = \frac{1}{2} \left[ (a+b) + (a-b)(\vec{\sigma}_1 \cdot \hat{n})(\vec{\sigma}_2 \cdot \hat{n}) + (c+d)(\vec{\sigma}_1 \cdot \hat{m})(\vec{\sigma}_2 \cdot \hat{m}) \right. \\ \left. + (c-d)(\vec{\sigma}_1 \cdot \hat{l})(\vec{\sigma}_2 \cdot \hat{l}) + e(\vec{\sigma}_1 + \vec{\sigma}_2) \cdot \hat{n} + f(\vec{\sigma}_1 - \vec{\sigma}_2) \cdot \hat{n} \right. \\ \left. + t\{(\vec{\sigma}_1 \cdot \hat{l})(\vec{\sigma}_2 \cdot \hat{m}) + (\vec{\sigma}_1 \cdot \hat{m})(\vec{\sigma}_2 \cdot \hat{l})\} + u\{(\vec{\sigma}_1 \cdot \hat{l})(\vec{\sigma}_2 \cdot \hat{m}) - (\vec{\sigma}_1 \cdot \hat{m})(\vec{\sigma}_2 \cdot \hat{l})\} \right].$$

The various quantities in this expression are as defined previously with  $t$  and  $u$  the TRI-violating functions of centre-of-mass energy  $E$  and scattering angle  $\theta$ . For identical particles, as is the case in p-p or n-n scattering, the Pauli principle requires

$$f = u = 0.$$

For n-p scattering the quantity P-A can be written in the following form<sup>12</sup>

$$P_Y(\theta) - A_Y(\theta) = -\frac{2}{\sigma_0} \text{Im}(d^*t + c^*u)$$

with  $\sigma_0$  the differential cross section for the scattering of unpolarized particles

$$\sigma = \frac{1}{2} (a^2 + b^2 + c^2 + d^2 + e^2 + f^2 + t^2 + u^2).$$

For the depolarization parameters one obtains the relation<sup>12</sup>

$$D_m^l(\theta) + D_l^m(\theta) = \frac{2}{\sigma_0} \text{Re}(c^*t + d^*u).$$

The TRI-violating functions  $t$  and  $u$  can be expanded in terms of partial waves. As derived by Binstock, Bryan and Gersten<sup>13</sup>

$$t(\theta) = \frac{1}{k} \sum_{j=1} (2j+1)[j(j+1)]^{-1/2} P_j^{(1)}(\cos \theta) \exp \left[ i(\delta_{j,j-1} + \delta_{j,j+1}) \right] \sin(2\lambda_j),$$

with  $2\lambda_j$  the TRI-violating mixing angle. For the case of p-p scattering the Pauli principle excludes spin-triplet even states and spin-singlet odd states. Retaining only the first term in the expansion one finds for n-p scattering

$$t(\theta) = \frac{1}{k} \frac{3\sqrt{2}}{2} \sin\theta \exp\left[i\{\delta(^3S_1) + \delta(^3D_1)\}\right] \sin(2\lambda_1),$$

and for p-p scattering

$$t(\theta) = \frac{1}{k} 5\sqrt{6} \sin\theta \cos\theta \exp\left[i\{\delta(^3P_2) + \phi_1 + \delta(^3F_2) + \phi_3\}\right] \sin(2\lambda_2),$$

with the  $\phi_j$ 's the Coulomb phase shifts for the  $l^{\text{th}}$  partial wave. If TRI violation is the result of short-range interactions such as in a one-boson-exchange model as proposed by Bryan and Gersten,<sup>14</sup> then the J=1 state is much more important than the higher J-states which leads to the above expressions and a potentially greater sensitivity of the n-p system over the p-p system. In previous analyses<sup>15</sup> of existing p-p and n-p elastic scattering data values of the time-irreversible phase parameters  $\lambda_1$  and  $\lambda_2$  were obtained, not inconsistent with zero but with large uncertainties.

Writing the differential cross sections in terms of the polarizations perpendicular to the scattering plane, i.e. along n, one obtains for the polarization-analyzing power difference

$$P_y(\theta) - A_y(\theta) = 2 \frac{\sigma^{+-} - \sigma^{+ -}}{\sigma^{++} + \sigma^{+-} + \sigma^{-+} + \sigma^{--}}.$$

Here  $\sigma^{+-}$  is the differential cross section for scattering from a polarization direction defined as spin-up to a polarization direction with spin-down, etc. A nonzero result will only be obtained if the spin-flip differential cross sections differ ( $\sigma^{++} \neq \sigma^{+-}$ ). Similarly one can write for the depolarization parameter

$$D(\theta) = \frac{\sigma^{++} - \sigma^{+-} + \sigma^{--} - \sigma^{-+}}{\sigma^{++} + \sigma^{+-} + \sigma^{--} + \sigma^{-+}}, \quad \text{note that } |D| < 1,$$

and consequently

$$P-A = (1-D)\epsilon$$

where

$$\epsilon = \frac{\sigma^{+-} - \sigma^{+ -}}{\sigma^{++} + \sigma^{+-}}.$$

The sensitivity to measuring TRI-violation in the N-N system scales with 1-D. If  $D = 1$  it follows that  $P-A = 0$ . Unfortunately previous hadronic tests of TRI have often been made under kinematical conditions where the depolarization parameter turned out to be close to unity.<sup>16</sup> Phase-shift predictions for the depolarization parameter D in n-p and p-p elastic scattering at 200, 500 and 800 MeV indicate that the p-p system is to be preferred over the n-p system except for the extreme backward angles.

An upper limit on the TRI-violating amplitude  $t$  in elastic p-p scattering at 579 MeV and six centre-of-mass angles between  $66^\circ$  and  $86^\circ$  has been presented recently.<sup>17</sup> The analysis is based on measurements of a set of sixteen polarization parameters allowing reconstruction of the scattering matrix in terms of the six amplitudes defined above. The average ratio of the upper limit on  $t^2$  gives  $t^2/(a^2 + b^2 + c^2 + d^2 + e^2 + t^2) = 0.0059$  (90% confidence limit). Analyzing these results in terms of the time irreversible phase parameter  $\lambda_2$  one finds  $|\lambda_2| = 0.016 \pm 0.010$ .<sup>18</sup> A P-A measurement for the n-p system at 800 MeV has been made by Bhatia et al.<sup>19</sup> at  $\theta_{c.m.} = 133^\circ$ . At this angle 1-D is greater than unity. The result obtained is P-A =  $0.011 \pm 0.019$  with an additional systematic uncertainty of  $\pm 0.02$ . This is the most sensitive test of TRI in the nucleon-nucleon system that exists to date. However, the comparison is based on charge-symmetry breaking to be energy independent, since it assumes the analyzing power equality  $A[\vec{H}(\vec{n}, p)n] = A[\vec{H}(n, p)n]$  at two different energies. Comparison of this datum with the model prediction of Binstock, Bryan and Gersten<sup>13</sup> establishes an upper limit on P-A an order of magnitude lower than the model prediction.

A new P-A measurement for the p-p system at 200 MeV is currently in progress at TRIUMF.<sup>20</sup> The experiment avoids the need to make absolute determinations of the polarimeter analyzing power and beam polarization by measuring the p-p polarization and analyzing power relative to those for p- $^{12}\text{C}$  elastic scattering. For a spin-zero target, parity conservation requires P-A = 0. The experiment has as objective a determination of the ratio of measured ratios  $(P_H/P_C)/(A_H/A_C)$  to an accuracy of  $\pm 0.004$  or less.

The only experiment to date which provides a comparison of the depolarization parameters  $D_Z^{x'}$  and  $D_X^{z'}$  for elastic p-p scattering at 430 MeV and a centre-of-mass scattering angle of  $66^\circ$  has been made by Händler et al.<sup>21</sup> The result for  $D_Z^{x'} + D_X^{z'} = 0.0019 \pm 0.009$  translates in a time irreversible phase parameter  $\lambda_2 < 0.1$ . However, as shown by Binstock, Bryan and Gersten<sup>13</sup> the scattering angle  $\theta_{c.m.} = 66^\circ$  is close to a zero of the parameter  $D_Z^{x'} + D_X^{z'}$  assuming only that a possible TRI-violating process is short range in nature.

### 3. ISOSPIN AND CHARGE SYMMETRY

#### 3.1 Introduction

Charge symmetry is a consequence of isotopic spin invariance, the first "internal symmetry" that was postulated in elementary particle physics shortly after the discovery of the neutron. Isotopic spin invariance is broken by the electromagnetic interaction and consequently one expects effects of order the fine structure constant  $\alpha = 1/137$ . Charge symmetry is a lesser symmetry because it only involves a rotation in isospin space through  $\pi$  or a reflection about the 1-2 plane of charge space. In the case of nucleons charge symmetry has as a

consequence that observables are unaffected by changing neutrons into protons and protons into neutrons.

The classification of the nucleon-nucleon interaction within the isospin formalism has been presented by Henley and Miller.<sup>22</sup> In brief one can distinguish four interactions. Of these only the interactions classified as (3) and (4) in Ref. 22 concern charge-symmetry breaking:

(3) Charge-asymmetric, charge-dependent interactions, which preserve symmetry under the interchange of nucleons  $i$  and  $j$  in isospin space, denoted by

$$V_{ij} = D \{ \tau_3(i) + \tau_3(j) \} .$$

In this and the following expression the quantities  $D$ ,  $E$ , and  $F$  represent functions of space and spin coordinates,  $\vec{t}(i)$  and  $\vec{t}(j)$  are the isospin operators for nucleons  $i$  and  $j$ , and  $\tau_3(i)$  and  $\tau_3(j)$  are the third components of the isospin operators. This interaction only affects the  $n$ - $n$  and  $p$ - $p$  systems; there is no isospin mixing since  $[T^2, T_3] = 0$ . The quantities  $\vec{T}$  and  $T_3$  are the total isospin operator and the third component of the total isospin operator, respectively.

(4) Charge-asymmetric, charge-dependent interactions, which are asymmetric under the interchange of nucleons  $i$  and  $j$  in isospin space, denoted by

$$V_{ij} = E \{ \tau_3(i) - \tau_3(j) \} + F \{ \vec{t}(i) \times \vec{t}(j) \}_3 .$$

This interaction only affects the  $n$ - $p$  system; it causes isospin mixing.

### 3.2 Evidence for Class IV Charge-Symmetry Breaking Interactions

#### Neutron-Proton Elastic Scattering:

Charge symmetry of the  $n$ - $p$  interaction leads to the complete separation of the isovector and isoscalar parts of the scattering matrix for  $n$ - $p$  elastic scattering. In the even (odd) partial waves the isovector part contains spin singlet (triplet) and the isoscalar part spin triplet (singlet) contributions only. The concept of charge symmetry forbids transitions between the two parts of the scattering matrix and thus between the spin triplet and singlet states. The triplet-singlet transition amplitude  $f_{TS}$  is thus forced to vanish. This restriction in turn leads to exactly equal polarizations of neutrons and protons in the scattering of initially unpolarized particles. Thus, for a given (neutron) scattering angle  $\theta$  in  $n$ - $p$  scattering, the concept of charge symmetry implies:

$$\Delta P(\theta) \equiv P_N(\theta) - P_p(\pi-\theta) \equiv 0 ,$$

i.e. the equality of scattered and recoil nucleon polarization. Exactly the same considerations hold for the analyzing powers  $A_N(\theta)$  and  $A_p(\pi-\theta)$  and their difference  $\Delta A$  in the scattering of polarized nucleons.

If on the other hand, charge symmetry is given up, isospin mixing via spin triplet-singlet transitions becomes possible and a non-zero difference  $\Delta A$  will in general be observed. Such a difference is directly proportional to the amplitude  $f_{TS}$  and thus to the existence of class IV charge-symmetry breaking interactions. From the detection of a non-vanishing analyzing power difference  $\Delta A$  the amplitude  $f_{TS}$  can be determined to the extent that the other interfering amplitude is known, since

$$\Delta A = \frac{2}{\sigma_0} \operatorname{Re} [b^* f_{TS}] ,$$

where the centre-of-mass n-p scattering amplitude is written as<sup>12</sup>:

$$M = \frac{1}{2} \left[ (a+b) + (a-b)(\vec{\sigma}_1 \cdot \hat{n})(\vec{\sigma}_2 \cdot \hat{n}) + (c+d)(\vec{\sigma}_1 \cdot \hat{m})(\vec{\sigma}_2 \cdot \hat{m}) + (c-d)(\vec{\sigma}_1 \cdot \hat{l})(\vec{\sigma}_2 \cdot \hat{l}) \right. \\ \left. + e(\vec{\sigma}_1 + \vec{\sigma}_2) \cdot \hat{n} + f_{TS}(\vec{\sigma}_1 - \vec{\sigma}_2) \cdot \hat{n} \right] .$$

The various quantities in this equation are as defined above.

La France et al.<sup>23</sup> have listed all the spin-dependent observables in the centre of mass which involve the spin triplet-singlet transition amplitude. Experimental considerations show that the next simplest quantity to be measured in n-p elastic scattering is the difference in the spin-correlation parameters  $C_{xz}(\theta)$  and  $C_{zx}(\theta)$ . The correlation parameter  $C_{xz}$  has the projectile spin transverse to the beam direction in the scattering plane and the target spin longitudinal with the incident beam direction, while for  $C_{zx}$  the reverse holds. Again charge symmetry leads to the equality of  $C_{xz}(\theta)$  and  $C_{zx}(\theta)$ , but if charge symmetry is broken then one will be able to measure a difference:

$$\Delta C(\theta) \equiv C_{xz}(\theta) - C_{zx}(\theta) .$$

This difference in the spin correlation parameters  $C_{xz}(\theta)$  and  $C_{zx}(\theta)$  is, like the difference in the analyzing powers, directly proportional to the spin triplet-singlet transition amplitude:

$$\Delta C = \frac{2}{\sigma_0} \operatorname{Im} [c^* f_{TS}] .$$

All other spin-dependent observables which involve the spin triplet-singlet transition amplitude require the measurement of the polarization of either one or both of the scattered nucleons.

Calculations of the charge-symmetry breaking effects on the analyzing powers of energies up to 460 MeV have been made by Cheung, Henley and Miller<sup>24</sup> and for energies up to 750 MeV by Gersten.<sup>25</sup> The differences in the analyzing powers were calculated as functions of angle and energy taking into account the direct electromagnetic effect (one photon exchange),  $\rho^0$ - $\omega$  meson mixing, and the neutron-proton mass difference effect in charged one pion exchange. Gersten<sup>25</sup> also included the neutron-proton mass difference effect in charged  $\rho$ -exchange.



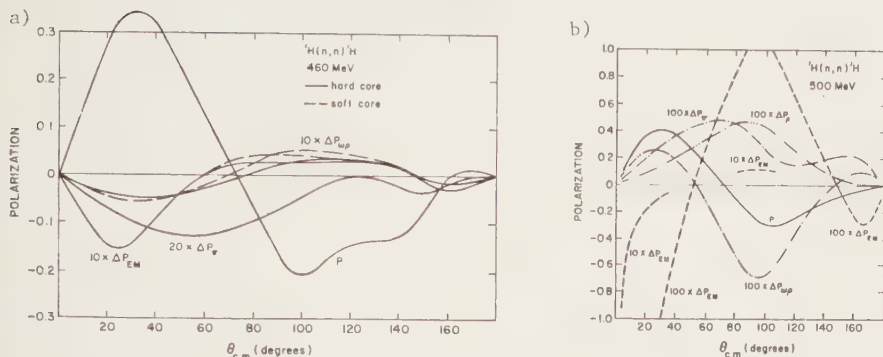


Fig. 2. Theoretical predictions for the difference in polarizations of scattered neutron and recoil proton in elastic scattering of unpolarized neutrons from unpolarized protons due to direct electromagnetic effects ( $\Delta P_{EM}$ ), due to  $\rho^0$ - $\omega$  meson mixing ( $\Delta P_{\omega\rho}$ ), due to the n-p mass difference effect in charged one pion exchange ( $\Delta P_{\pi}$ ) and in  $\rho$ -exchange ( $\Delta P_{\rho}$ ), a) by Cheung, Henley and Miller, ref. 24; b) by Gersten, ref. 25.

The latter approach is in terms of the bar phase shifts with values obtained in N-N phase-shift analyses which assume isospin conservation. The triplet-singlet mixing angles were calculated in the first Born approximation. Of importance at 500 MeV are  $^1P_1$ - $^3P_1$  and  $^1D_2$ - $^3D_2$  mixing. In general the absolute values of the triplet-singlet mixing angles are slowly increasing functions of energy. The 500 MeV predictions by these authors are shown in Fig. 2.

Two experiments to measure the difference  $\Delta A$  between the neutron and proton analyzing powers  $A_n$ - $A_p$  are currently in progress: at TRIUMF with 480 MeV incident neutrons<sup>26</sup> and at IUCF with 200 MeV incident neutrons.<sup>27</sup> Designed as a null-measurement, requiring no accurately known polarization standards, the TRIUMF experiment will determine the difference in angle at which  $A_n$  and  $A_p$  cross through zero ( $\sim 71^\circ$  c.m.). The two interleaved phases of the experiment consist of scattering polarized (unpolarized) neutrons from an unpolarized (polarized) proton target of the frozen spin type. The experiment is intended to provide an unambiguous test of class IV charge-symmetry breaking effects to the level of  $\Delta A = 0.001$ , corresponding to a laboratory angle difference at the zero crossing of  $\sim 0.05^\circ$ . Theoretical predictions for this angular difference by Cheung, Henley and Miller<sup>24</sup> and Gersten<sup>25</sup> are a factor 2.5 and 10, respectively, larger than the experimental accuracy aimed for in the experiment (see Fig. 3).

In the IUCF experiment, in addition to a determination of the displacement in the angle where  $A_n$  and  $A_p$  cross zero, information on the angular dependence of  $\Delta A$  in the range  $75^\circ$ - $120^\circ$  c.m. is obtained by measuring the ratio of the analyzing powers at different angles  $A_n(\theta_1)A_p(\theta_2)/A_n(\theta_2)A_p(\theta_1)$ . This ratio is again independent of beam and target polarization and differs from unity as a consequence of charge-symmetry breaking interactions. The experimental layout is depicted

in Fig. 4. Note that the cross-over angle at 200 MeV is close to 90° and therefore mainly dependent on  $^1P_1$ - $^3P_1$  mixing, while the angular dependence of the ratio of the analyzing powers will also be sensitive to  $^1D_2$ - $^3D_2$  mixing.

The Reaction  $np \rightarrow d\pi^0$ :

In the final state the total isospin equals one, and therefore under isospin conservation only the T=1 n-p component can contribute to the reaction. For the T=1 component certain symmetries hold. For instance the differential cross section is symmetric about 90° in the centre of mass (like  $pp \rightarrow d\pi^+$ ). Similar symmetry relations hold for the vector and tensor polarizations of the deuteron when scattering unpolarized neutrons from unpolarized

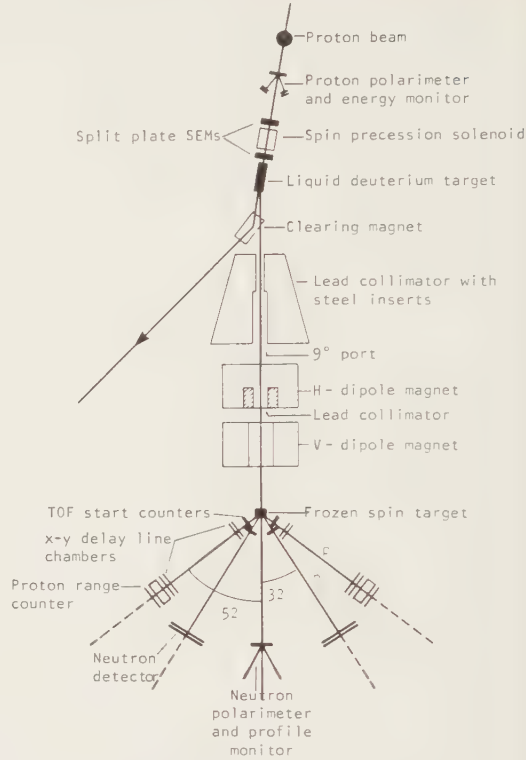


Fig. 3. Experimental layout of the test of charge symmetry in n-p elastic scattering at 480 MeV.

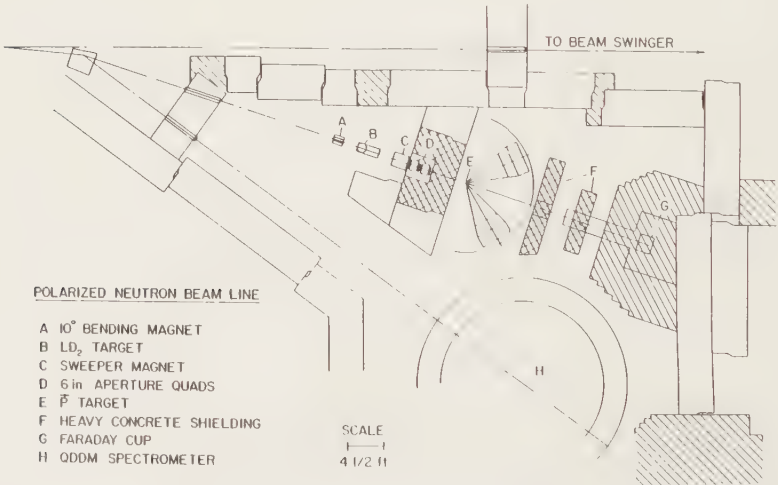


Fig. 4. Experimental layout of the test of charge symmetry in n-p elastic scattering at 200 MeV.

protons. It is to be noted that the vector polarization  $P_y$  and the tensor polarization components  $P_{xz}$  are odd functions in  $\theta$ , while the tensor polarization components  $P_{xx}$ ,  $P_{yy}$  and  $P_{zz}$  are even functions in  $\theta$ . When scattering polarized neutrons from unpolarized protons or unpolarized neutrons from polarized protons the analyzing powers are identical ( $A_n = A_p$ , like  $np \rightarrow np$ ). Unfortunately the crossover angle, where the analyzing power changes sign, varies rapidly and is only present at incident energies below 450 MeV, making a null experiment a very difficult task. Any forward-backward asymmetry of the differential cross section angular distribution points to the existence of an isospin-mixing amplitude or to the presence of class IV interactions.

The most recent measurement of the forward-backward asymmetry is the one by Hollas et al.<sup>28</sup> A nearly monoenergetic neutron beam of 795 MeV was incident on a liquid hydrogen target. The recoiling charged particles were momentum analyzed, a time-of-flight measurement allowed a determination of their rest mass. A complete angular distribution was obtained choosing  $3^\circ$  wide bins between  $2^\circ$  and  $178^\circ$  in the centre of mass. Defining the forward-backward asymmetry parameter  $A_{fb}$  as the differences in the integrated differential cross section from 0 to  $\pi/2$  and from  $\pi/2$  to  $\pi$  divided by the sum, no evidence for charge-symmetry breaking interactions was found to an order of 0.5% in the asymmetry parameter  $A_{fb}$ .

The angular distribution asymmetry has been calculated at 577 MeV by Cheung, Henley and Miller<sup>29</sup> taking into account charge-symmetry breaking contributions due to one photon exchange,  $\pi^0$ - $\eta$  and  $\rho^0$ - $\omega$  meson mixing, and the neutron-proton mass difference effect in charged one pion exchange. The dominant contribution is due to  $\pi^0$ - $\eta$  mixing. The predicted value for the asymmetry parameter  $A_{fb}$  at 577 MeV is -0.16%, while at 800 MeV the predicted value due to  $\pi^0$ - $\eta$  mixing alone is -0.11%.<sup>28</sup> Clearly experiments need to improve on the uncertainty in the asymmetry parameter  $A_{fb}$  (approximately by a factor 10) in order to provide quantitative information on charge-symmetry breaking. The main obstacle at present is the uncertainty in the correction for deuteron losses, since deuteron total reaction cross sections are poorly known at intermediate energies.

## References

- 1) E.H. Thorndike, Phys. Rev. 138 (1965) B586.
- 2) A.E. Woodruff, Ann. Phys. (N.Y.) 7 (1959) 65.
- 3) J.M. Potter, J.D. Bowman, C.F. Hwang, J.L. McKibben, R.E. Mischke, D.E. Nagle, P.B. Debrunner, H. Frauenfelder and L.B. Sorenson, Phys. Rev. Lett. 33 (1974) 1307; D.E. Nagle, J.D. Bowman, C. Hoffman, J. McKibben, R. Mischke, J.M. Potter, H. Frauenfelder and L. Sorenson, in High energy

- physics with polarized beams and polarized targets - 1978, ed. G.H. Thomas, AIPCP #51 (AIP, New York, 1979), p. 224.
- 4) R. Balzer, R. Henneck, Ch. Jacquemart, J. Lang, M. Simonius, W. Haeberli, Ch. Weddigen, W. Reichart and S. Jaccard, *Phys. Rev. Lett.* 44 (1980) 699; R. Balzer, W. Haeberli, R. Henneck, S. Jaccard, Ch. Jacquemart, J. Lang, W. Reinart, Th. Roser, M. Simonius and Ch. Weddigen, *SIN Newsletter* 13, (1980) 50.
  - 5) P. von Rossen, U. von Rossen and H.E. Conzett, in *Polarization phenomena in nuclear physics - 1980*, ed. G.G. Ohlsen et al., AIPCP #69 (AIP, New York, 1981) p. 1442.
  - 6) D.E. Nagle, J.D. Bowman, R. Carlini, R.E. Mischke, H. Frauenfelder, R.W. Harper, V. Yuan, A.B. McDonald and R. Talaga, in *High energy spin physics - 1982*, ed. G.M. Bunce, AIPCP #95 (AIP, New York, 1983), p. 150.
  - 7) N. Lockyer, T.A. Ronanowski, J.D. Bowman, C.M. Hoffmann, R.E. Mischke, D.E. Nagle, J.M. Potter, R.L. Talaga, E.C. Swallow, D.M. Alde, D.R. Moffett and J. Zyskind, *Phys. Rev. Lett.* 45 (1980) 1821.
  - 8) B. Desplanques, J.F. Donoghue and B.R. Holstein, *Ann. Phys. (N.Y.)* 124 (1980) 449.
  - 9) V.R. Brown, E.M. Henley and F.R. Krejs, *Phys. Rev. C* 9 (1974) 935; E.M. Henley and F.R. Krejs, *Phys. Rev. D* 11 (1975) 605.
  - 10) L.S. Kisslinger and G.A. Miller, *Phys. Rev. C* 27 (1983) 1602.
  - 11) G. Nardulli in *High energy spin physics - 1982*, ed. G.M. Bunce, AIPCP #95 (AIP, New York, 1983), p. 156.
  - 12) J. Bystricky, F. Lehar and P. Wintermiz, Université de Montréal Report CRMA-1127.
  - 13) J. Binstock, R. Bryan and A. Gersten, *Ann. Phys. (N.Y.)* 133 (1981) 355.
  - 14) R. Bryan and A. Gersten, *Phys. Rev. Lett.* 26 (1971) 1000; erratum 27 (1972) 1102.
  - 15) R. Zulkarneev, Kh. Murtazaev and V. Khachaturov, *Phys. Lett.* 61B (1976) 164 and references therein.
  - 16) H.E. Conzett, *Hadronic J.* 5 (1982) 714.
  - 17) E. Aprile, C. Eisenegger, R. Hausammann, E. Heer, R. Hess, C. Lechanoine-LeLuc, W.R. Leo, S. Morenzoni, Y. Onel, D. Rapin and S. Mango, *Phys. Rev. Lett.* 47 (1981) 1360.
  - 18) L.G. Greeniaus, private communication.
  - 19) T.S. Bhatia, G. Glass, J.C. Hiebert, L.C. Northcliffe, W.B. Tippens, B.E. Bonner, J.E. Simmons, C.L. Hollas, C.R. Newsom, P.J. Riley and R.D. Ransome, *Phys. Rev. Lett.* 48 (1982) 227.
  - 20) D.A. Hutcheon, private communication.
  - 21) R. Handler, S.C. Wright, L. Pondrom, P. Limon, S. Olsen and P. Kloeppel, *Phys. Rev. Lett.* 19 (1967) 933.

- 22) E.M. Henley and G.A. Miller, in *Mesons in Nuclei*, ed. M. Rho and D.H. Wilkinson (North-Holland, Amsterdam, 1979), vol. I.
- 23) P. La France, C. Lechanoine, F. Lehar, F. Perrot, L. Vinet and P. Winternitz, *Nuovo Cimento* A64 (1981) 179.
- 24) C.-Y. Cheung, E.M. Henley and G.A. Miller, *Nucl. Phys.* A305 (1978) 342.
- 25) A. Gersten, *Phys. Rev.* C24 (1981) 2174.
- 26) J. Birchall, N.E. Davison, H.P. Gubler, W.P. Lee, J.P. Svenne, W.T.H. van Oers, R. Abegg, C.A. Miller, E.B. Cairns, H. Coombes, C.A. Davis, P. Green, L.G. Greeniaus, W.J. McDonald, G.A. Moss, G. Roy, J. Soukup, G.M. Stinson, H.E. Conzett and G.R. Plattner, in *High energy spin physics - 1982*, AIP Conf. Proc. 95 (AIP, New York, 1983), p. 165.
- 27) S.E. Vigdor, A.D. Bacher, D. Duplantis, W.W. Jacobs, H.-O. Meyer, G.L. Moake, P. Schwandt, E.J. Stephenson, L.D. Knutson, P.A. Quin, J. Sowinski, B.P. Richwa and P.L. Jolivet, in *Polarization phenomena in nuclear physics - 1980*, AIP Conf. Proc. 69 (AIP, New York, 1981), p. 1455.
- 28) C.L. Hollas, C.R. Newsom, P.J. Riley, B.E. Bonner and G. Glass, *Phys. Rev.* C24 (1981) 1561.
- 29) C.-Y. Cheung, E.M. Henley and G.A. Miller, *Phys. Rev. Lett.* 43 (1979) 1215.



## THE DEUTERON PROPERTIES

T.E.O. ERICSON

CERN, 1211 Geneva 23, Switzerland

The low energy deuteron parameters are discussed in view of their physical information and their constraints on the description of the deuteron in terms of more exotic subsystems. Important recent progress has recently been achieved on the understanding of the root mean square radius, the quadrupole moment, the  $D/S$  parameter and the asymptotic  $S$  state amplitude. There is a strong model-independent interlinkage of various quantities, which holds independent of the detailed model. Strong evidence is found for quantitative dominance of pionic interactions, particularly for the  $D/S$  ratio and quadrupole moment.

Our understanding of  $NN$  interactions and their electromagnetic effects have traditionally been very heavily influenced by a handful of basic quantities in the deuteron. These are: the binding energy  $\epsilon$ , the magnetic moment  $\mu_d$ , the quadrupole moment  $Q$ , the "deuteron radius"  $r_d$ , the asymptotic value of the  $S$  wave function  $A_S$  and the asymptotic  $D/S$  ratio  $\eta$ .

Since similar quantities exist also in other nuclear systems, it is worthwhile to enquire why the present ones have become such extraordinary touchstones in nuclear physics. There are three basic reasons for this:

- first, they are all known to an experimental precision which is very high;
- second, most of them are strongly interlinked between themselves; this imposes strong constraints in any description;
- third, because of the highly well-defined conditions, it is routine to compare the predictions of these quantities in any serious model and to compare them to the very precise experimental values.

The last condition may sound trivial, but it is not. The fact that theoreticians return to a description of the same quantities in depth means that a number of smaller corrections are well understood. In this manner, the significance of the high experimental precision becomes fully relevant. These quantities rapidly separate theoretical chaff from wheat, and holds new approaches up to a rapid examination of their practical worth. This is of particular importance at the present moment, when the nature of  $NN$  interactions is being re-examined in the light of QCD. The numerical experimental values of the various quantities are given in Table 1 [excellent previous versions are found in Refs. 1 and 2] and are commented on below. While the main present developments concern  $Q$ ,  $r_d$ ,  $A_S$  and  $\eta$ , I will also discuss, for completeness,  $\epsilon$  and  $\mu_d$ .



Before this, however, it is useful to examine briefly the deuteron in the potential approach which, of course, has its limits. The usual deuteron equations for the coupled S and D states are

$$\begin{aligned} u'' &= [-\alpha^2 + U_{00}]u + U_{02}w \\ w'' &= [-\alpha^2 + 6/r^2 + U_{22}]w + U_{20}u, \end{aligned} \quad (1)$$

where the  $U_{ij} = MV_{ij}$  are the potentials. The asymptotic wave functions  $u$  and  $w$  are normalized so that

$$\begin{aligned} u &\rightarrow A_S e^{-\alpha r} \\ w &\rightarrow nA_S e^{-\alpha r} \end{aligned} \quad \text{as } r \rightarrow \infty \quad (2)$$

A crucial property of the potentials is the notoriously weak central interaction  $U_{00}$ . In fact, if one would substitute the attractive central OPEP interaction in the S state and ignore the D wave coupling, the  $\pi NN$  coupling constant must be increased by a factor of three to produce binding, quite apart from the fact that short-range interaction is repulsive. In the D state  $U_{22}$  is repulsive and does not produce binding. The deuteron binding is thus a crucial property of the S-D channel coupling. It is mainly produced by the OPEP tensor potential as was observed long ago by Glendenning and Kramer<sup>3</sup>. The asymptotic S and D wave normalizations are the deuteron "coupling constants". They are directly and externally measurable in various ways as a matter of principle. The S wave normalization governs in particular the radius  $r_d$ , while the quadrupole moment is proportional to  $A_S^2$  and also, very roughly, to  $n$ .

The S wave amplitude is related to the deuteron effective range  $\rho(-\epsilon, -\epsilon)$  by the relation

$$A_S^2 \approx A_S^2(1+n^2) \equiv \frac{2\alpha}{[1-\alpha\rho(-\epsilon, -\epsilon)]} \quad (3)$$

This quantity has proved difficult to determine directly with sufficient accuracy. On the other hand, the closely related value  $\rho(-\epsilon, 0)$ , the mixed effective range is directly measurable and is defined by

$$\rho(-\epsilon, 0) \equiv \frac{2}{\alpha} [1 - (\alpha a_t)^{-1}] \quad (4)$$

The triplet scattering length  $a_t$  is in practice fixed by the incoherent cross-section  $\sigma_0 = \pi(3a_t^2 + a_S^2)$ . The experimental values by Houk<sup>4</sup> and Dilg<sup>5</sup>,

2043.6(2.2) fm<sup>2</sup> and 2049.1(1.4) fm<sup>2</sup> are inconsistent within error bars. Since there is no obvious reason to discard any one of them, we use them both to obtain

$$\begin{aligned} \rho_{\text{toulk}}(-\epsilon, 0) &= 1.750(5) \\ \rho_{\text{Dilg}}(-\epsilon, 0) &= 1.760(5) \\ \hline \rho_{3V}(-\epsilon, 0) &= 1.755(4) \text{ (2ppt)} \end{aligned} \quad (5)$$

Models for the deuteron incorporating OPEP characteristically give the effective range  $\rho \approx 1.76$  fm to within some per cent, but the result has some model-dependence, and is far less accurate than experiments. The *difference*  $\delta\rho = \rho(-\epsilon, -\epsilon) - \rho(-\epsilon, 0)$  is, however, nearly zero, and a magnitude smaller than might have been dimensionally expected. This is a natural consequence of OPEP as pointed out by Noyes<sup>6</sup>. Klarsfeld et al.<sup>7</sup> in a recent manuscript, have found that this difference correlates very accurately with the exact value for the triplet scattering length  $a_t$  in numerous models (see Fig. 1).

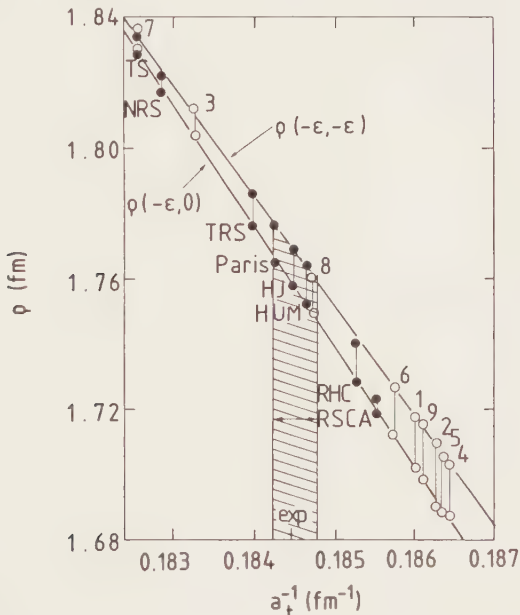


FIGURE 1

The deuteron effective range  $\rho(-\epsilon, -\epsilon)$  and the mixed effective  $\rho(-\epsilon, 0)$  versus  $a_t^{-1}$  in various models according to Klarsfeld et al.<sup>7</sup>. Note that the *difference*  $\delta\rho = [\rho(-\epsilon, -\epsilon) - \rho(-\epsilon, 0)]$  is very well determined by  $a_t^{-1}$  and that this difference is very model-independent in this variable.

Let us now return to experimental deuteron parameters and their interpretation in more detail.

*Binding energy*<sup>8</sup>

$$\epsilon = 2.224\,579(9) \text{ MeV} \quad (4 \text{ ppm}) \quad (6)$$

This quantity is known to a precision far outside any theoretical possibility, and it is in this sense irrelevant. It is, however, extremely important that theoretical deuteron descriptions have this quantity correct, even if this means some minor phenomenological adjustments at short range. The reason is that the deuteron scale parameter is the inverse wave number  $R \equiv \alpha^{-1}$ .

$$\alpha^{-1} \equiv R = 4.31896(2) \text{ fm} \quad (5 \text{ ppm}) \quad (7)$$

using relativistic kinematics. The non-relativistic value often used

$$\alpha_{\text{NR}}^{-1} \equiv R_{\text{NR}} = 4.31768(2) \text{ fm} \quad (8)$$

differs by 0.3 parts per thousand. This difference is nearly, but not quite irrelevant, since it does contribute about  $2 \times 10^{-3} \text{ fm}$  to the experimentally determined mixed effective range parameter  $\rho(-\epsilon, 0)$  known to about  $\pm 5 \times 10^{-3} \text{ fm}$ .

*Magnetic moment*<sup>9</sup>

$$\mu_d = 0.857\,406(1) \text{ n.m.} \quad (1 \text{ ppm}) \quad (9)$$

Once more this quantity is known to precision far beyond theoretical power. The most remarkable feature of the magnetic moment is that it is given to high accuracy as the sum of the neutron and proton values

$$\mu_n + \mu_p = 0.879\,696 \text{ n.m.} \quad (10)$$

The discrepancy is only

$$\Delta\mu_d = -0.02229 \text{ n.m.} \quad (11)$$

i.e., -2.6%. This, however, does not give full justice to the comparison, since there is a very substantial cancellation between  $\mu_n$  and  $\mu_p$ , which eliminates the isovector nuclear magnetic moment. A better measure of the scale would seem to be

$$\Delta\mu_d / (|\mu_n| + |\mu_p|) = -0.5\% \quad (12)$$

This result is most remarkable, since it means that whatever further descriptions are chosen, the nucleonic results must be preserved to within a fraction of a per cent.

Let us briefly examine various sources of corrections to the nucleonic sum. These fall into three categories.

A) Corrections assuming point nucleons. Since the magnetic moment occurs from currents, it is clear that contributions from orbital motion of the nucleons are important in principle. The fact that the deuteron is part of the time in a  $D$  state will generate a well-defined correction in any potential description, and this is the basis for the classical determination of the  $D$  state probability of the deuteron. However, even for pointlike nucleons, there are several additional, well-defined, corrections generated by minimal coupling from the LS and LL potentials. The physics of these corrections has been very well discussed by Scheerbaum<sup>10</sup>. It is in practice of very short range and therefore quite model-dependent with contributions of a few per cent.

B) Isobar ( $\Delta, N^*$ ) components enter the deuteron wave function. This depletes the nucleon content and the nucleon contributions to  $\mu_d$ . At the same time it adds the isobar contributions proportional to their probability and their magnetic moments. Both of these quantities are imperfectly known.

C) At short distances, the deuteron may be in a six-quark or more complex state. Like for the isobar case, the contribution will depend both on the probability and the magnetic moment of this state.

In view of the fact that the magnetic moment is only one single number, there are clearly too many possibilities for a reliable test of any of these contributions. In fact, it would not even be trivial to test the point nucleon assumption well. As a consequence, I cannot but agree with the statement of Thomas<sup>2</sup> in the Vancouver Conference: "An apparently innocuous, well-understood property has turned into a nightmare".

In spite of the many possibilities, the magnetic moment is still a major restriction. It is far from trivial to accommodate more than about 2% at most of any exotic admixture into the deuteron wave function without actively provoking a discrepancy in the magnetic moment (a fortuitous agreement could, of course, occur, but should then be explained).

Let us now consider the remaining quantities for which substantial experimental and theoretical progress has taken place recently.

#### *The deuteron radius $r_d$*

This quantity is determined from highly accurate values for the  $q^2$  term in the deuteron form factor as measured in the ratio of  $eD/ep$  scattering in the low  $q^2$  region. The deuteron charge radius  $\langle r_c^2 \rangle^{\frac{1}{2}}$  is in a sense the primary

number, but this is corrected for neutron and the proton form factors (or charge radii) so as to have an "intrinsic" deuteron radius. This defines the deuteron radius as

$$r_d^2 = \langle r_C^2 \rangle - \langle r_p^2 \rangle - \frac{3}{4} \frac{1}{M_p^2} + 6(dG_{en}/dq^2)_{q^2=0} \quad (13)$$

Both the proton and neutron form factors are known to a sufficient accuracy so that no new uncertainties of significance is introduced by this procedure. There are two determinations of  $r_d$ , inconsistent within the quoted accuracy\*). The determination of Bérard et al.<sup>12</sup> gives  $r_d = 1.9650(45)$  fm, while Simon et al.<sup>11</sup> find 1.9576(68) fm. There is no obvious preference of one with respect to the other, so that the average value is  $r_d = 1.9627(38)$  fm. This number includes meson-exchange contributions, etc., since no attempt has been made to include any many-body corrections.

One may well ask whether it is appropriate to introduce a definition of  $r_d$ , which implicitly assumes that the deuteron consists of nucleons. The nucleon size correction is about 7.5%, while the experimental numbers are quoted to a precision of 2 to 3 parts per thousand. While the mathematical definition of  $r_d$  causes no problem, it might well be questioned whether it has much sense to correct for nucleon size in the deuteron to a precision of a few per cent in the correction term. The answer to this is yes: the spatial regions which are affected by extended nucleon corrections extend to 4 to 8 fm which is very large. To a precision of a few per cent and even beyond in the correction, it is appropriate simply to subtract off the nucleon size. I have, however, not found a discussion about this point in the literature.

The deuteron radius is very closely related to the asymptotic S wave amplitude  $A_S$  in a nearly model-independent way, at least on the level of present accuracy.

The radius is related to the wave function by

$$r_d^2 = \frac{1}{4} \int_0^\infty r^2 (u^2 + w^2) dr + \text{MEC} + \text{ISOBAR} + \text{QUARKS, etc.} \quad (14)$$

The overwhelming bulk of the contribution comes from the asymptotic S state  $u \rightarrow v = A_S e^{-\alpha r}$  which gives

$$r_C^{dS} = \frac{1}{4} \alpha^{-\frac{3}{2}} A_S \approx 1.98 \text{ fm} \quad (15)$$

---

\*The definition of  $r_d$  by Simon et al.<sup>11</sup> differs from that of Bérard et al.<sup>12</sup> in that the Darwin-Foldy term  $3/4 M_p^{-2}$  has not been eliminated. In the numbers quoted below, the modern value for the neutron form factor has been used, introducing a small correction to Ref. 12.

i.e., the experimental value to about 1%. The following corrections must be considered: a) the D state contribution of  $+0.023$  fm, i.e.,  $+1.2\%$ ; this term is model-independent to present accuracy; b) the shape correction to  $u(r)$  inside the asymptotic region ( $-2 \pm 0.2\%$ ); this correction is not well investigated, but seems to be quite stable in different approaches (see below for a more detailed discussion); it is the main source of uncertainties; c) meson exchange corrections are of the order of  $+0.002$  to  $0.004$  fm<sup>13</sup>, i.e.  $+0.1$  to  $+0.2\%$ , and are not yet of importance in present discussions; d) isobar and quark effects contribute  $<0.1\%$ , the reason being that there are of short range and contribute only indirectly by a change in  $A_S$ <sup>14,15</sup>; this, however, is automatically included by using the *experimental* value for  $A_S$ .

In order to visualize the dependence of  $r_d$  with  $A_S$  in various well-known deuteron models or models for NN interactions, some of these results are displayed in Fig. 2 (unfortunately,  $r_d$  is unavailable in several models). The linear relation implied by the asymptotic wave function is clearly seen to be a

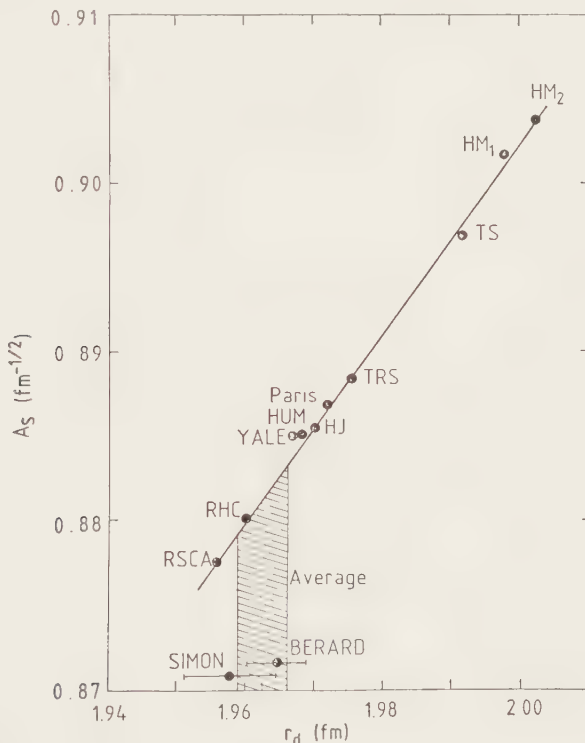


FIGURE 2

The variation of  $r_d$  with  $A_S$  for a number of current NN models. Note the very exact linear correlation independent of potential details. I am indebted to D.W.L. Sprung for several of the numerical values and to R. Machleidt for the information on the Bonn potential (HM). The same relation has been independently observed by Sprung, Klarsfeld and Martorell (private communication)<sup>16</sup>.

general feature nearly independent of other dynamical features. In order to see the shape correction more clearly, I show in Fig. 3 the percentage shape correction to  $r_d/A_S$  versus  $A_S$ . Since the correction is small, and not much precision is needed, a good guide to the functional dependence is given even by very crude S wave functions. From Hulthén wave functions, the correction is expected to be given by  $-\frac{5}{9}(\alpha\rho)^3$  to leading order in terms of the effective range. Indeed, the various points scatter closely around this line. In view of the precision, it is quite possible that the scatter reflects numerical inaccuracy rather than model dependence.

From these results, it is possible to obtain the first direct determination of the asymptotic S wave amplitude using Fig. 2, as indicated in Table II. This result, taken together with the result of Eq. (5) establishes *experimentally*

$$\delta\rho = -0.018(13) \text{ fm} \quad (16)$$

According to Fig. 1, the expected value of  $\delta\rho$  of  $+0.012$  fm has opposite sign and is nearly model-independent. The discrepancy of  $0.030(13)$  fm is slightly more than two standard deviations, so there is no major internal inconsistency in the data. In spite of this discrepancy, the present analysis establishes for the first time that direct experimental data give  $\delta\rho \approx 0$ .

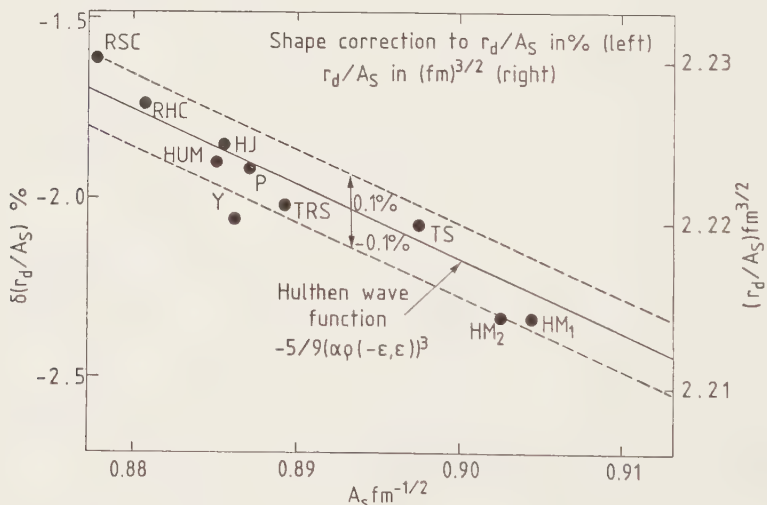


FIGURE 3

The percentage size correction of  $r_d/A_S$  versus  $A_S$  for the same models. Note the small model-dependence. The solid line is the size correction using Hulthén wave functions.



as is expected from OPEP. The "natural" magnitude of  $|\delta\rho|/\rho$  is about 5% while OPEP models in general give  $|\delta\rho|/\rho \leq 0.5\%$ . An elimination of the experimental inconsistencies would clearly be of considerable interest as a more accurate test.

#### *The D/S ratio $\eta$*

This quantity has been notoriously difficult to determine experimentally. In the past few years, three different methods of high precision have become available, so that this quantity now is known to a few per cent. The methods are all based on the orientation of the deuteron using tensor polarization, which singles out the D state. All but one of the experiments are first generation ones, so that it is not obvious that all precautions have been taken for high precision results both in the experiments and in the analysis. This was the topic of the deuteron workshop for one and a half days just before this Conference. The present results are given in Table III

Two words of caution must be given. First, the accuracy of the analytical extrapolation is not well established at the present high level of precision and may be a source of systematic error. This problem does not affect subCoulomb stripping, which therefore may be more useful for future improvements. Second, the accuracy of the average value is dominated by one single experiment<sup>18</sup>, and may give a too optimistic view of the actual precision once systematics are included.

#### *Quadrupole moment Q*

The standard literature value  $Q = 0.2860(15) \text{ fm}^2$  (5 ppt) is due to Reid and Vaid<sup>21</sup>. This is based on a theoretical analysis using variational techniques of highly accurate molecular beam experiments. A new value  $Q = 0.28590(30) \text{ fm}^2$  (1 ppt) has just become available<sup>20</sup>. This is based on an improved analysis by Bishop and Cheung<sup>22</sup>, as well as the realization that the variational techniques are exceptionally appropriate for the present case. The experimental value has now reached a precision which is presently outside theoretical reach.

With this survey of the experimental quantities, let us now turn to their significance.

As a first example, consider the question of the deuteron wave function as related to the experimental constraints. In a contribution to the Conference, Sprung et al.<sup>23</sup> explicitly construct the S and D wave functions using the following assumptions and procedures:

- take Q and  $r_d$  as constraints using inequalities (the MEC corrected value for Q, and the corrected  $r_d$  from Ref. 11 was used);
- assume  $\eta$  known;
- assume the long-range part of interaction known, whether OPEP or an improved OPEP based on theory;

- integrate  $u$  and  $w$  inwards from infinity consistent with the constraints to a value  $r = R$ ;
- vary  $\eta$  and insist on the validity of the inequalities which follow from the constraints.

Their conclusion is that  $\eta$  is constrained to a small band of possible values. They also conclude that  $u(r)$  is very well determined outside 1 fm, while  $w(r)$  is rather ill-determined inside about 1.6 fm. As an example for the Turreil-Reuben-Sprung potential  $\eta_{\text{TRS}}(R=1.6 \text{ fm}) = 2.67(5) \times 10^{-2}$ . In Fig. 4, their results are shown using OPEP with the Paris potential for comparison. The interest of this method is that it does not enquire into the short-range behaviour of the interaction. It is clear that such an approach yields a value for  $\eta$  in very good agreement with experiments, which implicitly implies that  $Q$  and  $r_d$  fix  $\eta$  to a considerable degree. This approach permits one to visualize the model-dependence of these quantities far better than in the past. Unfortunately, the method used loses its power in the region inside about 1.5 fm, and cannot be systematically extended to shorter distances; still, it is most instructive outside this range.

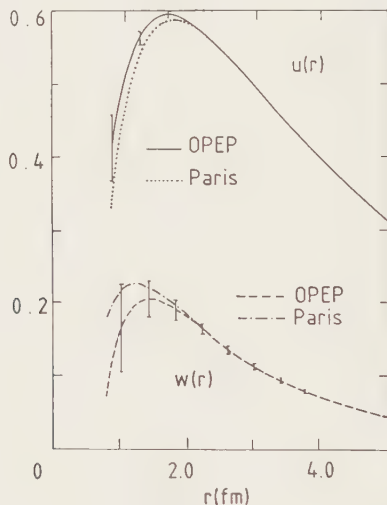


FIGURE 4

The S and D wave functions as constructed by Sprung et al.<sup>23</sup> using OPEP in the external region. The Paris wave functions are given for convenient comparison.

A second example is a recent explicit construction of  $\eta$  and  $Q$  by Rosa-Clot and myself<sup>20</sup>. Our purpose has been to obtain a very quantitative test of the accuracy of pionic effects in nuclear physics. For this we have developed a method that controllably eliminates contributions inside about 1 fm for these quantities.

The idea is most simply seen as follows, using a potential framework. The equation for the D wave

$$w^u = (\alpha^2 + 6/r^2 + U_{22})w + U_{20}u \quad (17)$$

has strong repulsion both because of the centrifugal barrier as well as due to the very important OPEP contribution to  $U_{22}$ . In this repulsive potential, the D wave is generated by the source function  $U_{20}u$  from the S state via the tensor potential. An *exact* formal solution for  $\eta$  can now be expressed using the *exact* regular solution  $\mathcal{F}_2(r)$  for the homogeneous D state equation.

$$\eta \equiv \int_0^\infty \eta(r) dr = M\sqrt{8} \int_0^\infty r \mathcal{F}_2(r) V_T(r) \tilde{u}(r) dr \quad (18)$$

Here  $\tilde{u} \rightarrow e^{-\alpha r}$  as  $r \rightarrow \infty$ . The idea is now that one does not need to know much about the S wave, and that  $\mathcal{F}_2(r)$  goes very fast to zero near the origin because of the strong repulsion.

In order to see the power of this formulation, Fig. 5 gives  $\eta(r)$  versus  $r$  for iterated pure OPEP and the Paris potential using the same  $\tilde{u}$ . The two agree to 4%, which is very remarkable as a starting approximation. Even the OPEP Born approximation is good to 20%. It is important that the region inside 1 fm is unimportant and controllable. The basic problem is not to improve the accuracy, but how not to spoil it.

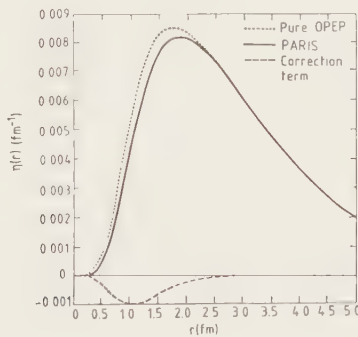


FIGURE 5

The integrand for the D/S ratio with iterated OPEP and with the Paris potential according to Eq. (18). The same  $\tilde{u}$  is used. Note that about one third of the integral originates between 1 and 2 fm and very little inside 1 fm. The OPEP value is an excellent first approximation (from Ericson and Rosa-Clot<sup>20</sup>).

The dependence of the exact  $S$  wave function is very weak indeed (see Fig. 6). Even a purely asymptotic wave gives poor but not unreasonable results, while realistic  $\tilde{u}(r)$  introduce errors of less than 1% with the uncertainty coming in the peak region of the integrand. It is very important to note that  $u$  and  $w$  are not required to normalize to unity, so that isobar-quark admixtures are easily accommodated with no change.

The corrections and uncertainties are the following.

A) The  $2\pi$  potential (-4.3%)

This contribution is theoretically well founded up to the exchange of  $\approx 7$  pion masses. The contributions are generated by a  $\pi N$  scattering (" $\Delta$ "),  $\pi\pi$  phase shifts (of which the well-determined  $P$  wave exchange ( $I=1, J=1$ ) is very dominant) and the crossed and uncrossed  $2\pi$  exchange between nucleons. These contributions are all accurately fixed apart from an over-all (improvable)  $\pm 15\%$  normalization uncertainty. The uncertainty in  $\eta$  from this source is about  $\pm 0.6\%$ . The theoretical contributions agree well with the results of the Paris potential even after the latter has had phenomenological adjustments inside 0.8 fm.

B) The  $\pi N$  coupling constants

To a precision of a few parts in a thousand the effective coupling constant is the weighted mean or charged and neutral pions

$$f^2 = \frac{2f_c^2 + f_0^2}{3} \quad \mu = \frac{2\mu_c + \mu_0}{3} \quad (19)$$

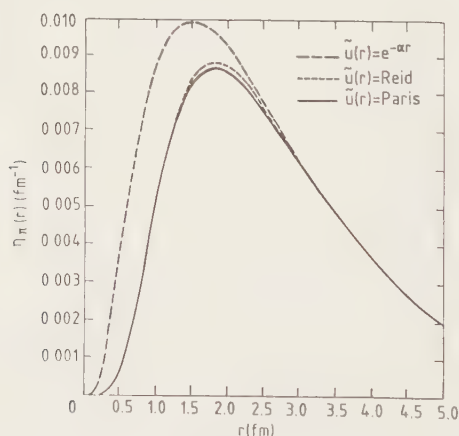


FIGURE 6

Dependence of the  $D/S$  integrand (18) on the  $S$  wave function. Even extremely poor wave functions like  $\exp(-\alpha r)$  give a fair result and normal wave functions introduce nearly negligible model dependence (from Ericson and Rosa-Clot<sup>20</sup>).

Until very recently the experimental neutral coupling indicated a pseudovector coupling with  $f_C^2 = f_0^2 = 0.0790^{24}$ . A recent new value of the  $\pi^0$  coupling constant from pp forward dispersion relations by Kroll<sup>25</sup> gives

$$f_{\text{exp}}^2 = 0.776(9) \quad (20)$$

This is -2% lower than previously and is consistent with the pseudoscalar coupling. With this new value, a major source of worry about consistency has been removed.

C) The  $\pi NN$  form factor

This quantity is the largest single uncertainty in the present analysis. The form factor can be parametrized for small  $t$  as

$$K(t) = \frac{\Lambda^2 - \mu^2}{\Lambda^2 + t} \quad (21)$$

corresponding to an equivalent uniform radius

$$R = \sqrt{10}/\Lambda \quad (22)$$

This parametrization is valid whatever the origin of the form factor, which could be due to extended quark bags. In a pion exchange language, the form factor requires at least a  $3\pi$  exchange.

The effect on the integrand for  $\eta$  is seen in Fig. 7 for various  $\Lambda$  and  $R$ . In view of the close agreement of  $\eta$  with theory, it is very awkward to accept a phenomenological  $\Lambda \lesssim 1000$  MeV, i.e., more than a -3% reduction. This indicates  $R \lesssim 0.65$  fm.

Other information on the form factors is hard to obtain, but  $NN$  scattering data indicate large  $\Lambda$ <sup>26</sup>, consistent with the present observation. Dispersion relations for  $\Lambda$  indicate it to be  $\geq 1000$ -1400 MeV/c<sup>27</sup>. On the other hand, quark bag models favour  $\Lambda \lesssim 700$  MeV/c<sup>28</sup>, indicating a conflict.

A similar analysis can be made of the quadrupole moment with  $Q = Q_1 + Q_2$

$$\begin{aligned} Q_1 &= 1/\sqrt{50} \int_0^\infty r^2 u w dr \\ Q_2 &= -1/20 \int_0^\infty r^2 w^2 dr \end{aligned} \quad (23)$$

The  $D$  state contribution is -6% of the total and is easy to evaluate to the required accuracy.

With the previous Green function technique, one can write  $Q_1$  identically as

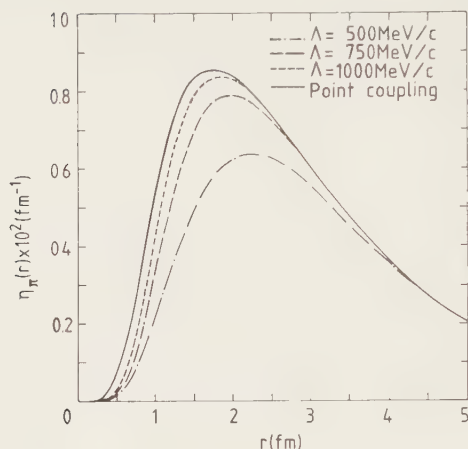


FIGURE 7

Dependence of the D/S integrand on the  $\pi NN$  form factor. The integrand decreases by 3.1%, 8.5% and 19% for the three cases, which correspond to  $R = 0.63$  fm,  $0.84$  fm and  $1.26$  fm. Note how the contributions are modified up to rather large  $r$  as soon as  $\Lambda \lesssim 1000$  MeV (from Ericson and Rosa-Clot<sup>20</sup>).

$$Q_1 \equiv A_S^2 \times (\text{constant}) \times \int_0^\infty F(r) \eta(r) dr \quad (24)$$

The integrand consists of a weight function  $F(r)$ , which is nearly model-independent apart from the very short-range region, and the previous integrand  $\eta(r)$  (see Fig. 8). As a consequence, one expects  $Q$  and  $\eta$  to contain very similar

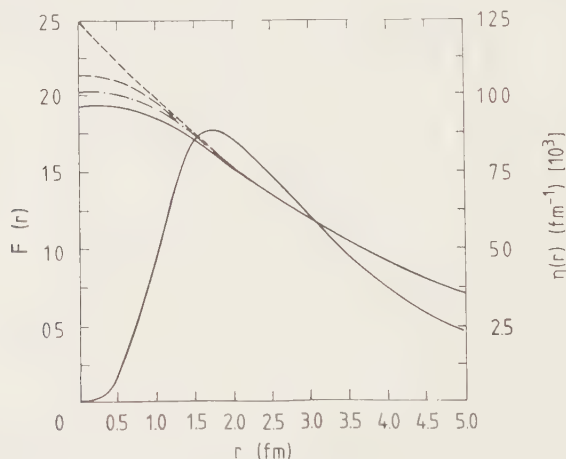


FIGURE 8

The quadrupole weight function  $F(r)$  and the D/S integrand. The folded value is nearly model-independent (from Ericson and Rosa-Clot<sup>20</sup>).

information, apart from the fact that the quadrupole moment emphasizes the intermediate range somewhat more. This is well borne out displaying  $Q/A_S^2$  versus  $\eta$  in units which removes the over-all proportionality of the integrands to the  $\pi NN$  coupling constant. Figure 9 shows that indeed standard major models give a very exact linear relation between these quantities. In fact, the curve is useful, for an early version of the Paris model had a point far off the curve to the right: on investigation, we were informed by the Paris group that this was due to numerical inaccuracies, and the correct point is indeed on the universal line. Quark models with small  $\Lambda$  are also on the line, but they appear out of scale to the left. Using the same  $f^2$  and  $A_S^2$  any other variation of  $Q$  and  $\eta$  will obey the approximate relationship

$$\frac{\Delta Q}{Q} \approx 1.7 \frac{\delta \eta}{\eta} \quad (25)$$

The experimental point in the Figure is obtained using the experimental value  $A_S 0.805^{29}$  and with  $f^2 = 0.078$ . The quadrupole moment is then corrected for MEC contributions according to Kohno<sup>13</sup>, giving the points indicated in the Figure. There is the possibility of a disagreement with *any* potential model, but this conclusion is based on only two standard deviations in  $\eta$ , which, in addition, may have an underestimated error. It is clearly important to increase the precision in  $\eta$  by a factor 2 to 3. In the meantime, accepting the validity of the

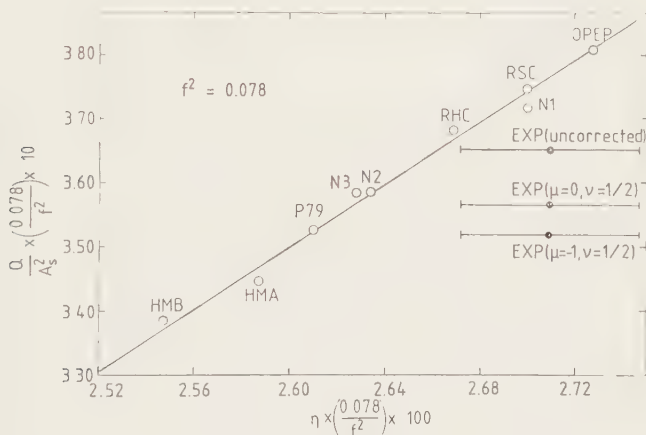


FIGURE 9

Variation of  $Q/A_S^2$  versus  $\eta$  in various standard approaches. Both  $Q$  and  $\eta$  have been corrected for the trivial proportionality to the  $\pi NN$  coupling constant in Born approximation. Note the universal linear correlation to high precision independent of detailed assumptions (from Ericson and Rosa-Clot<sup>20</sup>).



universal line, the quadrupole moment determines  $\eta$  more accurately. This leads to a value for  $\eta \approx 2.65 \times 10^{-2}$  using  $A_S = 0.880$ . This is consistent with the previously quoted value of Klarsfeld et al.

Finally, how is this related to the problem of bag sizes? Apart from the Stony Brook little bag, there is disagreement with data using quark bag form factors straightforwardly. This indicates that some modification in the thinking about two bags in interaction may be needed. A possible way out has been indicated by Guichon and Miller<sup>29</sup>. They observe that a bag is not an inert system. It is therefore logical to antisymmetrize the constituents of two interacting bags. In this way, they find that the corresponding Fock term substantially compensates the form factor effect. Using the condition of continuity in the probability current, they find that there is no problem even with the bag radii beyond 1 fm. In this case, the "form factor" becomes only an "effective form factor". This idea is an interesting one and is well worth to pursue further.

The conclusion of the present discussion is that we can now theoretically relate  $Q$  and  $\eta$  on the level of 1% and that the experimental precision in  $\eta$  must be improved to test this relation. As a by-product, the MEC contributions will be model-independently tested. Even as of now there can be no doubt that  $\eta$  and  $Q$  provide the best quantitative evidence for pions in nuclear physics, and this includes contributions both from rescattering and from the non-trivial region between 1 to 2 fm.

TABLE I  
Deuteron properties\*

$\epsilon = 2.24579(9)$ MeV	(4 ppm)
$\alpha^{-1} = R = 4.31896(2)$ fm	(5 ppm)
$\mu_d = 0.857406(1)$ n.m.	(1 ppm)
$r_d = 1.963(4)$ fm	(2 ppt)
$\rho_{av}(-\epsilon, -\epsilon) = 1.737(12)$ fm	(7 ppt) <sup>+</sup>
$A_S(\text{average}) = 0.8802(20)$	(2 ppt)
$\eta = 0.0271(4)$	(13 ppt)
$Q_d = 0.28590(30)$	(1 ppt)
*Comments are given in the text.	
+Note inconsistency with deduced value 1.767(4) from $\rho(-\epsilon, 0)$ .	

TABLE II

$A_S^{\text{exp}}(\text{Bérard}) = 0.8813(24)$	$\rho_B(-\epsilon, -\epsilon) = 1.744(14) \text{ fm}$
$A_S^{\text{exp}}(\text{Simon}) = 0.8772(36)$	$\rho_S(-\epsilon, -\epsilon) = 1.720(21) \text{ fm}$
$A_S^{\text{exp}}(\text{average}) = 0.8802(20) \text{ (2 ppt)}$	$\rho_{\text{av}}(-\epsilon, -\epsilon) = 1.737(12) \text{ fm} \text{ (7 ppt)}$
*Note that $A_S$ is about three times more accurate than $\rho(-\epsilon, -\epsilon)$ which is of considerable practical use!	

TABLE III  
Determinations of  $\eta$  by different methods

Method	$\eta \times 10^2$	Analysis
elastic ( $\vec{D}, p$ ) <sup>17</sup>	2.63(9)	Analytical extrapolation
$^2\text{H}(\vec{D}, p) ^3\text{H}$ <sup>18</sup>	2.72(4)	"
SubCoulomb Stripping <sup>19</sup>	2.71(8)	
Average <sup>20</sup>	2.71(4)	13 ppt

## REFERENCES

- 1) D.W.L. Sprung, in Few-Body Problems in Nuclear and Particle Physics (Quebec, 1975), p. 475.
- 2) A.W. Thomas, in Nucleon-Nucleon Interactions, AIP Conference Proceedings No. 41 (1978) p. 373.
- 3) N.K. Glendenning and G. Kramer, Phys. Rev. D6 (1962) 2159;
- 4) T.L. Houk, Phys. Rev. C3 (1971) 1886.
- 5) W. Dilg, Phys. Rev. C11 (1975) 103.
- 6) H.P. Noyes, Ann. Rev. Nucl. Sci. 22 (1972) 465.
- 7) S. Klarsfeld, J. Martorell and D.W.L. Sprung, Preprint (1983).
- 8) C. Van der Leun and C. Alderliesten, Nucl. Phys. A380 (1982) 261;

- 9) I. Lindgren, in *Alpha-, Beta- and Gamma-Ray Spectroscopy*, Vol. 2, ed. K. Siegbahn (Amsterdam, 1965), p. 1620.
- 10) R.R. Scheerbaum, *Phys. Rev. C* 11 (1975) 255.
- 11) G.G. Simon et al., *Nucl. Phys. A* 333 (1980) 381.
- 12) R.W. Bérard et al., *Phys. Lett.* 47B (1973) 355.
- 13) M. Kohno, *J. Phys. G: Nucl. Phys.* 9 (1983) L85.
- 14) E. Hadjimichael, *Nucl. Phys. A* 312 (1978) 341.
- 15) M.G. Vassanji et al., *J. Phys. G: Nucl. Phys.* 7 (1981) 1029.
- 16) S. Klarsfeld, J. Martorell and D.W.L. Sprung, Private communication.
- 17) J.T. Londergan et al., *Phys. Lett.* 120B (1983) 270.
- 18) I. Borbély et al., *Phys. Lett.* 109B (1982) 262.
- 19) R.P. Goddard et al., *Phys. Lett.* 118B (1982) 241.
- 20) T.E.O. Ericson and M. Rosa-Clot, *Nucl. Phys. A* 405 (1983) 497.
- 21) R.V. Reid and M.L. Vaida, *Phys. Rev. A* 7 (1973) 1841, *Phys. Rev. Lett.* 34 (1975) 1064E.
- 22) D.M. Bishop and L.M. Cheung, *Phys. Rev. A* 20 (1979) 381, and as cited and discussed in Ref. 20.
- 23) D.W.L. Sprung et al., Contributed paper to this Conference.
- 24) R.D. Viollier et al., *Phys. Lett.* 48B (1974) 99.
- 25) P. Kroll, *Physics Data* 22-1 (1981) Fachinform Zentrum Karlsruhe.
- 26) K. Holinde, *Physics Reports* 68 (1981) 121.
- 27) W. Nutt and B. Loiseau, *Nucl. Phys. B* 104 (1976) 98;  
B. Loiseau, Private communication.
- 28) A.W. Thomas, *Adv. in Nucl. Phys.* 13 (1983) 1.
- 29) P. Guichon and G.A. Miller, CERN Preprint TH. 3649 (1983).

## SEMI-PHENOMENOLOGICAL NUCLEON-NUCLEON POTENTIALS

J.J. de SWART, W.A. van der SANDEN, and W. DERKS

Institute for Theoretical Physics, University of Nijmegen, Toernooiveld 1,  
6525 ED NIJMEGEN, The Netherlands

A review is given of some of the properties of semiphenomenological nucleon-nucleon potentials. Special attention is paid to how they compare with low energy pp-polarization data and with phase shift analyses. Shown is that for all potentials holds, that the long and intermediate range parts of the  $I = 1$  tensorpotential are too strong, and of the  $I = 1$  spin-orbit potential are much too weak.

### 1. INTRODUCTION

In this review about the semiphenomenological description of the nucleon-nucleon (NN) interaction we want to limit ourselves to a discussion of the semiphenomenological NN-potentials. Omitted is therefore the discussion of work based upon dispersionrelations. We think here especially of the work of P. Kroll et al.<sup>1</sup>, of S. Furuichi et al.<sup>2</sup>, and of R. Viollier et al.<sup>3</sup>.

An NN-potential will be called semiphenomenological, when it is obviously not a purely phenomenological one, but when it is based on some underlying theory. Mostly this is some form of meson exchange, but lately also attempts are made to look at quark and/or gluon exchange. These latter potentials are, however, not yet in such a shape that they provide reasonable fits to the data. Any discussion of them will so be omitted.

Important ingredients of all semiphenomenological potential models are the parameters of these models. At present there exist no theory which allows us to calculate, in a parameterfree way, an NN-potential, which predicts realistic phase shifts. Therefore one must introduce in every calculation some free parameters, which are then fitted to the experimental data. It is of course obvious, that the more parameters one has at ones disposal, the easier it will be to get a satisfactory fit to the data. Let us divide these parameters into three sets. The first set will contain the physical parameters. That are the parameters which can be checked, independently, somewhere else in physics. An example is the pion-nucleon coupling constant. For some of these parameters NN scattering is perhaps the only place, where they can realistically be determined. The second set of parameters contains the purely phenomenological parameters. These are introduced to cover up our ignorance and are used at the same time to improve the fit to the data. We think here, for example, of the hard core radii

and of the descriptions of the short range forces. Finally we want to introduce a third set. This set contains those parameters for which it is hard to decide if they belong to either set one or set two. What to think of the mass and the coupling constant of a fictitious  $\sigma$ -particle? The  $\sigma$ -particle can in principle be related to a proper treatment of the broad  $\epsilon$ -meson<sup>4,5,6</sup>, but when this is not done, then we include the parameters in set three. Also the form factors are placed in this set.

## 2. THE POTENTIALS

Let us next mention and discuss shortly some of the (semi) phenomenological potentials. In fact it will be more a mentioning of the different groups working on such potentials. Each of these groups has constructed several potentials, but of course most potentials of the same group are based upon the same underlying philosophy. Let us state at the outset, that we have made a choice of the available potentials and that some are left out intentionally and some unintentionally. We think, however, that it is a fair representation of the presently available NN-potentials.

### 2.1. The Funabashi potentials<sup>7</sup>

These are OBE-potentials, where a rather restricted set of mesons ( $\pi$ ,  $\eta$ ,  $\rho$ ,  $\omega$  and two scalar mesons  $\sigma_0$  and  $\sigma_1$ ) is used. These potentials contain 3 to 4 free physical parameters, 1 or 2 purely phenomenological parameters, and 3 parameters of set three. In total about 8 parameters are used in the parameter fitting.

### 2.2. The Bonn potentials<sup>8,9</sup>

In the past the Bonn group constructed several different OBE-potentials<sup>8</sup>, all containing about 8 to 9 parameters. Six of these were physical (set 1) and the rest belonged to set 3. The newest potential<sup>9</sup> contains again 6 physical parameters, but now about 7 which belong to set 3. They use no purely phenomenological parameters of set 2. The total number of parameters used in their newest potential is about 13.

### 2.3. The Nijmegen potentials<sup>10,11</sup>

The OBE-potentials as constructed by the Nijmegen group can be divided into two different sets. The hard core potentials<sup>10</sup> Nhc have in total 14 parameters, 10 of these are coupling constants (set 1) and 4 are purely phenomenological hard cores (set 2). The soft core potential<sup>11</sup> Nsc has 12 physical parameters (set 1) and one cut-off parameter of set 3. This soft core potential has no purely phenomenological parameters of set 2 and has a total of 13 parameters.

### 2.4. The Paris potentials<sup>12,13</sup>

The first Paris potential<sup>12</sup> (P1) is of mixed origin (dispersion theory and OBE). Only one free parameter  $g_\omega$  belongs to set 1. The short range part is described purely phenomenologically and needs 12 parameters (set 2). This gives

a total of 13 parameters for this P1-potential.

The parametrized Paris potential<sup>13</sup> (P2) is much harder to classify. In their publication<sup>13</sup> the Paris group is very vague and sometimes contradictory about the procedure followed. This potential contains 2 parameters of set 1 and 132 parameters belonging to set 2. It is not clear to us (because it is nowhere clearly explained) how many of these 132 parameters are determined by theory and how many by fitting the data. It is very likely that not all of these parameters are used to fit the data. During the talk at Karlsruhe I was wondering if there were perhaps 100 fitted, or perhaps 50? A private discussion afterwards with B. Loiseau and M. Lacombe made it clear, that for each potential form *at least* one parameter was used. This makes for *at least* 14 purely phenomenological parameters of set 2. As a rough estimate for the total number of parameters effectively used in data fitting we would now like to guess about 20.

The important thing is really not the exact number of effective parameters, but that the parametrization changed for some of the potentials the dispersion theoretical intermediate range part.

#### 2.5. The Argonne potential<sup>14</sup>

The Argonne potential  $v_{14}$  is a purely phenomenological potential with a OPE-tail. The short and intermediate range parts of the potential are parametrized with 28 purely phenomenological parameters.

### 3. WHY DO PEOPLE CONSTRUCT POTENTIALS?

For a proper understanding and appreciation of the different potentials it is enlightening to look into the various motives of the different groups. These motives range from interests in high-energy physics to applications in nuclear physics. For some of these applications one wants very accurate fits to the data, for other applications a less good fit to the scattering data is perhaps sufficient.

Motives finding their origin in relativistic quantum mechanics are:

- (i) a determination of the various meson-nucleon coupling constants;
- (ii) the influence of possible form factors;
- (iii) a study of non-static effects, such as the energy and momentum dependence of the potential;
- (iv) a study of retardation effects.

The Paris potential P1 was motivated by dispersion theory. The  $\pi N$  scattering data, when properly analyzed and analytically continued, determine an important part of the long and intermediate range NN-forces.

The NN-forces are a special case of the more general baryon-baryon interaction. Especially the Nijmegen group started constructing NN-potentials, because they wanted information for use in the study of the YN-interaction ( $\Lambda N$ ,  $\Sigma N$ ,  $\Xi N$ ,

$\Delta\Delta$ , etc.).

For many groups the study of nuclear matter was a motive. In that case the influence of the closed  $N\Delta$  and  $\Delta\Delta$ -channels is probably very important. The Argonne group constructed a special potential  $v_{28}$  for that case.

#### 4. WHICH EQUATIONS ARE USED?

To calculate from the potentials the phase shifts two different methods can be distinguished. The groups working in coordinate space use the familiar Schrödinger equation

$$(\Delta + p^2) \psi(r) = 2mV\psi(r) \quad . \quad (1)$$

The groups working in momentum space use the Lippmann-Schwinger (LS-) equation for the scattering amplitude  $T$  (or equations equivalent to it)

$$T(\underline{p}_f, \underline{p}_i; p^2) = V(\underline{p}_f, \underline{p}_i; p^2) + \int \frac{d^3k}{(2\pi)^3} V(\underline{p}_f, \underline{k}; p^2) \frac{2m}{p^2 - k^2 + i\epsilon} T(\underline{k}, \underline{p}_i; p^2) \quad . \quad (2)$$

In both cases one can distinguish between non-relativistic and relativistic treatments of the kinematics. The difference is the relation between the cm-energy  $E$  and the relative momentum  $p$ . This is nonrelativistically  $E = p^2/2m$ , and relativistically  $E = (p^2 + m_1^2)^{\frac{1}{2}} + (p^2 + m_2^2)^{\frac{1}{2}} - m_1 - m_2$ .

As already stated above people often use relativistic forms of the LS-equation. These equations look different from (2), but can always be rewritten in the form (2). These relativistic LS-equations have been used in the past by and often carry the names of Blankenbecler and Sugar<sup>15</sup>, Logunov and Tavkhelidze<sup>16</sup>, Kadshevsky<sup>17</sup>, Thompson<sup>18</sup>, Partovi and Lomon<sup>19</sup>, Bryan and Gersten<sup>5</sup>, and many others.

The relativistic LS-equation has been used by the Bonn and Funabashi groups (also sometimes by the Nijmegen group). The great advantage of this method is, that any momentum dependence of the potential can be handled (as long as physical so that no divergences appear). However, there are also some drawbacks. The inclusion of the Coulomb-potential is very difficult and to my knowledge has never been done properly by any of these groups. Another disadvantage of the method is, that it is slower and less accurate than the calculations in coordinate space. Advocates of the calculations in momentum space often claim that the last statement above is incorrect. Still, we feel that the statement is correct, but it is perhaps more a matter of interpretation what one calls slow on a fast computer.

The Schrödinger equation is used by the Nijmegen group in its relativistic form. The Paris, Argonne, and Funabashi groups use the non-relativistic version. The biggest drawback of this method is, that one needs to approximate the momentum dependence of the potential, such that only terms linear in  $p^2$  are kept.



This is, unfortunately, quite a drastic approximation. However, when one has done this approximation, then the inclusion of the Coulomb potential is trivial and the existing codes are very fast and accurate (when carefully programmed).

## 5. ABOUT THE POTENTIAL FORMS

The spin dependence of all potentials can be written in the coordinate representation in the form

$$V = V_C + V_{\sigma_1 \cdot \sigma_2} + V_T S_{12} + V_{SO} \underline{L} \cdot \underline{S} + V_Q Q_{12} \quad (3)$$

The quadratic spin-orbit potential  $V_Q$  is treated differently by the different potentials.

Nijmegen and Paris use  $Q_{12} = \frac{1}{2} [(\underline{\sigma}_1 \cdot \underline{L})(\underline{\sigma}_2 \cdot \underline{L}) + (\underline{\sigma}_2 \cdot \underline{L})(\underline{\sigma}_1 \cdot \underline{L})]$  ,

Funabashi uses  $W_{12} = Q_{12} - \frac{1}{3} (\underline{\sigma}_1 \cdot \underline{\sigma}_2) L^2$  ,

and Argonne uses  $(\underline{L} \cdot \underline{S})^2 = \frac{1}{2} [Q_{12} - \underline{L} \cdot \underline{S} + L^2]$  .

The main difference between the potentials comes in the treatment of the central potential  $V_C$  and the spin-dependent potential  $V_{\sigma}$ . In order to get some feeling for these differences and also to get some feeling for how well one can calculate potentials at present, we will look at the recently derived improved Coulomb potential<sup>20</sup> which should be used in the relativistic Schrödinger equation. This potential includes the lowest order relativistic and recoil corrections to the ordinary Coulomb potential. Between two protons this improved Coulomb potential has the form

$$V = V_C + V_{\sigma_1 \cdot \sigma_2} + V_T S_{12} + V_{SO} \underline{L} \cdot \underline{S} \quad .$$

Well known are the expressions for  $V_T$ ,  $V_{LS}$ , and  $V_{\sigma}$ . The central potential  $V_C$  has the form

$$V_C = V_{CS} + V_{CE} \frac{p^2}{M^2} + \frac{1}{2M^2} (\Delta V_{Cd} + V_{Cd} \Delta) + V_{CL} L^2 \quad (4)$$

For point protons the static central potential is

$$V_{CS} = \frac{\alpha}{r} + [\lambda - \frac{1}{2} (1 + \kappa)] \frac{4\pi\alpha}{M^2} \delta^3(\underline{r}) \quad ,$$

the energy dependent ( $V_{CE}$ ) and momentum dependent ( $V_{Cd}$ ) central potentials are

$$V_{CE} = (\lambda + \frac{1}{2}) \frac{\alpha}{r} \quad \text{and} \quad V_{Cd} = (\lambda - 1) \frac{\alpha}{r} \quad ,$$

and the  $L^2$ -dependent central potential  $V_{CL}$  is

$$V_{CL} = \frac{2\lambda}{M^2} \frac{\alpha}{r^3} \quad .$$

In these expressions  $M$  and  $\kappa$  are the mass and anomalous magnetic moment of the proton and  $\lambda$  is an arbitrary parameter which depends on the gauge and on the retardation. We see therefore that this potential is not unique, but depends on the gauge and on the retardation. However, the observables are

unique in the lowest orders of  $\alpha$  and  $v/c$ . For example when applied to the realistic hydrogen atom the binding energies are correct up to order  $\alpha^4$ . Important to note is the freedom in the choice of  $\lambda$ . The potential becomes energy independent if one chooses  $\lambda = -\frac{1}{2}$ , the choice  $\lambda = 1$  removes the momentum dependence, and the choice  $\lambda = 0$  removes the  $L^2$ -dependence.

Similar results are also obtained<sup>21</sup> for the exchanges of massive neutral scalar and vector mesons. This example shows that the different potential forms  $V_i$  with  $i = C, \sigma, T, S0, Q$  are probably all energy dependent, momentum dependent and  $L^2$ -dependent. When we look at the different potential forms used by the different groups, then we note the following practical approximations.

In the Nijmegen hard core potentials  $V_i = V_{iS}(r)$  for all  $i$ . The Paris potential P1 uses

$$V_i = V_{iS}(r) + \frac{E}{M} V_{iE}(r) \quad \text{for } i = C \text{ and } \sigma.$$

The Paris potential P2 and the Nijmegen soft core potential use

$$V_i = V_{iS}(r) - \frac{1}{M} (\Delta V_{id} + V_{id}\Delta) \quad \text{for } i = C \text{ and } \sigma.$$

The Argonne potential uses

$$V_i = V_{iS}(r) + V_{iL}(r) L^2 \quad \text{for } i = C \text{ and } \sigma.$$

The Funabashi potential uses

$$V_i = V_{iS}(r) + \frac{1}{M} (\Delta V_{id} + V_{id}\Delta) + V_{iL}(r) L^2.$$

In this context it should be said that dispersion theory gives only energy dependent potentials and perhaps  $L^2$ -dependent. The difficulty with the energy dependent potentials is, that they are not very well suited for non-relativistic quantum mechanics. Such potentials give difficulties in many kinds of calculations. For this reason most groups have tried to stay away from energy dependent potentials. We feel that this has perhaps been an error.

Let us also make a remark about the tensor potential  $V_T(r)$ . The Argonne potentials, the Paris potential P1, and also the Paris  $N\bar{N}$ -potential have tensor potentials that are finite for  $r = 0$ . We have the feeling that that is unphysical and should be avoided. The reason for this feeling is, that for the triplet coupled channels the radial wave function  $\chi_\ell(r)$  will have a logarithmic singularity when  $r \rightarrow 0$ , then

$$\chi_\ell(r) \sim r^{\ell+1} + a r^p \ln r.$$

The exponent  $p$  is such that  $\chi_\ell$  is still zero when  $r \rightarrow 0$ , but this singularity will give in many computer codes accuracy problems for  $\ell > 0$ , unless treated very carefully. When not for physical reasons it is surely useful for practical reasons, when the phenomenological inner part of the tensor potentials are

chosen such that  $V_T(r = 0) = 0$ .

## 6. FIT TO THE EXPERIMENTAL DATA

One way to gauge the quality of the different NN-potentials is to see how well they describe the experimental data. For that one needs first of all a good phase shift analysis of all the data. In the past all groups used the Livermore phase shift analyses<sup>22</sup> MAW IX and X of 1968 and 1969. These are now rather outdated, especially for the np phases. Unfortunately there is at present not a single phase shift analysis used by all groups. Probably none of the available analyses have at present the required quality over the whole energy range to be a good standard.

(i) A fit to the phase shifts is made by minimizing

$$\chi_{pn}^2 = \sum_i \left[ \frac{\delta_i - \delta_i(\text{exp})}{\Delta \delta_i(\text{exp})} \right]^2,$$

where the  $\delta_i(\text{exp})$  are the phase shifts of the single energy analyses at several different energies. This is surely a good, first start when constructing a potential. This procedure has been followed in the construction of the Paris P1-potential and the Funabashi potentials. However, this method has some serious drawbacks, especially when the phase shift analysis used is in a false minimum. A nice example<sup>23</sup> of this is the difference in the  $^3S_1$  phase shift and the coupling parameter  $\epsilon_1$  between the MAW IX and X analyses.

(ii) A much better method is to make a fit to the experimental data using an existing phase shift analysis. The importance of this method was stressed very much in the talk<sup>6</sup> of one of us (J.J. de Swart) to the 1976 European Conference on the Few-Body Problem. When one is near the minimum in the  $\chi^2$ -surface, then one must calculate

$$\chi_e^2 = \chi_{\min}^2 + \frac{1}{2} \sum_{i,j} [\delta_i - \delta_i(\text{exp})] \frac{\partial^2 \chi}{\partial \delta_i \partial \delta_j} [\delta_j - \delta_j(\text{exp})],$$

where  $\chi_{\min}^2$  and  $(\partial^2 \chi)/(\partial \delta_i \partial \delta_j)$  must be obtained from the phase shift analysis. This quantity  $\chi_e^2$  gives then the  $\chi^2$  that would be obtained when one does a direct  $\chi^2$ -fit to the data. One of the first ones to use this method were Bryan and Gersten<sup>5</sup>. This method was used by the Nijmegen group, by the Bonn group, and probably also by the Argonne group. Also this method has its drawbacks. The fit suffers from the prejudices and inaccuracies of the phase shift analysis one uses. Examples of possible inadequacies of phase shift analyses are: the specific selection of data sets, the treatment of the higher partial waves, the treatment of the Coulomb interaction and of the Coulomb corrections, the choice of energy dependence, etc.

(iii) A method recently advocated by the Paris group<sup>24</sup> is to make a direct

comparison with the experimental data. The difference with the method described under (ii) escapes us. The difference could be that one can now select ones own data set. This has its advantages, but at the same time it makes almost impossible to compare the  $\chi^2$  for the different potentials. Moreover, one has no feeling for the goodness of the fit, unless also a phase shift analysis is performed, and  $\chi_{\min}^2$  given.

TABLE 1:  $\chi^2$  for some of the potentials.

	F <sup>7</sup>	B <sup>8</sup>	P1(pp) <sup>12</sup>	P1(np)	Nhc <sup>10</sup>	Nsc <sup>11</sup>
$\chi_{\text{ph}}^2(\text{i})$	6.4	2.85	2.5	3.7	-	-
$\chi_{\text{e}}^2(\text{ii})$	-	2.87	-	-	2.2	2.1
$\chi_{\text{e}}^2(\text{iii})$	P2 <sup>13</sup> : 2.0 (pp), 2.2 (np); A <sup>14</sup> : 1.64 (np)					

In table 1 is given the  $\chi^2$  for the different potentials. Important to note is that all entries, except P2 and A, are calculated with the MAW X-analysis. These latter potentials use more modern data and are so probably somewhat better especially for the np-data.

In order to illustrate the dangers of the last method (iii) and also as an introduction to the next topic we would like to treat the article<sup>24</sup> of J. Coté et al. about the analyzing power in pp-scattering at low energies. In this paper is claimed that "a direct comparison of theoretical predictions with data is more decisive then a comparison to phase shift analyses, ...". We would like to show that this is incorrect. In this paper the prediction of the Paris potential P2 is compared with the polarization data at 6.141 MeV<sup>25</sup>, 10 MeV<sup>26</sup>, and 16 MeV<sup>27</sup>. In Table 2 is given the  $\chi^2$  (P2) for the Paris P2-potential and the number N of datapoints in each set.

TABLE 2:  $\chi^2$  of the polarization data.

$E_L$	N	$\chi^2(\text{P2})$	$\chi_{\min}^2$ <sup>28</sup>
6.141	6	0.48	0.35
10	7	23.2	5.4
16	9	14.5	2.6

The Paris group calls the fit to the 6.141 MeV data excellent and the fit to the 16 MeV data very good. They come to the overall conclusion that the prediction of the Paris potential P2 is in good agreement with the experiments.

When this paper was published we had just finished in Nijmegen a phase shift analysis<sup>28</sup> of the same data. In that analysis only the <sup>3</sup>P-phases  $\Delta_T$  and  $\Delta_{LS}$

were searched for, the other phases were kept fixed at their best possible values. In Table 2 we give also the  $\chi_{\min}^2$  for these data sets. One expects to find  $\chi_{\min}^2 \approx N-2$  with an error of the order  $\sqrt{2N}$ . It is clear that  $\chi_{\min}^2$  for the 6.141 MeV data is *much* too low, due to an unknown, but large, systematic error in this very difficult experiment. This makes these data unfortunately useless and they should be removed from any proper dataset. A one standard deviation (sd) is obtained when  $\chi^2 = \chi_{\min}^2 + 1$ . This shows that the Paris potential prediction at 10 MeV is  $(23.2 - 5.4)^{\frac{1}{2}}$  sd = 4.2 sd off, and at 16 MeV is  $(14.6 - 2.6)^{\frac{1}{2}}$  sd = 3.5 sd off. A comparison with a phase shift analysis shows thus that the agreement with the data is not good, in contradiction with the Paris conclusion.

Quite important is to study: why the fit is not good, because in the same paper Coté et al. say: "These data are sensitive to the intermediate range of the NN-interaction, where the two-pion-exchange contribution is expected to play an important role". We fully agree with this statement. So what is going on?

#### 7. THE LONG AND INTERMEDIATE RANGE OF THE $I = 1$ TENSOR- AND SPIN-ORBIT POTENTIALS

From the discussion at the end of section 6 it is clear that the low energy  $^3P$ -phases  $\Delta_T$  and  $\Delta_{S0}$  are not correctly predicted by the P2-potential. We will study this better. We replace the 6.141 MeV and 10 MeV data by recently measured<sup>29</sup> much more accurate data at 5.05 MeV and 9.85 MeV. In Table 3 is given the  $\chi^2$  of single energy (se) and multi-energy (me) phase shift analyses, together with the predictions of the Nijmegen soft core potential<sup>11</sup> and the Paris P2-potential<sup>13</sup>, using only their  $\Delta_T$  and  $\Delta_{S0}$ .

TABLE 3:  $\chi^2$  of polarization data.

E	N	se	me	Nsc	P2
5.05	11	4.5	5.7	5.6	?
9.85	15	12.7	13	41	140
16	9	2.6	3.5	5.4	14.5

To understand what is going on it is sufficient to look at the very accurate 9.85 MeV data. These data show clearly that the Nsc potential is 5.3 sd off and the P2 potential 11 sd. Clearly both potentials are not good.

The  $I = 1$  tensorpotential can be studied with the help of the tensor combination  $\Delta_T$  of the  $^3P$ -phases, where

$$\Delta_T = \frac{5}{72} [-2\delta(^3P_0) + 3\delta(^3P_1) - \delta(^3P_2)] \quad .$$

TABLE 4:  $\Delta_T$  at several energies.

E	pp			np		
	exp <sup>30</sup>	Nsc <sup>11</sup>	P2 <sup>13</sup>	Nsc <sup>11</sup>	A <sup>14</sup>	B <sup>9</sup>
5.05	$0.41 \pm 0.02$	0.43		0.50	0.52	0.53
9.85	$0.94 \pm 0.01$	0.98	1.01	1.07	1.14	1.16
16	$1.58 \pm 0.05$	1.63	1.67	1.74	1.84	1.87

In Table 4 we give  $\Delta_T$  for several of the potentials together with the value (me) obtained in a multi-energy phase shift analysis and with errors of single energy phase shift analyses. At 9.85 MeV we note that Nsc is off  $\pm 4$  sd and P2 is off  $\pm 7$  sd. In order to be able to compare the Argonne and Bonn predictions with these pp data, we calculated with the Nsc potential also the tensor combination when the Coulomb interaction was omitted. That value is listed under Nsc (np). We note that the Argonne and Bonn predictions for  $\Delta_T$  are even worse. We come to the conclusion that: The long and intermediate range part of the  $I = 1$  tensor potential is too strong in all potential models considered.

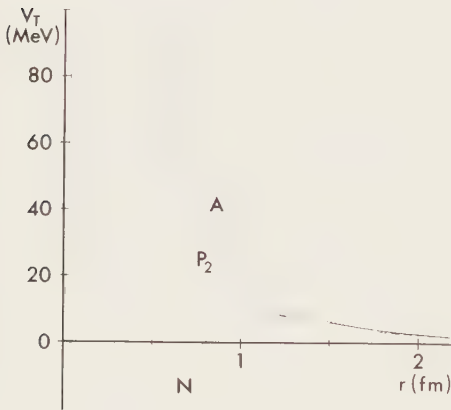


FIGURE 1  
The  $I = 1$  tensor potential.

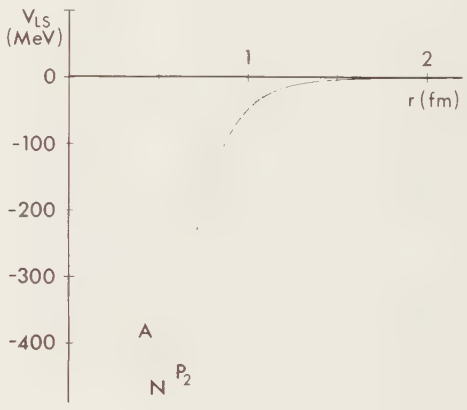


FIGURE 2  
The  $I = 1$  spin-orbit potential.

In Figure 1 we show the  $I = 1$  tensor potential for the Nijmegen Nsc, the Paris P2, and the Argonne  $v_{14}$  potentials. The most important contributions to this tensor potential come from the exchange of the  $\pi$ ,  $\rho$ , and  $\omega$  mesons. Very likely is, that the  $\pi^0$ -coupling constant is much lower than generally assumed.

The  $I = 1$  spin-orbit potential can be studied with the help of the combination

$$\Delta_{SO} = \frac{1}{12} [-2\delta(^3P_0) - 3\delta(^3P_1) + 5\delta(^3P_2)] \quad .$$

In Table 5 we give the predictions of the several potentials and the values obtained in single energy (se) and multi-energy (me) phase shift analyses.

TABLE 5:  $\Delta_{S0}$  at several energies.

E	se <sup>30</sup>	pp me <sup>30</sup>	Nsc <sup>11</sup>	P2 <sup>13</sup>	Nsc <sup>11</sup>	np A <sup>14</sup>	B <sup>9</sup>
5.05	0.06 ± 0.02	0.07	0.05		0.06	0.04	0.04
9.85	0.22 ± 0.02	0.21	0.14	0.15	0.17	0.11	0.12
16	0.31 ± 0.14	0.43	0.35	0.36	0.39	0.29	0.31

A comparison shows that the Paris P2 and the Nijmegen Nsc potentials have essentially the same wrong prediction. The predictions of the Argonne and Bonn potentials are also similar, but even further of the mark.

In Figure 2 we have made a plot of the Argonne, Nijmegen, and Paris spin-orbit potentials. Surprising is the fantastic agreement between the Paris P2 and Nijmegen Nsc potential. We come here to the conclusion that: In all potential models considered the tail of the  $I = 1$  spin-orbit potential is much too weak.

That this is not a small effect can be seen clearly at 9.85 MeV, where the Nsc and P2 potentials predict only 2/3 of the experimental  $\Delta_{S0}$ . An important feature of the spin-orbit potential is, that it does not have any one-pion-exchange contribution. The main contributions come from the broad  $\epsilon$  and  $\rho$  mesons (2 $\pi$ -exchange contribution) and the  $\omega$ -meson. Some or all of these contributions are obviously incorrect.

8. CONCLUSIONS

- (i) The low energy data are really a goldmine for information about the long- and intermediate range NN-interaction (see also ref. 31). More data in this energy region are required. In order to determine the  $\pi^0$ -coupling constant from the  $^1S_0$  data, more and accurate pp-cross sections are necessary in the  $T_L = 1$  to 5 MeV range and also in the 10 - 30 MeV range. Good asymmetry  $A(\theta)$  or polarization  $P(\theta)$  data in pp scattering in the range from 12 to 30 MeV are useful for a better understanding of the  $^3P$ -phases.
- (ii) It appears that we are getting a handle on the  $\pi^0$ -coupling constant. We believe, that  $g_{\pi^0}^2/4\pi$  is probably more in the neighborhood of 13.5 than of 14.4.
- (iii) In the next generation of potentials it will be necessary to take carefully account of the difference between pp and np. One must take account of the  $\pi^0$ - $\pi^\pm$  mass difference and one must try to include the charge independence breaking of the  $\pi N$  coupling constants. In order to be able to compare with the



very accurate experimental data it is essential that one uses relativistic kinematics. Moreover one must take account of the improved Coulomb potential and the vacuum polarization potential. For most of us this will mean, that we have to improve the computation accuracy of our programs quite a lot.

(iv) A tip for fitting the parameters of any model. In the  $^1S_0$ -wave one should fit the phase shift for pp at  $T_{\text{lab}} = 382.54$  keV. Including all possible electromagnetic corrections one should obtain here  $\delta_E = 14.608 \pm 0.001^\circ$ .

(v) It would be nice to have a standard and accurate phase shift analysis, which could be used by all groups for comparison purposes. However, such an analysis should not assume at the outset charge independence.

(vi) In the future a proper treatment of the NN-interaction will require a coupled channel approach, where one should include couplings to channels like  $\pi D$ ,  $N\Delta$ ,  $\Delta\Delta$ , NN, etc. Some first steps in this direction have already been taken <sup>32,14</sup>. However, we would like to warn, that this is probably hard to do correctly in a coordinate space formulation. The potentials are quite strongly momentum dependent. Because the  $\Delta$  is unstable under strong interactions several problems pop up. There is no clear  $N\Delta$ -threshold, only the  $NN_\pi$ -threshold. The off-diagonal potentials coupling the NN-channel to the  $N\Delta$ -channel do not have the form  $e^{-m\pi r}/r$ , but have a form that looks more like  $\sin m\pi r/r$ .

(vii) When one thinks of quark effects also couplings with colored channels should be included.

(viii) It is clear that the presently available semi-phenomenological NN-potentials are far from perfect. A lot of work can and must still be done to improve them.

#### ACKNOWLEDGEMENT

We would like to thank dr. R. Machleidt and dr. R.B. Wiringa for sending information and discussions.

#### REFERENCES

1. P. Kroll, Physics Data 22-1 (1981) (Fachinform.-Zentrum Karlsruhe); W. Grein and P. Kroll, Nucl.Phys. A 338 (1980) 332.
2. S. Furuichi et al., Nucl.Phys. A 193 (1972) 285 and references quoted therein.
3. R. Viollier et al., Phys.Lett. 48B (1974) 99.
4. J. Binstock and R. Bryan, Phys.Rev. D4 (1971) 1341.
5. R.A. Bryan and A. Gersten, Phys.Rev. D6 (1972) 3411.
6. J.J. de Swart, M.M. Nagels, Fortschr.Phys. 28 (1978) 215.

7. T. Obinata, M. Wada, *Prog.Theor.Phys.* 53 (1975) 732; 57 (1977) 1984; 61 (1979) 1697.
8. K. Holinde, R. Machleidt, *Nucl.Phys. A* 247 (1975) 495; A 256 (1976) 479; A 280 (1977) 429.
9. R. Machleidt, K. Holinde, contributions to this conference.
10. M.M. Nagels, T.A. Rijken, J.J. de Swart, *Phys.Rev. D* 12 (1975) 744; D15 (1977) 2547; D20 (1979) 1633.
11. M.M. Nagels, T.A. Rijken, J.J. de Swart, *Phys.Rev. D* 17 (1978) 768.
12. M. Lacombe, B. Loiseau, J.M. Richard, R. Vinh Mau, P. Pirès, R. de Tourreil, *Phys.Rev. D* 12 (1975) 1495.
13. M. Lacombe et al., *Phys.Rev. C* 21 (1980) 861.
14. R.B. Wiringa, R.A. Smith, T.L. Ainsworth, *Phys.Rev. C* (1983).
15. R. Blankenbecler, R. Sugar, *Phys.Rev.* 142 (1966) 1051.
16. A.A. Logunov, A.N. Tavkhelidze, *Nuov.Cim.* 29 (1963) 380.
17. V.G. Kadyshevsky, *Nucl.Phys. B* 6 (1968) 125; *Nuov.Cim.* 55 (1968) 275.
18. R.H. Thompson, *Phys.Rev. D* 1 (1970) 110.
19. M.H. Partovi, E.L. Lomon, *Phys.Rev. D* 2 (1970) 1999.
20. G.J. Austen, J.J. de Swart, *Phys.Rev.Lett.* 50 (1983) 2039.
21. G.J.M. Austen, Thesis University of Nijmegen, 1982.
22. M.H. MacGregor, R.A. Arndt, R.M. Wright, *Phys.Rev.* 173 (1968) 1272; 182 (1969) 1714.
23. P.S. Signell, J. Holdeman Jr., *Phys.Rev.Lett.* 27 (1971) 1393.
24. J. Coté, P. Pirès, R. de Tourreil, M. Lacombe, B. Loiseau, R. Vinh Mau, *Phys.Rev.Lett.* 44 (1980) 1031.
25. G. Bittner and W. Kretschmer, *Phys.Rev.Lett.* 43 (1979) 330.
26. J.D. Hutton et al., *Phys.Rev.Lett.* 35 (1975) 429.
27. P.A. Lovoi et al., in: *Proceedings of the 4th International Symposium on Polarization Phenomena in Nuclear Reactions*, eds: W. Gruber and W. König, Zürich 1975 (Birkhäuser, Basel, 1976), pp. 450-451.
28. W.A. van der Sanden, A.H. Emmen, and J.J. de Swart, internal report Nijmegen, THEF-NYM-80.4 (unpublished).
29. M.D. Barker et al., *Phys.Rev.Lett.* 48 (1982) 918.
30. W.A. van der Sanden et al., Comments on the P-wave parameters  $\Delta_{LS}$  and  $\Delta_T$  in p-p scattering below 30 MeV (in preparation).
31. T.E.O. Erikson, this volume.

32. H. Sugawara and F. von Hippel, Phys.Rev. 172 (1968) 1764;  
G.H. Niephaus et al., Phys.Rev. C20 (1979) 1096;  
A.M. Green and M.E. Sainio, J.Phys. G5 (1979) 503;  
J.A. Tjon and E. van Faassen, Phys.Lett. 120B (1983) 39 and preprint March 1983.

## THE NUCLEON-ANTINUCLEON INTERACTION

Carl B. DOVER

Brookhaven National Laboratory, Upton, New York, USA 11973

The current status of our understanding of the low energy nucleon-antinucleon ( $N\bar{N}$ ) interaction is reviewed. We compare several phenomenological models which fit the available  $NN$  cross section data. The more realistic of these models employ an annihilation potential  $W(r)$  which is spin, isospin and energy dependent. The microscopic origins for these dependences are discussed in terms of quark rearrangement and annihilation processes. It is argued that the study of  $NN$  annihilation offers a powerful means of studying quark dynamics at short distances. We also discuss how one may try to isolate coherent meson exchange contributions to the medium and long range part of the  $NN$  potential. These pieces of the  $NN$  interaction are calculable via the  $G$ -parity transformation from a model for the  $NN$  potential; their effects are predicted to be seen in  $NN$  spin observables, to be measured at LEAR. The possible existence of quasi-stable bound states or resonances of an  $N$  plus one or more nucleons is discussed, with emphasis on few-body systems.

### 1. INTRODUCTION

In contrast to the situation for the nucleon-nucleon ( $NN$ ) system, relatively little high precision data is available for the  $N\bar{N}$  system. This situation should change dramatically in the next few years, as the LEAR (Low-Energy-Antiproton Ring) facility comes on line at CERN. The present review may be considered as a "pre-LEAR perspective." My object is to critically appraise the current theories of the low energy  $N\bar{N}$  interaction, and point to some of the avenues of research which are likely to further enhance our understanding of the  $N\bar{N}$  problem.

Why is the  $N\bar{N}$  system so interesting? There are numerous reasons, some of which are discussed here. One tantalizing possibility is that one may be able to exploit the intimate relation (via the  $G$ -parity transformation) between the longer range (nominally  $r \geq 0.8 - 1$  fm, a typical "bag" radius) part of the  $N\bar{N}$  potential and that for the  $NN$  system. Repulsive coherences in the  $NN$  spin-orbit forces due to meson exchange, for instance, become attractive coherences of  $N\bar{N}$  tensor forces as a result of the  $G$ -parity transformation. The strong predicted spin and isospin dependence of the meson exchange ( $t$ -channel) part of the  $N\bar{N}$  potential should show up more readily in a comparison of spin observables in channels with different isospin structure ( $\bar{p}p \rightarrow \bar{p}p$  vs  $\bar{p}p \rightarrow \bar{n}n$ , for instance) than in total cross sections.

The extraction of useful constraints on the NN interaction from a study of the "crossed"  $N\bar{N}$  channel is hampered considerably by the presence of annihilation processes in the latter. Since the  $N\bar{N}$  system has baryon number  $B = 0$ , it can dissolve into a spray of mesons (the mean multiplicity of pions is about 5 at low energies), a mode of decay unavailable to the NN system with  $B = 2$ . For distances  $r < 1$  fm or so, the annihilation mechanism dominates, and one can obtain very little information on the structure of the real potential. In any case, a meson exchange description breaks down inside of 1 fm, since in this region the "bags" containing the N and  $\bar{N}$  overlap, and one probes the dynamics of internal quark degrees of freedom. The microscopic description of  $N\bar{N}$  annihilation at the quark level is a problem of high importance; we review several attempts to formulate a quark rearrangement model to account for the observed  $N\bar{N}$  branching ratios into various mesonic channels. In principle, detailed two meson interferometry studies should provide signatures of differing quark mechanisms operating in  $N\bar{N}$  annihilation.

The  $N\bar{N}$  system is an ideal entrance channel for accessing narrow "baryonium" states, if they exist. These could be either of "quasi-nuclear" type or ( $Q^2\bar{Q}^2$ ) composites. An abundant spectrum of such states is predicted theoretically, but the estimates for their width are unreliable. Since the experimental situation is murky, we do not enumerate the detailed properties of predicted baryonium spectra here. We content ourselves with the remark that the "color chemistry" of multi-quark systems ( $n \geq 4$  quarks) is of fundamental interest in nuclear and particle physics, and that the  $N\bar{N}$  channel offers the best window for studying the  $Q^2\bar{Q}^2$  sector.

In addition to questions relating to the  $N\bar{N}$  problem itself, we also consider how the characteristic signatures of the two-body problem (spin, isospin and energy dependences, ranges of real and imaginary potential, etc.) are transmitted to the many-body scenario. For instance, the marked spin dependence of the  $N\bar{N}$  annihilation potential  $W(r)$  which occurs in several models leads to strong excitation of isoscalar spin-flip ( $\Delta T=0$ ,  $\Delta S=1$ ) modes of nuclei in  $\bar{N}$  inelastic scattering. These are only weakly excited by the nucleon probe. We also investigate the possibility that relatively long-lived nuclear systems containing an  $\bar{N}$  may exist. Certain few-body systems are the most likely candidates, since one may take maximum advantage of spin-isospin selectivity in the absorptive potential and the influence of the long-range one pion exchange potential in systems where the nuclear core is not spin-isospin saturated.

## 2. BRIEF REVIEW OF $N\bar{N}$ DATA

The experimental situation in low energy  $N\bar{N}$  physics has been recently reviewed by Tripp<sup>1</sup> and Smith<sup>2</sup>. The emphasis of these reviews is on the evidence (for and against) pertaining to the existence of narrow "baryonium" states in  $N\bar{N}$  scattering. At the time of the Bressanone meeting<sup>1</sup>, earlier evidence for the S(1940) and other resonances in the  $N\bar{N}$  system was placed in question by a spate of negative results.

In the past year, the CERN-Heidelberg-Saclay group presented new results<sup>3</sup> on  $\bar{p}p$  elastic scattering and annihilation. This experiment had better mass resolution (0.4 MeV) than earlier attempts (typically about 1.5 MeV). A dip-bump structure was seen near 1936 MeV, perhaps indicating the resurrection of the S meson. Other recent results, discussed by Smith<sup>2</sup>, do not indicate a narrow structure near the S, although high mass resolution may well be critical. The S region could contain overlapping resonances (both potential and quark models give certain isospin or C-parity doublets, for instance), and high resolution studies at LEAR are necessary in order to clarify this very confused situation.

Resonant structures have also been looked for in backward ( $\theta \approx 180^\circ$ )  $\bar{p}p$  scattering. *A priori*, large angle scattering might appear to be quite promising for bump hunting, since cross sections are much smaller than in the forward direction, and a resonance might be expected to show up more readily. D'Andlau et al.<sup>4</sup> found evidence for structure in the S region, but a later higher precision experiment of Alston-Garnjost et al.<sup>5</sup> found only a smooth cross section at  $180^\circ$  as a function of momentum. The main problem is that the  $180^\circ$   $\bar{p}p$  cross section attains a diffraction maximum around  $p_{lab} \approx 510$  MeV/c, i.e. just the position of the tentative S meson. Interest in the  $180^\circ$  data has recently been rekindled by the Nijmegen group<sup>6</sup>, who have performed an optical model fit<sup>7</sup> to all the available  $N\bar{N}$  data (elastic and charge exchange angular distributions, total cross sections, and polarization data). A result of this fit is a good theoretical description of the diffractive background at  $180^\circ$ . When this background is subtracted from the data of Alston-Garnjost et al.<sup>5</sup>, there is still evidence for a narrow structure at 1940 MeV. This structure can be accommodated in a coupled channel framework<sup>6</sup> if the  $NN$  channel is coupled to a  $Q^2\bar{Q}^2$  "baryonium" channel. In ref. 6, this coupling is taken in the  $^{11}P_1$   $N\bar{N}$  wave as an example, but the data are not sufficient to actually determine the quantum numbers of the proposed resonance.

In addition to the S region, there has been recent evidence for an  $N\bar{N}$  resonance at  $2.02 \text{ GeV}/c^2$  in production experiments<sup>16,17</sup>. In ref. (16), an  $I = 1$  state was observed in the reactions  $\bar{p}p \rightarrow p_{fast} \bar{n}\pi^+\pi^-\pi^-$  and

$\bar{p}p \rightarrow \pi^+_{\text{fast}} \bar{p}n\pi^+\pi^-$  at 6 and 9 GeV/c. The mass spectra showing the 2.02 GeV/c<sup>2</sup> peak are shown in Fig. 1. The structure at 2.02 GeV/c<sup>2</sup>, as well as one in the S region, was also seen by Bodenkamp et al.<sup>9</sup> in the  $\gamma p \rightarrow p\bar{p}p$  photo-production reaction from 4.7 - 6.6 GeV, shown in Fig. 2. On the other hand, numerous attempts<sup>10</sup> to produce these states via baryon-exchange mechanisms have led to negative results. The experimental situation for  $\bar{N}N$  resonances thus remains unclear.

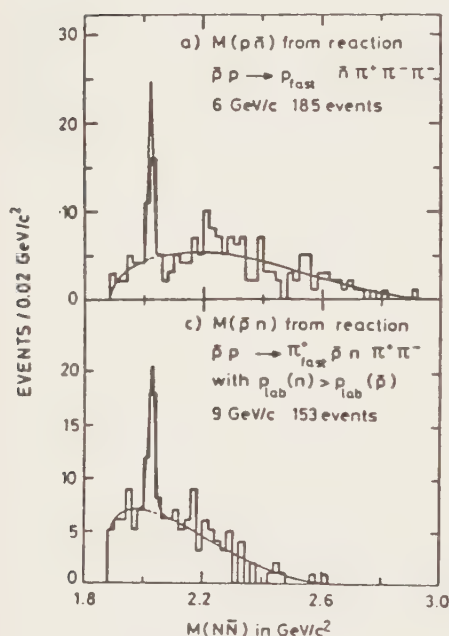


FIGURE 1

$\bar{N}N$  mass spectra from Azooz et al.<sup>8</sup>.

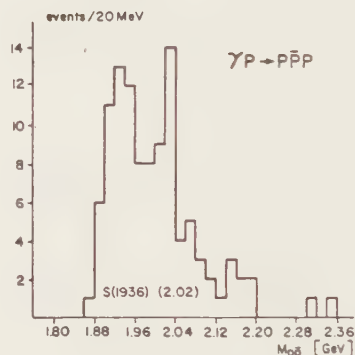


FIGURE 2

$\bar{N}N$  mass spectrum in photoproduction, from Bodenkamp et al.<sup>9</sup>.

There has been persistent evidence<sup>11,12</sup> for the emission of energetic  $\gamma$  rays ( $E > 100$  MeV) from  $\bar{p}p$  atoms. These transitions lead to the population of narrow ( $\Gamma < 20$ -30 MeV)  $\bar{N}N$  levels at masses of about 1210, 1638, 1694 and 1771 MeV, according to the group<sup>11</sup> at CERN. The statistical significance of these lines is at the 3 $\sigma$  level. In an experiment<sup>12</sup> at the Brookhaven AGS, evidence



at about the  $3\sigma$  level was obtained for the 1771 MeV state, but the statistics were insufficient to confirm or deny the other levels seen by the CERN group.

Numerous theoretical predictions exist for the spectrum of "baryonium" states coupled to the  $N\bar{N}$  channel. The quark model aspects have been reviewed in ref. (13), while considerations based on  $N\bar{N}$  potential models are treated in refs. (14) and (15). In the quark model, composites of type  $Q^2\bar{Q}^2$  are coupled to the  $N\bar{N}$  channel via the quark-antiquark annihilation mechanism depicted in Fig. 3(a). The spectrum of  $Q^2\bar{Q}^2$  states in the MIT bag model, as well as their relative couplings to  $N\bar{N}$ , have been worked out by Jaffe<sup>16</sup>. The spectrum of  $Q^2\bar{Q}^2$  bag states is shown in Fig. 4; the levels are grouped into trajectories A, B and C as defined by Jaffe<sup>16</sup>. Trajectory A is most strongly coupled to  $N\bar{N}$ , followed by B and C. Several candidates for the levels seen in the  $\gamma$  ray experiment are evident. One of the mechanisms for populating these levels by  $\gamma$  or  $\pi$  emission is shown in fig. 3(b). The branching ratios for  $\gamma$  emission to  $Q^2\bar{Q}^2$  states (relative to annihilation) have been evaluated by Ader et al.<sup>17</sup>. The dominant mechanism was found to be  $\gamma$  emission from a quark or antiquark

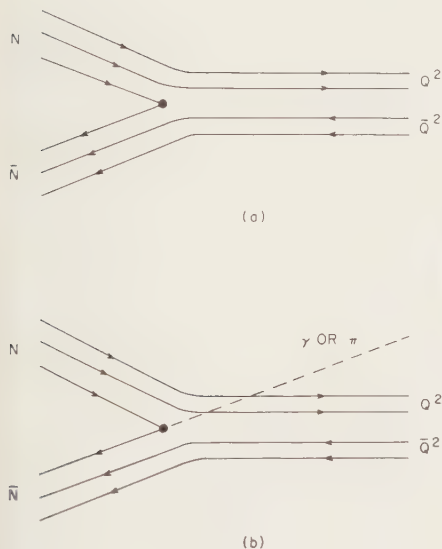


FIGURE 3

Mechanism for direct  $N\bar{N}$  coupling to  $Q^2\bar{Q}^2$  bag states ( ${}^3P_0$  model) is shown in (a); one of the processes for populating  $Q^2\bar{Q}^2$  states via  $\gamma$  or  $\pi$  emission is shown in (b).

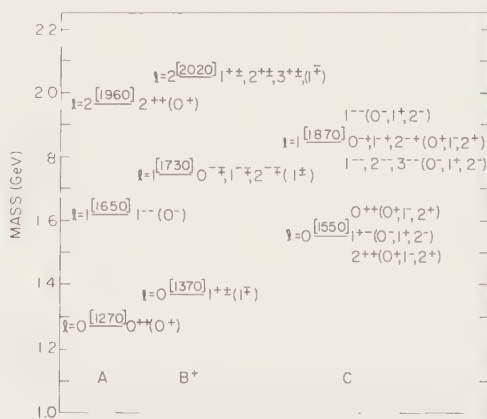


FIGURE 4

Spectrum of  $Q^2\bar{Q}^2$  states (labeled by  $J^PC(I^G)$ ) in the MIT bag model, after Jaffe<sup>16</sup>.

line, followed by  $Q\bar{Q}$  annihilation into the vacuum, rather than that shown in Fig. 3(b). Branching ratios of the order of a few times  $10^{-4}$  were obtained in the quark model, about an order of magnitude smaller than the results<sup>11</sup> from CERN. In the  $N\bar{N}$  potential model<sup>14</sup>, the channels of maximum attraction for each L correspond to the same quantum numbers as trajectory A in Fig. 4. The branching ratios for  $\gamma$  or  $\pi$  emission to  $N\bar{N}$  quasi-bound states were evaluated in ref. (17) in the context of the potential model; agreement with the experimental values is obtained, in contrast to the evaluation in the quark model. The significance of this fact is not clear at this point.

One of the first tasks at LEAR will be to confirm (or deny) the existence of narrow  $N\bar{N}$  bound states or resonances. If narrow states indeed exist, detailed information on decay branching ratios would greatly facilitate quantum number assignments. If narrow states are not found, much interesting physics could still emerge from the spectroscopy of broad mesons coupling strongly to the  $N\bar{N}$  channel. Firm evidence exists for broad structures in  $N\bar{N}$  total cross sections (T and U mesons) and high spin states<sup>18</sup> in the  $\bar{p}p + \pi^+\pi^-$  reaction.

### 3. THE REAL (NON-ANNIHILATION) PART OF THE $N\bar{N}$ INTERACTION

In the conventional picture of the NN interaction, the potential V is generated by meson exchange (t-channel). Such a picture is appropriate for the medium and long range parts of V. In phenomenological one boson exchange (OBE) models, for example ref. (19), contributions to V arise from exchanges of nonets of scalar, pseudoscalar and vector mesons. In the work of the Stony Brook<sup>20</sup> and Paris<sup>21</sup> groups, the  $\sigma$  and  $\rho$  exchange contributions of the OBE approach are replaced by isoscalar and isovector two pion exchange contributions evaluated by dispersion relation techniques. In either approach, a potential of the form  $V_{NN} = \sum_i V_i$  arises, where i refers to the quantum numbers of the various t-channel exchanges. If  $G_i$  is defined as the G-parity of the exchanged meson i, then the corresponding part of the  $N\bar{N}$  potential is just  $V_{NN} = \sum_i (-)^{G_i} V_i$ ; note that  $G = (-1)^n$  for a system of pions. This is the "G-parity transformation", which leads to a very close connection between the t-channel NN and  $N\bar{N}$  potentials, and fostered early hopes that an analysis of the  $N\bar{N}$  observables would provide additional constraints on the meson exchange picture of the NN force.

In practice, the usefulness of the G-parity transformation is limited to the medium and long range part of V. The short range part of the NN force is generally treated phenomenologically (by hard cores<sup>19</sup> or other parametrized cutoffs<sup>21</sup>, for instance), and it is not clear how to transform these

prescriptions into the NN sector. For  $r < 0.8 - 1$  fm, the representation of  $V$  as a local meson exchange potential breaks down, since the quark bags making up the  $N$  and  $\bar{N}$  start to overlap appreciably. The short range aspects of the NN and  $N\bar{N}$  systems demand a description in terms of quark dynamics. In addition, as we discuss in Sects. 4 and 5, the  $N\bar{N}$  system, having baryon number  $B = 0$ , easily annihilates into mesons (the  $N\bar{N}$  absorption cross section is about twice that for elastic scattering at low energies). The annihilation mechanism has no counterpart in the low energy NN system (here pions are only appreciably produced above 400 MeV kinetic energy). Thus the NN phenomenology provides no guidance as to how to construct the effective  $N\bar{N}$  annihilation potential  $V_{\text{ann}} + iW$ . The presence of strong absorption masks the sensitivity of the  $N\bar{N}$  observables to the short range real potential. Note also that the annihilation process (through dispersive corrections) generates a real potential  $V_{\text{ann}}$  as well as an imaginary part  $W$ . The magnitude of  $V_{\text{ann}}$  has not been reliably estimated theoretically; in principle, it could be comparable in size to the t-channel meson exchange potential at critical distances of order  $r \approx 1$  fm, although it is intrinsically of shorter range.

Is it possible to isolate the longer range effects of the t-channel meson exchange potential from an analysis of  $N\bar{N}$  observables? So far this has not been accomplished, since the available  $N\bar{N}$  data consist mostly of total cross sections (elastic, charge exchange and annihilation) and some angular distributions, which reflect mainly the strong absorption (geometric) aspects of the problem. Except for some crude data on  $\bar{p}p$  elastic polarization, no spin observables have been measured. These spin quantities hold the key to seeing the characteristic effects of t-channel exchanges in  $N\bar{N}$ , and hence establishing some connection to the NN problem.

We now indicate that the coherences present in the  $N\bar{N}$  potential provide signatures in the  $N\bar{N}$  spin observables, even in the presence of strong absorption.

Let us first review the coherence properties<sup>14</sup> of the NN system, and their effect on the observables. The most dramatic effect of coherence in the NN system is seen in the  $2I+1$ ,  $2S+1$   $^L_J = ^{33}\text{P}_0$  phase shift. Here, the one pion exchange potential (OPEP), dominated by its tensor component, is strongly attractive. On the other hand, the short range spin-spin, spin-orbit and vector meson exchange forces are all coherently repulsive. The competition between strong long range attraction and coherent short range repulsion leads to a sign change in the  $^{33}\text{P}_0$  phase shift near 200 MeV. The same mechanism holds also for other triplet-odd NN waves with  $J = L - 1$ . Partial waves for which an attractive OPEP is balanced against non-coherent short range

repulsion do not display a zero of the phase shift; an example is the  $^{13}\text{D}_2$  channel, where the phase remains close to the OPEP value and there is no zero. Deviations from OPEP predictions for peripheral NN partial waves are particularly interesting, since they register the coherent summed strength of  $\vec{g}_1 \cdot \vec{g}_2$ ,  $\vec{L} \cdot \vec{S}$  and vector exchange potentials.

In passing from the  $\bar{\text{N}}\bar{\text{N}}$  to the NN system, the G-parity transformation leads to a dramatic change in the pattern of coherence. For  $\bar{\text{N}}\bar{\text{N}}$ , the central, tensor and quadratic spin-orbit forces are fully coherent and attractive for isospin  $I = 0$  states with spin  $S = 1$  and  $L = J \pm 1$ . For fixed  $J$ , the channels of maximum attraction are  $^{13}\text{P}_0$ ,  $^{13}\text{S}_1 - ^{13}\text{D}_1$ ,  $^{13}\text{P}_2 - ^{13}\text{F}_2$ , etc. As mentioned earlier, these channels form a natural parity band with  $J^{\pi C} = 0^{++}, 1^{--}, 2^{++}$ , etc., which share the same quantum numbers as the "leading trajectory" of  $Q^2\bar{Q}^2$  states in the bag model.

The coherence of  $\bar{\text{N}}\bar{\text{N}}$  tensor forces for  $I = 0$  is most readily seen in spin observables. Some sample predictions from ref. (22) are shown in Figs. 5 and 6. In Fig. 5, we show an angular distribution for the  $\bar{\text{p}}\text{p}$  elastic polarization

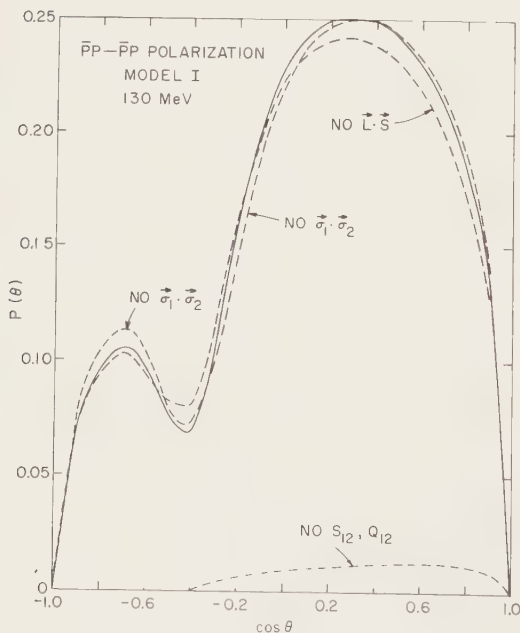


FIGURE 5

Elastic  $\bar{\text{p}}\text{p}$  polarization at 130 MeV, from ref. (14).

$P(\theta)$  at 130 MeV. If the spin-spin and spin-orbit parts of the  $\bar{\text{N}}\bar{\text{N}}$  potential are set to zero,  $P(\theta)$  remains essentially unchanged, while if tensor forces are neglected,  $P(\theta)$  almost vanishes. In contrast to the NN system, where  $P(\theta)$  arises predominantly from the spin-orbit potential, the polarization in  $\bar{\text{N}}\bar{\text{N}}$  is largely an effect of the coherent tensor force from meson exchange. The quantitative aspects of  $P(\theta)$  (and other spin observables) are influenced, however, by a possible strong spin-spin and tensor component in  $W(r)$ , which can cloud the simple and elegant interpretation based on meson exchange. In Fig. 6, we display predictions<sup>14</sup> for

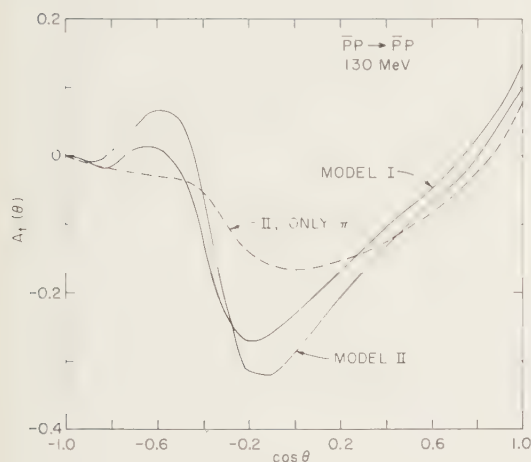


FIGURE 6  
Polarization transfer  $A_t$  at 130 MeV,  
from ref. (14).

$A_t$ , which may be measurable in future experiments at LEAR. Fig. 6 shows that the polarization transfer  $A_t$  is considerably enhanced if the coherent vector meson contribution is added to one pion exchange.

To summarize, a careful measurement of  $N\bar{N}$  spin observables could provide an important constraint on the summed strength of the  $\pi$ ,  $\omega$  and  $\rho$  tensor potentials (and also the coherent quadratic spin-orbit potentials). This information would be complementary to that obtained from

a study of the spin dependence in NN scattering.

#### 4. GEOMETRIC AND PHENOMENOLOGICAL MODELS OF $N\bar{N}$ ANNIHILATION

The G-parity transformation provides a means of obtaining the medium and long range parts of the  $N\bar{N}$  meson exchange potential from a model for the NN interaction. This is only part of the story, since annihilation processes in  $N\bar{N}$  are very strong. This is strikingly illustrated by considering the total  $\bar{p}p$  elastic and annihilation cross sections  $\sigma_E$  and  $\sigma_A$ , which can be represented<sup>23</sup> phenomenologically as

$$\begin{aligned}\sigma_E &= 28 + 17/p_{\text{lab}} \quad (\text{mb}) \\ \sigma_A &= 38 + 35/p_{\text{lab}} \quad (\text{mb})\end{aligned}\tag{1}$$

for  $p_{\text{lab}}$  in the range 0.5 - 2 GeV/c. We see that  $\sigma_A$  is very large (far exceeding the s-wave unitarity bound even at the lowest measured momenta) and that  $\sigma_E/\sigma_A \approx 1/2$  at low energies, unlike the result  $\sigma_E \approx \sigma_A$  which one might expect in the most naive geometric limit.

The qualitative features of  $\sigma_E$  and  $\sigma_A$  can already be understood<sup>14</sup> in the simplest sort of absorbing sphere model, based on the old continuum theory of nuclear reactions, as described by Blatt and Weisskopf<sup>24</sup>, for instance. In

this model, the annihilation potential  $W(r)$  is replaced by an incoming wave boundary condition at a strong absorption radius  $r = R$ :

$$[u'_\ell(r)/u_\ell(r)]_{r=R} = -iK, \quad K = (M(E-V_0))^{1/2} \quad (2)$$

Here,  $V_0$  is the depth of the real potential at  $r = R$  and  $M$  is the nucleon mass. In ref. (14), this model was used, with  $R \approx 1$  fm, to fit  $\sigma_E$  and  $\sigma_A$ . The model reproduces the monotone-decreasing cross sections rather well, in particular the ratio  $\sigma_A/\sigma_{EL}$ . The boundary condition model was one of the earliest approaches<sup>25</sup> to understanding the size of  $\bar{N}N$  cross sections. A recent application is due to Myhrer and Dalkarov<sup>26</sup>.

Higher partial waves play an important role, even at very low momenta. The s-wave region, which lies below 150 - 200 MeV/c, has not yet been explored experimentally; this is an important task for LEAR. The representation (1) of  $\sigma_A$  is reminiscent<sup>24</sup> of the "1/v law", but in fact has nothing to do with s-wave dominance. The signal that we are getting into the s-wave region is that  $\sigma_A$  drops significantly below the value obtained by simply extrapolating Eq. (1) to low momentum. An interesting quantity is  $\beta\sigma_A$ , where  $\beta = v/c$ ; as  $\beta \rightarrow 0$ ,  $\beta\sigma_A$  must approach a constant. From two recent optical models for fitting the  $\bar{N}N$  cross section data, we find<sup>27</sup>

$$\beta\sigma_A \approx \begin{cases} 28.21 + 0.192E + 0.0128E^2 & (\text{ref. 28}) \\ 32.83 + 0.096E & (\text{ref. 29}) \end{cases} \quad (3)$$

where  $\beta\sigma_A$  is in mb and  $E$  (lab kinetic energy) is in MeV. Eq. (3) holds for  $E < 10$  MeV. The average threshold value is about  $(\beta\sigma_A)_{\beta \rightarrow 0} \approx 30$  mb. This value could change significantly if narrow bound s-states exist close to the  $\bar{N}N$  threshold. These do not occur in refs. (28) and (29); there are instead deeply bound and very broad  $\bar{N}N$  s-states in these models.

The simple black disk or boundary condition models are sufficient for a semi-quantitative understanding of total cross sections, but provide no useful account of spin observables, isospin dependence, or large angle elastic or charge exchange scattering. For these quantities, which contain most of the interesting physics, the full optical model treatment is necessary.

An early optical model fit to the  $\bar{N}N$  data was carried out by Bryan and Phillips<sup>30</sup>. They used an OBE model for the t-channel meson exchange potential, and a local Woods-Saxon form

$$V_{\text{ann}}(r) + iW(r) = -(V_0 + iW_0)/(1 + \exp((r-R)/a)) \quad (4)$$

for the complex annihilation potential. They used  $V_0 = 0$ ,  $W_0 = 62$  GeV,  $R = 0$  and  $a = 1/6$  fm. This type of analysis was later redone by Dover and Richard<sup>28</sup>, who used the Paris potential<sup>21</sup> for the t-channel part, and also included a real annihilation potential. They fit the high precision  $\bar{p}p \rightarrow \bar{n}n$



charge exchange data<sup>31</sup> which had become available. A family of annihilation potentials was found which fit the data (Model I with  $V_0 = 21$  GeV,  $W_0 = 20$  GeV,  $R = 0$ ,  $a = 1/5$  fm and Model II with  $V_0 = W_0 = 500$  MeV,  $R = 0.8$  fm,  $a = 1/5$  fm are two examples; see Fig. 6). This family has the characteristic that the absorptive parts are comparable at around 1 fm. The enormous values (many GeV) attained by the annihilation potential at short distances are of no physical significance. The cross sections are insensitive to the potentials in this region, as long as absorption is sufficiently strong. A similar situation prevails in heavy ion reactions.

After the analysis of Dover and Richard<sup>28</sup> appeared,  $\bar{p}p$  backward ( $\theta = 174^\circ$ ) elastic scattering was measured with high precision by Alston-Garnjost et al<sup>5</sup>. Although ref. (28) was consistent with the earlier crude elastic data at backward angles, it now considerably underestimated the cross section. It proved impossible to remedy this situation by further variations of an annihilation potential of the type (4). The Paris group<sup>29</sup> reanalyzed the  $N\bar{N}$  data, including all differential cross section and polarization information, using a more flexible phenomenological form

$$W(r) = \{g_c(1 + f_c E) + g_{SS}(1 + f_{SS} E)\sigma_1 \cdot \sigma_2 + g_{TS_{12}} + \frac{g_{LS}}{2} \underline{L} \cdot \underline{S} \frac{1}{r} \frac{d}{dr}\} \frac{K_0(2mr)}{r} \quad (5)$$

The coefficients  $g_c$ ,  $g_{SS}$ ,  $g_T$ ,  $g_{LS}$  are adjusted separately for isospins  $I = 0, 1$ . The radial dependence is given in terms of the modified Bessel function  $K_0$  of range  $1/2m \approx 0.1$  fm (held fixed), which reduces to a Yukawa form for large  $r$ . The form (5) is rather general, incorporating arbitrary spin, isospin and energy ( $E$ ) dependence, as well as  $L$  and  $J$  dependence through the spin-orbit ( $\underline{L} \cdot \underline{S}$ ) and tensor ( $S_{12}$ ) terms. No real annihilation potential was considered, and an updated version<sup>32</sup> of the Paris potential was used for the t-channel exchange part. Further free parameters<sup>29</sup> are required to specify the short range cutoff.

A sample of the good fits to the  $N\bar{N}$  data obtained by the Paris group is shown in Fig. 7. Since numerous free parameters are involved in these fits, it is clear that they cannot all be uniquely determined from the limited data. In particular, since the only spin observable that has been measured (crudely) is  $P(\theta)$ , see Fig. 7, it is difficult to disentangle the effects of  $\sigma_1 \cdot \sigma_2$ ,  $\underline{L} \cdot \underline{S}$  and  $S_{12}$  terms. Nevertheless, some interesting conclusions can be drawn from this analysis. Firstly, the spin and isospin dependence of  $W(r)$  in ref. (29) is very strong. For s-waves, the values of  $W^{IS}$  stand in the ratio



$$W^{00} : W^{10} : W^{01} : W^{11} = \begin{cases} 1:0.81:0.11:0.073, & E = 0 \\ 0.92:1:0.15:0.035, & E = 100 \text{ MeV} \end{cases} \quad (6)$$

From Eq. (6), we see that  $W$  is an order of magnitude or so more absorptive in  $S = 0$  than in  $S = 1$  channels, whereas the isospin dependence is significant but not as strong as the spin dependence. Further, we note that  $W$  is strongly energy dependent. For instance, as  $E$  changes from 100 to 200 MeV,  $W^{00}$  increases by a factor 1.6. The strong spin dependence of  $W(r)$  has a dramatic consequence in  $\bar{N}$  inelastic scattering on nuclei<sup>33</sup>: isoscalar, spin-flip

( $\Delta S=1$ ) modes of nuclei, which are excited only very weakly in nucleon inelastic scattering, become very prominent in the  $\bar{N}$  inelastic response function.

Very recently, the Nijmegen group has presented a coupled model<sup>6,7</sup> for  $NN$  scattering. They solve the relativistic coupled channels Schrödinger equation (including the  $n$ - $p$  mass difference and Coulomb effects) with a potential matrix of the form

$$V = \begin{pmatrix} V & -V_A \\ \tilde{V} & 0 \end{pmatrix} \quad (7)$$

Here  $V = V_{NN} + V_{ph} + V_{coul}$  is the diagonal  $NN$  potential,  $V_{nuc}$  is the  $t$ -channel meson exchange potential (taken as the  $G$ -parity transformed Model D potential of ref. (19)),  $V_{coul}$  is the Coulomb potential and  $V_{ph}$  is a phenomenological energy independent real potential of the form

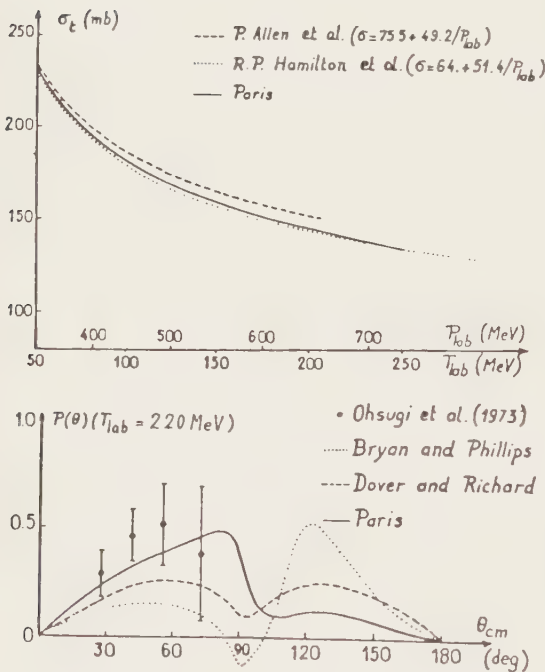


FIGURE 7

Optical model fits to  $\bar{p}p$  total cross section and elastic polarization, from the Paris group<sup>29</sup>.

$$V_{ph}(r) = (V_c + V_{SS} \sigma_1 \cdot \sigma_2 + V_{T12}^S m r + V_{SO} \frac{L \cdot S}{m_e r} \frac{d}{dr}) \times (1 + \exp(m_e r))^{-1} \quad (8)$$

with a range  $1/m_e = 0.31$  fm.

The potential  $V_A$ , which couples the  $N\bar{N}$  system to a set  $\{i\}$  of effective two-body annihilation channels, is chosen to be

$$V_A^{(i,I)}(r) = V(i,I) (1 + \exp(m_a r))^{-1}, \quad (9)$$

dependent on isospin, but not on  $L$ ,  $S$  or  $J$ . The range of  $V_A$  is  $1/m_a \approx 0.46$  fm. For each isospin, two annihilation channels were introduced ( $i = 1, 2$ ); the effective particles in these channels are taken to be spinless and of equal mass ( $2M_1 = 1700$  MeV and  $2M_2 = 420$  MeV). No interaction between these effective particles is included. All the absorptive in  $N\bar{N}$  are simulated by the coupled annihilation channels, so no explicit imaginary potential is introduced.

The quality of the Nijmegen fit<sup>7</sup> is illustrated for the polarization in Fig. 8. The Nijmegen model has a somewhat better  $\chi^2$  (1.5 vs. 2.8 per point) than the Paris model. Again, the requirement of fitting the  $\bar{p}p$  backward elastic data is very constraining.

Spin orbit and tensor terms (in  $W(r)$  or  $V_{ph}$ ) play an important role in obtaining a good fit to the  $180^\circ$  data.

By comparing the predicted polarizations (at almost the same energy) in Figs. 7 and 8, one sees that although the Paris and Nijmegen models agree reasonably well in the angular region where data exist, they differ strongly in their predictions for  $P(\theta)$  near  $\theta \approx 90^\circ$ . The Nijmegen model leads to large negative values of  $P(\theta)$  here (as large as  $\approx -0.7$ ), while  $P(\theta)$  remains positive at all angles for  $E \approx 220$  MeV. The situation is similar for other spin observables, but much less dramatic for total

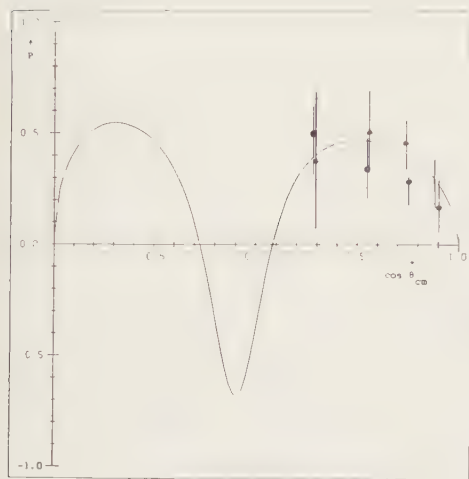


FIGURE 8

Fit to the elastic  $\bar{p}p$  polarization at 230 MeV, from the Nijmegen group<sup>7</sup>.

cross sections. The measurement of spin quantities at LEAR will be crucial in choosing between various theoretical models.

The importance of  $N\bar{N}$  spin measurements is also emphasized by a qualitative comparison of the spin and isospin dependence of the Nijmegen and Paris models. At any  $r$  and  $E$ , the potentials  $V_{ph}^{IS}$  of Eq. (8) for  $s$ -states are in the ratio

$$V_{ph}^{00} : V_{ph}^{10} : V_{ph}^{01} : V_{ph}^{11} = 1:0.05:0.88:0.28 \quad (10)$$

Comparing to Eq. (6), we see that  $V_{ph}$  displays a strong isospin dependence and a weaker spin dependence, the reverse of the situation for  $W$  in the Paris model. The off-diagonal elements  $V_A$ , which may be more directly comparable to  $W$ , are moderately isospin dependent but are taken to be independent of  $S$ , opposite to the trend displayed by  $W$  in ref. (29). It is clear that the present  $N\bar{N}$  data are insufficient to settle the fascinating question of the degree of spin and isospin dependence of  $N\bar{N}$  annihilation processes. Quantitative guidance from the quark/gluon picture is needed. Various other phenomenological models have been applied to the  $N\bar{N}$  system, although no fits as detailed as those of the Paris and Nijmegen groups have been done. We mention separable potential<sup>33</sup> models, which have some motivation in the context of quark rearrangement models. These topics are treated more extensively in the review<sup>34</sup> of A. M. Green.

## 5. MICROSCOPIC MODELS OF $N\bar{N}$ ANNIHILATION

In Chap. 4, we discussed a variety of phenomenological models for  $N\bar{N}$  annihilation. We now turn to a class of models motivated by quantum chromodynamics (QCD), in which annihilation is described in terms of confined quarks ( $Q$ ) and gluons ( $g$ ), either through  $Q\bar{Q}$  annihilation into  $g$ , or quark rearrangement processes. In principle,  $N\bar{N}$  annihilation should be a good test of quark/gluon dynamics at short distances. Our goal is to try to establish the connection between the microscopic and phenomenological forms of the annihilation potential. Aside from the geometrical aspects of the problem, which involve convolutions of bag model wave functions for quarks, we also study the spin, isospin and energy dependence predicted by various microscopic models. It is really these features which enable us to differentiate between models, since the geometrical aspects (effective size of the absorptive region) of the problem are common to all approaches.

The simplest QCD motivated approach to  $N\bar{N}$  annihilation is due to the Seattle group<sup>35</sup>, who consider quark-antiquark annihilation into one gluon. The process  $Q\bar{Q} \rightarrow g$  can only occur in the overlap volume of the bags confining

the quarks. The gluon is treated as a plane wave, and the bags are assumed to remain spherical as they overlap. The final state  $Q^2\bar{Q}^2g$  is considered as a "doorway state" leading to many complex reaction channels. It is assumed that this  $Q^2\bar{Q}^2g$  configuration never finds its way back into the elastic channel (the familiar "never come back" approximation in nuclear physics, valid when the number of compound nuclear levels is large). Thus one can simply sum over final  $Q^2\bar{Q}^2g$  states in order to obtain a model for  $W$ , without worrying how this configuration hadronizes into a final state containing color singlet mesons.

In ref. (35), the spatial wave function of the quarks was taken from the MIT bag model. A similar calculation using oscillator wave functions is given in ref. (36). The resulting<sup>35</sup>  $N\bar{N}$  absorptive potential  $W(r)$  contains central, spin-spin and tensor components, each of which has the form

$$W_i(r) = (\alpha_S^*/R) f_i(r/R) \quad (11)$$

$$f_i(r/R) = \sum_{n=0}^4 a_{ni} [2-(r/R)]^{n+4} \text{ for } r < 2R$$

where  $\alpha_S^*$  is an effective QCD coupling constant, and  $R$  is the bag radius. For  $r > 2R$ ,  $W(r)$  vanishes, since the spherical bags do not overlap.

The explicit spin-isospin dependence of the non-tensor part of  $W(r)$  is given<sup>36</sup> by the factor

$$W(r) \sim (243 + 9\sigma_{\bar{N}} \cdot \sigma_N - 27 \tau_{\bar{N}} \cdot \tau_N - 25 \sigma_{\bar{N}} \cdot \sigma_N \tau_{\bar{N}} \cdot \tau_N) \quad (12)$$

This can be used to give the ratios  $W^{IS}$ :

$$W^{00} : W^{10} : W^{01} : W^{11} = 0.18 : 0.65 : 1 : 0.49, \quad (13)$$

valid at all  $r$  and  $E$ .

Comparing with the result (6) for the phenomenological fit of the Paris group<sup>29</sup>, we see that the one gluon model is qualitatively different: for instance,  $W^{00}$  is now the weakest rather than the strongest component.

The one gluon model was applied<sup>35</sup> to total and integrated elastic and charge exchange cross sections, with good fits being obtained with

$$\alpha_S^* \approx 10, \quad R \approx 0.9 \text{ fm}, \quad (14)$$

although a reasonable description of the data may be obtained in the whole range  $0.6 \leq R \leq 1.1 \text{ fm}$ . These results yield a bag radius somewhat smaller than the original MIT model<sup>37</sup>.

The one gluon model of annihilation has geometrical features very similar to that of the other models we have discussed, as shown in Fig. 9. The solid curves meet in the region  $r \approx 0.7 - 0.8 \text{ fm}$ , which appears to define an effective  $N\bar{N}$  strong absorption radius. It is clear that the behavior of  $W(r)$  for  $r < 0.5 \text{ fm}$  is largely irrelevant; the data clearly do not constrain the

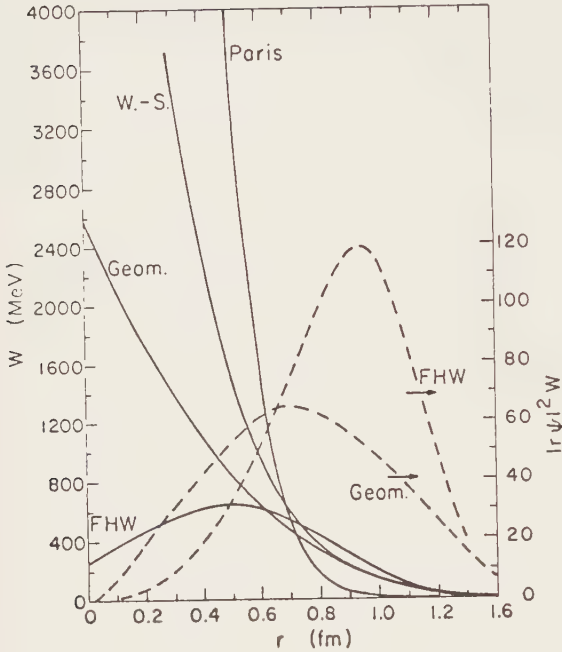


FIGURE 9

A comparison<sup>35</sup> of  $^1S_0$  pp absorptive potentials (solid lines) for the models of Dover-Richard<sup>28</sup> (W.-S.), the Paris group<sup>29</sup>, and the Seattle group<sup>35</sup>. For the latter, the  $QQ + g$  model (FHW) and a purely geometric model (Geom.) are shown. The dashed lines show the region of absorption (right-hand scale) for the atom 1s wave function. It is necessary to crank up

radial shape of  $W(r)$  in this region. Note that the effective radius for the Paris analysis<sup>29</sup> is much the same as that for other models, although the radius parameter appearing in Eq. (5) is only 0.1 fm. In speaking of the "range" of the annihilation potential, the physically meaningful quantity is the effective range, which depends on both the well depth and the range parameter describing the radial shape.

Although the one gluon model can be arranged to give the correct NN geometrical properties by varying  $R$  and  $\alpha_S^*$ , it has a number of faults, and is clearly not an adequate representation of the physics of NN annihilation. It is necessary to crank up

$\alpha_S^*$  to large values in order to get the correct magnitude for the cross sections. The resulting value (Eq. (14)) is an order of magnitude larger than the perturbative value  $\alpha_S \approx 1-2$ . Thus  $\alpha_S^*$  can only be considered as an effective coupling constant which simulates the summed influence of many higher order processes. Although higher order terms probably do not qualitatively alter the radial shape of  $W(r)$ , there is no reason to suspect that the particular spin-isospin structure (12) obtained from the one gluon process is preserved in higher order. In fact, one expects the spin dependence to be considerably altered by multigluon and quark rearrangement graphs. A hint that the one gluon analysis provides the wrong spin-isospin mixture is seen in its very poor fits to the backward elastic data, which are sensitive to spin effects. The polarization data, which might also be

illuminating, were not included<sup>35</sup> in the analysis. The one gluon model, through its neglect of any threshold effects relating to mesonic channels, yields an energy independent  $W(r)$ . Any sensible microscopic model which takes account of specific channels will yield an energy dependence in the corresponding one channel approximation. In the Paris model<sup>29</sup>, the fits are considerably improved by the energy dependence of  $W(r)$ .

We now turn to a consideration of quark rearrangement models. In these approaches, the final state is automatically "hadronized" into physical mesons, so detailed comparisons with  $N\bar{N}$  branching ratios into particular mesonic channels become feasible, as well as the description of total cross sections--possible already with far cruder models. This class of models has been reviewed by Green<sup>34</sup>, so we will be brief.

Recent efforts by Maruyama and Ueda<sup>38</sup> have focused on the quark rearrangement diagram shown in Fig 10. This mechanism produces three meson states composed of  $\pi$ ,  $\eta$ ,  $\omega$  and  $\rho$  mesons. Vector meson decay then leads to the correct pion multiplicity in the final state. The probability  $P$  for an  $N\bar{N}$  system in channel  $\{I,S\}$  to annihilate into mesons  $\alpha, \beta, \gamma$  is taken to be

$$P(I,S,\alpha,\beta,\gamma) = b(I,S)C(I,S,\alpha,\beta,\gamma)g_\alpha g_\beta g_\gamma V(\alpha,\beta,\gamma) \quad (15)$$

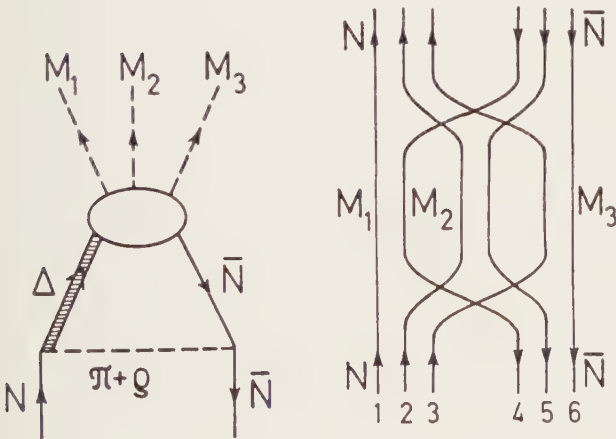


FIGURE 10

A quark rearrangement graph leading to a three meson intermediate state is shown on the right. An annihilation graph involving the  $\Delta$  resonance is shown on the left (from ref. (34)).

where  $C(I,S,\alpha,\beta,\gamma)$  is an  $SU(6)$  overlap factor,  $g_\alpha$  is the  $q\bar{q}$  coupling strength to meson  $\alpha$  (found to be approximately proportional to the mass  $m_\alpha$ ),  $V$  is the phase space factor (which generates an energy dependence), and  $b(I,S)$  takes account of initial state distortion effects. Eq. (15) was used<sup>38</sup> to fit the branching ratios for  $N\bar{N}$  annihilation into three mesons; a good fit is obtained with seven free parameters. If  $P$  in

Eq. (15) is summed over  $\alpha$ ,  $\beta$ ,  $\alpha$ , and identified with the absorptive strength  $W^{IS}$ , we obtain

$$W^{00} : W^{10} : W^{01} : W^{11} : = 1 : 0.57 : 0.44 : 0.36 \quad (16)$$

Comparing with Eq. (6), we see that  $W^{00}$  is largest, as in the fit<sup>29</sup> to the  $\bar{N}\bar{N}$  scattering data, but the spin dependence is not as dramatic.

Through the phase space factor  $V$ , the effective  $W$  becomes quite energy dependent in the quark rearrangement model. Some channels involving vector mesons ( $\rho^+\rho^-\pi^0$ ,  $\rho^+\rho^-\eta$ ,  $\omega\rho^+\rho^-$ , for instance) have very large  $SU(6)$  strengths  $C$ , but do not contribute much near  $E = 0$  due to their large mass. As  $E$  increases, these modes become dominant.

The quark rearrangement model has recently been refined by Green and his collaborators<sup>39, 40</sup>, in the form of a system of coupled equations for  $\bar{N}\bar{N}$  elastic and annihilation channels. The transition potential for  $\bar{N}\bar{N} \rightarrow M_1 M_2 M_3$  is non-local (and separable, if oscillator wave functions are used to calculate overlaps). In Eq. (39), a local approximation was applied to the equivalent one channel annihilation potential

$$V_{\text{ann}}^{IS}(r) + iW^{IS}(r) = \lambda e^{-\beta r^2} I(IS, E) \quad (17)$$

The function  $I$  is rapidly increasing with energy; thus it is possible in principle to have some relatively narrow  $\bar{N}\bar{N}$  bound states ( $E < 0$ ), while retaining very strong absorption at higher energies. If  $\lambda$  is adjusted phenomenologically, the  $\bar{N}\bar{N}$  data, including the backward elastic points, can be fitted well. It will be interesting to see whether or not the  $180^\circ$  fit can be reproduced when the full non-local coupled equations are solved. In ref. (40), the quark rearrangement model is generalized to include  $\bar{N}\bar{\Delta} + \bar{N}\Delta$  and  $\Delta\bar{\Delta}$  intermediate states. The spin-isospin dependence of  $I(IS, E)$  is rather similar to Eq. (16), i.e.  $W^{00}$  is strongest and  $W^{11}$  is weakest at  $E = 0$ , and  $W^{00}$  generally remains the largest for  $E > 0$ . This is qualitatively similar to the Paris result<sup>29</sup> of Eq. (6), except that the total spread in  $W^{IS}$  values is only a factor of 2-3, rather than an order of magnitude or more.

A problem with these models is that the overall strength cannot be reliably calculated (a rough estimate is given in ref. (40)). Thus, as with the one gluon model (where  $\alpha_S^* \approx 5-10 \alpha_S$ ), there is the danger that the effect of higher order corrections and other mechanisms is being simulated by varying the overall strength of the annihilation potential, and that one is in fact not testing the validity of the mechanism at hand. A key point is the spin-isospin dependence of  $W$ : different mechanisms at the quark level lead to quite distinct predictions for  $W^{IS}$ . Presently, the data are not sufficient



to obtain a sharp distinction between competing models: the measurement of spin observables in different isospin channels ( $\bar{p}p \rightarrow \bar{p}p$ ,  $\bar{n}n$  and  $\bar{n}p \rightarrow \bar{n}p$ ) is crucial to further progress.

## 6. THE $\bar{N}$ AS A PROBE OF THE NUCLEUS

We mention briefly a few possibilities: i)  $\bar{N}$  inelastic scattering, ii) quasi-stable few-body systems, iii) production of hypernuclei with  $\bar{N}$ 's.

The strong spin and isospin dependence of the  $\bar{N}$  absorptive potential  $W^{\text{IS}}$  should show up as a characteristic selectivity in  $\bar{N}$  inelastic scattering from nuclei. For instance, using the Paris model<sup>29</sup>, it has been predicted<sup>41</sup> that the isoscalar, spin flip ( $\Delta T=0$ ,  $\Delta S=1$ ) modes of nuclei are strongly excited with  $\bar{N}$ 's. In a model where  $W$  is spin-isospin independent, these modes are only weakly excited, as is the case for nucleon inelastic scattering.

Another consequence of the spin-isospin dependence of  $W$  is that some relatively long-lived few-body systems containing an  $\bar{N}$  may exist. For instance, if one believes that the two-body  $N\bar{N}$  absorption is smallest for  $I = S = 1$  ( $W^{11}$  in Eq. (6)), then one can try to exploit this selectivity by preparing the spin-isospin environment of an  $\bar{N}$  in a nucleus so as to emphasize this channel. The prototype reaction would involve a deuteron:

$$\bar{p} + (d)_{S=1, I=0} \rightarrow p + (\bar{p}n)_{S=1, I=1}, \quad (18)$$

for instance  ${}^6\text{Li}(\bar{p}, p)_{\bar{p}} {}^6\text{H}$ , where  ${}^6\text{H}$  has the cluster structure  $[\alpha \otimes (\bar{p}n)_{S=I=1}]_{I=+}$ . If an  $\bar{N}$  is attached to a core which is not spin-isospin saturated, the long range pion exchange term contributes to the Hartree field. In few-body systems, this effect will be relatively more important. The  $\bar{N}$  wave function would be localized in this region of long-range attraction, and the resulting nucleus might be relatively long-lived. For instance, one could ask whether the addition of a  $\bar{p}$  stabilizes the di-neutron: the relevant reaction would be  ${}^3\text{H}(\bar{p}, p)(\bar{p}nn)_{1/2^+, I=3/2}$ .

The coherent tensor forces which operate in the  $N\bar{N}$  system also crop up in the  $\bar{p}p \rightarrow \bar{\Lambda}\Lambda$  reaction. Here the coherence is due to  $(K, K^*)$  rather than  $(\pi, \rho)$  exchanges. The observed  $\bar{p}p \rightarrow \bar{\Lambda}\Lambda$  amplitudes display a marked spin dependence; large  $\Lambda$  and  $\bar{\Lambda}$  polarizations are seen. This leads to the possibility<sup>42</sup> that the  $(\bar{p}, \bar{\Lambda})$  reaction on nuclear targets may be used to directly populate unnatural parity states of  $\Lambda$  hypernuclei, for example the  $2^-$  member of the ground state doublet in  ${}^{12}_{\Lambda}\text{C}$ . These are not seen in the  $(K^-, \pi^-)$  reaction, since spin-flip is absent at  $0^\circ$ , and small at non-zero angles. Via the  $(\bar{p}, \bar{\Lambda}\gamma)$  reaction, one could observe the M1  $\gamma$  rays connecting  $\Lambda$  hypernuclear doublets, and thus obtain a handle on the spin dependence of the  $\Lambda N$  interaction. Note

that  $\bar{\Lambda}$ -nuclei could be formed in the  $(\bar{p}, \Lambda)$  reaction, but the cross sections at  $0^\circ$  are predicted<sup>42</sup> to be about 3 orders of magnitude smaller than for  $(\bar{p}, \bar{\Lambda})$  and the  $\bar{\Lambda}$  states are mostly rather broad.

The field of  $\bar{N}$ -nuclear interactions is a potentially fascinating one, and almost totally unexplored. We will have to leave it for a future talk.

#### ACKNOWLEDGEMENT

The author was supported by the U.S. Department of Energy under contract DE-AC02-76CH00016. Discussions with A. Gal, M. E. Sainio and R. Vinh Mau are gratefully acknowledged.

#### REFERENCES

- 1) R. D. Tripp, Proc. Fifth European Symposium on Nucleon-Antinucleon Interactions, Bressanone, Italy, June 1980.
- 2) G. A. Smith, Proc. Seventh Int. Conf. on Experimental Meson Spectroscopy, Brookhaven National Laboratory, Upton, New York, April, 1983.
- 3) C. Amsler et al., preprint CERN-EP/82-93, June, 1982.
- 4) Ch. D'Andlau et al., Phys. Lett. 58B (1975) 223.
- 5) M. Alston-Garnjost et al., Phys. Rev. Lett. 43 (1979) 1901.
- 6) P. H. Timmers, W. A. van der Sanden, and J. J. de Swart, Nijmegen preprint THEF-NYM-83.07.
- 7) P. H. Timmers, W. A. van der Sanden, and J. J. de Swart, Nijmegen preprint THEF-NYM-83.06.
- 8) F. Azooz et al., Phys. Lett. 122B (1983) 471.
- 9) J. Bodenkamp et al., Phys. Lett. B (to appear).
- 10) B. Barnett et al., Phys. Rev. D27 (1983) 493; J. Bensinger et al., Brookhaven preprint BNL-32091 (1982); Z. Ajaltouni et al., Nucl. Phys. B209 (1982) 301; A.D.J. Banks et al., Phys. Lett. 100B (1981) 191; S. U. Chung et al., Phys. Rev. Lett. 45 (1980) 1611.
- 11) B. Richter et al., Phys. Lett. 126B (1983) 284.
- 12) see the detailed discussion of the  $\gamma$  ray data by G. A. Smith in ref. 2.
- 13) L. Montanet, G. C. Rossi and G. Veneziano, Phys. Rep. 63 (1980) 149.
- 14) W. W. Buck, C. B. Dover and J. M. Richard, Ann. Phys. (N.Y.) 121 (1979) 47; C. B. Dover and J. M. Richard, Ann. Phys. (N.Y.) 121 (1979) 70.
- 15) I. S. Shapiro, Phys. Rep. C35 (1978) 129.
- 16) R. L. Jaffe, Phys. Rev. D17 (1978) 1445.

- 17) C. B. Dover, J. M. Richard and M. C. Zabek, *Ann. Phys. (N.Y.)* 130 (1980) 70.
- 18) E. Eisenhandler et al., *Nucl. Phys. B113* (1976) 1; A. A. Carter et al., *Nucl. Phys. B127* (1977) 202.
- 19) M. Nagels, T. Rijken and J. J. de Swart, *Phys. Rev. D12* (1975) 744.
- 20) A. D. Jackson, D. O. Riska and B. Verwest, *Nucl. Phys. A249* (1975) 397.
- 21) M. Lacombe et al., *Phys. Rev. D12* (1975) 1495.
- 22) C. B. Dover and J. M. Richard, *Phys. Rev. C25* (1982) 1952.
- 23) T. E. Kalogeropoulos, in *Proceedings of the IVth International Experimental Meson Spectroscopy Conference*, Northeastern University, Boston, 1974.
- 24) J. M. Blatt and V. F. Weiskopf, *Theoretical Nuclear Physics* (Wiley, New York, 1952).
- 25) J. S. Ball and G. F. Chew, *Phys. Rev. 109* (1958) 1385.
- 26) O. D. Dalkarov and F. Myhrer, *Nuovo Cimento A40* (1977) 152; W. B. Kaufmann, *Phys. Rev. C19* (1979) 440; A. Delville, P. Jasselette and J. Vandermeulen, *Am. J. Phys. 46* (1978) 907.
- 27) C. B. Dover and M. E. Sainio, unpublished calculations.
- 28) C. B. Dover and J. M. Richard, *Phys. Rev. C21* (1980) 1466.
- 29) J. Côté et al., *Phys. Rev. Lett. 48* (1982) 1319.
- 30) R. A. Bryan and R.J.N. Phillips, *Nucl. Phys. B5* (1968) 201.
- 31) R. P. Hamilton et al., *Phys. Rev. Lett. 44* (1980) 1179.
- 32) M. Lacombe et al., *Phys. Rev. C21* (1980) 861.
- 33) F. Myhrer and A. W. Thomas, *Phys. Lett. 64B* (1976) 59; A. M. Green, W. Stepień-Rudzka and S. Wycech, *Nucl. Phys. A399* (1983) 307; A. M. Green and S. Wycech, *Nucl. Phys. A377* (1982) 441.
- 34) A. M. Green, lectures at the International Summer School on the Nucleon-Nucleon Interaction and Nuclear Many-Body Problems, Jilin University, Changchun, China, July, 1983 (Helsinki preprint HU-TFT-83-17).
- 35) R. A. Freedman, W.Y.P. Hwang and L. Willets, *Phys. Rev. D23* (1981) 1103; M. A. Alberg et al., *Phys. Rev. D27* (1983) 536.
- 36) A. Faessler, G. Lübeck and K. Shimizu, University of Tübingen preprint (1982).
- 37) A. Chodos et al., *Phys. Rev. D10* (1974) 2599; T. DeGrand et al., *Phys. Rev. D12* (1975) 2060.
- 38) M. Maruyama and T. Ueda, *Nucl. Phys. A364* (1981) 297 and Osaka University preprint OUAM 82-12-1 (1982).

- 39) A. M. Green, J. A. Niskanen and J. M. Richard, Phys. Lett. 121B (1983) 101.
- 40) A. M. Green and J. A. Niskanen, Helsinki preprint HU-TFT-83-27 (June, 1983).
- 41) C. B. Dover, M. E. Sainio and G. E. Walker, Phys. Rev. C (submitted).
- 42) C. B. Dover, A. Gal and M. E. Sainio, in preparation.

## TWO NUCLEON PROBLEMS

Peter U. SAUER

Institute for Theoretical Physics, University Hannover, Hannover, Germany

The discussion session on "Two-Nucleon Problems" is summarized. New experimental data on the two-nucleon system below and above pion threshold and force models for their theoretical description are reviewed.

### 1. DEFINITION OF TWO NUCLEON PROBLEMS

Experimentally, the two-nucleon (NN) system is still being very actively studied below and above pion ( $\pi$ ) threshold. The relevant inelastic channels at intermediate energies are those with a single pion, i.e., pion-deuteron ( $\pi d$ ) and  $\pi NN$ . Single-baryon resonances of pion-nucleon scattering clearly operate as reaction mechanism in the inelastic channels. However, the nucleon is also a composite system with quark-gluon substructure determined by quantum chromodynamics (QCD), and QCD has ample room for dibaryon resonances of quark-gluon nature as an additional reaction mechanism. Thus, the two-nucleon system to be discussed is a system of coupled channels with composite clusters. On the theoretical side, two interacting nucleons still form the basic building block for any microscopic theory of nuclear phenomena. This is why the two-nucleon problem is fundamental for nuclear physics.

### 2. EXPERIMENTAL DATA

The new experimental data come mostly from spin experiments. Below pion threshold the proton-proton phase shifts are well established, the neutron-proton phase shifts still need improvement. Spin correlation experiments<sup>1</sup> are designed at energies below 50 MeV in order to determine - more independently - the  $^3S_1$  -  $^3D_1$  mixing parameter  $\epsilon_1$ , characteristic for the tensor force, and the  $^1P_1$  phase shift  $\delta$ . These phase shift parameters have been highly correlated in previous data. The sensitivity of the spin correlation  $A_{yy}$  on  $\epsilon_1$  and on  $\delta(^1P_1)$  is given in fig. 1. The bulk of the newly presented data refer to spin observables in the coupled NN- $\pi d$  system. The experiments are part of the search for dibaryon resonances. They are difficult to perform. In elastic  $\pi d$  scattering the data of the vector analyzing power<sup>2</sup>  $it_{11}$  shown in fig. 2 has been improved. The oscillatory behavior of the data in early measurements has now disappeared. The controversy on the corresponding tensor analyzing power<sup>3,4</sup>

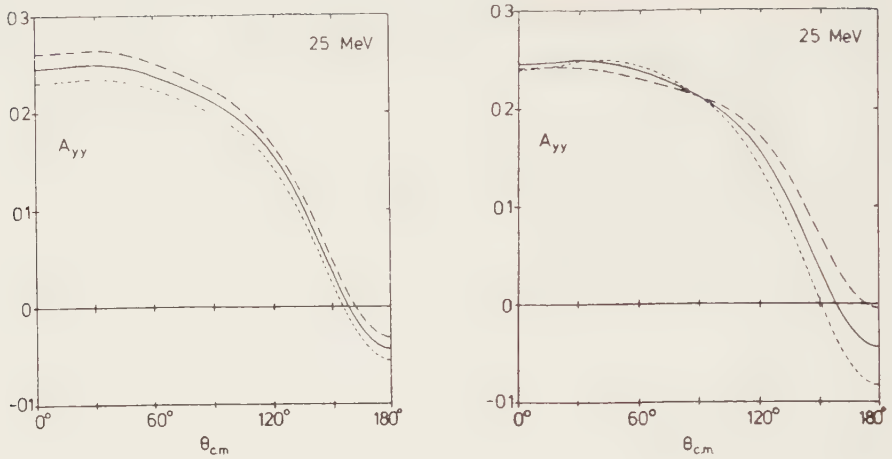


FIGURE 1

Sensitivity of the spin correlation parameter  $A_{yy}$  at 25 MeV to variations of the mixing parameter  $\epsilon_1$  and of the  $1p_1$  phase shift from ref. 1. Starting values are taken from the Paris potential. Left:  $\epsilon_1 = 1.60^\circ$  varied by  $\pm 0.50^\circ$ , right:  $\delta(1p_1) = -7.00^\circ$  varied by  $\pm 2.00^\circ$ .

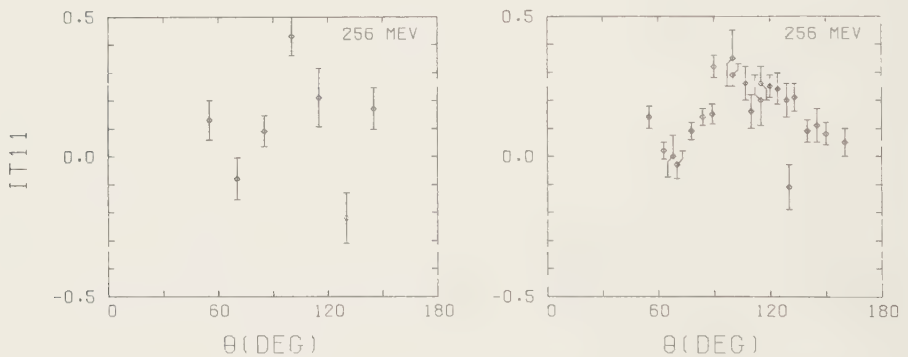


FIGURE 2

Example of data on the vector analyzing power  $it_{11}$  in elastic  $\pi d$  scattering from ref. 2. The data refer to 256 MeV pion energy. The scarce older data (left) have been substantially improved (right).

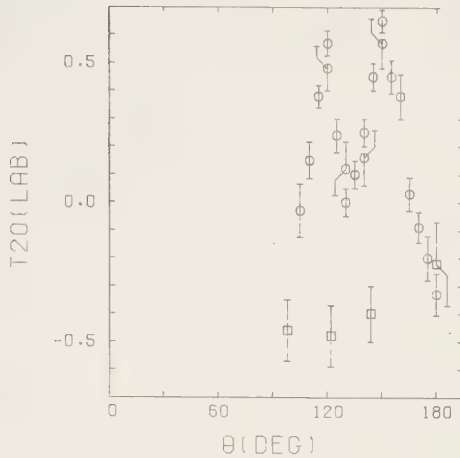


FIGURE 3

Angular distribution of the tensor analyzing power  $t_{20}^{lab}$  in elastic  $\pi$ d scattering. The data at 134 MeV pion energy (circles) taken from ref. 3 show a rapid variation and are in conflict with those of ref. 4 (squares) referring to 142 MeV pion energy.

$t_{20}$  of fig. 3 at around 140 MeV pion energy still remains. Pion production and absorption experiments<sup>5</sup>  $pp \leftrightarrow \pi d$  supplement the existing information on the two-nucleon system above pion threshold in an important way.

Do experimental data prove the existence of a resonance in the coupled NN- $\pi$ NN system? The use of standard techniques for establishing a resonance in a model-independent way, i.e., the search for peaks in cross sections<sup>6</sup>, the looping of scattering amplitudes in Argand plots<sup>7</sup>, the factorization of resonance residues<sup>8</sup>, has so far been inconclusive.

### 3. THE SEARCH FOR THE RELEVANT DEGREES OF FREEDOM IN THE TWO-NUCLEON SYSTEM

The theoretical discussion on two-nucleon problems centred around two questions:

- (1) Is the two-nucleon attraction at intermediate ranges to be understood in terms of meson exchanges or in terms of quark sharing between nucleonic clusters?
- (2) What is the status of force models which treat the coupled NN- $\pi$ NN system in a unified manner and which are based on the conventional nucleonic, isobaric and pionic degrees of freedom? Is their present failure in accounting for data evidence for dibaryon resonances of quark-gluon nature?



### 3.1. Intermediate range attraction of the two-nucleon interaction

The quark-gluon substructure of the composite nucleon is essential for the interaction when two nucleonic clusters overlap. At large separations meson exchange dominates the interaction. The small-distance phenomenology of the old meson theory is now to be replaced by a quark-gluon description<sup>9,10</sup>. A full QCD description of the two-nucleon interaction should yield the long-range meson exchange. There may be no conflict between these two descriptions. Duality suggests the equivalence<sup>11</sup> between all t-channel exchanges of one- and many-boson type and all s-channel poles realized by quark-gluon states. The dividing line in configuration space between the two seemingly different descriptions may only be a matter of convenience.

In practical terms, the meson-exchange picture of the two-nucleon force has been highly successful<sup>12-14</sup> in accounting for experimental data. It interprets the intermediate-range attraction as an effect of two-pion exchange. In contrast, nonrelativistic quark models with many-body confinement potentials<sup>15,16</sup>, i.e., without the unphysical long-range van-der-Waals force, also yield intermediate-range attraction as an effect of quark sharing between nucleonic clusters in the same way as atoms share electrons in molecular binding. An example taken from ref. 16 is given in fig. 4. These quark models are conceptually important, but at present are still qualitative. They are not yet able to compete with meson-exchange models for quantitative success.

### 3.2. Unified force model for the coupled NN- $\pi$ NN system

The standard force model designed to describe the two-nucleon system below and above pion threshold incorporates, besides the nucleonic degrees of freedom, pions in a one-pion approximation and important single-baryon resonances. E.g., the Hilbert space may consist as in fig. 5 of a nucleonic part and of sectors, in which one pion is added or in which a single nucleon is turned into a  $\Delta$ -isobar or a Roper-resonance R. Pions are created by vertices with baryons. The baryons are still bare ones. They have to be dressed for the pionic degree of freedom in order to become the physical nucleon,  $P_{33}$  and Roper resonances. The pion-nucleon interactions unaccounted for by isobars and the two-baryon interactions unaccounted for by the pion are added as unretarded two-body potentials which may be based either on heavy-meson exchange<sup>19,20</sup> or on a quark-gluon phenomenology<sup>21</sup>. The model respects three-particle unitarity. It is not microscopic in a fundamental sense, but it attempts a consistent description of a range of phenomena.

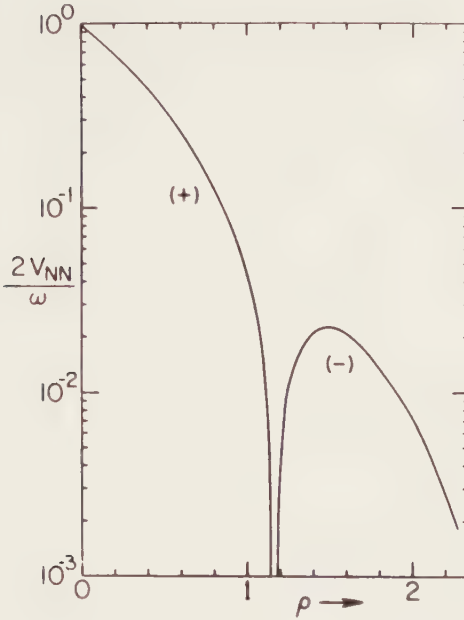


FIGURE 4

Effective potential between two nucleonic three-quark clusters taken from ref. 16. The orbital quark wave functions are those of a two-center harmonic oscillator. The effective potential is given in units of the oscillator quantum  $\omega$ , the cluster distance  $R$  in terms of the oscillator length  $a$ , i.e.,  $\rho = R/2a$ . The effective potential, presented by F. Lenz<sup>15</sup> for a corresponding two-meson model which can even be solved analytically, without the adiabatic approximation employed in ref. 16, shows the same features of intermediate-range attraction and short-range repulsion. Refs. 15 and 16 use many-body confinement potentials, in contrast refs. 17 and 18 use two-body confinement potentials. It cannot be excluded, that the intermediate-range attraction seen also in refs. 17 and 18 may merely be due to the unphysical van-der-Waals force arising from the employed quark hamiltonian.

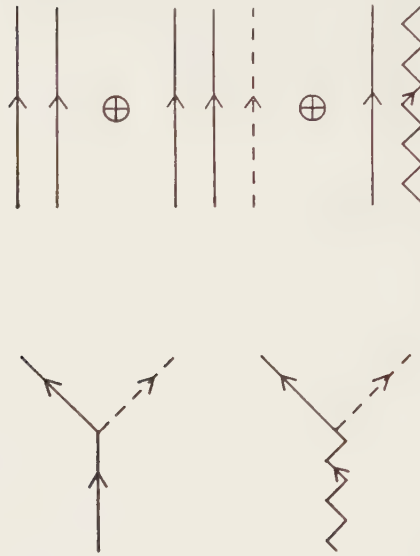


FIGURE 5

Hilbert space for the description of the two-nucleon system below and above pion threshold. The vertices which connect the baryonic sectors with the pionic sector are also shown. The solid line denotes the nucleon, the zig-zag line the isobar and the dashed line the pion.

Different groups use this model in different approximations. Broadly speaking they may be classified by the mechanism for pion production and pion **absorption**. One version bases this mechanism on the explicit  $\pi NN$  vertex of fig. 5 and is then faced with the problem of nucleon renormalization<sup>22</sup>. The other type<sup>22,23</sup> produces or absorbs a pion through the intermediary of the  $\Delta$ -isobar, which is in turn excited through an instantaneous transition potential from a purely nucleonic configuration.

The presence of the  $\Delta$ -isobar in the force model at least yields a pseudo-resonant behavior for partial wave amplitudes due to the  $N\Delta$ -branch cut, i.e., it yields a bump in cross sections, but no pole in the  $S$ -matrix. Besides this pseudoresonant behavior all versions of the force model may also develop dynamical resonances<sup>24</sup>, which, however, will not really catch our physics interest. They are no dibaryon resonances in the exciting sense. The physically interesting question is: Do we need - besides the conventional nucleonic, isobaric and pionic degrees of freedom - in addition explicit quark-gluon degrees of freedom in order to explain the experimental data in the coupled  $NN - \pi NN$  system?

The force model with the conventional nucleonic, isobaric and pionic degrees of freedom has had encouraging successes. Nevertheless, none of its approximative versions is at present able to account for all existing data. An example for the problems is given in fig. 6. Hope was expressed in the discussion that

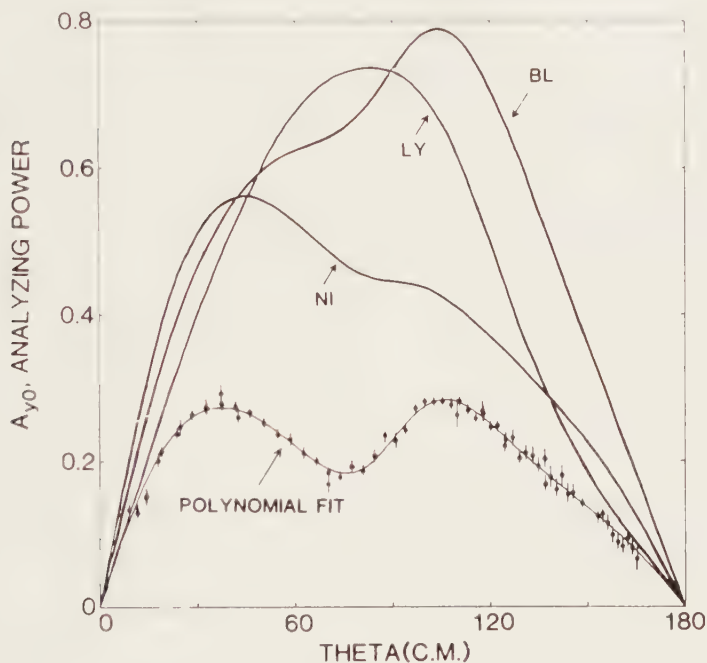


FIGURE 6

Analyzing power  $A_{y0}$  for the reaction  $\bar{p}p \rightarrow \pi^+ d$  at 793 MeV proton energy from ref. 25. The curves marked LY, BL and NI refer to theoretical predictions derived from refs. 26 (LY), 27 (BL) and 28 (NI). The force models of refs. 26 and 27 are of the first type version using the explicit  $\pi NN$  vertex, the one of ref. 28 of the second type version using the  $\Delta$ -isobar explicitly.

further tuning of the applied versions with respect to the parametrization of their dynamical input may make them work successfully throughout. However, neither the failure nor the possibility for ultimate success has been established yet for the conventional model. There was also a consensus that if the SIN measurement for the  $\pi d$  tensor analyzing power  $t_{20}$  of fig. 3 survived additional experimental scrutiny, then new physics and a signal for dibaryons of quark-gluon nature will have been found which would go beyond the dynamics of the conventional force model.

#### 4. NUCLEAR THEORY WITH THE FORCE MODEL BASED ON NUCLEONIC, ISOBARIC AND PIONIC DEGREES OF FREEDOM

There are two reasons for casting the experimental information of the two-nucleon system below and above pion threshold into the form of the force model of section 3.2. Firstly, one wants to check if the conventional degrees of freedom being used are the relevant ones for the two-nucleon reactions at intermediate energies. This task has not been completed yet. Secondly, the force model is to be used for a microscopic description of many-nucleon systems, i.e., for nuclear structure<sup>20,29</sup> with nonnucleonic degrees of freedom or for a microscopic derivation<sup>30</sup> of the pion-nucleus potential. This important aspect of the force model with nucleonic, isobaric and pionic degrees of freedom has received little attention in the past, has attracted only few contributions to this conference and was unfortunately not discussed.

#### ACKNOWLEDGEMENT

The rapporteur thanks the participants in the discussion for their contributions and for making the material they presented available to him. He especially thanks the chairman of the session for critically reading and improving the manuscript.

#### REFERENCES

- 1) R. Aures et al., "Measurement of the Spin Correlation Parameter  $A_{yy}$  for n-p Scattering in the Energy Range up to 50 MeV", contribution to this conference; M. Schöberl et al., "A Neutron-Proton Spin Correlation Experiment at 14 MeV Using a Polarized Proton Target", contribution to this conference.
- 2) G.R. Smith et al., "Measurements of  $it_{11}$  in  $\pi$ - $\bar{d}$  Scattering between 140 and 325 MeV", contribution to this conference.
- 3) V. Koenig et al., "Dibaryon Signals in the Tensor Polarization  $t_{20}$  in  $\pi$ - $\bar{d}$  Scattering", contribution to this conference.
- 4) W.S. Freeman et al., "Measurement of Tensor Polarization in Pion-Deuteron Elastic Scattering", contribution to this conference.
- 5) Kamal K. Seth, "Inelasticity in Nucleon-Nucleon Collisions and the Dibaryon Question", contribution to this conference.
- 6) Kamal K. Seth et al., "Search for Narrow Dibaryon Resonances", contribution to this conference.

- 7) I.M. Narodetskii and Yu. A. Simonov, *Sov. J. Nucl. Phys.* 28 (1978) 698;  
Yu. A. Simonov and M. van der Velde, *J. Phys.* G5 (1979) 493.
- 8) A.S. Rinat and J. Arvieux, *Phys. Lett.* 104B (1981) 182.
- 9) M. Bozoian and H.J. Weber, *Phys. Rev.* C28 (1983) 811.
- 10) Earle L. Lomon, "Effects of Quark Sub-Structure on Nucleon-Nucleon Scattering", contribution to this conference.
- 11) Yu. A. Simonov, contribution to this discussion.
- 12) J.J. de Swart, "Semiphenomenological Descriptions of the Nucleon-Nucleon Interaction", review talk presented at this conference.
- 13) M. Lacombe et al., *Phys. Rev.* C21 (1980) 861.
- 14) R. Machleidt and K. Holinde, "A Comprehensive and Consistent Meson-Exchange Model for the NN Interaction", contribution to this conference.
- 15) K. Yazaki, "Quantum Mechanical Scattering with Confining Interaction", review talk presented at this conference; F. Lenz, contribution to this discussion.
- 16) D. Robson, "A Many-Body Confinement Potential Model for Multi-Hadron Systems", contribution to this conference.
- 17) K. Maltman and N. Isgur, *Phys. Rev. Lett.* 23 (1983) 1827.
- 18) B. Silvestre-Brac et al., "Nonrelativistic 3-Quark Dynamical Solution of Faddeev Equation and the S-Wave Nucleon-Nucleon Scattering", contribution to this conference.
- 19) T.-S. H. Lee, *Phys. Rev. Lett.* 50 (1983) 1571.
- 20) H. Pöpping, P.U. Sauer and Zhang Xi-Zhen, "Two-Nucleon Force Model with  $\Delta$ - and  $\pi$ -Degrees of Freedom", contribution to this conference.
- 21) G.A. Miller and L.S. Kisslinger, *Phys. Rev.* C27 (1983) 1669.
- 22) I.R. Afnan, "The Nucleon-Nucleon Interaction", review talk presented at this conference.
- 23) P.U. Sauer, *Nucl. Phys.* A353 (1981) 3c; M. Betz and T.-S. H. Lee, *Phys. Rev.* C23 (1981) 375.
- 24) W.M. Kloet and J.A. Tjon, *Phys. Lett.* 106B (1981) 24;  
T. Ueda, *Phys. Lett.* 119B (1982) 281.
- 25) Kamal K. Seth et al., *Phys. Lett.* 126B (1983) 164.
- 26) C. Fayard et al., *Phys. Rev. Lett.* 45 (1980) 524;  
T. Mizutani et al., *Phys. Lett.* 107B (1981) 177.
- 27) B. Blankleider and I.R. Afnan, *Phys. Rev.* C24 (1981) 1572.
- 28) J. Niskanen, *Nucl. Phys.* A298 (1978) 417;  
J. Niskanen, *Phys. Lett.* 79B (1978) 190.

- 29) A.M. Green, Rep. Prog. Phys. 39 (1976) 1109.
- 30) T.-S. H. Lee and K. Ohta, Phys. Rev. C25 (1982) 3043.



Chapter IV

**THEORY AND CALCULATIONS  
IN FEW BODY SYSTEMS**



## THEORETICAL DESCRIPTION OF FEW-CLUSTER SYSTEMS

E.W. SCHMID

Institut für Theoretische Physik, Universität Tübingen,  
D-7400 Tübingen, W.-Germany

The transition from a (non-relativistic) quantum theory of particles to a quantum theory of clusters is discussed. Effective interactions given by the resonating group model, the orthogonality condition model and the fish bone optical model are reviewed. Special attention is paid to the appearance of three-body potentials. A hypothesis is made that three-body forces are a measure of the non-elementarity of the interacting bodies. The resonating group Faddeev method is formulated and numerical results on the breakup reaction  $d(\alpha, p)\alpha$  are presented.

### 1. INTRODUCTION

During the first two days of this conference we have learned that nucleons are formed by bags of quarks, which are surrounded by clouds of quark-antiquark pairs. This means that nucleons are composite particles and, consequently, should be treated as such. In earlier years, not having anything better on hand, we have treated them as pointlike particles interacting by a potential. We have assumed that such a potential exists and have considered it a challenge to investigate its off-shell behaviour. With a quark model, we have at least the hope that it might become possible to derive the effective interaction of nucleons from a more fundamental theory; preliminary attempts have produced promising results, already<sup>1,2</sup>.

Effective interactions of composite particles are obtained by the transition from a dynamical theory of the subparticles to a dynamical theory of the composite particles. In this two-level scheme the theory at the first level is defined by fundamental principles and by reasonable assumptions, while at the second level, the effective dynamical equation is derived. Unfortunately, this road is still rather stony for quarks and nucleons: i) at the first level we are not yet certain which assumptions are reasonable, ii) in making the transition to the second level we are not yet sure which approximations should be made and how to convert a complicated mathematical expression into a potential. What we need is more experience with composite particle dynamics and this need brings me to the topic of my talk.

There are clusters of nucleons, like  $t$ ,  ${}^3\text{He}$ ,  $\alpha$ ,  ${}^{16}\text{O}$ , which have rather stable ground states. We may try to treat them as elementary particles, study their effective interactions and investigate where and how the elementary particle

aspect breaks down. Also here, we are dealing with a two-level scheme. At the first level, we assume the Schrödinger equation for the nucleons, the Pauli principle and, as a reasonable assumption, some phenomenological N-N potential. At the second level, we are looking for a dynamical equation which effectively describes the relative motion of clusters. After having chosen the N-N interaction, the theory at the first level is well defined. We can study the transition to the second level and we can study general features of the effective interaction of clusters. Some of these features may be general enough to be relevant, also, in the constituent quark model of the nucleons. Knowing what we are looking for, we can now shop around and see what's on the market, already.

We shall briefly look at cluster decompositions of A-nucleon integral equations and then proceed to the resonating group model and to simplified versions of this model. Especially in the simplified versions, the structure of composite particle interactions will become transparent and it will be seen that there is a relation between energy-dependence of two-cluster potentials, three-cluster potentials and the probability density interpretation of the absolute square of a wave function. Finally we shall discuss the resonating group Faddeev method and present numerical results on d- $\alpha$  elastic and breakup scattering in which the  $\alpha$ -particle is treated as an elementary particle.

## 2. CLUSTER DECOMPOSITION OF A-PARTICLE INTEGRAL EQUATIONS

This important subject will be covered by the talk of K. Kowalski (Session IV.7). Therefore I can limit myself to a few remarks. There exist various forms of A-nucleon integral equations which are rigorously equivalent to the A-nucleon Schrödinger equation plus boundary condition. Their reduction to effective integral equations for clusters of nucleons has formally been done by several groups<sup>3-7</sup>. The advantage of this approach is that it starts from a rigorous theory and includes the effect of all possible reaction channels. The disadvantage is that the reduction is so complicated that it becomes difficult to find good approximations and even more difficult to perform numerical calculations. A major problem is caused by the Pauli principle. The mean free path of interpenetrating clusters becomes very short when the exchange of two nucleons, already, leads to a new cluster configuration. The indistinguishability of nucleons thus becomes an essential ingredient and the tedious task of antisymmetrizing sets of integral equations cannot be spared.

## 3. THE RESONATING GROUP MODEL AND RELATED MODELS

In the resonating group model, the reduction of the Schrödinger equation for particles to an effective equation for clusters is achieved by a restriction of

the space of wave functions<sup>8-10</sup>. In the so-called single-channel no-distortion approximation, one assumes that the ground state wave functions  $\phi_1, \phi_2 \dots$  of the clusters do not change when the clusters overlap and interact. Only the relative motion wave function  $\chi$ , as a function of the center of mass coordinates of the clusters, is considered to be free. Denoting the product  $\phi_1 \phi_2 \dots \phi_N$  by  $\Phi$  the restricted space of functions is given by  $\delta\psi = A\{\Phi\delta\chi\}$  where  $\delta\chi$  means all variations of  $\chi$  and  $A$  denotes antisymmetrization. The resonating group equation reads

$$\langle \Phi\delta\chi | A(H-E) | \Phi\chi \rangle = 0 \quad (1)$$

From its relative motion solutions  $\chi$  one gets the microscopic solution  $\psi$  as  $\psi = A\{\Phi\chi\}$ . The microscopic hamiltonian  $H$  contains a phenomenological N-N potential. When a hard core potential is used, the bra and ket states appearing in (1) are multiplied by Jastrow correlation functions.

The important feature of the resonating group method is that microscopic wave functions are properly antisymmetrized. This means, for instance, that one does not get twice the nuclear matter density when two  $\alpha$ -particles overlap. This is one of the reasons why in the  $\alpha$ - $\alpha$  system, for instance, the no-distortion approximation yields observables which are in good agreement with experiment.

The resonating group approximation may be improved by enlarging the function space. In the coupled-channels resonating group model, the function space is a sum of terms,  $\delta\psi = A\{\Phi_1\delta\chi_1 + \Phi_2\delta\chi_2 + \dots\}$ , where the  $\chi_1, \chi_2, \dots$  are relative motion states of the various channels. Eq. (1) becomes a matrix equation, in this case. If, in addition, internal motion states  $\tilde{\phi}_i$  are introduced which are not products of ground states of clusters, one gets the so-called distortion approximation, because the additional states can describe the distortion of clusters in the region of strong interaction. When there are more than 2 clusters, the distortion states are not necessarily square integrable, because of spectator motion, and the resonating group equation becomes complicated<sup>10</sup>.

Let us return to Eq. (1). After performing the integration over internal coordinates one gets

$$(T + V - E_r + k^T + k^V + K E_r) |\chi\rangle = 0 \quad (2)$$

where  $T$  is the relative motion kinetic energy operator,  $V$  is a double folding potential and  $E_r$  is the relative motion energy. The terms  $k^T$ ,  $k^V$  and  $K E_r$  are non-local potentials which arise from antisymmetrization together with microscopic kinetic energy, potential energy and energy, respectively.

The non-local potentials are rather complicated expressions, even when the cluster ground states are approximated by ground states of the harmonic oscillator shell model, as it is usually done. Nevertheless, these potentials have

been evaluated and used in bound state and scattering calculations for many systems of light nuclei; some illustrations will be presented in the subsequent talk by H.M. Hofmann.

We want to treat clusters as elementary particles. This means that we want to interpret Eq. (2) as an effective Schrödinger equation and  $\chi$  as a quantum mechanical wave function. Let us see whether this is possible. At the first level, we have a microscopic wave function  $\psi$  which we consider to be a quantum mechanical wave function. At the second level we have a relative motion function  $\chi$  and we want to ask whether  $|\chi|^2$  is a probability density. A probability interpretation implies correct normalization. We immediately see that we are in trouble, because  $\psi$  and  $\chi$  do not have the same norm. In the single-channel case, for instance, we have

$$\langle \psi | \psi \rangle = \langle \phi_\chi | A | \phi_\chi \rangle = \langle \chi | (1-K) | \chi \rangle . \quad (3)$$

Here,  $(1-K)$  is called overlap kernel and  $K$  is the norm kernel, which also appears in Eq. (2). The eigenstates  $u_i$  and eigenvalues  $\eta_i$  of  $K$  have been studied for many two-cluster systems and also for some three-cluster systems<sup>11</sup>. Eigenstates of  $K$  with eigenvalues equal to one are Pauli-forbidden relative motion states and satisfy Eqs. (1) and (2) at all energies; they appear only in the harmonic oscillator approximation.

It has been suggested by Friedman et al.<sup>12</sup> to perform an off-shell transformation by inserting  $(1-K)^{-\frac{1}{2}}$   $(1-K)^{\frac{1}{2}}$  in front of  $\chi$ , in Eq. (2), and by multiplying the equation by  $(1-K)^{-\frac{1}{2}}$  from the left\*. Separating out, again, the kinetic energy operator  $T$  and the folding potential  $V$ , one gets

$$(T + V - E_r + \bar{K}^T + \bar{K}^V) |\bar{\chi}\rangle = 0 , \quad (4)$$

$$|\bar{\chi}\rangle = (1-K)^{\frac{1}{2}} |\chi\rangle , \quad (5)$$

and new non-local potentials  $\bar{K}^T$  and  $\bar{K}^V$ . As can be seen from Eq. (3), the norm of  $\bar{\chi}$  is equal to the norm of the corresponding  $\psi$ . The interaction has become energy-independent hermitian, by the transformation; a wave packet state would now retain its norm at all times when it is described by Eq. (4) with  $E_r$  being replaced by  $i \hbar \partial/\partial t$ .

Saito<sup>14</sup> and Fließbach<sup>15</sup> have speculated that  $\bar{\chi}$  might be interpreted as a probability amplitude, which would mean that Eq. (4) is a Schrödinger equation. But here we have to be careful. Correct normalization is a necessary condition for a probability interpretation, but not a sufficient one. How can we find a

---

\*Fließbach and Walliser<sup>13</sup> have shown that this transformation remains meaningful in the harmonic oscillator limit, when the limit is defined in a proper way.

sufficient condition? We have to recall that a quantum mechanical probability density is, in principle, an observable. It must be possible to measure it, at least in a gedankenexperiment. When there are two clusters and we want to measure the probability density of finding their centers of masses at a certain (short) distance, we need a third body as a probe. The probe may be another cluster, or any particle. If we know its interaction with each one of the first two clusters, and if we know that the presence of the probe does *not* give rise to a three-body potential, then we can perform scattering experiments and deduce the relative probability distribution of the first two clusters by comparing experimental data with calculated cross sections. No three-body force means that the probe is interacting with each one of the two clusters as in free space, regardless of the presence of the other cluster; in a pictorial way, we can say that the spectator has an unblurred view of the two clusters. This gives us the sufficient condition we are looking for: Add a third particle, or cluster,  $c$  to a system of two clusters  $a, b$  and extract from the three-cluster effective interaction  $\bar{V}_{abc}$  the effective two-cluster interactions  $\bar{V}_{ab}$ ,  $\bar{V}_{bc}$  and  $\bar{V}_{ca}$ ,

$$(V + \bar{k}^T - \bar{k}^V \equiv) \bar{V}_{abc} = \bar{V}_{ab} + \bar{V}_{bc} + \bar{V}_{ca} + v_{abc}^{(3)} \quad (6)$$

When the remaining three-cluster potential  $v_{abc}^{(3)}$  is zero or negligible, Eq. (4) for the  $a, b$  system may be interpreted as a Schrödinger equation.

Let me put this into the form of a hypothesis: *Composite particles behave like elementary particles only when three- and multibody forces, in systems with a spectator, are small.* One could also say that three- and multibody forces, in systems with a spectator, are a measure of the non-elementarity of the interacting bodies. Let's use these statements as a guideline to learn more about three- and multibody forces.

What are the origins of multibody forces, in systems of nuclear clusters? First, there is the Pauli principle which gives rise to the three-body Pauli potential<sup>16</sup>. This potential is even present when one of the three clusters is a distinguishable particle<sup>17</sup>. A second origin are hard core correlations. When the phenomenological potential at the first level is a hard core potential, the effective two-cluster potentials tend to be less attractive in the interior region and a three-body potential tends to keep the clusters farther apart<sup>18,19</sup>. Third, there is channel coupling. In a  $p-n-\alpha$  system, for instance, the  $\alpha$ -particle will certainly no longer behave like an elementary particle when the  $t$ - $^3\text{He}$  channel is open. The channel-coupling interaction, which is a multibody force, signifies this fact. Fourth, there are distortions. When they are formally eliminated from the resonating group equation, one gets the so-called elimination potentials which are energy-dependent two- or multibody potentials<sup>10</sup>.



According to the above hypothesis, the elementary particle concept of clusters does not necessarily break down when clusters overlap. The appearance of multibody forces, when a spectator is introduced, is the important thing ! And even then one should not give up too early. It has been seen in a simplified version of the resonating group model<sup>17</sup> that the three-body Pauli potential mainly corrects for the improper normalization of the two-cluster relative motion function  $\chi$ . When an off-shell transformation according to Eq. (5) is performed, the effective potential becomes energy-independent and the three-body Pauli potential is greatly reduced. In the fish bone optical model with saturation<sup>18</sup>, which treats the second case in a somewhat simplified way, the off-shell transformation which makes the effective potential energy-independent also reduces the three-body force<sup>19</sup>.

There is a connection between an improper normalization of a subsystem wave function, energy-dependence of the subsystem interaction and multibody potentials. Since there are implications for the constituent quark model, let's see whether this connection holds true also for the elimination potentials which arise from cluster distortions.

The simplest case of an elimination potential is obtained when a square integrable, antisymmetric distortion state  $f$  is added to a single-channel (two-cluster) space,

$$\delta\psi = A\{\phi\delta\chi\} + \delta a f, \quad (7)$$

where  $\delta a$  is an arbitrary variation of the amplitude  $a$ . For simplicity we assume that  $f$  is orthogonal to all channel states (by having different spin or isospin, for instance). The resonating group equation then reads

$$\begin{aligned} \langle\phi\delta\chi|A(H-E)|\phi\chi\rangle + \langle\phi\delta\chi|(H-E)|f\rangle a &= 0, \\ \langle f|(H-E)|\phi\chi\rangle + \langle f|(H-E)|f\rangle a &= 0. \end{aligned} \quad (8)$$

Elimination of  $a$  leads to

$$\langle\phi\delta\chi|A(H-E)|\phi\chi\rangle - \frac{\langle\phi\delta\chi|H|f\rangle \langle f|H|\phi\chi\rangle}{\langle f|(H-E)|f\rangle} = 0. \quad (9)$$

In the second term we see the elimination potential  $V_{\text{eli}}$  which has the R-space representation

$$V_{\text{eli}}(\vec{R}', \vec{R}'') = - \langle\phi\vec{R}'|H|f\rangle \langle f|(H-E)|f\rangle^{-1} \langle f|H|\phi\vec{R}''\rangle. \quad (10)$$

When  $\langle f|H|f\rangle$  is a rather high energy, and when we are only interested in energies in the vicinity of the threshold energy  $E_0$ , we can make a Taylor expansion in  $E$  around  $E_0$  and truncate after the linear term,

$$V_{\text{eli}} = - \langle \vec{\phi} \vec{R}' | H | f \rangle \langle f | (H - E_0) | f \rangle^{-1} \langle f | H | \vec{\phi} \vec{R}'' \rangle - \\ - \langle \vec{\phi} \vec{R}' | H | f \rangle \langle f | (H - E_0) | f \rangle^{-2} \langle f | H | \vec{\phi} \vec{R}'' \rangle E_r + O(E_r^2) . \quad (11)$$

The second term on the right hand side has the same mathematical structure as the term  $K(\vec{R}', \vec{R}'')E_r$  in Eq. (2). Dropping  $O(E^2)$  we can combine these two terms, perform the off-shell transformation (5) and get a transformed equation for  $\bar{\chi}$  with an energy-independent potential.

What has this to do with renormalization of the relative motion function  $\chi$ ? Well, in the present case we have

$$\langle \psi | \psi \rangle = \langle \chi | (1-K) | \chi \rangle + |a|^2 . \quad (12)$$

Even when  $K$  were equal to zero,  $\langle \psi | \psi \rangle$  and  $\langle \chi | \chi \rangle$  would not be equal, because our function space has the "hidden corner"  $f$ , into which the system goes and re-emerges with probability  $|a|^2$ . When  $\chi$  satisfies Eq. (9) we can calculate  $a$  from the second line of Eq. (8) and insert it into Eq. (12). We get

$$\langle \psi | \psi \rangle = \langle \chi | (1-K) | \chi \rangle + \langle \chi \vec{\phi} | H | f \rangle \langle f | (H - E_0 - E_r) | f \rangle^{-2} \langle f | H | \vec{\phi} \chi \rangle . \quad (13)$$

We see now that, for  $E_r = 0$ , the operator which appears sandwiched between  $\langle \chi |$  and  $| \chi \rangle$ , in the second term on the right hand side, is just the operator which we have combined with  $K$  to perform the off-shell transformation (5). This means that, for  $E_r = 0$ , the norm of a solution  $\bar{\chi}$  of the transformed equation is equal to the norm of the microscopic state  $\psi$ , i.e. we have renormalized  $\chi$ .

The last question is how this is related to the appearance of a three-body potential, when a spectator is introduced. At the moment, there is only an intuitive answer: The spectator part of a wave equation is a potential *times* a wave function. When the latter contains a subsystem wave function with a norm defect, a three-body potential must appear to compensate for this defect. Going over from  $\chi \rightarrow \bar{\chi}$  means that this compensation is no longer necessary and we thus are eliminating one of the reasons for having a three-body force.

In a constituent quark model for the N-N interaction (forgetting relativistic corrections, for the moment), the state  $f$  might be identified with a  $\Delta$ - $\Delta$  configuration and  $\langle f | (H - E_0) | f \rangle$  would be around 600 MeV. The Taylor expansion (11) and the off-shell transformation (5) would then help to make the N-N interaction of the quark model comparable with energy-independent phenomenological N-N interactions.

The present simple example can be generalized to several distortion states and to distortion states which are not orthogonal to channel states. The simple example above has been given to demonstrate that the nuclear cluster model can indeed help us to understand some general features of composite particle

interactions.

We have already mentioned a few times that there are simplified models which are related to the resonating group model. Because of their simplicity, these models sometimes give a better insight into the structure of composite particle interactions than the more correct resonating group model. In the following we will take a brief look at orthogonality condition models and at the fish bone optical model.

Saito<sup>20</sup> studied resonating group wave functions and found that the Pauli principle produces some almost energy-independent nodes. In his orthogonality condition model he reproduces these nodes by a non-local potential which forces the wave function to be orthogonal to Pauli-forbidden and almost Pauli-forbidden eigenstates of the norm kernel. Neudatchin et al.<sup>21</sup> and Friedrich et al.<sup>22</sup> found that the Pauli-forbidden states can rather well be represented by bound states of a (deep) local potential. The orthogonality condition with respect to these bound states is automatically satisfied by two-cluster scattering states. Kukuĭn, Neudatchin and Pomerantsev<sup>23</sup> have extended the orthogonality condition model from two to three clusters. In their method, the Pauli-forbidden states of the two-cluster subsystems, together with any motion of the spectator cluster, are shifted to infinite energy by a non-local potential.

The two- and three-cluster orthogonality condition models have been extended to include also the effect of partly Pauli-forbidden norm kernel eigenstates by the fish bone optical model<sup>17</sup>, which reads

$$(T+V-E_r)|\bar{\chi}\rangle - \sum_{i,j} |u_i\rangle \langle u_i|(T+V-E)|u_j\rangle \bar{M}_{ij} \langle u_j|\bar{\chi}\rangle = 0 \quad (14)$$

The first term has the same origin as the direct part of the resonating group interaction, but  $V$  is now considered to contain fitting parameters. The second term approximates the exchange potentials  $\bar{K}^T + \bar{K}^V$  of Eq. (4) by an expansion of  $(T+V-E)$  on the basis  $|u_i\rangle$  of norm kernel eigenstates. The expansion is modified by the matrix  $\bar{M}_{ij}$ . The matrix contains the eigenvalues  $\eta_i$  of the norm kernel and introduces the Pauli effect into the equation. It reads

$$\bar{M}_{ij} = 1 - \frac{1-\eta_i}{\sqrt{(1-\bar{\eta}_i)(1-\bar{\eta}_j)}} \quad i \leq j, \text{ symmetric} \quad (15)$$

with

$$\bar{\eta}_i = \begin{cases} 0 & \text{if } \eta_i = 1 \\ \eta_i & \text{if } \eta_i \neq 1 \end{cases} .$$

The energy  $\epsilon$  is the energy at which the Pauli-forbidden eigenstates of the norm kernel become bound state solutions of the equation. In practice, one chooses

$\epsilon$  to be a large positive energy. If a certain residual interaction term is added to Eq. (14), if  $V$  is chosen to be equal to the double folding potential and if  $\epsilon = E_r$ , then Eq. (14) becomes identical to the off-shell transformed resonating group equation. It has been seen by comparison with Saito's model that the effect of the partly Pauli-forbidden states is essentially a barrier effect<sup>24</sup>, which may be interesting for heavy ion grazing collisions.

Eq. (14) is valid for two or more clusters; it has been extended to also include hard core correlations<sup>18</sup>. The evaluation of the exchange interaction is straightforward when the eigenstates and eigenvalues of the norm kernel are known. With the fish bone optical model, some investigations on three-body forces have been done. In an application to the bound state of three  $\alpha$ -particles<sup>25</sup> it has been seen that the effective three-body Pauli potential is very strong when the off-shell transformation (5) is not carried out. The three-body Pauli potential becomes much smaller by off-shell transformation. Nevertheless, some 7 MeV overbinding were obtained for the  $3\alpha$  system, as compared to the experimental binding energy of  $^{12}\text{C}$ , which may be due to the neglect of the saturation effect; almost the same amount of overbinding has been obtained by Smirnov et al.<sup>26</sup> in a calculation with the energy-independent (deep) local  $\alpha$ - $\alpha$  potential. In the  $\Lambda$ - $\alpha$ - $\alpha$  system, the three-body Pauli potential of the fish bone optical model has a simple mathematical form and can be evaluated without difficulty. It has been found<sup>25</sup> that, after off-shell transformation, it decreases the binding energy of  $^9_\Lambda\text{Be}$  by 0.05 - 0.2 MeV, depending on the choice of the effective  $\Lambda$ - $\alpha$  potential.

The three-body potential arising from hard core correlations has only been studied in the  $\Lambda$ - $\Lambda$ - $\alpha$  system where the Pauli principle has no effect<sup>19</sup>. It has been found that it decreases the binding energy by 0.5 MeV which is about 5% of the relative binding energy of the three bodies.

Concluding this section we may say that tightly bound nuclear clusters do behave *approximately* like elementary particles at energies which are well below the threshold where the clusters can break up. There is a striking similarity between the effective interaction of nuclear clusters and the interaction of nucleons: In both cases we have to accept the fact that three-body forces are non-zero<sup>27,28</sup>, even though they may be rather small when the off-shell behaviour of the two-body forces is chosen properly. The general investigation of three-body forces is only at the beginning and may become a promising field in the near future.

#### 4. THE RESONATING GROUP FADDEEV METHOD

In few-body physics it has always been a challenge to study the off-shell behaviour of interactions by solving the Faddeev equations and comparing the

results with experimental data. In the preceding section of my talk we have seen that the possibility of treating clusters as elementary particles depends to a large extent on the proper choice of this off-shell behaviour. For testing the elementary particle concept of clusters we want to combine the resonating group method and the Faddeev method. There are difficulties which we want to overcome in the following way.

- 1) We decompose the resonating group potential of the three-body system into three subsystem potentials and a remaining three-body potential. By applying the off-shell transformation (5) we install proper normalization of subsystem wave functions and reduce the strength of the three-body potential; the reduced three-body potential is neglected.
- 2) We replace the two-cluster resonating group potentials by potentials of the fish bone optical model and use its fitting parameters to reproduce experimental two-body data.
- 3) We compare the two-cluster potentials of the resonating group model and of the fish bone optical model by looking at wave functions. The resonating group wave functions are not uniquely defined because of the uncertainty of the phenomenological microscopic interaction. If the wave functions of the fish bone optical model lie within the range of this uncertainty, we can call the method a resonating group Faddeev method.
- 4) By a unitary interpolation method we reproduce phase shifts and wave functions of the two-cluster potentials of the fish bone optical model by rank- $r$  separable potentials; when Pauli-forbidden positive energy bound states are present they are reproduced too.
- 5) With the separable potentials, we perform Faddeev calculations and check whether the results are sensitive to the (undetermined) two-body phase shifts at high energies.
- 6) We calculate cross sections and analyzing powers and compare them with experimental data.

In the case of  $d-\alpha$  scattering with breakup into  $n-p-\alpha$  this procedure has been tested by K. Hahn et al.<sup>30</sup>. The  $n-p$  interaction was chosen to be a rank-1 separable potential for the  $^3S_1 - ^3D_1$  partial wave. A charge symmetric  $N-\alpha$  potential has been constructed by fitting the fish bone optical model (14), with a Woods Saxon direct potential including a spin-orbit term, to reproduce experimental  $n-\alpha$  phase shifts of the  $^2S_{1/2}$ ,  $^2P_{3/2}$  and  $^2P_{1/2}$  partial waves in the energy range 0-18 MeV (c.m.). The comparison of the fish bone optical model wave functions with resonating group wave functions shows a slight difference at short distances. This difference is mainly due to the fact that a Woods Saxon shape has been chosen as spherical part of the direct potential, while the corresponding res. group potentials were of gaussian shape. The Woods Saxon

shape has been preferred, however, because hard core correlations tend to make the direct potentials more similar to a Woods Saxon shape than to a gaussian shape<sup>31</sup>. The potentials of the fish bone optical model have been approximated by separable potentials of rank-3 for the  ${}^2S_{1/2}$  wave and rank-2 for the  ${}^2P_{3/2}$  and  ${}^2P_{1/2}$  waves. The separable potentials reproduce wave functions with high accuracy in the elastic energy region; the  ${}^2S_{1/2}$  potential also reproduces the Pauli-forbidden bound state at (chosen) +500 MeV. With the separable interactions the Faddeev equations have been solved (without Coulomb interaction) by Doleschall's code, for incident deuteron energies of 7.5 and 12 MeV (Lab).

Special emphasis has been put on point 5 of the above program, because the whole method would break down if the three-body observables were sensitive to the unknown high-energy behaviour of two-cluster phase shifts. In order to test this sensitivity, new separable potentials of rank-4 for the  ${}^2S_{1/2}$  wave and rank-3 for the  ${}^2P_{3/2}$  and  ${}^2P_{1/2}$  waves have been constructed which are wave function equivalent to the old potentials in the range 0-18 MeV (c.m.) but differ in the range 50-200 MeV (c.m.) by up to 50 degrees of phase shift. The Faddeev calculation has been repeated with the new potentials and no sensitivity of the observables has been found. This result may seem surprising, at first sight, but let us recall that the two sets of potentials are not only phase equivalent, at low energies, but wave function equivalent. A three-nucleon calculation by Fiedeldey<sup>32</sup>, in which the deuteron wave function has been kept fixed, seems to confirm the present finding.

The N- $\alpha$  phase shifts in the range 18-50 MeV may have some influence on the observables of d- $\alpha$  scattering at  $E_d = 7.5$  and 12 MeV (Lab). This is related to the question of whether distortions of the  $\alpha$ -particle, i.e. square integrable states of the d- ${}^3\text{He}$  and d-t channel, play an important role. A sensitivity check in this energy range, however, has not yet been performed.

Let us take a look now at the resonating group Faddeev results and compare them with the results of two d- $\alpha$  Faddeev calculations in which phenomenological N- $\alpha$  potentials have been employed. In all three calculations, the N- $\alpha$  potentials used reproduce rather well the experimental phase shifts of the elastic energy region. However, there is a difference in the half off-shell behaviour, which is depicted in Fig. 1, for the  ${}^2S_{1/2}$  partial wave. The full line shows the N- $\alpha$  wave function at 10 MeV for the potential used in the resonating group Faddeev calculation. The first node signifies orthogonality with respect to one Pauli-forbidden state. The broken line has been calculated with the phenomenological potential used by Charnomordic et al.<sup>33</sup>, in their d- $\alpha$  Faddeev calculation, and the dotted line has been calculated with another phenomenological potential. It is seen that the broken line is rather similar to the resonating



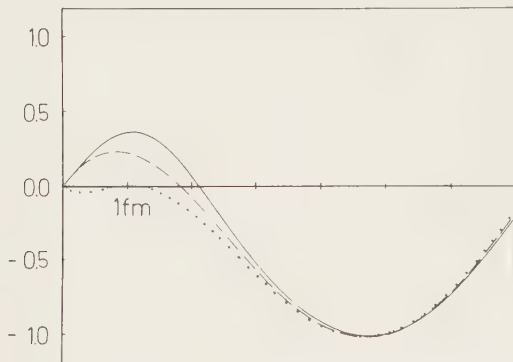


FIGURE 1

Comparison of N- $\alpha$  wave functions at  $E = 10$  MeV (c.m.); full line: resonating group model, broken and dotted line: phenomenological models.

group wave function, while the dotted line is not. Also, the second phenomenological potential produces phase shifts which, above 30 MeV, are too large in comparison with resonating group phase shifts. If the resonating group model is good and the Pauli principle has a significant influence on d- $\alpha$  scattering, we should expect good agreement with experiment in case of the resonating group Faddeev calculation, a little less good agreement in Charnomordic's calculation and worse agreement in the

third calculation. As is seen in Fig. 2, this is just what we get !

There is one more reason why the result of the phenomenological model by Charnomordic et al. agrees so well with experiment: In the  $^2P_{3/2}$  and  $^2P_{1/2}$  waves their potentials overestimate a little the probability of finding the nucleon inside the  $\alpha$ -particle, while in the  $^2S_{1/2}$  potential this probability is a little underestimated. In the elastic scattering cross section, these effects partly compensate<sup>34</sup>. The result of the third calculation demonstrates that it can be dangerous to work with phenomenological potentials.

Fig. 3 shows a breakup cross section of the resonating Faddeev calculation in comparison with the result obtained for the phenomenological potential by Charnomordic et al.. Further results will be given in Ref. 30. A d- $\alpha$  breakup calculation with a phenomenological N- $\alpha$  potential has also been performed by Koike<sup>35</sup>. In Koike's calculations the best agreement with experiment is obtained<sup>36</sup> when the  $^2S_{1/2}$  potential has a bound state at -300 MeV. In a Faddeev calculation, the effect of this large negative energy is similar to the effect of the choice  $\epsilon = +500$  MeV, in Hahn's calculation.

## 5. CONCLUSION AND OUTLOOK

We have studied the possibility of treating tightly bound nuclear clusters as elementary particles with the consequence that their motion is then described by a Schrödinger equation. We have seen that this is approximately possible in certain models, like the single-channel resonating group model. We have made the hypothesis that the appearance of three- and multicenter forces signifies



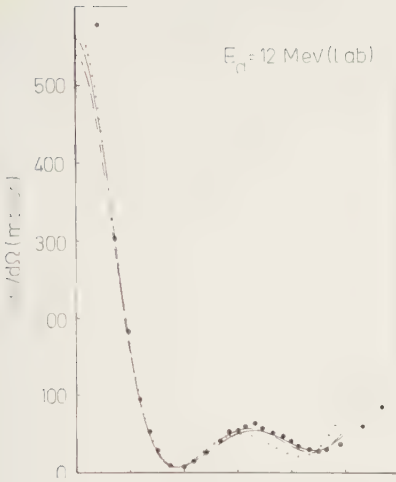


FIGURE 2

The  $d$ - $\alpha$  elastic differential cross section; full line: resonating group  $N$ - $\alpha$  potential, broken and dotted lines: phenomenological  $N$ - $\alpha$  potentials.



FIGURE 3

Differential cross section of the  $d(\alpha, p\alpha)n$  reaction; full line: resonating group  $N$ - $\alpha$  potential, broken line:  $N$ - $\alpha$  potential of Ref. 33.

the limit where the elementary particle concept breaks down. The resonating group Faddeev method allows us to perform scattering calculations with three clusters and to test the off-shell property of effective interactions. In a Faddeev calculation on  $d$ - $\alpha$  scattering it has been seen that the Pauli principle, which is effectively included in the interaction, has a strong influence on the three-body observables.

We may finally ask whether it is possible to apply the resonating group Faddeev method to three clusters of quarks or to other composite particle models. The answer seems to be yes. Resonating group potentials for two clusters of quarks have already been derived<sup>2</sup>. Progress has also been made in a self-regularizing non-linear spinor field theory. As has been shown by Stumpf and collaborators<sup>37</sup>, it is possible to derive from the general functional equation of the quantized spinor field an equation for the energy which is restricted to equal times for all fields. This equation corresponds to a Schrödinger equation for fermions with polarization clouds. When the polarization clouds are formally eliminated, effective potentials arise which are energy-dependent and contain three- and multibody components. If microscopically

derived potentials are brought into an energy-independent hermitian form, we may hope that three-body forces become small and may be neglected. We have seen that the input needed for a resonating group Faddeev calculation consists mainly of subsystem wave functions for a chosen set of energies, from which the separable potentials are then constructed. This input can be supplied even when the effective interactions are given by very complicated analytic expressions or by numerical arrays.

## REFERENCES

- 1) I.T. Obukhovskiy, V.G. Neudatchin, Yu.F. Smirnov and Yu.M. Tchuvil'skiy, *Phys. Lett.* 88B (1979) 231.
- 2) A. Faessler, F. Fernandez, G. Lübeck and K. Shimizu, *Phys. Lett.* 112B (1982) 201; A. Faessler and F. Fernandez, *Phys. Lett.* 124B (1983) 145.
- 3) G. Cattapan, L. Lovitch and V. Vanzani, Structural properties of multi-cluster equations derived from N-body scattering theory, Preprint 1983.
- 4) Gy. Bencze, W.N. Polyzou and E.F. Redish, *Nucl. Phys.* A390 (1982) 253.
- 5) R. Goldflam and K.L. Kowalski, *Phys. Rev.* C22 (1980) 2341.
- 6) W.N. Polyzou, A.G. Gibson and C. Chandler, *Phys. Rev.* C26 (1982) 1878.
- 7) K.L. Kowalski, Recent developments in few particle scattering theory, this volume.
- 8) J.A. Wheeler, *Phys. Rev.* 52 (1937) 1083 and 1107.
- 9) K. Wildermuth and Th. Kanellopoulos, *Nucl. Phys.* 7 (1958) 150; K. Wildermuth and W. McClure, *Cluster Representations of Nuclei* (Springer, Berlin, 1966); K. Wildermuth and Y.C. Tang, *A Unified Theory of the Nucleus*, in: *Clustering Phenomena in Nuclei*, Vol. 1 (Vieweg, Braunschweig, 1977).
- 10) E.W. Schmid, *Phys. Rev.* C21 (1980) 691; E.W. Schmid, N-Cluster dynamics and effective interaction of composite particles. II. The interaction, Preprint 1980 (rejected by the referees of *Phys. Rev. C*).
- 11) D.A. Zaikin, *Nucl. Phys.* A170 (1971) 584; H. Horiuchi, *Progr. Theor. Phys. Suppl.* 62 (1977) 90; K. Kato and H. Bando, *Progr. Theor. Phys.* 59 (1978) 774.
- 12) W.A. Friedman and H. Feshbach, in: *Racah Memorial Contributions* (North Holland, Amsterdam, 1968).
- 13) T. Fließbach and H. Walliser, *Nucl. Phys.* A377 (1982) 84.
- 14) S. Saito, *Progr. Theor. Phys. Suppl.* 62 (1977) 11.
- 15) T. Fließbach, *Z. Phys.* A272 (1975) 39.
- 16) E.W. Schmid, Two- and three-body interactions of composite particles, Preprint 1977 (rejected by the referee of *Nucl. Phys.*).

- 17) E.W. Schmid, *Z. Phys.* A302 (1981) 311.
- 18) Y. Akaishi, H. Klar, S. Maeda, S. Saito, E.W. Schmid and G. Spitz, contribution to this conference.
- 19) S. Maeda and E.W. Schmid, contribution to this conference.
- 20) S. Saito, *Progr. Theor. Phys.* 41 (1969) 705.
- 21) V.I. Kukulin, V.G. Neudatchin and Yu.F. Smirnov, *Nucl. Phys.* A245 (1975) 429.
- 22) B. Buck, H. Friedrich and C. Wheatley, *Nucl. Phys.* A275 (1977) 246.
- 23) V.I. Kukulin, V.G. Neudatchin and V.N. Pomerantsev, *J. Phys. G: Nucl. Phys.* 4 (1978) 1409.
- 24) E.W. Schmid, S. Saito and H. Fiedeldey, *Z. Phys.* A303 (1982) 37.
- 25) E.W. Schmid, M. Orłowski and Bao Cheng-guang, *Z. Phys.* A308 (1982) 237.
- 26) Yu.F. Smirnov, I.T. Obukhovskiy, Yu.M. Tchuvil'skiy and V.G. Neudatchin, *Nucl. Phys.* A235 (1974) 289.
- 27) Ch. Hajduk and P.U. Sauer, *Nucl. Phys.* A369 (1981) 321; Ch. Hajduk, thesis (University of Hannover, 1982).
- 28) I. Slaus, Y. Akaishi and H. Tanaka, *Phys. Rev. Lett.* 48 (1982) 993.
- 29) R. Kircher and E.W. Schmid, *Z. Phys.* A299 (1981) 241.
- 30) K. Hahn, P. Doleschall and E.W. Schmid, Resonating group Faddeev approach to deuteron-alpha scattering, to be published.
- 31) G. Spitz, H. Klar and E.W. Schmid, contribution to this conference.
- 32) H. Fiedeldey, *Nuovo Cimento Lett.* 9 (1974) 301.
- 33) B. Charnomordic, C. Fayard and G.H. Lamot, *Phys. Rev.* C15 (1977) 864.
- 34) K. Hahn, contribution to this conference.
- 35) Y. Koike, *Nucl. Phys.* A337 (1980) 23.
- 36) K. Wick, private communication.
- 37) H. Stumpf, *Z. Naturforsch.* 37a (1982) 1295; D. Grosser and T. Lauxmann, *J. Phys. G: Nucl. Phys.* 8 (1982) 1505; D. Grosser, B. Hailer, L. Hornung, T. Lauxmann and H. Stumpf, A method of calculating bound states in a unified model, to be published; H. Stumpf, Discussion of the two-fermion sector in unified field model with indefinite metric I, II, to be published.



## RESONATING GROUP CALCULATIONS IN NUCLEAR FEW CLUSTER SYSTEMS\*

Hartmut M. HOFMANN

Institute for Theoretical Physics, University of Erlangen-Nürnberg,  
D-8520 Erlangen, W-Germany

Several theoretical techniques, applicable to scattering systems, are presented and connexions between a recent algebraic approach and a variational ansatz are demonstrated. The results of these techniques are compared with experimental data. It is shown that diverse cluster decompositions have to be taken into account in order to reproduce the data.

### 1. INTRODUCTION

Nuclear few cluster systems are well studied experimentally<sup>1</sup>. Theoretically different approaches contribute to our present understanding of these systems. All these approaches show two sides, one is the conceptual idea, the other the technical performance. In comparison with experiment the last property is the crucial one, and I will elucidate this fact a bit.

The simplest nuclear few cluster problem is the deuteron, consisting of the elementary clusters "proton" and "neutron", thereby neglecting quark degrees of freedom. Due to this simple structure, the deuteron can be solved by various methods without any restrictions e.g. on the complexity of the force. Proceeding along these lines, where one treats all individual nucleons on a democratic basis, the technical difficulties increase so rapidly, that nuclear systems with mass numbers beyond 3 or 4 are no more feasible in Fadeev-type calculations. Hence, one has to restrict the complexity of the problem and to consider only the main components of the wave functions. One very fruitful idea, developed by Wildermuth<sup>2</sup>, is to cluster nucleons, which means, that the orbital wave function of the nucleons is symmetric under permutations within one cluster and all nucleons inside a cluster are in relative s-states.

These restrictions on the complexity of the wave functions enforce the use of effective forces. Just to illustrate this, let us consider the deuteron as one cluster, neglecting the d-state component of the wave function. Since the tensor force is known to contribute appreciably to the binding energy of the deuteron, an "s-wave-deuteron" is usually unbound with realistic nucleon-nucleon potentials. Therefore one has to modify the central part of the force

---

\*) Supported by the Deutsche Forschungsgemeinschaft

in order to bind the deuteron appropriately. There are several potentials in the literature<sup>3,4</sup> giving reasonable binding energies for a simple ansatz of the wave function for light nuclei. This change of the central parts of the potential is most obvious in the transition from the model potential of ref. 4 to the realistic nucleon-nucleon potential of ref. 5.

However, we should keep in mind that effective forces depend on energy either directly or via the modelspace dependence. With these restrictions on the wave functions, we can now return to our original problem, the description of nuclear systems, as few cluster systems. The aim is to find an approximate solution to the many body hamiltonian in the form of known internal functions and unknown relative motion wave functions. I do not want to discuss systems with more than 2 fragments, as these are already discussed before<sup>6</sup>.

Even with this restriction to binary fragmentations, various techniques of resonating group calculations cover too wide a range of nuclear systems to be discussed here. Therefore I will describe only those methods, which are applied to scattering systems and not solely to bound states, because cluster calculations provide the unique microscopic description of reactions between complex nuclei, beyond DWBA. Furthermore, the much simpler bound state calculations do not give substantial more insight into nuclear structure problems than extended shell model calculations<sup>7</sup>.

With the above restriction to binary fragmentations the ansatz for the wave function reads schematically

$$\Psi(1, \dots, N) = A \sum_{s=1}^M \phi_1^s(1, \dots, N_1) \phi_2^s(N_1+1, \dots, N) X_{\text{rel}}^s(R_{\text{rel}}) \quad (1)$$

where A is the total antisymmetrizer and s denotes a multi-index characterizing each channel by fragmentation, excitation of the fragments, orbital angular momentum L and channel spin  $S_c$  coupled to total angular momentum J.  $\phi_i^s$  denotes the internal function of fragment i in channel s and  $X_{\text{rel}}^s$  is the unknown relative motion wave function to be determined from the Schrödinger equation

$$H(1, \dots, N) \Psi(1, \dots, N) = E \Psi(1, \dots, N) \quad (2)$$

projected onto the space of trial functions. This differential equation in 3N-coordinates is reduced to a system of M coupled equations, depending on the relative coordinates only. This reduction is achieved by, loosely speaking, integrating over the internal coordinates. These multi-dimensional integrations represent the main technical barrier for the solution of eq. (2) with totally antisymmetrized cluster wave functions, thus setting the limits on the complexity of systems accessible to actual calculation. The solution of

the remaining equations is intimately connected with the method of integrating over internal coordinates. Two main approaches, in use now, will be described in the next chapter. Chapter 3 is devoted to a comparison of theoretical results with experimental data. And finally novel approaches are sketched and physical problems manageable with the new techniques are discussed.

## 2. THEORETICAL METHODS

The different methods to reduce the N-particle Schrödinger equation, eq. (2), to a system of equations for  $\chi_{rel}$  can be arranged into two classes: In the first class, the relative vector of the two fragments is taken as a generator coordinate and the resulting integro-differential equations for  $\chi_{rel}$  are solved numerically; in the second class, the wave functions  $\chi_{rel}$  are expanded into a suitable set of functions and the resulting equations for the expansion coefficients are solved algebraically. In the following all formulas are written explicitly for the single channel case only to make their structure as evident as possible. In the more channel case, all equations are understood as matrix equations in the space of channels.

### 2.1. Generator Coordinate Techniques

The generator coordinate techniques are beautifully described in great detail by Tang<sup>8</sup>, so I can restrict my discussion to the essentials of the method: Multiplying the total wave function by an appropriate but arbitrary wave function  $Z$  for the c.m.-motion eq. (1) can be converted into

$$\Psi = A \{ \int \phi_1 \phi_2 \delta(\underline{R}_{rel} - \underline{R}') Z(\underline{R}_{cm}) \} \chi_{rel}(\underline{R}') d\underline{R}' \quad (3)$$

and eq. (2) reduces to

$$\int [H(\underline{R}, \underline{R}') - E N(\underline{R}, \underline{R}')] \chi_{rel}(\underline{R}') d\underline{R}' = 0 \quad (4)$$

with

$$H(\underline{R}, \underline{R}') = \langle \phi_1 \phi_2 \delta(\underline{R}_{rel} - \underline{R}) Z | H | A [ \phi_1 \phi_2 \delta(\underline{R}_{rel} - \underline{R}') Z ] \rangle \quad (5)$$

and an analogous equation for the norm kernel  $N(\underline{R}, \underline{R}')$ . Since the internal wave functions  $\phi_1$  and  $\phi_2$  are already antisymmetrized, it is advantageous to decompose the total antisymmetrizer into

$$A = A_1 A_2 \quad A' = A_1 A_2 (1 + A'') \quad (6)$$

Note, that  $A$  in eq. (5) can be replaced by  $A'$ , thus one can separate  $H$  into two parts

$$H(\underline{R}, \underline{R}') = H_D(\underline{R}, \underline{R}') + H_E(\underline{R}, \underline{R}') \quad (7)$$

Realizing, that  $H_D(\underline{R}, \underline{R}')$  contains a  $\delta$ -function, eq. (4) can be converted into<sup>8</sup>



$$[-\hbar^2/2\mu \nabla_R^2 + V_D(R) - (E - E_1 - E_2)] X_{rel}(R) + \int K(R, R') X_{rel}(R') dR' = 0 \quad (8)$$

with  $E_i$  the binding energy of the fragment  $i$  and

$$K(R, R') = H_E(R, R') - E N_E(R, R') \quad (9)$$

Choosing harmonic oscillator wave functions for  $\phi_1$ ,  $\phi_2$  and  $Z$  all necessary integrations to determine the kernels can be performed analytically using shell-model techniques. With the kernels and  $V_D$  known, eq. (8) can be solved by various numerical techniques<sup>8</sup>.

This method is well suited to describe single channel problems for energies up to 50 MeV and large mass numbers<sup>9</sup>, e.g.  $^{16}O + ^{28}Si$ . However, for coupled channels the calculation of the kernels becomes tedious and new techniques, c.f. chapter 4, seem to be more efficient. Just recently, a first calculation with two different cluster fragmentations is reported for the  $^7Li$ -system<sup>10</sup>, which will be discussed in chapter 3.

## 2.2 The Algebraic Expansion Methods

The algebraic methods are characterized by an ansatz for the relative motion wave function  $X_{rel}(R)$  in eq. (1) in terms of regular, and irregular Coulomb waves and appropriate  $L^2$ -functions covering the interaction region. This method was first applied to nuclear scattering systems<sup>11</sup> by Hackenbroich. He obtained convincing results for light nuclear systems, ranging from  $A = 4$  to  $A = 12$ , with his refined resonating group method, which will be described briefly along the lines of ref. 12.

For the relative motion wave function with orbital angular momentum  $l$  an ansatz is chosen as follows

$$X_{rel}^1(R) = F_1(R) + a \tilde{G}_1(R) + \sum_{i=1}^n b_i W_i(R) \quad (10)$$

where  $F_1$  and  $\tilde{G}_1$  are the regular and regularized irregular Coulomb waves, respectively, and  $W_i$  are  $L^2$ -functions, to take care of the interaction region. Note, that  $G_1$  has to be regularized, so that  $X_{rel}$  has the right boundary condition for  $R = 0$ . The elements of the reactance matrix  $a$  and the coefficients  $b_i$  are the variational parameters which are determined from

$$\delta \{ \langle \Psi | H - E | \Psi \rangle - 1/2 a \} = 0 \quad (11)$$

Rewriting the translationally invariant hamiltonian as

$$H = H_1 + H_2 + \sum_{i=1}^{N_1} \sum_{j=N_1+1}^N V_{ij} - \frac{Z_1 Z_2 e^2}{R} + \frac{Z_1 Z_2 e^2}{R} + T_{rel} \quad (12)$$

where  $H_1$  and  $H_2$  are the internal hamiltonians of fragment 1 and 2, respectively, the next two terms are the short ranged interaction between the two fragments and the last two terms determine the asymptotic hamiltonian if

the two fragments are far from each other. All the integrals in eq. (11) exist<sup>12</sup>, if the fragment functions  $\phi_i$  of eq. (1) are eigenstates of  $H_i$  in eq. (12) to the energy  $E_i$  and if the Coulomb waves are eigenfunctions of the asymptotic hamiltonian to the energy  $E_{rel} = E - E_1 - E_2$ . This means that the thresholds are fixed once the interaction and the internal wave functions of the fragments are chosen.

In order to solve the variational eq. (11) we change our notation

$$\psi = f + a g + \sum_i b_i \bar{w}_i \quad (13)$$

where the functions on the right hand side of eq. (13) contain the relative motion part and all internal functions. Now we diagonalize the norm-matrix and the hamiltonian in the space of the functions  $\bar{w}_i$  and denote the eigenfunctions with  $w_i$ , which satisfy

$$\langle w_i | w_j \rangle = \delta_{ij}; \quad \langle w_i | H | w_j \rangle = e_i \delta_{ij} \quad (14)$$

The variational eq. (11) can be cast into the form

$$\langle g | H' | f \rangle + a \langle g | H' | g \rangle + \sum_i b_i^* \langle g | H' | w_i \rangle = 0 \quad (15a)$$

$$\langle w_i | H' | f \rangle + a \langle w_i | H' | g \rangle + \sum_j b_j^* (e_i - E) \delta_{ij} = 0 \quad (15b)$$

where eqs. (14) and  $H' = H - E$  have been used. Eliminating  $b_j^*$  from eqs. (15), one finds

$$a = - \langle g | \tilde{H} | f \rangle^T \langle g | \tilde{H} | g \rangle^{-1} \quad (16)$$

with the definition

$$\tilde{H} = H' - \sum_i H' | w_i \rangle (e_i - E)^{-1} \langle w_i | H' \quad (17)$$

Interpreting eq. (16) as a matrix equation, as implicitly always assumed, the reactance matrix is obviously not symmetric, hence, a unitary S-matrix is not guaranteed; the set of functions  $w$  being incomplete. Therefore, one has to use a Kato correction<sup>12,13</sup>, leading to

$$a = - 2 \langle f | \tilde{H} | f \rangle - \langle g | \tilde{H} | f \rangle^T \langle g | \tilde{H} | g \rangle^{-1} \langle g | \tilde{H} | f \rangle \quad (18)$$

with an obviously symmetric matrix  $a$ . All matrix elements necessary for the evaluation of eq. (16) or (18) resp. can be calculated analytically by generating function techniques<sup>12,14</sup> using Jacobian coordinates if the functions  $w_i$  are given by

$$w_i^1(R) = R^{1+1} \exp(-\beta_i R^2) \quad (19)$$

and if the potentials are given in terms of Gaussians<sup>5</sup>, and if the Coulomb functions in the interaction region are expanded in terms of  $w_i$ .

For this technique, a chain of flexible computer programs exists, which allows to treat central, spin-orbit, tensor and Coulomb potentials for systems with many coupled channels belonging to different cluster decompositions of up to four clusters. However, due to the increasing number of matrix elements, the nucleon number is limited to about 12. Furthermore, the non-orthogonality of the functions  $w_i$ , together with the monotonic change in shape of  $w_i$  with  $\beta_i$ , creates severe technical problems, if the excitation energy exceeds 20 - 30 MeV, thus limiting the range of energies accessible. When adding in the expansion eq. (13) functions of the type  $w_i(R) * R^{2k}$ , with  $k = 1, 2$  the above techniques can still be used and much higher energies can be reached. First model calculations demonstrate that 100 MeV excitation energy can be treated without technical problems<sup>15</sup>.

Another method, which has no obvious limitations for the energy range, was recently developed by Filippov<sup>16</sup> and Smirnov<sup>17</sup>. In the following the essentials of their approach will be given and compared with the refined resonating group method.

Starting from the ansatz eq. (1), the relative motion wave function is expanded in terms of harmonic oscillator wave functions  $R_{n1}$

$$X_{rel}^1(R) = \sum_{n=0}^{\infty} C_{n1} R_{n1}(R) \quad (20)$$

where the coefficients  $C_{n1}$  depend on energy. In the following we restrict our considerations to potential scattering only and suppress the index 1 in order to make the formulas as transparent as possible. With the expansion, eq. (20), the Schrödinger equation (2) is converted into the  $n$ -representation:

$$\sum_m (H_{nm} - \delta_{nm} E) C_m = 0; \quad n = 0, 1, 2, \dots \quad (21)$$

For a short ranged potential, the hamiltonian for large  $n$  contains only the kinetic energy, which has non-zero matrix elements  $T_{n, n-1}, T_{nn}, T_{n, n+1}$ . Assuming that the potential matrix  $V$  can be cut off at a finite dimension  $M$ , eq. (21) can be broken into two parts

$$\sum_{m=0}^M (H_{nm} - E \delta_{nm}) C_m = -\delta_{nM} T_{n, M+1} C_{M+1}; \quad n = 1, \dots, M \quad (22)$$

and the equation of free motion. Diagonalizing the  $M$ -dimensional hamiltonian matrix with an orthogonal matrix  $U$ , eq. (22) gives in obvious notation

$$\sum_n (e_i - E) U_{in} C_n = -U_{iM} T_{M, M+1} C_{M+1}; \quad i = 1, \dots, M \quad (23)$$

which can be solved for  $C_M$ , using the orthogonality of  $U$

$$C_M = \sum_{i=1}^M U_{iM}^2 / (E - e_i) T_{M, M+1} C_{M+1} \quad (24)$$

Now, for free waves the coefficients  $C_n$  are given by

$$C_n^0 = C_n^{\text{reg}} + \tan \delta C_n^{\text{irreg}} \quad (25)$$

where  $C_n^{\text{reg}}$  and  $C_n^{\text{irreg}}$  are known functions<sup>17</sup>. Assuming, that for  $n \geq M$  the coefficients  $C_n$  are equal to the free ones  $C_n^0$ , eq. (24) can be solved for  $\tan \delta$

$$\tan \delta = - (C_M^{\text{reg}} + s C_{M+1}^{\text{reg}}) / (C_M^{\text{irreg}} + s C_{M+1}^{\text{irreg}}) \quad (26a)$$

with the abbreviation

$$s = \sum_{i=1}^M U_{iM}^2 T_{M M+1} / (e_i - E) \quad (26b)$$

Note, that in potential scattering  $\tan \delta$  is just the reactance matrix as discussed earlier. The only unknown quantities in eq. (26) are the energies  $e_i$  and the matrix  $U$ , resulting from the diagonalisation of the hamiltonian, eq. (22), in the  $M$ -dimensional space.

It is not clear to me, what the approximation of the coefficients  $C_n$  by the free ones really means. Therefore I want to demonstrate, that eq. (26) can be obtained from the variational principle eq. (11) with the ansatz

$$X_{\text{rel}}(R) = \sum_{n=0}^M C_n R_n(R) + F'(R) + a G'(R) \quad (27)$$

where  $F'$  and  $G'$  are the regular and irregular Coulomb waves, respectively, minus the first  $M$  expansion terms, eg.

$$G'(R) = \sum_{n=M+1}^{\infty} C_n^{\text{irreg}} R_n(R) \quad (28)$$

Taking  $C_n$  and  $a$  as variational parameters and following along the lines of eq. (12 - 16) we find

$$a = - \langle G' | \tilde{H} | F' \rangle^T \langle G' | \tilde{H} | G' \rangle^{-1} \quad (29)$$

where now  $\tilde{H}$  is given by

$$\tilde{H} = H' - \sum_{i,n,m}^M H' | R_n \rangle U_{ni} (e_i - E)^{-1} U_{mi} \langle R_m | H' \quad (30)$$

Note the formal equality of eq. (29 - 30) and (16 - 17). Taking into account that  $F$  and  $G$  satisfy  $H^- | F \rangle = 0$ , a typical matrix element can be evaluated using eq. (28) and (22).

$$\begin{aligned} \langle G' | H' | F' \rangle &= \langle G' | H' | F - \sum_{n=0}^M C_n^{\text{reg}} R_n \rangle = \\ &= - \langle G' | H' | \sum_{n=0}^M C_n^{\text{reg}} R_n \rangle = - C_{M+1}^{\text{irreg}} T_{M M+1} C_M^{\text{reg}} \end{aligned} \quad (31)$$

Inserting the matrix elements according to eq. (31) into eq. (29) leads straightforward to eq. (26). Thus it is shown, that the two approaches are



### 3. COMPARISON WITH EXPERIMENT

Recently, most effort of theoretical few cluster studies has been concentrated on the  $A = 7$  systems  ${}^7\text{Li}$  and  ${}^7\text{Be}$ . Therefore I will pick these systems as typical examples. The interest in these systems arose because of their keyrole in the understanding of the present solar neutrino problem<sup>18</sup>, and because of the nuclear physics problems emerging from the rich structure of states and resonances at low energies with high orbital angular momenta<sup>19</sup>.

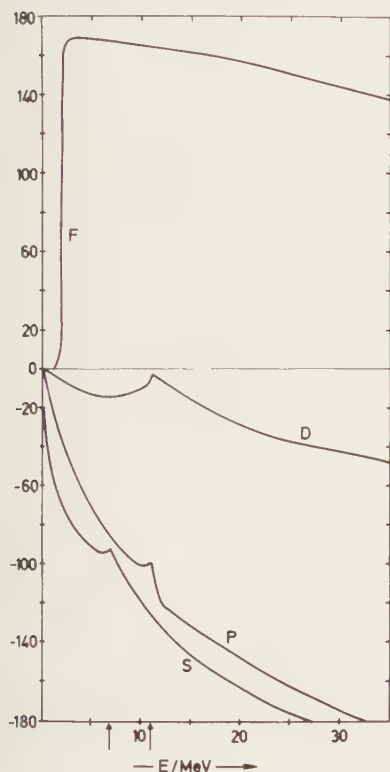


Figure 2a  
Calculated  $t$ - ${}^4\text{He}$  phase shifts,  
adopted from ref. 10. The arrows  
indicate the  ${}^6\text{Li}$ - $n$  thresholds.

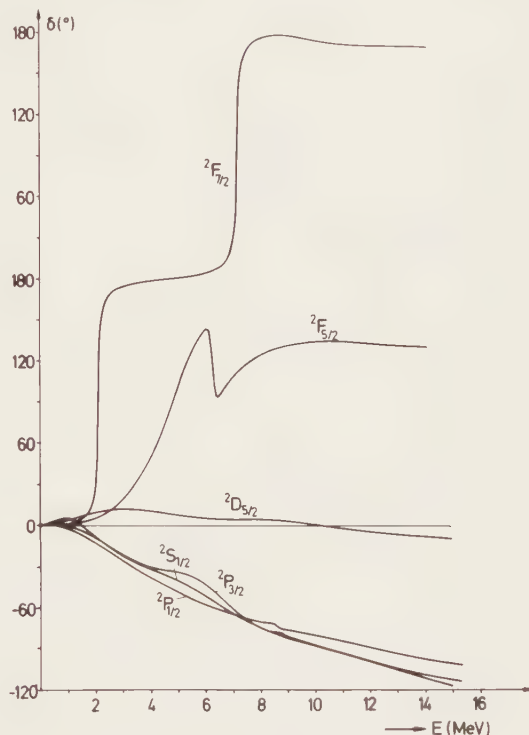


Figure 2b  
Calculated  ${}^3\text{He}$ - ${}^4\text{He}$  phase shifts,  
adopted from ref. 21.

This rich structure, together with the many low-lying thresholds, raise the main technical difficulties, which prevented till now thorough theoretical studies. On the other side the many thresholds open a wide field for experimental investigations, compare fig. 1 for the experimental situation.

Two groups reported recently multichannel calculations for the systems  ${}^7\text{Li}$  and  ${}^7\text{Be}$ , one using the techniques of chapter 2.1<sup>10,20</sup> and the other those of

chapter 2.2<sup>21</sup>, respectively.

Let us first compare the input of the two calculations. Since it is common believe, that the cluster structure of the  ${}^7\text{Li}$  ground state is predominately  $\alpha+t$ , the lowest threshold, both groups took the (4,3)-cluster structures into account. Also the next threshold,  ${}^6\text{Li}$ -nucleon, is found in both calculations, see fig. 1, afterwards the input differs. A central force only is used in ref.

10 and 20, hence, with the cluster structure  $\alpha+d$  for  ${}^6\text{Li}$  there are only two low-lying positive parity states, the ground state with  $\alpha+d$  in relative s-state and one excited state with relative d-wave. In contrast to that, ref. 21 employs central, spin-orbit and tensor forces, hence, the d-wave state splits into three J -states  $3^+$ ,  $2^+$  and  $1^+$  with roughly the experimental energies, see fig. 1.

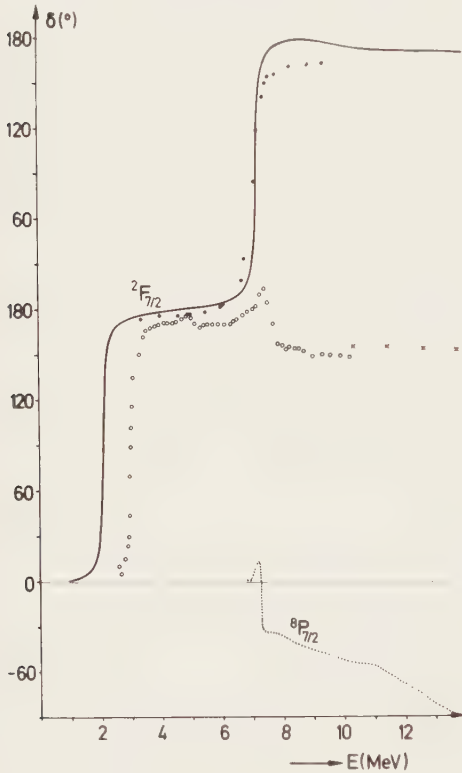


Figure 3a

The large  $7/2^-$ -phase shifts for  ${}^3\text{He}$ - ${}^4\text{He}$  (full line) and  ${}^6\text{Li}$ -p channels (dotted line). The data are from refs. 22, 23, 26.



Figure 3b

Same as fig. 3a, but the  ${}^5\text{Li}$ -d channels omitted in the calculation.

Furthermore, the (5,2)-cluster structures are taken into account in ref. 21, whereas it is claimed<sup>10,20</sup> that it is a good approximation to omit these structures, because of the Pauli principle. I will demonstrate in the following that this is not the case.

In fig. 2 phase shifts for elastic scattering of t (resp.  ${}^3\text{He}$ ) on  ${}^4\text{He}$  for the two calculations are displayed, demonstrating the advantages of both approaches, large energy range versus more detailed description. In comparison



with experimental data, we find, cf. fig. 3a, that a detailed description is essential in reproducing the data. I will just pick this example to demonstrate that in the understanding of the detailed experimental information it is vital to include the (5,2)-cluster-structures.

At low energies a beautiful  $L = 3$  resonance in the (4,3)-channels appears in all calculations. The calculations without (5,2)-structures, cf. fig. 2a and fig. 3b, show no second resonance, contrary to experiment<sup>22,23</sup>, whereas the full calculation, cf. fig. 3a, exhibits the resonance, even at the right energy.

Let us examine the situation in more detail. Fig. 3b shows that the resonance occurs within the (6,1)-structures in the  ${}^6\text{Li}^*(3^+)$ -p channel  ${}^8\text{p}_{7/2}$ , i.e. in a channel with channel spin  $7/2$ . Together with the internal orbital angular momentum of the  ${}^6\text{Li}$  excited state of  $l = 2$ , the spin  $S$  has to be  $3/2$ , thus leading to a Young tableau for the orbital symmetry of  $[4,2,1]$ . Now the tensor force does not conserve spin (neither orbital symmetry), therefore some small coupling effect can be seen in the  ${}^3\text{He}$ -phase-shifts at the resonance energy, cf.

fig. 3b. This tiny effect corresponds just to the occurrence of threshold states, as discussed in ref. 24. Here, however, we observe a tremendous effect; we find in the full calculation (and in the experimental data) the resonance just in the initially non-resonant channel. Hence, the coupling between the resonance and the (4,3)-channel has to be mediated by a strong force, the central force being the only strong one. Here the (5,2)-channels come into play. The  ${}^5\text{Li}$ -d  $S_c = 3/2$  channel decomposes into spin  $S = 3/2$  and  $S = 1/2$  components. Hence, in the interaction region, this (at the resonance still closed) channel brings about a mixing of the  ${}^4\text{He} - {}^3\text{He}$  spin  $1/2$  channel with the  ${}^6\text{Li}^*$ -p spin  $3/2$  channel via the central force. This situation is illustrated in fig. 4, where the total spin-isospin symmetries according to Littlewood's rules are indicated by Young tableaux for the dominant orbital symmetries.

This example demonstrates that a cluster decomposition, which contains other symmetries than those considered already (or mixes those symmetries) may be necessary in order to reproduce the behaviour of the experimental data. As

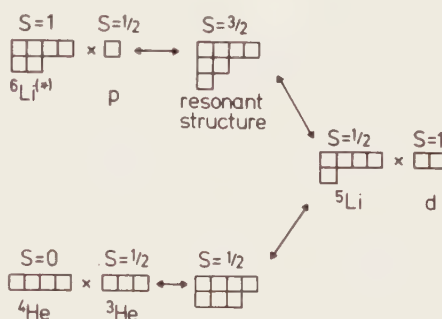


Figure 4

Young tableaux for the  $7/2^-$  resonance. The arrows indicate couplings via central forces.

another, typical example we show in fig. 5 that a multistructure calculation allows to reproduce experimental data in different channels simultaneously.

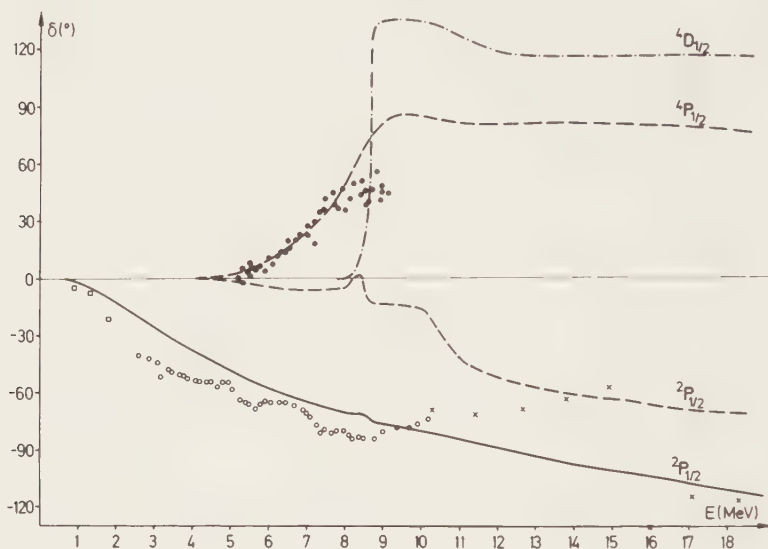


Figure 5

Comparison of calculated<sup>21</sup> and experimental<sup>22,25,26</sup>  $1/2^-$  phase shifts for  $^3\text{He}$ - $^4\text{He}$  (full line),  $^6\text{Li}$ -p (dashed lines) and  $^5\text{Li}$ -d channels (dashed-dotted line).

In fig. 6 the analysing power in elastic  $^3\text{He}$ - scattering at 8 and 10 MeV is displayed, indicating that also experimental observables are neatly reproduced. The deviation between data and calculation at 10 MeV is due to the cutoff in orbital angular momentum at  $l = 3$  in the  $^3\text{He} - ^4\text{He}$  channels and  $l = 2$  in the  $^6\text{Li} - p$  channels. This cutoff had to be applied in order to reduce the computing time<sup>21</sup> necessary.

#### 4. OUTLOOK

The above examples show the versatility of the cluster-model in the description of light nuclear systems. We are still, however, left with the problem, that the two approaches do not yet combine all advantages, i.e. large energy range, higher mass number and faster calculation techniques to allow for more cluster structures or more coupled channels.

It seems to me that the techniques proposed to calculate the matrix elements, either for the integral kernels or for the algebraic method should give ample space to reach the above aim. Using harmonic oscillator functions or those described below eq. (19), the larger energy range seems easily accessible. It should be noted, that already in the most recent calculations by

Tang<sup>10</sup> the integral transforms technique<sup>28</sup> is employed. But, this is still along the lines of reducing the antisymmetrizer in a double coset decomposition<sup>29</sup> and calculating all possible different radial matrix elements.

A possible major step in the direction of higher mass numbers and more efficient calculations is the use of SU(3)-recoupling techniques, studied by Hecht and Zahn<sup>30,31</sup> for norm kernels. In this approach one has no more to calculate all different matrix elements from a double coset expansion (a number which increases rapidly from  $^{12}\text{C}$  to  $^{16}\text{O}$ ), but the matrix elements themselves are calculated by SU(3)-recoupling coefficients, because in the cases considered there is a one-to-one correspondence between the irreducible representations of the groups  $S_n$  and SU(3).

Even for different oscillator parameters calculational procedures are proposed<sup>31</sup>. Till now, however, no efficient way of calculating interaction matrix elements via SU(3)-recoupling coefficients seems to be known in the general case. Therefore, only a gradual transition to the new methods seems to be possible.

With the expansion of the relative motion wave function in terms of harmonic oscillator wave functions, high energies, up to the medium energy range, are accessible. Cluster reactions like  $^3\text{He}(^4\text{He}, \pi)^7\text{Li}$ <sup>32</sup> are waiting for a consistent description. In this extended energy range several questions arise: The crucial one, are the systems still dominated by a few cluster decompositions and can these be approximated by binary fragmentations of eventually unstable particles, e.g.  $^5\text{Li}$  - d channels in the example discussed.

If this question is answered in the affirmative, then the interaction to be chosen is on the agenda. As discussed in the introduction, the restriction of the total Hilbert space to cluster-decompositions, i.e. a subspace, leads

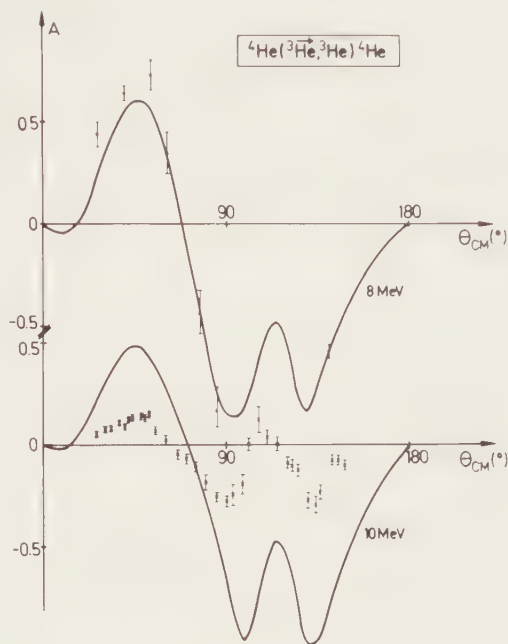


Figure 6

Comparison of calculated  $^3\text{He}$  analyzing powers<sup>21</sup> with data at 8 MeV<sup>27</sup> and 10 MeV<sup>26</sup>.

unavoidable to the use of effective forces, which depend on the model space considered. All present interactions have been tested in small model spaces only and have to be studied in other spaces now.

To illustrate the problem: At low energies there are thresholds of dominant cluster decompositions or of channels studied experimentally, which have to be reproduced using simple internal wave functions. Due to the absence of tensor force contributions in symmetric clusters, the central force is always enhanced compared to the realistic nucleon-nucleon force determined from scattering experiments. This fact will lead to too attractive phase shifts at larger energies, an example is provided by the  $l = 4$  phase shift in elastic  $^3\text{He} - ^3\text{He}$ -scattering<sup>33</sup>. Therefore, if we want to describe higher energies we have to use central forces with a core, thus loosing binding energy. But, far from all dominating thresholds the exact threshold position should not matter.

In conclusion, there is still an open field for studies in nuclear few cluster systems.

#### Acknowledgement

Fruitful discussions with J. Burger, T. Mertelmeier, T.H. Seligman and W. Zahn are gratefully acknowledged.

#### REFERENCES

- 1) G.R. Plattner, in *Few Body Systems and Nuclear Forces*, Lecture Notes in Physics 87, eds. H. Zingl, M. Haftel and H. Zankel (Springer, Berlin, 1978) pp 376 - 392
- 2) K. Wildermuth and W. McClure, *Cluster Representation of Nuclei* (Springer, Berlin, 1966); K. Wildermuth and Y.C. Tang, *A unified theory of the nucleus in: Clustering Phenomena in Nuclei*, Vol.1, eds. K. Wildermuth and P. Kramer (Vieweg, Braunschweig, 1977)
- 3) D.M. Brink and E. Boeker, *Nucl. Phys. A* 91 (1967) 1  
A.B. Volkov, *Nucl. Phys.* 74 (1965) 33
- 4) H. Eickemeier and H.H. Hackenbroich, *Z. Phys.* 195 (1966) 412
- 5) H. Eickemeier and H.H. Hackenbroich, *Nucl. Phys. A* 169 (1971) 407
- 6) E. Schmid, *Theoretical Description of Few Cluster Systems*, this volume
- 7) A.G.M. van Hees, *One particle-hole excitations in p- and fp-shell nuclei*, Ph. D.-Thesis, Utrecht 1981
- 8) Y.C. Tang, *Microscopic description of the nuclear cluster theory in: Topics in Nuclear Physics*, Lecture Notes in Physics 145, eds. T.T.S. Kuo and S.S.M. Wong (Springer, Berlin, 1981) pp 572 - 693
- 9) K. Langanke, *Phys. Lett.* 104 B (1981) 112
- 10) Y. Fujiwara and Y.C. Tang, *Channel coupling effects in the resonating group study of the seven-nucleon system*, University of Minnesota, 1983

- 11) For a complete reference see: Hans H. Hackenbroich memorial volume, Nucl. Phys. A 286 (1977) iii - v
- 12) H.H. Hackenbroich, Reactions involving light nuclei, in: Symp. on Present Status and Novel Developments in the Nuclear Many Body Problem, eds. F. Calogero and C.C. Degli Atti (Editrice Compositori, Bologna 1973)
- 13) G. John, Anwendung der Theorie der symmetrischen Gruppe auf Zustände und Reaktionen der leichten Kerne BMW-FB K 71-20, ZAED Leopoldshafen 1971
- 14) H.H. Hackenbroich, Z. Phys. 231 (1970) 216
- 15) H.M. Hofmann, to be published
- 16) G.F. Filippov, V.S. Vasilevski and T.P. Kovalenko, Algebraic version of the resonating group method, preprint TP-81-1071 Kiev 1981
- 17) Y. Smirnov and Y. Nechaev, Kinam 4 (1982) 445
- 18) J.N. Bahcall, W.F. Heubner, S.H. Lubow, P.D. Parker and R.K. Ulrich, Rev. Mod. Phys. 54 (1982) 767
- 19) F. Ajzenberg-Selove, Nucl. Phys. A 320 (1979) 1
- 20) Y. Fujiwara and Y.C. Tang, Three-cluster resonating group method in the coupled channel formalism, University of Minnesota, preprint 1983
- 21) H.M. Hofmann, T. Mertelmeier and W. Zahn, Nucl. Phys. in print
- 22) R.J. Spiger and T.A. Tombrello, Phys. Rev. 163 (1967) 964
- 23) N. Jarmie, F.D. Correll, R.E. Brown, R.A. Hardekopf and G.G. Ohlsen, Elastic Scattering of Tritons by Helium - 4, LA-Report, LA-8492 (1980)
- 24) H.H. Hackenbroich and T.H. Seligman, Phys. Lett. 41 B (1972) 102
- 25) C. Petitjean, L. Brown and R.G. Seyler, Nucl. Phys. A 129 (1969) 209
- 26) Y.-W. Lui, O. Karban, A.K. Basak, C.O. Blyth, J.M. Nelson and S. Roman, Nucl. Phys. A 297 (1978) 189
- 27) D.D. Armstrong, L.L. Catlin, P.W. Keaton jr. and L.R. Veaser, Phys. Rev. Lett. 23 (1969) 135
- 28) T.H. Seligman and W. Zahn, J. Phys. G 2 (1976) 79
- 29) T.H. Seligman, Double coset decompositions of finite groups and the many body problem, Burg, Basel 1974
- 30) K.T. Hecht, E.J. Reske, T.H. Seligman and W. Zahn, Nucl. Phys. A 356 (1981) 146
- 31) W. Zahn, Cluster Modes and SU(3) Symmetry, Burg, Basel 1981
- 32) L. Bimbot, M.P. Combes, J.C. Jourdain, Y. le Bornec, F. Reide, A. Willis, N. Willis, J.F. Germond and C. Wilkin, Phys. Lett. 114 B (1982) 311
- 33) H.M. Hofmann and W. Zahn, Nucl. Phys. A 368 (1981) 29



## EFFECTIVE INTERACTIONS IN TWO- AND THREE-CLUSTER SYSTEMS

E.W. SCHMID

Institut für Theoretische Physik, Universität Tübingen,  
D-7400 Tübingen, W.-Germany

### 1. INTRODUCTION

A preconference on "Effective Interactions in Two- and Three-Cluster Systems" was held at the University of Tübingen\* during the week Aug. 15-21, 1983. There were 20 invited talks (60 min.) and discussion sessions. A summary follows.

### 2. RESONATING GROUP INTERACTIONS

The resonating group model may be seen as an approach to describe nuclear bound and excited states, as well as single- and multichannel scattering, by an equation for the relative motion of nuclear fragments, called clusters. In the resonating group equation, the clusters appear as structureless point-masses. All information on the internal structure of the clusters, on the forces acting between the nucleons and on the Pauli principle are incorporated in the effective interaction. The effective interaction is rather complicated, especially in systems with more than two clusters. Much work has been done in finding methods by which the complicated exchange kernels can be derived.

#### 2.1. Technical Progress

H. HOFMANN (Universität Erlangen, W.-Germany) reported on progress in the further development of Hackenbroich's method. The latter is a generalization of the Hulthén-Kohn variational method to the multichannel case. All matrix elements of the linear equation, which represents the resonating group equation, are calculated by a very flexible computer code which, however, requires an expansion of all wave functions and potentials into superpositions of gaussian functions or polynomial-times-gaussian functions. Especially the regular and (cut off) irregular Coulomb functions are represented, in the region of interaction, by sums of gaussian functions of different width. This technique has worked perfectly well in all low energy applications. For higher

---

\*The preconference was organized by the Department of Physics, Hokkaido University, Sapporo, Japan, by the Institut für Kernphysik der Technischen Universität, Wien, Austria, and by the Institut für Theoretische Physik der Universität, Tübingen, W.-Germany. It was sponsored by the Deutsche Forschungsgemeinschaft.



energies it becomes numerically unstable. H. Hofmann and his collaborators are now using a different expansion basis which is of the polynomial-times-gaussian type. The code can now be used also at intermediate energies. Some difficulties in the evaluation of long ranged operators, like electromagnetic transition operators, have also been overcome<sup>1</sup>. Some critical thought has been given to the use of phenomenological N-N potentials. A realistic potential with tensor- and spin-orbit components does not bind a harmonic oscillator  $\alpha$ -particle without configuration mixing. A simple description of cluster ground states, however, is needed to perform complicated coupled-channel calculations. H. Hofmann uses a purely central N-N potential for the internal motion of clusters and a realistic N-N potential for the relative motion. The philosophy behind this procedure is that phenomenological N-N potentials are effective potentials anyway, and that many features of nuclear reactions are more sensitive to a correct dynamical treatment than to details of the potential.

Y. FUKUSHIMA (Fukuoka University, Japan) reported on a new computer code which evaluates the exchange kernels of a multi-cluster system in analytic form. The code uses a complex generator coordinate technique. The N-N potential may have a tensor- and a spin-orbit part. Since the code can give the decomposition of the exchange kernels according to the particle exchange character, it can also be used for systematic studies of the Pauli effect. The code will be available for public use at the Computer Center of the University of Tokyo.

In a method presented by S. OKABE (Hokkaido University, Japan, and Universität Siegen, W.-Germany) the resonating group kernels are evaluated by expanding them into a set of orthonormalized wave functions which are created by permutation operators and which are classified by the concept of particle exchange<sup>2</sup>. The expansion is supposed to converge rapidly.

The strength of effective three-cluster forces arising from hard core correlations has been discussed by S. NAKAICHI-MAEDA (Hokkaido University, Japan, and Universität Tübingen, W.-Germany). The Jastrow correlation factor affects the shape of two-cluster effective interactions and it leads to an effective three-cluster interaction when three clusters are present<sup>3</sup>. In the  $\Lambda$ - $\Lambda$ - $\alpha$  system the three-body force decreases the binding energy of around 10 MeV by 0.5-0.7 MeV, depending on the hard core radius of the  $\Lambda$ -N potential. It is seen that an off-shell transformation which renormalizes the relative motion wave functions is crucial for getting this relatively small three-body force effect.

## 2.2. New Applications

A resonating group calculation on the  $\alpha$ -decay width of  $^{212}\text{Po}$  has been discussed by K. WILDERMUTH (Universität Tübingen, W.-Germany). The test function space used for this calculation<sup>4</sup> consists of shell model configurations in the

interior region and  $\alpha$ - $^{208}\text{Pb}$  relative motion states in the transition region, taking advantage of the fact that the resonating group equation does not require orthogonal test function spaces. The addition of the  $\alpha$ - $^{208}\text{Pb}$  states is crucial for a fast convergence of the theoretical description. The calculation yields satisfying agreement with the experimental decay width and demonstrates that even a heavy nuclear system can be treated by the resonating group model. With a computer more powerful than the UNIVAC 1100/80 used for this calculation it would even be possible, and desirable, to enlarge the test function space.

Y. FUJIWARA (University of Michigan, USA) reported on a coupled reaction channel treatment<sup>5</sup> of a three-cluster system  $A+B+C$ , in which  $A$  is an  $\alpha$ -particle and  $B, C$  are two  $s$ -shell clusters. The full three-cluster resonating group kernels are evaluated in analytic form. The coupled reaction channels are  $(A+B)+C$ ,  $(A+C)+B$ , and  $(B+C)+A$ , where the bound subsystems  $(A+B)$  etc. are either ground states or excited states. For an initial study, the method has been applied to the seven nucleon system with  $\alpha, d, n$  for  $A, B, C$  and  $^3\text{H}+\alpha$ ,  $n+^6\text{Li}$  and  $n+^6\text{Li}^*$  as coupled channels. Calculations have been performed with one, two and three channels. Two features are exhibited quite clearly: i) Pauli resonances arising from the almost Pauli-forbidden states are present in the single- and two-channel calculations and nearly disappear in the full three-channel calculation, ii) keeping cluster radii fixed is not sufficient to prevent nuclear collapse in a multichannel calculation.

A coupled reaction channel calculation on  $\pi$ - $^3\text{He}$  scattering has been formulated by T. KATAYAMA (Hokkaido University, Japan, and Universität Hannover, W.-Germany). The coupled channels are  $NNN$ ,  $\pi NNN$  and  $\Delta NN$ . The aim of the calculation is a microscopic understanding of pion absorption in nuclei.

A resonating group Faddeev calculation<sup>6</sup> on  $d$ - $\alpha$  elastic scattering and  $\alpha(d, \alpha p)n$  breakup scattering has been discussed by K. HAHN (Universität Tübingen, W.-Germany). Comparison with results of similar calculations with phenomenological  $N$ - $\alpha$  potentials shows that the Pauli principle plays an important role. Phenomenological models give good results when the off-shell behaviour of the chosen potentials is in approximate agreement with the off-shell behaviour of resonating group potentials.

### 3. SIMPLIFIED CLUSTER INTERACTIONS

The effective cluster interactions appearing in the resonating group model are rather complicated expressions. There are two reasons why one tries to simplify them: i) by extracting dominant terms and neglecting the rest one can get a better understanding of their physical content, ii) one needs simple potentials for many practical applications, like analysis of experimental data etc..

The need for better potentials in phenomenological models has clearly been demonstrated by H. OBERHUMMER (Technische Universität Wien, Austria) who showed that in (off-shell sensitive!) cluster transfer reactions the absolute values of experimental and calculated cross sections sometimes differ by several orders of magnitude, even when the shapes agree rather well<sup>7</sup>.

A class of simplified resonating group model potentials are the equivalent local potentials. H. HORIUCHI (Kyoto University, Japan) gave a report on his derivation of local potentials by the WKB method<sup>8</sup>. The potentials derived from the resonating group equation automatically incorporate the orthogonality condition of scattering states with respect to Pauli-forbidden states. As a consequence, the local potentials are deep. A detailed analysis shows that the one-nucleon exchange process dominates in the total exchange process, in the whole spatial region and at all energies. When volume integrals are used for making a comparison, the energy dependence and mass number dependence of the equivalent local potentials agree well with those of phenomenological potentials for light ion scattering. Horiuchi criticized approaches which lead to shallow effective cluster potentials and emphasized that the main effect of the Pauli principle is to shorten the wave length of the relative motion wave function in the region of overlap and, consequently, to deepen the effective potential. His local potentials do not show a Pauli barrier<sup>9</sup>. This may be due to the limited accuracy of the WKB calculation, or due to the possibility that the Pauli barrier is only present in the fish bone optical model where it has been found.

R. LIPPERHEIDE (Hahn-Meitner Institut, Berlin, W.-Germany) discussed an inversion method<sup>10</sup> which is based on the Bargmann method. Instead of considering fixed angular momentum and continuous energy he considers fixed energy and continuous complex angular momentum. The inversion is achieved for two classes of scattering functions which have the form of certain rational (nonrational) functions in the complex angular momentum plane. If the phase shifts for fixed energy  $E$  and integer angular momentum  $\ell$ , calculated from some original potential or taken from experiment, are interpolated by these rational (nonrational) functions, the corresponding local potential can be calculated in a simple manner. Lipperheide presented many examples of inversion calculations in nuclear and atomic scattering and compared the results with those of other inversion techniques.

H. FIEDELDEY (University of South Africa) showed that the local potentials derived by Horiuchi are good approximations to  $\ell$ -dependent, exactly Wronskian equivalent local potentials. Although the latter potentials are exactly phase equivalent, they are not wave function equivalent. They can be made wave

function equivalent by introducing an additional velocity dependent term. This term can be absorbed by the kinetic energy part of the wave equation if one allows the reduced mass to depend on the distance<sup>11</sup>. In a typical resonating group example, the mass has its full value at the origin, drops to 70-80% of its value at intermediate distances and gets its full value again at larger distances. Of course, one has to know the resonating group wave functions, and not only the phase shifts, to determine the mass function.

Another class of potentials which can be used for inverting resonating group scattering functions is given by the fish bone optical model<sup>12</sup>. H. KLAR (Universität Tübingen, W.-Germany) showed numerical results. He considered three cases of a resonating group model for  $\alpha$ - $\alpha$  scattering. The three cases differ by the choice of the N-N interaction: a) a purely attractive gaussian potential with Serber exchange mixture, b) same as (a) but different width for singlet and triplet interaction, c) the Volkov-I potential. In each one of the three cases, the fitting parameters of the fish bone optical model were adjusted to reproduce the phase shifts for fixed  $\ell$  and  $0 < E \leq 20$  MeV. Then the wave functions of the fish bone optical model were compared with the corresponding resonating group wave functions. Fig. 1 shows the result for  $\ell = 2$  and 4 MeV\*.

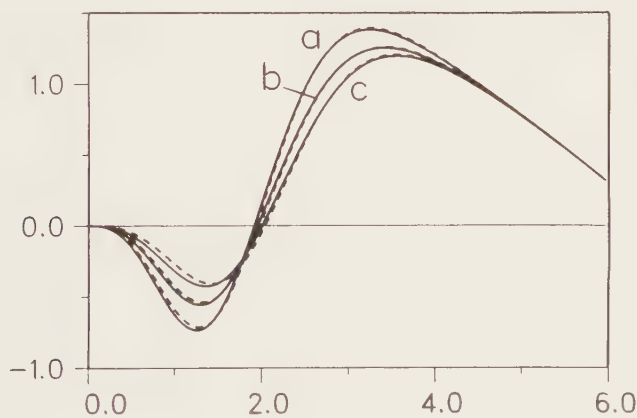


FIGURE 1

Relative motion wave functions of  $\alpha$ - $\alpha$  scattering at  $\ell = 2$  and 4 MeV (c.m.) are shown. Full lines: resonating group model with three different N-N potentials (see text). Broken lines: corresponding phase-equivalent fish bone optical model.

\*In order to exhibit the essential feature, the depths of the N-N potentials have been modified so that the three phase shift curves intersect at 4 MeV.

It is seen that the fish bone optical model, while only using phase shifts and norm kernel information as input, reproduces rather accurately resonating group wave functions. The wave functions of the three resonating group cases differ much more from each other than the wave functions of the fish bone optical model differ from the corresponding resonating group wave functions! Similar results were obtained for  $\ell = 0$  and 4 and for other energies.

G. SPITZ (Universität Tübingen, W.-Germany) showed that the effect of a hard core in the N-N potential can be incorporated in the fish bone optical model<sup>13</sup>. He solved the eigenvalue problem of the resonating group norm kernel with Jastrow correlations and calculated the shape of the direct potential for the  $n-\alpha$  and  $\alpha-\alpha$  systems. Only a slight modification of the calculated direct potential was needed to fit the experimental phase shifts.

H. LEEB (Technische Universität Wien, Austria) reported on a consistency check of optical model potentials<sup>14</sup>. When a  $\pi-\alpha$  optical potential is a physical quantity, rather than a mathematical parametrization of experimental cross sections, and when the same is true for a  $\pi-^{16}\text{O}$  potential and an  $\alpha-^{16}\text{O}$  potential, then it should be possible to describe  $\pi-^{20}\text{Ne}$  scattering by these three potentials, provided that  $^{20}\text{Ne}$  is well-described by an  $\alpha-^{16}\text{O}$  quasi-molecular state, and provided that three-body forces in the  $\pi-\alpha-^{16}\text{O}$  system are small. The numerical calculations are based on  $\pi-\alpha$ ,  $\pi-^{16}\text{O}$  and  $\pi-^{20}\text{Ne}$  potentials given by R.H. Landau and on the three-cluster fish bone optical model. Results indicate that there is consistency, even though the calculations are incomplete because the transition of the target nucleus into states of the  $\alpha-^{16}\text{O}$  rotational band has not yet been considered.

A numerical study by R. KIRCHER (Universität Tübingen, W.-Germany) shows that the unitary interpolation method<sup>15</sup> is a powerful tool for converting potentials into rank- $r$  separable potentials, when phase shifts as well as wave functions have to be reproduced in a given energy range.

#### 4. SPECIAL TOPICS

An interesting report on "anomalons" was given by Y.C. TANG (University of Minnesota, USA). Anomalons are nuclear fragments, produced in relativistic heavy ion collisions, with an anomalously short mean free path in nuclear emulsions. The nature of such objects is not yet fully understood. Tang et al. have made the hypothesis<sup>16</sup> that anomalons are excited nuclei in a quasi-molecular state with very large radius. The observation of a large asymmetric fission yield in the interaction of relativistic Au projectiles with nuclear emulsions seems to support the hypothesis. Tang proposes quantitative studies on the characteristics of the potential energy surface of medium and heavy nuclei and on the

excitation mechanism and probability of quasi-molecular states associated with the second minimum of the potential energy surface.

H. TANAKA and Y. AKAISHI (Hokkaido University, Japan) gave a report on three-nucleon forces. There is direct experimental evidence for the existence of a three-nucleon force, because the  $n$ - $n$  effective range parameters derived from the  $d(n,p)nn$  and the  $d(\pi^-, \gamma)nn$  reactions are not equal. The theoretical investigation of boson exchange processes yields a tentative mathematical form of the three-nucleon potential, which has been tested by ATMS calculations on the ground and excited states of the  $\alpha$ -particle. It is seen that the three-body force offers the simplest remedy to the discrepancy between experiment and models with only two-body potentials. The three-body force also enhances the meson exchange current effect and tends to bring the second maximum of the charge form factor of the  $\alpha$ -particle into agreement with experiment.

S. ORYU (Science University of Tokyo, Japan) presented test results on bound state Faddeev calculations which include a screened Coulomb potential. The calculations were done for the ground state of  ${}^9_{\Lambda}\text{Be}$  with a fish bone model  $\alpha$ - $\alpha$  potential and a local  $\Lambda$ - $\alpha$  potential of gaussian shape. The computer code uses a generalized separable expansion method and is rather flexible as to the choice of subsystem potentials.

Y. KOIKE (Osaka University, Japan) has extended his Faddeev code to separable potentials of higher rank and gave a survey on  $n$ - $d$  breakup results.

#### REFERENCES

- 1) H. Hofmann, Resonating Group Calculations in Few Cluster Systems, this volume.
- 2) S. Okabe, Nucl. Phys. A404 (1983) 179.
- 3) S. Nakaichi-Maeda and E.W. Schmid, Effective Interactions in the  $\Lambda$ - $\alpha$  and  $\Lambda$ - $\Lambda$ - $\alpha$  Systems, submitted to Z. Phys. A.
- 4) T. Steinmayer, W. Sünkel and K. Wildermuth, Phys. Lett. B125 (1983) 437.
- 5) Y. Fujiwara and Y.C. Tang, Three-Cluster Resonating-Group Method in the Coupled-Channel Formalism, submitted to Phys. Lett. B.
- 6) K. Hahn, P. Doleschall and E.W. Schmid, Resonating Group Faddeev Approach to Deuteron-Alpha Scattering, to be published.
- 7) F. Brunner, H.H. Müller, C. Dörninger and H. Oberhummer, Nucl. Phys. A398 (1983) 84.
- 8) H. Horiuchi, K. Aoki and T. Wada, Microscopic Study of Local Potential between Nuclei on the Basis of the Resonating Group Method, preprint 1983.
- 9) E.W. Schmid, S. Saito and H. Fiedeldey, Z. Phys. A306 (1982) 37.



- 10) R. Lipperheide and H. Fiedeldey, Z. Phys. A301 (1981) 81.
- 11) H. Fiedeldey and S.A. Sofianos, Equivalent Local and Velocity-Dependent Potentials for Nucleon-Alpha Scattering, to be published in Z. Phys..
- 12) E.W. Schmid, Z. Phys. A297 (1980) 105, Z. Phys. A302 (1981) 311.
- 13) G. Spitz, H. Klar and E.W. Schmid, The  $n$ - $\alpha$  and  $\alpha$ - $\alpha$  Direct Potential in the Fish Bone Optical Model with Saturation, contribution to this conference.
- 14) H. Leeb and E.W. Schmid, A Cluster Approach to Pion-Nucleus Scattering, to be published.
- 15) D.J. Ernst, C.M. Shakin and R.M. Thaler, Phys. Rev. C8 (1973) 46; R. Kircher and E.W. Schmid, Z. Phys. A299 (1981) 241.
- 16) Y.C. Tang, in Proc. of the Sixth High-Energy Heavy-Ion Study and Second Workshop on Anomalons, Lawrence Berkeley Laboratory, University of California, 1983.



RELATIVISTIC EFFECTS IN FEW NUCLEON SYSTEMS

Franz GROSS

Dept. of Physics, College of William and Mary, Williamsburg, VA 23185, USA

The discussion session on relativistic effects was moderated by Professor Walter Glöckle, of the Universität Bochum. This report is divided into two main sections on (1) relativistic few body equations and (2) relativistic calculations of matrix elements. In some places the discussion is incorporated into the text, but a number of issues pertaining to the first topic are summarized separately in part 1.3.

1. RELATIVISTIC FEW BODY EQUATIONS

Relativistic equations can be written in the following very general form

$$M = V + V G M$$
 (1)

where  $M$  is the scattering amplitude,  $V$  is the kernel or relativistic potential, and  $G$  the propagator. If  $V$  is in some sense small, Eq. (1) can be solved by iteration as shown diagrammatically in Fig. 1 for two particles. We see that the equation can be regarded as a means of summing a generalized Born series, or summing an infinite number of diagrams. If  $V$  is small, the solution to (1) will not differ significantly from taking  $V$  alone, and the equation is not

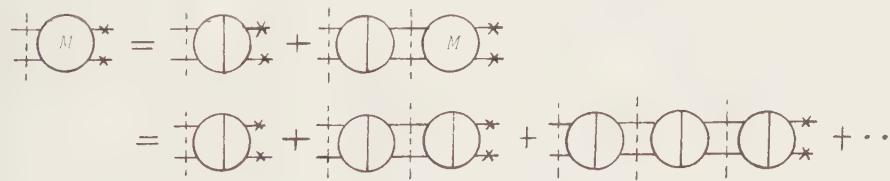


FIGURE 1

doing much for us. However, when  $V$  is large, the Born series will not exist, but the solution to (1) will. In this sense relativistic equations enable us to treat non-perturbative problems.

Eq. (1) is so general that almost any equation fits that form. Relativistic equations are defined by the rules used to determine the propagator and the kernel. Three major methods exist for defining  $G$  and  $V$ , and a review of these serves to introduce the reader to the major approaches to the relativistic few body problem. After this review, the issues of convergence will be discussed.

1.1. Methods of Constructing Relativistic Equations

a. Methods Based on Feynman Diagrams

In this method it is assumed that a subclass of relativistic Feynman diagrams will give a reasonable account of the dynamics. The subclass most commonly chosen is the sum of all ladders and crossed ladders. The ladder sum up to 6th order is shown in Fig. 2; the 6 additional crossed ladder diagrams which

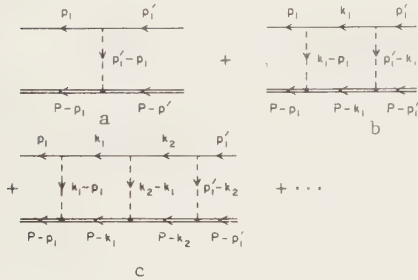


FIGURE 2

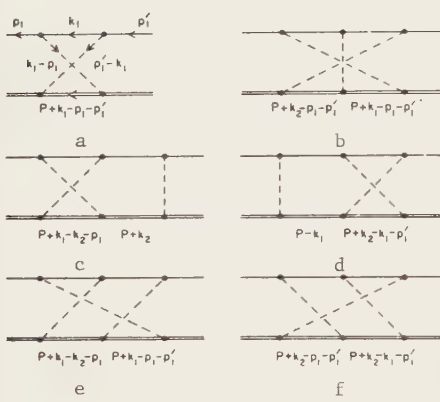


FIGURE 3

is shown in Fig. 4. The kernel now contains more terms, but diagram 4c and d are usually treated together and are referred to as the subtracted box for obvious reasons. Note that, if  $G$  were unconstrained, the subtracted box would be exactly zero. Equations which use constrained two body propagators are the BBS<sup>2</sup>, Todorov<sup>3</sup>, and an equation I introduced<sup>4</sup> in which one of the two particles is restricted to its mass shell, which I will refer to as  $G_1$ .

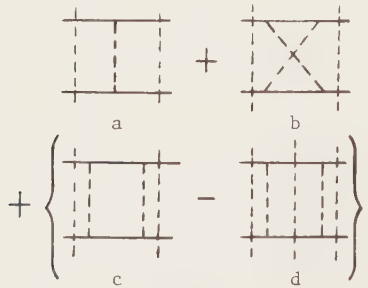


FIGURE 4

must be added to the ladder sum to this order are shown in Fig. 3.

I will describe three different choices of  $G$  which correspond to three different ways of summing these diagrams. The Bethe-Salpeter (BS) equation<sup>1</sup> uses the full, unconstrained propagator for  $G$ , so that irreducible terms which make up  $V$  are those given in Figs. 2a, 3a, b, e, f. If any of the other diagrams shown in Figs. 2 and 3 were included in  $V$ , we would be double counting; diagrams 2b and 3c, d are all obtained by iterating 2a and 3a; diagram 2c is obtained by iterating 2a twice.

Alternatively, we may constrain the two-body propagator in some way, as indicated by the vertical dashed lines shown in Fig. 1. In this case only part of the box diagram, 2b, or the other diagrams 2e, 3c, d are included when  $V$  is iterated. The 4th order kernel for an equation with a constrained propagator

is shown in Fig. 4. The kernel now contains more terms, but diagram 4c and d are usually treated together and are referred to as the subtracted box for obvious reasons. Note that, if  $G$  were unconstrained, the subtracted box would be exactly zero. Equations which use constrained two body propagators are the BBS<sup>2</sup>, Todorov<sup>3</sup>, and an equation I introduced<sup>4</sup> in which one of the two particles is restricted to its mass shell, which I will refer to as  $G_1$ .

For those who dislike derivations based on diagrams, I present an alge-

braic discussion. Let  $\hat{G}$  be a propagator corresponding to a different prescription from that employed in Eq. (1), with corresponding potential  $\hat{V}$ . Then it is easy to demonstrate that Eq. (1) follows from the two equations:

$$\begin{aligned} M &= \hat{V} + \hat{V} \hat{G} M & (a) \\ \hat{V} &= V + V (G - \hat{G}) \hat{V} & (b) \end{aligned}$$

This "derivation" shows that either Eq. (1) or Eq. (2a) can be used to calculate  $M$ ; Eq. (2b) merely tells how to obtain one kernel from the other. If  $G = G$  (BS), and  $\hat{G}$  is one of the constrained propagators, then the iteration of Eq. (2b) generates the diagrams shown in Fig. 4. However, the constrained equations should not be regarded as an approximation to the BS equation. From a relativistic point of view, both are equally good starting points and the question of which equation is "best" will depend on other criteria.

The extension of relativistic equations to more than two bodies is a subject of increasing importance. All of the equations mentioned above can be extended but the BS equation is more complicated than the others; for  $N$  particles the BS equation has  $4(N-1)$  integration variables while the constrained equations (in common with non-relativistic equations) have only  $3(N-1)$ . It is important that any  $N$  body system of equations satisfy the cluster property, which means that any subsystem of  $n < N$  particles must be dynamically independent of the others when the others are beyond the range of the forces. Only the BS and the  $G_1$  equations satisfy this requirement; the latter was recently proved for the 3 body system<sup>5</sup>.

### b. Methods Based on Time or $\tau$ Ordered Diagrams

A second method of defining  $G$  and  $V$  is based in consideration of time-ordered or  $\tau$ -ordered diagrams. It is possible to formulate field theory on the light front, which loosely speaking refers to quantizing fields at equal values of  $\tau = t - z$  (the velocity of light  $c$  is taken to be unity). The variable conjugate to  $\tau$  is  $p_+ = E + p_z$ , which now plays the role of the energy. This approach bears a close formal resemblance to old fashioned time ordered perturbation theory, where the fields are quantized at equal times. The equation for one boson exchange in the context of the light front is known as

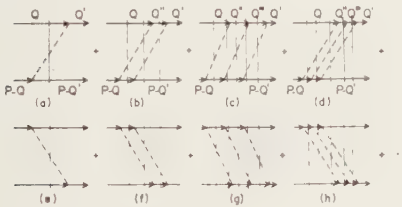


FIGURE 5

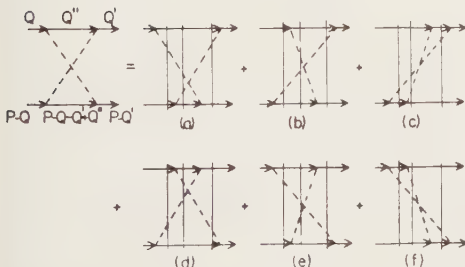


FIGURE 6

as the Weinberg Equation<sup>6</sup>, and several authors have used these techniques in recent years<sup>7-10</sup>.

While there is some formal resemblance between  $\tau$  ordered diagrams and time ordered diagrams there is a profound difference which cannot be overemphasized. The  $\tau$  ordered formalism is manifestly covariant at every step while time ordered perturbation theory breaks covariance. This is related to the fact that  $\tau$  is invariant under boosts in the  $z$  direction, while  $t$  is not. A disadvantage of the light front formulation is that it breaks manifest rotational invariance.

Bhalerao and Gurvitz<sup>11</sup> have recently discussed what they refer to as a "noninstantaneous approximation to the Bethe-Salpeter equation". While based on a time ordered formalism, and hence not strictly covariant, it is also similar to the way in which  $V$  would be constricted in the Weinberg equation. Contributions to  $V$  in the 6th order ladder approximation are shown in Fig. 5 (diagrams in which the nucleons are moving backward in time must also be included). To these must be added the crossed ladder diagrams, some of which are shown in Fig. 6. Note that a single Feynman diagram generates a large number of time or  $\tau$  ordered diagrams.

An advantage of these formulations is that they can be readily extended to  $N > 2$  bodies. Namyslowski and Weber<sup>12</sup> have shown that the three body Weinberg equation satisfies the cluster property.

### c. Methods Based on the Poincaré Algebra

The third method that I wish to review is based on consideration of the Poincaré Algebra. The Poincaré, or inhomogeneous lorentz group is described by 10 generators:

H	(time translation - energy)
$\vec{P}$	(space translations - momentum)
$\vec{J}$	(rotations - angular momentum)
K	(boosts)

These generators satisfy a closed algebra which can be used to determine some of the generators in terms of the others. An explicit construction for generators which satisfy this algebra for a many body system was first given by Bakamjian and Thomas (BK) in 1953<sup>13, 14</sup>. They assume that independent conjugate position and momentum operators exist for each particle, which for two particles can be denoted by  $\{\vec{r}_1, \vec{p}_1\}$  and  $\{\vec{r}_2, \vec{p}_2\}$ . Then conjugate pairs of total  $\{\vec{R}, \vec{P}\}$  and relative  $\{\vec{r}, \vec{p}\}$  position and momentum operators are defined which commute with each other. To construct the generators, a mass operator  $M$ , which contains the interaction  $v$  is first constructed.

$$M = (m_1^2 + p^2)^{1/2} + (m_2^2 + p^2)^{1/2} + v(r, p) \quad (3)$$

Note that it is assumed that  $v$  depends only on the relative position and momentum. In terms of  $M$  and  $\vec{L} \equiv \vec{r} \times \vec{p}$ , the Poincaré generators become

$$\begin{aligned} H &= (M^2 + P^2)^{1/2} \\ \vec{J} &= \vec{R} \times \vec{P} + \vec{L} \\ \vec{K} &= \frac{1}{c} (\vec{R}, H) - \frac{\vec{v} \times \vec{P}}{c + H} \end{aligned} \quad (4)$$

Note that any interaction  $v$  can be used as the basis for a relativistic theory, and hence this approach makes no restrictions on the dynamics. In this way it is different from the two approaches described above.

The BK procedure can be extended to  $N > 2$  bodies, but the resulting generators do not satisfy the cluster property and hence are unsatisfactory. Recently Coester and Polyzou<sup>15</sup>, using ideas developed by Socolov, have found a way to extend the BK construction to an arbitrary number of particles in such a way that the cluster property is satisfied. The construction gives  $H$  and  $\vec{K}$  as a sum of terms

$$\begin{aligned} H &= H_0 + V_2 + V_3 + \dots + V_N \\ \vec{K} &= \vec{K}_0 + \vec{K}_2 + \vec{K}_3 + \dots + \vec{K}_N \end{aligned} \quad (5)$$

where  $H_i$  and  $\vec{K}_i$  are interaction terms involving  $i$  particles. Hence the construction permits arbitrary interactions involving  $2, 3, \dots, N$  bodies.

#### d. Other Methods

Recently, Glöckle and Müller<sup>16</sup> have obtained a relativistic equation by starting with the form of the generators obtained from a Lagrangian field theory. They introduce a transformation which separates the  $NN$  sector from the  $NN\pi$  and other sectors by block diagonalizing the generators. This method provides an interesting bridge between the methods described in parts (a) and (c) above. The two body equation they obtain has a second order kernel identical to the  $G_1$  equation, but the propagator contains only positive energy contributions from the nucleons, a consequence of the diagonalization procedure.

Another approach to the relativistic  $N$  body problem has been given by Lindsay and Noyes<sup>17</sup>. They refer to their method as a "zero range scattering theory"; it gives unitary 3 and 4 body equations which depend only on two-particle physical observables as input. Numerical results have been obtained for three-particle bound states, elastic scattering and rearrangement of bound pairs with a third particle, and amplitudes for breakup into states of three free particles.

#### 1.2. Convergence

It is important to know how well any of these procedures converge to the result it is trying to obtain. For the wave equations based on either Feynman or time ( $\tau$ ) ordered diagrams, this reduces to the question of how rapidly the infinite series for the kernel  $V$  converges. For methods based on the Poincaré

algebra, this reduces to assessing the validity of the  $(v/c)^2$  expansions on which applications of this method usually rely.

For scalar particles, it has been known for many years that there are significant cancellations between ladder and crossed ladder diagrams. Recently<sup>18</sup> it was shown that this cancellation is exact in the limit where one of the two particles has spin zero and infinite mass  $M$ , regardless of the mass  $m$  or spin of the other particle. In this case one obtains the exact result for the ladder and crossed ladder sum by using the  $G_1$  equation, where the heavy particle is the one restricted to its mass shell and the kernel is given by one boson exchange (OBE). Stated in other language, when  $M \rightarrow \infty$ , the higher order terms in  $V$  cancel, leaving only the second order term corresponding to OBE. This means that in 4th order the subtracted box (Fig. 4c and d) cancels the crossed box, (Fig. 4b). In the  $M \rightarrow \infty$  limit, a one body equation (Dirac for spin  $\frac{1}{2}$ , Klein Gordon for spin 0) is obtained for the light particle. This cancellation is not obtained for the BS equation; since there is no subtracted box in 4th order, there is nothing to cancel the crossed box. The implications of this result are clear; the BS equation is less convergent than the equations with a restricted propagator.

The same<sup>4, 19</sup> cancellation has also been observed to work in 4th order for two spin  $\frac{1}{2}$  particles in QED and for a realistic theory of pseudoscalar isovec-

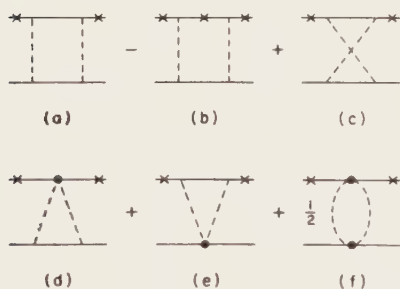


FIGURE 7

tor pions interacting with spin  $\frac{1}{2}$  nucleons in a manner consistent with chiral symmetry<sup>18</sup>. The latter example includes a  $\gamma^5 \pi NN$  coupling and a  $\sigma$ -like  $NN2\pi$  contact term necessary to preserve chiral symmetry to order  $g^2$ . The terms which contribute to the 4th order kernel are shown in Fig. 7; the heavy dot in the figure is the  $\sigma$  contact interaction. When these diagrams are regularized by including form factors at the vertices (for consistency, the  $\sigma$  contact term includes a form factor

which is the square of the form factor at the  $\pi NN$  vertex), they cancel in the  $M \rightarrow \infty$  limit. The leading isovector exchange term,  $\tau_1 \cdot \tau_2$ , cancels when the subtracted box (Fig. 7a and b) and crossed box (Fig. 7c) are added, and the leading isoscalar exchange part which remains is cancelled by the diagrams involving the contact term. This cancellation was demonstrated for an entire family of equations with restricted propagators in reference<sup>18</sup>, but only in the case when one particle was restricted to its mass shell was the potential resulting



after the cancellation energy independent and local (to order  $M^{-1}$ ).

Bhale Rao and Gurvitz (BG) do not observe this cancellation in their equation<sup>11</sup>. It is instructive to see why this is so<sup>20</sup>. For spinless particles, their propagator is identical to the  $G_1$  propagator but their potential is different. If we denote the three momentum of the final state by  $p$ , and the initial state by  $p'$ , then the second order potential in the two cases is

$$\begin{aligned} V_{2a} &= -\frac{g^2}{2\omega} \left[ \frac{1}{\omega + \Delta E} + \frac{1}{\omega - \Delta E} \right] \\ V_{2b} &= -\frac{g^2}{\omega} \left[ \frac{1}{\omega + \Delta E} \right] \end{aligned} \quad (6)$$

where  $V_a$  is the  $G_1$  potential and  $V_b$  the BG potential, and

$$\begin{aligned} \Delta E &= E' - E \\ \omega &= \left( \mu^2 + (p - p')^2 \right)^{1/2} \end{aligned} \quad (7)$$

and  $E = (M^2 + p^2)^{1/2}$ . When the initial and final states are both on shell,  $|p| = |p'|$  and  $\Delta E = 0$ . Hence the two choices are equal on shell. The first place where this difference can show up in the physical scattering amplitude is in 4th order, where the two theories give

$$\begin{aligned} V_{4a} &= V_{4-} + V_{2a} G V_{2a} \\ V_{4b} &= V_{4-} + V_{2b} G V_{2b} \end{aligned} \quad (8)$$

where  $V_{4-}$  is the contribution from the crossed box, equal in both cases when  $M \rightarrow \infty$ . Hence

$$\begin{aligned} V_{4a} &= V_{4-} + (V_{2a} - V_{2b}) G (V_{2a} - V_{2b}) \\ &\quad + (V_{2a} - V_{2b}) G V_{2b} + V_{2b} G (V_{2a} - V_{2b}) + V_{2b} G V_{2b} \\ &= V_{4b} + \Delta V G \Delta V + \Delta V G V_{2b} + V_{2b} G \Delta V \end{aligned} \quad (9)$$

A calculation of the additional terms on the right hand side of (9) shows that they are precisely what is needed to cancel  $V_{4b}$ , giving the famous  $V_{4a} = 0$ . I interpret this result as a demonstration that the BG approach is not as convergent as the  $G_1$  approach since the choice  $V_{2b}$  leads to a 4th order potential  $V_{4b}$  which is not small, while  $V_{2a}$  gives a potential  $V_{4a}$  which is small. The BG approach suffers from a difficulty similar to that of the BS equation.

Numerical studies of convergence tend to confirm these observations. Numerical phase shifts for four different choices of coupling constant for a meson mass  $\mu = m_\pi$  are given in Figs. 8 and 9, taken from reference<sup>21</sup>. Fig. 8 shows the BS equation and Fig 9 the BBS equation, and in both cases  $V_2$  is the second order kernel (OBE) while  $V_2 + V_4$  is the full kernel up to 4th order. The differences between  $V_2$  and  $V_2 + V_4$  are significantly smaller for the BBS equation (particularly for case (d) where the coupling constant is large) suggesting a much



better convergence for the BBS. This is a consequence of the cancellations described above, which the BBS equation also enjoys. One puzzle remains, however.

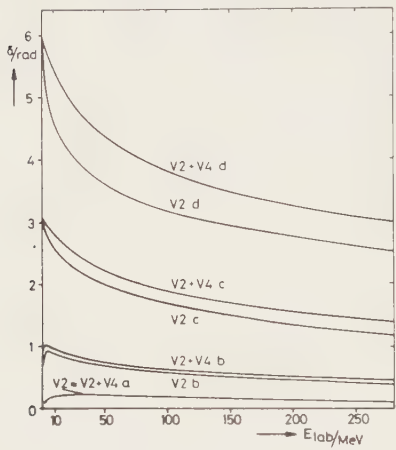


FIGURE 8

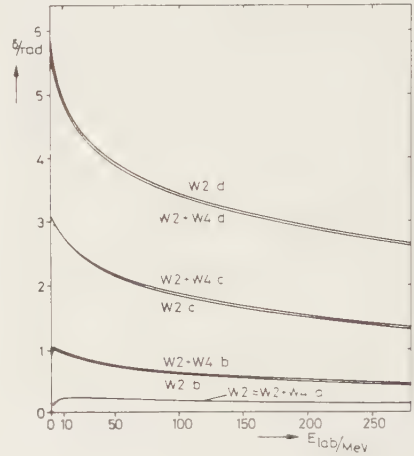


FIGURE 9

When the numerical phase shifts for the  $G_1$  equation are compared to the BBS equation (using the second order kernel) significant differences are found. This is hard to understand, because both the BBS and the  $G_1$  equation have the same cancellation and should therefore converge rapidly. Perhaps they are converging to different final results, opening up the possibility that these equations are not equivalent, even when the kernel is calculated to infinite order, as has often been assumed.

1.3. Discussion

Three main issues emerged from the discussion which grew out of the ideas reviewed in this section.

The first pertains to the use of equations which are constructed from consideration of the Poincaré algebra, as presented in Sec. c. What value are such equations when the dynamics is completely arbitrary? A rather clear and useful answer was given by Coester and Wiringa<sup>22</sup>. They point out that such equations enable us to determine the size of some relativistic effects, without claiming to give a unique or complete answer, and without fixing the size of 3 and 4 body forces, some of which could be of relativistic origin. In a paper presented to the conference, they estimate the size of relativistic corrections to the binding energy of the triton and alpha particle arising from terms involving the two body interaction only. Expanding their results to order  $m^{-1}$ , they obtain for the leading relativistic corrections

$$\Delta M_3 = - \sum_{i=1}^3 \frac{p_i^4}{8m^3} - \frac{1}{16m^2} \sum_{ij} \left\{ (p_i^2 + p_j^2), \quad V_{ij} \right\} \tag{a}$$

$$\Delta M_4 = - \sum_{i=1}^{\infty} \frac{p_i^4}{8m^3} - \frac{1}{16m^2} \sum_{i,j} \left\{ (p_i^2 + p_j^2), v_{ij} \right\} \\ + \frac{1}{36m} \sum_{i,j,k} \left\{ [v_{ij}, v_{jk}], (\vec{x}_k - \vec{x}_j) \right\} \cdot (\vec{p}_i + \vec{p}_j + \vec{p}_k) \quad (b) \quad (10)$$

where  $v_{ij}$  is the two body interaction between particles  $i$  and  $j$  related to  $v$  of Eq. (3) by

$$v = \frac{1}{m} (m^2 + p^2)^{1/2} \quad v (m^2 + p^2)^{1/2} \quad (11)$$

The same terms also give a correction to the deuteron binding energy. If  $V$  is rescaled so as to absorb this correction, fixing the deuteron binding energy at its correct value, the relativistic corrections obtained from equations (10) increase the binding of the triton (alpha) from  $-6.9 \pm 0.1$  MeV ( $-22.4 \pm 0.4$  MeV) to  $-8.6 \pm 0.5$  MeV ( $-26.7 \pm 1.4$  MeV). They conclude that these relativistic effects are comparable in size to the three-body forces calculated in reference<sup>23</sup>.

Glöckle pointed out that the expansion in powers of  $m^{-1}$  can be quite inaccurate. Müller<sup>24</sup> found that the  $p/m$  expansion gave a result almost twice as big as an exact calculation of the relativistic corrections to first order.

A second issue concerns the criteria by which one should judge whether any particular relativistic equation will be suitable for nuclear physics. I have emphasized the desirability of having an equation which is convergent and satisfies the cluster property. Another desirable feature, suggested in the discussion, is that the equation should have no solutions with negative mass. T.E.O. Ericson also suggested that solutions of the equation should be independent of the mixing between  $\gamma^5$  and  $\gamma^5 \gamma^4$  couplings for the pion. This is motivated by the observation that it is possible to transform from one of these couplings to another by a unitary transformation. However, to make this transformation exact requires that contact terms involving pion fields of all orders be included. Most equations treat the interaction exactly only to small finite order, treating higher order interactions approximately, and hence are unlikely to be able to satisfy this requirement exactly.

Finally, S. Brodsky suggested that, because the nucleon is composite, it is doubtful that the field theory of nucleons and mesons should be taken so seriously. He argued that the underlying quark degrees of freedom must be taken into account, and that in the long range domains where the compositeness of the nucleon can be ignored, non-relativistic equations are sufficient. The alternative view is that the ultimate usefulness of meson theory will depend on the effective confinement radius  $R$ . If  $R$  is small (less than 0.5fm) meson theory may be quite successful in describing a large class of nuclear phenomena and in such a case it will be necessary to have a relativistic theory, since small  $R$  implies

large momenta and significant effects due to relativity. In any case, relativistic meson theories will play a useful role by providing a calculable alternative against which to compare models which treat quark degrees of freedom explicitly. Ironically, the more serious and careful the attempt to explain nuclear phenomena using relativistic meson theory, the more likely discrepancies are to be taken seriously and the more rapid will be our progress toward isolating effects which require explicit treatment of the underlying quark degrees of freedom.

## 2. RELATIVISTIC CALCULATIONS OF MATRIX ELEMENTS

Obtaining solutions for wave functions and scattering amplitudes is only part of the goal in nuclear physics; once obtained, they must be used to calculate matrix elements which describe how few body systems interact with probes, such as electrons, pions, and protons. In what follows I will focus on interactions with electrons, which are assumed to take place through the one photon exchange approximation. This requires a calculation of matrix elements of the current operator, which are related to form factors. The techniques employed parallel the different techniques discussed in Sec. 1 above.

The current operator must be consistent with the dynamics assumed for the underlying few body relativistic equations. This is best illustrated by an ex-

ample. In the context of the  $G_1$  equation, assume that the dynamics are satisfactorily described by the OBE kernel (Fig. 10a), the subtracted box (Fig. 10b) which will be drawn with a small circle on the second particle to indicate that it is the sum of two terms Fig. 4c, d, and the crossed box (Fig. 10c). Then, if the mesons are neutral, the current operator is as shown in Fig. 11a-c. If the meson is charged, the additional diagrams shown in Fig. 11d-f must be added. The point is that the current operator is uniquely determined; it will contain precisely those terms which are in the kernel, suitably modified to include the photon interaction.

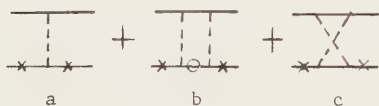


FIGURE 10

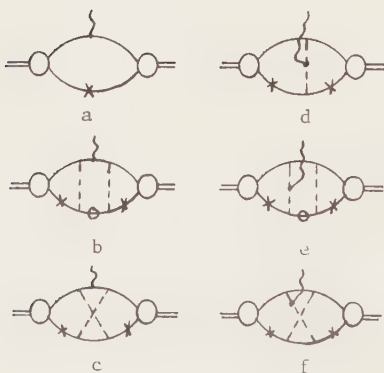


FIGURE 11

These remarks imply that the two meson exchange current can be expected to be important, since experience has

taught us over the last decade that the two meson exchange diagrams are important in the nuclear force.

This approach has recently been attacked by Gurvitz<sup>25</sup>. However, I believe<sup>26</sup> that his arguments are wrong, and that there are none of the ambiguities or large effects he claims to find.

The current operator can also be determined in the context of approaches which use the Poincaré algebra. Here, as has been emphasized by Coester<sup>27</sup>, the current operator must be consistent with the Poincaré algebra and with the wave functions used. In particular, to order  $(v/c)^2$  the current operators must satisfy the commutation relations

$$\begin{aligned} i [H, \rho] &= - \vec{\nabla} \cdot \vec{j} \\ i [\vec{K}, \rho] &= - \vec{j} + i [H, \rho] \vec{x} \\ i [K_i, j_k] &= - \delta_{ik} \rho + i [H, j_k] x_i \end{aligned} \quad (12)$$

Friar has recently completed a detailed comparison of the deuteron form factors obtained using this method with results obtained using Feynman diagrams<sup>28</sup>. He finds that a unique answer cannot be obtained unless one uses a deuteron wave function consistent with the current operator. For example, if  $|\phi\rangle$  is a deuteron wave function consistent with the operator  $\rho$ , and we introduce a unitary transformation such that

$$\begin{aligned} U|\phi\rangle &= |\phi_A\rangle \\ U\rho U^{-1} &= \rho_A \end{aligned} \quad (13)$$

then

$$\langle \phi' | \rho | \phi \rangle = \langle \phi' | \rho_A | \phi_A \rangle \quad (14)$$

which is merely the statement that matrix elements are invariant under unitary transformations. However, when faced with any given phenomenological wave function  $|\psi\rangle$  obtained from a fit to the NN phase shifts, it may not be clear whether to calculate  $\langle \psi' | \rho | \psi \rangle$  or  $\langle \psi' | \rho_A | \psi \rangle$  or another matrix element using some other unitary transformation of  $\rho$ . I emphasize that a relativistic approach in which both the wave function and  $\rho$  are calculated using the same dynamics will not suffer from these problems.

What experimental evidence do we have for relativistic effects? This is a difficult question to answer, because relativistic effects are intertwined with other aspects of the dynamics. However, the electro-disintegration of the deuteron to a threshold final state<sup>29</sup>, which is usually cited as evidence for the existence of meson-exchange currents, is more properly evidence of relativistic effects<sup>30</sup>. And in a paper presented to this conference, and published elsewhere<sup>31</sup>, Cambi, Mosconi, and Ricci have shown how a relativistic correction seems to have resolved the long standing discrepancy in the forward photodisin-

tegration of the deuteron. For a discussion, see the account given by Gibson in his talk at this conference<sup>32</sup>.

#### ACKNOWLEDGEMENTS

I would like to acknowledge helpful discussion with W. Glöckle and F. Coester. This work was supported in part by the U.S. National Science Foundation.

#### REFERENCES

- 1) E. E. Salpeter and H. A. Bethe, Phys. Rev. 84 (1951) 1232
- 2) R. Blankenbecler and R. Sugar, Phys. Rev. 142 (1966) 1051
- 3) I. T. Todorov, Phys. Rev. D 10 (1971) 2351
- 4) F. Gross, Phys. Rev. 186 (1969) 1448
- 5) F. Gross, Phys. Rev. C 26 (1982) 2226
- 6) S. Weinberg, Phys. Rev. 150 (1966) 1313
- 7) J. M. Namyslowski, Proceedings of the Graz Conference (1978) Lecture Notes in Physics #82, Ed. by Zingl et al, (Springer-Verlag) p.41
- 8) G. P. Lepage and S. J. Brodsky, Phys. Rev. D 22 (1980) 2157
- 9) M. Chemtob, Nucl. Phys. A336 (1980) 299
- 10) L. L. Frankfurt and M. I. Strikman, Nucl. Phys. B148 (1979) 107
- 11) R. S. Bhalerao, and S. A. Gurvitz, Phys. Rev. C 28 (1983) 383
- 12) J. M. Namyslowski and H. J. Weber, Zeit. fur. Physick A295 (1980) 219
- 13) R. Bakamjian and L. H. Thomas, Phys. Rev. 92 (1953) 1300
- 14) R. Fong and J. Sucher, J. of Math. Phys. 5 (1964) 456
- 15) F. Coester and W. N. Polyzou, Phys. Rev. D 26 (1982) 1348
- 16) W. Glöckle and L. Müller, Phys. Rev. C 23 (1981) 1183; L. Müller, Nucl. Phys. A360 (1981) 331
- 17) H. P. Noyes, Phys. Rev. C 26 (1982) 1858, J. Lindesay, SLAC-PUB-2932
- 18) F. Gross, Phys. Rev. C. 26 (1982) 2203
- 19) A. R. Neghabian and W. Glöckle, Can. J. of Phys. 61 (1983) 85
- 20) W. Glöckle, private communication;
- 21) L. Müller and W. Glöckle, Nucl. Phys. B 146 (1978) 393
- 22) F. Coester and R. B. Wiringa, contribution to this conference.
- 23) J. Carlson, V. R. Pandharipande and R. B. Wiringa, Nucl. Phys. A401 (1983) 59
- 24) See table 1 in the second paper of Ref. 16.
- 25) R. S. Bhalerao and S. A. Gurvitz, Phys. Rev. Lett. 47 (1981) 1815; S. A. Gurvitz, Weizmann Institute of Science report WIS-81/47 Oct-PH
- 26) F. Gross and B. D. Keister, Phys. Rev. C 28 (1983) 823
- 27) F. Coester and A. Ostebee, Phys. Rev. C 11 (1975) 1836
- 28) J. Friar, Phys. Rev. C 22 (1980) 796
- 29) M. Bernheim, et al, Nucl. Phys. A365 (1981) 349

- 30) See F. Gross, Invited Talk at the Delhi Conference, 29 Dec. 1975 - 3 Jan. 1976, in "Few Body Dynamics", Proceedings of the VII Int. Conference, Ed. A. N. Mitra, et al (North Holland) p. 523
- 31) A. Cambi, B. Mosconi, and P. Ricci, Phys. Rev. Lett. 48 (1982) 462
- 32) B. F. Gibson, "Electromagnetic and Weak Interactions in Few-Nucleon Systems", Invited talk at this conference.





## THE GREEN'S - FUNCTION MONTE-CARLO METHOD IN FEW-BODY CALCULATIONS

JOHN G. ZABOLITZKY

Institut für Theoretische Physik Universität zu Köln, W.-Germany

The few body Schrödinger equation is solved for the ground state without approximations by means of the Green's - Function Monte-Carlo method. The results are subject to only statistical error which may be made arbitrarily small in the case of many-Boson systems, and hopefully sufficiently small in the case of Fermions. The method is outlined and selected results for light atomic nuclei, droplets of Helium atoms and small molecules are given.

### 1. INTRODUCTION

In spite of the zero temperature regime being an almost negligible part of physical phenomena, the ground-state solution to the many-body Schrödinger equation is of considerable importance in several branches of physics and chemistry. In previous years for most cases of physical interest solutions free of approximations have been rather scarce. The equivalence between the Schrödinger equation and the diffusion equation has at least been recognized by 1949 by Metropolis, Ulam and Fermi<sup>1</sup> opening up the possibility of approximation-free computer simulations by solving an equivalent diffusion problem. An efficient algorithm, the Green's-Function Monte-Carlo method (GFMC) has been devised by Kalos and collaborators<sup>2-7</sup> more than 10 years ago. Applications have been mainly to infinite systems<sup>4-7</sup> approximated by finite systems with periodic boundary conditions. There is only a small number of calculations reported because of insufficient computational resources. In the present paper I review applications to few-body systems with particular emphasis on the problems arising in the case of Fermions as opposed to Bosons.

### 2. THE GREEN'S-FUNCTION MONTE-CARLO METHOD

Since it is not possible here to indulge in a detailed discussion I will briefly outline the basic ideas. For the moment let me consider a problem of  $N$  interacting Bosons governed by the Schrödinger equation

$$\left( -\nabla_R^2 + V(R) \right) \psi(R) = E \psi(R) \quad (1)$$

where the interaction  $V(R)$  is local but not necessarily pair-additive.  $R$  denotes the coordinate vector of the  $N$ -body system in  $3N$  dimensional space, i.e. represents the coordinates  $r_1 \dots r_N$ . Assuming the interaction  $V(R)$  bounded from below a shift of the energy scale may be introduced so that  $V(R) > 0$  and  $E_0 > 0$ . For a Bose ground state wavefunction we furthermore have  $\psi(R) \geq 0$ . The bounding of  $V(R)$  is not essential but simplifies the discussions. If the Green's function

$$\left( -\nabla_{R_1}^2 + V(R_1) \right) G(R, R_1) = \delta^{3N}(R - R_1) \quad (2)$$

were known, one could obtain the Ground-state wavefunction iteratively in the  $n \rightarrow \infty$  limit of

$$\psi^{(n+1)}(R) = E_t \int dR_1 G(R, R_1) \psi^{(n)}(R_1) \quad (3)$$

where  $E_t$  is some suitably chosen constant of dimension energy. The ground-state energy may then be estimated from

$$E_0 \xrightarrow{n \rightarrow \infty} E_t \frac{\int dR \psi^{(n)}(R)}{\int dR \psi^{(n+1)}(R)} \quad (4)$$

In order to have a stable iteration it is seen that the trial energy  $E_t$  should be some estimate of the eigenvalue  $E_0$ .

Eqs. (3) and (4) are rather trivial if one uses the spectral representation of the Green's function and the wavefunction,

$$\begin{aligned} G(R, R_1) &= \sum \langle R | i \rangle \frac{1}{E_i} \langle i | R_1 \rangle \\ \psi^{(n)}(R) &= \sum \langle R | i \rangle c_i^{(n)} \\ c_i^{(n+1)} &= \frac{E_t}{E_i} c_i^{(n)} = \left( \frac{E_t}{E_i} \right)^{n+1} c_i^{(0)} \end{aligned} \quad (3')$$

Since  $E_t/E_i$  is largest for the smallest  $E_i = E_0$  the iteration (3) converges to the ground state.

Obviously, the Green's function eq. (2) is unknown and cannot be computed. However, in a Monte-Carlo scheme, there is no need to compute values of functions but one instead performs a random walk where it is only required to

sample from functions. It is therefore sufficient to construct a second random walk process yielding the desired Green's function. This may be achieved by introducing a small domain  $d \in \mathbb{R}^{3N}$  and defining a Green's-function pertaining to constant potential  $U$  within  $d$ , which is assumed to be zero on the boundary of and outside  $d$ , where  $d$  and  $U$  may depend parametrically upon  $R_0$ ,

$$\left( -\nabla_1^2 + U(R_0) \right) G_U(R_1, R_0) = \delta^{3N}(R_1 - R_0) \quad (5)$$

For any reasonably shaped domain  $d$ , eq. (5) may be solved analytically.

Multiplying eq. (2) by  $G_U(R_1, R_0)$  and eq. (5) by  $G(R, R_1)$  and subtracting we obtain

$$\begin{aligned} G(R, R_0) &= G_U(R, R_0) + \int_{\partial d(R_0)} \left( -\frac{\partial G_U(R_1, R_0)}{\partial n} \right) G(R, R_1) dR_1 \\ &+ \int_{d(R_0)} (U(R_0) - V(R_1)) G_U(R_1, R_0) G(R, R_1) dR_1 \\ &= G_U(R, R_0) + \int_{d(R_0)} K(R_1, R_0) G(R, R_1) dR_1 \end{aligned} \quad (6)$$

If  $U$  is chosen to bound  $V(R)$  from above within the domain  $d$  it is easily shown that the norm of the integral kernel  $K$  is smaller than one, i.e. eq.(6) may be solved for  $G$  by iteration which is equivalent to summing the Neumann series.

In a Monte-Carlo algorithm this iteration translates into a random walk with transition probability  $K$ . Furthermore it may be shown that  $G$ ,  $G_U$ ,  $K$  are all non-negative. Therefore, all quantities occurring so far may be interpreted as probability densities for "pointers"  $R$  in  $3N$  dimensional space. Eqs. (3) and (6) may then immediately be translated into a Monte-Carlo algorithm to be executed on a computer. The positive wavefunction  $\Psi(R)$  is then represented by the probability density of finding a "pointer"  $R_i$  at  $R$  in  $dR$ . This probability of course is a probability only for the purposes of the Monte-Carlo scheme and must not be confused with the physical probability density which is as always given by  $|\Psi(R)|^2$ . Importance sampling may be used profitably to speed up the calculation.

The algorithm sketched so far is immediately applicable to few-Boson systems. In the case of Fermions a problem arises since the wavefunction may not be

chosen positive everywhere. Formally this problem may be circumvented by decomposing the wavefunction

$$\Psi_F(R) = \Psi_+(R) - \Psi_-(R), \quad \Psi_+(R) > 0 \quad \Psi_-(R) > 0 \quad (7)$$

Since the Green's functions are symmetric regardless of statistics it is then still possible to execute the Bose algorithm for the positive and negative parts, eq. (7), separately. If the first iterate is chosen antisymmetric one would assume that eq. (3) preserves this property. However, below the Fermion ground state there is a symmetric eigenstate of the Hamiltonian for any reasonable physical system. It is seen in eq. (3') that this symmetric state will get amplified by a factor of  $E_{\text{Fermi}}/E_{\text{Bose}}$  in each iteration. In a Monte-Carlo scheme admixture of statistical noise can never be avoided. This admixture will accordingly grow exponentially and destroy the calculation.

At first sight a remedy seems to be the projection onto some suitably chosen antisymmetric trial state  $\Psi_{\text{FT}}$  and evaluation of the energy from

$$E_{\text{tr}} = \langle \Psi_{\text{FT}} | H | \Psi \rangle / \langle \Psi_{\text{FT}} | \Psi \rangle \quad (8)$$

Obviously, symmetric noise in  $\Psi$  will not contribute to eq. (8). However, the variance of the energy estimator eq. (8) will involve the square of the trial state which is symmetric and therefore does receive a contribution from symmetric noise, i.e. the variance will grow exponentially. Nevertheless calculations are possible and have been performed at a significant expense of computer time<sup>8</sup> employing this so-called "method of transient estimators". At present there is no general solution to this problem in sight in spite of significant efforts<sup>9</sup> but increasing computational power.

A rigorously non-exact but for electrons rather accurate method is the so-called "fixnode approximation" where one assumes the nodal surfaces of the Fermion wavefunction to be known<sup>10,11</sup>. Nodal surfaces may conveniently be described by specifying trial wavefunctions, usually determinants. The problem then reduces entirely to a Bose problem within that part of space where the trial function is positive. Resulting energies are variational, i.e. upper bounds to the Schrödinger eigenvalue. The wavefunction could be optimized by varying the nodal surfaces. However, no scheme is known to do that in a systematic fashion.

### 3. RESULTS AND DISCUSSION

There are a number of cases where Fermion problems reduce to Bose problems. In one spatial dimension the nodal surface of an antisymmetric wavefunction is always rigorously known and no Fermion problem arises. In three-dimensional space in the case of strictly local interactions independent of internal degrees of freedom of the particles considered (spin and isospin) whenever the number of particles is smaller than the degeneracy (two for electrons, four for nucleons) the problem is equivalent to a Bose problem. In that case antisymmetry is maintained via the internal degrees of freedom whereas the spatial part of the wavefunction is symmetric.

In table 1 I give results for three and four nucleons interacting via the Malfliet-Tjon V potential<sup>12</sup>, in comparison with other methods. It is seen that everyone agrees on the triton, but that straight-forward integral equation approaches can not be brought to sufficient accuracy on the alpha particle. Presumably this is due to technical problems like insufficient numbers of partial waves, meshpoints, etc. The very nice agreement between the exact GFMC and other methods lends enhanced credibility to these other methods which are approximate but about two to three orders of magnitude faster to execute on a computer. Table 2 shows similar results in the presence of a strong three-body force<sup>12</sup>. Also there are shown results from two entirely independent GFMC calculation done by two different groups<sup>12</sup> which agree within statistical error as they should.

Table 1 N-body ground states from MTV potential

Method	N = 3 E/MeV	N = 4 E/MeV
GFMC	- 8.26 $\pm$ 0.01	- 31.3 $\pm$ 0.2
Variational	- 8.22 $\pm$ 0.02	- 31.19 $\pm$ 0.05
Feddeev (-Yakubasky)	- 8.253	- 28
Coupled-Cluster		- 31.24
ATMS		- 31.3

Table 2 same as table 1, with three-body force

Method	N = 3 E/MeV	N = 4 E/MeV
GFMC 1	- 9.05 $\pm$ 0.05	- 37.09 $\pm$ 0.06
GFMC 2	- 9.00 $\pm$ 0.08	- 37.2 $\pm$ 0.2
Variational	- 8.79 $\pm$ 0.07	- 36.2 $\pm$ 0.25

Consider next the problem of  $N$   $^4\text{He}$  atoms interacting via the Aziz et al HFDHE2 potential<sup>13</sup>. In fig.1 I show the density profiles for various values of  $N$ . The solid lines are GFMC calculations whereas the dashed lines come from variational calculations which may more easily be extended to larger values of  $N$ . It is seen that saturation is attained at about  $N=40$  at the proper value known from the infinite fluid. Fig.2 shows the resulting r.m.s. radii. Very small systems are more diffuse because of loose binding and therefore exhibit an increase in radius. The energies per particle for  $N \geq 20$  may be fitted to about 1/2 % accuracy by

$$E(N)/N = -7.02 + 18.8 x - 11.2 x^{2/3} \quad (9)$$

$$x = N^{-1/3}$$

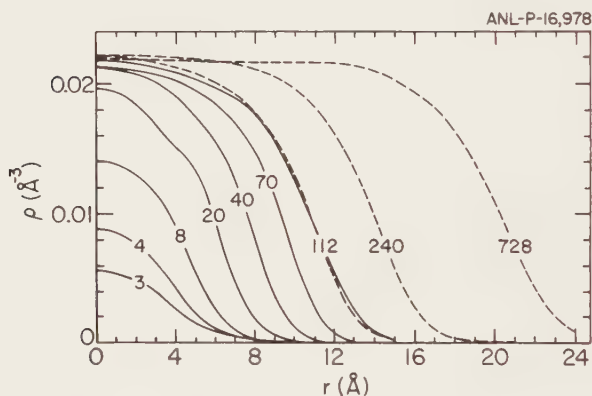


FIGURE 1 Density profiles for droplets of  $N$   $^4\text{He}$  atoms

This formula extrapolates very well to the infinite fluid giving  $-7.02$   $^{\circ}\text{K}$ /particle in comparison to experimental  $-7.12$   $^{\circ}\text{K}$ /particle and a surface tension of  $0.30$   $\text{K}\text{\AA}^{-2}$  (experimentally  $0.27$   $\text{K}\text{\AA}^{-2}$ ). Differences are attributed to deficiencies of the Hamiltonian (no three-body force, non-uniqueness of HFDHE2 potential).

As the last example let me consider the LiH molecule in the clamped-nuclei approximation, i.e. a four-electron problem in an external field generated by the fixed nuclei. This is just one particular example out of several molecules studied. Table 3 shows results for the correlation energies (difference between Schrödinger eigenvalue and self-consistent-field (SCF) or Hartree-Fock value) obtained from various methods. Currently, the Coupled-Cluster result in two-body cluster approximation is the most accurate result available<sup>13</sup>. The

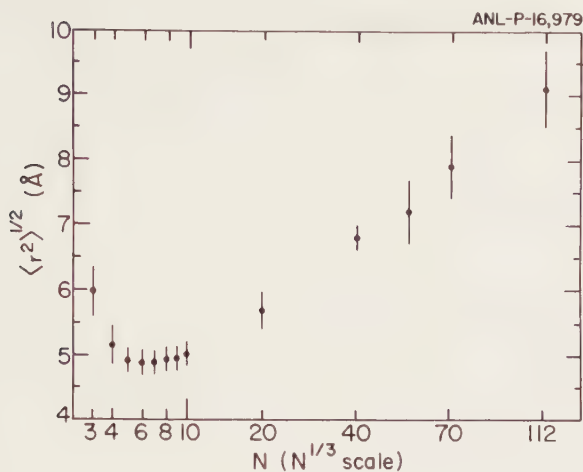


FIGURE 2 Radii of droplets of  $N$   $^4\text{He}$  atoms

GFMC has been carried out<sup>11</sup> in the fixnode approximation only yielding a statistical error of 2 mHartrees. The error due to the fixnode approximation is seen to be of the order 1-5 mHartrees.

Table 3

$E_{\text{SCF}}$	-7.987	323	Hartree
$E^{\text{CC}(2)}$	-0.081	54	Hartree
$E^{\text{FN-MC}}$	-0.080	$\pm 0.002$	Hartree
$E^{\text{EXP}}$	-0.083	20	Hartree

As a last application let me mention that for light nuclei it is also possible to carry out calculations with explicit inclusion of the mesonic degrees of freedom, i. e. describing nuclei as systems of nucleons interacting not via potentials but meson fields<sup>14</sup>.

#### REFERENCES

- 1) N. Metropolis, S. Ulam, J.Am.Stat.Ass. 44 (1949) 335
- 2) M. H. Kalos, Phys.Rev. 128 (1962) 1891
- 3) M. H. Kalos, J.Comp.Phys. 1 (1966) 127  
M. H. Kalos, Nucl.Phys. A 126 (1969) 609



- 4) M. H. Kalos, Phys.Rev. A 2 (1970) 250  
M. H. Kalos, D. Levesque, L. Verlet, Phys.Rev. A 9 (1974) 2178
- 5) D. M. Ceperley and M. H. Kalos, in: Monte Carlo Methods in Statistical Physics, ed. K. Binder (Springer, Berlin, 1979)
- 6) P. A. Whitlock, D. M. Ceperley, G. V. Chester, M. H. Kalos, Phys.Rev. B 19 (1979) 5598
- 7) M. H. Kalos, M. A. Lee, P. A. Whitlock, G. V. Chester, Phys.Rev. B 24 (1981) 115
- 8) D. Ceperley, B. J. Alder, Phys.Rev.Lett. 45 (1980) 566  
M. A. Lee, K. E. Schmidt, M. H. Kalos, G. V. Chester, Phys.Rev.Lett. 46 (1981) 728  
D. Ceperley, private communication
- 9) D. Arnou, M. H. Kalos, M. A. Lee, K. E. Schmidt, J.Chem.Phys. 77 (1982) 1  
D. M. Ceperley, Proceedings of the NATO ARW on Monte Carlo Methods in Quantum problems (1982), to be published  
M. H. Kalos, Proceedings of the NATO ARW on Monte Carlo Methods in Quantum problems (1982), to be published  
U. Helmbrecht and J. G. Zabolitzky, unpublished
- 10) J. B. Anderson, J.Chem.Phys. 65 (1976) 4121  
J. W. Moskowitz, K. E. Schmidt, M. A. Lee, M. H. Kalos, J.Chem.Phys. 77 (1982) 349
- 11) P. J. Reynolds, D. M. Ceperley, B. J. Alder, W. A. Lester, J.Chem.Phys. 77 (1982) 5593
- 12) V. R. Pandharipande, J. G. Zabolitzky, S. C. Pieper, R. B. Wiringa, U. Helmbrecht, Phys.Rev.Lett. 50 (1983) 1676
- 13) K. Szalewicz, B. Jeziorski, H. J. Monkhorst, J. G. Zabolitzky, J.Chem.Phys. 78 (1983) 1420  
J. G. Zabolitzky, B. Jeziorski, K. Szalewicz, H. J. Monkhorst, J.Chem.Phys., to be published
- 14) L. Szybisz and J.G.Zabolitzky, Proceedings of the NATO ARW on Monte Carlo Methods in Quantum problems (1982) to be published  
L. Szybisz, J. G. Zabolitzky, to be published

## RANDOM NUMBER METHOD IN FEW BODY CALCULATION

Yoshinori AKAISHI

Department of Physics, Hokkaido University, Sapporo 060, Japan

A review is given about the quasi-random number (QRN) method and the ATMS method. QRN is a numerical method for multiple integrations and ATMS is a variational method of solving few-nucleon systems with realistic two- and three- nucleon interactions. Accuracy of ATMS is demonstrated in few-body calculations. Energy levels, momentum distributions and charge form factor of the alpha particle are presented on the basis of realistic two-nucleon and semi-realistic three-nucleon potentials. Property of  $\Lambda$ - $\alpha$  potential is discussed with an extended ATMS method.

### 1. INTRODUCTION

An advantage of studying few-nucleon problems is feasibility of solving them up for realistic nuclear interactions with singular repulsive cores and strong tensor forces. The alpha particle is a tightly bound system with strong correlations and is a stable unit of cluster in nuclei. Therefore, by solving the four-nucleon problem we could obtain rich information on correlated structure of nucleus which leads us to realistic treatments of nuclei. One of such treatments is the cluster theory with saturation discussed by Schmid<sup>1</sup> where NN correlations play an important role. Thus, four-nucleon problem is one of the most interesting and challenging subjects.

The Faddeev theory is successfully applied to three-nucleon systems, but at least in the present stage it is not a practical method for system of four nucleons interacting with complicated realistic potentials. So, we should pay attention to variational approaches. In the case of central NN potential with hard core pioneer works were done by Schmid, Tang and Herndon<sup>2</sup> with Jastrow-type correlation function and Monte Carlo integration method. Some progresses have been accumulated along the variational approach. Pandharipande et al.<sup>3</sup> developed their Variational Monte-Carlo method and applied it to realistic four nucleon systems. The present author and others<sup>4</sup> proposed the ATMS method to construct variational wave functions for realistic interactions, where ATMS is an abbreviation of Amalgamation of Two-body correlations into Multiple Scattering process. Tanaka and Nagata<sup>5</sup> introduced in ATMS calculation the Quasi-Random Number (QRN) method for multiple integration which is much more effective than the Monte Carlo one. In this paper calculations which use QRN are reviewed in connection with ATMS.

## 2. QUASI-RANDOM NUMBER METHOD

The QRN method was presented by Richtmyer and by Haselgrove<sup>6</sup> and used by Tanaka and Nagata<sup>5</sup> in few-body calculation. Let  $I$  be a multiple integral,

$$I \equiv \int_{-\infty}^{\infty} dX_1 \cdot \int_{-\infty}^{\infty} dX_d F(X_1, \dots, X_d) = \int_0^1 dx_1 \cdot \int_0^1 dx_d f(x_1, \dots, x_d). \quad (1)$$

The last is obtained by such transformation as

$$X_i = c \tan \pi(x_i - 0.5) \quad \text{or} \quad X_i = c \log(x_i / (1 - x_i)) \quad \text{etc.} \quad (2)$$

We extend  $f$  to a periodic function  $g$  as

$$g(\vec{x}) = f(\vec{x}), \quad g(-x_i) = f(x_i) \quad \text{and} \quad g(\vec{x} + 2\vec{n}) = g(\vec{x}), \quad (3)$$

where  $\vec{n} = (n_1, \dots, n_d)$  is  $d$ -dimensional vector with any integer  $n_i$ . The second derivative of  $g$  must be bounded variation. The function  $g$  can be expanded into Fourier series of the period 2 ;

$$g(\vec{x}) = \sum_{\vec{m}} a(\vec{m}) \exp(i \pi \vec{m} \vec{x}).$$

The coefficient  $a(\vec{0})$  is just the integral value  $I$ .

We make a summation with quasi-random numbers starting from a set of irrational numbers  $\vec{\alpha} = (\alpha_1, \dots, \alpha_d)$ ,

$$S_1(N) \equiv \sum_{n=-N}^N g(n \vec{\alpha}) = (2N+1) a(\vec{0}) + D_1(N). \quad (4)$$

where  $D_1(N) = \sum_{\vec{m}} a(\vec{m}) \sin(\pi(N+0.5)\vec{m} \vec{\alpha}) / \sin(0.5 \pi \vec{m} \vec{\alpha})$ .

Haselgrove showed that  $D_1$  remains to be  $O(N^0)$  and not so large for well-selected set of  $\vec{\alpha}$ . Therefore,

$$S_1(N)/(2N+1) \text{ converges to } I \text{ with error } O(N^{-1}). \quad (5)$$

When we use a double summation  $S_2(N) \equiv \sum_{n=0}^N S_1(n)$ ,

$$S_2(N)/(N+1)^2 \text{ converges to } I \text{ with error } O(N^{-2}). \quad (6)$$

It should be remembered that the error of Monte Carlo (MC) integration is  $O(N^{-1/2})$  and is statistical one, that is, the probability of getting  $I$  within one standard deviation is 68 %.

Figure 1 shows a comparison between QRN and MC given by Tanaka and Nagata<sup>5</sup>. QRN error for double sum case is smaller than MC one by about  $10^{-2}$  factor at 50,000 sampling estimate. QRN converges very rapidly compared to MC. There might arise a question why such large difference occurs, because integration procedure is similar between MC and QRN except that MC uses random numbers and QRN does quasi-random numbers. Tanaka found that QRN error damps moderately, while MC deviation fluctuates frequently between positive and negative sides and its damping is slow. This difference comes from two facts. Integrand of QRN is always symmetric (periodic), while that of MC is not. Double summation defined in QRN gentles such fluctuation appeared in MC case.

Thus, QRN is a very effective method of numerical multiple integration and

is fully used in ATMS calculations of sections 4 to 6. It is noted that usefulness of QRN depends on the choice of a irrational number set and a transformation: The parameter of Eq.(2) should be so adjusted that integrand becomes as flat as possible.

### 3. ATMS METHOD

ATMS<sup>4</sup> constructs a variational wave function in the form

$$\psi = F \phi \quad (7)$$

on the basis of multiple scattering theory<sup>7</sup>, where  $\phi$  is a simple initial wave function. The multiple scattering operator  $F$  is given by

$$F = 1 + \sum_{(ij)} (Q/e)g(ij) F_{ij}, \quad (8a)$$

$$F_{ij} = 1 + \sum_{(kl)} (Q/e)g(kl) F_{kl}. \quad (8b)$$

From Eq.(8b) we get coupled algebraic equations

$$(F_{ij}-1) = -\sum_{(kl)} \eta(kl) - \sum_{(kl)} \zeta(kl) (F_{kl}-1) \quad (9)$$

by replacing the operator  $(Q/e)g$  with two-body correlation functions  $-\eta$  and  $-\zeta$  which are obtained from on-shell and off-shell solutions of Bethe-Goldstone equation. With Eq.(8a) and solutions of Eq.(9) we have a function  $F$  which is a correlation representation of the multiple scattering operator.

ATMS wave function is improved under Ritz's variational principle and therefore, ATMS energy is a strict upper-bound. In the ATMS method the many-body dynamical and the variational treatments are unified. The former reduces substantially the number of variational parameters and the latter supplies deficiencies in many-body treatment.

A recent progress in ATMS formalism is the inclusion of D-state term in the off-shell correlation. Tanaka and Sakai<sup>8</sup> solved Eq.(9) with  $\zeta = \zeta_S + \zeta_D S_{ij}$  and got a more reasonable expression of  $F$ . The importance of D-state term was well-known in on-shell case but disregarded in off-shell case so far. The new term brings an additional binding of about 3 MeV in ATMS calculation of the alpha particle for realistic interaction with tensor force.

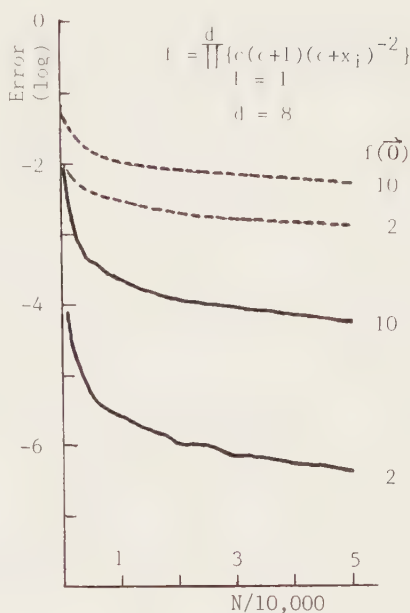


FIGURE 1

A comparison of errors of QRN(solid) and MC(dashed).

## 4. ACCURACY OF ATMS

Maeda et al.<sup>9</sup> applied ATMS to systems of three and four point- $\alpha$  particles interacting via a state-independent potential with repulsive core<sup>10</sup>.

Figure 2 shows the upper and lower bounds for three  $\alpha$  system. It is known that Temple's lower bound<sup>11</sup> comes usually far below Hall-Post's lower bound<sup>12</sup>. This is because Temple's bound ( $E_L$ ) involves  $\langle H^2 \rangle$  which is extremely sensitive to short-range correlation functions. The best of Jastrow-type wave function can make Temple's bound come above Hall-Post's one. The ATMS result is much more remarkable: The gap between upper ( $E_U$ ) and lower bounds is less than 0.2 MeV. This clearly demonstrates the high accuracy of ATMS.

The variational method is often criticized that its wave function is rather poor even when its energy is good. Schmid et al.<sup>13</sup> derived an upper bound formula to the impurity. Suppose that the variational wave function is expanded on exact eigenfunctions of  $H$ . The impurity  $B(E)$  in the wave function from mixing of eigenstates higher than a given energy  $E$  is bounded as

$$B(E) \leq B_U(E) \equiv G (E_1 - E_U) / (E - E_U)^2, \quad G \equiv E_U - E_L, \quad (10)$$

where  $G$  is the gap and  $E_1$  the first excited-state energy. The maximum total

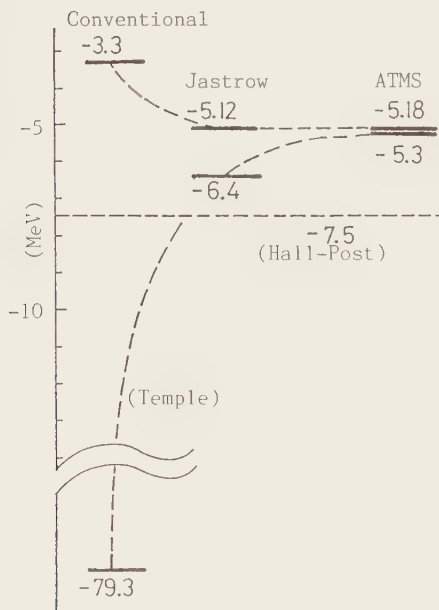


FIGURE 2  
Upper and lower bounds for three  $\alpha$  system.

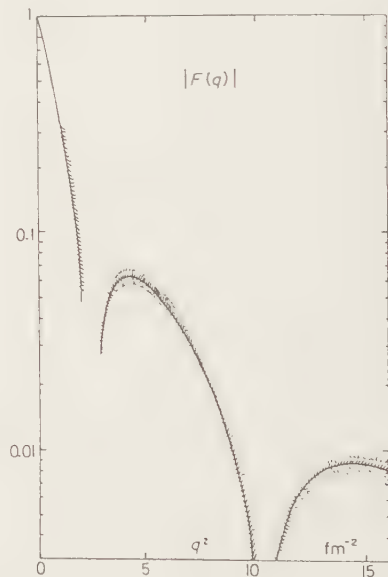


FIGURE 3  
ATMS error of form factor  
for three  $\alpha$  system.

impurity of ATMS is 3.4 % for three  $\alpha$  system. ATMS might seem to be too crude to discuss the small component of charge form factor at high momentum transfer. But by Eq.(10) the impurity decreases drastically as  $E$  increases, for example, it becomes less than 0.1 % at  $E = 17$  MeV. The error of charge form factor at high momentum transfer, which is mainly contamination of high-energy eigenstates, is restricted to be small enough in ATMS and is bounded in the shaded area of Fig.3. Temple's lower bound is a severe test of how well short-range correlations are described. The variational wave function is reliable when the gap  $G$  is small enough as in the case of ATMS.

For four nucleon system with Malfliet-Tjon's (V) potential<sup>14</sup>, we can make a comparison<sup>17</sup> of various methods, that is, the Faddeev-Yakubovsky (F-Y) theory<sup>15</sup>, the Variational Monte Carlo (VMC) method<sup>3</sup>, the Coupled Cluster Method (CCM)<sup>16</sup>, the Green Function Monte Carlo (GFMC) method<sup>17</sup> and ATMS.

TABLE Results for four-nucleon system.

Method	Energy (MeV)		rms radius (fm)	
F-Y	-28		Tjon <sup>18</sup>	
VMC	-31.19 $\pm$ 0.05		Carlson et al. <sup>19</sup>	
CCM(3)	-31.24	1.36	Zabolitzky	
CCM(4)	-31.36	1.39	Zabolitzky	
GFMC	-31.3 $\pm$ 0.2	1.36	Zabolitzky <sup>17</sup>	
ATMS	-31.36( $E_U$ )	-32.8( $E_L$ )	1.40	Maeda

GFMC value -31.3 $\pm$ 0.2 MeV is accepted as an exact energy. F-Y does not include the effect of higher-wave interaction. VMC may be the best value of Jastrow-type correlation function. CCM(3) is more reliable than CCM(4)<sup>16</sup>. ATMS gives -31.36 MeV as the upper bound and -32.8 MeV as the lower bound. It is known that the ratio  $(E_O - E_L)/(E_U - E_O)$  is very large for singular potential<sup>2</sup>, and so two bounds of ATMS may allow the estimation of the exact energy with smaller error than GFMC.

## 5. ALPHA PARTICLE

### 5.1. Energy levels and three-body force

Figure 4 shows up ATMS results<sup>20</sup> obtained with the Hamada-Johnston (H-J) potential<sup>21</sup> and also with the Fujita-Miyazawa (F-M) three-body force<sup>22</sup>.

In the case of only H-J the ground-state energy is -20.6 MeV (Exp. -29.0 MeV without Coulomb). The total potential energy is -151.7 MeV and the largest contribution (-70.2 MeV) comes from the tensor force. The total kinetic energy is 131.1 MeV and is three times as large as that (about 50 MeV) of harmonic

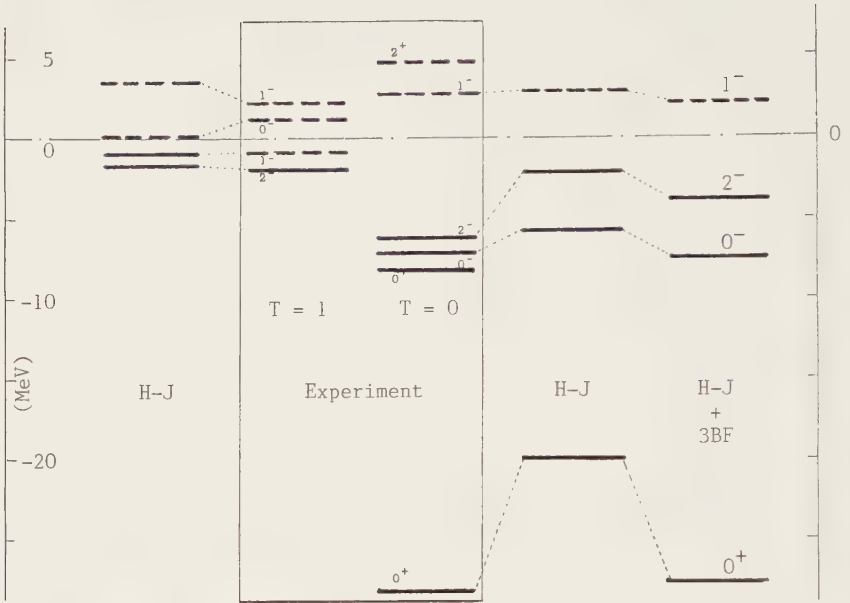


FIGURE 4 Energy levels of the alpha particle calculated with H-J and with H-J plus F-M three-body force.

oscillator model. This means that strong correlations exist.

The F-M three-body force brings about 8 MeV energy gain and reduces the rms radius from 1.65 fm to 1.47 fm (Exp. 1.44 fm). The gain 8 MeV is 30 % of the binding energy and might seem to be too large. But it is only 5 % of the potential energy -152 MeV from H-J. The three-body force contribution in the alpha particle is about 7 times as large as that in the triton<sup>23</sup>. A factor 4 comes from the ratio of numbers of nucleon trios and the contribution per trio is enhanced by the compactness of the alpha particle. In the excited states situation is very similar to that in the triton due to their 3N + N structures. Thus, the three-body force gives energy gains just required, that is, about 8 MeV for the ground state and about 1 or 2 MeV for the excited states<sup>23</sup>.

The F-M three-body force is not very realistic, but it should be stressed that the energy levels of the alpha particle can provide valuable phenomenological informations on the three-body force. The present F-M three-body force should be regarded as a semi-realistic three-body force determined from ATMS calculation of the alpha particle.

Lomnitz-Adler et al.<sup>3</sup> obtained the ground-state energy of  $-22.9 \pm 0.5$  MeV for Reid soft core (RSC) potential<sup>24</sup> by VMC. Sakai and Katayama<sup>25</sup> got -21.1 MeV



for RSC by ATMS. The ATMS result is poor compared with one by VMC and  $-24.9$  MeV by CCM<sup>16</sup>. ATMS with off-shell D-state term mentioned in section 3 should be examined. Carlson, Pandharipande and Wiringa<sup>26</sup> investigated thee- and four-nucleon systems by VMC with Urbana and Argonne potentials and three-body forces. It is noted that the Tucson three-body force<sup>27</sup> gives  $-6$  to  $-8$  MeV contribution in the alpha particle, and its  ${}^4\text{He}/{}^3\text{H}$  ratio is about 6.

## 5.2. Momentum distribution

Nucleon momentum distribution in the alpha particle is calculated for RSC by ATMS. Short-range correlation manifests itself at around  $p = 3 \text{ fm}^{-1}$  as seen in Fig. 5a. The D-state correlation is of almost same magnitude at this momentum region as stressed by Zabolitzky and Ey<sup>28</sup>. The total kinetic energy can be calculated by  $\text{K.E.} = (A-1)/2 \cdot \int dp n(p) (\hbar^2/2M)p^2$ , where the center-of-mass motion is completely removed. Enhancement of kinetic energy is about 80 % which comes half from the short-range correlation and half from the D state. If we use a relativistic kinetic energy in the above equation, total kinetic energy reduces from 90 MeV to 82 MeV. Thus, correlations in the alpha particle is so strong that relativistic treatment would be required in final stage of investigation.

Momentum distributions of two-nucleon center motion and of two-nucleon

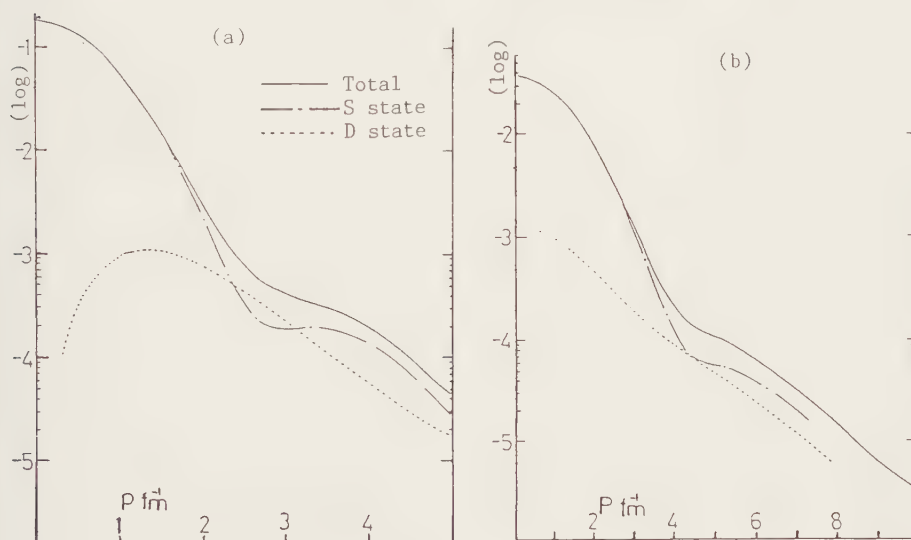


FIGURE 5

Momentum distributions of single nucleon (a) and two-nucleon center (b) in the alpha particle calculated with RSC.

relative motion are also calculated in the alpha particle. They have prominent high-momentum components coming from correlations, which may play important roles in high-energy proton-nucleus collision<sup>29</sup>.

The momentum distributions are well parametrized as

$$n(p) = N \{ \exp(-p^2/(2a)) + s \exp(-p^2/(2at)) \} \quad (11)$$

with  $(a \text{ fm}^{-2}, s, t) = (0.42, 0.01, 8)$  for nucleon,  $(0.42 \times 3, 0.01, 8)$  for NN center and  $(0.42/4, 0.015, 6)$  for NN relative momenta.

### 5.3. Charge form factor

Sick<sup>30</sup> pointed out the pronounced central depressions of the point proton densities of  $^3\text{He}$  and  $^4\text{He}$ . Any realistic NN interaction can not reproduce the depression, and the three-body force is invoked. Fable de la Rippelle<sup>31</sup> presented an interesting idea that F-M type three-body force might realize the central depression. Nogami et al<sup>32</sup>., however, found that at least 3 times stronger three-body force than F-M is required to reproduce the data.

The tensor component of three-body force, which was disregarded in the above considerations, is main origin of the energy gain in the alpha particle. Our aim is to reproduce simultaneously the binding energy and the charge form factor. Katayama et al.<sup>33</sup> performed ATMS calculation of the  $^4\text{He}$  charge form factor and investigated both effects of meson-exchange currents and the three-body force. Figure 6a is the charge density distribution obtained with H-J,

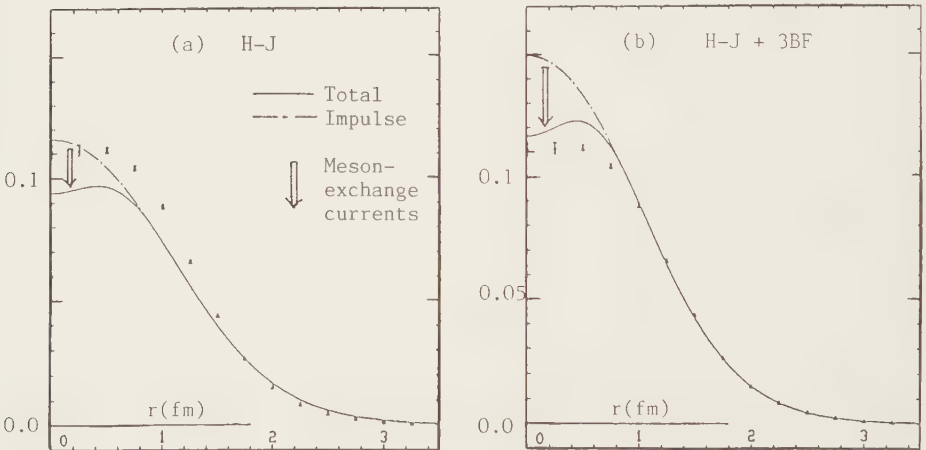


FIGURE 6  
Charge density distribution of the alpha particle  
calculated with H-J and with H-J plus F-M three-body force.

where rms radius is considerably large. Meson-exchange currents decrease charge density at central region. Figure 6b shows the effect of the F-M three-body force which reproduces the alpha particle energy and rms radius as discussed in 5.1. The proton density distribution is not depressed but raised at the central region by the three-body force. At the same time, however, the effect of meson exchange currents is enhanced by about 50 %. Thus, the three-body force can contribute to the central depression through the enhancement of meson-exchange currents. It should be remarked that at the central region of  ${}^4\text{He}$  the charge density is depressed but the proton density is not.

In the case of  ${}^3\text{He}$  Hadjimichael et al.<sup>34</sup> obtained an excellent agreement with the experiment. There we can see similar effects of meson-exchange currents and three-body force.

## 6. $\Lambda$ - $\alpha$ POTENTIAL

Kurihara et al.<sup>35</sup> extended ATMS to scattering problem by formulating a new theory in which particle-nucleus effective potential is microscopically constructed from realistic interactions. The  $\Lambda$ - $\alpha$ potential obtained from Dalitz's  $\Lambda\text{N}$  potential<sup>36</sup> shows a pronounced central repulsion<sup>37</sup> due to hard core of the  $\Lambda\text{N}$  potential and compactness of the alpha particle. Maeda and Schmid<sup>38</sup> made a careful calculation with Jastrow-type correlation function and found a central rise coming from the many-body correlation. Schmid discussed the importance of such central repulsion or rise in relation to the saturation of many-body system.

## 7. CONCLUSIONS

QRN is a very useful method of numerical integration in few-body problems. Actually, by QRN 9-, 10- and 12-dimensional integrations are carried out at each point for charge form factor, momentum distributions and  $\Lambda$ - $\alpha$  effective potential, respectively. ATMS connected with QRN is much more feasible than the Variational Monte Carlo and the Green Function Monte Carlo methods. Accuracy of ATMS is unambiguously demonstrated by small gap between upper and lower bounds to the energy. An upper bound formula to the impurity shows that ATMS wave function is also highly accurate at high momentum part.

The alpha particle is a strongly correlated system: D state and short-range correlations are important ingredients of realistic alpha particle and should be taken into account in refinement of nuclear models like cluster. Momentum distributions can provide information on short-range correlations and more detailed experimental data<sup>39</sup> at around  $p = 3$  to  $4 \text{ fm}^{-1}$  are waited for.

The three-body force plays an important role in reproducing the ground- and

excited-state energies of the alpha particle. Conversely, the energy levels are valuable data for phenomenological determination of the three-body force. The same three-body force has a favourable effect on the charge form factor.

New development would be expected on Kurihara et al.'s (KAT) scattering theory.

#### ACKNOWLEDGMENTS

The author would like to thank Prof. H. Tanaka, Prof. E.W. Schmid, Dr. S. Nakaichi-Maeda, Dr. T. Katayama and Mr. Y. Kurihara for valuable discussions and collaborations.

#### REFERENCES

- 1) E.W. Schmid, Theoretical description of few cluster systems, this volume.
- 2) E.W. Schmid, Y.C. Tang and R.C. Herndon, Nucl. Phys. 42 (1963) 95;  
65 (1965) 203.
- 3) J. Lomnitz-Adler, V.R. Pandharipande and R.A. Smith, Nucl. Phys.  
A361 (1981) 399.
- 4) Y. Akaishi, M. Sakai, J. Hiura and H. Tanaka, Prog. Theor. Phys. Suppl.  
No.56 (1974) 6.
- 5) H. Tanaka and H. Nagata, Prog. Theor. Phys. Suppl. No.56 (1974) 121.
- 6) C.B. Haselgrove, Math. Comp. 15 (1961) 323.
- 7) K.M. Watson, Phys. Rev. 89 (1953) 575.  
K.A. Brueckner and C.A. Levinson, Phys. Rev. 97 (1955) 1344.
- 8) H. Tanaka and M. Sakai, private communication.
- 9) S. Maeda, Y. Akaishi and H. Tanaka, Prog. Theor. Phys. 64 (1980) 1315.
- 10) S. Ali and A.R. Bodmer, Nucl. Phys. 80 (1966) 99.
- 11) G. Temple, Proc. Roy. Soc. A119 (1928) 276.
- 12) R.L. Hall and H.R. Post, Proc. Phys. Soc. 90 (1967) 381.
- 13) Y. Akaishi, S. Nakaichi and E.W. Schmid, Prog. Theor. Phys. 66 (1981) 211.
- 14) R.A. Malfliet and J.A. Tjon, Nucl. Phys. A127 (1969) 161.
- 15) L.D. Faddeev, Soviet Phys.-JETP 12 (1961) 1014.  
O.A. Yakubovsky, Soviet J. Nucl. Phys. 5 (1967) 937.
- 16) H. Kümmel, K.H. Lührmann and J.G. Zabolitzky, Phys. Report 36C (1978) 1.  
J.G. Zabolitzky, Phys. Lett. 100B (1981) 5.
- 17) J.G. Zabolitzky and M.H. Kalos, Nucl. Phys. A356 (1981) 114.  
J.G. Zabolitzky, K.E. Schmidt and M.H. Kalos, Phys. Rev. C25 (1982) 1111.
- 18) J.A. Tjon, Phys. Lett. 56B (1975) 217.

- 19) J. Carlson and V.R. Pandharipande, Nucl. Phys. A371 (1981) 301.
- 20) M. Sakai et al., Prog. Theor. Phys. Suppl. No.56 (1974) 32; 108.  
M. Sakai, Prog. Theor. Phys. 63 (1980) 180.
- 21) T. Hamada and I.D. Johnston, Nucl. Phys. 34 (1962) 382.
- 22) J. Fujita and H. Miyazawa, Prog. Theor. Phys. 17 (1957) 360.
- 23) M. Sato, Y.Akaishi and H.Tanaka, Prog. Theor. Phys. Suppl. No.56 (1974) 76;  
Prog. Theor. Phys. 66 (1981) 930.
- 24) R.V. Reid, Ann. of Phys. 50 (1968) 411.
- 25) M. Sakai and T. Katayama, contribution to this conference.
- 26) J. Carlson V.R. Pandharipande and R.B. Wiringa, Nucl. Phys. A401 (1983) 59.  
R.B. Wiringa, Nucl. Phys. A401 (1983) 86.
- 27) S.A. Coon and W. Glöckle, Phys. Rev. C23 (1981) 1790.
- 28) J.G. Zabolitzky and W. Ey, Phys. Lett. 76B (1978) 527.
- 29) T. Fujita and J. Hüfner, Nucl. Phys. A314 (1979) 317.  
Y. Haneishi and T. Fujita, preprint.
- 30) I. Sick, Lecture Notes in Physics (Springer-Verlag, 1978) Vol.87 p.236.
- 31) M. Fabre de la Ripelle, C. R. Acad. Sci. Ser. B288 (1979) 325.
- 32) Y. Nogami, N. Ohtsuka and L. Consoni, Phys. Rev. C23 (1981) 1759.  
T.K. Das and H.T. Coelho, Phys. Rev. C26 (1982) 697; 2288.
- 33) T. Katayama, Y. Akaishi and H. Tanaka, Prog. Theor. Phys. 67 (1982) 236.
- 34) E. Hadjimichael, R. Bornais and B. Goulard, Phys. Rev. Lett. 48 (1982) 583;  
Phys. Rev. C27 (1983) 831.
- 35) Y. Kurihara, Y. Akaishi and H. Tanaka, Prog. Theor. Phys. 67 (1982) 1483.
- 36) R.H. Dalitz, R.C. Herndon and Y.C. Tang, Nucl. Phys. B47 (1972) 109.
- 37) Y. Kurihara, Y. Akaishi and H. Tanaka, contribution to this conference.
- 38) S. Maeda and E.W. Schmid, contribution to this conference.
- 39) V.A. Goldstein and Eh.L. Kuplennikov, R.I. Jibuti and R.Ya. Kezerashvili,  
Nucl. Phys. A355 (1981) 333.  
S. Rock et al., Phys. Rev. C26 (1982) 1592.



## RECENT RESULTS OF CALCULATIONS IN THE FOUR-NUCLEON SYSTEM

A.C. FONSECA

Centro de Física Nuclear da Universidade de Lisboa, Av.Gama Pinto 2, 1699  
Lisboa, Portugal

A review on the most recent calculations of the four nucleon system is presented. A summary of the developments involving the methods used to solve the four-particle Schrodinger equation is provided that covers the Integral Equation Approach of Yakubovsky and Alt, Grassberger and Sandhas, Variational, Coupled-Cluster, Green's Function Monte Carlo, Hyperspherical, ATMS and Resonating Group methods. Whenever possible results obtained with different methods are compared. Relativistic effects and three-body force effects are discussed.

### 1. INTRODUCTION

In the past the four-nucleon problem has been the source of a great number of theoretical work. The aim has been to understand the boundstate and scattering properties of the system in terms of the forces between the constituent particles. Here we review the progress that has been achieved on this subject since the last Few-Body Conference in Eugene<sup>1</sup>; for other reviews on results and calculation methods see refs. 2-6. Since the solution of formally exact four-body equations only became possible in the last decade, and the need to understand the experimental data goes well beyond in time, different methods have been developed to solve the four-particle Schrodinger equation such as variational, coupled cluster, resonating group, hyperspherical and Monte Carlo methods. Therefore we will address each of these methods separately and report the latest advances concerning bound state and scattering calculations. Whenever possible results obtained with different methods are compared.

### 2. INTEGRAL EQUATION APPROACH

Although there are many formulations of the four-body problem that fall in this category, only the work of Yakubovsky<sup>7</sup> and Alt, Grassberger and Sandhas<sup>8</sup> (AGS) has lead to practical calculations of the four-nucleon system. The corresponding equations, once expressed in the appropriate momentum variables, are a set of



two coupled three vector variable integral equations whose kernel involves all lower particle subsystem amplitudes\*. From the computational point of view the advantage of Yakubovsky or AGS equations over other four-body formulations is that each time one represents the subsystem amplitudes in a separable form one reduces the dimensionality of the equation. Therefore, using the experience gained in the solution of the three-body problem, the standard procedure has been to express the two-body t-matrix as a finite sum of separable terms leading to two-vector variable four-body integral equations. Although these equations have been solved in the past<sup>9</sup> they involve considerable numerical effort which may be saved if the underlying 3+1 and 2+2 subamplitudes are accurately represented as operators of rank  $N$  ( $N$  small). The resulting four-body equations after partial wave decomposition are a set of coupled one continuous variable integral equations that are readily solved numerically. Beyond the model calculation of Kharchenko and Levashev<sup>10</sup> where the sensitivity of threshold scattering results to the parameters of the NN interaction is studied, all recent work on the integral equation approach has used the four-nucleon problem as a "theoretical laboratory" to develop and test several approximation methods used in the solution of the equations. Since a realistic four-nucleon calculation requires the correct description of many subamplitudes in many partial waves, as predicted by Tjon<sup>2</sup>, progress has been slow and not a single realistic calculation has been reported since the Eugene conference. Therefore we review some of the effort and the difficulties encountered in this field.

Although the two stage separable expansion approach described above has been widely used in the past<sup>2</sup>, considerable improvement on the speed of the calculation is gained when the Generalized Unitary Pole Expansion (GUPE)<sup>11</sup> or the Energy Dependent Pole Expansion (EDPE)<sup>12</sup> are used to represent the 3+1 and 2+2 subamplitudes compared to the Hilbert-Schmid Expansion<sup>13</sup> (HSE). The accuracy of the GUPE method is tested in a recent work by Sofianos et.al.<sup>14</sup> where the  $\alpha$ -particle binding energy is calculated for a variety of local and separable nucleon-nucleon potentials. The results are compared with similar calculations

---

\* They are the two-body and the 3+1 and 2+2 subamplitudes

using the EDPE or the HSE. They find that both GUPE and EDPE require similar computing times for a converged calculation and are about 15-20 times faster than HSE. They also find that GUPE is faster than EDPE for the same  $N$ . Typically  $N=3$  terms per subamplitude are required for a converged calculation. The EDPE method has also been shown to be very accurate in a bound state calculation<sup>15</sup> with central plus tensor forces between pairs. They find that  $N=2$  terms per subamplitude yield a four-nucleon binding energy that agrees within better than 1.5% with the results of Gibson and Lehman<sup>9</sup> where the corresponding two-variable integral equation is solved numerically.

Since it takes in general more terms to represent the 2+2 subamplitudes than the 3+1, Haberzettl and Sandhas<sup>16</sup> were able to formulate AGS equations in a way that the contribution of the 2+2 subsystem is calculated exactly through the convolution method. In this approach all four-body amplitudes can be calculated from the solution of single integral equation for the reaction  $(3)+1 \rightarrow (3)+1$  where  $(3)$  is a bound state of three particles. They also went on to show that for single term separable approximation for two and 3+1 subamplitudes the resulting equations are similar to those obtained by Fonseca and Shanley<sup>17</sup> from an extended nonrelativistic field-theoretical Lee model. Recently<sup>18</sup> the feasibility of such treatment has been shown in a four-boson binding energy calculation with one term in the expansion of the 3+1 subamplitude and also in a contribution to this conference<sup>19</sup>.

Although GUPE and EDPE methods work extremely well in the negative energy region it has been shown that above breakup threshold both methods fail to reproduce the three-body  $t$ -matrix (3+1 subamplitude in the four-body sector) even for large  $N$  ( $N > 6$ )<sup>20-21</sup>. Therefore a new breed of separable expansion methods were developed (SE1 and SE2 in ref. 20) which have a stronger energy dependence built in the effective three-body form factors. It is found that for  $N=6$  the SE2 method reproduces over the whole energy domain the three-body amplitude of Aaron, Amado and Yam's<sup>22</sup> three-boson model. Although below breakup threshold two-body unitarity is satisfied for any  $N$ , above breakup threshold only the converged result satisfies two- and three-body unitarity. From past experience it is expected that less number of terms may be needed to reproduce more realistic three-body amplitudes; nevertheless it is not clear at this stage how many terms may be required to get a converged four-body result in this energy region.

In spite of the progress achieved in the search for accurate approximation methods that may lead to the solution of four-body integral equations with less numerical effort, one is still in this domain far from being able to undertake realistic four-nucleon bound state calculations as those that are now possible with other methods. The advantage of the integral equation approach lies in scattering region where with present day computers one may be able to perform calculations involving central + tensor forces between pairs together with exact treatment of the 2+2 subsystem contributions through the convolution method in addition to s - and p - wave 3+1 subamplitudes as suggested in refs. 19 and 23. Nevertheless the problems one experiences in the expansion of three-body operators in a separable form may be the source of future difficulties concerning the accuracy of calculations at energies well above breakup threshold. The other alternative involves the solution of a two variable integral equation which in the scattering region may require powerfull real axis integration procedures to overcome the presence of running singularities along the axis of integration.

3. GREEN'S FUNCTION MONTE CARLO METHOD

In the Green's function Monte Carlo (GFMC) method the four-particle Schrodinger equation is solved exactly subject only to statistical sampling errors which may be made arbitrarily small. Although at present the method can only be used to calculate the space symmetric part of the  $\alpha$ -particle wave function emerging from the solution of the Schrodinger equation with local central potentials between pairs, the results are useful since they can be used as benchmarks for other few-body methods. In addition to the extreme accuracy of the calculation this method has the advantage that a three-body force can be easily incorporated. In the work of ref. 24 the calculation of the binding energy of four nucleons interacting via the Malfliet-Tjon potential  $V$  is reported. They obtain  $-31.3 \pm 0.2 \text{ MeV}$

TABLE I Results for the four-body system, two-body forces only.

Method	Energy/MeV	Source
GFMC	$-31.3 \pm 0.2$	Ref. 24
Variational	$-31.19 \pm 0.05$	Ref. 25
Faddeev-Yakubovsky	-28	Ref. 26
Coupled-cluster	-31.24	Ref. 27
ATMS	-31.3	Ref. 28

for  $E_\alpha$  and an rms point mass radius of  $1.36 \pm 0.01 \text{ fm}$ . The calculated point mass distribution is given and does not exhibit a central depression. In Table I the binding energy is compared with the results of other calculations. This

clearly indicates that insufficient number of two-body partial wave amplitudes are taken in the solution of Yakubovsky equations.

In a subsequent calculation<sup>29</sup> a three-body force is included that is independent of spin and isospin. The chosen interaction is model I given in ref. 25 and is about 10 times as strong as one would obtain from some models of two-pion exchange three-body forces. The four-nucleon binding energy becomes  $-37.09 \pm 0.06$  MeV which indicates that the three-body force accounts for 5.8 MeV more binding. The resulting point mass distribution is shown in Fig. 1 and exhibits a central depression as is expected from calculations involving the experimental charge form factor. The Figure also shows a comparison with the results of the corresponding variational calculation of ref. 25 where the calculated binding energy with the three-body force is  $-36.2 \pm 0.25$  MeV.

Although the GFMC cannot deal at this time with realistic four-nucleon calculations it leads to very accurate boundstate results that make possible to assess the numerical approximations involved in Yakubovsky and other numerical methods like truncation of partial-wave expansions, separable expansion of integral kernels, mesh sizes, etc.

#### 4. COUPLED-CLUSTER METHOD

The accuracy of the coupled-cluster method for the groundstate of the  $\alpha$ -particle is tested<sup>27</sup> and the results compared with the GFMC calculation of ref 24. The coupled cluster method decomposes the Schrodinger equation into a coupled set of "subsystem amplitudes" describing the motion of one-,two-,three,...,particle subsystems embedded in the many-body system under study. Upon truncation at the N-body level,  $N < A$  (A is the total number of particles in the system) a

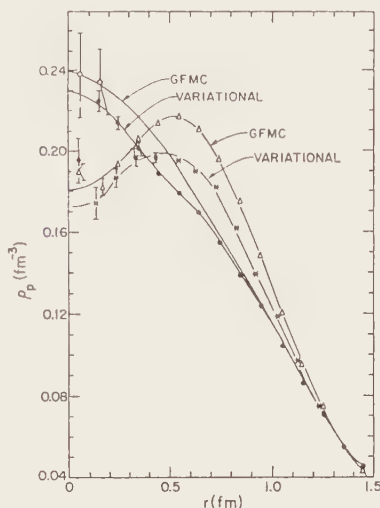


FIG. 1. Point proton density for the four-body system. O—two-body forces only, GFMC result of Ref. 24; ●—same, variational result of Ref. 25; Δ—two- and three-body forces, Ref. 29; ▲—same, variational result of Ref. 25

closed set of one-body, two-body,..., N-body equations is obtained which may be solved numerically. At the N=2-body truncation level an exact solution of the coupled one - and two-body equations is possible. At the N=3 - body truncation level some small inhomogeneous terms of the three-body equation are neglected and the coupled set of one -, two-and three-body equations is solved involving only a few controlled numerical approximations. On the N=4 - body truncation level actual solution of a four-body equation is not possible any more and the approximations involved in the solution of the coupled equations may lead to less accurate results than those obtained at the N=3 - body truncation level. Using Malfliet-Tjon potential V and the N=3 truncation level Zabolitzky gets -31.24 MeV for the  $\alpha$ -particle binding energy and 1.36 fm for the mass radius which compares favorably with the GFMC results shown in Table I. Binding energy and rms calculations are also reported for other two-body potentials. Again at the N=3 truncation level one gets -33.4 MeV and 1.55 fm for the Malfliet-Tjon I/II potential and -24.4 MeV and 1.60 fm for the Reid potential. Since the accuracy of the calculation does not depend critically on the potential, one may expect the results to be accurate to the 0.4 MeV/0.05 fm level for the N=3 truncation. No Coulomb repulsion is included in the above calculation.

Again comparing with the work of ref.23 where the Yakubovsky equations are solved with the Reid potential one finds that Tjon's calculation yields -19.5 MeV for the binding energy which is underbound relative to the coupled-cluster result. This is in part due to the discard of other than s-partial waves in the two-body t-matrix but also to the neglect of higher terms in the expansion of the underlying subamplitudes.

## 5. VARIATIONAL MONTE CARLO METHOD

Like any of the methods described in sections 3 and 4 the variational Monte Carlo method that was developed for nucleon-matter calculations is easy to use with Hamiltonians containing two-and three-body forces. Therefore we review the results of two recent publications<sup>25,30</sup> where four-nucleon bound state calculations with realistic two-body interactions are presented and the effect of adding a three-body force is studied. In the work of ref. 25 the three-body

forces used may be regarded as pedagogical models and the aim there is to develop some intuition for the effect that a "reasonable" three-body force has on the binding energy, rms radius and point mass density of the  $\alpha$ -particle. The parameters of the three-body force are adjusted to obtain the triton binding energy with either the Reid  $v_8$  or the Urbana  $v_{14}$  two-nucleon interactions. It is found that these models tend to overbind the  ${}^4\text{He}$  nucleus and that the resulting point mass density though improved in the right direction still does not have a deep enough dip. Depending on the details of the potentials used the contribution of the three-body force to the four-nucleon binding energy ranges from 6 to 12 MeV extra binding. Although a more realistic calculation is undertaken in ref.20 where two-pion exchange three-body forces are considered together with the Urbana  $v_{14}$  two-nucleon potential, the conclusions remain similar to those of ref.25. Models fitted to the  ${}^3\text{He}$  binding energy produce overbinding of the  ${}^4\text{He}$  nucleus by  $\sim 3$  MeV, while models fitted to  ${}^4\text{He}$  binding energy underbind the three-body nuclei by  $\sim 0.5$  MeV. The Tucson three-body force<sup>31</sup> is reported to give 7.2 MeV extra binding leading to  $E_\alpha = -29.3$  MeV which is already one MeV beyond the experimental results. The charge radii are well explained with the three-body force but the point mass distributions and electromagnetic form factors still show large discrepancies as shown in Fig. 2.

## 6. ATMS METHOD

The essential feature of ATMS (Amalgamation of the Two-nucleon correlations into the Multiple scattering process) is that the strong correlations between the particles under the realistic interactions are taken into account in their independent pair motion, and are included in a trial wave function through the process of multiple scattering. Thus the characteristics of the interaction are included in terms of two-body correlation functions. For details on realistic calculations see ref. 6 and 32. Recent work on this field involves some tests on the accuracy of the charge form factors obtained from ATMS calculations<sup>33</sup> as well as a comparison<sup>34</sup> with results obtained from the solution of Yakubovsky integral equations using the two stage separable expansion approach described in Section 2. The work involves the calculation of the binding energy for a



system of four  $\alpha$ -particles interacting with the Ali-Bodmer potential. While the ATMS method gives an upper bound of -11.1 MeV and a Temple lower bound of -11.9 MeV, the Yakubovsky approach with two terms in the HSE of the s-wave parts of the 3+1 and 2+2 subamplitudes and two terms (one attractive and one repulsive) in the UPE expansion of the underlying two-body amplitudes yields -8.3 MeV. The difference represents the effect of including higher partial wave components of the subsystem transition amplitudes which in the integral equation approach involves a great numerical effort.

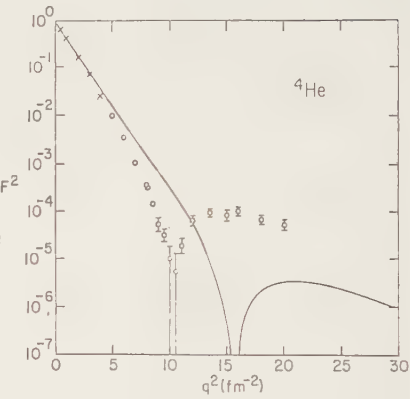


Fig. 2

Charge form factor with two - and three-body forces.

Computing times are also compared indicating that ATMS bound state calculations are not only more accurate but also ten times faster. Three-body force (3BF) and meson exchange current (MEC) contributions to the  $^4\text{He}$  charge form factor are also studied in the frame work of the ATMS approach<sup>35</sup>, where the four-nucleon wave function is obtained from the solution of the nuclear Hamiltonian including the 3BF of ref. 36 and Hamada-Johnston two-nucleon potential. The results are shown in Table II for the binding energy, rms radius and other important features of the charge form factor. In Fig. 3 and 4 the effects are graphically shown for the charge form factor and point mass density. They find that the introduction of the 3BF is crucial to enlarge the meson exchange current contribution. This may be attributed to the changes that the 3BF introduces in the nuclear density near the center where contributions from MEC become important.

Table II. Properties of the  $^4\text{He}$  wave functions and the  $^4\text{He}$  charge form factors with and without effects of the meson exchange currents and the three-body force.

	$P(D)$ [%]	Energy [MeV]	$\sqrt{r_{\text{max}}^2}$ [fm]	$\sqrt{r_{\text{ch}}^2}$ [fm]	$q_{\text{min}}^2$ [fm <sup>-2</sup> ]	$q_{\text{max}}^2$ [fm <sup>-2</sup> ]	$F_{\text{ch}}^{\text{max}}$ [ $\times 10^{-3}$ ]	$F_{\text{ch}}^{\text{max (b)}}$ [ $\times 10^{-3}$ ]
H-J only	12.74	-20.6	1.66	1.83	13.1	17.0	0.985	
+MEC				1.84	10.4	15.0	4.05	4.82
+3BF	16.12	-28.5	1.46	1.65	14.2	18.5	1.64	
+3BF+MEC				1.67	11.4	16.8	5.68	6.88
Experiment		-29.1	1.42	1.67	10.	14~16	8.9 $\pm$ 1.1	



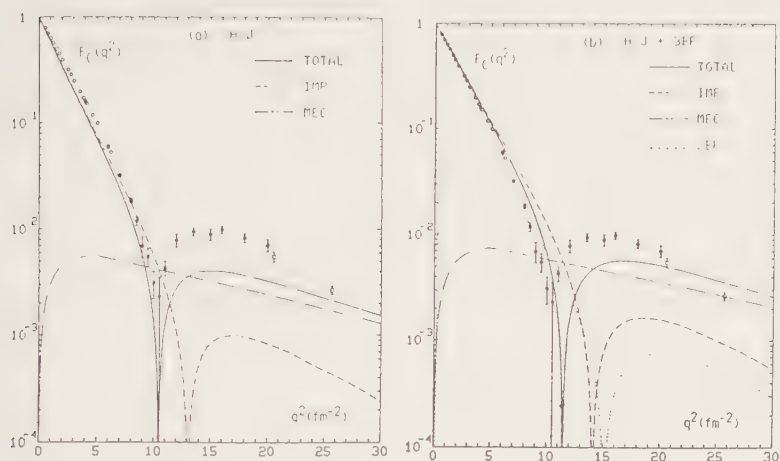


Fig. 3. Effects of meson exchange currents on the  ${}^4\text{He}$  charge form factor  $F_c(q^2)$  for (a) the H-J potential, and (b) the H-J plus the 3BF potential. In (b) the 3BF effect on the impulse term is also shown by the dotted line.

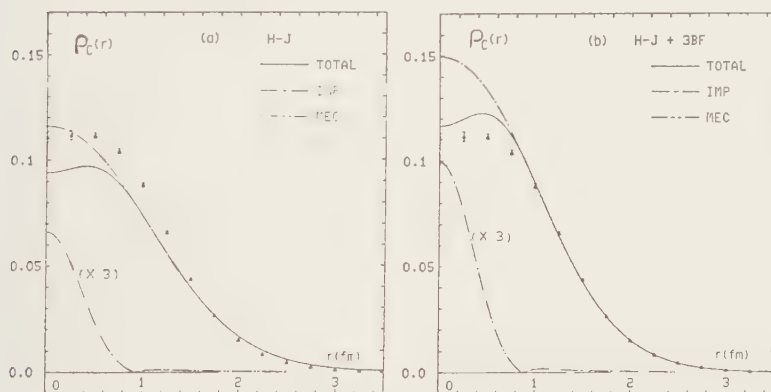


Fig. 4. Effects of meson exchange currents on the  ${}^4\text{He}$  charge density  $\rho_c(r)$  for (a) the H-J potential, and (b) the H-J plus the 3BF potential. The two-dot dashed line shows the meson exchange current contributions multiplied with the factor 3.

## 7. HYPERSPHERICAL METHOD

In the hyperspherical method the four-nucleon wave function denoted by  $\psi(\xi, \Omega)$  depends on the hyperradius  $\xi$  and on a set of 8 angles. The solution of the four-body Shrodinger equation involves an expansion of  $\psi$  in Hyperspherical Harmonics leading to an infinite set of coupled differential equations in the variable  $\xi$ <sup>37-38</sup>. To the exception of the work in ref. 39 where the numerical methods and the accuracy for the calculation are tested with central potentials

that are superpositions of Gaussians or Yukawa terms, all other work<sup>40-42</sup> involves realistic NN interactions. Particular concern is taken to check the convergence of the calculation<sup>40</sup> by comparing with the corresponding variational or coupled-cluster results. As in most other calculations they find that realistic local two-body potentials between pairs underbind  ${}^4\text{He}$  by as much as 8 MeV and that changes in the off shell nucleon-nucleon interaction cannot be responsible for such disagreement<sup>41</sup>. Using the potentials of Biedenharn et.al.<sup>43</sup> the effect of the tensor force on the  ${}^4\text{He}$  binding energy and rms radius is studied keeping the singlet interaction fixed and changing the percentage of the deuteron D-state  $P_D({}^2\text{H})$ . It is found that the percentage of D-state in  ${}^4\text{He}$  grows linearly with  $P_D({}^2\text{H})$  while the percentage of the S' state  $P_{S'}({}^4\text{He})$  decreases as  $P_D({}^2\text{H})$  grows.

## 8. MULTICHANNEL CALCULATIONS

The low energy spectrum of  ${}^4\text{He}$  is analysed in the frame work of a multichannel resonating group calculation<sup>44</sup> with Eikemeier-Hackenbroich potential. The well established resonance states are confirmed and at low energies a broad  $J^\pi = 1^-$ ,  $T = 0$  resonance is proposed. The level sequence  $J^\pi = 0^-, 2^-, 1^-$  for the lower lying ( $T = 0$ ) states and  $J^\pi = 2^-, 1^-$  (triplet),  $1^-$  (singlet),  $0^-$  for the higher lying ( $T = 1$ ) states agree with experiment except for the  $1^-$  (singlet) and  $0^-$  ordering. The differences observed in the mirror reactions  ${}^2\text{H}(\text{d}, \vec{p}){}^3\text{H}$  and  ${}^2\text{H}(\text{d}, \vec{n}){}^3\text{He}$  are explained in terms of the Coulomb potential alone. Since this work cannot at this stage be reproduced in a more exact approach it is hard to know if the agreement with experiment and the resulting conclusions depend on the potential used or on the method through which the results are obtained. Nevertheless concerning the charge symmetric fourbody reactions mentioned above Zankel<sup>45</sup> has shown independently that a good deal of the observed differences can be explained by Coulomb interference effects. Cluster calculations using the generator coordinator method<sup>46</sup> and an effective Gaussian nucleon-nucleon potential reproduce extremely well the available low energy scattering data, but again this may depend on the potential used.

Finally using the (N/D) approach<sup>47</sup> the correlation among s-wave low-energy four-nucleon observables is studied. It is found that the Triton binding energy, its asymptotic normalization parameter, the deuteron exchange left hand cut and the nucleon-triton (N,t) scattering length control the low energy N-t system. Relativistic corrections to the  $\alpha$ -particle binding energy are shown to be small although the corrections to the kinetic energy and potential exceed 5 MeV. This

is because of considerable cancelation between the various contributions. For the Afnan and Tang potential  $E_{\alpha} = -33.3$  MeV and  $\delta E_{\alpha} = +0.6$  MeV.

## 9. CONCLUSIONS

Recent work indicates that at the present time one can have access to four-nucleon wave functions and binding energies that are accurate within one or two tenths of an MeV. For realistic interactions the most accurate methods are the ATMS and the Coupled Cluster although for central potentials the GFMC takes the lead. Due to the number of subamplitudes and partial waves involved in a realistic four-nucleon calculation, the integral equation approach is still far from providing accurate bound state results compared to those obtained by other methods. Nevertheless in the scattering region, in spite of the excellent fits to the data that one and multichannel cluster methods show, the integral equation approach is still the one we have to hope for in order to have access to an exact scattering solution for a given two-body potential. The two-stage separable expansion method may still be effective in that region if the four-body observables are shown to converge there, particularly above breakup threshold.

Independently of the method used to solve the equations one finds that realistic two-body potentials underbind the  ${}^4\text{He}$  nuclei, give too large a r.m.s. radius and lead to charge form factors and point mass density distributions that do not fit the data even after MEC are added. In spite of the uncertainties concerning the calculation of the 3BF and its compatibility with the chosen 2BF it is now accepted that the 3BF affects the  $\alpha$ -particle binding energy by 6-12 MeV depending on the two- and three-body potentials used. The net result is a slight overbinding of  ${}^4\text{He}$  but a correct r.m.s. radius. The charge form-factor and point mass density move in the right direction but one still has room for MEC corrections or quark effects. Nevertheless one should be extremely careful in avoiding overcounting whenever adding MEC or quark effects together with a 3BF. Finally in order to compare results obtained with different methods and understand the approximations involved in four-nucleon calculations of any kind it is advisable that a realistic benchmark calculation with 2BF and 3BF may be decided upon.

## REFERENCES

- 1) The Few-Body Problem, Proceedings of the Ninth International Conference on the Few-Body Problem, Eugene, 1980, edited by F.S. Levin (North-Holland, Amsterdam 1981)..

- 2) J.A. Tjon in Proceedings of the Eighth International Conference on Few-Body Systems and Nuclear Forces II, Graz 1978, edited by H. Zingl, M. Haftel and H. Zankel (Springer, Berlin, 1978); in Proceedings of the Ninth International Conference on the Few-Body Problem, Eugene 1980, edited by F.S. Levin [Nuc]. Phys. A353, (1981) | (North-Holland, Amsterdam 1981).
- 3) A.C. Fonseca in Proceedings of the European Symposium on Few-Body Problems in Nuclear and Particle Physics, Sesimbra, 1980, (Centro de Física Nuclear da Universidade de Lisboa publication, 1980).
- 4) I.M. Narodetsky Riv. Nuovo Cimento 4,1(1981).
- 5) H. Kümmel, K.H. Lührmann and J.G. Zabolitzky, Phys. Rep. C36, 1(1978).
- 6) See also the articles on Prog. Theor. Phys. Suppl. 56 (1974).
- 7) O.A. Yakubovsky, Yad. Fiz. 5, 1312(1967) [Sov. J. Nucl. Phys. 5, 937(1967)].
- 8) P. Grassberger and W. Sandhas Nucl. Phys. B2, 181(1967); E.O. Alt, P. Grassberger and W. Sandhas, J.I.N.R. Report No. E4-6688, (1972).
- 9) B.F. Gibson and D.R. Lehman, Phys. Rev. C14, 685(1976); Phys. Rev. C18, 1042 (1978).
- 10) V.F. Kharchenko and V.P. Levashev, Nucl. Phys. A343, 249(1980).
- 11) A. Casei, H. Haberzettl and W. Sandhas, Phys. Rev. C25, 1728(1982).
- 12) S. Sofianos, N.J. McGurk and H. Fiedeldey, Nucl. Phys. A318, 295(1979).
- 13) S. Weinberg, Phys. Rev. B133, 232(1964).
- 14) S.A. Sofianos, H. Fiedeldey, H. Haberzettl and W. Sandhas Phys. Rev. C26, 228(1982)
- 15) S.A. Sofianos, H. Fiedeldey and H. Haberzettl, Phys. Rev. C22, 1772(1980).
- 16) H. Haberzettl and W. Sandhas, Phys. Rev. C24, 359(1981).
- 17) A.C. Fonseca and P.E. Shanley, Phys. Rev. C14, 1343(1976).
- 18) H. Haberzettl and S.A. Sofianos, Phys. Rev. C27, 2411(1983).
- 19) A.C. Fonseca in Proceedings of the Tenth International Conference on Few-Body Problem, Karlsruhe 1983; "Four-Body calculation of the four-nucleon system; bound state and scattering results" CFNUL preprint (submitted to Phys. Rev.C)
- 20) A.C. Fonseca. H. Haberzettl and E. Cravo, Phys. Rev. C27, 939(1983).
- 21) D. Eyre Technical Report, National Research Institute for Mathematical Sciences, P.O.Box 395, Pretoria South Africa.
- 22) R. Aaron, R.D. Amado and Y.Y. Yam, Phys. Rev. 136, B650(1964).
- 23) J.A. Tjon, Phys. Rev. Lett. 40, 1239(1978).
- 24) J.G. Zabolitzky and M.H. Kalos, Nucl. Phys. A356, 114(1981).
- 25) J. Carlson and V.R. Pandharipande, Nucl. Phys. A371, 301(1981).

- 26) J.A. Tjon, Phys. Lett. 56B, 217(1975).
- 27) J.G. Zabolizky, Phys. Lett. 100B, 5(1981).
- 28) S. Nakaichi, Y. Akaishi and H. Tanaka, Prog. Theor. Phys. 64,1315(1980).
- 29) J.G. Zabolizky, K.E. Schmidt and M.H. Kalos, Phys. Rev. C25,111(1982).
- 30) J. Carlson, V.R. Pandharipande and R.B. Wiringa Nucl. Phys. A401,59(1983).
- 31) S.A. Coon and W. Glockle, Phys. Rev. C23, 1790(1981) and references therein
- 32) M. Sakai, Prog. Theor. Phys., 63, 180(1980).
- 33) Y. Akaishi, S. Nakaichi and E. Sohmid, Prog. Theor. Phys. 66, 211(1981).
- 34) S. Nakaichi-Maeda, Y. Akaishi and H. Tanaka, Prog. Theor. Phys. 64,1315(1980).
- 35) T. Katayama, Y. Akaishi and H. Tanana, Prog. Theor. Phys. 67, 236(1982).
- 36) J. Fujita and H. Miyazawa, Prog. Theor. Phys. 17,360(1957).
- 37) J.L. Ballot and M. Fabre de la Ripelle, Ann. Phys. (N.Y.) 127, 62(1980).
- 38) V.D. Ėfros. Yad Fiz. 27, 845(1978). [Sov. J. Nucl. Phys. 27,448(1978)].
- 39) J.L. Ballot, Z. Phys. A302, 347(1981).
- 40) B.A. Fomin and V.D. Ėfros, Yad. Fiz. 31, 1441 (1980) [Sov. J. Nucl. Phys. 31,748(1980)]; Phys. Lett. 98B, 389(1981); Yad Fiz. 34, 587(1981) [Sov. J. Nucl. Phys., 34,327(1981)].
- 41) B.A. Fomin, Yad. Fiz. 33,1155(1981) [Sov. J. Nucl. Phys. 33,612(1981)].
- 42) B.A. Fomin and V.D. Ėfros, Yad. Fiz. 34,868(1981) [Sov. J. Nucl. Phys. 34, 485(1981)].
- 43) L.C. Biedenharn, J.M. Blatt, and M.H. Kalos, Nucl. Phys. 6, 359(1958).
- 44) H.M. Hofmann, W. Zahn and H. Stöwe, Nucl. Phys. A357, 139 (1981)
- 45) H. Zankel in Proceeding of the Fifth International Symposium on Polarization Phenomena in Nuclear Physics, AIP Conf. Proc. 69, 1413 (1980)
- 46) H. Furutani, Prog. Theor. Phys. 65, 586 (1981)
- 47) S. Adhikari, Phys. Rev. C24, 16 (1981)
- 48) A.I. Veselov and L. A. Kondratyuk, Yad. FIZ. 36, 342 (1982) (Sov. J. Nucl. Phys. 36, 2 (1982))



## THREE NUCLEON FORCES

Bruce H.J. McKELLAR

School of Physics, University of Melbourne, Parkville, Victoria 3052,  
Australia

and

Walter GLÖCKLE

Institut für Theoretische Physik II, Ruhr-Universität,  
D-4630 Bochum 1, W-Germany

This report is derived from both the invited review paper on Three Nucleon Potentials given by BHJMcK at Few Body-X, and from the discussions at the international workshop on Three Nucleon Forces organised by WG and held at Ruhr-Universität Bochum, on 18th and 19th August 1983. It attempts at the same time to provide a record of the content of the review paper and to summarise results presented at the workshop.

### 1. INTRODUCTION

The concept of the three nucleon potential was advanced very soon after Yukawa's proposal that mesons mediated the two nucleon force<sup>1</sup>. The construction of the  $\Delta$  mediated  $\pi\pi\pi$  exchange 3 nucleon potential by Fujita and Miyazawa<sup>2</sup>, and the realisation by Brown, Green and Gerace<sup>3</sup> that current algebra constraints could play an important role in determining the meson exchange three nucleon potentials ushered in the present era of meson-theoretic 3NP.

For more than a decade this work on the construction of increasingly sophisticated meson theoretic 3NP was not matched by a corresponding sophistication of calculations of the effects of the 3NP in many body systems. Now that has changed, and much of the international workshop on three nucleon forces was devoted to reports of "state of the art" calculations of the effects of 3NP in few nucleon systems and in nuclear matter.

In part this interest in the effects of 3NP in nuclear systems has been generated by the growing realisation that nuclear physics with two nucleon potentials fails — we cannot reproduce the binding energy and radius of  $^3\text{H}$ , nor the binding energy and equilibrium density of nuclear matter, nor any equilibrium properties of nuclei in between these extremes with just two body forces. And we now have enough confidence in our numerical methods, and in the two nucleon potential input, to suggest that what is missing is physics rather than adequate technical skill.



It seems that the  $\pi\pi$ E-3NP, which has received the most theoretical attention so far, is not capable of repairing all of these deficiencies<sup>4</sup>. This has already generated work on the meson theoretic construction of shorter range potentials and on the construction of empirical 3NP with the desired properties. Undoubtedly the next Few Body conference will hear of many more such developments.

In this report we first of all review the meson theoretic construction of three nucleon potentials, then discuss applications in the three nucleon problem. Then we review applications to other many nucleon systems and describe attempts to develop empirical 3NP. Finally we discuss a number of alternative approaches to three nucleon potentials and draw some conclusions.

## 2. MESON THEORETIC THREE NUCLEON POTENTIALS

### 2.1 The Two pion Exchange Three Nucleon Potential ( $\pi\pi$ E-3NP)

The  $\pi\pi$ E-3NP, illustrated in figure 1, has been the subject of most meson theoretic studies of the potential, from the work of Fujita and Miyazawa to work contributed to this conference<sup>5</sup>. The key ingredient required to construct

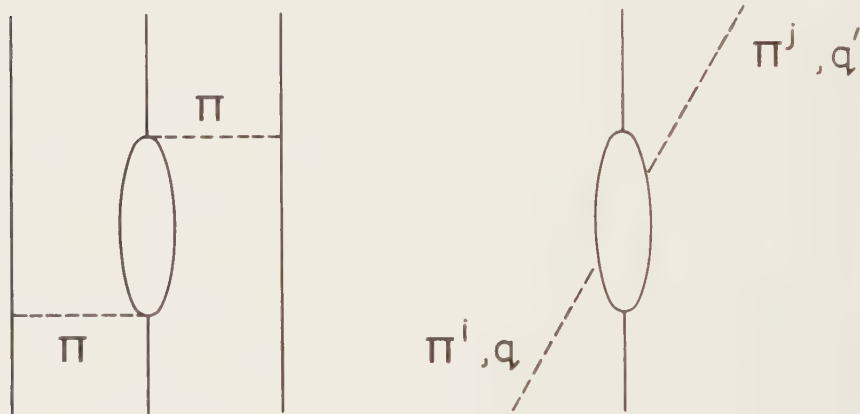


Fig.1(a) The  $\pi\pi$ E-3NP

(b) The underlying  $\pi$ N Scattering amplitude

the  $\pi\pi$ E-3NP is the  $\pi$ N scattering amplitude of figure 1(b) which is required for off mass shell pions. Two basic approaches which differ significantly in philosophy have been used to obtain information about this amplitude.

The first is the *model independent* philosophy which seeks to obtain the

maximum information about the off shell amplitude from general results which hold independently of any dynamical model of the amplitude. For the  $\pi\pi\text{E-3NP}$  this approach has been exploited most extensively by the Tucson-Melbourne group<sup>6</sup>, and the resulting potential has been extensively used in calculations.

The alternative approach in the *model making* approach which seeks to construct a dynamical model for the  $\pi\text{N}$  scattering amplitude of figure 1(b). This is the approach of Drell and Huang<sup>7</sup> and Fujita and Miyazawa. It was used in the 60's by Nogami and his collaborators<sup>8</sup>, and is represented in the contributions to this conference from Robilotta et al.<sup>5</sup> Both approaches were discussed extensively (and advocated ardently) at the workshop, and we therefore review the advantages and disadvantages of each.

The technique of including resonance states in the Hilbert Space ( $\Delta$ 's in the wavefunction) has been advocated as a way of including the three nucleon forces, and it is appropriate to compare this method with the  $\pi\text{N}$  amplitude methods in this section.

Before doing so we should define the kinematic structure of the  $\pi\text{N}$  scattering amplitude  $T \propto 1-S$ , of figure 1(b) which we write in the usual isospin and spin decomposition as

$$T^{ij} = T^{(+)} \delta_{ij} + T^{(-)} i \epsilon_{ijk} \tau_k \quad (1)$$

$$T^{(\pm)} = F^{(\pm)} + B^{(\pm)} [\not{q}, \not{q}'] \quad (2)$$

The amplitudes  $T^{ij}$  are understood to be sandwiched between the Dirac Spinors  $x$  Pauli isospinors of the initial and final nucleons. The invariant amplitudes  $F^{(\pm)}$ ,  $B^{(\pm)}$  are functions of four variables — the usual kinematic variables  $v = \frac{1}{4m} (p + p') \cdot (q + q')$  and  $t = (q - q')^2$  but also  $q^2$  and  $q'^2$  since the pions of interest are off mass shell. (The relatively small extent to which the nucleons are off shell because of the nuclear binding is customarily ignored). Brown and Green<sup>9</sup> have suggested that typical "masses" of the virtual pions important in nuclear processes are from  $-\mu^2$  to  $-15\mu^2$ , which are relatively small on the typical hadronic mass scale of 1 GeV. An extension of their arguments suggests that  $|v| \lesssim \frac{1}{2}\mu$  and  $0 \gtrsim t \gtrsim -15\mu^2$ . We should therefore ask what is known about  $F^{(\pm)}$  and  $B^{(\pm)}$  in this kinematic region.

First of all, in the nearby on shell  $(v, t)$  plane where  $q^2 = q'^2 = \mu^2$  the subthreshold expansion<sup>10</sup> extrapolates the amplitudes from the physical region to the  $(v, t)$  region of interest. However we need the amplitudes off the pion mass shell, so we must use the subthreshold expansion in the on shell plane as a constraint on the off pion mass shell extrapolations which are necessary.

The off mass shell extrapolation is further constrained by the soft pion

theorems established from PCAC and current algebra by Adler<sup>11</sup> and Weinberg<sup>12</sup>. These constraints apply only to  $\bar{F}^{(+)}$  — the amplitude  $F^{(+)}$  with the pseudo-vector nucleon pole term subtracted — and are usefully visualised on the  $\nu = 0$  hyperplane<sup>13</sup> illustrated in figure 2.  $\bar{F}^{(+)}$  is obviously symmetric under the interchange  $q^2 \leftrightarrow q'^2$ , which is the operation of reflection in the plane WXC in figure 2. Adler's consistency condition constrains  $\bar{F}^{(+)}$  to vanish at the points marked A and A' in the figure, and Weinberg's double soft pion limit fixes the value of  $\bar{F}^{(+)}$  at the point W to be  $-\sigma/f_\pi^2$ , where  $\sigma$  is the  $\pi N \sigma$  term and  $f_\pi$  is the  $\pi$  decay constant ( $f_\pi \sim 93$  MeV with this normalisation convention). If one assumes that  $\bar{F}^{(+)}$  ( $\nu = 0$ ) is a linear function of  $t$ ,  $q^2$  and  $q'^2$  these soft pion constraints determine  $\bar{F}^{(+)}$  everywhere on the plane WAA'. In particu-

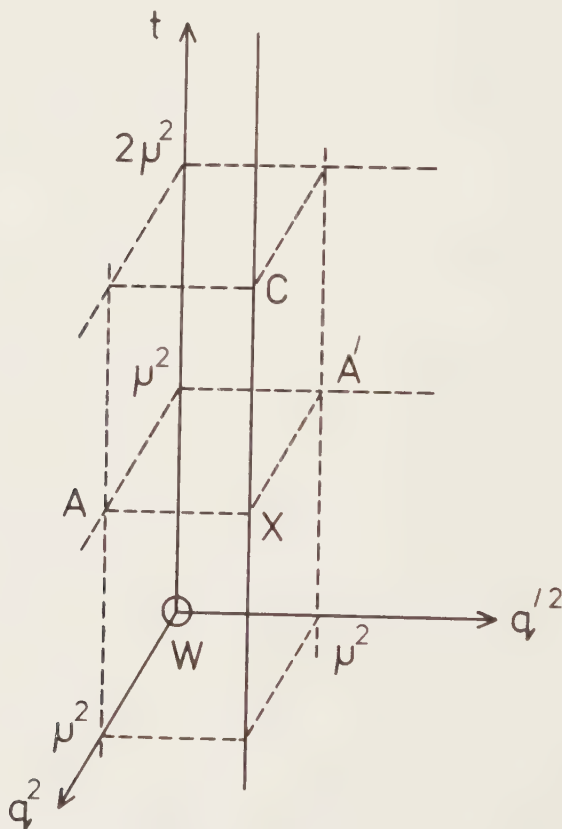


Fig.2 The  $\nu = 0$  hyperplane in  $\nu$ ,  $t$ ,  $q^2$ ,  $q'^2$  space

lar they fix  $\bar{F}^{(+)}$  to be  $+\sigma/f_\pi^2$  at the Cheng Dashen point C, which is the intersection of the "soft pion plane" WAA' and the on shell line  $q^2 = q'^2 = \mu^2$  (XC). This permits the determination of  $\sigma$  from the on shell amplitude — up to possible correction terms of order  $t^2$ .

From this point on the two possible approaches to the  $\pi N$  amplitude of figure 1(b) part company. In the *model independent approach* used in the construction of the Tucson-Melbourne potential<sup>6</sup> the fact that relatively small values of the arguments (on the hadronic scale) are apparently the most important in applications is used to suggest that a knowledge of  $T$  up to quadratic terms in nucleon 3-momenta will suffice. This means that for  $\bar{F}^{(+)}$  the linear approximation in  $\nu$ ,  $t$ ,  $q^2$ , and  $q'^2$  suffices and as crossing symmetry prohibits the appearance of odd powers of  $\nu$  the linear approximation in the  $\nu = 0$  hyperplane is adequate for this amplitude. To fix the  $\bar{F}^{(+)}$  amplitude in this approximation we need its value at one point outside the soft pion plane WAA'. In ref.6 the point X was used, because the amplitude had been directly evaluated at this point using dispersion relations<sup>14</sup>. However any other point on the on shell line would, in principle, serve just as well.

Using this information the model independent approach is able to fix the coefficients  $\alpha$ ,  $\beta$ , and  $\gamma$  in the expansion of  $\bar{F}^{(+)}$ ,

$$\bar{F}^{(+)} = \alpha + \beta t + \gamma(q^2 + q'^2) \quad (3)$$

without constructing a model for the amplitude. It is important to recognise that to this order the effects of all of the resonances (in all channels) are already included in these coefficients.

In the approximation of keeping only the terms quadratic in nucleon momenta, the other major invariant amplitude which contributes to the  $\pi\pi E$ -3NP is the spin flip amplitude  $B^{(-)}$ . Since the covariant multiplying this amplitude is already quadratic in the nucleon momenta we need only the constant term in the expansion of  $B^{(-)}$  which can be taken directly from the subthreshold expansion. However, since the subthreshold expansion is on pion mass shell the "constant" term in that expansion is really of the form  $\alpha + \gamma(q^2 + q'^2)$  with  $q^2 = q'^2 = \mu^2$ , one needs to make a model calculation to verify that the term  $2\gamma\mu^2$  is indeed a small correction.

In this sense one can say that the Tucson-Melbourne potential is independent of a detailed dynamical model of the underlying  $\pi N$  scattering amplitude. This has the advantage that, to the order considered, all resonant contributions are automatically included. The disadvantages of not having a detailed dynamical model for the  $\pi N$  amplitude are that such a model is in fact required if one wishes to include effects of higher order in the nucleon momenta, or if one

wishes to consider three body exchange currents. (In the latter case some model independent low energy theorem results would presumably be obtainable, but one would need explicit models to go beyond them.)

There is a systematic way to graft models for the higher order terms onto the model independent amplitude. To do this one writes the amplitude in the form

$$T = T_{\text{pole}} + \Delta T + q' \cdot C \cdot q \tag{4}$$

where  $T_{\text{pole}}$  is the nucleon pole,  $\Delta T$  contains the current algebra terms and the terms required to satisfy the soft pion theorems, and  $q' \cdot C \cdot q$  contains the resonance contributions. If the latter are included using a dispersion relation for  $C$  (rather than for  $q' \cdot C \cdot q$ ) one is guaranteed to not disturb the soft pion results.

The alternative *model making* approach is represented in the contributions to Few Body  $X$  by the papers of Robilotta et al.<sup>5</sup> This approach is also closely related to the coupled channel calculations which include  $\Delta$  resonant states in the nuclear wavefunction<sup>15</sup>. We represent a typical dynamical model of the  $\pi N$  amplitude in figure 3, where we also indicate the correspondence between the terms of the model and those of the PCAC Current Algebra model independent approach.

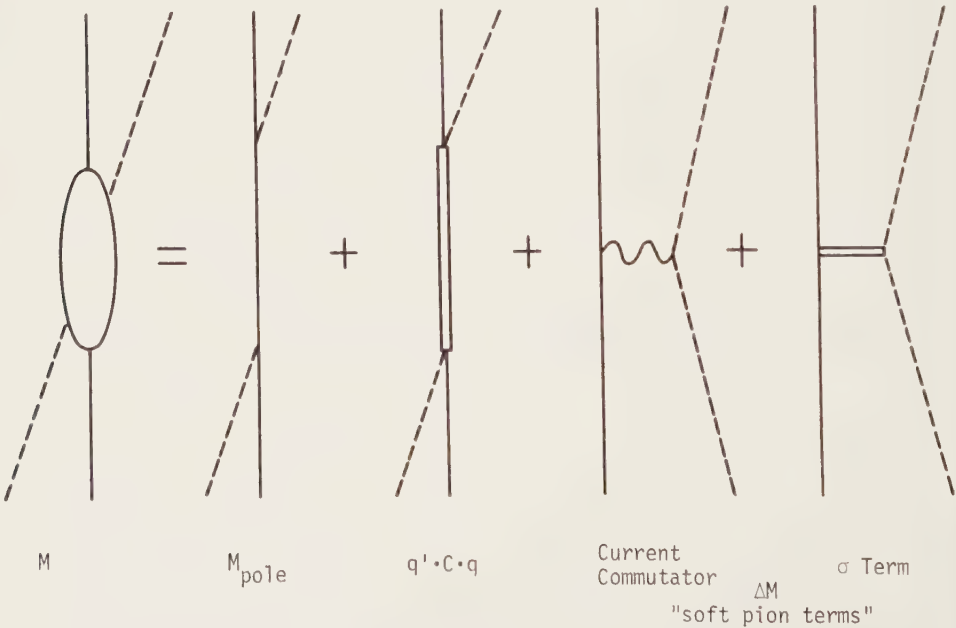


Figure 3: The model of Robilotta et al. for the  $\pi N$  amplitude.

Dynamical models for the  $\pi N$  scattering amplitude do overcome some of the disadvantages of the model independent approach — in particular they offer a mechanism for going beyond terms quadratic in the nucleon momenta. However the models constructed up to now have suffered from two difficulties

(i) they do not satisfy the soft pion constraints at the points A, A' and W of figure 2.

(ii) they are not truly dynamical, in that the  $\sigma$  term is included in an ad hoc way and is not represented by exchange of a physical (or fictitious) particle. Furthermore, the work of Shimizu, Polls and Muther<sup>14</sup> has raised the possibility that the  $\Delta$  resonance alone may not be sufficient, and that higher resonances may contribute significantly. Once model making is started, there is always the possibility of adding more diagrams, and one should look for criteria which decide where to stop.

If, instead of expanding the model it is contracted to just the nucleon and  $\Delta$  pole terms, this suggests that three nucleon forces can be incorporated into the calculations of nuclear physics if the Hilbert space is extended to include states in which some particles are  $\Delta$ 's<sup>15</sup>. This idea, the  $\Delta$ 's in the wave function approach, has been recently revived and pursued vigorously by the Hannover group in a coupled channel calculation of the three nucleon system<sup>16</sup>. This method has several advantages.

(i) Additional three body forces, such as that of figure 4(a), originally discussed by Fujita, Kawai and Tanifuji<sup>17</sup>, are automatically generated.

(ii) Those terms of higher order in momenta which correspond to non static propagation of the  $\Delta$  are readily included, and significantly alter the 3NP contribution to the energy.

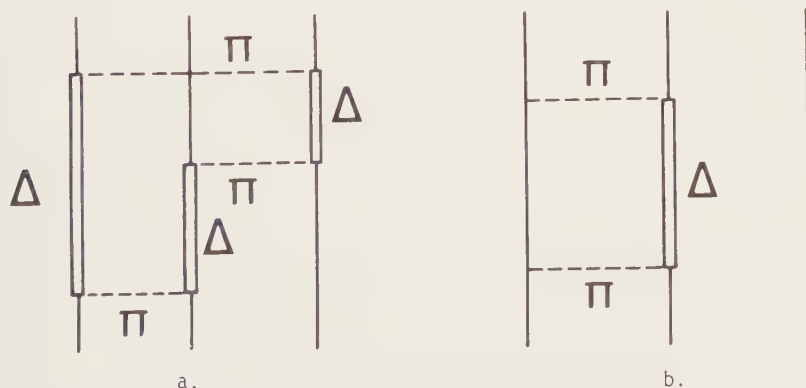


Figure 4. Additional effects included in  $\Delta$  in the wave function calculations.

a. The  $3\pi E - 3NP$  of Fujita, Kawai and Tanifuji.

b. The dispersion effect on the two body potential contribution to the energy.

(iii) Dispersion corrections to the two body force contribution arising from the diagrams of figure 4(b) are readily included and tend to cancel the effects of three body forces. In the conventional approach with potentials and only nucleon states in the Hilbert space, these dispersion effects can be included only by taking the energy dependence of the two pion exchange two nucleon potential seriously<sup>18</sup>, and finding ways to handle this energy dependence in many nucleon problems.

(iv)  $\pi$  and  $\rho$  exchange can be readily included.

Despite these advantages the  $\Delta$ 's in the wave function approach also has its short comings.

(i) The implied  $\pi N$  amplitude does not provide a good representation of the  $\pi N$  amplitude in the subthreshold region. To convince oneself of this one can use the tables of Olsson and Osypowski<sup>19</sup>, multiplying the  $\Delta$  amplitude in those tables by 1.37 to allow for the different choice of  $\pi N \Delta$  coupling constant. Some coefficients are listed in table I.

TABLE I  
Coefficients  $f_i^{(+)}$ ,  $b_i^{(-)}$  in the subthreshold expansion

		$a_1 + a_2 t + (a_3 + a_4 t)v^2 + (a_5 + a_6 t)v^4 + a_7 t^2 + ..$							
		i	1	2	3	4	5	6	7
$F^+$	model	-2.12	1.10	1.00	0.19	0.23	0.030	-0.017	
	expt	-1.45	1.18	1.14	0.15	0.20	0.034	0.001±0.04	
$B^-$	model	7.08	-0.15	1.23	-0.074	0.25	-0.023	.003	
	expt	10.33	0.20	1.04	-0.063	0.27	-0.030	.004	

(ii) The implied  $\pi N$  amplitude does not satisfy the off pion mass shell constraints of current algebra and PCAC.

(iii) The  $\pi N$  amplitude implied by the  $\Delta$ 's in the wavefunction approach in which the  $\Delta$  is on its mass shell differs significantly from the corresponding Feynman amplitude in which the  $\Delta$  propagates off its mass shell. In particular off mass shell ambiguities exist in the latter amplitude, but appear in the former only when the contact terms in the Hamiltonian are included<sup>20</sup>. While it may be argued that Olsson and Osypowski<sup>19</sup> found that the subthreshold expansion in  $\pi N$  scattering is well reproduced when the off mass shell term makes a small contribution, in their analysis of photoproduction<sup>21</sup> they found that that a large contribution from the off mass shell term was required. This should influence the  $\rho$  meson exchange contributions to the amplitude in a significant way<sup>20</sup>.

For these reasons one cannot escape the conclusion that, even in a  $\Delta$ 's in



the wavefunction calculation one cannot avoid including explicit three nucleon forces — which one would expect to contribute to the energy with about the same strength as the  $\Delta$  contributions themselves.

## 2.2 The $\pi$ - $\rho$ Exchange Three Nucleon Potential ( $\pi\rho$ E-3NP)

The importance of including  $\rho$  exchange terms as well as  $\pi$  exchange terms in the  $NN \rightarrow N\Delta$  transition potential was recognised quite early in the development of the  $\Delta$ 's in the wavefunction approach<sup>15</sup>, but  $\rho$  exchange contributions were included in explicit three body potentials only quite recently<sup>22,23</sup>. There were two contributions to the conference<sup>24,25</sup> and a presentation to the workshop on this subject. The  $\rho N \rightarrow \pi N$  amplitude has obvious relations to the  $\pi$  photoproduction amplitude, which has been discussed by Ellis in a contribution to this conference<sup>26</sup>.

Once again model independent<sup>23,24</sup> and model making<sup>22,25</sup> approaches to the construction of the amplitude are possible. The relationship between these approaches is illustrated in figure 5, which is to be compared to figure 3.

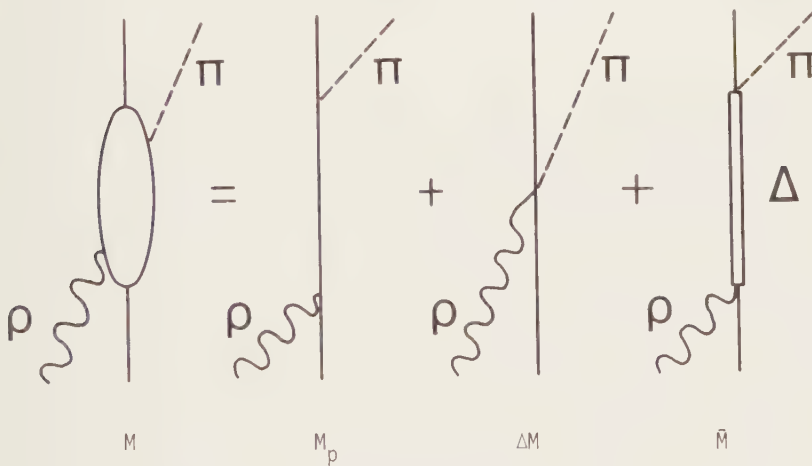


Figure 5: The  $\rho N \rightarrow \pi N$  scattering amplitude

In the model independent approach chiral symmetry breaking terms, analogous to the  $\sigma$  term in the  $\pi N$  scattering amplitude, arise in the same way that these terms appeared for the  $\pi$  photoproduction amplitude studied by McMullen and Scadron<sup>27</sup>. However, in contrast to the  $\pi N$  case, this time the chiral symmetry breaking terms do not contribute in a numerically significant way. Thus there is not such a difference between the two approaches for the  $\rho\pi$ E-3NP as there is for the  $\pi\pi$ E-3NP.

The term of lowest order in  $k$ , which one may have expected to dominate the 3NP, arises from the analogue Kroll-Ruderman term in  $\pi$  photoproduction<sup>28</sup>. This may be regarded as a contribution from the backward propagating nucleon in the  $\gamma_5$  coupling scheme, which is how Kroll and Ruderman originally derived the term. It may alternatively be regarded as arising from minimal substitution in the  $\gamma_5\gamma_\mu$  coupling scheme — as pointed out e.g. by Dombey and Read<sup>29</sup>, in the photoproduction case.

This minimal substitution is, in the present context,

$$\frac{g}{2m} \bar{\psi} \gamma_\mu \gamma_5 \tau_i \psi \partial^\mu \phi_i \rightarrow \frac{g}{2m} \bar{\psi} \gamma_\mu \gamma_5 \tau_i \psi (\partial^\mu \delta_{ij} - i \frac{g}{2} \rho_k^\mu \epsilon_{ijk}) \phi_j \quad (5)$$

Ellis, Coon and McKellar choose to emphasise the "backward propagating" nature of the term, and to work with  $\gamma_5$  coupling, whereas Robilotta et al. emphasise the "contact" or seagull interaction arising from the minimal substitution. The final contribution to the amplitude, is in the soft  $\rho$  limit ( $k \rightarrow 0$ )

$$M_{ij}^{ij} = \frac{-gg}{4m} i_{ij} i_{ijk} \tau_k + O(k) \quad (6)$$

for space like  $v$ .

Robilotta and Isidro Filho, and earlier McKellar, Coon and Scadron<sup>23</sup> claimed that this would be the major contribution to the  $\rho\pi E$ -3NP. However, at least in the case of nuclear matter the contribution of the Kroll-Ruderman term is suppressed relative to that from the  $\Delta$  by the spin-flip, isospin-flip nature of the Kroll-Ruderman 3NP. The contribution of the  $\Delta$  is further enhanced by tensor correlations in the wave function, and Ellis, Coon and McKellar<sup>24</sup> found that the  $\Delta$  gives the dominant contribution, although the Kroll-Ruderman term is not insignificant.

Two rather subtle points arise when considering the  $\rho N \rightarrow \pi N$  amplitude, and the related 3NP. The first is the treatment of the  $\pi$  pole in the  $\rho N \rightarrow \pi N$  amplitude. As can be seen in figure 6 this may be regarded as a  $\rho\pi$  force or a  $\pi\pi$  force. As there are two possibilities for the former the only simple way to treat this diagram without double counting is to regard it as a  $\pi\pi E$ -3NP. Thus in constructing a 3NP from the  $\rho N \rightarrow \pi N$  amplitude we must subtract both the forward propagating nuclear poles and the  $t$  channel  $\pi$  pole from  $\rho N \rightarrow \pi N$  amplitude before constructing the potential.

The other subtlety is that one must ensure that the  $\Delta$  contributes explicitly to the background term only — i.e. to terms of order  $k^2$ ,  $q^2$  or  $q \cdot k$ . This is readily achieved with derivative coupling, as long as one writes  $M_\nu = k \cdot C_\nu \cdot q$  and disperses  $C$  rather than  $M$ . Should one adopt the alternative of dispersing

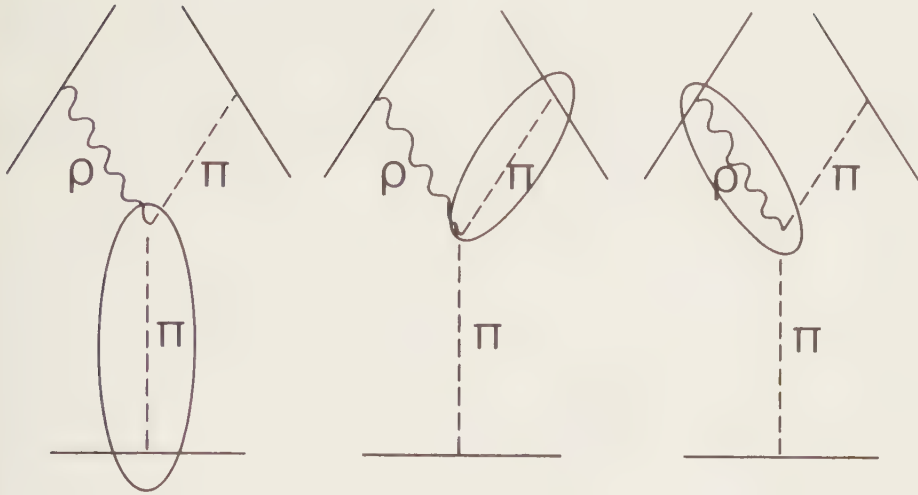


Figure 6: 3 Ways to regard the  $\pi$  pole in the  $\rho N \rightarrow \pi N$  amplitude as contributing to the 3NP.

$M$ , then one obtains a contribution to the  $M_0^{ij}$  amplitude proportional to  $\underline{\sigma} \cdot \underline{k} \delta^{ij}$  — this is however just what is required to cancel the backward propagating Born term in  $M_0^{ij}$  in the soft pion limit. This cancellation is embodied in the Fubini, Furlan, Rosetti relation<sup>30</sup>, which is the photoproduction analogue of the Adler zero in the  $\pi N$  scattering amplitude.

The net result of the detailed analysis of the  $\rho N \rightarrow \pi N$  amplitude by Ellis, Coon and McKellar is that the  $\rho\pi E$ -3NP is given to quite a good approximation by the sum of the Kroll-Ruderman term, discussed by McKellar, Coon and Scadron and by Robilotta and Isidro Filho, and the  $\Delta$  contribution introduced by Martzloff, Loiseau and Grangé.

### 2.3 The $\rho\rho$ Exchange Three Nucleon Potential

The  $\rho\rho E$ -3NP was also introduced by Martzloff, Loiseau and Grangé, in the  $\Delta$  dominance approximation. In the non relativistic limit the resulting potential is of the form  $((\underline{\sigma}_1 \times \underline{k}) \times \underline{k}) \cdot ((\underline{\sigma}_2 \times \underline{k}') \times \underline{k}')$  in momentum space. However in this case, as emphasised by McKellar, Coon and Scadron<sup>23</sup>, the backward propagating Born terms do not cancel but give the  $\rho$  meson equivalent to Thompson scattering. These give a 3NP proportional to  $(\underline{\sigma}_1 \times \underline{k}) \cdot (\underline{\sigma}_2 \times \underline{k}')$  — of lower order in the momenta than the  $\Delta$  term.

There is also an additional contribution from the current commutator terms. These give rise to spin and isospin flip terms in the  $\rho N \rightarrow \rho N$  amplitude which are in the non relativistic limit

$$M_{\mu\nu}^{ij} = \frac{ig_{\rho}^2}{2m} (1 + \kappa_{\rho}) \epsilon^{ijk} \tau_k \epsilon_{\mu\nu\lambda} \sigma^{\lambda} \quad (7)$$

for space like  $\mu, \nu, \lambda$ , and were discovered by Beg in his analysis of "isovector photon" scattering<sup>31</sup>. If one were to make models for this term, it is given by figure 7 — it arises from the  $\rho$  meson pole in the  $t$  channel.

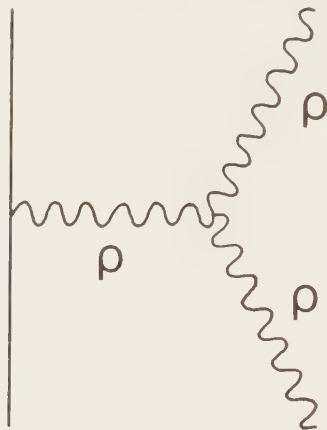


Figure 7: The  $\rho$  meson pole in the  $\rho N \rightarrow \rho N$  amplitude which gives rise to the Beg term in the amplitude.

However, Ellis, Coon and McKellar<sup>24</sup> have found that these terms, although of lower order in the nuclear momenta, nevertheless contribute much less to the energy than the  $\Delta$  term. This is partly a consequence of the strong magnetic coupling of the  $\rho$  meson, both to the nucleon and to the  $N$ - $\Delta$  transition amplitude — the effective expansion parameter is not  $k/m$  but  $\kappa_{\rho} k/m$ , which for  $k/m \sim 1/2$  is greater than unity.

This "breakdown" of the  $k/m$  expansion could even signal the breakdown of the potential approach to the nuclear many body problem. Less dramatically it could be confined to the  $\rho\rho E$ -3NP, which according to ref.24 makes a small contribution of the total energy in nuclear matter. Clearly this is a problem which should receive further study.

#### 2.4 The Form Factor Problem

It is clearly unphysical to extend the Yukawa terms  $\frac{e^{-mr}}{r}$  implied by the meson propagators down to very small values of  $r$ . We know in the two nucleon problem it is necessary to take into account other exchanges with the same quantum numbers as those of the meson, and that it is common in OBEP models to take these exchanges into account through form factors at the meson nucleon vertex<sup>32</sup>.

The same solution to the problem has been used for 3NP. The difficulty is that the numerical results obtained are very sensitive to the assumed form factors. This observation<sup>33</sup> has been revived in a new form in the contribution to this conference by Robilotta, Isidro Filho, Coelho and Das<sup>5</sup>. They point out that the form factor, which was introduced to moderate the short distance behaviour of the potential, in fact influences the potential at quite large distances — certainly up to 2 fm.

Part of the reason for this extension of the influence of the form factor to large distances is that the radial potential is not in general the Fourier Transform of  $\frac{1}{k^2 + \mu^2}$  but rather the Transform of  $\frac{k^2}{k^2 + \mu^2}$ . When this is modulated by a form factor, the  $k^2$  in the numerator ensures that the short range part of the potential, with a range  $\Lambda^{-1}$  where  $\Lambda$  is the cut off in the form factor, has a factor  $\Lambda^2$  which greatly enhances the contribution.

To illustrate this consider the simple case of a square root form factor  $\sqrt{\frac{\Lambda^2 - k^2}{\Lambda^2 + k^2}}$ , when the potential in configuration space behaves like

$$v(r) = \text{F.T.} \left[ \frac{k^2}{k^2 + \mu^2} \cdot \frac{\Lambda^2 - \mu^2}{\Lambda^2 + k^2} \right] \propto \mu^2 \frac{e^{-\mu r}}{r} - \Lambda^2 \frac{e^{-\Lambda r}}{r}, \quad (8)$$

which is plotted in figure 8 for  $\Lambda = 6\mu$ .

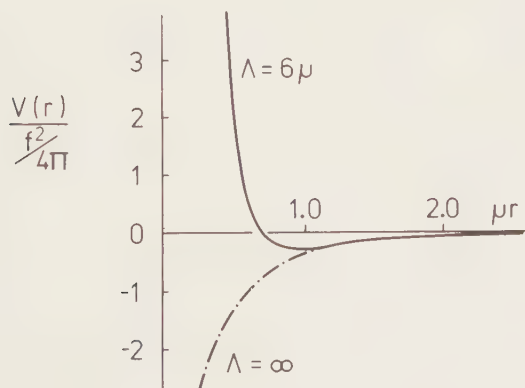


Figure 8: Showing the influence of the form factor on the radial dependence of the potential (after A. Cass<sup>33</sup>).

It should be emphasised that this is a physical effect — the one pion exchange channel, and hence the  $\pi NN$  form factor, receives contributions from  $3\pi$  exchange which does indeed have quite a long range. A number of attempts have been made to calculate the expected behaviour of the form factor; a dispersion relation<sup>34</sup> calculation, fitted with a monopole form gives  $\Lambda = 5.5\mu$ ; fits to the average differential cross section for np Charge Exchange and  $\bar{p}p$  charge exchange<sup>35</sup> suggest a smaller  $\Lambda = 4.1\mu$  in the monopole fit; and a recent self consistent attempt to fit a number of form factors<sup>36</sup> used the parameterisation

$$F(q) \propto \frac{1}{1 + q^2/\Lambda_1^2} \frac{1}{1 + (q^2/\Lambda_2^2)^n \ln^3(1 + \beta q^2/\Lambda_{QCD}^2)} \quad (9)$$

and obtained for the  $\pi NN$  form factor with  $n = 2$ ,  $\Lambda_1 = 1 \text{ GeV}$ ,  $\Lambda_2 = 9.49 \text{ GeV}$ . In the latter two cases information about the large  $q^2$  behaviour of the form factor from the constituent interchange model in the first case, and from QCD in the other<sup>37</sup> was used to constrain the parameterisation.

All of these analyses, while they differ in details, serve to suggest that the small  $q^2$  behaviour of the form factor may be able to be fixed by theoretical and experimental work.  $\Lambda \sim 5.6\mu$  (700-800 MeV) would seem to be a reasonable value to adopt, and for these values the form factor does induce significant changes in the potential in the 1-2 fm region.

We believe that these effects are physical rather than spurious, and should not be discarded in the way proposed by Robilotta et al. However results obtained for the effects of three body forces will depend sensitively on the behaviour of the form factor, and more effort could usefully be devoted to fixing the form factor from independent studies.

### 3. EFFECTS OF THREE BODY FORCES IN THE THREE NUCLEON SYSTEM

#### 3.1 Contribution to the Binding Energy

There are a number of approaches to the calculation of the Binding Energy of the triton, and by now many of these methods have been used to include the effects of a 3NP, including the Faddeev scheme, the variational Monte Carlo method, the ATMS method and the hyperspherical harmonic method. To facilitate a comparison of results obtained in these calculations we will present detailed results only for those calculations which use a comparable 3NP — we choose to make this comparison with calculations done using the Tucson-Melbourne  $\pi\pi E$ -3NP, with a monopole form factor with a cut off parameter  $\Lambda \sim 6\mu$ .

In the Faddeev equation approach, the 3NP may in principle be incorporated into the Faddeev or equivalent equations in a variety of ways<sup>38</sup>. Because the 3NP,  $W$ , does not introduce physically distinct amplitudes, it is possible to

split  $T_W$ , the partial T matrix in which the last interaction is the 3NP, in various ways giving different generalisations of the Faddeev Equations. One method which has been exploited in practice for the  $2\pi E$ -3NP<sup>39</sup> has been to utilise the fact that this particular W may be written, in a natural way, as the sum of three terms

$$W = W_1 + W_2 + W_3 \quad (10)$$

where the subscript labels the nucleon which is the active scatterer. It is then possible to associate  $W_1$  with  $V_1$  (the two body interaction between 2 and 3) and define a partial T matrix by

$$T = (V_1 + W_1) + (V_1 + W_1) G_0 T \quad (11)$$

from which the wavefunction

$$\Psi = (1 + P_{12}P_{23} + P_{13}P_{32})\psi \quad (12)$$

where

$$\psi = G_0 T(P_{12}P_{23} + P_{13}P_{32})\psi \quad (13)$$

may be constructed in the usual way.

The T matrix including three body forces can be expressed in terms of that generated from two body forces only, which we call  $t$ , by solution of

$$T = t + (1 + t G_0) W_1(1 + G_0 T) . \quad (14)$$

In a momentum space approach to the three nucleon problem the material variables are the Jacobi co-ordinates, whereas the natural coordinates for a meson exchange 3NP are the meson momenta — which depend on both of the Jacobi momenta for the initial and final states, and so the 3NP has a complicated partial wave expansion<sup>40,41,42</sup>.

The  $(j\ell)$  convention for labelling the three body states is adopted, so that the states are  $[[\lambda \times \tilde{s}]^j \times [\lambda \times \frac{1}{2}]^{\tilde{j}}]^J [t \times \frac{1}{2}]^T$ . The  $^1S_0$ ,  $^3S_1$ ,  $^3S_1$ - $^3D_1$  two body states generate the 5 channel truncation of the Hilbert Space.

Glöckle's method<sup>39</sup> of computing the energy including the 3NP used a truncation of  $W_1$  to the first three channels, a solution of (14) to first order in  $W_1$ , the Reid potential for  $V$  and the solution of (13) in momentum space. He used the Tucson-Melbourne  $\pi\pi E$ -3NP and obtained the result quoted in Table II.

Glöckle found that the results are sensitive to the choice of cut off in the form factor.  $\Lambda = 5.8\mu$  gives  $E_3 = 1.3$  MeV, but  $\Lambda = 7.1\mu$  gives  $E_3 = 1.9$  MeV.

Muslim, Kim and Ueda<sup>40</sup>, and Bömelburg<sup>41</sup>, calculated  $E_3$  perturbatively, from



$$E_3 = \frac{\langle \psi | W(1+P) | \psi \rangle}{\langle \psi | (1+P) | \psi \rangle} \quad (15)$$

using a 5 channel calculation of  $\psi$ . These results, given in table II, are comparable, but with a residual numerical discrepancy which needs to be understood. They obtain a negligible net  $E_3$ , s and p wave terms cancelling against each other.

It is interesting to compare these results with the result  $E_3^D = 0.65$  MeV obtained by Torre et al.<sup>43</sup>. They solve the Faddeev equations in configuration space truncated to 12 channels, using the Tourreil-Sprung two nucleon interaction, and a square root form factor with  $\Lambda = \sqrt{10}\mu$ . The small result could perhaps be attributed to the longer range form factor, were it not for the fact that the convergence of the partial wave expansion of (15) has been called into question by some recent work of Bömelburg et al.<sup>44,45</sup>. An 18 channel result, quoted in table II is obtained which is again very small. However they find quite large individual contributions, even up to the last channel, which fluctuate in sign. For example

$$\langle \#1 | W_3(1+P) | \#1 \rangle = -0.164 \text{ MeV} \quad (16a)$$

$$\langle \#1 | W_3(1+P) | \#18 \rangle = 0.330 \text{ MeV} \quad (16b)$$

Where  $|\#1\rangle = |^1S_0, S_{1/2}; \frac{1}{2}\rangle$  has 44% of the normalisation,

and  $|\#18\rangle = |^3D_2, d_{5/2}; \frac{1}{2}\rangle$  has just +0.1% of the normalisation.

There is thus no reason to expect that the omitted channels give small contributions. The calculation must either be extended, or a way found of evaluating matrix elements (or more directly  $E_3$ ) without recourse to a partial wave expansion of the P operator.

One method which has the advantage of not requiring such partial wave expansion is the direct evaluation of the matrix elements through Monte Carlo integration. Wiringa<sup>46</sup>, and Carlson, Pandharipande and Wiringa<sup>47</sup> have used this technique in conjunction with a variational calculation, revarying the parameters of the wavefunction after including the three body force, so their result goes beyond perturbation theory in W. They found a relatively large net effect from the three body force, 1.15 MeV attraction.

Wiringa<sup>48</sup> reported more recent calculations to the workshop, in which the Monte Carlo method of evaluating the expectation value of the Hamiltonian is used in conjunction with a three body wave function obtained from Faddeev calculations<sup>49</sup>. Using the two body Reid potential, the binding energy of the triton is significantly lowered by the new wave function, but the contribution of the  $\pi\pi$ E-3NP to the potential is not changed.

Wiringa<sup>46,48</sup> also reported an interesting effect when the two body potential is altered. Table III shows some of his results.

TABLE II

Results of Triton Binding Energy Calculations. The Reid Potential is used for the two body potential, and the Tucson-Melbourne  $\pi\pi\text{E}$ -3NP with a monopole form factor and  $\Lambda \sim 6\mu$  is used for the three body potential. Energies are in MeV.

	$E_1$	$E_2^S$	$E_3^D$	$E_3$	$E_{\text{tot}}$	Comment
GLÖCKLE ref. 42	-7.02	-	-	-1.28	-8.30	3 Channel W
MUSLIM, KIM and UEDA ref. 40	-6.98	+1.03	-0.96	+0.07	-6.91	5 Channel
BÖMELBURG ref. 41	-7.02	0.90	-0.70	0.20	-6.82	5 Channel
BÖMELBURG GLÖCKLE ref. 44	-7.02	-	-	-0.16	-7.18	18 Channel
CARLSON PANDHARIPANDE WIRINGA ref.47 , 48	-6.62	0.38	-1.53	-1.15	-7.77	Variational Wave function
WIRINGA ref.48	-7.08	0.28	-1.43	-1.15	-8.23	Faddeev Wave Function Monte Carlo Integral

It will be observed that as the repulsive core in the two body potential is weakened, increasing the two body binding energy, the three body potential contribution becomes more repulsive, leading to a somewhat smaller total binding energy. The physical reason for this is the larger probability that two nucleons are a short distance from each other, and so feel more of the short range repulsion in the  $\pi\pi\text{E}$ -3NP.

TABLE III

Dependence of Triton Binding Energy calculations on the Two Body Potential.

Two Body Potential	$E_2$	$E_3^S$	$E_3^D$	$E_3$	$E_{\text{tot}}$
Reid V 14	-7.08	0.28	-1.43	-1.15	-8.23
Argonne V 14	-7.29	0.41	-1.35	-0.94	-8.23
Supersoft Core	-7.38	0.58	-1.25	-0.67	-8.05

Now we see that we are entering *terra incognita* — the  $\pi\pi\text{E}$ -3NP was constructed to be a good approximation to the long range part of the 3NP. Physical effects which depend on its short range properties are likely to be altered by shorter range parts of the 3NP, which must now be included. One can either

utilise the  $\pi pE$ -3NP and the  $\rho pE$ -3NP discussed above, or a phenomenological approach, which we describe below, in which one tries to fix the short range behaviour of the 3NP to fit the observed binding energy discrepancies in  $^3H$ ,  $^4He$  and heavier nuclei.

Hajduk et al.<sup>50</sup> have applied the  $\Delta$  coupled channels approach to the triton. They find a considerable dispersion effect in the two body interaction, and a significant effect from a non static  $\Delta$  propagator. With  $\Lambda = 7\mu$  and monopole form factors their results are summarised in Table IV.

TABLE IV

Contributions to the energy of  $^3H$  in a  $\Delta$  coupled channels approach<sup>50</sup>.

Interaction	Two Body Dispersion Energy	Three Body Energy	Total Energy
$\pi\pi$	2.1	-1.4	0.7
$\pi\rho$	-2.2	0.5	-1.7
$\rho\rho$	0.7	0.1	0.8
Total	0.6	-0.8	-0.2

Once again, there are almost complete cancellations of individual terms, leading to a small final result. The advantages and disadvantages of the  $\Delta$  coupled channel approach as a representation of three body force effects has been discussed above. A consequence of the cancellations and the small final result from this approach is that it is important to include three body forces, such as the s wave  $\pi\pi E$ -3NP, the Kroll-Ruderman  $\pi pE$ -3NP, and off  $\Delta$  mass shell terms in the  $\Delta$  coupled channels calculation, and we see this as the desirable next step.

### 3.2 The Doublet Scattering Length

Torre et al.<sup>43</sup> have calculated the effect of the p wave part of the Tucson-Melbourne  $\pi\pi E$ -3NP on the doublet scattering length. They found that the large Reid soft core value ( $a_2 = 1.5$  fm) was reduced to 1.0 fm — a step in the right direction, but not far enough to agree with the experimental value of 0.65 fm. Delfino<sup>51</sup>, in a report to the Bochum workshop, showed that one could explain this result on the basis of the work of Girard and Fuda<sup>52</sup> which related  $a_2$  to the energy  $E_v$  of the virtual state of the triton, which is below a n-d threshold in the second sheet. Delfino then exploited this connection to obtain  $a_2$  including the full Tucson-Melbourne  $\pi\pi E$ -3NP, averaged over the spin isospin state with the triton quantum numbers. He used a separable Unitary Pole Approximation to the Malfliet-Tjon potentials I and III as the two body interaction. His results are summarised in Table V.

TABLE V

Binding Energy of the bound and virtual states of  $^3\text{H}$ , and the doublet scattering length. (after Delfino<sup>51</sup>).

	$E_3$	$E_V$	$a_2$
without 3NP	-8.50 MeV	-0.49 MeV	0.8 fm
with 3NP	-9.05 MeV	-0.47 MeV	0.5 fm

### 3.3 The Charge Form Factor of $^3\text{He}$

One of the intuitive arguments in favour of a non trivial 3NP effect in three nucleon systems is the observation of the dip in the central charge density, or equivalently a "large" secondary maximum in the charge form factor<sup>53</sup>. However calculations with present three nucleon potentials do not reproduce the observed charge form factor. As an example we show in figure 9 the results of Carlson, Pandharipande and Wiringa<sup>47</sup> for the charge form factor of  $^3\text{He}$ . The

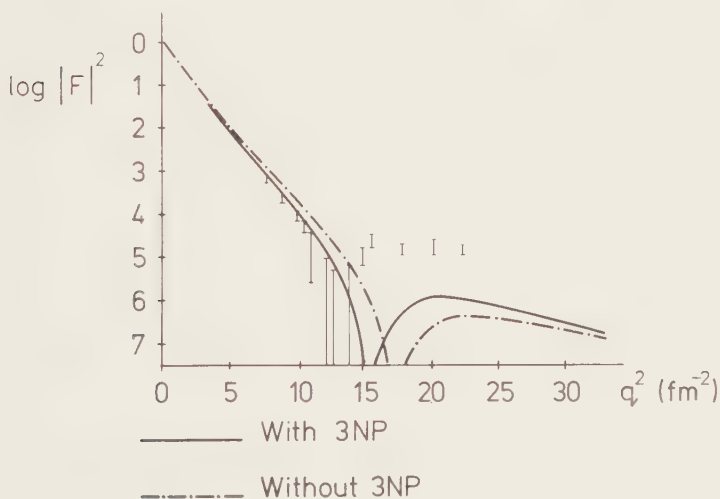


Figure 9

The Charge Form Factor of  $^3\text{He}$ , for the Reid Potential with and without the Tucson-Melbourne  $\pi\pi\text{E}$ -3NP (after ref.47).

minimum is moved to smaller  $q$ , and the height of the secondary maximum is increased, but neither of these trends is sufficient for the calculated charge form factor to be in agreement with the observations. Possibly it is necessary to look to exchange current effects, or quark effects, to resolve the discrepancy between calculated and observed form factors.

### 3.4 Effects of three body forces in break up reactions

Slaus, Akaishi and Tanaka<sup>54</sup> noted the discrepancy between the  $n$ - $n$  scattering length extracted from different reactions. In particular

$$\begin{aligned} a_{nn}(\text{nd} \rightarrow \text{pnn, knock out}) &= -20.7 \pm 0.2 \text{ fm} \\ \langle a_{nn}(\pi^- d \rightarrow nn) &= -18.6 \pm 0.48 \text{ fm} \\ \langle a_{nn}(\text{nd} \rightarrow \text{pnn, pick up}) &= -16.73 \pm 0.47 \text{ fm}. \end{aligned}$$

They then suggested that including three body forces in the analysis of the break up reaction increases  $a_{nn}$  extracted from knock out reactions, and decreases  $a_{nn}$  extracted from pick up reactions, thus removing the discrepancy. However Meier<sup>55</sup>, in a paper presented at the Bochum workshop, reported calculations suggesting that the effect of the 3NP on the extracted value of  $a_{nn}$  is angle dependent, and that a succinct statement of the effects of 3NP on  $a_{nn}$  was impossible to make.

Meier<sup>55</sup> and Bömelburg, Glöckle and Meier<sup>45</sup> give results that the 3NP could have effects in star, collinear and quasifree scattering regions in the  $pnn$  final state phase space. These effects are predicted to be small ( $\lesssim 13\%$ ) and will be difficult to see<sup>56</sup>, but this seems to be a useful way to look for effects of the 3NP.

Two warnings are in order. Since the angle dependence of the 3NP is one of its important attributes, one may have expected either the star or the collinear configurations to display an enhanced cross section, and the other to show a suppressed cross section. However, in the calculations it is found that the cross section for both configurations is enhanced by the  $\pi\pi\text{E}$ -3NP. Thus one must guard against being led astray by intuition.

Almost as important is the warning that one should not stake too much on the present calculations. Both the two body force (an UPA to the Malfeit-Tjon) and the three body force (spin-isospin matrix element of the Tucson-Melbourne  $\pi\pi\text{E}$ -3NP) are subject to improvement. This process makes significant changes in the calculation of  $E_3$ . Whether similar changes occur in the break up reaction will only be known when more extensive calculations are done and the present approximations are superseded.

## 4. NUCLEAR MATTER

Nuclear Matter has been the traditional testing ground for three body forces. Since the last Few Body Conference there have been two significant developments in calculations of  $E_3/N$ , the contribution of the 3NP to the binding energy per nucleon in symmetric nuclear matter.

In the first of this Wiringa et al.<sup>46-48</sup> have calculated  $E_3/N$  in the variational Monte Carlo approach, using the FHNC(4)/SOC method to include spin and isospin dependent correlations in the wavefunction. This relaxes the "effective potential approximation" used in earlier evaluations of the contribution of the 3NP to nuclear matter<sup>6</sup>, and allows contributions from all of the various spin-isospin components of the 3NP. Of the results obtained by Wiringa et al.<sup>46-48</sup>, we illustrate in figure 10 those obtained using the Tucson-Melbourne  $\pi\pi E$ -3NP, again with monopole form factors and  $\Lambda = 6\mu$ , and those obtained using a phenomenological 3NP which we discuss in more detail below.

It will firstly be noted that the "realistic two body potentials underbind nuclear matter at the observed density ( $k_F = 1.36 \text{ fm}^{-1}$ ), but predict saturation at too high a density and too large a binding energy. Including the Tucson-Melbourne  $\pi\pi E$ -3NP produces 1.9 MeV additional binding energy at the observed density, but exacerbates the undersirable features of the two body potential saturation curves. The calculated saturation point is shifted to higher density and greater binding energy. Presumably one should look to a force which enhances the short distance repulsion to decrease the equilibrium density and binding energy.

It is possible that the  $\pi\pi E$ -3NP will have this effect. Ellis et al.<sup>24,57</sup> have reported calculations of the effect of this potential in nuclear matter, calculating the effects of tensor correlations using the effective potential approximation, but allowing double exchange terms in the matrix element of  $W$  to estimate the importance of the Kroll-Ruderman terms. Table VI is abstracted from their results.

TABLE VI

Contributions of  $\pi\pi E$ ,  $\pi\rho E$  and  $\rho\rho E$ -3NP to the binding energy of nuclear matter (after Ellis et al.<sup>24,57</sup>).

3N Potential	Contribution to $E_3/N$ at $k_F = 1.36$
$\pi\pi E$	-3.60 MeV
$\pi\rho E$ , Kroll-Ruderman	+0.56 MeV
$\pi\rho E$ , $\Delta$	+2.27 MeV
$\rho\rho E$	-0.12 MeV
Total	-0.89 MeV

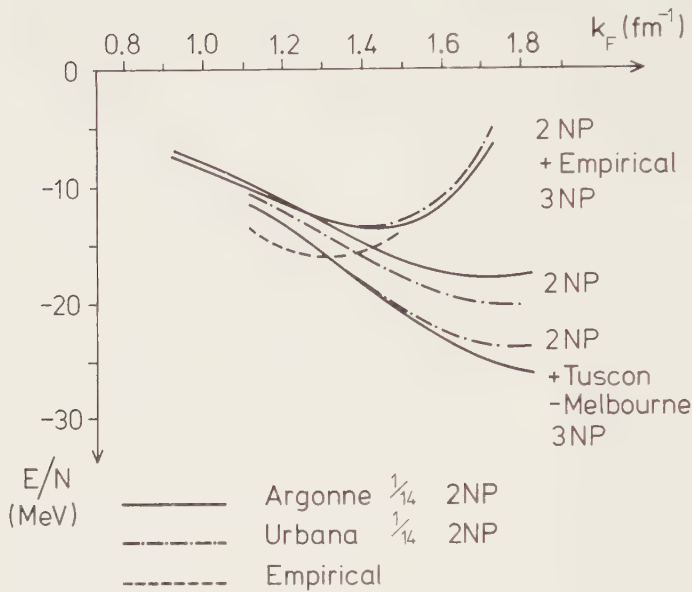


Figure 10

The saturation curves for the binding energy of nuclear matter, using two body potentials with meson theoretic and phenomenological 3NP (after ref. 46-48).

Note firstly that this approximate method, applied to the  $\pi\pi$ E-3NP gives 80% more binding energy than the more exact calculations of Wiringa et al. Note also that much of the attractive energy from  $\pi\pi$  exchange is cancelled by a repulsive contribution from  $\pi\rho$  exchange. Finally note that the  $\Delta$  contribution dominates the Kroll-Ruderman term, but that the Kroll-Ruderman term makes a significant contribution and should be retained.

It will be interesting to see how the inclusion of further correlations in the evaluation of the matrix elements of these shorter range terms in the meson exchange 3NP alters these results. We hope that the results of such a calculation will be available in the near future.



5. THREE NUCLEON POTENTIALS IN THE  $\alpha$  PARTICLE

The influence of 3NP in the  $\alpha$  particle is expected to be greater than its influence in the three nucleon system, simply because there are now many more triples which can interact through the 3NP. Three body forces in the  $\alpha$  particle have been studied by Coon et al.<sup>58</sup>, Tanaka et al.<sup>59,60</sup> and Wiringa et al.<sup>46-48</sup>. To illustrate the effects, Table VII gives the results obtained by Wiringa et al using the Tucson-Melbourne  $\pi\pi$ E-3NP, comparing the results with those obtained in the triton and nuclear matter. While the three body force does not provide enough additional binding for the triton, there is a slight tendency to overbind which is more pronounced in nuclear matter.

TABLE VII

Results obtained for  $^3\text{H}$ ,  $^4\text{He}$  and Nuclear matter by Wiringa et al,<sup>46-48</sup> for two body forces only, and with three body forces included.

	Two body interaction	Argonne $V_{14}$	Urbanna $V_{14}$
$^3\text{H}$	$E_2$	$-7.0 \pm 0.1$	$-7.2 \pm 0.1$
	$E_3$	-1.1	-0.9
	$E_{\text{tot}}$	$-8.1 \pm 0.1$	$-8.1 \pm 0.1$
$^4\text{He}$	$E_2$	$-22.1 \pm 0.3$	$-23.8 \pm 0.2$
	$E_3$	-7.7	-6.5
	$E_{\text{tot}}$	$-29.8 \pm 0.5$	$-29.3 \pm 0.5$
Nuclear Matter	$E_2/N$	-18.1	-20.0
	$E_3/N$	-9.5	-4.5
	$E_{\text{tot}}/N$	-27.6	-24.5

Tanaka<sup>60</sup> has emphasised the significance of the excited states of the  $\alpha$  particle as a probe of the structure of the three nucleon potential. The number of s state triples, and the spatial wave functions both change in going from the ground state to the excited states, as does the magnitude of the discrepancy when two body forces alone are used — it is about 6 MeV for the ground state and about 2 MeV for the excited states. Both Sato et al.<sup>61</sup> and Wiringa et al.<sup>46-48</sup> have studied the spectrum of excited states, and both have proposed to use this as an ingredient in the determination of the parameters of a phenomenological three body potential.

These investigations show promise that this may be a way of investigating the structure of the three body force provided we can satisfy ourselves that the

contribution from four body forces<sup>62</sup> is either negligible or reliably estimated!

## 6. OTHER APPLICATIONS OF THREE BODY FORCES

At a few body conference it is perhaps appropriate to emphasise the applications of 3NP to the traditional few body problems. There are however two other recent applications of the 3NP which are interesting because they emphasise different qualitative features of the interaction.

Andō and Bandō<sup>63</sup> have calculated the contribution of the three body force to the spin orbit splitting of one particle and one hole states in  $^{16}\text{O}$  and  $^{40}\text{Ca}$ . Using the 3NP of Martzolf et al.<sup>22</sup> they obtained a three body force contribution 20-30% of that obtained from two body potentials. Similar results were obtained using the Tucson-Melbourne potential when a large cut off ( $\Lambda \sim 8.5\mu$  in a monopole form factor) was used, but at  $\Lambda \sim 6\mu$  the 3NP contribution was dramatically reduced. We believe this work is important because it demonstrates that the spin orbit splitting is sensitive to the 3NP. With further work it could help us to decide between different models of the 3NP.

Coon, McCarthy and Vary<sup>64</sup> investigated the influence of 3NP on the magnetic transition form factors of  $^{17}\text{O}$ , which have been difficult to understand in the conventional shell model with only two body interactions<sup>65</sup>. They found that the Tucson-Melbourne  $\pi\pi\text{E}$ -3NP, in conjunction with meson exchange currents, was able to give a reasonable approximation to the observed form factors. Perhaps even more interesting was the fact that they showed that the Tucson-Melbourne  $\pi\pi\text{E}$ -3NP gave significantly better agreement than the Fujita-Miyazawa  $\pi\pi\text{E}$ -3NP. These results hold out the hope that we may have in the magnetic form factors not only evidence for the three body force, but a means of differentiating between different three body forces.

Both of these results are indications that one may find out more about the 3NP by looking at nuclear properties other than the binding energy. Further work along these lines should be encouraged.

## 7. PHENOMENOLOGICAL THREE BODY FORCES

It is clear that the short distance properties of the 3NP are not well determined by existing meson theoretic models. This of course parallels the situation of the two nucleon potential, where the short distance potential is not fixed by the meson theory, and is often parameterised.

A similar approach to the 3NP has been suggested by Wiringa et al.<sup>46-48</sup>, and by Tanaka and his collaborators<sup>59-61</sup>. In this approach a simple parameterised 3NP is written down, and the parameters are varied to obtain the best fit to data, usually chosen to be the  $A = 3$  and  $A = 4$  systems, and for Wiringa et al.<sup>46-48</sup> these systems with the saturation properties of nuclear matter. To

date a satisfactory fit to all of these data has not yet been obtained. That may be indicative of at least one of the following three difficulties:

(i) The form chosen for the 3NP may not be the appropriate one. An exhaustive study of the possible spin-isospin covariants has not been performed, as far as we are aware, but Ellis et al.<sup>24</sup> found 22 spin covariants to quadratic order in the nuclear momenta in their study of the  $\pi p$ -3NP. This is an indication that there is a rich field of possible structures waiting to be explored in constructing phenomenological potentials.

(ii) Four Body potentials<sup>62</sup>, or even multibody potentials<sup>66</sup>, may be important. The conventional argument<sup>62</sup> is that such potentials have negligible effects at normal nuclear matter densities. But the density dependence of such potentials is dramatic<sup>66</sup>, and they could influence the saturation properties of nuclear matter.

(iii) At short distances the potential concept may break down completely and we must deal directly with the quarks, rather than working with nucleons and mesons. This possibility has been argued forcefully at this conference, but we believe its relevance to "soft" nuclear physics at low momentum transfer remains to be established.

## 8. OTHER APPROACHES TO THE THREE BODY FORCE

It is intuitively clear that there are close connections between the two nucleon potential and the three nucleon potential, and that in an ideal world one would like to see both potentials obtained in a consistent way from the same underlying theory. The work of Fonsca and Peña<sup>67</sup> provides an attempt to do this in a model in which the 2NP is obtained in the Born-Oppenheimer molecular approach to the  $NN\pi$  system. At the present stage this model cannot be regarded as realistic, it may be interesting to relate it to the more conventional meson theoretic potentials in an attempt to learn more about the interrelationship between the 2NP and the 3NP.

Orlowski and Kim<sup>68</sup> have pointed out that an energy dependence in the two body potential introduces a three body potential when imbedded in the three body problem. In a qualitative sense one must anticipate this, because the introduction of the third particle will alter the energy of the two body subsystem. However there are difficulties involved in constructing a consistent set of three body equations for energy dependent potentials<sup>69</sup> and the prescription used by Orlowski and Kim, which is to set  $E_{12} = E_3 - q^2$  does not seem to overcome these difficulties. In general energy dependence of the two body potential reflects the suppression of degrees of freedom — in the case of interest to Orlowski and Kim these are the quark degrees of freedom — and it may be more straightforward to retain these degrees of freedom in the three

body problem or to project them out at the point, rather than construct a consistent set of three body equations for energy dependent potentials.

## 9. CONCLUSIONS

There is an increasing body of evidence that two nucleon potentials are not enough to account for the behaviour of many nucleon systems. Three nucleon potentials are the obvious next step to introduce in trying to understand that behaviour.

At present results obtained using  $\pi\pi$  exchange three nucleon potentials, which should dominate the long range behaviour of the 3NP show a great deal of sensitivity to the short range, or large momentum transfer properties, of the 3NP. The immediate task facing those who construct the 3NP in a fundamental way is to improve our understanding of the short distance régime of the 3NP. The construction of 3NP with heavier meson exchanges is one step which has been taken, but we would predict that, before Few Body XI, the quark model will be invoked to try to understand this part of the potential.

For those who use the 3NP we suggest two lines of approach that seem to us to be capable of providing useful insights into the presence and the nature of the 3NP. The first is in the study of break up reactions in the three body system, the second is the incorporation of the 3NP beyond the effective potential approximation in the construction of matrix elements of one body operators in many body systems, which has applications to spin orbit splitting and electromagnetic form factors. It is possible that these processes will be more sensitive to 3NP than the binding energy of many body systems.

Of course when we are satisfied we have understood the 3NP, and even before, we will need to start to worry about the effects of four body forces!

## REFERENCES

- 1) H. Primakoff and T. Holstein, Phys. Rev. 55 (1939) 1218.
- 2) I. Fujita and H. Miyazawa, Prog. Theor. Phys. 17 (1957) 360.
- 3) G.E. Brown, A.M. Green and W.J. Gerace, Nucl. Phys. A115 (1968) 435.
- 4) R.B. Wiringa, invited paper, Bochum Workshop (1983).
- 5) M.R. Robilotta, M.P. Isidro Filho, H.T. Coelho and T.K. Das, Contributions to this conference (pp. 226, 229) and Phys. Rev., to be published.
- 6) S.A. Coon, M.D. Scadron, P.C. McNamee, B.R. Barrett, D.W.E. Blatt and B.H.J. McKellar, Nucl. Phys. A317 (1979) 242;  
S.A. Coon and W. Glöckle, Phys. Rev. C 23 (1981) 1790 give some corrections to the potential.
- 7) S. Drell and K. Huang, Phys. Rev. 91 (1953) 1527.

- 8) R. Bhaduri, Y. Nogami and C.K. Ross, Phys. Rev. C 2 (1970) 2082;  
B.A. Loiseau, Y. Nogami and C.K. Ross, Nucl. Phys. A165 (1971) 601.
- 9) G.E. Brown and A.M. Green, Nucl. Phys. A137 (1969) 1.
- 10) G. Höhler, H.P. Jakob and R. Straus, Nucl. Phys. B39 (1972) 237;  
H. Nielsen and G.C. Dades, Nucl. Phys. B72 (1974) 310.
- 11) S. Adler, Phys. Rev. 137 (1965) B1022.
- 12) S. Weinberg, Phys. Rev. Lett. 17 (1966) 616.
- 13) S.A. Coon, private communication.
- 14) K. Shimizu, A. Polls, H. Müther and A. Faessler, Nucl. Phys. A364 (1981) 461.
- 15) See e.g. A.M. Green, Rep. Prog. Phys. 39 (1976) 1109.
- 16) Ch. Hajduk, P.U. Sauer and W. Strueve, Nucl. Phys. A405 (1983) 581;  
Ch. Hajduk, P.U. Sauer and S.N. Yang, Nucl. Phys. A405 (1983) 605.
- 17) I. Fujita, M. Kawai and M. Tamifuji, Nucl. Phys. 29 (1962) 252.
- 18) G.N. Epstein and B.H.J. McKellar, Lett. Nuovo Cim. 5 (1972) 807; Phys. Rev. D10 (1974) 2169; W.N. Cottingham, M. Lacombe, B. Loiseau, J.M. Richard and R. Vinh Mau, Phys. Rev. D8 (1973) 800.
- 19) M.G. Olsson and E.T. Osypowski, Nucl. Phys. B101 (1975) 136.
- 20) G. Ball and B.H.J. McKellar, University of Melbourne preprint UM-P-77/38 (1977); B.H.J. McKellar, G. Ball and R.G. Ellis, to be published.
- 21) M.G. Olsson and E.T. Osypowski, Nucl. Phys. B87 (1975) 399.
- 22) M. Martzolf, B. Loiseau and P. Grangé, Phys. Lett. 92B (1980) 46.
- 23) B.H.J. McKellar, S.A. Coon and M.D. Scadron, University of Arizona preprint (1981).
- 24) R.G. Ellis, S.A. Coon and B.H.J. McKellar, Contributions to this conference and R.G. Ellis, invited paper, Bochum Workshop (1983).
- 25) M.R. Robilotta and M.P. Isidro Filho, Contributions to this conference and Sao Paulo preprint IFUSP/P-380 (1982).
- 26) R.G. Ellis, contribution to this conference.
- 27) J.T. MacMullen and M.D. Scadron, Phys. Rev. D20 (1979) 1069, 1081.
- 28) N. Kroll and M.A. Ruderman, Phys. Rev. 93 (1954) 233.
- 29) N. Dombey and B.J. Read, Nucl. Phys. B60 (1973) 65.
- 30) S. Fubini, G. Furlan and C. Rossetti, Nuovo Cim. 40 (1965) 1161.
- 31) M.A.B. Beg, Phys. Rev. 150 (1966) 1276.
- 32) See e.g. K. Holinde, Phys. Rep. 68 (1981) 121.

- 33) A. Cass, Ph.D. Thesis, University of Melbourne (1980); D.W.E. Blatt, Ph.D. Thesis, University of Sydney (1974), and references 6 and 8.
- 34) A. Cass and B.H.J. McKellar, *Nucl. Phys.* B166 (1980) 399.
- 35) A. Cass and B.H.J. McKellar, *Phys. Rev.* D18 (1978) 3269.
- 36) U. Kaulfuss and M. Gari, Bochum preprint (1983).
- 37) See S. Brodsky, invited paper at this conference.
- 38) B.H.J. McKellar and R. Rajaraman, in "Mesons and Nuclei" (Edited by M. Rho and D. Wilkinson, North Holland Pub. Co., Amsterdam 1979) p. 357.
- 39) W. Glöckle, *Nucl. Phys.* A381 (1982) 343.
- 40) S. Muslim, Y.E. Kim and T. Ueda, *Nucl. Phys.* A393 (1983) 399.
- 41) A. Bömelburg, *Phys. Rev.* C28 (1983) 403.
- 42) See the paper by S.A. Coon and W. Glöckle in ref.6.
- 43) J. Torre, J.J. Benayoun and J. Chauvin, *Z. für Physik* A100 (1981) 319.
- 44) A. Bömelburg and W. Glöckle, Bochum Preprint (1983), and A. Bömelburg, invited paper, Bochum Workshop (1983), *Phys. Rev. C* (in print).
- 45) A. Bömelburg, W. Glöckle and W. Meier, contribution to this conference.
- 46) R.B. Wiringa, *Nucl. Phys.* A401 (1983) 86.
- 47) J. Carlson, V.R. Pandharipande and R.B. Wiringa, *Nucl. Phys.* A401 (1983) 59.
- 48) See ref.4, and R.B. Wiringa, paper presented at 3rd International Conference on Recent Progress in Many Body Theories (1983).
- 49) J.L. Friar, E.L. Tomusiak, B.F. Gibson and G.L. Payne, *Phys. Rev.* C24 (1980) 677.
- 50) Ch. Hajduk, invited paper, Bochum Workshop (1983); S.N. Yang, invited paper, Bochum Workshop (1983); See also ref.16.
- 51) A. Delfino, invited paper, Bochum Workshop (1983).
- 52) B.A. Girad and M.G. Fuda, *Phys. Rev.* C19 (1979) 579.
- 53) J.L. Friar, B.F. Gibson and G.L. Payne, *Comments Nucl. Part. Phys.* 11 (1983) 51.
- 54) I. Slaus, Y. Akaishi and H. Tanaka, *Phys. Rev. Lett.* 48 (1982) 993.
- 55) W. Meier, invited paper, Bochum Workshop (1983).
- 56) M. Karus et al. contribution to this conference.
- 57) R.G. Ellis, S.A. Coon and B.H.J. McKellar, TRIUMF preprint (1983).
- 58) S.A. Coon, J.G. Zabolitzky and D.W.E. Blatt, *Z. Phys.* A281 (1977) 137.

- 59) H. Tanaka (editor), *Prog. Theor. Phys. Supp.* 56 (1974); T. Katayama, Y. Akaishi and H. Tanaka, *Prog. Theor. Phys.* 67 (1982) 236.
- 60) H. Tanaka, invited paper, Bochum Workshop (1983).
- 61) M. Sato, Y. Akaishi and H. Tanaka, *Prog. Theor. Phys.* 66 (1981) 930.
- 62) D.W.E. Blatt and B.H.J. McKellar, *Phys. Rev. C* 11 (1975) 2040.
- 63) K. Andō and H. Bandō, *Prog. Theor. Phys.* 66 (1981) 227.
- 64) S.A. Coon, R.J. McCarthy and J.P. Vary, *Phys. Rev. C* 25 (1982) 756.
- 65) R.J. McCarthy and J.P. Vary, *Phys. Rev. C* 25 (1982) 73.
- 66) B.H.J. McKellar and R. Rajaraman, *Phys. Rev. Lett.* 31 (1973) 1063; *Phys. Rev. C* 10 (1974) 871; D.W.E. Blatt and B.H.J. McKellar *Phys. Rev. C* 12 (1975) 637.
- 67) A.C. Fonseca and M.T. Peña, contributions to this conference. and A.C. Fonseca, invited paper, Bochum Workshop.
- 68) M. Orlowski and Y.E. Kim, contributions to this conference.
- 69) B.H.J. McKellar and McKay, *Austr. Journal of Physics* (to be published)





## RECENT DEVELOPMENTS IN FEW-PARTICLE SCATTERING THEORY<sup>\*</sup>

K.L. KOWALSKI

Department of Physics, Case Western Reserve University, Cleveland, Ohio  
44106 USA

Work since 1980 on dynamically complete scattering theories in reviewed.

### 1. INTRODUCTION

Few-body methods are distinguished from conventional ones by their representation of a complete description of the physics. The latter ones, about which we have a lot to say, provide a self-consistent calculational scheme only after the particular truncation of the physics characteristic of the method has been imposed. Nonetheless, conventional methods have been of interest lately because they are viable and people do calculate with them (two attributes that have been painfully absent from few-body efforts for  $N > 4$ ) and because the clean extraction of the low-order approximations they suggest from full sets of scattering integral equations has proven to be fairly difficult.

How good are the standard algorithms and what should we look for in attempting to improve upon them? A hint can be found in the following observation<sup>1</sup>:

"...When the standard methods are applied to real reactions they can give acceptable results only because of the flexibility introduced by the use of effective interactions. These difficulties should be borne in mind when evaluating the apparent success of nuclear reaction theories."

Can we define and then systematize the calculation of these effective interactions? Most of this review is dedicated to work over the last three years attempting to answer this question based on  $N$ -particle scattering theory. The last reviews are given at Eugene<sup>2</sup>. Ref. 3 can serve as an introduction to the concepts and the notation used here. The otherwise excellent review in Ref. 4 ignores the formulation of Chandler and Gibson (C-G)<sup>5-7</sup>. Many of the ideas implicit in the C-G approach are valuable in sorting out the ambiguities endemic to truncated multichannel problems.

### 2. THE OPTICAL POTENTIAL

Although the optical potential (OP) is the archtypical effective interaction, it means quite different things to different people. By whatever criterion, there has been an extraordinary surge of interest of late in the OP. A major portion of this new work is a completion and modernization of the type of OP formalized by Feshbach<sup>8</sup> for distinguishable particles.

<sup>\*</sup>This work was supported in part by the National Science Foundation.

A two-body effective interaction (EI),  $U(\vec{p}', \vec{p})$  generates the amplitude for the elastic scattering of two composite objects:

$$T(\vec{p}', \vec{p}) = U(\vec{p}', \vec{p}) + \int (d\vec{p}'') \frac{U(\vec{p}', \vec{p}'') T(\vec{p}'', \vec{p})}{E - E'' + i\epsilon} . \quad (2.1)$$

An OP differs from an arbitrary EI by its singularity and reality structure; its antihermitian part is supposed to reflect the loss of flux from the elastic channel due to inelastic processes. This is equivalent to the stipulations

$$V_{\text{opt}}(z^*)^\dagger = V_{\text{opt}}(z) \quad , \quad (\text{h.a.}) \quad , \quad (2.2a)$$

$$\text{Disc } \{V_{\text{opt}}\} \text{ Elastic cut} = 0 \quad , \quad (2.2b)$$

upon the OP operator  $V_{\text{opt}}(z)$ , where  $z$  is a complex energy, which ensures that  $V_{\text{opt}}(z)$  is hermitian below the inelastic threshold. While it is easy to find EI's satisfying (2.2b) by separating out the discontinuity across the elastic unitarity cut<sup>9</sup>, the hermitian analyticity (h.a.) requirement (2.2a) is more difficult to satisfy.

The Feshbach<sup>8</sup> formalism is a neat realization of (2.1) - (2.2) for the scattering of two bound clusters ( $\beta$ ) of distinguishable particles, where for the elastic operator,  $T_{\beta,\beta}(z) = V^\beta + V^\beta G(z) V^\beta$  ,

$$T_{\beta,\beta}(z) = V_{\text{opt}}(\beta, z) + V_{\text{opt}}(\beta, z) G_\beta(z) P_\beta T_{\beta,\beta}(z) \quad , \quad (2.3)$$

$$V_{\text{opt}}(\beta, z) = V^\beta + V^\beta Q_\beta [z - Q_\beta H Q_\beta]^{-1} Q_\beta V^\beta \quad , \quad (2.4)$$

where  $z$  is taken to be  $E + i0$  in the scattering limit. [The validity of the renowned (2.4) above the threshold for rearrangement reactions has been called in question by Tobocman<sup>10</sup>.] The projection-operator technique removes the elastic unitarity cut structure from  $V_{\text{opt}}(\beta, z)$  and the hermiticity of  $V^\beta$  implies (2.2a) for  $V_{\text{opt}}(\beta, z)$  which is therefore hermitian for  $z$  not in the spectrum of  $Q_\beta H Q_\beta$  that, for simplicity, we take to be below the inelastic threshold. The pole singularities of  $V_{\text{opt}}(\beta, z)$  can be identified with resonant structure<sup>8</sup>.

Apart from interpretational questions (energy averaging, e.g.), the major problem with (2.4) is its calculation and a systematic way of doing this was proposed only recently<sup>9,11</sup>. We emphasize that the definition of (2.4) is entirely independent of any formalism used to calculate it. Particle identity presents a formidable obstacle to the generalization of (2.3) and (2.4). Feshbach's 1962 paper<sup>8</sup> includes identity in the projection operator formalism to obtain an effective (total) Hamiltonian, but not an optical potential<sup>12c,12d</sup>

For the generalization of (2.3), (2.4) one requires a (anti-) symmetrized transition operator,  $T(\hat{\beta})$ , formed from a class ( $\hat{\beta}$ ) of exchange-equivalent

rearrangement operators,  $T^{\beta, \bar{\beta}}, \beta \in \hat{\beta}$ ,

$$T(\hat{\beta}) = \sum_{\beta \in \hat{\beta}} A_{\beta, \bar{\beta}}^{\dagger} T^{\beta, \bar{\beta}}, \quad (2.5)$$

where  $A_{\beta, \bar{\beta}}$  is an exchange operator corresponding to the permutation that maps the canonical partition,  $\bar{\beta}$ , into  $\beta \in \beta$ . Note that  $T(\hat{\beta})$  depends on the off-shell form of  $T^{\beta, \bar{\beta}}$  as well as  $\bar{\beta}$ , although the scattering amplitudes depend on neither. An antisymmetrized OP operator,  $U(\hat{\beta}, z)$ , can be defined in terms of  $T(\hat{\beta}, z)$  as<sup>13</sup>

$$T(\hat{\beta}, z) = U(\hat{\beta}, z) + U(\hat{\beta}, z) G_{\bar{\beta}}(z) T(\hat{\beta}, z). \quad (2.6)$$

Only matrix elements of

$$V_{\text{opt}}(\hat{\beta}, z) \equiv P_{\bar{\beta}} U(\hat{\beta}, z) P_{\bar{\beta}} \quad (2.7)$$

are required in the elastic scattering problem but different off-shell extensions of  $T_{\beta, \bar{\beta}}(z)$  still yield different OP's<sup>12,13</sup>. The "symmetrical" AGS<sup>14</sup> off-shell extension,

$$G = \delta_{b,a} G_a + G_b T_{b,a}^{\text{AGS}} G_a, \quad (2.8)$$

yields an OP satisfying (2.2) and so that below the inelastic threshold the elastic scattering is described by a hermitian potential. This does not work for the so-called post or prior extensions, which yield effective interactions satisfying neither (2.2a) or (2.2b), because the  $T_{b,a}^{(\pm)}(z)$  are not h.a., while the  $T_{b,a}^{\text{AGS}}(z)$  are<sup>12a</sup>. AGS is not unique in this respect and any nonpathological, "symmetrical",  $T_{b,a}$  will generate an OP with the desired properties<sup>12</sup>; Bencze and Chandler<sup>6</sup> have generalized the work of Ref. 9 using such a  $T_{b,a}$ . The connected-kernel (CK) OP formalism proposed Ref. 10 using a C-G-type coupling scheme is a trivial application of the work of Refs. 6,9. The OP's introduced by Adhikari<sup>15</sup> are incorrectly defined in terms of the inversion of an operator that cannot possess an inverse.

In view of the proposals of Ref. 16, we show how easy it is to satisfy only (2.2b). If we introduce the channel coupling scheme  $V^a = \sum V^{a,c}$ , then the post transition operators, satisfy<sup>9</sup>

$$T^{(+)} = \Gamma \hat{G} S \hat{G}^{-1} + \Gamma \hat{G} P T^{(+)} \quad (2.9)$$

where  $\hat{G} = (G_a \delta_{a,b})$ ,  $S_{a,b} = 1$ ,  $P = (P_{\alpha} \delta_{a,b} \delta_{a,\alpha})$ ,  $P_{\alpha}$  is a two-cluster bound state projector, and  $(Q = I - P)$

$$\Gamma = V + V \hat{G} Q \Gamma = V + \Gamma \hat{G} Q V. \quad (2.10)$$

We assume nonidentical particles for simplicity. Clearly  $\Gamma$  satisfies (2.2b) but not (2.2a).  $T_{\alpha,\alpha}^{(+)}$  is half-shell equivalent to

$$\tilde{T}_{\alpha,\alpha}^{(+)} = \Gamma_{\alpha,\alpha} + \Gamma_{\alpha,\alpha} G_{\alpha} P_{\alpha} \tilde{T}_{\alpha,\alpha}^{(+)} \quad (2.11)$$

so  $\Gamma_{\alpha,\alpha}$  is a non-h.a., formalism-dependent (on the choice of  $V$ ) EI. With the prior extension we obtain similar results but with  $\Gamma$  replaced by  $\Gamma^t$  (given by (2.10) with  $V \rightarrow V^t, t \equiv \text{transpose}$ ). It is trivial to extend this to the antisymmetrized case<sup>9</sup>.

The antisymmetrized forms of  $\Gamma^t$  appropriate to a given Pauli-equivalent set of two-cluster partitions are the "new class of OP's" proposed by Adhikari, Kozack and Levin<sup>16</sup>, but according to our requirements for an OP the  $\Gamma, \Gamma^t$  are not OP's but EI's. Even in the nonidentical case  $\Gamma_{\alpha,\alpha}$  is quite distinct from the Feshbach  $U_{\alpha,\alpha}$  and depends upon the choice of  $V^a, c$ . Approximate  $\Gamma, \Gamma^t$  may give rise to  $\tilde{T}_{\alpha,\alpha}^{(\pm)}$  that violate unitarity even below the inelastic threshold: (2.2b) is not enough. The preceding discussion also shows that the particular wave function formalism used in Ref. 16 is really irrelevant and provides no preferred status to  $\Gamma, \Gamma^t$ .

Note that the same approximate  $\Gamma$ , e.g., will yield different on-shell elastic amplitudes depending upon whether (2.11) or the standard<sup>9</sup> OP formalism is used. The general properties of  $\Gamma$  and implicitly  $\Gamma^t$  (cf. Ref. 17) are studied in Ref. 9.

Finally, we note that Bencze and Chandler<sup>18</sup> have shown that the curious energy-independent OP<sup>19</sup> is the abstract form of Feshbach's OP appropriate for time-dependent scattering theory and thus carries no new physical content. Identity and unitarity questions still remain unanswered in this formalism.

The properties of  $V_{\text{opt}}^{\text{AGS}}(\hat{\beta}, z)$  have been investigated using conventional, Refs. 10,12,20-22, and CK, Refs. 9,13,23, techniques. This OP satisfies (2.2), includes all effects of particle identity, is formalism independent, incorporates the Feshbach resonance structure, and is related to the antisymmetrized Feshbach effective Hamiltonian by a nondynamical transformation.

These last properties, along with some applications to multiple l2c and inelastic scattering<sup>22</sup> have been developed using the conventional formal operator algebra that would involve illegitimate operator inversions if the scattering limit (S.L.)  $z \rightarrow E + i0$  were taken prematurely. For example, although the "solution"  $[1 - V^\alpha G_\alpha(z)]^{-1} V^\alpha$  of the LS equation  $T_{\alpha,\alpha}(z) = V^\alpha + V^\alpha G_\alpha(z) T_{\alpha,\alpha}(z)$  does not exist in the S.L., for complex  $z$  it can be rearranged to yield the "closed form",  $T_{\alpha,\alpha}(z) = V^\alpha + V^\alpha G(z) V^\alpha$ , which is well defined on the cut. Alternatively, this heuristic procedure can be discussed in terms of LS nonuniqueness as merely an algorithm for projecting out all but the desired particular solution<sup>11</sup>. Tobocman<sup>10</sup> has questioned this and has insisted, in effect, but without substantiation, that all intermediate inversions must also be S.L.-defined. The assessments of various OP's in Ref. 10 appear incorrect in that they are based upon irrelevant criteria. Unitarity necessarily requires the S.L. and one must be careful; e.g. the treatment in Ref. 24 is not generally correct.

All of the recent work<sup>12c,20,22,25</sup> combining identity with multiple scattering (MS) formalisms fail to achieve this while taking identity into account in all of the intermediate scatterings. The Green's function  $G_\beta$  for the two-cluster channel of interest that appears in all of the constituent operators in Refs. 12c,20,22 contains no restriction on the permutation symmetry of the  $\beta$ -cluster states. Thus, any approximation scenario necessarily involves uncertain assumptions about the role of these unsymmetrical states. Surprisingly, the well-known KMT<sup>26</sup> formalism has the same defect even in the case where projectile identity is ignored. The tricks that have been proposed<sup>12c,20,22,26</sup> in the KMT case in order to retain a MS structure pay the steep price of re-entering the full Hilbert space and bringing back improperly symmetrized target states. The cumulant-type expansions used in Refs. 12c,20,22 for either the AGS-or-post-generated OP's with identity also have the serious shortcoming of failing to identify the role of the heavy-particle exchange terms. This is not the case in Ref. 25, but here the avoidance of antisymmetrized subsystem operators requires an unphysical split of the two-nucleon potentials into direct and exchange parts. The virtues of the post off-shell extension (as contrasted to AGS) put forth in Refs.<sup>12c,20,22,27</sup> are based on circular reasoning concerning the generation of the "correct" MS structure; this is ambiguous because of the unsymmetrized-target-state problem. It appears one really needs a full-blown N-particle formalism to give credence to some of the MS approximations to the OP with full account of particle identity<sup>23</sup>.

A natural low-order approximation to  $V_{\text{opt}}^{\text{AGS}}$  yields an equation for the projected wave function that is tantalizing close to that of the RGM method. This "close encounter" is deceptive because the two methods refer to different associations with the elastic transition operator (see Sec. 3).

### 3. EFFECTIVE INTERACTIONS FOR REARRANGEMENT

A spate of articles<sup>15b,28</sup> have recently appeared concerning the widely used coupled-reaction channel (CRC) method motivated by ambiguities in the definition of the approximation and the related difficulty of recovering some version of the CRC from an N-body theory.

Ultimately the CRC method defines a set of EI's,  $U_{\alpha\beta}(A)$ , referring to a distinguished set  $A = \{\alpha, \beta, \dots\}$  of two-cluster channels characterized by the projectors  $P_\alpha, P_\beta, \dots$ , the union of whose ranges span the relevant model space. The rearrangement transition operators are then determined from

$$T_{\alpha\beta} = U_{\alpha\beta}(A) + \sum_{\gamma \in A} U_{\alpha\gamma}(A) G_\gamma P_\gamma T_{\gamma\beta}, \quad (3.1)$$

where either  $U_{\alpha\beta}(A)$  is given and (3.1) determines  $T_{\alpha\beta}$ , or a given off-shell extension for  $P_\alpha T_{\alpha\beta} P_\beta$  specifies  $U_{\alpha\beta}(A)$ .

It is easy to construct (for specious reasons)  $U_{\alpha\beta}(A)$  that lead to ill-defined (3.1). For example, the hermitian choice [Ref. 28d, Eq. (6.13)]

$$U_{\alpha\beta}^{\text{wrong}} = V^{\beta} - \delta_{\alpha\beta} G_P^{-1} \quad (3.2)$$

implies  $1 - U^{\text{wrong}} \hat{G} = S G^{-1} \hat{G}$ , so Eqs. (3.1) cannot be inverted. (In Ref. 15 it is implicitly assumed that  $S^{-1}$  exists.) This is why the "recovery" in Ref. 28d of the wave function form of the CRC within an otherwise correct formalism is incorrect. The reason<sup>29q</sup> that this recovery attempt is incorrect is that the  $U_{\alpha\beta}$  for a formalism designed for the projections,  $P_{\beta}|\psi^{(+)}\rangle$  of the full wave function is being forced to yield approximate wave equations for the components,  $|\psi_{\beta}\rangle$ , of the wave function in the model space  $H_{\pi}$ . This strategy is contradictory and does cause difficulties in Ref. 28l but is really irrelevant to the primary thrust of Ref. 28d.

More promising choices for  $U_{\alpha\beta}(A)$  can be obtained in a less ad hoc manner. The traditional way is to attempt the consistent solution of the Schrödinger (wave) equation in  $H_{\pi}$ <sup>28a</sup>, but this is plagued by the nonorthogonality (N-0) and possibly, overcompleteness (O-C) difficulties that have sparked much of the recent controversy. Dealing with this is an important aspect of the C-G theory<sup>5-7,28k</sup>. The device of the Moore-Penrose (M.P.) generalized inverse<sup>29</sup> has also proven to be effective in the two-cluster CRC case<sup>28p,q</sup>.

O-C occurs when there are components such that  $\sum^{(A)} P_{\beta}|\hat{\phi}_{\beta}\rangle = 0$ , so that the  $P_{\beta}$  are not independent. It is in such cases that the M.P. inverse,  $M^{-1}$ , of the bounded operator  $\sum^{(A)} P_{\beta}$ , e.g.,  $M^{-1}(\sum^{(A)} P_{\beta}) = P_{\pi}$ , where  $P_{\pi}$  is the projector onto  $H_{\pi}$ , is introduced to deal with the N-0 contributions.

A major question is whether O-C appears for physically realistic situations. The arguments of Cotanch and Vincent<sup>30</sup> strongly suggest that it does not; the counterexample posed in Ref. 28p violates translational invariance. When  $A =$  Pauli-class  $\hat{\beta}$ , it has been shown<sup>12b</sup> that no O-C occurs.

Birse and Redish<sup>28p,q</sup> clarify several CRC-related issues by providing a unique definition  $|\psi_{\beta}\rangle = P_{\beta} M^{-1}|\psi^{(+)}\rangle$  of the components and a reciprocal mapping to the projections  $|\bar{\psi}_{\beta}\rangle = P_{\beta}|\psi^{(+)}\rangle$ . Most of their work is based on the expectation that O-C is or "almost is" a problem. Their effective interaction is found to be

$$U_{\alpha\beta}^{\text{BR}} = P_{\alpha} V^{\alpha} P_{\pi} M^{-1} P_{\beta} \quad (3.3)$$

where  $V^{\alpha} = P_{\pi}(H - H_{\alpha})P_{\pi}$ , and  $H$  is the  $P_{\pi}$ -space effective Hamiltonian. Although (3.3) is non-h.a., it is free of A-class elastic unitarity cuts and because  $H$  is hermitian is expected to generate the correct model space unitarity relations; a direct proof using (3.1) and (3.3) would be more convincing. Birse<sup>28q</sup> has extended the result of Ref. 12d from  $\hat{\beta}$  to an arbitrary set  $A$  by finding an expres-



sion for  $U_{\alpha\beta}^{\text{AGS}}$ , defined by (3.1) with AGS for  $T_{\alpha,\beta}$ <sup>13,28d</sup>.

There has been much interest in the comparison of the (low-order) CRC (RGM) with approximations to connected-kernel (C-K) equations or to other approaches. Some numerical tests<sup>31</sup> indicate that CRC (RGM) calculations for a three-body system are superior to undistorted C-K calculations on the same  $L^2$  function space, but seem only to imply that a specific technique designed for a particular formalism (CRC) does not work equally well with other formalisms. Overall the CRC (RGM) is regarded useful enough to investigate its possible improvement and/or justification by embedding it within a full scattering theory.

This embedding has been accomplished<sup>28k</sup> in what is certainly a super-CRC formalism, viz. the C-G method<sup>5</sup>; this approach is compared with other methods in Ref. 28p. An attempt<sup>28m</sup> to salvage some of Ref. 15b results in a general CRC formalism that bears some similarity to the C-G method.

The approach of Ref. 28d with a h.a. EI free of the model-space unitarity cuts is complete in the sense of providing a set of C-K equations for the EI. [The reduction procedure of Ref. 28g reproduces some results of Ref. 28d and proposes clustered sets of successive effective interaction equations. Cf. Ref. 28c.] Although it is clear what approximation to  $U_{\alpha\beta}^{\text{AGS}}$  yields the low-order CRC, it is not at all evident how to recover this from the C-K formalism. The study of systematic approximations to the C-K equations for  $U_{\alpha\beta}^{\text{AGS}}$  has only begun<sup>23</sup>; note that although approximate solutions will be free of A-space unitarity cuts, the h.a. property may not be preserved.

Birse and Redish<sup>28p</sup> show how the lowest-order approximation ( $H \approx H$ ) to their version of the CRC is a distorted version of the so-called precursor BRS equations in the wave function form advocated by Levin<sup>32</sup>. The low-order CRC is recovered in the pole approximation (basically the famous BSA) via a suitable choice of distorting potentials, thus rendering irrelevant much, but not all, of the speculation about CRC vs. C-K. The physical circumstances under which this constitutes a good approximation are not specified, nor is the equivalent approximation to the undistorted C-K equations. The freedom of choice of distorting potential is dynamically ad hoc and so the demonstration of Ref. 28p is not a true embedding proof; nevertheless, these results may lead to C-K equation-based improvements to the CRC and at the very least indicate the inequivalence of the naive BSA to the CRC. Recent numerical work seems to suggest that the undistorted BSA is a poor representation of the physics<sup>33</sup>.

#### 4. FURTHER C-K APPLICATIONS TO REACTION THEORY

The formulation of the CRC (RGM) seems simplest in terms of wave function equations, and insight has been achieved using wave function formalisms obtained from C-K theories<sup>16,28p,32</sup>. Levin<sup>32</sup> has exploited the equations<sup>34</sup> involving

the components<sup>3</sup>

$$\psi_{\alpha}^{(b)} > = (G^t \hat{G}^{-1})_{b\alpha} |\hat{\psi}_{\alpha}^{(b)} >, \quad (4.1)$$

where  $G^t = \hat{G} + \hat{G} V^t G^t$  and  $\bar{V}S = VS$ , that are referred<sup>32</sup> to as "true" in that if  $b = \beta$  (two-cluster), then only  $|\psi_{\alpha}^{(\beta)} >$  contributes asymptotically to the  $\alpha \rightarrow \beta$  transition. This nonunique attribute, is probably better designated well-labeled<sup>3</sup> and requires that the kernel  $K^t = \hat{G} V^t$  become connected after a finite number of iterations<sup>34</sup>. The C-K equations for  $|\psi_{\alpha}^{(b)} >$  are somewhat cumbersome because of the t-operation and because  $T^{(-)} = \hat{G}^{-1} S \hat{G} V^t (G^t \hat{G}^{-1})$  the relationship to physical transition amplitudes is a bit contorted. This leads to the complications encountered in Ref. 32. The seemingly more natural (e.g.,  $T^{(+)} = VGS\hat{G}^{-1}$ ) choice of components  $(G\hat{G}^{-1})_{b,\alpha} |\hat{\psi}_{\alpha}^{(b)} >$  is<sup>3</sup> independent of  $b$  (not well-labeled or "true") and equal to  $|\hat{\psi}_{\alpha}^{(+)} >$ . Given the operator representation  $G^t \hat{G}^{-1}$  the antisymmetrization of formalism is easy<sup>16</sup> when  $V$  is label transforming.

Few-cluster models for reactions derive their physical validity in circumstances where a few ( $n_0$ ) clusters of particles are so tightly bound (clusters  $\sim \hat{O}$  = dominant<sup>35</sup> partition) that the possibility of their breakup can be ignored in the explicit dynamics but may be represented implicitly via the intercluster EI's. Ref. 36a (PR) is an ambitious attempt at a physically consistent theory of few-cluster models; Ref. 36b is a BLKT-type version of PR, while some of the relevant mathematical equations are discussed in Refs. 29, 36c. A version of the PR formalism with an explicit MS structure is obtained in Ref. 36d for arbitrary  $n_0$  as well as  $n_0 = 3$  specializations. The PR (and BRS) approach for  $n_0 = 3$  is also explored in Ref. 36e. This may be viewed as the formal recovery of ad hoc three-cluster models. We do not review the considerable work on the latter.

A different (based on two-particle-connected equations<sup>37</sup>) approach to few-cluster models is adopted by Vanzani et al<sup>28g,o,35,37</sup>. The limitations arising from indexing by chains of partitions (COP) have been removed and the leading few-cluster model equations directly involve the relevant physical transition amplitudes.

## 5. N-PARTICLE SCATTERING THEORY

Chains of Partitions: The scattering equations proposed by Yakubovsky, et al<sup>3,4</sup> are labeled by COP and involve a complex organization of operators leading to intimidating derivations partly due to the fact that the combinatorics of COP have not been worked into as convenient forms as that for partitions. A significant step towards understanding the COP structure is taken in Ref. 38 and is studied further in Refs. 37, 39. An important technical advance involves the decompositions of the partition-labeled operators  $V_a, H_a, G_a$ , etc, into chain-elementary-components<sup>38</sup> which have been placed into convenient forms in Ref. 39 and

then exploited to develop chain-elementary C-K resolvent equations representing the scattering in its most finely-decomposed form and from which all of the various scattering equations can be derived<sup>39</sup>. The infamous Yakubovsky<sup>40</sup> recurrence relations are circumvented and the inductive development advocated by Sandhas<sup>41</sup> is justified. Haberkott<sup>42</sup> has found partial decoupling of the AGS equations so the only transition operators appearing are labeled by those two-cluster partitions corresponding to a definite split  $(n, N-n)$  of the  $N$  particles into clusters of fixed numbers of particles. This is achieved via EI's that contain the suppressed channels. In the case of identical particles, a reduction to a single integral equation is obtained. Some combinatoric results relevant to COP equations for identical particles, have been obtained by Karlsson<sup>43</sup>.

Partition-Labeled Theories: The structure underlying scattering theory can be expressed in terms of graph and lattice theories. The former codifies our intuitive notions of connectivity while the latter is exploited to study the properties of sets of partitions. The classification of partition-labeled  $N$ -particle operators by their connectivity leads to nontrivial combinatorial problems that are investigated in Ref. 44 using the partition lattice; these results have been applied in quantum field theory and relativistic quantum mechanics<sup>45</sup>.

A number of papers<sup>46</sup> depend crucially upon the remarkable properties, Refs. 36c, 44, 46d, of the matrix<sup>17</sup>  $\bar{\Delta}_{a,b}$  ( $\bar{\Delta}_{a,b} = 1$  if  $a \not\supset b$  and  $= 0$ , if  $a \supset b$ ) and its various submatrices, square or nonsquare. These results are used in Ref. 46c to invert the BRS equations to obtain the Rosenberg equations and to derive the Watson-type multiple scattering equations with a connected-kernel (but  $N$ -body constituent operators) obtained first in Ref. 46b. New inversion properties of the restrictions of  $\bar{\Delta}$  are proven in Ref. 46d and these are exploited to obtain new C-K equations for the antisymmetrized transition operators that possess relatively little or no coupling. In Refs. 46a,b (The derivation of the BRS equations there is not "new".) great emphasis is placed upon the attainment of  $N(N-1)/2$  rather than  $(2^{N-1} - 1)$  C-K equations for the two-cluster amplitudes that are dynamically equivalent to the BRS equations; the "inframinimal" claims here do not contradict the minimal coupling theorem<sup>47</sup> and the realistic case of identical particles causes problems unanticipated in Refs. 46a,b. [The inference<sup>48</sup> that the minimal set of two-cluster partitions is also maximal is false.] The essential simplicity of Rosenberg's equations and their multiparticle extensions<sup>46c</sup> can be appreciated via graphical arguments<sup>4,49</sup>.

C-G Theory: A number of important developments and applications of the G-G<sup>5</sup> theory have taken place since 1980<sup>6,7,50</sup>. Elementary derivations of the C-G

equations (and variants) for the projected transition operators  $T_{ba} \equiv P_b T_{ba}^{(-)} P_a$  have appeared<sup>7,51</sup> that depend on the existence of  $X^{-1} = \left( \sum^A P_a \right)^{-1}$ , where  $A$  is some set of partitions (In the C-G theory  $A = \text{all}$  and  $X = JJ^*$ ; in Ref. 51,  $A = \text{all two-clusters}$ ,  $X \equiv M$ .) If this is the case, then since  $I = X^{-1} \sum^A G_c P_c G_c^{-1}$  and  $T_{ba}^{(-)} = V^a + V^b G I V^a = G_b^{-1} G V^a$ , we obtain the C-G equations

$$T_{ba} = P_b V^a P_a + P_b V^b X^{-1} \sum_c G_c P_c T_{ca} \quad (5.1)$$

C-G type equations have been found<sup>50</sup> that do not contain  $X^{-1}$ ; a C-K version of the C-G equations has been derived<sup>7</sup> that appears, however, to possess some complications with identity. The real spirit, and the possibly tremendous power, of the C-G approach is to circumvent the C-K problem via the construction of an appropriate sequence of approximate transition operators that do satisfy C-K integral equations<sup>50</sup>. At this stage C-G seem to be in the unique position of having formulated a comprehensive scattering theory replete with a well-defined and consistent set of approximations and a solid backdrop of rigorous mathematical theorems.

Pathologies: Bugbears persist in few-particle scattering theory. Spurious solutions are a potential, but possibly not serious problem for reduced C-K equations with kernels of high connectivity; factorizations indicating possible spuriousities are obtained in Refs. 52. Some of the spuriousities pointed out by Chandler are characteristic of Federbush model rather than the reduced C-K equations<sup>53</sup>.

Bencze and Chandler<sup>54</sup> have shown that the much-abused Lippmann identity (L.I.) holds in the weak topology, disproving earlier claims<sup>55</sup>; the L.I. is studied in Ref. 46b, and in Ref. 56 the L.I. is taken as a weak limit and used to derive the LS equations.

A few years ago the very foundation of standard C-K theory was threatened by the seeming existence of scattering solutions of the homogeneous C-K integral equations for some special situation<sup>57a</sup>. These arguments were shown to imply a contradiction with a known theorem<sup>57b</sup> and, more incisively, to involve the violation of the necessary requirement

$$\lim_{\epsilon \rightarrow 0} K(\epsilon) |\Psi(\epsilon)\rangle = K(\epsilon \rightarrow 0) |\Psi\rangle \quad , \quad (5.2)$$

where  $K(\epsilon)$  is the relevant (singular at  $\epsilon \rightarrow 0$ ) kernel and  $|\Psi\rangle = \lim |\Psi(\epsilon)\rangle$ , leading to  $K(\epsilon \rightarrow 0) |\Psi\rangle \neq |\Psi\rangle$  and no paradox. [It is claimed in Ref. 46b that the results of Ref. 57a result from an improper use of the L.I.] K.S.P.<sup>57c</sup> claim to demonstrate that (5.2) is not necessary for the type of problems (e.g., two particles in an external field and, in general, noninteracting subsystems of  $N$  particles) they consider. They also claim Sloan's<sup>57b</sup> observation actually supports their argument. K.S.P. propose scattering integral equations that

presumably do not have the difficulties that bother them. Evidently we will hear more about this as time goes on. We should also hear more about the problems, also involving singular limits, that are claimed by Tobocman<sup>10</sup> to exist in manipulations of more conventional operator groupings.

N  $\geq$  4: Ref. 58 contains a review of the 4-nucleon scattering problem and describes calculations carried out using Hilbert-Schmidt (H.S.) techniques. Noyes<sup>59</sup> has proposed an N = 4 version of his N = 3 zero-range scattering theory.

Much recent N = 3 work concerns separable representations of the off-shell input into the N = 4 equations<sup>60</sup>. For the N = 3 system itself, calculations using a new iterative technique<sup>61</sup> and the HS method<sup>62</sup> have appeared. Eyre et al.<sup>63</sup> have used a cluster-expansion formalism to carry out model calculations employing an elastic channel EI. The tests of the single-scattering approximation to the Watson and KMT OP's for  $\pi$ -d scattering in Refs. 64 converged poorly enough to call the MS series for the  $\pi$ -A OP into question; it would be interesting to compare this with the results for a factored  $tp^{65}$ .  $L^2$ -discretization techniques<sup>31</sup> are used with some success in an N = 3 model in Ref. 66 for treating continuum effects in contrast to the failure of the finite-basis expansions for the N = 3 BKLT equation<sup>67</sup>. In more formal work, Kouri<sup>68</sup> finds Faddeev-type equations with BKLT effective interactions; the spectral properties of non-self-adjoint Hamiltonians in quasi-Faddeev equations are investigated in Ref. 69; the AGS equations with a three-body potential is reconsidered in Ref. 70 looking at the effect of a  $V_3$  bound state.

A distinctive three-body approximation formalism for local potentials in coordinate space has been formulated in Ref. 71 employing the method of the partially separable, N = 2 t-matrix of Ref. 72a that also has been applied to potentials with absorption<sup>72b</sup> (See also Ref. 73). Separable approximations to N = 2 t-matrices are studied in Ref. 74a which is a critical study of a previously proposed technique<sup>74b</sup>, while Ref. 74c consists of the detailed elaboration of a method<sup>74d</sup> that seems to possess remarkable convergence properties, exact bound-state/on -half-off-shell characteristics, and the possibility of generalization to multiparticle amplitudes. New iterative techniques for N = 2 are proposed in Refs. 75.

Other Results: The N-body permutation symmetries are confronted with the single transition operator  $V + V G V$  in Ref. 76a; this leads to a variational calculational strategy<sup>76b</sup>. Multiparticle variational principles have also been proposed in Ref. 77. The semi-classical expansion of N-body Green's functions is developed in Ref. 78a and applied<sup>78b</sup> to obtain N = 3 spectral sum rules; such sum rules were previously found<sup>78c</sup>. Refs. 79 contain recent results on time delay. In Ref. 80, H is approximated by a sequence of self-adjoint bound-

ed operators leading to a general scattering theory of approximations. A necessary condition to obtain resolvents such as that in (2.4) from scattering equations is proposed in Ref. 81. An interesting proof of the unitarity of the  $[1,N]$  Pade approximant has been given by Balazs<sup>82</sup>. New results for scattering on a line are obtained in Ref. 83. Rigorous characteristics of low-energy scattering are studied by Bolle *et al*<sup>84</sup>. The BKLT equations which play a significant role in the review of "calculable" methods in many-body scattering in Ref. 48, have been applied to reactive scattering in Ref. 85.

## REFERENCES

- 1 ) P.E. Hodgson, *Nuclear Reactions and Nuclear Structure* (Oxford University Press, London 1971), p. 59.
- 2 ) F.S. Levin, *Nucl. Phys.* A353 (1981) 143c; L.P. Kok, *ibid* 171c.
- 3 ) K.L. Kowalski, in *Lecture Notes in Physics*, 87, (1978) 393.
- 4 ) I.M. Narodetsky and O.A. Yakubovsky, ITEP-1, Moscow (1980).
- 5 ) C. Chandler and A.G. Gibson, *J. Math. Phys.* 18 (1977) 2336; *ibid.* 19 (1978) 1610. See Refs. 6,7 for readable introductions to the two-Hilbert space method and for further references.
- 6 ) Gy. Bencze and Chandler, *Phys. Rev. C* 25 (1982) 136.
- 7 ) W.N. Polyzou, A.G. Gibson, and C. Chandler, *Phys. Rev. C* 26 (1982) 1878.
- 8 ) H. Feshbach, *Ann. Phys. (N.Y.)* 5 (1958) 357; *ibid.* 19 (1962) 287.
- 9 ) K.L. Kowalski, *Phys. Rev. C* 23 (1981) 597.
- 10) W. Tobocman, CWRU preprint (May 1983).
- 11) K.L. Kowalski, *Ann. Phys. (N.Y.)* 120 (1979) 328.
- 12a) A. Picklesimer and K.L. Kowalski, *Phys. Letters* 95B, (1980) 1. (b) K.L. Kowalski and A. Picklesimer, *Phys. Rev. Letters* 46 (1981) 228; *Nucl. Phys.* A369 (1981) 336. (c) A. Picklesimer *Phys. Rev. C* 24 (1981) 1400. (d) K.L. Kowalski and A. Picklesimer, *Ann Phys. (N.Y.)* 139 (1982) 215.
- 13) R. Goldflam and K.L. Kowalski *Phys. Rev. Lett.* 44 (1980) 1044; *Phys. Rev. C* 22 (1980) 949.
- 14) E.O. Alt, P. Grassberger, and W. Sandhas, *Nucl. Phys.* B2 (1967) 167.
- 15) S.K. Adhikari, (a) *Phys. Rev. C* 25 (1982) 118; (b) *ibid.* C 27 (1983) 2543.
- 16) S.K. Adhikari, R. Kozack, and F.S. Levin, Contribution to this Conference.
- 17) K.L. Kowalski, *Phys. Rev. C* 16 (1977) 7.
- 18) Gy. Bencze and C. Chandler, *Phys. Lett.* 112B (1982) 295.
- 19) Z.Y. Ma, K.C. Tam, and T.T.S. Kuo, *Nucl. Phys.* A394 (1983) 60.
- 20) A. Picklesimer and R.M. Thaler, *Phys. Rev. C* 23 (1981) 42.
- 21) K.L. Kowalski, *Phys. Rev. C* 24 (1981) 1915.
- 22) A. Picklesimer, P.C. Tandy, and R.M. Thaler, *Phys. Rev. C* 25 (1982) 1215.
- 23) K.L. Kowalski, *Phys. Rev. C* 25 700 (1982).
- 24) F. Cannata, J.P. Dedonder, and F. Lenz, *Ann. Phys. (N.Y.)* 143 (1982) 84.



- 25) S.A. Curvitz, Phys. Rev. C 22 (1980) 964; *ibid* C 24 (1981) 29.
- 26) A.K. Kerman, H. Mc Manus, and R.M. Thaler, Ann. Phys. (N.Y.) 8 (1959) 551; H. Feshbach, A. Gal, and J. Hüfner, *ibid.* 66 (1971) 20; E.R. Siciliano and R.M. Thaler, Phys. Rev. C 16 (1977) 1322; P.C. Tandy and R.M. Thaler, *ibid.* C 22 (1980) 232.
- 27) A. Picklesimer, P. Tandy, R.M. Thaler, Phys. Rev. C 25 (1982) 1233.
- 28) (a) N. Austern, Phys. Lett. 90B (1980) 33; *ibid.* 109B (1982) 210; (b) Y. Hahn, *ibid.* 97B (1980) 1; Nucl. Phys. A 389 (1982) 1; (c) G. Cattapan, L. Lovitch, and V. Vanzani, Nuovo Cimento, 58A (1980) 275; (d) R. Goldflam and K.L. Kowalski Phys. Rev. C 22 (1980) 2341; (e) G. Cattapan and V. Vanzani, Lett. Nuovo Cimento 31 (1981) 585 (f) Nuovo Cimento 62A, (1981) 226; (g) *ibid.* 68A (1982) 368; (h) Gy. Bencze, Phys. Lett. 98B (1981) 331; (i) M. Kawai, M. Ichimura and N. Austern, Z. Phys. A 303 (1981) 215; (j) F.S. Levin and C.T. Li, Phys. Lett. 100B (1982) 245; (k) Gy. Bencze, C. Chandler and A.G. Gibson, Nucl. Phys. A 390 (1982) 461; (l) R. Goldflam, Phys. Rev. C 26 (1982) 34; (m) W. Tobocman, Phys. Rev. C 27 (1983) 976; (n) E.W. Schmid, Z. Phys. A 311 (1983) 67; (o) V. Vanzani, Czech. J. Phys. B 32 (1982) 277; Proc. 1983 RCNP Int. Symp on Lt. Ion Reaction Mech. (Osaka 1983); (p) M.C. Birse and E.F. Redish, Nucl. Phys. A (t.b.p.) (q) M.C. Birse, Phys. Rev. C (t.b.p.).
- 29) W.N. Polyzou, J. Math. Phys. 22 (1981) 798.
- 30) R.S. Cotanch and C.M. Vincent, Phys. Rev. C 14 (1976) 1739.
- 31) F. Sohre and E.W. Schmid, Z. Natf. 309 (1975) 271; Z.C. Kuruoglu and F.S. Levin, Phys. Rev. Letters, 48 (1982) 899.
- 32) F.S. Levin, Ann. Phys. (N.Y.) 130 (1980) 139.
- 33) S.K. Adhikari, Phys. Rev. C 24 (1981) 379; W. Tobocman, Nucl. Phys. A 369 (1981) 17.
- 34) Gy. Bencze and P.C. Tandy, Phys. Rev. C 16 (1977) 564.
- 35) R.M. Dixon and E.F. Redish, J. Math. Phys. 21 (1980) 372; G. Cattapan, L. Lovitch, and V. Vanzani, Nuovo Cimento A72 (1982) 333.
- 36) (a) W.N. Polyzou and E.F. Redish, Ann. Phys. (N.Y.) 119 (1979) 1; (b) R. Goldflam, K.L. Kowalski, and W. Tobocman J. Math. Phys. 21 (1980) 1888; (c) W.N. Polyzou, *ibid.* 21 (1980) 506; (d) R. Goldflam and K.L. Kowalski Phys. Rev. C 21 (1980) 483; (e) Gy. Bencze, W.N. Polyzou, and E.F. Redish, Nucl. Phys. A 390 (1982) 253.
- 37) V. Vanzani Lett. Nuovo Cimento. 16 (1977) 1; *ibid.* A54 (1980) 141; G. Cattapan, L. Lovitch, and V. Vanzani IFDD 17-83.
- 38) Benoist-Gueutal and M.L'Huillier, J. Math. Phys. 23 (1982) 1823.
- 39) G. Cattapan and V. Vanzani, Preprint DEPD 22-83; Contrib., this Conf. Vol. II, p. 172.
- 40) O.A. Yakubovsky, Sov. J. Nucl. Phys. 5 (1967) 937.
- 41) W. Sandhas, Acta. Phys. Aust. Suppl. 13 (1974) 679; Czech. J. Phys. B 25 (1975) 251.
- 42) H. Haberzettl, Phys. Rev. Letters, 47 1367 (1981).
- 43) B.R. Karlsson, J. Math. Phys. 23 421 (1981).
- 44) K.L. Kowalski, W.N. Polyzou and E.F. Redish J. Math. Phys. 22 (1981) 1965.
- 45) K.L. Kowalski, Phys. Rev. C 20 (1979) 2526; F. Coester and W.N. Polyzou, Phys. Rev. C 27 (1982) 1348.
- 46) (a) A. Picklesimer, P. Tandy, R.M. Thaler, Phys. Rev. C 26 (1982) 315; (b)



- Ann. Phys. (N.Y.), 145, (1983) 207; (c) K.L. Kowalski and A. Picklesimer, J. Math. Phys. 24 (1983) 294; (d) Phys. Rev. C 26, 1835 (1982).
- 47) K.L. Kowalski, Phys. Rev. C 16, (1977) 2073.
- 48) E.F. Barrett, B.A. Robson, and W. Tobocman, Rev. Mod. Phys. 55 (1983) 155.
- 49) K.L. Kowalski, Phys. Rev. C 27, (1983) 489; A. Picklesimer, *ibid.* C 27 (1983) 1927.
- 50) C. Chandler and A.G. Gibson preprints, Contrib. Vol. II, p. 158.
- 51) W. Tobocman, Phys. Rev. C 27 (1983) 1405.
- 52) S.K. Adhikari, Phys. Rev. C 25 (1982) 128; G. Cattapan and V. Vanzani, Lett. Nuovo Cimento, 33 (1982) 367.
- 53) C. Chandler, Nucl. Phys. A301 (1978) 1; C. Chandler and I.H. Sloan, *ibid.* A361 (1981) 521.
- 54) Gy. Bencze and C. Chandler, Phys. Lett. 90A (1982) 162.
- 55) S. Mukherjee, Phys. Lett. 81A (1981) 207; *ibid.* 83A (1983) 1.
- 56) W. Tobocman, Phys. Rev. C 27 (1982) 88.
- 57) (a) V.V. Komarov, et al., Phys. Rev. C 22 (1980) 976; (b) I.H. Sloan, *ibid.* C 23 (1981) 2189; L.D. Faddeev and O.A. Yakubovsky, Sov. J. Nucl. Phys. 33 (1981) 331; (c) V.V. Komarov, V.L. Shablov and A.M. Popova, *ibid.* 34 (1981) 182; HU-TFT preprint 82-55 and references cited therein; Prog. Theor. Phys. 66 (1981) 940.
- 58) I.M. Narodetsky ITEP - 121 (1980), ITEP-13 (1981), ITEP-76 (1981).
- 59) H.P. Noyes, Phys. Rev. C 26 (1982) 1858.
- 60) A. Casel, et al. Phys. Rev. C 25 (1982) 1738; S.A. Sofianos, et al. *ibid.* C 26 (1982) 228; H. Haberzettl and S.A. Sofianos, *ibid.* C 27 (1983) 2411. Y. Matsui, *ibid.* C 26 (1982) 2620; A.C. Fonseca, *ibid.* C 27 (1983) 939.
- 61) L. Tomio and S.K. Adhikari, Phys. Rev. C 22 (1980) 2359.
- 62) K. Möller and I.M. Narodetsky, ITEP-17 (1983).
- 63) D. Eyre, et al., Phys. C 24 (1981) 2409; D. Eyre and T.A. Osborn, *ibid.* C 26 (1982) 1369.
- 64) I.R. Afnan and A.T. Stelbovics, Phys. Rev. C 23 (1981) 845; H. Garcilazo and G. Mercado, *ibid.* C 25 (1982) 2596.
- 65) H. Kottler and K.L. Kowalski, Phys. Rev. 138 (1965) B619; D.L. Weiss and D.J. Ernst, *ibid.* C 26 (1982) 605; K.L. Kowalski and S.C. Pieper, *ibid.* C 4 (1971) 74. The forward-scattering calculations here were inappropriately labeled FSA and refer simply to the usual on-shell IA with the d cm-motion treated correctly.
- 66) D. Eyre and H.G. Miller, TWISK-309 (1983).
- 67) W. Tobocman, Phys. Rev. C 24 (1981) 2743.
- 68) D.J. Kouri, Phys. Rev. C 22 (1980) 422.
- 69) J.W. Evans and D.K. Hoffman, J. Math. Phys. 22 (1981) 2858.
- 70) W. Glöckle and R. Brandenburg, Phys. Rev. C 27 (1983) 83.
- 71) T. Sasakawa, et al., Phys. Rev. C 27 (1983) 18.
- 72) (a) T. Sasakawa, et al., Phys. Rev. C 26 (1982) 42; (b) T. Sasakawa, *ibid.* C 28 (1983) 439.
- 73) W. Cassing, et al., Phys. Rev. C 26 (1982) 22.

- 74) (a) J. Heidenbauer and W. Plessas, *Phys. Rev. C* 27 (1983) 63; (b) D.J. Ernst, *et al.*, *ibid.* C 8 (1973) 46; (c) Oryu, *ibid.* C 27 (1983) 2500; (d) *ibid.* *Prog. Theor. Phys.* 62 (1979) 847.
- 75) Y. Hahn and R. Luddy, *Phys. Rev. C* 24 (1981) 1; L. Tomio and S.K. Adhikari, *ibid.* C 24 (1981) 43; J. Horacek and T. Sasakawa, *J. Math. Phys.* to be published).
- 76) (a) B.G. Giraud and M.A. Nagarajan, *J. Physique* 41 (1980) 477; (b) M.A. Nagarajan and B.G. Girard, *Phys. Rev. C* 27 (1983) 232.
- 77) R. Goldflam, *et al.*, *Nucl. Phys.* A359 (1981) 122.
- 78) (a) S.F.J. Wilk, *et al.*, *Phys. Rev. A* 24 (1981) 2187; (b) D. Bolle and T.A. Osborn, *ibid.* A 26 (1982) 3062; (c) T.A. Osborn, *et al.*, *Phys. Rev. Lett.* 45 (1980) 1987.
- 79) D. Wardlow, *et al.*, *J. Chem. Phys.* 76 (1982) 4916; D. Bollé and F. Gesztesy, 1983 preprint.
- 80) H. Kröger, *J. Math. Phys.* 24 (1983) 1509.
- 81) V.V. Komarov, *et al.* preprint HU-TFT-82-56.
- 82) L.A.P. Balázs, *Phys. Rev. D* 26 (1982) 1671.
- 83) D. Bollé, F. Gesztesy and S.F.J. Wilk, 1983 preprint.
- 84) D. Bollé and S.F.J. Wilk *J. Math. Phys.* (t.b.p.) S. Albeverio, *et al.*, *Ann. Phys. (N.Y.)* (t.b.p.).
- 85) Y. Shimia, M. Baer, and D.J. Kouri, *Chem. Phys. Lett.* 94 (1983) 321.



## TRENDS IN THEORETICAL FEW-BODY PHYSICS

L.P. KOK

Institute for Theoretical Physics, University of Groningen, The Netherlands

A.S. RINAT

Weizmann Institute of Science, Rehovot, Israel

In accepting to discuss 'Trends in theoretical few-body physics' we did not feel called to prophesy developments in the future. We rather interpreted our task as giving an opinion on some questions related to nuclear few-body systems:

1. To what extent do we understand standard phenomena which have been the theme of nuclear few-body conferences during the past twentyfive years?
2. Can one observe or foresee a change in attitude towards these phenomena?
3. If so, will new tools be needed for their description?

One difficulty is the personal bias which will go into our answers. Indeed, we were prepared to hear in discussions judgements and emphases, that differed from ours.

However, we did not foresee a second difficulty which presented itself in the course of the conference, and which originated in its format. Virtually all points originally selected by us in relation to the three questions rose frequently and were dealt with at length by invited speakers as well as in various discussion sessions. Naturally, we felt uneasy as our time approached: We relied on the expertise of the members of an ad hoc panel (I.R. Afnan, C.E. DeTar, and Yu.A. Simonov), and their capacity to further elucidate and giving perspective while avoiding repetitions.

< 1960

When trying to establish a trend, some historical perspective seems indispensable. We thus mention that before 1960 'Few-body Nuclear Physics' meant  $A \geq 4$ . Schrödinger equations for nuclei can not be solved exactly, and as a consequence nuclear physics became a discipline of model making par excellence. The nucleus  $^4\text{He}$  is the lightest system to which a model, in case the shell model, was applied.

Some of us may recall from nuclear physics meetings in the sixties the presence of a discernable group of specialists, dealing with the  $A=2$ , the

nucleon-nucleon, system. Their interest had little to do with nuclear physics proper and their progress had hardly any impact on the formulation of nuclear models.

The above-mentioned interest has not waned, and an echo we heard in the talk by Bugg<sup>1</sup>. He reported that pp elastic scattering for  $T_p^{\text{lab}} \leq 800$  MeV is essentially understood. That is, for  $I = 1$  we have at our disposal a set of phase shifts and mixing parameters (or alternatively of helicity parameters) smoothly varying with  $T_p$ . These satisfactorily account for all observables and do not require additional data. The latter would only provide checks, and barring surprises, do not contain additional information. Notice that 'satisfactory status' does not require that these phase parameters result from a (known) effective potential  $V_{NN}$  which incidentally itself is never free of adjustable parameters.

We agree of course with Bugg that we are close to a satisfactory representation of data in terms of phase parameters. However, later on we shall express dissatisfaction when placing the nucleon-nucleon system in a wider 'few-body' context, which is actually very desirable.

Another topic of continued interest is the deuteron and some of its ground-state properties. Accuracy of data like the asymptotic D/S ratio and the quadrupole moment cause renewed interest, which is also due to its link with the role of pions in the  $A=2$  system<sup>2,3</sup>.

Back to the early days of nuclear physics, one should in all fairness acknowledge the existence of the  $A=3$  system. It served mainly as a testing ground for variational calculations of the binding energy. In addition, one cannot take leave of the past, without emphasizing the ground-state isovector magnetic moment of the  $A=3$  system, which is about 8% larger than can be predicted with purely nucleonic degrees of freedom<sup>4</sup>. More than three decades ago it was known that mesic degrees of freedom occasionally influence static (or near-static) nuclear properties. One could not speak of a trend then, but indications for what may have been in stock were inescapable<sup>5</sup>.

> 1960

With the advent of Fadde'ev theory it became feasible to give a nonrelativistic description of three-body systems<sup>6</sup>, in particular when pairs of particles interact through short-range forces.

With satisfaction one may look back on the realization of a program to calculate through the  $Nd$  system. This task has in essence been completed, in spite of a few unsettled problems, like a practical way to exactly include the Coulomb interaction in a momentum-space description of the  $ppn$  system<sup>7,8</sup>.

In addition we still live with the persistent underbinding of  ${}^3\text{H}$  with pair-forces alone, and which has given rise to intensive studies of purely nucleonic three-body forces  $V_3$ , and  $\Delta$  admixtures<sup>9</sup> - again an insufficiency of nucleonic degrees of freedom. However, it may be in place to emphasize that a large body of elastic Nd data is well accounted for by the action of pair forces alone. This agreement constrains the strength of a possible three-body force.

No property illustrates the three questions above more than the interpretation of the various electro-magnetic form factors of deuteron,  ${}^3\text{H}$  and  ${}^3\text{He}$ , and  ${}^4\text{He}$ . Using the impulse approximation and the Fadde'ev solutions for nonrelativistic bound-state wave functions produces, for instance for the triton, discrepancies<sup>10</sup> for  $q \geq (3-3.5)\text{fm}^{-1}$ . Understanding was subsequently sought in contributions due to relativity, two-body or many-body meson-exchange forces,  $\Delta$ -admixture effects, etc. Whatever the cause, nonrelativistic potential models are bound to fail when nuclei are probed at increasing momentum transfers.

We shall come back to these foreseen and observed failures after completing a list of outgrows and pay-offs of Fadde'ev theory. First in line are quasi three-body systems like  $\text{pn}{}^4\text{He}$ . In Plattner's lucid review<sup>11</sup> one finds summarized the state of art, achievements, and intrinsic shortcomings of such postulated extensions. A similar model has been explored in a simultaneous description of  $X(d,d')X'$ ;  $X(d,p)Y$ ;  $X(d,n)Z$ ;  $X(d,\text{pn})X$  reactions<sup>12</sup>. One certainly gained insight and could substantiate in these models the workings of a standard distorted-wave Born formalism.

Next in line are the generalizations to  $A \geq 4$ . It is indeed possible to carry out reliable calculations of the  ${}^4\text{He}$  binding energy<sup>13</sup>, but contrary to the situation for  $A=3$ , reactions amongst four nucleons can only be performed in an approximate sense which still requires improvements to become satisfactory<sup>14</sup>.

Having understood the mathematical complexities which Fadde'ev overcame for  $A=3$ , many authors<sup>8,15</sup> attempted to formulate a theory for reactions amongst clusters with  $A=A_1+A_2=A'_1+A'_2 \geq 4$ . In fact, much room has been reserved for these topics in previous meetings. With no numerical progress reported at the present, these reaction theories may eventually find themselves outside the mainstream. We refer to Kowalski's appraisal<sup>16</sup> of the present status of N-particle theory and its connections with more traditional reaction theories.

In this connection we should mention cluster models, which also have a venerable history, and which are altogether alive. Hofmann<sup>17</sup> and Schmid<sup>17</sup> presented reviews with a survey of the prevailing status, of the sharpening of tools and - last but not least - numerical results.

> 1975

Reactions amongst few nucleons involving pions came into focus after 1975. In the center stands the  $NN\pi$  system, with emphasis originally on its role in the description of  $(\pi, \pi)$ ,  $(\pi, 2N)$ , ... reactions.

Due to the relative simplicity of the system, and the unique, multiple ways its channels can be reached experimentally, the  $NN\pi$  system has been, and still is intensively studied. A large number of contributions to this conference on  $\pi d \rightarrow \pi d$ ;  $NN \rightarrow \pi d$ ;  $NN \rightarrow NN$ ;  $\pi d, NN \rightarrow NN\pi$  contain detailed information, in principle stored in newer data for p or d analyzing powers, cross sections for reactions with polarized proton beams and/or targets, polarization transfers and the like. Also here the aim is a representation of data by amplitudes which couple various channels.

Of course, this notion is at the heart of theoretical descriptions, which produce a coupled-channel description reminiscent of, but far more complex than Fadde'ev theory. The status of theory and a comparison with (some of the) data have been given by Afnan<sup>18</sup> and Arvieux<sup>19</sup>. It is likely that interest in the reactions above will persist for some time to come, not in the least due to the availability of  $\bar{d}$  targets. These data are in need and may help to, for instance, pinpoint what helicity amplitude(s) cause(s) the underestimate of  $\sigma(\theta)$  for  $NN \rightarrow \pi d$ <sup>20</sup>. There is still abundant interest in the various elastic  $\pi d$  polarization data, in particular in  $t_{20}$ , on which experimental consensus is badly needed<sup>21,22</sup>.

Finally, in the review talk of Locher<sup>23</sup>, and at several other occasions during this meeting dibaryons were discussed, which may decay to virtually any channel of the  $NN\pi$  system.

Proponents and contestants agree on the energy behavior of all partial-wave amplitudes  $f_{\alpha\beta}^J(s)$ , which describe the transition  $\alpha \rightarrow \beta$  through  $N\Delta$  intermediate states: For  $\Delta$  energies  $s_{\Delta}^{\frac{1}{2}} \approx m_{\Delta}$ , the amplitudes for all  $\alpha, \beta$  and several  $J$  will show pseudo-resonance behavior with masses and widths dependent on the (average)  $N$  spectator energy, the  $N\Delta$  orbital momentum barrier and possibly on  $\alpha, \beta$ .

If dibaryons exist, one ideally likes to identify them from (indirectly) extracted amplitudes, making minimal assumptions, like the presence of a smooth background.

In the case at hand one knows that pseudo and genuine resonances produce similar  $s$  behavior in  $f_{\alpha\beta}^J(s)$ . It thus seems very hard to interpret data without a theory, i.e., to isolate a resonance amplitude from  $f$  without knowing that part of it has a nonsmooth, resonance behavior. At least on two accounts it is dangerous to interpret the difference between data and some theoretical (or even with some assumed) background as an indirect signal of dibaryons. (1) There is



spread in predictions by various authors, which entails a corresponding spread in extracted resonance parameters; (2) Minor theoretical uncertainties (role of small  $\pi N$  waves, changes in parametrization of input) may disproportionately influence selected spin observables, leading in turn to a similarly large discrepancy.

It is likely that data taking and interpretations including dibaryons will continue for a while: Prospects to settle the issue do not look bright. Interest may just pass away, if no further striking evidence or consequences will be forwarded.

A word on ongoing  $\pi d(NN) \rightarrow NN\pi$  experiments may be in place here<sup>24</sup>. Whatever the information implied, it is unlikely that these will ever form a sufficient data base to really decide on the dibaryon issue.

We thus seem to have satisfactory and fairly complete descriptions of low-energy nuclear few-body systems. One may safely expect continued activity in the study of these systems at higher energies where pions play a role. Our picture of even the simplest of those systems is as yet not in a satisfactory state.

The experiments which have been drawn into our sphere of interest and should be continued next, deal with the lightest nuclei, but few-body physics is not a regime with a fixed baryon-number and a fixed description. For higher energies, ever smaller distances are probed, descriptions in terms of pointlike hadrons will break down and the QCD description will become indispensable.

Realistic QCD calculations are still not feasible. It thus seems natural to invoke approximations, which hopefully keep some essential features in a manageable framework. Nonrelativistic quark models and bag models are examples of those approximate short cuts.

Let us start with models of isolated hadrons. The survey by Thomas should impress an audience, how far a particular version, namely the cloudy bag model<sup>25</sup>, goes. It accounts of a number of static and nonstatic properties of baryons, like masses, vector and axial-vector form factors and the like. Furthermore, by postulating that chiral-invariance is partially restored by a pseudo-scalar field, which is then associated with pointlike pions (or the full pseudo-scalar octet in the  $SU_3 \times SU_3$  case). These communicate with hadrons, and this enables a description of meson baryon scattering within the scope of that model. A more complete list of successful applications can be found in the paper of Thomas<sup>25</sup>. During this conference other models were discussed, of which we mention the compound bag model by Simonov<sup>26</sup>.

The applicability of bag models to few-body systems requires foremost a description of the two-nucleon system. For bag center separations

$r > 2R_{\text{bag}}$  there are no difficulties. However, the very notion of overlapping bags can in principle only be spelled out, if the approximations to QCD leading to the single-hadron 'bag Lagrangian' are understood and can be made explicit. This then conceivably permits a generalization to  $q^6$ ,  $q^9$ , ... systems. Such a derivation has as yet not been given and consequently one can only guess whether partially overlapping bags resemble coalescing soap bubbles or have alternative shapes. Whatever choice will be deemed most realistic it enables a calculation of  $V_{\text{NN}}^{\text{eff}}(r)$  as a Van der Waals or Lennard-Jones potential<sup>27</sup>. For the shortest ranges it replaces potentials constructed from (multiple) boson exchange, while for increasing  $r$  equivalence with the latter will probably result<sup>28</sup>. As a check serves the  $q^9$  system, for which one should find  $V^{\text{eff}}(ijk) \approx V^{\text{eff}}(ij) + V^{\text{eff}}(jk) + V^{\text{eff}}(ki)$ .

The same reasoning, calculation and consistency tests apply to nonrelativistic quark models with confining forces<sup>29</sup>. Thus, in principle, a confining potential for  $q^6$ ,  $q^9$ , ... ought to be derived. However, for these quark models one intuitively guesses the sufficiency of a cluster model<sup>30</sup> with as total confining force the sum of pair confining forces. When this picture is adopted a solvable model results<sup>31</sup>.

All these considerations are of no relevance when few-body systems are probed at very high energies. High-momentum-transfer form factors are 'ultimately' governed by scaling laws, essentially counting the number of spectator quarks<sup>32</sup>.

For decreasing momentum transfers there is a domain where dynamical effects will modify counting rules. For still lower  $q^2$ , results may be expected which are equivalent to those obtained from the impulse approximation with nonrelativistic target wave functions, supplemented by meson-exchange corrections, etc.<sup>33</sup>.

There are somewhat diverging opinions on where the two pictures are expected to join. Brodsky<sup>34</sup> maintains that the characteristic length of QCD forces one to use the full QCD machinery down to small  $q^2$ , which nuclear physicists still thought to be their realm. Gross<sup>35</sup> and others believe that on the basis of Bethe-Salpeter-like equations, the notion of wave functions can be given meaning and can be used to 'medium  $q^2$  ranges'.

For some time to come we may well be stuck for medium range  $q^2$  values with an ultimately undesirable hybrid. It may just be convenient to continue usage of, say a deuteron 'wave function', giving (non-interfering) probability amplitudes to find for given  $q^2$  a  $N^2$  or a  $q^6$  configuration. It is clearly desirable to devise a model where this makes sense, and experiments which allow the measurement of these probabilities.

We certainly convey the impression of all participants when observing that the wide scope of present experiments on few-body nuclei, causes a new orientation. When the substructure of hadrons has to be taken into account, the same will be the case for the language of description. If the latter is unadulterated QCD specialists will have to be called in. One may then expect that participants in few-body meetings will no more have a common language.

If, however, manageable approximations to QCD will suffice, and these will allow treatment of  $A \geq 2$  systems, one can look forward to an exciting new trend, both in the selection of experiments and in their interpretation.

#### REFERENCES

- 1) D.V. Bugg, invited talk, these proceedings.
- 2) T.E.O. Ericson, invited talk, these proceedings.
- 3) S.Klarsfeld, J. Martorell, and D.W.L. Sprung, preprint (1983);  
D.W.L. Sprung et al., Few Body X, Conference Contributions Book.
- 4) See, e.g., R.J. Blin-Stoyle, *Fundamental Interactions and the Nucleus* (North-Holland, Amsterdam, 1973).
- 5) A.E. Cox et al., Nucl. Phys. 74 (1965) 497;  
H.P. Noyes, Nucl. Phys. 74 (1965) 508.
- 6) L.D. Fadde'ev, for example: *Mathematical Aspects of the Three Body Problem in Quantum Scattering Theory*, Steklov Math. Inst., Leningrad Publ. 69 (1963) [Transl. D. Davey and Co., New York, 1965].
- 7) C. Chandler, Nucl. Phys. A353 (1981) 129c.
- 8) L.P. Kok, Nucl. Phys. A353 (1981) 171c.
- 9) Few Body X, Conference Contributions Book.  
Shin Nan Yang and P.U. Sauer.
- 10) R.G. Arnold et al., Phys. Rev. Lett. 35 (1975) 776; 40 (1978) 1429.
- 11) G.R. Plattner, invited talk, these proceedings.
- 12) A.S. Reiner (Rinat) and A.I. Jaffe, Phys. Rev. 161 (1967) 935;  
J.P. Farrall et al., Ann. of Phys. (N.Y.) 96 (1976) 33.
- 13) See, for example, J.A. Tjon, Nucl. Phys. A353 (1981) 47c.
- 14) A.C. Fonseca, invited talk, these proceedings.
- 15) See, for example, F.S. Levin, Nucl. Phys. A353 (1981) 143c, and Ref. 16.
- 16) K.L. Kowalski, invited talk, these proceedings.
- 17) H.M. Hofmann, invited talk, these proceedings.

- E.W. Schmid, invited talk, these proceedings.
- 18) I.R. Afnan, invited talk, these proceedings.
- 19) J. Arvieux, invited talk, these proceedings.
- 20) A.S. Rinat and Y. Starkand, *Nucl. Phys.* A397 (1983) 381;  
T. Mizutani et al., *Phys. Lett.* B107 (1981) 177.
- 21) G.R. Smith et al., *Few Body X, Conference Contributions Book*.
- 22) V. König et al., *Few Body X, Conference Contributions Book*,  
W.S. Freeman et al., *ibid*.
- 23) M.P. Locher, invited talk, these proceedings.
- 24) C.E. Waltham et al., *Few Body X, Conference Contributions Book*.
- 25) A.W. Thomas, invited talk, these proceedings.
- 26) Yu.A. Simonov, invited talk, these proceedings; and preprint ITEP-93  
(Moscow, 1983).
- 27) R. Liberman, *Phys. Rev.* D16 (1977) 1542;  
C.E. DeTar, *Phys. Rev.* D17 (1978) 323.
- 28) H.J. Weber, *Z. Phys.* A297 (1980) 26.
- 29) N. Isgur and G. Karl, *Phys. Lett.* B72 (1977) 109.
- 30) M. Harvey, *Nucl. Phys.* A352 (1980) 301, 326;  
A. Faessler et al., *Phys. Lett.* B112 (1982) 201.
- 31) K. Maltman and N. Isgur, *Phys. Rev. Lett.* 50 (1983) 1827.
- 32) S. Brodsky and B. Chertok, *Phys. Rev.* D14 (1976) 3003.
- 33) See, for example, H. Arenhövel, *Proceedings ICOHEPANS 9*;  
*Nucl. Phys.* A374 (1982) 521.
- 34) S. Brodsky, discussion during Discussion Session DS5 of this conference.
- 35) F. Gross, discussion during Discussion Session DS5 of this conference, and,  
for example, W.W. Buck and F. Gross, *Phys. Rev.* D20 (1979) 2361.

Chapter V  
SPECIAL TOPICS



## FEW BODY PROBLEMS IN ATOMIC AND MOLECULAR PHYSICS

T. K. LIM

Department of Physics and Atmospheric Science, Drexel University,  
Philadelphia, Pennsylvania 19104, U.S.A.\*

In this article, I present a short summary and review of recent developments in the application of traditional few-body methods to atomic and molecular physics, proffering selective examples which demonstrate the new insights being obtained in the description of processes occurring in these areas of few-body physics.

### 1. INTRODUCTION

When the invitation from the organizers of this conference came to hand, it was immediately clear to that the task of reviewing all recent exciting work in atomic and molecular physics with few-body associations would be an immense undertaking. It had been shared by 5 reviewers at Oregon<sup>1-5</sup> and was beyond me working alone. Thus I decided, in order not to shortchange anyone, that I would stick firmly by the title of the talk and even narrow further its scope by excluding from consideration work which did not in some way involve theoretical methods familiar to few-nucleon physicists and linked with the substance of our international conferences.

Before I begin, let me set the stage for the rest of this review by sketching the rough outlines of its presentaion. This contribution is broken up into 3 main sections; according to my prescription they are titled "atomic physics" (including under this umbrella term all systems wherein the electron is recognized as a separate entity and the dominant interaction is Coulombic), "molecular physics" (wherein the existence of the electron is denied and atoms are taken to be elementary objects and the interaction is atom-atom), and "chemical physics" (wherein the electron exists but its motion is inextricably linked to that of the heavier nuclei and the interaction is complicated). Within each section are 2 subsections corresponding to bound-state (or spectroscopy) calculations, and collision (or continuum) calculations.

### 2. ATOMIC PHYSICS

#### 2.1 Bound States

---

\*Work supported under grants PHY78-19375 and PHY83-06584 from the NSF and by the Alexander von Humboldt-Stiftung.



In the glory days when the Faddeev Equations had just been introduced their application in atomic physics was carried out on  $H^-$  by Ball, Chen and Wong<sup>6</sup>. The method was promptly derailed. The "problem of 3 charged particles" had reared its ugly head and bitten the few-body community. Ball, et al. could not achieve true convergence for the eigenvalue of the ground state. Others have tried with different separable expansions for the Coulombic interaction to describe various 2-electron atoms but with little success. In recent years, only Colegrave and King have persisted in using the Faddeev approach but, in a recent communication, they have reluctantly acknowledged that even with expansions which include  $1s, 2s, 3s, 2p$  and  $3p$  states  $H^-$  still presents problems although the heavier systems such as  $He$ ,  $Li^+$  and  $Be^{2+}$  appear to yield the sought-after convergence<sup>7</sup>. There the matter rests and there is where I shall leave it since the question of the correct Faddeev-type approach to 3 charged particles remains unresolved<sup>8</sup>.

The alternative connected-kernel approach of Baer, Kouri, Levin and Tobocman (the BKLT method or the Channel Coupling Array, CCA, method as it is usually labelled when applied to atomic structure calculations) has also had its share of problems<sup>9</sup>. When applied to the ungerade-triplet excited  $H_2$  state, CCA yielded unphysical behavior in the potential-energy curve of  $H-H$ . At small  $H-H$  separations, the potential became infinitely attractive indicating a "catastrophic" collapse of the system. In addition, when the expansion basis through which CCA equations were solved was increased there was non-monotonic behavior in the energy. The situation was equally bleak for  $H_2^+$ . However, because of reluctance to give up on what had started off as a promising tool, Levin and his collaborators eventually showed that non-monotonicity is not inherent in CCA<sup>10</sup>. In addition, physically acceptable results for the potential-energy functions can be obtained when an appropriate nodal condition is imposed on each CCA wave function. Then, just when the future seemed rosy once more for CCA, it has again been dealt a setback<sup>11</sup>. An attempt to describe the  $H_3^+$  ground state received mixed results. In the CCA calculations with 9 channels retained the energy curves showed strong fluctuations and in some cases unphysical behavior resurfaced. It appears that the jury is still out on the CCA and much remains to be done to clarify its general use in atomic physics.

With regard to another stalwart in the stable of few-body methods, Haftel and Mandelzweig have recently developed exact solutions of 1-dimensional coupled differential equations and applied their technique to the equations arising from the hyperspherical harmonics, H.H, formulation of the bound state of the 3-body Coulomb system<sup>12</sup>. Their results for the energy of the ground state of the  $He$  atom are in excellent agreement with those which Shoucri and Darling

obtained through direct numerical integration of the Schroedinger Equation<sup>13</sup>. This is a happy augury for the H.H approach but this must be tempered, however by the poorer results for more loosely-bound systems such as  $H^-$  and the positronium ion. It is obvious that the full power of their method cannot be realized until correlations, reflecting cusp behavior, are built into the H.H wave functions. Two special features should be noted in the Haftel-Mandelzweig work. First, their method allows for an iterative procedure to improve results. Second, they have evaluated the Faddeev wave functions for the ground states of the 3 systems and, in the process, discovered significant e-e correlations which are clearly manifested by the nodes in these functions (see e.g. Figure 1). No such nodes appear in the Schroedinger wave functions. It also bears mentioning here that Sasakawa and Sawada have discovered analytical expressions for various bound-state and scattering parameters in the H.H treatment of the 3-body Coulomb problem when the global momentum  $K_m$  is restricted to 0 and  $2^{14}$ . Although it would seem that few physical situations can be represented by such a model, this work should nevertheless find relevance as a useful test of numerical computations. It should also encourage attempts to generalize the treatment to larger  $K_m$  values especially now that computer programs are available which can perform algebraic analysis.

The e-e correlations which I highlighted in the last paragraph assume even more significance in the excited states of He. In fact, Herrick and Kellmann have postulated that "intrashell" states of doubly excited He,  $He^{**}$ , i.e. states in which the 2 electrons have the same principal quantum number, constitute supermultiplets and that the origin of the supermultiplet pattern arises out of a physical situation in which the near constants of the motion correspond to a linear triatomic molecule: the angular momentum of a rigid linear rotor and the bending motions of an  $XYX$  vibrator. This picture of 2 electrons so strongly correlated that they are localized at roughly the same

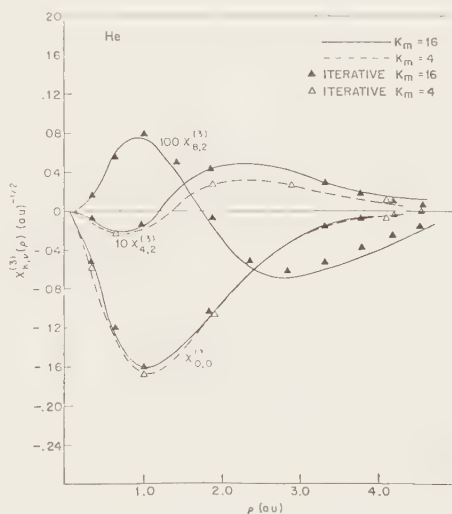


Fig. 1. Faddeev He ground-state wave function in the e-e channel. From ref. 12 with permission.

distance from but on opposite sides of the nucleus, undergoing large-amplitude bending vibrations together with collective rotations is confirmed by computations of the conditional probability densities for the electrons from high-quality configuration-interaction functions<sup>15,16</sup>. (See Figures 2 and 3).

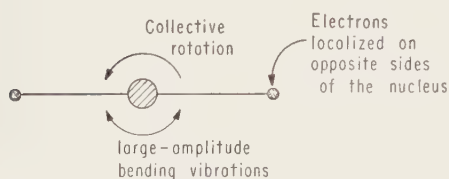


Fig. 2. The molecular picture of electron correlation in doubly-excited states of 2-electron atoms. From ref. 16 with permission.

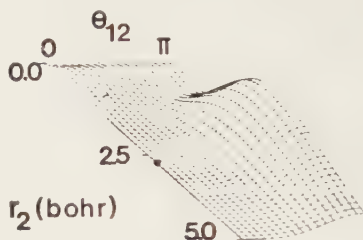


Fig. 3. The conditional probability density for the  $1S^e$  state of  $\text{He}^{**}$ . The large dot indicates the position of electron 1. From ref. 16 with permission.

The molecular picture comes as a surprise to all of us who have been brought up to believe sacrosanct the independent-particle characteristics of the electrons in atoms. The appearance of molecule-like collective motion in  $\text{He}^{**}$  leads now to the obvious question about its likelihood in many-electron systems and elsewhere. Berry, et al. have found that "intrashell" states for other 2-e systems with heavier nuclei revert back to independent-particle behavior so it seems that this collectivity is not widespread. However, its mere presence in  $\text{He}^{**}$ , so unexpected, raises the possibility of "bizarre" behavior in other areas, e.g. independent-particle motion in highly-excited vibrational states of small polyatomic molecules.

## 2.2. Continuum States

It would be safe to say that no area of few-body physics offers as much challenge to the theoretician as the successful development of a general 3-body theory for Coulombic systems. While other citadels of resistance to solution have succumbed, the edifice of the correct 3-charged-particle theory remains unscaled. Work goes on, nevertheless, to probe various aspects of charged-particle systems and processes, and 4 areas of activity deserve special mention here.

The first is the work of Burger, Sandhas and Alt on e-H scattering below breakup<sup>17</sup>. By including a "polarization" term which mimics the third-order quasi-Born contribution to the effective potential, they find excellent fits to data at 8.7 eV; lower energy data can already be described with the first-order quasi-Born approximation.

The second pertains to (e,2e) coincidence theory<sup>1d</sup>. The flood of data continues unabated both for small as well as large momentum transfers. Weigold and McCarthy and their collaborators have already shown that experiments at large momentum transfer correspond to symmetric geometry of the 2 outgoing electrons and can be handled via the distorted-wave impulse approximation, DWIA<sup>4,18</sup>. Although they have extended their analysis of (e,2e) on H to more exotic systems such as Ne and even methanol, CH<sub>3</sub>OH, that does not excite me as much as the success of Byron and Joachain in reproducing the much more detailed data of Ehrhardt, et al. for asymmetric geometry and on He<sup>19</sup>. The eikonal-Born series expansion evaluated to the second Born term, which they used, is able to follow the data in locating the 2 peaks in the triple differential cross section although the absolute magnitudes are not as well duplicated. The same approximation, applied to the symmetric (e,2e) data, offers no improvement to the first Born and signals that the full series expansion is necessary here, a distinct nuisance.

The third area of activity is concerned with the behavior of the cross section for electron impact ionization i.e. the cross section of electron-ion breakup induced by collision with a second electron, at threshold. It has been generally accepted that this cross section near threshold obeys a simple power law. In Wannier's classical phase-space derivation, the value of the exponent in the case of H is the ridiculous number 1.1268!<sup>20</sup> Experimental data are hard to come by. Whatever there was seemed to support Wannier<sup>21</sup>. Now, however, Temkin, arguing that the cross section behavior is independent of the specifics of the region where all 3 charged particles are close together but rather manifest the influence of long-range forces so that the threshold behavior is dependent only upon the final product wave function of the 2 e's, has extracted an entirely new form for the threshold expression<sup>22</sup>. Wannier theory stresses a strong correlation in the motion of the escaping e's. Thus their energy distribution is equal; this is not so in Temkin theory. Another specific prediction in Wannier theory is that the e's escape in opposite directions; no such statement is made by Temkin theory. These and other conflicting implications of the 2 theories should be amenable to experimental verification. A recent attempt by Donahue, et al., in the face of formidable difficulties, shows that their yield-curve data is unable to discriminate between the 2 protagonist theories<sup>23</sup>. Worse still, Baum, et al. find that neither law fits their data<sup>24</sup>. However, their experimental points are well above threshold. Whichever side will prevail eventually must hinge on, yes, you have guessed it!, a correct general theory of 3 charged particles<sup>25</sup>. The conflict has spilled over into positron-H impact ionization as well; for this process, Temkin's law is unch-

anged but Wannier theory predicts an exponent of  $2.65^{26}$ . An indirect consequence of all this is that Pelikan and Klar have used Klar's hyperspherical-coordinates approach, set up initially to study the threshold law, to calculate elastic positron-H scattering, and in the process, confirmed Armour's proof that there is no positron-H bound state<sup>27,28</sup>. Thus has a seemingly easy problem been finally solved!

The last area of activity on the continuum problem for 3 charged particles which I wish to cover is Bottcher's work on the wave-packet-time-dependent description of electron impact ionization<sup>29</sup>. Attracted by the burning interest in the threshold law, Bottcher adapted the technique first popularized in treating chemical dissociation. In his method, an electron is localized in a wave-packet some distance from and is set moving towards the target. Using the alternating-gradients method to reduce the 3-dimensional problem to a sequence of 1-dimensional problems, Bottcher has solved the time-dependent Schroedinger Equation to deduce the amplitudes for ionization. Because he has had to use a great spread in energy for his wavepacket, the threshold law is difficult to extract. Indeed, Bottcher's results indicate that both Wannier and Temkin mechanisms are present near threshold, perhaps a clear case of sitting on the fence! And on that note, it is timely for me to move on to places where few-body theory has had more unqualified successes.

### 3. MOLECULAR PHYSICS

#### 3.1 Bound States

My definition of molecular physics tailors this subsection to consideration of the bound states of rare-gas molecular clusters where the interactions are mainly pairwise between structureless atoms, are central and, at long range, are of the van der Waals  $r^{-6}$  type. The original impetus for the study of such molecules came from the problem of homogeneous nucleation where the development of a molecular theory of condensation is urgently needed<sup>30,31</sup>. A first step in that direction is to understand the stability of small or microclusters of the rare gas atoms. The most extensive study in this area has been conducted by the Hokkaido group, my other collaborators and me<sup>32-34</sup>.

We began with small clusters of  $^4\text{He}$  because the renowned Efimov Effect was expected to be manifest in its 3-atom configuration. As a result, we found that it is possible to transplant successfully both Faddeev and variational methods into this new "terrain". And as they say, the rest is history! Our most recent work involved the application of Faddeev-Yakubovsky theory to the  $^4\text{He}$  tetramer, i.e. the collection of 4  $^4\text{He}$  atoms. Using Sofianos' energy-dependent-pole-expansion method<sup>35</sup>, we generated separable expansions for the (3+1) and (2+2)

subamplitudes, found good convergence and a bound ground state at -0.4 K with a realistic He-He potential. The success of Sofianos' expansion and recent work which has unearthed two other expansion techniques whose utility may surpass the one we used, makes us hopeful that we have the necessary tools to describe the quantum dynamics of 4-atom clusters<sup>36</sup>.

Our foray into fermionic  $^3\text{He}$  clusters using our trusted variational method, the ATMS method, has revealed that, like  $n^3$  and  $n^4$ , the trimer and tetramer of  $^3\text{He}$  are not bound. The evidence we have collected suggests that the smallest  $^3\text{He}$  molecule is very probably the octomer and that Fermi statistics will force its ground state to have non-zero orbital angular momentum<sup>34</sup>.

Faddeev-type approaches, although exact in principle, are much less so in practice because of the calculational approximations one must rely upon. For these integral-equation methods high accuracy, when it matters, is still elusive. And that is why the Green's Function Monte Carlo, GFMC, method of Kalos and his collaborators is one of the more pleasing developments in few-body theory during the last few years<sup>37</sup>. The method allows exact solution for the ground state of the Schroedinger Equation subject only to statistical sampling errors which may be made arbitrarily small. The technique is discussed in great detail elsewhere in this volume. Suffice it to say here that GFMC involves an iterational procedure and Kalos, et al. accelerate it towards a solution with an importance function which embodies as much physical knowledge as possible about the system to which it is being applied. Many-body forces provide no extra difficulty. Unfortunately, a considerable number of iterations are required and it is imperative to pick a good importance function. While yielding useful benchmarks for the few-body system, it has, in the process, confirmed the accuracy of ATMS. There are difficulties associated with the application of GFMC to fermionic systems so much still has to be done here before GFMC has the corner on all ground state calculations.

As for our old friend, the H.H approach, there was an abortive attempt to use it on the  $^4\text{He}$  trimer<sup>38</sup>. Only recently have 2 groups revived efforts to apply H.H to ground states of van der Waals molecules<sup>39</sup>. These are not well enough along the way for me to report any results.

As I have discussed previously, graphical illustrations of few-body wave functions can play a significant role in greater understanding of these systems. The molecular wave functions extracted from Faddeev and GFMC methods cannot easily produce conditional probability densities a la Berry, et al.; GFMC e.g. cannot even yield good 1-particle density functions. However, Bao, et al. have recently computed these densities, labelling them as correlated densities to better suggest their significance, by using an expansion in harmonic-oscillator



states to solve the Schrodinger Equation<sup>40</sup>. The pairwise potential chosen for their study of few-body systems is that appropriate for alpha-cluster models of light nuclei. However, its characteristics sufficiently resemble those for van der Waals molecules that one can extend their conclusions to the latter. The correlated densities reveal startling features about the shapes and modes of motion in microclusters. For example, different definite geometric shapes can coexist within a state; the second  $0^+$  state in the 4-body system has an admixture of square and tetrahedral structures while the  $0^+$  ground state of the 5-body system moves back and forth between a trigonal bipyramid and a square pyramid. Is there independent-particle behavior present? Bao, et al. are unable accurately to peel out the characteristics of higher levels so the answer is we do not know yet. The study reveals how each successive atom added ensures the emergence of new geometrical structures and may elucidate the physics of small droplet formation.

To illustrate the wider implications of few-body bound-state work and to close this section, I mention that March has linked our work on  $^4\text{He}$  trimers to his own work and concluded that 3-body correlations expected in liquid  $^4\text{He}$  can imply the absence of a Bose-Einstein condensate even though there is superfluidity<sup>41</sup>.

### 3.2. Continuum States

I arrive now at molecular collision processes. The prototypical example is atom-diatom scattering. In the best believe-it-or-not fashion, the first accurate computation of 3-dimensional atom-diatom collisions involving a system interacting via van der Waals potentials was accomplished just 2 years ago when Haftel and I applied Faddeev-AGS theory to 3 "helium-like" atoms with 1 bound 2-atom state<sup>42</sup>. The numerical technique used was the Ebenhoh solution for 3 identical spinless particles. Venturing where no few-body theorist had ever gone before, because none had chosen to!, we found a resemblance of our results to those of some 1-dimensional models popularly used in chemistry and therefore a strong suggestion that the collisional behavior of 3-dimensional systems may be qualitatively described by 1-dimensional models after all. We evaluated the breakup, i.e. collision-induced dissociation, cross section and by time-reversal invariance the cross section for recombination. Then by appropriately folding in a Boltzmann factor we recovered the termolecular recombination rate. Having chosen parameters with some relevance to chemical systems, we extracted results which spanned the experimental rates in H-H-He, H-H-Ar and H-H-H<sub>2</sub> collisions. Furthermore, by analyzing the multiple-scattering series, we observed that features familiar to physicists, such as "quasifree scattering" and "final-state interaction", are resurrected in molecular physics and in



point of fact, inverse final-state interaction is the "resonance mechanism" suggested by chemists as the way for recombination to occur!

To extend these studies to processes in real van der Waals systems such as the heavier rare gases, one is immediately faced with the problem of many 2-atom bound states because of the more attractive forces involved. A realistic calculation is out of the question right now but, by using the Ernst-Shakin-Thaler separable-expansion technique, Haftel and I have considered 2 reasonable models, one with spin-dependent Morse potentials to mimic the situation in systems of H atoms while the second has spin-independent Hulthen potentials. In both, 2 or 3 bound vibrational states exist in the 2-atom systems. Our models now have more structure than those normally devised to study few-nucleon processes and we begin to observe phenomena not previously encountered. In particular, we show conclusively for both models that the higher the initial state in the diatom the higher the dissociation probability, i.e. that there exists vibrational enhancement, when the incident energy is low<sup>43</sup>. (See Figure 4).

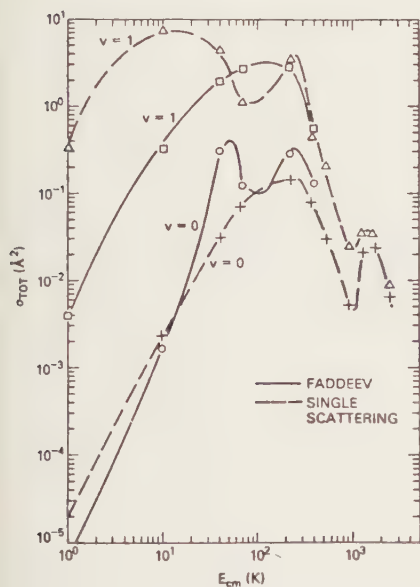


Fig. 4. The total breakup cross section for 2 vibrational states in the Hulthen atom-diatom model.

Increasing the incident energy does not reverse this property, i.e. there is no vibrational inhibition at higher energy. This reversal, however, had been found to occur in a number of reliable collinear calculations<sup>44</sup> with like potentials. Thus, we have determined that vibrational inhibition is an artifact of collinearity and the clash of theory with experiment is now removed. As for 4-atom processes, Maeda and I have used Faddeev-Yakubovsky theory to extract the atom-tri-atom scattering length for <sup>4</sup>He. We attribute the large value of -116 Å to the presence of a resonance-like state in the tetramer<sup>45</sup>. We are pressing on with this work in the belief that few-body methods can help bridge the gap between physics and chemistry. Nothing demonstrates how reasonable that belief is better than the work to be discussed in the next section.

#### 4. CHEMICAL PHYSICS

##### 4.1 Bound States

I shall highlight here only one work, the Manz, et al. study of a 1-dimensional system of  $\text{HI}$ <sup>46</sup>. These authors developed a picture of an H atom oscillating rapidly between 2 slow partners of I atoms to describe the 4 loosely-bound states near the breakup threshold when they solved directly the Schrodinger Equation transformed by the use of hyperspherical coordinates. Their results show that these states are located in the saddle-point region of a minimum-free potential, the first such occurrences ever predicted!

##### 4.2 Continuum States

Three groups have signalled new advances in the few-body treatment of collision processes in chemical systems<sup>47-49</sup>. Manz and Romelt and their collaborators have used hyperspherical coordinates and their method of S-matrix propagation to attack collinear collisions involving vibrationally inelastic, reactive and dissociative processes<sup>47</sup>. Their results were extremely accurate and I await with interest attempts to verify the technique's utility in 3 dimensions. The first successful solution of BKLT equations for reactive scattering for a realistic potential and 3-finite-mass atoms has also been reported; converged results were obtained for the collinear  $\text{H}+\text{H}_2$  exchange reaction<sup>48</sup>. Prospects for the application of BKLT elsewhere have improved considerably since Shima and Baer discovered the appropriate basis sets for the solution of the algebraic equations which arise in BKLT. Finally, on the third front, Micha and Kuruoglu have developed new "multichannel" Faddeev Equations applicable to chemical systems<sup>49</sup>. Earlier uses of the Faddeev formalism here had been limited by the need to assume dominance by pairwise forces in the systems studied. Micha and Kuruoglu circumvented this problem by including spin so that a non-diagonal electronic representation could be engaged to reduce the general interaction matrix to the sum of diatomic ones. The first application of these new equations to 3-dimensional  $\text{H}+\text{H}_2$  scattering reveal the presence of resonances in agreement with previous results.

#### 5. CONCLUSIONS

It has always been felt that, beyond their precincts, few-body methods would play an important role in nuclear physics because they could serve as a theoretical laboratory to examine approximation schemes and calculational techniques whose final destination would be many-body nuclear reactions. The irony, as we have seen in this review, is that they are perhaps more likely to find application and success in molecular physics and, perish the thought!, in chemistry.

## REFERENCES

- 1) A. Kuppermann, Nucl. Phys. A353 (1981) 286.
- 2) W. P. Reinhardt, Nucl. Phys. A353 (1981) 295.
- 3) D. A. Micha, Nucl. Phys. A353 (1981) 309.
- 4) E. Weigold, Nucl. Phys. A353 (1981) 327.
- 5) K. C. Kulander, Nucl. Phys. A353 (1981) 341.
- 6) J. S. Ball, J. C. Y. Chen and D. Y. Wong, Phys. Rev. 173 (1968) 202.
- 7) R. K. Colegrave and A. M. King, J. Phys. B14 (1981) L539.
- 8) S. P. Merkuriev, Acta Phys. Austriaca Suppl. 23 (1981) 89.
- 9) F. S. Levin, Nucl. Phys. A353 (1981) 143.
- 10) W. K. Ford and F. S. Levin, Phys. Lett. 109B (1982) 155; W. K. Ford, J. Shertzer and F. S. Levin, Chem. Phys. Lett. 96 (1983) 223.
- 11) F. S. Levin, private communication.
- 12) M. I. Haftel and V. B. Mandelzweig, Ann. Phys. 150 (1983) 48.
- 13) R. M. Shoucri and B. T. Darling, Phys. Rev. A12 (1975) 2272.
- 14) T. Sasakawa and T. Sawada, contribution to this conference.
- 15) D. R. Herrick and M. E. Kellman, Phys. Rev. A21 (1980) 418.
- 16) R. Berry, G. S. Ezra and G. Natanson, in: New Horizons of Quantum Chemistry, eds. P. -O. Lowdin and B. Pullman (D. Reidel, Dordrecht, Holland, 1983) p. 77-94.
- 17) H. Burger, W. Sandhas and E. Alt, contribution to this conference.
- 18) E. Weigold, in: Momentum-Wave Functions-1982, ed. E. Weigold (AIP, New York, 1982) pp. 1-4; I. E. McCarthy, this volume, pp. 5-18.
- 19) C. J. Joachain, in: Recent Developments in Electron-Atom and Electron-Molecule Collision Processes, ed. W. Eissner (Daresbury, Daresbury, 1982) pp. 50-56; H. Ehrhardt, M. Fischer and K. Jung, Zeit. Phys. A304 (1982) 119.
- 20) G. H. Wannier, Phys. Rev. 90 (1953) 817.
- 21) E. Schubert, A. Schuck, K. Jung and S. Geltman, J. Phys. B12 (1979) 967.
- 22) A. Temkin, Phys. Rev. Lett. 49 (1982) 365.
- 23) J. B. Donahue, et al., Phys. Rev. Lett. 48 (1982) 1538.
- 24) G. Baum, et al., J. Phys. B14 (1981) 4377.
- 25) A. R. P. Rau, in: Invited Papers, XIII ICPEAC, eds. J. Eichler, I. Hertel and N. Stolterfoht (North-Holland, Holland, 1983) in print.
- 26) H. Klar, J. Phys. B14 (1981) 4165.

- 27) E. A. G. Armour, Phys. Rev. Lett. 48 (1982) 1578.
- 28) E. Pelikan and H. Klar, Zeit. Phys. A310 (1983) 153.
- 29) C. Bottcher, J. Phys. B15 (1982) L463.
- 30) M. R. Hoare and P. Pal, Adv. Phys. 20 (1971) 161.
- 31) D. H. Levy, Adv. Chem. Phys. 47 (1981) 323.
- 32) S. Nakaichi, T. K. Lim, Y. Akaishi and H. Tanaka, J. Chem. Phys. 78 (1983) 2103 and references therein.
- 33) S. Nakaichi, T. K. Lim, Y. Akaishi and H. Tanaka, Phys. Rev. A26 (1982) 32.
- 34) S. Nakaichi-Maeda, T. K. Lim and Y. Akaishi, J. Chem. Phys. 77 (1982) 5581.
- 35) S. Sofianos, N. J. McGurk and H. Fiedeldey, Nucl. Phys. A318 (1979) 295.
- 36) S. A. Sofianos, H. Fiedeldey, H. Haberzettl and W. Sandhas, Phys. Rev. C26 (1982) 228; A. C. Fonseca, H. Haberzettl and E. Cravo, Phys. Rev. C27 (1983) 939; H. Haberzettl and S. A. Sofianos, Phys. Rev. C27 (1983) 2411.
- 37) J. G. Zabolitzky and M. H. Kalos, Nucl. Phys. A356 (1981) 114.
- 38) S. Bosanac and J. N. Murrell, Mol. Phys. 26 (1973) 349.
- 39) J. Frey and B. J. Howard, and J. Levinger, private communication.
- 40) C. G. Bao, Nucl. Phys. A373 (1982) 1; C. G. Bao, T. K. Lim and W. Q. Chao, submitted to Nucl. Phys.
- 41) N. H. March, Contemp. Phys. 24 (1983) 373; J. Chem. Phys. 79 (1983) 529.
- 42) T. K. Lim, J. M. Yuan and M. I. Haftel, Chem. Phys. Lett. 81 (1981) 87; M. I. Haftel and T. K. Lim, J. Chem. Phys. 77 (1982) 4515.
- 43) M. I. Haftel and T. K. Lim, contribution to this conference.
- 44) P. M. Hunt and S. Sridharan, J. Chem. Phys. 77 (1982) 4022.
- 45) S. Nakaichi-Maeda and T. K. Lim, Phys. Rev. A28 (1983) 692.
- 46) J. Manz, et al., Chem. Phys. Lett. 93 (1982) 184.
- 47) G. Haake, J. Manz and J. Romelt, J. Chem. Phys. 73 (1980) 5040; J. Manz and J. Romelt, Chem. Phys. Lett. 77 (1981) 172; J. Romelt, Chem. Phys. Lett. 87 (1982) 259.
- 48) Y. Shima and M. Baer, Chem. Phys. Lett. 91 (1982) 43; Y. Shima, M. Baer and D. J. Kouri, Chem. Phys. Lett. 94 (1983) 321; Y. Shima, D. J. Kouri and M. Baer, J. Chem. Phys. 78 (1983) 6666; Y. Shima and M. Baer, J. Phys. B16 (1983) 2169.
- 49) Z. C. Kuruoglu and D. A. Micha, J. Chem. Phys. in print and private communication.

## ELECTROMAGNETIC AND WEAK INTERACTIONS IN FEW-NUCLEON SYSTEMS

B. F. GIBSON

Theoretical Division, Los Alamos National Laboratory  
Los Alamos, New Mexico 87545

Selected problems in electroweak interactions are reviewed. Processes where exact numerical calculations might provide insight are emphasized.

### 1. INTRODUCTION

One fundamental question facing physicists today is that of how we unify the basic forces of nature: gravitational, electromagnetic, strong nuclear, and weak nuclear. Although progress toward an answer has been made, the candidate "Grand Unified Theories" are so far just that, candidate theories. Along the path, nuclear physics has contributed significantly to our overall knowledge of the strong force and is in a position to contribute to our knowledge of the weak force. Another fundamental question concerns our understanding of the structure of nuclei. These multibaryon systems comprise most of the mass and energy of the visible universe. Element synthesis is crucially based upon nuclear structure. The energy of our solar system is produced by nuclei. Interactions of nuclei involve all the forces of nature. Thus, to comprehend our universe, we must understand the structure of nuclear systems. But there exist various levels of understanding. Just as one would not attempt to study liquid argon to learn about QED, one does not expect to extract significant knowledge about QCD from studying the binding of the neutron and proton to form deuterium. Likewise, one does not attempt to calculate the structure of complex crystals starting from first principles; solid state is an important and viable field of physics independent of quantum electrodynamics.

Particle physics seeks an understanding of elementary particle interactions at very high energies (ultra short distances). In contrast, nuclear physics strives to describe the nucleus at energies and interparticle distances corresponding to conditions which one might picture as two bags barely overlapping. Here, in a region that the particle physicist finds difficult to describe quantitatively with asymptotically free theories, the nuclear physicist finds simplification and order in terms of nucleons and meson exchange. However, it is the possibility of speculating about the transition from the remarkably successful picture of the nucleus as a composite system of interacting nucleons to one of a quark soup that intrigues many physicists. But one must first define the limits of validity for the description of nuclear phenomena in terms

of physically observable baryons and mesons before evidence for quark degrees of freedom in nuclei can be critically evaluated. Recall two nuclear physics successes of the last decade: 1) the perfection of model calculations based solely upon nucleon degrees of freedom to the point that comparison of results with experimental data revealed the inadequacies of the assumption and demonstrated the undeniable need to expand the model to include meson exchange currents - a new degree of freedom; 2) the perfection of realistic nucleon-nucleon potential model calculations to the extent that a comparison of binding energy estimates with well established experimental results revealed discrepancies that could only be accounted for by the introduction of three-body forces. In each case detailed, precision calculations were required in comparison with numerous experimental data before one could establish that these small but significant effects were genuine. Thus, nuclear physics seeks the appropriate degrees of freedom with which to describe nuclear systems and their interactions. The ultimate test of our intellect will be whether we possess the capability to calculate all of the nuclear phenomena which we have the ability to measure.

It is this goal of understanding all we can measure which gives few-body investigations there special place in physics. Not only can experimentalists perform kinematically complete measurements, but theorists can produce exact calculations. Why the emphasis on exact calculations? First, one can test model theories by direct comparison with data. That is, approximations can be controlled, and disagreement between theory and experiment should imply some physics (not harmonic oscillator space) is missing. Second, one can find insight into novel, qualitative features of structure or reactions. For example, a folding model, two-body equation description of  ${}^3\text{H}$  will not yield the infinite binding which exact equations produce for zero range forces. Similarly, a DWBA calculation of  ${}^3\text{H}(\gamma, d)n$  fails to account for the 40% of the cross section near the peak energy which comes from coupling to the three-body channel. Third, one can generate benchmark solutions with which to test approximate procedures before launching involved studies of heavier nuclei. Unfortunately, much hard work is required to solve the exact equations for  $A \geq 3$ , especially the scattering problem, which accounts for a dearth of published continuum results. Yet, the intuition and understanding from such endeavors are most rewarding.

Two particularly useful classes of nuclear reactions are those involving electromagnetic and weak probes. Despite the auspicious title provided for my talk, there is not time allotted to provide even a catalog of experiments to be done. My remarks must necessarily be truncated to a rather subjective view of recent developments. (My apologies if your favorite piece of physics has been

omitted.) In contrast to some previous speakers, I shall consider the quantum hadrodynamic model of Walecka - the nucleon-plus-meson exchange picture of few-nucleon systems. I will not address that energy and momentum region where quark effects might become visible. I hope thereby to adhere to that area of experiment where exact calculations might contribute significantly to our understanding of nuclear physics.

## 2. ELECTROMAGNETIC INTERACTIONS

This field of physics covers a wide variety of reactions: photodisintegration, radiative capture, elastic and inelastic electron scattering, etc. Experiments may be kinematically complete or incomplete. The QED interaction operator is reasonably well understood. Elastic electron scattering yields our best picture of the charge density of the nucleus. It was the discrepancy between theory and experiment in the case of thermal  $np \rightarrow {}^2\text{H}\gamma$  that led the push for including meson exchange currents in our description of nuclei.<sup>1</sup>

Let us begin with an examination of the  ${}^2\text{H}(\gamma, p)n$  reaction for  $0^\circ$  outgoing protons, a topic which drew considerable attention at the Eugene meeting. At low energy, the number of partial waves dominating in the continuum is quite limited. Consequently, one does not lose sight of the physics in summing a large number of multipole matrix elements. The interaction between a photon and a proton charge can be represented ( $\hbar=c=1$ ) by<sup>2</sup>

$$H_{\text{int}}^e = \vec{j}(\vec{r}) \cdot \vec{\epsilon} \exp(i\vec{k} \cdot \vec{r})$$

and the interaction of a photon with a nucleon magnetic moment can be represented by

$$H_{\text{int}}^m = \frac{e\hbar}{2M} \vec{k} \times \vec{\epsilon} \cdot \vec{\sigma} \exp(i\vec{k} \cdot \vec{r})$$

where  $\vec{k}$  is the photon momentum and  $\vec{\epsilon}$  is its polarization;  $\vec{j}$  is the nonrelativistic nucleon current operator,  $\vec{r}$  is the nucleon center-of-mass position, and  $\vec{\sigma}$  is the nucleon spin operator. The current interaction can be separated into electric and magnetic parts, and when working with exact initial and final states of the same Hamiltonian, the "electric" components<sup>2</sup> of the matrix element

$$M_{fi} = \langle f | \int d^3r \vec{j}(\vec{r}) \cdot \vec{\epsilon} \exp(i\vec{k} \cdot \vec{r}) | i \rangle$$

can be shown,<sup>3</sup> through the use of current conservation, to be identical to those of the long wave length limit series

$$M_{fi} = (E_f - E_i) \sum_L i^L \langle f | \vec{\epsilon} \cdot \vec{r} (\vec{k} \cdot \vec{r})^{L-1} / L! | i \rangle.$$

This  $\vec{\epsilon} \cdot \vec{r}$  form of the E1 photodisintegration operator<sup>4</sup> contains all relevant



meson exchange corrections. However, it does not include the relativistic component of the dipole operator,<sup>5</sup> which will be seen to be important in the  $0^\circ$  cross section.

The data of Hughes et al.<sup>6</sup> which were confirmed by Gilot et al.<sup>7</sup> appear at first sight to disagree with all reasonable two-nucleon potential models (see Fig. 1). They have drawn considerable theoretical attention.<sup>8</sup> But consider

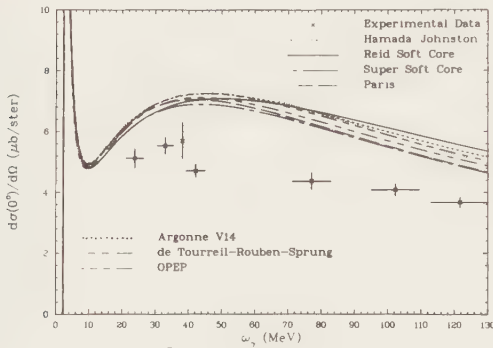


Fig. 1.  ${}^2\text{H}(\gamma, p)n$  without spin-orbit; data from Ref. 6 and 7.

what is happening physically. A photon with polarization perpendicular to the beam ( $\vec{k} \cdot \vec{\epsilon} = 0$ ) strikes a deuteron. Classically the  $\vec{E}$  field lies at right angles to the incident wave; it cannot produce a force on the proton along the direction ( $0^\circ$ ) of the beam defined by  $\vec{k}$ . Quantum mechanically, the photon brings in  $L=1$ , the proton and neutron go off back-to-back in the final state, colinear with the incident beam, and therefore have  $L=0$ . Hence the transition is forbidden, unless there is spin involved. In a central force model of the reaction, one finds  $d\sigma/d\Omega \sim \sin^2\theta$  for the  $\vec{\epsilon} \cdot \vec{r}$  operator; higher electric multipoles merely add higher powers of  $\sin^2\theta$ . The reaction is nonzero only because of i) the deuteron D-state, ii) noncentral forces in the np continuum, iii) the relativistic spin dependence of the photodisintegration operator, and iv) meson exchange and other non-Siegert terms in the interaction Hamiltonian. It is (i) and (ii) which lead to the nonzero impulse approximation result shown in Fig. 1. It is (iii), the relativistic spin-orbit contribution to the E1 operator which accounts for most of the discrepancy between the data and that impulse approximation result (see Fig. 2), as was first pointed out by Cambi et al.<sup>9</sup> This  $(v/c)^2$  relativistic correction<sup>5</sup> due to the induced electric moment of a moving magnetic moment ( $\frac{\vec{v}}{c} \times \vec{\mu} \rightarrow \frac{\hbar}{4m} \frac{\vec{p} \times \vec{\sigma}}{c^2} 2\mu_N$ ) becomes important at  $0^\circ$  because that part of the E1 transition operator which dominates the  $90^\circ$  cross section (and thus the total cross section) vanishes. The 20% correction from this unambiguous term in the operator is the dominant correction; uncertainties in the meson exchange current corrections are of the order of  $\pm 6-7\%$ . Thus, we see how relativistic effects can be visible in low energy physics. Before leaving the two-body problem, let me note that there is reported to this conference<sup>10</sup> an interesting preliminary result for a measurement of  $t_{20}$ , the tensor polarization of recoil deuterons in  ${}^2\text{H}(e, e'){}^2\text{H}$ . Such information is needed to separate the monopole and

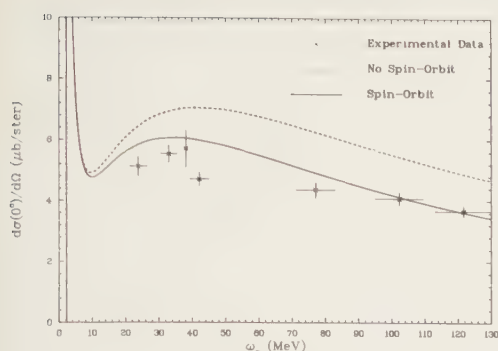


Fig. 2.  ${}^2\text{H}(\gamma, p)n$  for SCC model; data from Ref. 6 and 7.

the reaction  ${}^2\text{H}(\gamma, n_{\text{pol}})n$  was measured at an angle of  $90^\circ$  for  $6 \leq E_\gamma \leq 13$  MeV. Disagreement with published theoretical calculations was found. A similar claim<sup>14</sup> has been made for measurement of the cross section asymmetry for deuteron photodisintegration with linearly polarized photons of  $80 \leq E_\gamma \leq 600$  MeV for center-of-mass proton angles of  $75^\circ$ - $150^\circ$ .

Let us now turn our attention to the study of elastic electron scattering from  ${}^3\text{H}$  and  ${}^3\text{He}$ . It is this process that yields direct information about the square of the trinucleon ground-state wave function in terms of the charge and magnetic form factors. Recall that the cross section for this simple process can be written as<sup>15</sup>

$$\frac{d\sigma}{d\Omega} = \frac{d\sigma}{d\Omega}_{\text{Mott}} \{ F_{\text{ch}}^2(q^2) + \mu^2 \eta^2 [1 + 2(1 + \eta^2) \tan^2(\theta/2)] F_{\text{mag}}^2(q^2) \} / (1 + \eta^2)$$

$$\frac{d\sigma}{d\Omega}_{\text{Mott}} = \left( \frac{Z\alpha}{2E} \right)^2 \frac{\cos^2(\theta/2)}{\sin^4(\theta/2) [1 + (2E/M) \sin^2(\theta/2)]},$$

where  $\eta = q/(2M)$ ,  $q = k_e - k'_e$  is the momentum transfer,  $M$  is the trinucleon mass, and  $k_e \cdot k'_e = \cos \theta$ . The charge form factor  $F_{\text{ch}}(q^2)$  is defined in impulse approximation by<sup>16</sup>

$$F_{\text{ch}}(q^2) = \frac{1}{Ze} \langle \psi | \rho_{\text{ch}}(\vec{r}, \vec{r}_j) \exp(i\vec{q} \cdot \vec{r}) | \psi \rangle,$$

where

$$\rho_{\text{ch}}(\vec{r}, \vec{r}_j) = \sum_{j=1}^3 \left[ \frac{1}{2}(1 + \tau_z^j) f_{\text{ch}}^p(\vec{r} - \vec{r}_j) + \frac{1}{2}(1 - \tau_z^j) f_{\text{ch}}^n(\vec{r} - \vec{r}_j) \right]$$

and  $\psi$ ,  $f_{\text{ch}}^p$ ,  $f_{\text{ch}}^n$  are the trinucleon wave function and charge densities of the proton and neutron respectively. Relativistic corrections of order  $(v/c)^2$  include the usual Darwin-Foldy and spin-orbit terms.<sup>5</sup> Meson-exchange-current

quadrupole charge form factors of the deuteron. In addition, Bohannon and Heller<sup>11</sup> have reported model problem numerical studies for the extension of the soft-photon theorem for bremsstrahlung discussed at the Graz meeting.<sup>12</sup> Finally, Holt et al.<sup>13</sup> have raised a new question concerning deuteron photodisintegration.

The neutron polarization in

corrections are of the same order and are intimately connected.<sup>17</sup> The magnetic moment form factor is perhaps more easily described in momentum space

$$F_{\text{mag}}(q^2) = \langle \psi | \hat{\epsilon} \cdot \vec{J} | \psi \rangle, \quad \hat{\epsilon} \cdot \vec{q} = 0$$

where

$$\vec{J}_{\text{impl}} = \vec{J}_{\text{conv}} + \vec{J}_{\text{mom}}$$

$$\vec{J}_{\text{conv}} = \sum_{j=1}^3 \frac{1}{2M} [\vec{p}_j \exp(i\vec{q} \cdot \vec{r}_j) + \exp(i\vec{q} \cdot \vec{r}_j) \vec{p}_j] \frac{1}{2} (1 + \tau_z^j) f_{\text{ch}}^p(q^2)$$

$$\vec{J}_{\text{mom}} = \sum_{j=1}^3 \frac{i}{2M} \vec{\sigma}_j \times \vec{q} \exp(i\vec{q} \cdot \vec{r}_j) \left[ \frac{1}{2} (1 + \tau_z^j) \mu_p f_{\text{mag}}^p(q^2) + \frac{1}{2} (1 - \tau_z^j) \mu_n f_{\text{mag}}^n(q^2) \right].$$

This operator is of order  $(v/c)$  and relativistic corrections are  $(v/c)^3$ . The isovector meson-exchange-current correction cannot be neglected, being the same order in  $(v/c)$  as the impulse current. I wish only to make two points concerning the trinucleon form factors, which have been of intense interest since Collard's original experiment.<sup>18</sup> First, recent measurement<sup>19</sup> of the  $^3\text{He}$  charge form factor below  $q^2 = 4 \text{ fm}^{-2}$ , when combined with the world's data, indicates that  $\langle r_{\text{ch}}^2(^3\text{He}) \rangle^{1/2} = 1.875 \pm .011 \text{ fm}$  in contrast to that reported by Dunn et al.<sup>20</sup> (The magnetic rms radius is about  $1.95 \text{ fm}$ .<sup>21</sup>) Work in progress<sup>22</sup> on  $^3\text{H}$  appears

to yield  $\langle r_{\text{ch}}^2(^3\text{H}) \rangle^{1/2}$  somewhat lower than Collard's original value ( $1.70 \text{ fm}$ ). An rms radius as small as  $1.65 \text{ fm}$  would not be inconsistent with point charge radii differences produced in Faddeev calculations ( $\Delta r_{\text{ch}} \approx 0.20 \text{ fm}$ ),<sup>23</sup> because studies of the  $^3\text{He}$  charge form factor including a Coulomb interaction between protons indicate that the Coulomb repulsion increases  $\Delta r_{\text{ch}}$  by a small but not insignificant  $0.03 - 0.04 \text{ fm}$ .<sup>24</sup> Definitive  $^3\text{H}$  experiments are needed. Second, the magnetic form factor data are shown in Fig. 3. Theoretical results came tantalizingly close to the data. However, as has been pointed out by Lehman, it is disconcerting to see that the

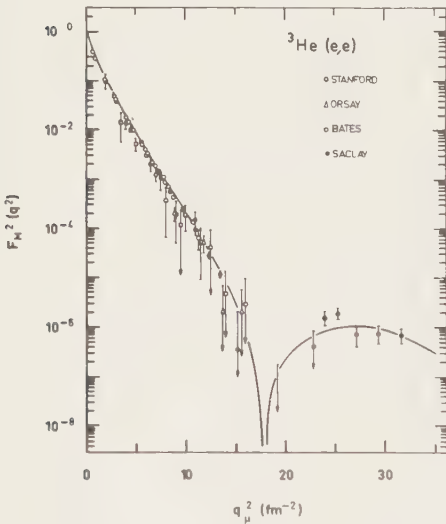


Fig. 3.  $F_M^2(q^2)$  for  $^3\text{He}$  from Ref. 25; curve is a best fit.

magnetic moments from these calculations do not agree (see Table I).<sup>26</sup>

In contrast to elastic scattering, inelastic electron scattering, especially coincidence experiments such as  $^3\text{He}(e, e'p)d$  and  $^3\text{He}(e, e'p)np$ , yields information

about the overlap of the ground-state wave function and the wave function of a nucleon moving freely relative to a deuteron or pair of nucleons in a scattering state. These overlaps define the structure of the  ${}^3\text{H} \rightarrow \text{nd}$ ,  ${}^3\text{He} \rightarrow \text{pd}^*$  etc. vertices, which can be described in terms of asymptotic normalization constants, momentum distributions, and related quantities.<sup>30</sup> To be specific we consider the  ${}^3\text{He}(e, e'p)d$  experiment of Jans et al.,<sup>31</sup> although there also exist new data by Kozlovsky et al.<sup>32</sup> The general form of the coincidence cross section is

$$\frac{d\sigma}{dE_e d\Omega_e d\Omega_p} = \frac{d\sigma}{d\Omega_{ep}} F(E_e, \Omega_e, \Omega_p) \frac{3}{2} \{ |f_0(q)|^2 + 2|f_2(q)|^2 \}$$

where  $d\sigma/d\Omega_{ep}$  is the half-off-shell ep scattering cross section,  $F(E_e, \Omega_e, \Omega_p)$  is a kinematic factor, and  $\frac{3}{2}\{\dots\}$  is the momentum distribution. It is  $\{\dots\}$  which is usually called the spectroscopic factor. A closely related quantity is the fraction of pd component in the trinucleon wave function:

$$P_{pd} = 2\pi \int_0^\infty q^2 dq \{ |f_0(q)|^2 + |f_2(q)|^2 \}$$

The momentum distribution amplitudes  $f_0(q)$  and  $f_2(q)$  are the  $\ell=0,2$  components of the overlap of the ground state wave function with the continuum state of a nucleon of momentum  $\vec{q}$  moving freely relative to a deuteron:

$$\begin{aligned} &{}_A \langle \text{nd}; \vec{q}, \frac{1}{2}m_p \mid m_d \mid {}^3\text{H}; \frac{1}{2}m \rangle \\ &= \sqrt{\frac{3}{2}} \sum_{\ell=0} \sum_{J=1/2, 3/2} \langle \frac{1}{2}m_n \mid m_d \mid JM_J \rangle \langle \frac{1}{2}m_p \mid JM_J \mid \frac{1}{2}m \rangle \sqrt{4\pi} Y_{\ell m}^{[1]}(\hat{q}), \end{aligned}$$

where spin and isospin quantum numbers have been suppressed. These amplitudes are directly related to the asymptotic normalization constants  $C_\ell^1$  of the trinucleon ground state wave function<sup>30,33</sup>

$$\begin{aligned} \lim_{\rho \rightarrow \infty} \psi(\vec{r}, \vec{\rho}) &= C_S^1 \sqrt{\frac{\mu}{2\pi}} \frac{e^{-\mu\rho}}{\rho} \sqrt{4\pi} [[Y^{[0]}(\hat{\rho}) \times \chi_{\frac{1}{2}}^{[1]}(1)]^{\frac{1}{2}} \times \phi_d^{[1]}(r)]^{\frac{1}{2}} \frac{\eta'}{\sqrt{2}} \\ &= C_D^1 \sqrt{\frac{\mu}{2\pi}} \frac{e^{-\mu\rho}}{\rho} \left( 1 + \frac{3}{\mu\rho} + \frac{3}{\mu^2\rho^2} \right) \\ &\quad \times \sqrt{4\pi} [[Y^{[2]}(\hat{\rho}) \times \chi_{\frac{1}{2}}^{[1]}(1)]^{\frac{3}{2}} \times \phi_d^{[1]}(\vec{r})]^{\frac{1}{2}} \frac{\eta'}{\sqrt{2}} \end{aligned}$$

by

$$C_\ell^1 = i^\ell \{ 2\pi i \mu^{\frac{1}{2}} \lim_{q \rightarrow i\mu} (q - i\mu) f_\ell(q) \}.$$

A question of recent interest is whether one can extrapolate from the measured ( $q=0$ ) distorted wave quantity<sup>34</sup>

$$D_2 = \lim_{q \rightarrow 0} \{ -f_2(q) / [q^2 f_0(q)] \}$$

Table I. Breakdown of magnetic moment calculations

	SSC <sup>27</sup>	Paris <sup>28</sup>	RSC <sup>29</sup>
impulse	-1.760	-1.77	-1.826
pair-graph	-0.344	-0.29	-0.563
pion-graph	-0.082	-0.03	-0.202
$\Delta$ -graph	-0.144	-0.05*	-0.024

\*from coupled-channel calculation.

to the pole position ( $i\mu$ ) where  $C_S^1$  and  $C_D^1$  are defined. That is, if one defines a theoretical distorted wave quantity

$$\tilde{D}_2 = -C_D^1/(\mu^2 C_S^1) ,$$

is  $\tilde{D}_2 \cong D_2$ ? Simple separable model studies indicate that the answer is yes, although not as well as in the case of the deuteron. Separable model results for the  $^3\text{H} \rightarrow \text{nd}$  momentum distribution are plotted in Fig. 4 along with data extracted from the  $^3\text{He}(e,e'p)d$  experiment of Saclay. There is an absolute uncertainty in the extraction of the order of 10-15% due to the assumption of pole dominance and the ambiguity associated with the half-off-shell ep cross section. Within this framework, both the 4% and 7% deuteron D-state models are consistent with experiment for  $q \leq 100$  MeV/c, the expected range of validity for the pole dominance assumption. Such is also the case for more sophisticated models like the Reid soft core.<sup>31,35</sup> Thus, pole dominance is not a valid assumption at higher momentum transfer. (Incidentally, for the  $^3\text{He}(e,e'p)np$  reaction<sup>31</sup> where the detected proton does not have a high energy relative to the np pair, neglect of 3-body final state interactions will likely destroy any agreement between theory and experiment.) The inclusive quasielastic cross sections are also most interesting. There are systematic disagreements between theory and data.<sup>36</sup> Time does not permit delving into this subject.

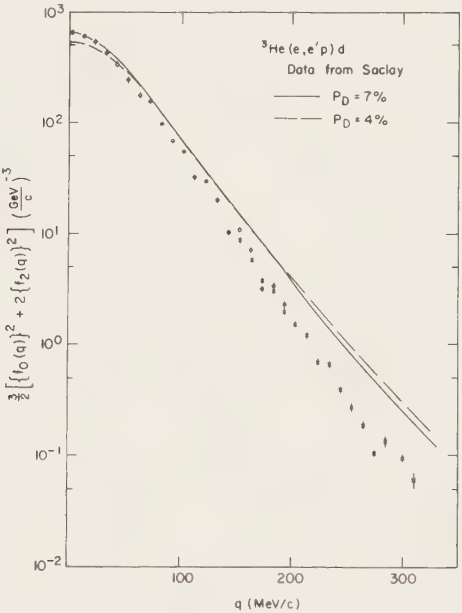


Fig. 4. Momentum distribution for  $^3\text{H} \rightarrow \text{nd}$  with data from  $^3\text{He}(e,e'p)d$ .

does not have a high energy relative to the np pair, neglect of 3-body final state interactions will likely destroy any agreement between theory and experiment.) The inclusive quasielastic cross sections are also most interesting. There are systematic disagreements between theory and data.<sup>36</sup> Time does not permit delving into this subject.

Before leaving the A=3 isodoublet, let me point out some recent interesting

results in the realm of photonuclear physics. In a preprint concerning the  $^2\text{H}(p,\gamma)^3\text{He}$  capture reaction, King et al.<sup>37</sup> have reported measurement of angular distributions from 6.5 to 16 MeV (see Fig. 5). A sensitivity to the D-state components of the  $^3\text{He}$  wave function is noted. One caution in any analysis of such data to extract angular distribution coefficients: All higher partial wave contributions should be summed in any analysis because the trinucleons,

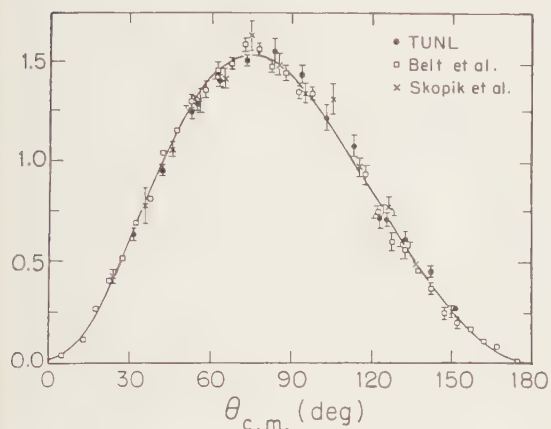


Fig. 5. Angular distribution for  $^2\text{H}(p,\gamma)^3\text{He}$ ; data from Ref. 37-39.

like the deuteron, are large objects; the multipole series does not converge rapidly and the sum of an infinite number of individually negligibly small terms is not vanishingly small.<sup>40</sup> Skopik et al.<sup>39</sup> have just published an  $^3\text{He}(e,d)e^+p$  measurement which implies that E2 strength near the peak of the  $^3\text{He}(\gamma,d)p$  cross section is small, less than 2% of the total cross section. A preprint by Torre et al.<sup>41</sup> shows reasonable results for magnetic exchange current contributions to the  $nd \rightarrow ^3\text{H}\gamma$  thermal neutron capture reaction.<sup>42</sup> In the higher energy region, the question of time reversal invariance in the  $^3\text{He}\gamma \leftrightarrow pd$  reaction has again come to the forefront. Sober et al.<sup>43</sup> have remeasured at Bates differential cross sections for  $^3\text{He}(\gamma,d)p$  in the photon energy range of 150-350 MeV for center-of-mass angles of  $60^\circ$  and  $90^\circ$ . The absolute uncertainty for this gas target experiment in which recoil deuterons are detected is quoted as less than 6%. (Preliminary results can be found in Briscoe et al.<sup>44</sup>) These results are significantly higher than those of Saclay and Bonn<sup>45</sup> and lower than those of Caltech and Frascati.<sup>46</sup> The detail balance converted cross sections agree well with the recent TRIUMF data<sup>47</sup> and with new data from the UCLA-Saclay collaboration,<sup>48</sup> although the agreement is poor with older published results.<sup>44</sup> There is no evidence for a violation of time reversal invariance. Finally, interesting Coulomb effects were found in the  $^3\text{He}(\gamma,2p)n$  reaction for photon energies between 80 and 120 MeV, when the two protons are emitted in close proximity.<sup>49</sup>

In the  $A=4$  area, the significant difference between the  $^4\text{He}(\gamma,p)^3\text{H}$  and  $^4\text{He}(\gamma,n)^3\text{He}$  cross sections in the 24-32 MeV photon energy range is the most interesting phenomena. The cross sections are shown in Fig. 6 (solid lines) as



they were evaluated by Calarco, Berman, and Donnelly.<sup>50</sup> The shaded bands indicate their estimates of the uncertainties in the individual cross sections.

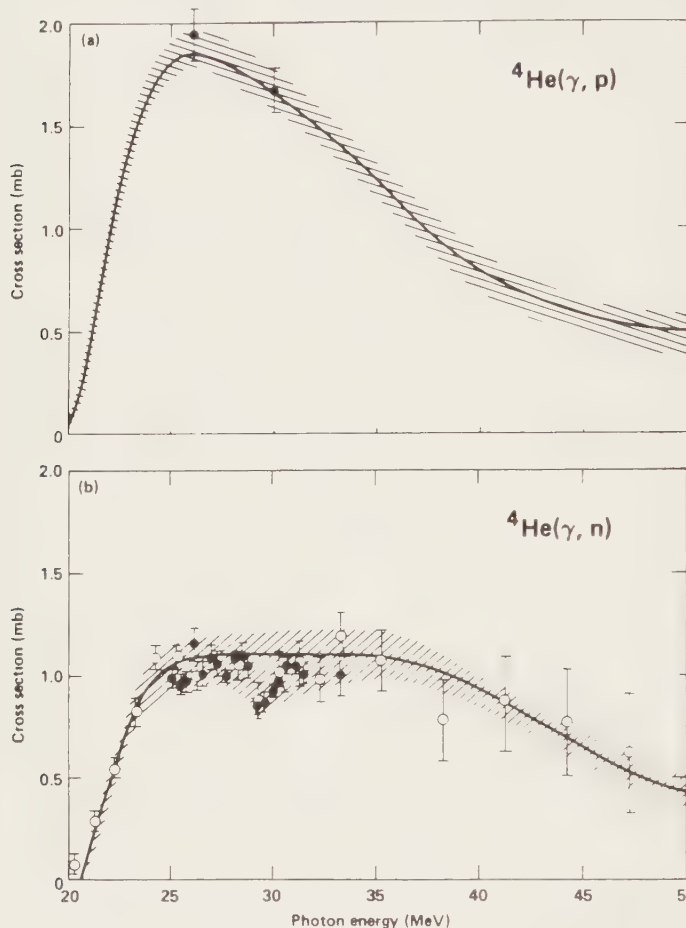


Fig. 6 The  ${}^4\text{He}(\gamma, p){}^3\text{H}$  and  ${}^4\text{He}(\gamma, n){}^3\text{He}$  cross section evaluation (solid lines); data in (a) from Ref. 51, open circles in (b) from Ref. 52, closed circles in (b) from Ref. 53.

to date predict only small differences in the two cross sections.<sup>50</sup> Other information concerning this energy region is becoming available. Angular distributions for the  ${}^3\text{H}(p, \gamma){}^4\text{He}$  reaction have been reported by McBroom et al.<sup>54</sup> In addition, Weller et al.<sup>55</sup> have reported a first measurement of polarized neutron capture on  ${}^3\text{He}$  at  $E_n = 9$  MeV, which corresponds to a photon energy of 27.3 MeV. The polarized and unpolarized angular distribution data lead Weller et al. to the conclusion that there is little E2 or spin-flip E1 contributing to

The data points are from Ref. 51-53; these references also contain the data included in the cross section evaluation. It is clear that the cross sections differ substantially below 30 MeV. Because the reaction mechanism is dominated by the E1 ( $\Delta S=0, \Delta T=1$ ) transition, the inequality of the cross section implies the existence of strong isospin mixing in the four-nucleon  $J^\pi=1^-$  states. Calarco et al. have interpreted the large deviation of the cross section ratio  $R=\sigma(\gamma, p)/\sigma(\gamma, n)$  from a value of 1 in terms

of a charge asymmetry in the nuclear force, because continuum calculations published



the cross section.

The photodisintegration of the alpha particle is more complex than that of, say,  $^3\text{He}$  where one has only two open channels (pd and ppn).<sup>56</sup> Here one has 5 distinct open channels, and there exist known excited states of  $^4\text{He}$ .<sup>57</sup> However, at the low energies relevant to the ratio puzzle, the dominant E1 transition is saturated by the  $^4\text{He}(\gamma, n)^3\text{He}$  and  $^4\text{He}(\gamma, p)^3\text{H}$  reaction channels.<sup>58</sup> The  $^4\text{He}(\gamma, d)d$  channel contributes only to even multipoles because of the equal mass and charge of the final-state deuterons, while the multiparticle channels  $^4\text{He}(\gamma, d)np$  and  $^4\text{He}(\gamma, n)npp$  do not connect to the  $T=0$   $^4\text{He}$  ground state for any final-state isospin value other than the  $T=1$  of the  $n^3\text{He}$  and  $p^3\text{H}$  channels. These multiparticle final states are therefore suppressed relative to two-body final states of the same isospin, just as one sees experimentally and theoretically for the trinucleons.<sup>56</sup> Based upon this knowledge that only 2-body channels are important, a bound-state shell model calculation was used to illustrate the point that, if all three  $J^\pi = 1^-$  states ( $T=1, S=0$ ;  $T=1, S=1$ ;  $T=0, S=1$ ) were properly mixed via Coulomb and/or a small charge asymmetry in the NN force, the measured ratio  $R$  could be understood.<sup>59</sup> Such a model would appear to be in conflict with the results of Ref. 55. However, recent R-matrix work by Dodder and Hale<sup>60</sup> on fitting of the strong interaction cross sections (elastic scattering, charge exchange, etc.) indicates that Coulomb mixing of the type discussed in Ref. 59 does lead to significant mixing in the  $J^\pi=1^-$  levels. Such an R-matrix calculation would be expected to yield a ratio of  $R \gg 1$ .

### 3. WEAK INTERACTIONS

The unified theory of the electroweak interactions is one of the great achievements of physics. The WSG<sup>61</sup> or Standard Model unifies the weak interactions and electromagnetism in a renormalizable framework. Predictions of weak-neutral-current effects agree with experiment. Despite the notable successes, rigorous testing of the theory lies ahead. It is for this reason that experimentalists must strive for improved  $\mu^-$  and neutrino facilities. Nuclear targets will play a key role in studies of the structure of the weak interactions, because nuclear selection rules and the variety of available transitions make nuclei excellent filters or analyzers for sorting out components of the weak interaction. Recall that nuclear experiments demonstrated V-A was to be and not S-P-T.

In order to be specific, let me restrict my remarks to neutrino physics. Tests of  $\mu$ -e universality, induced pseudoscalar coupling, CVC, etc. with muons are of no less importance<sup>62</sup> as are parity nonconservation studies in  $\vec{p}p$ ,  $\vec{p}d$  scattering and  $np \rightarrow d\gamma$ .<sup>63-65</sup> Even so, there is not time to provide a complete

review of the underlying theory. It is assumed that there exists an effective Lagrangian description of the  $\nu_e \leftrightarrow e^-$ ,  $\nu_e \leftrightarrow \nu_e$ , and  $e^- \leftrightarrow e^-$  processes mediated by the  $\gamma$ , charged  $W$ , and the neutral  $Z$  bosons. The heavy bosons are so massive that those couplings are point-like, and one writes a four-point interaction description: leptonic current times hadronic current. The hadronic currents<sup>66</sup> are of the V-A form  $J_\mu = J_\mu^5 + J_\mu^V$  with the charge-changing currents being the raising and lowering parts of the isovector operator  $J_\mu^{(\pm)} = J_\mu^1 \pm iJ_\mu^2$ . Correspondingly, the electromagnetic current has the isospin structure  $J_\mu^Y = J_\mu^3 + J_\mu^V$ , and the conserved-vector-current theory (CVC) tells us that the vector part of the charge-changing current is just  $J_\mu^{(\pm)} = J_\mu^1 \pm iJ_\mu^2$ . CVC relates this aspect of the weak and electromagnetic current; this was the first part of the electroweak unification. The Standard Model is, in essence, an extended CVC with the addition of a neutral weak current of the form  $J_\mu^{(0)} = J_\mu^3 - 2\sin^2\theta_W J_\mu^Y$ . We believe that the interaction of leptons with the bosons is understood; therefore one is studying the hadronic aspects of the electroweak interaction in nuclear investigations.

Because the momentum transfer is small in conventional processes such as  $\beta$ -decay,  $e^-$ -capture, and  $\mu^-$ -capture, neutrino studies are valued for their potential to explore the weak interaction form factors over an extended region of momentum transfer  $q$ . The Standard Model predicts that the electromagnetic and weak interaction processes are related for all  $q$ . There are simple (theoretically) tests of this remarkable concept.<sup>66</sup> Consider  $(\nu_e \nu_e')$ ,  $(\bar{\nu}_e, \bar{\nu}_e')$ , and  $(e, e')$  scattering from a  $T=0$ ,  $J^\pi=0^+$  nucleus such as  $^4\text{He}$  (either the elastic scattering or the inelastic scattering to the 20 MeV  $T=0$ ,  $J^\pi=0^+$  first excited state). Because we have  $T=0$ ,  $J_\mu^{(0)} = -2\sin^2\theta_W J_\mu^Y$ ; the weak neutral current is pure vector in WSG and is directly proportional to the e.m. current. Thus, there is a direct relation between neutrino scattering and electron scattering. In particular one has

$$d\sigma_{\nu_\ell \nu_\ell'} \equiv d\sigma_{\bar{\nu}_\ell \bar{\nu}_\ell'} = \sin^4\theta_W \frac{G^2 q^4}{2\pi^2 \alpha^2} d\sigma_{ee'}^{\text{ERL}},$$

where ERL refers to the extreme relativistic limit ( $E_e \gg m_e$ ). This result holds for all  $q$ , all  $\theta$  independent of the nuclear structure. It is a true test of the unification of the electroweak interactions. The neutrino and electron cross sections must be identical if the Standard Model is correct.

I close with cursory mention of weak interaction physics and the deuteron. First a reminder:  $\mu^- d \rightarrow \nu n n$  may provide the cleanest measurement of the nn scattering length. Second, parity nonconservation in  $\vec{\gamma} d \rightarrow n p$  and in  $\vec{p} d$  elastic scattering yield information about  $T=1$  parts of the weak interaction not avail-

able from  $T=0$   $\vec{p}p$  experiments. Third,  $\nu$ - $^2\text{H}$  and  $\bar{\nu}$ - $^2\text{H}$  scattering and reactions are interesting testing grounds of electroweak coupling to more than one nucleon, that is exchange currents. In addition, the elastic scattering is sensitive to axial vector isoscalar coupling which is identically zero in the Standard Model. Donnelly<sup>67</sup> has investigated this in some detail and found that for  $E_\nu \cong 150$  MeV the sensitivity of the cross section to any such nonstandard term can be enhanced by a large factor over vector coupling. Furthermore, the interference with the vector coupling is destructive for neutrinos and constructive for antineutrinos, providing a clean signal.

#### ACKNOWLEDGEMENT

I wish to thank J. L. Friar, D. R. Lehman and J. D. Walecka for many profitable discussions. In addition, I am in debt to B. L. Berman, W. J. Briscoe, J. R. Calarco, T. W. Donnelly, B. Frois, L. Heller, Y. E. Kim, R. P. Redwine, P. U. Sauer, and D. M. Skopik, for supplying information included. This work was performed under the auspices of the U. S. Dept. of Energy.

#### REFERENCES

1. H. A. Bethe and C. Longmire, *Phys. Rev.* 77 (1950) 647; N. Austern and E. Rost, *Phys. Rev.* 117 (1960) 1506; A. Cox et al. *Nucl. Phys.* 74 (1965) 481; G. E. Brown and D. O. Riska, *Phys. Lett.* 38B (1972) 193; M. Gari and A. H. Huffman, *Phys. Rev. C* 7 (1973) 944.
2. R. G. Sachs and N. Austern, *Phys. Rev.* 81 (1951) 705.
3. L. L. Foldy, *Phys. Rev.* 96 (1953) 178.
4. A. J. F. Siegert, *Phys. Rev.* 52 (1937) 787.
5. W. A. Barker and F. N. Glover, *Phys. Rev.* 99 (1955) 317; J. L. Friar, Mesonic vs. Relativistic Effects, in: *Mesons in Nuclei*, eds. M. Rho and D. H. Wilkinson (North Holland, Amsterdam, 1979) pp 597-623; J. L. Friar, *Nucl. Phys.* A353 (1981) 233c.
6. R. J. Hughes et al. *Nucl. Phys.* A267 (1976) 329.
7. J. F. Gilot et al. *Phys. Rev. Lett.* 47 (1981) 304.
8. H. Arenhövel and W. Fabian, *Nucl. Phys.* A282 (1977) 397; E. L. Lomon, *Phys. Lett.* 68B (1977) 419; M. L. Rustgi et al. *Phys. Rev. C* 20 (1979) 24; M. Gari and B. Sommer, *Phys. Rev. Lett.* 41 (1978) 22; E. Hadjimichael, *Phys. Lett.* 85B (1979) 17; W. Jaus and W. S. Woolcock, *Nucl. Phys.* A365 (1981) 477.
9. A. Cambi et al. *Phys. Rev. Lett.* 48 (1982) 462.
10. M. E. Schulze et al. Measurement of tensor polarization of the recoil deuteron in electron-deuteron elastic scattering, this conference.
11. G. E. Bohannon and L. Heller, Extension of the Soft-Photon Theorem for Bremsstrahlung (to be published).
12. L. Heller, *Lecture Notes in Physics* 87 (1978) 68.
13. R. J. Holt et al. *Phys. Rev. Lett.* 50 (1983) 577.

14. V. G. Gorbenko et al. Nucl. Phys. A381 (1982) 330.
15. M. N. Rosenbluth, Phys. Rev. 79 (1950) 615.
16. L. I. Schiff, Phys. Rev. 133 (1964) B802.
17. J. L. Friar, Phys. Rev. C 27 (1983) 2078.
18. H. Collard et al. Phys. Rev. 138 (1965) B57.
19. D. M. Skopik (private communication).
20. P. C. Dunn et al. Phys. Rev. C 27 (1983) 71.
21. J. S. McCarthy et al. Phys. Rev. C 15 (1977) 1396.
22. D. Beck, D. M. Skopik, and W. Turchnitz (private communication).
23. J. A. Tjon et al. Phys. Rev. Lett. 25 (1970) 540; G. Gignoux and A. Laverne, Phys. Rev. Lett. 29 (1972) 436; G. L. Payne et al. Phys. Rev. C 22 (1980) 823.
24. G. L. Payne et al. Phys. Rev. C 22 (1980) 832; J. L. Friar et al. Phys. Rev. C 24 (1981) 665.
25. J. M. Cavedon et al. Phys. Rev. Lett. 49 (1982) 986; B. Frois, Experiments on few nucleon systems with low and medium energy electrons, this conference.
26. D. R. Lehman, Bull. Am. Phys. Soc. 27 (1982) 694 (and private communication).
27. E. Hadjimichael et al., Phys. Rev. C 27 (1983) 831.
28. Ch. Hajduk et al. Nucl. Phys. A (in print); The electromagnetic structure of the three-nucleon bound states, this conference.
29. M. A. Maize and Y. E. Kim, Nucl. Phys. A (in print); Meson-exchange currents, current conservation and magnetic form factor of  $^3\text{He}$ , this conf.
30. B. F. Gibson and D. R. Lehman, Structure of the  $^3\text{H} \rightarrow n + d(d^*)$  vertexes (to be published).
31. E. Jans et al. Phys. Rev. Lett. 49 (1982) 974.
32. I. V. Kozlovsky et al. Nucl Phys, A368 (1981) 493.
33. J. L. Friar et al. Phys. Rev. C 25 (1982) 1616.
34. L. D. Knutsen et al. Phys. Rev. Lett. 35 (1975) 1570.
35. A. E. L. Dieperink et al. Phys. Lett. 63B (1976) 261.
36. D. R. Lehman, Phys. Rev. C 3 (1971) 1827; H. Meier-Hajduk et al. Nucl. Phys. A395 (1983) 332.
37. S. E. King et al. Effects of the  $^3\text{He}$  D-state in the  $^2\text{H}(p,\gamma)^3\text{He}$  reaction (to be published).
38. B. D. Belt et al. Phys. Rev. Lett. 24 (1970) 1120.
39. D. M. Skopik et al. Phys. Rev. C 28 (1983) 52.
40. B. F. Gibson and J. S. O'Connell, Phys. Lett. 32B (1970) 331.
41. J. Torre and B. Goulard, Meson exchange currents and radiative thermal neutron capture by the deuteron (to be published).
42. J. S. Merritt et al. Nucl Sci. Eng. 34 (1968) 195; E. T. Jurney et al. Phys. Rev. C 25 (1982) 2810.
43. D. I. Sober et al. The two-body photodisintegration of  $^3\text{He}$  between 150 and 350 MeV (to be published).

44. W. J. Briscoe et al. *Phys. Rev. Lett.* 49 (1982) 187.
45. P. E. Argan et al. *Nucl. Phys. A* 237 (1975) 447; H. J. Gassen et al. *Z. Phys. A* 303 (1981) 35.
46. C. A. Heusch et al. *Phys. Rev. Lett.* 37 (1976) 405; P. Picozza et al. *Nucl. Phys. A* 157 (1970) 190.
47. R. Abegg et al. *Phys. Lett.* 118B (1982) 55.
48. B. H. Silberman et al. (private communication).
49. C. A. Peridier et al. *Z. Phys. A* 310 (1983) 317.
50. J. R. Calarco et al. *Phys. Rev. C* 27 (1983) 1866.
51. J. R. Calarco et al. (private communication).
52. B. L. Burman et al. *Phys. Rev. C* 22 (1980) 2273.
53. L. Ward et al. *Phys. Rev. C* 24 (1981) 317.
54. R. C. McBroom et al. *Phys. Rev. C* 25 (1982) 1644.
55. H. R. Weller et al. *Phys. Rev. C* 25 (1982) 2111.
56. B. F. Gibson, *Nucl. Phys. A* 353 (1981) 85c.
57. W. E. Meyerhof and T. A. Tombrello, *Nucl. Phys. A* 109 (1968) 1.
58. A. N. Gorbunov, *Proc. P. N. Lebedev Physics Inst.* 71 (1974) 1 (*Nauka*, Moscow; translation: Consultants Bureau, New York).
59. B. F. Gibson, *Nucl. Phys. A* 195 (1972) 449.
60. G. M. Hale (private communication).
61. S. Weinberg, *Phys. Rev. Lett.* 19 (1967) 1264 and *Phys. Rev. D* 5 (1972) 1412; A. Salam and J. C. Ward, *Phys. Lett.* 13 (1964) 168; S. L. Glashow et al. *Phys. Rev. D* 2 (1970) 1285.
62. J. D. Walecka, Muon capture reaction ( $\mu^-, \nu_e$ ) with nuclei, in: *Proceedings of the Second LAMPF II Workshop*, eds. H. Thiessen, T. Bhatia, R. Carlini, and N. Hintz (Los Alamos, LA-9572-C, 1972) pp 440-453; Semileptonic weak interactions in nuclei, in: *Muon Physics II*, eds. V. Hughes and C. Wu (Academic Press, New York, 1975) pp 113ff.
63. E. M. Henley, *Annu. Rev. Nucl. Sci.* 19 (1969) 367; E. Fischback and D. Tadic, *Phys. Rept.* 6 (1973) 124; M. Gari, *ibid* 6 (1973) 318; M. Box et al. *J. Phys. G* 1 (1975) 493.
64. B. Desplanques et al. *Ann. Phys. (N.Y.)* 124 (1980) 449.
65. J. M. Potter, et al. *Phys. Rev. Lett.* 33 (1974) 1307; B. Balzer et al. *Phys. Rev. Lett.* 44 (1980) 699; N. Lockyer et al. *Phys. Rev. Lett.* 45 (1980) 1821; V. M. Lobashov et al. *Nucl. Phys. A* 197 (1972) 241 (and private communication); J. F. Cavaignec et al. *Phys. Lett.* 67B (1977) 148.
66. J. D. Walecka, Neutrino Interactions with nuclei, in: *Proceedings of the Second LAMPF II Workshop*, eds. H. Thiessen, T. Bhatia, R. Carlini, and N. Hintz (Los Alamos, LA-9572-C, 1982) pp 560-583; Weak interactions with nuclei, in: *Proceedings of the Third LAMPF II Workshop*, eds. H. Thiessen and T. Bhatia (to be published).
67. T. W. Donnelly, Highlights of nuclear physics with neutrinos, in: *Proceedings of the Los Alamos Neutrino Workshop*, eds. F. Boehm and G. J. Stephenson, Jr. (Los Alamos, LA-9358-C, 1981). pp 11-32; Intermediate energy elastic neutrino scattering from nuclei, *ibid* pp 75-95.



## MOLECULAR SYSTEMS WITH MUONS OR MONOPOLES

Giovanni FIORENTINI

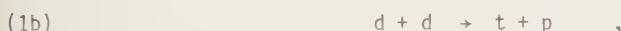
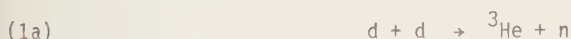
Istituto Nazionale di Fisica Nucleare and  
 Istituto di Fisica dell'Università, 56100, Pisa, Italy

I discuss recent developments in the field of exotic molecules. Particularly I will concentrate on muonic molecules, three body systems consisting of two Hydrogen nuclei and one negative muon, and systems which contain a magnetic monopole in addition to electrons and atomic nuclei.

### 1. INTRODUCTION

I will discuss recent developments in the field of "exotic" molecular systems. Particularly I will concentrate on muonic molecules, three body systems consisting of two hydrogen nuclei and one negative muon, and what I would like to call monopolic molecules, systems which contain a magnetic monopole in addition to electrons and atomic nuclei.

Muonic molecules  $((X-\mu-X'))$ ;  $X, X' = p, d$  or  $t$ ) are in essence shrunked versions of the  $H_2^+$  molecular ion, with a typical scale of lengths given by the muon Bohr radius,  $a_\mu = a_0 m_e/m_\mu \sim 250$  fm, and with binding energies of up to few hundreds eV. They are interesting by itself as a pure three body Coulomb problem, which can be studied, both theoretically and experimentally, to a high degree of precision. Beyond this, the study of muonic molecules is particularly important in connection with several fields of physics: the study of muon capture,  $\mu^- + p \rightarrow \nu_\mu + n$ , when the muon is bound in the  $(p-\mu-p)$  molecule, is important in order to determine basic parameters of the weak interaction theory. Study of the two mirror fusion reactions,



when the two deuterons are bound in the  $(d-\mu-d)$  molecule can yield interesting information on charge symmetry violations in the p-wave d-d interaction near threshold. Also, the spectroscopy of muonic molecules is a sensitive tool to investigate the tail of the nucleon-nucleon potential. Finally, it has been pointed out that the fusion reactions occurring in muonic molecules - the so called muon catalyzed fusion - can be of interest for practical applications. In this respect it is worth mentioning the encouraging (preliminary) results of an experiment in progress at LAMPF.



There are several reviews covering the different aspects of the physics of muonic molecules<sup>1-17</sup>, but for the developments of the last two years. For this reason I will mainly discuss most recent developments.

Whereas the study of muonic molecules started in the fifties, the subject of monopolic molecules is much more recent. The possibility that magnetic monopoles bind to atomic and molecular systems has been considered recently in the context of the renewed interest for magnetic monopoles. Grand Unification Theories predict the existence of very massive monopoles,  $m_M \sim 10^{17}$  GeV. These should reach Earth with very low velocity,  $v_M/c \sim 10^{-5} \div 10^{-3}$ , i.e. a velocity smaller than that of the atomic electrons. Consequently, non-trivial interactions of the monopole with matter occur. This chemistry of monopoles has to be studied in order to plan for significant searches of monopoles. This is a point I would like to stress: any search of slow monopoles, unless it relies on a direct measurement of the monopole magnetic field, is strongly affected by the way monopoles interact with matter. We will see that monopoles can indeed bind to simple atomic systems, the essential mechanism being the attraction between the electron magnetic moment and the monopole magnetic field. The molecular systems one forms in this way have some similarity with muonic molecules.

## 2. ENERGY LEVELS AND FORMATION PROCESSES OF MUONIC MOLECULES (THEORY)

The theoretical spectroscopy of muonic molecules is a field which has been mastered by Russian physicists since the beginning. Ya. Zeldovich in the early times, later S.S. Gershtein and more recently L.I. Ponomarev and his collaborators have developed methods of calculation of higher and higher accuracy. Particularly, in the last few years the group of Ponomarev was able to describe the full spectrum of molecular levels with an accuracy of some meV on typical energies of order  $e^2/a_\mu \sim 5000$  eV<sup>18,19</sup>. Some results are summarized in table I and II, where  $(J,v)$  denote the rotational and vibrational quantum numbers. A few points are to be remarked:

- 1) In contrast to the case of electronic molecules, there are very few rotational and vibrational levels. This is a consequence of the different ratio  $m_{\text{lepton}}/m_{\text{nucleus}}$  in the two cases.
- 2) The  $(p-\mu-p)$  system has just two levels, with  $J = 0$  and  $J = 1$ . These correspond, as a consequence of the Pauli principle, to "para" and "ortho" states respectively. The different nuclear spin content of the two states has important consequences when discussing the problem of muon capture.
- 3) The  $(J,v) = (1,1)$  levels of the  $(d-\mu-d)$  and  $(d-\mu-t)$  have very small binding energies, in the range of eV, comparable to the typical energies of

TABLE I

The mesomolecular spectrum according to (a) the perturbative calculation; (b) the truncation method. The energies are in eV. (From Ref. 18).

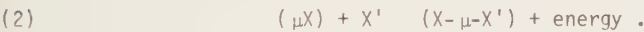
(a)	<i>Jv</i>	(ppμ)	(pdμ)	(ptμ)	(ddμ)	(dtμ)	(ttμ)
	00	253.55	221.49	213.85	324.99	319.09	362.89
	01	—	—	—	35.66	34.70	83.68
	10	107.33	98.79	101.30	226.74	232.61	289.19
	11	—	—	—	1.96	0.85	45.15
	20	—	—	—	85.34	103.16	172.79
	30	—	—	—	—	—	48.90

(b)	<i>Jv</i>	(ppμ)	(pdμ)	(ptμ)	(ddμ)	(dtμ)	(ttμ)
	00	252.95	221.52	213.97	325.04	319.15	362.95
	01	—	—	—	35.80	34.87	83.88
	10	106.96	97.40	99.01	226.61	232.44	289.15
	11	—	—	—	1.91	0.64	45.24
	20	—	—	—	86.32	102.54	172.65
	30	—	—	—	—	—	48.70

electronic systems. This suggests that resonant interactions between muonic and electronic molecules can occur (see below). It was very hard to establish theoretically the existence of these states, since it needed an accuracy of at least .1 eV in the calculations.

Formation of muonic molecules occurs through collisions:



The formation reactions are classified according to the way the binding energy of the muonic molecule is released. Besides the usual Auger process (Fig. 1a), it is also possible to have energy transfer through the excitation of the vibrational and rotational levels of ordinary molecules (Fig. 1b). This latter process is only possible if the mesomolecule has weakly bound levels, with a binding energy  $E_b$  smaller than the dissociation energy of the Hydrogen molecules, a few eV. This is what occurs for the case of (d-μ-d) and (d-μ-t) systems, as we noted above. Due to the quantization of the vibrational and rotational energy this process can only occur if a resonance condition among  $E_b$ , the kinetic energy of the muonic atom,  $E_{kin}$ , and the quantum jumps of the electronic molecule,  $\Delta E$ , is satisfied (see Fig. 2):

(3a)  $E_{kin} = E_{res}$

(3b)  $E_{res} = \Delta E - E_b.$

TABLE II  
Hyperfine structure of the (dd $\mu$ ) mesomolecule (a) and of the (dt $\mu$ ) mesomolecule (b), from Ref. 19. F is the total spin, the index N labels the different states with the same F,  $\mathcal{E}_{Jv}^N$  is the hyperfine energy shift, in eV, w is the relative probability of forming the (J,v,F,N) state of the mesomolecule starting from a specific spin state of the mesoatom.

(a)					
$Jv$	$F$	$N$	$\mathcal{E}_{Jv}^N$ (eV)	$w_{Jv}^N$ ( $\uparrow\downarrow$ )	$w_{Jv}^N$ ( $\uparrow\uparrow$ )
00	$\frac{1}{2}$	1	0	0.1667	0.1667
		1	-0.0286	0.8333	0.0833
		1	0.0191	0	0.7500
01	$\frac{1}{2}$	1	0	0.1667	0.1667
		1	-0.0246	0.8333	0.0833
		1	0.0164	0	0.7500
10	$\frac{1}{2}$	{1	-0.0169	0.2213	0.0560
		{2	0.0070	0.0565	0.1384
	$\frac{3}{2}$	{1	-0.0180	0.4436	0.1115
		{2	0.0084	0.1119	0.2774
	$\frac{5}{2}$	1	0.0097	0.1667	0.4167
		1	-0.0159	0.2222	0.0555
11	$\frac{1}{2}$	{1	-0.0159	0.2222	0.0555
		{2	0.0077	0.0555	0.1389
	$\frac{3}{2}$	{1	-0.0161	0.4444	0.1111
		{2	0.0079	0.1112	0.2778
	$\frac{5}{2}$	1	0.0082	0.1667	0.4167
		1	0.0082	0.1667	0.4167

(b)					
$Jv$	$F$	$N$	$\mathcal{E}_{Jv}^N$ (eV)	$w_{Jv}^N$ ( $\uparrow\downarrow$ )	$w_{Jv}^N$ ( $\uparrow\uparrow$ )
00	0	1	0.0173	0	0.1111
		{1	0.0282	0.0096	0.3301
		{2	-0.1107	0.9904	0.0032
01	0	1	0.0463	0	0.5556
		{1	0.0239	0	0.1111
		{2	0.0312	0.0043	0.3319
10	1	{1	-0.1123	0.9957	0.0014
		{2	0.0439	0	0.5556
	2	{1	0.0277	0.0007	0.0368
		{2	-0.1039	0.1104	0.0002
	3	{1	0.0162	0.0000	0.1111
		{2	0.0249	0.0031	0.1101
11	1	{3	-0.1035	0.3303	0.0010
		{4	0.0406	0.0000	0.1111
	2	{1	0.0273	0.0056	0.1833
		{2	-0.1041	0.5499	0.0019
	3	{3	0.0447	0.0000	0.1852
		1	0.0433	0	0.2593
11	0	{1	0.0445	0.0001	0.0370
		{2	-0.1424	0.1110	0.0000
	1	{1	0.0407	0.0000	0.1111
		{2	0.0439	0.0002	0.1110
	2	{3	-0.1422	0.3331	0.0001
		{4	0.0501	0.0000	0.1111
11	3	1	0.0443	0.0004	0.1851
		2	-0.1424	0.5552	0.0001
		3	0.0511	0.0000	0.1852
11	3	1	0.0508	0	0.2593
		2	-0.1424	0.5552	0.0001
		3	0.0511	0.0000	0.1852

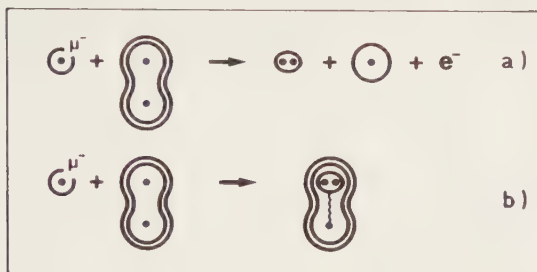


FIGURE 1

Formation of the mesomolecule: a) through the Auger (non resonant) process  
b) through the resonance process

It is intuitively clear that the resonant structure can be used as a tool in order to perform accurate determinations of the energy levels of muonic molecules. Also it is clear that under suitable conditions the resonant process can considerably increase the rate of formation of muonic molecules. Several recent developments in the field of muonic molecules are grounded on this idea.

The formation of muonic molecules via the two mechanisms has been studied in detail by Ponomarev and his collaborators<sup>20-21</sup>. The same group also calculated the rate of the ortho-para transition in the (p- $\mu$ -p) system, which is important for the study of muon capture<sup>22</sup>.

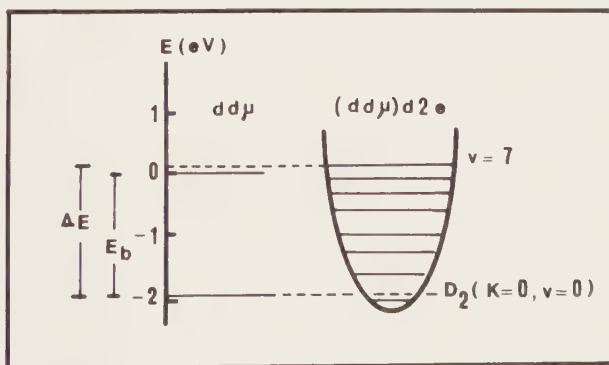


FIGURE 2

Scheme of the resonant formation for  $(dd\mu)$

### 3. THE (p- $\mu$ p) MOLECULAR ION: A PROBE FOR THE STRUCTURE OF THE WEAK HAMILTONIAN

The V-A theory predicts a strong dependence of the muon capture rate,

$$(4) \quad \mu^- + p \rightarrow \nu_\mu + n,$$

on the spin state of the muon relative to the proton. Measurements in gas deal essentially with muons bound around the proton in the singlet, is atomic state, and thus give information on  $\Lambda_s$ , the capture rate in the singlet state. In order to get informations on the capture rate in the triplet,  $\Lambda_t$ , it is necessary to use high density targets, so that the (p- $\mu$ -p) molecule can be formed. The muon capture rates in the ortho and para state are, respectively<sup>23</sup>:

$$(5a) \quad \Lambda_{om} = 2\gamma_o (3/4 \Lambda_s + 1/4 \Lambda_t)$$

$$(5b) \quad \Lambda_{pm} = 2\gamma_p (1/4 \Lambda_s + 3/4 \Lambda_t)$$

where  $\gamma_o$  and  $\gamma_p$  are factors connected with the overlap probability of the muon and one of the protons ( $2\gamma_o = 1.009 \pm .001$ ;  $2\gamma_p = 1.143 \pm .001$ ).

Clearly, in order to disentangle between the contribution of  $\Lambda_s$  and  $\Lambda_t$  it is necessary to know the molecular state of the muon when the measurement takes place. It is well established that the molecule is formed in the ortho state<sup>24</sup>. The transition probability to the para state, though expected to be small<sup>25,22</sup>, can however have significant effects on the interpretation of the results. Recently an experiment has been performed<sup>26</sup>, with such an accuracy that it is possible to recognize in the data even the effect of the ortho-para transition. The main results of the experiment, by a Saclay-Bologna-CERN collaboration, are reported in table III. A few comments are in order:

- i) the reported value for the capture rate,  $\Lambda_{cap}$ , is more accurate than previous measurements by a factor of at least two.
- ii) For the first time it was possible to get a measurement of the transition rate from the ortho to the para state,  $\Lambda_{op}$ . This value is fairly consistent with the theoretical calculation.
- iii) By using the measured value of  $\Lambda_{op}$  one gets a value of the capture rate from the ortho-molecule which is in agreement with the predictions of the standard weak interaction theory. The agreement, however, gets worse if one would use the theoretical value of  $\Lambda_{op}$ <sup>22</sup>.

TABLE III

Results of the Bologna-Saclay-CERN collaboration on muon capture in (p- $\mu$ -p) from Refs. 26. The theoretical value of  $\Lambda_{op}$  is from Ref. 22. We report the reaction rates in units of s<sup>-1</sup>.

	$\Lambda_{cap}$	$\Lambda_{op}$	$\Lambda_{om}$
Experiment	460 $\pm$ 20	(4.1 $\pm$ 1.4)10 <sup>4</sup>	531 $\pm$ 33
Theory		(7.1 $\pm$ 1.2)10 <sup>4</sup>	502

An independent analysis of the same data by E. Zavattini<sup>27</sup> shows clearly the significance of the experimental data in order to test the basic assumptions of the standard weak interaction theory. The results of his analysis can be summarized as follows:

- i) by assuming muon-electron universality, one derives a value of the induced pseudoscalar term\*,  $m_\mu f_p(q^2) = -8.7 \pm 1.9$  at  $q^2 = -.87 m_\mu^2$ , which is in good agreement with the prediction of PCAC (-8.1 $\pm$ 1).
- ii) Alternatively, by assuming the PCAC prediction for  $f_p$  one derives  $f_A^{(\mu)}(0) = -1.24 \pm 0.04$ , which is in very good agreement with the value measured with electrons in the neutron decay:  $f_A^{(e)}(0) = -1.250 \pm .009$ . This is a test of the muon-electron universality to the level of 3%.

These conclusions are the main result one can today draw from the muon capture experiments in Hydrogen. Their importance stems from the fact that no nuclear physics consideration is involved. It will be interesting the comparison with an experiment on muon capture in deuterium\*\*, by the Saclay-Bologna-CERN collaboration, which is presently being analysed. Preliminary results<sup>28</sup> give a value of the capture rate in the doublet state,  $\Lambda_{c,d} = 498 \pm 37$  s<sup>-1</sup>, which is in disagreement with the theoretical prediction by 2-3 standard deviations.

#### 4. THE (d- $\mu$ -d) SYSTEM: A PROBE FOR THE STUDY OF NUCLEAR FORCES.

As a consequence of the existence of the weakly bound states with (J,v) = (1,1), it is possible to perform accurate experimental determination of the

\* I am using the (usual) notations of ref. 23 for the various coupling constants and form factors.

\*\* When a negative muon is stopped in deuterium, the (d $\mu$ ) atoms which are formed initially can bind to another deuteron to form (d- $\mu$ -d). However, the (d- $\mu$ -d) ions are quickly destroyed as a consequence of the nuclear fusion reaction. In this way the muon is left again free and it forms again a (d $\mu$ ) atom. In conclusion, most of the time the muon is bound in an atomic state, and not in a molecular one, as it occurs in liquid Hydrogen.

binding energy<sup>21</sup>. One measures the formation rate of the muonic molecule as a function of the temperature of the target, i.e. as a function of the kinetic energy of the  $(d\mu)$  atom involved in the reaction. By studying this dependence it is possible to deduce the resonance energy  $F_{res}$  of eqs. 3 and thus to derive the binding energy. Actually the experimental study of the mesomolecule formation occurs through the detection of the nuclear fusion reaction which occurs in the mesomolecule. The nuclei bound in the muonic molecule behave as if they were in a plasma with a density  $\rho \sim (a_0 m_e / m_\mu)^{-3}$ , which is about  $10^7$  times the liquid Hydrogen density, and with a temperature corresponding to their vibrational energy,  $KT_{ef} = E_{vib} \sim 100$  eV. Under such extreme conditions, comparable to those inside a white dwarf, the nuclei fuse rapidly, the fusion rate being order of magnitude faster than the muon decay rate and the rate of molecular formation. In summary, through the observation of the nuclear fusion reactions one gets informations about the energy levels of the muonic molecule.

In this way a few years ago it was possible to measure the binding energy of the  $(J=1, v=1)$  level of the  $(d-\mu-d)$  molecule<sup>29</sup>:

$$(6) \quad E_b = (2.196 \pm 0.003) \text{ eV} .$$

More recently, effects associated with the hyperfine structure of the  $(d-\mu-d)$  molecule have been observed by an SIN-Wien collaboration<sup>30</sup>. Through the analysis of their experiment it should be possible to derive the full spectrum of the hyperfine sublevels of the  $(1,1)$  level with an accuracy of about 1 meV.

Beyond their intrinsic interest, these measurements are of importance in order to establish the very long range part of the interaction potential between hadrons, i.e. at distances larger than the pion Compton wavelength. I would like to discuss this point in some detail. In the last few years several authors pointed out that long range interactions between hadrons could arise from the exchange of new (hypothetical) light particles or from the exchange of two gluons. Muonic molecules are of interest for the study of these anomalous interactions<sup>31</sup>. This occurs since the two hadrons are at distance large enough to neglect the contribution of the (not understood) short range part of the hadronic interaction and still small enough that the effect of the anomalous interaction can be detected. For example, measurements of the hyperfine structure of the  $(d-\mu-d)$  molecule with an accuracy of the order of 1 meV can be sensitive to the exchange of a pseudoscalar particle with mass up to 1 MeV if its coupling constant is  $g_{ps}^2 \gtrsim 10^{-1}$  <sup>31</sup>.

Ponomarev and his collaborators<sup>32</sup> pointed out that the measurement of the



branching ratio of reactions (1) when the deuterons are bound in the muonic molecule can be quite interesting in order to test the charge symmetry of nuclear reactions. Indication of violation of this symmetry in the p-wave interaction of two deuterons have been obtained in low energy d-d scattering. However the extraction of the p-wave contribution to the cross section is quite difficult. On the contrary, this contribution can be directly measured when the fusion proceeds from the muonic molecule. The point is that: i) the muonic molecule is mainly formed in the  $(J,v) = (1,1)$  state as a consequence of the dominance of the resonant formation process, ii) electromagnetic transitions to lower states are slower than the rate for fusion, iii) since the total P-parity equals  $(-1)^J$ , the angular momentum  $L$  of the relative nucleus motion is odd for  $J=1$  and the dominant contribution arises from the p-wave. In conclusion, it looks that muonic molecules can be used as a "multipole-meter" in the study of fusion reactions.

Also, the experimental study of the SIN-Wien group<sup>30</sup>, is of importance for the interpretation of experiments on muon capture in deuterium, particularly for the knowledge of the spin state of the  $(\mu d)$  atom when capture takes place. For the first time it was possible to accurately measure the rate of the hyperfine transition in collisions of the  $(\mu d)$  atoms with deuterium and to deduce a value for collisions with hydrogen.

Thus the long missing experimental information on the hyperfine populations of  $(\mu d)$  atoms is provided (at least at low temperature), not only for pure  $D_2$ , but also for H/D mixtures.

## 5. THE $(d-\mu-t)$ MOLECULE. ENERGY FROM MUON CATALYZED FUSION?

The resonant formation mechanism (Fig. 1b) can occur also in this system and it was theoretically estimated, already in 1977<sup>33</sup>, that in a suitable mixture of deuterium and tritium a muon could catalyse about one hundred nuclear fusion reactions, during its lifetime. In order to appreciate this number, let me remember that in the Alvarez experiment<sup>34</sup> where muon catalyzed fusion was observed for the first time the yield of detected fusions per muon was at the level of  $10^{-2}$ .

An experiment performed at Dubna<sup>35</sup> obtained a lower limit for the molecular formation rate,  $\lambda_{dt\mu} \gtrsim 2 \cdot 10^8 \text{ s}^{-1}$ , which supports the idea that a muon can catalyze a lot of fusions in suitable conditions.

Recently an experiment has been performed at LAMPF<sup>36</sup>, which provides very nice, quantitative data on the catalysis in deuterium-tritium. By working at high deuterium-tritium density (up to 60% of liquid Hydrogen density), copious 14-MeV neutron production was observed, demonstrating up to 70 fusions per

muon. On this grounds it was possible to derive that, under optimal conditions, a muon will catalyze about one hundred fusions, at least for a temperature of the target  $\lesssim 543$  °K. The main results of the experiment are reported in Figs. 3-4 and in Table IV.

It is worth observing that the bottle-neck of the chain is the sticking of the muon to the  $^4\text{He}$  nucleus produced in the fusion. The measured value of the (effective) sticking probability,  $w_s^{\text{exp}} = (7.6 \pm .5)10^{-3}$  <sup>36</sup>, which is in fair agreement with the theoretical prediction <sup>37</sup>  $w_s^{\text{th}} = (9 \pm 1)10^{-3}$ , implies that no matter how fast are all the other reactions one cannot hope for more than 150 fusions per muon.

TABLE IV  
Parameters critical to muon catalysis in deuterium-tritium mixtures

Parameter	Theory	Previous Experiment <sup>35</sup>	LAMPF Experiment <sup>36</sup>
Fusion rate	$10^{12}\text{s}^{-1}$	--	--
Rate of atomic capture in Hydrogen	$\sim 10^{11}\text{s}^{-1}$	--	--
Rate of transfer to tritium $\lambda_{dt}$	$2 \times 10^8\text{s}^{-1}$	$(2.9 \pm 0.4) \times 10^8\text{s}^{-1}$	$(2.8 \pm 0.1) \times 10^8\text{s}^{-1}$
Mesomolecule formation rates:	$3 \times 10^4\text{s}^{-1}$ (non-resonant) $= 10^8\text{s}^{-1}$ (resonant, max) (temp. dependent)	$> 10^8\text{s}^{-1}$ (no temp. dep. seen)	temp. dependent dt $\mu$ -d and dt $\mu$ -t parts:
$\lambda_{dt\mu-d}$	--	--	$(6.9 \pm 0.4) \times 10^8\text{s}^{-1}$ (534K)
$\lambda_{dt\mu-t}$	--	--	$(3.0 \pm 0.3) \times 10^8\text{s}^{-1}$ (534K)
Probability of sticking to He $w_s$	$\begin{cases} 0.0091 \\ 0.0086 \end{cases}$	--	$(7.6 \pm 0.5) \times 10^{-3}$
Relative He/H capture probability	$\sim 2$	--	$\sim 6$ (tentative)
Rate of transfer to Helium, $\lambda_m$	$5 \times 10^8\text{s}^{-1}$	--	$\sim 4 \times 10^8\text{s}^{-1}$ (tentative)
Optimal tritium concentration	$\sim 0.5$	--	$\sim 0.5$ (broad peak)
Optimal efficiency $\eta_{\mu}^{\text{opt}}$	$\sim 50$	--	$90 \pm 9$ fusions/ $\mu$ (534K)

Notes:

- 1) Statistical errors are shown; the systematic error is  $\pm 12\%$ .
- 2) Consistent with convention,  $\lambda_m$ ,  $\lambda_{dt}$ ,  $\lambda_{dt\mu}$  and  $\eta_{\mu}^{\text{opt}}$  are normalized to liquid hydrogen density.
- 3) The reported value of  $w_s$  is based specifically on a study of an equimolar d-t mixture at room temperature. An attempt to analyze the target gas was abortive so that one cannot rule out the possibility that impurities in the gas lead to an artificially large value of  $w_s$ .

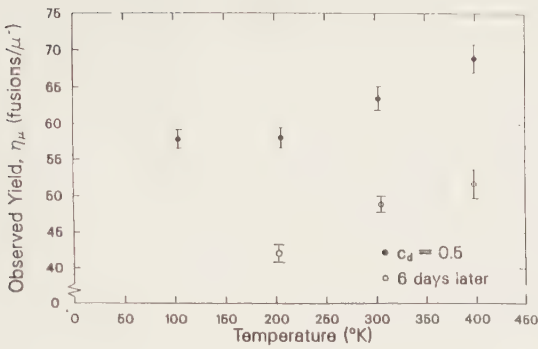


FIGURE 3

Absolute muon catalyzed fusion yield ( $\eta_\mu$ ) for an equimolar mixture of deuterium and tritium at 0.6 LHD showing temperature dependence and poisoning effect of helium-3 arising from tritium decay, from Ref. 36.

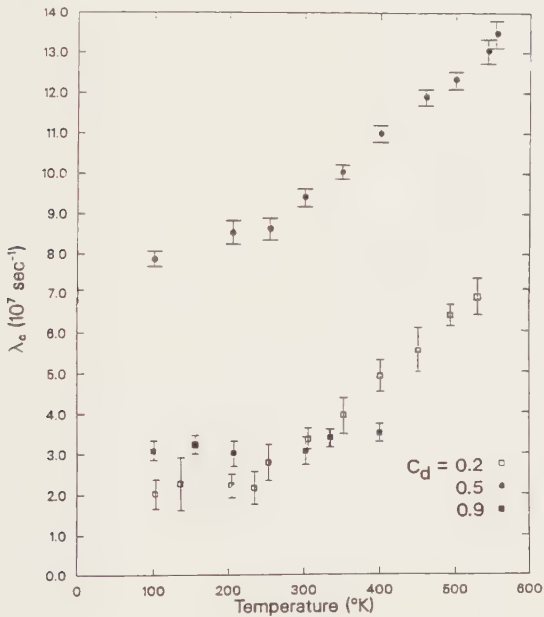


FIGURE 4

Muon catalysis cycle rate ( $\lambda_c$ ) as a function of deuterium concentration and temperature, from Ref. 36.

It is worth reporting that it has been estimated that 100-200 fusions per muon would be enough in order to build a reactor with a positive energy balance<sup>38</sup>.

Also independently of this, the LAMPF experiment is quite interesting since it opens the way to study the spectroscopy of the (d- $\mu$ -t) molecule, and more generally it gives informations on the kinetics of muons in deuterium-tritium mixtures. One can expect to have a quite clear experimental picture thanks to the additional informations which will arise from extensions of the LAMPF experiment, already scheduled for the fall, and from other experiments planned and/or in preparation at SIN, Dubna and Leningrad.

## 6. MONOPOLE CHEMISTRY

Over a half century ago Dirac invented the magnetic monopole on theoretical grounds. Recently there has been a renewed interest in the monopole problems for three reasons: i) The grand unification theories predict magnetic monopoles, ii) Cabrera<sup>39</sup> reported the observation of a candidate event and iii) Rubakov's theoretical analysis<sup>40</sup> demonstrated that monopoles should catalyze proton decay.

It is natural and interesting to investigate the interactions of monopoles with matter, particularly in order to devise methods for the detection of magnetic monopoles. In this respect it is important the possibility that monopoles bind to atomic systems.\*

Thirty years ago a preliminary investigation was performed by Malkus<sup>15</sup>, who suggested that chemical binding might be possible, but a definite conclusion was not reached. Recently quantitative investigations have been performed on the simplest monopole-atom system, namely the one consisting of a monopole, one proton and one electron. It has been proved that an infinite number of bound states exist for these system<sup>42</sup>, the binding energy of the most tightly bound state being about 1.6 eV<sup>46</sup>. Qualitatively, these results can be understood easily. The attraction between the atom and the monopole is due to the interaction between the magnetic moment of the electron and the magnetic field of the monopole, ( $q_M/R^2$ ;  $q_M e = \frac{1}{2} \hbar c$ ). This results, at large monopole-atom distances  $R$ , in an interaction:

$$V \approx \frac{1}{2} \hbar^2 (m_e R^2) .$$

This interaction will be regularized at distances  $R \lesssim a_0$  as a consequence of the finite size of the electron orbit. Thus the motion of the atom occurs in a potential falling as  $R^{-2}$  at large distances and regular at the origin. This

\*Bound states of monopoles with nuclei also exist. See refs. 41-44.

potential has infinitely many bound states. Simply by dimensional considerations, the binding energy has to be of the order of  $\frac{1}{2} \hbar^2 / (m_e a_0^2)$ , i.e. in the eV range.

Clearly, all this can be viewed as an initial investigation of monopole chemistry. If monopoles do exist in nature, their rarity will demand novel physical and chemical methods of experimental investigation. For these reasons, it will be necessary to study the interactions of monopoles with systems more complicated than atomic Hydrogen. Also, it is necessary to have estimates of the transition rates between the different levels of the monopole-atom system and to evaluate the cross section for the formation of bound states. In conclusion, there is a large field to be explored, with a problematics very similar to that one has in the study of muonic atoms and muonic molecules.

## 7. CONCLUSIONS

Let me summarize the main points of this discussion:

- i) Essentially thanks to the efforts of Ponomarev's group one has now a detailed understanding of the spectroscopy of muonic molecules.
- ii) The LAMPF experiment has produced interesting (preliminary) results on the kinetics of muon reactions in deuterium-tritium mixtures. Some of the results, particularly the temperature dependence of the formation rates of the (d- $\mu$ -t) molecule, are not understood theoretically. Additional experimental data, particularly at higher temperature, will be quite useful.
- iii) The study of muon capture in (p- $\mu$ -p) system is now at such a level of precision that it is possible to get unambiguous tests of the basic assumptions of weak interaction theory. It comes out that the weak interaction theory is in agreement with the experiment. On the other hand, the not complete agreement with the experiment and the calculation of the ortho-para transition rate should be clarified.
- iv) The study of the interactions of slow monopole with matter has shown that monopoles can form quite exotic molecular states. This opens a new field, which is worth investigating in order to plan for decisive searches of monopoles and which has many similarities with the field of muonic molecules.

## ACKNOWLEDGEMENTS

It is really a pleasure to thank Profs. Leonid Ponomarev and Emilio Zavattini to whom I am very much indebted for the many things I have learnt from them during several years.

I would also like to thank Profs. Bertin, Bracci, Breunlich, Duclos, Jones, Petitjean and Vitale for informing me of their results prior to publication and/or for conversations we have had on several times.

## REFERENCES

- 1) Ya.B. Zeldovich, and S.S. Gerstein, *Usp.Fiz.Nauk* 71 (1960) 581  
(English transl. *Sov.Phys.-Uspekhi* 3 (1961) 593)
- 2) S.S. Gerstein, and L.I. Ponomarev, in "Muon Physics", Eds. V.W. Hughes, and C.S. Wu, Academic Press, New York, 1975, v. III, p. 141
- 3) V.P. Dzhelepov, *Atomnaja Energija* 14 (1963) 27
- 4) E.H.S. Burhop, in "Electronic and Ionic Impact Phenomena", Eds. H.S.W. Massey, E.H.S. Burhop, and H.B. Gilbody, Oxford, 1974
- 5) A. Bertin, A. Vitale, and A. Placci, *Riv. Nuovo Cimento* 5 (1975) 423
- 6) A. Bertin et al., *Nuovo Cimento* 72A (1982) 225
- 7) "Mesons in Matter", Proceedings of the Int. Symposium on Meson Chemistry and Mesomolecular Processes in Matter, 7-10 June, 1977
- 8) L.I. Ponomarev, *Proc. VI Int. Conference of Atomic Physics*, Riga, 17-22 August 1978, Plenum Press, New York (1979)
- 9) S.I. Vinitsky, and L.I. Ponomarev, *Physics of Elementary Particles and Atomic Nuclei*, 13 (1982) 1336, Moscow, Energoatomizdat
- 10) S.Tesh, *Kernenergie Bd. 25* /1981/ 97
- 11) J. Meyer-ter-Vehn, *Physik. Blätter* 35 (1979) 211
- 12) L.I. Ponomarev, X. European Conference on Controlled Fusion and Plasma Physics, Moscow, 14-19 September, 1981, Proceedings, p. 66, p. 11
- 13) L. Bracci, and G. Fiorentini, *Phys.Rep.* 86 (1982) 170
- 14) J. Rafelski, Int. School of Exotic Atoms, Erice, 25 March - 5 April 1979, "Exotic Atoms '79", Eds. K.J. Crowe, E. Duclos, G. Fiorentini, and G. Torelli, Plenum Press, New York, (1979)
- 15) W.H. Breunlich, *Nucl.Phys.* A353 (1981) 201
- 16) G. Fiorentini, *Nucl.Phys.* A374 (1982) 607
- 17) L.I. Ponomarev, to be published in the Proceedings of the 3<sup>rd</sup> Int. Conference on Emerging Nuclear Energy Systems, Helsinki, Finland, June 1983
- 18) V. Melezhik et al., *JETP* 52 (1981) 353,  
S. Vinitsky et al., *JETP* P55 (1982) 400, and  
for a comprehensive review of the method of calculation see  
L.I. Ponomarev, *Sov. Journ. of Particles & Nuclei* 13 (1982) 557
- 19) D.D. Bakalov et al., *JETP, Zh. Eksp.Teor.Fiz.* 79 (1980) 1629
- 20) L.I. Ponomarev and M.P. Faifman, *JETP* 44 (1976) 886
- 21) S. Vinitsky et al. *JETP* 47 (1978) 444
- 22) D.D. Bakalov et al., *Nucl.Phys.* A384 (1982) 302
- 23) see: H. Primakoff, in *Muon Physics Vol. II*, Academic Press (1975)  
(S.C. Wu & W.H. Hughes Eds.)
- 24) see: E. Zavattini in *Muon Physics, Vol. III*, Academic Press (1975)  
(S.C. Wu & W.H. Hughes Eds.)

- 25) S. Weinberg, Phys.Rev.Lett. 4 (1976) 585
- 26) G. Bardin et al., Nucl.Phys. A352 (1981) 365  
G. Bardin et al., Phys.Lett. 104B (1981) 320  
see also: G. Bardin, Ph.D. thesis, Univ. of Paris-Sud (1982)  
and J. Martino, Ph.D. thesis, Univ of Paris-Sud (1982)
- 27) E. Zavattini, Lectures given at the S. Miniato Conference on intermediate Energy Physics, Aug. 1983, to be published in the Proceedings of the Conference
- 28) Private communication by A. Bertin and A. Vitale
- 29) V.B. Bystritsky et al., JETP, 49 (1979) 232
- 30) P. Kammel et al., Phys.Lett. 112B (1982) 319  
P. Kammel et al., "First Observation of Muonic Hyperfine effects in pure deuterium", to be published in Phys.Rev. A  
see also: P. Kammel, Ph.D. thesis, Univ. of Wien (1982)
- 31) L. Bracci, G. Fiorentini and R. Tripiccion, Nucl.Phys. B217 (1983) 215
- 32) L.N. Bogdanova et al., Phys.Lett. 115B (1982) 171
- 33) S.S. Gershtein & L.I. Ponomarev, Phys.Lett. 72B (1977) 80
- 34) L.W. Alvarez et al., Phys.Rev. 105 (1957) 1127  
see also L.W. Alvarez, in Adventures in Experimental Physics  $\alpha$  (1972)
- 35) V.M. Bystritsky et al., Phys.Lett. 94B (1980) 476
- 36) S. Jones et al., "Experimental investigation of muon catalysed fusion in high density deuterium tritium mixtures", presented at the 3<sup>rd</sup> Intern. Conf. on Emerging Nuclear Energy Systems, Helsinki, Finland (1983)
- 37) S.S. Gershtein et al., JETP 53 (1981) 872
- 38) Yu.V. Petrov, Nature 285 (1980) 466 and Proc. XIV, LNPI Winter School (1978) Leningrad
- 39) B. Cabrera, Phys.Rev.Lett. 48 (1982) 1378
- 40) V.A. Rubakov, JETP Letters 33 /1981) 644
- 41) L. Bracci and G. Fiorentini, Phys.Lett. 129B (1983) 29
- 42) L. Bracci and G. Fiorentini, Phys.Lett. 124B (1983) 493 and Pisa Preprint IFUP TH 83/2, to be published in Nucl.Phys. B
- 43) K. Olanssen et al., DESY preprint 83-041 (1983)  
J. Makino et al., Osaka preprint OUAM-82-11-2 (1982)
- 44) J.S. Trefil et al., Nature 302 (1983) 111
- 45) W.V.R. Malkus, Phys.Rev. 83 (1951) 899
- 46) Th.W. Ruijgrok, T.A. Tjon and T.T. Wu, DESY preprint, DESY 83-026 (1983)





## FEW-BODY PROBLEM IN CELESTIAL MECHANICS

Stanley F. DERMOTT

Center for Radiophysics and Space Research, Cornell University, Ithaca, New York 14853-0355, U.S.A.\*

The approaches taken by solar system dynamicists to various outstanding problems has changed considerably in recent years. Some problems for which few-body approaches have been tried in the past are now thought to involve collective phenomena. Observed features in Saturn's rings associated with resonances are examples. On the other hand, the problem of the origin of the Kirkwood gaps in the asteroid belt, for which a number of a many-body approaches (involving collisions or gas friction) have been tried, probably has a few-body solution and may involve chaos.

### 1. INTRODUCTION

Celestial mechanics prior to this century was concerned largely with the production of planetary ephemerides. A direct product of the analyses of the observed orbits was a determination of the planet and the satellite masses. One of the more famous indirect products had a part in one of the greatest advances in physical science. In the early decades of this century the orbits of the planets were so well determined and their motions so well understood that it was clear that certain deviations from keplerian motion could not be accounted for by perturbations due to the other planets or by any effects associated with classical Newtonian gravitational theory. I am, of course, referring to the perihelion advance of the planet Mercury which was to be accounted for by Einstein's general theory of relativity. It was also established early in this century that the orbit of the Moon is gradually expanding due to tidal friction in the Earth's oceans and, to a lesser extent, the Earth's solid body.

The classical approach to solar system dynamics may still unlock some secrets. There appear to be small, but still unexplained, changes in the orbits of Uranus and Neptune<sup>1</sup>. Since the recent discovery of the satellite of Pluto<sup>2</sup>, we now know that the mass of Pluto is far too small to account for these observations. It is a natural speculation, therefore, that comparatively massive, unseen, bodies exist beyond the orbit of Pluto. As yet, however, there is little else to support this view. Observations of the motions of the Pioneer spacecraft as they leave the solar system could yield some useful information.

---

\*This research was supported by NASA grant NAGW-392.

Recent discoveries and recent theoretical advances, some of which preceded the exploration of the planets by spacecraft, and the results from the Voyager missions to the outer planets have pushed solar system dynamics once more to the forefront of planetary science. Topics of particular current interest which I will discuss in this talk include the origin and the evolution of resonances in the solar system, the structure of the Saturnian and Uranian ring systems and the origin of the Kirkwood gaps in the asteroid belt. Apart from the widespread interest in these special problems, it is now recognized by the planetary science community that an understanding of the dynamical evolution of the planetary and satellite systems must precede any discussion of their nature and origin. This new attitude was undoubtedly born on 8 March 1979 - the day on which Voyager 1 discovered the spectacular volcanism on Io, a phenomenon which had been predicted, on dynamical grounds, by Peale and his colleagues<sup>3</sup>.

## 2. SOME DEFINITIONS

In celestial mechanics, the orbit of a satellite is described by the elements  $a$ ,  $e$ ,  $I$ ,  $\Omega$  and  $\tilde{\omega}$ , where  $a$  is the semimajor axis,  $e$  the eccentricity,  $I$  the inclination,  $\Omega$  the longitude of the ascending node and  $\tilde{\omega}$  the longitude of the pericenter. The position in the orbit is given by the mean longitude

$$\lambda = \int_0^t n \, dt + \varepsilon \quad (1)$$

where  $n$ , the mean motion of the satellite, is equal to  $2\pi/P$  where  $P$  is the satellite's orbital period, and  $\varepsilon$  is the longitude at epoch<sup>4</sup>.

The magnitudes and the phases of the perturbations of a satellite's near-keplerian orbit are determined by the disturbing potential  $U$  of the perturbing satellite. For a satellite moving in a total potential  $V$ , we may define  $U$  as  $U = V - GM/r$ , where  $GM/r$  is the potential of the planet at the radial distance  $r$  of the satellite.  $U$  can be expanded as an infinite summation of terms, a Fourier series, with the general form

$$U = \sum S \cos \phi \quad (2)$$

where the argument  $\phi$  has the form

$$\phi = [(p+q)\lambda' - p\lambda - (g\tilde{\omega} + g'\tilde{\omega}' + f\Omega + f'\Omega')] \quad (3)$$

where  $p$ ,  $q$ ,  $g$ ,  $g'$ ,  $f$  and  $f'$  are integers and the orbital elements of the perturbing satellite are denoted by primed quantities. The requirement of rotational invariance gives us the single restriction

$$q = g + g' + f + f' \quad (4)$$

A satellite (or, of course, a planet or an asteroid) is trapped in a resonance if some argument  $\phi$ , the resonant argument, librates rather than circulates. The integer  $q$ , the order of the resonance, largely determines the strength  $S$  of the resonance: as  $|q|$  increases in integral steps,  $|S|$  decreases in steps of  $\approx e, e', \sin I$  or  $\sin I'$ . Since, in the solar system, eccentricities and inclinations are small, only low-order resonances are important and first-order ( $q = 1$ ) resonances are dominant. Examples of known resonances in the solar system are given in Table 1.

TABLE 1  
RESONANCES IN THE SOLAR SYSTEM<sup>5,6</sup>

System	Resonance Variable $\phi$	Resonance Type
<u>Planets</u>		
Neptune <sub>8</sub> - Pluto <sub>9</sub>	$2\lambda_8 - 3\lambda_9 + \tilde{\omega}_9$ $(4\lambda_8 - 6\lambda_9 + 2\Omega_9)?$	Co-rotational
<u>Asteroids</u>		
Trojans - Jupiter'	$\lambda - \lambda'$	1:1 Leading/Lagging tadpoles
Thule - Jupiter'	$3\lambda - 4\lambda' + \tilde{\omega}$	Co-rotational
Hilda - Jupiter'	$2\lambda - 3\lambda' + \tilde{\omega}$	Co-rotational
Griqua - Jupiter'	$\lambda - 2\lambda' + \tilde{\omega}$	Co-rotational
Alinda - Jupiter'	$\lambda - 3\lambda' + 2\tilde{\omega}$	Co-rotational
<u>Jupiter</u>		
Io <sub>1</sub> - Europa <sub>2</sub> - Ganymede <sub>3</sub>	$\lambda_1 - 3\lambda_2 + 2\lambda_3$	Laplace
Io <sub>1</sub> - Europa <sub>2</sub>	$\lambda_1 - 2\lambda_2 + (\tilde{\omega}_1 \text{ or } \tilde{\omega}_2)$	Lindblad
Europa <sub>2</sub> - Ganymede <sub>3</sub>	$\lambda_2 - 2\lambda_3 + \tilde{\omega}_2$	Lindblad
<u>Saturn</u>		
Mimas <sub>1</sub> - Tethys <sub>3</sub>	$2\lambda_1 - 4\lambda_3 + \Omega_1 + \Omega_3$	Inclination
Enceladus <sub>2</sub> - Dione <sub>4</sub>	$\lambda_2 - 2\lambda_4 + \tilde{\omega}_2$	Lindblad/Co-rotational
Titan <sub>6</sub> - Hyperion <sub>7</sub>	$3\lambda_6 - 4\lambda_7 + \Omega_7$	Lindblad
Dione <sub>4</sub> - Dione B'	$\lambda_4 - \lambda'$	1:1 Leading tadpole
Tethys <sub>3</sub> - Telesto'	$\lambda_3 - \lambda'$	1:1 Leading tadpole
Tethys <sub>3</sub> - Calypso'	$\lambda_3 - \lambda'$	1:1 Lagging tadpole
Janus <sub>10</sub> - Epimetheus <sub>11</sub>	$\lambda_{10} - \lambda_{11}$	1:1 Horseshoe
Ring features - satellites	Various	Lindblad/Inclination

### 3. CO-ROTATIONAL RESONANCE

Since the dynamics of rings is now an important branch of solar system dynamics<sup>7</sup>, planetary scientists have had to familiarize themselves with the

terminology and methods of galactic dynamics. Resonances are now classified as either co-rotational or Lindblad. Consider the simple case where the resonant argument has the form

$$\phi = (p+q)\lambda' - p\lambda - q\tilde{\omega}' \quad (5)$$

In the stable configuration  $\phi$  librates (ie. oscillates) about  $\pi$ . If  $q = 1$  (first-order resonance), then all conjunctions ( $\lambda = \lambda'$ ) of the satellites take place near the apocenter of the perturbing satellite (primed quantities). Thus, the existence of the resonance guarantees that the separation of the satellites at conjunction is close to a maximum. (If  $q = 2$  (second-order resonance), then only every other conjunction takes place near apocenter, and so forth). Resonances can involve the motions of nodes or even combinations of the motions of nodes and of pericenters, but these cases are too complex to discuss here.

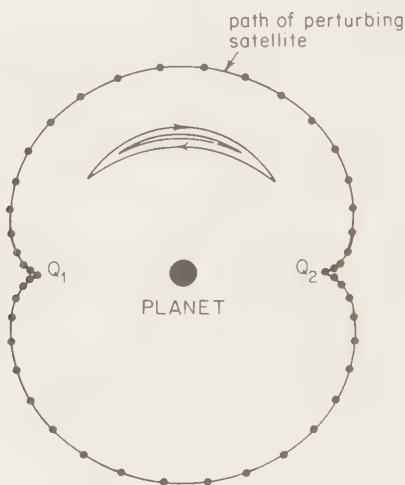


FIGURE 1

The dynamics of co-rotation resonance. A satellite trapped in resonance librates (or oscillates) about a longitude which is stationary in a reference frame co-rotating with the pattern speed of the disturbing potential. In this frame, the path of the perturbing satellite is closed and stationary. The example shown here is the 3:2 ( $\approx n/n'$ ) resonance. Points marked on the path of the perturbing satellite denote positions at equal time intervals. (Copyright University of Arizona Press).

Differentiating equation (5) with respect to time and rearranging, we obtain

$$\frac{\dot{n}' - \dot{\omega}'}{\dot{n} - \dot{\omega}'} = \frac{p}{p + q} \quad (6)$$

Thus, the mean motions relative to the motion of the pericenter are **exactly** commensurate. It follows that, in a frame rotating with the mean motion  $n$  of the perturbed satellite, the path of the perturbing satellite is closed (see Figure 1). The gravitational influence of the perturbing satellite on the orbit of the other satellite can now be modeled by spreading the mass of the perturbing satellite along its closed path in such a way that the line density at any one point is proportional to the time spent in that part of the path. In Figure 1, the positions of the perturbing satellite are marked at equal time intervals; thus the spacing of these marks is a measure of the line density. The line density distribution represents the disturbing potential, and in this type of resonance, which is called a **co-rotational** resonance, the resonant satellite co-rotates with the pattern speed of the disturbing potential.

The example shown is the 3:2 resonance  $[(p+q)/p = 3/2]$  for which the line density is a maximum at the points marked  $Q_1$  and  $Q_2$ . Different values of  $p$  and  $q$  give rise to different distributions of mass, but in all cases, if the orbital eccentricity of the perturbing satellite is not zero, then the line density distribution is not uniform. It is this longitudinal nonuniformity which gives rise to the forces that stabilize the resonance. Consider a satellite displaced from the equilibrium point. If the satellite is displaced towards the planet, then its mean motion will be greater than the resonant mean motion  $n$  and, as shown in Figure 1, it will drift in the prograde sense. The force on the satellite due to the mass distribution at  $Q_1$  will then have a greater effect than that at  $Q_2$ , and will act to increase the angular momentum of the satellite. But, since mean motion decreases with increasing angular momentum, the net effect of the force is to reverse the sense of drift. In this way, we see that a displaced satellite can librate about a longitude that is fixed in the rotating reference frame<sup>8</sup>.

Rearranging equation (6), we obtain

$$\frac{n'}{n} = \frac{p}{p+q} + \frac{q}{(p+q)n} \frac{\dot{\omega}'}{\omega'} \quad (7)$$

and, since  $\dot{\omega}'/n \ll p/(p+q)$ , satellites in resonance have near-commensurate mean motions. Roy and Ovenden, in a seminal paper<sup>9</sup>, pointed out that the structure of the solar system is determined not by Bode's law, which I regard as discredited<sup>10</sup>, but by resonant gravitational interactions. They proved that the number of pairs of near-commensurate mean motions in the solar system is too great to be ascribed to chance. We can conclude from this either that the mechanism of formation of the planets and the satellites was such as to favor orbits with commensurate mean motions or that the present, markedly non-random, distribution of orbits is the result of orbital evolution since the time of

planet and satellite formation. This conclusion alone has motivated much of the recent research in solar system dynamics.

#### 4. LINDBLAD RESONANCE

In co-rotation resonance, the free eccentricities are large compared with the forced eccentricities and the libration of the resonant argument  $\phi$  is determined by changes in the mean motion of the perturbed satellite. If the eccentricity of the perturbed satellite is very small, then another type of resonance, called **Lindblad** resonance, is possible in which an eccentricity is forced on the orbit of the satellite and the motion of  $\phi$  is determined by the motion of the pericenter of the forced orbit.



FIGURE 2

Formation of waves in rings by nearby satellites. Arrows on the ring particle paths show the direction of motion of the particles with respect to the perturbing satellite. For clarity I assume here that the outer strand of particles is perturbed only by the outer satellite; in fact both satellites sometimes act on the same particles at the same time, and at all times each satellite acts on all strands. Damping of the excited waves by particle collisions results in the formation of a narrow ring. (Copyright University of Arizona Press).

This type of resonance is best explained in terms of waves on narrow rings. Consider a narrow ring of particles which is perturbed by a small nearby satellite (see Figure 2). On encounter with a nearby satellite, a ring particle briefly experiences an attractive force in the direction of the satellite. For a particle initially moving in a circular orbit, this causes (a) the excitation of a small eccentricity  $e$ , given by

$$e = 2.24 \frac{m'}{M} \left| \frac{a}{x} \right|^2$$

where  $M$  is the mass of the planet and  $x$  is the separation of the perturbing satellite and the ring, and (b) a change in the semimajor axis of the ring particle in such a direction that the particle appears to have been repelled by the satellite.



If the excited eccentricity is damped by inter-particle collisions, then the change in the mean semimajor axis of the ring particles when averaged over a large number of repeated encounters with the perturbing satellite is not zero and the satellite exerts a continuous repulsive torque on the ring particles. If a ring is bounded by two small satellites, then its width will be reduced until the torques due to the satellites are countered by those produced by viscous forces, or inter-particle collisions, in the ring. This is the Goldreich-Tremaine<sup>13,14</sup> narrow ring model which was developed to account for the recently discovered rings of Uranus<sup>7</sup>. The satellites involved in such a process are now commonly referred to as shepherding satellites. We do not know if the narrow uranian rings are associated with shepherding satellites, but Voyager observations of Saturn's narrow F-ring have shown that this narrow ring appears to be bounded by two small satellites. Voyager 2 will have its closest approach to Uranus on 24 January 1986: the returned images are eagerly awaited.

In a frame co-rotating with the perturbing satellite, all particles initially moving in circular orbits must follow identical paths after encounter. It follows that each satellite generates a standing wave of amplitude  $A = ea$  and wavelength  $\lambda = 3\pi x$ . In the inertial frame, each particle moves in an independent keplerian ellipse, but the pericenters of these elliptical orbits and the phases of the particles on the orbits are such that the locus of the particles is a sinusoidal wave that moves through the ring with the angular velocity of the perturbing satellite.<sup>8,11</sup>

If the waves survive from one encounter to the next, then there is the possibility of resonance. This will occur wherever the local ring circumference is an integral number of wavelengths, that is wherever

$$2\pi a/\lambda = p+1 \quad (9)$$

where  $p$  is an integer  $\geq 0$ . Consecutive perturbations will then be in phase and a wave with an amplitude significantly  $> A$  may result.

The magnitude of the forced eccentricity, in the absence of damping and assuming that  $q = 1$ , is given by,

$$e = \left| \frac{m'/M \ f(p)n}{(p+1)n' - pn} \right| \quad (10)$$

Thus  $e$  increases markedly as the exact resonance is approached. At the exact resonance, the phase of the response changes by  $180^\circ$ . Similar behavior is observed in any driven harmonic oscillator. For particles outside the exact resonance, conjunction always occurs at apocenter, whereas for particles inside the exact resonance, conjunction always occurs at pericenter. Thus, the satellite excites a wave pattern of  $p+1$  equally spaced loops which co-rotate

with the perturbing satellite (see Figure 3).



FIGURE 3

Dynamics of Lindblad resonance. Ring particle paths are shown in a reference frame co-rotating with the perturbing satellite. (Copyright of Nature (MacMillan Journals Ltd.)).

The particle path pattern shown in Figure 3 is one of streamline flow for which interparticle collisions are a minimum. If a ring has a sufficiently high surface density, then the longitudinal variation of the gravitational potential associated with the  $p+1$  loops at a Lindblad resonance can act on the orbits of the other ring particles to generate a spiral density wave with  $p+1$  arms.<sup>7,8</sup> Outside the region of exact resonance, the particle paths in a frame co-rotating with the perturbing satellite are closed and contain the same number of waves. However, each closed path is displaced longitudinally with respect to its neighbor, and it follows from geometrical considerations that a spiral density wave must result (see Figure 4). The whole pattern is stationary in the co-rotating reference frame. Thus, the gravitational potential

associated with the spiral arms acts on the ring particles with the same frequency as the disturbing potential and the pattern is self-enhancing.

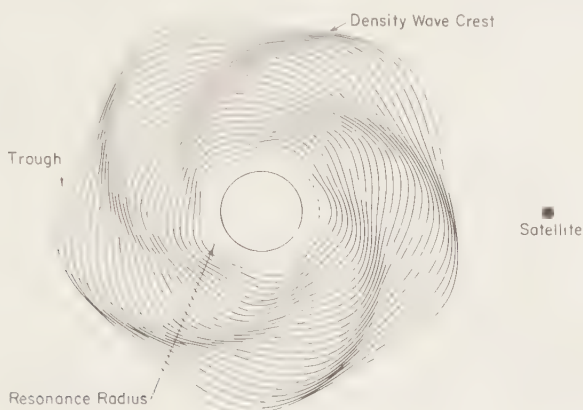


FIGURE 4

Schematic diagram of the particle path pattern and the associated trailing spiral density wave generated by the  $p = 4$  Lindblad resonance. If the ratio of the resonant mean motions is  $p/(p+1)$ , then  $p+1$  spiral arms are generated. (Copyright University of Arizona Press).

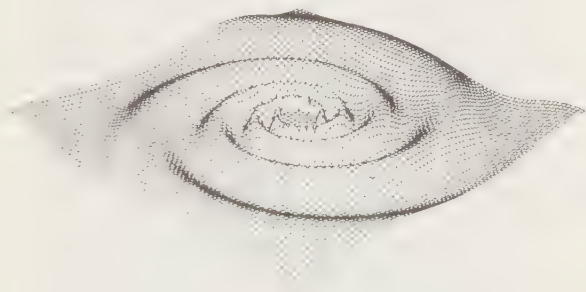


FIGURE 5

Dynamics of spiral bending waves. Schematic diagram of the variation of the vertical displacement with angle and radius for a two-armed spiral. (Copyright Academic Press).

The vertical analog of Lindblad resonance which is excited when a satellite orbit is inclined to the ring plane has been described by Shu et al.<sup>15</sup> (see Figure 5). A most remarkable example of this type of resonance was discovered by the Voyager spacecraft in Saturn's A-ring. The radial distance of the resonance location is given by

$$a = (GM)^{1/3} n^{-2/3} \quad (11)$$

where  $n$  satisfies

$$(p+q)n' - pn - \dot{\omega} - (q-1)\dot{\omega}' = 0 \quad (12)$$

or

$$(p+q)n' - pn - \dot{\Omega} - (q-1)\dot{\Omega}' = 0 \quad (13)$$

The locations of the different types of resonance associated with the same near-commensurate ratio of mean motions,  $n'/n \approx p/(p+q)$ , are usually well separated since  $\dot{\omega}$  and  $\dot{\Omega}$  are quite different. This is the case, for example, for the 5:3 resonance with Mimas and this resonance gives rise to two types of spiral density wave which have actually been observed (see Figure 6). The bending wave ( $\dot{\Omega}, \dot{\Omega}'$  case) on the left in Figure 6 is the most prominent since the raised corrugations of the ring give rise to a striking pattern of bright slopes and dark shadows. The Lindblad wave ( $\dot{\omega}, \dot{\omega}'$  case) on the right is not quite so prominent since it lies in the plane of the disk.

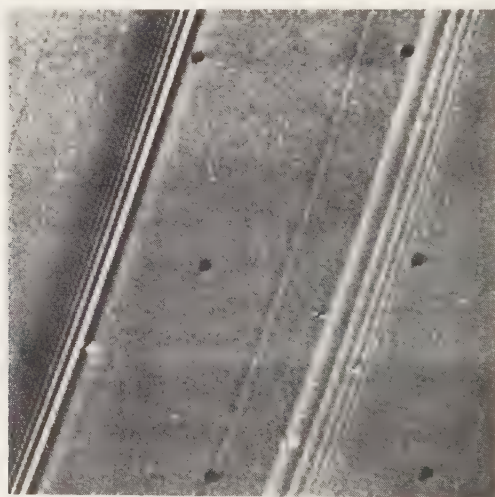


FIGURE 6

Voyager 2 image showing two prominent wave patterns in the outer A ring of Saturn. The feature on the left is a spiral bending wave and that on the right is a spiral density wave. Both features are associated with the 5:3 resonance with Mimas. The image shown is about 975 km across.

The study of density waves in Saturn's rings is now a very active subject. Much of the terminology that we use has been taken from galactic dynamics, but there are a number of important differences between the two subjects. The orbital period of a particle in Saturn's rings is  $\approx 8$  hours, whereas galactic

rotation periods are  $\approx 10^8$  years. Particles in Saturn's rings may have completed  $10^{12}$  orbits and the discussion of equilibrium configurations is appropriate, whereas in galactic dynamics the configurations develop over a very small number of rotations. Secondly, Saturn's rings have an optical depth of unity and each particle suffers, on average, one collision for each revolution of the planet. In galactic dynamics, stellar collisions can be discounted. However, it is already apparent that insights gained from the study of galaxies have wide application to ring problems. In time, perhaps, the flow of information may reverse direction, but this has yet to happen.

Before leaving this topic, I must mention that Lindblad resonances are not only important in ring systems but can involve pairs of satellites. In some cases, for example, that of Io and Europa, these simple resonances can give rise to equally spectacular effects. Io rotates so as to keep one face permanently turned towards Jupiter and, to a first approximation, the tidal bulge raised on Io by Jupiter is  $\approx 15$  km in height and is stationary on Io. However, there are small variations in the tide height due to Io's orbital eccentricity and these amount to  $\approx 100$  m. The heating associated with the repeated flexing of an imperfectly elastic, solid body can be large. However, the tidal forces also act to circularize the orbit and, if the orbital eccentricity is "free", then it rapidly decays and the heating event is short-lived and insignificant. But the orbital eccentricity of Io is forced to have the value 0.0041 by the perturbations associated with the 2:1 Lindblad resonance with Europa. In this case, the heat source does not decay and is sufficient to drive the observed volcanism<sup>3</sup>. The deposition rate on Io from both surface flows and volcanic plumes is observed to be about 0.1 cm/year and is sufficient to have recirculated a mass equal to the mass of the satellite during the lifetime of the solar system.

## 5. KIRKWOOD GAPS

There are several puzzling aspects to the distribution of resonances in the solar system. Although there is an excess of near-commensurabilities in the solar system as a whole, the exact resonances are largely confined to two satellite systems. The jovian and saturnian systems are virtually saturated with first-order resonances, whereas the uranian system does not contain a single exact resonance of any kind. Amongst the planets, Neptune and Pluto provide the only example of an exact resonance and this isolated case is consistent with a random distribution of planetary mean motions.

Consideration of the distribution of asteroidal mean motions only serves to deepen the mystery. The region between the 2:1 jovian resonance at 3.27 AU

and Jupiter contains comparatively few asteroids and these tend to be trapped in first-order resonances with Jupiter. These asteroids are the Hilda group at the 3:2 resonance, Thule at the 4:3 resonance and the Trojans at the 1:1 resonance (these asteroids are co-orbital with Jupiter). In sharp contrast, the resonant locations within the main asteroid belt (between 2.2 AU and 3.27 AU) are almost free of asteroids. These gaps in the distribution of mean motions were discovered by Kirkwood in 1867 and are now known to exist at the 3:1, 5:2, 7:3, 9:4, 11:5, 13:6 and 8:3 resonances.

Goldreich<sup>16</sup> suggested that the preference for resonance amongst pairs of mean motions in the satellite systems is the result of orbital evolution due to tidal dissipation in the planets. According to this hypothesis, the mean motions were initially random, but decreased, at different rates, as tidal forces fed angular momentum into the satellite orbits. After appreciable orbital evolution, pairs of mean motions attained commensurability and were captured in resonances. Goldreich's achievement was to show<sup>16</sup> that some resonances are stable under the action of tidal forces. In terms of Figure 3, this stability can be understood as a displacement of the stable longitude in the rotating reference frame, analogous to the lag produced by friction in a driven harmonic oscillator. The torque exerted by the resonance compensates for the difference between the tidal torques on the two satellites, the satellite orbits can then evolve in tandem and the exact resonance is maintained.

Since the tides raised by the planets on the sun have negligible effects on their orbits, the tidal hypothesis can certainly account for the lack of resonances in the planetary system. Yoder's outstanding work<sup>17,18</sup> on the origin and the evolution of the Laplace resonance shows that it is now almost certain that tidal dissipation in Jupiter has resulted in appreciable evolution of the orbits of Io, Europa and Ganymede. The internal structure of Uranus is quite different to those of Jupiter and Saturn (which are similar) and it is possible that tidal dissipation in that planet has been insufficient to appreciably change the orbits of its satellites. This could account for the lack of resonances in the uranian satellite system. However, I now consider that the difference between the distribution of resonances amongst the satellite systems of Jupiter, Saturn and Uranus and amongst the planets may have a more fundamental origin. This new insight arises from recent work by Wisdom<sup>19</sup> on the origin of the Kirkwood gaps

Wisdom's work<sup>19,20,21</sup> is the first major application of the techniques of non-linear dynamics to specific solar system problems and is both very exciting and timely. The origin of at least one of the Kirkwood gaps, the 3:1 gap at 2.5 AU, appears to have been solved and the chaotic tumbling of the



saturnian satellite Hyperion, which has recently been observed by the Voyager spacecraft, has already been accounted for<sup>21</sup>.

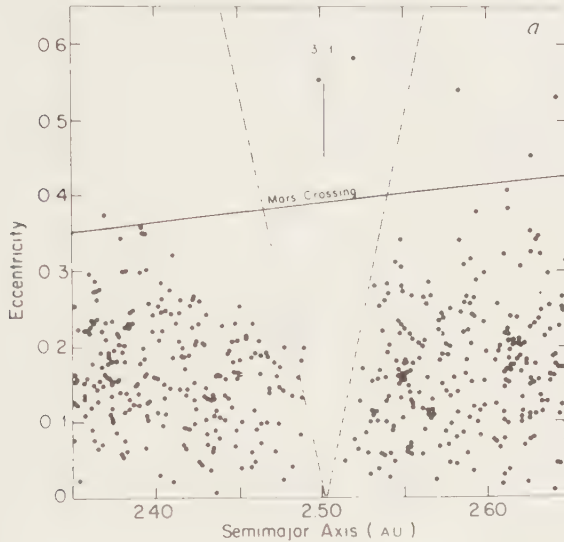


FIGURE 7

Kirkwood gaps in the asteroid belt. Distribution of the orbital eccentricities and semimajor axes of asteroids near the 3:1 resonance with Jupiter at 2.50 AU. The dashed lines represent the libration width associated with the leading term in the expansion of the disturbing function. If the asteroids lie above the Mars crossing line, then they may be removed by close planetary encounters. (Copyright of Nature (MacMillan Journals Ltd.)).

The fundamental question addressed in this work concerns the separation of the resonances. The classical approach to solar system problems is to expand the disturbing function  $U$  in a Fourier-like series (equation (2)). The high-frequency terms in this series are then removed by averaging and the problem is reduced to a study of the equations of motion when only a single term, that associated with the resonant argument  $\phi$ , is retained in the disturbing function. The circumstances under which this approach is not valid are now, to some extent, understood and appear to be well-described by the resonance overlap criterion<sup>22</sup>.

If an asteroid is trapped in some resonance of strength  $S$ , and the libration amplitude of the associated resonant argument  $\phi$  is a maximum, then the range  $\delta n$  (or  $\delta a$ ) through which the mean motion (or the semimajor axis) oscillates is also a maximum. We have<sup>23</sup>



$$\xi_n = 2 \left( \frac{12 |s|}{a^2} \right)^{1/2} \quad (14)$$

and we refer to this range as the libration width. For the 3:1 resonance with Jupiter at 2.50 AU,  $|s|^{1/2} \propto e$  and the libration region in the  $a$ - $e$  plane is V-shaped - see Figure 7. It is clear from Figure 7 that that region in  $a$ - $e$  space where resonance is possible is almost devoid of asteroids and that those few asteroids that remain in the resonance region tend to have very high eccentricities, high enough indeed, for their orbits to cross that of Mars. This diagram alone is strong evidence that the Kirkwood gaps have been produced by the direct gravitational action of Jupiter on the **present** distribution of asteroidal orbits. The myriad other hypotheses involving primordial processes that operated in the accretion disk, the statistics of libration, or the effects of friction can be discounted<sup>23</sup>.

The strongest resonances that can exist at the 3:1 ( $= p+q/p$ ) location have resonant mean motions  $n_1$  and  $n_2$  given by

$$(p+q)n' - pn_1 - \dot{\bar{q}}\bar{\omega} = 0 \quad (15)$$

$$(p+q)n' - pn_2 - \dot{\bar{q}}\bar{\Omega} = 0 \quad (16)$$

Their separation  $n_1 - n_2$  is given by

$$n_1 - n_2 = \frac{\bar{q}}{p} (\dot{\bar{\Omega}} - \dot{\bar{\omega}}) \quad (17)$$

In the asteroid belt, the rates of motion of the pericenters and the nodes,  $\dot{\bar{\omega}}$  and  $\dot{\bar{\Omega}}$ , are determined by the comparatively weak gravitational attractions of Jupiter and the other planets and are very low ( $\approx 2 \cdot 10^{-4}$  rad/year). Hence,  $n_1 - n_2$  is less than the half-sum of the libration widths of the two resonances and the resonances overlap. Wisdom, using a novel mapping technique that accurately describes the character of the motion, has shown that in these circumstances quasi-periodic orbits are unlikely and the motion is mostly chaotic<sup>19,20</sup>. The mappings show that the chaotic orbit diffuses through phase space and that, from time to time, on a timescale of  $\approx 10^5$  years, the eccentricity reaches very high values. The orbit then crosses that of Mars and, in some cases, even that of the Earth and the asteroid is eventually removed by close planetary encounters. It seems probable, that this mechanism has been responsible for the formation of at least the 3:1 Kirkwood gap. It could also be responsible for the delivery of meteorites from the asteroid belt to the Earth.

$\dot{\omega}$  and  $\dot{\Omega}$  are also very small for the planetary orbits and again the libration regions of the low-order resonances would overlap. For this reason, we would not expect any low-order resonances amongst the planets to have long-term stability<sup>23</sup>. This could account for the lack of exact resonances in the planetary system. However, for satellites moving about a markedly oblate planet  $\omega$  and  $\dot{\Omega}$  can be high and if the orbital eccentricities and inclinations are low and the satellite-planet mass ratios are small, then the exact resonances may be well separated. We calculate that this separation clearly occurs only in the satellite system of Saturn. It is striking that the saturnian system is virtually saturated with exact first-order resonances. For the uranian system, which is devoid of exact resonances of any kind, we find that the dynamical oblateness  $J_2$  is so low and the satellites are so distant from the planet that, with the observed orbital eccentricities, the exact low-order resonances would overlap. This could account for the lack of exact resonances in the uranian system<sup>23</sup>.

## REFERENCES

- 1) P.K. Seidelmann, The ephemerides: past, present and future, in: Dynamics of the solar system, IAU symposium No. 81, ed. R.L. Duncombe (D. Reidel, Dordrecht, 1979) pp. 99-114.
- 2) J.W. Christy and R.S. Harrington, *Astron. J.* 83 (1978) 1005.
- 3) S.J. Peale, P. Cassen and R.T. Reynolds, *Science* 203 (1979) 892.
- 4) W.M. Kaula, *An Introduction to Planetary Physics: The Terrestrial Planets* (John Wiley, New York, 1968).
- 5) R. Greenberg, Orbital resonances among Saturn's satellites, in: *Saturn*, ed. T. Gehrels (University of Arizona Press, Tucson, 1984).
- 6) S.J. Peale, *Ann. Rev. Astron. Astrophys.* 14 (1976) 215.
- 7) A. Brahic and R. Greenberg (eds.), *Planetary Rings* (University of Arizona Press, Tucson, 1984).
- 8) S.F. Dermott, Dynamics of narrow rings, in: *Planetary Rings*, eds. A. Brahic and R. Greenberg (University of Arizona Press, Tucson, 1984).
- 9) A.E. Roy and M.W. Ovenden, *Mon. Not. R. astron. Soc.* 141 (1954) 232.
- 10) S.F. Dermott, *Nature Physical Sciences* 244 (1973) 18.
- 11) S.F. Dermott, *Nature* 290 (1981) 454.
- 12) W.H. Julian and A. Toomre, *Astrophys. J.* 146 (1966) 810.
- 13) P. Goldreich and S. Tremaine, *Nature* 277 (1979) 97.
- 14) P. Goldreich and S. Tremaine, *Ann. Rev. Astron. Astrophys.* 20 (1982) 249.

- 15) F.H. Shu, J.N. Cuzzi and J.L. Lissauer, *Icarus* 53 (1983) 185.
- 16) P. Goldreich, *Mon. Not. R. astr. Soc.* 130 (1965) 159.
- 17) C.F. Yoder, *Nature* 279 (1979) 747.
- 18) C.F. Yoder and S.J. Peale, *Icarus* 47 (1981) 1.
- 19) J. Wisdom, *Astron. J.* 87 (1982) 577.
- 20) J. Wisdom, *Icarus* (in print).
- 21) J. Wisdom, S.J. Peale and F. Mignard, *Icarus* (in print).
- 22) B.V. Chirikov, *Phys. Rep.* 52 (1979) 263.
- 23) S.F. Dermott and C.D. Murray, *Nature* 301 (1983) 201.

Chapter VI

EXPERIMENTS ON  
FEW NUCLEON SYSTEMS



## FEW BODY EXPERIMENTS WITH POLARIZED BEAMS AND POLARIZED TARGETS

James E. SIMMONS

Los Alamos National Laboratory, Los Alamos, NM 87545, U. S. A.

A survey is presented concerning recent polarization experiments in the elastic p-d, p-<sup>3</sup>He, and p-<sup>4</sup>He systems. Mention is made of selected neutron experiments. The nominal energy range is 10 to 1000 MeV. Recent results and interpretations of the p-d system near 10 MeV are discussed. New experiments on the energy dependence of back angle p-d tensor polarization are discussed with respect to resolution of discrepancies and difficulty of theoretical interpretation. Progress is noted concerning multiple scattering interpretation of forward p-d deuteron polarization. Some new results are presented concerning the p-<sup>3</sup>He system and higher energy p-<sup>4</sup>He polarization experiments.

### 1. INTRODUCTION

It is my object here to make a broad survey of few body polarization phenomena that have been reported in the past few years. Energies will be in the range of about 10 to 1000 MeV. Requirements of time and space will limit my subject matter to the elastic channels in nucleon interactions with deuterium, helium-3, and helium-4. Excellent reviews cover prior elements of my subject: At the Few Body Conference in Eugene, Grüebler<sup>1</sup> discussed three- and four-body systems at lower energies ( $\sim 10$  MeV); at the Santa Fe Polarization Conference, Igo<sup>2</sup> discussed polarization experiments at intermediate energies ( $\sim 1000$  MeV); at Graz, Ohlsen<sup>3</sup> reviewed polarization effects in the three-body system, with emphasis on break-up phenomena. At the Santa Fe conference Kloe<sup>4</sup> compared theory with experiment.

### 2. LOW ENERGY NUCLEON-DEUTERON SCATTERING

I turn first to a very recent experiment concerning the literal subject of my talk. Schmelzer et al.<sup>5</sup> have submitted a contribution to this conference on the measurement of the spin correlation parameter  $C_{yy}$  in d-p scattering at incident deuteron energy  $T_d = 10$  MeV. This is a difficult measurement in which a vector polarized deuteron beam was scattered from a thin (70  $\mu$ m) LMN-type polarized proton target. The experimental results for  $C_{yy}$  are shown in Fig. 1. The five data cover the angular range of  $\theta_{c.m.}$  (proton) from 75 to 135°. These values represent slight changes from the published values. Three curves are also shown; two of these are Faddeev calculations with Coulomb corrections. The solid curve was from Stolk and Tjon<sup>6</sup> using a local N-N interaction; it gives a

good qualitative prediction for the data. The dashed curve is from Fayard et al.<sup>7</sup> with separable interaction; it is not so good. The dot-dash curve is a prediction from the phase shift analysis of Schmelzbach et al.<sup>8</sup> in 1972; it lies between the other two. It is expected that refinement of such data will help to define the nature of the off-shell N-N interaction. Comparison to prior work at Grenoble in Birmingham is noted in Ref. 5.

The Zurich group (ETHZ) has made a significant contribution to understanding proton-deuteron scattering for equivalent proton energies in the range 8.5 to 22.7 MeV. A detailed account of their analyzing power measurements with polarized proton and deuteron beams was published this year by Gruebler et al.<sup>9</sup> Sawada et al.<sup>10</sup> at Tsukuba have also made a series of accurate analyzing power measurements near  $T_d = 20$  MeV (published this year). These efforts have cleared up certain discrepancies, produced complementary information, and brought greater confidence to the experimental situation.

Comparison of such p-d data to theory is based on the Faddeev equations.<sup>11</sup> To the extent that the N-N interactions are known, with correct inclusion of the Coulomb force, the Faddeev equations may be integrated to give exact values of the p-d wave functions. On the whole, the method provides remarkable predictions for N-d scattering below 50 MeV. In the following paragraphs we illustrate the comparison between theory and experiment at  $T_p = 10$  MeV equivalent energy. Figure 2 shows the proton analyzing power  $A_Y^p$  at  $T_p = 10$  MeV as given by Doleschall et al.<sup>12</sup> For this and the following figure the Faddeev predictions are given by four curves labelled in a common fashion. All curves are calculated for n-d scattering using separable potentials. The S-wave interactions include a repulsive core. All curves include a two-term singlet S-wave ( $2^1S_0R$ ) and P-waves. The four curves are summarized as follows: Dashed, with two term tensor (2T2R); dot-dash, with four term tensor (4T4); continuous, same as preceding but with all D-waves; dotted, same as preceding but with approximate Coulomb corrections. In principle, the dotted curve should give the best representation of the data; the continuous curve is next best. In Fig. 2 we see a good prediction for  $A_Y^p$  from the full n-d calculation (solid curve); inclusion of Coulomb corrections (dotted curve) is somewhat better at small angles, but a little less

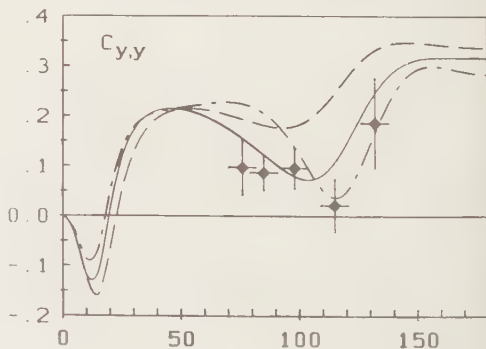


Fig. 1. Spin correlation parameter  $C_{yy}$  for p(d,p)d at  $T_d = 10$  MeV. Data from Ref. 5. For curves see text.



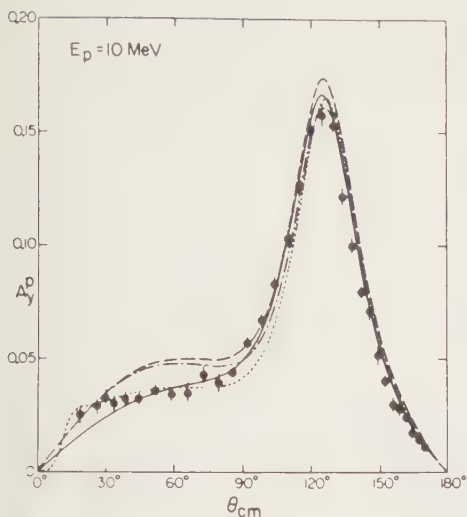


Fig. 2. Proton analyzing power for  $d(p,p)d$  at  $T_p = 10$  MeV. Data from Ref. 12. The dotted curve is the full Faddeev calculation.

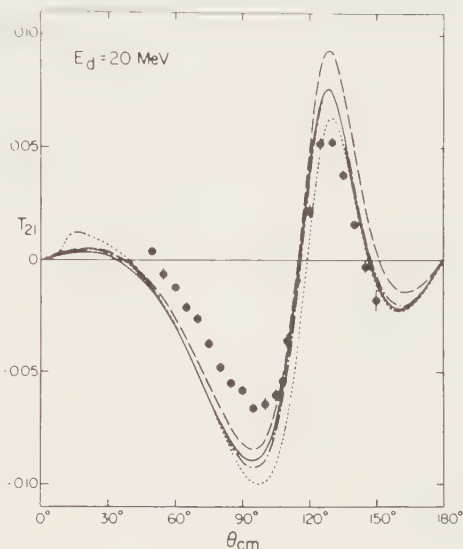


Fig. 3. Tensor analyzing power  $T_{21}$  for  $p(d,p)d$  at  $T_d = 20$  MeV. Data from Ref. 10. Dotted curve is the full Faddeev calculation.

good at larger angles. The four-term tensor interaction definitely improves the fit for angles less than  $90^\circ$ ; this is related to superior representation of the  $\epsilon_1 \ ^3S_1 - \ ^3D_1$  mixing parameter.

As another example, Fig. 3 shows  $T_{21}$ , a deuteron tensor analyzing power at  $T_d = 20$  MeV. This parameter is determined by XZ components of beam polarization, and the data are from Tsukuba<sup>10</sup> where the necessary control of spin quantization direction was available. The Faddeev predictions are from Ref. 12 with the same definitions as above. There seem to be relatively serious discrepancies between the Faddeev predictions and the data, and it is not obvious which curve does best. Doleschall et al. note that the way the Coulomb corrections are treated could have a significant effect on  $T_{21}$  and some of the other parameters. Kloet<sup>4</sup> has also emphasized the importance of Coulomb effects.

Further work on the Coulomb questions appeared this year by Zankel and Hale,<sup>13</sup> who made calculations for the n-d and p-d  $A(\theta)$ , parameter including Coulomb distortion effects. Comparison was made to precision n-d data of Tornow et al.<sup>14</sup> and p-d data of Ref. 9. The conclusion was that 5% differences occur at the back angle peak of  $A(\theta)$  that are not obtained from simpler correction procedures.

Space does not permit further examples of the low energy p-d analyzing powers. Suffice it to say that the 4T4R predictions of Ref. 12 provide good predictions for the tensor analyzing powers  $T_{20}$  and  $T_{22}$  near  $T_d = 20$  MeV;

comparison was not as good for the vector analyzing power  $iT_{11}$ .

Sperisen et al.<sup>15,16</sup> at ETHZ have recently published two papers on a series of measurements of polarization transfer observables in p-d scattering at  $T_p = 10$  MeV. In the second paper measurements were made for the  $d(\vec{p}, \vec{d})p$  process; three vector-vector and seven vector-tensor parameters were obtained. The Faddeev predictions for these observables showed little sensitivity to the form of the tensor force or to additional D-waves or the Coulomb force. There were indications of sensitivity to P-waves in the vector to tensor observables. Figure 4 shows three of these. The curves showing

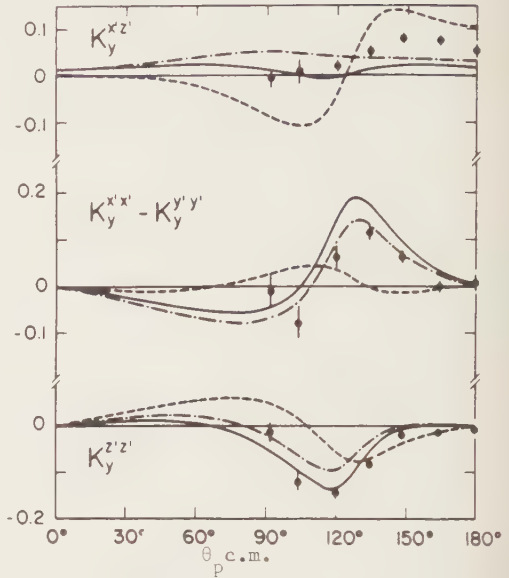


Fig. 4. V-T polarization transfer parameters in  $d(p,d)p$  at  $T_p = 10$  MeV. Data from Ref. 16. Dashed curves have no P-waves; others do.

Faddeev predictions are not the same as for Figs. 2 and 3. The dashed curves contain no P-waves; they do not agree with the data. The other two curves include P-waves and variants of the tensor force; they have a qualitative resemblance to the data, but deviations are still observed. The P-wave sensitivity of these parameters was a very interesting finding and encouraged the expectation that further analysis of these results would lead to better understanding of the N-N interaction in the Faddeev context.

Much effort has been put into low energy N-d scattering experiments (of which I have mentioned but a small part here). Such experiments were done at Lawrence Berkeley Laboratory (LBL) as described by Conzett.<sup>17</sup> Work at Los Alamos was described in Ref. 3. Shimizu et al.<sup>18</sup> have made  $\vec{p}$ -d analyzing power measurements at Kyoto at 65 MeV. Further work from that laboratory is being reported to this conference by Hatanaka et al.<sup>18</sup> on d-p tensor measurements; rather good agreement is reported with theory employing the Graz interactions. Brock et al.,<sup>29</sup> Romero et al.,<sup>20</sup> and Watson et al.,<sup>21</sup> at Davis have reported n-d analyzing power measurements giving partial reference to recent neutron work.

At Karlsruhe a significant neutron-deuteron scattering program has been underway at the cyclotron accelerator for energies up to 50 MeV. Quite recently Schwarz et al.<sup>22</sup> published results for precision n-d differential cross sections from 2.5 to 30 MeV. New results from this group will be reported to the

conference by Brady et al.<sup>22</sup> on the n-d analyzing power from 14 to 50 MeV. Such data will be important for understanding the basic interaction and the role of Coulomb effects.

The exploitation of the Faddeev method for the explanation of low energy elastic scattering has been a major success of the past decade. The general qualitative agreement between theory and experiment is most impressive. We hope that additional knowledge might be gained about the on-shell N-N interaction in this way, owing partly to the enhanced effects that occur in some observables of the N-d system. From my viewpoint, it is not obvious that this has happened. Nor does it appear that new insights have been gained with respect to the off-shell N-N interaction from the elastic system. In this connection, R. Brown<sup>23</sup> has called my attention to the importance of breakup studies to off-shell effects and to new experiments of this kind currently underway at Indiana. The calculational complexity of the Faddeev method is partly to blame for these circumstances. For significant improvement to occur from this state it appears that the calculations must be made more accurate with respect to current understanding of the N-N interaction.

I have not found any recent publications on the phase shift analysis of the low energy p-d system. Reference 8 (1972) was one of the most complete. This undoubtedly derives from the complexity of the problem and the relative success of the Faddeev approach. At  $T_p = 10$  MeV alone, almost 400 data on 21 independent observables over a broad range of angles exist. Perhaps this is the time to reconsider this question. Would it be possible to calculate higher partial waves or some of the inelasticity parameters from the Faddeev method? This might make phase-shift analyses more feasible while keeping the theoretical input reasonably small. If by this means the mass of data on N-d scattering from 5 to 50 MeV could be compactly described, this would be a significant accomplishment.

### 3. INTERMEDIATE ENERGY p-d POLARIZATION

Nucleon-deuteron scattering may be considered as dividing into two regions: the forward direction where the incoming particle scatters individually from the two constituents of the deuteron, and backward angles where the incoming particle exchanges with one of the particles picking up the other to form an outgoing deuteron. Nucleon exchange was identified thirty years ago by Christian and Gammel<sup>24</sup> as the significant physical process for low energy N-d backward scattering. Its importance continues into the intermediate energy range. At energies near 600 MeV, however, another process becomes important and enhances backward scattering --  $\Delta(1232)$  formation in the intermediate state. It is the same process that drives the  $pp \rightarrow nd$  reaction to a peak at that energy, as described by Barry<sup>25</sup> and others.

Berthet et al.<sup>26</sup> have measured backward p-d scattering from 0.6 up to 2.7 GeV. Their data overlaps the enhancement in the scattering at 600 MeV. Beyond 600 MeV an experimental decline was observed to 2.2 GeV where a new change of slope was seen. They compared existing data on the backward scattering from 200 to 2000 MeV using nucleon exchange (ONE) and pion exchange (OPE) models. They found that neither model was adequate by itself. In unpublished work Laget and Lecolley<sup>27</sup> have formulated a model that employs a coherent sum of ONE and OPE, which apparently does give good predictions for p-d backward scattering at intermediate energies.

Measurements of the back angle tensor analyzing power  $T_{20}(180)$  have generated much interest in the past few years. Earlier this year Arvieux et al.<sup>28</sup> reported such measurements using the polarized deuteron beam at Saturne-2 over the energy range  $T_d = 0.3$  to 3.0 GeV. Their experimental arrangement had good signal to background for detection of protons over the full energy range and deuterons over a part of it. Their results are shown in Fig. 5. There is a good deal of information on this figure of which I can discuss but a part. Their experimental data are seen in the lower part of the figure as solid dots (proton detection) or open squares (deuteron detection).

A prominent feature of the data in Fig. 5 is the dip in  $T_{20}$  near  $T_d = 1.5$  GeV. The nature of this dip was predicted by Vasan<sup>10</sup> some time ago on the basis of ONE. This calculation is indicated by the dotted curve in Fig. 5,

but the position comes too high in energy. Keister and Tjon<sup>30</sup> have investigated relativistic effects in the ONE model; their pseudovector calculation is comparable to that of Vasan; their pseudoscalar calculation is not consistent with the data. A second feature of the data is a dip of lesser magnitude near  $T_d = 1.4$  GeV, which has not been seen or predicted heretofore. The model of Ref. 27 included nucleon and pion exchange in a coherent fashion. This prediction is shown as the dashed curve and describes well the dip at  $T_d = 0.5$  GeV; however, by 1.2 GeV it has climbed far above the data.

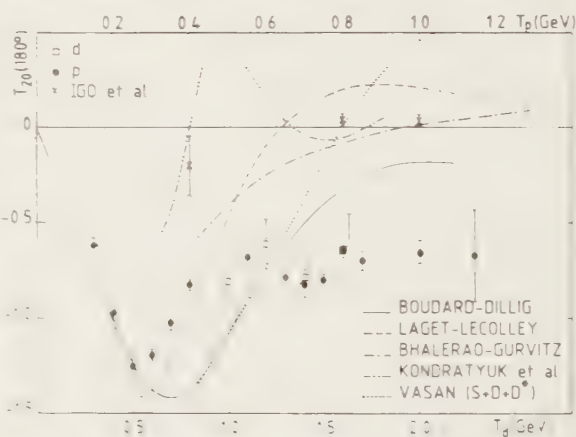


Fig. 5. Back angle tensor analyzing power  $T_{20}$  vs  $T_d$  for p(d,p)d at intermediate energies. Dots and squares Ref. 28; crosses Ref. 31.

Significant on Fig. 5 are the data points from Argonne of Igo et al.<sup>31</sup> shown as crosses at  $T_p = 0.4, 0.8$ , and  $1.0$  GeV. These points are consistent with zero and are in complete disagreement with those of the Saturne group. Something went wrong at Argonne, which was probably related to the difficult problem of detecting low energy deuterons from back angle scattering. It must be noted that these problems pertain only to back angle scattering. Argonne and Saturne are in excellent agreement on forward-scattering measurements. We see that this very interesting experiment from Saturne has resolved an experimental discrepancy and provided new data for theoretical comparison.

In the forward scattering of nucleons from deuterium at intermediate energies two regions are identified. At small angles the scattering occurs singly from the constituent nucleons. At momentum transfers near  $-t = 0.3$  (GeV/c)<sup>2</sup> double scattering becomes important, and the scattering decreases less rapidly. The deuteron D-state must be involved<sup>32</sup> to obtain a quantitative explanation of the process.

Measurement of the polarization parameters is essential to the verification of the validity of multiple scattering theory.

Figure 6 shows one example of the many polarization measurements of the UCLA group and their collaborators, as reported by Bleszynski et al.<sup>33</sup> Shown is the tensor analyzing power  $P_{yy}$  at  $T_p$  (equiv.) = 800 MeV, where  $y$  is parallel to the  $z$ -axis scattering plane. The experiments were done at the Argonne ZGS machine with a polarized deuteron beam incident on a liquid hydrogen target. The data show a rise to a substantial peak near  $-t = 0.25$  (GeV/c)<sup>2</sup>, at the onset of double scattering, then a sharp decline and a broad minimum.

There are two significant theoretical predictions in Fig. 6, which were described in Ref. 33, and in greater detail in Alberi et al.<sup>34</sup> The dashed curve represents a Glauber model calculation including the deuteron D-states and current N-N amplitudes. It represents well the forward peak but undershoots the data at larger values of  $-t$ . The solid curve gives results of a complete systematic multiple scattering calculation<sup>33,34</sup> of which the most significant new elements are corrections to the eikonal approximation. These corrections allow additional diffraction effects and phase changes for the nucleon wave as it

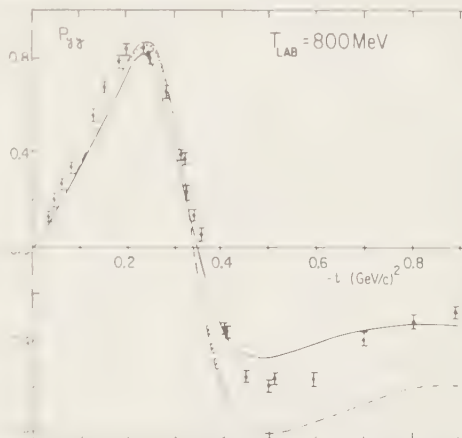


Fig. 6. Tensor analyzing power  $P_{yy}$  in  $p(d,d)p$  at  $T_p$  (equiv.) = 800 MeV. Data and M.S. curves Ref. 33.



propagates from the first to the second scattering. The solid curve gives a significantly improved representation of the data in the region of larger momentum transfer. Note that the experiments at Argonne<sup>33</sup> also yield values for  $P_y$  and  $P_{xx}$  at 800 MeV and other energies.

It may be noted that the Saturne group<sup>28</sup> has obtained  $A_{yy}$  ( $=P_{yy}$ ) data at  $T_p$  (equiv.) = 600 MeV over the whole angular range, with good agreement to the Argonne data at forward angles. At the moment, however, there is no theoretical model that can give a qualitative explanation of a growing mass of N-d data at both forward and backward angles.

In closing this section, I would like to mention some very recent results from the UCLA collaboration in  $d(\vec{p}, \vec{p})d$  polarization transfer at 500 and 800 MeV.

In a contribution to this conference Sun et al.<sup>35</sup> describe the measurements that were done at LAMPF in the polarized external proton beam. The preliminary results for two parameters,  $D_{LL}$  and  $D_{SL}$ , are shown in Fig. 7 at  $T_p = 800$  MeV. The nomenclature is such that L means longitudinal and S means perpendicular to L in the plane of scattering. The dashed curves are preliminary multiple scattering calculations of the type mentioned above.<sup>33</sup> The interesting point is that these curves do not represent the data well.

New effects may be showing up here. Dr. Igo informs me that the p-d program is, on this very date, being pursued at LAMPF at 800 MeV in a HRS experiment with polarized proton beam, polarized deuteron target, and final state proton polarization measurement. The long range objective is determination of the elastic amplitudes at 800 MeV.

#### 4. UPDATE ON N- $^3\text{He}$ SCATTERING

In a contribution to this conference by Verheijen et al.,<sup>36</sup> the Manitoba group have continued low energy p-  $^3\text{He}$  analyzing power studies with a polarized  $^3\text{He}$  gas target. By optical pumping, polarizations of about 16% were achieved. New data at 30 and 35 MeV were obtained. In addition, a phase-shift analysis was performed on all available data at seven energies between 19.5 and 35 MeV. A good representation of the existing data was obtained but with no claim to uniqueness. Reference to prior work is given in Müller et al.<sup>37</sup> I note also that Brady et al.<sup>38</sup> of the Karlsruhe group have submitted a contribution to the

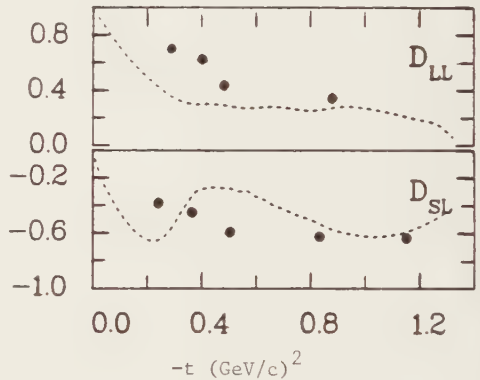


Fig. 7. Polarization transfer in  $d(p,p)d$  at  $T_p = 800$  MeV. Preliminary data from Ref. 35.

conference on preliminary results on the  $n-^3\text{He}$  analyzing power at eleven energies between 16 and 50 MeV.

At higher energy very recent results are becoming available on  $p-^3\text{He}$  scattering from Hasell et al.<sup>39</sup> in a collaboration of Manitoba and others at TRIUMF. Differential cross sections and

analyzing powers were measured with the polarized proton beam at four energies between 200 and 515 MeV. Evidence for interference between double and triple scattering was seen in the cross sections. An example of the analyzing power data at  $T_p = 200$  MeV is shown in Fig. 8. The curve represents a Glauber-theory prediction with up to three scatterings. At this stage in the development of the model, agreement is reasonable out to about  $40^\circ$  c.m.

In terminating this section, I note the  $p-^3\text{He}$  back angle differential cross section measurements of Berthet et al.<sup>40</sup> at Saturne-2 for  $T_p$  between 700 and 1700 MeV. They observed two structures associated with delta and possibly heavy baryon excitation.

## 5. SOME RESULTS IN $N-^4\text{He}$ SCATTERING

I have not found many recent publications in low energy  $N-^4\text{He}$  polarization work. Most recent is a measurement by York et al.<sup>41</sup> at TAMU on neutron- $^4\text{He}$  analyzing power at 50 MeV. The  $d(\vec{d}, \vec{n})^3\text{He}$  reaction at  $0^\circ$  was used as the polarized neutron source. Their data show a clear minimum in  $A(\theta)$  at  $110^\circ$  c.m. and a strong maximum at  $135^\circ$ . In a report to the conference, Doll et al.<sup>42</sup> of the

Karlsruhe group describe their measurements for  $n-^4\text{He}$   $A(\theta)$  at eleven energies up to 50 MeV. Shown in Fig. 9 is an example of their data at  $T_n = 40$  MeV. The solid points are their work, the open ones are proton data of Plattner et al.<sup>43</sup> The dashed curve is for  $n-^4\text{He}$  phase shift prediction and the other is for  $n-^4\text{He}$ . At back angles there is excellent agreement between the two data sets. Near  $90^\circ$  a very interesting charge-dependent difference develops that

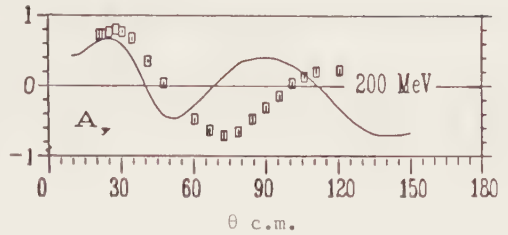


Fig. 8. Analyzing power in  $^3\text{He}(\vec{p}, p)^3\text{He}$  at  $T_p = 200$  MeV. Data and M.S. curve from Ref. 39.

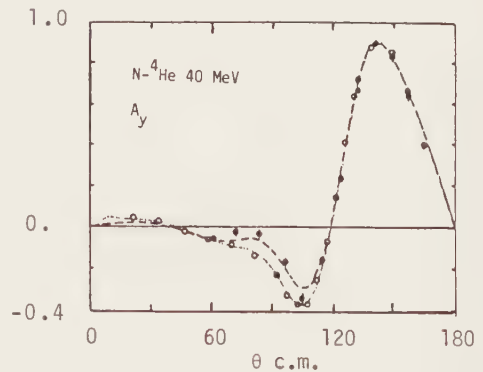


Fig. 9.  $N-^4\text{He}$  analyzing power at  $T_N = 40$  MeV. Dots preliminary neutron data Ref. 42; open circles proton data Ref. 43. Dashed curve is  $n-^4\text{He}$  PSA.



will be important in clarifying the way in which Coulomb corrections are employed. In this connection, I note the recent paper of Fröhlich et al.<sup>44</sup> who treat such Coulomb differences explicitly for the  $N-^4\text{He}$  system; references are also given to prior phase-shift analyses.

At intermediate energy the most timely results in  $p-^4\text{He}$  scattering come from TRIUMF. Most recently Moss et al.<sup>45</sup> reported measurement of the rotation parameter ( $R$ ) at 500 MeV. In a somewhat earlier work the same group<sup>46</sup> published measurements for the differential cross section and analyzing power for  $p-^4\text{He}$  scattering at 200, 350, and 500 MeV over the full angular range.

In a very recent paper, Sherif<sup>47</sup> has discussed these results (not  $R$ ) in an optical model (OM) with exchange effects. The  $^4\text{He}$  target nucleus may be thought to consist of a proton plus triton cluster, and the associated heavy particle stripping (HPS) mechanism is calculated by the distorted wave Born approximation. Thus the total interaction is OM + HPS. The chief focus is on the exchange effects, manifested through HPS, with the object of reproducing the back angle cross section and analyzing power.

At 350 MeV, the differential cross section data are reproduced rather well. The case for the  $p-^4\text{He}$  analyzing power at  $T_p = 350$  MeV is shown in Fig. 10; the data are from Ref. 46. The short dashed curve is the optical model alone; it does well out to  $90^\circ$  c.m. The long dashed curve represents exchange

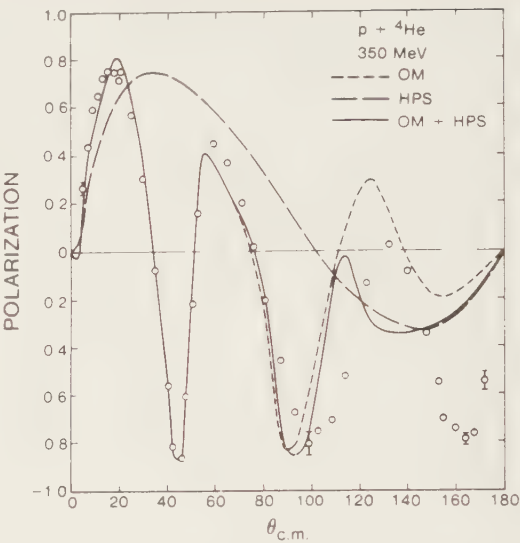


Fig. 10.  $p-^4\text{He}$  analyzing power at  $T_p = 350$  MeV. Data from Ref. 46. Optical model predictions from Ref. 47.

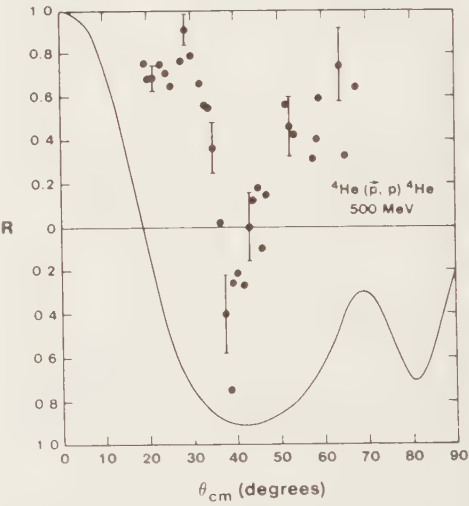


Fig. 11.  $p-^4\text{He}$  rotation parameter at  $T_p = 500$  MeV. Data and optical predictions from Ref. 45.

through heavy particle stripping. The solid curve gives the complete interaction. Unfortunately HPS does not help very much; agreement in the large angle region is lacking.

Data for the  $p-{}^4\text{He}$  spin rotation parameter from Ref. 45 are shown in Fig. 11 at  $T_p = 500$  MeV. Carbon scattering was employed in the polarimeter. To the best of my knowledge this is the first such measurement for  $p + {}^4\text{He}$  above  $\sim 50$  MeV. The parameter has definite structure with a negative minimum near  $40^\circ$  c.m., rising to large positive values to either side. Also shown on the figure is a prediction for  $R$  from results of a standard optical model fit to the differential cross section and analyzing power in the forward hemisphere. The prediction is poor.

In a current preprint Greben and Gourishankar<sup>48</sup> have carefully examined  $p-{}^4\text{He}$  scattering at 500 MeV in the optical model context. Their considerations of the data set led them to a model with a more pronounced attractive tail in the real central potential and to reduced spin orbit potentials than some prior models. In this manner they achieved excellent fits in the forward hemisphere for  $d\sigma/d\Omega$ ,  $A$  and  $R$ . They emphasize the value of  $R$  data in arriving at good optical model parameters.

A substantial amount of theoretical activity has occurred in the past few years concerning intermediate energy  $p-{}^4\text{He}$  scattering. Brief mention of some of this follows. Auger et al.<sup>49</sup> investigated intermediate isobaric states in the multiple scattering model. Wallace and Alexander<sup>50</sup> studied correlation effects with inclusion of isobar states in the context of multiple scattering. Alexander and Landau<sup>51</sup> described a microscopic optical model for energies near 200 MeV. Arnold et al.<sup>52</sup> presented a relativistic optical model for energies in the range 0.5 to 1.5 GeV.

Knowledge of the  $p-{}^4\text{He}$  system at intermediate energies is in a state of development. Experimentally the system is fairly simple, both to measure and with respect to the number of observables (3). With the theoretical interest now evident we may expect significant increase in our understanding in the next few years.

#### REFERENCES

- 1) W. Grüebler, Nucl. Phys. A353 (1981) 31c, Few Body Conference, Eugene (1980).
- 2) G. J. Igo, A. I. P. Conf. Proc. No. 69 (1981) 1157, Santa Fe Polarization Symposium (1980).
- 3) G. G. Ohlsen, Lecture Notes in Physics, vol. 87 (II), Ed. H. Zingl (Springer 1978) pg. 295, Few Body Conference, Graz, 1978.
- 4) W. M. Kloet, A. I. P. Conf. Proc. No. 69 (1981) 1132, Santa Fe Polarization Symposium (1980).
- 5) R. Schmelzer et al., Phys. Lett. 120B (1983) 297, and R. Schmelzer et al., Karlsruhe Conf. Abstracts, (1983) 249 (unpublished).

- 6) C. Stolk and J. A. Tjon, Nucl. Phys., A295 (1978) 384.
- 7) C. Fayard et al., in Proc. 3rd Session d'Etudes de Physique Nucleaire (La Toussuire 1975) LYCN 7502.
- 8) P. A. Schmelzbach et al., Nucl. Phys. A197 (1972) 273.
- 9) W. Grüebler et al., Nucl. Phys. A398 (1983) 445.
- 10) M. Sawada et al., Phys. Rev. C 27 (1983) 1932.
- 11) P. Doleschall, Nucl. Phys. A201 (1973) 264.
- 12) P. Doleschall et al., Nucl. Phys. A380 (1982) 72.
- 13) H. Zankel and G. M. Hale, Phys. Rev. C 27 (1983) 419.
- 14) W. Tornow et al., Phys. Rev. Lett. 49 (1982) 312.
- 15) F. Sperisen et al., Phys. Lett. 102B (1981) 9.
- 16) F. Sperisen et al., Phys. Lett. 110B (1982) 103.
- 17) H. E. Conzett, Lecture Notes in Physics, vol 87 (II), Ed. H. Zingl (Springer 1978) pg. 477, Few Body Conf. Graz, 1978.
- 18) H. Shimizu et al., Nucl. Phys. A382 (1982) 242.  
K. Hatanaka, Karlsruhe Conf. Abstracts (1983) 246 (unpublished).
- 19) J. E. Brock et al., Nucl. Phys. A382 (1982) 221.
- 20) J. L. Romero et al., Phys. Rev. C 25 (1982) 2214.
- 21) J. W. Watson et al., Phys. Rev. C 25 (1982) 2219.
- 22) P. Schwarz et al., Nucl. Phys. A398 (1982) 1.  
F. P. Brady et al., Karlsruhe Conf.
- 23) R. E. Brown, Private Communication (1983).
- 24) R. S. Christian and J. L. Gammel, Phys. Rev. 91 (1953) 100.
- 25) G. W. Barry, Annals of Physics 73 (1972) 482.
- 26) P. Berthet et al., J. Phys. G 8 (1982) L111.
- 27) J. M. Laget and J. F. Lecolley, Abstracts Versailles (1983) 425 (unpublished).
- 28) J. Arvieux et al., Phys. Rev. Lett. 50 (1983) 19.
- 29) S. S. Vasan, Phys. Rev. D 8 (1973) 4092.
- 30) B. D. Keister and J. A. Tjon, Phys. Rev. C 26 (1982) 578.
- 31) G. Igo et al., Phys. Rev. Lett. 43 (1979) 425.
- 32) V. Franco and R. J. Glauber, Phys. Rev. Lett. 22 (1969) 370.
- 33) M. Bleszynski et al., Phys. Lett. 106B (1981) 42, and Priv. Comm.
- 34) G. Alberi et al., Annals of Physics 142 (1982) 299.
- 35) Sun Tsu-Hsun et al., Karlsruhe Conf.
- 36) P. J. T. Verheijen et al., Karlsruhe Conf.
- 37) D. Müller et al., Nucl. Phys. A311 (1978) 1.
- 38) F. P. Brady et al., Karlsruhe Conf.
- 39) D. K. Hasell, Thesis Univ. Manitoba (1983).
- 40) P. Berthet et al., Phys. Lett. 106B (1981) 465.
- 41) R. L. York et al., Phys. Rev. C 27 (1983) 46.
- 42) P. Doll et al., Karlsruhe Conf.
- 43) G. R. Plattner et al., Phys. Rev. C 5 (1972) 1158.
- 44) J. Fröhlich et al., Nucl. Phys. A384 (1982) 97.
- 45) G. A. Moss et al., Nucl. Phys. A392 (1983) 361.
- 46) G. A. Moss et al., Phys. Rev. C 21 (1980) 1932.
- 47) H. S. Sherif et al., Phys. Rev. C. 27 (1983) 2759.
- 48) J. M. Greben and R. Gourishankar, U. Alberta Preprint TRI-PP-83-18, To be Pub. in Nucl. Phys. A405 (1983) 445.
- 49) J. P. Auger et al., J. Phys. G. 7 (1981) 1627.
- 50) S. J. Wallace and Y. Alexander, Phys. Lett. 90B (1980) 346.
- 51) Y. Alexander and R. N. Landau, Phys. Lett. 84B (1979) 292.
- 52) L. G. Arnold et al., Phys. Rev. C. 19 (1979) 917.

## NUCLEAR FEW CLUSTER STUDIES

Gian-Reto PLATTNER

Institut für Physik, Universität Basel, CH-4056 Basel,  
Switzerland

Two topics from the wide field of nuclear few cluster studies are reviewed in this talk\*. They were chosen after a search revealed their prevalence in the literature from 1979-1983.

Recent developments in the experimental and theoretical study of the six-nucleon system are discussed first. It is concluded that sufficiently comprehensive data sets are available to test the various theoretical models, which all show distinct deficiencies and must be improved. It is recommended that new experiments should only be carried out if the resolution of a specific, well-defined problem is attempted.

The larger part of the talk is devoted to a critical review of the "molecular" (two-body) aspects of the interaction between lighter heavy ions (in particular  $^{12}\text{C}+^{12}\text{C}$ ). Such few-body aspects of HI collisions have never before been discussed at a Few Body Conference. An attempt is made to define the present status of the "molecular state" concept and to suggest directions for further, more conclusive experimental studies, based on well-tested methods used in few-body nuclear physics.

### 1. THE $A = 6$ SYSTEM (particularly $^6\text{Li}$ )

Interest: very strong correlations between the six nucleons;

$2n+2p \rightarrow \alpha$ -particle,  $n+p \rightarrow$  deuterons, i.e. strong cluster effects.

#### 1.1. New developments concerning the $A=6$ ground and excited states.

##### Experiment

a) New data on electron scattering form factors <sup>1</sup>.

Now available  $l^{-6}$  for  $q \lesssim 3\text{fm}^{-1}$ :

$^6\text{Li}$  gs ( $1^+, 0$ ) CO, M1 form factors;

$^6\text{Li}^*$  ( $3^+, 0$ ) C2,  $^6\text{Li}^*$  ( $0^+, 1$ ) M1,  $^6\text{Li}^*$  ( $2^+, 1$ ) M1+E2+M3;

$^6\text{Li}$  continuum form factors near  $\alpha+d$ ,  $^3\text{H}+^3\text{He}$  thresholds;

---

\*In order to comply with the editor's page limits while still covering the complete contents of the 45' talk, I have chosen to present the material with only a minimum of prose, in much the same way as it appeared on the original transparencies.

- b) New data<sup>7</sup> on  $\alpha$ +d photo capture to  ${}^6\text{Li}$  gs for  $1\text{ MeV} < E_{\text{cm}} < 8\text{ MeV}$ ;  
 c) New data<sup>8,9</sup> on QFS of p on d in  ${}^6\text{Li}$ , from which is deduced by DWIA: d momentum distribution in  ${}^6\text{Li}$ .

#### Interpretation

- a) "Phenomenological"  $\alpha$ +d cluster model<sup>1</sup> with H.O. wave functions fitted to A=6 data;  
 b) "microscopic"  $\alpha$ +d cluster model<sup>10</sup> with resonating group (RGM) relative motion plus H.O. cluster wave functions. None of the parameters fitted to A=6 data.

Note: Both cluster models include a degree of freedom corresponding to alignment or distortion of the deuteron cluster in  ${}^6\text{Li}$ . Both use fully antisymmetrized wave functions and include the full Coulomb interaction.

- c) Three-body (Faddeev)  $\alpha$ +n+p model<sup>11-13</sup>. The  $\alpha$ , n and p considered as elementary and pointlike, relative motion wave functions calculated by the Faddeev equations with realistic phenomenological NN and N $\alpha$  interactions, including the NN tensor force, but neglecting the Coulomb interaction. No free parameter fitted to A=6 data.

#### Results of these experimental and theoretical studies:

- "phenomenological" cluster model yields excellent fits to the known e.m. form factors (fig. 1).

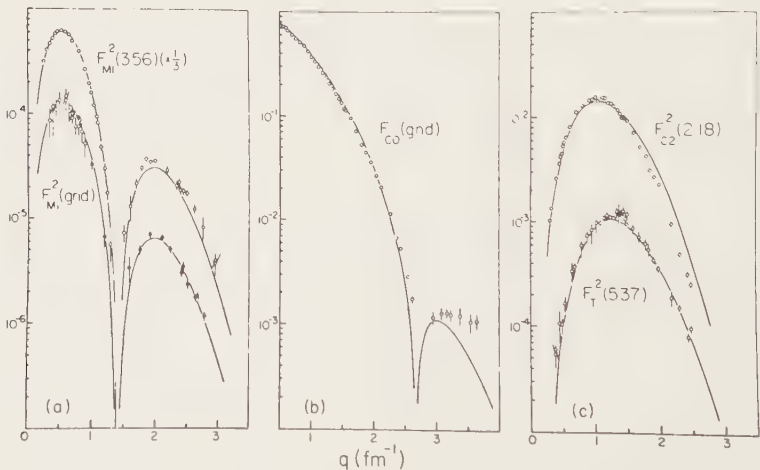


FIGURE 1

conclusion: deuteron in  ${}^6\text{Li}$  must be stretched and aligned along the  $\alpha$ -d axis in order to achieve agreement with the data.

- "microscopic" RGM cluster model study of  ${}^6\text{Li}$  concentrates on the gs CO form factor and the  $\alpha$ +d elastic scattering phase shifts, which are qualitatively well reproduced (fig. 2).

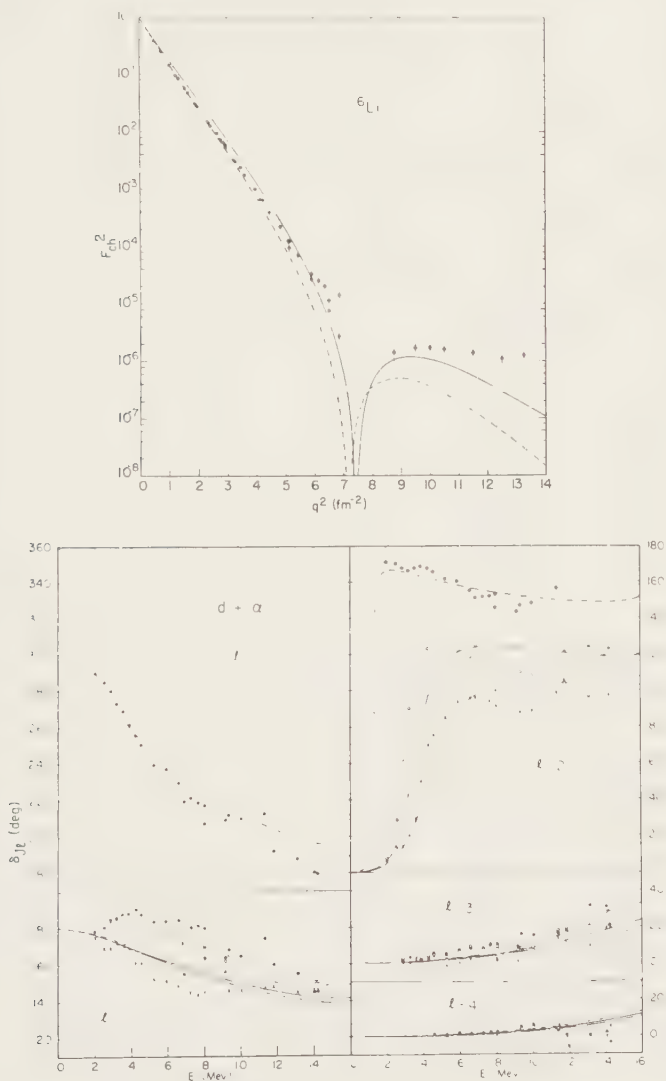


FIGURE 2

conclusion: deuteron in  ${}^6\text{Li}$  must be deformed. However, in this model this amounts to a compression, increasing with decreasing  $\alpha$ -d separation. Gain in the variational value of the  $\alpha$ -d separation energy by distortion is 1.6 MeV! (i.e.  ${}^6\text{Li}$  without distortion would be unbound).

- three-body model reproduces the d momentum distribution in  ${}^6\text{Li}$  reasonably well (fig. 3). Detailed predictions are given for the  $\ell=0$  and  $\ell=2$  parts of the gs wave function, including a projection

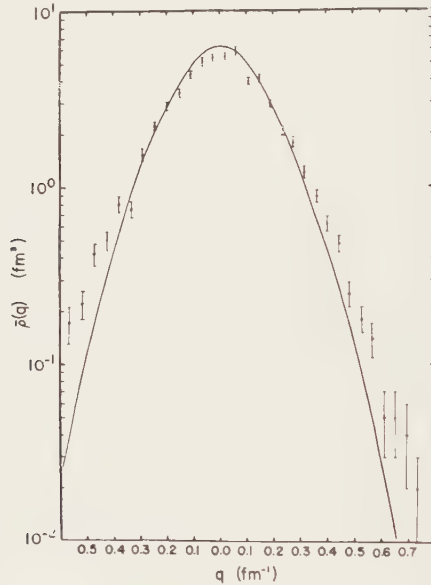


FIGURE 3

of the full  $A=6$  wave functions onto  $(\ell_J)^n$  shell model states. Conclusion:  $\ell=2$  part of gs wave function is very small ( $P_D \sim 5 \cdot 10^{-4}!$ ), reduced by one order of magnitude by  $S_1$ - $D_1$  NN tensor interaction, has a node near 1.6 fm induced by the tensor coupling. Shell model orbital probabilities are very different from conventional shell-model predictions because of large sd-shell admixtures ( $\sim 12\%$ ).



My remarks and criticisms

- cluster models indicate clearly a deformation of the deuteron cluster, but "stretching and alignment" as well as "compression" lead to better agreement with data. How realistic are the specific distortions?

- three-body model underbinds  ${}^6\text{Li}$  by 0.5 MeV. Maybe an indication of  $\alpha$ -core polarization effects?

- Coulomb interaction is important in  ${}^6\text{Li}$ . Detailed quantitative results of three-body model will only be trustworthy with Coulomb interaction included.

- all three models reproduce only part of the available data on  ${}^6\text{Li}$  ground and excited states. No full comparison with all of the empirical information!

- all models should be compared to all of the existing empirical information (within reach of the model). Fold realistic charged particle densities into three-body model wave functions to obtain rms radius, form factors aso.

- remember: the  $\alpha+d$  probability in  ${}^6\text{Li}$  is a purely formal quantity which will never be measured, since its practical definition is impossible.

1.2. New developments concerning the  ${}^6\text{Li}$  continuum (mainly  $\alpha+n+p$ )Experiments

A large set of kinematically complete data on  $\alpha+d$  breakup, with polarized and unpolarized deuterons, at many energies and angles, including QFS and FSI kinematics has been measured <sup>14-17</sup>.

Interpretation

Three-body (Faddeev) calculations <sup>14-17</sup>, neglect the Coulomb interaction (except for "outer" Coulomb corrections of doubtful validity) and also the NN tensor interaction (see however contribution <sup>18</sup> to this conference).

My impression

- Spectacular successes and failures in close relation (see e.g. contributions <sup>19-22</sup> to this conference);

- data set provides ample information to test calculations, while continuum Faddeev calculations in the  $A=6$  system are not yet as fully developed as in the three-nucleon case.

### 1.3. Closing remarks

I conclude this section on the  $A=6$  system by expressing my strong belief, that new experimental investigations should only be undertaken in this field if the resolution of a specific, well defined problem is attempted. On the other hand, all existing theoretical models show distinct deficiencies which can be eliminated in the near future. Once such more realistic models with "quantitative" predictive power become available, it will be the right time to study specific aspects of the structure of  ${}^6\text{Li}$  (e.g. D-state) or of the underlying interactions (e.g. off-shell properties of the  $N-\alpha$  interaction, NN-tensor interaction, meson exchange contributions to e.m. form factors, existence or non-existence of three-body forces).

## 2. STRUCTURES IN LIGHT HEAVY ION (H.I.) REACTIONS

2.1. Trajectories of collision partners in light H.I. collisions with  $E_{\text{cm}} \sim 0-30$  MeV are spatially localized, i.e. quasiclassical. Collisions can thus be roughly divided into three categories, each giving rise to a particular type of structure in the cross-section, studied as a function of bombarding energy:

- "distant" encounters: Coulomb plus long-range tail of internuclear interaction, reaction time is short ( $\Delta t \sim 10^{-22}$  s), energy transfer is  $\sim 0$ , internal degrees of freedom of collision partners are not excited, lead to:

gross structure (refraction, diffraction) with  $\Gamma \sim 5$  MeV, "quasi-optical" phenomena;

- "grazing" encounters, strong internuclear interaction, reaction time is longer ( $\Delta t \sim 5 \cdot 10^{-21}$  s), energy transfer into internal degrees of freedom (collective excitations, few-body rearrangements, "molecular" states?), lead to:

intermediate structure (IS) with  $\Gamma \sim 50-500$  keV, "few-body" phenomena, surface interactions;

- "head-on" encounters, very strong interaction, long reaction time ( $\Delta t \sim 10^{-20}$  s), transfer of the available cm. energy into internal degrees of freedom (full or partial fusion, slow preequilibrium processes, compound nucleus formation), lead to:

fine structure with  $\Gamma < 10$  keV, "many-body" phenomena.

All three types of collisions occur simultaneously above the Coulomb barrier: we observe strong interference between various structures:

- gross structure seen in elastic scattering, not in reactions;
- fine structure usually not resolved in experimental studies;
- intermediate structure ( $\equiv$  few body phenomena) seen in elastic and inelastic scattering and rearrangement (direct) reactions, if coupling to many-body degrees of freedom is weak for grazing encounters, i.e. if number of open channels, carrying high energy and large angular momentum, is small in grazing collisions.

Experiments confirm these considerations, as shown in

- fig. 4: gross and intermediate structure in  $^{12}\text{C}+^{12}\text{C}$  and  $^{16}\text{O}+^{16}\text{O}$  elastic scattering, gross structure only in  $^{14}\text{N}+^{14}\text{N}$  (too many open channels) <sup>23</sup>;

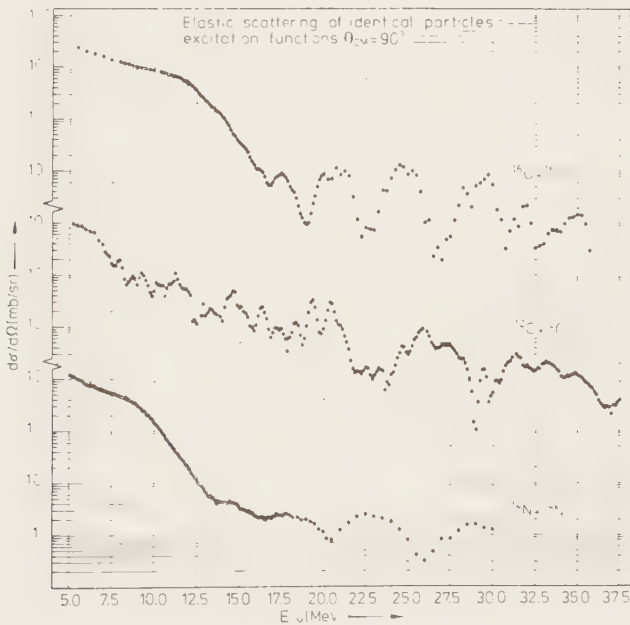


FIGURE 4

- fig. 5 : IS in  $^{12}\text{C}+^{12}\text{C}$  induced reactions (no gross structure!) <sup>24</sup>;

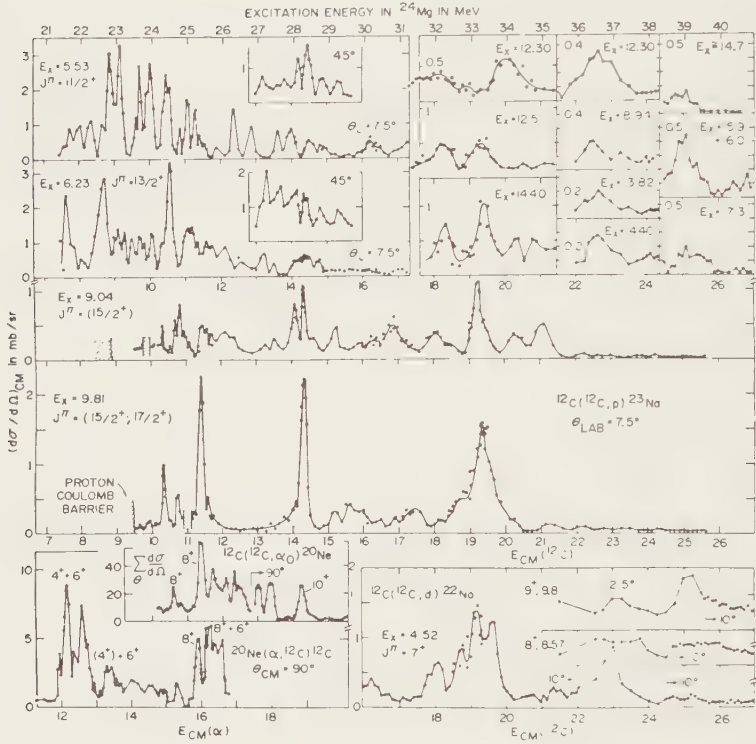


FIGURE 5

Excitation functions for various  $^{12}\text{C}+^{12}\text{C}$  induced reactions on a common energy scale ( $E_x$  of  $^{24}\text{Mg}$ ). The channels are labelled in the figure.

- fig. 6: the available (tentative) information <sup>25</sup> on the J-values of the IS proves that these are surface phenomena (corresponding for  $^{12}\text{C}+^{12}\text{C}$  to a distance of interaction  $R \sim 6 \pm 0.5$  fm), since  $E_{\text{cm}} \sim J(J+1) R^{-2}$  for semiclassical grazing trajectories (a possible exception are the IS's on or below the Coulomb barrier, which might correspond to phenomena occurring at larger separations).

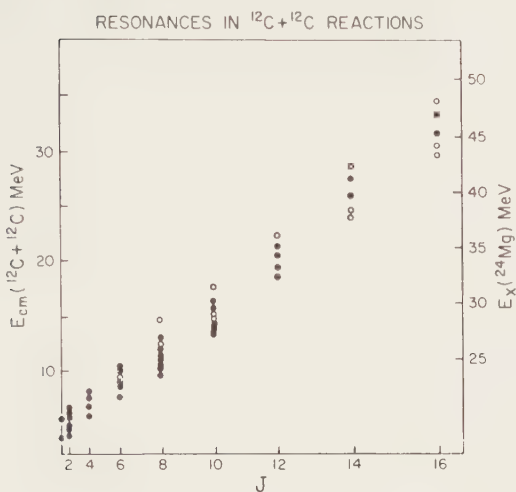


FIGURE 6

- fig. 7: "counting" the number of open channels for grazing collisions explains, why  $^{12}\text{C}+^{12}\text{C}$  shows the most pronounced IS (lowest number of open channels) <sup>26</sup>;

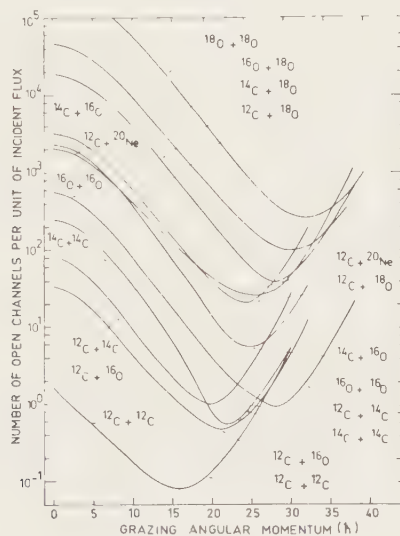


FIGURE 7

Conclusion: - gross structures are two-body "optical" effects, no exotic explanations needed;

- fine structure (if observed) is a many-body statistical, compound nuclear effect;

- intermediate structure is a surface few-body phenomenon. A detailed understanding of the corresponding reaction mechanisms and the underlying nuclear structure requires considerable deductive experimental studies.

## 2.2. Study of the intermediate structure

First interpretation (1960, year of discovery of IS in  $^{12}\text{C}+^{12}\text{C}$  H.I. reactions by a Chalk River Group <sup>27</sup>):

- IS caused by "molecular resonances", induced by a long range interaction of a novel kind <sup>28</sup> (neutron exchange?, deformation of  $^{12}\text{C}$ ?), fig. 8 shows the original  $^{12}\text{C}+^{12}\text{C}$  data <sup>27</sup>.

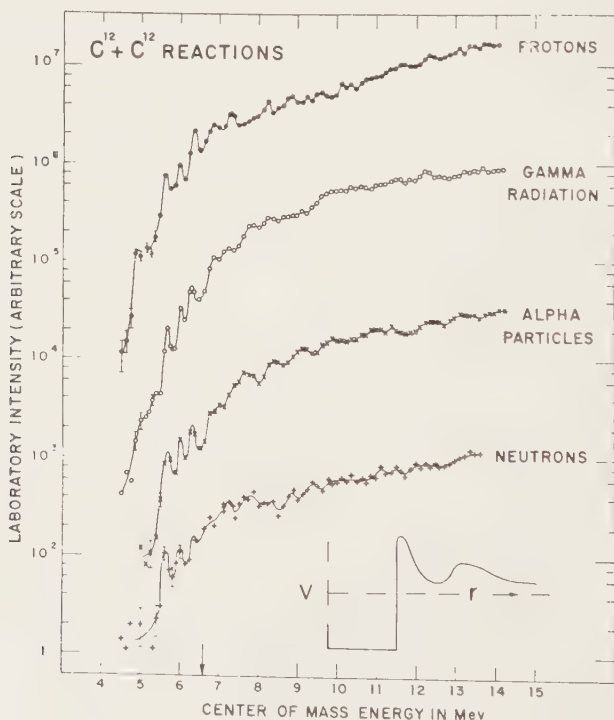


FIGURE 8

This fascinating conjecture is now 23 years old, but the H.I. physics community has been unable to prove or disprove it! In my opinion the reason is a deplorable lack of deductive (rather than inductive) investigations:

- deductive: forward, from conjecture to observation, from cause to effect, yields positive evidence
- inductive: backwards, from observed effect to hypothetical cause, yields interesting conjectures but no proof that they are correct!

Instead of a careful test of the "molecular" state hypothesis, there was a great, but uncoordinated rush towards other systems and higher energies. IS was discovered [see recent reviews<sup>25,29,30</sup>]:

- below, on and above the Coulomb barrier,
- in ~20 composite systems from  $A=20$  to 60,
- in elastic, inelastic scattering and reactions to very many final states, including protons, neutrons,  $\gamma$ ,  $\alpha$ , deuterons, excited residual nuclei, total cross sections.

Malicious characterization: A great mess! in which the few careful investigations are polluted by a great deal of sloppy work (see the introduction to ref. 29 and ref. 31 as an indication that this is also felt within the H.I. community!).

2.3. Possibilities for a deductive approach (a few-body physicists list).

- a) Which of the many IS correspond to a true resonance?
  - unambiguous assignment of a unique angular momentum  $J$  for the whole bump;
  - proof of the existence of a pole in the reaction amplitude (e.g. phase shift analysis, R-matrix analysis of the prominent decay channels).
- b) What are the reduced partial widths  $\gamma^2$  of an identified resonance for decay into the prominent channels?
  - quantitative R- or S-matrix analysis;
  - cross-checks on the results by observing closed reaction loops

(e.g.  $^{12}\text{C}+^{12}\text{C} \rightarrow ^{20}\text{Ne}+\alpha$ ,  $^{12}\text{C}+^{12}\text{C} \rightarrow ^{16}\text{O}+^8\text{Be}$ ,  $^{20}\text{Ne}+\alpha \rightarrow ^{16}\text{O}+^8\text{Be}$ );



- proof that "molecular reduced widths" (i.e. two-body  $^{12}\text{C}+^{12}\text{C}$ ,  $^{12}\text{C}+^{12}\text{C}^*$ ,  $^{12}\text{C}^* + ^{12}\text{C}^*$ ) are dominant. Study of decay widths  $\Gamma$  is not conclusive, since these are asymptotic rather than internal-structure quantities.

c) What are the electromagnetic properties of (a series of) true resonances with large "molecular" widths?

- observe  $\gamma$ -transitions into, from and between the suspected "molecular" states;
- deduce size and e.m. moments of wave functions;
- deduce overlap between members of conjectured "molecular" rotational band.

This is no simple task, but less will not do!

#### 2.4. What is the present status (in $^{12}\text{C}+^{12}\text{C}$ )?

- existence of IS established up to  $E_{\text{cm}} \sim 40$  MeV (total  $\sim 80$  bumps), compound nuclear (thermally equilibrated) statistical origin excluded for most of the structure.
- existence of resonance pole proven for  $\sim 5$  bumps (fig. 9 as an example: phase shift analysis of elastic  $^{12}\text{C}+^{12}\text{C}$  scattering <sup>32</sup>).

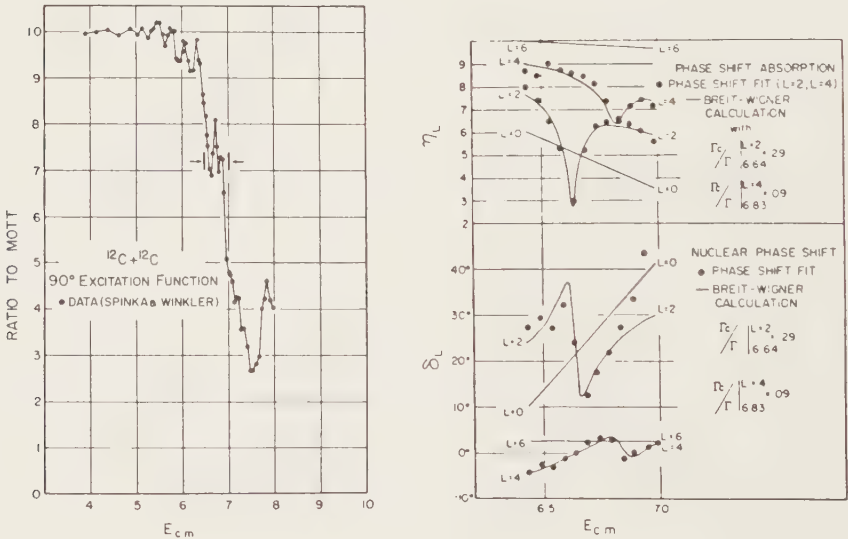


FIGURE 9

Excitation function and corresponding phase shift parameters

- reliable J-values assigned for  $\sim 2/3$  of the bumps.
- estimates (and a few quantitative determinations) available for "molecular" decay - and reduced widths in  $\sim 2/3$  of the cases:

$$\Gamma(^{12}\text{C}+^{12}\text{C})/\Gamma_{\text{tot}} \sim 0.1-0.2 \quad [\text{refs. } 32-34],$$

but  $\Gamma(^{12}\text{C}+^{12}\text{C})/\Gamma_{\text{Wigner}} \sim 0.01-0.05$  !! [ref. <sup>35</sup>].

- No systematic investigations of reduced partial widths, total width not accounted for by quantitative studies of all strong decay channels, particularly the single and mutual inelastic channels.
- Search for e.m. transitions between conjectured members of "molecular band" fails to detect expected  $\gamma$ /particle branching ratio by an order of magnitude <sup>36-38</sup>.
- Very strong decay of composite system into  $\alpha + {}^20\text{Ne}$  and  $\text{N} + {}^23\text{Na}/{}^23\text{Mg}$  is observed, not very suggestive of simple molecular configurations.

## 2.5. My provocative conclusions

There exists at present no conclusive, positive, deductive empirical evidence for any kind of interpretation of IS in light H.I. reactions.

Nuclear "molecular" states are not likely to be the dominant structure, but may play a certain role.

To quote a recent review <sup>25</sup>: "... the term nuclear molecular state has become almost universal in the literature. It should be pointed out, however, that the terminology, although universally accepted, implies more than is actually known about these states"!

All the available evidence points to a much more complicated interplay of many different kinds of structure.

It is not clear at all, that the IS observed at different energies and in different channels have a common origin. The structures below and on the Coulomb barrier in  ${}^{12}\text{C}+{}^{12}\text{C}$  may well be more likely candidates for prominent few-body phenomena than IS at higher energies.

## 2.6. Theoretician's ideas

The prevalent theoretical concept <sup>39</sup> to explain IS is that of a fragmented "giant resonance", i.e. a "simple" (two-body) state in

the entrance channel spread by weak coupling over the more complex few- to many-body states of the composite system:

- the simple state is taken to be a shape resonance, i.e. a single particle state in the mean ion-ion potential;
  - the more complex states are taken to be similar two-body states of the two ions; however, one or both ions are thought to be excited to their low-lying collective states;
  - in this way, energy and angular momentum are transferred from orbital to intrinsic degrees of freedom of the collision partners.
- Figs. 10 and 11 show two complementary pictorial representations of such a process, by which a  $^{12}\text{C}+^{12}\text{C}$  state with angular momentum  $J$  couples to a  $^{12}\text{C}+^{12}\text{C}^*(2^+)$  state with the same  $J$ , transferring  $\Delta E = 4.4$  MeV and  $\Delta l = 2$  from orbital to intrinsic degrees of freedom.

Note that in fig. 11 the separation of the two ions (the moment of inertia) is assumed to be constant, so that a "resonant" coupling is possible only in a limited region of energies, where the total (orbital + intrinsic) energies and angular momenta can be identical for the  $^{12}\text{C}+^{12}\text{C}$  and the  $^{12}\text{C}+^{12}\text{C}^*(2^+)$  "aligned" ( $J=l+2$ ) states.

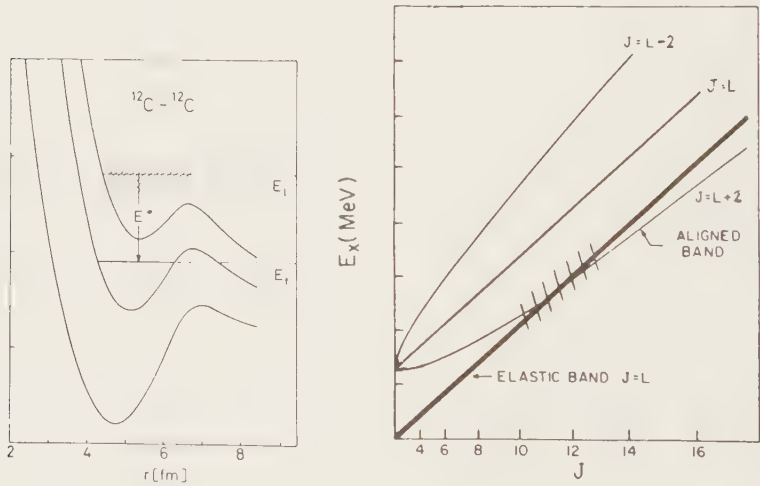


FIGURE 10

FIGURE 11

This description has been shown to yield qualitative agreement with experiment, but does not yield <sup>40-44</sup> a detailed description of the data.

Reactions cannot be calculated in any detailed way. A quantitative representation of the data should not be expected! In the process of giant-resonance fragmentation the coupling to a collective intrinsic degree of freedom is only a first step:

- in further steps, mutual inelastic excitation, excitation of  $\alpha$ -particle substructures, of more and more complex structures all the way to complete fusion into a highly excited compound nucleus will occur!

- each intermediate state will thus be further fragmented into more complex states, so that one expects a long chain of (*resonant*) couplings, linking the initial two-body "molecular" states to the full dynamics of the 24-nucleon problem (for  $^{12}\text{C}+^{12}\text{C}$ );

- the composite system has a chance to decay during all of these intermediate steps, thus feeding a great variety of reaction channels.

The situation is very reminiscent of (nucleon induced) preequilibrium-processes, which can only be described in terms of statistical models.

## 2.7. My conclusions

The "nuclear molecular state" is only a fleeting doorway state, which makes up for but a few percent of the total wave function (remember the small values of the reduced "molecular widths"!):

- most probably its only relation to atomic molecules is the two-cluster aspect of the first few steps in the fragmentation process;

- the question of its existence is thus relegated to the level of semantics and may well be a question without a definitive answer!

It is sad that the exciting conjecture of full-fledged, long-lived nuclear molecules in light H.I. interactions seems to have little chance of surviving. Should the researchers in the field prove me wrong, this would indeed be a great - but welcome - surprise for me!

## REFERENCES

- 1) J.C. Bergström et al., Phys.Rev.C25(1983)1156.
- 2) L. Lapikas, Proc.Conf.Modern Trends in elastic electron scattering, Amsterdam (unpublished).
- 3) J.C. Bergström et al., Nucl.Phys.A327(1979)439.
- 4) G.C. Li et al., Nucl.Phys.A162(1971)583.
- 5) J.C. Bergström, Nucl.Phys.A327(1979)458 and refs. cited there.
- 6) J.C. Bergström, Phys.Rev.C21(1980)2496 and refs. cited there.
- 7) R.G.H. Robertson et al., Phys.Rev.Lett.47(1981)1867.
- 8) D. Albrecht et al., Nucl.Phys.A338(1980)477.
- 9) S. Barbarino et al., Phys.Rev.C21(1980)1104.
- 10) H. Kanada et al., Nucl.Phys.A389(1982)285.
- 11) D.R. Lehmann and Mamta Rajan, Phys.Rev.C25(1982)2743.
- 12) D.R. Lehmann, Phys.Rev.C25(1982)3146.
- 13) D.R. Lehmann and W.C. Parke, Phys.Rev.C28(1983)364.
- 14) Yasuro Koike, Nucl.Phys.A337(1980)23.
- 15) M. Bruno et al., Nucl.Phys.A386(1982)269.
- 16) L. Glantz et al., Nucl.Phys.A390(1982)365.
- 17) I. Slaus et al., Nucl.Phys.A397(1983)205.
- 18) I. Slaus et al., The sensitivity of the  $d+\alpha$  breakup to np forces, this conference.
- 19) M.S.A.L. Al-Ghazi et al., Measurement of  $A_y$  and  $A_{yy}$  in the  ${}^3\text{He}(\vec{d},p){}^n\text{He}$  reaction at 14.8 MeV, this conference.
- 20) H. Oswald et al., Measurement of the excitation function and angular distribution of the  ${}^4\text{He}(\vec{d},p\alpha){}^n$  breakup reaction at low energies, this conference.
- 21) C. Heinrich et al., Angular distribution of neutron-proton final state interaction in the reaction  $D(\vec{d},p\alpha){}^n$ , this conf.
- 22) M. Ishikawa et al.,  ${}^4\text{He}(\vec{d},p){}^n\text{He}$  reaction and Faddeev calculations, this conference.
- 23) D.A. Bromley, Quasimolecular heavy ion interactions, in: Nuclear Reactions induced by heavy ions (North Holland, Amsterdam, 1970)p.52.
- 24) E.R. Cosman et al., Phys.Rev.Lett.35(1975)265.
- 25) T.M. Cormier, Resonances in heavy ion nuclear reactions, in: Annual Review of Nuclear and Particle Science, Vol.32, eds. J.D. Jackson, H.E. Gove and R.F. Schwitters (Annual Reviews Inc., Palo Alto, 1982)pp.271-308.
- 26) F. Haas and Y. Abe, Phys.Rev.Lett.46(1981)1667.
- 27) E. Almquist et al., Phys.Rev.Lett.4(1960)515.
- 28) E. Vogt and H. McManus, Phys.Rev.Lett.4(1960)518.

- 29) Resonances in Heavy ion reactions, Lecture Notes in Physics, Vol. 156, ed. K.A. Eberhard (Springer, Heidelberg, 1981).
- 30) R. Bass, Nuclear reactions with heavy ions (Springer, Heidelberg, 1980).
- 31) J.P. Schiffer, Resonances in sd-shell nuclei, in ref.29,p.177.
- 32) S.K. Korotky et al., Phys.Rev.C20(1979)1014.
- 33) R.J. Ledoux et al., Phys.Rev.C27(1983)1103.
- 34) K.A. Erb et al., Phys.Rev.C22(1980)507.
- 35) W. Treu et al., Phys.Rev.C28(1983)237.
- 36) R.L. McGrath et al., Phys.Rev.C24(1981)2374.
- 37) V. Metag et al., Phys.Rev.C25(1982)1486.
- 38) E. Adelberger et al., Annual report 1982, MPI Heidelberg,p.126.
- 39) H. Feshbach, J.Phys.(Paris) Colloque 5(1976)177.
- 40) B. Imanishi, Phys.Lett.27B(1968)267.
- 41) H. Fink et al., Nucl.Phys.A188(1972)259.
- 42) Y. Abe et al., Prog.Theor.Phys.Suppl.68(1980)303.
- 43) O. Tanimura, Nucl.Phys.A309(1978)233 and refs. cited there.
- 44) Y. Abe, Molecular resonances and strong absorption, in: Clustering Aspects of Nuclear Structure and Nuclear Reactions, ed. W.T.H. Van Oers, J.P. Svenne, J.S.C. McKee and W.R. Falk (AIP, New York, 1978) pp. 132-143.





## ELECTRON SCATTERING AND FEW NUCLEON SYSTEMS

B. Frois

DPh-N/HE, CEN Saclay, 91191 Gif-sur-Yvette Cedex, France

Recent results obtained by electron scattering in the few-nucleon systems ( $A \leq 4$ ) are presented. In particular, new experimental data have measured the tensor polarization  $T_{20}$ , the magnetic form factor  $B(q^2)$  and the electrodisintegration of deuterium. A brief overview of the experimental situation is given together with a status of the theoretical interpretation.  $^3\text{He}$  charge and magnetic form factors are discussed. New theoretical results indicate that three body forces improve considerably the saturation properties of  $^3\text{He}$ ,  $^4\text{He}$  and nuclear matter, but are not able to reconcile experiment and theory for the charge form factors of  $^3\text{He}$  and  $^4\text{He}$ . Calculations of meson exchange effects with different theoretical approaches bring the theory into reasonable agreement with the experimental charge and magnetic form factors of  $^3\text{He}$ . Recent results of the measurements of the two and three body break-up of  $^3\text{He}$  are discussed.

### 1. INTRODUCTION

The structure of few nucleons systems is of particular interest for a quantitative understanding of the nature of elementary interactions between nuclear constituents. Even the simplest properties of few-nucleon systems such as their binding energies, density distributions, quadrupole and magnetic moments cannot be accurately determined by considering only the interactions between nucleons in the framework of a potential theory.

We are now in a situation very close to the one of atomic physics after the discovery of the Lamb shift, thirty five years ago. At that time, an interaction between charges was no longer sufficient to describe such a small effect. The modification of the field due to the presence of photons was needed to build a theory. To day, nuclear physics is in a similar situation. The interaction between nucleons is not sufficient to build a theory. One has now striking experimental evidence of the presence of meson exchanges, such as a factor of 10 enhancement in electrodisintegration of deuterium or in the magnetic form factor of  $^3\text{He}$ . Similar observations have also been made with photodisintegration experiments. But, the difficulty of the meson theory is that the strong couplings involved make the calculations of short range processes very difficult. This explains why for a long time nuclear physics has progressed in a phenomenological way without much reference to the meson theory. This situation is now changing rapidly. At distances  $r \gtrsim 1\text{fm}$  the experimental observations have firmly established the mesonic exchange nature of the nucleon-nucleon in-

teraction, but the short range part,  $r < 0.8$  fm is out of the reach of meson theory. This is precisely the region which is relatively easy to describe within the quark picture of nuclear forces. Quark theory being valid only on a scale of small distances would then provide a theory just where the meson description is no longer tractable. Quark models are now in a rather primitive state and any argumentation is very speculative. But, there is now an urgent need for unambiguous informations on the processes occurring at small internucleon distances, between 0.1 and 1 fm in the few nucleons systems.

High energy electrons are by far the best tool to study these processes. They interact with any charge or current in the nucleus by the exchange of a virtual photon which penetrate in the nucleus, transferring any required amount of energy or momentum transfer selected, by adjustment of experimental kinematical conditions.

The reaction mechanism is fully interpretable in a quantitative way because the total charge and current are conserved during the reaction.

The virtual photon will "see" the spatial distribution of the nuclear charge and magnetization by mapping out their form factors. The only requirement will be that the photon has a sufficiently small wavelength matched to the size of the spatial fluctuations that one wants to study :

$$\text{Approximately :} \quad q \sim \frac{1.5}{\Delta r}$$

where  $\Delta r$  expressed in fm is the size of the spatial fluctuations to be observed and  $q$  (in  $\text{fm}^{-1}$ ) is the value of the momentum transferred to the nucleus by the virtual photon.

A charged meson exchange will be "seen" by the photons as an enhancement or a decrease of the form factors at specific momentum transfers. For example, the pionic pair current dominates the magnetic form factor of  $^3\text{He}$  in the momentum range  $3 < q^2 < 10 \text{ fm}^{-2}$ .

By selecting carefully the kinematical conditions, one can separate by a combination of measurements the longitudinal and the transverse form factors.

In this talk, I will give a very brief overview of the developments in the field of electron scattering during essentially the last two years. A large number of experimental data have become recently available stimulating a great theoretical activity. It is obvious that in 30 minutes, I cannot make an extensive review of all the work done recently in this field. So, the main emphasis of my talk will be to discuss what we have learned from these data and the present limitations of their interpretations.

## 2. ELASTIC ELECTRON SCATTERING FROM DEUTERIUM

The unpolarized cross section for elastic electron deuterium cross section

is given by the expression :

$$\frac{d\sigma}{d\Omega} = \left( \frac{d\sigma}{d\Omega} \right)_{\text{Mott}} \cdot \left[ A(q^2) + B(q^2) \tan^2 \frac{\theta}{2} \right]$$

where  $A(q^2)$  and  $B(q^2)$  are relativistically invariant structure functions of deuterium related to  $F_C$ ,  $F_Q$ ,  $F_M$ , the charge, quadrupole and magnetic form factors of deuterium.  $A(q^2)$  is well determined experimentally up to very large momentum transfers<sup>2</sup> and is one of the evidences that one has reached quark degrees of freedom. The interpretation of the comparison between theory and experiment has been called the "Gordian knot" by Gari and Hyuga<sup>2</sup>. The theoretical uncertainties are large. One has to treat correctly a relativistic problem up to the order  $\frac{1}{M^3}$  at least, where baryon resonances and isoscalar meson exchange processes such as  $\pi$ ,  $\rho$ ,  $\omega$  and  $\rho$ ,  $\pi$ ,  $\gamma$  must be taken into account properly. On top of these difficulties, the insufficient knowledge of the neutron charge form factor prevent definitive conclusions. From the experimental point of view a separation of the contributions of the charge and quadrupole form factors would be extremely useful to shed some light on this problem. An experiment is being carried out at Bates laboratory using an unpolarized beam of electrons scattered from an unpolarized deuterium target with the detection of the polarization of recoil deuterons to measure the tensor polarization  $T_{20}$ .

$T_{20}$  is independent of the nucleon form factors. In principle this is an ideal experiment to separate the charge and quadrupole form factors of deuterium. But it is more sensitive to the meson-exchange currents than to the details of the nucleon-nucleon potentials. Figure 1 presents the calculation of Haftel, Mathelitsch and Zingl<sup>3</sup> for three different well known potentials. The difference is very small without MEC and it turns out to be even smaller with the inclusion of MEC.

Preliminary data measured by Schulze et al.<sup>5</sup> at MIT-Bates laboratory are shown on figure 2 together with three theoretical predictions. The data are in excellent agreement with the Paris potential, while they are inconsistent with the other two separable potentials.

An interesting experiment which is not planned for the moment anywhere, because of its great difficulty, is the scattering of polarized electrons by a polarized deuterium target. Cheung and Woloshyn<sup>7</sup> have made recently some calculations showing a great sensitivity to the neutron form factor. With the present polarized targets this experiment seems very difficult, but there is no reason to exclude this possibility.

The lack of sensitivity of  $T_{20}$  to the percentage of D state  $P_D$  is unfortunate, because it is a measure of the tensor force component of the nucleon nucleon interaction. Even if it is not directly a physical observable,  $P_D$  is well

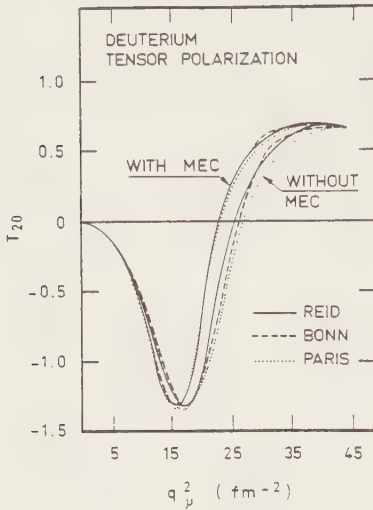


FIGURE 1

Deuterium tensor polarization  $T_{20}$ , calculated for three different potentials by Haftel, Mathelitsch and Zingl<sup>3</sup>. Only the pair current has been taken into account in the calculation.

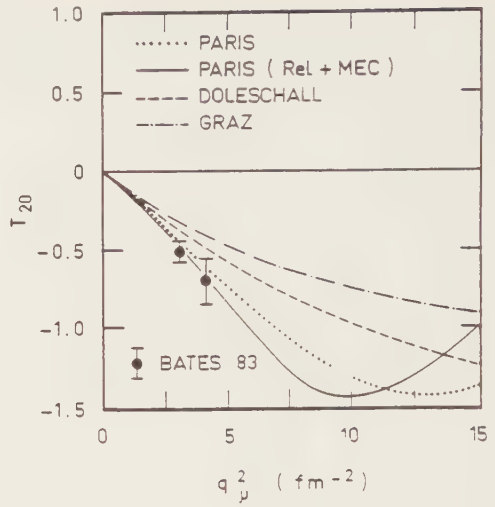


FIGURE 2

Deuterium tensor polarization  $T_{20}$ . The experimental data are preliminary results from Schulze et al.<sup>5</sup>

defined in terms of the potentials used in nuclear calculations. So it is of fundamental importance to find experiments that are sensitive to  $P_D$  since it would give a measure of the difference between various realistic models. This problem has been discussed in particular by Lomon<sup>8</sup> and also by Allen and Fiedelney<sup>9</sup> from the point of view of elastic electron scattering from deuterium. Their conclusions show that due to the absence of knowledge of the neutron form factor and because of theoretical uncertainties, it is clear that one cannot make a discrimination between potentials without some ambiguity. However, the magnetic form factor  $F_M$  which is related to the structure function  $B(q^2)$  by  $B(q^2) = \frac{4}{3} n(n+1) F_M^2(q^2)$  is less sensitive to the neutron form factor than  $A(q^2)$ . Furthermore,  $F_M$  is very sensitive to  $P_D$ . Lomon<sup>8</sup> finds a factor 2 between the magnetic form factors at  $q^2 = 26 \text{ fm}^{-2}$  predicted by the potentials FL 1 ( $P_D = 4.57 \%$ ) and FL 15 ( $P_D = 7.55 \%$ ), while neglecting  $G_{EN}$  would make only a 10 % difference between the theoretical predictions for these two potentials. Meson exchanges are playing an important role at such momentum transfers, but

in a naïve expectation one would not expect a dramatic difference between the MEC calculated for different potentials. So precise measurements of the magnetic form factor should be sensitive to different nucleon-nucleon potentials.

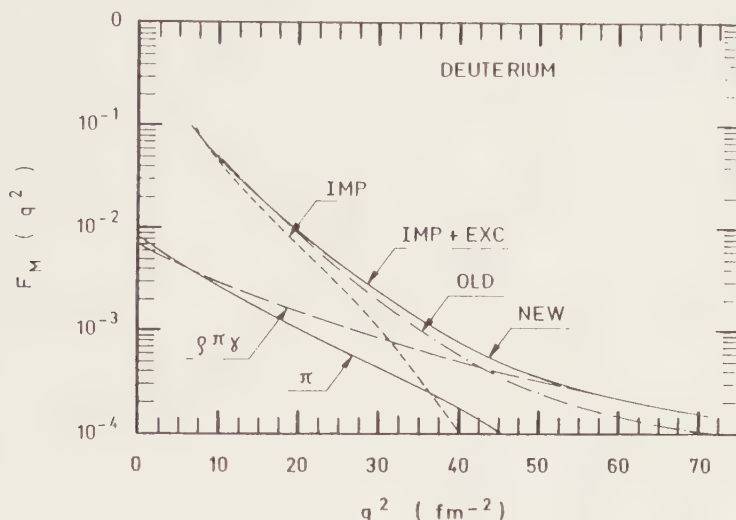


FIGURE 3

The magnetic form factor  $F_M$  predicted by Gari<sup>11</sup>. The impulse approximation (IMP) is shown together with the contribution of  $\pi$  and  $\rho\pi\gamma$  meson exchange. The sum of the impulse approximation and the meson exchange is shown for two values of the  $\rho$  coupling constant 0.38(OLD) and 0.56(NEW).

The meson exchange current in deuterium are isoscalar for elastic scattering, which implies that they are already relativistic corrections of order  $\frac{1}{M^2}$  and  $\frac{1}{M^3}$ . Gari and Hyuga<sup>10</sup> have derived the expressions of the  $\pi\rho\omega$  and  $\rho\pi\gamma$  exchanges. Figure 3 shows a new calculation of Gari<sup>11</sup> for the Reid soft core potential ( $P_D = 6.47\%$ ) where he has redone the calculation of reference 10, increasing the  $\rho\pi\gamma$  coupling constant from 0.38 to 0.56 because of an improvement in the experimental determination of the decay of the  $\rho$  meson  $\rho \rightarrow \pi + \gamma$  performed by Berg et al.<sup>12</sup>. At low momentum transfers, the meson exchanges have a small effect. The  $\rho\pi\gamma$  and the pionic pair term are of equal magnitude. When the momentum transfer increases, the contribution of the  $\rho\pi\gamma$  increases also and it is the dominant contribution for  $q^2 > 30 \text{ fm}^{-2}$ . The impulse approximation contribution drops at  $40 \text{ fm}^{-2}$ , mainly because of the shape of the nucleon form factor of Iachello, Jackson and Landé<sup>3</sup> used in this calculation. So, the region  $q^2 > 40 \text{ fm}^{-2}$  would be extremely interesting to measure, but it is at present

not feasible with existing electron accelerators. The separation of  $B(q^2)$  from  $A(q^2)$  requires measurements at backward angles as close as possible to  $180^\circ$ , because of the factor  $\tan^2 \frac{\theta}{2}$ . At such large scattering angle one has to separate  $B(q^2)$  from the electrodisintegration of deuterium, which is relatively difficult at high incident energy. To have a large count rate, liquid targets must be used with a large thickness, limiting quickly the experimental resolution to unacceptable values. At forward angles  $B(q^2)$  has a negligible contribution and in the cross section observed the electrodisintegration is negligible, so the measurement of  $A(q^2)$  is much easier.

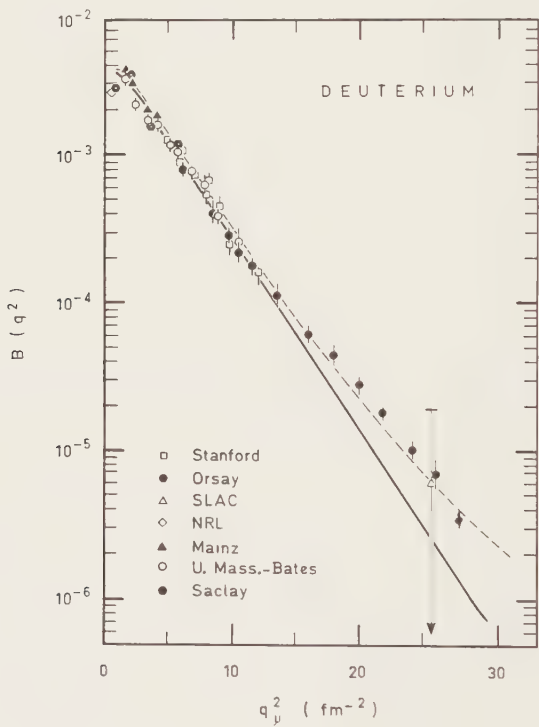


FIGURE 4  
The structure function  $B(q^2)$  of deuterium predicted by Gari<sup>11</sup>.

Up to now the maximum momentum transfer measured for  $B(q^2)$  was  $15 \text{ fm}^{-2}$ , while only one upper limit was determined<sup>14</sup> for  $q^2 = 26 \text{ fm}^{-2}$ . New measurements

have been recently done by Parker, Peterson et al.<sup>15</sup> at Bates laboratory in the region  $1.6 \text{ fm}^{-2} < q^2 < 10.52 \text{ fm}^{-2}$ , and by Auffret et al.<sup>16</sup> between  $5 < q^2 < 26 \text{ fm}^{-2}$  at Saclay. The results of both groups are preliminary, they agree fairly well with each other and with previously existing data. Figure 4 gives a comparison of these new data with the calculation of Gari<sup>11</sup> for the Reid-soft-core potential. The experimental data are in good agreement with this calculation. The impulse approximation prediction at this momentum transfer is a factor 3 smaller, while the  $\rho\pi\pi$  represents 50 % of the cross section. The experimental uncertainty is of the order of 20%, for  $q^2 = 26 \text{ fm}^{-2}$ . One has really to await the final analysis of these data to make definitive conclusions. Nevertheless, it seems that the theoretical prediction is on the right track, and that the isoscalar meson exchanges are correctly estimated, since, the same calculation explains also reasonably  $A(q^2)$  up to even much higher momentum transfers.

### 3. ELECTRODISINTEGRATION OF DEUTERIUM AT THRESHOLD

In the previous discussion, meson exchanges have a slowly increasing contribution and they represent at  $26 \text{ fm}^{-2}$  about 65 % of the cross section. This is certainly no longer a simple correction, but because of the experimental and theoretical uncertainties, it will be difficult to make quantitatively a very accurate estimate of the various contributions. A major difficulty is the  $\frac{1}{M^2}$  order of the correction; one should in principle make the same correction for the wave function of the deuteron to be consistent. The situation is completely different for the electrodisintegration cross section at threshold and backward angle. This is an M1 transition, where the meson exchanges are of isovector nature and of the order  $\frac{1}{M}$ . They are constrained by low-energy theorems, and one expects to have a much better theoretical control of the processes involved.

This reaction is the inverse of the radiative capture of thermal neutrons :



Without meson exchange the theory shows a 10 % disagreement with the experimental result. In 1972 Riska and Brown<sup>17</sup> have explained this difference by a one pion exchange. This was the first time that an electromagnetic process was used to show the existence of a virtual pion exchanged between two nucleons. But, the electrodisintegration of deuterium is much more interesting. Hockert and al.<sup>18</sup> have shown in 1973 that there is a strong interference between the  $^3D_1-^1S$  and  $^3S-^1S$  transitions. In the region of the minimum of the nuclear contribution  $q^2 \sim 11 \text{ fm}^{-2}$ , the meson exchange currents are a factor 10 larger than the nuclear contribution. The cross section at  $155^\circ$  is dominated by the exchange of one pion, the pion current and the pair current. Recently a detailed



investigation of the electrodisintegration cross section at threshold has been done by Leidemann and Arenhövel<sup>19</sup>, and by Mathiot<sup>20</sup>. I will not discuss these calculations here but I would like to mention the main elements which play an important role in the calculations.

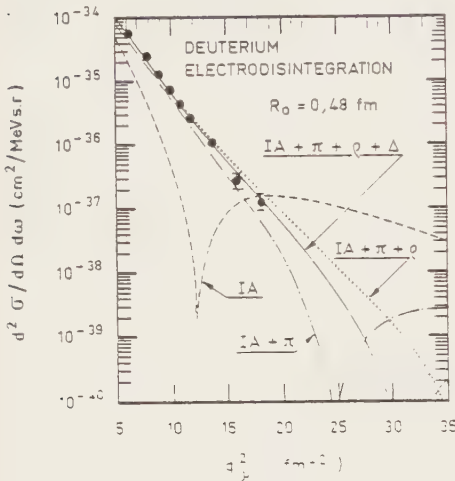


FIGURE 5

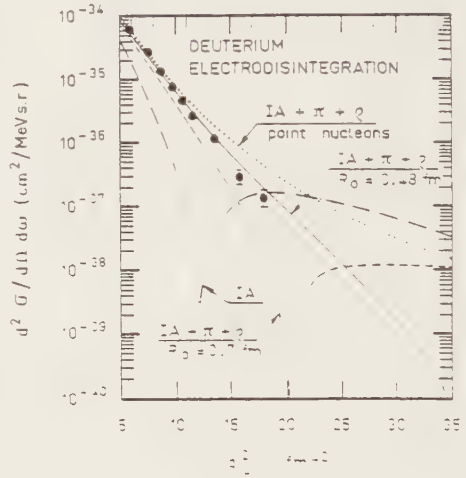


FIGURE 6

The electrodisintegration cross section of deuterium calculated with the Paris potential for  $E_{np} = 1.5$  MeV. The comparison with the experimental data is indicative since the data correspond to integration between 0 and 3 MeV. The effects of the  $\pi$ ,  $\rho$ ,  $\Delta$  meson exchange currents are shown. The form factor  $F_1^V$  has been used. Figure 6 indicates the variation of the cross section as a function of the  $\pi NN$  hadronic form factor.

The choice of electromagnetic form factor for the nucleon has a considerable effect. In principle the continuity equation requires using  $G_E^V$  in place of  $F_1^V$ . The vertex form factors  $\pi NN$  and  $\rho NN$  have also a strong influence on the shape of the theoretical predictions. Leidemann and Arenhövel have made a quantitative estimate directly comparable to the experiment by calculating the electrodisintegration cross section integrated over 3 MeV. They have also included different multipoles, Mathiot<sup>20</sup> has calculated only the value of the cross section at  $E_{np} = 1.5$  MeV which is reasonably close to the average value integrated over 3 MeV. He estimates this approximation to be better than 10 % at  $6 \text{ fm}^{-2}$  which is sufficient for a discussion of the main effects observed. But he keeps only the transition to the  $^1\text{So}$  state, which creates a minimum going to zero in the cross section, while Leidemann and Arenhövel<sup>19</sup> will fill this minimum by

the contribution of other multipoles. Both calculations find an equally good agreement with the existing data<sup>20-23</sup> up to  $q^2 \approx 10 \text{ fm}^{-2}$ . But at  $18 \text{ fm}^{-2}$ , the calculation of Mathiot gives a much better agreement with the data than the one of Leidemann and Arenhovel. Figure 5 is the prediction of Mathiot together with the data of Bernheim et al.<sup>21</sup>. Though the comparison is not quantitatively accurate, because it is not integrated over 3 MeV, the difference is estimated to be invisible on such a small plot in a logarithmic scale. Without MEC, the cross section is much too small, with  $\pi$  one gets closer to the experimental result. The addition of the  $\rho$  makes the cross section too large. The effect of the  $\Delta$  is to

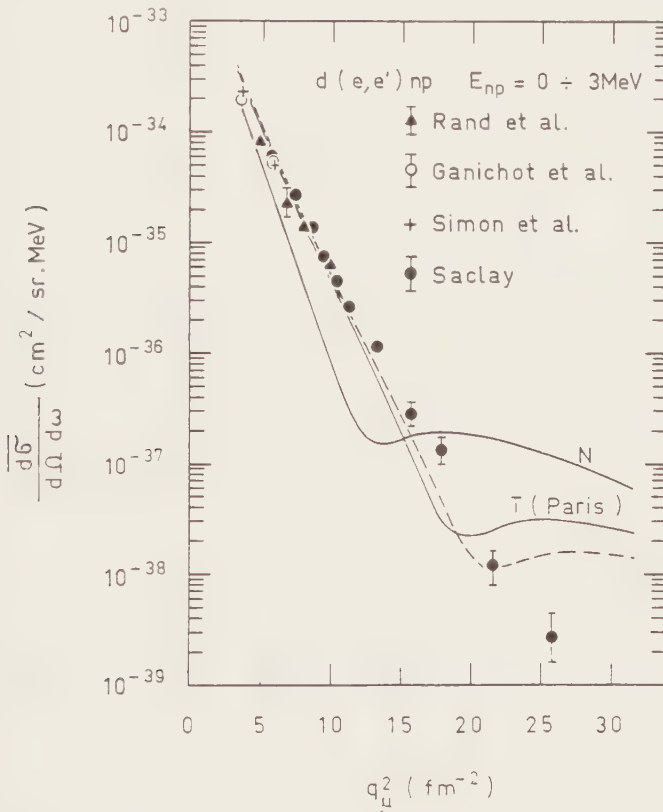


FIGURE 7

Electrodisintegration cross section at threshold integrated for  $E_{np}$  between 0 and 3 MeV. The data are from reference 25. The theoretical calculations are from Leidemann and Arenhovel<sup>19</sup>. The curve N does not include MEC, while T includes the MEC for the Paris potential, the dashed line is the same calculation with  $G_{EN} = 0$ . The form factor  $G_E$  has been used.

bring the theory close to the experimental data. Mathiot has chosen  $F_1^V$  contrary to Leidemann and Arenhovel. He does not predict a minimum before  $31 \text{ fm}^{-2}$ . But his calculation shows one of the effect of one of the most important theoretical uncertainty. By taking different values of the  $\pi\text{NN}$  form factor which Mathiot relates to a nucleon size, the minimum of the form factor is shifted from  $20 \text{ fm}^{-2}$  to  $q^2 \sim 37 \text{ fm}^{-2}$  (figure 6). The value  $R_0 = 0.48 \text{ fm}$  which gives a reasonable agreement with the data corresponds to  $\Lambda = 1.25 \text{ GeV}$ , where  $\Lambda$  is the mass scale parameter defined by :

$$F_{\pi\text{NN}}(k) = \frac{\Lambda_\pi^2 - m_\pi^2}{\Lambda_\pi^2 + k^2}$$

This very large effect of the  $\pi\text{NN}$  form factor is at present the largest phenomenological adjustment of the theory.

Figure 7 shows the existing data<sup>21-24</sup> with the latest data taken by Clemens and al.<sup>25</sup> at Saclay up to  $26 \text{ fm}^{-2}$ , together with the prediction of Leidemann and Arenhövel, with the form factor  $G_E^V$  for the nucleon.

Mathiot and Riska have investigated recently this ambiguity in the choice of  $G_E$  and  $F_1$ . They have explained that while the continuity equation needs  $G_E^V$ , there are additional purely transverse  $\pi$  and  $\rho$  meson exchange currents for M1 transitions. They demonstrate that for observables that *depend only on the transverse part* of the pion and  $\rho$  meson exchange current, a correction arises which can be taken into account by replacing the form factor  $G_E^V$  by  $F_1^V$  in the nucleon electromagnetic current. In other words the pion and the rho currents requires  $G_E^V$  while the pair terms require  $F_1^V$ .

On figure 7 the dashed line is the Paris potential prediction without the neutron form factor. It is interesting to see such a large effect, but one would need the same calculation with  $F_1^V$  instead of  $G_E^V$  before reaching a definitive conclusion.

From these results, one sees that a reasonable agreement can be reached between experiment and theory when a form factor is used for the  $\pi\text{NN}$  vertex. However this form factor is adjusted to reproduce the data and has not been determined with sufficient accuracy from a fundamental point of view.

When Hockert et al.<sup>18</sup> obtained a reasonable agreement between their theoretical calculation and the experimental data of Rand et al.<sup>24</sup> up to  $10 \text{ fm}^{-2}$ , it was a break through. For the first time a large effect of the pion exchange could be measured unambiguously, because it was by chance the only relevant contribution. The purely nucleonic transition is cancelled at relatively low momentum transfer because of a destructive interference between the  $^3S_1 - ^1S_0$  and

the  $^3D_1 - ^1S_0$  transitions. This is quite in contrast with the magnetic form factor of deuterium where the purely nucleonic contribution vanishes only at  $35 \text{ fm}^{-2}$  and has not yet been seen because of the absence of a suitable electron beam of at least 1.5 GeV. In 1973 the pion exchange was the only "short range" interaction visible experimentally. It was sufficient to consider only a pion exchange between point nucleons to reproduce fairly accurately the experimental data. Today, the experimental situation is completely different, much shorter range interactions are observed, typically between 0.3 and 1 fm. One is getting the benefits of twenty years of technical developments for measuring small cross sections. The new electrodisintegration data of Clemens et al.<sup>25</sup> are typical. A cross section as small as  $2.5 \cdot 10^{-39} \text{ cm}^2/\text{sr}$  has been measured with 30 % accuracy at  $q^2 = 26 \text{ fm}^{-2}$ . Figure 5 shows that in this momentum range, the cross section is probably entirely due to the  $\rho$  meson exchange contribution. The situation is now exactly the opposite of the region measured by Rand et al.<sup>24</sup> up to  $10 \text{ fm}^{-2}$  where the  $\rho$  meson-exchange and the  $\Delta$  currents are almost cancelled by the effect of the finite size in which the  $\pi NN$  interaction takes place.

These results emphasize the importance of studying such an isovector magnetic transition. The various currents which contribute to the cross section have strong destructive interferences which occur successively at different momentum transfers. So measurements at specific momentum transfers single out the different contributions of the meson exchanges. Electron scattering is here just a microscope which looks at an object with larger and larger magnification. With the very high momentum transfers measured recently the short range part of the nucleon-nucleon interaction is now the major part of the effects observed.

#### 4. $d(e,e'p)n$ and $d(\gamma,p)n$

Another, very interesting aspect of the electrodisintegration of deuterium is the measurement in coincidence of the electron and the proton which has been discussed in great detail by Arenhövel<sup>27</sup> recently. Following his notation, the  $d(e,e'p)n$  cross section is a function of the longitudinal (L) and transverse (T) cross sections.

$$\frac{d^3\sigma}{dk'd\Omega_e d\Omega_p} = (\sigma_L + \sigma_T + \sigma_{LT} \cos \phi_{np} + \sigma_{TT} \cos \phi_{np})$$

where  $\phi_{np}$  is the angle between the plane defined by the momenta of the proton and the neutron, and the plane defined by the momenta of the incoming and outgoing electron. In the impulse approximation, the differential cross section can be factorized into an elementary cross section and a spectral function which is directly the energy and momentum distribution of the bound proton.

If such a factorization were possible, the momentum distribution of the proton in deuterium could be extracted directly, giving a possibility of evaluating the S/D ratio, but Arenhövel<sup>27</sup> has shown that the factorization is not better than 20 %, and therefore a very crude approximation.

Three experiments have been carried out recently at Saclay for different kinematics<sup>28,29</sup> which are indicated below :

Saclay kinematics for d(e,e'p)n

$k_e$ (MeV/c)	$k_{e'}$ (MeV/c)	$\theta_e$ (deg)	$ \vec{q} _{LAB}$ (MeV/c)	$E_{np}$ (MeV)	Proton momentum (MeV/c)
500	395	59	450	51	5-175
500	353	44,4	350	114	155-375
560	360	25	279	179	300-500

Figure 8 gives the momentum distribution  $\rho(p)$  for the Reid soft core poten-

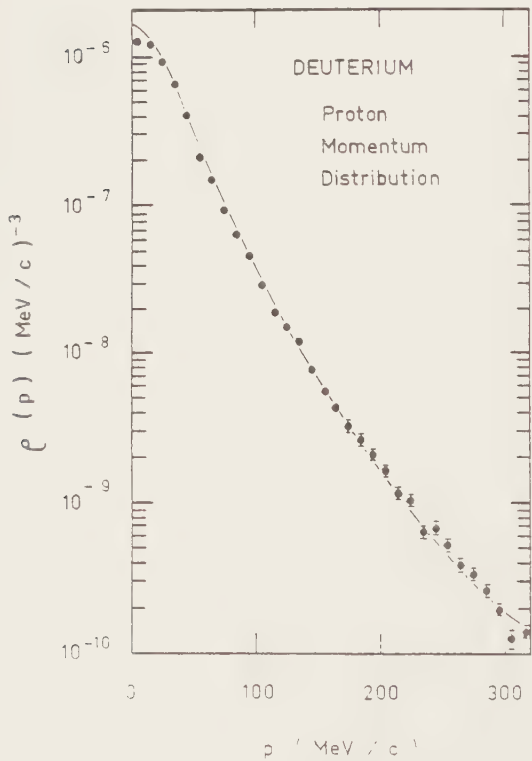


FIGURE 8  
The momentum distribution of deuterium calculated by Arenhövel<sup>27</sup> with the Reid soft core potential. This is not the result of an impulse approximation, but of an unfolding of the experimental cross sections of Bernheim et al.<sup>28</sup> for meson exchange currents and final state interactions. No renormalization of either the calculation or the data is needed.

tial up to 300 MeV/c. The experimental data<sup>28</sup> are in excellent agreement with the calculation of Arenhövel where the final state interaction and meson exchange effects have been unfolded point by point. This is a much nicer way to plot experimental data, but the experimental information is modified by corrections which depend on the model used. For the kinematic region of the experimental results shown on figure 7, the final state interactions and the meson exchange corrections are probably well known enough to enable such unfolding procedure. However, it is preferable to make directly a comparison of the experimental cross section to the theory, giving up the idea of extracting unambiguously a momentum distribution.

Figure 9 shows the latest results from Saclay<sup>29</sup> together with the theoretical prediction<sup>27</sup> for the Reid soft core potential. The curve labelled (N) has been obtained by taking only the meson exchange contributions for electric transitions by using Siegert's theorem. The curve labeled N + MEC + IC includes meson-exchange and isobar currents and final state n-p interactions. The curve BA corresponds to the Born approximation, and agrees poorly with the data.

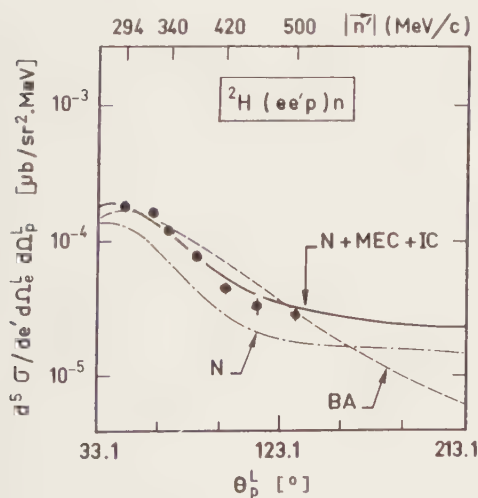


FIGURE 9  
New results of  $d(e,e'p)n$  from  
Saclay experiment<sup>29</sup>.  
 $E_{np} = 179$  MeV.  $\Delta$  contributions  
are important for this  
kinematical condition.

The large effect off the meson exchanges seen in figure 9 comes almost exclusively from  $\sigma_T$ . An interesting feature of this kinematic region is the large effect of the  $\Delta$ .

The dependence on the potential used in the calculation is rather small, though for the higher momentum part the Paris potential or the De Toureil Sprung potential give a very slightly better agreement.

A different theoretical approach has been followed by Laget<sup>30</sup> who has extended to virtual photons calculations carried out initially for real photons. This method

is based on the non-relativistic reduction of the Feynman diagrams such as the ones shown in the insert of figure 10.

The calculations are in excellent agreement with a large number of experimental data for processes involving virtual and real pions. In these calculations, the  $\pi NN$  form factor and the  $\rho$  coupling constant were determined by a fit<sup>33</sup> to the photodisintegration cross section at a scattering angle of  $90^\circ$  for energies between 100 and 500 MeV. Figure 10 shows the excellent description of the experimental data by the mechanisms assumed by Laget. The recent Bonn data<sup>32</sup> in the  $\Delta$  region are in very good agreement with this calculation.

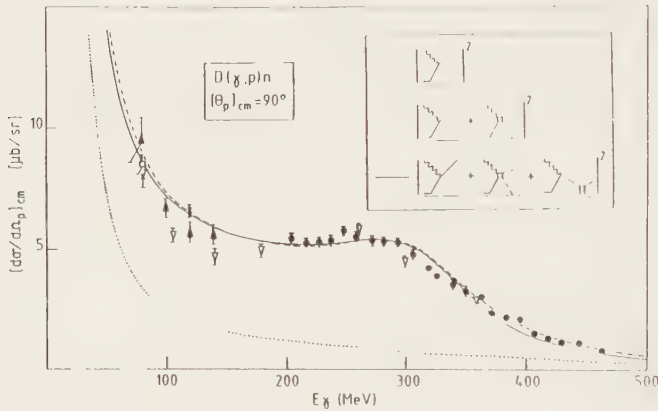


FIGURE 10  
 $d(\gamma, p)n$  at  $90^\circ$ . The data in the  $\Delta$  region have been measured recently at Bonn<sup>32</sup>.

Below the pion threshold the cross section does not depend on the  $\rho$  exchange, while the  $\Delta N \rightarrow NN$  transition is strongly modified in the  $\Delta$  region ( $E_\gamma \sim 300$  MeV). The pion and the  $\rho$  exchanges are decoupled which make their determination reliable. The values fitting the photodisintegration data at  $90^\circ$  are  $\Lambda_\pi \simeq 1$  GeV and  $G_\rho^2/G_\pi^2 \simeq 1.3$ . Once these two values have been adjusted, the photo and the electrodisintegration cross sections are determined without any further assumption. The predictions<sup>31</sup> for the angular distributions of the photodisintegration of deuterium and  $^3\text{He}$  are in excellent agreement with the experimental data, the electrodisintegration is also well reproduced. With 300 MeV photons one can see large effects in the  $\Delta$  region while a much larger energy is required for electrons for coincidence experiments to map out the  $q, \omega$  plane.

5. ELASTIC ELECTRON SCATTERING FROM  $^3\text{He}$  AND  $^3\text{H}$

From a theoretical point of view, the wave functions obtained either by three body calculations in  $\{r\}$  space and in  $\{q\}$  space, are now in good agreement with



each other. However these calculations fail completely to explain the form factors of  ${}^3\text{He}$  measured by electron scattering. It is clear that there are other effects. Very recently, the effects of three body forces and meson exchanges have been calculated, and the situation appears much clearer than at the previous few-body conference.

Elastic electron scattering measures the structure functions  $A(q^2)$  and  $B(q^2)$  just as in the case of deuterium. Since the ground state of  ${}^3\text{He}$  has a  $\frac{1}{2}$  spin the only form factors which contribute to  $A(q^2)$  are the charge and the magnetic form factors. The structure function  $A(q^2)$  of  ${}^3\text{He}$  has been determined up to  $q^2 = 80 \text{ fm}^{-2}$ . The magnetic part in  $A(q^2)$  for very large  $q$  is not known, but predicted to be important. The magnetic form factor has been measured recently by Cavedon et al.<sup>39</sup> but only up to  $32 \text{ fm}^{-2}$ , which means that it is impossible now to correct  $A(q^2)$  for magnetic scattering and to extract the charge form factor for  $q > 32 \text{ fm}^{-2}$ . The calculation of Katayama<sup>35</sup> is in good agreement for  $q^2 > 65 \text{ fm}^{-2}$ . The major problem is in the region  $15 \text{ fm}^{-2} \leq q \leq 65 \text{ fm}^{-2}$ . This discrepancy is found with all the potentials and all the existing numerical methods used to solve the three body bound state problem. Sick<sup>42</sup> has shown at the Graz conference that admitting that  $A(q^2) \equiv F_{\text{Ch}}^2(q^2)$  and with meson exchange corrections, an inverse Fourier transform would determine a hole in the charge distribution of  ${}^3\text{He}$ . A considerable theoretical effort has been to calculate the effects of a three body force. Blomelburg and Glöckle<sup>43</sup> have carefully evaluated the convergence of the calculation for the binding energy of  ${}^3\text{H}$  with the Tucson<sup>44</sup> three body force. They start from the Faddeev equations in a partial wave decomposition, getting the triton wavefunction from a five channel solution with the Reid potential. Their conclusions are that the main corrections to the binding energy comes from channel 1 and 2. With eighteen partial waves they get a negligible result of  $-0.158 \text{ MeV}$  additional attraction. But their striking result is the lack of convergence of the result. It is clear that even with eighteen partial waves, the final result is not yet reached. This is probably caused by the angular dependence of the three body force which makes partial wave expansions converge very slowly. There are also large cancellations between the different contributions of the three-body force. This explains why there has been significant differences between theoretical predictions.

A variational method does not have this problem and gives an exact upper bound to the binding energy of the nucleus. The recent results of Carlson, Pandharipande and Wiringa<sup>45</sup> (CPW) and Wiringa<sup>46</sup> have been obtained with reliable many body techniques. A comparison of the saturation properties of  ${}^3\text{H}$ ,  ${}^4\text{He}$  and nuclear matter shows that if a three-body force is the only missing ingredient it should provide a  $1.5 \text{ MeV}$  attraction in  ${}^3\text{H}$  a  $5.4 \text{ MeV}$  attraction

in  ${}^4\text{He}$  and a 4.5 MeV repulsion in nuclear matter with the Urbana  $V_{14}$  potential<sup>45</sup>. This means that there must be two parts in the three-body force an attractive one and a repulsive to decrease the binding energy of nuclear matter. In a first attempt to reconcile the theory with the experimental data of  $A(q^2)$  Carlson and Pandharipande have shown that the three-body force that would give a fit to the data of the charge form factor of  ${}^3\text{He}$  would underbind nuclear matter by 10 MeV which is completely unacceptable. An excellent agreement for the binding energies and the charge radii is found with a three-body force in which the attractive part is the Tucson two pion exchange, while the short range part has a phenomenological shape with two parameters.

These results show that major improvements are obtained in the saturation properties. Furthermore, the Coulomb energy found theoretically  $\sim 700$  keV leaves very little to be explained by nuclear charge asymmetry. Nevertheless it should be noted that these improvements based only on a three-body force are not completely satisfactory because  ${}^4\text{He}$  is now overbound by  $\sim 1$  MeV. The charge form factor  ${}^3\text{He}$  and  ${}^4\text{He}$  are still not quantitatively explained by the Argonne or the Urbana  $V_{14}$  potentials with three-body interactions.

A recent calculation by Hadjimichael, Bornais, Goulard has proposed an explanation in terms of both a three-body force and meson exchange currents.<sup>54</sup> The calculation has been made with the wave functions of the Grenoble group<sup>54</sup>. The agreement obtained is impressive up to  $40 \text{ fm}^{-2}$ . (Figure 11) The charge radii are equal to 1.92 fm ( ${}^3\text{He}$ ) and 1.71 fm ( ${}^3\text{H}$ ) in very close agreement to

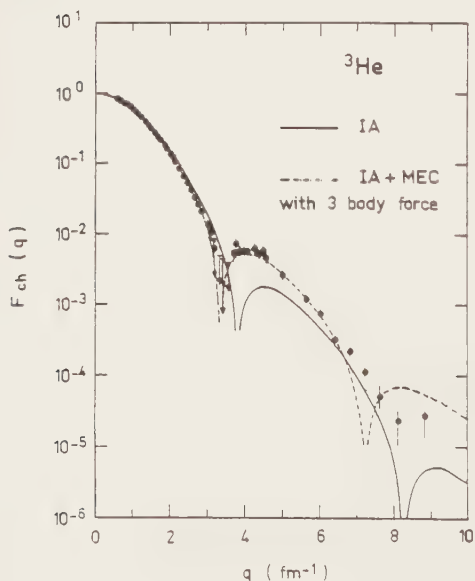


FIGURE 11

${}^3\text{He}$  charge form factor calculated with two body and three-body forces. Meson exchange currents have also been included in this calculation<sup>50</sup>. The experimental data have been obtained at Stanford by McCarthy et al.<sup>37</sup>, and at SLAC by Arnold et al.<sup>38</sup>.

the most recent values  $^3\text{He}$  ( $1.935 \pm 0.030$  Dunn et al.<sup>40</sup>;  $1.958 \pm 0.018$  Ottermann<sup>49</sup> and  $^3\text{H}$  ( $1.67 \pm 0.05$  Beck et al.<sup>47</sup>). The major source of uncertainty is coming from the fact that MEC are of relativistic order ( $1/M^2$ ). Nevertheless this calculation shows that MEC are likely to explain much of the disagreement between theory and experiment for the charge form factor of  $^3\text{He}$ . The results of Struerve, Hajduk and Sauer<sup>51</sup> including also relativistic corrections of the single nucleon charge the nucleon  $\Delta$  transition charge and the pion sea-gull process to the order  $1/M^2$ , also is in much better agreement with the experimental data.

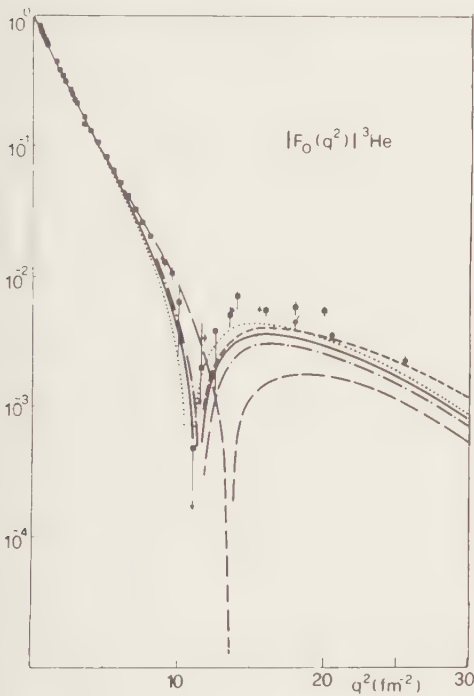


FIGURE 12

$^3\text{He}$  charge form factor in a model where the pair current is calculated with a quark model by Beyer et al.<sup>52</sup>

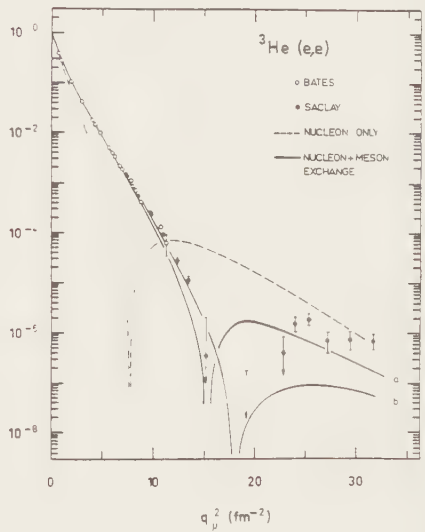


FIGURE 13

$^3\text{He}$  magnetic form factor. The experimental data are compared to purely nucleonic contribution (dashed line and the calculations of Hadjimichael et al.(a) and Riska (b).

An interesting new approach has been followed by Beyer et al.<sup>52</sup> where the pair current is evaluated within a quark constituent model. Again the amplitude of the second maximum can be fairly well reproduced. (Figure 12) These different results show that the  $^3\text{He}$  obtained with modern potentials are probably fairly accurate but the problems left are all concerning the short distance

interactions both in the two body force and in the three-body force.

In the magnetic form factor of  $^3\text{He}$  and  $^3\text{H}$ , MEC can be calculated in a much more reliable way. They are of order  $(1/M)$  because it is an M1 magnetic isovector transition exactly as in the case of the electrodisintegration of deuterium at threshold. The new data of Dunn et al.<sup>40</sup> at MIT-Bates, have determined the magnetic form factor at  $\theta = 160^\circ$  for momentum transfers between 0,7 and  $11 \text{ fm}^{-2}$  while the data of Cavedon et al.<sup>39</sup> have been measured at  $\theta = 155^\circ$  between 7 and  $32 \text{ fm}^{-2}$  at Saclay. In the overlapping region there is an excellent agreement between the two experiments. Because of the change of sign of the form factor, the location of the minimum is well determined around  $18 \text{ fm}^{-2}$ . The data have been corrected for the charge contribution Coulomb distortion by a phase shift analysis which has been described by Cavedon et al.<sup>39</sup> so the data are really representing a form factor and can be directly compared to theoretical calculations. Figure 13 shows the comparison of the experimental data to a calculation by Riska<sup>53</sup> with a phenomenological wave function and the calculation of Hadjimichael, Bornais, Goulard<sup>54</sup> with the wave functions of the Grenoble group. The agreement at momentum transfer lower than  $15 \text{ fm}^{-2}$  is very good, but at high momentum transfer it is very difficult to disentangle the origin of the disagreement for Hadjimichael et al.<sup>50</sup> while for Riska it is probably only an incorrect behaviour of the wave function at high  $q$ . The cross section at  $q^2 \approx 7.5 \text{ fm}^{-2}$  is coming only from meson exchange currents. The dominant contributions at low  $q$  is the pair current, at higher momentum transfer around  $q^2 \approx 30 \text{ fm}^{-2}$  the pair current cancels the  $\Delta$  current and there is considerable interference between the different diagrams.

Similar agreements are obtained by Struve et al.<sup>51</sup> and Maize and Kim<sup>55</sup>, but their calculations differ in the choice of electromagnetic or hadronic form factor. In particular Maize and Kim have discussed the effect of the neutron form factor. The agreement obtained at low  $q$  shows that we understand well the  $\pi$  exchange. At higher momentum transfer, the situation will require a deeper analysis and will be an excellent testing ground for the description of short range processes.

An accurate comparison between  $^3\text{He}$  and  $^3\text{H}$  is needed. In the charge form factor, meson exchange currents are expected to cancel even at high momentum transfer. However, in the quark model of Beyer et al.<sup>52</sup> for the pair current ( $\pi\bar{N}\bar{N}$ ) there is no such cancellation, the quark pair effect is nearly equal and additive for both nuclei.

## 6. $^3\text{He}$ (e,e'p)

The electrodisintegration of  $^3\text{He}$  by means of the (e,e'p) reaction has been studied recently by Jans et al.<sup>56</sup> up to 20 MeV.

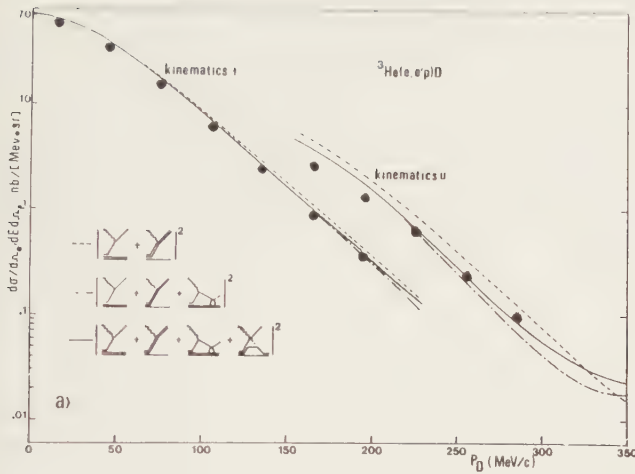


Figure 14  
 ${}^3\text{He}(e,e'p)$ . The experimental data have been measured by Jans et al.<sup>56</sup>

The measurements have been made for two kinematical regions in which the proton momentum varies approximately between 20 and 290 MeV. Meson exchanges and final state interactions are important and do not allow a direct extraction of the proton momentum distribution. Figure 14 shows the results of Jans et al.<sup>56</sup> together with the calculations of Laget<sup>31</sup>. Laget has used the same momentum function to calculate the  ${}^3\text{He}(e,e')$  cross section of Day et al.<sup>58</sup> at 3.26 GeV and 7.26 GeV. A good agreement is obtained for the 3.26 GeV data, while at 7.26 GeV there is a significant deviation. Sick et al.<sup>59</sup> have shown that for inclusive  ${}^3\text{He}(e,e')$  data between 0.5 and 14 GeV electron energy, a clear  $y$  scaling is observed assuming that electrons have been scattered off nucleons only. This shows that up to momentum transfers of  $q^2 \sim 1.5 \text{ (GeV/c)}^2$  the concept of nucleonic constituents is a relevant one. The large deviation observed between the experimental result and the theoretical calculation for  $F(y)$  shows that there are some important theoretical problems at such high momentum transfers. (Figure 15).  $F(y)$  can be directly related to the momentum distribution of the nucleon,  $y$  being the component of the nucleon momentum parallel to  $q$ . Final state interactions are too small to explain the large deviations in the region of high momentum transfers. It is obvious that some important effect is missing in the present calculations. An increase of the momentum space density at large momentum seems to be needed in particular. However, there is at present no really satisfactory theoretical interpretation of these data.

## 7. CONCLUSION

Electron scattering experiments have measured recently important effects of

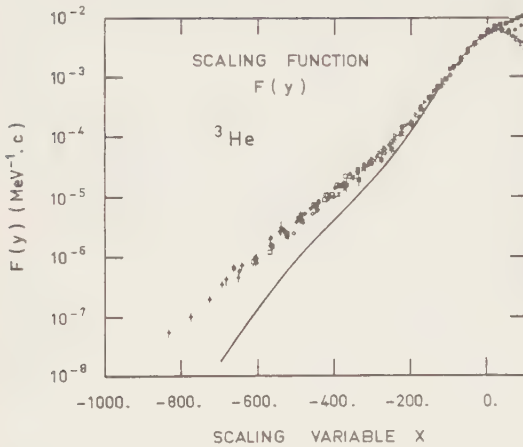


FIGURE 15

The scaling function  $f(y)$  for  ${}^3\text{He}$  determined by Sick et al.<sup>59</sup> The solid line is a Faddeev calculation without final state interactions. The experimental data have been measured at SLAC by Day et al.<sup>58</sup>

interactions at very small distances. Meson exchange currents are playing an important role, but the phenomenological adjustment of the hadronic form factor does not allow at present an unambiguous interpretation. The merit of this phenomenological approach is that a wide variety of processes involving either virtual or real photons is well described, using exactly the same hadronic form factors and the same values of the meson coupling constants.

The real problem is now to derive these quantities from a fundamental point of view and not to extract them by a fit to the experimental data. It is hoped that quark models will be a better theoretical description. The  $\rho$ -meson exchange, for example, is a short range interaction occurring at about 0.3 fm where nucleons are strongly overlapping. At such short distances the concept of  $\rho$  exchange might not be an appropriate one. It might be possible to use already a description based on an interaction between six quarks. Hybrid models are now investigated and will be discussed at this conference. Kisslinger<sup>26</sup> has already used such a model for the calculation of the magnetic form factor of deuterium and the electrodisintegration at threshold. At large distances two nucleons are considered, while at short distances the dynamical aspects are described by a system of six quarks. Such models are only in their infancy, and they are only qualitative at present, but their concept is attractive and it is clear that they will be improved in a near future.

#### REFERENCES

- 1) R.G. Arnold et al. Phys. Rev. C21 (1980) 1426.
- 2) M. Gari and H. Hyuga, Nucl. Phys. A264 (1976) 409.
- 3) M.I. Haftel, L. Mathelitsch and H.F.K. Zingl Phys. Rev. C22 (1980) 1285

- 4) J.A. Tjon and M.J. Zuilhof, *Phys. Lett.* 84B (1979) 31
- 5) M.E. Schulze et al. private communication
- 6) E.J. Stephenson et al. *Nucl. Instr. and Methods* 178 (1980) 345
- 7) C.Y. Cheung and R.M. Woloshyn, *Phys. Lett.* 127B (1983) 147
- 8) E.L. Lomon, *Annals of Physics* 125B (1980) 309
- 9) L.J. Allen and H. Fiedeldey, *Phys. Rev.* C24 (1981) 1734
- 10) M.Gari and H. Hyuga *Nucl. Phys.* A264 (1976) 409
- 11) M.Gari, private communication
- 12) D. Berg et al., *Phys. Rev. Lett.* 44 (1980) 706
- 13) F. Iachello, A. Jackson and A. Landé, *Phys. Lett.* 43B (1973) 193
- 14) R.E. Rand et al. *Phys. Rev.* D8 (1973) 3229  
F.Martin et al. *Phys. Rev. Lett.* 38 (1977) 1320
- 15) B. Parker, G.A. Peterson et al., private communication
- 16) S. Auffret et al. to be published
- 17) D.O. Riska and G.E. Brown *Phys. Lett.* 38B (1972) 994
- 18) J. Hockert et al. *Nucl. Phys.* 217 (1973) 14
- 19) W. Leidemann and H.Arenhövel, *Nucl. Phys.* A393 (1983) 385
- 20) J.F. Mathiot, preprint Orsay (1983) IPNO/Th83-16  
J.F. Mathiot and D.O. Riska, preprint 1983, University of Helsinki
- 21) M. Bernheim et al. *Phys. Rev. Lett.* 46 (1981) 402
- 22) G.G. Simon et al. *Phys. Rev. Lett.* 37 (1976) 739  
G.G. Simon et al. *Nucl. Phys.* A324 (1979) 277
- 23) D. Ganichot et al. *Nucl. Phys.* A178 (1972) 545
- 24) R.E. Rand et al. *Phys. Rev. Lett.* 18 (1967) 469
- 25) J.C. Clemens et al. to be published
- 26) L.S. Kisslinger, *Phys. Lett.* 112B (1982) 307
- 27) H. Arenhövel, *Nucl. Phys.* A384 (1982) 287 and references therein.
- 28) M. Bernheim et al. *Nucl. Phys.* A365 (1981) 349
- 29) P. Barreau et al. communication to this conference
- 30) J.M. Laget, *Phys. Rep.* 69 (1981) 1
- 31) J.M. Laget, Symposium on "Delta-nucleus dynamics" Argonne May 2-4, 1983



- 32) B.A. Mecking, Conference on "New Horizons in Electromagnetic Nuclear Physics" held at Charlottesville April 1982, edited by J.V. Noble and R. R. Whitney. J. Arends et al. Univ. of Bonn, preprint 1983
- 33) J.M. Laget, Nucl. Phys. A312 (1978) 265
- 34) W. Fabian and H. Arenhövel, Nucl. Phys. A314 (1979) 253
- 35) T. Katayama et al., University of Hokkaido preprint
- 36) H. Collard et al., Phys. Rev. 138 (1965) 357
- 37) J.S. McCarthy, et al., Phys. Rev. C15 (1977) 1396
- 38) R.G. Arnold et al., Phys. Rev. Lett. 40 (1978) 1429
- 39) J.M. Cavedon et al., Phys. Rev. Lett. 49 (1982) 986
- 40) P. Dunn et al., Phys. Rev. 27 (1983) 71
- 41) M. Bernheim et al., Lett. al Nuovo Cimento 5 (1972) 431
- 42) I. Sick, Lecture Notes in Physics 87, edited by H. Zingl et al. Springer Berlin 1978, 276.
- 43) A. Bömelburg, preprint 1983 Ruhr-Universität Bochum, Institut für Theoretische Physik
- 44) S.A. Coon et al. Nucl. Phys. A317 (1979) 242  
S.A. Coon and W. Glöckle Phys. Rev. C23 (1981) 1790
- 45) J. Carlson, V.R. Pandharipande and R.B. Wiringa Nucl. Phys. A401 (1983) 59
- 46) R.B. Wiringa, Nucl. Phys. A401 (1983) 86
- 47) P.H. Beck et al., Phys. Rev. C25 (1982) 1152
- 48) I. Sick, Phys. Lett. 64B (1976) 33
- 49) C. Otterman, Thesis Mainz 1983
- 50) E. Hadjimichael, R. Bornais and B. Goulard Phys. Rev. C27 (1983) 831
- 51) W. Struve, Ch. Hajduk and P. Sauer, comm. to this conference
- 52) M. Beyer et al., Phys. Lett. 122B (1983) 1
- 53) D. Riska Nucl. Phys. A350 (1980) 227
- 54) J. Torre et al., Z. Phys. A300 (1981) 319
- 55) M.A. Maize and Y.E. Kim, preprint 1983, Purdue University
- 56) E. Jans et al., Phys. Rev. Lett. 49 (1982) 974
- 57) Ch. Hajduk et al., Nucl. Phys. A322 (1979) 329  
R.A. Brandenburg et al., Phys. Rev. C12 (1975) 1368
- 58) D. Day et al., Phys. Rev. Lett. 43B (1979) 1143
- 59) I. Sick et al., Phys. Rev. Lett. 45 (1980) 871 and private communication

## TRENDS IN EXPERIMENTAL FEW BODY PHYSICS

Ingo SICK

Department of Physics, University of Basel, Basel, Switzerland

In this paper I summarize some of the results of the discussion session on experimental few body physics. Given the wide variety of contributions, ideas and questions brought up, no attempt will be made to present them all. Rather, I will try to use the input from this discussion in order to formulate some forward-looking ideas concerning the topics brought up.

The first subject I would like to discuss concerns an experimental technique: the design of *new polarimeters* to measure the tensor polarization of high-energy deuterons.

Investigations of most of the interesting observables of reactions between light nuclei today involve the measurement of polarization. While we have excellent sources of polarized light nuclei, good vector-polarized targets and good analyzers for scattered vector-polarized particles, polarimeters for tensor-polarized deuterons are still at a rather unsatisfactory stage of development. In particular, it is still rather difficult to analyze the deuteron tensor polarization for energies  $E_d > 50$  MeV. Given the great interest in measuring tensor polarization observables, a major effort to improve this situation is called for.

In order to demonstrate the need for such polarimeters, I want to mention two ongoing experiments. In the search for dibaryon states<sup>1</sup>, a topic of intense recent activity relating to the predicted 6-quark states of the 2-nucleon system, several experimental groups<sup>2,3</sup> are presently trying to observe tensor polarization observables in  $\pi$ -d elastic scattering. In order to measure the deuteron d-state wave function at intermediate and short range, an e-d scattering experiment involving a measurement of  $T_{20}$  is presently under way<sup>4</sup>. The deuteron d-state wave function, a quantity of fundamental interest for few-body physics and the understanding of the nucleon-nucleon interaction, is an observable that has

kept nuclear physicists busy for a long time. While we have today very good information on the large-radius part<sup>5</sup> (asymptotic normalization, derived from the quadrupole moment and subcoulomb  $\vec{d}$  elastic scattering), the shorter-range part of the wave function is still largely unconstrained by experiment.

All experiments mentioned above measure the deuteron polarization by slowing down the high energy deuteron to energies  $< 10$  MeV where the  ${}^3\text{He}(\vec{d}, p)$  reaction at  $\theta = 0^\circ$  provides a sensitive analyzer<sup>6</sup>. For energies  $E_d > 50$  MeV this technique leads to a figure of merit (the ratio of detected to incident particles times  $T_{20}$  of reaction) that is much too low.

The first systematic studies of improved polarimeters with higher figure of merit are presently under way. Recent measurements performed at Saturne<sup>7</sup> show that at energies of 200-700 MeV  $\vec{d}$ -Ca and  $\vec{d}$ -Ni elastic scattering yield values of  $A_y$  and  $A_{yy}$  which, as a function of scattering angle, oscillate around an average value that for angles  $\theta > 20^\circ$  approaches 0.8. Such large analyzing powers can be understood qualitatively as a consequence of the nuclear absorption and spin-orbit forces in diffraction or rainbow scattering. Given this mechanism, one can expect that the analyzing powers are largely independent of energy, target and, most important, excitation energy of the residual nucleus. Under these circumstances, one has a chance of designing an efficient polarimeter, and detailed calculations of the figure of merit (not obviously large due to the small d-nucleus cross section at  $\theta > 20^\circ$ ) should be carried out.

The most promising candidate for a polarimeter of high figure of merit at present probably involves  $\vec{d}$ -p scattering at backward angles<sup>8</sup>. The analyzing power  $T_{20}$  is large ( $\sim -0.8$ ) and largely independent of energy up to  $E_d = 2$  GeV. This large value of  $T_{20}$  results from an interference between neutron exchange and forward nuclear scattering amplitude. A systematic study carried out at IUCF shows that among the reactions involving light targets ( $A < 12$ )  $p$ - $\vec{d}$  scattering probably yields the highest figure of merit.

Polarimeters based on  $p$ - $\vec{d}$  scattering clearly merit detailed studies in the future. A major effort should be devoted to the problem of isolating elastic (rather than breakup) scattering with reasonable angular resolution. For energies  $E_d > 100$  MeV, where the

back-scattered deuteron has enough energy to be detected, this technique is a very promising one, and lets us hope for polarimeters 10 times better than the ones actually in use.

A second topic discussed concerns our knowledge on an understanding of *D-states in light nuclei*. The effect of the nucleon-nucleon tensor force leads to D-state probabilities of order 10%; some of these, those for the deuteron in particular, have received extensive attention, others, those of  $A = 3, 4$  systems, have been studied very little.

D-states in light nuclei are of great importance in a number of ways: 1) For the understanding of the structure of light nuclei, wave function components of probability  $\sim 10\%$  are clearly vital. 2) The D-states add higher momentum components to the wave function, which dominate when studying configuration mixing and small wave function components in heavier nuclei by transfer reactions at momentum transfers  $> 400$  MeV/c. 3) Our understanding of D-states and non-nucleonic degrees of freedom is strongly interdependent. In particular  $N \rightarrow \Delta$  transitions imply in general  $S \leftrightarrow D$  state transitions (due to the large spin of the  $\Delta$ ). Understanding the non-nucleonic degrees of freedom in light nuclei, where one has the best chance given the comparatively good knowledge of the nucleonic wave function, requires a detailed understanding of D-states.

Above, we have discussed some of the open questions concerning the deuteron. The  $A=3$  D-state recently has come into sharper focus and a number of communications to this conference deal with it.

In particular the data on the magnetic form factor<sup>9</sup> of  $^3\text{He}$  shows a large effect of the S-D transition; however, as mentioned above, meson exchange currents give a similar, opposite, effect on  $F_M(q)$ . This is a general property of M1 observables, and concerns both  $A=2$  and  $A=3$ . The asymptotic normalization of the  $^3\text{He}$ -D-state wave function has been investigated by transfer reactions<sup>10,11</sup> that allow to study one particular D-state amplitude, namely the one where the transferred nucleon has  $L=2$  relative to the deuteron center of mass. Reactions between light nuclei, less subject to nuclear structure uncertainties and more likely to allow access to other than long-range properties (asymptotic normalizations) only start to be exploited.

Several contributions to this conference<sup>12-14</sup> investigate this

topic. Here, I would like to discuss one piece of work that concentrates on the  $\vec{d} + p \rightarrow {}^3\text{He} + \gamma$  reaction. This reaction presents a number of features<sup>15</sup> that make it unique for the determination of properties of the  ${}^3\text{He}$  D-state. Inducing the reaction with tensor polarized deuterons allows to enhance D-state effects to the point where they can be isolated cleanly from the "noise" of S-state contributions. At  $E_{\text{CM}} \sim 10\text{--}15$  MeV, where the capture cross section peaks, the process is overwhelmingly dominated by the E1-amplitude, a multipolarity that due to the Siegert theorem does not get contributions from meson exchange currents. Moreover, the energy is low enough so that modern Faddeev calculations can be used to solve without approximation the continuum 3-body problem<sup>16</sup>.

Faddeev calculations<sup>17</sup> for  $p + \vec{d}$  capture confirm that the above features are indeed realized: The  $T_{20}$  observable depends on the  ${}^3\text{He}$  D-state only, is zero for D-state probability zero, and is not sensitive to the deuteron D-state. Meson exchange current contributions are negligibly small. The only problem:  $T_{20}$  is very small,  $\sim 0.03$ , and difficult to measure!

At Basel, we recently have performed such a  $p + \vec{d}$  experiment<sup>15</sup>, using the tensor-polarized  $\vec{d}$ -beam of SIN, a  $\text{LH}_2$  target and two NaI detectors. The measured analyzing power for  $E_d = 30$  MeV,  $\theta = 90^\circ$ , amounts to  $A_{yy} = 0.028 \pm 0.003$  and is quite close to the value 0.0342 calculated by J. Torre, who performed a Faddeev calculation for both  $p + \vec{d}$  and  ${}^3\text{He}$ , using the Reid soft core NN-interaction. Conclusions on the difference will have to await a more definitive data reduction. The degree to which internal parts of the D-state wave function are explored by this experiment also remains to be studied.

The above example shows us basically the following: With the experimental tools available today one can select observables that depend on the physical quantity of interest only, such that the physics of interest can be isolated without too many complications from other, poorly understood, aspects. For the future, we obviously would like to find similar observables relating to, e.g., the  ${}^4\text{He}$  D-state which is predicted to have a probability of  $\sim 10\%$ . A candidate for instance is the reaction  $\vec{n} + {}^3\text{He} \rightarrow {}^4\text{He} + \gamma$  (with both partners polarized such as to get tensor polarization observables).

Model calculations for such processes are needed before experiments, or more quantitative numerical calculations, will be done.

One other theme of the discussion session I would like to come back to concerns the *three body force (3BF)*. This subject has been around for a long time, but has somehow not been taken all that seriously; presumably, in the absence of good ways to derive a 3BF theoretically, it seemed too easy a means to "fix" problems not explained in terms of two body forces (2BF). Contrary to atomic physics<sup>18</sup> the experimental evidence was not solid and specific enough to prove the need for a 3BF.

In the recent past, we have witnessed a revived interest in the 3BF. Two reasons for this come to mind. The theoretical description of 3BF's have achieved a much higher degree of understanding, so that we have today a better idea what 3BF's could look like<sup>19</sup>. In addition, we now have a number of observables which can be calculated using very sophisticated techniques and well controlled approximations; if the experimental results cannot be explained in terms of empirical 2BF's, then we feel compelled to introduce new ideas, like a 3BF. The revival of interest in a 3BF is clearly documented in a number of contributions to this conference<sup>20</sup>.

Recent attempts to observe the effects of 3BF's have largely concentrated on integral observables measured at low energy. In particular, the comparison between N-N scattering lengths as determined from 2- and 3-body reactions was advocated<sup>21</sup> as a tool to look for 3BF's; if a discrepancy is found between the two determinations, this could indicate the presence of a 3BF (although in a rather non-specific way). The binding energy of nuclear matter and light nuclei, treated on the same footing by variational calculations, is another observable that has received increasing attention<sup>22</sup>. The sensitivity of form factors at high momentum transfer to the short-range structure of wave functions of light nuclei also has been studied<sup>23</sup> in connection with the 3BF.

When predicting effects of 3BF's in nuclear systems, a number of theoretical difficulties arise. The lowest-order diagram expected to contribute to the largest-range 3BF is the one of two consecutive one pion exchanges connecting 3 nucleons, with a  $\Delta$  in the intermediate state. This diagram indeed provides something like a 0.5 MeV change of the binding energy of  $^3\text{He}$ , and its effects on



the nuclear configuration (a preference of triangular over collinear 3-nucleon configurations) is helpful in explaining the  $^3\text{He}$  charge form factor. However, the higher-order diagrams do not appear to be negligible, and the convergence of the calculations is at present an open question. This state of affairs basically reflects the fact that a 3BF gets us into the domain of non nucleonic (and quark) degrees of freedom, a field of nuclear physics that is still quite unexplored.

When looking to future activities concerning the 3BF we should ask, whether experiments can provide additional, more constraining evidence. This is possible, I think, if we respect a number of considerations discussed below. These are based on the fact that the effects of a 3BF in general are small relative to those of a 2BF. If we want to extract a 3BF in circumstances, where observables dominated by 2BF's can be calculated with limited accuracy only, then we should find ways to enhance the 3BF. How can we do that?

The first point to make concerns the range of the 3BF, which is smaller than the one of the 2BF. Thus, observables connected to the short range behaviour of the interaction are necessary in order to enhance the signal/noise (3BF/2BF) ratio. This implies projectile or reaction product energies of order 100 MeV in order to achieve small enough a wave length,  $\sim 0.5$  fm. This point -- which would suggest that zero-energy observables like scattering lengths are not optimal! -- should be taken quite seriously in the future. The actual progress in the techniques for "exact" 3-body calculations at positive energies suggests, that such experiments can in a near future be quantitatively interpreted.

A second point concerns the fact that 3BF's, which are most effective on nucleons that are very close together, will have their largest effect at large nuclear densities. The  $A=3,4$  bound states have the highest nucleon densities occurring in nature, and the dominating  $\ell=0$  wave function components enhance the overlap of nucleons at small radii. Experiments searching for effects of 3BF's thus should preferably involve the  $A=3,4$  bound states.

A third point is inspired by the properties of the lowest order (dominant?) 3BF alluded to above. The preference of triagonal over collinear arrangements of 3 nucleons is a signature one should certainly look for when trying to isolate 3BF's. The study of angular



correlations in reactions between 3 nucleons then seems particularly promising.

Of course, the above mentioned ideas to enhance the effects of 3BF's are effective only if the experimental results can be compared to theoretical calculations of good quality, calculations that do not make dangerous approximations when predicting the 2BF "background". With reference to existing calculations, this implies two specific points: The D-state of the  $A=3$  (sub-) system must be treated correctly; much of the signature of a 3BF will come from angular correlations of the 3 nucleons, and these can only be predicted if the full angular complexity of the 3N wave function is included, much of which is due to the D-state. By the same token, calculations based on separable interactions do not look like a viable approach; the loss of angular information that occurs when approximating  $V(\vec{r}_1 - \vec{r}_2)$  by  $V(r_1) \cdot V(r_2)$  forbids meaningful conclusions on 3BF effects. A need for Faddeev calculations at positive energies (100 MeV) using realistic NN interactions (Paris, RSC, ..) is thus evident. Although such calculations are very difficult, the request for such calculations does not seem inappropriate. One such calculation (at  $E_{CM} = 15$  MeV) has been done<sup>16</sup>, and various theoretical groups are at present tooling up for similar ones.

When respecting the above "rules" to enhance the signal/noise ratio, we should have a fair chance to detect the effects of nuclear 3-body forces.

#### REFERENCES

- 1) M.P. Locher, Nucl. Phys. ... (this volume)
- 2) R.H. Holt et al., Phys. Rev. Lett. 47 (81) 472
- 3) J. Ulbricht et al., Phys. Rev. Lett. 48 (82) 311
- 4) M.E. Schulze et al., Contributions to Few Body X
- 5) T.E.O. Ericson, Nucl. Phys. ... (this volume)
- 6) R.J.Holt et al., Phys. Rev. Lett. 43 (79) 1229
- 7) J. Arvieux, priv. com.
- 8) E.J. Stephenson et al., IUCF Annual Report, 1982, p. 163

- 9) J.M. Cavedon et al., Phys. Rev. Lett. 49 (83) 986
- 10) L.D. Knutson et al., Phys. Rev. C2 (81) 411
- 11) N. Seichert et al., Contributions to Few Body X
- 12) A. Arriaga, F.D. Santos, Contributions to Few Body X
- 13) K. Hatanaka et al., Contributions to Few Body X
- 14) S.E. King et al., Phys. Rev. Lett. 51 (83) 877
- 15) J. Jourdan et al., to be publ.
- 16) J. Torre et al., Phys. Rev. Lett. 40 (78) 511
- 17) J. Torre, priv. com.
- 18) A. Teitsma, P.A. Egelstaff, Phys. Rev. A21 (80) 367
- 19) S.A. Coon et al., Nucl. Phys. A317 (79) 242
- 20) A. Bömelburg et al., Contributions to Few Body X  
     A.C. Fonseca, M.T. Peña, Contributions to Few Body X  
     R.G. Ellis et al.,                   "       "   "   "  
     H.T. Coelho, T.K. Das,               "       "   "   "  
     M.R. Robilotta, M.P. Isodro Filho,   "   "   "  
     R.J. Slobodrian,                   "       "   "   "  
     M. Karus et al.,                   "       "   "   "
- 21) I. Slaus et al., Phys. Rev. Lett. 48 (82) 993
- 22) J. Carlson et al., to be publ.
- 23) P.U. Sauer, Nuov. Cim. 76A (83) 309

## CONCLUDING REMARKS FOR THE FEW BODY X CONFERENCE

Earle LOMON

Center for Theoretical Physics, Laboratory for Nuclear Science and Department of Physics, Massachusetts Institute of Technology, Cambridge, Massachusetts 02139

Unfortunately Professor Weidenmüller has been too ill to attend and, with the advantage of his breadth of knowledge and his wisdom, deliver the scheduled concluding remarks. We all regret this; no one more than I, as I attempt to substitute for him. Not having been given this responsibility until recently I have not taken notes and am unable to summarize all aspects of the conference as they deserve. Instead, I will make some general remarks and discuss issues relating to the role of hadronic and quark-gluon aspects in few-nucleon physics.

This has been an excellent conference. We have all had the opportunity to learn much and be stimulated into thinking of interesting and useful directions of research. We owe this to the excellent planning and organization for which we warmly thank Drs. Zeitnitz and Klages, the International Advisory Committee, the Scientific Organizing Committee, the University, and the very pleasant and helpful staff at the registration, travel and banking desks that successfully responded to a wide variety of requests. I personally liked the absence of parallel sessions and the provision of discussion sessions. Although this meant that we worked long hours and that some interesting contributions could not be given orally, it enabled a more complete interaction to take place. This was very advantageous in cross-fertilizing our ideas and bringing balance to our efforts. By the way, the best discussion sessions were those that left the most time for spontaneous discussion.

In this meeting we were once more impressed with the range of few particle physics. We examined a broad range of systems from a few quarks to the interaction of shepherd satellites with planetary rings. And once again we have seen how techniques developed for one system can be applied to another. One example is the readiness to treat molecules bound by magnetic monopoles on the basis of the methods used for muonic molecules. Also we have seen several examples of nuclear methods being applied to few quark systems.

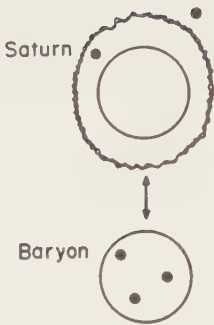


FIGURE 1

Range of few body problems; a few quarks in a bag to planetary rings and shepherd satellites.

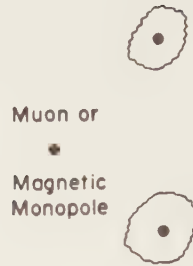


FIGURE 2

Many body techniques have multiple applications. Similar calculations will predict properties of molecules bound by muons or magnetic monopoles.

#### PROGRESS SINCE 1980 - EXPERIMENTAL

There has been a remarkable number of important experiments in the past few years reaching meaningfully higher levels of accuracy or measuring new observables. These have been with both electromagnetic and hadronic probes. In particular the new intermediate energy accelerators have extended their range of measurements and have completed or continued programs of importance. We have, from the Bates Accelerator Lab, the first elastic electron deuteron tensor polarization  $t_{20}(q^2)$  ever and are promised more precision and higher momentum transfer in the near future. Even the present data as shown in Fig. 3 is of some value in limiting the nuclear force model and the meson exchange currents. When higher momentum transfer data is available for comparison it will enable a separation of these two aspects.

At the Saclay Linear Accelerator the magnetic scattering,  $B(q^2)$  has been extended importantly in momentum transfer with useful precision as shown in Fig. 4. This places new limits on a combination of model dependence and meson exchange current effects. Present electron accelerators are tantalizingly just out of reach of momentum transfers ( $q^2 \approx 40 \text{ fm}^{-2}$ ) at which a clear separation of these two aspects should be available.

In hadronic reactions there has been considerable progress in obtaining complete sets of data for nucleon-nucleon reactions, elastic and inelastic involving  $NN\pi$  and  $d\pi$  final states. This work has mainly been for laboratory nucleon energies up to 800 MeV, but there is also some data from Saturne II at higher energies. In this range we now know the  $pp$  phases quite well and have a good start on the  $I=0$  phases. We have been reminded by a few experiments at

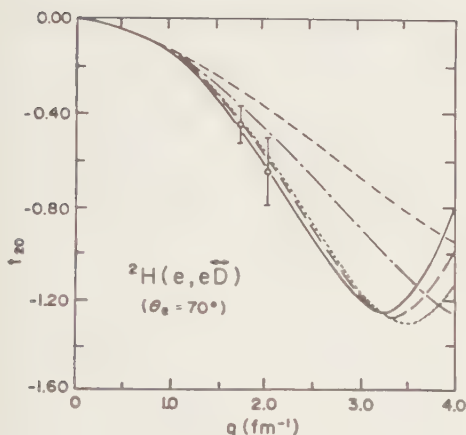


FIGURE 3

Tensor polarization  $t_{20}$  in elastic electron-deuteron scattering. The data points are from M. Schulze et al. submitted for publication to Phys. Rev. Lett. The curves represent predictions of different potential models with (TOT) or without (IA) meson exchange current corrections: Paris, TOT, (—); Paris, IA, (....), FL 4.6, TOT, (—); GrazI, TOT, (— · —); GrazI, IA (-----).

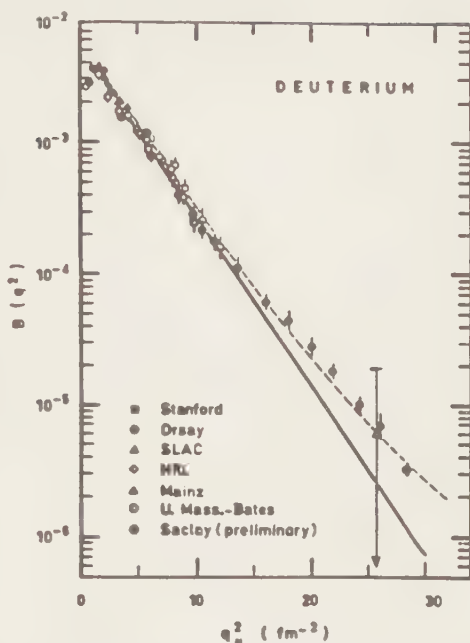


FIGURE 4

The magnetic elastic electron-deuteron scattering  $B(q^2)$ . The sources of the experimental values are indicated on the graph, including the recent preliminary data from Saclay. The curves represent the result of the Paris potential with (---) and without (—) meson exchange current corrections.

$E_L \leq 50$  MeV that there are still important improvements in data and comparison with theory that are to be made at low energies. Low energy polarization has been a surprisingly good test of the accuracy of the Paris potential.

The  $\pi D$  backward tensor polarization experiments have puzzled us with hints of structure and very different results from SIN and LAMPF, as illustrated by Fig. 5. As the measurements are at slightly different energies and angles it is possible that they are compatible. It is of great importance to the question of dibaryons that these investigations be pursued until there is agreement.

In proton-deuteron, pion-deuteron and electromagnetic and hadronic experiments on the  $He^3$  and  $He^4$  we have seen how precision experiments can be brought to bear on physical questions of importance - asymptotic D states, nuclear form factors and reaction mechanisms. Figure 6 illustrates one example of the remarkable precision now possible.

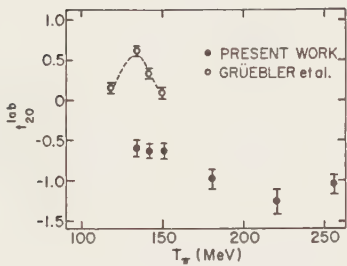


FIGURE 5  
Tensor polarization in  $\pi$ -d scattering. The figure is from E. Ungricht et al, submitted for publication to Phys. Rev. Lett. The excitation function at  $\theta_d=18^\circ$  (solid dots) is compared with the results of W. Gruebler et al, Phys. Rev. Lett. 49, 444 (1982), at  $\theta_d=15^\circ$  (open circles). The angular acceptances are  $\pm 1.5^\circ$  and  $\pm 2.5^\circ$  respectively.

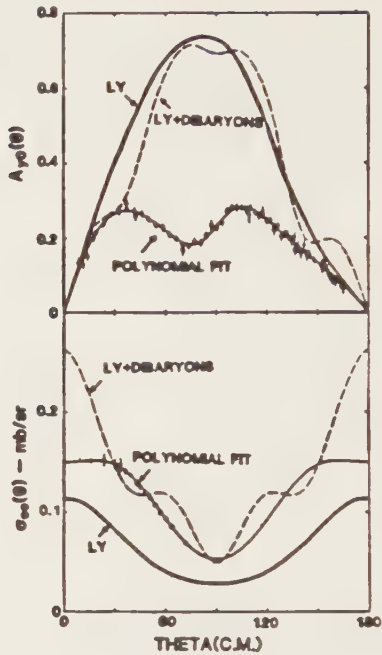


FIGURE 6  
Differential cross section and analyzing power for  $pp+d\pi$  from K. Seth et al, Phys. Lett. 126B, 164 (1983).

PROGRESS SINCE 1980 - THEORETICAL

Among the more mature issues - accurate calculations of few body bound and scattering states, reactions in a non-relativistic coupled cluster framework, and relativistic and meson-exchange current corrections - progress has been slow and painful. Brilliant theoretical work has established rigorous procedures which have found only a few applications. Calculations which cover new ground, even in less rigorous formulations, have not been abundant in the past three years. It is to be recommended that theoreticians calculate some key quantities in the future, though it be hard work and be model dependent. Three body continuum calculations with realistic interactions and two-pion exchange current corrections are examples of long neglected areas.

In the new area that involves the effect of quark and gluon degrees of freedom we have the solid technology of asymptotic momentum transfer and quark counting results from high energy theory. Stan Brodsky has described many of

them, especially the use of the infinite momentum frame, to us at this meeting. At the LAMPF II workshop a few weeks ago Glennys Farrar described the derivation of many relations among hadron-hadron reactions and their absolute prediction at asymptotic momentum transfers.

However we have only started to deal with prediction of medium momentum transfer reactions in which the very critical dynamics of transition from asymptotic freedom to confinement takes place. Many interesting ideas are being tried to deal with this very difficult situation, but time is needed to evaluate their effectiveness. I believe that few hadron interactions at intermediate energy will be very sensitive to many important aspects of quark-gluon dynamics. Consequently this field of inquiry should be energetically pursued before the next conference. I shall address the rest of my remarks to some considerations of what must go into such research.

#### HOW DO WE SEE QUARKS?

Because quarks and gluons are presumed to be confined we must carefully consider the criteria for experimentally identifying and analyzing their effects. There are two classes of situations.

i) Effects which qualitatively may be explained on either a "classical" (hadron field phenomena) or a q.c.d. basis:

These must be examined theoretically from both points of view. If both views yield adequate quantitative success then two important criteria must be invoked. One criterion is the simplicity of the description. The other, of equal importance, is the microscopic and parameter free aspects of the explanation. A model with a few parameters often provides a simple description of data which may be better understood by a difficult numerical calculation starting from first principles or known parameters.

In Figures 7 and 8 are the results of alternative explanations of the now famous "EMC effect" of the ratio of deep inelastic muon and electron scattering on iron versus deuterium. In Figure 7 the theoretical ingredients are quark bag coalescence, sea-quarks and fraction of momentum carried by gluons. In Figure 8 the ingredients are two-nucleon correlations and pion currents. The fits are roughly of the same quality and both are parameterized. In order to be convinced of the implications much work needs to be done experimentally and theoretically. Experimental investigation of A dependence and spin dependence would be useful as well as increased accuracy. Both types of theory must strive to explain the experimental results with more basic input or more extensive cross-referencing to other phenomena.



An older story is that of the structure seen in nucleon-nucleon scattering. At least for the lowest energy cases, the  $^1D_2$  and the  $^3F_3$ , the more natural, more quantitative explanation seems to be the "classical" effect of channel coupling, whether resonant or not.

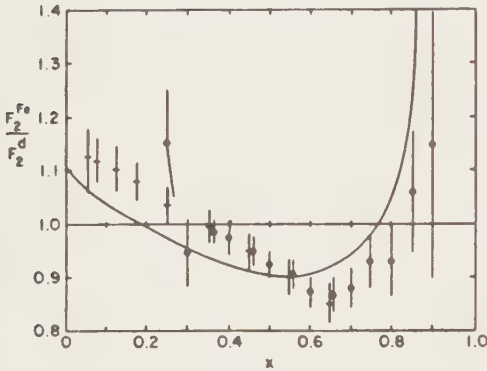


FIGURE 7

The EMC effect analyzed in terms of quark-gluon distribution. The figure is from C.E. Carlson and T.J. Havens, Phys. Rev. Lett. 51, 261 (1983). The experimental points are the ratios of the iron to deuterium form factors for deep inelastic muon (crosses) and electron (dots) scattering. The curve is given by the model of the reference.

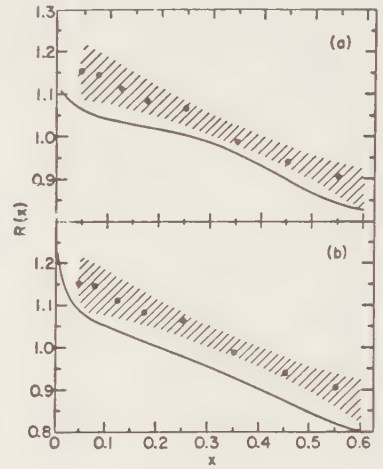


FIGURE 8

The EMC effect analyzed in terms of nucleon distributions and meson exchange currents. The experimental values are as in Fig. 7. The curve is the model of E.L. Berger, F. Coester and R.B. Wiringa.

ii) Effects qualitatively indicating the quark-gluon degrees of freedom:

Such a "smoking gun" has not yet definitely appeared. One experimental candidate is the anomalon, if all its supposed characteristics stand the test of cleaner experiments. If the property of persistence remains as well as the anomalously large cross section, it seems to me that the only present explanations which are adequate are those involving hidden color.

It is my belief that the search for intermediate energy structure in few hadron systems is a most promising way of finding clear signatures of quark-gluon degrees of freedom. In spite of the disappointments with the lowest energy nucleon-nucleon structures,  $q^4$ - $q$ ,  $q^6$ ,  $q^9$ ,  $q^n$ g, etc. systems should show

their asymptotically free properties at appropriate energies and momentum transfers. Present indications are that the lowest energy structures due to these degrees of freedom are in the 1-5 GeV range and some of these "exotics" may already have been identified in meson-meson and meson-baryon systems. Although some may be seen as narrow peaks, we must expect in general to find these by complete sets of experiments and phase shift analysis. Such analysis will also identify properties important to their relationship to quark-gluon states - spin and parity, width, shape, inelastic channels and relative spacing. For instance the 11% NN and 9%  $\Delta\Delta$  content of the  $^1S_0$  and  $^3S_1$  configurations of the lowest six-quark state implies a strong enhancement of two-pion production, while the color magnetic splitting is about 70 MeV. When several such structures are identified and compared they can provide a very strong verification of the color degrees of freedom. From their details they can tell us much about quark dynamics.

#### THE NEED FOR CLASSICAL AND Q.C.D. DESCRIPTIONS

Figure 9 schematically indicates the range and probable overlap of regions in which hadrons or quarks and gluons dominate. Beyond 2 fm. one-pion exchange dominates, while between 1 and 2 fm. two-pion exchange is most important. We know of many results from first principles, quantitatively explained by one- and two-pion and  $\omega$  exchange from first principles. In this conference Franz Gross has several times reminded us of this in connection with both strong forces and electromagnetic form factors. On the other hand there is much evidence from high energy physics, experimental and theoretical, that quark and

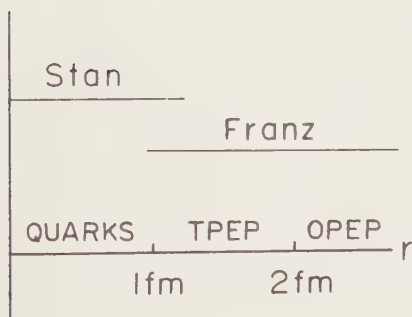


FIGURE 9  
Ranges of dominance of hadronic clusters and of asymptotic freedom of quarks and gluons.

gluon degrees of freedom have asymptotically free behavior over scales of about 1 fm. Because high order q.c.d. is difficult it follows that it may be operationally necessary to use both classical and q.c.d. methods to describe few-

body and nuclear characteristics in detail. Both elements will be simultaneously needed at intermediate energies and momentum transfers. Effective clustering into hadrons may take place before full confinement, just outside the range of asymptotic freedom. This is analogous to the appearance of alpha-particle clusters in the nuclear surface which can largely be described by particle-hole corrections to the shell model. If so, the analytical situation may be quite tractable.

#### ASYMPTOTIA?

There has been some disagreement as to at how low a momentum transfer and energy asymptotic freedom is a good approximation. It should be noted that asymptotic behavior and structure can coexist over a wide region. In nuclear physics we have the situation that in regions with many resonances, averaging or subtracting these resonances produces simple, statistically asymptotic results. Gerhard Høhler cites dispersion relation evidence in pion-nucleon reaction consistent with this view. I hazard a prediction that in the 1-10 GeV/c region we will see both many structures due to quark-gluon systems and a background rapidly becoming asymptotic. This would make medium energy hadron physics a field of great promise for the future.

#### IS DISPERSION THEORY RELEVANT IN Q.C.D.?

Finally I want to raise a question rarely heard. Dispersion relations, which associate analytical singularities with asymptotic (in configuration space) mass spectra, have played a role of great importance in hadronic physics. The Paris potential is a case in point. Internal structure of nuclei can be described by anomalous thresholds. Are dispersion relations of any value in our present day quark-gluon physics?

The proofs of dispersion relations depend on the free field hypothesis at large distances. Confinement precludes this assumption for quark and gluon fields. Does this destroy the results for the hadrons? Are there any similar analytic markers of quarks and gluons in transition amplitudes? Do the relevant singularities become spread over the range determined by confinement? The answers to these questions may give us new techniques for making predictions in the asymptotic freedom to confinement transition region.

In closing I once again thank the organizers of this conference for the pleasant and informative meeting we have had.

# TABLE OF CONTENTS

## FEW BODY PROBLEMS IN PHYSICS - BOOK OF CONTRIBUTED PAPERS

PREFACE	vii
I. THE NUCLEON-NUCLEON-INTERACTION AND RELATED PROBLEMS	1
N-N Experiments with Polarized Beam and Target at Saturne II	
F. Lehar, J. Bystricky, J. Deregel, J. Fabre, L. van Rossum, J.M. Fontaine, F. Perrot, J. Ball, T. Hasegawa, C.R. Newson, J. Yonnet, W. Leo, Y. Onel, A. Penzo, H. Azaiez	3
Elastic and Inelastic Scattering of Neutrons on Protons at SIN	
J. Franz, G. Nicklas, E. Rössle, G. Rupp, H. Schmitt, L. Schmitt, H. Woolverton	7
The Differential Cross Section for Proton-Proton Elastic Scattering at $90^\circ$ c.m. between 300 and 500 MeV	
D.F. Ottewell, E.G. Auld, W. Falk, G. Giles, G. Jones, G.J. Lolos, B.J. McParland, P. Walden, W. Ziegler	11
Measurement of the Analyzing Power for the $pp \rightarrow d\pi^+$ Reaction in the Region 500 - 800 MeV	
W.B. Tippens, T.S. Bhatia, G. Glass, J.C. Hiebert, R.A. Kenefick, L.C. Northcliffe, J.G.J. Boissevain, J.J. Jarmer, J.E. Simmons, D. Fitzgerald, J. Holt, A. Mokhtari, G.E. Tripard	13
Measurement of the Spin Correlation Parameters $A_{11}$ and $A_{S1}$ for the $pp \rightarrow d\pi^+$ Reaction in the Region 500 - 800 MeV	
D.B. Barlow, A. Saha, T.S. Bhatia, G. Glass, J.C. Hiebert, R.A. Kenefick, S. Nath, L.C. Northcliffe, W.B. Tippens, J.G.J. Boissevain, J.J. Jarmer, J.E. Simmons, R.H. Jeppesen, G.E. Tripard	15
Measurement of the Spin Correlation Parameter $A_{nn}(0)$ for the $pp \rightarrow d\pi^+$ Reaction in the Region 500 - 800 MeV	
W.B. Tippens, T.S. Bhatia, G. Glass, J.C. Hiebert, R.A. Kenefick, L.C. Northcliffe, J.G.H. Boissevain, J.J. Jarmer, J.E. Simmons, D. Fitzgerald, J. Holt, A. Mokhtari, G.E. Tripard	17
The Energy Dependence of the $D_{NN}$ Parameter and of the Moduli of the Transversity Amplitudes at $\Theta_{cm} = 90^\circ$ for pp Elastic Scattering between 0.9 and 1.5 GeV/c	
C.L. Hollas, D.J. Cremans, R.D. Ransome, P.J. Riley, B.E. Bonner, M.W. McNaughton, S. Wood	19

$D_{SS}$ ,  $D_{LS}$ ,  $D_{LL}$  and  $P$  for pp Elastic Scattering at  
699 and 750 MeV

D.J. Cremans, C.L. Hollas, K.H. McNaughton,  
P.J. Riley, R.F. Rodebaugh, Shen-wu Xu,  
B.E. Bonner, M.W. McNaughton, O.B. Van Dyck,  
Sun Tsu-hsun, S.E. Turpin, B. Aas, H. Ohnuma,  
G. Weston

21

The  $170^0$ -to- $90^0$  Cross Section Ratio for the Neutron-  
Proton Elastic Scattering

A. Bol, C. Dupont, P. Leleux, P. Lipnik,  
P. Macq, A. Ninane

23

The Neutron-Proton Capture at Extreme C.M. Angles

A. Bol, C. Dupont, P. Leleux, P. Lipnik,  
P. Macq, A. Ninane

25

Measurements of the Neutron-Proton Analyzing  
Power between 17 and 50 MeV

F.P. Brady, P. Doll, J. Hansmeyer, W. Heeringa,  
J.C. Hiebert, H.O. Klages, P. Plischke,  
J. Wilczynski

27

Polarization in Neutron-Proton Scattering at 25 MeV

M.D. Barker, D. Holslin, P.A. Quin, W. Haeberli

31

Measurement of the Spin Correlation Parameter  $A_{yy}$   
for  $\vec{n}-\vec{p}$  Scattering in the Energy Range up to 50 MeV

R. Aures, A. Bischoff, F.P. Brady, P. Doll,  
E. Finckh, W. Heeringa, K. Hofmann, H.O. Klages,  
J. Wilczynski, B. Zeitnitz

33

A Neutron-Proton Spin Correlation Experiment at  
14 MeV using a Polarized Proton Target

M. Schöberl, S. Berber, H. Hilbert, R. Köppel,  
H. Kuiper, R. Pferdenges, R. Schmelzer,  
G. Mertens, W. Tornow

35

Reconstruction of Proton-Proton Partial Wave Amplitudes  
using  $O(4)$  Expansions

J. Bystricky, P. La France, F. Lehar, F. Perrot,  
P. Winternitz

37

Elastic pp Scattering through Large Angles at Medium  
Energies

N.F. Golovanova, V. Iskra

39

The Potential-Free Approach to the Construction of  
the NN-Wave Functions

V.E. Troitsky

41

Amplitude Reconstruction for pp Scattering at 800 MeV

R.F. Rodebaugh, B.E. Bonner

43

Realistic Off-Shell Behaviour for Separable N-N potentials	
J. Haidenbauer, W. Plessas	45
The Momentum and Energy-Dependence of Separable Potentials	
M.W. Kermode, Z. Melhem	47
0-50 MeV Phase Shifts and the Behaviour of T-Matrices in Negative Energies by the Separable Energy-Dependent Approximations to square well Potentials	
K. Miyagawa	49
Nucleon-Nucleon Interactions Reflected to the Three-Nucleon Properties	
S. Ishikawa, T. Sawada, T. Sasakawa	51
Off-Shell Scattering by the Coulomb Potential	
B. Talukdar, D.K. Ghosh	53
On a Combined Variable-Phase-Off-Shell Scattering Theory	
B. Talukdar, S.R. Bhattaru	55
A Comprehensive and Consistent Meson-Exchange Model for the NN-Interaction	
R. Machleidt, K. Holinde	57
A Meson Exchange Model for N-N Polarization at 2 GeV/c	
I. Hulthage, F. Myhrer	61
Meson-Exchange Hamiltonian for Nucleon-Nucleon Scattering up to 2 GeV	
T.-S.H. Lee	63
Two Pion Exchange potential in Momentum Space	
I. Arisaka, K. Nakagawa, M. Wada	65
The Two-Body weak Axial Charge Density Operator in the Hard-Pion Model	
H.-U. Jäger, M. Kirchbach, E. Truhlik	67
Determination of the Long Range Part of the Deuteron Wave Function	
D.W.L. Sprung, J. Martorell, S. Klarsfeld	69
The Deuteron as a Probe of the NN Force	
T.E.O. Ericson, M. Rosa-Clot	73

Model of Angular Extrapolation in d+p Elastic Scattering	
J.T. Londergan, C.E. Price, E.J. Stephenson	75
Relation Between Q and $\eta$ for the Deuteron	
M.N. Butler, D.W.L. Sprung	77
The Deuteron Asymptotic D/S Ratio in the Framework of the OBE Model for the NN Interaction	
R. Machleidt, K. Holinde	79
The Relativistic Corrections to the Deuteron Quadrupole Moment	
A.F. Krutov, V.E. Troitsky	81
Deuteron Properties of a Model with Isobar Coupling	
E. Lomon	83
Electric Dipole Moment of the Deuteron	
Y. Aharonov, Y. Avishai	85
The Determination of the Asymptotic S-State Amplitude for the Deuteron	
M.W. Kermode, L.J. Allen, A. McKerrell, J.P. McTavish	87
The Connection Between the Asymptotic Deuteron Charge Form Factor and the Asymptotic np-Scattering $^3S_1$ -Phase	
A.F. Krutov, V.E. Troitsky	89
Photodisintegration of the Deuteron Near Threshold	
L. Črepinšek, H.F.K. Zingl	91
Cross Section Asymmetry of the Deuteron Photodisintegration at $E_\gamma = 29$ MeV and 38.6 MeV	
M.P. De Pascale, G. Giordano, G. Matone, P. Picozza, D. Babusci, R. Bernabei, L. Casano, S. D'Angelo, M. Mattioli, D. Prosperi, C. Schaerf, S. Frullani, B. Girolami	95
Relativistic Corrections to the Forward Cross Section for $d(\gamma, p)n$	
A. Cambi, B. Mosconi, P. Ricci	97
Low Energy Theorem Calculations of $np \rightarrow d\gamma$	
H.W. Fearing	99
A Modern Potential Model Calculation of Proton-Proton Bremsstrahlung	
H.W. Fearing, R.L. Workman	101



# SYMMETRIES IN THE NUCLEON-NUCLEON-INTERACTION

## Parity Nonconservation in Elastic $\vec{\alpha}$ Scattering

Ch. Jacquemart, J. Lang, R. Mueller,  
F. Nessi-Tedaldi, Th. Roser, M. Simonius,  
J. Sromicki, W. Haeberli, S. Jaccard

103

## Charge Dependence of Nuclear Forces

T.E.O. Ericson, G.A. Miller

107

## Parity Violation in N-N Interaction Tested in the Decay of $^{19}\text{F}$

K. Elsener, W. Gruebler, V. König, P.A. Schmelzbach,  
J. Ulbricht, J. Donaldson, M. Merdzan, W.Z. Zhang,  
D. Singy, C. Forstner

109

## Effects of Charge-Dependent Neutron-Proton Interaction in Two- and Three-Nucleon Systems

Shin Nan Yang, P.U. Sauer

111

# N- $\bar{\text{N}}$ -INTERACTION

## $p\bar{p}$ Annihilation Potential at Low Energy from the Quark Rearrangement Model

S. Furui, A. Faessler

113

## A Quark Rearrangement Model for Low-Energy Annihilation

M. Maruyama, T. Ueda

115

## Cross-Section Estimation for High Angular Momentum $N\bar{N}$ Bound State Production

J.C. Anjos, M.F. Barroso, L.P. Rosa, Z.D. Thomê

117

## $p\bar{p}$ Annihilation in an S-Wave Quark rearrangement Model

A.M. Green, J.A. Niskanen

119

## Phase Shift Analysis and Discrete Ambiguities of Nucleon- Antinucleon Scattering

A. Gersten

123

# II. PION-FEW NUCLEON SYSTEMS

## DIBARYON RESONANCE PROBLEM

## HYPERNUCLEAR SYSTEMS

125

## Is the Pion a Klein-Gordon-Particle ?

M. Bawin, M. Jaminon

127

J/ $\psi$ Pair Production in $\pi p$ and $pp$ Collisions	
B.A. Li, K.F. Liu	129
Production of Vector Meson Pairs in Hadronic Collisions	
B.A. Li, K.F. Liu	131
Pion Distributions in Free and Bound Nucleon	
M. Sawicki	133
$\pi N$ Scattering in the Model with Bare $\Delta$	
B. Golli, M. Rosina	135
The $\pi N$ Data Base Star System	
B.M.K. Nefkens	137
Methods of $\pi N$ Partial Wave Analysis	
G. Höhler	141
Two-Nucleon Force Model with $\Delta$ - and $\pi$ -Degrees of Freedom	
H. Pöpping, P.U. Sauer, Z. Xi-Zhen	145
Possible Quark $\Delta$ Substructure Effects in $\pi d$ Polarization	
A.S. Rinat	149
Peripheral Nucleon-Nucleon Inelasticity Parameters at Medium Energies	
M. Lacombe, B. Loiseau, S. Morioka, R. Vinh Mau	151
The Low Type Equations for the Pion-Two-Nucleon Interaction Problem	
T.I. Kopaleishvili, A.I. Machavariani	153
NN-Scattering at 400 - 1000 MeV in OBE- $\pi NN$ Dynamics and Dibaryons	
T. Ueda	155
Spin Dependence in the Inclusive $NN \rightarrow NN\pi$ Reaction	
R.R. Silbar, J. Dubach, M.M. Sternheim, W.M. Kloet	157
Exact Integral Equations for $\pi N$ Elastic Scattering and One- $\pi$ Production	
R.F. Alvarez-Estrada	159
Results for the Half-Off-Shell Continuation of the On-Shell $\pi N$ T-Matrix	
M.J. Reiner	161

Measurements of Polarization Parameters in pp  
Elastic Scattering at 560 MeV

E. Aprile, P. Bach, G. Cantale, S. Degli-Agosti,  
E. Heer, R. Hess, C. Lechanoine-Leluc, W. Leo,  
S. Morenzeni, Y. Onel, D. Rapin, S. Mango

163

Inelasticity in Nucleon-Nucleon Collisions and the  
Dibaryon Question

K.K. Seth

165

Dibaryon Signals in the Tensor Polarization  $t_{20}$  in  
 $\pi^+$ -d Scattering ?

V. Koenig, W. Gruebler, J. Ulbricht,  
P.A. Schmelzbach, J. Donaldson, M. Merdzan,  
K. Elsener, D. Singy, W.Z. Zhang, A. Chisholm

169

Measurements of  $iT_{11}$  in  $\pi$ -d<sub>pol</sub> Scattering between  
140 and 325 MeV

G.R. Smith, E.L. Mathie, E.T. Boschitz,  
M. Meyer, F. Vogler, M. Daum, S. Mango,  
J.A. Konter

173

Measurement of Tensor Polarization in Pion-Deuteron  
Elastic Scattering

W.S. Freeman, D.F. Geesaman, R.J. Holt,  
J.R. Specht, E. Ungricht, B. Zeidman,  
E.J. Stephenson, J.D. Moses, M. Farkhondeh,  
S. Gilad, R.P. Redwine

177

The Study of Differential Cross Sections of the  
 $\pi^+$ D  $\rightarrow$  PP Reaction at Pion Energies 280, 300, 330,  
357, 390, 420 and 450 MeV

M.Ja. Bork ski, V.G. Gaditsky, G.E. Gavrilov,  
V.A. Gordeev, Yu.S. Grigor'ev, V.P. Koptev,  
A.G. Krivshich, S.P. Griglov, L.G. Kudin,  
A.Yu. Majorov, Yu.A. Malov, G.V. Scherbakov,  
I.I. Strakovsky, L.N. Uvarov

179

Energy Dependent Partial Wave Analysis of the  
 $\pi^+$ D  $\rightarrow$  PP Reaction in the Region  $S = 2.09 - 2.42$  GeV

A.V. Kravtsov, M.G. Ryskin, I.I. Strakovsky

181

The Polarization Observables  $D_{NN}$ , P and A for  
 $\bar{p}p \rightarrow \bar{p}\pi^+n$  at 800 MeV

B.E. Bonner, M.W. McNaughton, O.B. van Dyck,  
S.E. Turpin, D.J. Cremans, C.L. Hollas, P.J. Riley,  
R.F. Rodebaugh, B. Aas, G.S. Weston

183

Spin-Spin Correlations and Spin-Asymmetries for the  
Reaction  $\bar{p}p \rightarrow p\pi^+$  at Intermediate Energies

C.E. Waltham, R. Shypit, D.A. Axen, F. Entezami,  
M. Comyn, D. Healey, G.A. Ludgate, G.D. Wait,  
D.V. Bugg, J.A. Edgington, N.R. Stevenson

185

First Measurement of  $K_{NN}$  in the Reaction  $\bar{p}p \rightarrow \bar{d}\pi^+$   
at 800 MeV

S.E. Turpin, B.E. Bonner, O.B. van Dyck,  
M.W. McNaughton, D.J. Cremans, C.L. Hollas,  
K.H. McNaughton, P.J. Riley, R.F. Rodebaugh,  
Xu Shin-wu, B. Aas, G.S. Weston

189

A Novel Technique for Measuring the Vector Polarization  
of a Deuteron

B.E. Bonner, M.W. McNaughton, O.B. van Dyck,  
S.E. Turpin, C.L. Hollas, D.J. Cremans, P.J. Riley,  
R.F. Rodebaugh, B. Aas, G.S. Weston

191

Relativistic Calculation of all Spin Observables  
in  $pp \rightarrow d\pi$

M.P. Locher, A. Švarc

193

Effects of  $^1D_2$  Dibaryon Formation in  $\pi d$   
Scattering

H.G. Dosch, S.C.B. Andrade, E. Ferreira,  
G. Perez

195

Energy Dependence of the  $pp \rightarrow \pi d$  Observables  $A_{y0}$   
and  $A_{xz}$

F. Foroughi, B. Favier, A. Berdoz

197

Resonances in  $\pi$ -d Scattering within the Faddeev  
Framework

I.R. Afnan, B.C. Pearce

199

Advantages of Amplitude Analysis in  $90^\circ_{CM}$  Geometry  
for P-P Scattering and Resonance Criteria

M. Furić, A. Švarc, Ž. Bajzer

201

Dibaryon Resonances and Aligned Coupling States  
of Nucleon and  $\Delta$  Isobar

T. Otofujii, K. Sakai, S. Saito, M. Yasuno, H. Kanada

203

Phase Shift Analysis of P-P Scattering and Diproton  
Resonance

H. Abe, H. Kanada

205

Search for Narrow Dibaryon Resonances

K.K. Seth, A. Saha, D. Kielczewska,  
S. Iversen, M. Aartuso, D. Barlow, L. Casey,  
D. Godman, M. Kaletka, R. Seth, J. Stuart,  
T.S. Bhatia

207

A Search for  $T = 0$  Dibaryonic Resonances

M.P. Combes, J.L. Ballot, P. Berthet, R. Frascaria,  
M. L'Huillier, C.F. Perdrisat, B. Tatischeff,  
N. Willis, J. Banaigs, J. Berger, A. Codino,  
J. Duflo, F. Plouvin, E. Aslanides, F. Hibou, O. Bing  
R. Beurtey, M. Boivin, D. Hutcheon, Y. Le Bornec,  
F. Fabbri, G. Piccozza, L. Satta, J. Yonnet

209

Electrodesintegration of Deuteron as a Method for S-Dibaron Resonances Searching	
A.M. Popova, Yu.A. Popov, E.K. Shabalina	211
A Dramatic Anomaly in Pion Production in $\vec{p} + d$ Collisions	
D. Kielczewska, K.K. Seth, A. Saha, S. Iversen, D. Barlow, M. Kaletka	213
On Charmed Dibaryon Systems	
G. Bhamathi	215
Test of Charge Independence in the Pion-Nucleon System by Use of the Triangle Inequalities	
M.E. Sadler, S. Adrian, F.O. Borcharding, W.J. Briscoe, A. Eichon, D.H. Fitzgerald, G.J. Kim, A. Mokhtari, B.M.K. Nefkens, G. Olah, C.J. Seftor, D.I. Sober, T. Walker, J.A. Wightman	217
Sensitivity of Charge Asymmetry Parameter to Coulomb Effects in $\pi^\pm$ -d Elastic Scattering	
J. Fröhlich, B. Saghai	219
Charge-Symmetry Analysis of Low-Energy Elastic $\pi^\pm$ D scattering	
R. Rockmore, B. Saghai	221
Radiative Corrections in Few-Body Hadronic Interactions	
B. Saghai	223
The Reaction $\vec{p} + d \rightarrow t + \pi^+$ at Intermediate Energies	
R. Abegg, D.A. Hutcheon, C.A. Miller, J. Arvieux, J.M. Cameron, C.A. Davis, A. Hussein, G.A. Moss, W.C. Olsen, G. Roy, J. Uegaki, I. van Heerden	225
Differential Cross Section for Elastic $\pi^\pm$ Helium Isotopes Scattering	
G. Fournier, A. Gerard, J. Miller, J. Picard, B. Saghai, P. Vernin, P.Y. Bertin, B. Coupat, E.W.A. Lingeman, K.K. Seth	227
On the Possibility of the Ramsauer Effect in Inelastic $\pi$ He <sup>4</sup> Scattering at Low Energies	
F. Nichitiu, M. Sapozhnikov	229
Quasi-Free Scattering of $\pi^+$ and $\pi^-$ from <sup>3</sup> He and <sup>4</sup> He at Energies from 350 to 475 MeV	
R.C. Minehart, J. Boswell, P.C. Gugelot J. Källne, J. McCarthy, L. Orphanos, C. Smith, R.R. Whitney, P.A.M. Gram	231

Study of the ( $\pi p^3\text{H}$ ), ( $\pi^2 p^2 n$ ) and ( $3pn$ ) ReactionsInduced by Pions on  $^4\text{He}$  at 156 MeV

F. Balestra, S. Bossolasco, M.P. Bussa, L. Busso,  
P. Davolio, L. Ferrero, R. Garfagnini, G. Gervino,  
D. Panzieri, G. Piragino, F. Tosello, I.V. Falomkin,  
V.I. Lyashenko, V.A. Panyushkin, G.B. Pontecorvo,  
M.G. Sapozhnikov, Yu.A. Shcherbakov, A. Maggiora

233

## Coherent Pion Production on Deuterium by Medium

Energy Neutrons

W. Dutty, J. Franz, E. Rössle, H. Schmitt, L. Schmitt,  
O. Dumbrajs

235

## Backward Pion Production in Proton-Deuteron

Scattering

J. Mahalanabis, P. Bandyopadhyay

237

 $\pi^+/\pi^-$  Absorption in  $^3\text{He}$  at 120 MeV

G. Backenstoss, S. Cierjacks, M. Furić, M. Izycki,  
S. Ljungfelt, U. Mankin, T. Petković, G. Schmidt,  
M. Steinacher, H. Ullrich, P. Weber, H.J. Weyer,  
K. v. Weymar

239

Pion Absorption on  $^3\text{He}$  at 65 MeV

K.A. Aniol, R.R. Johnson, R. Tacik, W. Gyles,  
B. Barnett, H.W. Roser, D. Ashery, J. Alster,  
M. Moinester, A. Altman, J. Lichtenstadt,  
D.R. Gill, J. Vincent, B. Sobie, H. Gubler,  
S. Levinson

243

## Some Results on Correlated Pairs Emitted After Negative

Pion Absorption at Rest in  $^{12}\text{C}$ 

C. Cernigoi, R. Cherubini, D. Gill, N. Grion,  
G. Pauli, R. Rui

245

## Isospin Dependence of Pion Absorption on

Nucleon Pairs

R.R. Silbar, E. Piasetzky

247

 $\pi^0$ -Photoproduction on the  $^3\text{H}/^3\text{He}$  Isodoublet

B. Bellinghausen, H.J. Gassen, G. Nöldeke, E. Reese,  
T. Reichelt, P. Stipp, J. Hartfiel, S. Hilger, R. Mutius

249

## Gauge Invariance and Current Algebra in Pion

Photoproduction

R.E. Ellis

251

Contribution of Non-Linear Interaction to Nuclear  
Matter

K. Nakagawa, I. Arisaka, M. Wada

253

HYPERNUCLEAR FEW BODY SYSTEMS

A Comment on the  $\Lambda$ -Nucleon Force in Hypertriton

Y. Sunami, H. Narumi 255

Repulsive Core Effect of  $\Lambda$ -N Interaction on  
 $\Lambda$ - $\alpha$  Potential I

Y. Kurihara, Y. Akaishi, H. Tanaka 257

Microscopic Three-Cluster Model of Light  
 $\Lambda$ -Hypernuclei

T. Motoba, H. Bandō, K. Ikeda 259

Study of  $^{21}_{\Lambda}\text{Ne}$ -Hypernucleus by Microscopic Three-  
Cluster Model

T. Yamada, K. Ikeda, H. Bandō, T. Motoba 261

Effect of Pauli Principle to the Width of  $\Sigma$   
Excitation

E. Satoh, M. Kimura 263

Kaon-Induced Deuteron Disintegration

O.V. Maxwell 265

$\Delta$ -Isobar Excitation in Carbon Nuclei at  
4.4 + 10.7 GeV/c in Charge-Exchange Reaction  
( $^3\text{He}, t$ )

V.G. Ableev, A.P. Kobushkin, A.B. Kurepin,  
D.K. Nikitin, A.A. Nomofilov, N.M. Piskunov,  
V.I. Sharov, I.M. Sitnik, E.A. Stokovskij,  
L.N. Strunov, G.G. Vorobjov, S.A. Zaporozhets 267

Kaon Electroproduction in Few Nucleon Systems

S.R. Cotanch, S.S. Hsiao 269

III. ELECTROMAGNETIC INTERACTION

FORMFACTORS 271

The Electromagnetic Structure of the Three Nucleon  
Bound States

W. Struve, Ch. Hajduk, P.U. Sauer 273

Bremsstrahlung Weighted and Integrated Photo-  
disintegration Cross-Section of the Alpha Particle

S. Sanyal, S.N. Mukherjee 275



The $(\gamma, p)$ -to $(\gamma, n)$ Ratio in ${}^4\text{He}$ and Charge Symmetry Breaking	
H.R. Weller, L.C. Biedenharn, P.P. Delsanto, N.R. Roberson, D.R. Tilley	277
The ${}^3\text{He}$ Charge Form Factor: A Simple Theoretical Approach	
E.A. Bartnik, H. Haberzettl, W. Sandhas	279
${}^6\text{Li}$ as a Two-Cluster System and its Photoabsorption Calculations	
M.A.K. Lodhi, K.E. Wald	281
Estimate of $p+d \rightarrow {}^3\text{He}+\gamma\gamma$ Contribution to the Radiative Capture Reaction $p+d \rightarrow {}^3\text{He} + \gamma$ at $T_p = 450$ MeV	
F. Prats, W.J. Briscoe	283
Estimate of $p+d \rightarrow {}^3\text{He} e^- e^+$ Cross Section at $T_p = 450$ MeV	
F. Prats, W.J. Briscoe	285
Electromagnetic Form Factors of Bound Nucleons	
Il-Tong Cheon	287
Meson-Exchange Currents, Current Conservation, and Magnetic Form Factor of ${}^3\text{He}$	
M.A. Maize, Y.E. Kim	289
Three-Nucleon Bound State Obtained from Triquark Nucleon Models	
E. Harper, H.J. Weber	291
New Estimate of Nuclear Charge Asymmetry in the $A = 3$ Bound State	
S.A. Coon	293
Electromagnetic Transitions in the Framework of the Refined Resonating Group Model	
H.M. Hofmann, T. Mertelmeier	295
The ${}^3\text{He}$ Asymptotic D/S State Ratio and the Tensor Analysing Powers of the $p(\vec{d}, \gamma){}^3\text{He}$ Reaction	
A. Arriaga, F.D. Santos	297
Photon Scattering by the Proton and Deuteron in the $\Delta$ -Region	
K.P. Schelhaas, B. Ziegler, E. Hayward	299

Measurement of the Tensor Polarization of the  
Recoil Deuteron in Electron-Deuteron Elastic  
Scattering

M.E. Schulze, D. Beck, M. Farkhondeh, S. Gilad,  
S. Kowalski, R.P. Redwine, W. Turchinets,  
R.J. Holt, J.R. Specht, K. Stephenson,  
B. Zeidman, R.M. Laszewski, E.J. Stephenson,  
J.D. Moses, M.J. Leitch, R. Goloskie, D.P. Saylor

303

Exclusive Electrodesintegration of  $^2\text{H}$  Far Away Off  
the Quasielastic Region

P. Barreau, M. Bernheim, P. Bradu, A. Bussiere,  
G.P. Capitani, E. de Sanctis, S. Frullani,  
F. Garibaldi, Z.E. Meziani, J. Morgenstern,  
J. Mougey, S. Turck-Chieze

305

Structure of the Deuteron Electromagnetic Current  
and the Continuity of Nuclear and Quark Dynamics

S. Glazek

307

IV. THEORY AND CALCULATIONS IN NUCLEAR FEW BODY PROBLEMS

309

A Dispersive Approach to Bound State Equations

T. Jaroszewicz

311

A New Integral Equation for Three-Body Scattering  
in Configuration Space

J.L. Friar, B.F. Gibson, W.H. Klink, G.L. Payne,  
W.N. Polyzo

313

From Few-Body to Many Bodies

M. Fabre de la Ripelle

315

A Fourth Generation Three-Body Problem

A.N. Mitra

319

A Minimal Unitary (Covariant) Scattering  
Theory

J.V. Lindesay, A. Markevich

321

Tabakin-Like Separable Kernels for the NN  
Bethe-Salpeter Equation

G. Rupp, L. Streit, J.A. Tjon

323

$L^2$  Discretization Approximations in a Soluble  
Three-Particle Model

Z.C. Kuruoglu, F.S. Levin

325

Vibrational Enhancement of Total Breakup Cross  
Sections

M.I. Haftel, T.K. Lim 329

Numerical Solution of a Singular Three-Body  
Equation

L.R. Dodd 331

On the Solution of the Integral Equations  
with Bounded Kernels

C. Daskaloyannis 333

Three-Body Theory of Reactions

T. Sasakawa, T. Sawada, J. Horacek 335

Inclusion of Weak NN Interaction in the Three  
Nucleon Scattering Theory

Y. Avishai 339

Relativistic Effects in the Binding Energies  
of Few-Body Nuclei

F. Coester, R.B. Wiringa 343

A New Chain-of-Partitions Labelled Approach to  
N-Body Scattering

G. Cattapan, V. Vanzani 345

Sum Rules for Few-Particle Scattering in Two  
Dimensions

D. Bollé, C. Danneels, T.A. Osborn 349

Few-Body Techniques in Many-Body Perturbation  
Theory

B. Cheng-guang 351

Nuclear-Coulomb Scattering Length as a Limit  
of Renormalized t-Matrix from Negative Energies

M.A. Navrotsky 353

Coulomb-Modified Scattering Parameters and Entire  
Coulomb Wave Functions

J.W. de Maag, L.P. Kok, H. van Haeringen 355

One-Dimensional Faddeev Equations for a Three  
Body System with Coulomb Interactions

P.A. Massaro 359

Inequalities for and Zeros of the Coulomb T-Matrix  
in Momentum Space

H. van Haeringen, L.P. Kok 361

Exact Solution for Truncated Three-Body Coulomb Problem	
T. Sasakawa, T. Sawada	363
Does n-d Doublet Scattering Show Any Indication of the Efimov Effect Near the Three-Body Threshold ?	
V.S. Bhasin, W. Sandhas	365
On the Numerical Evaluation of the Input Integrals in the CG-Equations for a Six Boson Problem	
C. Chandler, A.G. Gibson	369
Equations for the Elastic Scattering Amplitudes at Low Energies	
V.B. Belyaev, V.V. Pupyshev	373
Scattering Lengths in Nonrelativistic Three-Body Systems	
F. Gesziesy, G. Karner	375
Correlations Inside A 4 Structureless $\alpha$ -Particles System	
B. Cheng-guang, T.K. Lim, C. Wei-qin	377
Effective Interactions in the $\Lambda$ - $\alpha$ and $\Lambda$ - $\Lambda$ - $\alpha$ Systems	
S. Maeda, E.W. Schmid	379
A Study on the Energy Dependence of the n-d Elastic Scattering	
Y. Koike	381
Proton Deuteron Breakup Reaction Near the Threshold	
H. Kröger, A.M. Nachabe, R.J. Slobodrian	385
New Results on NN Interactions from pd Desintegration	
V.V. Komarov, A.M. Popova, V.V. Zatekin	387
Magnetic Dipole Effects on p-n-n Final States	
R.J. Slobodrian	389
Nuclear-Coulomb pd Scattering Length in the Model with Separable Interaction	
S.A. Shadchin, M.L. Zepalova	391
Coulomb Distortion to Proton-Deuteron Tensor Polarized Cross Sections and the Nucleon Exchange Singularity	
G. Berthold, H. Zanke	393

Off-Shell Effects in Second-Order Nucleon-Deuteron  
Polarizations

H. Zankel, W. Plessas 395

Scattering Lengths in Nucleon-Deuteron  
Scattering

H. Zankel, L. Mathelitsch 397

S-Wave Proton-Deuteron Scattering Lengths

J.L. Friar, B.F. Gibson, G.L. Payne 399

Generalized Separable Expansion Amplitudes  
of p-p, p- $\alpha$  and  $\alpha$ - $\alpha$  Scatterings in Realistic  
Short Range Force Plus Coulomb Force

S. Oryu, R. Kircher, Y. Takatsuka, H. Kamada 401

Cluster Excitation in Energetic Hadron-Nucleus  
Collisions

V.I. Komarov, B. Kühn, H. Müller, S. Tesch 403

Cluster Expansion for Three-Body Bound States

D. Eyre, J.P. Svenne 405

The n- $\alpha$  and  $\alpha$ - $\alpha$  Direct Potential in the Fish  
Bone Optical Model with Saturation

G. Spitz, H. Klar, E.W. Schmid 407

Two- and Three-Cluster Fish Bone Model with  
Saturation

Y. Akaishi, S. Saito, H. Klar, S. Maeda,  
E.W. Schmid, G. Spitz 409

Virtual Breakup Effect of Triton ( $^3\text{He}$ ) Cluster  
on  $\alpha$ -t ( $^3\text{He}$ ) Scattering

T. Kajino, T. Matsuse, A. Arima 411

p- $^3\text{He}$  Scattering with Full Spin Dependence and  
Some Antisymmetry

R.H. Landau 413

Three-Particle Nature of  $3/2^+$  Resonance in  $^5\text{He}$

V.I. Kukulin, V.M. Krasnopol'sky, V.T. Voronchev 417

A Fish Bone Optical Model Calculation on  $\pi^+ - ^{20}\text{Ne}$   
Scattering

H. Leeb, E.W. Schmid 419

Analysis of Proton- $^3\text{He}$  Scattering by Separable  
Potential

L. Beltramin, R. DeI Frate, G. Pisent 421

Off Shell Effects in the Reactions  $d+\alpha \rightarrow d+\alpha$  and  
 $d+\alpha \rightarrow n+p+\alpha$

K. Hahn 425

Three-Body Potential Among Alpha Particles

O. Portilho, D.A. Agrelo, S.A. Coon 427

Four-Nucleon Scattering in the K-Matrix  
 Approximation

S.A. Sofianos, H. Fiedeldey, W. Sandhas 429

A=4 Level Structure from an R-Matrix Analysis  
 of the Four Nucleon SYS

G.M. Hale, D.C. Dodder 433

The Four-Nucleon Bound State with Paris and  
 Reid Potentials I

T. Katayama, M. Sakai 435

The Four-Nucleon Bound State with Paris and  
 Reid Potentials II

T. Katayama, M. Sakai 437

Correlations Between Four-Nucleon Observables

V.P. Levashev 439

$^4\text{He}$  Calculations in Large Harmonic Oscillator  
 Bases

R. Ceuleneer, P. Vandepuette 441

Four-Body Calculation of the Four Nucleon System:  
 Binding Energies and Scattering Results

A.C. Fonseca 443

Structure of the  $^3\text{H}+n+d(^*)$  Vertexes

B.F. Gibson, D.R. Lehman 447

New Effective Nuclear Force with Finite-Range  
 Three-Body Terms and Cluster Structure of Light-  
 Nuclei

A. Tohsaki-Suzuki 449

Exchange Symmetry in Nuclear Reaction Models

R. Kozack, F.S. Levin 453

Detailed Study of the Structure of Low-Lying  
 States in  $^6\text{Li}-^6\text{He}-^6\text{Be}$  Nuclei in the Model for  
 Three Composite Particles

V.M. Krasnopolsky, V.T. Voronchev, V.I. Kukulin,  
 P.B. Sazonov 455

Calculation of the Momentum Distribution of the Alpha-Deuteron Motion in ${}^6\text{Li}$	457
R. Beck, F. Dickmann	
A New Class of Antisymmetric Optical Potentials	459
S.K. Adhikari, R. Kozack, F.S. Levin	
Realistic Three-Body Models for Nuclear Reactions	461
G. Bencze, P. Doleschall, G. Cattapan, V. Vanzani	
A New Qualitative Optical Model Analysis for Elastic Scattering Data	465
J.M. Greben	
Application of a Unified Theory of Rearrangement Reactions to (p,d)-Reactions	467
J.M. Greben	
Unitary Potential Description of the Low- Energy Pion Elastic Scattering on ${}^4\text{He}$	469
M.Kh. Khankhasayev	
The Influence of the Pion Absorption Channel on the Low-Energy ( $\pi, {}^4\text{He}$ ) Scattering	471
V.B. Belyaev, M.Kh. Khankhasayev	
Analyticity, Normalizable Resonance State and Stripping to the Continuum	473
V.J. Menon, A.V. Lagu	
${}^{14}\text{C}$ : Two Neutrons and an Excitable Core	475
W.-M. Wendler, M. Micklinghoff, A. Lindner	
Study of Spin-Dependent Effects in the ${}^{116}\text{Sn}(\vec{d}, p){}^{117}\text{Sn}$ Reaction	477
C. Lapointe, J. Birchall, N. Videla, J. Knudson, J.S.C. McKee, H.E. Conzett, R.M. Larimer, D. Eversheim, C. Rioux, S. Roman, J. Brown	
Dwa Analysis of the ${}^3\text{He}(d, dd)p$ Reaction Including Both Processes of d-d and d-p Quasi-Free Scatterings	479
Y. Kudo, Y. Yamashita	
V. THREE NUCLEON FORCES	481
Possible Effects of the Two-Pion-Exchange Three- Nucleon Force in the Three-Nucleon System	483
A. Bömelburg, W. Glöckle, W. Meier	



Energy-Dependent Off-Shell and Phase Equivalent Potentials and the Tri-Nucleon Properties

M. Orłowski, Y.E. Kim 487

Molecular Calculation of the One Pion Three-Nucleon Three-Body Force

A.C. Fonseca, M.T. Pena 489

Three-Nucleon Force due to  $\rho\pi$  Exchange

R.G. Ellis, S.A. Coon, B.H.J. McKellar 491

Dynamical Symmetries and the Two-Pion Exchange Three-Nucleon Potential

M.R. Robilotta, M.P. Isidro Filho, H.T. Coelho, T.K. Das 493

Dynamical Symmetries and the Pion-Rho Exchange Three-Nucleon Potential

M.R. Robilotta, M.P. Isidro Filho 495

Comparative Study of the Trinucleon Ground State with Various Trinucleon Forces

H.T. Coelho, T.K. Das, M.R. Robilotta, M. Isidro Filho 497

Form Factors and the S-Wave Two-Pion Exchange Three-Nucleon Potential

M.R. Robilotta, M.P. Isidro Filho, H.T. Coelho, T.K. Das 499

Evidence of Three Body Forces Obtainable from Three Nucleon Final States

R.J. Slobodrian 501

Search for Three-Body Force Effects in the Reaction

${}^2\text{H}(\vec{p}, pp)n$  at  $E_p = 14.1$  MeV

M. Karus, M. Buballa, J. Helten, B. Laumann, R. Melzer, P. Niessen, H. Oswald, G. Rauprich, J. Schulte-Uebbing, C. Thomas, H. Paetz gen. Schieck 505

VI. EXPERIMENTS IN FEW NUCLEON SYSTEMS

507

The Spin Rotation Parameters  $D_{NN}$ ,  $D_{SL}$ ,  $D_{SS}$ ,  $D_{LS}$ ,  $D_{LL}$  and  $P$  for  $\vec{p}d \rightarrow \vec{p}d$  Elastic Scattering at 500 and 800 MeV

S. Tsu-hsun, B.E. Bonner, M.W. McNaughton, O.B. van Dyck, G.S. Weston, B. Aas, M. Bleszynski, G.J. Igo, H. Ohnuma, D.J. Cremans, C.L. Hollas, K.H. McNaughton, P.J. Riley, R.F. Rodebaugh, S.E. Turpin

509

Spin Correlation Parameters in the  $pp \rightarrow \pi d$   
Reaction and Direct Reconstruction of Scattering  
Amplitudes at  $\Theta = \pi/2$  at Five Energies

E. Aprile, P. Bach, G. Cantale, S. Degli-Agosti,  
E. Heer, R. Hees, C. Lechanoine-Leluc, W. Leo,  
Y. Onel, D. Rapin, P.-Y. Rascher, P. Sormani,  
J. Jaccard, S. Mango

511

Analyzing Power for  $\pi \pm p$  Elastic Scattering Between  
471 and 687 MeV/c

D.H. Fitzgerald, W.J. Briscoe, A. Eichon, G.A. Kim,  
A. Mokhtari, B.M.K. Nefkens, J.A. Wightman, S. Adrian,  
M.E. Sadler, T. Walker

513

The Analysing Power of the  $\vec{p}p \rightarrow \pi^+d$  Reaction at Inter-  
mediate Energies

G. Giles, E.G. Auld, G. Jones, G.J. Lolos,  
B.J. McParland, W. Ziegler, D. Ottewell, P. Walden,  
W.R. Falk

515

Comparison of the  ${}^3\text{He}(p,2p)d$  and  ${}^3\text{He}(p,pd)p$  Reactions

A. Bracco, H.P. Gubler, D.K. Hasell, W.T.H. van Oers,  
M.B. Epstein, D.A. Krause, D.J. Margaziotis,  
R. Abegg, C.A. Miller, A.W. Stetz

517

Measurement of  $A_y$  and  $A_{yy}$  in the  ${}^4\text{He}(\vec{d},p)n$   ${}^4\text{He}$  Reaction  
at 14.8 MeV

M.S.A.L. Al-Ghazi, J. Birchall, C. Lapointe,  
J.S.C. McKee, N. Videla

519

Acceleration of Deuterons Polarized in the Horizontal  
Plane by the RCNP Cyclotron and Measurements of the  
Tensor Analyzing Power  $A_{xz}$  at 56 MeV

K. Hatanaka, N. Matsuoka, H. Sakai, T. Saito,  
K. Hosono, M. Kondo, K. Imai, H. Shimizu,  
K. Nisimura

523

Tensor Analyzing Powers for the  $\vec{d}-p$  Elastic  
Scattering at 56 MeV

K. Hatanaka, N. Matsuoka, H. Sakai, T. Saito,  
K. Hosono, M. Kondo, Y. Koike, K. Imai,  
H. Shimizu, K. Nisimura, A. Okihana

525

Analyzing Power of the Elastic  $\vec{n}-d$  Scattering  
from 14 MeV to 50 MeV

F.P. Brady, P. Doll, E. Finckh, W. Heeringa,  
K. Hofmann, H.O. Klages, W. Nitz, J. Wilczynski

527

Low Energy Measurements of the Backward Elastic  
 $n-d$  Cross Section

G. Janson, L. Glantz, A. Johansson, I. Koersner

529

Polarized Deuteron Elastic Scattering at 10 MeV  
from a Polarized Proton Target

R. Schmelzer, S. Berber, H. Hilmert, R. Köppel,  
H. Kuiper, R. Pferdmenges, M. Schöberl,  
H. Zankel

531

Three Body Forces and the  $d+p+p+n$  Reaction  
Close to Threshold

A.M. Nachabe, R.J. Slobodrian, P. Bricault,  
R. Roy, J. Pouliot, L. Potvin, B.K. Sinha,  
H. Kröger

533

$^3\text{He}(p,p)^3\text{He}$  Analyzing Powers and Phase Shift  
Analysis Between 25 and 35 MeV

P.J.T. Verheijen, R.H. McCamis, C. Lapointe  
W.T.H. van Oers

535

Measurement of the Analyzing Power of the Elastic  
 $n-^3\text{He}$  Scattering up to 50 MeV

F.P. Brady, P. Doll, B. Haesner, W. Heeringa, K. Hofmann,  
P. Jany, H.O. Klages, Chr. Maier, J. Wilczynski

537

Spin-Polarization Observables at the  $J=3/2^+$   
Resonance in the Reactions  $^3\text{H}(d,n)^4\text{He}$  and  
 $^3\text{He}(d,p)^4\text{He}$

H.E. Conzett

539

Analyzing Power Measurement and Phase Shift Ana-  
lysis for the  $n-^4\text{He}$  System up to 50 MeV

P. Doll, B. Haesner, J.C. Hiebert, H.O. Klages,  
H. Krupp, P. Plischke, H. Wilczynski, H. Zankel

543

The Quasi Free Process in the  $^3\text{He}(d,dd)p$  Reaction

A. Okihana, K. Fukunaga, S. Kakigi, T. Ohsawa,  
S. Kato, S. Tanaka

545

Elastic Scattering of  $\alpha$  Particles on p, d,  $^3\text{He}$ ,  $^4\text{He}$   
Nuclei at 7 GeV/c

J. Banaigs, J. Berger, A. Codino, J. Duflo,  
L. Goldzahl, F. Plouin, F.L. Fabbri, P. Picozza,  
L. Satta, M. Boivin, P. Berthet, R. Frascaria

547

Cluster Structure of  $^{10}\text{B}$

M. Bartel, O. Bohn, H. Brückmann, D. Gola,  
D. Grossmann, C. Heinrich, F. Schmidt, K. Wick

549

Proton Analyzing Power and Cross Section Measure-  
ment in the  $D(\vec{p},2p)n$  Reaction for a Symmetric Con-  
figuration in the CM

B. Favier, F. Foroughi, C. Nussbaum

551

Reaction Mechanism of the Five-Body Breakup  
 $^{16}\text{O}(n,4\alpha)n$

B. Antolković, S. Zulj

553

Multiple-Scattering Effect in the  ${}^3\text{He}(p,pp){}^2\text{H}$   
Reaction at 65 MeV

S. Kakigi, K. Fukunaga, T. Ohsawa, A. Okihana,  
H. Nakamura-Yokota, T. Sekioka, S. Tanaka,  
S. Kato

555

Measurement of the Excitation Function and Angular  
Distribution of the  ${}^4\text{He}(\bar{d},p\alpha)n$  Breakup Reaction at  
Low Energies

H. Oswald, M. Buballa, J. Helten, M. Karus,  
B. Laumann, R. Melzer, P. Niessen, G. Rauprich,  
J. Schulte-Uebbing, C. Thomas, H. Paetz gen.Schieck,  
Y. Koike

557

Three-Body Collisions in the Final State of a Four-  
Body Reaction

J. Krug

559

${}^6\text{Li}$  Levels Excited by the  ${}^9\text{Be}(p,\alpha)$  Reaction at  
 $E_p = 30$  and  $50$  MeV

Th. Delbar, Gh. Gregoire, G. Paič

561

Angular Distribution of Neutron-Proton Final State  
Interaction in the Reaction  $D(\alpha,p\alpha)N$

C. Heinrich, M. Bartel, O. Bohn, H. Brückmann,  
D. Gola, D. Grossmann, F. Schmidt, K. Wick,  
Y. Koike

563

The Sensitivity of the  $d+\alpha$  Breakup to n-p Forces

I. Slaus, I. Supek, Y. Koike, J.M. Lambert,  
P.A. Treado, F.D. Correll, R.E. Brown,  
R.A. Hardekopf, N. Jarmie

565

Isospin-Forbidden  ${}^2\text{H}(d,d)np$  and  ${}^4\text{He}(d,\alpha)np$   
Reactions

M. Ishikawa, S. Seki, K. Furuno, Y. Tagishi,  
M. Sawada, T. Sugiyama, T. Murayama, J. Sanada

567

${}^4\text{He}(d,p){}^4\text{He}$  Reaction and Faddeev Calculations

M. Ishikawa, S. Seki, K. Furuno, Y. Tagishi,  
M. Sawada, T. Sugiyama, K. Matsuda, T. Murayama,  
N.X. Dai, J. Sanada, Y. Koike

569

VII. FEW QUARK SYSTEMS

571

A Many-Body Confinement Potential Model for  
Multi-Hadron Systems

D. Robson

573

Chiral Symmetry Breaking and the Pion: (I) a  
Chiral Effective Hamiltonian

V. Bernard, R. Brockmann, M. Schaden,  
W. Weise, E. Werner

577

Chiral Symmetry Breaking and the Pion: (II) its Mass, Radius and Leptonic Decay	
V. Bernard, R. Brockmann, M. Schaden, W. Weise, E. Werner	581
DI-Hyperon State in the Potential Quark Model	
M. Oka, K. Shimizu, K. Yazaki	585
Pionic and E.M. Couplings of Hadrons: a Uni- fied View	
A.N. Mitra	587
The Nonrelativistic Quark Model and Spectra of Baryons and Mesons	
S. Ono	593
Baryon Spectra in a Relativistic Quark Model with Pion Field	
T. Hatsuda	597
On the $1^3P_J$ Splittings of Bottonium	
D.S. Kulshreshtha	599
E 1 and M 1 Transitions of Bottonium	
D.S. Kulshreshtha	601
Possible Explanation of $\rho^0 \rho^0$ Production in $J/\psi$ Radiative Decay	
B.-A. Li, K.-F. Liu	603
A Unified Dynamical Theory of Quark Degrees of Freedom in Nuclei	
Y.E. Kim, M. Orlowski	605
Effects of Quark Sub-Structure on Nucleon-Nucleon Scattering	
E.L. Lomon	609
Many Baryon Forces and Currents Derived from the Quark Structure of Nucleons	
P.U. Sauer, U.-J. Wiese	611
An Extended P-Matrix Analysis of Nucleon-Nucleon Scattering	
B.L.G. Bakker, M. van der Velde	613
Dependence of the Three-Body Observables on the Way of "Confinement" Introduction into the Quark Compound Bag Model	
A. Abdurakhmanov, B. Akhmadkhodjaev, E.B. Gandy1, A.L. Zubarev	617

The Meson Degrees of Freedom in the Quark Bag Model and NN-Interaction at Low and Intermediate Energies	619
A.N. Safronov	
Nonlinear Pion Field Effects in Chiral Bag Models	621
G. Kalbermann, J.M. Eisenberg	
Ro-Meson Coupling to the Nucleon in the Chiral Bag Model	625
E. Oset	
Divergence of the Nucleon Selfenergy in the Chiral Bag Model	627
E. Oset	
Quark Dynamics in Chiral Bags	629
H. Høgaasen, F. Myhrer	
Recoil Corrections in Bag Models	631
R. Goldflam, M. Betz	
Quantum Fluctuations in the Bag and Nucleon Observables	635
O.V. Maxwell, V. Vento	
On the Center-of-Mass Motion in MIT Bag Model	637
S. Saito, T. Otofujii, M. Yasuno	
Recoil Corrections in Bag Model Calculations of $D_{13}(1520)$ Photoproduction and the Proton Mag- netic Moment	639
Ch. Hajduk, B. Schwesinger	
Axial Form Factors in the Bag Model	641
W.N. Cottingham, B. Loiseau, O.V. Maxwell	
Relativistic Surface Motion of the Bag and Con- struction of Meson-Baryon-Formfactors	643
U.-G. Meißner	
3-Quark Irreducible Force in Nucleon	645
E.A. Bartnik, J.M. Namysłowski	
Quark Pauli Effects in Light Nuclei	649
A. Watt, M.H. Storm	
Scattering and Cluster Properties in Relativistic Models of Directly Interacting Confined Quarks	651
W.N. Polyzou, F. Coester	

Can the Bag Radius of the Nucleon be small, say .5 - .7 FM ?	
J.A. Parmentola	653
A Covariant Theory with a Confined Quantum	
H.P. Noyes, G. Pastrana	655
Quark Model and The Nucleon-Nucleon Interaction	
A. Faessler, F. Fernandez, G. Lübeck, K. Shimizu	657
Short Range Part of the NN Interaction from Quark Exchange Kernels: High or Low Repulsive Core ?	
Y. Suzuki, K.T. Hecht	661
Quark-Gluon Versus Meson Exchange I the Short- Range Part of the NN Interaction	
K. Holinde	663
Quark-Gluon Versus Meson Exchange II NN Scattering Phase Shifts	
C. Elster, K. Holinde	665
Non Relativistic 3-Quark Dynamical Solution of Faddeev Equation and the S-Wave Nucleon-Nucleon Scattering	
B. Silvestre-Brac, A.K. Jain, C. Gignoux	667
Quark Model and B-N Spin-Orbit Coupling	
W. Fan, H. Yin	669
Extension of the Refined Resonating Group Method to the Six Quark System	
J. Burger, H.M. Hofmann	671
Equivalent Velocity-Dependent Potentials for the Short-Range NN Interaction from Quark Exchange Kernels	
S.A. Sofianos, H. Fiedeldey	673
Color Van Der Waals Force in the Coupled Channel Approach	
K.F. Liu	675
An Analysis on the Color Van der Waals Force	
W. Fan, H. Yin, Z. Fei, K. Xing-Nan	677
Deep Inelastic Lepton Scattering and the Quark Structure of Nuclei	
J.P. Vary, H.J. Pirner	679



Charge Form Factor of  $^3\text{He}$  in a Quark Cluster Model

J.P. Vary, S.A. Coon, H.J. Pirner

683

## P-odd Effects in Proton-Proton Scattering and the Compound Bag Model

M.M. Musakhanov, Z.Z. Israilov

687

## Kaon Scattering and the Cloudy Bag Model

R.C. Barrett, B.K. Jennings, E.A. Veit, A.W. Thomas

689

## Determination of Parameters of Deuteron Six-Quark Component

V.G. Ableev, Kh. Dimitrov, A. Filipkowski,  
A.P. Kobushkin, D.K. Nikitin, A.A. Nomofilov,  
N.M. Piskunov, V.I. Sharov, I.M. Sitnik,  
E.A. Strokovsky, L.N. Strunov, L. Vizireva,  
G.G. Vorobiev, S.A. Zaporozhets

691

## VIII. ATOMIC AND MOLECULAR FEW BODY SYSTEMS

693

## Mesic Molecular Effects in the Capture of Negative Pions Stopped in Gaseous Hydrogen Isotopes

K.A. Aniol, D.F. Measday, M.D. Hasinoff,  
H.W. Roser, A. Bhageri, F. Entezami,  
C. Virtue, J. Stadlbauer, M. Salomon,  
D.H. Horvath, B.C. Robertson

695

Nuclear Structure Effects in the Atomic  $1s2s$  $^3S_1$  Hyperfine Multiplet of  $\text{Li}^+$ J. Kowalski, R. Neumann, S. Noehte, H. Suhr,  
G. zu Putlitz

697

## Method of Continued Fraction and Application to Atomic Physics

J. Horacek, T. Sasakawa

699

## Faddeev-Hahn Equations in some Problems of Atomic and Mesoatomic Physics

S.E. Brenner, E.M. Gandy, A.L. Zubarev,  
R.A. Sultanov

701

## Two Particles Atomic Radiative Recombination Scaling Law

G. Mezzorani, G. Puddu, P. Quarati

703

## First Order Quasiparticle Calculations for Electron-Hydrogen Collisions

H. Bürger, W. Sandhas, E.O. Alt

707

Electron-Hydrogen Quasiparticle Calculations with Polarization Effect	
H. Bürger, W. Sandhas	709
Potentials Obtained by Inversion of e-He Atomic Scattering Data	
H. Bürger, L.J. Allen, H. Fiedeldey, S.A. Sofianos, R. Lipperheide	711
Channel Coupling Array Calculations of the $H_3^+$ Ground State	
F.S. Levin, J. Shertzer	713
Channel Coupling Array Calculations of $H_2$ Ungerade States	
J. Shertzer, E. Bernstein, F.S. Levin	715
$^4He$ Atom-Diatom Scattering Analysis Using the FCM Technique for Realistic Diatomic Potentials	
S. Huber	717
TABLE OF CONTENTS OF FEW BODY PROBLEMS IN PHYSICS - BOOK OF INVITED REVIEW TALKS AND REPORTS ON THE DISCUSSION SESSIONS	719
LIST OF PARTICIPANTS	723
AUTHOR INDEX	749



## LIST OF PARTICIPANTS

ABEGG, R.  
TRIUMF  
UBC CAMPUS  
4004 WESBROOK MALL  
VANCOUVER, B.C. V6T 2A3  
CANADA

AFNAN, I.R.  
SCHOOL OF PHYSICAL SCIENCES  
THE FLINDERS UNIVERSITY OF SOUTH AUST.

BEDFORD PARK, S.A. 5042  
AUSTRALIA

AKAISHI, Y.  
DEPARTMENT OF PHYSICS  
FACULTY OF SCIENCE  
HOKAIDO UNIVERSITY, KITA-10 NISHI-3  
SAPPORO 060  
JAPAN

ALBINSKA, M.-M.  
KERNFORSCHUNGSZENTRUM KARLSRUHE GMBH  
INSTITUT FUER KERNPHYSIK III  
POSTFACH 3640  
7500 KARLSRUHE  
WEST-GERMANY

ALBINSKI, J.  
KERNFORSCHUNGSZENTRUM KARLSRUHE GMBH  
INSTITUT FUER KERNPHYSIK III  
POSTFACH 3640  
7500 KARLSRUHE  
WEST-GERMANY

ALLEN, L.J.  
DEPARTMENT OF PHYSICS  
UNIVERSITY OF SOUTH AFRICA  
P.O. BOX 392  
PRETORIA 0001  
SOUTH AFRICA

ALT, E.O.  
INSTITUT FUER PHYSIK  
JOHANNES-GUTENBERG UNIVERSITAET  
JAKOB-WELDER-WEG 11  
6500 MAINZ  
WEST-GERMANY

ALVAREZ-ESTRADA, R.F.  
DEPARTAMENTO DE FISICA TEORICA  
FACULTAD DE CIENCIAS FISICAS  
UNIVERSIDAD COMPLUTENSE  
MADRID-3  
SPAIN

ANIOL, K.A.  
TRIUMF  
4004 WESBROOK MALL

VANCOUVER, BC V6T 2A3  
CANADA

ANSALDO, E.J.  
PHYSICS DEPARTMENT  
UNIVERSITY OF B.C.

VANCOUVER, B.C. V6T 1W5  
CANADA

ANTOLKOVIC, B.  
INST. "RUDJER BOSKOVIC"  
BIJENICKA 54  
P.O. BOX 1016  
41004 ZAGREB  
YUGOSLAVIA

ANZALDO, A.M.  
KERNFORSCHUNGSZENTRUM KARLSRUHE GMBH  
INR  
POSTFACH 3640  
7500 KARLSRUHE  
WEST-GERMANY

ARENHOEVEL, H.  
INSTITUT FUER KERNPHYSIK  
UNIVERSITAET MAINZ  
POSTFACH 3980  
6500 MAINZ  
WEST-GERMANY

ARISAKA, I.  
CHIBA INSTITUTE OF TECHNOLOGY  
2-17-1 TSUDANUMA

NARASHINO-SHI 275  
JAPAN

ARNOLD, R.C.  
AMERICAN UNIVERSITY  
C/O STANFORD LINEAR ACCELERATOR CENTER  
P.O. BOX 4349  
STANFORD, CALIFORNIA 94305  
USA

ARVIEUX, J.  
LABORATOIRE NATIONAL SATURNE  
CEN SACLAY  
  
91191 GIF-SUR-YVETTE CEDEX  
FRANCE

AUFLEGER, S.  
INSTITUT FUER KERNPHYSIK  
UNIVERSITAET MAINZ  
POSTFACH 3980  
6500 MAINZ 1  
WEST-GERMANY

AURES, R.  
KERNFORSCHUNGSZENTRUM KARLSRUHE GMBH  
INSTITUT FUER KERNPHYSIK I  
POSTFACH 3640  
7500 KARLSRUHE  
WEST-GERMANY

AVISHAI, Y.  
CRN - DEPARTEMENT DE PHYSIQUE  
NUCLEAIRE THEORIQUE  
  
67037 STRASBOURG CROENENBOURG  
FRANCE

BACKENSTOSS, G.  
INSTITUT FUER PHYSIK  
EXPERIMENTALPHYSIK  
KLINGELBERGSTR. 82  
4056 BASEL  
SWITZERLAND

BAIER, H.  
INSTITUT FUER RADIUMFORSCHUNG  
UND KERNPHYSIK  
BOLTZMANNASSE 3  
1090 WIEN  
AUSTRIA

BAJZER, Z.  
INST. "RUDJER BOSKOVIC"  
BIJENICKA 54  
P.O. BOX 1016  
41001 ZAGREB  
YUGOSLAVIA

BAKKER, B.L.G.  
DEPARTMENT OF PHYSICS AND ASTRONOMY  
FREE UNIVERSITY AMSTERDAM  
DE BOELELAAN 1081  
1081 HV AMSTERDAM  
THE NETHERLANDS

BALDIN, A. M.  
J.I.N.R.  
DUBNA  
HEADPOSTOFFICE BOX 79  
101000 MOSCOW  
USSR

BAO, CHENG-GUANG  
INSTITUTE OF HIGH ENERGY PHYSICS  
ACADEMIA SINICA  
P.O. BOX 918(4)  
PEKING  
THE PEOPLES REPUBLIC OF CHINA

BARRETT, R.C.  
PHYSICS DEPARTMENT  
UNIVERSITY OF SURREY  
GUILDFORD  
SURREY GU2 5XH  
ENGLAND

BAWIN, M.  
INSTITUT DE PHYSIQUE B5  
UNIVERSITE DE LIEGE  
SART TILMAN  
4000 LIEGE 1  
BELGIUM

BECK, R.  
KERNFORSCHUNGSZENTRUM KARLSRUHE GMBH  
INSTITUT FUER KERNPHYSIK III  
POSTFACH 3640  
7500 KARLSRUHE  
WEST-GERMANY

BENCZE, G.  
CENTRAL RESEARCH INSTITUTE FOR PHYSICS  
RESEARCH INSTITUTE FOR PARTICLE AND  
NUCLEAR PHYSICS, P.O.B. 49  
1525 BUDAPEST 114  
HUNGARY

BERDOZ, A.  
INSTITUT DE PHYSIQUE  
AV. A.L. BREGUET 1  
  
2000 NEUCHÂTEL  
SUISSE

BERGSTROM, J.C.  
ACCELERATOR LABORATORY  
UNIVERSITY OF SASKATCHEWAN  
  
SASKATOON, SASK. S7N 0W0  
CANADA

BERNY, L.  
TECHNION  
AVE. JERUSALEM 98/28  
P.O. BOX 2250  
GIRIAT - YAH, HAIFA 29000  
ISRAEL

BERTHOLD, G.H.  
INSTITUT FUER THEORETISCHE PHYSIK  
UNIVERSITAET GRAZ  
UNIVERSITAETSPLATZ 5  
8010 GRAZ  
AUSTRIA

BOL, A.  
INSTITUT DE PHYSIQUE  
UNIVERSITE DE LOUVAIN  
2 CHEMIN DU CYCLOTRON  
1348 LOUVAIN-LA-NEUVE  
BELGIUM

BHAMATHI, G.  
DEPARTMENT OF THEORETICAL PHYSICS  
UNIVERSITY OF MADRAS  
GUINDY CAMPUS  
MADRAS - 600025  
INDIA

BOLSTERLI, H.  
T-9  
MS B279  
LOS ALAMOS NATIONAL LABORATORY  
LOS ALAMOS, NM 87545  
USA

BHASIN, V.S.  
DEPARTMENT OF PHYSICS AND ASTROPHYSICS  
UNIVERSITY OF DELHI

BORBELY, I.  
CENTRAL RESEARCH INSTITUTE  
FOR PHYSICS  
P.O. BOX 49  
1525 BUDAPEST 114  
HUNGARY

DELHI 110007  
INDIA

BIALY, J.  
KERNFORSCHUNGSZENTRUM KARLSRUHE GMBH  
IK III / ZYKLOTRON  
POSTFACH 3640  
7500 KARLSRUHE  
WEST-GERMANY

BOSCHITZ, E.  
UNIVERSITAET KARLSRUHE  
IEKP

7500 KARLSRUHE  
WEST-GERMANY

BIRCHALL, J.  
DEPARTMENT OF PHYSICS  
UNIVERSITY OF MANITOBA

BRADY, F.P.  
DEPARTMENT OF PHYSICS  
UNIVERSITY OF CALIFORNIA

WINNIPEG, MANITOBA R3T 2N2  
CANADA

DAVIS, CA 95616  
USA

BISCHOFF, A.  
KERNFORSCHUNGSZENTRUM KARLSRUHE GMBH  
INSTITUT FUER KERNPHYSIK I  
POSTFACH 3640  
7500 KARLSRUHE  
WEST-GERMANY

BRAEUER, K.  
INSTITUT FUER THEORETISCHE PHYSIK  
DER UNIVERSITAET TUEBINGEN  
AUF DER MORGENSTELLE 14  
7400 TUEBINGEN  
WEST-GERMANY

BOEMELBURG, A.  
INSTITUT FUER THEORETISCHE PHYSIK II  
UNIVERSITAETSSTR. 150

BRANDENBURG, R.  
INSTITUT FUER THEORETISCHE PHYSIK  
RUHR-UNIVERSITAET BOCHUM

4630 BOCHUM-QUERENBURG  
WEST-GERMANY

4630 BOCHUM 1  
WEST-GERMANY

BOERKER, G.  
INSTITUT FUER EXPERIMENTALPHYSIK I  
RUHR-UNIVERSITAET BOCHUM  
UNIVERSITAETSSTRASSE  
4630 BOCHUM  
WEST-GERMANY

BREUNLICH, W.  
INSTITUT FUER RADIUMFORSCHUNG  
BOLTZMANNGASSE 3

1090 WIEN  
AUSTRIA

BOERSMA, H.J.  
NATUURKUNDIG LABORATORIUM  
DER VRIJE UNIVERSITEIT  
DE BOELELAAN 1081  
1081 HV AMSTERDAM  
NETHERLANDS

BRISCOE, W.J.  
THE GEORGE WASHINGTON UNIVERSITY  
DEPARTMENT OF PHYSICS

WASHINGTON, DC 20052  
USA

BROCKMANN, R.  
INSTITUT FUER THEORETISCHE PHYSIK  
UNIVERSITAET REGENSBURG  
UNIVERSITAETSSTR. 31  
8400 REGENSBURG  
WEST-GERMANY

BRODSKY, S.J.  
SLAC  
P.O. BOX 4349  
STANFORD, CA 94305  
USA

BUECHE, G.  
KERNFORSCHUNGSZENTRUM KARLSRUHE GMBH  
IK II  
POSTFACH 3640  
7500 KARLSRUHE  
WEST-GERMANY

BUERGER, H.  
PHYSIKALISCHES INSTITUT  
UNIVERSITAET BONN  
ENDENICHER ALLEE 11-13  
5300 BONN 1  
WEST-GERMANY

BUGG, D.V.  
RUTHERFORD LABORATORY  
CHILTON, DIDCOT  
OXON OX11 0QX  
GREAT BRITAIN

BURGER, J.  
INSTITUT FUER THEORETISCHE PHYSIK III  
UNIVERSITAET ERLANGEN-NUERNBERG  
GLUECKSTR. 6  
8520 ERLANGEN  
WEST-GERMANY

BYSTRICKY, J.  
C.E.N. - SACLAY  
DPH-PE/S.E.E.

91191 GIF-SUR-YVETTE CEDEX  
FRANCE

CANTALE, G.  
UNIVERSITY OF GENEVA  
32, BD. D'YVOY  
1211 GENEVE 3  
SWITZERLAND

CATTAPAN, G.  
ISTITUTO DI FISICA GALILEO GALILEI  
UNIVERSITA DEGLI STUDI DI PADOVA  
VIA F. MARZOLO, 8  
35100 - PADOVA  
ITALY

CAVEDON, J.-M.  
IRF-DPH-N/HE  
CEN SACLAY  
91191 GIF-SUR-YVETTE  
FRANCE

CERNIGOI, C.  
ISTITUTO DI FISICA  
UNIVERSITA DEGLI STUDI DI TRIESTE  
VIA A. VALERIO 2  
TRIESTE  
ITALY

CEULENEER, R.  
FACULTE DES SCIENCES  
UNIVERSITE DE L'ETAT A MONS  
19, AVENUE MAISTRIAU  
7000 MONS  
BELGIUM

CHANDLER, C.  
DEPARTMENT OF PHYSICS AND ASTRONOMY  
UNIVERSITY OF NEW MEXICO  
ALBUQUERQUE, NM 87131  
USA

CHATTERJEE, A.  
UNIVERSITY COLLEGE OF SCIENCE  
DEPARTMENT OF PHYSICS  
92, ACHARYA PRAFULLA CHANDRA ROAD  
CALCUTTA - 700 009  
INDIA

CITRON, A.  
KERNFORSCHUNGSZENTRUM KARLSRUHE GMBH  
INSTITUT FUER KERNPHYSIK II  
POSTFACH 3640  
7500 KARLSRUHE  
WEST-GERMANY

CLOSE, F.E.  
RUTHERFORD LABORATORY  
CHILTON DIDCOT

OXFORDSHIRE OX11 0QX  
ENGLAND

COELHO, H.T.  
DEPARTAMENTO DE FISICA  
UNIVERSIDADE FEDERAL DE PERNAMBUCO  
50000 RECIFE, PE  
BRASIL

COESTER, F.  
ARGONNE NATIONAL LABORATORY  
BLDG 203  
ARGONNE, ILL. 60439  
USA



CONZETT, H.E.  
LAWRENCE BERKELEY LAB.  
UNIVERSITY OF CALIFORNIA

BERKELEY, CA 94720  
USA

COON, S.A.  
PHYSICS DEPARTMENT  
UNIVERSITY OF ARIZONA  
BLDG 81  
TUCSON, AZ 85721  
USA

COTANCH, S.R.  
DEPARTMENT OF PHYSICS  
NORTH CAROLINA STATE UNIVERSITY  
BOX 5367  
RALEIGH, NC 27650  
USA

CRAVO, E.  
CENTRO DE FISICA NUCLEAR  
UNIVERSIDADE DE LISBOA  
AV. PROF. GAMA PINTO 2  
1699 LISBOA  
PORTUGAL

DANNEELS, C.L.R.J.  
KATHOLIC UNIVERSITY OF LOUVAIN  
INSTITUUT VOOR THEORETISCHE FYSIKA  
CELESTIJNENLAAN 200 D  
3030 LEUVEN  
BELGIUM

DASGUPTA, S.S.  
UNIVERSITY OF BURDWAN  
6A, SEVEN TANKS LANE

CALCUTTA 700,030  
INDIA

DASKALOYANNIS, C.  
DEPARTMENT OF THEORETICAL PHYSICS  
UNIVERSITY OF OXFORD  
1 KEBLE ROAD  
OXFORD OX1 3NP  
GREAT BRITAIN

DE MAAG, J.W.  
INSTITUTE FOR THEORETICAL PHYSICS  
UNIVERSITY OF GRONINGEN  
P.O. BOX 800  
GRONINGEN  
THE NETHERLANDS

DE SWART, J.J.  
INSTITUTE FOR THEORETICAL PHYSICS  
UNIVERSITY OF NIJMEGEN  
TOERNOOIVELD  
6526 ED NIJMEGEN  
THE NETHERLANDS

DELFINO, A.  
INSTITUT FUER EXPERIMENTALPHYSIK  
RUHR-UNIVERSITAET BOCHUM  
UNIVERSITAETSSTR. 150  
4630 BOCHUM  
WEST-GERMANY

DERMOTT, S.  
CRSR  
SPACE SCIENCES  
CORNELL UNIVERSITY  
ITHACA, N.Y. 14853  
USA

DETAR, C.  
UNIVERSITY OF UTAH  
PHYSICS DEPARTMENT  
201 JFB (PHYSICS)  
SALT LAKE CITY, UT 84112  
USA

DICKMANN, F.  
KERNFORSCHUNGSZENTRUM KARLSRUHE GMBH  
IK III  
POSTFACH 3640  
7500 KARLSRUHE  
WEST-GERMANY

DIETRICH, K.  
PHYSIKDEP. DER TUM  
JAMES FRANCK STRASSE  
8046 GARCHING  
WEST-GERMANY

DILLIG, M.  
INSTITUT FUER THEORETISCHE PHYSIK  
UNIVERSITAET ERLANGEN  
GLUECKSTR.6  
8520 ERLANGEN  
WEST-GERMANY

DING, DA-ZHAO  
INSTITUTE OF ATOMIC ENERGY  
P.O. BOX 275(10)  
PEKING  
BEIJING  
THE PEOPLE'S REPUBLIC OF CHINA

DODD, L.R.  
DEPARTMENT OF MATHEMATICAL PHYSICS  
UNIVERSITY OF ADELAIDE  
G.P.O., BOX 498  
ADELAIDE, S.A. 5001  
SOUTH AUSTRALIA

DOLESCHALL, P.  
CENTRAL RESEARCH INSTITUTE FOR PHYSICS  
P.O. BOX 49  
1525 BUDAPEST  
HUNGARY

DOLL, P.  
KERNFORSCHUNGSZENTRUM KARLSRUHE GMBH  
INSTITUT FUER KERNPHYSIK I  
POSTFACH 3640  
7500 KARLSRUHE  
WEST-GERMANY

ENGELMANN, A.R.  
UNIVERSITY OF UPPSALA  
QUANTUM CHEMISTRY GROUP  
BOX 518  
751 20 UPPSALA  
SWEDEN

DOVER, C.  
DEPARTMENT OF PHYSICS  
BROOKHAVEN NATIONAL LABORATORY

ERICSON, T.E.O.  
CERN

UPTON, N.Y. 11973  
USA

1211 GENEVE 23  
SWITZERLAND

DUCK, I.  
RICE UNIVERSITY

EVERSHEIM, P.D.  
INSTITUT FUER STRAHLEN- UND KERN-  
PHYSIK DER UNIVERSITAET BONN  
NUSSALLEE 14-16  
5300 BONN 1  
WEST-GERMANY

HOUSTON, TEXAS 77251  
USA

DUMBRAJS, O.  
INSTITUT FUER THEORETISCHE KERNPHYSIK  
UNIVERSITAET KARLSRUHE  
POSTFACH 6380  
7500 KARLSRUHE 1  
WEST-GERMANY

EYRE, D.  
NATIONAL RESEARCH INSTITUTE FOR  
MATHEMATICAL SCIENCES OF THE CSIR  
P.O. BOX 395  
PRETORIA 0001  
REPUBLIC OF SOUTH AFRICA

DUPONT, C.  
INSTITUT DE PHYSIQUE  
UNIVERSITE DE LOUVAIN  
2 CHEMIN DU CYCLOTRON  
1348 LOUVAIN-LA-NEUVE  
BELGIUM

FABRE DE LA RIFELLE, M.  
DIVISION DE PHYSIQUE THEORIQUE  
INSTITUT DE PHYSIQUE NUCLEAIRE  
B.P. NO 1  
91406 ORSAY CEDEX  
FRANCE

DUSSEL, O.  
DPTO. DE FISICA - CNEA  
AVENIDA DEL LIBERTADOR 8250  
  
1429 BUENOS AIRES  
REPUBLICA DE ARGENTINA

FAESSLER, A.  
INSTITUT FUER THEORETISCHE PHYSIK  
UNIVERSITAET TUEBINGEN  
AUF DER MORGENSTELLE  
7400 TUEBINGEN  
WEST-GERMANY

EDGINGTON, J.A.  
DEPARTMENT OF PHYSICS  
QUEEN MARY COLLEGE  
MILE END ROAD  
LONDON E1 4NS  
UNITED KINGDOM

FALK, W.R.  
PHYSICS DEPARTMENT  
UNIVERSITY OF MANITOBA

WINNIPEG, R3T 2N2  
CANADA

ELLIS, R.G.  
TRIUMF  
4004 WESBROOK MALL  
UBC CAMPUS  
VANCOUVER, B.C. V6T 2A3  
CANADA

FEARING, H.W.  
TRIUMF  
UNIVERSITY OF BRITISH COLUMBIA

VANCOUVER, B.C.  
CANADA

ENGELHARDT, H.-D.  
UNIVERSITAET KARLSRUHE  
IEKP

7500 KARLSRUHE  
WEST-GERMANY

FERREIRA, E.  
DEPARTAMENTO DE FISICA  
PONTIFICIA UNIVERSIDADE CATOLICA  
CAIXA POSTAL 38071  
RIO DE JANEIRO 22452  
BRASIL

FIEDELDEY, H.  
PHYSICS DEPARTMENT  
UNIVERSITY OF SOUTH AFRICA  
P.O. BOX 392  
PRETORIA 001  
REPUBLIC OF SOUTH AFRICA

FIER, H.-P.  
INSTITUT FUER THEORETISCHE PHYSIK I  
DOMAGKSTR. 71

4400 MUENSTER  
WEST-GERMANY

FINCKH, E.  
PHYSIKALISCHES INSTITUT  
UNIVERSITAET ERLANGEN-NUERNBERG  
ERWIN-ROMMEL-STR. 1  
8520 ERLANGEN  
WEST-GERMANY

FIORENTINI, G.  
INFN & PHYSICS DEPT. PISA  
ISTITUTO DI FISICA  
PIAZZA TORRICELLI 2  
56100 PISA  
ITALY

FONSECA, A.C.  
CENTRO FISICA NUCLEAR  
AV. GAMA PINTO 2

1699 LISBOA  
PORTUGAL

FONTAINE, J.-M.  
CEN-SACLAY  
91191 GIF-SUR-YVETTE CEDEX  
FRANCE

FOROUGH, F.  
INSTITUT DE PHYSIQUE  
1 RUE A.L. BREGUET

2000 NEUCHATEL  
SUISSE

FRIED, H.M.  
PHYSICS DEPARTMENT  
BROWN UNIVERSITY

PROVIDENCE, RI 02912  
USA

FROELICH, J.  
INSTITUT FUER THEORETISCHE KERNPHYSIK  
UNIVERSITAET KARLSRUHE  
POSTFACH 6380  
7500 KARLSRUHE  
WEST-GERMANY

FROIS, B.  
DFHN/HE  
CEN SACLAY

91191 GIF-SUR-YVETTE  
FRANCE

FUJIWARA, Y.  
SCHOOL OF PHYSICS AND ASTRONOMY  
TATE LAB. OF PHYS., UNIV. OF MINNESOTA  
116 CHURCH ST., S.E.  
MINNEAPOLIS, MINNESOTA 55455  
USA

FUKUSHIMA, Y.  
DEPARTMENT OF APPLIED PHYSICS  
FUKUOKA UNIVERSITY

FUKUOKA 814-01  
JAPAN

FURUI, S.  
INSTITUT FUER THEORETISCHE PHYSIK  
DER UNIVERSITAET TUEBINGEN  
AUF DER MORGENSTELLE 14  
7400 TUEBINGEN  
WEST-GERMANY

GALSTER, S.  
KERNFORSCHUNGSZENTRUM KARLSRUHE GMBH  
MEP  
POSTFACH 3640  
7500 KARLSRUHE  
WEST-GERMANY

GEMMEKE, H.  
KERNFORSCHUNGSZENTRUM KARLSRUHE GMBH  
IK I  
POSTFACH 3640  
7500 KARLSRUHE  
WEST-GERMANY

GENZ, H.  
INSTITUT FUER THEORETISCHE KERNPHYSIK  
UNIVERSITAET KARLSRUHE  
POSTFACH 6380  
7500 KARLSRUHE 1  
WEST-GERMANY

GERSTEN, A.  
DEPARTMENT OF PHYSICS  
BEN-GURION UNIVERSITY

BEER-SHEVA  
ISRAEL

GIBBS, W.  
T-5, MS-B283  
LOS ALAMOS NATIONAL LABORATORY  
LOS ALAMOS, NM 87545  
USA

GIBSON, B.F.  
T-5, MS-B283  
LOS ALAMOS NATIONAL LABORATORY  
LOS ALAMOS, NM 87545  
USA

GIBSON, A.G.  
DEPARTMENT OF MATHEMATICS  
UNIVERSITY OF NEW MEXICO  
ALBUQUERQUE, NM 87131  
USA

GILAD, S.  
MASSACHUSETTS INSTITUTE OF TECHNOLOGY  
LABORATORY FOR NUCLEAR SCIENCE  
ROOM 26-405  
CAMBRIDGE, MA 02139  
USA

GILES, G.L.  
TRIUMF  
VANCOUVER, B.C. V8W-2Y2  
CANADA

GILS, H.J.  
KERNFORSCHUNGSZENTRUM KARLSRUHE GMBH  
IK III  
POSTFACH 3640  
7500 KARLSRUHE  
WEST-GERMANY

GLAZEK, S.  
INSTITUTE OF THEORETICAL PHYSICS  
WARSAW UNIVERSITY  
HOZA 69  
00-681 WARSAW  
POLAND

GLOECKLE, W.  
INSTITUT FUER THEORETISCHE PHYSIK  
RUHRUNIVERSITAET BOCHUM  
UNIVERSITAETSTR. 150  
4630 BOCHUM  
WEST-GERMANY

GOLA, D.  
I. INSTITUT FUER EXPERIMENTALPHYSIK  
ZYKLOTRON  
LURUPER CHAUSSEE 149  
2000 HAMBURG 50  
WEST-GERMANY

GOLLI, B.  
DEPARTMENT OF PHYSICS  
E. KARDELJ UNIVERSITY  
JADRANSKA 19, P.O. BOX 39  
61111 LJUBLJANA  
YUGOSLAVIA

GOTOW, K.  
PHYSICS DEPARTMENT  
VIRGINIA POLYTECHNIC INSTITUTE AND  
STATE UNIVERSITY  
BLACKSBURG, VA 24061  
USA

GOUWELDOOS, M.  
NATUURKUNDIG LABORATORIUM DER  
VRIJE UNIVERSITEIT  
DE BOELELAAN 1081  
1081 HV AMSTERDAM  
THE NETHERLANDS

GREAVES, P.D.  
EDITORIAL OFFICE OF 'NUCLEAR PHYSICS'  
C/O NORDITA  
BLEGDAMSVEJ 17  
2100 COPENHAGEN 0  
DENMARK

GREBEN, J.M.  
PHYSICS DEPARTMENT  
UNIVERSITY OF ALBERTA

EDMONTON, ALBERTA T6G 2J1  
CANADA

GREEN, A.M.  
RESEARCH INSTITUTE FOR THEORETICAL  
PHYSICS, UNIVERSITY OF HELSINKI  
SILTAVUORENPENGER 20  
00170 HELSINKI 17  
FINLAND

GREENIAUS, L.G.  
NUCLEAR RESEARCH CENTER  
UNIVERSITY OF ALBERTA  
TRIUMF  
EDMONTON, ALBERTA T6G 2N5  
CANADA

GROSS, F.L.  
DEPARTMENT OF PHYSICS  
WILLIAM AND MARY

WILLIAMSBURG, VA 23185  
USA

GRUEBLER, W.  
LABORATORIUM FUER KERNPHYSIK  
EIDGENOESSISCHE TECHNISCHE HOCHSCHULE  
HOENGERBERG  
8093 ZUERICH  
SWITZERLAND

GUARALDO, C.  
LABORATORI NAZIONALI DI FRASCATI  
CASELLA POSTALE 13

00044 FRASCATI  
ITALY

*List of Participants*

657c

GUßLER, H.P.  
TRIUMF  
4004 WESBROOK MALL  
UBC CAMPUS  
VANCOUVER, B.C. V6T 2A3  
CANADA

GYARMATI, B.  
INSTITUTE OF NUCLEAR RESEARCH  
HUNGARIAN ACADEMY OF SCIENCES  
BEM TER 18/C  
4001 DEBRECEN PF. 51  
HUNGARIAN

HABERZETTL, H.  
PHYSIKALISCHES INSTITUT  
UNIVERSITAET BONN  
ENDENICHER ALLEE 11-13  
5300 BONN 1  
WEST-GERMANY

HAEBERLI, W.  
PHYSICS DEPARTMENT  
UNIVERSITY OF WISCONSIN  
1150 UNIVERSITY AVENUE  
MADISON, WISC. 53705  
USA

HAFTEL, M.I.  
NAVAL RESEARCH LABORATORY  
CODE 6651  
  
WASHINGTON, D.C. 20375  
USA

HAHM, K.  
INSTITUT FUER THEORETISCHE PHYSIK  
UNIVERSITAET TUEBINGEN  
AUF DER MORGENSTELLE 14 D  
7400 TUEBINGEN  
WEST-GERMANY

HAIDENBAUER, J.  
INSTITUT FUER THEORETISCHE PHYSIK  
UNIVERSITAET GRAZ  
UNIVERSITAETSPLATZ 5  
8010 GRAZ  
AUSTRIA

HAJDUK, H.  
DEPARTMENT OF PHYSICS  
SUNY

STONY BROOK, NEW YORK 11794  
USA

HAJDUK, C.  
INSTITUT FUER THEORETISCHE PHYSIK  
UNIVERSITAET HANNOVER  
APPELSTR. 2  
3000 HANNOVER  
WEST-GERMANY

HALE, G.M.  
LOS ALAMOS NATIONAL LABORATORY  
GROUP T-2  
MS 243  
LOS ALAMOS, N.M. 87545  
USA

HANCOCK, A.D.  
CERN  
EP DIVISION  
BATIMENT 2 / R023  
1211 GENEVE 23  
SWITZERLAND

HANNEMANN, M.  
INSTITUT FUER PHYSIK  
JOHANNES-GUTENBERG UNIVERSITAET  
JAKOB-WELDER WEG 11  
6500 MAINZ 1  
WEST-GERMANY

HANSMEYER, J.  
  
UNTER DEN ULMEN 124  
  
5000 KOELN  
WEST-GERMANY

HARPER, E.P.  
PHYSICS DEPARTMENT  
THE GEORGE WASHINGTON  
UNIVERSITY  
WASHINGTON D.C. 20052  
USA

HARTT, K.  
DEPARTMENT OF PHYSICS  
UNIVERSITY OF RHODE ISLAND  
  
KINGSTON, RHODE ISLAND 02881  
USA

HEERINGA, W.  
KERNFORSCHUNGSZENTRUM KARLSRUHE GMBH  
INSTITUT FUER KERNPHYSIK I  
POSTFACH 3640  
7500 KARLSRUHE  
WEST-GERMANY

HEINRICH, C.  
I. INSTITUT FUER EXPERIMENTALPHYSIK  
ZYKLOTRON  
LURUPER CHAUSSEE 149  
2000 HAMBURG 50  
WEST-GERMANY

HELLER, L.  
LOS ALAMOS NATIONAL LABORATORY  
MS B283  
  
LOS ALAMOS, NM 87545  
USA

HIEBERT, J.C.  
CYCLOTRON INSTITUTE  
TEXAS A & M UNIVERSITY

COLLEGE STATION, TX 77843  
USA

HINES, K.C.  
UNIVERSITY OF MELBOURNE  
SCHOOL OF PHYSICS

PARKVILLE, VICTORIA 3052  
AUSTRALIA

HINTERBERGER, F.  
INSTITUT FUER STRAHLEN- UND KERN-  
PHYSIK DER UNIVERSITAET BONN  
NUSSALLEE 14-16  
5300 BONN 1  
WEST-GERMANY

HOEHLER, G.  
INSTITUT FUER THEORETISCHE KERNPHYSIK  
UNIVERSITAET KARLSRUHE  
POSTFACH 6380  
7500 KARLSRUHE  
WEST-GERMANY

HOFMANN, H.M.  
INSTITUT FUER THEORETISCHE PHYSIK  
UNIVERSITAET ERLANGEN  
GLUECKSTR. 6  
8520 ERLANGEN  
WEST-GERMANY

HOFMANN, K.  
KERNFORSCHUNGSZENTRUM KARLSRUHE GMBH  
INSTITUT FUER KERNPHYSIK I  
POSTFACH 3640  
7500 KARLSRUHE  
WEST-GERMANY

HOLLAS, C.L.  
LANL  
LAMPF VISITORS CENTER MS H 831  
THE UNIVERSITY OF TEXAS AT AUSTIN  
LOS ALAMOS, NM 87544  
USA

HORACEK, J.  
CHARLES UNIVERSITY  
DEPARTMENT OF MATHEMATICAL PHYSICS  
VYSOCANSKA 231  
19000 PRAHA 9  
CSSR

HORIUCHI, H.  
DEPARTMENT OF PHYSICS  
FACULTY OF SCIENCE  
KYOTO UNIVERSITY  
KYOTO 606  
JAPAN

HUBER, H.S.  
DEPARTMENT OF CHEMISTRY & PHYSICS  
BEAVER COLLEGE

GLENSIDE, PA 19038  
USA

JAHN, H.  
KERNFORSCHUNGSZENTRUM KARLSRUHE GMBH  
INR  
POSTFACH 3640  
7500 KARLSRUHE  
WEST-GERMANY

JAIN, A.K.  
INSTITUT SCIENCE NUCLEAIRE DE GRENOBLE  
UNIVERSITY OF GRENOBLE  
53 - AVENUE DES MARTYRS  
38026 - GRENOBLE CEDEX  
FRANCE

JANS, E.  
NIKHEF - K  
POSTBUS 4395

AMSTERDAM  
THE NETHERLANDS

JANY, P.  
KERNFORSCHUNGSZENTRUM KARLSRUHE GMBH  
INSTITUT FUER KERNPHYSIK I  
POSTFACH 3640  
7500 KARLSRUHE  
WEST-GERMANY

JEREMIE, H.  
DEPARTEMENT DE PHYSIQUE  
UNIVERSITE DE MONTREAL  
CP 6128  
MONTREAL H3C 3J7  
CANADA

JOHANSSON, A.  
TANDEM ACCELERATOR LABORATORY  
BOX 533

75121 UPPSALA  
SWEDEN

JONES, B.  
DEPARTMENT OF PHYSICS  
UNIVERSITY OF BRITISH COLUMBIA  
6224 AGRICULTURE ROAD  
VANCOUVER, B.C. V6T 2A6  
CANADA

KAMKE, D.  
INSTITUT FUER EXPERIMENTALPHYSIK I  
RUHR-UNIVERSITAET BOCHUM  
UNIVERSITAETSSTR. 150, GEBAEUDE NB  
4630 BOCHUM 1  
WEST-GERMANY

*List of Participants*

659c

KARLSSON, B.R.  
TANDEM ACCELERATOR LABORATORY  
P.O. BOX 533

75121 UPPSALA  
SWEDEN

KATAYAMA, T.  
C/O PROF. DR. P.U. SAUER  
INSTITUT FUER THEORETISCHE PHYSIK  
UNIVERSITAET HANNOVER, APPELSTR. 2  
3000 HANNOVER 1  
WEST-GERMANY

KECSKEMETI, J.  
CENTRAL RESEARCH INSTITUTE  
FOR PHYSICS  
P.O. BOX 49  
1525 BUDAPEST 114  
HUNGARY

KEIZER, P.H.M.  
NIKHEF - K  
P.O. BOX 4395  
  
1009 AJ AMSTERDAM  
THE NETHERLANDS

KERMODE, M.W.  
DAMTP  
LIVERPOOL UNIVERSITY  
P.O. BOX 147  
LIVERPOOL L69 3BX  
GREAT BRITAIN

KHADKIKAR, S.B.  
PHYSICAL RESEARCH LABORATORY  
NAVRANGPURA

AHMEDABAD - 380 009  
INDIA

KHANKHASAYEV, M.  
JOINT INSTITUTE FOR NUCLEAR RESEARCH  
LABORATORY OF THEORETICAL PHYSICS  
HEAD POST OFFICE, P.O. BOX 79  
MOSCOW  
UDSSR

KIM, Y.E.  
DEPARTMENT OF PHYSICS  
PURDUE UNIVERSITY

WEST LAFAYETTE, INDIANA 47907  
USA

KING, SING-NAN  
INSTITUTE OF ATOMIC ENERGY  
P.O. BOX 275(18)  
PEKING  
BEIJING  
THE PEOPLE'S REPUBLIC OF CHINA

KIONTKE, S.  
KERNFORSCHUNGSZENTRUM KARLSRUHE GMBH  
INSTITUT FUER KERNPHYSIK I  
POSTFACH 3640  
7500 KARLSRUHE  
WEST-GERMANY

KIRCHBACH, M.  
JOINT INSTITUTE FOR NUCLEAR RESEARCH  
LTF  
HEAD POST OFFICE, P.O. BOX 79  
MOSCOW  
UDSSR

KIRCHER, R.  
INSTITUT FUER THEORETISCHE PHYSIK  
UNIVERSITAET TUEBINGEN  
AUF DER MORGENSTELLE 14  
7400 TUEBINGEN  
WEST-GERMANY

KLAGES, H.-O.  
KERNFORSCHUNGSZENTRUM KARLSRUHE GMBH  
INSTITUT FUER KERNPHYSIK I  
POSTFACH 3640  
7500 KARLSRUHE  
WEST-GERMANY

KLOET, W.M.  
INSTITUTE FOR THEORETICAL PHYSICS  
SOR BONNELAAN 4  
  
UTRECHT  
THE NETHERLANDS

KLOSE, W.  
KERNFORSCHUNGSZENTRUM KARLSRUHE GMBH  
POSTFACH 3640

7500 KARLSRUHE  
WEST-GERMANY

KLUGE, W.  
KERNFORSCHUNGSZENTRUM KARLSRUHE GMBH  
IK II  
POSTFACH 3640  
7500 KARLSRUHE  
WEST-GERMANY

KNUTSON, L.D.  
PHYSICS DEPARTMENT  
UNIVERSITY OF WISCONSIN  
1150 UNIVERSITY AVENUE  
MADISON, WI 53706  
USA

KOCH, R.  
INSTITUT FUER THEORETISCHE KERNPHYSIK  
UNIVERSITAET KARLSRUHE  
POSTFACH 6380  
7500 KARLSRUHE 1  
WEST-GERMANY



KOCH, H.  
IK 2  
KERNFORSCHUNGSZENTRUM KARLSRUHE  
POSTFACH 3640  
7500 KARLSRUHE  
WEST-GERMANY

KOENIG, V.  
LABORATORIUM FUER KERNPHYSIK  
ETHZ  
HOENGGGERBERG  
8093 ZUERICH  
SWITZERLAND

KOHNO, M.  
INSTITUT FUER THEORETISCHE PHYSIK  
UNIVERSITAET REGENSBURG  
  
8400 REGENSBURG  
WEST-GERMANY

KOIKE, Y.  
RESEARCH CENTER FOR NUCLEAR PHYSICS  
OSAKA UNIVERSITY  
  
IBARAKI, OSAKA, 567  
JAPAN

KOK, L.P.  
INSTITUTE FOR THEORETICAL PHYSICS  
UNIVERSITY OF GRONINGEN  
P.O. BOX 800  
9700 AV GRONINGEN  
THE NETHERLANDS

KOWALSKI, K.L.  
DEPARTMENT OF PHYSICS  
CASE WESTERN RESERVE UNIVERSITY  
UNIVERSITY CIRCLE  
CLEVELAND, OHIO 44106  
USA

KROEGER, H.  
FACULTE DES SCIENCES ET DE GENIE  
DEPARTEMENT DE PHYSIQUE  
UNIVERSITE LAVAL  
QUEBEC, P.Q. G1K 7P4  
CANADA

KROLL, P.  
FACHBEREICH PHYSIK  
UNIVERSITAET WUPPERTAL  
GAUSS-STR. 20  
5600 WUPPERTAL 1  
WEST-GERMANY

KRUG, J.  
INSTITUT FUER EXPERIMENTALPHYSIK I  
RUHR-UNIVERSITAET BOCHUM  
UNIVERSITAETSSTR. 150  
4630 BOCHUM 1  
WEST-GERMANY

KRUPP, H.  
KERNFORSCHUNGSZENTRUM KARLSRUHE GMBH  
INSTITUT FUER KERNPHYSIK I  
POSTFACH 3640  
7500 KARLSRUHE  
WEST-GERMANY

KRUPPA, A.T.  
INSTITUTE OF NUCLEAR RESEARCH  
HUNGARIAN ACADEMY OF SCIENCE  
  
4001 DEBRECEN PF. 51  
HUNGARY

KUDO, Y.  
DEPARTMENT OF PHYSICS  
OSAKA CITY UNIVERSITY  
SUGIMOTO-CHO, SUMIYOSHI-KU  
OSAKA 558  
JAPAN

KUEHN, B.  
ZENTRALINSTITUT FUER KERNFORSCHUNG  
ROSSENDORF  
POSTFACH 19  
8051 DRESDEN  
DDR

KUHLMANN, E.  
INSTITUT FUER EXPERIMENTALPHYSIK  
RUHR-UNIVERSITAET BOCHUM  
UNIVERSITAETSSTR. 150  
4630 BOCHUM  
WEST-GERMANY

KUIPER, H.  
PHYSIKALISCHES INSTITUT  
UNIVERSITAET ERLANGEN-NUERNBERG  
ERWIN-ROMMEL-STR. 1  
8520 ERLANGEN  
WEST-GERMANY

KULSHRESHTHA, D.S.  
DEPARTMENT OF PHYSICS  
UNIVERSITY OF KAISERSLAUTERN  
  
6750 KAISERSLAUTERN  
WEST-GERMANY

KUTI, J.  
DEPARTMENT OF PHYSICS  
UNIVERSITY OF CALIFORNIA AT SAN DIEGO  
9-019  
LA JOLLA, CA 92093  
USA

KUZMICHEV, V.E.  
PHYSIKALISCHES INSTITUT  
UNIVERSITAET BONN  
ENDENICHER ALLEE 11-13  
5300 BONN 1  
WEST-GERMANY

LACOMBE, M.  
INSTITUT DE PHYSIQUE NUCLEAIRE  
DIVISION DE PHYSIQUE THEORIQUE  
B.P. NO. 1  
91406 ORSAY  
FRANCE

LAGU, A.V.  
DEPARTMENT OF PHYSICS  
BANARAS HINDU UNIVERSITY  
  
VARANASI - 221005  
INDIA

LANDAU, R.H.  
DEPARTMENT OF PHYSICS  
OREGON STATE UNIVERSITY  
  
CORVALLIS, OREGON 97331  
USA

LAPOINTE, C.  
PHYSICS DEPARTMENT  
UNIVERSITY OF MANITOBA

WINNIPEG, MANITOBA R3T 2N2  
CANADA

LEE, T.-S. H.  
PHYSICS DIVISION  
ARGONNE NATIONAL LABORATORY  
  
ARGONNE, ILL. 60439  
USA

LEEB, H.  
INSTITUT FUER KERNPHYSIK  
TECHNISCHE UNIVERSITAET WIEN  
SCHUETTELSTRASSE 115  
1020 WIEN  
AUSTRIA

LEHAR, F.  
D.PH.P.E. - CEN-SACLAY  
BAT. 141  
B.P. 2  
91191 GIF-SUR-YVETTE CEDEX  
FRANCE

LEHMAN, D.R.  
DEPARTMENT OF PHYSICS  
THE GEORGE WASHINGTON UNIVERSITY  
  
WASHINGTON, D.C. 20052  
USA

LEKKAS, P.  
INSTITUT FUER EXPERIMENTALPHYSIK I  
RUHR-UNIVERSITAET BOCHUM  
UNIVERSITAETSSTRASSE  
4630 BOCHUM  
WEST-GERMANY

LELEUX, P.  
INSTITUT DE PHYSIQUE  
UNIVERSITE DE LOUVAIN  
2 CHEMIN DU CYCLOTRON  
1348 LOUVAIN-LA-NEUVE  
BELGIUM

LENZ, F.  
  
SIN  
  
5234 VILLIGEN  
SWITZERLAND

LETOURNEUX, J.  
LABORATOIRE DE PHYSIQUE NUCLEAIRE  
UNIVERSITE DE MONTREAL  
C.P. 6128  
MONTREAL H3C 3J7  
CANADA

LEVIN, F.S.  
PHYSICS DEPARTMENT  
BROWN UNIVERSITY

PROVIDENCE, RI 02912  
USA

LIM, T.K.  
DEPARTMENT OF PHYSICS AND  
ATMOSPHERIC SCIENCE  
DREXEL UNIVERSITY  
PHILADELPHIA, PA 19104  
USA

LINDESAY, J.  
STANFORD LINEAR ACCELERATOR CENTER  
BIN 81  
P.O. BOX 4349  
STANFORD, CA 94305  
USA

LINDNER, A.  
1. INSTITUT FUER EXPERIMENTALPHYSIK  
UNIVERSITAET HAMBURG  
JUNGIUSSTR. 9  
2000 HAMBURG 36  
WEST-GERMANY

LIU, K. F.  
DEPT. OF PHYSICS &  
ASTRONOMY  
UNIVERSITY OF KENTUCKY  
LEXINGTON, KY 40506  
USA

LOCHER, M.  
  
SIN  
  
5234 VILLIGEN  
SWITZERLAND

LODHI, M.A.K.

DEPARTMENT OF PHYSICS  
TEXAS TECH. UNIVERSITY  
BOX 4180  
LUBBOCK, TX 79409  
USA

MAHALANABIS, J.

THEO. NUC. PHYS. DIV.  
SAHA INSTITUTE OF NUCLEAR PHYSICS  
92 A.P.C. ROAD  
CALCUTTA 700009  
INDIA

LOISEAU, B.

DIV. DE PHYSIQUE THEOR.  
IPN  
B.P.1  
91406 ORSAY  
FRANCE

MAIER, C.

KERNFORSCHUNGSZENTRUM KARLSRUHE GMBH  
INSTITUT FUER KERNPHYSIK I  
POSTFACH 3640  
7500 KARLSRUHE  
WEST-GERMANY

LOLOS, G.J.

TRIUMF  
4004 WESBROOK MALL

MANDELZWEIG, V.B.

RAHAT INSTITUTE OF PHYSICS  
HEBREW UNIVERSITY

VANCOUVER, B.C. V6T 2A3  
CANADA

JERUSALEM 91904  
ISRAEL

LOMON, E.

MASS. INST. OF TECH.  
6 - 304

MARGAZIOTIS, D.J.

CALIFORNIA STATE UNIVERSITY  
LOS ANGELES  
745 ILIFF ST.  
PACIFIC PALISADES, CA 90272  
USA

CAMBRIDGE, MA 02139  
USA

LOVAS, I.

CENTRAL RESEARCH INSTITUTE  
FOR PHYSICS  
P.O. BOX 49  
1525 BUDAPEST 114  
HUNGARY

MARTORELL, J.

DEPARTAMENTO DE FISICA  
ATOMICA Y NUCLEAR  
UNIVERSIDAD DE PALMA DE MALLORCA  
PALMA DE MALLORCA  
SPAIN

LOVITCH, L.

ISTITUTO DI FISICA  
UNIVERSITA DI FERRARA  
VIA PARADISO, 12  
44100 FERRARA  
ITALY

MASCHOW, R.

KERNFORSCHUNGSZENTRUM KARLSRUHE GMBH  
IK I  
POSTFACH 3640  
7500 KARLSRUHE  
WEST-GERMANY

LUEBCKE, W.

INSTITUT FUER EXPERIMENTALPHYSIK I  
RUHR-UNIVERSITAET BOCHUM  
UNIVERSITAETSSTRASSE  
4630 BOCHUM  
WEST-GERMANY

MASSARO, P.A.

DIPART. DI FISICA DELL'UNIVERSITA  
SEZIONE I N F N  
VIA AMENDOLA 173  
70126 BARI  
ITALY

MACHLEIDT, R.

INSTITUT FUER THEORETISCHE KERNPHYSIK  
UNIVERSITAET BONN  
NUSSALLEE 14-16  
5300 BONN  
WEST-GERMANY

MATHELITSCH, L.

INSTITUT FUER THEORETISCHE PHYSIK  
UNIVERSITAET GRAZ  
UNIVERSITAETSPLATZ 5  
8010 GRAZ  
AUSTRIA

MACQ, P.

INSTITUT DE PHYSIQUE  
UNIVERSITE DE LOUVAIN  
2 CHEMIN DU CYCLOTRON  
1348 LOUVAIN-LA-NEUVE  
BELGIUM

MATHIE, E.L.

SIN

5234 VILLIGEN  
SWITZERLAND

MATHUR, V.S.  
DEPARTMENT OF PHYSICS  
BANARAS HINDU UNIVERSITY

VARANASI, 221005  
INDIA

MATTHAEY, H.  
KERNFORSCHUNGSZENTRUM KARLSRUHE GMBH  
IK II  
POSTFACH 3640  
7500 KARLSRUHE  
WEST-GERMANY

MCKEE, J.S.C.  
DEPARTMENT OF PHYSICS  
UNIVERSITY OF MANITOBA

WINNIPEG, MANITOBA R3T 2N2  
CANADA

MCKELLAR, B.H.J.  
SCHOOL OF PHYSICS  
UNIVERSITY OF MELBOURNE

PARKVILLE, VIC. 3052  
AUSTRALIA

MEIER, W.  
INSTITUT FUER THEORETISCHE PHYSIK II  
RUHR-UNIVERSITAET

4630 BOCHUM  
WEST-GERMANY

MEISSNER, U.G.  
INSTITUT FUER THEORETISCHE PHYSIK II  
RUHR-UNIVERSITAET BOCHUM  
UNIVERSITAETSSTR. 150  
4630 BOCHUM  
WEST-GERMANY

MERTELMEIER, T.  
INSTITUT FUER THEORETISCHE PHYSIK  
UNIVERSITAET ERLANGEN-NUERNBERG  
GLUECKSTR. 6  
8520 ERLANGEN  
WEST-GERMANY

MILLER, G.  
PHYSICS DEPARTMENT  
UNIVERSITY OF WASHINGTON  
FM-15  
SEATTLE, WA 98195  
USA

MINEHART, R.C.  
PHYSICS DEPARTMENT  
UNIVERSITY OF VIRGINIA  
MC CORMICK ROAD  
CHARLOTTESVILLE, VA 22901  
USA

MITRA, A.N.  
DEPARTMENT OF PHYSICS  
DELHI UNIVERSITY  
244 TAGORE PARK  
DELHI - 110009  
INDIA

MIZUTANI, T.  
DEPARTMENT OF PHYSICS  
VIRGINIA POLYTECHNIC INSTITUTE AND  
STATE UNIVERSITY  
BLACKSBURG, VIRGINIA 24061  
USA

MORAVCSIK, M.J.  
INSTITUTE OF THEORETICAL SCIENCE  
UNIVERSITY OF OREGON

EUGENE, OREGON 97403  
USA

MORIOKA, S.  
DIVISION DE PHYSIQUE THEORIQUE  
I.P.N.  
B.P. NO. 1  
91406 ORSAY CEDEX  
FRANCE

MOSCONI, B.  
ISTITUTO DI FISICA TEORICA  
DELL UNIVERSITA DI FIRENZE  
LARGO ENRICO FERMI, 2  
50125 FIRENZE  
ITALY

MOSS, G.A.  
NUCLEAR RESEARCH CENTRE  
UNIVERSITY OF ALBERTA

EDMONTON, ALBERTA T6G 2N5  
CANADA

MOSZKOWSKI, S.A.  
DEPARTMENT OF PHYSICS  
UNIVERSITY OF CALIFORNIA

LOS ANGELES, CA 90024  
USA

MUJICA, V.  
UPPSALA UNIVERSITY  
QUANTUM CHEMISTRY GROUP  
BOX 518  
751 20 UPPSALA  
SWEDEN

MUKHOPADHYAY, D.  
INSTITUT FUER THEORETISCHE PHYSIK  
PHILOSOPHENWEG 19

6900 HEIDELBERG  
WEST-GERMANY

MULDERS, P.J.  
CENTER FOR THEORETICAL PHYSICS, 6-405  
MASSACHUSETTS INSTITUTE OF TECHNOLOGY

CAMBRIDGE, MA 02139  
USA

MYHRER, F.  
DEPARTMENT OF PHYSICS  
UNIVERSITY OF SOUTH CAROLINA

COLUMBIA, SC 29208  
USA

NAKAGAWA, K.  
PHYSICAL SCIENCE LABORATORIES  
NIHON UNIVERSITY  
7-24-1 NARASHINO-DAI FUNABASHI  
CHIBA  
JAPAN

NAKAICHI-MAEDA, S.  
INSTITUT FUER THEORETISCHE PHYSIK  
UNIVERSITAET TUEBINGEN  
AUF DER MORGENSTELLE 14  
7400 TUEBINGEN 1  
WEST-GERMANY

NAKANO, K.  
DESY  
PAVILLON  
LURUPER CHAUSSEE  
2000 HAMBURG  
WEST-GERMANY

NAMYSLOWSKI, J.M.  
INSTITUTE OF THEORETICAL PHYSICS  
WARSAW UNIVERSITY  
UL. HOZA 69  
00-681 WARSAW  
POLAND

NATH, S.  
CYCLOTRON INSTITUTE  
TEXAS A&M UNIVERSITY

COLLEGE STATION, TX 77843  
USA

NEFKENS, B.M.K.  
UCLA  
PHYSICS DEPARTMENT  
405 HILGARD AVENUE  
LOS ANGELES, CALIFORNIA 90024  
USA

NENCKA-FICEK, H.  
INSTYTUT FIZYKI MOLEKULARNEJ  
POLSKIEJ AKADEMII NAUK  
SMOLUCHOWSKIEGO 17/19  
POZNAN  
POLAND

NESSI-TEDALDI, F.  
LABORATORIUM FUER KERNPHYSIK  
EIDG. TECHNISCHE HOCHSCHULE  
HOENGERBERG  
8093 ZUERICH  
SWITZERLAND

NICKLAS, G.  
FAKULTAET FUER PHYSIK  
UNIVERSITAET FREIBURG  
HERMANN-HERDER-STR. 3  
7800 FREIBURG  
WEST-GERMANY

NINANE, A.  
INSTITUT DE PHYSIQUE  
UNIVERSITE DE LOUVAIN  
2 CHEMIN DU CYCLOTRON  
1348 LOUVAIN-LA-NEUVE  
BELGIUM

NISKANEN, J.A.  
RESEARCH INSTITUTE FOR THEOR. PHYSICS  
UNIVERSITY OF HELSINKI  
SILTAVUORENPENGER 20 C  
00170 HELSINKI 17  
FINLAND

NITZ, W.  
KERNFORSCHUNGSZENTRUM KARLSRUHE GMBH  
INSTITUT FUER KERNPHYSIK I  
POSTFACH 3640  
7500 KARLSRUHE  
WEST-GERMANY

NOGAMI, Y.  
PHYSICS DEPT. THEORY GROUP  
MC MASTER UNIVERSITY

HAMILTON, ONTARIO L8S 4M1  
CANADA

NORTHCLIFFE, L.C.  
CYCLOTRON INSTITUTE  
TEXAS A&M UNIVERSITY

COLLEGE STATION, TX 77843  
USA

NOYES, H.P.  
STANFORD LINEAR ACCELERATOR CENTER  
BIN 81  
P.O. BOX 4349  
STANFORD, CA 94305  
USA

OEHM, W.  
PHYSIKALISCHES INSTITUT, AVZ I  
UNIVERSITAET BONN  
ENDENICHER ALLEE 11-13  
5300 BONN 1  
WEST-GERMANY

OHKUBO, S.  
DEPARTMENT OF APPLIED SCIENCE  
KOCHI WOMEN'S UNIVERSITY

KOCHI 780  
JAPAN

OKA, M.  
CENTER FOR THEORETICAL PHYSICS  
MASSACHUSETTS INSTITUTE OF TECHNOLOGY  
RM. 6-412A  
CAMBRIDGE, MA 02139  
USA

OKABE, S.  
UNIVERSITAET GH SIEGEN  
FACHBEREICH PHYSIK

5900 SIEGEN 21  
WEST-GERMANY

OKUMUSOGLU, N.T.  
FIZIK BOELUEMUE  
DEPARTMENT ON PHYSICS  
19 MAYIS UENIVERSITESI  
ATAKUM, SAMSUN  
TURKEY

ONEL, Y.  
DEPT. DE PHYS. NUCLEAIRE  
UNIVERSITE DE GENEVE  
32, BD D'YVOY  
1211 GENEVE 4  
SWITZERLAND

ONO, S.  
CERN  
THEORY DIVISION  
  
GENEVE  
SWITZERLAND

ORLOWSKI, M.K.L.  
PURDUE UNIVERSITY  
DEPARTMENT OF PHYSICS

WEST LAFAYETTE, IN 47907  
USA

ORYU, S.  
DEPARTMENT OF PHYSICS  
FACULTY OF SCIENCE AND TECHNOLOGY  
SCIENCE UNIVERSITY OF TOKYO  
NODA, CHIBA 278  
JAPAN

OSET, E.  
DPTO. DE FISICA ATOMICA Y NUCLEAR  
FACULTAD DE CIENCIAS  
UNIVERSIDAD DE VALLADOLID  
VALLADOLID  
ESPANA

OSMAN, A.  
THEORETICAN NUCLEAR PHYSICS  
PHYSICS DEPARTMENT  
FACULTY OF SCIENCE, CAIRO UNIVERSITY  
CAIRO  
EGYPT

OSWALD, H.  
INSTITUT FUER KERNPHYSIK  
UNIVERSITAET KOELN  
ZUELPICHER STR. 77  
5000 KOELN 41  
WEST-GERMANY

OTTEWELL, D.F.  
TRIUMF  
4004 WESBROOK MALL

VANCOUVER, B.C. V6T 2A3  
CANADA

PACE, E.  
I.N.F.N. SEZIONE SANITA  
ISTITUTO SUPERIORE DI SANITA  
VIALE REGINA ELENA 299  
00161 ROMA  
ITALY

PAETZ GEN. SCHIECK, H.  
INSTITUT FUER KERNPHYSIK  
UNIVERSITAET KOELN  
ZUELPICHER STR. 77  
5000 KOELN 41  
WEST-GERMANY

PAIANO, G.P.  
ISTITUTO DI FISICA  
UNIVERSITA DI BARI  
VIA AMENDOLA 173  
70126 BARI  
ITALY

PAIC, G.  
INST. "RUDJER BOSKOVIC"  
BIJENICKA 54  
P.O. BOX 1016  
41001 ZAGREB  
YUGOSLAVIA

PARMENTOLA, J.  
DEPARTMENT OF PHYSICS AND ASTRONOMY  
UNIVERSITY OF PITTSBURGH

PITTSBURGH, PA. 15260  
USA

PAYNE, G.L.  
PHYSICS DEPARTMENT  
305 VAN  
UNIVERSITY OF IOWA  
IOWA CITY, IOWA 52242  
USA

PENA, M.T.  
CENTRO DE FISICA NUCLEAR DA  
UNIVERSIDADE DE LISBOA  
AV. PROF. GAMA PISITO, 2  
1699 LISBOA CODEX  
PORTUGAL

PERROT, F.  
D.PH. NME  
CEN SACLAY

91191 GIF-SUR-YVETTE CEDEX  
FRANCE

PICOZZA, P.  
LABORATORI NAZIONALI DI  
FRASCATI DELL'INFN  
CASELLA POSTALE 13  
00044 FRASCATI (ROME)  
ITALY

PILKUHN, H.  
INST. FUER THEOR. KERNPHYSIK  
UNIVERSITAET KARLSRUHE  
POSTFACH 6380  
7500 KARLSRUHE  
WEST-GERMANY

PIRNER, H.J.  
INSTITUT FUER THEORETISCHE PHYSIK  
UNIVERSITAET HEIDELBERG  
PHILOSOPHENWEG 19  
6900 HEIDELBERG  
WEST-GERMANY

PISENT, G.  
ISTITUTO DI FISICA DELL'UNIVERSITA  
VIA MARZOLO 8  
35100 PADOVA  
ITALY

PLATTNER, G.R.  
INSTITUT FUER THEORETISCHE PHYSIK  
UNIVERSITAET BASEL  
KLINGELBERGSTR. 82  
4056 BASEL  
SWITZERLAND

PLENDL, H.S.  
DEPARTMENT OF PHYSICS  
FLORIDA STATE UNIVERSITY  
TALLAHASSEE, FLORIDA 32306  
USA

PLESSAS, W.  
INSTITUT FUER THEORETISCHE PHYSIK  
UNIVERSITAET GRAZ  
UNIVERSITAETSPLATZ 5  
8010 GRAZ  
AUSTRIA

PLISCHKE, P.  
UNIVERSITAET KARLSRUHE  
IEKP  
POSTFACH 6380  
7500 KARLSRUHE  
WEST-GERMANY

POEPPING, H.  
INSTITUT FUER THEORETISCHE PHYSIK  
UNIVERSITAET HANNOVER  
APPELSTR. 2  
3000 HANNOVER 1  
WEST-GERMANY

POLYZOU, W.N.  
DEPARTMENT OF PHYSICS  
AND ASTRONOMY  
UNIVERSITY OF IOWA  
IOWA CITY, IOWA 52242  
USA

POULIOT, J.  
PHYSICS DEPARTMENT  
LAVAL UNIVERSITY

STE-FOY, P.Q. G1K 7P4  
CANADA

PRESTON, M.A.  
DEPARTMENT OF PHYSICS  
UNIVERSITY OF SASKATCHEWAN

SASKATOON S7N 0W0  
CANADA

PRORIOL, J.  
LABORATOIRE DE PHYSIQUE COPUSCULAIRE  
UNIVERSITE DE CLERMONT II  
LES CEZEAX  
63170 AUBIERE  
FRANCE

QUARATI, P.  
DIPARTIMENTO FISICA  
UNIVERSITA DI CAGLIARI  
VIA OSPEDALE 72  
09100 CAGLIARI  
ITALY

RANSOME, R.D.  
CERN  
EP DIV.

1211 GENEVE 23  
SWITZERLAND

RASHID, K.  
NUCLEAR PHYSICS DIVISION  
PAKISTAN INST. OF SCIENCE AND TECHN.  
P.O. NILORE  
RAWALPINDI  
PAKISTAN



RAYCHAUDHURI, P.  
DEPARTMENT OF APPLIED MATHEMATICS  
UNIVERSITY OF CALCUTTA  
  
CALCUTTA-700009  
INDIA

REBEL, H.  
KERNFORSCHUNGSZENTRUM KARLSRUHE GMBH  
INSTITUT FUER KERNPHYSIK III  
POSTFACH 3640  
7500 KARLSRUHE  
WEST-GERMANY

REDISH, E.F.  
DEPARTMENT OF PHYSICS  
UNIVERSITY OF MARYLAND  
  
COLLEGE PARK, MD 20742  
USA

REICHEL, T.  
PHYSIKALISCHES INSTITUT  
UNIVERSITAET BONN  
NUSSALLEE 12  
5300 BONN  
WEST-GERMANY

REINER, M.J.  
DEPARTMENT OF PHYSICS  
HOLLINS COLLEGE

HOLLINS COLLEGE, VIRGINIA 24020  
USA

REMANE, E.  
KERNFORSCHUNGSZENTRUM KARLSRUHE GMBH  
INSTITUT FUER KERNPHYSIK I  
POSTFACH 3640  
7500 KARLSRUHE  
WEST-GERMANY

REUSCHER, M.  
KERNFORSCHUNGSZENTRUM KARLSRUHE GMBH  
INSTITUT FUER KERNPHYSIK I  
POSTFACH 3640  
7500 KARLSRUHE  
WEST-GERMANY

REVAI, J.  
CENTRAL RESEARCH INSTITUTE  
FOR PHYSICS  
P.O. BOX 49  
1525 BUDAPEST 114  
HUNGARY

RICHARD, J.M.  
DIVISION DE PHYSIQUE THEORIQUE  
INSTITUT DE PHYSIQUE NUCLEAIRE  
  
91406 ORSAY  
FRANCE

RICHARDSON, J.R.  
TRIUMF  
UBC  
4004 WESBROOK MALL  
VANCOUVER, B.C. V6T 2A3  
CANADA

RILEY, P.J.  
DEPARTMENT OF PHYSICS  
RLM 5.208  
UNIVERSITY OF TEXAS  
AUSTIN, TEXAS 78712  
USA

RINAT, A.S.  
WEIZMANN INSTITUTE OF SCIENCE  
DEPARTMENT OF PHYSICS

REHOVOT 76100  
ISRAEL

ROBSON, D.  
PHYSICS DEPARTMENT  
FLORIDA STATE UNIVERSITY

TALLAHASSEE, FL 32301  
USA

ROCKMORE, R.  
PHYSICS DEPARTMENT  
RUTGERS UNIVERSITY

PISCATAWAY, N.J. 08854  
USA

RODNEY, W.S.  
DIVISION OF PHYSICS  
NATIONAL SCIENCE FOUNDATION  
1800 G. STREET, NW  
WASHINGTON, DC 20550  
USA

ROESSLE, E.  
FAKULTAET FUER PHYSIK  
HERMANN-HERDER-STRASSE 3

7800 FREIBURG  
WEST-GERMANY

ROSA-CLOT, M.  
ISTITUTO DI FISICA  
UNIVERSITA DI PISA  
PIAZZA TORRICELLI 2  
56100 PISA  
ITALY

ROSER, T.  
LABOR FUER KERNPHYSIK  
ETH ZUERICH  
HOENGERBERG  
8093 ZUERICH  
SWITZERLAND

ROY, R.  
PHYSICS DEPARTMENT  
LAVAL UNIVERSITY

SAINTE-FOY, P.Q. G1K 7P4  
CANADA

RUIJGROK, TH.W.  
INSTITUTE FOR THEORETICAL PHYSICS  
PRINCETONPLEIN 5  
P.O. BOX 80.006  
3508 TA UTRECHT  
THE NETHERLANDS

RUPP, G.  
ZIF  
UNIVERSITAET BIELEFELD  
WELLENBERG 1  
4800 BIELEFELD 1  
WEST-GERMANY

SADLER, M.E.  
ABILENE CHRISTIAN UNIVERSITY  
BOX 7646  
915/677-1911  
ABILENE, TEXAS 79699  
USA

SAGHAI, B.  
INSTITUT DE RECHERCHE FONDAMENTALE  
D.P.H.N-HE  
CEN-SACLAY  
F-91191 GIF-SUR-YVETTE CEDEX  
FRANCE

SAMPAIO, A.A.  
CENTRO DE FISICA NUCLEAR  
UNIVERSIDADE DE LISBOA  
AV. PROD. GAMA PINTO, 2  
1699 LISBOA CODEX  
PORTUGAL

SANDHAS, W.  
PHYSIKALISCHES INSTITUT  
UNIVERSITAET BONN  
ENDENICHER ALLEE 11-13  
5300 BONN  
WEST-GERMANY

SASAKAWA, T.  
DEPARTMENT OF PHYSICS  
TOHOKU UNIVERSITY

980 SENDAI  
JAPAN

SATOH, E.  
CHIBA-KEIZA COLLEGE  
4-3-30 , TODOROKI-CHO  
CHIBA-SHI  
CHIBA 260  
JAPAN

SAUER, P.U.  
INSTITUT FUER THEORETISCHE PHYSIK  
TU HANNOVER  
APPELSTR. 1  
3000 HANNOVER  
WEST-GERMANY

SAUERLAND, T.  
INSTITUT FUER EXPERIMENTALPHYSIK  
RUHRUNIVERSITAET BOCHUM  
POSTFACH 10 21 48  
4630 BOCHUM  
WEST-GERMANY

SAWICKI, M.  
SLAC  
STANFORD UNIVERSITY  
P.O. BOX 4349  
STANFORD, CA 94305  
USA

SCHATZ, G.  
KERNFORSCHUNGSZENTRUM KARLSRUHE GMBH  
INSTITUT FUER KERNPHYSIK III  
POSTFACH 3640  
7500 KARLSRUHE  
WEST-GERMANY

SCHECK, F.  
INSTITUT FUER PHYSIK  
UNIVERSITAET MAINZ  
POSTFACH 3980  
6500 MAINZ  
WEST-GERMANY

SCHIERHOLZ, G.  
DESY  
NOTKESTR. 85  
2000 HAMBURG 52  
WEST-GERMANY

SCHMELZER, R.  
PHYSIKALISCHES INSTITUT  
UNIVERSITAET ERLANGEN-NUERNBERG  
ERWIN-ROMMEL-STR. 1  
8520 ERLANGEN  
WEST-GERMANY

SCHMID, E.W.  
INSTITUT FUER THEORETISCHE PHYSIK  
UNIVERSITAET TUEBINGEN  
AUF DER MORGENSTELLE 14  
7400 TUEBINGEN  
WEST-GERMANY

SCHMITT, H.  
FAKULTAET FUER PHYSIK  
UNIVERSITAET FREIBURG  
HERMANN-HERDER-STR. 3  
7800 FREIBURG I. BR.  
WEST-GERMANY

SCHOEBERL, M.  
 PHYSIKALISCHES INSTITUT  
 UNIVERSITAET ERLANGEN-NUERNBERG  
 ERWIN-ROMMEL-STR. 1  
 8520 ERLANGEN  
 WEST-GERMANY

SILBAR, R.R.  
 T-5, MS-B283  
 LOS ALAMOS NAT. LAB.  
  
 LOS ALAMOS, NM 87545  
 USA

SCHULZ, R.  
 KERNFORSCHUNGSZENTRUM KARLSRUHE GMBH  
 INSTITUT FUER KERNPHYSIK I  
 POSTFACH 3640  
 7500 KARLSRUHE  
 WEST-GERMANY

SIMMONS, J.E.  
 PHYSICS DIVISION  
 MAIL STOP D456  
 LOS ALAMOS NATIONAL LABORATORY  
 LOS ALAMOS, NM 87545  
 USA

SCHWEIGER, W.  
 INSTITUT FUER THEORETISCHE PHYSIK  
 UNIVERSITAET GRAZ  
 UNIVERSITAETSPLATZ 5  
 8010 GRAZ  
 AUSTRIA

SIMONIUS, M.  
 LABORATORIUM FUER KERNPHYSIK  
 ETH  
 HOENGGERBERG  
 8093 ZUERICH  
 SWITZERLAND

SEICHERT, M.  
 SEKTION PHYSIK  
 UNIVERSITAET MUEENCHEN  
 AM COULOMBWALL 1  
 8046 GARCHING  
 WEST-GERMANY

SIMONOV, YU.A.  
 INST. THEOR. EXPER. PHYSICS  
 ATOMIC ENERGY COMM.  
 B. CHEREMUSHKINSKAYA UL. 89  
 117259 MOSCOW U-259  
 UDSSR

SEKI, R.  
 DEPARTMENT OF PHYSICS AND ASTRONOMY  
 CALIFORNIA STATE UNIVERSITY  
  
 NORTHRIDGE, CA 91330  
 USA

SLAUS, I.  
 INST. "RUDJER BOSKOVIC"  
 BIJENICKA 54  
 P.O. BOX 1016  
 41001 ZAGREB  
 YUGOSLAVIA

SESMA, J.  
 DEPARTAMENTO DE FISICA TEORICA  
 FACULTAD DE CIENCIAS  
 UNIVERSIDAD DE ZARAGOZA  
 ZARAGOZA  
 SPAIN

SLOBODRIAN, R.J.  
 DEPARTEMENT DE PHYSIQUE  
 UNIVERSITE LAVAL  
 CITE UNIVERSITAIRE  
 STE. FOY, QUE. G1K 7P4  
 CANADA

SETH, K.K.  
 PHYSICS DEPARTMENT  
 NORTHWESTERN UNIVERSITY  
  
 EVANSTON, IL 60201  
 USA

SMITH, G.  
  
 SIN  
  
 5234 VILLIGEN  
 SWITZERLAND

SHIBATA, T.-A.  
 CERN  
 EP-DIVISION  
  
 1211 GENEVE 23  
 SWITZERLAND

SMITH, R.A.  
 DEPARTMENT OF PHYSICS  
 TEXAS A&M UNIVERSITY  
  
 COLLEGE STATION, TEXAS 77843  
 USA

SICK, I.  
 INSTITUT FUER THEORETISCHE PHYSIK  
 UNIVERSITAET BASEL  
 KLINGELBERGSTR. 82  
 4056 BASEL  
 SWITZERLAND

SOFIANOS, S.A.  
 PHYSICS DEPARTMENT  
 UNIVERSITY OF SOUTH AFRICA  
 P.O.BOX 392  
 0001 PRETORIA  
 REPUBLIC OF SOUTH AFRICA

SPITZ, G.R.  
 INSTITUT FUER THEORETISCHE PHYSIK  
 UNIVERSITAET TUEBINGEN  
 AUF DER MORGENSTELLE 14  
 7400 TUEBINGEN 1  
 WEST-GERMANY

SPRUNG, D.W.L.  
 DEPARTMENT OF PHYSICS  
 THEORY GROUP  
 MCMASTER UNIVERSITY  
 HAMILTON, ONTARIO L8S 4M1  
 CANADA

STEPHAN, M.  
 INSTITUT FUER EXPERIMENTALPHYSIK I  
 RUHR-UNIVERSITAET BOCHUM  
 UNIVERSITAETSSTRASSE  
 4630 BOCHUM  
 WEST-GERMANY

STEPHENSON, E.J.  
 INDIANA UNIVERSITY CYCLOTRON FACILITY  
 2401 MILO B, SAMPSON LANE  
  
 BLOOMINGTON, INDIANA 47405  
 USA

STEWART, N.M.  
 PHYSICS DEPARTMENT  
 BEDFORD COLLEGE  
 UNIVERSITY OF LONDON, REGENTS PARK  
 LONDON NW1,4NS  
 ENGLAND

STINGL, M.  
 INST. FUER THEOR. PHYSIK I  
 UNIVERSITAET MUENSTER  
 DOMAGKSTR. 71  
 4400 MUENSTER  
 WEST-GERMANY

STREIT, L.  
 ZENTRUM FUER  
 INTERDISZIPLINAERE FORSCHUNG  
 WELLENBERG 1  
 4800 BIELEFELD 1  
 WEST-GERMANY

SUZUKI, Y.  
 DEPARTMENT OF PHYSICS  
 NIIGATA UNIVERSITY  
 IKARASHI  
 NIIGATA 950-21  
 JAPAN

SVARC, A.  
  
 SIN  
  
 5234 VILLIGEN  
 SWITZERLAND

SVENNE, J.P.  
 DEPARTMENT OF PHYSICS  
 UNIVERSITY OF MANITOBA  
  
 WINNIPEG, MANITOBA R3T 2N2  
 CANADA

TALUKDAR, B.  
 DEPARTMENT OF PHYSICS  
 VISVA-BHARATI UNIVERSITY

SANTINIKETAN 731235, WEST BENGAL  
 INDIA

TANAKA, H.  
 DEPT. OF PHYSICS, FACULTY OF SCIENCE  
 HOKKAIDO UNIVERSITY  
 KITA 10, NISHI 8  
 SAPPORO 060  
 JAPAN

TANG, Y.C.  
 SCHOOL OF PHYSICS AND ASTRONOMY  
 UNIVERSITY OF MINNESOTA  
 148 PHYSICS BUILDING  
 MINNEAPOLIS, MINN. 55455  
 USA

TATISCHEFF, B.  
 INSTITUT DE PHYSIQUE NUCLEAIRE  
 CNRS,IN2P3  
 BOITE POSTALE NO. 1  
 91406 ORSAY CEDEX  
 FRANCE

TEODORO, M.R.  
 INSTITUTO DE FISICA - UFRGS  
 AV. LUIZ ENGLERT S/NO  
 PORTO ALEGRE - RS  
 90.000 BRASIL  
 BRASIL

THALHEIM, H.-O.  
 INSTITUT FUER PHYSIK  
 JOHANNES-GUTENBERG UNIVERSITAET  
 JAKOB-WELDER WEG 11  
 6500 MAINZ 1  
 WEST-GERMANY

THOMAS, A.W.  
 DIVISION TH  
 CERN

1211 GENEVE 23  
 SWITZERLAND

THOME, Z.D.  
 PROGRAMA DE ENG. NUCLEAR, COPPE/UFRJ  
 UNIVERSIDADE FEDERAL DO RIO DE JANEIRO  
 CAIXA POSTAL 68 509 - CEP 21 944  
 RIO DE JANEIRO  
 BRASIL

TOHSAKI-SUZUKI, A.  
PHYSICS LABORATORY, FACULTY OF  
TEXTILE SCIENCE AND TECHNOLOGY  
SHINSHU UNIVERSITY  
TOKIDA, UEDA, NAGANO PRE. ZIP 386  
JAPAN

TOKER, G.  
DEPARTMENT OF NUCLEAR PHYSICS  
THE WEIZMANN INSTITUTE OF SCIENCE  
REHOVOT 76100  
ISRAEL

TOSTEVIN, J.A.  
PHYSICS DEPARTMENT  
UNIVERSITY OF SURREY

GUILDFORD, SURREY GU2 5XH  
ENGLAND

ULBRICHT, J.  
ETH - ZUERICH  
LABORATORIUM FUER KERNPHYSIK  
HOENGERBERG  
8093 ZUERICH  
SWITZERLAND

ULLRICH, H.  
KERNFORSCHUNGSZENTRUM KARLSRUHE GMBH  
IK II  
POSTFACH 3640  
7500 KARLSRUHE  
WEST-GERMANY

UMLAND, E.A.  
TW BONNER NUCLEAR LABORATORY  
RICE UNIVERSITY

HOUSTON, TEXAS 77251  
USA

URBANO, J.N.  
INSTITUT FUER KERNPHYSIK  
KFA - JUELICH  
POSTFACH 1913  
5170 JUELICH 1  
WEST-GERMANY

VAN FAASSEN, E.E.H.  
INSTITUUT VOOR THEORETISCHE FYSICA  
PRINCETON PLEIN 5  
P.O. BOX 80006  
3508 TA UTRECHT  
THE NETHERLANDS

VAN GEFFEN, F.M.M.  
NATUURKUNDIG LABORATORIUM  
VRIJE UNIVERSITEIT  
DE BOEELAAN 1081  
1081 HV AMSTERDAM  
THE NETHERLANDS

VAN OERS, W.T.H.  
TRIUMF  
4004 WESBROOK MALL

VANCOUVER, B.C. V6T 2A3  
CANADA

VAN WAGENINGEN, R.  
NATUURKUNDIG LABORATORIUM  
DER VRIJE UNIVERSITEIT  
DEL BOEELAAN 1081  
1081 HV AMSTERDAM  
THE NETHERLANDS

VANZANI, V.  
ISTITUTO DI FISICA  
UNIVERSITA DI PADOVA  
VIA MARZOLO, 8  
35100 PADOVA  
ITALY

VEIT, E.A.  
TRIUMF  
UNIVERSITY OF BRITISH COLUMBIA  
4004 WESBROOK MALL  
VANCOUVER, B.C. V6T 2A3  
CANADA

VIOLIER, R.D.  
INSTITUTE FOR THEORETICAL PHYSICS  
UNIVERSITY OF BASEL  
KLINGELBERGSTR. 82  
4056 BASEL  
SWITZERLAND

VOGELZANG, J.  
NATUURKUNDIG LABORATORIUM  
DER VRIJE UNIVERSITEIT  
DE BOEELAAN 1081  
1081 HV AMSTERDAM  
THE NETHERLANDS

VON WITSCH, W.  
INST. FUER STRAHLEN- UND KERNPHYSIK  
UNIVERSITAET BONN  
NUSSALLEE 14-16  
5300 BONN  
WEST-GERMANY

WADA, M.  
PHYSICAL SCIENCE LABORATORIES  
COLLEGE OF SCIENCE AND TECHNOLOGY  
NIHON UNIV., 7-24-1 NARASHINO-DAI  
FUNABASHI (274)  
JAPAN

WAGNER, M.  
INSTITUT FUER PHYSIK  
JOHANNES-GUTENBERG UNIVERSITAET  
JAKOB-WELDER WEG 11  
6500 MAINZ 1  
WEST-GERMANY

WALTER, R.  
PHYSICS DEPARTMENT  
DUKE UNIVERSITY

DURHAM, N.C. 27706  
USA

WATT, A.  
DEPARTMENT OF PHYSICS  
UNIVERSITY OF GLASGOW

GLASGOW, G12 8QQ  
SCOTLAND

WEBER, H.J.  
DEPARTMENT OF PHYSICS  
UNIVERSITY OF VIRGINIA  
MC CORMICK ROAD  
CHARLOTTESVILLE, VA 22901  
USA

WEDDIGEN, C.  
KERNFORSCHUNGSZENTRUM KARLSRUHE GMBH  
IK II  
POSTFACH 3640  
7500 KARLSRUHE  
WEST-GERMANY

WEIDENMUELLER, H.A.  
MAX-PLANCK-INSTITUT FUER KERNPHYSIK  
POSTFACH 10 39 80

6900 HEIDELBERG  
WEST-GERMANY

WEISE, W.  
INSTITUT FUER THEORETISCHE PHYSIK  
UNIVERSITAET REGENSBURG

8400 REGENSBURG  
WEST-GERMANY

WELLER, H.R.  
PHYSICS DEPARTMENT  
DUKE UNIVERSITY

DURHAM, NORTH CAROLINA 27706  
USA

WICK, K.  
I. INSTITUT FUER EXPERIMENTALPHYSIK  
UNIVERSITAET HAMBURG  
LURUPER CHAUSSEE 149  
2000 HAMBURG 50  
WEST-GERMANY

WIESE, U.-J.  
INSTITUT FUER THEORETISCHE PHYSIK  
UNIVERSITAET HANNOVER  
APPELSTR. 2  
3000 HANNOVER  
WEST-GERMANY

WILCZYNSKI, J.  
KERNFORSCHUNGSZENTRUM KARLSRUHE GMBH  
INSTITUT FUER KERNPHYSIK I  
POSTFACH 3640  
7500 KARLSRUHE  
WEST-GERMANY

WILK, S.  
DEPARTMENT OF PHYSICS  
UNIVERSITY OF MANITOBA

WINNIPEG, MANITOBA R3T 2N2  
CANADA

WIRINGA, R.  
ARGONNE NATIONAL LABORATORY  
DEPARTMENT OF PHYSICS  
9700 SOUTH CASS AVENUE  
ARGONNE, ILL. 60439  
USA

WIRZBA, A.  
NIELS BOHR INSTITUT  
BLEGDAKSVEJ 17

2100 KOPENHAGEN  
DENMARK

WOCHLE, J.  
KERNFORSCHUNGSZENTRUM KARLSRUHE GMBH  
INSTITUT FUER KERNPHYSIK I  
POSTFACH 3640  
7500 KARLSRUHE  
WEST-GERMANY

WOOLVERTON, H.L.  
FAKULTAET FUER PHYSIK  
HERMANN-HERDER-STR. 3

7800 FREIBURG  
WEST-GERMANY

WU, C.-E.  
DEPARTMENT OF PHYSICS  
GUANGXI UNIVERSITY

NANNING, GUANGXI  
THE PEOPLES REPUBLIC OF CHINA

YANG, S.N.  
DEPARTMENT OF PHYSICS  
NATIONAL TAIWAN UNIVERSITY

TAIPEI, TAIWAN 107  
TAIWAN

YAZAKI, K.  
UNIVERSITY OF TOKYO  
FACULTY OF SCIENCE, DEP. OF PHYSICS  
7-3-1 HONGO, BUNKYO-KU  
TOKYO 113  
JAPAN

ZABOLITZKY, J.G.  
INSTITUT FUER THEORETISCHE PHYSIK  
UNIVERSITAET ZU KOELN  
ZUELPICHER STRASSE 77  
5000 KOELN 41  
WEST-GERMANY

ZICKENDRAHT, W.  
UNIVERSITAET MARBURG  
FACHBEREICH PHYSIK  
RENTHOF 5  
3550 MARBURG  
WEST-GERMANY

ZANKEL, H.  
INSTITUT FUER THEORETISCHE PHYSIK  
UNIVERSITAET GRAZ  
UNIVERSITAETSPLATZ 5  
8010 GRAZ  
AUSTRIA

ZIEGER, A.  
MAX PLANCK INSTITUT FUER CHEMIE  
KERNPHYSIKALISCHE ARBEITSGRUPPE  
SAARSTR. 23  
6500 MAINZ  
WEST-GERMANY

ZEITNITZ, B.  
KERNFORSCHUNGSZENTRUM KARLSRUHE GMBH  
INSTITUT FUER KERNPHYSIK I  
POSTFACH 3640  
7500 KARLSRUHE  
WEST-GERMANY

ZIEGLER, B.  
MAX-PLANCK-INSTITUT FUER CHEMIE  
KERNPHYSIKALISCHE ABTEILUNG  
SAARSTRASSE 23  
6500 MAINZ  
WEST-GERMANY

ZHANG, XI-ZHEN  
INSTITUTE OF ATOMIC ENERGY  
P.O. BOX 275  
PEKING  
THE PEOPLES REPUBLIC OF CHINA

ZINGL, H.  
INSTITUT FUER THEORETISCHE PHYSIK  
UNIVERSITAET GRAZ  
UNIVERSITAETSPLATZ 5  
8010 GRAZ  
AUSTRIA





## AUTHOR INDEX

AFNAN, I.R., 257c  
 AKAISHI, Y., 409c  
 ARNOLD, R.G., 119c  
 ARVIEUX, J., 141c  
 AVISHAI, Y., 211c

BRODSKY, S.J., 3c  
 BUGG, D.V., 227c

CLOSE, F.E., 55c

DE SWART, J.J., 299c  
 DERKS, W., 299c  
 DERMOTT, S.F., 535c  
 DETAR, C., 129c  
 DOVER, C.B., 313c

ERICSON, T.E.O., 281c

FIORENTINI, G., 519c  
 FONSECA, A.C., 421c  
 FROIS, B., 583c

GIBSON, B.F., 503c  
 GLÖCKLE, L., 435c  
 GROSS, F., 387c

HOFMANN, H.M., 363c  
 HÖHLER, G., 209c

JONES, G., 157c

KOK, L.P., 481c  
 KOWALSKI, K.L., 465c  
 KUTI, J., 25c

LIM, T.K., 491c  
 LOCHER, M.P., 243c  
 LOMON, E., 613c

McKELLAR, B.H.J., 435c  
 MULDER, P.J., 99c

NEFKENS, B.M.K., 193c

PLATTNER, G.-R., 565c

RINAT, A.S., 481c

SAUER, P.U., 335c  
 SCHMID, E.W., 347c, 379c  
 SICK, I., 605c  
 SIMMONS, J.E., 553c  
 SIMONOV, Yu.A., 109c

THOMAS, A.W., 69c

VAN DER SANDEN, W.A., 299c  
 VAN OERS, W.T.H., 267c

YAZAKI, K., 87c

ZABOLITZKY, J.G., 401c









MICHIGAN STATE UNIV. LIBRARIES



31293002384455